BEILSTEIN JOURNAL OF ORGANIC CHEMISTRY

Organo-fluorine chemistry IV

Edited by David O'Hagan

Imprint

Beilstein Journal of Organic Chemistry
www.bjoc.org
ISSN 1860-5397
Email: journals-support@beilstein-institut.de

The *Beilstein Journal of Organic Chemistry* is published by the Beilstein-Institut zur Förderung der Chemischen Wissenschaften.

Beilstein-Institut zur Förderung der Chemischen Wissenschaften
Trakehner Straße 7–9
60487 Frankfurt am Main
Germany
www.beilstein-institut.de

BEILSTEIN JOURNAL OF ORGANIC CHEMISTRY

Preparation of imidazo[1,2-*a*]-*N*-heterocyclic derivatives with *gem*-difluorinated side chains

Layal Hariss[1], Kamal Bou Hadir[2], Mirvat El-Masri[1], Thierry Roisnel[3], René Grée[*3] and Ali Hachem[*1]

Full Research Paper

Open Access

Address:
[1]Laboratory for Medicinal Chemistry and Natural Products, Lebanese University, Faculty of Sciences (1) and PRASE-EDST, Hadath, Beirut, Lebanon, [2]American University of Beirut, Department of Chemistry, Beirut 11-0236, Lebanon and [3]Université de Rennes 1, Institut des Sciences Chimiques de Rennes, CNRS UMR 6226, Avenue du Général Leclerc, 35042 Rennes Cedex, France

Email:
René Grée[*] - rene.gree@univ-rennes1.fr; Ali Hachem[*] - ahachem@ul.edu.lb

* Corresponding author

Keywords:
aerobic oxidative coupling; imidazo[1,2-*a*]-*N*-heterocycles; *gem*-difluoroalkyl derivatives; propargylic fluorides

Beilstein J. Org. Chem. **2017,** *13,* 2115–2121.
doi:10.3762/bjoc.13.208

Received: 07 July 2017
Accepted: 27 September 2017
Published: 10 October 2017

This article is part of the Thematic Series "Organofluorine chemistry IV".

Guest Editor: D. O'Hagan

Abstract

Using an aerobic oxidative coupling, different new imidazo[1,2-*a*]-*N*-heterocycles with *gem*-difluroroalkyl side chains have been prepared in fair yields by the reaction of *gem*-difluoroenones with aminopyridines, -pyrimidines and -pyridazines. Condensed heterocycles of this type play an important role as key core structures of various bioactive compounds. Further, starting with a chloroimidazopyridazine derivative, Pd-catalyzed coupling reactions as well as nucleophilic substitutions have been performed successfully in order to increase the molecular diversity.

Introduction

Nitrogen-containing heterocyclic compounds are frequently found in bioactive naturally occurring compounds, as well as in the synthetic pharmacopeia. Imidazo[1,2-*a*]pyridine is an important heterocyclic system present in many molecules featuring diverse biological activities, such as antiviral, antimicrobial, antitumor, anti-inflammatory, antiparasitic, hypnotic, etc. [1-5]. It is recognized as a key scaffold due to its broad occurrence in a number of drug candidates and drugs, such as zolpidem [6] (**1a**, used in the treatment of insomnia), and alpidem [6] (**1b**, an anxiolytic agent). Some imidazopyridine derivatives also act as β-amyloid formation inhibitors, GABA and benzodiazepine receptor agonists, and cardiotonic agents [7-10]. Further, the biological activities of imidazo[1,2-*a*]pyridines proved to be strongly depending upon the nature of substituents at C2 and C3 positions. For instance, the 3-aroylimidazo[1,2-*a*]pyridines **1c** demonstrated also good anticancer

properties [11,12], while imidazo[1,2-*a*]pyrimidines **2** are also known for their antituberculosis activity [13], and imidazopyridazine **3** acts as a sirtuin modulator [14].

On the other hand, the incorporation of fluorine or fluorinated groups into organic molecules has been widely recognized as a general strategy toward drug development in pharmaceutical research. This is connected to fluorine's electronegativity, size, and lipophilicity [15,16], which can strongly improve the biological properties of molecules through, for instance, increase of metabolic stability and bioavailability for many drugs and pharmacological tools. So, the preparation of fluorinated molecules is a very attractive research area for organic and medicinal chemists [17-20].

Our research program aims to synthesize new fluorinated molecules based on the easy access and the versatility of fluorinated propargylic derivatives [21]. Thus, taking into account the known biological properties of the imidazo-fused *N*-heterocycles, we became interested in the preparation of new derivatives of this type possessing *gem*-difluorinated side chains as indicated in Figure 1. Such new fluorinated heterocycles could be of interest for bioorganic and medicinal chemistry studies.

Several synthetic approaches for imidazopyridines are available, but only a few examples have been reported to date for the construction of this scaffold with introduction of fluorine [22], trifluoromethyl [23] or trifluoroethyl groups [24]. Herein, we report the synthesis of imidazo[1,2-*a*]pyridines, imidazo[1,2-*a*]pyrimidines, and imidazopyridazines with fluorinated side chains following an efficient strategy developed by Hajra et al. [25]. This methodology, developed for the synthesis of 3-aroylimidazopyridines, involves a copper(II) acetate-catalyzed aerobic oxidative amination and it proceeds through a tandem Michael addition followed by an intramolecular oxidative amination. Therefore, our target molecules **A** could be synthesized by the oxidative coupling of 2-aminopyridines with α,β-unsaturated ketones **B**, themselves easily accessible from *gem*-difluoropropargylic alcohols **C** through a base-mediated isomerization process (Scheme 1) [26,27].

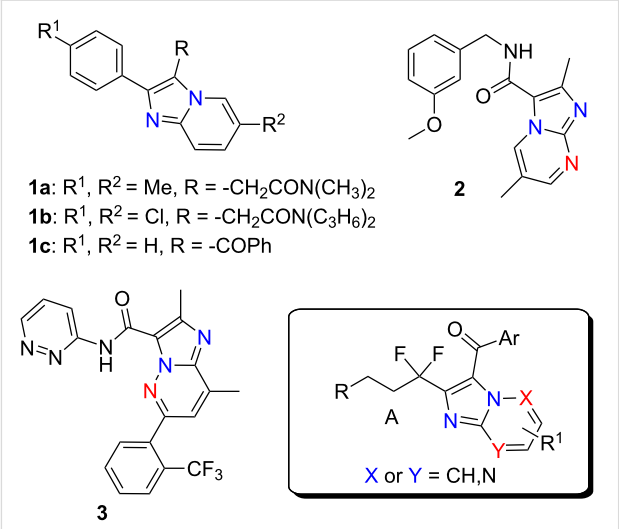

Figure 1: Representative examples of bioactive imidazo[1,2-*a*]pyridines, imidazo[1,2-*a*]pyrimidines, imidazopyridazines and our target molecules.

Results and Discussion

The required propargylic alcohols **5a**–**e** (type **C**, Scheme 1) were obtained in 27–73% yields by reaction of the lithium salt of the easily accessible *gem*-difluoro propargylic derivatives **4** [28] with aromatic aldehydes. Then, the DBU-mediated isomerization afforded the desired enones **6a**–**e** in 21–66% yields (Scheme 2 and Table 1).

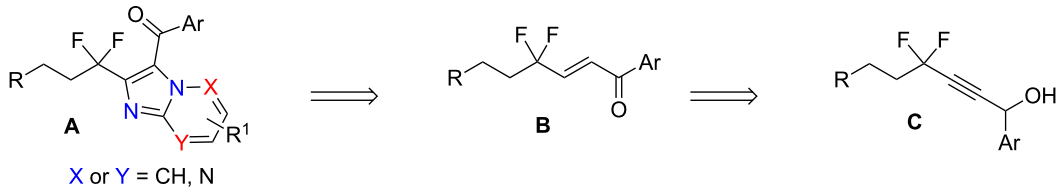

Scheme 1: Retrosynthetic scheme for the preparation of our target molecules **A**.

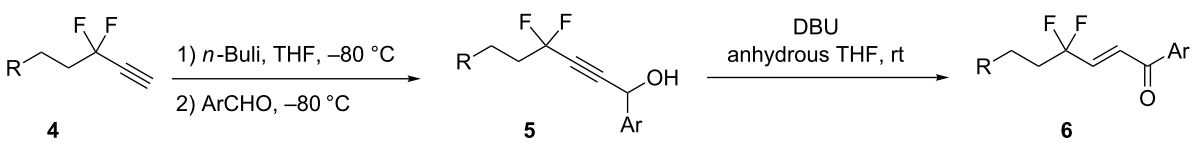

Scheme 2: Synthesis of enones **6** with a *gem*-difluoroalkyl side chain.

Table 1: Synthesis of enones **6a–e**.

Entry	R	Ar	**5**: yield (%)	**6**: yield (%)
1	Ph	Ph	**5a** (73%)	**6a** (62%)
2	Ph	*o*-PhBr	**5b** (70%)	**6b** (60%)
3	Ph	2-naphthaldehyde	**5c** (71%)	**6c** (50%)
4	Ph	*p*-anisaldehyde	**5d** (27%)	**6d** (21%)
5	CH_2OBn	Ph	**5e** (65%)	**6e** (66%)

For the synthesis of the desired nitrogen heterocycles, we started our study by reacting **6a** with 2-aminopyridine in the presence of $AlCl_3$ and I_2 under an O_2 atmosphere [29]. However, only a poor yield was obtained (20%, Scheme 3).

Then, we found that $Cu(OAc)_2{\cdot}H_2O$ (10 mol %) and 1,10-phenanthroline (10 mol %) in chlorobenzene at 160 °C under an O_2 atmosphere, following the conditions recently reported by Hajra et al. [25], gave **7a** in 62% yield (Table 2, entry 1). Having these optimized conditions in hand, and to explore the substrate scope, different substituted 2-aminopyridines were successfully employed to afford the tandem oxidative cyclization products **7** in 32–65% yields. On the other hand, enones **6** with two different R groups (Table 2, entries 1, 2, 3, 6, 8, and 9)

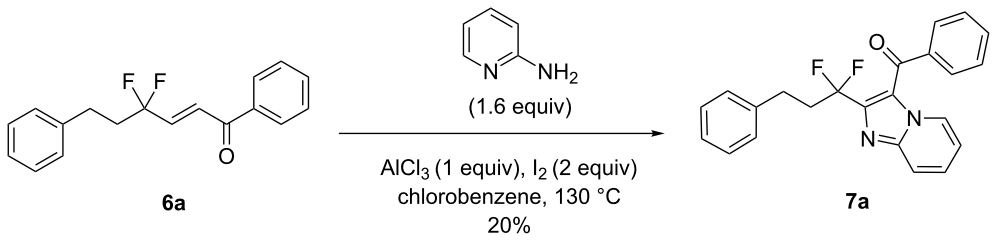

Scheme 3: Synthesis of **7a**.

Table 2: Preparation of different imidazo[1,2-*a*]-*N*-heterocyclic derivatives.

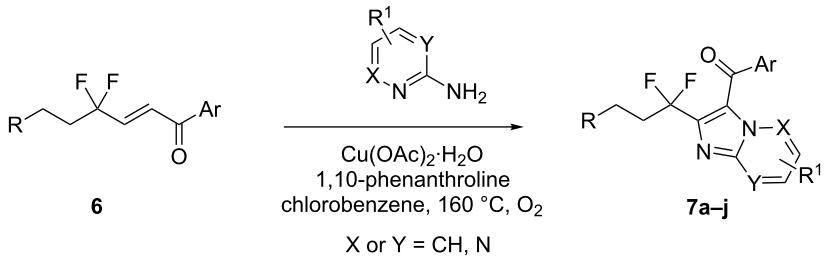

Entry	Product	Ar	R	R^1	X	Y	Time	Yield (%)
1	**7a**	Ph	Ph	H	CH	CH	25 h	62
2	**7b**	Ph	Ph	7-Me	CH	CH	20 h	60
3	**7c**	Ph	Ph	6-Br	CH	CH	46 h	60
4	**7d**	Ph	Ph	H	CH	N	30 h	57
5	**7e**	Ph	Ph	6-Cl	N	CH	24 h	53
6	**7f**	Ph	$-CH_2OBn$	H	CH	CH	33 h	55
7	**7g**	Ph	$-CH_2OBn$	H	CH	N	29 h	36
8	**7h**	*o*-BrPh	Ph	H	CH	CH	4 h	65
9	**7i**	2-naphthaldehyde	Ph	H	CH	CH	3.5 h	59
10	**7j**	*p*-MeOPh	Ph	H	CH	CH	6 h	32

were well tolerated under the optimized conditions affording the tandem products **7** in fair to moderate yields, although lower yields were obtained in the cases of **7j** and **7g** (32% and 36%, respectively). Moreover, two other important heterocyclic frameworks, imidazo[1,2-*a*]pyrimidines **7d** and imidazo[1,2-*b*]pyridazines **7e**, have been synthesized by the same method albeit in slightly decreased yields (Table 2, entries 4 and 5).

The structures of molecules **7** are in full agreement with their spectroscopical (NMR) and analytical data (HRMS). For the imidazopyridines, the structure of **7a** was confirmed by X-ray analysis (Figure 2) [30] and the other derivatives were proposed by analogy. In the same way as for the imidazopyridazines, the structure of **7e** was established by X-ray analysis [30] and this was extended to the other derivatives. These results unambiguously demonstrate the regiochemistry of the reaction. These cascade reactions proceed first through a Michael addition of the primary amine on the enone, followed by an intramolecular cyclization by the pyridine/pyrimidine nucleus. Unfortunately, no crystal structure could be obtained for the imidazopyrimidines and therefore the corresponding structures **7d** and **7g** were proposed by analogy.

These oxidative coupling conditions appeared compatible with the first isomerization step, therefore, the possibility of a "one-pot" reaction was considered. Indeed, by heating alcohol **5a** (Table 1, entry 1) with 2-aminopyridine and DBU (1,8-diazabicycloundec-7-ene) under the same conditions as mentioned above, the desired imidazopyridine derivative **7a** was isolated in 33% yield (Scheme 4). This one-pot process gives an overall yield very close to the two-step reaction (38%).

Further, the halogen-substituted substrate **7e** appeared as an attractive precursor to increase the molecular diversity around this scaffold. In order to explore this possibility, we performed two Suzuki–Miyaura reactions, as representative examples of Pd-catalyzed coupling processes (Table 3). They gave the target molecules **8** and **9** in 46% and 53% yields, respectively. On the other hand, two nucleophilic substitution reactions using phenol

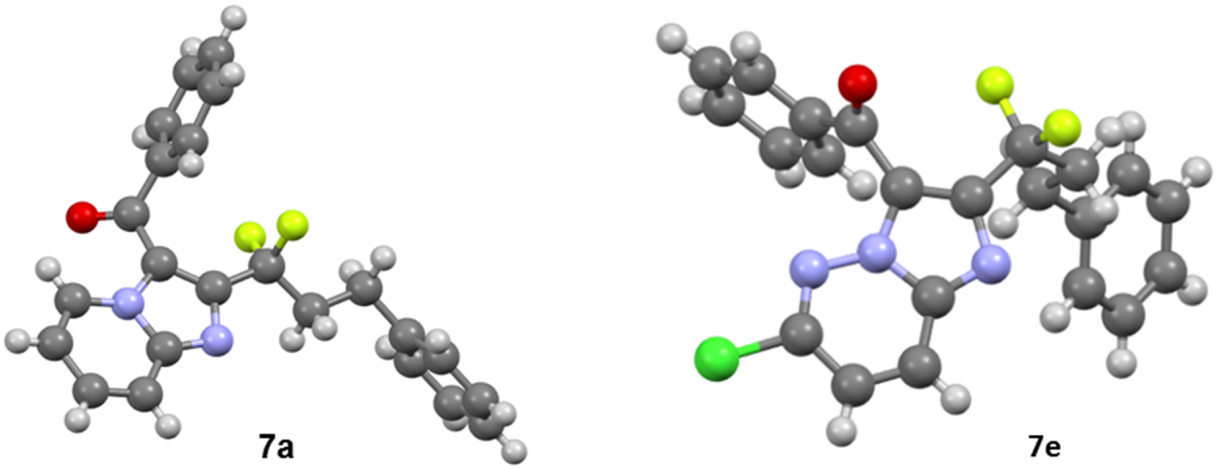

Figure 2: Structures of **7a** and **7e** by X-ray crystallography analysis.

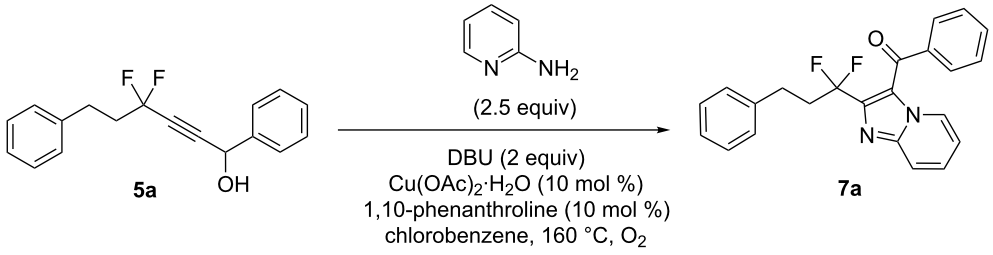

Scheme 4: One-pot synthesis of **7a**.

Table 3: Coupling and substitution reactions.

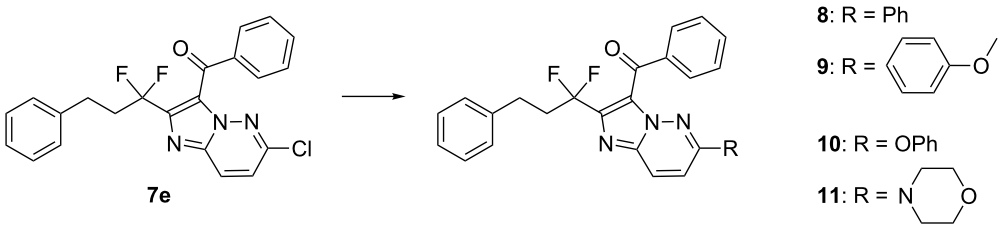

Entry	Product	R	Conditions	Yield (%)
1	**8**	Ph	$PhB(OH)_2$, Na_2CO_3, $PdCl_2(dppf)_2$, $EtOH/H_2O$, 16 h	46
2	**9**	*p*-MeOPh	methoxyphenylboronic acid, Na_2CO_3, $PdCl_2(dppf)_2$, $EtOH/H_2O$, 16 h	53
3	**10**	PhO	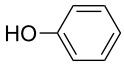 K_2CO_3, DMF, 120 °C, 5 h	73
4	**11**		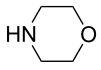 NEt_3, EtOH, reflux, 2 days	23

and morpholine gave the expected heterocycles **10** and **11** in 73% and 23% yields, respectively.

Conclusion

In summary, we developed a short and completely regioselective method for the synthesis of imidazo[1,2-*a*]-*N*-heterocycles with *gem*-fluorinated side chains starting from easily accessible propargylic fluorides. Although the yields are only moderate to fair, this short (1–2 steps) method offers significant flexibility to prepare focused libraries of molecules with this core structure. Such new fluorine-containing heteroaromatic frameworks would be of much interest for biological studies in different areas of life sciences.

Experimental

Representative procedure for the synthesis of imidazopyridine 7a

The syntheses of propargylic fluorides **5** and enones **6** were performed in a similar way as described before [26].

Synthesis of 4,4-difluoro-1,6-diphenylhex-2-yn-1-ol (5a)

To a solution of *gem*-difluoro intermediate **4** [28] (500 mg, 2.77 mmol, 1 equiv) in anhydrous THF (6 mL) cooled at −80 °C was added dropwise under nitrogen a 2.5 M solution of *n*-BuLi in hexanes (1.3 mL, 3.30 mmol, 1.2 equiv). The mixture was stirred for 1 h at a temperature below −80 °C before dropwise addition of the aldehyde (0.35 mL, 3.33 mmol, 1.2 equiv) in anhydrous THF (4 mL). The reaction mixture was stirred for additional 45 min at $t < -80$ °C and then allowed to warm to rt for 2 h. The mixture was then treated with a saturated ammonium chloride solution and extracted with ethyl acetate. The combined organic phases were washed with water, dried over Na_2SO_4 and concentrated in vacuo. The crude product was purified by chromatography on silica gel, using a mixture of petroleum ether/ethyl acetate as eluent. After purification by chromatography on silica gel, propargylic alcohol **5a** was obtained as a colorless oil (580 g, 73% yield); R_f 0.46 (petroleum ether/AcOEt 8:2); ^{1}H NMR ($CDCl_3$, 300 MHz) δ 7.59–7.25 (m, 10H), 5.54 (t, J_{HF} = 3.9 Hz, 1H), 2.99–2.93 (m, 2H), 2.54–2.38 (m, 2H), 2.83 (br s, 1H); ^{13}C NMR ($CDCl_3$, 75 MHz) δ 139.7, 138.9 (t, ^4J = 1.1 Hz), 128.8, 128.7 (2C), 128.5 (2C), 128.3 (2C), 126.5, 126.3, 125.9, 114.1 (t, ^1J = 233.4 Hz), 87.0 (t, ^3J = 6.8 Hz), 79.1 (t, ^2J = 40.9 Hz), 64.0 (t, ^4J = 1.8 Hz), 40.8 (t, ^2J = 26.1 Hz), 28.9 (t, ^3J = 4.0 Hz); ^{19}F NMR ($CDCl_3$, 282 MHz) δ −83.45 (td, J_{FH} = 14.6, 3.9 Hz); HRMS (ESI) *m*/*z* $[M + Na]^+$: calcd. for $C_{18}H_{16}OF_2Na$, 309.10614; found, 309.1060 (0 ppm); *m*/*z* $[M - HF + Na]^+$: calcd. for $C_{18}H_{15}OFNa$, 289.09991; found, 289.0992 (2 ppm).

Synthesis of (*E*)-4,4-difluoro-1,6-diphenylhex-2-en-1-one (6a)

The previous difluoropropargylic alcohol **5a** (540 mg, 1.88 mmol, 1 equiv) was dissolved in THF (4 mL), then DBU (0.42 mL, 2.82 mmol, 1.5 equiv) was added and the reaction mixture was stirred at room temperature. After 2 h, ^{19}F NMR

showed 100% conversion and the reaction mixture was neutralized with a saturated solution of NH_4Cl. After extraction with ethyl acetate, the organic phases were washed with water, dried (Na_2SO_4) and concentrated in vacuo. The crude product was purified by chromatography on silica gel, using a mixture of petroleum ether/ethyl acetate as eluent. Enone **6a** was isolated as a colorless oil (335 mg, 62% yield); R_f 0.43 (petroleum ether/AcOEt 9:1); ^{1}H NMR ($CDCl_3$, 500 MHz) δ 8.04 (m, 2H), 7.66–7.64 (m, 1H), 7.57–7.52 (m, 2H), 7.35–7.28 (m, 6H), 6.97 (m, 1H), 2.93–2.92 (m, 2H), 2.41–2.35 (m, 2H); ^{13}C NMR ($CDCl_3$, 125 MHz) δ 188.93, 139.8, 138.3 (t, ^2J = 27.1 Hz), 136.7, 133.5, 128.7 (2C), 128.6 (2C), 128.5 (2C), 128.1 (2C), 127.6 (t, ^3J = 7.5 Hz), 126.3, 120.6 (t, ^1J = 240.4 Hz), 38.9 (t, ^2J = 25.9 Hz), 28.2 (t, ^3J = 4.3 Hz); ^{19}F NMR ($CDCl_3$, 282 MHz) δ −98.84 (m); HRMS (ESI) *m*/*z* [M + Na]$^+$: calcd. for $C_{18}H_{16}OF_2Na$, 309.10614; found, 309.1059 (1 ppm).

Synthesis of (2-(1,1-difluoro-3-phenylpropyl)imidazo[1,2-*a*]pyridin-3-yl)(phenyl)methanone (**7a**)

A mixture of 2-aminopyridine (20 mg, 0.21 mmol, 1.2 equiv), enone **6a** (51 mg, 0.17 mmol, 1 equiv), $Cu(OAc)_2{\cdot}H_2O$ (3.6 mg, 0.02 mmol, 10 mol %), and 1,10-phenanthroline (2.5 µL, 0.02 mmol, 10 mol %) in chlorobenzene (1 mL) was stirred in a reaction tube at 160 °C under an O_2 atmosphere. After 25 h, ^{19}F NMR monitoring indicated complete consumption of the starting material. The reaction mixture was cooled to room temperature, filtered and extracted with dichloromethane. The filtrate was concentrated and the crude product was purified by column chromatography on silica gel, using petroleum ether/ethyl acetate as eluent. **7a** was isolated as white crystals (32 mg, 62% yield); R_f 0.46 (petroleum ether/EtOAc 7:3); Mp: 117 °C; ^{1}H NMR ($CDCl_3$, 300 MHz) δ 8.76 (d, *J* = 6.9 Hz, 1H), 7.89 (s, 1H), 7.86 (s, 1H), 7.75 (d, *J* = 9.0 Hz, 1H), 7.64 (t, *J* = 7.3 Hz, 1H), 7.53–7.43 (m, 3H), 7.26–7.13 (m, 5H), 7.02 (t, *J* = 6.7 Hz, 1H), 2.72–2.65 (m, 4H); ^{13}C NMR ($CDCl_3$, 75 MHz) δ 187.9, 146.1, 145.1, 140.4, 139.5 (t, ^3J = 2.1 Hz), 133.3 (2C), 129.5, 128.4 (2C), 128.3 (3C), 128.2 (2C), 127.3, 126.0, 120.6, 120.3 (t, ^1J = 239.8 Hz), 118.2, 114.7, 39.3 (t, ^2J = 25.1 Hz), 28.3 (t, ^3J = 4.4 Hz); ^{19}F NMR ($CDCl_3$, 282 MHz) δ −90.93 (t, *J* = 15.7 Hz); HRMS (ESI) *m*/*z* [M + Na]$^+$: calcd. for $C_{23}H_{18}N_2OF_2Na$, 399.12794; found, 399.1279 (0 ppm); *m*/*z* [M + H]$^+$: calcd. for $C_{23}H_{19}N_2OF_2$, 377.14599; found, 377.1454 (2 ppm); *m*/*z* [M – HF + Na]$^+$: calcd. for $C_{23}H_{17}N_2OFNa$, 379.12171; found, 379.1216 (0 ppm).

One pot synthesis of (2-(1,1-difluoro-3-phenylpropyl)imidazo[1,2-*a*]pyridin-3-yl)(phenyl)methanone (**7a**)

A mixture of 2-aminopyridine (25 mg, 0.26 mmol, 2.5 equiv), alcohol **5a** (30 mg, 0.10 mmol, 1 equiv), DBU (0.03 mL, 0.20 mmol, 2 equiv), $Cu(OAc)_2{\cdot}H_2O$ (2.1 mg, 0.01 mmol, 10 mol %), and 1,10-phenanthroline (1.4 µL, 0.01 mmol, 10 mol %) in chlorobenzene (1 mL) was stirred in a reaction tube at 160 °C under an O_2 atmosphere. After 4 h monitoring by ^{19}F NMR indicated the disappearance of the starting material. Thus the mixture was cooled to room temperature, filtered, washed and extracted with dichloromethane. The organic phase was concentrated and the crude product was purified by column chromatography on silica gel, using petroleum ether/ethyl acetate as eluent. Imidazopyridine **7a** was isolated in 33% yield.

Supporting Information

Supporting Information File 1

Experimental details and characterization data of new compounds with copies of ^{1}H, ^{13}C and ^{19}F NMR spectra.
[http://www.beilstein-journals.org/bjoc/content/supplementary/1860-5397-13-208-S1.pdf]

Acknowledgements

This work was financially supported by the Research Grant Program at Lebanese University (Lebanon). We thank all members of the two teams (Beirut and Rennes) for fruitful discussion and kind help. We thank CRMPO (Rennes) for the mass spectral analysis.

References

1. Lhassani, M.; Chavignon, O.; Chezal, J.-M.; Teulade, J.-C.; Chapat, J.-P.; Snoeck, R.; Andrei, G.; Balzarini, J.; De Clercq, E.; Gueiffier, A. *Eur. J. Med. Chem.* **1999,** *34,* 271. doi:10.1016/S0223-5234(99)80061-0 and references cited therein.
2. Pericherla, K.; Kaswan, P.; Pandey, K.; Kumar, A. *Synthesis* **2015,** *47,* 887. doi:10.1055/s-0034-1380182 and references cited therein.
3. Koubachi, J.; El Kazzouli, S.; Bousmina, M.; Guillaumet, G. *Eur. J. Org. Chem.* **2014,** 5119. doi:10.1002/ejoc.201400065 and references cited therein.
4. Basilio-Lopes, A.; de Aquino, T. M.; Mongeot, A.; Bourguignon, J.-J.; Schmitt, M. *Tetrahedron Lett.* **2012,** *53,* 2583. doi:10.1016/j.tetlet.2012.02.117 and references cited therein.
5. Rao, N. S.; Kistareddy, C.; Balram, B.; Ram, B. *Pharma Chem.* **2012,** *4,* 2408. and references cited therein.
6. Langer, S. Z.; Arbilla, S.; Benavides, J.; Scatton, B. *Adv. Biochem. Psychopharmacol.* **1990,** *46,* 61. and references cited therein.
7. Humphries, A. C.; Gancia, E.; Gilligan, M. T.; Goodacre, S.; Hallett, D.; Marchant, K. J.; Thomas, S. R. *Bioorg. Med. Chem. Lett.* **2006,** *16,* 1518. doi:10.1016/j.bmcl.2005.12.037
8. Fuchs, K.; Romig, M.; Mendla, K.; Briem, H.; Fechteler, K. Novel beta-amyloid inhibitors, method for producing the same and the use thereof as medicaments. WO Patent WO2002014313, July 21, 2001.

9. Davey, D.; Erhardt, P. W.; Lumma, W. C., Jr.; Wiggins, J.; Sullivan, M.; Pang, D.; Cantor, E. *J. Med. Chem.* **1987,** *30,* 1337. doi:10.1021/jm00391a012
10. Fookes, C. J. R.; Pham, T. Q.; Mattner, F.; Greguric, I.; Loch, C.; Liu, X.; Berghofer, P.; Shepherd, R.; Gregoire, M.-C.; Katsifis, A. *J. Med. Chem.* **2008,** *51,* 3700. doi:10.1021/jm7014556
11. Tung, Y.-S.; Coumar, M. S.; Wu, Y.-S.; Shiao, H.-Y.; Chang, J.-Y.; Liou, J.-P.; Shukla, P.; Chang, C.-W.; Chang, C.-Y.; Kuo, C.-C.; Yeh, T.-K.; Lin, C.-Y.; Wu, J.-S.; Wu, S.-Y.; Liao, C.-C.; Hsieh, H.-P. *J. Med. Chem.* **2011,** *54,* 3076. doi:10.1021/jm101027s
12. Hseih, H.-P.; Chao, Y.-S.; Liou, J.-P.; Chang, J.-Y.; Tung, Y.-S. Antitumor compounds. U.S. Patent US7,456,289, Dec 15, 2005.
13. Moraski, G. C.; Markley, L. D.; Hipskind, P. A.; Boshoff, H.; Cho, S.; Franzblau, S. G.; Miller, M. J. *ACS Med. Chem. Lett.* **2011,** *2,* 466. doi:10.1021/ml200036r
14. Casaubon, R. L.; Narayan, R.; Oalmann, C.; Vu, C. B. Substituted bicyclic azaheterocycles and analogues as sirtuin modulators. WO Patent WO2,013,059,587, Oct 19, 2012.
15. Hudlicky, M., Ed. *Chemistry of Organic Fluorine Compounds II: A Critical Review;* ACS Monograph, Vol. 187; American Chemical Society: Washington, DC, 1995.
16. Kitazume, T.; Yamazaki, T. *Experimental Methods in Organic Fluorine Chemistry;* Gordon and Breach Science Publishers: Tokyo, 1998.
17. Qing, F.-L.; Zheng, F. *Synlett* **2011,** 1052. doi:10.1055/s-0030-1259947 and references cited therein. See for a recent review article.
18. Gillis, E. P.; Eastman, K. J.; Hill, M. D.; Donnelly, D. J.; Meanwell, N. A. *J. Med. Chem.* **2015,** *58,* 8315. doi:10.1021/acs.jmedchem.5b00258 and references cited therein. See for a recent review article.
19. Zhou, Y.; Wang, J.; Gu, Z.; Wang, S.; Zhu, W.; Aceña, J. L.; Soloshonok, V. A.; Izawa, K.; Liu, H. *Chem. Rev.* **2016,** *116,* 422. doi:10.1021/acs.chemrev.5b00392 and references cited therein. See for a recent review article.
20. Yerien, D. E.; Bonesi, S.; Postigo, A. *Org. Biomol. Chem.* **2016,** *14,* 8398. doi:10.1039/c6ob00764c and references cited therein. See for a recent review article.
21. Hachem, A.; Grée, D.; Chandrasekhar, S.; Grée, R. *Synthesis* **2017,** *49,* 2101. doi:10.1055/s-0036-1589484 and references cited therein.
22. Liu, P.; Gao, Y.; Gu, W.; Shen, Z.; Sun, P. *J. Org. Chem.* **2015,** *80,* 11559. doi:10.1021/acs.joc.5b01961
23. Monir, K.; Bagdi, A. K.; Ghosh, M.; Hajra, A. *J. Org. Chem.* **2015,** *80,* 1332. doi:10.1021/jo502928e
24. Zhu, M.; Han, X.; Fu, W.; Wang, Z.; Ji, B.; Hao, X.-Q.; Song, M.-P.; Xu, C. *J. Org. Chem.* **2016,** *81,* 7282. doi:10.1021/acs.joc.6b00950
25. Monir, K.; Bagdi, A. K.; Mishra, S.; Majee, A.; Hajra, A. *Adv. Synth. Catal.* **2014,** *356,* 1105. doi:10.1002/adsc.201300900
26. Nasr El Dine, A.; Khalaf, A.; Grée, D.; Tasseau, O.; Fares, F.; Jaber, N.; Lesot, P.; Hachem, A.; Grée, R. *Beilstein J. Org. Chem.* **2013,** *9,* 1943. doi:10.3762/bjoc.9.230
27. Nasr El Dine, A.; Grée, D.; Roisnel, T.; Caytan, E.; Hachem, A.; Grée, R. *Eur. J. Org. Chem.* **2016,** 556. doi:10.1002/ejoc.201501347
28. Pujari, S. A.; Kaliappan, K. P.; Valleix, A.; Grée, D.; Grée, R. *Synlett* **2008,** 2503. doi:10.1055/s-2008-1078179
29. Xing, M.-M.; Xin, M.; Shen, C.; Gao, J.-R.; Jia, J.-H.; Li, Y.-J. *Tetrahedron* **2016,** *72,* 4201. doi:10.1016/j.tet.2016.05.052
30. CCDC 1549632 (for compound **7a**) and CCDC 1549633 (for compound **7e**) contain the supplementary crystallographical data for this paper. These data can be obtained free of charge from the Cambridge Crystallographic Data Centre.

License and Terms

BEILSTEIN JOURNAL OF ORGANIC CHEMISTRY

Synthesis and application of trifluoroethoxy-substituted phthalocyanines and subphthalocyanines

Satoru Mori[1] and Norio Shibata[*1,2]

Review

Open Access

Address:
[1]Department of Nanopharmaceutical Sciences, Nagoya Institute of Technology, Gokiso, Showa-ku, Nagoya 466-8555, Japan and [2]Department of Life Science and Applied Chemistry, Nagoya Institute of Technology, Gokiso, Showa-ku, Nagoya 466-8555, Japan

Email:
Norio Shibata[*] - nozshiba@nitech.ac.jp

* Corresponding author

Keywords:
aggregation; fluorine; phthalocyanine; subphthalocyanine; trifluoroethoxy

Beilstein J. Org. Chem. **2017,** *13,* 2273–2296.
doi:10.3762/bjoc.13.224

Received: 08 July 2017
Accepted: 12 October 2017
Published: 27 October 2017

This article is part of the Thematic Series "Organo-fluorine chemistry IV".

Guest Editor: D. O'Hagan

Abstract

Phthalocyanines and subphthalocyanines are attracting attention as functional dyes that are applicable to organic solar cells, photodynamic therapy, organic electronic devices, and other applications. However, phthalocyanines are generally difficult to handle due to their strong ability to aggregate, so this property must be controlled for further applications of phthalocyanines. On the other hand, trifluoroethoxy-substituted phthalocyanines are known to suppress aggregation due to repulsion of the trifluoroethoxy group. Furthermore, the electronic characteristics of phthalocyanines are significantly changed by the strong electronegativity of fluorine. Therefore, it is expected that trifluoroethoxy-substituted phthalocyanines can be applied to new industrial fields. This review summarizes the synthesis and application of trifluoroethoxy-substituted phthalocyanine and subphthalocyanine derivatives.

Introduction

Phthalocyanines [1-3] are analogues of porphyrin condensed with four isoindoline units via a nitrogen atom and exhibit a deep blue color due to their wide 18π electron conjugation. Among them, the most fundamental phthalocyanine copper complex, which does not have a substituent on its periphery, is known as a blue organic pigment called phthalocyanine blue [4-7]. Phthalocyanines have long been used as a blue pigment for, e.g., road signs and bullet trains because they can be manufactured cheaply, are very robust and are difficult to discolor [8]. Conventional pigments are intended for the use as colorants, so only coloring characteristics such as color tone, stability, solubility and others, have been regarded as being important. However, as the development of optoelectronics advanced in recent years, the term “functional dyes” was proposed [9-11]. Functional dye is a generic name for dyes that exceed the framework of coloration and show various chemical and physical responses. In modern times, unlike the concept of colorants in the past, dyes have been developed for various applications based on their unique functions. Phthalocyanines are also expected to be applied as functional dyes. A series of compounds having a macrocyclic π-conjugated system including porphyrin are known as functional dyes. In particular, phthalo-

cyanines have a wide range of functions and are expected to serve as novel material in the future. Besides blue organic pigments such as ink and colorants, it is expected to be widely applied to electronic devices in the medical field such as color filters for liquid crystal screens [12,13], storage media [14], dye-sensitized solar cells [15,16], photodynamic cancer treatment method [17] and other applications.

Incidentally, fluorine is one of the elements that is expected to improve the state-of-the-art science technology [18]. Fluorine is located at the top right of the periodic table of elements excluding the noble gas elements of group 18. The size of fluorine is approximately 23% larger than hydrogen and has the highest electronegativity (4.0) among all the elements [19,20]. Therefore, substituting fluorine for a single hydrogen atom in the structure of an organic compound may cause noticeable changes in the dipole moment although the change in the chemical structure is small [21,22]. As a result, compounds into which fluorine has been introduced may show beneficial changes in their properties. In addition, among the chemical bonds formed by carbon, fluorine bonds have the highest binding energy [23], such that fluorine-containing compounds often show resistance to metabolism and oxidation compared to non-fluorinated compounds. In addition to their stability, perfluorinated compounds exhibit non-tackiness, low friction, and the ability to repel water and oil [24]. Therefore, they are used as functional materials such as fluorocarbon polymer. Fluorine is also an important key element in the fields of medical and agricultural chemistry [25-31]. As described above, fluorine is considered an essential element for next-generation science technology, and many researchers have studied methods for the synthesis of fluorine-containing compounds.

By introducing a fluorine atom, phthalocyanines are also expected to become novel functional materials that reflect the specific properties of the fluorine atom. Fluorine-containing phthalocyanines have been found to behave differently from non-fluorine phthalocyanines due to the specific properties of fluorine [32]. For example, since phthalocyanines have a conjugate planar structure with high symmetry, it is very difficult to dissolve them in ordinary organic solvents. For this reason, fluorine is often introduced to improve the solubility of phthalocyanine in organic solvents [33-35]. Although ordinary phthalocyanines are known to be slightly soluble compounds, fluorine-containing phthalocyanines show high solubility in various organic solvents. Furthermore, they are thermally and chemically stable due to a strong carbon–fluorine bond [36-38]. Moreover, due to the strong electronegativity of fluorine, fluorinated phthalocyanines show interesting electrochemical behavior [39,40]. As described above, since the properties of fluorine-containing phthalocyanines change considerably due to the strong electronegativity of fluorine, their development as unprecedented new functional materials is expected. Among other fluorine-containing phthalocyanines, trifluoroethoxy-substituted phthalocyanines (TFEO-Pcs) having a trifluoroethoxy group (-OCH_2CF_3) at the periphery of the phthalocyanine can be conveniently synthesized from trifluoroethanol (CF_3CH_2OH). First, tetrakis(trifluoroethoxy)phthalonitrile (**2**) is synthesized by reacting commercially available tetrafluorophthalonitrile (**1**) with trifluoroethanol. Thereafter, tetramerization is carried out as a general synthesis of phthalocyanine to induce TFEO-Pc (Scheme 1). Since TFEO-Pcs have a large number of fluorine atoms, their solubility in organic solvents is extremely high. Therefore, TFEO-Pcs can be easily purified by silica gel column chromatography. In addition, when a phthalocyanine is substituted with an electron-donating group, such as an alkoxy group, the electron density in the phthalocyanine macrocycle increases, making it easily oxidized and becoming unstable. On the other hand, TFEO-Pcs are compounds that are stable and easy to handle because the electron density in the macrocycle does not increase due to the strong electron-withdrawing action of the fluorine atoms. By utilizing the robust-

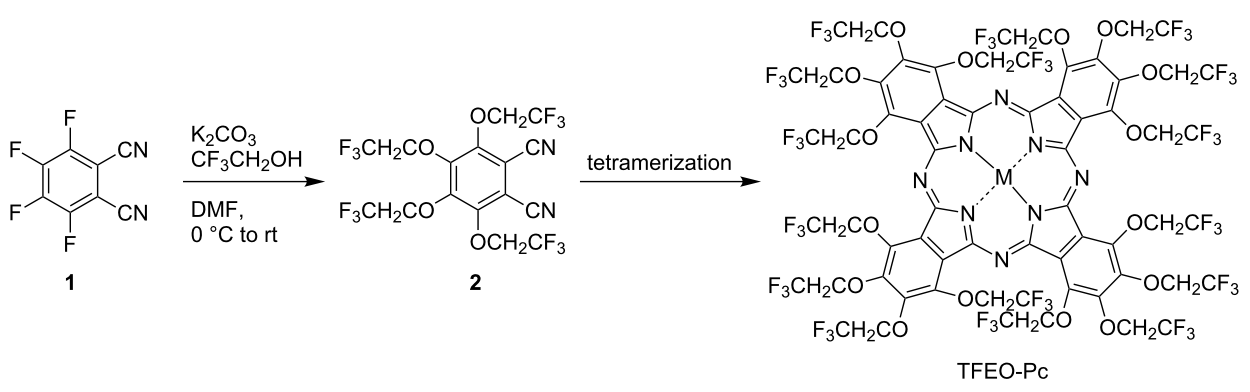

Scheme 1: Synthesis of trifluoroethoxy-substituted phthalocyanine.

ness and high solubility of TFEO-Pcs, it is possible to synthesize various phthalocyanine derivatives that are difficult to synthesize conventionally due to the weak solubility of phthalocyanine. Due to the strong electronegativity of the fluorine atom, an electron-deficient π-conjugated system is formed, so it is expected that phthalocyanine, which originally acts as an electron donor, will exhibit an electron acceptor property. Thus, it is expected that TFEO-Pcs can be developed as unique functional molecules [41]. This review summarizes the synthesis of various TFEO-Pc derivatives and the effect of fluorine on their properties.

Review

Properties of trifluoroethoxy-substituted phthalocyanines

Research on TFEO-Pc has taken place since the 1990s [42]. The early stages of this research focused on spectroscopic investigations of metal-free phthalocyanine and its zinc complex which showed the most fundamental spectroscopic properties among the phthalocyanines [43,44]. Trifluoroethoxy-substituted zinc phthalocyanine (TFEO-ZnPc) shows a very strong absorption peak called the Q band in the longer wavelength region greater than 700 nm. It is red-shifted compared with the unsubstituted phthalocyanine zinc complex due to the influence of the oxygen atom directly connected to the phthalocyanine macrocycle. The phenomenon of solvatochromism [45,46] is defined by the polarity of the solvent, and the Q band is shifted to a shorter wavelength region in a highly polar solvent. In addition to the Q band, in solvatochromism, a small absorption peak forms on the slightly shorter wavelength side than the Q band which is caused by vibrational progression of the Q band and a broad peak referred to as the Soret band in the 300–400 nm region. Unlike the strong absorption of the Q band, the emission of fluorescence by TFEO-ZnPc is not very strong, and the Stokes shift is small, about 10 nm. On the other hand, metal-free trifluoroethoxy-substituted phthalocyanine (TFEO-H_2Pc) shows a split in the Q band due to its low symmetry [47]. In metal-free phthalocyanine, the four pyrrole units in the center of the macrocycle have two protons. Therefore, metal-free phthalocyanine has the ability to donate and accept protons [48-50]. The protonation/deprotonation of the nitrogen atom in phthalocyanines easily modifies its chemical and electronic properties. And this protonation/deprotonation phenomenon is expected to be applied to chemical sensors [51]. Due to the strong electronegativity of fluorine, the acidity of these pyrrole rings is increased in TFEO-H_2Pc. For this reason, it is susceptible to deprotonation, whereas protonation hardly occurs.

Trifluoroethoxy-substituted nickel phthalocyanine (TFEO-NiPc) and trifluoroethoxy-substituted iron phthalocyanine (TFEO-FePc) were compared with non-fluorinated alkoxy-substituted phthalocyanines [52]. A slightly bathochromic shift of the Q band was observed for TFEO-Pcs relative to non-fluorinated alkoxylated phthalocyanines. Although the melting points of non-fluorinated alkoxylated phthalocyanines are lower than 200 °C, TFEO-NiPc does not melt below 300 °C. Phthalocyanine iron complexes, which are substituted by non-fluorinated alkoxy groups at all peripheries, are easily oxidized and unstable, so these cannot even be synthesized. On the other hand, TFEO-FePc is stabilized by the strong electronegativity of fluorine and has been successfully isolated. In measurements of cyclic voltammetry, iron phthalocyanines with an alkoxy group show a lower first oxidation potential than unsubstituted iron phthalocyanine, but TFEO-FePc shows a more difficult oxidation process than unsubstituted iron phthalocyanine. Furthermore, it is known that iron phthalocyanines easily form a μ-oxo dimer [53] that is connected face-to-face via oxygen, but a spectroscopic investigation revealed that it is difficult to form when using TFEO-FePc. This remarkable stability of TFEO-FePc is due to the low energy of the highest occupied molecular orbital (HOMO) [54] caused by the strong electronegativity of fluorine.

A noteworthy feature of the compounds od the TFEO-Pc series is their high solubility in various organic solvents. This high solubility is suitable for the investigation of the spectroscopic properties of phthalocyanines. TFEO-Pc is soluble not only in general organic solvents but also in liquid carbon dioxide (CO_2) and supercritical CO_2 [55]. These forms of CO_2 have attracted attention as solvents which do not discharge volatile organic compounds (VOCs), and are expected to replace organic solvents as a countermeasure to VOC emissions [56-58]. Phthalocyanines that show solubility in CO_2 are useful for industrial applications because they can be applied without using an organic solvent [59,60]. The plus and minus signs shown in Table 1 express solubility, where (+) means readily soluble, (−) means sparingly soluble, (++) means very high solubility, and (±) means moderate solubility. After conducting solubility studies on various phthalocyanines, only phthalocyanine in which all positions were substituted with trifluoroethoxy groups showed high solubility in both liquid CO_2 and supercritical CO_2. On the other hand, phthalocyanine without any trifluoroethoxy groups such as *tert*-butyl-substituted zinc phthalocyanine (*t*-Bu-ZnPc) or perfluorinated zinc phthalocyanine (F-ZnPc), showed low solubility in both forms of CO_2 while phthalocyanine with zinc as the central metal tended to have higher solubility than metal-free phthalocyanine.

TFEO-Pc also shows high solubility in Solkane® 365 mfc, which is a type of fluorine-based solvent. Solkane® 365 mfc is a proven candidate solvent that does not deplete ozone, allowing

Table 1: Solubility of phthalocyanines in liquid CO_2 and supercritical CO_2.

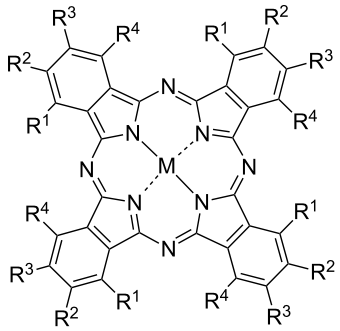

TFEO-ZnPc: M = Zn, R^1–R^4 = OCH_2CF_3
3a: M = Zn, R^1 = R^4 = OCH_2CF_3, R^2 = R^3 = H
3b: M = Zn, R^1 = R^4 = H, R^2 = R^3 = OCH_2CF_3
F-ZnPc: M = Zn, R^1–R^4 = F
t-Bu-ZnPc: M = Zn, R^2 or R^3 = *tert*-Bu, R^1 = R^4 = R^3 or R^2 = H
TFEO-H_2Pc: M = H_2, R^1–R^4 = OCH_2CF_3
3c: M = H_2, R^1 = R^4 = OCH_2CF_3, R^2 = R^3 = H

compound	in liquid CO_2	in supercritical CO_2
TFEO-ZnPc	++	+
3a	+	–
3b	±	–
F-ZnPc	–	–
t-Bu-ZnPc	–	–
TFEO-H_2Pc	+	–
3c	±	–

the use of Solkane® 365 mfc as an alternative to organic solvents to reduce the environmental burden [61,62]. An unsymmetrical type of TFEO-ZnPc with ethynyl group (**4**) shows high solubility in Solkane® 365 mfc while a Glaser-type coupling reaction catalyzed by copper with Solkane® 365 mfc as the medium have been reported (Scheme 2) [63]. In this way, TFEO-

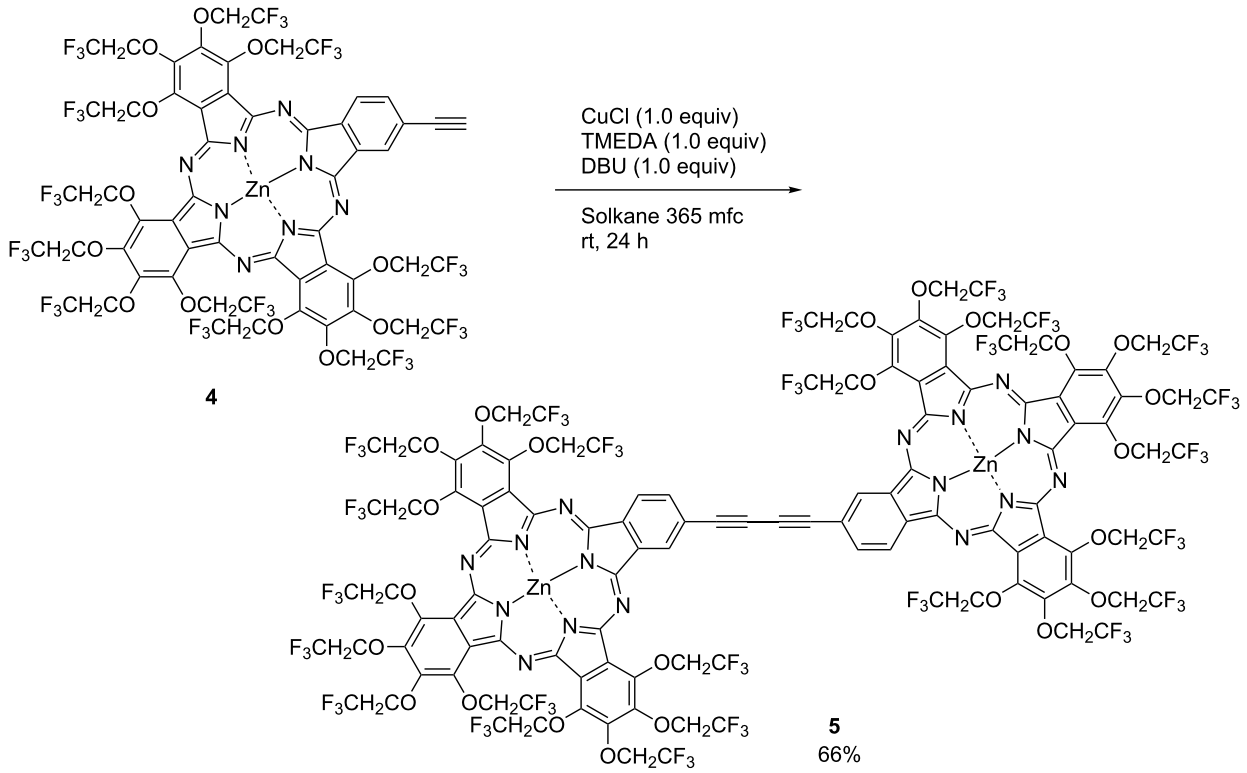

Scheme 2: Synthesis of trifluoroethoxy-substituted binuclear phthalocyanine **5** in Solkane® 365 mfc.

Pc can be chemically modified in Solkane® 365 mfc, making it very useful and allowing its expansion to industrial applications.

Phthalocyanine is usually composed of four isoindoline units. The functionality of phthalocyanine can be enhanced by selectively modifying one of the four units. However, it is difficult to selectively modify the targeted position in the four units using chemical reactions [64,65]. This is because the selective reaction of phthalocyanine is unexplored and removal of byproducts after the reaction is difficult due to its aggregation properties. On the other hand, TFEO-Pcs have high solubility, and chemical modification and purification are easy. For example, the synthesis of unsymmetrical TFEO-Pcs, which are also referred to as A_3B type phthalocyanines, and their cross-coupling reaction catalyzed by palladium between A_3B type TFEO-Pcs and acetylenes have been reported (Scheme 3) [66,67]. A_3B type phthalocyanines are synthesized by mixing two types of phthalonitrile, but symmetric A_4 and A_2B_2 types are simultaneously produced as byproducts. It is usually difficult to remove these symmetrical A_4 and A_2B_2 type Pc isomers from A_3B type Pc, but TFEO-Pcs can be easily purified by silica gel column chromatography. The extension of π-conjugation by a palladium-catalyzed cross-coupling reaction after a tetramerization reaction proceeds with high yield. Furthermore, since TFEO-Pcs are not only easy to purify but also do not aggregate, their identification by NMR, MS, UV–vis and IR is easy. Consequently, various TFEO-Pcs can be conveniently prepared, setting a path for the development of more functional materials.

Synthesis of di- and trinuclear trifluoroethoxy-substituted phthalocyanines and investigation of their aggregation properties

Di- or trinuclear phthalocyanines can be highly functionalized compared with mononuclear phthalocyanines by chemically modifying each unit unsymmetrically caused by an electronic interaction between each unit [68]. In addition, since it is possible to separate charges in dimer-type phthalocyanines, they are expected to be applied to new electron or energy transfer systems [69] such as solar cell materials as well as photocatalysts for organic reactions. A phthalocyanine dimer in which TFEO-Pcs are directly linked by C–C bonds has been reported (Scheme 4) [70,71]. This homodimer was synthesized by a palladium-catalyzed homo-coupling reaction of two A_3B type monoiodinated TFEO-ZnPcs. There are two positions where the substituent can be introduced into the phthalocyanine, at the α-position near the center of the macrocycle and at the β-position on the outer side of the macrocycle. Even though a TFEO-Pc homodimer connected at the β-position (**7a**) was obtained, the dimer connected at the α-position (**8a**) could not be synthesized due to the repulsion of each unit (Figure 1). Considering that the *tert*-butyl-substituted phthalocyanine dimer connected at the α-position (**8b**) could be synthesized, the repulsive effect of the trifluoroethoxy groups is very strong. Furthermore, the same structural dimer of TFEO-Pc and *tert*-butyl-substituted phthalocyanine **7b** was synthesized by the Suzuki coupling reaction. These dimers show a new absorption peak in the longer wavelength region than the Q band which is not observed in the monomer. This suggests intramolecular electronic coupling between each unit [72]. The authors noted that this

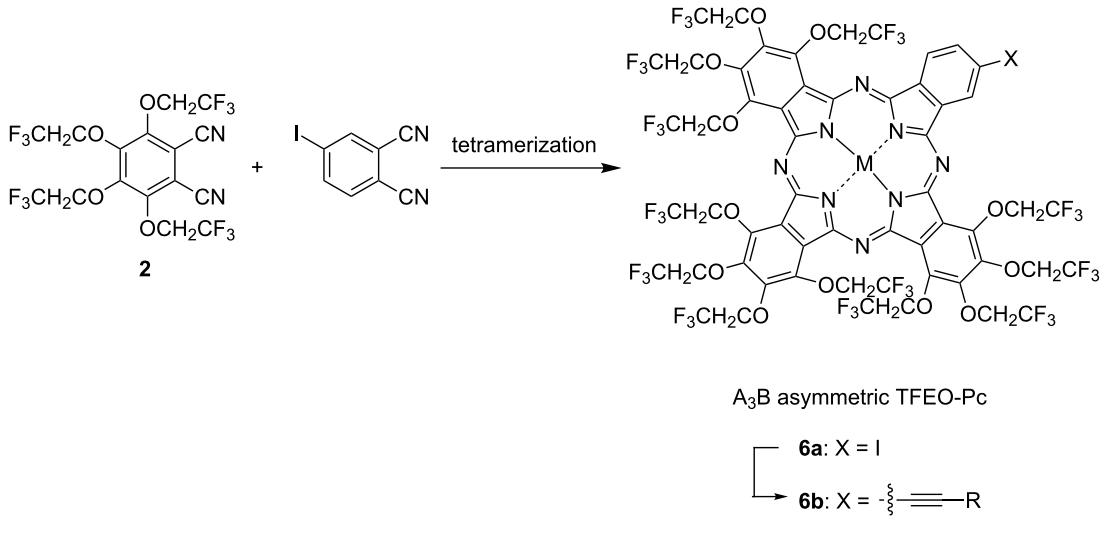

Scheme 3: Synthesis of trifluoroethoxy-substituted unsymmetrical phthalocyanines.

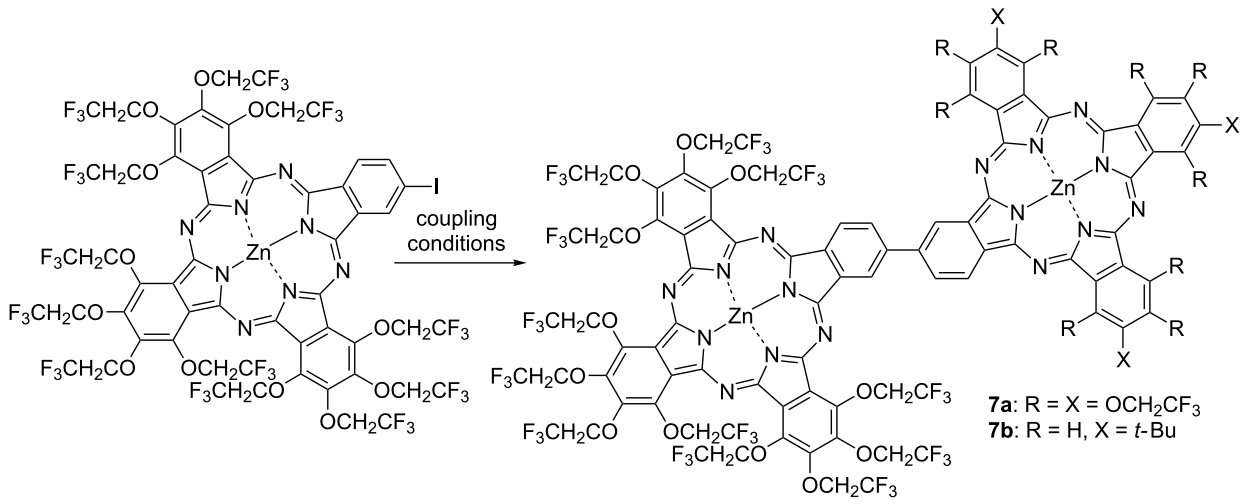

Scheme 4: Synthesis of trifluoroethoxy-substituted phthalocyanine dimers linked at the β-position.

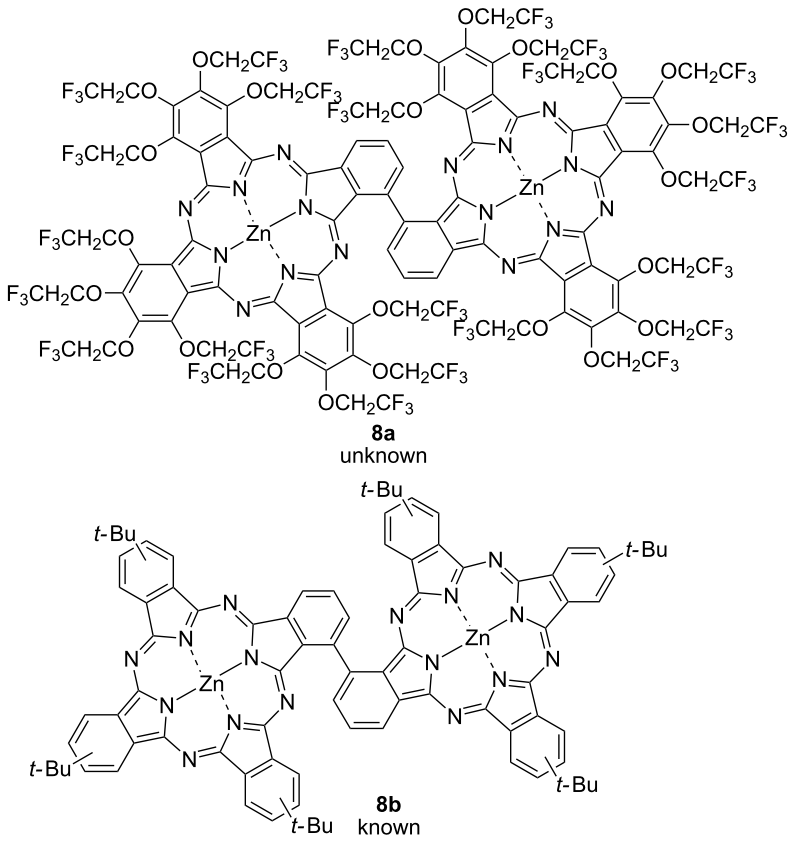

Figure 1: Structure of trifluoroethoxy-substituted phthalocyanine dimers linked at the α-position.

intramolecular electronic coupling is likely to be dependent on the overall planarity of the molecules.

Rigid TFEO-Pc dimers with a diacetylene moiety as a linker have also been reported [73,74]. There are reports of dimers via two kinds of diacetylene linkers, via a butadiyne and via an aryldiacetylene moiety (Figure 2). Such binuclear phthalocyanines that are connected via a rigid acetylene linker synthesized by Glaser or Sonogashira reactions have attracted attention due to their interesting effects resulting from further expan-

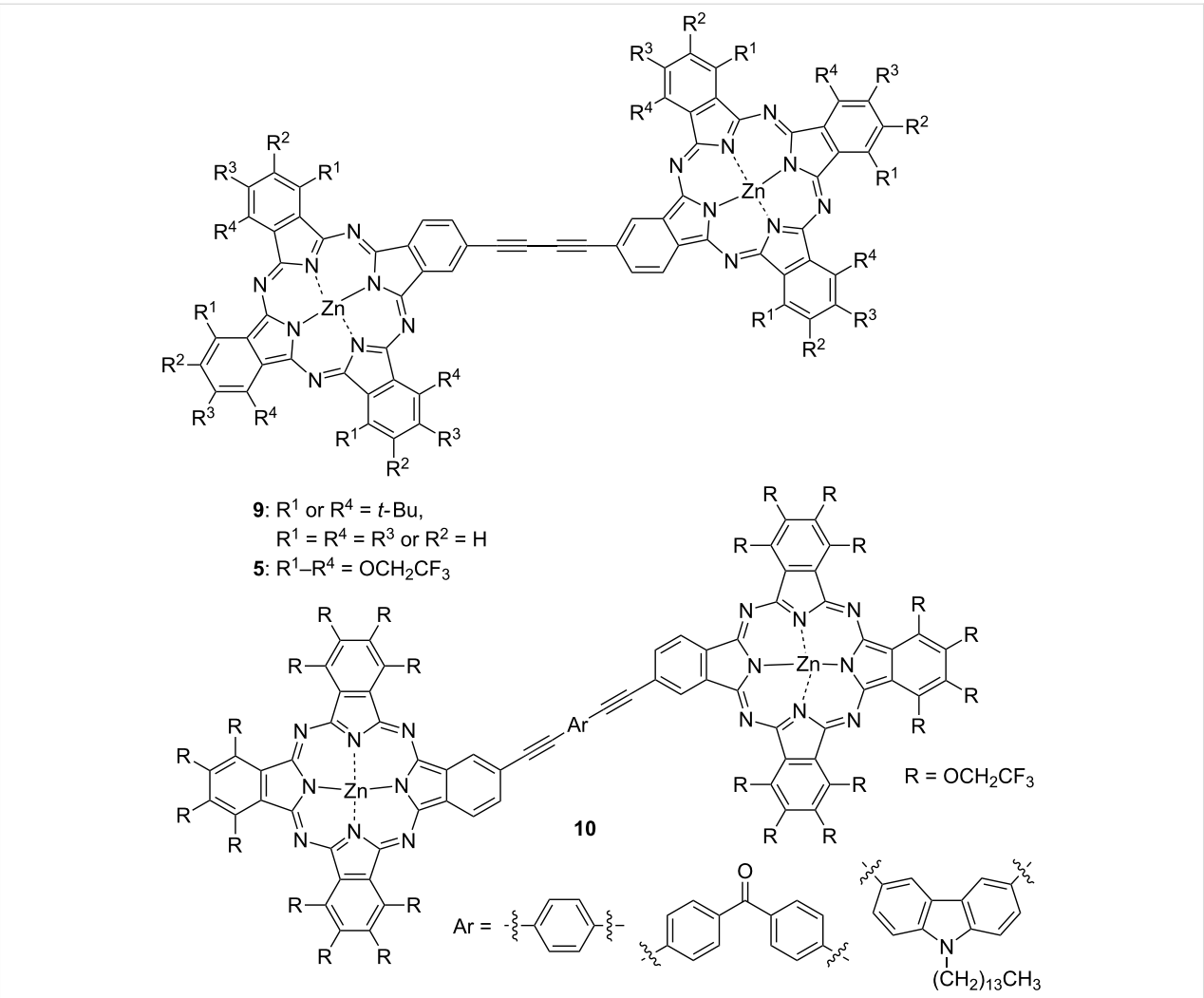

Figure 2: Structure of trifluoroethoxy-substituted dimer via a diacetylene linker.

sion of conjugation. The electronic interaction between the covalently connected chromophore unit leads to important changes in the absorption spectra and so these dimers are expected to serve as attractive building blocks for the construction of multicomponent photoinduced electron transfer supramolecular systems [75,76]. However, phthalocyanine dimers with high rigidity and flatness exhibit a stronger aggregation effect as π-conjugation expands. For example, a *tert*-butyl-substituted phthalocyanine dimer connected via diacetylene linker (**9**) strongly aggregates in solution although *tert*-butyl-substituted mononuclear phthalocyanine does not show any aggregation effect [74]. The aggregation behavior can be estimated from the UV–vis spectra. Phthalocyanine, which is free from aggregation, exhibits a sharp Q band, but the Q band of aggregated phthalocyanine is broadened and shifts to the shorter wavelength region (Figure 3) [77]. The dimer shows a broad Q band in trifluorotoluene which is a typical absorption peak of phthalocyanine aggregates. However, the Q band becomes sharp after the addition of 1% pyridine to the solution [78]. This phenomenon occurs because pyridine coordinates vertically to the central metal of the phthalocyanine and inhibits a stacking interaction between phthalocyanines. Thus, the change in the spectral shape after the addition of pyridine strongly suggests the aggregation behavior of phthalocyanine. On the other hand, binuclear phthalocyanine connected via a diacetylene linker with trifluoroethoxy substituent **5** shows a sharp Q band peak in trifluorotoluene. The absorption spectrum of the dimer does not change even when pyridine is added. This result demonstrates that phthalocyanine does not aggregate in solution.

It is known that intramolecular aggregation is preferred in binuclear phthalocyanines connected via a flexible linker such as an sp^3 carbon bond or an ether bond that can rotate freely because of an entropic advantage [79,80]. So these dimers form a folded structure in a so-called closed clamshell conformation. However, not only intermolecular interactions but also intramolecular

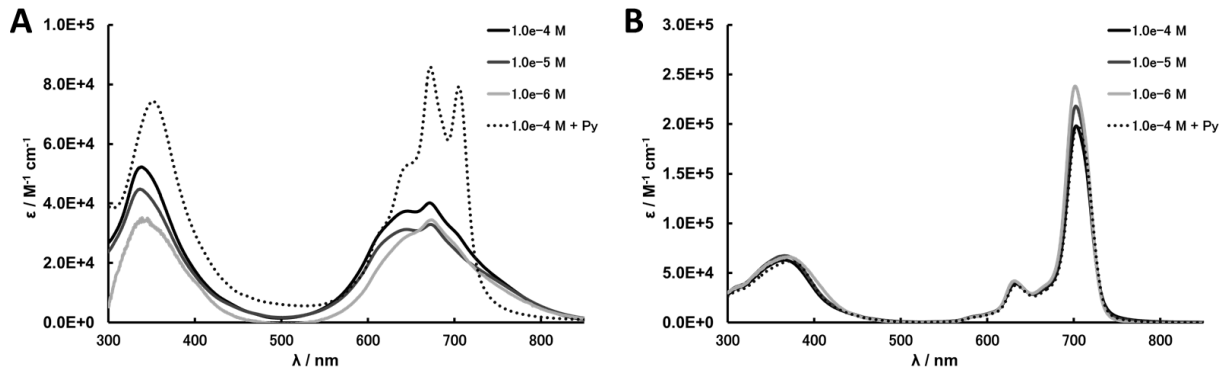

Figure 3: UV–vis spectra of **9** (A) and **5** (B).

aggregation can be suppressed due to strong repulsion by the introduction of a trifluoroethoxy group into the flexible binuclear phthalocyanine, which always adopts an open clamshell conformation. Binuclear phthalocyanines connected via a flexible triazole linker that are substituted by a *tert*-butyl (**11**) [81] or trifluoroethoxy (**12**) [82] group have been reported. These dimers were synthesized from A_3B type phthalocyanines containing an ethynyl group and 1,4-bis(azidomethyl)benzene via a so-called "double-click reaction" [83] catalyzed by CuI. The examination of the spectroscopic properties of these dimers revealed that the *tert*-butyl-substituted phthalocyanine dimer showed a Q band significantly broadened around 700 nm. Furthermore, the shape of the Q band became sharp after the addition of pyridine, as a result of an aggregated dimer caused by an intramolecular stacking interaction and the adoption of a closed clamshell conformation (Figure 4). On the other hand, the trifluoroethoxy-substituted phthalocyanine dimer showed a sharp Q band at around 700 nm. Since there was no change in

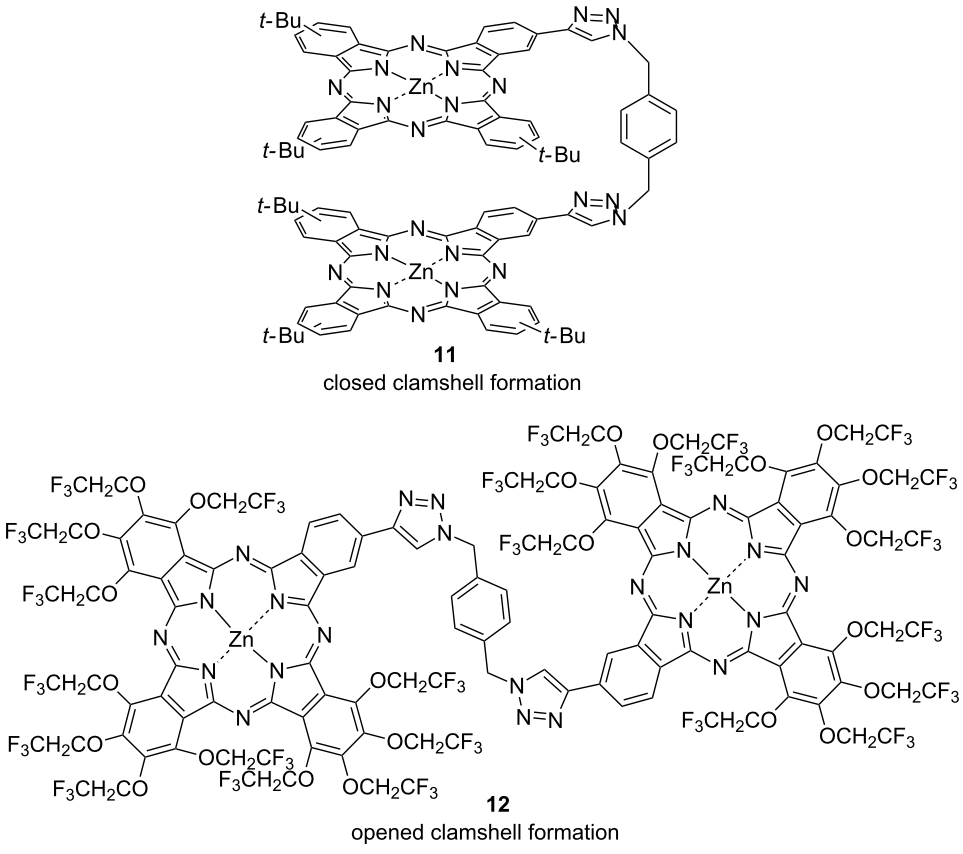

Figure 4: Structure of binuclear phthalocyanines linked by a triazole linker.

the spectral structure, even when pyridine was added, this dimer always assumed an opened clamshell conformation caused by the repulsive effect of the trifluoroethoxy group. More interestingly, similar aggregation behaviors were also suggested for trinuclear phthalocyanines that can aggregate more easily [84]. These trinuclear phthalocyanines were synthesized by a triple click reaction. The *tert*-butyl-substituted trimer **14** exhibited aggregation behavior by an intramolecular stacking interaction between the units (Figure 5). On the other hand, the trifluoroethoxy-substituted trimer **13** did not exhibit such aggregation behavior and adopted a "windmill-like molecular structure" by the repulsive action of the trifluoroethoxy group. Thus, it was found that not only the binuclear phthalocyanine connected via a flexible linker but also the trinuclear phthalocyanine can com-

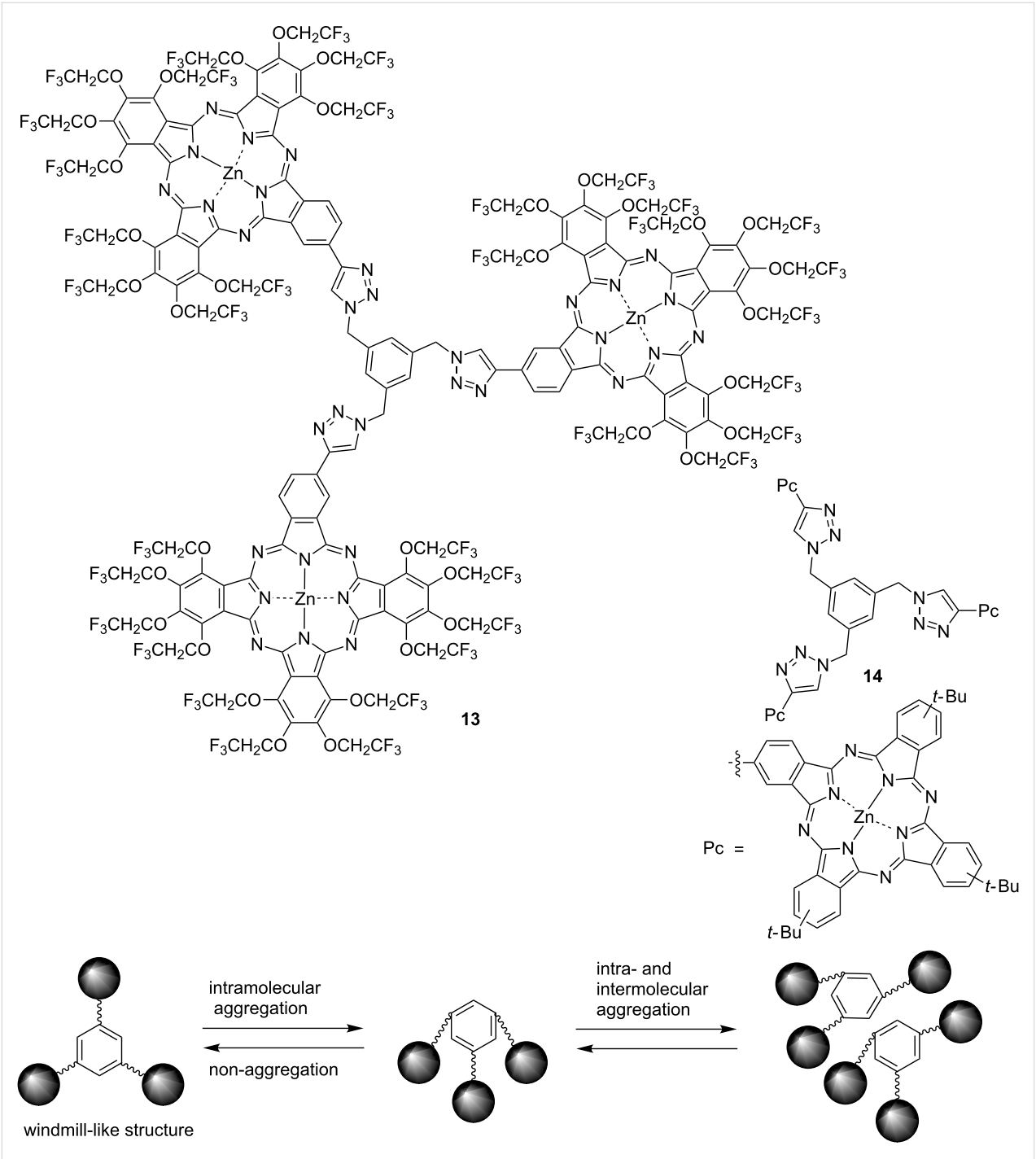

Figure 5: Structure of trinuclear phthalocyanines linked by a triazole linker, and windmill-like molecular structure vs aggregated structure.

pletely suppress the intermolecular stacking interaction by introduction of a trifluoroethoxy group into the periphery of phthalocyanine.

Application of trifluoroethoxy-substituted phthalocyanines to biology

Phthalocyanines are expected to be applied to medical fields [85,86] such as biological image probes and as agents for photodynamic therapy because of their excellent spectroscopic properties, allowing phthalocyanine to be a useful medical dye because it absorbs light of long wavelengths with high tissue transparency. However, ordinary phthalocyanines cause the deterioration of spectroscopic properties and solubility by forming aggregates, so it is necessary to suppress this aggregation [87]. As described above, the ability of the trifluoroethoxy group in suppressing the aggregation of phthalocyanine is extremely remarkable. Therefore, it is expected that an effective medical dye can be developed by using this excellent aggregation suppressing effect. On the other hand, improving the biocompatibility of phthalocyanine is as important as suppressing its aggregation property. It is also necessary to improve the water solubility of the lipophilic phthalocyanine in order to increase its biocompatibility [88,89]. One frequent method to increase the water solubility of phthalocyanine involves the combination of a biomolecule such as a sugar [90,91] or a peptide [92]. For example, TFEO-Pcs conjugated with peptides (**15**) have been reported [93]. A_3B type TFEO-Pc was successfully condensed with peptides by palladium-catalyzed cross-coupling reactions in good yield (Scheme 5). These TFEO-Pc-peptide conjugates, which show a sharp Q band in the UV–vis spectrum, do not aggregate in solution. These dyes are expected to be developed into medical imaging probes.

Phthalocyanine is expected to be used not only as a biological imaging agent but also in cancer treatment. Photodynamic therapy (PDT) is a laser cancer therapy that introduces organic dyes into cancer cells and kills them by reactive oxygen species with cytotoxicity generated by light irradiation [94,95]. In addition to reducing the psychological burden of the patients because this process does not require surgical operation, damage to normal cells can be minimized by irradiating the laser only to the target tumor cells. The features of ideal PDT agents include, among others: i) strong absorption in the red wavelength region; ii) non-aggregation property; iii) high biocompatibility; iv) good selectivity to cancer cells; v) high quantum yield of singlet oxygen [96]. Since the PDT activity of phthalocyanine is remarkably decreased by aggregation, TFEO-Pc, which has a non-aggregation property, is expected to be a highly active PDT drug. Incidentally, improving drug selectivity for cancer cells is a problem in developing cancer therapeutic drugs. Phthalocyanines have the capacity to accumulate in cancer cells due to the EPR (enhanced permeation and retention) effect [97,98]. This is a phenomenon in which new blood vessels around cancer cells allow macromolecules to pass easily through cells, causing the accumulation of molecules around cancer cells as a result. This effect is more likely to occur with a long residence time of the compound in blood. The residence time in blood is prolonged by increasing the water solubility of the drug. An ideal PDT drug would improve the water solubility of TFEO-Pc. In 2006, TFEO-ZnPcs were conjugated with deoxyribonucleosides **16** and **17** for possible use in PDT [99]. The deoxyribonucleoside unit is expected to enhance the water solubility of the phthalocyanine, facilitating its incorporation into cancer cells which undergo active cell division. These TFEO-ZnPc/deoxyribonucleoside hybrids were synthesized from unsymmetrical A_3B-type TFEO-ZnPc under Sonogashira cross-coupling conditions (Scheme 6). UV–vis absorption measurements suggested that the deoxyribonucleoside-linked TFEO-Pcs had a non-aggregation property, as expected. Unfortunately, it was also found that these conjugates gradually decomposed under light irradiation, so their application as an anticancer agent was discontinued.

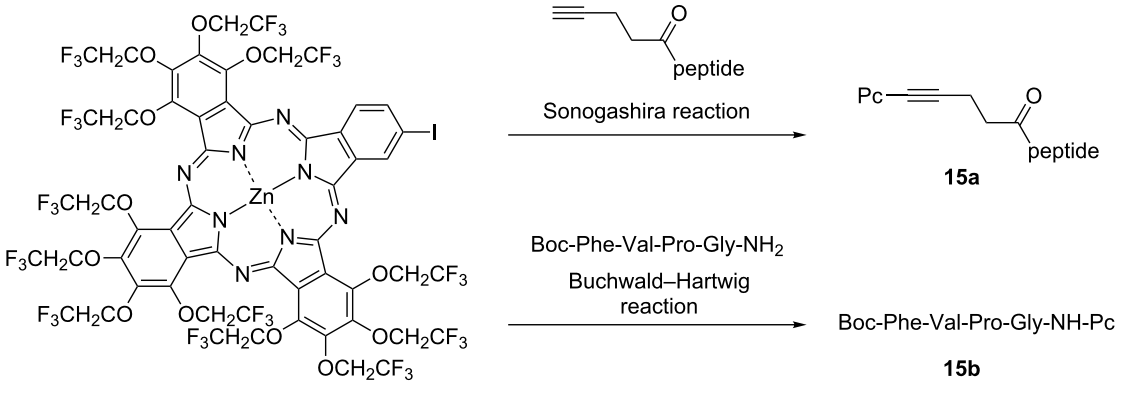

Scheme 5: Synthesis of trifluoroethoxy-substituted phthalocyanines conjugated with peptides.

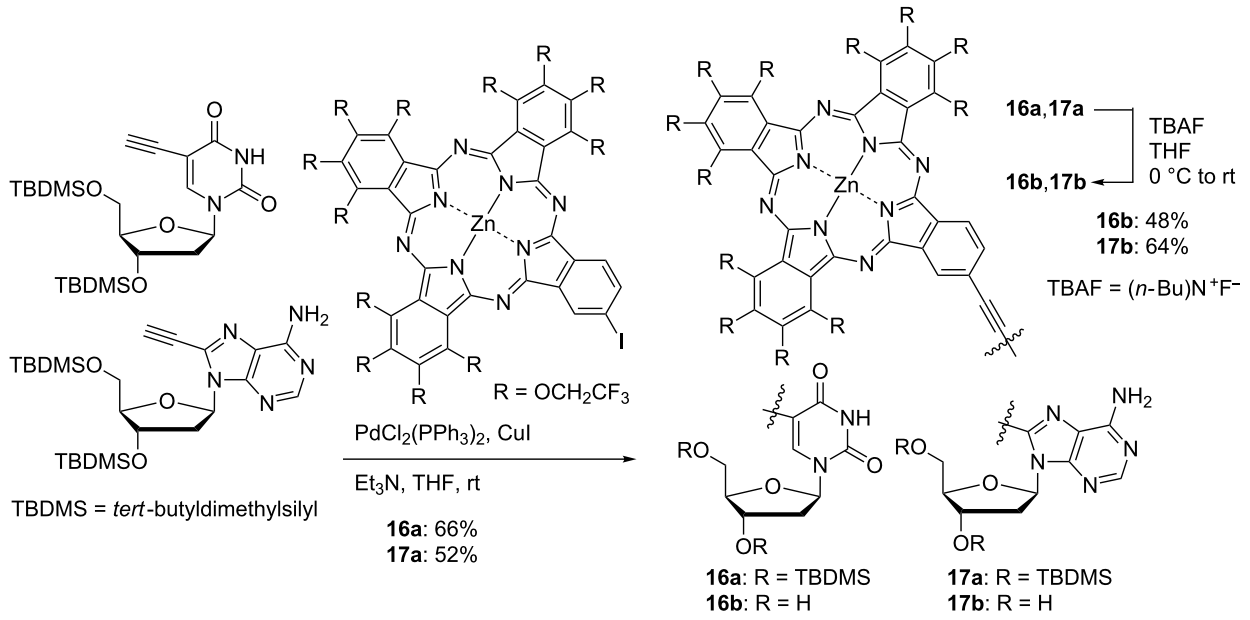

Scheme 6: Synthesis of trifluoroethoxy-substituted phthalocyanines conjugated with deoxyribonucleosides.

After that TFEO-ZnPc/cyclodextrin conjugates **18** were reported under similar conditions (Scheme 7) [100]. That study revealed that cyclodextrin-linked TFEO-Pcs have a non-aggregation property and sufficient water solubility, similar to the deoxyribonucleoside conjugates. An in vitro investigation showed that cyclodextrin-linked TFEO-Pcs were ideal PDT

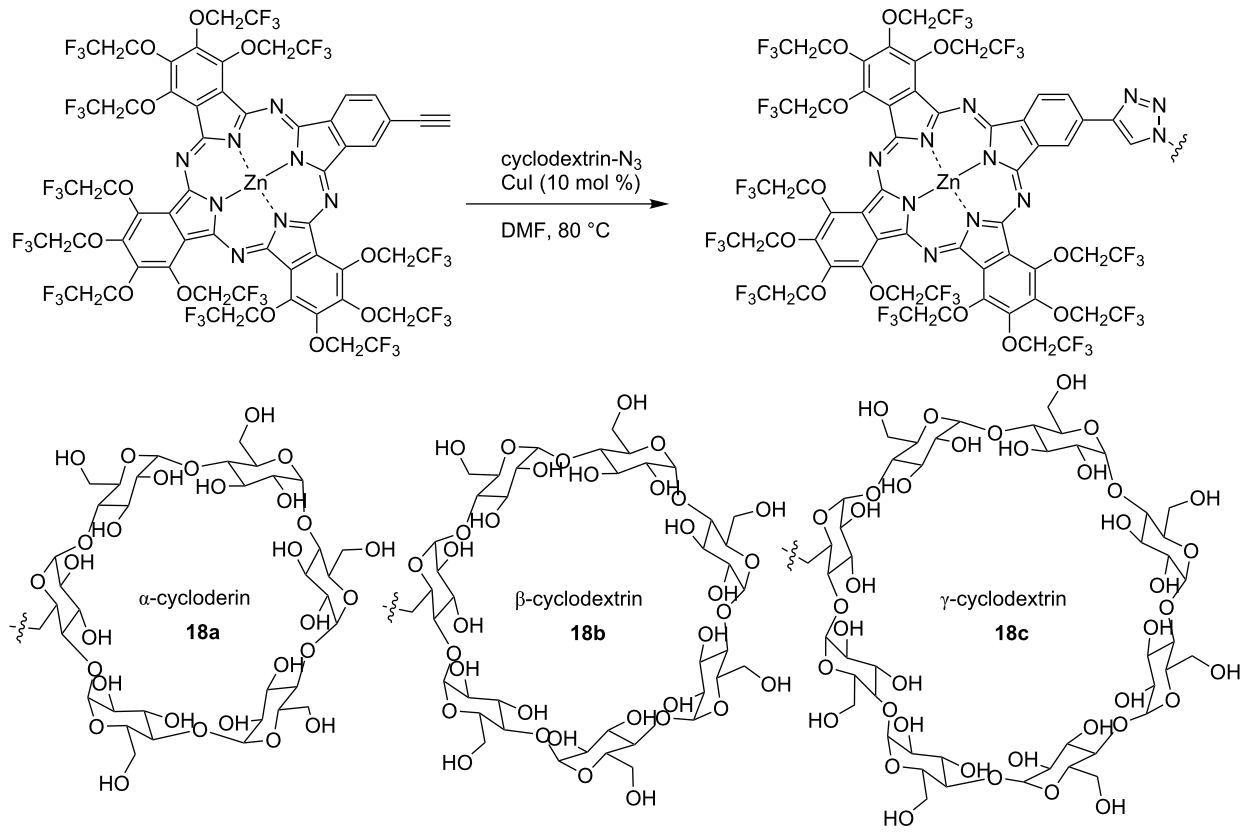

Scheme 7: Synthesis of trifluoroethoxy-substituted phthalocyanines conjugated with cyclodextrin.

drugs that exhibits high cytotoxicity under light irradiation while displaying little cytotoxicity in the dark (Table 2). On the other hand, interestingly, the fluorine-free *tert*-butylated derivative showed cytotoxicity even in the dark. This result suggests that the trifluoroethoxy group reduces the cytotoxicity of the phthalocyanine. Subsequently, an in vivo investigation was also conducted. Chicken embryos transplanted with cancer cells were treated with PDT by a cyclodextrin conjugate and proved 17 days later. The cancer cells of embryos treated with PDT had shrunk to about half the size of untreated embryos. On the other hand, when cancer cells were not irradiated with light after administration of the cyclodextrin conjugate, these cells were almost of the same size as at unprocessed embryos. These results suggest that the cyclodextrin conjugate does not display cytotoxicity when not irradiated with light. Therefore, the cyclodextrin conjugate has the potential to be effective and very safe.

Application of trifluoroethoxy-substituted phthalocyanines to functional materials

Development for organic thin-film solar cells

The introduction of trifluoroethoxy groups imparts not only a non-aggregation property and high solubility but also an electron-deficient π space and thermal or chemical stability to the phthalocyanine. For these reasons, it is expected that TFEO-Pcs will be developed for the application in functional dyes with higher performance and in new industrial fields. An interesting example involves investigations on energy transfer between the phthalocyanine and the fullerene [101]. Normally, phthalocyanine plays the role as a donor type molecule in the field of organic semiconductors [102]. For example, a hybrid compound consisting of phthalocyanine and fullerene **20a** causes the transfer of energy from the phthalocyanine unit to the fullerene unit when irradiated by light (Figure 6) [103,104]. However, such energy transfer does not occur in the hybrid of TFEO-ZnPc and fullerene **20b** because the strong electron-withdrawing property of fluorine reverses the relationship between the electronic states of both units [105]. It was suggested that TFEO-Pc has an orbital energy closer to that of [6,6]-phenyl-C_{61}-butyric acid methyl ester (PCBM) [106,107], which is a known acceptor molecule, than to poly(3-hexylthiophene-2,5-diyl) (P3HT) [107], which is a known donor molecule. It can thus be concluded that TFEO-Pc can play a role as an acceptor-type semiconductor. In general, organic semiconductors have a greater abundance of donor-type molecules than acceptor-type molecules. Therefore, the structural development of acceptor

Table 2: Comparison of IC_{50} values with laser PDT among phthalocyanine conjugated with cyclodextrin against B16-F10.

	IC_{50} (μM)		
compound	drug only	PDT[a]	effective ratio[b]
19: β-CD-*t*-Bu-Pc	16.7	1.10	15.2
18a: α-CD-TFEO-Pc	≥50	1.29	≥38.8
18b: β-CD-TFEO-Pc	≥50	1.12	≥44.6
18c: γ-CD-TFEO-Pc	≥50	1.25	≥40.0

[a]PDT comprised laser irradiation. [b]Effective ratio shows ratio vs drug only.

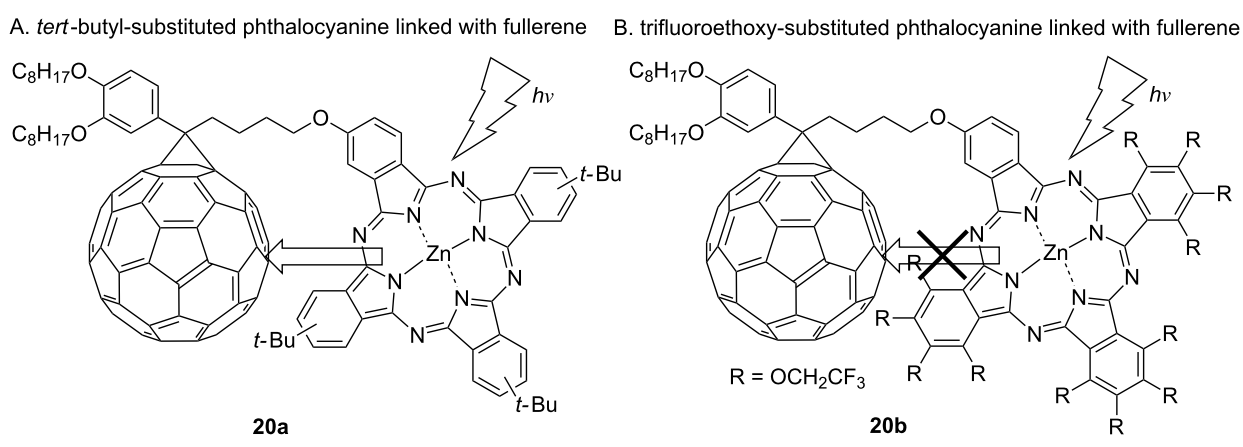

Figure 6: Direction of energy transfer of phthalocyanine–fullerene conjugates.

molecules is restricted. TFEO-Pcs could be developed as a new acceptor-type molecule.

In fact, solar cells that utilize the ability of TFEO-Pc to accept energy have been developed. A planar heterojunction organic thin-film solar cell was prepared by using P3HT as the donor and TFEO-ZnPc as the acceptor [108,109]. Photoelectric conversion was observed in a wide absorption region, suggesting that TFEO-Pcs might be used as a substitute for fullerene in solar cells. In addition, the influence of the number of introduced trifluoroethoxy groups on the performance of solar cells has been investigated. The open circuit voltage (V_{OC}), short circuit current density (J_{SC}) and fill factor (FF) of heterojunction solar cells using various TFEO-Pcs were estimated and their conversion efficiency (E_{ff}) was compared (Table 3). The solar cell that used phthalocyanine with a single trifluoroethoxy group introduced at the β-position, rather than trifluoroethoxy full-coated phthalocyanine, showed the best performance. In the development of organic thin-film solar cells, dye material needs a moderate aggregation property for effective energy transfer [110]. Therefore, it is considered that the performance of solar cells that use per(trifluoroethoxy)phthalocyanine, which exhibits a strong repulsion effect, will be low. It is expected that phthalocyanine will be put to practical use within solar cells by improving the orientation control in thin films.

Development for fluorinated polymer dyes

Fluoropolymers are widely used from household products to aerospace materials because they show excellent stability, as well as non-adhesive, electrical and optical properties due to the specific properties of fluorine [24,111]. Material development studies of compounds that combine the properties of fluoropolymers and the spectroscopic properties of phthalocyanines have been conducted [112,113]. TFEO-Pc-supported fluoropolymers **23** that combine the properties of a fluorinated polymer and the spectroscopic properties of a phthalocyanine have been developed [114]. A_3B TFEO-ZnPc **4** and fluorinated polymer **22** were condensed by a click reaction between azide and alkyne groups (Scheme 8). The graft ratio of the TFEO-ZnPc-supported fluoropolymer was calculated from the area ratio of ^{19}F NMR, and the resulting fluorinated copolymers showed different grafting ratios (from 10 to 72%) depending on the reaction conditions. A thermogravimetric analysis showed a weight loss of more than 90% at 210 °C for the precursor before condensation of TFEO-ZnPc, whereas the TFEO-ZnPc-supported fluoropolymer showed only 5% weight loss at 300 °C. It was suggested that introduction of TFEO-ZnPc into a fluoropolymer markedly improves its thermal stability. In addition, the TFEO-ZnPc-supported fluoropolymer showed significantly lower fluorescence than monomeric TFEO-ZnPc. This suggests a strong electronic interaction among TFEO-Pc units, allowing for its application in photonic devices.

Synthesis of double-decker phthalocyanines and investigation of the repulsive effect of trifluoroethoxy substituents

The properties of trifluoroethoxylated phthalocyanine depend on the number of substituted trifluoroethoxy groups and their

Table 3: Characteristics of phthalocyanine/P3HT heterojunction organic thin-film solar cells.

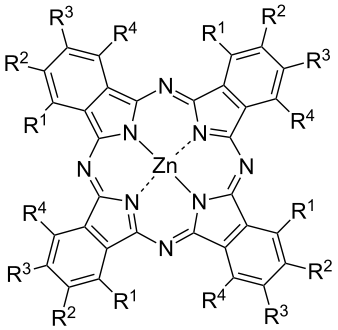

TFEO-ZnPc: R^1–R^4 = OCH_2CF_3
21a: $R^1 = R^4 = OCH_2CF_3$, $R^2 = R^3 = H$
21b: $R^1 = R^4 = H$, $R^2 = R^3 = OCH_2CF_3$
21c: R^1 or $R^4 = OCH_2CF_3$, $R^2 = R^3 = R^1$ or $R^4 = H$
21d: R^2 or $R^3 = OCH_2CF_3$, $R^1 = R^4 = R^3$ or $R^2 = H$

	E_{ff} (%)	FF	V_{oc} (V)	J_{sc} (mA/cm^2)
P3HT only	2.4×10^{-3}	0.41	0.22	2.7×10^{-2}
TFEO-ZnPc	3.3×10^{-2}	0.29	0.24	0.48
21a	6.8×10^{-3}	0.26	0.21	0.13
21b	8.1×10^{-5}	0.15	0.53	1.1×10^{-3}
21c	1.2×10^{-2}	0.32	0.35	0.10
21d	7.1×10^{-2}	0.38	0.42	0.45

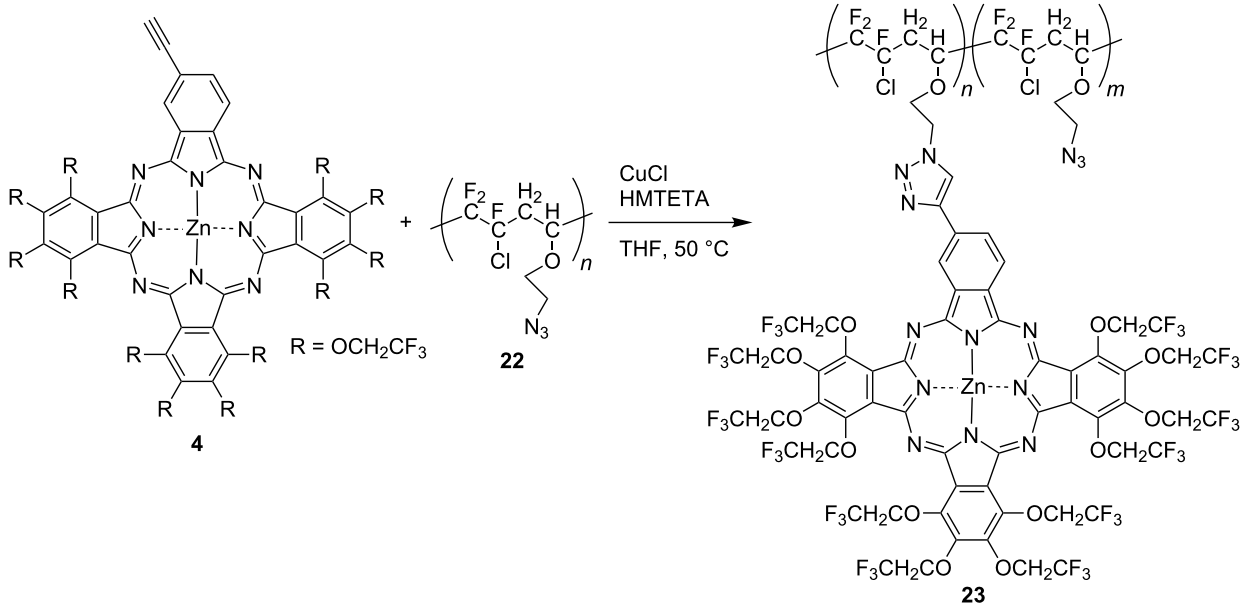

Scheme 8: Synthesis of fluoropolymer-bearing phthalocyanine side groups.

substitution positions. Various trifluoroethoxylated phthalocyanines having a different number of substituents and substituted positions have been reported [115-118]. The effect of the substitution of the trifluoroethoxy groups on the aggregation properties has been investigated by a synthetic study of trifluoroethoxy-substituted double-decker type phthalocyanines **25** and **26** [119]. When a rare earth element is used as the central metal of the phthalocyanine, it is known that phthalocyanine macrocycles form a double-decker phthalocyanine (DDPc) in which two macrocycles are coordinated above and below the metal [120,121]. The double-decker structure can be regarded as a phthalocyanine which forcibly formed an aggregate by a rare earth element. Therefore, when TFEO-Pc showing a non-aggregation property by a strong repulsion effect is used, it is interesting to know whether the formation of DDPc is possible or not. First, it was investigated whether the phthalocyanine can be synthesized by using phthalonitrile in which one trifluoroethoxy group was introduced at the α- or β-position (Scheme 9). The target DDPc was successfully obtained in moderate yield by heating trifluoroethoxy-substituted phthalonitrile in the presence of DBU and a lanthanoid acetylacetone complex in *n*-octanol. Next, the synthesis of DDPc using a phthalonitrile having two trifluoroethoxy groups at the α- or β-position was investigated. Even though, β-disubstituted trifluoroethoxylated DDPcs were obtained with the same yield as the mono-substituted product. The reaction did not proceed in the case of the α-disubstituted product. Furthermore, DDPc could also not be synthesized using phthalonitrile in which all four positions were trifluoroethoxylated. These results suggest that a trifluoroethoxy group substituted at the α-position has a greater repulsion effect than substituted at the β-position of the phthalocyanine. In the case of α-disubstituted phthalocyanine, it is believed that the repulsion effect is too high to obtain a double-decker type structure. Among the DDPcs obtained, β-trifluoroethoxy-substituted DDPcs showed a strong aggregation behavior despite the presence of pertrifluoroethoxy substitutions.

Synthesis and optical properties of trifluoroethoxy-substituted subphthalocyanines

Subphthalocyanines [122-125] are phthalocyanine analogues unlike phthalocyanines which are planar compounds composed of four isoindoline units, and are cone-shaped distorted molecules composed of three isoindoline units. The only central element of subphthalocyanine is boron, and it has a ligand in the axial direction on the boron. Since subphthalocyanines have excellent spectroscopic properties and a unique three-dimensional structure, it is expected that they will be applied to various fields [126-128], alongside phthalocyanines. However, the solubility of subphthalocyanines is not very high despite of the non-aggregation phenomenon due to their three-dimensional structure. On the other hand, since trifluoroethoxy-substituted subphthalocyanines (TFEO-subPcs) have high solubility due to the influence of fluorine and are easy to handle, it is expected that various derivatives as well as TFEO-Pcs will be developed. TFEO-subPc is synthesized by cyclotrimerisation of tetrakis(trifluoroethoxy)phthalonitrile (**2**) in the presence of boron trichloride in *p*-xylene under reflux conditions (Scheme 10) [129]. There are two methods to synthesize sub-

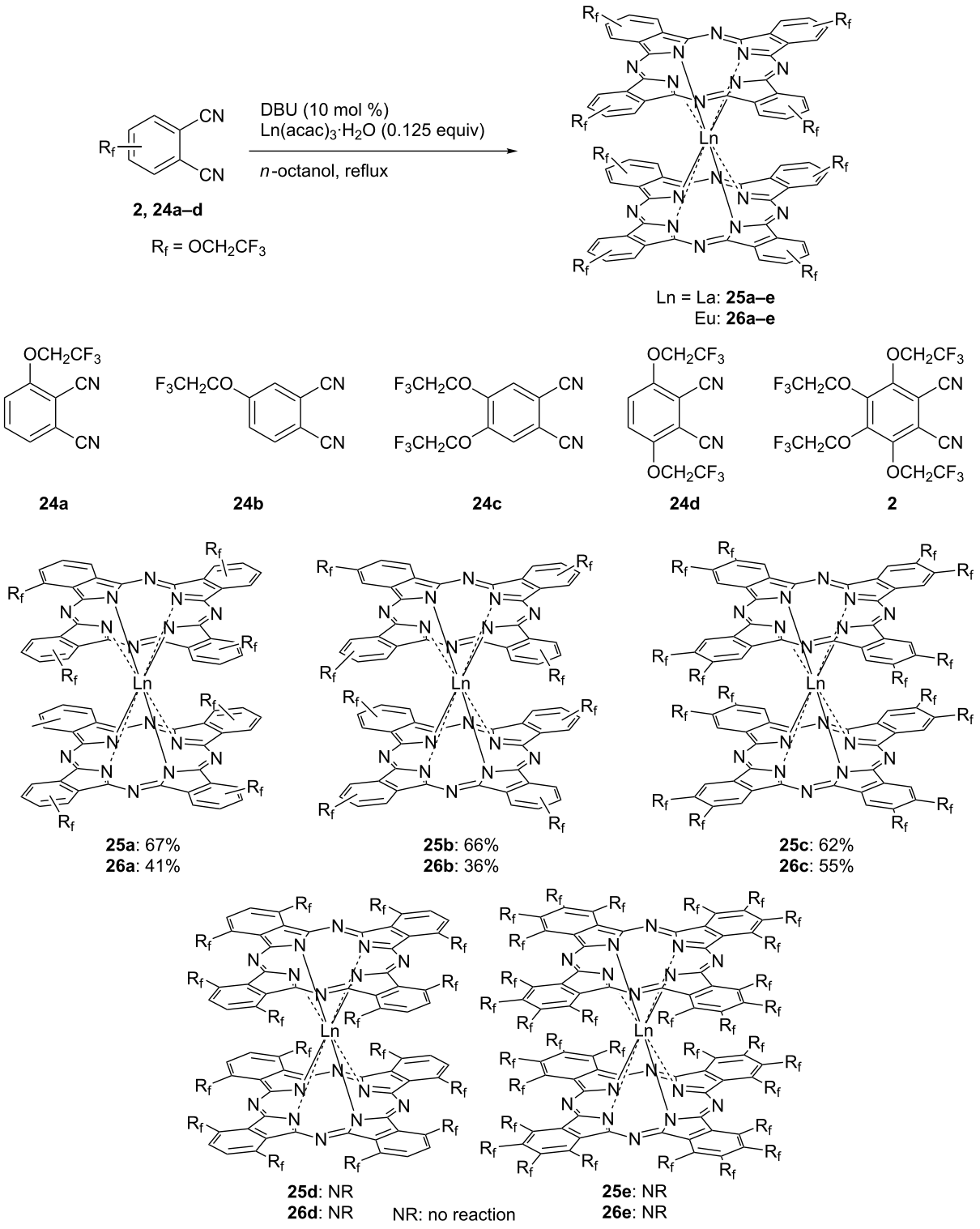

Scheme 9: Synthesis of trifluoroethoxy-substituted double-decker type phthalocyanines.

phthalocyanine derivatives, mainly peripheral functionalization and substitution of axial positions. Among them, substitution reactions at the axial position can easily deliver many subphthalocyanine derivatives by coordinating various chemical species with one subphthalocyanine as a foothold. However, it is known that axial substitution reactions proceed with low

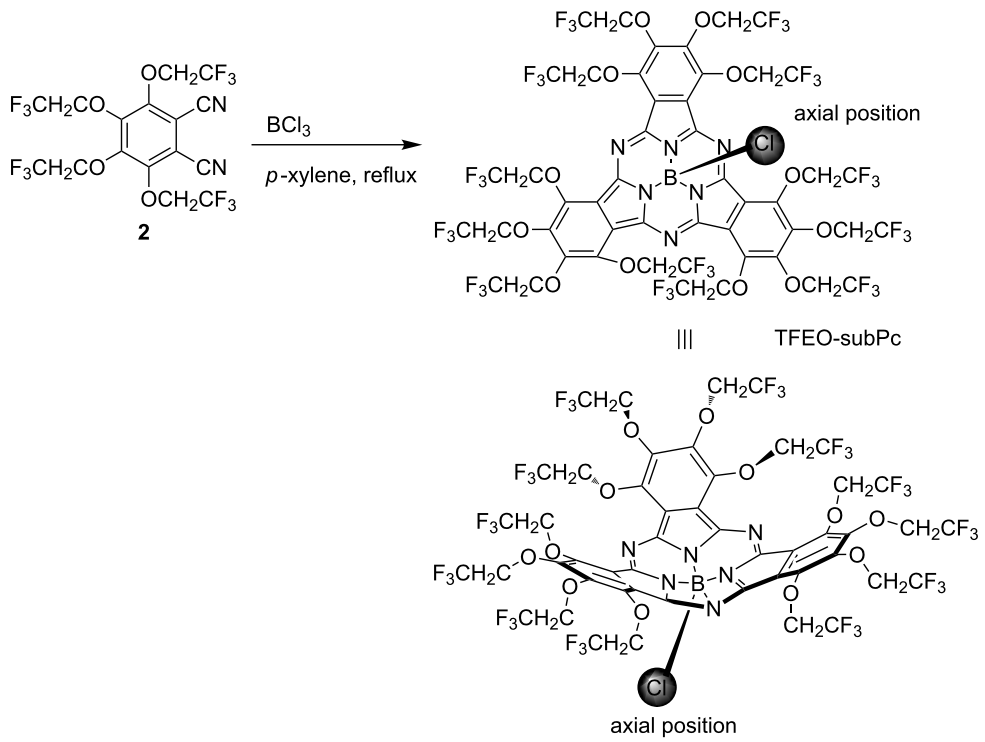

Scheme 10: Synthesis of trifluoroethoxy-substituted subphthalocyanine.

yield with ordinary subphthalocyanine [130]. On the other hand, TFEO-subPc remarkably improves the substitution activity at its axial position, and the axial substitution reaction of alcohols proceeds with high yield under the classical reaction conditions of heating in the presence of triethylamine in toluene. Unsubstituted subphthalocyanine (H-subPc) and perfluorinated subphthalocyanine (F-subPc) were also synthesized, and the efficiency of the axial substitution reaction with triethylene glycol was compared (Table 4). The yield of the substitution reaction of H-subPc was only 5%, and the reaction did not proceed in the case of F-subPc. On the other hand, in TFEO-subPc, the substitution reaction at the axial position proceeded successfully, and the target substitution was obtained at a rate of 68%. This is because the stability of subphthalocyanine and the reactivity of the substitution reaction at the axial position are improved by the introduction of a trifluoroethoxy group.

Table 4: Comparison of axial ligand substitution reactivity of subphthalocyanines.

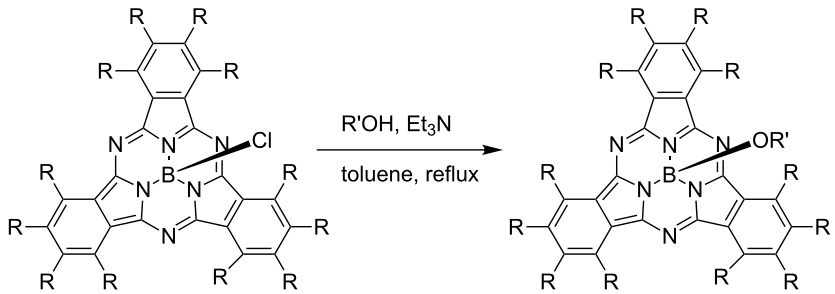

entry	subPc	R	R'OH	yield (%)
1	H-subPc	H	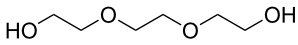	5
2	F-subPc	F		NR
3	TFEO-subPc	OCH_2CF_3		68

Using this high reactivity of axial substitution, hybrid dyes in which the axial position of TFEO-subPc is substituted with fullerene **27** or phthalocyanine **28** intended to construct energy transfer systems have been synthesized (Figure 7). In the previous section, it was explained that the hybrid dye of TFEO-ZnPc and fullerene does not cause energy transfer between units, but in this case, the TFEO-subPc unit acts as a donor.

A composite of subphthalocyanine was synthesized by using the high axial position substitution activity of TFEO-subPc. TFEO-subPc homodimers **29** substituted at the axial position in the *ortho*-, *meta*-, or *para*-position were synthesized by reacting TFEO-subPc with catechol, resorcinol or hydroquinone in toluene in the presence of triethylamine (Scheme 11) [131]. The synthesis of H-subPc homodimer **30** was attempted using the same method, but the target substance was obtained. This is a good example showing the high activity of the axial substitution reaction of TFEO-subPc. The synthesis of the heterodimer of TFEO-subPc with H-subPc or F-subPc was also attempted. However, since the substitution activity on the axial position of H-subPc and F-subPc was unsatisfactory, the reaction did not progress as expected. Therefore, the activation method for the axial position using trifluoromethanesulfonate reported by Torres et al. was investigated [132]. The reaction proceeded successfully and the desired heterodimers **32** and **33** were obtained (Scheme 12). The investigation of these spectroscopic

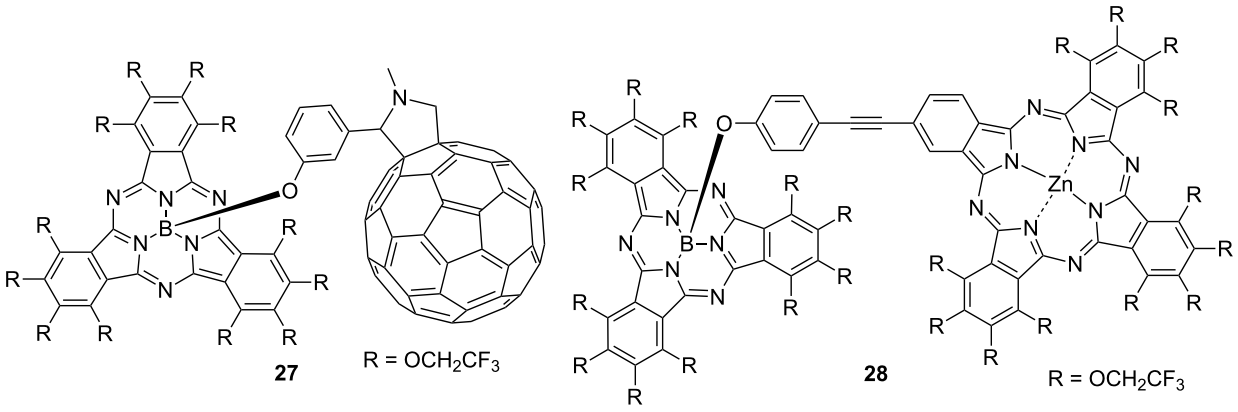

Figure 7: Structure of axial ligand substituted subphthalocyanine hybrid dyes.

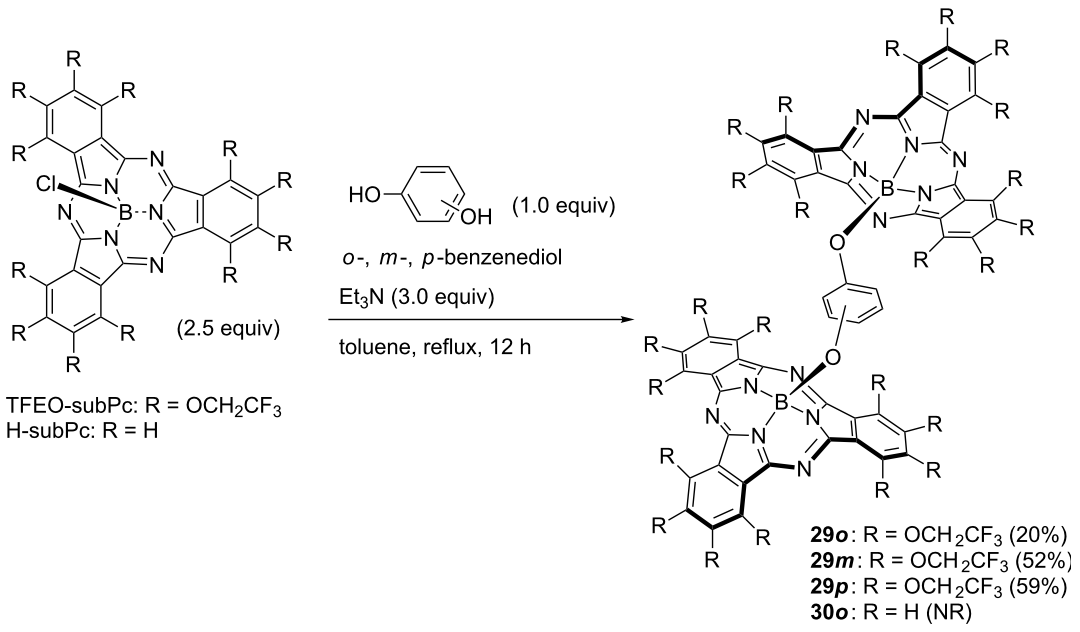

Scheme 11: Synthesis of subphthalocyanine homodimers.

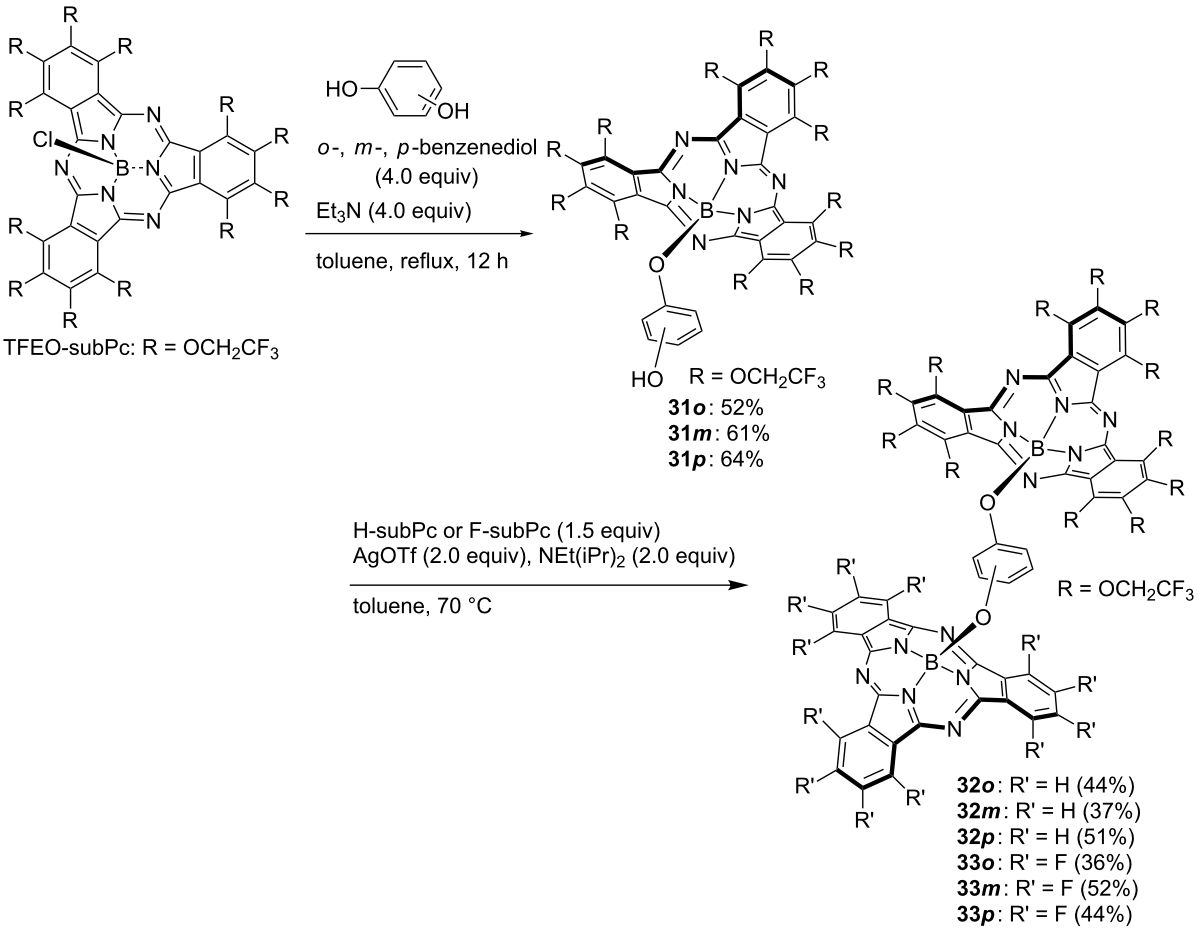

Scheme 12: Synthesis of subphthalocyanine heterodimers.

properties revealed that energy transfer occurs between units in the TFEO-subPc and H-subPc heterodimer. Since the UV–vis spectra of a heterodimer are the sum of the absorption spectra of the respective units, it is suggested that each unit has an independent π-conjugate system. On the other hand, the fluorescence quantum yield decreased as a whole and the fluorescence derived from H-subPc was remarkably quenched. These results suggest energy transfer from the H-subPc unit to the TFEO-subPc unit (Figure 8) [133]. Subsequently, an unsymmetrical subphthalocyanine trimer composed of TFEO-subPc, F-subPc and H-subPc with phloroglucinol as a linker by the axial substitution reaction, has also been reported [134]. The synthesis of this trimer was carried out by the following sequential method. First, the axial position of TFEO-subPc-Cl was substituted with phloroglucinol under reflux conditions in toluene in the presence of triethylamine. Next, the connection of F-SubPc under reflux conditions was attempted, but the reaction did not proceed because of the poor axial reactivity. Therefore, the axis substitution reaction for F-SubPc was carried out after activating its axial position by silver triflate to obtain an intermediate dimer. Finally, H-SubPc was condensed by the axial substitution reaction using the activation method by silver triflate to induce the desired trimer **34**. Even in the trimer, an investigation of the spectroscopic properties suggested the transfer of energy between units. Each unit had an independent absorption property, but the fluorescence peak corresponding to H-subPc was quenched. This result suggests energy transfer from the H-subPc unit to fluorine-containing units. The relationship of HOMO and LUMO energy levels of SubPcs estimated from electrochemical measurements and DFT calculations is as follows: H-SubPc > TFEO-SubPc > F-SubPc. From these results, energy transfer between units is assumed as three patterns: from H-subPc to the TFEO-subPc or F-subPc unit, and from TFEO-subPc to the F-subPc unit.

Synthesis and optical investigation of trifluoroethoxy-substituted benzene-fused phthalocyanines

One of the binuclear phthalocyanines that have attracted attention in recent years is the benzene-fused phthalocyanine dimer

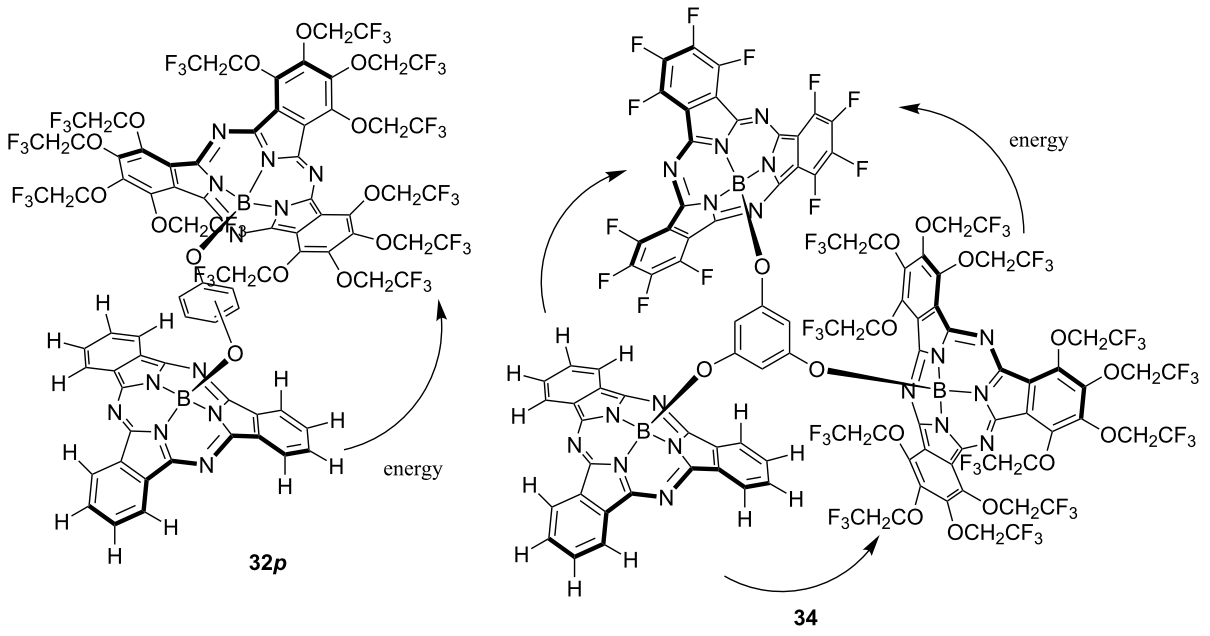

Figure 8: Energy transfer between subphthalocyanine units.

in which two phthalocyanines are fused together, having a common benzene ring. The benzene-fused dimer shows strong absorption in the near infrared region due to its large conjugated planar π-systems, and exhibits interesting features such as a strong electronic interaction between each unit through a common benzene ring. The benzene-fused phthalocyanine dimer was first reported in 1987, and various benzene-fused dimer derivatives have been reported ever since [135,136]. Although various benzene-fused phthalocyanine dimers (Pc-Pcs) and benzene-fused subphthalocyanine dimers (subPc-subPcs) have been reported (Figure 9) [137-140], there is only one report of a benzene-fused phthalocyanine and a subphthalocyanine heterodimer (Pc-subPc). In 2014, a trifluoroethoxy-substituted Pc-subPc was reported and its properties were compared with homodimers [141]. This heterodimer was synthesized by a stepwise synthesis method in which a phthalocyanine unit was first synthesized and then a subphthalocyanine unit was formed (Scheme 13). The synthesis of

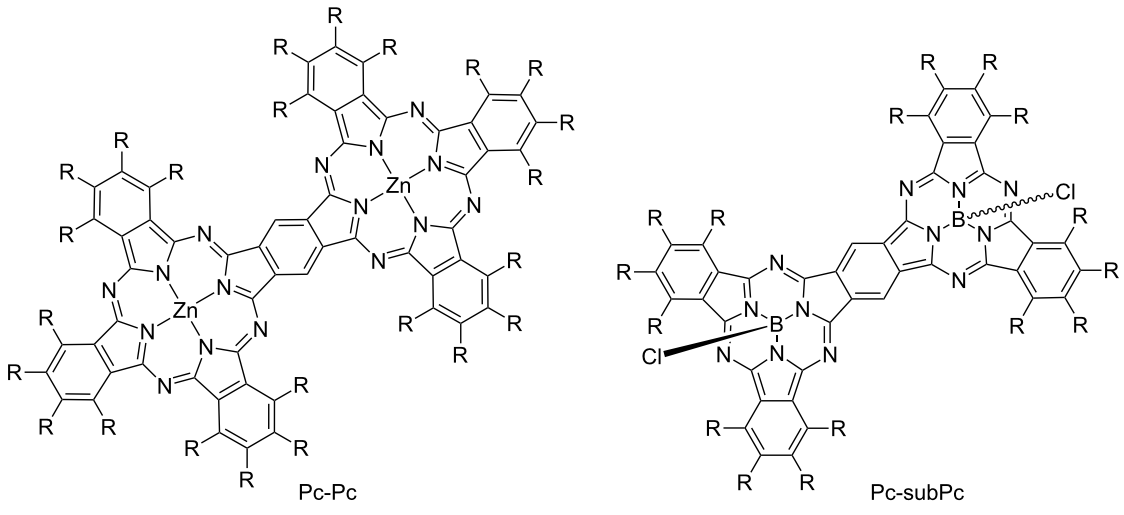

Figure 9: Structure of phthalocyanine and subphthalocyanine benzene-fused homodimers.

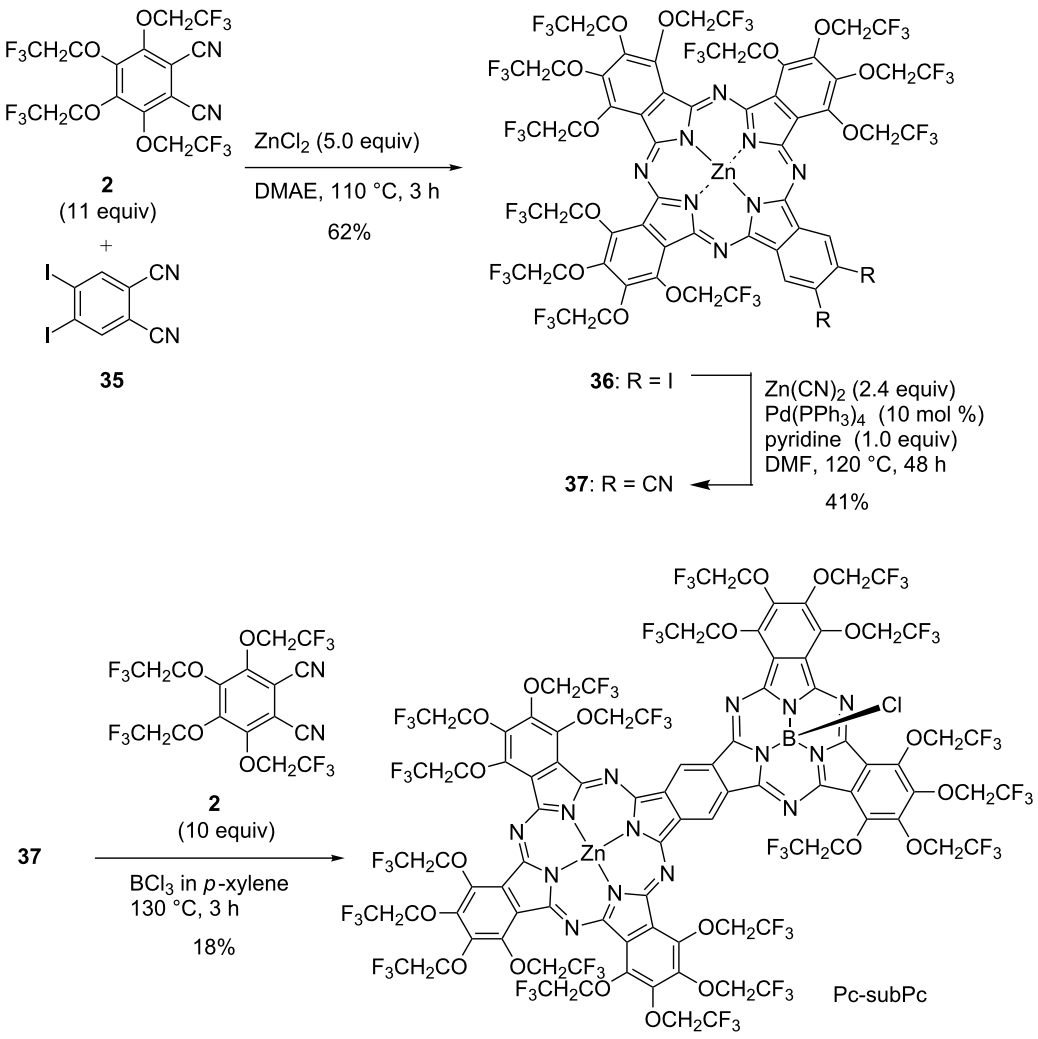

Scheme 13: Synthesis of a phthalocyanine and subphthalocyanine benzene-fused heterodimer.

Pc-subPc was carried out as follows. First, A_3B type diiodophthalocyanine **36** was synthesized by an unsymmetrical synthesis using diiodophthalonitrile **35** and trifluoroethoxyphthalonitrile **2**, and then iodides were converted to cyano groups by a coupling reaction. Finally, dicyanophthalocyanine **37** was reacted with **2** in the presence of boron trichloride to obtain trifluoroethoxy-substituted Pc-subPc. Although Pc-subPc was synthesized via a two-step statistical unsymmetric synthesis, it can be easily purified by silica gel column chromatography due to the aggregation inhibitory effect caused by the trifluoroethoxy group. The structure of Pc-subPc was confirmed by X-ray crystal structural analysis, having both a planar structure derived from phthalocyanine and a cone-shaped structure derived from subphthalocyanine (left of Figure 10). In the UV–vis absorption spectrum, Pc-subPc shows an absorption band around 800 nm which is located between the absorption bands of Pc-Pc and subPc-subPc (right of Figure 10). This result is consistent with a decrease in the HOMO–LUMO gap due to the conjugate expansion of each dimer, and it can be said that Pc-subPc is a dye showing intermediate spectroscopic properties between Pc-Pc and subPc-subPc.

Conclusion

This review is a summary of research on trifluoroethoxy-substituted phthalocyanines and subphthalocyanines. Due to the specific properties of fluorine, the aggregation behavior of phthalocyanine is alleviated, and various beneficial properties such as solubility and spectroscopic properties are enhanced. Since trifluoroethoxy-substituted phthalocyanines and subphthalocyanines are easy to handle, it is possible to obtain diverse derivatives and to fully demonstrate their functions. They are also expected to be developed into new material fields due to their high

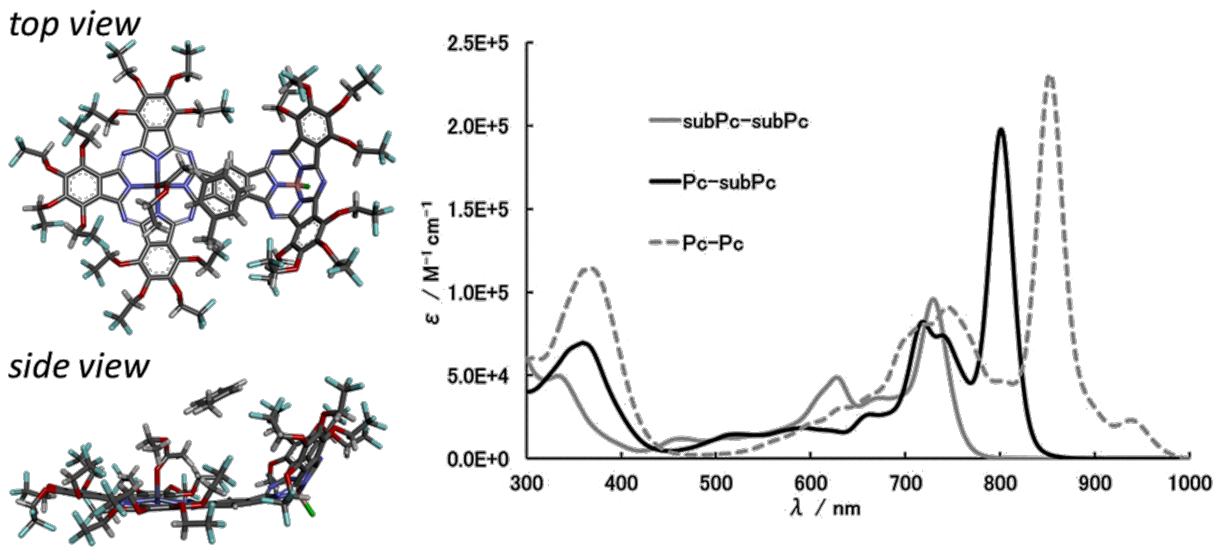

Figure 10: X-ray crystallography of Pc-subPc (left) and UV–vis spectra of benzene-fused dimers.

stability, high solubility and high lipophilicity. By combining the characteristics of fluorine and the functionalities of phthalocyanine, it is expected that new applications of phthalocyanines can be explored in furture.

Acknowledgements

This research is partially supported by JSPS KAKENHI Grant Number JP16H01017 in Precisely Designed Catalysts with Customized Scaffolding, and the Asahi Glass Foundation.

References

1. Lever, A. B. P.; Milaeva, E. R.; Speier, G. In *Phthalocyanines, Properties and Applications;* Leznoff, C. C.; Lever, A. B. P., Eds.; VCH: New York, 1993; Vol. 3, pp 1–69.
2. de la Torre, G.; Nicolau, M.; Torres, T. In *Handbook of Advanced Electronic and Photonic Materials;* Nalwa, H. S., Ed.; Wiley: Chichester, 2001; Vol. 5, pp 1–111.
3. Erk, P.; Hengelsberg, H. Applications of Phthalocyanines. In *The Porphyrin Handbook;* Kadish, K. M.; Smith, K. M.; Guilard, R., Eds.; Academic Press: San Diego, 2003; pp 105–149. doi:10.1016/B978-0-08-092393-2.50009-3
4. Dent, C. E.; Linstead, R. P. *J. Chem. Soc.* **1934,** 1027–1031. doi:10.1039/jr9340001027
5. Tianyong, Z.; Chunlong, Z. *Dyes Pigm.* **1997,** *35,* 123–130. doi:10.1016/S0143-7208(97)84839-5
6. Lelu, S.; Novat, C.; Graillat, C.; Guyot, A.; Bourgeat-Lami, E. *Polym. Int.* **2003,** *52,* 542–547. doi:10.1002/pi.1029
7. Defeyt, C.; Vandenabeele, P.; Gilbert, B.; Van Pevenage, J.; Cloots, R.; Strivay, D. *J. Raman Spectrosc.* **2012,** *43,* 1772–1780. doi:10.1002/jrs.4125
8. Gregory, P. *J. Porphyrins Phthalocyanines* **2000,** *4,* 432–437. doi:10.1002/(SICI)1099-1409(200006/07)4:4<432::AID-JPP254>3.0.CO;2-N
9. Chemistry of Functional Dyes. In *Proceedings of the Second International Symposium on Chemistry of Functional Dyes,* Yoshida, Z.; Shirota, Y., Eds.; Mita Press: Tokyo, Japan, 1993; Vol. 2.
10. Tokita, S.; Matsuoka, M.; Kogo, Y.; Kihara, H. *Molecular Design of Functional Dyes-PPP Molecular Orbital Method and Its Applications;* Maruzen: Tokyo, 1989.
11. Kim, S.-H., Ed. *Functional Dyes;* Elsevier: Amsterdam, Netherlands, 2006.
12. Choi, J.; Kim, S. H.; Lee, W.; Yoon, C.; Kim, J. P. *New J. Chem.* **2012,** *36,* 812–818. doi:10.1039/c2nj20938a
13. Kim, Y. D.; Kim, J. P.; Kwon, O. S.; Cho, I. H. *Dyes Pigm.* **2009,** *81,* 45–52. doi:10.1016/j.dyepig.2008.09.006
14. Rollet, F.; Morlat-Thérias, S.; Gardette, J.-L.; Fontaine, J.-M.; Perdereau, J.; Polack, J.-D. *J. Cultural Heritage* **2008,** *9,* 234–243. doi:10.1016/j.culher.2008.04.001
15. Cid, J.-J.; García-Iglesias, M.; Yum, J.-H.; Forneli, A.; Albero, J.; Martínez-Ferrero, E.; Vázquez, P.; Grätzel, M.; Nazeeruddin, M. K.; Palomares, E.; Torres, T. *Chem. – Eur. J.* **2009,** *15,* 5130–5137. doi:10.1002/chem.200801778
16. O'Regan, B. C.; López-Duarte, I.; Martínez-Díaz, M. V.; Forneli, A.; Albero, J.; Morandeira, A.; Palomares, E.; Torres, T.; Durrant, J. R. *J. Am. Chem. Soc.* **2008,** *130,* 2906–2907. doi:10.1021/ja078045o
17. Bonnett, R. *Chem. Soc. Rev.* **1995,** *24,* 19–33. doi:10.1039/cs9952400019
18. Berger, R.; Resnati, G.; Metrangolo, P.; Weber, E.; Hulliger, J. *Chem. Soc. Rev.* **2011,** *40,* 3496–3508. doi:10.1039/c0cs00221f
19. Sen, K. D.; Jørgensen, C. K. *Electronegativity;* Springer: New York, 1987. doi:10.1007/BFb0029833
20. Nagle, J. K. *J. Am. Chem. Soc.* **1990,** *112,* 4741–4747. doi:10.1021/ja00168a019
21. O'Hagan, D.; Rzepa, H. S. *Chem. Commun.* **1997,** 645–652. doi:10.1039/a604140j
22. Park, B. K.; Kitteringham, N. R. *Drug Metab. Rev.* **1994,** *26,* 605–643. doi:10.3109/03602539408998319
23. O'Hagan, D. *Chem. Soc. Rev.* **2008,** *37,* 308–319. doi:10.1039/B711844A

24. Ameduri, B.; Boutevin, B. *Well Architectured Fluoropolymers: Synthesis, Properties and Applications;* Elsevier: Amsterdam, 2004.
25. Ismail, F. M. D. *J. Fluorine Chem.* **2002,** *118,* 27–33. doi:10.1016/S0022-1139(02)00201-4
26. Purser, S.; Moore, P. R.; Swallow, S.; Gouverneur, V. *Chem. Soc. Rev.* **2008,** *37,* 320–330. doi:10.1039/B610213C
27. Isanbor, C.; O'Hagan, D. *J. Fluorine Chem.* **2006,** *127,* 303–319. doi:10.1016/j.jfluchem.2006.01.011
28. Bégué, J.-P.; Bonnet-Delpon, D. *J. Fluorine Chem.* **2006,** *127,* 992–1012. doi:10.1016/j.jfluchem.2006.05.006
29. Kirk, K. L. *J. Fluorine Chem.* **2006,** *127,* 1013–1029. doi:10.1016/j.jfluchem.2006.06.007
30. Hagmann, W. K. *J. Med. Chem.* **2008,** *51,* 4359–4369. doi:10.1021/jm800219f
31. Ojima, I., Ed. *Fluorine in Medicinal Chemistry and Chemical Biology;* Wiley-Blackwell: New York, 2009. doi:10.1002/9781444312096
32. Stuzhin, P. A. Fluorinated Phthalocyanines and Their Analogues. In *Fluorine in Heterocyclic Chemistry;* Nenajdenko, V., Ed.; Springer: Heidelberg, 2014; Vol. 1, pp 621–681. doi:10.1007/978-3-319-04346-3_15
33. Boyle, R. W.; Rousseau, J.; Kudrevich, S. V.; Obochi, M. O. K.; van Lier, J. E. *Br. J. Cancer* **1996,** *73,* 49–53. doi:10.1038/bjc.1996.9
34. Ünlü, S.; Yaraşır, M. N.; Kandaz, M.; Koca, A.; Salih, B. *Polyhedron* **2008,** *27,* 2805–2810. doi:10.1016/j.poly.2008.05.036
35. Selçukoğlu, M.; Hamuryudan, E. *Dyes Pigm.* **2007,** *74,* 17–20. doi:10.1016/j.dyepig.2006.01.009
36. Moons, H.; Loas, A.; Gorun, S. M.; Doorslaer, S. V. *Dalton Trans.* **2014,** *43,* 14942–14948. doi:10.1039/C4DT00621F
37. Bao, Z.; Lovinger, A. J.; Brown, J. *J. Am. Chem. Soc.* **1998,** *120,* 207–208. doi:10.1021/ja9727629
38. Yoon, S. M.; Song, H. J.; Hwang, I.-C.; Kim, K. S.; Choi, H. C. *Chem. Commun.* **2010,** *46,* 231–233. doi:10.1039/B914457A
39. Meiss, J.; Merten, A.; Hein, M.; Schuenemann, C.; Schäfer, S.; Tietze, M.; Uhrich, C.; Pfeiffer, M.; Leo, K.; Riede, M. *Adv. Funct. Mater.* **2012,** *22,* 405–414. doi:10.1002/adfm.201101799
40. Cnops, K.; Zango, G.; Genoe, J.; Heremans, P.; Martinez-Diaz, M. V.; Torres, T.; Cheyns, D. *J. Am. Chem. Soc.* **2015,** *137,* 8991–8997. doi:10.1021/jacs.5b02808
41. Mori, S.; Shibata, N. *J. Synth. Org. Chem., Jpn.* **2016,** *74,* 154–166. doi:10.5059/yukigoseikyokaishi.74.154
42. Kobayashi, H.; Matsumoto, K.; Sonoda, T. In *Proceedings of the 2nd International Symposium on the Chemistry of Functional Dye,* Kobe; Mita Press: Osaka, Japan, 1992; pp 290–295.
43. Kobayashi, N.; Sasaki, N.; Higashi, Y.; Osa, T. *Inorg. Chem.* **1995,** *34,* 1636–1637. doi:10.1021/ic00111a004
44. Weitman, H.; Schatz, S.; Gottlieb, H. E.; Kobayashi, N.; Ehrenberg, B. *Photochem. Photobiol.* **2001,** *73,* 473–481. doi:10.1562/0031-8655(2001)073<0473:SPOTAB>2.0.CO;2
45. Hiroaki, I.; Yutaka, K.; Akiyuki, M. *Chem. Lett.* **2004,** *33,* 862–863. doi:10.1246/cl.2004.862
46. Reichardt, C. *Chem. Rev.* **1994,** *94,* 2319–2358. doi:10.1021/cr00032a005
47. Kobayashi, N.; Ogata, H.; Nonaka, N.; Luk'yanets, E. A. *Chem. – Eur. J.* **2003,** *9,* 5123–5134. doi:10.1002/chem.200304834
48. Liu, J.-B.; Zhao, Y.; Zhao, F.-Q.; Zhang, F.-S.; Tang, Y.-W.; Song, X.-q.; Zhou, F.-T. *Acta Phys.-Chim. Sin.* **1996,** *12,* 202–207.
49. Beeby, A.; FitzGerald, S.; Stanley, C. F. *J. Chem. Soc., Perkin Trans. 2* **2001,** 1978–1982. doi:10.1039/B102937C
50. Honda, T.; Kojima, T.; Kobayashi, N.; Fukuzumi, S. *Angew. Chem., Int. Ed.* **2011,** *50,* 2725–2728. doi:10.1002/anie.201006607
51. Leclaire, J.; Dagiral, R.; Fery-Forgues, S.; Coppel, Y.; Donnadieu, B.; Caminade, A.-M.; Majoral, J.-P. *J. Am. Chem. Soc.* **2005,** *127,* 15762–15770. doi:10.1021/ja054797b
52. Eberhardt, W.; Hanack, M. *Synthesis* **1997,** 95–100. doi:10.1055/s-1997-1495
53. Nemykin, V. N.; Chernii, V. Ya.; Volkov, S. V.; Bundina, N. I.; Kaliya, O. L.; Li, V. D.; Lukyanets, E. A. *J. Porphyrins Phthalocyanines* **1999,** *3,* 87–98. doi:10.1002/(SICI)1099-1409(199902)3:2<87::AID-JPP108>3.0.CO;2-G
54. Iida, N.; Tanaka, K.; Tokunaga, E.; Mori, S.; Saito, N.; Shibata, N. *ChemistryOpen* **2015,** *4,* 698–702. doi:10.1002/open.201500165
55. Das, B.; Tokunaga, E.; Shibata, N.; Kobayashi, N. *J. Fluorine Chem.* **2010,** *131,* 652–654. doi:10.1016/j.jfluchem.2010.01.004
56. Jessop, P. G.; Ikariya, T.; Noyori, R. *Chem. Rev.* **1999,** *99,* 475–494. doi:10.1021/cr970037a
57. Cooper, A. I. *J. Mater. Chem.* **2000,** *10,* 207–234. doi:10.1039/a906486i
58. Oakes, R. S.; Clifford, A. A.; Rayner, C. M. *J. Chem. Soc., Perkin Trans. 1* **2001,** 917–941. doi:10.1039/b101219n
59. Hay, J. N.; Khan, A. *J. Mater. Sci.* **2002,** *37,* 4743–4752. doi:10.1023/A:1020874532674
60. Hoggan, E. N.; Flowers, D.; Wang, K.; DeSimone, J. M.; Carbonell, R. G. *Ind. Eng. Chem. Res.* **2004,** *43,* 2113–2122. doi:10.1021/ie0308543
61. Xu, X.-H.; Kusuda, A.; Tokunaga, E.; Shibata, N. *Green Chem.* **2011,** *13,* 46–50. doi:10.1039/C0GC00619J
62. Xu, X.-H.; Azuma, A.; Taniguchi, M.; Tokunaga, E.; Shibata, N. *RSC Adv.* **2013,** *3,* 3848–3852. doi:10.1039/c3ra00132f
63. Kusuda, A.; Xu, X.-H.; Wang, X.; Tokunaga, E.; Shibata, N. *Green Chem.* **2011,** *13,* 843–846. doi:10.1039/c1gc15106a
64. Kobayashi, N.; Kondo, R.; Nakajima, S.; Osa, T. *J. Am. Chem. Soc.* **1990,** *112,* 9640–9641. doi:10.1021/ja00182a034
65. Wang, A.; Long, L.; Zhang, C. *Tetrahedron* **2012,** *68,* 2433–2451. doi:10.1016/j.tet.2012.01.004
66. Tian, M.; Wada, T.; Kimura-Suda, H.; Sasabe, H. *J. Mater. Chem.* **1997,** *7,* 861–863. doi:10.1039/a701606i
67. Tian, M.; Wada, T.; Sasabe, H. *J. Heterocycl. Chem.* **2000,** *37,* 1193–1202. doi:10.1002/jhet.5570370528
68. de la Torre, G.; Bottari, G.; Sekita, M.; Hausmann, A.; Guldi, D. M.; Torres, T. *Chem. Soc. Rev.* **2013,** *42,* 8049–8105. doi:10.1039/c3cs60140d
69. Maya, E. M.; Vázquez, P.; Torres, T. *Chem. – Eur. J.* **1999,** *5,* 2004–2013. doi:10.1002/(SICI)1521-3765(19990702)5:7<2004::AID-CHEM2004>3.0.CO;2-P
70. Ali, H.; Baillargeon, P.; van Lier, J. E. *Tetrahedron Lett.* **2008,** *49,* 7253–7255. doi:10.1016/j.tetlet.2008.09.160
71. Ali, H.; van Lier, J. E. *Tetrahedron Lett.* **2009,** *50,* 337–339. doi:10.1016/j.tetlet.2008.11.035
72. Dodsworth, E. S.; Lever, A. B. P.; Seymour, P.; Leznoff, C. C. *J. Phys. Chem.* **1985,** *89,* 5698–5705. doi:10.1021/j100272a025
73. Tian, M.; Zhang, Y.; Wada, T.; Sasabe, H. *Dyes Pigm.* **2003,** *58,* 135–143. doi:10.1016/S0143-7208(03)00062-7
74. Yoshiyama, H.; Shibata, N.; Sato, T.; Nakamura, S.; Toru, T. *Chem. Commun.* **2008,** 1977–1979. doi:10.1039/b800918j

75. Vigh, S.; Lam, H.; Janda, P.; Lever, A. B. P.; Leznoff, C. C.; Cerny, R. L. *Can. J. Chem.* **1991,** *69,* 1457–1461. doi:10.1139/v91-215
76. García-Frutos, E. M.; O'Flaherty, S. M.; Maya, E. M.; de la Torre, G.; Blau, W.; Vázquez, P.; Torres, T. *J. Mater. Chem.* **2003,** *13,* 749–753. doi:10.1039/b210707d
77. Kobayashi, N.; Lever, A. B. P. *J. Am. Chem. Soc.* **1987,** *109,* 7433–7441. doi:10.1021/ja00258a030
78. Huang, X.; Zhao, F.; Li, Z.; Huang, L.; Tang, Y.; Zhang, F.; Tung, C.-H. *Chem. Lett.* **2007,** *36,* 108–109. doi:10.1246/cl.2007.108
79. Leznoff, C. C.; Marcuccio, S. M.; Greenberg, S.; Lever, A. B. P.; Tomer, K. B. *Can. J. Chem.* **1985,** *63,* 623–631. doi:10.1139/v85-102
80. Leznoff, C. C.; Svirskaya, P. I.; Khouw, B.; Cerny, R. L.; Seymour, P.; Lever, A. B. P. *J. Org. Chem.* **1991,** *56,* 82–90. doi:10.1021/jo00001a019
81. Yoshiyama, H.; Shibata, N.; Sato, T.; Nakamura, S.; Toru, T. *Org. Biomol. Chem.* **2008,** *6,* 4498–4501. doi:10.1039/b814169j
82. Yoshiyama, H.; Shibata, N.; Sato, T.; Nakamura, S.; Toru, T. *Org. Biomol. Chem.* **2009,** *7,* 2265–2269. doi:10.1039/b902905b
83. Durmaz, H.; Sanyal, A.; Hizal, G.; Tunca, U. *Polym. Chem.* **2012,** *3,* 825–835. doi:10.1039/C1PY00471A
84. Das, B.; Umeda, M.; Tokunaga, E.; Toru, T.; Shibata, N. *Chem. Lett.* **2010,** *39,* 337–339. doi:10.1246/cl.2010.337
85. Allémann, E.; Rousseau, J.; Brasseur, N.; Kudrevich, S. V.; Lewis, K.; van Lier, J. E. *Int. J. Cancer* **1996,** *66,* 821–824. doi:10.1002/(SICI)1097-0215(19960611)66:6<821::AID-IJC19>3.0.CO;2-5
86. Liu, K. J.; Gast, P.; Moussavi, M.; Norby, S. W.; Vahidi, N.; Walczak, T.; Wu, M.; Swartz, H. M. *Proc. Natl. Acad. Sci. U. S. A.* **1993,** *90,* 5438–5442. doi:10.1073/pnas.90.12.5438
87. Mantareva, V.; Kussovski, V.; Angelov, I.; Wöhrle, D.; Dimitrov, R.; Popova, E.; Dimitrov, S. *Photochem. Photobiol. Sci.* **2011,** *10,* 91–102. doi:10.1039/B9PP00154A
88. De Filippis, M. P.; Dei, D.; Fantetti, L.; Roncucci, G. *Tetrahedron Lett.* **2000,** *41,* 9143–9147. doi:10.1016/S0040-4039(00)01638-5
89. Li, H.; Jensen, T. J.; Fronczek, F. R.; Vicente, M. G. H. *J. Med. Chem.* **2008,** *51,* 502–511. doi:10.1021/jm070781f
90. Ribeiro, A. O.; Tomé, J. P. C.; Neves, M. G. P. M. S.; Tomé, A. C.; Cavaleiro, J. A. S.; Iamamoto, Y.; Torres, T. *Tetrahedron Lett.* **2006,** *47,* 9177–9180. doi:10.1016/j.tetlet.2006.10.155
91. Zorlu, Y.; Dumoulin, F.; Bouchu, D.; Ahsen, V.; Lafont, D. *Tetrahedron Lett.* **2010,** *51,* 6615–6618. doi:10.1016/j.tetlet.2010.10.044
92. Sibrian-Vazquez, M.; Ortiz, J.; Nesterova, I. V.; Fernández-Lázaro, F.; Sastre-Santos, A.; Soper, S. A.; Vicente, M. G. H. *Bioconjugate Chem.* **2007,** *18,* 410–420. doi:10.1021/bc060297b
93. Ali, H.; Ait-Mohand, S.; Gosselin, S.; van Lier, J. E.; Guérin, B. *J. Org. Chem.* **2011,** *76,* 1887–1890. doi:10.1021/jo102083g
94. Nyman, E. S.; Hynninen, P. H. *J. Photochem. Photobiol., B: Biol.* **2004,** *73,* 1–28. doi:10.1016/j.jphotobiol.2003.10.002
95. Kuimova, M. K.; Botchway, S. W.; Parker, A. W.; Balaz, M.; Collins, H. A.; Anderson, H. L.; Suhling, K.; Ogilby, P. R. *Nat. Chem.* **2009,** *1,* 69–73. doi:10.1038/nchem.120
96. Macdonald, I. J.; Dougherty, T. J. *J. Porphyrins Phthalocyanines* **2001,** *5,* 105–129. doi:10.1002/jpp.328
97. Greish, K. Enhanced Permeability and Retention (EPR) Effect for Anticancer Nanomedicine Drug Targeting. In *Cancer Nanotechnology Methods and Protocols;* Grobmyer, S. R.; Moudgil, B. M., Eds.; Springer Protocols, Vol. 624; Humana Press: Totowa, New Jersey, 2010; pp 25–37. doi:10.1007/978-1-60761-609-2_3
98. Erbas, S.; Gorgulu, A.; Kocakusakogullari, M.; Akkaya, E. U. *Chem. Commun.* **2009,** 4956–4958. doi:10.1039/B908485A
99. Reddy, M. R.; Shibata, N.; Kondo, Y.; Nakamura, S.; Toru, T. *Angew. Chem., Int. Ed.* **2006,** *45,* 8163–8166. doi:10.1002/anie.200603590
100. Obata, T.; Mori, S.; Suzuki, Y.; Kashiwagi, T.; Tokunaga, E.; Shibata, N.; Tanaka, M. *J. Cancer Ther.* **2015,** *6,* No. 53220. doi:10.4236/jct.2015.61008
101. D'Souza, F.; Ito, O. *Coord. Chem. Rev.* **2005,** *249,* 1410–1422. doi:10.1016/j.ccr.2005.01.002
102. Mishra, A.; Bäuerle, P. *Angew. Chem., Int. Ed.* **2012,** *51,* 2020–2067. doi:10.1002/anie.201102326
103. Linssen, T. G.; Dürr, K.; Hanack, M.; Hirsch, A. *J. Chem. Soc., Chem. Commun.* **1995,** 103–104. doi:10.1039/C39950000103
104. Sukeguchi, D.; Yoshiyama, H.; Singh, S. P.; Shibata, N.; Nakamura, S.; Toru, T.; Hayashi, Y.; Soga, T. *Heterocycl. Commun.* **2009,** *15,* 263–272. doi:10.1515/HC.2009.15.4.263
105. Sukeguchi, D.; Yoshiyama, H.; Shibata, N.; Nakamura, S.; Toru, T.; Hayashi, Y.; Soga, T. *J. Fluorine Chem.* **2009,** *130,* 361–364. doi:10.1016/j.jfluchem.2008.11.005
106. Guo, J.; Liang, Y.; Szarko, J.; Lee, B.; Son, H. J.; Rolczynski, B. S.; Yu, L.; Chen, L. X. *J. Phys. Chem. B* **2010,** *114,* 742–748. doi:10.1021/jp909135k
107. Dang, M. T.; Hirsch, L.; Wantz, G. *Adv. Mater.* **2011,** *23,* 3597–3602. doi:10.1002/adma.201100792
108. Yamada, I.; Umeda, M.; Hayashi, Y.; Soga, T.; Shibata, N. *Jpn. J. Appl. Phys.* **2012,** *51,* 04DK09. doi:10.1143/JJAP.51.04DK09
109. Yamada, I.; Iida, N.; Hayashi, Y.; Soga, T.; Shibata, N. *Jpn. J. Appl. Phys.* **2013,** *52,* 05DA07. doi:10.7567/JJAP.52.05DA07
110. Rand, B. P.; Cheyns, D.; Vasseur, K.; Giebink, N. C.; Mothy, S.; Yi, Y.; Coropceanu, V.; Beljonne, D.; Cornil, J.; Brédas, J.-L.; Genoe, J. *Adv. Funct. Mater.* **2012,** *22,* 2987–2995. doi:10.1002/adfm.201200512
111. Hougham, G.; Cassidy, P. E.; Johns, K.; Davidson, T., Eds. *Fluoropolymers: Synthesis and Applications;* Plenum Publishers: New York, 1999; Vol. 1–2.
112. Gritsenko, K. P.; Dimitriev, O. P.; Kislyk, V. V.; Getsko, O. M.; Schrader, S.; Brehmer, L. *Colloids Surf., A* **2002,** *198–200,* 625–632. doi:10.1016/S0927-7757(01)00977-3
113. Wang, J.-W.; Shen, Q.-D.; Bao, H.-M.; Yang, C.-Z.; Zhang, Q. M. *Macromolecules* **2005,** *38,* 2247–2252. doi:10.1021/ma047890d
114. Tillet, G.; De Leonardis, P.; Alaaeddine, A.; Umeda, M.; Mori, S.; Shibata, N.; Aly, S. M.; Fortin, D.; Harvey, P. D.; Ameduri, B. *Macromol. Chem. Phys.* **2012,** *213,* 1559–1568. doi:10.1002/macp.201200076
115. Kondratenko, N. V.; Nemykin, V. N.; Lukyanets, E. A.; Kostromina, N. A.; Volkovan, S. V.; Yagupolskii, L. M. *J. Porphyrins Phthalocyanines* **1997,** *1,* 341–347. doi:10.1002/(SICI)1099-1409(199710)1:4<341::AID-JPP37>3.0.CO;2-K
116. Winter, G.; Heckmann, H.; Haisch, P.; Eberhardt, W.; Hanack, M.; Lüer, L.; Egelhaaf, H.-J.; Oelkrug, D. *J. Am. Chem. Soc.* **1998,** *120,* 11663–11673. doi:10.1021/ja981644y
117. Gao, L.; Qian, X. *J. Fluorine Chem.* **2002,** *113,* 161–165. doi:10.1016/S0022-1139(01)00539-5
118. Sukeguchi, D.; Yoshiyama, H.; Shibata, N.; Nakamura, S.; Toru, T. *Heterocycl. Commun.* **2009,** *15,* 195–202. doi:10.1515/HC.2009.15.3.195

119. Mori, S.; Ogawa, N.; Tokunaga, E.; Shibata, N. *J. Porphyrins Phthalocyanines* **2014,** *18,* 1034–1041. doi:10.1142/S1088424614500862
120. Ishikawa, N.; Sugita, M.; Ishikawa, T.; Koshihara, S.; Kaizu, Y. *J. Am. Chem. Soc.* **2003,** *125,* 8694–8695. doi:10.1021/ja029629n
121. Ye, T.; Takami, T.; Wang, R.; Jiang, J.; Weiss, P. S. *J. Am. Chem. Soc.* **2006,** *128,* 10984–10985. doi:10.1021/ja060029o
122. Kobayashi, N. *J. Porphyrins Phthalocyanines* **1999,** *3,* 453–467. doi:10.1002/(SICI)1099-1409(199908/10)3:6/7<453::AID-JPP157>3.0.CO;2-2
123. Claessens, C. G.; González-Rodríguez, D.; Torres, T. *Chem. Rev.* **2002,** *102,* 835–854. doi:10.1021/cr0101454
124. Torres, T. *Angew. Chem., Int. Ed.* **2006,** *45,* 2834–2837. doi:10.1002/anie.200504265
125. Shimizu, S.; Kobayashi, N. *Chem. Commun.* **2014,** *50,* 6949–6966. doi:10.1039/C4CC01526F
126. Sastre, A.; Torres, T.; Díaz-García, M. A.; Agulló-López, F.; Dhenaut, C.; Brasselet, S.; Ledoux, I.; Zyss, J. *J. Am. Chem. Soc.* **1996,** *118,* 2746–2747. doi:10.1021/ja9533050
127. González-Rodríguez, D.; Torres, T.; Guldi, D. M.; Rivera, J.; Echegoyen, L. *Org. Lett.* **2002,** *4,* 335–338. doi:10.1021/ol0169022
128. Mutolo, K. L.; Mayo, E. I.; Rand, B. P.; Forrest, S. R.; Thompson, M. E. *J. Am. Chem. Soc.* **2006,** *128,* 8108–8109. doi:10.1021/ja061655o
129. Shibata, N.; Das, B.; Tokunaga, E.; Shiro, M.; Kobayashi, N. *Chem. – Eur. J.* **2010,** *16,* 7554–7562. doi:10.1002/chem.201000373
130. Claessens, C. G.; Gonzalez-Rodríguez, D.; Rodríguez-Morgade, M. S.; Medina, A.; Torres, T. *Chem. Rev.* **2014,** *114,* 2192–2277. doi:10.1021/cr400088w
131. Mori, S.; Ogawa, N.; Tokunaga, E.; Shibata, N. *Dalton Trans.* **2015,** *44,* 19451–19455. doi:10.1039/C5DT02279G
132. Guilleme, J.; González-Rodríguez, D.; Torres, T. *Angew. Chem., Int. Ed.* **2011,** *50,* 3506–3509. doi:10.1002/anie.201007240
133. Kossanyi, J.; Chahraoui, D. *Int. J. Photoenergy* **2000,** *2,* 9–15. doi:10.1155/S1110662X00000027
134. Mori, S.; Ogawa, N.; Tokunaga, E.; Tsuzuki, S.; Shibata, N. *Dalton Trans.* **2016,** *45,* 908–912. doi:10.1039/C5DT04500B
135. Leznoff, C. C.; Lam, H.; Marcuccio, S. M.; Nevin, W. A.; Janda, P.; Kobayashi, N.; Lever, A. B. P. *J. Chem. Soc., Chem. Commun.* **1987,** 699–701. doi:10.1039/c39870000699
136. Kobayashi, N. *J. Chem. Soc., Chem. Commun.* **1991,** 1203–1205. doi:10.1039/c39910001203
137. Claessens, C. G.; Torres, T. *Angew. Chem., Int. Ed.* **2002,** *41,* 2561–2565. doi:10.1002/1521-3773(20020715)41:14<2561::AID-ANIE2561>3.0.CO;2-3
138. Fukuda, T.; Stork, R. J.; Potucek, R. J.; Olmstead, M. M.; Noll, B. C.; Kobayashi, N.; Durfee, W. S. *Angew. Chem., Int. Ed.* **2002,** *41,* 2565–2568. doi:10.1002/1521-3773(20020715)41:14<2565::AID-ANIE2565>3.0.CO;2-G
139. Kobayashi, N.; Lam, H.; Nevin, W. A.; Janda, P.; Leznoff, C. C.; Koyama, T.; Monden, A.; Shirai, H. *J. Am. Chem. Soc.* **1994,** *116,* 879–890. doi:10.1021/ja00082a007
140. Zango, G.; Zirzlmeier, J.; Claessens, C. G.; Clark, T.; Martínez-Díaz, M. V.; Guldi, D. M.; Torres, T. *Chem. Sci.* **2015,** *6,* 5571–5577. doi:10.1039/C5SC01709B
141. Shibata, N.; Mori, S.; Hayashi, M.; Umeda, M.; Tokunaga, E.; Shiro, M.; Sato, H.; Hoshi, T.; Kobayashi, N. *Chem. Commun.* **2014,** *50,* 3040–3043. doi:10.1039/C3CC49831J

License and Terms

BEILSTEIN JOURNAL OF ORGANIC CHEMISTRY

Comparative profiling of well-defined copper reagents and precursors for the trifluoromethylation of aryl iodides

Peter T. Kaplan, Jessica A. Lloyd, Mason T. Chin and David A. Vicic*§

Full Research Paper

Open Access

Address:
Department of Chemistry, Lehigh University, 6 E. Packer Ave., Bethlehem, PA 18015, USA

Email:
David A. Vicic* - vicic@lehigh.edu

* Corresponding author
§ Phone: 1-610-758-3466, Fax: 1-610-758-6536

Keywords:
benchmarking; copper; fluorine; fluoroalkylation; trifluoromethylation

Beilstein J. Org. Chem. **2017,** *13,* 2297–2303.
doi:10.3762/bjoc.13.225

Received: 28 June 2017
Accepted: 07 October 2017
Published: 30 October 2017

This article is part of the Thematic Series "Organo-fluorine chemistry IV".

Guest Editor: D. O'Hagan

Abstract

A number of copper reagents were compared for their effectiveness in trifluoromethylating 4-iodobiphenyl, 4-iodotoluene, and 2-iodotoluene. Yields over time were plotted in order to refine our understanding of each reagent performance, identify any bottlenecks, and provide more insight into the rates of the reactions. Interestingly, differences in reactivity were observed when a well-defined [$LCuCF_3$] complex was employed directly or generated in situ from precursors by published reports. Relative reactivities were also found to highly dependent on the nature of the iodoarenes.

Introduction

Selectively fluorinated molecules that bear the trifluoromethyl group have great importance in the life sciences and materials fields as well as discovery chemistry in general [1-3]. Consequently, transition-metal-catalyzed methods for preparing aromatic trifluoromethyl compounds from readily available aryl halides are an area that has seen rapid growth in the past ten years. Copper is one of the most successfully used metals for mediating the trifluoromethylation of aryl halides, and the active form of the reagents is typically a copper(I) complex bearing a trifluoromethyl ligand, i.e., [$L_nCu–CF_3$]. Sporadic examples of trifluoromethylation 'catalysis' using copper have been observed [4-9], but these reactions typically only work for aryl iodides and have a low substrate scope, low turn-over values, and/or involve decarboxylation reactions at high temperatures. Stoichiometric trifluoromethylating agents are therefore more commonly used in benchtop trifluoromethylation chemistry. Ancillary ligands (L) are known to play a large role in the reactivity of such [$L_nCu–CF_3$] reagents, and recent work has focused on developing new ligands that not only allow for better control of reactivity but also provide stability to facilitate meaningful comparative studies, such as structural and electrochemical ones [2]. *N*-Heterocyclic carbene (NHC) complexes of copper such as **A1** (Scheme 1) were the first well-defined and structurally characterized copper–CF_3 complexes that display

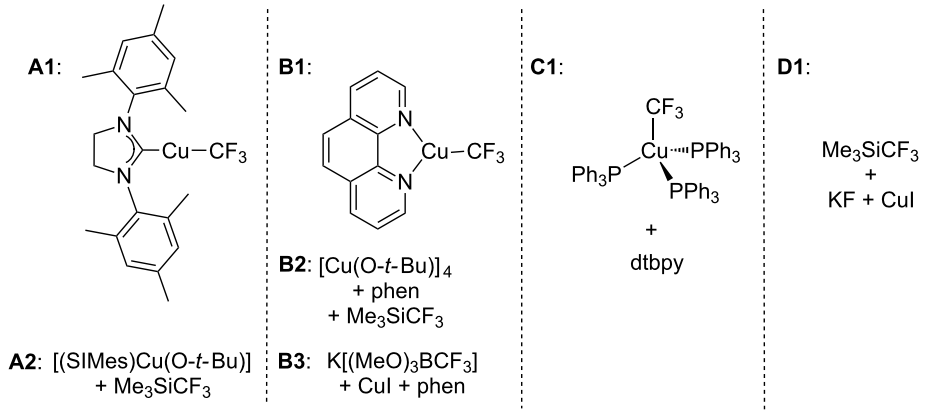

Scheme 1: Reagents and precursors used for trifluoromethylation reactions.

activity for the trifluoromethylation of aryl halides [10,11]. [(SIMes)$CuCF_3$] (**1**, SIMes = 1,3-bis(2,4,6-trimethylphenyl)-4,5-dihydroimidazol-2-ylidene), which is in equilibrium with [$(SIMes)_2Cu$][$Cu(CF_3)_2$] (**2**), can either be used directly or prepared in situ through the reaction of [(SIMes)Cu(O-*t*-Bu)] (**3**) with Me_3SiCF_3 (Scheme 2) [10]. Phenanthroline complexes of copper **B1** were reported shortly after the NHC counterparts [5,12] and have reached much success in chemical synthesis due to the ease of preparation and the low cost of the phenanthroline ancillary ligand. [(phen)$CuCF_3$] can now be purchased commercially, or prepared in situ by a variety of methods including the reaction of [Cu(O-*t*-Bu)]$_4$ with Me_3SiCF_3 and phen (**B2**, Scheme 1) [12] or by reaction of [$(MeO)_3BCF_3$] with CuI and phen (**B3**, Scheme 1) [8]. The compound [$(PPh_3)_3CuCF_3$] has been for a long time [13], however, its trifluoromethylating ability and structure determination was not reported until 2011. Trifluoromethylations with [$(PPh_3)_3CuCF_3$] are only efficient when the reactions are performed in neat aryl iodode [14]. Less side-products and higher yields are observed for trifluoromethylations with [$(PPh_3)_3CuCF_3$] when dtbpy (dtbpy = 4,4′-di-*tert*-butylbipyridine) is added to reaction mixtures (**C1**) to presumably generate a dtbpy complex of $CuCF_3$ [14]. Finally, conditions that generate "ligandless" [$CuCF_3$] (**D1**, for example) are also amenable for the trifluoromethylation of aryl iodides [15], but it is unclear how the reactivity profile of the ligandless complex compares to systems **A**–**C** described in Scheme 1. An important issue is that only single time point yields have been reported for systems **B**–**D**, and the significantly different reaction conditions employed for each system have made it impossible to truly compare reagent performance based on the available literature data. For this reason, we sought to run trifluoromethylation reactions with systems **A**–**D** under both identical and the reported optimal reaction conditions in order to track how yields change over time for each reagent for comparative studies. We also sought to explore whether there were differences in reactivity when a well-defined [$LCuCF_3$] complex was employed directly or generated in situ by published reports. If so, it will be informative to know the extent of differences in reagent performance over time.

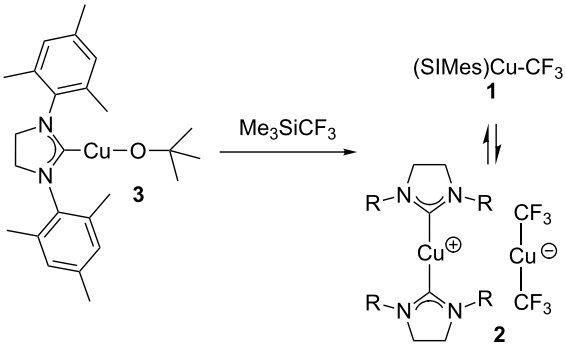

Scheme 2: Preparation of [$(SIMes)_2Cu$][$Cu(CF_3)_2$].

Results and Discussion

Because the phenanthroline-based system described as **B1** (Scheme 1) is the most widely used reagent for trifluoromethylations, we modeled our "standard" comparative conditions similar to those reported by Hartwig in 2011 [12]. These conditions involve reacting 4-iodo-1,1'-biphenyl with a [Cu–CF_3] source at 50 °C in DMF (Scheme 3). Somewhat more diluted reaction conditions relative to the published procedure were used to ensure homogeneity for all the different complexes described in Scheme 1. Conversions to 4-(trifluoromethyl)-1,1'-biphenyl were then monitored by gas chromatography relative to a calibrated internal standard. Experiments were performed in tripli-

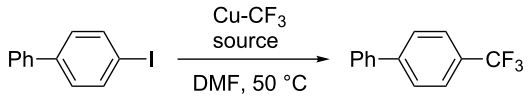

Scheme 3: General protocol for reactions described in Figure 1.

cate, and the average yields over time are plotted graphically in Figure 1.

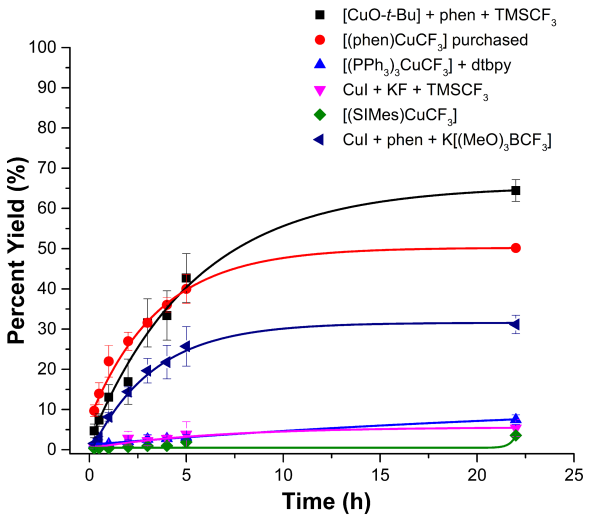

Figure 1: Yields of 4-(trifluoromethyl)-1,1'-biphenyl over time for the systems described in Scheme 1. These runs represent "standard" conditions described in Scheme 3 and the Experimental section. Yields were monitored by gas chromatography relative to a calibrated internal standard.

As shown in Figure 1, conditions where the [(phen)$CuCF_3$] was generated in situ (**B2**) provided the best yields of 4-(trifluoromethyl)-1,1'-biphenyl after 24 hours, with yields and conversion of aryl iodide (data not shown) both near 65%. When commercially purchased [(phen)$CuCF_3$] (**B1**) was used, yields up to the five hour mark were comparable to those of **B2**, but were ≈15% lower after the full 24 hours. Yields of product were 50%, with consumption of biphenyl iodide at 62%. Importantly, traditional single time point yields would not be able to highlight the loss of activity at the longer reaction times. The related phen system **B3**, which uses K[$(MeO)_3BCF_3$] as the trifluoromethyl source, performed significantly lower than **B1** and **B2** and gave a final overall yield of 31%. Consumption of the biphenyl iodide was found to be 51%. The data is intriguing because systems **B1**, **B2**, and **B3** are all expected to involve [(phen)$CuCF_3$] as the active trifluoromethylating agent, yet there are clear differences in reactivities for only slight changes in chemical components in the reaction mixtures. For the same conditions in DMF at 50 °C, **A1**, **C1**, and **D1** all performed poorly relative to [(phen)$CuCF_3$] and gave product yields less than 10% (Figure 1).

We then compared **B2**, the highest performing [(phen)$CuCF_3$] system in DMF, to the performance of isolated **A1** and in situ generated (**A2**) [(SIMes)$CuCF_3$] as well as to the [$(PPh_3)_3CuCF_3$ + dtbpy] combination (**C1**) under their reported optimized solvent conditions to explore the effect of the solvent on the lower performing systems in Figure 1 [10,14]. The results are shown in Figure 2 and highlight the fact that the solvent plays a key role in reagent performance, even for reasonably comparable $LCuCF_3$ complexes. The system **C1** shows high yields at early reaction times, but then suffers a severe leveling out effect after approximately ten hours. Based on the data, it is tempting to suggest that system **C1** might be worthy of a thorough mechanistic analysis, as if one can fully understand why the reagent suffers a rapid deactivation then a performance improvement may be possible. System **A1**, on the other hand, displays sluggish reactivity at early reaction times, but steadily produces 4-(trifluoromethyl)-1,1'-biphenyl in yields that are slightly higher than **C1** after 30 hours. [(SIMes)Cu(CF_3)], generated in situ from [(SIMes)Cu(O-*t*-Bu)] and $TMSCF_3$ (**A2**) afforded the highest yields at extended reaction times. It is interesting to note here, for the trifluoromethylation of 4-iodobiphenyl with SIMes copper complexes under the reported literature conditions, that the better performer was not the isolated and well-defined $LCu–CF_3$ complex, but instead the $LCu–CF_3$ complex generated in situ from the copper *tert*-butoxide precursor. This trend in reactivity mirrors that which was observed for the phen-based systems **B1** and **B2** in Figure 1. The reported optimized conditions for **A1** and **A2**, however, involve using copper as the limiting agent with a five-fold excess of aryl halide [4]. Therefore, while yields of the SIMes-based systems can provide good yields of product, the phen-based systems remain far more practical. Ligandless

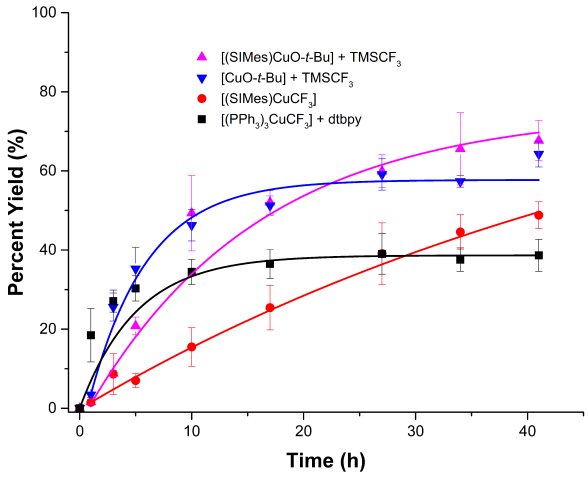

Figure 2: Yields of 4-(trifluoromethyl)-1,1'-biphenyl over time for the systems described in Scheme 1. Conditions for **C1**: [$(PPh_3)_3Cu(CF_3)$] + dtbpy: toluene, 80 °C. Conditions for **A1**: [(SIMes)Cu(CF_3)] and **A2** ([(SIMes)Cu(O-*t*-Bu)] + $TMSCF_3$: DMI/benzene (1.5:7.5), 50 °C. DMI = 1,3-dimethyl-2-imidazolidinone. Conditions for **B2**: [$(Cu(O\text{-}t\text{-}Bu))_4$ + phen +$TMSCF_3$: DMF, 50 °C. Yields were monitored by gas chromatography relative to a calibrated internal standard.

$CuCF_3$ was also tested under the reported optimized reaction conditions [15], but in our hands the protocol afforded $CHCF_3$ as the major fluorine-containing product.

Because our group has developed the NHC-based copper reagents for trifluoromethylation reactions [10,11], we were interested in comparing the effects of electronics and sterics of the aryl halides using the NHC-based systems **A1** and **A2** with the phen system **B2**. First, in order to explore reactivities with more electron rich aryl iodides, we investigated the use of 4-iodotoluene as a substrate for trifluoromethylation reactions. Because the product 1-methyl-4-(trifluoromethyl)benzene had similar retention times as the solvents in the gas chromatography analyses, we monitored the reactions of the iodotoluenes by quantitative ^{19}F NMR spectroscopy. Using the same solvent systems employed for the reactions in Figure 2, conversions were measured over a 22 hour period (Figure 3). In this case, [(SIMes)Cu(CF_3)] performed just as well as the [(phen)Cu(CF_3)] generated in situ at the 22 hour mark. However, the yield versus time plot revealed that the phen-based reagent was clearly better at early reaction times. The plots revealed other interesting information. For the electron-rich aryl iodides, the reactivity difference for the SIMes copper complexes was opposite from what was observed previously in Figure 2. Here, the isolated and well-defined [(SIMes)Cu(CF_3)] outperformed the in situ-generated counterpart, although at the five hour mark both performed equally well. Single time point yields would not have been able to identify the leveling out of reactivity of **A2** for the more electron-rich aryl halide. Moreover, an induction period was observed for both **A1** and **A2**. We noted a detection limit of approximately 2% with our NMR spectrometer, so we believe this induction period with the electron-rich substrates is real and not stemming from the different analytical method used for determining yields for Figure 2 and Figure 3. Why an induction period is observed for the iodotoluenes but not for the iodobiphenyl substrate is still not well-understood and is currently under investigation.

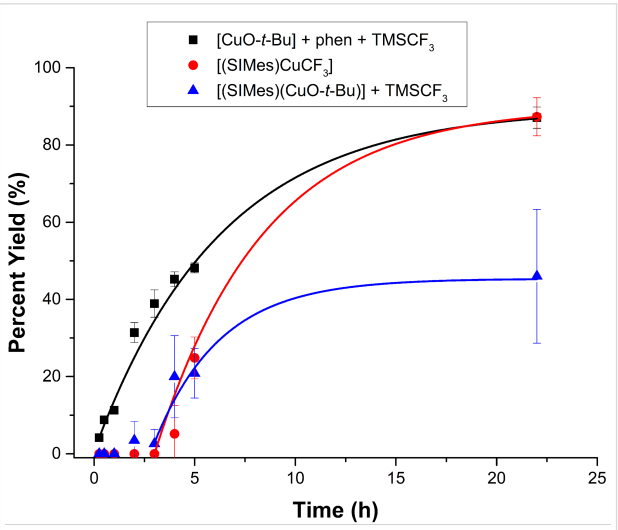

Figure 3: Reaction of 1-iodo-4-methylbenzene with systems **A1**, **A2**, and **B2** to produce 1-methyl-4-(trifluoromethyl)benzene. Conditions for **B2**: DMF, 50 °C. Conditions for **A1** and **A2**: DMI/benzene (1.5:7.5), 50 °C. Yields were calculated by ^{19}F NMR spectroscopy versus an internal standard.

Reactions were then run with 2-iodotoluene in order to gauge steric effects in the trifluoromethylation reactions. It should be noted here that the promoting effect of *ortho* substituents in trifluoromethylation reactions is well-known. For example, the rate of trifluoromethylation of *o*-MeC_6H_4Br was found to be 3.5 times faster than that for bromobenzene by $CuCF_3$ in DMF [16]. Figure 4 describes the results of the trifluoromethylations of 2-iodotoluene with systems **A1**, **A2**, and **B2**. For this iodoarene substrate, the phen- and the NHC-based copper reagents performed nearly equally well at almost all time periods. The well-defined and isolated **A1** again showed a noticeable induction period, whereas the induction period for **A2** was short.

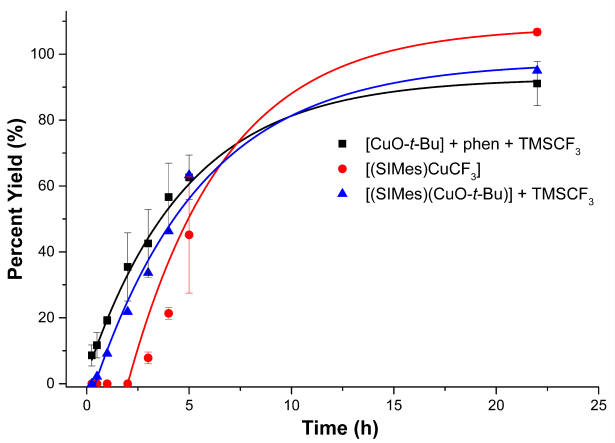

Figure 4: Reaction of 2-iodotoluene with systems **A1**, **A2**, and **B2** to produce 1-methyl-2-(trifluoromethyl)benzene. Conditions for **B2**: DMF, 50 °C. Conditions for **A1** and **A2**: DMI/benzene (1.5:7.5), 50 °C. Yields were calculated by ^{19}F NMR spectroscopy versus an internal standard.

Conclusion

In summary, we have determined that in DMF the best trifluoromethylating agent was generated in situ using the [Cu(O-*t*-Bu)]$_4$/Me_3SiCF_3/phen combination. However, when optimized solvents were employed, other metal complexes and precursors approached and even exceeded the [(phen)Cu(CF_3)] system, albeit with much higher metal loadings. In order to rigorously assess future trifluoromethylating agents and minimize issues of reproducibility, we encourage others to provide comparative data (yields versus time) for any newly developed trifluoromethylation reaction with a well-established reagent

using identical reaction vessels and performed by the same experimentalist. The work shown here reveals the importance of comparing trifluoromethylation reactions using a number of different variables (solvent, sterics, and electronics) in order to adequately describe a catalyst's performance for the community. Explicit benchmarking in catalysis science is rarely reported in the literature (less than 500 mentions in approximately 1×10^6 articles describing catalytic phenomena) [17], and as methodologies for trifluoromethylation reactions continue to develop it will be important to have protocols for assessing new reagents.

Experimental

General

[(Phen)Cu(CF_3)] was purchased from Aspira Scientific (Lot #40C906, 90% purity) and used without further purification. All other copper reagents were prepared according to reported procedures and were verified by ^{1}H NMR and ^{19}F NMR for purity. Copper salt precursors were purchased from Sigma-Aldrich. Trimethyl(trifluoromethyl)silane (99% purity) was purchased from SynQuest Labs, Inc. and used without further purification. All other chemicals were verified by ^{1}H NMR for purity and used without further purification. Purity of reagents used, CuCl (97%), KF (≥99%), 1,10-phenanthroline (≥99%), NaO-*t*-Bu (98%), KO-*t*-Bu (98%), K_2CO_3 (≥99%), undecane (≥99%), fluorobenzene (≥99%), 4-iodobiphenyl (97%), 4-iodotoluene (97%), 2-iodotoluene (97%), and 4,4′-di-*tert*-butyl-2,2′-dipyridyl (98%). All solvents were purified by passing through activated alumina and/or copper in a solvent purification system supplied by Pure Process Technology or purchased anhydrous from Fisher Scientific (toluene, acetonitrile, DMF, and DMI). The quantitative analyses were accomplished using a Shimadzu GC-2010 Plus Gas Chromatograph and flame ionization detector (FID). A Rxi-5ms (fused silica), low-polarity phase, crossbond diphenyl dimethyl polysiloxane, 15.0 m length column was used. Parameters were: injection volume of 4.0 μL, 25:1 split ratio, linear velocity of 57.0 cm/s, total flow of 65.3 mL/min, and temperature program starting at 40 °C held for one minute, followed by a temperature ramp of 20.0 °C per minute to the final temperature of 250 °C which was held for 4 minutes. All peaks were well separated. All manipulations were performed using standard Schlenk and high vacuum techniques or were performed in a nitrogen filled glovebox. The quantitative NMR analyses were accomplished using a Bruker Ascend 400 MHz spectrometer by ^{19}F NMR spectra referenced to internal standard of fluorobenzene. Solution ^{1}H NMR spectra were recorded at ambient temperature on a Bruker Ascend 400 MHz spectrometer and referenced to residual proton solvent signals. ^{19}F NMR spectra were recorded on the Bruker Ascend NMR spectrometer operating at 376 MHz and referenced to trifluorotoluene set at δ −63.7. All graphical data were treated with a best fit curve generated by the Origin 9.0.0 program. The exponential fit with function ExpGro1 was selected for all data.

Updated procedure for the preparation of [(SIMes)$_2$Cu][Cu(CF$_3$)$_2$] (2): A solution of [(SIMes)Cu(O-*t*-Bu)] (220 mg, 0.50 mmol) and $CF_3Si(CH_3)_3$ (0.110 mL, 0.74 mmol) in 6.0 mL THF was stirred at room temperature. The conversion to product was monitored by ^{19}F NMR spectroscopy, and after 1.5 h the volatiles were evaporated on a high vacuum line. The white residue was filtered and washed twice with 5 mL toluene and then twice with 5 mL of pentane. The yield of [(SIMes)$_2$Cu][Cu(CF$_3$)$_2$] was 81%. The spectroscopic data matched literature values [10]. ^{1}H NMR (25 °C, CD_2Cl_2) δ 1.84 (s, 12H), 2.39 (s, 6H), 3.80 (s, 4H), 6.89 (s, 4H); ^{19}F NMR (25 °C, CD_2Cl_2) δ −31.33 (s, 3F).

Updated procedure for the preparation of [(SIMes)Cu(O-*t*-Bu)] (3): A suspension of [(SIMes)CuCl] (330 mg, 0.81 mmol) and *t*-BuONa (78 mg, 0.81 mmol) in 6.0 mL THF was stirred for 2 h at room temperature and then filtered through a pad of Celite. The Celite was washed two times with 4 mL of THF. The solvents were then removed on a high vacuum line, and the resulting light yellow residue was dissolved in benzene and then filtered again through a pad of Celite. The Celite was washed two times with 4 mL of benzene, and the filtrate was evaporated on a high vacuum line. The resulting white solid was washed with pentane, filtered, and dried. Yield 92%. The spectroscopic data matched literature values [10]. ^{1}H NMR (C_6D_6) δ 1.31 (s, 9H), 2.12 (s, 6H), 2.14 (s, 12H), 3.01 (s, 4H), 6.73 (s, 4H).

General procedure for the standard conditions of trifluoromethylation of 4-iodobiphenyl (systems A1, B1, and C1 in Figure 1**).** To a 20 mL vial was added copper trifluoromethyl reagent (0.28 mmol) in 5.4 mL of DMF. In the case of [(PPh_3)$_3$CuCF$_3$] [14], 77.2 mg (0.28 mmol) of dtbpy was also added. Then 67.1 mg (0.23 mmol) of 4-iodobiphenyl and 60.5 μL (0.28 mmol) of undecane as internal standard, were added to the vial. The solution was then allowed to stir for five minutes. Then 0.6 mL aliquots were taken and transferred into 5 mL air-tight ampules fitted with a stirring bar. The ampules were sealed and placed in an oil bath at 50 °C. The reactions were removed from the oil bath at various time intervals and quenched with 0.6 mL of methanol in air. Aliquots of each solution were injected into a GC-FID and the reactions were monitored for the formation of the 4-trifluoromethylbiphenyl product.

General procedure for the standard conditions of trifluoromethylation of 4-iodobiphenyl using in situ generated reagents (systems B2, B3, and D1 in Figure 1**).** The prepara-

tion of each reagent (**B2**, **B3**, and **D1**) is described below. After preparation of the reagent, 60.50 μL (0.2851 mmol) of undecane was added as internal standard. Each solution was allowed to stir for five minutes, and then 0.60 mL aliquots were taken and transferred into 5 mL air-tight resealable ampules. The ampules were sealed and placed in an oil bath at 50 °C and the solutions were stirred. The reactions were removed from the oil bath at various time intervals and quenched with 0.6 mL of methanol in air. Aliquots of each solution were injected into a GC-FID and the reactions were monitored for the formation of the 4-trifluoromethylbiphenyl product.

Generation of B2 in Figure 1**:** For the generation of (phen)$CuCF_3$ in situ, a vial was charged with 28.4 mg (0.28 mmol) of CuCl, 32.3 mg (0.28 mmol) of KO-*t*-Bu, and 51.5 mg (0.28 mmol) of 1,10-phenanthroline in 5.4 mL of DMF. The solution was stirred for 0.5 h before the addition of 0.042 mL (0.28 mmol) of $(Me)_3SiCF_3$. The solution was stirred for an additional hour before the introduction of 0.23 mmol of 4-iodobiphenyl.

Generation of B3 in Figure 1**:** A vial was charged with 0.232 mmol of 4-iodobiphenyl, 53.6 mg (0.28 mmol) of CuI, 60.5 mg (0.28 mmol) of [K][$B(OMe_3)(CF_3)$] [8], and 51.5 mg (0.28 mmol) of 1,10-phenanthroline in 5.4 mL of DMF.

Generation of D1 in Figure 1**:** A vial was charged with (0.23 mmol) of 4-iodobiphenyl, 53.6 mg (0.28 mmol) of CuI, 16.7 mg (0.28 mmol) of KF, and 0.042 mL (0.28 mmol) of $(Me)_3SiCF_3$ in 5.4 mL of DMF as solvent.

General procedure for the 'best' conditions of trifluoromethylation of 4-iodobiphenyl (systems **A1**, **A2**, and **C1** in Figure 2)

Reaction conditions employing $[(SIMes)_2Cu][Cu(CF_3)_2]$ (system A1): A vial was charged with 1.15 mmol of 4-iodobiphenyl and 105 mg (0.12 mmol) of $[(SIMes)_2Cu][Cu(CF_3)_2]$ in 5.4 mL of DMI/benzene (1.5:7.5) with 60.5 μL (0.29 mmol) of undecane, as internal standard. After the solution was allowed to stir for five minutes, 0.6 mL aliquots were taken and transferred into 5 mL air-tight ampules. The ampules were sealed and placed in an oil bath at 50 °C. The reactions were removed from the oil bath at various time intervals and quenched with 0.6 mL of methanol in air. Aliquots of each solution were injected into a GC-FID and the reactions were monitored for the formation of the 4-trifluoromethylbiphenyl product.

Reaction conditions employing [(SIMes)Cu(O-*t*-Bu)] + $TMSCF_3$ (system A2): A vial was charged with 1.15 mmol of 4-iodobiphenyl, 106 mg (0.24 mmol) of [(SIMes)Cu(O-*t*-Bu)] and 0.053 mL (0.359 mmol) of $(Me)_3SiCF_3$ in 5.4 mL of DMI/benzene (1.5:7.5) with 60.5 μL (0.29 mmol) of undecane, as internal standard. After the solution was allowed to stir for five minutes, 0.6 mL aliquots were taken and transferred into 5 mL air-tight ampules. The ampules were sealed and placed in an oil bath at 50 °C. The reactions were removed from the oil bath at various time intervals and quenched with 0.6 mL of methanol in air. Aliquots of each solution were injected into a GC-FID and the reactions were monitored for the formation of the 4-trifluoromethylbiphenyl product.

Reaction conditions employing $[(PPh_3)_3CuCF_3]$ (system C1): A vial was charged with 0.31 mmol of 4-iodobiphenyl, 264 mg (0.29 mmol) of $(PPh_3)_3CuCF_3$, and 85.0 mg (0.32 mmol) of dtbpy in 5.4 mL of toluene with 60.5 μL (0.29 mmol) of undecane, as internal standard. After the solution was allowed to stir for five minutes, 0.6 mL aliquots were taken and transferred into 5 mL air-tight ampules. The ampules were sealed and placed in an oil bath at 80 °C. The reactions were removed from the oil bath at various time intervals and quenched with 0.6 mL of methanol in air. Aliquots of each solution were injected into a GC-FID and the reactions were monitored for the formation of the 4-trifluoromethylbiphenyl product.

General procedure for the trifluoromethylation of 2-iodotoluene and 4-iodotoluene (system **A1**, **A2** and **B2** in Figure 3 and Figure 4)

Reaction conditions employing $[(SIMes)_2Cu][Cu(CF_3)_2]$ (system A1): A vial was charged with 270 mg (1.20 mmol) of 2-iodotoluene or 4-iodotoluene and 105 mg (0.12 mmol) of $[(SIMes)_2Cu][Cu(CF_3)_2]$ in 5.4 mL of DMI/benzene (1.5:7.5) with 90.0 μL (0.95 mmol) of fluorobenzene, as internal standard. After the solution was allowed to stir for five minutes, 0.6 mL aliquots were taken and transferred into 5 mL air-tight ampules. The ampules were sealed and placed in an oil bath at 50 °C. The reactions were removed from the oil bath at various time intervals and quenched with 0.6 mL of methanol in air. Each aliquot was monitored by ^{19}F NMR spectroscopy for formation of the respective 2-trifluoromethyltoluene or 4-trifluoromethyltoluene product.

Reaction conditions employing [(SIMes)Cu(O-*t*-Bu)] + $TMSCF_3$ (system A2): A vial was charged with 270 mg (1.20 mmol) of 2-iodotoluene or 4-iodotoluene, 106 mg (0.24 mmol) of [(SIMes)Cu(O-*t*-Bu)] and 0.053 mL (0.36 mmol) of $(Me)_3SiCF_3$ in 5.4 mL of DMI/benzene (1.5:7.5) with 90.0 μL (0.95 mmol) of fluorobenzene, as internal standard. After the solution was allowed to stir for five minutes, 0.60 mL aliquots were taken and transferred into 5 mL

air-tight ampules. The ampules were sealed and placed in an oil bath at 50 °C. The reactions were removed from the oil bath at various time intervals and quenched with 0.6 mL of methanol in air. Each aliquot was monitored by ^{19}F NMR spectroscopy for formation of the respective 2-trifluoromethyltoluene or 4-trifluoromethyltoluene product.

Reaction conditions employing [(phen)Cu(O-*t*-Bu)]$_4$ + TMSCF$_3$ (system B2): For the generation of (phen)CuCF$_3$ in situ, a vial was charged with 28.4 mg (0.28 mmol) of CuCl, 32.3 mg (0.28 mmol) of KO-*t*-Bu, and 51.5 mg (0.28 mmol) of 1,10-phenanthroline. To the vial, 5.4 mL of DMF was added. The solution was stirred for 0.5 h before the addition of 0.042 mL (0.28 mmol) of Me_3SiCF_3. The solution was stirred for an additional hour before the introduction of 52.1 mg (0.23 mmol) of 2-iodotoluene or 4-iodotoluene and 90.0 μL (0.95 mmol) of fluorobenzene, as internal standard. After the solution was allowed to stir for five minutes, 0.60 mL aliquots were taken and transferred into 5 mL air-tight ampules. The ampules were sealed and placed in an oil bath at 50 °C. The reactions were removed from the oil bath at various time intervals and quenched with 0.6 mL of methanol in air. Each aliquot was monitored by ^{19}F NMR spectroscopy for formation of the respective 2-trifluoromethyltoluene or 4-trifluoromethyltoluene product.

Acknowledgements

D.A.V. thanks the Office of Basic Energy Sciences of the U.S. Department of Energy (DE-SC0009363) for support of this work.

References

1. Tomashenko, O. A.; Grushin, V. V. *Chem. Rev.* **2011,** *111,* 4475–4521. doi:10.1021/cr1004293
2. Wang, H.; Vicic, D. A. *Synlett* **2013,** *24,* 1887–1898. doi:10.1055/s-0033-1339435
3. Roy, S.; Gregg, B. T.; Gribble, G. W.; Le, V.-D.; Roy, S. *Tetrahedron* **2011,** *67,* 2161–2195. doi:10.1016/j.tet.2011.01.002
4. Schareina, T.; Wu, X.-F.; Zapf, A.; Cotté, A.; Gotta, M.; Beller, M. *Top. Catal.* **2012,** *55,* 426–431. doi:10.1007/s11244-012-9824-0
5. Oishi, M.; Kondo, H.; Amii, H. *Chem. Commun.* **2009,** 1909–1911. doi:10.1039/b823249k
6. Weng, Z.; Lee, R.; Jia, W.; Yuan, Y.; Wang, W.; Feng, X.; Huang, K.-W. *Organometallics* **2011,** *30,* 3229–3232. doi:10.1021/om200204y
7. Nakamura, Y.; Fujiu, M.; Murase, T.; Itoh, Y.; Serizawa, H.; Aikawa, K.; Mikami, K. *Beilstein J. Org. Chem.* **2013,** *9,* 2404–2409. doi:10.3762/bjoc.9.277
8. Knauber, T.; Arikan, F.; Roeschenthaler, G.-V.; Goossen, L. J. *Chem. – Eur. J.* **2011,** *17,* 2689–2697. doi:10.1002/chem.201002749
9. Chen, Q.-Y.; Wu, S.-W. *J. Chem. Soc., Chem. Commun.* **1989,** 705–706. doi:10.1039/c39890000705
10. Dubinina, G. G.; Ogikubo, J.; Vicic, D. A. *Organometallics* **2008,** *27,* 6233–6235. doi:10.1021/om800794m
11. Dubinina, G. G.; Furutachi, H.; Vicic, D. A. *J. Am. Chem. Soc.* **2008,** *130,* 8600–8601. doi:10.1021/ja802946s
12. Morimoto, H.; Tsubogo, T.; Litvinas, N. D.; Hartwig, J. F. *Angew. Chem., Int. Ed.* **2011,** *50,* 3793–3798. doi:10.1002/anie.201100633
13. Usui, Y.; Noma, J.; Hirano, M.; Komiya, S. *Inorg. Chim. Acta* **2000,** *309,* 151–154. doi:10.1016/S0020-1693(00)00248-6
14. Tomashenko, O. A.; Escudero-Adán, E. C.; Martínez Belmonte, M.; Grushin, V. V. *Angew. Chem., Int. Ed.* **2011,** *50,* 7655–7659. doi:10.1002/anie.201101577
15. Urata, H.; Fuchikami, T. *Tetrahedron Lett.* **1991,** *32,* 91–94. doi:10.1016/S0040-4039(00)71226-3
16. Konovalov, A. I.; Lishchynskyi, A.; Grushin, V. V. *J. Am. Chem. Soc.* **2014,** *136,* 13410–13425. doi:10.1021/ja507564p
17. Bligaard, T.; Bullock, R. M.; Campbell, C. T.; Chen, J. G.; Gates, B. C.; Gorte, R. J.; Jones, C. W.; Jones, W. D.; Kitchin, J. R.; Scott, S. L. *ACS Catal.* **2016,** *6,* 2590–2602. doi:10.1021/acscatal.6b00183

License and Terms

BEILSTEIN JOURNAL OF ORGANIC CHEMISTRY

Homologated amino acids with three vicinal fluorines positioned along the backbone: development of a stereoselective synthesis

Raju Cheerlavancha[1], Ahmed Ahmed[1], Yun Cheuk Leung[1], Aggie Lawer[1], Qing-Quan Liu[2], Marina Cagnes[3], Hee-Chan Jang[3], Xiang-Guo Hu[2] and Luke Hunter[*1]

Full Research Paper

Open Access

Address:
[1]School of Chemistry, The University of New South Wales, Sydney NSW 2052, Australia, [2]National Engineering Research Center for Carbohydrate Synthesis, Jiangxi Normal University, Nanchang, China and [3]School of Chemistry, The University of Sydney, Sydney NSW 2006, Australia

Email:
Luke Hunter[*] - l.hunter@unsw.edu.au

* Corresponding author

Keywords:
amino acids; conformation; deoxyfluorination; fluorine; stereochemistry

Beilstein J. Org. Chem. **2017,** *13,* 2316–2325.
doi:10.3762/bjoc.13.228

Received: 26 June 2017
Accepted: 09 October 2017
Published: 01 November 2017

This article is part of the Thematic Series "Organo-fluorine chemistry IV".

Associate Editor: K. N. Allen

Abstract

Backbone-extended amino acids have a variety of potential applications in peptide and protein science, particularly if the geometry of the amino acid is controllable. Here we describe the synthesis of δ-amino acids that contain three vicinal C–F bonds positioned along the backbone. The ultimately successful synthetic approach emerged through the investigation of several methods based on both electrophilic and nucleophilic fluorination chemistry. We show that different diastereoisomers of this fluorinated δ-amino acid adopt distinct conformations in solution, suggesting that these molecules might have value as shape-controlled building blocks for future applications in peptide science.

Introduction

The incorporation of unnatural amino acids into a peptide structure can potentially reduce conformational disorder and hence improve the binding affinity of the peptide for its biological target. For example, conformationally rigid amino acids such as **1** (Figure 1) have been shown to dramatically affect the secondary structure of peptides within which they are contained, with consequent implications for the peptides' biological potency and selectivity [1]. A more subtle example of this concept is provided by the amino acid β-methylphenylalanine (**2**), which exerts conformational bias through acyclic means; steric interactions associated with the β-methyl group can affect the topography of peptides which once again affects the biological affinity and selectivity [2].

Extending the idea of acyclic shape control, amino acids with homologated backbones (e.g., **3**–**5**, Figure 1) [3-10] provide op-

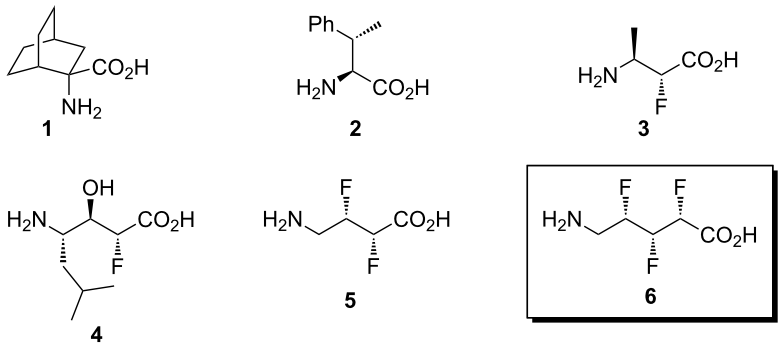

Figure 1: Examples of conformationally biased amino acids [1-10]. Compound **6** is a target of this work.

portunities for functionalisation in ways not possible in natural α-amino acids. There is the ability to place heteroatoms along the amino acid backbone, or to incorporate two or more functionalised side chains per amino acid residue, and this results in a variety of stereochemical configurations that can affect the conformation. Organofluorine chemistry offers a particular attraction here, since fluorinated molecules (e.g., **3**–**5**) tend to adopt predictable conformations due to hyperconjugative and/or dipole–dipole interactions associated with the C–F bond [11-15].

Such a progression in the study of fluorinated amino acids develops into the concept of α,β,γ-trifluoro-δ-amino acids (e.g., **6**, Figure 1). δ-Amino acids such as **6** are of special interest because they have the same backbone length as a dipeptide of α-amino acids, and thus may potentially be substituted for a two amino acid unit in a natural peptide without changing the overall length of the peptide [16]. The presence of three vicinal fluorine atoms on the amino acid backbone of **6** gives rise to eight possible stereoisomeric forms, which presents a synthetic challenge of stereocontrol. As an initial contribution towards the study of such compounds, we recently published a synthesis of two diastereoisomers of **6** (in protected form) [17]. We now disclose full details of the various synthetic approaches that were investigated towards the target **6**, and the extensive troubleshooting that was required even within the approach that was ultimately successful. We also present here, for the first time, a qualitative NMR *J*-based conformational analysis of the free amino acids including **6**.

Results and Discussion

Early in our efforts to develop a successful synthesis of **6**, we realized that it might be possible to construct the repeating $(CHF)_n$ motif within the target molecule via an iterative synthetic approach (Scheme 1, boxed). We reasoned that an aldehyde such as **7** could undergo electrophilic fluorination, mediated by a chiral organocatalyst [18-20], to generate the fluorinated aldehyde **8** as a single stereoisomer. Then, if the carbon chain of **8** could be extended by one atom to give the homologated aldehyde **9**, fluorination could be repeated and the cycle could continue until the desired number of fluorine atoms was installed. This hypothetical approach had several attractions, including (i) the flexibility of being able to generate amino acids of different backbone lengths (e.g., **5**, **6**, Figure 1) via a unified strategy; (ii) an ability to access any stereoisomer of the target molecules (provided that the stereoselectivity in each fluorination step was catalyst-controlled); (iii) the lower toxicity of the electrophilic fluorination reagent NFSI (compared with nucleophilic fluorination reagents such as DeoxoFluor).

Accordingly, two aldehyde substrates (**7a** and **7b**) were prepared [21,22], containing either a phthalimide or a Boc protecting group. Electrophilic fluorination was attempted according to the method developed by Jørgensen and co-workers (Scheme 1) [20]. Thus, the aldehyde **7a** (or **7b**) was treated with *N*-fluorobenzenesulfonimide in the presence of the chiral organocatalyst **10**, and after a certain period the fluorinated aldehyde product **8** was reduced in situ. Initial studies with substrate **7a** (containing the phthalimide protecting group) suggested that the undesired difluorinated compound **12** was formed as the major product. An additional complication was that the phthalimide protecting group of **12** seemed to be at least partially sensitive to sodium borohydride [23]. In contrast, the substrate **7b** (containing the Boc protecting group) was successfully converted into the desired fluorohydrin **11**, albeit in poor yield. The optical purity of **11** was established through Mosher ester analysis (see Supporting Information File 1).

With the fluorohydrin **11** in hand (Scheme 1), the next task was to extend the carbon chain by one atom. The alcohol **11** was first converted into the corresponding tosylate (Scheme 1), but when this tosylate was subsequently treated with cyanide the undesired disubstituted product **14** was formed in 40% yield. Unfortunately, despite varying the reaction stoichiometry it was

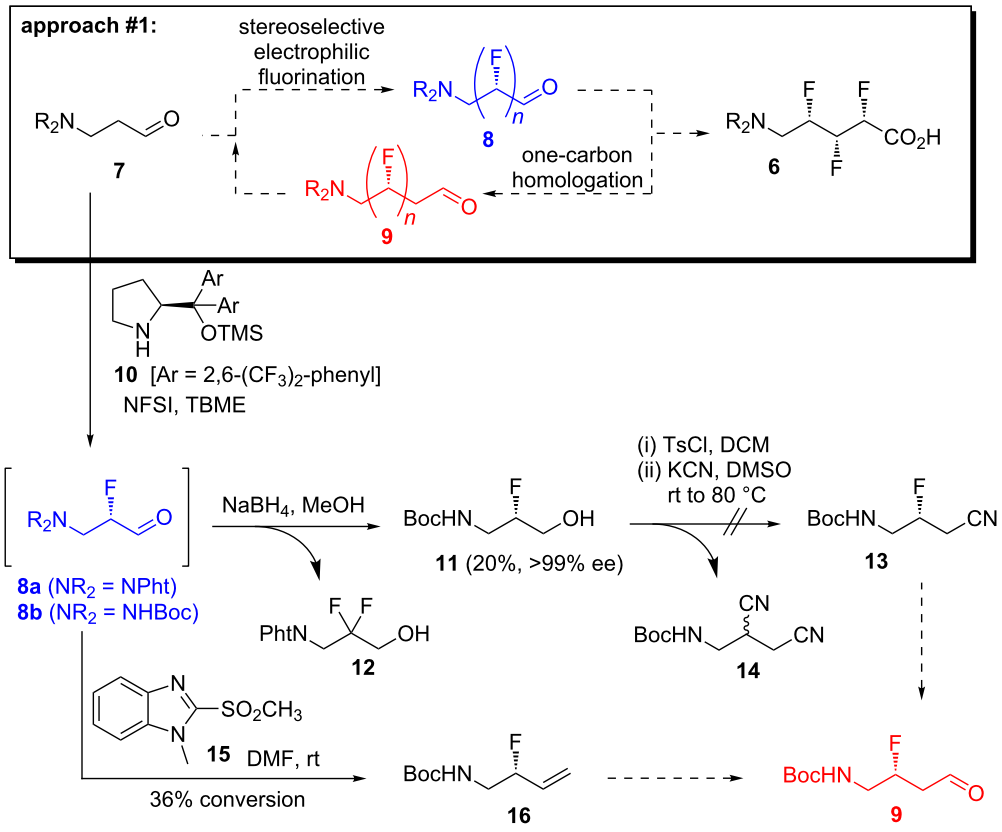

Scheme 1: The first synthetic approach.

not possible to isolate any of the desired product **13**. It is possible that varying the reaction solvent might alter the reactivity profile, but this was not investigated in this study. We did explore a triflate leaving group in this reaction (not shown), but this gave a complex mixture of products upon treatment with cyanide. As a further disappointment, the disubstituted product **14** appeared to be racemic, which implied that an elimination–addition sequence had taken place, which in turn suggested that intermediates such as **9** might be rather unstable.

An alternative strategy for extending the carbon backbone was needed. Grubbs and co-workers recently showed that β-fluoroaldehydes (e.g., **9**, Scheme 1) can be synthesized in one step from allylic fluorides (e.g., **16**) via Wacker-type oxidation [24]. Other methods for converting allylic fluorides into β-fluoroaldehydes are also known [25,26]. Therefore we turned our attention to converting the fluorinated aldehyde **8b** (Scheme 1) into the allylic fluoride **16**. The crude fluorinated aldehyde **8b** was treated with a variety of olefination reagents (e.g., Tebbe; Wittig; reagent **15** [27]). Unfortunately, however, the desired allylic fluoride **16** was either not formed or was very unstable, which meant that the subsequent Wacker-type oxidation [24] to **9** could not be attempted.

Concurrent with the homologation attempts described above (Scheme 1), some model studies were performed (Table 1) to ascertain the feasibility of performing α-fluorinations on other β-fluorinated carbonyl compounds besides **9**. Thus, β-fluoroaldehyde **17** which was synthesized by an independent method (see Supporting Information File 1) was treated with NFSI and catalyst **10** according to Jørgensen's fluorination protocol [20] (Table 1, entry 1). However, this resulted in a complex mixture of products within which the desired α,β-difluorinated product could not be identified. The alternative model substrate **18** (see Supporting Information File 1) was next investigated (Table 1, entry 2). Unfortunately, however, compound **18** proved unstable to silica and so it was not possible to obtain sufficiently pure material for a meaningful α-fluorination test reaction to be performed. The low stability of β-fluoroaldehydes appeared to be a general phenomenon, and so an attempt was next made to generate such a substrate in situ via the oxidation of β-fluoroalcohol **19** (Table 1, entry 3), followed immediately by a fluorination reaction. However, this did not yield any of the desired vicinal difluorinated material. It is possible that alternative electrophilic fluorinating reagents such as Selectfluor [28] could give different results, but this was not investigated in this work.

Table 1: Attempted α-fluorination of β-fluorocarbonyl compounds.

Entry	Substrate	Conditions	Outcome
1	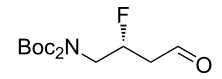 **17**	(i) **10**, NFSI, TBME, rt; (ii) $NaBH_4$, MeOH	complex mixture
2	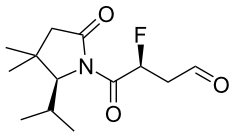 **18**	substrate **18** decomposed on silica, so no α-fluorination reactions could be attempted	N/A
3	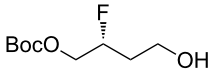 **19**	(i) PCC; (ii) **10**, NFSI, TBME, rt; (iii) $NaBH_4$, MeOH	starting material **19** recovered
3	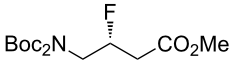 **20**	KO*t*-Bu, NFSI, THF, rt	starting material **20** recovered
4	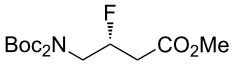 **20**	KHMDS, NFSI, THF, −78 °C	complex mixture

In a final attempt to develop an iterative fluorination/homologation strategy (Scheme 1, boxed), we considered whether an ester could be employed as the repeating unit, instead of an aldehyde. Accordingly, the model ester **20** (see Supporting Information File 1) was treated with an electrophilic fluorine source under basic conditions (Table 1, entries 3 and 4). Unfortunately, however, these attempts either returned unreacted starting material, or gave rise to a complex mixture of products, rather than the desired α,β-difluorinated ester.

Since major difficulties were encountered in both of the key steps of the proposed iterative fluorination/homologation approach (Scheme 1, boxed), we were forced to conclude that this was not a viable route to α,β,γ-trifluoro-δ-amino acids **6**.

The next approach that was investigated is shown in Scheme 2. Having learned that homologation reactions involving fluorinated substrates were not facile, we decided to start the new approach with a full-length carbon chain in the form of piperidinedione **21**. We envisaged that a sequence of reactions – two electrophilic fluorinations [29-31] followed by reduction and deoxyfluorination – would deliver the target molecule **6**.

Accordingly, two piperidinedione substrates (**21a** and **21b**) were prepared [32,33], containing a Boc or a benzyl protecting group, respectively (Scheme 2). Substrate **21a** was first treated with Selectfluor in acetonitrile according to a mild protocol developed by Smith and co-workers for the α-fluorination of ketones [31]. However, ^{1}H NMR and ^{19}F NMR analysis of the crude reaction mixture revealed that the only identifiable product was the undesired *gem*-difluorinated compound **25** (Scheme 2), which was obtained along with a significant amount of unreacted starting material **21a** (see Supporting Information File 1). When the alternative substrate **21b** was exposed to a variety of different electrophilic fluorinating conditions (Scheme 2), a new reaction outcome was observed: in this case, the only identifiable product was the undesired dimeric species **26**, which was consistently obtained in reasonably high yields (see Supporting Information File 1). This product presumably arose through aldol condensation of the readily enolisable ketone **22** with another molecule of **21**. Overall then, it was concluded that approach #2 was not a viable strategy for synthesising target **6**. Alternative substrates based on the piperidine-2,5-dione scaffold might prove more tractable in the future, but this has not yet been investigated in our laboratories.

Since the first two approaches to target **6** (Scheme 1 and Scheme 2) were unsuccessful, we reasoned that a better-precedented synthetic method was needed. O'Hagan and co-workers have previously reported a concise method for synthesising compounds that contain three vicinal C–F bonds [34]; their method commences with an epoxy alcohol, which undergoes three successive nucleophilic substitutions with fluoride (i.e., deoxyfluorination of the alcohol, epoxide ring opening with fluoride, then deoxyfluorination). We therefore sought to apply O'Hagan's method to the target **6b** (Scheme 3, boxed).

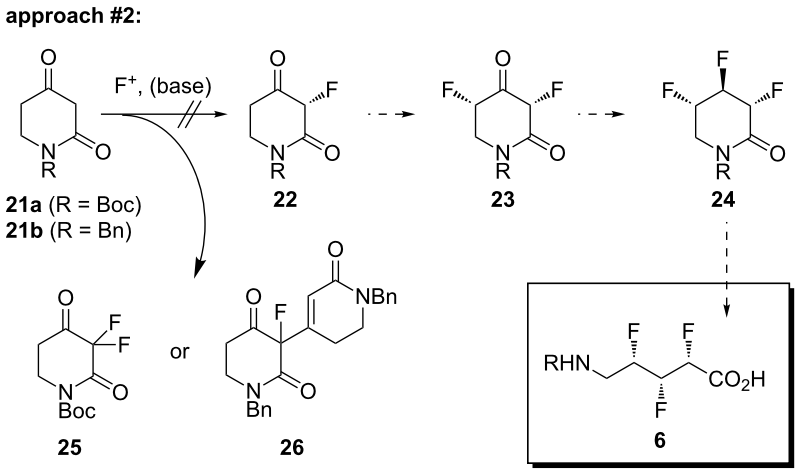

Scheme 2: The second synthetic approach.

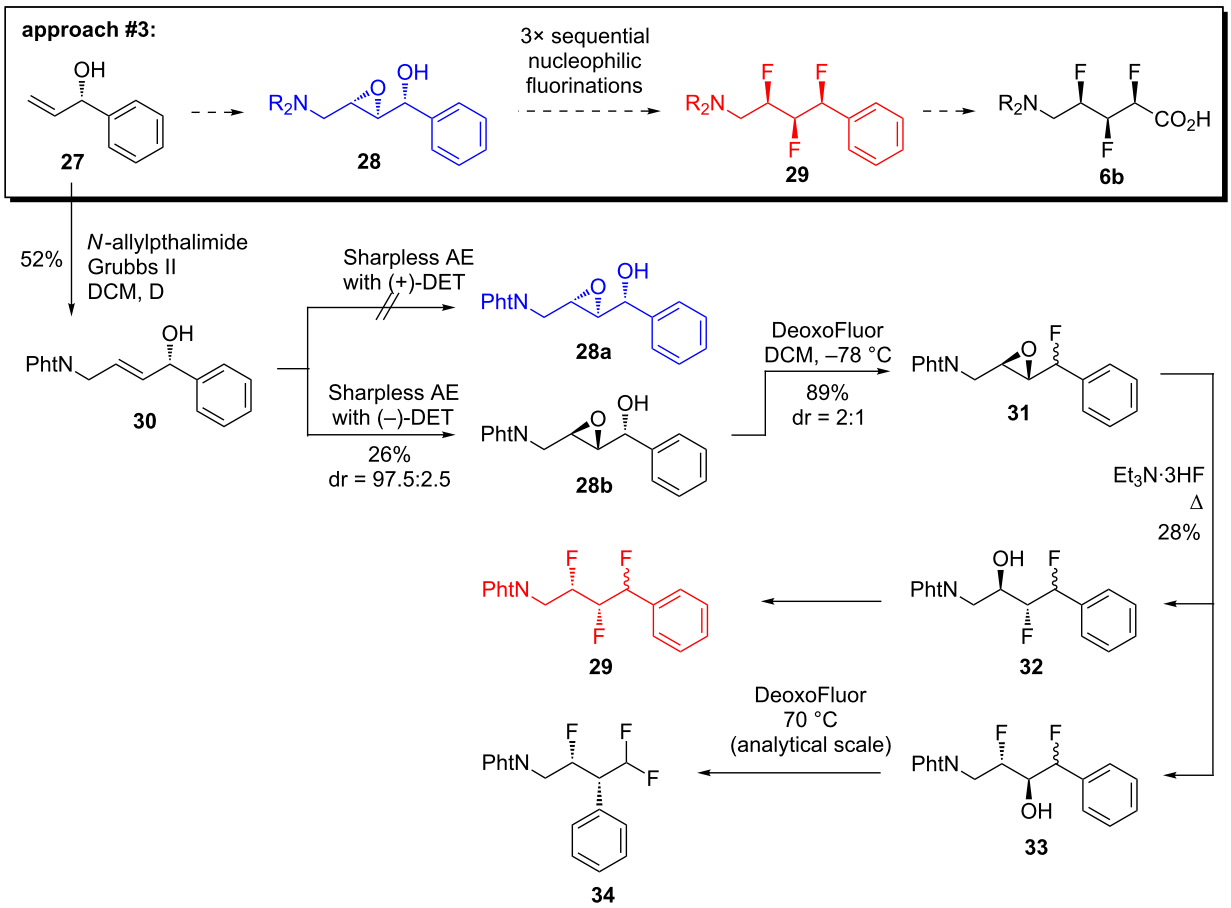

Scheme 3: The third synthetic approach.

Accordingly, the enantiopure allylic alcohol **27** [35] was extended through a cross-metathesis reaction to deliver the disubstituted alkene **30** (Scheme 3). Compound **30** became the substrate for an attempted Sharpless asymmetric epoxidation reaction using (+)-DET (Scheme 3); however, none of the desired product **28a** was observed in this case, presumably due to a sub-

strate/catalyst mismatch effect. Therefore, the epoxidation reaction was re-attempted using (−)-DET (Scheme 3); this successfully afforded the *syn*,*anti*-epoxy alcohol **28b** with good stereoselectivity, albeit in poor yield. One reason for the low yield of **28b** was the difficulty in its chromatographic separation from the byproducts of the epoxidation reaction. Nevertheless, a sufficient quantity of **28b** was obtained to proceed some way with the synthesis. Compound **28b** was treated with Deoxo-Fluor at low temperature, in order to affect a deoxyfluorination of the benzylic alcohol. This reaction gave the product **31** in high yield, but unfortunately with poor stereoselectivity, presumably due to a competing S_N1-type reaction mechanism [36,37]. This reaction was not fully optimised; instead, the available quantity of the fluoroepoxide **31** was carried forward so that some idea could be obtained about the feasibility of the subsequent steps in the synthesis. Thus, the fluoroepoxide **31** (as a mixture of diastereoisomers) was treated with $Et_3N{\cdot}3HF$ according to O'Hagan's method [34] (Scheme 3). This did effect epoxide-opening to some extent, but the reaction was rather unsatisfactory because it was low-yielding and non-regioselective, which made full characterisation of the product mixture (**32**/**33**) impossible. Nevertheless, an analytical-scale final fluorination reaction was attempted (Scheme 3) because this was anticipated to converge some of the compounds into a simpler product mixture. Analysis of the crude reaction mixture by ^{19}F NMR revealed that the desired product **29** may have been formed in small quantity. However, there was clear evidence that a *gem*-difluorinated compound had also formed: presumably this was compound **34** arising through neighbouring group participation and migration of the phenyl group [38]. A similar problem was encountered in the synthesis of α,β-difluorinated-γ-amino acids (e.g., **5**, Figure 1), which was being investigated in parallel [5,6].

At this stage, it was clear that O'Hagan's method [34] (Scheme 3) was the most promising strategy that had been examined so far. But four major obstacles remained: first, the starting material **27** was volatile and difficult to stockpile; second, the purification of epoxy alcohol **28b** was troublesome; third, the fluorination of **28b** proceeded with poor stereoselectivity; and fourth, the final fluorination reaction suffered from an undesired rearrangement side-reaction. We subsequently found that all four of these problems could be solved by making a single change to the synthesis: namely, by introducing a *p*-nitro group onto the aryl ring of the starting material, **35** (Scheme 4) [17].

A benefit of the *p*-nitro group immediately became apparent: the starting material **35** [35] (Scheme 4) was less volatile and hence easier to stockpile than its unsubstituted counterpart **27** (Scheme 3). Compound **35** was carried through the same set of reactions that were described previously for substrate **27** (Scheme 3). Thus, **35** underwent a cross metathesis reaction to furnish **36** in good yield (Scheme 4). Compound **36** then became the substrate for a Sharpless asymmetric epoxidation reaction, which delivered **37** with very high stereoselectivity (Scheme 4). The *p*-nitro group of **37** played another useful role here: compound **37** was rather insoluble, so it could be efficiently purified simply by triturating the crude product mixture with toluene, a procedure which afforded **37** in much higher yield than was obtained for the epoxy alcohol **28b** lacking the *p*-nitro group (Scheme 3). Compound **37** then underwent the first deoxyfluorination reaction to give compound **38a** in excellent yield (Scheme 4). The presence of the *p*-nitro group did improve the stereoselectivity of this reaction somewhat, but it was found that the inclusion of the additive TMS-morpholine [36,37] was also required to ensure a high diastereoisomeric excess of **38a**. The epoxide **38a** was then ring-opened using $Et_3N{\cdot}3HF$ to deliver the difluorodiol **39a** as a mixture of regioisomers. This mixture subsequently converged during the next deoxyfluorination reaction (Scheme 4). Gratifyingly, the *p*-nitro group of **39a** was found to completely shut down the neighbouring group participation pathway; the desired trifluoroalkane **40a** was obtained in good yield with no evidence of rearrangement or epimerization.

It was also possible to modify the synthesis shown in Scheme 4 to produce the all-*syn* trifluoroalkane **40b**. Thus, the alcohol **37** underwent a Mitsunobu-type inversion of configuration, and O'Hagan's series of three consecutive fluorination reactions [34] were subsequently applied to successfully deliver the all-*syn* trifluoroalkane **40b** (Scheme 4) [17].

Trifluoroalkanes **40a** and **40b** (Scheme 4) were advanced intermediates along the route towards the target trifluorinated amino acids (**6**). To complete the synthesis, the final requirements were to oxidise the aryl moiety into a carboxylic acid, and to deprotect the amino group. However, the *p*-nitro group of **40a**,**b** now posed a complication, because aryl oxidation reactions are only facile for electron-rich systems [39,40]. Unsurprisingly, when the oxidation reaction was attempted under standard $NaIO_4/RuCl_3$ conditions [39,40] with the nitroaryl substrate **40a**, no reaction was observed and the starting material was recovered intact.

Therefore, in order to identify a suitable method converting **40a**,**b** into **6a**,**b** (Scheme 4), model studies was undertaken using the simplified substrate **41** (Table 2). Initially, attempts were made to reduce **41** into the corresponding aniline **42**, with a view to its subsequent elaboration, e.g., via diazotization. However, a variety of reduction conditions resulted either in no observable reaction (Table 2, entries 1 and 2), or else in defluo-

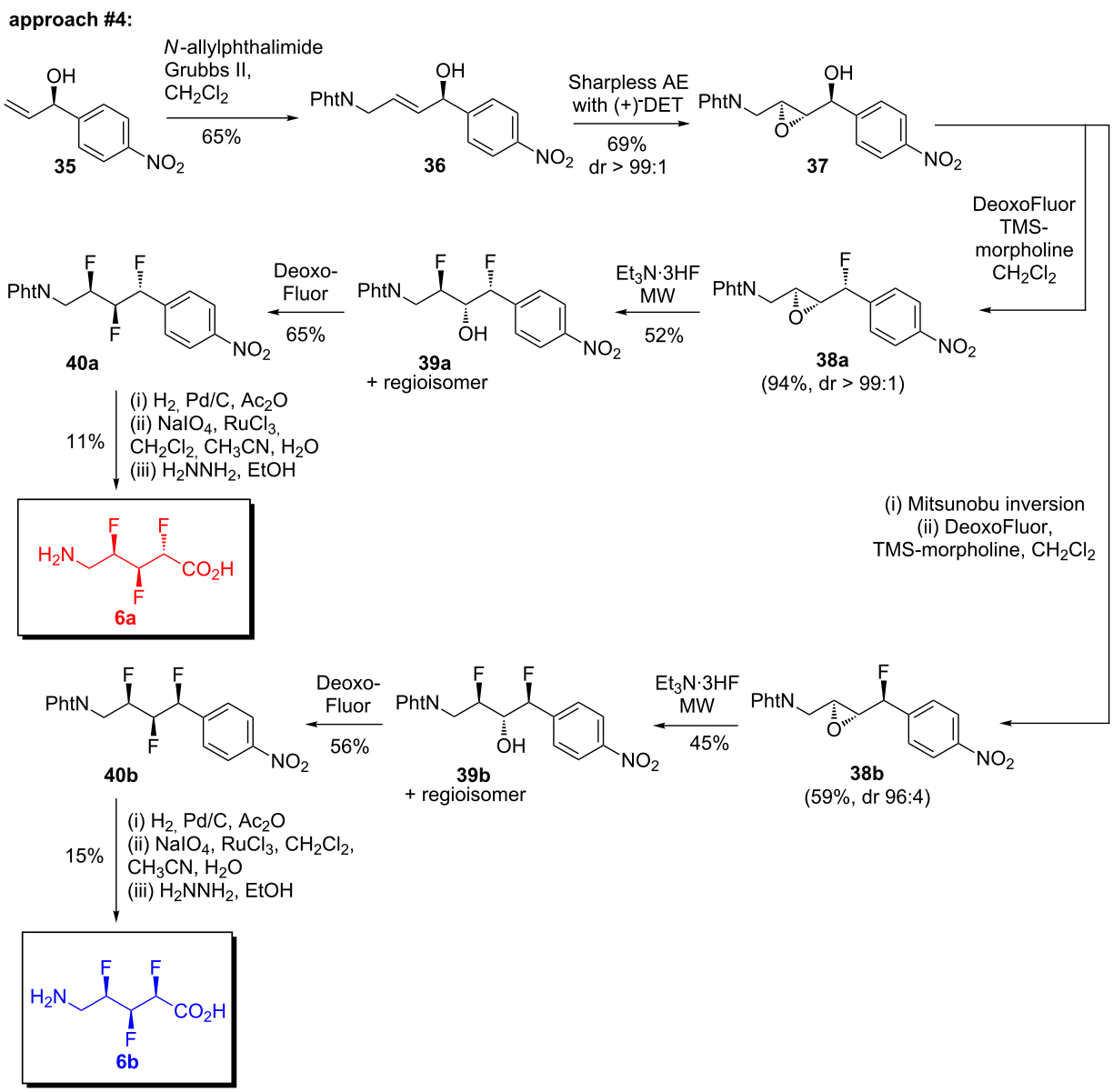

Scheme 4: The fourth synthetic approach (partially reproduced from ref. [17]).

rination at the benzyl position (Table 2, entry 3). The latter proceess is precedented [41]. Since none of the reductions to arylamines were successful, an alternative approach was investigated in which the nitroarene group would be converted into the corresponding acetanilide **43**. If this approach were successful, it was envisaged that the acetanilide **43** could be directly oxidised to carboxylic acid **44**, thereby bypassing any diazotization process. Hydrogenation of **41** with 10% Pd/C in the presence of acetic anhydride allowed the isolation of acetanilide **43** in moderate yields (Table 2, entries 4−6). It was found that the acetic anhydride solvent needed to be freshly distilled in every case in order for the reaction to be successful. The reaction duration was another significant determinant of the yield of **43** (Table 2, entries 4−6), since the over-reduced (i.e., benzylic defluorination) product was still produced in varying amounts. The subsequent oxidation of **43** was successfully achieved using sodium metaperiodate and ruthenium chloride (Table 2) [39,40], with the desired carboxylic acid **44** being obtained in 31% yield.

Having established the conditions necessary for the conversion of the nitroaryl group in model system **41** (Table 2), the procedure could now be applied to the trifluoroalkanes **40a**,**b** (Scheme 4). Thus, compound **40a** was dissolved in freshly

Table 2: Model studies that informed the final steps of the synthesis.

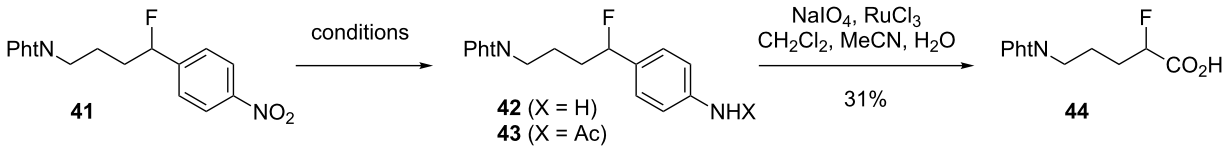

Entry	Conditions	Outcome
1	$Na_2S_2O_4$, aq HCl, rt, 20 h	no reaction
2	$Na_2S_2O_4$, HCl, ethanol, reflux, 4 h	no reaction
3	Pd/C, ammonium formate, THF, 5 h	defluorination of **41** observed by ^{1}H and ^{19}F NMR analysis of crude reaction mixture
4	H_2, 10% Pd/C, Ac_2O, 3 h	**43** (38%)
5	H_2, 10% Pd/C, Ac_2O, 5 h	**43** (58%)
6	H_2, 10% Pd/C, Ac_2O, 18 h	**43** (21%)

distilled acetic anhydride and subjected to hydrogenation over Pd/C (Scheme 4). The reaction was monitored by TLC at short time intervals in order to avoid over-reduction. The starting material was consumed within 5 h, but the expected acetanilide product (see Supporting Information File 1) was accompanied by varying quantities of a side-product that was tentatively identified either as an alternative rotamer of the acetanilide, or the corresponding imide (i.e., $ArNAc_2$, see Supporting Information File 1). Although the formation of this imide would be unexpected, it was reasoned that it might still be a suitable substrate for the subsequent oxidation reaction. Accordingly, the product of the hydrogenation reaction was next treated with sodium metaperiodate and ruthenium trichloride (Scheme 4), and gratifyingly this delivered the desired trifluorinated carboxylic acid (see Supporting Information File 1) in moderate yield. Finally, the pthalimide group was removed with hydrazine to give the target amino acid **6a** (Scheme 4). The modest overall yield for this three-step sequence can be partially attributed to the challenge of purifying the penultimate and final compounds, which were of low molecular weight and very polar. Nevertheless, the first synthesis of a δ-amino acid containing three vicinal fluorines on the backbone had been successfully completed. The all-*syn* target **6b** was then obtained in a similar fashion from **40b** (Scheme 4).

The ^{1}H and ^{19}F NMR spectra of **6a** and **6b** were simulated (see Supporting Information File 1) in order to measure the spin–spin coupling constants and thereby gain information on the solution-state conformations (Figure 2). For **6a**, the observed *J* values about the Cα–Cβ and Cβ–Cγ bonds are interme-

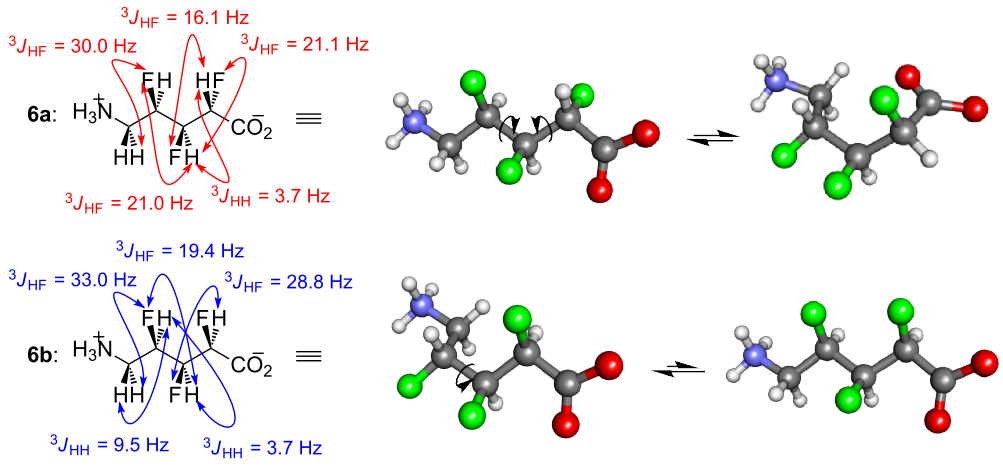

Figure 2: Selected *J* values and the inferred molecular conformations of **6a** and **6b**.

diate in magnitude [42], suggesting that conformational averaging is occurring about both of these bonds. In contrast, the *J* values about the Cγ–Cδ bond of **6a** fall clearly into either *gauche* or *anti* ranges [42], suggesting that this part of the molecule is relatively rigid in solution. Overall, the pattern of large, small and intermediate *J* values is consistent with two major conformations of **6a** existing in equilibrium (Figure 2). The first conformer (left) has an extended zigzag structure. This matches the geometry that was observed in the X-ray crystal structure for the *anti*,*syn*-trifluoroalkane **40a** [17]. The second conformer (right) has a bent shape which provides *gauche* alignments between all pairs of vicinal C–F and C–N bonds, whilst avoiding any 1,3-dipolar repulsions [11,12,43].

The observed *J* values for the all-*syn* trifluoro amino acid **6b** also allowed its solution conformation to be deduced (Figure 2). The *J* values about the Cα–Cβ and Cγ–Cδ bonds of **6b** mostly fall clearly into *gauche* or *anti* ranges, suggesting that these segments of the molecule are relatively rigid in solution. In contrast, the *J* values about the Cβ–Cγ bond of **6b** are more intermediate in magnitude (e.g., $^3J_{HH}$ = 3.7 Hz), suggesting that conformational averaging could be occurring about this bond. Overall, the pattern of large, small and intermediate *J* values is consistent with two conformations of **6b** existing in equilibrium (Figure 2). The first conformer (left) has a bent structure. This provides *gauche* alignments between all pairs of vicinal C–F and C–N bonds, whilst avoiding 1,3-dipolar repulsion [11,12,43]. The second suggested conformer of **6b** (right) has an extended zigzag structure. This geometry is counterintuitive, because although it provides *gauche* alignments between all pairs of vicinal C–F and C–N bonds, it includes an unfavourable parallel alignment of the Cα–F and Cγ–F bonds. The extended conformer of **6b** may be a minor contributor only.

Conclusion

Full details have been presented of the efforts that were required to identify and optimise a synthetic route towards the δ-amino acids **6a** and **6b**, molecules which contain three vicinal C–F bonds positioned stereospecifically along the backbone. Several synthetic approaches towards these challenging targets were investigated, involving both electrophilic and nucleophilic fluorination chemistry. The ultimately successful approach involved a modification of O'Hagan's method [34], in which a stereochemically-defined epoxy alcohol precursor underwent three sequential nucleophilic deoxyfluorination reactions. The solution-state geometries of amino acids **6a** and **6b** were probed through qualitative NMR *J*-based analyses, revealing that **6a** and **6b** exhibit distinct conformational behaviour. This suggests that these fluorinated backbone-extended amino acids might enjoy future applications, for example as shape-controlled building blocks for incorporation into bioactive peptides [16].

Supporting Information

Supporting Information File 1

Synthetic procedures and characterisation data of intermediated, NMR spectra and NMR simulations for **6a**,**b**.
[http://www.beilstein-journals.org/bjoc/content/supplementary/1860-5397-13-228-S1.pdf]

Acknowledgements

L.H. thanks the Australian Research Council for funding (ARC DE120101653; ARC DP140103962).

References

1. Cowell, S. M.; Lee, Y. S.; Cain, J. P.; Hruby, V. J. *Curr. Med. Chem.* **2004,** *11,* 2785–2798. doi:10.2174/0929867043364270
2. Kover, K. E.; Jiao, D.; Fang, S.; Hruby, V. J. *J. Org. Chem.* **1994,** *59,* 991–998. doi:10.1021/jo00084a014
3. Mathad, R. I.; Gessier, F.; Seebach, D.; Jaun, B. *Helv. Chim. Acta* **2005,** *88,* 266–280. doi:10.1002/hlca.200590008
4. Hu, X.-G.; Lawer, A.; Peterson, M. B.; Iranmanesh, H.; Ball, G. E.; Hunter, L. *Org. Lett.* **2016,** *18,* 662–665. doi:10.1021/acs.orglett.5b03592
5. Hunter, L.; Jolliffe, K. A.; Jordan, M. J. T.; Jensen, P.; Macquart, R. B. *Chem. – Eur. J.* **2011,** *17,* 2340–2343. doi:10.1002/chem.201003320
6. Wang, Z.; Hunter, L. *J. Fluorine Chem.* **2012,** *143,* 143–147. doi:10.1016/j.jfluchem.2012.06.016
7. Yamamoto, I.; Jordan, M. J. T.; Gavande, N.; Doddareddy, M. R.; Chebib, M.; Hunter, L. *Chem. Commun.* **2012,** *48,* 829–831. doi:10.1039/C1CC15816C
8. Absalom, N.; Yamamoto, I.; O'Hagan, D.; Hunter, L.; Chebib, M. *Aust. J. Chem.* **2015,** *68,* 23–30. doi:10.1071/CH14456
9. Hunter, L.; Butler, S.; Ludbrook, S. B. *Org. Biomol. Chem.* **2012,** *10,* 8911–8918. doi:10.1039/c2ob26596f
10. Hu, X.-G.; Thomas, D. S.; Griffith, R.; Hunter, L. *Angew. Chem., Int. Ed.* **2014,** *53,* 6176–6179. doi:10.1002/anie.201403071
11. O'Hagan, D. *Chem. Soc. Rev.* **2008,** *37,* 308–319. doi:10.1039/B711844A
12. Hunter, L. *Beilstein J. Org. Chem.* **2010,** *6,* No. 38. doi:10.3762/bjoc.6.38
13. Thiehoff, C.; Rey, Y. P.; Gilmour, R. *Isr. J. Chem.* **2017,** *57,* 92–100. doi:10.1002/ijch.201600038
14. Zimmer, L. E.; Sparr, C.; Gilmour, R. *Angew. Chem., Int. Ed.* **2011,** *50,* 11860–11871. doi:10.1002/anie.201102027
15. Fox, S. J.; Gourdain, S.; Coulthurst, A.; Fox, C.; Kuprov, I.; Essex, J. W.; Skylaris, C.-K.; Linclau, B. *Chem. – Eur. J.* **2015,** *21,* 1682–1691. doi:10.1002/chem.201405317
16. Lawer, A.; Tai, J.; Jolliffe, K. A.; Fletcher, S.; Avery, V. M.; Hunter, L. *Bioorg. Med. Chem. Lett.* **2014,** *24,* 2645–2647. doi:10.1016/j.bmcl.2014.04.071
17. Cheerlavancha, R.; Lawer, A.; Cagnes, M.; Bhadbhade, M.; Hunter, L. *Org. Lett.* **2013,** *15,* 5562–5565. doi:10.1021/ol402756e
18. Beeson, T. D.; MacMillan, D. W. C. *J. Am. Chem. Soc.* **2005,** *127,* 8826–8828. doi:10.1021/ja051805f

19. Steiner, D. D.; Mase, N.; Barbas, C. F., III. *Angew. Chem., Int. Ed.* **2005,** *44,* 3706–3710. doi:10.1002/anie.200500571
20. Marigo, M.; Fielenbach, D.; Braunton, A.; Kjærsgaard, A.; Jørgensen, K. A. *Angew. Chem., Int. Ed.* **2005,** *44,* 3703–3706. doi:10.1002/anie.200500395
21. Wisniewska, H. M.; Swift, E. C.; Jarvo, E. R. *J. Am. Chem. Soc.* **2013,** *135,* 9083–9090. doi:10.1021/ja4034999
22. Delfourne, E.; Kiss, R.; Le Corre, L.; Dujols, F.; Bastide, J.; Collignon, F.; Lesur, B.; Frydman, A.; Darro, F. *J. Med. Chem.* **2003,** *46,* 3536–3545. doi:10.1021/jm0308702
23. Horii, Z.-I.; Iwata, C.; Tamura, Y. *J. Org. Chem.* **1961,** *26,* 2273–2276. doi:10.1021/jo01351a031
24. Chu, C. K.; Ziegler, D. T.; Carr, B.; Wickens, Z. K.; Grubbs, R. H. *Angew. Chem., Int. Ed.* **2016,** *55,* 8435–8439. doi:10.1002/anie.201603424
25. Katcher, M. H.; Sha, A.; Doyle, A. G. *J. Am. Chem. Soc.* **2011,** *133,* 15902–15905. doi:10.1021/ja206960k
26. Miró, J.; del Pozo, C.; Toste, F. D.; Fustero, S. *Angew. Chem.* **2016,** *128,* 9191–9195. doi:10.1002/ange.201603046
27. Ando, K.; Kobayashi, T.; Uchida, N. *Org. Lett.* **2015,** *17,* 2554–2557. doi:10.1021/acs.orglett.5b01049
28. Nyffeler, P. T.; Durón, S. G.; Burkart, M. D.; Vincent, S. P.; Wong, C.-H. *Angew. Chem., Int. Ed.* **2005,** *44,* 192–212. doi:10.1002/anie.200400648
29. Enders, D.; Huttl, M. R. M. *Synlett* **2005,** 991–993. doi:10.1055/s-2005-864813
30. Kwiatkowski, P.; Beeson, T. D.; Conrad, J. C.; MacMillan, D. W. C. *J. Am. Chem. Soc.* **2011,** *133,* 1738–1741. doi:10.1021/ja111163u
31. Bonnefous, C.; Payne, J. E.; Roppe, J.; Zhuang, H.; Chen, X.; Symons, K. T.; Nguyen, P. H.; Sablad, M.; Rozenkrants, N.; Zhang, Y.; Wang, L.; Severance, D.; Walsh, J. P.; Yazdani, N.; Shiau, A. K.; Noble, S. A.; Rix, P.; Rao, T. S.; Hassig, C. A.; Smith, N. D. *J. Med. Chem.* **2009,** *52,* 3047–3062. doi:10.1021/jm900173b
32. Andrés, M.; Buil, M. A.; Calbet, M.; Casado, O.; Castro, J.; Eastwood, P. R.; Eichhorn, P.; Ferrer, M.; Forns, P.; Moreno, I.; Petit, S.; Roberts, R. S. *Bioorg. Med. Chem. Lett.* **2014,** *24,* 5111–5117. doi:10.1016/j.bmcl.2014.08.026
33. Ward, R. A.; Bethel, P.; Cook, C.; Davies, E.; Debreczeni, J. E.; Fairley, G.; Feron, L.; Flemington, V.; Graham, M. A.; Greenwood, R.; Griffin, N.; Hanson, L.; Hopcroft, P.; Howard, T. D.; Hudson, J.; James, M.; Jones, C. D.; Jones, C. R.; Lamont, S.; Lewis, S.; Lindsay, N.; Roberts, K.; Simpson, I.; St-Gallay, S.; Swallow, S.; Tang, J.; Tonge, M.; Wang, Z.; Zhai, B. *J. Med. Chem.* **2017,** *60,* 3438–3450. doi:10.1021/acs.jmedchem.7b00267
34. Brunet, V. A.; Slawin, A. M. Z.; O'Hagan, D. *Beilstein J. Org. Chem.* **2009,** *5,* No. 61. doi:10.3762/bjoc.5.61
35. Štambaský, J.; Malkov, A. V.; Kočovský, P. *J. Org. Chem.* **2008,** *73,* 9148–9150. doi:10.1021/jo801874r
36. Bio, M. M.; Waters, M.; Javadi, G.; Song, Z. J.; Zhang, F.; Thomas, D. *Synthesis* **2008,** 891–896. doi:10.1055/s-2008-1032181
37. Bresciani, S.; O'Hagan, D. *Tetrahedron Lett.* **2010,** *51,* 5795–5797. doi:10.1016/j.tetlet.2010.08.104
38. Banik, S. M.; Medley, J. W.; Jacobsen, E. N. *Science* **2016,** *353,* 51–54. doi:10.1126/science.aaf8078
39. Gao, Y.; Hanson, R. M.; Klunder, J. M.; Ko, S. Y.; Masamune, H.; Sharpless, K. B. *J. Am. Chem. Soc.* **1987,** *109,* 5765–5780. doi:10.1021/ja00253a032
40. Schüler, M.; O'Hagan, D.; Slawin, A. M. Z. *Chem. Commun.* **2005,** 4324–4326. doi:10.1039/b506010a
41. Hudlicky, M. *J. Fluorine Chem.* **1989,** *44,* 345–359. doi:10.1016/S0022-1139(00)82802-X
42. O'Hagan, D.; Rzepa, H. S.; Schüler, M.; Slawin, A. M. Z. *Beilstein J. Org. Chem.* **2006,** *2,* No. 19. doi:10.1186/1860-5397-2-19
43. Scheidt, F.; Selter, P.; Santschi, N.; Holland, M. C.; Dudenko, D. V.; Daniliuc, C.; Mück-Lichtenfeld, C.; Hansen, M. R.; Gilmour, R. *Chem. – Eur. J.* **2017,** *23,* 6142–6149. doi:10.1002/chem.201604632

License and Terms

BEILSTEIN JOURNAL OF ORGANIC CHEMISTRY

Fluorination of some highly functionalized cycloalkanes: chemoselectivity and substrate dependence

Attila Mário Remete[1], Melinda Nonn[2], Santos Fustero[3], Matti Haukka[4], Ferenc Fülöp[*1,2] and Loránd Kiss[*1]

Full Research Paper

Open Access

Address:
[1]Institute of Pharmaceutical Chemistry, University of Szeged, H-6720 Szeged, Eötvös u. 6, Hungary, [2]MTA-SZTE Stereochemistry Research Group, Hungarian Academy of Sciences, H-6720 Szeged, Eötvös u. 6, Hungary, [3]Departamento de Química Orgánica, Facultad de Farmàcia, Universidad de Valencia, Av. Vicente Andrés Estellés, s/n 46100 Valencia, Spain and [4]Department of Chemistry, University of Jyväskylä, FIN-40014, Jyväskylä, Finland

Email:
Ferenc Fülöp[*] - fulop@pharm.u-szeged.hu; Loránd Kiss[*] - kiss.lorand00@gmail.com

* Corresponding author

Keywords:
amino acids; chemoselectivity; fluorine; functionalization; stereoisomers

Beilstein J. Org. Chem. **2017,** *13,* 2364–2371.
doi:10.3762/bjoc.13.233

Received: 26 July 2017
Accepted: 12 October 2017
Published: 06 November 2017

This article is part of the Thematic Series "Organo-fluorine chemistry IV".

Guest Editor: D. O'Hagan

Abstract

A study exploring the chemical behavior of some dihydroxylated β-amino ester stereo- and regioisomers, derived from unsaturated cyclic β-amino acids is described. The nucleophilic fluorinations involving hydroxy–fluorine exchange of some highly functionalized alicyclic diol derivatives have been carried out in view of selective fluorination, investigating substrate dependence, neighboring group assistance and chemodifferentiation.

Introduction

Fluorinated molecules exert an ever-increasing impact in medicinal chemistry thanks to their valuable biological properties. Numerous drugs introduced to the market nowadays contain fluorine, and their number is expected to continuously increase in years to come [1,2]. Therefore, there is a high demand in synthetic organic and medicinal chemistry for both, the synthesis of novel fluorinated biomolecules and the development of selective and controlled efficient fluorination procedures. This high interest is clearly demonstrated by the number of various published papers on the field, and related recent comprehensive reviews [3-12]. The nucleophilic fluorination with commercially available organic fluorinating agents (e.g., DAST, Deoxofluor, Fluolead, XtalFluor-E or XtalFluor-M) is a widely used approach for the introduction of a fluorine atom into an organic molecule. The most common approach is the exchange of a hydroxy group for fluorine, taking place, in general, by inver-

sion [13-18]. Although fluorination based on hydroxy–fluorine interconversion seems to be an eloquent, simple and efficient procedure for the creation of a certain fluorinated organic molecule, regio- and stereoselectivity, stereocontrol and substrate influence remain a challenge in the case of highly functionalized frameworks.

Results and Discussion

Our aim in this study was to explore the chemical behavior of some alicyclic, highly functionalized vicinal diol derivatives (accordingly possessing two fluorine precursor moieties in their structures) under fluorination protocols. During the past two decades multifunctionalized amino acids and their analogous derivatives have gained considerable interest in pharmaceutical chemistry as bioactive compounds. Some derivatives (e.g., peramivir, oseltamivir or laninamivir) are known as antiviral drugs [19-22], while other cyclopentane β-amino acids (e.g., icofungipen, cispentacin) are relevant antifungal agents [19]. Therefore we have selected some five and six-membered alicyclic dihydroxylated β-amino ester stereo- and regioisomers as model compounds [23-26], derived from cyclopentene or cyclohexene β-amino acids. These were used in order to evaluate their behavior in fluorination in view of selectivity and to explore substrate dependency and chemodifferentiation. Based on the different stereochemical structures of the selected model diols as well as the nature of the *N*-protecting group used, we expected differences in their chemical behavior under fluorination conditions. In a former investigation on oxirane opening reactions of various epoxycycloalkane β-aminocarboxylates [27], a high substrate dependence and directing effect of the functional groups has been observed. These results led us to perform similar investigations with the above mentioned dihydroxylated cyclic β-amino acid esters.

Our study started with the fluorination of racemic dihydroxylated cyclopentane *cis*- or *trans*-β-amino acid esters (±)-**1** and (±)-**4** [23-26]. The preliminary investigations were performed with the commercially available fluorinating agents mentioned above in various solvents (e.g., PhMe, THF, and CH_2Cl_2) at different temperatures. Hereby Deoxofluor in CH_2Cl_2 with or without adding DBU was found to be the most suitable reagent. The diol derivatives, obviously, are expected to deliver the corresponding difluorinated products. In spite of this anticipation, the treatment of dihydroxylated amino acid ester (±)-**1** with 1.5 equiv of Deoxofluor after 70 min afforded through intramolecular cyclization a compound which was identified on the basis of 2D NMR analysis as oxazoline derivative (±)-**2** as the sole product in 71% yield. When the same reaction was carried out in the presence of 4 equiv DBU as the base [28] the reaction time could be decreased to 10 min with a slightly increased yield of the product (Scheme 1). This observation led us to conclude that out of the two hydroxy groups only that attached to C-3 takes part in the reaction and is substituted via the amide O-atom. Increasing the amount of Deoxofluor to 4 equiv resulted in the exclusive formation of the fluorine-containing oxazoline derivative (±)-**3**. Note that the addition of DBU did not have a significant effect on this reaction. When isolated hydroxyoxazoline (±)-**2** is subjected to the fluorination protocol compound (±)-**3** was obtained in a modest yield (15%) that could be slightly increased to 25% by the addition of DBU to the reaction mixture (Scheme 1).

In contrast to (±)-**1**, its stereoisomer (±)-**4**, afforded in the reaction with 1.5 equiv of Deoxofluor in the presence of 4 equiv of DBU, according to 2D NMR and X-ray data fluorohydrine derivative (±)-**5** through chemodifferentiation in a moderate yield (Scheme 2, Figure 1).

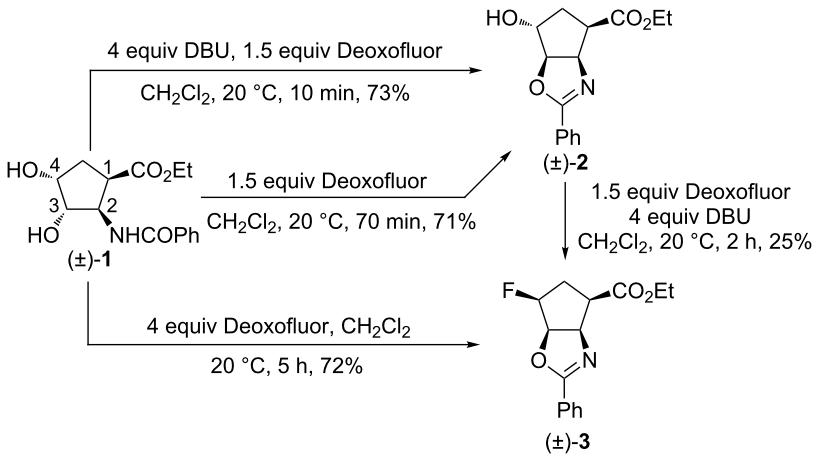

Scheme 1: Fluorination of diol derivative (±)-**1**.

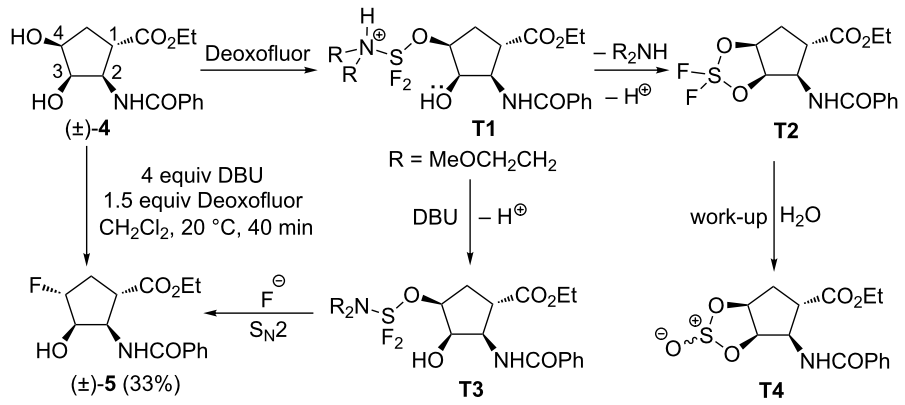

Scheme 2: Fluorination of diol derivative (±)-**4**.

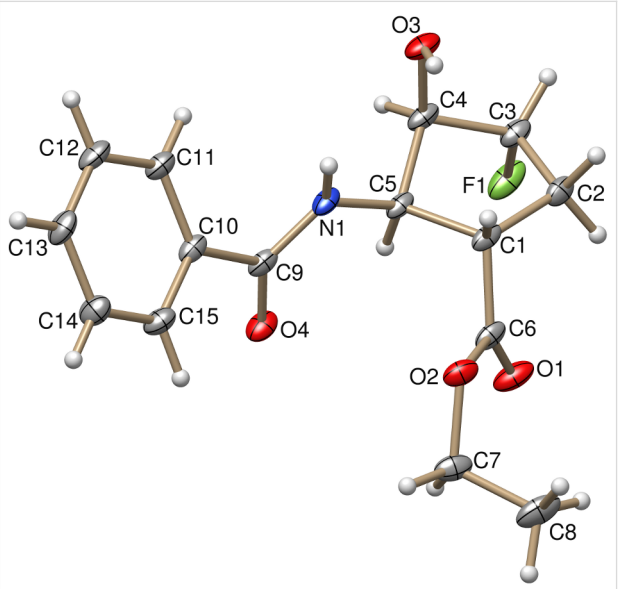

Figure 1: X-ray structure of fluorohydrine derivative (±)-**5**.

This result indicated that in the case of compound (±)-**4**, the C-4 hydroxy group is transformed into a leaving group on interaction with Deoxofluor, followed by a fluoride attack to give (±)-**5**. Of note, the role of DBU was found to be crucial in this reaction, since without the addition of the base the formation of sulfite derivative **T4** was detected (Scheme 2).

The vicinal fluorohydrine moiety is a relevant unit in a series of valuable biomolecules such as amino acids, heterocyclic natural products and nucleosides [29-36]. Therefore, the fluorinated β-amino acid derivative (±)-**5**, obtained through transformation of (±)-**4** with chemodiscrimination of the alcoholic groups, might represent a promising bioactive framework.

As the fluorination of the five-membered diol stereoisomers (±)-**1** and (±)-**4** proved to be highly substrate dependent and on the basis of our earlier findings on substrate determinant fluorinations [37], we next investigated the effect of the nature of the *N*-protecting group on this reaction. The treatment of *N*-Cbz-protected dihydroxylated cyclopentane β-amino ester (±)-**6** with Deoxofluor under various conditions provided an unidentifiable mixture of products. However, the reaction of diol (±)-**6** with 1.5 equiv of Deoxofluor in the presence of DBU as the base furnished aziridine derivative (±)-**7** within 10 min through intramolecular cyclization via the carbamate N-atom (Scheme 3). Again, only the selective transformation of the C-3 hydroxy group with the fluorinating agent took place, without the involvement of the C-4 OH group. Unfortunately, all further attempted fluorinations of hydroxylated aziridine (±)-**7** under various conditions using for example XtalFluor, $Et_3N{\cdot}HF$, and pyridine·HF and applying an efficient approach earlier developed by our group, proved to be unsuccessful ([18] and references cited therein).

Due to the biological relevance of six-membered β-amino acid derivatives (e.g., tilidin, oryzoxymicin, BAYY9379) [19], we continued our synthetic investigations by selecting some cyclohexane β-amino acid esters as model compounds. Thus, diol (±)-**8** [23-26] derived from dihydroxylation of *cis*-2-aminocyclohex-4-ene carboxylic acid was treated with 1 equiv of Deoxofluor in CH_2Cl_2. Again, through chemodiscrimination of the alcoholic groups in positions 4 and 5, oxazine derivative (±)-**9** was formed as the single product through intramolecular cyclization involving the nucleophilic amide O-atom (Scheme 4).

Upon treatment of diol (±)-**8** with excess Deoxofluor (4 equiv), in addition to the expected fluorinated oxazine (±)-**10**, a highly unsaturated amino ester (±)-**11** was formed as the major product. The two compounds were separated by column chromatography and product (±)-**11** was identified to be a cyclohexadiene amino acid ester. A relatively simple way of its formation is depicted in Scheme 5. Specifically, after transformation of the

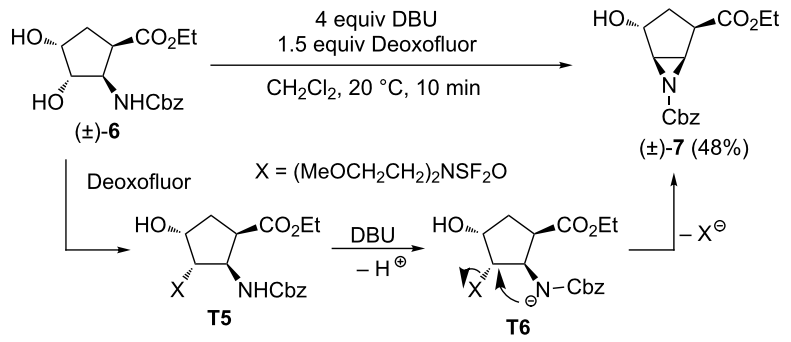

Scheme 3: Fluorination of diol derivative (±)-**6**.

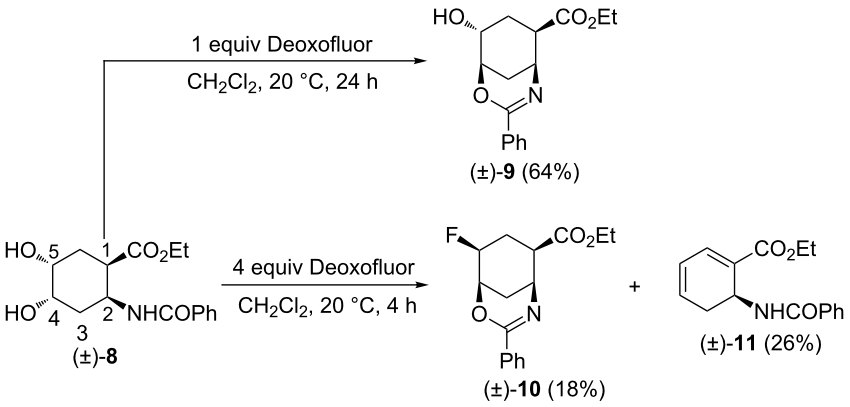

Scheme 4: Fluorination of cyclohexane-derived diol (±)-**8**.

alcoholic group at C-4 in (±)-**8** into a leaving group, an intramolecular cyclization takes place to afford oxazine (±)-**9**. Subsequently, this oxazine, in the presence of an excess Deoxofluor gives fluorinated derivative (±)-**10**. Finally, in the presence of fluoride as base, deprotonation (**T9**), followed by oxazine-ring opening through olefinic-bond migration (**T10**) then gives the highly conjugated amino acid ester (±)-**11** (Scheme 5).

Noteworthy, the presence of DBU in the experiment of (±)-**8** with Deoxofluor did not have a significant effect on the ratio of

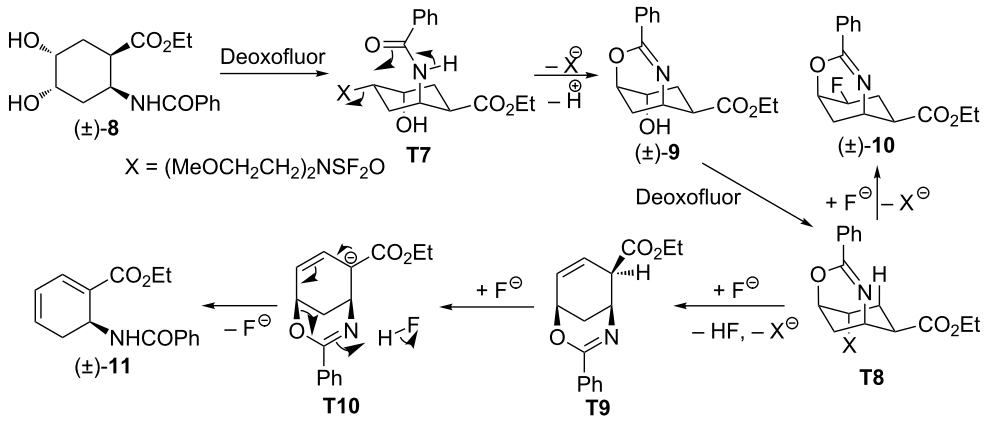

Scheme 5: Proposed route for the formation of compounds (±)-**10** and (±)-**11**.

the products. However, in the presence of the base the yields of (±)-**10** and (±)-**11** decreased to 10% and 17%, respectively.

Unfortunately and surprisingly, diol (±)-**12** (derived from *trans*-2-aminocyclohex-4-ene carboxylic acid) [23-26] a stereoisomer of (±)-**8**, in the reaction with either 1 equiv or excess of Deoxofluor did not give any identifiable product. However, according to earlier observations on the effect of DBU the reaction in the presence of this base afforded keto ester (±)-**13** in 41% yield. In contrast to the stereoisomer (±)-**8**, reaction of diol (±)-**12** with Deoxofluor took place at the C-5 hydroxy group leading to intermediate **T11**. The latter, in the presence of DBU, gave enol **T12** which immediately converted to keto amino ester (±)-**13** (Scheme 6).

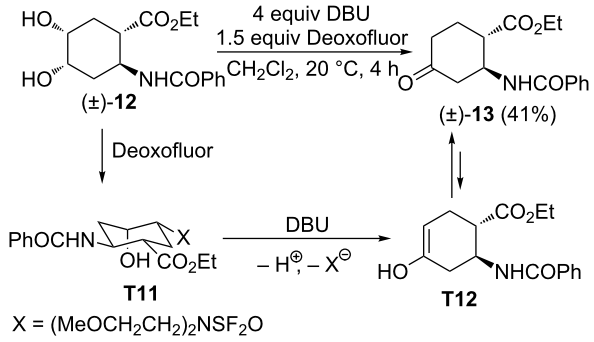

Scheme 6: Fluorination of diol derivative (±)-**12**.

Subsequently, we investigated the behavior of other six-membered diol isomers in this reaction. The diol derivative (±)-**14** (derived from *cis*-2-aminocyclohex-3-ene carboxylic acid), underwent intramolecular cyclization upon treatment with 1 equiv of Deoxofluor providing isomers (±)-**15** and (±)-**16** in nearly 2:1 ratio that could be separated and isolated by chromatography. This experimental observation indicates that in the case of diol (±)-**14** both alcoholic groups are transformed into the corresponding good leaving groups upon treatment with Deoxofluor. When (±)-**14** was treated with an excess of Deoxofluor, somewhat surprisingly, the fluorinated isoxazoline derivative (±)-**17** was formed with the fluorine attached to the β-position relative to the ester function, whereas the N-atom is located in the γ-position through a β to γ flip (Scheme 7).

The formation of isoxazolines (±)-**15** and (±)-**16** in the presence of 1 equiv of Deoxofluor involves rather simple reaction steps as only one of the hydroxy groups is transformed into a leaving group in each case (**T13** and **T14**, respectively). In contrast, when using the fluorinating reagent in excess, both hydroxy groups are converted to leaving groups to afford intermediate **T15**. The latter affords aziridinium ion **T16** through intramolecular reaction with the amide nitrogen. The subsequent aziridine-ring opening by reaction with fluoride results in amide intermediate **T17** which undergoes an intramolecular cyclization to give (±)-**17** (Scheme 8). A similar aziridinium opening reaction with fluoride can be found in [38,39].

Interestingly, when changing the *N*-protecting group from benzoyl in (±)-**14** to Cbz ((±)-**18**), the fluorination with Deoxofluor provided, analogously to the five-membered compound (±)-**6** (Scheme 3), aziridine (±)-**19** in 60% yield (Scheme 9).

Diol (±)-**20** (derived from *trans*-2-aminocyclohex-3-ene carboxylic acid), a stereoisomer of (±)-**14**, furnished selectively one single cyclized product in the presence of 1 equiv of Deoxofluor, namely oxazoline derivative (±)-**21** (Scheme 10). This is in high contrast to the transformation of (±)-**14** (Scheme 7). Interestingly, when (±)-**20** is treated with Deoxofluor in excess, again, differently from its all-*cis* counterpart (±)-**14**, two fluorinated oxazolines in nearly 1:1 ratio are obtained: (±)-**22** as the expected product, with the ring N-atom in the β-position to the ester group and compound (±)-**23**, having the N-atom in the

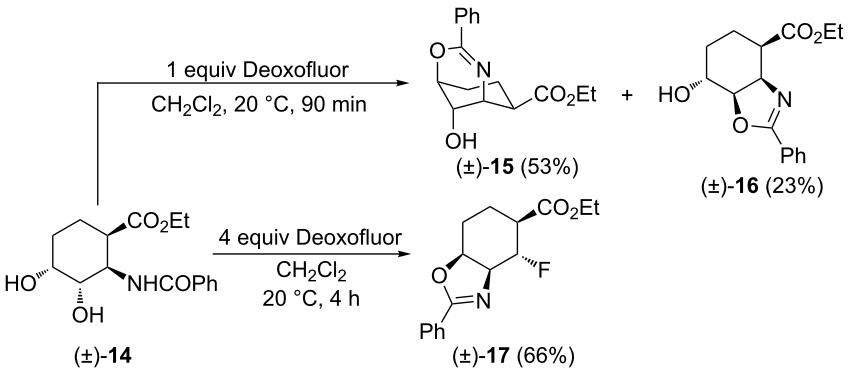

Scheme 7: Fluorination of diol derivative (±)-**14**.

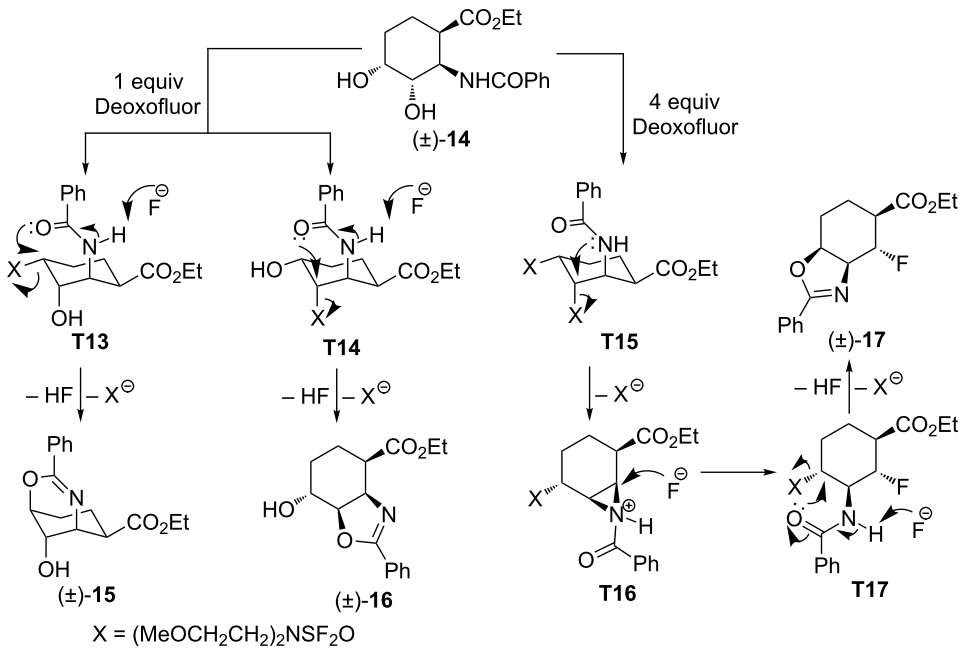

Scheme 8: Proposed route for the formation of compounds (±)-**15**, (±)-**16** and (±)-**17**.

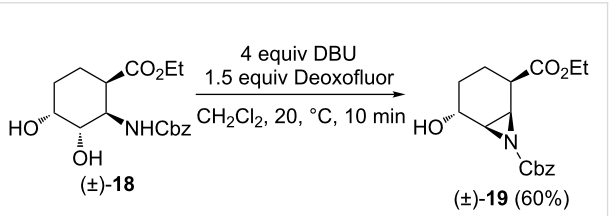

Scheme 9: Fluorination of *N*-Cbz-protected diol derivative (±)-**18**.

γ-position relative to the carboxylate. The latter being formed by *N*-migration, through an aziridinium ion opening reaction with fluoride.

Finally, the fluorination protocol was applied to commercially available *meso*-compound **24** having a cyclohexane framework. However, the treatment of **24** with various amounts of Deoxofluor gave only unidentifiable products whereas the reaction in the presence of DBU, afforded ketoester (±)-**25** (see also Scheme 6) in 48% yield (Scheme 11).

Conclusion

In conclusion, the chemical behavior of the alcoholic functions of some vicinal diol derivatives towards fluorination has been investigated under various conditions. The fluorination reactions of the highly functionalized cycloalkanes were found to be highly substrate dependent, taking place with chemodiscrimina-

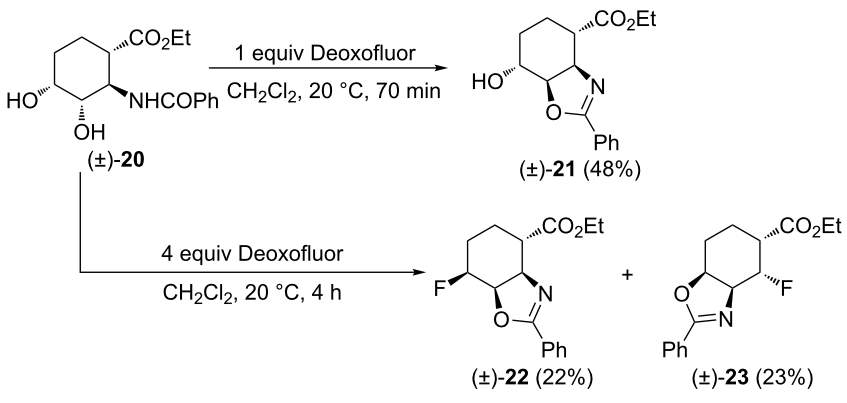

Scheme 10: Fluorination of diol derivative (±)-**20**.

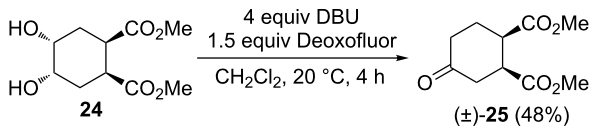

Scheme 11: Fluorination of meso diol derivative **24**.

tion of the two hydroxy groups. The stereochemical arrangement of the functional groups deeply influenced the selectivity of the transformations. Further investigations of other substrates in view of selectivity and substrate-directing effects are currently being studied in our research group.

Experimental

General information

Chemicals were purchased from Sigma–Aldrich and the solvents were used as received. Melting points were determined with a Kofler apparatus. Elemental analyses were carried out with a Perkin–Elmer CHNS-2400 Ser II elemental analyzer. Silica gel 60 F254 was purchased from Merck. The NMR spectra were acquired at room temperature on a Bruker Avance 400 spectrometer with 11.75 T magnetic field strength (^{1}H frequency: 400.13 MHz, ^{19}F frequency: 376.50 MHz, ^{13}C frequency: 100.76 MHz, respectively) in $CDCl_3$ or DMSO-d_6 solution, using the deuterium signal of the solvent to lock the field. The ^{1}H and ^{13}C chemical shifts are given relative to TMS and ^{19}F chemical shifts are referenced to $CFCl_3$ (0.00 ppm).

General procedures for fluorination

Method A: To a solution of dihydroxylated compound (0.50 mmol) in 10 mL anhydrous CH_2Cl_2 under an Ar atmosphere, 50% Deoxofluor in toluene was added (amount given in the text) and the reaction mixture was stirred at 20 °C for the time given in the text. The solution was then diluted with CH_2Cl_2 (30 mL) and washed with saturated aqueous $NaHCO_3$ solution (2 × 20 mL). The organic layer was dried (Na_2SO_4) and concentrated. The crude product was purified by column chromatography on silica gel (*n*-hexane/EtOAc or *n*-hexane/acetone).

Method B: To a solution of dihydroxylated compound (0.50 mmol) in 15 mL anhydrous CH_2Cl_2 under an Ar atmosphere, 4 equiv DBU and 1.5 equiv 50% Deoxofluor in toluene were added and the solution was stirred at 20 °C for the time given in the text. The solution was then diluted with CH_2Cl_2 (30 mL) and washed with saturated aqueous $NaHCO_3$ solution (2 × 20 mL). The organic layer was dried (Na_2SO_4) and concentrated. The crude product was purified by column chromatography on silica gel (*n*-hexane/EtOAc or *n*-hexane/acetone).

Supporting Information

Supporting Information File 1

Characterization data and copies of NMR spectra.
[http://www.beilstein-journals.org/bjoc/content/supplementary/1860-5397-13-233-S1.pdf]

Acknowledgements

We are grateful to the Hungarian Research Foundation (NKFIH Nos. K 115731 and K 119282) for financial support. The financial support of the GINOP-2.3.2-15-2016-00014 project is also acknowledged. This research was supported by the EU-funded Hungarian grant EFOP-3.6.1-16-2016-00008.

ORCID® iDs

Santos Fustero - https://orcid.org/0000-0002-7575-9439

References

1. Wang, J.; Sánchez-Roselló, M.; Aceña, J. L.; del Pozo, C.; Sorochinsky, A. E.; Fustero, S.; Soloshonok, V. A.; Liu, H. *Chem. Rev.* **2014,** *114,* 2432. doi:10.1021/cr4002879
2. Zhou, Y.; Wang, J.; Gu, Z.; Wang, S.; Zhu, W.; Aceña, J. L.; Soloshonok, V. A.; Izawa, K.; Liu, H. *Chem. Rev.* **2016,** *116,* 442. doi:10.1021/acs.chemrev.5b00392
3. Ahrens, T.; Kohlmann, J.; Ahrens, M.; Braun, T. *Chem. Rev.* **2015,** *115,* 931. doi:10.1021/cr500257c
4. Cresswell, A. J.; Davies, S. G.; Roberts, P. M.; Thomson, J. E. *Chem. Rev.* **2015,** *115,* 566. doi:10.1021/cr5001805
5. O'Hagan, D.; Deng, H. *Chem. Rev.* **2015,** *115,* 634. doi:10.1021/cr500209t
6. Liu, X.; Xu, C.; Wang, M.; Liu, Q. *Chem. Rev.* **2015,** *115,* 683. doi:10.1021/cr400473a
7. Ni, C.; Hu, M.; Hu, J. *Chem. Rev.* **2015,** *115,* 765. doi:10.1021/cr5002386
8. Champagne, P. A.; Desroches, J.; Hamel, J.-D.; Vandamme, M.; Paquin, J.-F. *Chem. Rev.* **2015,** *115,* 9073. doi:10.1021/cr500706a
9. Liang, T.; Neumann, C. N.; Ritter, T. *Angew. Chem., Int. Ed.* **2013,** *52,* 8214. doi:10.1002/anie.201206566
10. Campbell, M. G.; Ritter, T. *Chem. Rev.* **2015,** *115,* 612. doi:10.1021/cr500366b
11. Charpentier, J.; Früh, N.; Togni, A. *Chem. Rev.* **2015,** *115,* 650. doi:10.1021/cr500223h
12. Yang, X.; Wu, T.; Phipps, R. J.; Toste, F. D. *Chem. Rev.* **2015,** *115,* 826. doi:10.1021/cr500277b
13. Bresciani, S.; Slawin, A. M. Z.; O'Hagan, D. *J. Fluorine Chem.* **2009,** *130,* 537. doi:10.1016/j.jfluchem.2009.03.003
14. Gouverneur, V.; Müller, K., Eds. *Fluorine in Pharmaceutical and Medicinal Chemistry: From Biophysical Aspects to Clinical Applications;* Imperial College Press: London, 2012.
15. Kiss, L.; Forró, E.; Fustero, S.; Fülöp, F. *Org. Biomol. Chem.* **2011,** *9,* 6528. doi:10.1039/c1ob05648d
16. Kiss, L.; Forró, E.; Fustero, S.; Fülöp, F. *Eur. J. Org. Chem.* **2011,** 4993. doi:10.1002/ejoc.201100583
17. Kiss, L.; Nonn, M.; Sillanpää, R.; Fustero, S.; Fülöp, F. *Beilstein J. Org. Chem.* **2013,** *9,* 1164. doi:10.3762/bjoc.9.130

18. Nonn, M.; Kiss, L.; Haukka, M.; Fustero, S.; Fülöp, F. *Org. Lett.* **2015,** *17,* 1074. doi:10.1021/acs.orglett.5b00182
19. Kiss, L.; Fülöp, F. *Chem. Rev.* **2014,** *114,* 1116. doi:10.1021/cr300454h
20. Mooney, C. A.; Johnson, S. A.; 't Hart, P.; van Ufford, L. Q.; de Haan, C. A. M.; Moret, E. E.; Martin, N. I. *J. Med. Chem.* **2014,** *57,* 3154. doi:10.1021/jm401977j
21. Schade, D.; Kotthaus, J.; Riebling, L.; Kotthaus, J.; Müller-Fielitz, H.; Raasch, W.; Koch, O.; Seidel, N.; Schmidtke, M.; Clement, B. *J. Med. Chem.* **2014,** *57,* 759. doi:10.1021/jm401492x
22. Tian, J.; Zhong, J.; Li, Y.; Ma, D. *Angew. Chem., Int. Ed.* **2014,** *53,* 13885. doi:10.1002/anie.201408138
23. Benedek, G.; Palkó, M.; Wéber, E.; Martinek, T. A.; Forró, E.; Fülöp, F. *Eur. J. Org. Chem.* **2008,** 3724. doi:10.1002/ejoc.200800345
24. Benedek, G.; Palkó, M.; Wéber, E.; Martinek, T. A.; Forró, E.; Fülöp, F. *Tetrahedron: Asymmetry* **2009,** *20,* 2220. doi:10.1016/j.tetasy.2009.09.001
25. Kiss, L.; Nonn, M.; Forró, E.; Sillanpää, R.; Fustero, S.; Fülöp, F. *Eur. J. Org. Chem.* **2014,** 4070. doi:10.1002/ejoc.201402121
26. Cherepanova, M.; Kiss, L.; Fülöp, F. *Tetrahedron* **2014,** *70,* 2515. doi:10.1016/j.tet.2014.02.063
27. Remete, A. M.; Nonn, M.; Fustero, S.; Fülöp, F.; Kiss, L. *Molecules* **2016,** *21,* 1493. doi:10.3390/molecules21111493
28. L'Heureux, A.; Beaulieu, F.; Bennett, C.; Bill, D. R.; Clayton, S.; LaFlamme, F.; Mirmehrabi, M.; Tadayon, S.; Tovell, D.; Couturier, M. *J. Org. Chem.* **2010,** *75,* 3401. doi:10.1021/jo100504x
29. Hu, X.-G.; Lawer, A.; Peterson, M. B.; Iranmanesh, H.; Ball, G. E.; Hunter, L. *Org. Lett.* **2016,** *18,* 662. doi:10.1021/acs.orglett.5b03592
30. Hunter, L.; Jolliffe, K. A.; Jordan, M. J. T.; Jensen, P.; Macquart, R. B. *Chem. – Eur. J.* **2011,** *17,* 2340. doi:10.1002/chem.201003320
31. Patel, A. R.; Liu, F. *Aust. J. Chem.* **2014,** *68,* 50. doi:10.1071/CH14256
32. Yadav, Y. S.; Reddy, B. V. S.; Ramesh, K.; Kumar, G. G. G. K. S. N.; Grée, R. *Tetrahedron Lett.* **2010,** *51,* 1578. doi:10.1016/j.tetlet.2010.01.059
33. Qiu, X.-L.; Xu, X.-H.; Qing, F.-L. *Tetrahedron* **2010,** *66,* 789. doi:10.1016/j.tet.2009.11.001
34. Wójtowicz-Rajchel, H. *J. Fluorine Chem.* **2012,** *143,* 11. doi:10.1016/j.jfluchem.2012.06.026
35. Si, C.; Fales, K. R.; Torrado, A.; Frimpong, K.; Kaoudi, T.; Vandeveer, H. G.; Njoroge, F. G. *J. Org. Chem.* **2016,** *81,* 4359. doi:10.1021/acs.joc.6b00305
36. Singh, U. S.; Mishra, R. C.; Shankar, R.; Chu, C. K. *J. Org. Chem.* **2014,** *79,* 3917. doi:10.1021/jo500382v
37. Kiss, L.; Nonn, M.; Sillanpää, R.; Haukka, M.; Fustero, S.; Fülöp, F. *Chem. – Asian J.* **2016,** *11,* 3376. doi:10.1002/asia.201601046
38. Pasco, M.; Moumné, R.; Lecourt, T.; Micouin, L. *J. Org. Chem.* **2011,** *76,* 5137. doi:10.1021/jo2001512
39. Davies, S. G.; Fletcher, A. M.; Frost, A. B.; Roberts, P. M.; Thomson, J. E. *Org. Lett.* **2015,** *17,* 2254. doi:10.1021/acs.orglett.5b00880

License and Terms

BEILSTEIN JOURNAL OF ORGANIC CHEMISTRY

Hydrolysis, polarity, and conformational impact of C-terminal partially fluorinated ethyl esters in peptide models

Vladimir Kubyshkin* and Nediljko Budisa*

Full Research Paper

Open Access

Address:
Biocatalysis group, Institute of Chemistry, Technical University of Berlin, Müller-Breslau-Strasse 10, Berlin 10623, Germany

Email:
Vladimir Kubyshkin* - kubyshkin@win.tu-berlin.de; Nediljko Budisa* - nediljko.budisa@tu-berlin.de

* Corresponding author

Keywords:
conformation; ester bond; hydrolysis; peptides; polarity

Beilstein J. Org. Chem. **2017,** *13,* 2442–2457.
doi:10.3762/bjoc.13.241

Received: 04 August 2017
Accepted: 19 October 2017
Published: 16 November 2017

This article is part of the Thematic Series "Organo-fluorine chemistry IV".

Guest Editor: D. O'Hagan

Abstract

Fluorinated moieties are highly valuable to chemists due to the sensitive NMR detectability of the ^{19}F nucleus. Fluorination of molecular scaffolds can also selectively influence a molecule's polarity, conformational preferences and chemical reactivity, properties that can be exploited for various chemical applications. A powerful route for incorporating fluorine atoms in biomolecules is last-stage fluorination of peptide scaffolds. One of these methods involves esterification of the C-terminus of peptides using a diazomethane species. Here, we provide an investigation of the physicochemical consequences of peptide esterification with partially fluorinated ethyl groups. Derivatives of *N*-acetylproline are used to model the effects of fluorination on the lipophilicity, hydrolytic stability and on conformational properties. The conformational impact of the 2,2-difluoromethyl ester on several neutral and charged oligopeptides was also investigated. Our results demonstrate that partially fluorinated esters undergo variable hydrolysis in biologically relevant buffers. The hydrolytic stability can be tailored over a broad pH range by varying the number of fluorine atoms in the ester moiety or by introducing adjacent charges in the peptide sequence.

Introduction

Fluorine is a rare element in natural biochemical settings [1]. Notwithstanding several prominent fluoro-organic metabolites in nature [2,3], fluorine is virtually absent from natural biopolymers such as proteins and nucleic acids. Therefore, organofluorine groups lack a natural background in spectroscopic observations of biological samples. This feature is especially beneficial for NMR applications because the sole stable fluorine isotope (^{19}F) has the third largest magnetogyric ratio among the nuclei measured by NMR (after ^{3}H and ^{1}H hydrogen isotopes); as a result, ^{19}F NMR experiments are remarkably sensitive [4].

Fluorine-containing groups can be incorporated into biopolymers by various approaches, including those that utilize biosynthesis [5-7], enzymatic conversion [8], chemical synthesis [9,10], and ligation reactions [11]. Depending on the research target, ^{19}F NMR measurements can be used to study

ligand–protein [12] and protein–protein interactions [13]; membrane proteins [14-16] and membrane-associated peptides [17,18]; equilibria among conformations of RNA [19], DNA [20], and peptide nucleic acids (PNA) [21]; and many others. Particularly recent is the development of peptide-based contrast agents for ^{19}F imaging [22].

In polypeptides, the incorporation of fluorine can significantly alter the properties of the native molecule. The hydrophobicity [23,24], conformational equilibria [25], and the thermodynamic [26-29] and kinetic [30,31] folding profiles can be altered by the presence of even a single fluorinated amino acid in the sequence. Perhaps the most studied molecules exhibiting such effects are the proline analogues, with the proline-to-fluoroproline exchange providing the first proof-of-principle and experimental basis for a number of subsequent conceptual studies [32]. For example, these were used to demonstrate the impact of non-canonical amino acids in proteins [33]. Fluoroproline-containing sequences were also applied as collagen mimics to dissect collagen-stabilizing forces [34,35].

However, the impact of fluorine labeling on polypeptides is still not fully understood and it may appear controversial in the literature. For example, a donor–acceptor type enhancement of the face-to-face stacking of phenyl- and pentafluorophenyl groups has been suggested [36]; though, subsequent studies of α-helical [37], peptoid [38], and collagen-mimicking models [39] did not support this suggestion. Though, this was reported later in a context of a hydrophobic core of model protein structures [40]. Furthermore, the influence of the fluorinated groups on lipophilicity remains uncertain, especially in biochemical literature.

The impact of partially fluorinated alkyl groups on the polarity of small molecules was recently investigated in a series of model studies by Huchet and others [41-44]. These investigations demonstrated the checkmark-shape of the lipophilicity (log*P)* changes upon increasing the number of fluorine atoms in the terminal aliphatic alkyl fragment (Figure 1A; see also remark on page S2 in Supporting Information File 1). While a methyl group is lipophilic, the incorporation of one, two or three fluorine atoms produces a non-additive increase in the molecular dipole. On the other hand, the linear increase in the molecular volume due to the hydrogen-to-fluorine exchange increases the lipophilicity. As the result of these two opposite tendencies, the log*P* value decreases with incorporation of each moiety in the following order: $RCH_3 > RCF_3 > RCHF_2 \geq RCH_2F$. The polarity and lipophilicity are among the most important effects of fluorination, as these parameters strongly impact other important biological properties, such as the potential distribution in biochemical compartments and the metabolic stability [44,45].

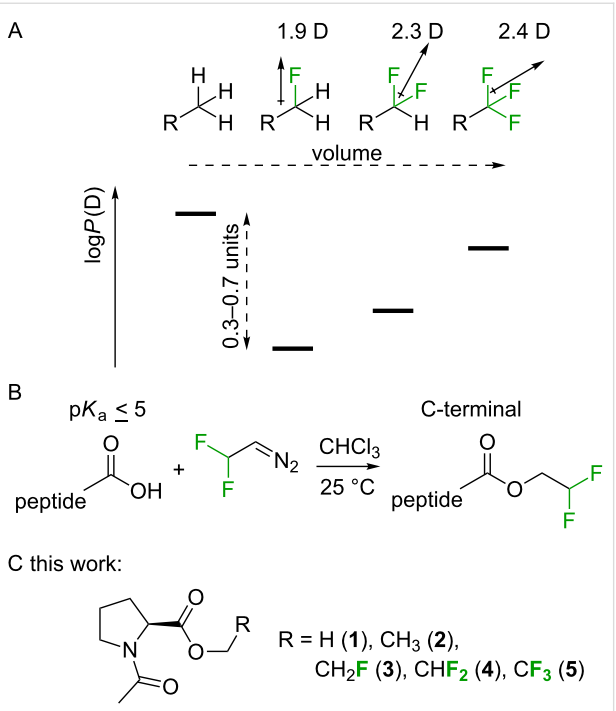

Figure 1: A. Dependence of the lipophilicity (log*P*) on the number of fluorine atoms in a partially fluorinated terminal alkyl group demonstrates a characteristic checkmark-shape [41]. B. Selective labeling of carboxylic acids (C-terminus in peptides) with 2,2-difluorodiazoethane yields 2,2-difluoroethyl esters [46]. C. Esters of *N*-acetylproline studied herein.

Considering the variety of spectroscopic applications, a labeling strategy that allows specific incorporation of a fluorinated moiety into a modular peptide fragment is highly desirable. Several recent efforts have been made to achieve this goal [9,47]. Fluorinated diazoalkanes have shown particularly promising results in small molecule functionalization [48], and these have a potential to be used for biomacromolecular functionalization as well [49]. As an example, we recently discovered the selective formation of 2,2-difluoroethyl esters upon treatment of small molecules and peptide substrates with 2,2-difluorodiazoethane (Figure 1B) [46]. The transformation was carried out in chloroform, which certainly limited the substrate scope. Nonetheless, due to the high acidity of the C-terminal carboxylic group [50], a number of C-terminally modified peptides were readily prepared by this method with full conversion. The availability of the C-terminal 2,2-difluoroethanol-esterified peptides also enables the investigation of the impact of partial fluorination on target peptides. Of particular importance are investigations of the hydrolytic stability of the partially fluorinated esters and the possible conformational impact on the peptide. Thus, we herein report results from

studies of *N*-acetylproline esters, which were used as models for C-terminally modified peptides (Figure 1C). In addition, the conformational impact is examined using several oligopeptides.

Results and Discussion

Synthesis

The synthesis of the C-terminal esters was performed starting from *N*-acetylproline (**6**), which was prepared as described previously [50]. The reference methyl and ethyl esters **1** and **2** were prepared by stirring of **6** in acidic alcohol (methanol or ethanol, respectively) at room temperature overnight (Scheme 1A). We attempted to employ the same procedure for esterification of **6** in trifluoroethanol. However, this resulted in a very low yield of the desired product **5** (4%). The monofluoro- and trifluoroethyl esters **3** and **5** were then prepared via the corresponding chloranhydride, which was generated as described (Scheme 1B) [51]. The drawback of this method is that generation of chloranhydride from *N*-acetylated proline leads to partial epimerization of the residue.

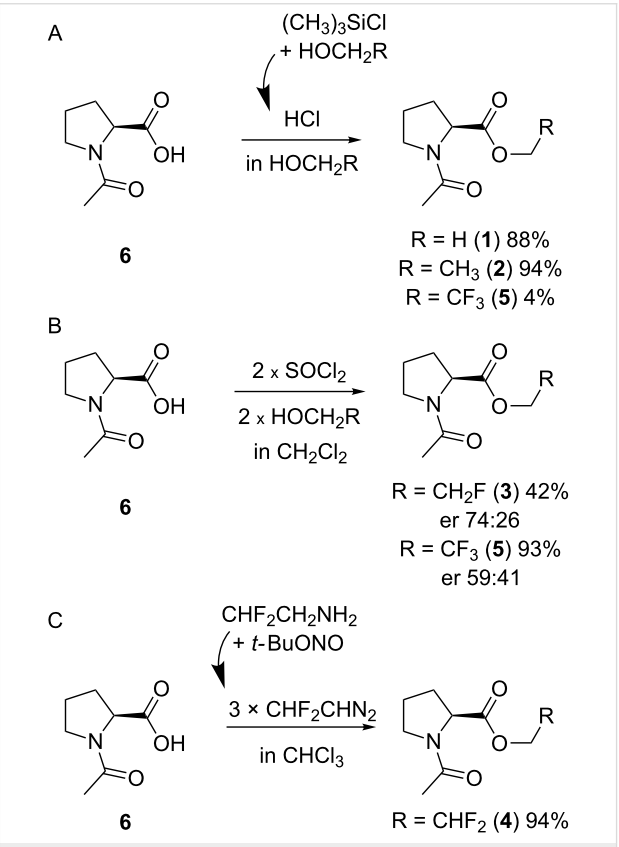

Scheme 1: Synthesis of the model compounds.

Finally, ester **4** was prepared by treatment of **6** with 3 equivalents of the 2,2-difluorodiazoethane (Scheme 1C). The reaction was performed smoothly using chloroform as a solvent giving a good yield (94%). We also attempted to perform the reaction in an acetonitrile/water (1:1) mixture. However, only a very low yield (15%) was obtained with 2,2-difluorodiazoethane generated directly in the solvent mixture. Therefore, we tried generating 2,2-difluorodiazoethane in acetonitrile with subsequent addition of this solution to an aqueous solution of the substrate. Although the yield increased, it remained low (20%). The poor yields in the aqueous medium are explained by the high reactivity of the diazomethane species, which favors nonspecific reactions in water [52]. Very recently, more specific diazomethane reagents for water-tolerant esterification have also been developed [53]. During the revision of this paper Peng et al. reported on esterification of carboxylic acids using 2,2-difluorodiazoethane, which was performed in a number of aprotic organic solvents, including acetonitrile [54].

Hydrolytic stability

The kinetic stability of the ester linkage in the aqueous medium is of critical importance, as it further defines the time window for the reactions with the corresponding esters under the biologically relevant conditions of aqueous buffers. Hydrolysis of the C-terminal esters has been fairly well described in the literature [55-57], indicating the hydrolysis occurs via a pseudo-first order reaction in a buffered medium assuming that [HO^-] is constant (Equations 1–3):

$$\mathrm{AcProOCH_2R + HO^- \longrightarrow AcProO^- + HOCH_2R}$$

$$-\frac{\mathrm{d[AcProOCH_2R]}}{\mathrm{dt}} = k[\mathrm{HO^-}][\mathrm{AcProOCH_2R}] = k_{\mathrm{apparent}}[\mathrm{AcProOCH_2R}] \quad (1)$$

$$k_{\mathrm{apparent}} = k[\mathrm{HO^-}] \quad (2)$$

$$\tau_{1/2} = \frac{\ln 2}{k_{\mathrm{apparent}}} \sim \frac{1}{[\mathrm{HO^-}]} \quad (3)$$

Particularly interesting is the dependence of the hydrolysis rate on the nature of the alkyl group of the ester; it has been demonstrated that ethyl esters hydrolyze approximately 2–3 times slower compared with the methyl esters [58], whereas methyl esters hydrolyze approximately 30 times slower compared with the 3'-tRNA esters in aminoacyl-tRNA [59]. Clearly, the hydrolysis rate depends on the electron donating/withdrawing effect of the alkyl moiety R, indicating a significantly compromised kinetic stability is likely for the partially fluorinated ester groups.

Next, we determined the half-life values following the above mentioned kinetic model for esters **1**–**5** in aqueous medium at

pH 11 and 298 K (Figure 2). In accordance with previous reports, we found that the ethyl ester hydrolyzed 3 times slower compared with the methyl ester, whereas the introduction of the first fluorine atom dropped the half-life by a factor of approximately 8. For the subsequent fluorine atoms, the hydrolysis rate increased by a factor of 3–4 for each appended fluorine atom. The trifluoroethyl ester **5** delivered the fastest hydrolysis rate with a half-life of only 6.4 ± 1.7 min. Extrapolation to pH 8.0 gives a value of 107 ± 28 hours. (This procedure requires multiplication by 1000.) We experimentally determined the half-life of **5** at pH 8 to be 102 ± 2 hours, which agrees well with the extrapolation. The mutual consistency of the values determined with different kinetic modes (minutes at pH 11, days at pH 8) provides a good indication of their accuracy.

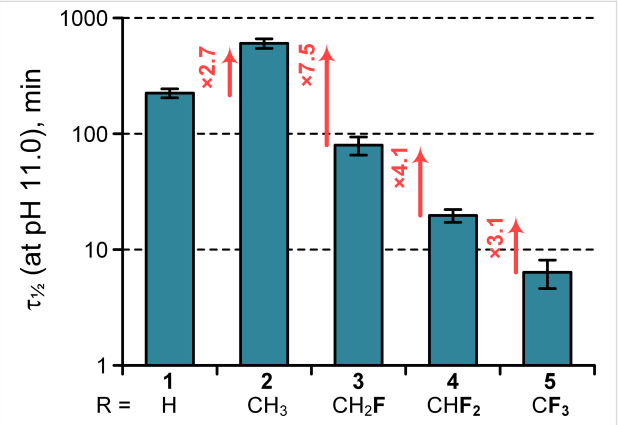

Figure 2: Kinetics of the C-terminal ester hydrolysis.

These data show that chemical modification with the terminally fluorinated ethyl esters **3**–**5** is possible over the course of days at physiologically relevant pH < 8. In fact, this stability enables further determination of several physicochemical properties for the examined compounds in water; for example, partitioning can be safely measured. It is also notable that the hydrolysis rate of the C-terminal trifluoroethyl or difluoroethyl esters may suggest a mechanism of self-cleavage for a potential drug molecule under physiological conditions, in addition to the most common path mediated by the esterases [60]. Though, the susceptibility of the fluorine-bearing esters towards natural esterases is still unknown, and systematic investigation of this issue is lacking in the literature. Notably, pH-programmed decomposition of fluoro-organic molecules has been recently reported for few other cases [61,62].

Lipophilicity

To characterize the lipophilicity, esters **1**–**5** were subjected to 24 hours of partitioning between octan-1-ol and water at 298 K. The resulting partition is illustrated in Figure 3. In accordance with previous observations, the log*P* values exhibit the checkmark-shape: the lipophilicity decreased with the introduction of the first polar C–F bond, and with the introduction of subsequent fluorine atoms, the lipophilicity increased due to the increase in molecular volume. The lipophilicity of 2,2-difluoroethyl derivative **4** is nearly identical to that of parent ethyl ester **2**, and the relative difference in the log*P* from the increase (**5** vs **4**, Δlog*P* = +0.53 ± 0.13) and decrease (**3** vs **4**, Δlog*P* = −0.45 ± 0.13) in the number of fluorine atoms are equivalent to one methyl group difference (**2** vs **1**, Δlog*P* = +0.44 ± 0.08). The amplitude of the change is similar to that reported recently for the corresponding fluorinated ethanols [63]. Importantly, C-terminal esterification maintains a much higher lipophilicity compared with the C-terminal amide **7** (Table 1).

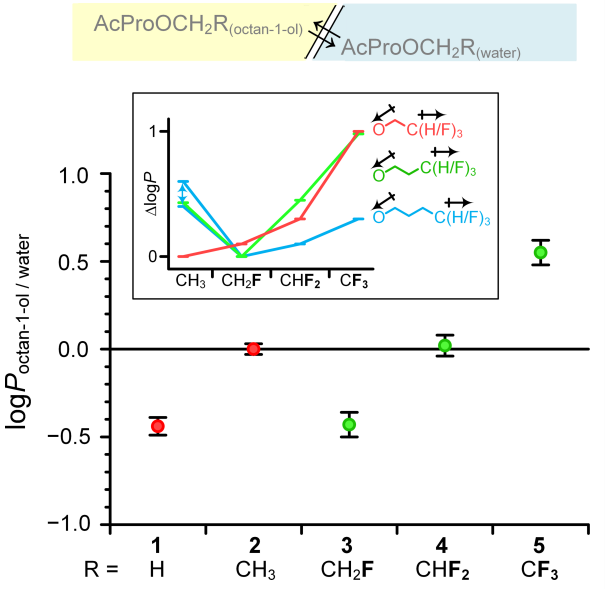

Figure 3: Partitioning of the esters **1**–**5** between octan-1-ol and water. Insert: comparison with the other partially fluorinated propoxy and methoxy groups from references [41,44].

The observed checkmark shape differs from that previously reported for an isolated partially fluorinated methyl group at the end of a saturated aliphatic chain. In the latter case, the methyl group is the most lipophilic, more than a trifluoromethyl group; and the same has been reported for the partially fluorinated propyl ethers $OCH_2CH_2CF_nH_{3-n}$ (log*P*: $CH_3 > CF_3 > CHF_2 \geq CH_2F$) [41,44] (see insert on Figure 3). In contrast, among the partially fluorinated methyl ethers OCF_nH_{3-n}, the lipophilicity of the methoxy group is the lowest, while the fluoromethoxy group is the most lipophilic (log*P*: $CF_3 > CHF_2 > CH_2F \approx CH_3$) [44,64]. These differences were explained by the mutual intramolecular compensation of the C–O dipole and the dipole from the partial fluorination [65]. Thus, the polar effect from the fluorine-bearing region becomes less prominent as the number of the C–C bonds to the polar fragments decreases. The

Table 1: Summarized properties of the analyzed compounds as determined by NMR at 298 K.

compound		$\tau_{1/2}$, min (aq buffer)	log*P* (octan-1-ol/water)
1	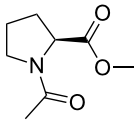	224 ± 20 (pH 11.0)	−0.44 ± 0.05
2	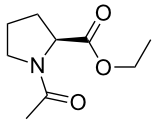	603 ± 58 (pH 11.0)	0.00 ± 0.03
3	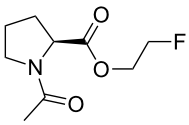	80 ± 14 (pH 11.0)	−0.43 ± 0.07
4	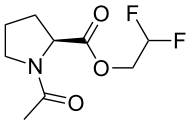	19.7 ± 2.5 (pH 11.0)	+0.02 ± 0.06
5	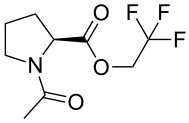	6.4 ± 1.7 (pH 11.0) 6112 ± 70 (pH 8.0)	+0.55 ± 0.07
7	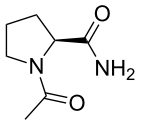	–	−1.57 ± 0.10

partially fluorinated ethoxy moieties reported here represent an intermediate situation between the partially fluorinated methoxy and propoxy/higher alkoxy groups (log*P*: $CF_3 > CHF_2 \approx CH_3 > CH_2F$).

Amide isomerism

The tertiary amide bond in *N*-acylprolyl can exist in two conformational states, s-*trans* and s-*cis* (Scheme 2), with the former being thermodynamically preferred in most cases [66,67]. The intrinsic contextual preference in the amide isomerism around the proline residue is usually characterized using small molecular models such as esters of *N*-acetylproline, similar to those in this study [35,68,69]. Within this model, the *trans*-amide prevalence is not large, and both rotameric states are readily observed in NMR spectra. In the *N*-acylprolyl models, the nature of the terminal groups can influence the amide isomerism. The most important factor is the presence of the C-terminal charge, which reduces the *trans*-amide stability [50,70]. Nonetheless, when the charge is eliminated, the influence of the C-terminal moiety may become negligible. For instance, we recently observed identical parameters for the amide rotation around the glycyl–prolyl amide bond in $AcGlyGlyProGlyGlyNH_2$ [71] and AcGlyProOMe [68] compounds when measured in deuterium oxide.

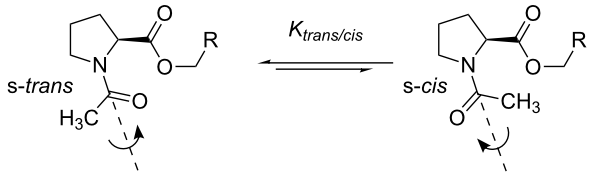

Scheme 2: Amide isomerism in the *N*-acetylprolyl fragment.

For **1**–**5**, we found the *trans/cis* ratios ≈ 5 for all five esters when measured in aqueous medium; the kinetic parameters of the amide rotation were also nearly identical (Table 2). We then noticed that the *trans/cis* ratios measured for the fluorine-labeled esters **3**–**5** in nonpolar solvents (such as benzene) were systematically higher relative to the reference compounds **1** and **2**. We tested the relative increase in the *trans*-amide preference $\Delta\Delta G$ as a function of solvent (Equation 4) and found a dependence of this parameter on the dielectric constant, as would be expected from an electrostatic interaction between the polar alkoxy group and the amide moiety (Figure 4).

$$\begin{aligned}&\Delta\Delta G(-\mathrm{R1}/-\mathrm{R2};\mathrm{solvent})\\&=\Delta G_{trans/cis}(-\mathrm{R1})-\Delta G_{trans/cis}(-\mathrm{R2})\\&=-RT\ln\frac{K_{trans/cis}(-\mathrm{R1})}{K_{trans/cis}(-\mathrm{R2})}\end{aligned}\tag{4}$$

A somewhat similar situation has been recently reported by Siebler et al. for the C-terminal amide in dimethylamido *N*-acetylproline, where the conformational equilibrium rendered the s-*cis* conformation remarkably more polar compared with the s-*trans* counterpart (Scheme 3A), which leads to an elevated *trans/cis* ratio in nonpolar solvents such as dioxane and chloroform [72]. In contrast to this situation, in methyl ester **1**, the dependence of the *trans/cis* ratio on the solvent is known to be marginal [73,74].

To explain the elevated *trans/cis* ratio observed with partially fluorinated esters **3**–**5**, we simulated the dipolar moment of compound **5** by DFT modelling. The dipolar moment for the lowest energy structure predicted a strong preference in favor of the less polar s-*cis* conformation ($\Psi = +101$, $\mu = 2.3$ D) over the s-*trans* ($\Psi = +157$, $\mu = 5.8$ D; Scheme 3B). Semi-empirical simulation of the four-state model (see Scheme 3A) also predicted a higher polarity for the s-*trans* conformational states ($\mu = \parallel 4.6, \perp 7.1$ D) compared to the s-*cis* ($\mu = \parallel 4.7, \perp 3.7$ D)

Table 2: Summarized conformational properties of the compounds **1**–**5** as measured by NMR.

	structure	amide isomerism					α-CH multiplicity:[a] dd, J_{HH} = Hz			
		in D_2O			in C_6D_6		in D_2O		in C_6D_6	
		$K_{trans/cis}$[a]	$k \cdot 10^3$, s^{-1} (310 K)[b]		$K_{trans/cis}$[a]	$k \cdot 10^3$, s^{-1} (298 K)[b]				
			trans→ *cis*	*cis*→ *trans*		*trans*→ *cis*	*cis*→ *trans*	*trans*	*cis*	*trans*	*cis*
1	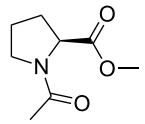	4.94 ± 0.05	7.0 ± 0.5[c]	33 ± 2[c]	5.10 ± 0.10	67 ± 2	342 ± 10	8.5, 4.7	8.7, 2.5	8.1, 3.7	8.6, 2.6
2	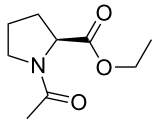	4.60 ± 0.08	6 ± 1	20 ± 5	4.67 ± 0.03	67 ± 2	309 ± 14	8.7, 4.5	8.8, 2.4	8.3, 3.6	8.5, 2.7
3	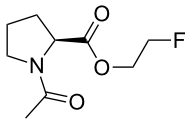	4.74 ± 0.04	7 ± 1	30 ± 2	6.80 ± 0.04	52 ± 2	348 ± 11	9.1, 4.6	8.9, 2.7	8.2, 4.2	8.4, 2.6
4	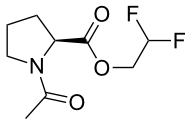	4.95 ± 0.05	7 ± 1	32 ± 4	9.06 ± 0.26	47 ± 2	430 ± 17	9.3, 4.7	8.8, 2.5	8.0, 3.9	8.7, 2.5
5	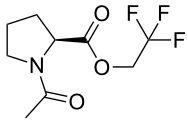	5.48 ± 0.14	6 ± 1	35 ± 5	10.04 ± 0.15	48 ± 2	477 ± 13	9.2, 4.7	8.8, 2.4	8.0, 4.1	8.7, 2.6

[a]Determined in ^1H (and ^{19}F) one-dimensional NMR spectra, analyte 50 ± 10 mM, 298 K; [b]measured by ^1H and $^{19}F\{^1H\}$ EXSY NMR at 50 ± 10 mM analyte concentration; [c]as reported in [69].

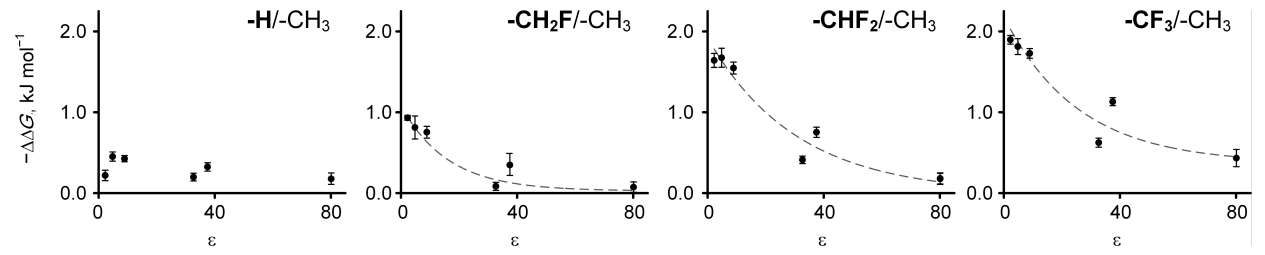

Figure 4: Enhancement of the *trans/cis* thermodynamic preferences in the ester models as a function of the solvent dielectric constant, ε. The *trans/cis* ratios were determined from the ^1H and ^{19}F NMR spectra at 298 K. Solvent set: C_6D_6, $CDCl_3$, CD_2Cl_2, CD_3OD, CD_3CN, D_2O. For details see Table S1 in Supporting Information File 1.

counterpart due to the conformational contribution of the terminal fluorinated moiety. Both predictions clearly contradict the experimentally observed tendencies.

A possible problem with the existing models is that they assume a defined orientation for the fluorine-bearing moiety. However, this moiety may be rather flexible, similar to the parent esters **1** and **2**. This conclusion is suggested by the log*P* differences between esters **3**–**5**, which are nearly identical to those between the parent alcohols (mono, di- and trifluoroethanols) [63,75]. It is therefore apparent that in contrast to **1** and **2**, a more complex equilibrium should be considered for compounds **3**–**5** that

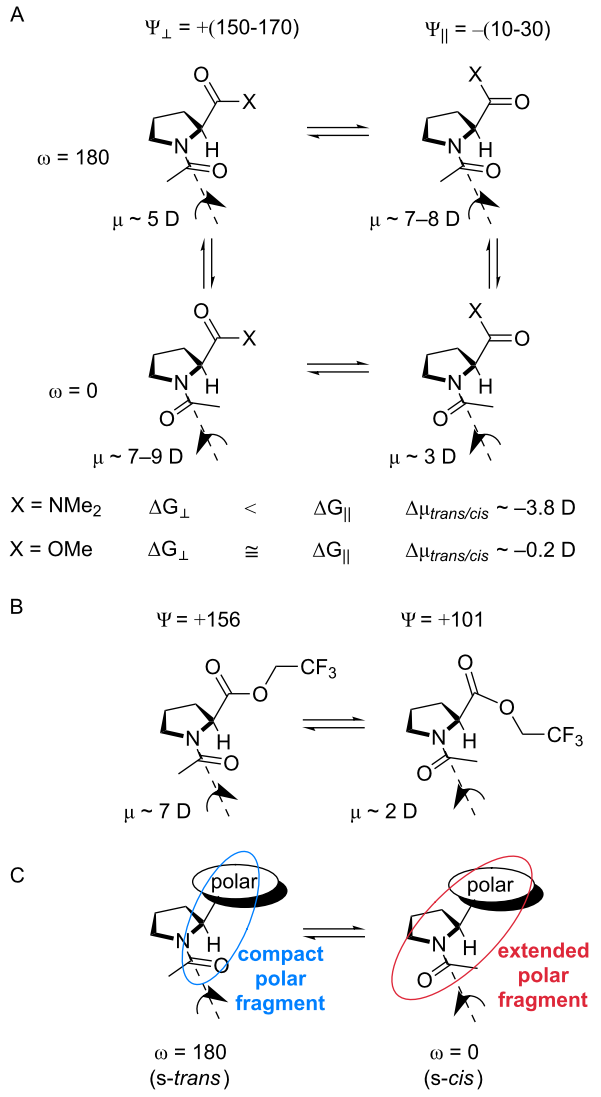

Scheme 3: A. Four-state conformational equilibrium model used by Siebler et al. [72] for explanations of the elevated *trans/cis* ratio in non-polar solvents, which occurs for X = $N(CH_3)_2$ and does not occur for X = OCH_3. B. The two-state lowest energy model. C. The simplistic explanation of the C-terminal polarity effect observed for the partially fluorinated esters **3**–**5**.

involves at least three mutually orienting dipoles in a complex energy landscape. This may be very challenging for computational analysis since the amplitude of the effect is only ≤2 kJ mol^{-1}. At this point, we can propose a simplistic perception of this complex interaction based on the fact that in the s-*trans* conformation, the amide carbonyl group is moved towards the carboxyalkyl moiety, which increases the interaction between the mutually orienting dipoles within a more compact structure (Scheme 3C). As the result, the gradual increase in the polarity from the most distant partially fluorinated moiety leads to an increase in the effect in the order **3** < **4** < **5** (Figure 4).

An alternative explanation for the elevated *trans/cis* ratio is strengthening of the n→π* interaction between the carbonyl groups. For example, Hodges and Raines reported elevated *trans/cis* ratios in phenyl esters of *N*-formylproline containing electron withdrawing substituents (X in Scheme 4A) when measured in chloroform [76]. The *trans*-amide preference was enhanced by 2.2 kJ mol^{-1} for X = NO_2 relative to X = $N(CH_3)_2$. Thus, it is possible that in the case of the esters **3**–**5**, the electron-withdrawing effect of fluorine atoms leads to a similar enhancement of the n→π* interaction between the carbonyl groups due to the higher electrophilicity of the carboxyl carbon atom (Scheme 4B). Nonetheless, this explanation does not explain why, despite the electrophilicity of the carboxyl group indicated by the hydrolysis experiments (Figure 2), the exchange of the ethyl group by the methyl group enhances the hydrolysis rate while only marginally impacts the *trans/cis* ratio. Furthermore, it is unclear why a polar solvent quenches the enhancement of the electrophilicity of the C-terminal carbonyl, which requires the differential solvation of two rotamers. This differential solvation may be explained by the polarity of the two rotamers; thus, the polarity model expressed in Scheme 3 cannot be dismissed.

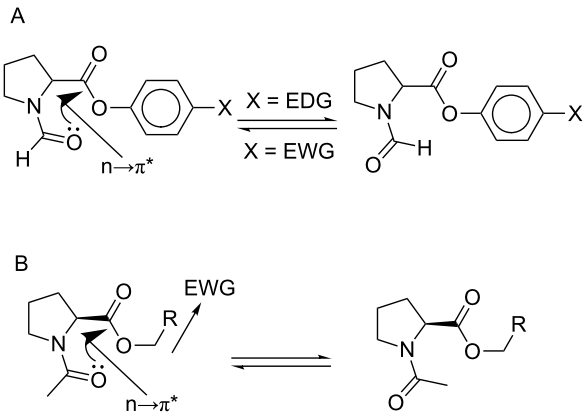

Scheme 4: Elevation of the *trans/cis* ratio in derivatives of *N*-acyl proline may result from the enhanced n→π* interaction between the carbonyl-groups. EWG = electron-withdrawing group, EDG = electron-donating group.

Additional factors, such as multipolar interactions [77] and especially the polar surface exposure [78], may also be considered. Further understanding of the relevant interactions requires more detailed studies and experimental models. Nonetheless, the experimental observations and the simple description proposed herein (Scheme 3C) suggest that the amide bond of the *N*-acetylproline fragment can function as an intramolecular probe of the C-terminal ester group polarity. Notably, the predicted flexibility of the partially fluorinated alkoxy groups in the presence of other strong dipoles is inconsistent with the

concept of conformational adaptors elaborated by Müller et al. quite recently [44,65].

Side chain conformation

The side-chain conformations of proline are restricted by the pyrrolidine ring structure. The two main envelope conformations are *exo*- and *endo*- (alternatively designated as *up*-/*down*-, respectively), in which by the C^4-ring atom is oriented toward or away from the carboxyl group orientation, respectively [79,80]. This conformational equilibrium manifests in the χ angles, which is reflected by the *J*-coupling observed between the α-CH and β-CH_2 groups in the ^{1}H NMR spectra ($J_{\alpha\beta}$) [81,82]. A recent analysis of the $J_{\alpha\beta}$ values by Braga et al. was used to quantify the pucker equilibrium in compound **1** [74]. We examined the values of $J_{\alpha\beta}$ for compounds **1**–**5** in a polar (deuterium oxide) and nonpolar (benzene-d_6) solvents. The observed $J_{\alpha\beta}$ values are consistent with those reported previously [74,83], and the value differences likely reflect a change of only a few percent due to the contribution from the two conformations. This result indicates that the C-terminal partially fluorinated ester has a negligible influence on the side chain conformation of the prolyl moiety.

Conformation of short oligopeptides

We then examined how the properties observed this far impact the conformational properties of a peptide chain. As described above, the C-terminal charge has a large effect on the stability of the *trans*-amide alignment of the peptide bond. It has been demonstrated that removing the terminal charge enhances the stability of the polyproline-II helical fold in collagen-mimicking [84] or polyproline sequences [70] and significantly shifts the equilibrium of short model sequences in favor of the polyproline-II over the β-structure conformation [85]. Reaction with 2,2-difluorodiazoethane esterifies and thus eliminates the charge of the C-terminal carboxyl group, thereby enhancing the polyproline-II stability. This effect contrasts with the effects of other terminal modifications, such as aromatic amino acids, which reduce the polyproline-II fold stability [86].

We then prepared hexaproline peptide **8a**, which was subsequently esterified with the diazomethane reagent to give **8b**. Methyl ester **8c** was also prepared for comparison (Scheme 5A). Measured circular dichroism (CD) spectra for the hexapeptides **8a**–**c** (Figure 5, top) demonstrate strong negative bands at 204 nm and weak positive bands at 227 nm, which indicate a polyproline-II fold. Remarkably, this spectral shape was observed for all three hexaproline peptides **8a**–**c**, while some increase of the negative band amplitude was only observed for the methanol samples. Overall, this model suggests a small conformational impact from the C-terminal 2,2-difluoroethylation or methylation as compared to the parent peptide **8a**.

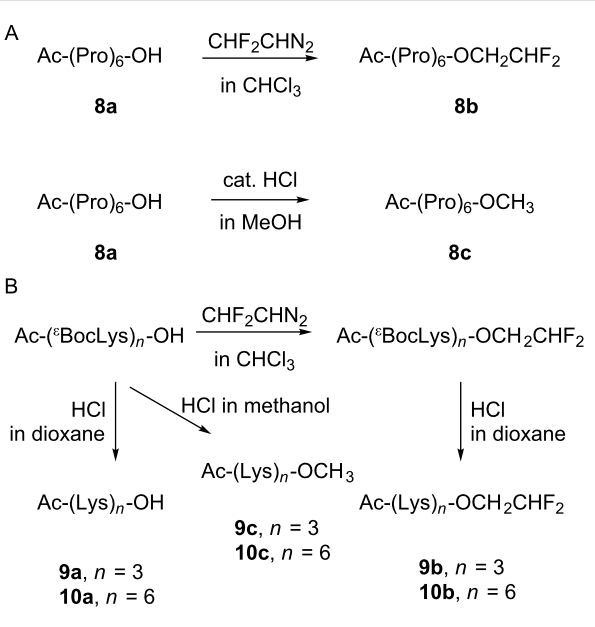

Scheme 5: Synthesis of the model peptides.

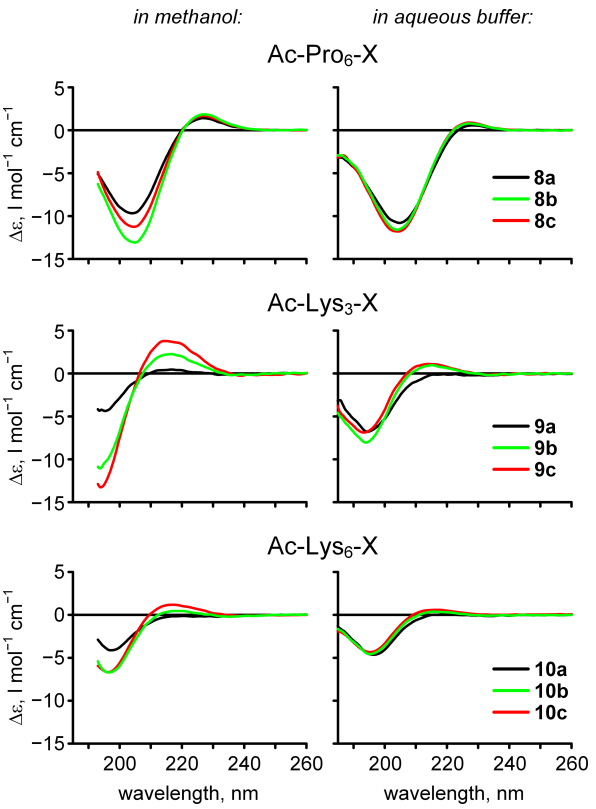

Figure 5: Mean residue molar circular dichroism (Δε) of peptides **8**–**10** in methanol (left) and aqueous phosphate buffer (right, 50 mM buffer, pH 7.0) samples. Recorded at 298 K and 100 μM peptide.

These findings motivated assessment of a model system with a more dynamic structure. For example, it has been shown that

oligolysine sequences favor a polyproline-II fold in short stretches [87]. We prepared tri- and hexalysine peptides without (**9a**, **10a**) and with (**9b**, **10b**) the C-terminal difluoroethyl ester, as well as the methyl esters (**9c**, **10c**) as shown in Scheme 5B. The CD spectra of these peptides (Figure 5) revealed a negative band at ≈195 nm and a band at ≈216 nm, thus enabling measurement of the conformational impact. This band was clearly positive for the esterified peptides **9b**,**c** and **10b**,**c** in contrast to the parent non-esterified peptides **9a** and **10a**. This is especially seen in the shortest trilysine sequence, where the esterification significantly increases the charge density, and thus the extended polyproline-II helix can be stabilized via the charge repulsion forces. Longer hexalysine sequences exhibited the same effect, albeit to a lower extent. Predictably, the C-terminal charge has a decreasing effect as the length of the peptide increases.

An independent refinement of these conclusions can be found in diffusion measurements conducted by ^{1}H DOSY (diffusion ordered spectroscopy). We previously applied a simple set of equations for estimation of the diffusion coefficients of an oligomeric hydrophobic polyproline-II helix [71]. Here, we combined these equations in order to derive Equation 5, which describes diffusion as a function of molecular weight assuming pure deuterium oxide solution at 298 K. This equation considers molecules to be rigid spheres, as it is based on the Stokes–Einstein relationship. The 'coil' state significantly contributes to the conformational flexibility, which results in a diffusion deceleration [88]. We used the simple criterion of the difference between the experimental log*D* and the 'theoretical' log*D* derived from Equation 5 (MW – molecular weight in Da, log*D* in log m^2 s^{-1}) (Figure 6). The increase in these values indicates a 'coil' contribution in the molecular conformation. However, it should be kept in mind that the diffusion data describes the overall disorder of the peptide body, including the side chain conformations; in contrast, CD represents only the backbone.

$$\log D_{\text{theor.}} = -8.524 - \frac{1}{3}\log(\text{MW} + 8.9) \qquad (5)$$

The diffusion data (Figure 6) indicated that the hexaproline peptides **8a**–**c** are rather rigid, the trilysine peptides **9a**–**c** are somewhat more flexible, and the hexalysine peptides **10a**–**c** are characterized by remarkable molecular disorder. In all cases, the C-terminal esterification reduced the level of disorder, although, the effect is hardly distinguishable from experimental error values. Overall, these results demonstrate that the side-chain disorder may play a more significant role in the peptide diffusion properties, than the backbone rigidity induced by an eliminated terminal charge.

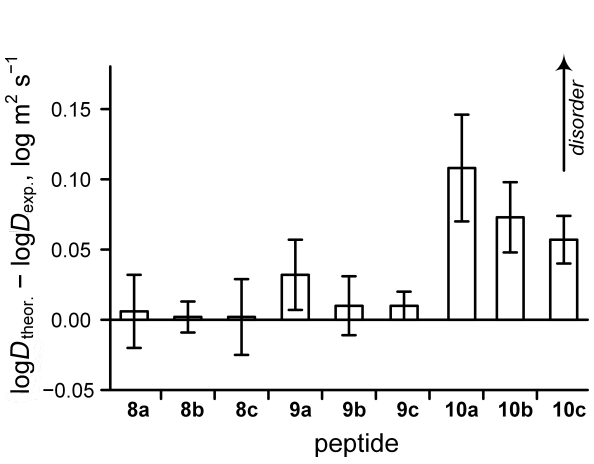

Figure 6: Conformational analysis of the peptides by ^{1}H DOSY NMR (D_2O, 298 K). The theoretical values were calculated according to Equation 5 assuming deuterium oxide viscosity and 298 K.

The conformational impact of the C-terminal esterification described here is also expected to be generic, as the polyproline-II structure is preferred by various oligopeptide sequences [89,90] and is highly abundant in the unfolded protein states [91].

Hydrolytic stability in peptides

Finally, we tested hydrolytic stability in esterified peptides **8b**, **9b** and **10b** by observing hydrolysis of the ester using ^{19}F NMR in buffered deuterium oxide (pH 7). We expected pseudo-first order kinetics as for the hydrolysis of esters **1**–**5** at pH 11. Nonetheless, for the peptide esters **8b**, **9b** and **10b**, the experimental decay (Figure 7) of the ester concentration resembled pseudo-zero order kinetics, which was also observed for another amino acid ester hydrolysis not shown here.

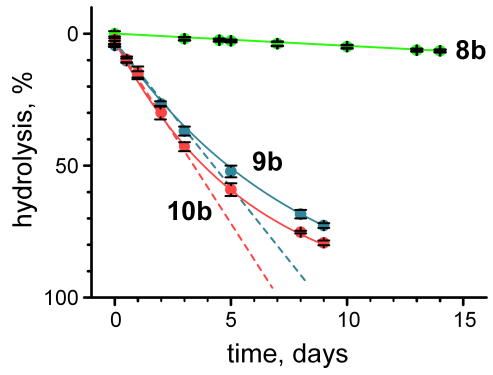

Figure 7: Hydrolysis of the C-terminal 2,2-difluoroethyl esters of the oligopeptides in buffered deuterium oxide at 298 K and pH 7. Dashed lines reflect the pseudo zero-order kinetic behavior of hydrolysis during the initial stages of this process.

Both fittings to the zero (Equations 6 and 7) and first order (Equations 1–3) kinetic models demonstrated fairly good agreement with each other (see Experimental).

$$-\frac{\mathrm{d[peptideOCH_2CHF_2]}}{\mathrm{dt}} = k_{\mathrm{apparent}} \quad (6)$$

$$\tau_{1/2} = \frac{1}{2k_{\mathrm{apparent}}} \quad (7)$$

Notably, the half-life (Equation 7) of oligoproline **8b** (152 ± 14 days) demonstrated a good agreement with the half-life of monoproline peptide **4** extrapolated to pH 7.0 (137 ± 17 days). The half-life values for the oligolysine peptides **9b** and **10b** were much shorter at 5.0 ± 0.5 and 4.0 ± 0.3 days, respectively. These results can be explained by the increased local concentration of negatively charged hydroxide ions resulting from the positive charge, which causes ester hydrolysis. The accelerated hydrolysis of oligolysine esters can potentially lead to partial 2,2-difluoroethyl ester hydrolysis during the CD sample handling, and thus explain somewhat reduces CD intensity compared to the methyl ester samples (Figure 5).

This result also suggests that the hydrolysis rate of a C-terminal ester in peptides can be well tailored by installing proximal charges in the molecule. This conclusion is of particular importance due to growing interest in modifying potential peptide therapeutics with positively charged residues for improved cell permeability [92]. Though, the charge-induced hydrolysis acceleration from the proximal lysine charge (**9b**, **10b** vs **8b**, factor ≈ 30) is lower than the α-NH_2/NH_3^+ hydrolysis acceleration in the classical studies of α-amino acid esters (factor ≈ 100–150) [58]. The hydrolysis rate can thus be further tuned by changing the proximity of the positive charge to the ester group. Further investigations of the peptide ester hydrolysis catalyzed by the proximal charges may be very beneficial for understanding of the role of ribosome electrostatics during translation termination [93,94], which is an ester hydrolysis reaction performed by bulk water [95].

Conclusion

We have described the properties of C-terminal partially fluorinated ethyl esters of *N*-acetylproline. The hydrolytic stability decreases up to two orders of magnitude as the number of fluorine atoms in the ester group increases. Furthermore, the measured lipophilicity values follow the characteristic checkmark-shape, while the side chain conformation was not affected. The amide isomerism remained unchanged in polar aqueous medium. Conversely, in the nonpolar solvents, the equilibrium between the two conformers was shifted toward a more compact arrangement of the polar groups in the s-*trans* rotamer.

In oligopeptides, the C-terminal 2,2-difluoroethylation increased the polyproline-II structural contribution. The effect was seen most prominently in a short oligolysine peptide. The hydrolytic stability of the ester bond in the peptide depends on the charge of the peptide, as it was impaired in the positively charged oligolysine peptides compared with the neutral oligoproline. These results suggest the potential application of late-stage C-terminal esterification with partially fluorinated groups as a tool in peptide and therapeutic design, as well as in ^{19}F NMR applications.

Experimental

Synthesis of model compounds

Esterification in acidic alcohols

N-Acetylproline (150 mg, 0.95 mmol) was dissolved in absolute alcohol (methanol, ethanol or 2,2,2-trifluoroethanol, 2 mL) and trimethylsilyl chloride (0.1 mL, 0.8 mmol) was added. The mixture was stirred for 21 hours at room temperature, solvent was removed under reduced pressure, and the crude material was purified on a short silica gel (≈11 g) column using an ethyl acetate/methanol 39:1 as the eluent. 143 mg of **1** was obtained as a clear oil (yield 88%), R_f = 0.53 (ethyl acetate/methanol 39:1). 167 mg of **2** was obtained as a clear oil (yield 94%), R_f = 0.61 (ethyl acetate/methanol 39:1). 10 mg of **5** was obtained as a clear oil (yield 4%), R_f = 0.74 (ethyl acetate/methanol 39:1).

Esterification via chloranhydrides

Compound **3**: *N*-acetylproline (101 mg, 0.64 mmol) was dissolved in anhydrous dichloromethane (3 mL) and the resulting solution was cooled down in an ice bath. Thionyl chloride (0.1 mL, 1.38 mmol, 2.2 equiv) was added, followed by 2-fluoroethanol (80 µl, 1.38 mmol, 2.2 equiv). The mixture was stirred at ambient temperature for 14 hours. The solvent was removed under reduced pressure, and the resulting crude material was subjected to a silica gel (20 g) column purification using an ethyl acetate/methanol 39:1 eluent. 55 mg of **3** was obtained as a clear oil (yield 42%), R_f = 0.63 (ethyl acetate/methanol 39:1).

Compound **5** was obtained in an analogous procedure to **3** starting from *N*-acetylproline (100 mg, 0.64 mmol), thionyl chloride (0.1 mL, 1.4 mmol, 2.2 equiv) and trifluoroethanol (0.12 mL, 1.6 mmol, 2.5 equiv). 141 mg of the product was obtained as a clear oil (yield 93%), R_f = 0.73 (ethyl acetate/methanol 39:1).

Esterification with diazoalkanes

No special precautions were applied when working with 2,2-difluorodiazoethane except for performing all work in a fume hood and maintaining conventional lab protection.

The procedure in chloroform involved mixing 2,2-difluoroethylamine (160 mg, 1.97 mmol, 3 equiv) in chloroform (5 mL), *tert*-butyl nitrite (90% purity, 260 mg, 2.27 mmol, 3.5 equiv) and acetic acid (2.5 μL, 0.044 mmol, 7 mol %). The resulting yellowish mixture was refluxed for 10 min. The reflux was stopped, and the mixture was allowed to stand at room temperature for 2 min. Then, a solution of *N*-acetylproline (100 mg, 0.64 mmol) in chloroform (1.5 mL) was added. The mixture was stirred at room temperature for the next 12 hours. Volatiles were removed under reduced pressure; the crude material was purified on a short (21 g) silica gel column using ethyl acetate/methanol 39:1 mixture as the eluent. 132 mg of **4** was obtained as a clear oil (yield 94%), R_f = 0.69 (ethyl acetate/methanol 39:1).

The procedure in acetonitrile/water was performed using same proportions as those in the chloroform reaction. The amine and nitrite were mixed in acetonitrile (2.5 mL), followed by the addition of *N*-acetylproline (2 mg) for activation. The mixture was refluxed for 10 min, and after the heating was stopped, this solution was added to a solution of *N*-acetylproline in water (2.5 mL). The mixture was stirred at room temperature for 16 hours. Then, trifluoroacetic acid (0.1 mL) was added, and the mixture was stirred for an additional hour to quench residual diazo compound. The solution was then freeze-dried. Purification of the crude material on a silica gel column afforded 30 mg of **4** as a clear oil (yield 20%). When the diazo compound was generated in an acetonitrile/water (1:1) mixture (4.5 mL), no heating was applied, and *N*-acetylproline was added to the yellowish mixture 5 min after mixing the amine with the nitrite. From this run, 21 mg of **4** was isolated after silica gel purification (yield 15%).

Physical chemistry

Hydrolytic stability

Aqueous potassium phosphate buffer (100 mM) at pH 11.0 or 8.0 was mixed with 1:10 (v/v) deuterium oxide to give 550 μL of 91 mM buffer. The analyte **1**–**5** was added from a 200 mM stock solution in deuterium oxide to give 0.5 mM analyte. The first NMR spectra were collected within 4 min following addition of the analyte. The monitoring was continued by recording ^{1}H and ^{19}F NMR spectra at regular time points until >50% hydrolysis. Ambient temperature was maintained at 298 ± 1 K. The decay of the integral intensity of the analyte was quantified by integration. Plotting the logarithm of the intensity versus time delivered the kinetic constant, which was converted to the half-life time (squared correlation coefficient > 0.90). The experiments were performed in triplicate.

Partitioning

To 4–5 mg analyte, octan-1-ol (1.00 mL) and deionized water (1.00 mL) were added. The mixture was shaken gently at ambient temperature (298 ± 2 K) for 24 hours. Each phase (200 μL) was sampled using identical NMR tubes, and acetonitrile-d_3 (300 μL) was added to each sample. The NMR measurements were performed by ^{1}H or ^{19}F detection at 298 K using calibrated 90-degree pulses and one-scan experiments in order to ensure complete pre-relaxation. The same acquisition parameters were used for the octan-1-ol and water samples; for processing, only the zero phase was adjusted. The spectra were baseline corrected, and equivalent resonances were integrated. The ratio between the signal intensities was considered as the partitioning constant. The partitioning experiments were performed in triplicate. Subsequent addition of water and octan-1-ol was performed in forward and reverse manner, and the resulting partitioning constants were identical within experimental error.

Conformational analysis

The amide rotational thermodynamic and kinetic measurements were performed by NMR as described in [50,68]. The equilibrium ratio between the rotameric states was obtained from the ^{1}H, ^{19}F and ^{19}F{^{1}H} (inverse-gated decoupling) spectra at 298 K by integration. The kinetics was measured in ^{1}H and/or ^{19}F{^{1}H} z-cross-relaxation experiments at either 310 K (for deuterium oxide samples) or 298 K (for benzene samples). The $J_{\alpha\beta}$-coupling values were obtained by visual inspection of the α-CH resonances in the ^{1}H NMR spectra, and the accuracy was defined by the length of the time domain spectrum at approximately 0.3 Hz. The semi-empirical calculations were performed by using the PM6 algorithm from the MOPAC package. DFT geometry optimization of the **5** amide rotamers was performed using B88-PW91 GGA with the DZVP basis set.

Characterization of model compounds

^{1}H and ^{13}C NMR spectra were assigned using ^{1}H{^{19}F} inverse-gated decoupled, ^{1}H{^{13}C} dept45, ^{1}H{^{13}C} HSQC, ^{1}H-^{13}C HMBC, ^{1}H NOESY/EXSY and ^{19}F{^{1}H} HOESY experiments. For the minor s-*cis* conformation, only chemical shifts and, when possible, multiplicities are given. The enantiomeric ratio (er) was measured in ^{19}F{^{1}H} inverse-gated decoupled NMR spectra of the dichloromethane-d_2 solutions containing 40 mM analyte (550 μL) recorded upon addition of an equivalent amount of europium(III) tris-[3-(heptafluoropropylhydroxymethylene)-D-camphorate] in the same solvent (200 μL) as the shifting reagent. The spectra were measured at 298 K.

Methyl *N*-acetylprolinate (1): ^{1}H NMR (D_2O, 700 MHz) δ s-*trans*, 4.37 (dd, J_{HH} = 8.5, 4.7 Hz, α-CH), 3.69 (s, 3H, OCH_3), 3.60 and 3.56 (two m, 2H, δ-CH_2), 2.23 and 1.95 (two m, β-CH_2), 2.05 (s, 3H, CH_3C=O), 1.94 (m, 2H, γ-CH_2); s-*cis*, 4.63 (dd, J_{HH} = 8.7, 2.5 Hz, α-CH), 3.73 (s, OCH_3), 3.47 (ddd, J_{HH} = 11.6, 8.5, 3.5 Hz, δ-CH), 3.41 (dt, J_{HH} = 11.4, 8.4 Hz, δ-CH), 2.27 and 2.15 (two m, β-CH_2), 1.93 (s, CH_3C=O), 1.89 and 1.79 (two m, γ-CH_2); $^{13}C\{^1H\}$ NMR (D_2O, 126 MHz) δ s-*trans*, 175.0 (s, CO_2), 173.0 (s, N-C=O), 59.0 (s, α-CH), 52.9 (s, OCH_3), 48.4 (s, δ-CH_2), 29.2 (s, β-CH_2), 24.2 (s, γ-CH_2), 21.2 (s, CH_3); s-*cis*, 174.6 (s, CO_2), 173.4 (s, N-C=O), 60.7 (s, α-CH), 53.2 (s, OCH_3), 46.6 (s, δ-CH_2), 30.6 (s, β-CH_2), 22.3 (s, γ-CH_2), 21.2 (s, CH_3); HRMS (ESI-orbitrap): $[M + H]^+$ calcd for $C_8H_{14}NO_3$, 172.0968; found, 172.0968; $[\alpha]_D^{25}$ −83 (*c* 2.0, $CHCl_3$).

Ethyl *N*-acetylprolinate (2): ^{1}H NMR (D_2O, 700 MHz) δ s-*trans*, 4.34 (dd, J_{HH} = 8.7, 4.5 Hz, α-CH), 4.15 (m, 2H, OCH_2), 3.59 and 3.56 (two m, 2H, δ-CH_2), 2.24 and 1.95 (two m, β-CH_2), 2.04 (s, 3H, CH_3C=O), 1.94 (m, 2H, γ-CH_2), 1.19 (t, J_{HH} = 7.2 Hz, 3H, CH_3); s-*cis*, 4.61 (dd, J_{HH} = 8.8, 2.4 Hz, α-CH), 4.20 (q, J_{HH} = 7.2 Hz, OCH_2), 3.47 (ddd, J_{HH} = 11.5, 8.7, 3.7 Hz, δ-CH), 3.41 (dt, J_{HH} = 11.5, 8.3 Hz, δ-CH), 2.28 and 2.15 (two m, β-CH_2), 1.93 (s, CH_3C=O), 1.90 and 1.80 (two m, γ-CH_2); $^{13}C\{^1H\}$ NMR (D_2O, 176 MHz) δ s-*trans*, 174.7 (s, CO_2), 173.0 (s, N-C=O), 62.6 (s, OCH_2), 59.3 (s, α-CH), 48.5 (s, δ-CH_2), 29.3 (s, β-CH_2), 24.3 (s, γ-CH_2), 21.2 (s, CH_3), 13.2 (s, CH_3); s-*cis*, 174.2 (s, CO_2), 173.3 (s, N-C=O), 63.0 (s, OCH_2), 60.8 (s, α-CH), 46.7 (s, δ-CH_2), 30.7 (s, β-CH_2), 22.3 (s, γ-CH_2), 21.2 (s, CH_3), 13.2 (s, CH_3); HRMS (ESI-orbitrap): $[M + H]^+$ calcd for $C_9H_{16}NO_3$, 186.1125; found, 186.1120; $[\alpha]_D^{25}$ −81 (*c* 2.0, $CHCl_3$).

2-Fluoroethyl *N*-acetylprolinate (3): ^{1}H NMR (D_2O, 500 MHz) δ s-*trans*, 4.63 (dm, J_{HF} = 47 Hz, 2H, CH_2F), 4.41 (dd, J_{HH} = 9.1, 4.6 Hz, 1H, α-CH), 4.37 (ddd, J_{HH} = 5.1, 3.0 Hz, J_{HF} = 30 Hz, 2H, OCH_2), 3.62 and 3.59 (two m, 2H, δ-CH_2), 2.26 and 1.98 (two m, 2H, β-CH_2), 2.05 (s, 3H, CH_3C=O), 1.96 (m, 2H, γ-CH_2); s-*cis*, 4.69 (dd, J_{HH} = 8.9, 2.7 Hz, α-CH), 4.65 (m, CH_2F), 4.43 (m, OCH_2), 3.49 (ddd, J_{HH} = 11.6, 8.6, 3.5 Hz, δ-CH), 3.42 (dt, J_{HH} = 11.4, 8.2 Hz, δ-CH), 2.31 and 2.20 (two m, β-CH_2), 1.95 (s, CH_3C=O), 1.91 and 1.81 (two m, γ-CH_2); $^{13}C\{^1H\}$ NMR (D_2O, 126 MHz) δ s-*trans*, 174.2 (s, CO_2), 173.0 (s, N-C=O), 81.9 (d, J_{CF} = 165 Hz, CH_2F), 64.9 (d, J_{CF} = 19 Hz, OCH_2), 59.1 (s, α-CH), 48.4 (s, δ-CH_2), 29.2 (s, β-CH_2), 24.3 (s, γ-CH_2), 21.2 (s, CH_3); s-*cis*, 173.8 (s, CO_2), 173.4 (s, N-C=O), 82.3 (m, CH_2F), 65.2 (d, J_{CF} = 19 Hz, OCH_2), 60.7 (s, α-CH), 46.6 (s, δ-CH_2), 30.6 (s, β-CH_2), 22.3 (s, γ-CH_2), 21.2 (s, CH_3); ^{19}F NMR (D_2O, 471 MHz) δ −224.3 (tt, J_{FH} = 47, 30 Hz, s-*trans*), −224.6 (tt, J = 47, 30 Hz, s-*cis*); HRMS (ESI-orbitrap): $[M + H]^+$ calcd for $C_9H_{15}FNO_3$, 204.1030; found, 204.1028; $[\alpha]_D^{25}$ −45 (*c* 2.0, $CHCl_3$), er 74:26.

2,2-Difluoroethyl *N*-acetylprolinate (4): ^{1}H NMR (D_2O, 500 MHz) δ s-*trans*, 6.07 (tt, J_{HH} = 3.4 Hz, J_{HF} = 54 Hz, 1H, CHF_2), 4.43 (dd, J_{HH} = 9.3, 4.7 Hz, 1H, α-CH), 4.38 (ddt, J_{HH} = 3.4, 2.1 Hz, J_{HF} = 15 Hz, 2H, OCH_2), 3.61 and 3.58 (two m, 2H, δ-CH_2), 2.27 and 1.99 (two m, 2H, β-CH_2), 2.05 (s, 3H, CH_3C=O), 1.96 (m, 2H, γ-CH_2); s-*cis*, 6.11 (tt, J_{HH} = 3.2 Hz, J_{HF} = 54 Hz, CHF_2), 4.74 (dd, J_{HH} = 8.8, 2.5 Hz, α-CH), 4.44 (m, OCH_2), 3.50 (ddd, J_{HH} = 11.6, 8.6, 3.4 Hz, δ-CH), 3.43 (dt, J_{HH} = 11.5, 8.3 Hz, δ-CH), 2.32 and 2.20 (two m, β-CH_2), 1.95 (s, CH_3C=O), 1.92 and 1.80 (two m, γ-CH_2); $^{13}C\{^1H\}$ NMR (D_2O, 126 MHz) δ s-*trans*, 173.4 (s, CO_2), 173.0 (s, N-C=O), 113.0 (t, J_{CF} = 240 Hz, CHF_2), 63.0 (t, J_{CF} = 27 Hz, OCH_2), 58.9 (s, α-CH), 48.4 (s, δ-CH_2), 29.2 (s, β-CH_2), 24.3 (s, γ-CH_2), 21.1 (s, CH_3); s-*cis*, 173.4 (s, N-C=O), 173.0 (s, CO_2), 113.0 (m, CHF_2), 63.3 (d, J_{CF} = 27 Hz, OCH_2), 60.6 (s, α-CH), 46.6 (s, δ-CH_2), 30.6 (s, β-CH_2), 22.3 (s, γ-CH_2), 21.2 (s, CH_3); ^{19}F NMR (D_2O, 471 MHz) δ −126.92 (dtd, J_{FF} = 292 Hz, J_{FH} = 53, 15 Hz, 1F, s-*trans*), −126.93 (dtd, J_{FF} = 292 Hz, J_{FH} = 53, 15 Hz, 1F, s-*trans*), −127.20 (dt, J_{FH} = 54, 15 Hz, s-*cis*); HRMS (ESI-orbitrap): $[M + H]^+$ calcd for $C_9H_{14}F_2NO_3$, 222.0936; found, 222.0933; $[\alpha]_D^{25}$ −76 (*c* 2.0, $CHCl_3$).

2,2,2-Trifluoroethyl *N*-acetylprolinate (5): ^{1}H NMR (D_2O, 700 MHz) δ s-*trans*, 4.78 (q, J_{HF} = 8.7 Hz, 2H, OCH_2), 4.59 (dd, J_{HH} = 9.2, 4.7 Hz, 1H, α-CH), 3.63 and 3.59 (two m, 2H, δ-CH_2), 2.29 and 2.01 (two m, 2H, β-CH_2), 2.06 (s, 3H, CH_3C=O), 1.98 (m, 2H, γ-CH_2); s-*cis*, 4.78 (dd, J_{HH} = 8.8, 2.4 Hz, α-CH), 4.71 (m, OCH_2), 3.50 (ddd, J_{HH} = 11.6, 8.8, 3.3 Hz, δ-CH), 3.43 (dt, J_{HH} = 11.5, 8.1 Hz, δ-CH), 2.33 and 2.22 (two m, β-CH_2), 1.97 (s, CH_3C=O), 1.94 and 1.82 (two m, γ-CH_2); $^{13}C\{^1H\}$ NMR (D_2O, 176 MHz) δ s-*trans*, 173.4 (s, N-C=O), 172.6 (s, CO_2), 122.9 (q, J_{CF} = 277 Hz, CF_3), 60.9 (q, J_{CF} = 36 Hz, OCH_2), 58.8 (s, α-CH), 48.3 (s, δ-CH_2), 29.1 (s, β-CH_2), 24.3 (s, γ-CH_2), 21.1 (s, CH_3); s-*cis*, 173.4 (s, N-C=O), 172.2 (s, CO_2), 122.9 (q, J_{CF} = 276 Hz, CF_3), 61.3 (d, J_{CF} = 36 Hz, OCH_2), 60.5 (s, α-CH), 46.6 (s, δ-CH_2), 30.6 (s, β-CH_2), 22.3 (s, γ-CH_2), 21.2 (s, CH_3); ^{19}F NMR (D_2O, 471 MHz) δ −73.6 (t, J_{FH} = 9 Hz, s-*trans*), −73.7 (t, J_{FH} = 8 Hz, s-*cis*); HRMS (ESI-orbitrap): $[M + H]^+$ calcd for $C_9H_{13}F_3NO_3$, 240.0842; found, 240.0837; $[\alpha]_D^{25}$ −13 (*c* 2.0, $CHCl_3$), er 59:41.

Synthesis of the peptides

$Ac(Pro)_6OH$ (**8a**) and $Ac(^{\varepsilon}BocLys)_nOH$ (*n* = 3, 6) peptides were synthesized on pre-loaded 2-chlorotrityl resin conventionally. The esterification with 2,2-difluorodiazoethane was performed as described in [46]. Alternatively, the procedure was performed as follows: *tert*-Butyl nitrite (≈ 6 μL) and 2,2-

difluoroethylamine (≈ 11 μL) were mixed in chloroform (100 μL), and this mixture was shaken at room temperature for 10 min. It was then added to the peptide (25 μmol; in this example 18.4 mg of Ac($^{\varepsilon}$BocLys)$_3$OH) soaked in chloroform (100 μL). The resulting mixture was shaken at room temperature for approximately 10 hours. Volatiles were removed with nitrogen gas, and the residue was freeze-dried from an acetonitrile/water mixture to afford the target peptides. The Boc-protected peptides were purified on a silica gel column using a dichloromethane/methanol 9:1 → 1:0 gradient elution. The Boc deprotection was performed as follows. The peptide (3–4 mg) was mixed with 4 M hydrogen chloride in dioxane (100 μL), and the turbid mixture was shaken at room temperature for 20 min. Water (100 μL) was added, resulting a clear solution, which was shaken for an additional 20 min. The mixture was then freeze-dried from water to afford target peptides **9a**,**b** or **10a**,**b**.

The esterification of **8a** with methanol was performed as follows. Ac(Pro)$_6$OH (**8a**, 5.6 mg) was dissolved in methanol (0.5 mL), and trimethylsilyl chloride (0.08 mL) was added. The mixture was shaken at room temperature for 24 hours. Volatiles were removed with nitrogen gas, and the residue was freeze-dried from water. No HPLC purification has been applied in order to avoid ion-pairing agent contaminations and hydrolysis of the esters. Additionally, full conversion was observed in the synthesis of peptides **8b** and **8c**.

Oligolysine peptides were esterified as follows. A peptide Ac($^{\varepsilon}$BocLys)$_n$OH (n = 3, 6; 3 mg) was dissolved in methanol (1 mL), and trimethylsilyl chloride (0.08 mL) was added. The mixture was shaken at ambient temperature for 20 hours. Solvent was removed with nitrogen gas, and the residues were freeze-dried from deuterium oxide (0.2 mL) to afford target peptides **9c**, **10c**.

Characterization of the peptides

Mass spectra were recorded using high-resolution electrospray-orbitrap mass spectrometry ionization (HRMS) for all peptides except hexalysine peptides **10a**–**c**, which produced no distinguishable molecular ions. For cationic peptides **9a**–**c** and **10a**–**c**, additional MALDI–TOF analysis confirmed the molecular assignment.

Diffusion coefficients were determined in a ^{1}H stimulated echo experiment with bipolar gradients and a spoil pulse. The settings were as follows: 298 K, deuterium oxide, 700 MHz, Δ = 30 ms, $\delta/2$ = 2 ms, spoil pulse 0.5 ms, 128 array experiments with linear gradient increase. The reported error value is the distance between the midpoint and the top of the log$D$ projection peak. Experimental log$D$ values were compared to the calculated ones (Equation 5).

Circular dichroism spectra were recorded in a 1 mm quartz cell at 298 K in methanol (HPLC grade) or aqueous potassium phosphate buffer (50 mM, pH 7.01 at 297 K). The peptide concentration was 100 μM as determined gravimetrically. The mean residue absorption difference $\Delta\varepsilon$ was calculated assuming 6 residues for peptides **8a**–**c**, **10a**–**c** and 3 residues for peptides **9a**–**c**. Hydrolysis was measured in deuterium oxide solution of a 150 mM potassium phosphate buffer. The buffer pH 7.01 was adjusted in water at 298 K. It was then lyophilized, then dissolved in deuterium oxide. The peptides were dissolved in the buffer, and the resulting samples were kept at 298 ± 2 K, while the ^{19}F NMR measurements were conducted at several time points. The starting concentrations of the analytes were 8 mM for **8b**, 5 mM for **9b** and 2.5 mM for **10b**. The half-life was calculated using the first (zero) order kinetic model.

Ac(Pro)$_6$OH, **8a**. HRMS: calcd for $[M + H]^+$ 643.3450, for $[M + Na]^+$ 665.3269; found, 643.3443 and 665.3257; log$D$, calcd for [M] −9.462; found, −9.468 ± 0.026.

Ac(Pro)$_6$OCH$_2$CHF$_2$, **8b**. HRMS: calcd for $[M + H]^+$ 707.3574, for $[M + Na]^+$ 729.3394; found, 707.3566 and 729.3377; log$D$, calcd for [M] −9.475; found, −9.477 ± 0.011; $\tau_{½}$ = 152 ± 14 (139 ± 20) days (buffered deuterium oxide, pH 7.0).

Ac(Pro)$_6$OCH$_3$, **8c**. HRMS: calcd for $[M + H]^+$ 657.3606, for $[M + Na]^+$ 679.3426; found, 657.3599 and 679.3416; log$D$, calcd for [M] −9.465; found, −9.467 ± 0.027.

Ac(Lys)$_3$OH·3HCl, **9a**. HRMS: calcd for $[M + 3H]^{3+}$ 149.1093; found, 149.1096; MALDI–TOF: calcd for $[M + H]^+$ 445.3; found, 445.2; log$D$, calcd for $[M + 3H^+]$ −9.410; found, −9.442 ± 0.025.

Ac(Lys)$_6$OH·6HCl, **10a**. MALDI–TOF: calcd for $[M + H]^+$ 829.6; found, 829.5; log$D$, calcd for $[M + 6H^+]$ −9.499; found, −9.607 ± 0.038.

Ac(Lys)$_3$OCH$_2$CHF$_2$·3HCl, **9b**. HRMS: calcd for $[M + 3H]^{3+}$ 170.4468; found, 170.4474; MALDI–TOF: calcd for $[M + H]^+$ 509.3; found, 509.2; log$D$, calcd for $[M + 3H^+]$ −9.429; found, −9.439 ± 0.021; $\tau_{½}$ = 5.0 ± 0.3 (4.5 ± 0.5) days (buffered deuterium oxide, pH 7.0).

Ac(Lys)$_6$OCH$_2$CHF$_2$·6HCl, **10b**. MALDI–TOF: calcd for $[M + H]^+$ 893.6; found, 893.6; log$D$, calcd for $[M + 6H^+]$ −9.510; found, −9.583 ± 0.025; $\tau_{½}$ = 4.0 ± 0.3 (3.7 ± 0.3) days (buffered deuterium oxide, pH 7.0).

$Ac(Lys)_3OCH_3 \cdot 3HCl$, **9c**. HRMS: calcd for $[M + 3H]^{3+}$ 153.7812; found , 153.7812. MALDI–TOF: calcd for $[M + H]^+$ 459.3; found, 459.6; log*D*, calcd for $[M + 3H^+]$ −9.415; found, −9.425 ± 0.010.

$Ac(Lys)_6OCH_3 \cdot 6HCl$, **10c**. MALDI–TOF: calcd for $[M + H]^+$ 843.6; found, 844.3; log*D*, calcd for $[M + 6H^+]$ −9.502; found, −9.559 ± 0.017.

Supporting Information

Supporting Information File 1

Amide equilibrium constants (Table S1) and copies of the NMR and CD spectra.
[http://www.beilstein-journals.org/bjoc/content/supplementary/1860-5397-13-241-S1.pdf]

Acknowledgements

VK acknowledges DFG research group 1805 for a postdoctoral position. Enamine Ltd. (Kyiv, Ukraine) is thanked for provision of 2,2-difluoroethylamine. Dr Oleg Babii (KIT, Karlsruhe) is gratefully acknowledged for MALDI-TOF analysis.

ORCID® iDs

Vladimir Kubyshkin - https://orcid.org/0000-0002-4467-4205
Nediljko Budisa - https://orcid.org/0000-0001-8437-7304

References

1. Budisa, N.; Kubyshkin, V.; Schulze-Makuch, D. *Life* **2014,** *4,* 374–385. doi:10.3390/life4030374
2. O'Hagan, D.; Harper, D. B. *J. Fluorine Chem.* **1999,** *100,* 127–133. doi:10.1016/S0022-1139(99)00201-8
3. O'Hagan, D.; Schaffrath, C.; Cobb, S. L.; Hamilton, J. T. G.; Murphy, C. D. *Nature* **2002,** *416,* 279. doi:10.1038/416279a
4. Ulrich, A. S. *Prog. Nucl. Magn. Reson. Spectrosc.* **2005,** *46,* 1–21. doi:10.1016/j.pnmrs.2004.11.001
5. Merkel, L.; Budisa, N. *Org. Biomol. Chem.* **2012,** *10,* 7241–7261. doi:10.1039/C2OB06922A
6. Holzberger, B.; Rubini, M.; Möller, H. M.; Marx, A. *Angew. Chem., Int. Ed.* **2010,** *49,* 1324–1327. doi:10.1002/anie.200905978
7. Völler, J.-S.; Dulic, M.; Gerling-Driessen, U. I. M.; Biava, H.; Baumann, T.; Budisa, N.; Gruic-Sovulj, I.; Koksch, B. *ACS Cent. Sci.* **2017,** *3,* 73–80. doi:10.1021/acscentsci.6b00339
8. Holzberger, B.; Marx, A. *Bioorg. Med. Chem.* **2009,** *17,* 3653–3658. doi:10.1016/j.bmc.2009.03.063
9. Pandey, A. K.; Naduthambi, D.; Thomas, K. M.; Zondlo, N. J. *J. Am. Chem. Soc.* **2013,** *135,* 4333–4363. doi:10.1021/ja3109664
10. Kubyshkin, V. S.; Mykhailiuk, P. K.; Afonin, S.; Grage, S. L.; Komarov, I. V.; Ulrich, A. S. *J. Fluorine Chem.* **2013,** *152,* 136–143. doi:10.1016/j.jfluchem.2013.03.002
11. Ye, L.; Larda, S. T.; Li, Y. F. F.; Manglik, A.; Prosser, R. S. *J. Biomol. NMR* **2015,** *62,* 97–103. doi:10.1007/s10858-015-9922-y
12. Hawk, L. M. L.; Gee, C. T.; Urick, A. K.; Hu, H.; Pomerantz, W. C. K. *RSC Adv.* **2016,** *6,* 95715–95721. doi:10.1039/C6RA21226C
13. Tressler, C. M.; Zondlo, N. J. *Biochemistry* **2017,** *56,* 1062–1074. doi:10.1021/acs.biochem.6b01020
14. Didenko, T.; Liu, J. J.; Horst, R.; Stevens, R. C.; Wüthrich, K. *Curr. Opin. Struct. Biol.* **2013,** *23,* 740–747. doi:10.1016/j.sbi.2013.07.011
15. Kinde, M. N.; Bondarenko, V.; Granata, D.; Bu, W.; Grasty, K. C.; Loll, P. J.; Carnevale, V.; Klein, M. L.; Eckenhoff, R. G.; Tang, P.; Xu, Y. *Proc. Natl. Acad. Sci. U. S. A.* **2016,** *113,* 13762–13767. doi:10.1073/pnas.1609939113
16. Ye, L.; Eps, N. V.; Zimmer, M.; Ernst, O. P.; Prosser, R. S. *Nature* **2016,** *533,* 265–268. doi:10.1038/nature17668
17. Wadhwani, P.; Strandberg, E.; van der Berg, J.; Mink, C.; Bürck, J.; Ciriello, R. A. M.; Ulrich, A. S. *Biochim. Biophys. Acta, Biomembr.* **2014,** *1838,* 940–949. doi:10.1016/j.bbamem.2013.11.001
18. Afonin, S.; Glaser, R. W.; Sachse, C.; Salgado, J.; Wadhwani, P.; Ulrich, A. S. *Biochim. Biophys. Acta, Biomembr.* **2014,** *1838,* 2260–2268. doi:10.1016/j.bbamem.2014.03.017
19. Granquist, L.; Virta, P. *J. Org. Chem.* **2015,** *80,* 7961–7970. doi:10.1021/acs.joc.5b00973
20. Nakamura, S.; Yang, H.; Hirata, C.; Kersaudy, F.; Fujimoto, K. *Org. Biomol. Chem.* **2017,** *15,* 5109–5111. doi:10.1039/c7ob00706j
21. Kiviniemi, A.; Murtola, M.; Ingman, P.; Virta, P. *J. Org. Chem.* **2013,** *78,* 5153–5159. doi:10.1021/jo400014y
22. Kirberger, S. E.; Maltseva, S. D.; Manulik, J. C.; Einstein, S. A.; Weegman, B. P.; Garwood, M.; Pomerantz, W. C. K. *Angew. Chem., Int. Ed.* **2017,** *56,* 6440–6444. doi:10.1002/anie.201700426
23. Salwiczek, M.; Nyakatura, E. K.; Gerling, U. I. M.; Ye, S.; Koksch, B. *Chem. Soc. Rev.* **2012,** *41,* 2135–2171. doi:10.1039/C1CS15241F
24. Kubyshkin, V.; Afonin, S.; Kara, S.; Budisa, N.; Mykhailiuk, P. K.; Ulrich, A. S. *Org. Biomol. Chem.* **2015,** *13,* 3171–3181. doi:10.1039/C5OB00034C
25. Afonin, S.; Kubyshkin, V.; Mykhailiuk, P. K.; Komarov, I. V.; Ulrich, A. S. *J. Phys. Chem. B* **2017,** *121,* 6479–6491. doi:10.1021/acs.jpcb.7b02852
26. Naduthambi, D.; Zondlo, N. J. *J. Am. Chem. Soc.* **2006,** *128,* 12430–12431. doi:10.1021/ja0648458
27. Steiner, T.; Hess, P.; Bae, J. H.; Wiltschi, B.; Moroder, L.; Budisa, N. *PLoS One* **2008,** *3,* e1680. doi:10.1371/journal.pone.0001680
28. Arnold, U.; Raines, R. T. *Org. Biomol. Chem.* **2016,** *14,* 6780–6785. doi:10.1039/C6OB00980H
29. Huhmann, S.; Nyakatura, E. K.; Erdbrink, H.; Gerling, U. I. M.; Czekelius, C.; Koksch, B. *J. Fluorine Chem.* **2015,** *175,* 32–35. doi:10.1016/j.jfluchem.2015.03.003
30. Torbeev, V. Y.; Hilvert, D. *Proc. Natl. Acad. Sci. U. S. A.* **2013,** *110,* 20051–20056. doi:10.1073/pnas.1310414110
31. Roderer, D.; Glockshuber, R.; Rubini, M. *ChemBioChem* **2015,** *16,* 2162–2166. doi:10.1002/cbic.201500342
32. Newberry, R. W.; Raines, R. T. *Top. Heterocycl. Chem.* **2016,** *48,* 1–25. doi:10.1007/7081_2015_196
33. Agostini, F.; Völler, J.-S.; Koksch, B.; Acevedo-Rocha, C. G.; Kubyshkin, V.; Budisa, N. *Angew. Chem., Int. Ed.* **2017,** *56,* 9680–9703. doi:10.1002/anie.201610129
34. Barth, D.; Milbrandt, A. G.; Renner, C.; Moroder, L. *ChemBioChem* **2004,** *5,* 79–86. doi:10.1002/cbic.200300702
35. Shoulders, M. D.; Raines, R. T. *Annu. Rev. Biochem.* **2009,** *78,* 929–958. doi:10.1146/annurev.biochem.77.032207.120833

36. Waters, M. L. *Curr. Opin. Chem. Biol.* **2002,** *6,* 736–741. doi:10.1016/S1367-5931(02)00359-9
37. Butterfield, S. M.; Patel, P. R.; Waters, M. L. *J. Am. Chem. Soc.* **2002,** *124,* 9751–9755. doi:10.1021/ja026668q
38. Gorske, B. C.; Blackwell, H. E. *J. Am. Chem. Soc.* **2006,** *128,* 14378–14387. doi:10.1021/ja065248o
39. Cejas, M. A.; Kinney, W. A.; Chen, C.; Vinter, J. G.; Almond, H. R., Jr.; Balss, K. M.; Maryanoff, C. A.; Schmidt, U.; Breslav, M.; Mahan, A.; Lacy, E.; Maryanoff, B. E. *Proc. Natl. Acad. Sci. U. S. A.* **2008,** *105,* 8513–8518. doi:10.1073/pnas.0800291105
40. Pace, C. J.; Gao, J. *Acc. Chem. Res.* **2013,** *46,* 907–915. doi:10.1021/ar300086n
41. Huchet, Q. A.; Kuhn, B.; Wagner, B.; Fischer, H.; Kansy, M.; Zimmerli, D.; Carreira, E. M.; Müller, K. *J. Fluorine Chem.* **2013,** *152,* 119–128. doi:10.1016/j.jfluchem.2013.02.023
42. Vorberg, R.; Trapp, N.; Zimmerli, D.; Wagner, B.; Fischer, H.; Kratochwil, N. A.; Kansy, M.; Carreira, E. M.; Müller, K. *ChemMedChem* **2016,** *11,* 2216–2239. doi:10.1002/cmdc.201600325
43. Huchet, Q. A.; Schweizer, W. B.; Kuhn, B.; Carreira, E. M.; Müller, K. *Chem. – Eur. J.* **2016,** *22,* 16920–16928. doi:10.1002/chem.201602643
44. Huchet, Q. A.; Trapp, N.; Kuhn, B.; Wagner, B.; Fischer, H.; Kratochwil, N. A.; Carreira, E. M.; Müller, K. *J. Fluorine Chem.* **2017,** *198,* 34–46. doi:10.1016/j.jfluchem.2017.02.003
45. Stepan, A. F.; Kauffman, G. W.; Keefer, C. E.; Verhoest, P. R.; Edwards, M. *J. Med. Chem.* **2013,** *56,* 6985–6990. doi:10.1021/jm4008642
46. Mykhailiuk, P. K.; Kishko, I.; Kubyshkin, V.; Budisa, N.; Cossy, J. *Chem. – Eur. J.* **2017,** *23,* 13279–13283. doi:10.1002/chem.201703446
47. Bume, D. D.; Pitts, C. R.; Jokhai, R. T.; Lectka, T. *Tetrahedron* **2016,** *72,* 6031–6036. doi:10.1016/j.tet.2016.08.018
48. Mertens, L.; Koenigs, R. M. *Org. Biomol. Chem.* **2016,** *14,* 10547–10556. doi:10.1039/C6OB01618A
49. Mix, K. A.; Aronoff, M. R.; Raines, R. T. *ACS Chem. Biol.* **2016,** *11,* 3233–3244. doi:10.1021/acschembio.6b00810
50. Kubyshkin, V.; Durkin, P.; Budisa, N. *New J. Chem.* **2016,** *40,* 5209–5220. doi:10.1039/C5NJ03611A
51. Hargaden, G. C.; Müller-Bunz, H.; Guiry, P. J. *Eur. J. Org. Chem.* **2007,** 4235–4243. doi:10.1002/ejoc.200700227
52. McGrath, N. A.; Andersen, K. A.; Davis, A. K. F.; Lomax, J. E.; Raines, R. T. *Chem. Sci.* **2015,** *6,* 752–755. doi:10.1039/C4SC01768D
53. Mix, K. A.; Raines, R. T. *Org. Lett.* **2015,** *17,* 2358–2361. doi:10.1021/acs.orglett.5b00840
54. Peng, S.-Q.; Zhang, X.-W.; Zhang, L.; Hu, X.-G. *Org. Lett.* **2017,** *19,* 5689–5692. doi:10.1021/acs.orglett.7b02866
55. Schuber, F.; Pinck, M. *Biochimie* **1974,** *56,* 383–390. doi:10.1016/S0300-9084(74)80146-X
56. Schuber, F.; Pinck, M. *Biochimie* **1974,** *56,* 391–395. doi:10.1016/S0300-9084(74)80147-1
57. Schuber, F.; Pinck, M. *Biochimie* **1974,** *56,* 397–403. doi:10.1016/S0300-9084(74)80148-3
58. Hay, R. W.; Porter, L. J.; Morris, P. J. *Aust. J. Chem.* **1966,** *19,* 1197–1205. doi:10.1071/CH9661197
59. Wolfenden, R. *Biochemistry* **1963,** *2,* 1090–1092. doi:10.1021/bi00905a031
60. Laizure, S. C.; Herring, V.; Hu, Z.; Witbrodt, K.; Parker, R. B. *Pharmacotherapy* **2013,** *33,* 210–222. doi:10.1002/phar.1194
61. Kubyshkin, V.; Kheylik, Y.; Mykhailiuk, P. K. *J. Fluorine Chem.* **2015,** *175,* 73–83. doi:10.1016/j.jfluchem.2015.03.008
62. Vorberg, R.; Carreira, E. M.; Müller, K. *ChemMedChem* **2017,** *12,* 431–437. doi:10.1002/cmdc.201700027
63. Linclau, B.; Wang, Z.; Compain, G.; Paumelle, V.; Fontenelle, C. Q.; Wells, N.; Weymouth-Wilson, A. *Angew. Chem., Int. Ed.* **2016,** *55,* 674–678. doi:10.1002/anie.201509460
64. Kondratov, I. S.; Logvinenko, I. G.; Tolmachova, N. A.; Morev, R. N.; Kliachyna, M. A.; Clausen, F.; Daniliuk, C. G.; Haufe, G. *Org. Biomol. Chem.* **2017,** *15,* 672–679. doi:10.1039/C6OB02436J
65. Müller, K. *Chimia* **2014,** *68,* 356–362. doi:10.2533/chimia.2014.356
66. MacArthur, M. W.; Thornton, J. M. *J. Mol. Biol.* **1991,** *218,* 397–412. doi:10.1016/0022-2836(91)90721-H
67. Fischer, G. *Chem. Soc. Rev.* **2000,** *29,* 119–127. doi:10.1039/A803742F
68. Kubyshkin, V.; Budisa, N. *Org. Biomol. Chem.* **2017,** *15,* 6764–6772. doi:10.1039/C7OB01421J
69. Berger, G.; Chab-Majdalani, I.; Hanessian, S. *Isr. J. Chem.* **2017,** *57,* 292–302. doi:10.1002/ijch.201600106
70. Kuemin, M.; Schweizer, S.; Ochsenfeld, C.; Wennemers, H. *J. Am. Chem. Soc.* **2009,** *131,* 15474–15482. doi:10.1021/ja906466q
71. Kubyshkin, V.; Budisa, N. *Org. Biomol. Chem.* **2017,** *15,* 619–627. doi:10.1039/C6OB02306A
72. Siebler, C.; Maryasin, B.; Kuemin, M.; Erdmann, R. S.; Rigling, C.; Grünenfelder, C.; Ochsenfeld, C.; Wennemers, H. *Chem. Sci.* **2015,** *6,* 6725–6730. doi:10.1039/C5SC02211H
73. Eberhardt, E. S.; Loh, S. N.; Hinck, A. P.; Raines, R. T. *J. Am. Chem. Soc.* **1992,** *114,* 5437–5439. doi:10.1021/ja00039a072
74. Braga, C. B.; Ducati, L. C.; Tormena, C. F.; Rittner, R. *J. Phys. Chem. A* **2014,** *118,* 1748–1758. doi:10.1021/jp5007632
75. O'Hagan, D.; Young, R. J. *Angew. Chem., Int. Ed.* **2016,** *55,* 3858–3860. doi:10.1002/anie.201511055
76. Hodges, J. A.; Raines, R. T. *Org. Lett.* **2006,** *8,* 4695–4697. doi:10.1021/ol061569t
77. Pollock, J.; Borkin, D.; Lund, G.; Purohit, T.; Dyguda-Kazimierowicz, E.; Grembecka, J.; Cierpicki, T. *J. Med. Chem.* **2015,** *58,* 7465–7474. doi:10.1021/acs.jmedchem.5b00975
78. Arnott, J. A.; Planey, S. L. *Expert Opin. Drug Discovery* **2012,** *7,* 863–875. doi:10.1517/17460441.2012.714363
79. Kang, Y. K. *J. Phys. Chem. B* **2007,** *111,* 10550–10556. doi:10.1021/jp073411b
80. Wu, D. *AIP Adv.* **2013,** *3,* 032141. doi:10.1063/1.4799082
81. Cai, M.; Huang, Y.; Liu, J.; Krishnamoorthy, R. *J. Biomol. NMR* **1995,** *6,* 123–128. doi:10.1007/BF00211775
82. Feytens, D.; Chaume, G.; Chassaing, G.; Lavielle, S.; Brigaud, T.; Byun, B. J.; Kang, Y. K.; Miclet, E. *J. Phys. Chem. B* **2012,** *116,* 4069–4079. doi:10.1021/jp300284u
83. DeRider, M. L.; Wilkens, S. J.; Waddell, M. J.; Bretscher, L. E.; Weinhold, F.; Raines, R. T.; Markley, J. L. *J. Am. Chem. Soc.* **2002,** *124,* 2497–2505. doi:10.1021/ja0166904
84. Babu, I. R.; Ganesh, K. N. *J. Am. Chem. Soc.* **2001,** *123,* 2079–2080. doi:10.1021/ja002165d
85. He, L.; Navarro, A. E.; Shi, Z.; Kallenbach, N. R. *J. Am. Chem. Soc.* **2012,** *134,* 1571–1576. doi:10.1021/ja2070363
86. Lin, Y.-J.; Chu, L.-K.; Horng, J.-C. *J. Phys. Chem. B* **2015,** *119,* 15796–15806. doi:10.1021/acs.jpcb.5b08717
87. Rucker, A. L.; Creamer, T. P. *Protein Sci.* **2002,** *11,* 980–985. doi:10.1110/ps.4550102
88. Evans, R.; Deng, Z.; Rogerson, A. K.; McLachlan, A. S.; Richards, J. J.; Nilsson, M.; Morris, G. A. *Angew. Chem., Int. Ed.* **2013,** *52,* 3199–3202. doi:10.1002/anie.201207403
89. Tiffany, M. L.; Krim, S. *Biopolymers* **1968,** *6,* 1379–1382. doi:10.1002/bip.1968.360060911

90. Mezei, M.; Fleming, P. J.; Srinivasan, R.; Rose, G. D. *Proteins: Struct., Funct., Bioinf.* **2004,** *55,* 502–507. doi:10.1002/prot.20050
91. Shi, Z.; Chen, K.; Liu, Z.; Kallenbach, N. R. *Chem. Rev.* **2006,** *106,* 1877–1897. doi:10.1021/cr040433a
92. Bedewy, W.; Liao, H.; Abou-Taleb, N. A.; Hammad, S. F.; Nasr, T.; Pei, D. *Org. Biomol. Chem.* **2017,** *15,* 4540–4543. doi:10.1039/c7ob00430c
93. Indrisiunaite, G.; Pavlov, M. Y.; Heurgué-Hamard, V.; Ehrenberg, M. *J. Mol. Biol.* **2015,** *427,* 1848–1860. doi:10.1016/j.jmb.2015.01.007
94. Kazemi, M.; Himo, F.; Åquist, J. *ACS Catal.* **2016,** *6,* 8432–8439. doi:10.1021/acscatal.6b02842
95. Schmeing, T. M.; Huang, K. S.; Strobel, S. A.; Steitz, T. A. *Nature* **2005,** *438,* 520–524. doi:10.1038/nature04152

License and Terms

BEILSTEIN JOURNAL OF ORGANIC CHEMISTRY

Diastereoselective Mannich reactions of pseudo-C_2-symmetric glutarimide with activated imines

Tatsuya Ishikawa[1], Tomoko Kawasaki-Takasuka[1], Toshio Kubota[2] and Takashi Yamazaki[*1]

Full Research Paper

Open Access

Address:
[1]Division of Applied Chemistry, Institute of Engineering, Tokyo University of Agriculture and Technology, 2-24-16 Nakamachi, Koganei 184-8588, Japan and [2]Department of Biomolecular Functional Engineering, Ibaraki University, Nakanarusawa 4-12-1, Hitachi 316-8511, Japan

Email:
Takashi Yamazaki* - tyamazak@cc.tuat.ac.jp

* Corresponding author

Keywords:
chiral oxazolidinones; diastereoselectivity; Mannich reactions; pseudo-C_2 symmetry; trifluoromethyl

Beilstein J. Org. Chem. **2017,** *13,* 2473–2477.
doi:10.3762/bjoc.13.244

Received: 22 September 2017
Accepted: 09 November 2017
Published: 21 November 2017

This article is part of the Thematic Series "Organo-fluorine chemistry IV".

Guest Editor: D. O'Hagan

Abstract

As an extension of the boron enolate-based aldol reactions, the oxazolidinone-installed bisimide **1a** from 3-(trifluoromethyl)glutaric acid was employed for Mannich reactions with tosylated imines **2** as electrophiles to successfully obtain the corresponding adducts in a stereoselective manner.

Introduction

During these decades, we have been keenly interested in the 3-(trifluoromethyl)glutaric acid derivatives and developed a couple of routes to get successful access to such target molecules with a variety of substituents at the 2-position [1-3]. Previously, the oxazolidinone-installed bisimide **1a** was employed for the crossed aldol reactions by the way of boron enolate which allowed the isolation of optically active lactones in good to excellent yields [4,5]. One of the most intriguing features of this protocol is the fact that the enantiomers at the lactone part were readily obtained only by the selection of the tertiary amines employed in the reaction. It is quite apparent that this success is, at least in part, based on its inherent pseudo-C_2 symmetric structure [6-8] which enables the formation of plural stereogenic centers by a single operation. These promising results prompted us to extend this aldol protocol to its relative, Mannich reactions [9-13] whose details are reported in this article.

Results and Discussion

On the basis of our previous study [4], the chiral glutarimide **1a** was employed as the starting material and optimization of reaction conditions with benzaldehyde-based imines **2** was performed (Table 1). Lithium enolate by the action of LDA to **1a** was found to be ineffective as long as the imines with benzyl (**2aa**) or Boc (**2ab**) as substituents R were employed (Table 1, entries 1 and 2).

Table 1: Optimization of reaction conditions.

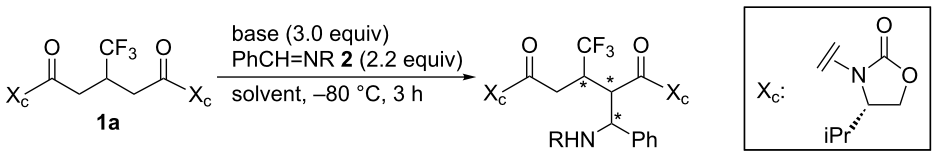

Entry	Solvent	Base	R	Yield[a] (%)	DS[b]
1	THF	LDA	$PhCH_2$ (**2aa**)	NR	–
2	THF	LDA	Boc (**2ab**)	NR	–
3	THF	LDA	Ts (**2ac**)	85 (**3a**)	69:18:(13)
4	THF	NaHMDS	Ts (**2ac**)	59 (**3a**)	38:43:(19)
5	THF	LiHMDS	Ts (**2ac**)	80 (**3a**)	27:62:(11)
6[c]	DCM	DIPEA	Ts (**2ac**)	NR	–
7[d]	THF	LDA	Ts (**2ac**)	96 [75] (**3a**)	73:17:(10)
8[d,e]	THF	LDA	Ts (**2ac**)	91 (**4a**)	73:21:(6)

[a]All yields were determined by ^{19}F NMR and in the bracket isolated yields are given. NR: no reaction. [b]Diastereoselectivities (DS) were determined by ^{19}F NMR and in the parentheses the sum of the other minor stereoisomers is given. [c]$TiCl_4$ (3.0 equiv) was used as a Lewis acid. [d]The reaction was continued for 6 h. [e]Substrate **1b** with the phenylglycine-derived oxazolidinone part was employed instead of **1a**.

However, the attachment of the stronger electron-withdrawing 4-toluenesulfonyl (Ts) moiety attained efficient activation of the imine **2ac** to afford the desired Mannich product **3a** in 85% yield as determined by ^{19}F NMR (Table 1, entry 3). NaHMDS (Table 1, entry 4) or LiHMDS (Table 1, entry 5) instead of LDA worked properly affording **3a** in a yield of 59 or 80%, respectively. The product **3a** theoretically consists of 8 diastereomers and usually 2 isomers predominated with a couple of minor peaks whose sum is given in parentheses (for example, in the case of entry 3 (Table 1), four small peaks were observed in addition to the major two). It is interesting to note that MHMDS (M: Li or Na) and LDA furnished a different isomer as the major product. We have also prepared the titanium enolate [14], but the reaction did not proceed at all (Table 1, entry 6). As the separation of product **3a** from unreacted substrate **1a** proved to be difficult, the reaction time was extended from 3 h to 6 h. After this time the consumption of **1a** was complete and the yield of **3a** was almost quantitative (Table 1, entry 7). Because the employment of the phenylalanine-based oxazolidinone as the chiral auxiliary under the same conditions gave similar results as the one obtained from valine (Table 1, entries 8 vs 7), we decided the conditions in entry 7 (Table 1) as the best of all tested and investigated the structural scope of imines **2** at the next stage (Table 2).

As mentioned above, LDA and LiHMDS proved to work in a complementary manner in terms of their diastereoselectivity towards products **3**. Therefore, we next tried to use both bases for the reaction with **1a** and the resultant enolate was treated with a variety of tosylimines **2** (Table 2). For better overview entry 1 in Table 2 contains the same data as entry 7 in Table 1. It is assumed that the differences between the spectroscopically determined yields to the isolated ones originate from the tedious separation process of the products **3** from the byproduct, 4-toluenesulfonamide (4-$MeC_6H_4SO_2NH_2$) **5** produced by the hydrolysis of the unreacted imines **2** [15]. As expected, aromatic sulfonylimines with electron-withdrawing substituents **2bc**–**dc** acted nicely as electrophiles to furnish the desired adducts **3b**–**d** in high to excellent isolated yields where the complementary formation of the diastereomers was usually observed (Table 2, entries 3–8). Aromatic imines with electron-donating groups, **2fc** and **2gc**, as well as the heteroaromatic imine **2ec** sometimes required longer reaction times, but worked without any significant problems (Table 2, entries 9–14). As a general trend, LiHMDS tended to afford lower chemical yields the reason for which was not clear at present. Imines from aliphatic aldehydes **2hc** and **2ic** could be used in a similar manner but the steric effect due to the branched structure in the latter affected the reaction to some extent (Table 2, entries 15 and 16). As described above, facile isolation of **3** was sometimes hampered by contamination of the substrate **1a** and/or 4-toluenesulfonamide **5** which is noticed by the absence of isolated yields shown in brackets in Table 2.

The configuration of the major diastereomer of **3a** (Table 2, entry 1) was unambiguously determined by X-ray crystallographic analysis (Figure 1) [16].

Based on this information a possible reaction mechanism was formulated as depicted in Scheme 1. It is well-known that

Table 2: Scope and limitation of the present Mannich reactions.

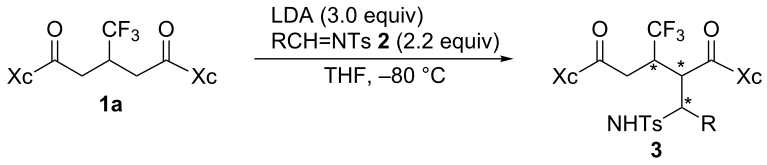

Entry	Base	R	Time (h)	Yield[a] (%)	Product	DS[b]
1	LDA	Ph (**2ac**)	3.0	96 [75]	**3a**	73:17:(10)
2	LiHMDS	Ph (**2ac**)	6.0	96[74]	**3a**	27:63:(10)
3	LDA	4-BrC_6H_4- (**2bc**)	6.0	93 [91]	**3b**	62:17:(21)
4	LiHMDS	4-BrC_6H_4- (**2bc**)	6.0	84 [62]	**3b**	26:61:(13)
5	LDA	4-$O_2NC_6H_4$- (**2cc**)	6.0	quant [92]	**3c**	65:13:(22)
6	LiHMDS	4-$O_2NC_6H_4$- (**2cc**)	6.0	64 [45]	**3c**	49:44:(7)
7	LDA	3-FC_6H_4- (**2dc**)	6.0	89 [78]	**3d**	81:6:(13)
8	LiHMDS	3-FC_6H_4- (**2dc**)	6.0	84 [72]	**3d**	33:51:(16)
9	LDA	2-furyl- (**2ec**)	8.0	95 [55]	**3e**	51:22:(27)
10	LiHMDS	2-furyl- (**2ec**)	6.0	48	**3e**	28:57:(15)
11	LDA	4-MeC_6H_4- (**2fc**)	8.0	quant [66]	**3f**	51:16:(33)
12	LiHMDS	4-MeC_6H_4- (**2fc**)	6.0	51	**3f**	28:64:(8)
13	LDA	4-MeOC_6H_4- (**2gc**)	6.0	86	**3g**	34:31:(35)
14	LiHMDS	4-MeOC_6H_4- (**2gc**)	6.0	26	**3g**	38:29:(33)
15	LDA	Et (**2hc**)	6.0	93	**3h**	39:36:(25)
16	LDA	iPr (**2ic**)	6.0	23	**3i**	37:17:(46)

[a]All yields were determined by ^{19}F NMR and in the bracket the isolated yields are given. [b]Diastereoselectivities (DS) were determined by ^{19}F NMR for the crude mixture and in the parentheses the sum of the other minor stereoisomers is given.

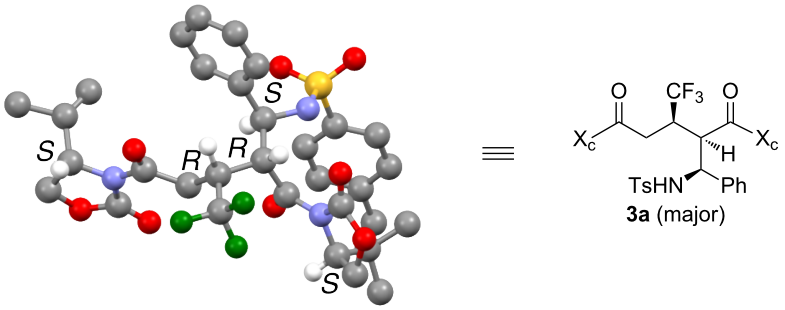

Figure 1: Crystallographic analysis of the major diastereomer of **3a** (some hydrogen atoms are omitted for clarity). Each color represents the following atoms: gray, carbon; white, hydrogen; blue, nitrogen; red, oxygen; green, fluorine; yellow, sulfur.

oxazolidinone-derived imides in general construct bidentate chelation when they are converted to the corresponding metal enolates [17]. The subsequent reactions occur so as to avoid unfavorable steric repulsive interaction with the oxazolidinone substituent, the iPr group in our case (**Int-a**). The selection of the two enantiotopic enolates should be explained on the basis of the Cieplak effect [18,19] for the enolate conformation with the allylic hydrogen possessing the same plane for making the steric bias minimum (**Int-b**) [20,21]. The most important argument for this effect is the stabilization of the forming electron-deficient $\sigma^{*\neq}$ orbital in the transition state by the electron donation from the neighboring orbital. In our case, possible electron donation is expected either by the $\sigma_{C\text{-}C}$ in **TS(*pro-R,si*)** or $\sigma_{C\text{-}CF3}$ in **TS(*pro-R,re*)**. Because the former orbital is more electron-rich, imines as electrophiles should approach from the *si* face of the *pro-R* enolate (E: an appropriate electrophile in Scheme 1). The same orbital interaction would be operative when the electrophile came closer from the *re* face of the

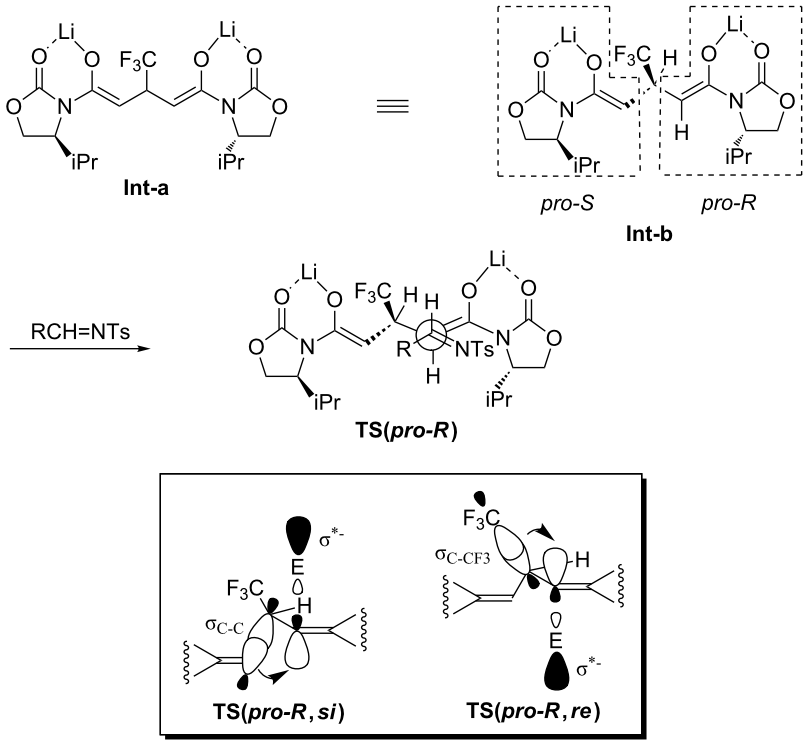

Scheme 1: Explanation of the construction of the main stereoisomers.

pro-S enolate which suffered from the existence of the sterically demanding iPr group. As a result, the major reaction pathway was considered to follow the transition state **TS(*pro-R*,*si*)** where the *si* face of imines seemed to match favorably with a construction of the least sterically demanding conformation, leading to formation of the obtained diastereoisomer **3a**.

Conclusion

As shown above, the oxazolidinone-installed imide from 3-(trifluoromethyl)glutaric acid **1a** was found to afford the corresponding adducts **3** in good to excellent chemical yields in a stereoselective fashion when its enolate was subjected to a solution containing tosylated imines **2** as electrophiles. Further work is going on in this laboratory to utilize the thus obtained adducts **3** and the results will be reported in due course.

Supporting Information

Supporting Information File 1

Experimental procedures, characterization data, copies of ^{1}H and ^{13}C NMR spectra for the new compounds, and crystallographic analysis data are available.
[http://www.beilstein-journals.org/bjoc/content/supplementary/1860-5397-13-244-S1.pdf]

ORCID® iDs

Takashi Yamazaki - https://orcid.org/0000-0002-1460-3086

References

1. Yamazaki, T.; Haga, J.; Kitazume, T.; Nakamura, S. *Chem. Lett.* **1991,** *20,* 2171–2174. doi:10.1246/cl.1991.2171
2. Yamazaki, T.; Haga, J.; Kitazume, T. *Chem. Lett.* **1991,** *20,* 2175–2178. doi:10.1246/cl.1991.2175
3. Shinohara, N.; Haga, J.; Yamazaki, T.; Kitazume, T.; Nakamura, S. *J. Org. Chem.* **1995,** *60,* 4363–4374. doi:10.1021/jo00119a013
4. Watanabe, Y.; Yamazaki, T.; Kubota, T. *Org. Lett.* **2010,** *12,* 268–271. doi:10.1021/ol902592t
5. Watanabe, Y.; Yamazaki, T.; Kubota, T. *Org. Lett.* **2010,** *12,* 1648. doi:10.1021/ol100413b
6. Gao, X.; Han, H.; Krische, M. J. *J. Am. Chem. Soc.* **2011,** *133,* 12795–12800. doi:10.1021/ja204570w
7. Linclau, B.; Cini, E.; Oake, C. S.; Josse, S.; Light, M.; Ironmonger, V. *Angew. Chem., Int. Ed.* **2012,** *51,* 1232–1235. doi:10.1002/anie.201107370
8. Ikeuchi, K.; Ido, S.; Yoshimura, S.; Asakawa, T.; Inai, M.; Hamashima, Y.; Kan, T. *Org. Lett.* **2012,** *14,* 6016–6019. doi:10.1021/ol302908a
9. Arend, M.; Westermann, B.; Risch, N. *Angew. Chem., Int. Ed.* **1998,** *37,* 1044–1070. doi:10.1002/(SICI)1521-3773(19980504)37:8<1044::AID-ANIE1044>3.0.CO;2-E
10. Huguenot, F.; Brigaud, T. *J. Org. Chem.* **2006,** *71,* 2159–2162. doi:10.1021/jo052323p

11. Han, X.; Kwiatkowski, J.; Xue, F.; Huang, K.-W.; Lu, Y. *Angew. Chem., Int. Ed.* **2009,** *48,* 7604–7607. doi:10.1002/anie.200903635
12. Mei, H.; Dai, Y.; Wu, L.; Soloshonok, V. A.; Han, J.; Pan, Y. *Eur. J. Org. Chem.* **2014,** 2429–2433. doi:10.1002/ejoc.201400118
13. Yin, L.; Brewitz, L.; Kumagai, N.; Shibasaki, M. *J. Am. Chem. Soc.* **2014,** *136,* 17958–17961. doi:10.1021/ja511458k
14. Franck, X.; Seon-Meniel, B.; Figadère, B. *Angew. Chem., Int. Ed.* **2006,** *45,* 5174–5176. doi:10.1002/anie.200600927
15. Because of their close Rf values, after evaporation of the volatiles from the chromatographically separated fractions containing these two compounds **3** and **5**, this diastereomer mixture was dissolved in an appropriate amount of CH_2Cl_2 where hexane was added slowly to precipitate the sulfonamide **5**.
16. CCDC 1575731 contains the supplementary crystallographic data for the major diastereomer of **3a**. All data can be acquired free of charge from The Cambridge Crystallographic Data Centre via http://www.ccdc.cam.ac.uk/data_request/cif.
17. Evans, D. A.; Ennis, M. D.; Mathre, D. J. *J. Am. Chem. Soc.* **1982,** *104,* 1737–1739. doi:10.1021/ja00370a050
18. Cieplak, A. S.; Tait, B. D.; Johnson, C. R. *J. Am. Chem. Soc.* **1989,** *111,* 8447–8462. doi:10.1021/ja00204a018
19. Cieplak, A. S. *Chem. Rev.* **1999,** *99,* 1265–1336. doi:10.1021/cr980381n
20. Johnson, F. *Chem. Rev.* **1968,** *68,* 375–413. doi:10.1021/cr60254a001
21. Hoffmann, R. W. *Chem. Rev.* **1989,** *89,* 1841–1860. doi:10.1021/cr00098a009

BEILSTEIN JOURNAL OF ORGANIC CHEMISTRY

Syntheses, structures, and stabilities of aliphatic and aromatic fluorous iodine(I) and iodine(III) compounds: the role of iodine Lewis basicity

Tathagata Mukherjee[1,§], Soumik Biswas[1], Andreas Ehnbom[1], Subrata K. Ghosh[1], Ibrahim El-Zoghbi[2], Nattamai Bhuvanesh[1], Hassan S. Bazzi[*2] and John A. Gladysz[*1]

Full Research Paper

Open Access

Address:
[1]Department of Chemistry, Texas A&M University, P.O. Box 30012, College Station, Texas, 77842-3012, USA, and [2]Department of Chemistry, Texas A&M University at Qatar, P.O. Box 23874, Doha, Qatar

Email:
Hassan S. Bazzi[*] - bazzi@tamu.edu; John A. Gladysz[*] - gladysz@mail.chem.tamu.edu

* Corresponding author
§ Present address: Dr. Tathagata Mukherjee, Intel Corporation, Hillsboro, Oregon

Keywords:
chlorination; copper mediated perfluoroalkylation; crystal structure; DFT calculations; fluorous; hypervalent iodine; nucleophilic substitution; polar space group

Beilstein J. Org. Chem. **2017,** *13,* 2486–2501.
doi:10.3762/bjoc.13.246

Received: 23 August 2017
Accepted: 25 October 2017
Published: 23 November 2017

This article is part of the Thematic Series "Organo-fluorine chemistry IV".

Guest Editor: D. O'Hagan

Abstract

The title molecules are sought in connection with various synthetic applications. The aliphatic fluorous alcohols $R_{fn}CH_2OH$ ($R_{fn} = CF_3(CF_2)_{n-1}$; n = 11, 13, 15) are converted to the triflates $R_{fn}CH_2OTf$ (Tf_2O, pyridine; 22–61%) and then to $R_{fn}CH_2I$ (NaI, acetone; 58–69%). Subsequent reactions with NaOCl/HCl give iodine(III) dichlorides $R_{fn}CH_2ICl_2$ (n = 11, 13; 33–81%), which slowly evolve Cl_2. The ethereal fluorous alcohols $CF_3CF_2CF_2O(CF(CF_3)CF_2O)_xCF(CF_3)CH_2OH$ (x = 2–5) are similarly converted to triflates and then to iodides, but efforts to generate the corresponding dichlorides fail. Substrates lacking a methylene group, $R_{fn}I$, are also inert, but additions of TMSCl to bis(trifluoroacetates) $R_{fn}I(OCOCF_3)_2$ appear to generate $R_{fn}ICl_2$, which rapidly evolve Cl_2. The aromatic fluorous iodides 1,3-$R_{f6}C_6H_4I$, 1,4-$R_{f6}C_6H_4I$, and 1,3-$R_{f10}C_6H_4I$ are prepared from the corresponding diiodides, copper, and $R_{fn}I$ (110–130 °C, 50–60%), and afford quite stable $R_{fn}C_6H_4ICl_2$ species upon reaction with NaOCl/HCl (80–89%). Iodinations of 1,3-$(R_{f6})_2C_6H_4$ and 1,3-$(R_{f8}CH_2CH_2)_2C_6H_4$ (NIS or I_2/H_5IO_6) give 1,3,5-$(R_{f6})_2C_6H_3I$ and 1,2,4-$(R_{f8}CH_2CH_2)_2C_6H_3I$ (77–93%). The former, the crystal structure of which is determined, reacts with Cl_2 to give a 75:25 $ArICl_2$/ArI mixture, but partial Cl_2 evolution occurs upon work-up. The latter gives the easily isolated dichloride 1,2,4-$(R_{f8}CH_2CH_2)_2C_6H_3ICl_2$ (89%). The relative thermodynamic ease of dichlorination of these and other iodine(I) compounds is probed by DFT calculations.

Introduction

A number of fluorous alkyl iodides, usually of the formula $R_{fn}CH_2CH_2I$ or $R_{fn}I$ ($R_{fn} = CF_3(CF_2)_{n-1}$), are commercially available and have seen abundant use as building blocks in fluorous chemistry [1-3]. Fluorous aryl iodides, such as $R_{fn}C_6H_4I$ or $R_{fn}(CH_2)_mC_6H_4I$ species, are also often employed as intermediates (typically m = 2, 3 and $n \geq 6$ [1-3]), but only a few have been commercialized [4]. Many research groups have described the syntheses of other types of fluorous alkyl [5-8] and aryl [9-12] iodides [13-17]. The former are ubiquitous by virtue of the large number of perfluoroalkyl iodides $R_{fn}I$ that have been shown to undergo free radical additions to alkenes [7,8].

In previous papers, we have reported convenient preparations of a variety of fluorous alkyl iodides [13-15], aryl iodides [16,17], and hypervalent iodine(III) derivatives [16-19]. The latter have included aliphatic iodine(III) bis(trifluoroacetates) [18,19] and dichlorides [17], and aromatic iodine(III) bis(acetates) [16] and dichlorides [17]. The bis(carboxylates) have been employed as recyclable reagents for oxidations of organic substrates [16,18,19], and some of the dichlorides are depicted in Scheme 1. Others have described additional fluorous iodine(III) species [11,20-22].

Recently, our attention has been directed at two potential applications of iodine containing fluorous compounds. One involves new approaches to phosphorus–carbon bond formation using fluorous alkyl and aryl iodides [23,24]. The other involves the use of fluorous iodine(III) dichlorides for free radical chlorinations [25]. In this regard, phenyl iodine(III) dichloride ($PhICl_2$) is an effective free radical chlorinating agent for hydrocarbons [26,27]. Importantly, the mechanism does not involve the liberation of Cl_2, followed by the textbook sequence of steps. Rather, hydrogen abstraction is effected by a species other than the chlorine radical Cl·, presumably PhICl· [26,27].

One potential attraction of fluorous iodine(III) dichlorides as chlorinating agents would be the recovery and recycling of the fluorous iodide byproduct. Towards this end, higher fluorophilicities are usually advantageous. To a first approximation, these are maximized by increasing the lengths and quantities of the $(CF_2)_n$ segments, and decreasing the lengths and quantities of any $(CH_2)_m$ segments [1-3]. However, longer $(CF_2)_n$ segments are often coupled with lower absolute solubilities [1,28], a logical consequence as one approaches the macromolecular limit of polytetrafluoroethylene. Fluorophilicities are typically quantified by fluorous/organic liquid/liquid phase partition coefficients [1-3]. The most common solvent combination is perfluoro(methylcyclohexane) ($CF_3C_6F_{11}$) and toluene.

The objective of this study was to bridge several strategic gaps regarding highly fluorophilic building blocks for the formation of (1) phosphorus–carbon bonded species, and (2) iodine(III) dichloride reagents. For example, aliphatic species of the formula $R_{fn}CH_2CH_2ICl_2$ are unstable [17]. However, analogs with one less methylene group, $R_{fn}CH_2ICl_2$, have been isolated for n = 8 and 10 as depicted in Scheme 1 [17,20]. Although partition coefficients are not available for the iodide $R_{f8}CH_2I$ (the byproduct that would form in most chlorination reactions),

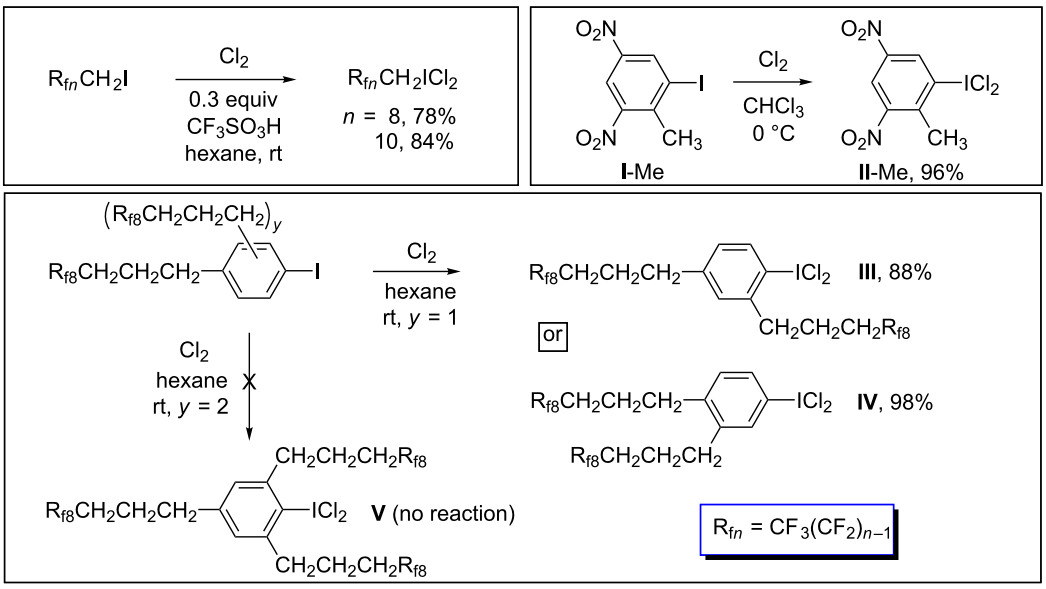

Scheme 1: Some previously reported iodine(III) dichlorides relevant to this work.

they would fall between those of $R_{f8}I$ (88.5:11.5 for $CF_3C_6F_{11}$/toluene [29]) and $R_{f8}(CH_2)_3I$ (50.7: 49.3 [30]). These rather modest fluorophilicities would presumably be lower for the more polar dichlorides $R_{fn}CH_2ICl_2$ – a possible disadvantage for reactions in fluorous solvents. In any case, higher homologs that would have more biased partition coefficients were sought.

In the same vein, literature data prompted interest in certain fluorous aromatic iodine(III) dichlorides. For example, the non-fluorous iodine(III) dichloride **II**-Me (Scheme 1) [31], which features two strongly electron-withdrawing nitro groups and a mildly electron-donating methyl group, is easily isolated in analytically pure form from the reaction of the corresponding aryl iodide and Cl_2, even though the nitro groups render the iodine atom less Lewis basic and thermodynamically less prone to oxidation. The Hammett σ values associated with CF_2CF_3 and $CF_2CF_2CF_3$ substituents (σ_p 0.52; σ_m 0.47–0.52 [32]) suggest that R_{fn} groups are less electron withdrawing than nitro groups (σ_p 0.81; σ_m 0.71). Therefore, similar fluorous compounds of the formula $(R_{fn})_2C_6H_3ICl_2$ were seen as realistic targets. The less fluorophilic homologs **III** and **IV** (Scheme 1), which feature three methylene or $CH_2CH_2CH_2$ "spacers" that electronically insulate the arene ring from the perfluoroalkyl groups, have been previously isolated [17].

As described below, the pursuit of the preceding objectives has met with both success and some unanticipated speed bumps, for which parallel computational studies have provided valuable insight. Regardless, these efforts have resulted in a number of practical preparations that will soon be utilized in further applications [23], and defined various physical properties and stability limits that are useful guides for future research.

Results

Syntheses and reactions, $R_{fn}CH_2I$ (n = 11, 13, 15). To the authors' knowledge, no fluorous alkyl iodides of the formula $R_{fn}CH_2I$ are commercially available. Thus, as shown in Scheme 2, a sequence previously employed for lower homologs (n = 8, 10 [13]) was investigated. The commercially available alcohols $R_{fn}CH_2OH$ (n = 11, 13, 15) were first converted to the triflates $R_{fn}CH_2OTf$ using pyridine and triflic anhydride (Tf_2O) in (trifluoromethyl)benzene ($CF_3C_6H_5$), an amphoteric solvent that is usually able to dissolve appreciable quantities of both fluorous and non-fluorous solutes [33]. The reactions with n = 11 and 13 were conducted at 0 °C, and work-ups gave the expected triflates in 60–61% yields. In contrast, only traces of product were obtained with n = 15, presumably due to the poor solubility of the alcohol in virtually any medium. However, the solubilities of fluorous compounds are often highly temperature dependent [28,34], and an analogous reaction at room temperature gave $R_{f15}CH_2OTf$ in 22% yield. The triflates were white solids with some solubility in acetone. They were characterized by IR and NMR (^1H, $^{13}C\{^1H\}$, $^{19}F\{^1H\}$) spectroscopy and microanalyses as summarized in the experimental section.

The triflates were treated with NaI in acetone at 75 °C. Over the course of 24 h, high conversions to the corresponding fluorous iodides $R_{fn}CH_2I$ were realized, although at rates much slower than with non-fluorous analogs. Work-ups afforded the products as analytically pure white solids in 58–69% yields, which were characterized analogously to the triflates. All were to some degree soluble in acetone, but as the perfluoroalkyl group lengthened, appropriate cosolvents were required to achieve significant concentrations. In order to obtain ^{13}C NMR spectra (n = 13, 15), C_6F_6 – which is technically a non-fluorous solvent [35] but is nonetheless often effective with fluorous solutes – was employed.

Importantly, these fluorous aliphatic iodides were more fluorophilic than those mentioned in the introduction. Representative partition coefficients were determined as described in the experimental section. Those for $R_{f15}CH_2I$ ranged from >99:<1 for $CF_3C_6F_{11}$/toluene to 87:13 for $CF_3C_6F_{11}$/acetone. The $CF_3C_6F_{11}$/toluene partition coefficient of $R_{f11}CH_2I$ was also >99:<1.

Next, CH_3CN/C_6F_6 solutions of the fluorous aliphatic iodides (n = 11, 13) were treated with aqueous NaOCl and conc. HCl. The combination of HCl and a mild oxidant generates Cl_2, providing a "greener" synthetic approach to iodine(III) dichlorides [36-38]. Accordingly, the target molecules $R_{fn}CH_2ICl_2$ precipitated in 33–81% yields. However, the poor solubilities of these pale yellow powders precluded further purification by the usual protocols. Microanalyses confirmed the presence of chlorine.

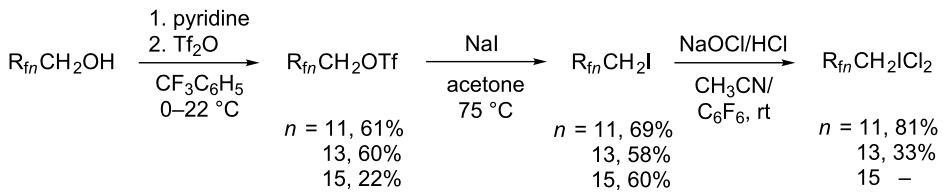

Scheme 2: Syntheses of fluorous compounds of the formula $R_{fn}CH_2X$.

When ^{1}H NMR spectra were recorded in acetone-d_6, new CH_2 signals 1.37–1.38 ppm downfield of those of the precursors $R_{fn}CH_2I$ were apparent. However, the NMR samples slowly became greenish yellow, suggestive of dissolved Cl_2, and the starting iodides were usually evident. The use of Cl_2 in place of NaOCl/HCl did not give better results.

Syntheses and reactions, $R_{fOx}CH_2I$ (x = 2–5). There is an ongoing effort in fluorous chemistry to decrease reliance on perfluorooctyl containing building blocks, which are associated with a variety of environmental issues [39]. One approach is to switch to related ethereal phase tags or "ponytails" [40,41]. Accordingly, oligomeric fluorous ethers that terminate in CH_2OH groups, $CF_3CF_2CF_2O(CF(CF_3)CF_2O)_xCF(CF_3)CH_2OH$, are commercially available. These are abbreviated $R_{fOx}CH_2OH$, and the ethereal oxygen atoms have essentially no Lewis base character. In some cases, $CF_2CF_2OCF(CF_3)CF_2OCF(CF_3)$-segments have been found to impart higher fluorophilicites than similar perfluoroalkyl groups [42]. However, the multiple $CF(CF_3)$ stereocenters are disadvantageous, as they render such compounds mixtures of diastereomers, presenting an impediment to crystallization. In some cases, NMR spectra do not differentiate the diastereomers, and in other cases more complex signal patterns are evident.

As shown in Scheme 3, the oligomeric alcohols (x = 2–5) were elaborated as described for the non-ethereal alcohols $R_{fn}CH_2OH$ and a previous report involving the lower non-oligomeric homolog $R_{fO1}CH_2OH$ (x = 1 [5]). They were first converted to the triflates $R_{fOx}CH_2OTf$ using pyridine and triflic anhydride (Tf_2O). These were soluble in hexane/ethyl acetate and isolated as analytically pure colorless oils in 84–93% yields. Subsequent reactions with NaI in acetone (70–75 °C, x = 2,4,5) gave the corresponding iodides $R_{fOx}CH_2I$ as colorless liquids in 81–91% yields. Unfortunately, efforts to oxidize these compounds to the corresponding iodine(III) dichlorides using the conditions in Scheme 1 and Scheme 2 were unsuccessful. NMR analyses of crude reaction mixtures showed only starting material.

Attempted syntheses of $R_{fn}ICl_2$. Prior to the efforts described in the previous sections, iodine(III) dichlorides derived from perfluoroalkyl iodides $R_{fn}I$ were considered as targets. Since these lack sp^3 carbon–hydrogen bonds, they are not susceptible to possible chlorination or other degradation under free radical chlorination conditions. However, no reactions were observed when $R_{fn}I$ were treated with Cl_2 or NaOCl/HCl.

Nonetheless, perfluoroalkyl iodides $R_{fn}I$ (n = 6–8, 10, 12) can be oxidized using various recipes (e.g., 80% H_2O_2 in trifluoroacetic acid anhydride) to the iodine(III) bis(trifluoroacetates) $R_{fn}I(OCOCF_3)_2$ in high isolated yields [18,19,21]. It was thought that these might, in turn, react with TMSCl as sketched in Scheme 4 to provide "back door" entries to the target compounds $R_{fn}ICl_2$. Indeed, when these reactions were carried out, the samples exhibited the appropriate characteristic bright yellow colors (n = 6, 8). However, upon work-up only the original perfluoroalkyl iodides $R_{fn}I$ were isolated. Hence, it is concluded that the target compounds are thermodynamically and kinetically unstable with respect to Cl_2 elimination, consistent with the failure of the direct reaction and a lower Lewis basicity of the iodine atom as compared to $R_{fn}CH_2I$.

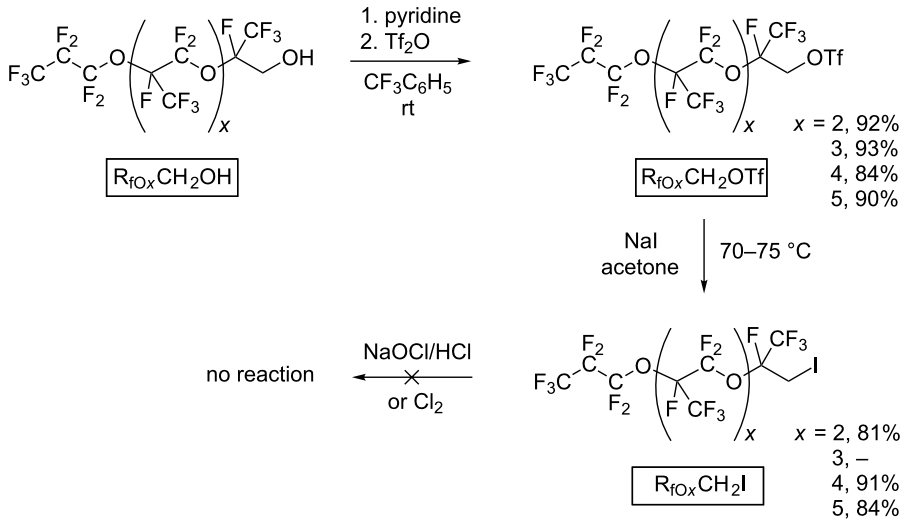

Scheme 3: Syntheses of fluorous compounds of the formula $CF_3CF_2CF_2O(CF(CF_3)CF_2O)_xCF(CF_3)CH_2X'$.

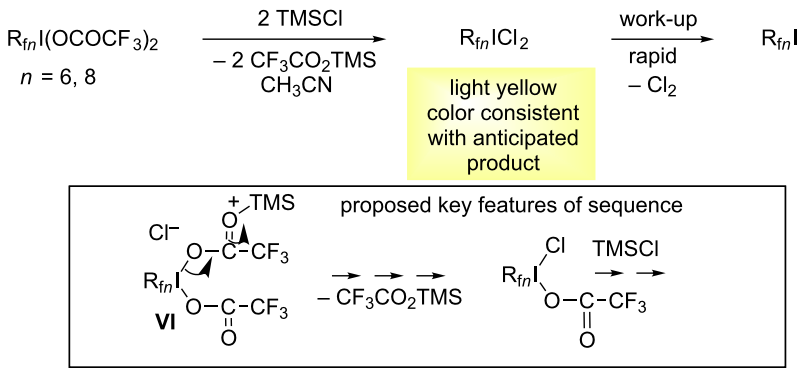

Scheme 4: Attempted syntheses of aliphatic fluorous iodine(III) dichlorides $R_{fn}ICl_2$.

After these experiments were carried out, we became aware of the isolation of CF_3ICl_2 ($R_{f1}ICl_2$) from the reaction of CF_3IClF and TMSCl at −40 °C [43]. This route is conceptually similar to that shown in Scheme 4, and a crystal structure of CF_3ICl_2 could even be obtained. However, consistent with our observations, the compound decomposed above −35 °C.

Syntheses and reactions, aryl iodides with one perfluoroalkyl group. Aromatic compounds are challenging to render highly fluorophilic [16,30,44]. For example, the singly-phase-tagged arene $C_6H_5CH_2CH_2CH_2R_{f8}$ gives a 49.5:50.5 $CF_3C_6F_{11}$/toluene partition coefficient. Values for doubly tagged analogs fall into the range (90.7–91.2):(9.3–8.8) (*o*, *m, p*-isomers), and that for the triply tagged species 1,3,5-$C_6H_3(CH_2CH_2CH_2R_{f8})_3$ is >99.7:<0.3 [30]. As noted above, longer perfluoroalkyl segments increase fluorophilicities, as do shorter methylene segments (compare the partition coefficients of $C_6H_5R_{f8}$ (77.5:22.5) or 1,4-$(R_{f8})_2C_6H_4$ (99.3:0.7) with the preceding examples [29]). Thus, in considering various fluorous aryliodine(III) dichloride targets, initial efforts were directed at systems with at least two R_{fn} substituents per arene ring. Given the ready isolation of the dinitro-substituted aryliodine(III) dichloride **II**-Me in Scheme 1 [31], this was seen as a surefire objective.

However, this was not to be, so the results in this and the following section are presented in inverse chronological order, focusing first on arenes with one R_{fn} substituent. As shown in Scheme 5 (top), the commercially available *meta* diiodide 1,3-$C_6H_4I_2$ was treated with copper (1.0 equiv) and $R_{f6}I$ (0.5 equiv; a deficiency to help suppress dialkylation) in DMSO at 110 °C. Similar recipes have previously been used to couple aryl iodides and $R_{fn}I$ building blocks [45,46]. Work-up gave the target compound 1,3-$R_{f6}C_6H_4I$ in 60% yield (based upon limiting $R_{f6}I$).

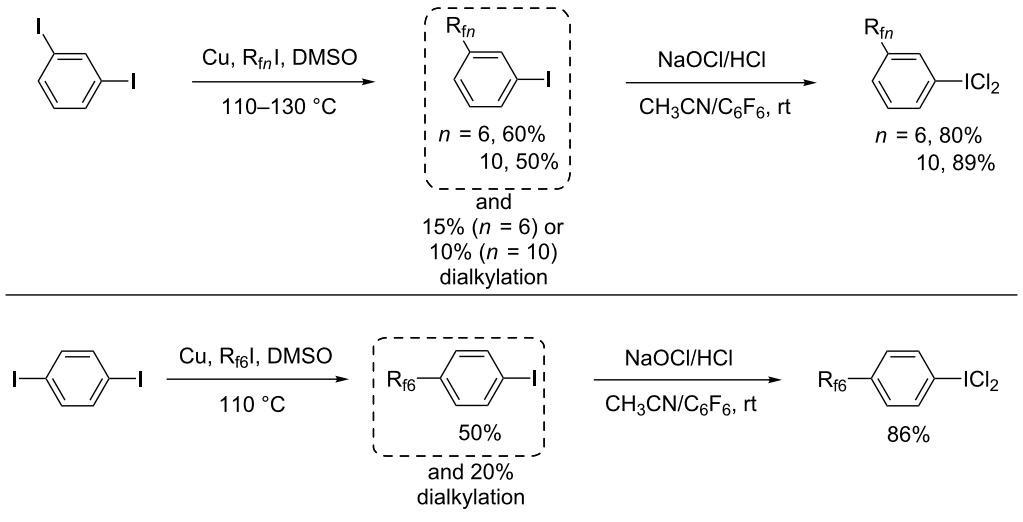

Scheme 5: Syntheses of aromatic fluorous compounds with one perfluoroalkyl group.

Some of the previously reported dialkylation product 1,3-$(R_{f6})_2C_6H_4$ was also formed [47,48], but was easily separated due to its differential fluorophilicity (extraction of a CH_3CN solution with perfluorohexane). An analogous procedure with $R_{f10}I$ gave the higher homolog 1,3-$R_{f10}C_6H_4I$ in 50% yield [9], and a lesser amount of what was presumed to be the dialkylation product. The analogous *para* diiodide 1,4-$C_6H_4I_2$ gave parallel chemistry, as illustrated by the reaction with $R_{f6}I$ to give 1,4-$R_{f6}C_6H_4I$ (50% [4,12]) in Scheme 5 (bottom).

The three aryl iodides $R_{fn}C_6H_4I$ thus obtained were treated with NaOCl/HCl per the sequence in Scheme 2. As shown in Scheme 5, work-ups gave the corresponding iodine(III) dichlorides $R_{fn}C_6H_4ICl_2$ as pale yellow powders in 80–89% yields. Although these were clean by NMR, only one gave a correct microanalysis. As illustrated in Figure S1 (Supporting Information File 1), $CDCl_3/C_6F_6$ solutions of 1,3-$R_{f6}C_6H_4ICl_2$ and 1,4-$R_{f6}C_6H_4ICl_2$ containing an internal standard were monitored by ^{1}H NMR. Slow partial evolution of Cl_2 to give the iodides 1,3-$R_{f6}C_6H_4I$ and 1,4-$R_{f6}C_6H_4I$ was observed (7% and 27% conversion over 60 h, respectively).

Syntheses and reactions, aryl iodides with two perfluoroalkyl groups. In a previously reported procedure [48], the diiodide 1,3-$C_6H_4I_2$ was treated with copper (5.1 equiv) and $R_{f6}I$ (2.2 equiv) in DMSO at 140 °C. As shown in Scheme 6 (top), the bis(perfluorohexyl) adduct 1,3-$(R_{f6})_2C_6H_4$, which was the undesired byproduct in Scheme 5 (top), was isolated in 75% yield. Subsequent iodination using NIS in fuming H_2SO_4/CF_3CO_2H afforded the "all *meta*" iodide 1,3,5-$(R_{f6})_2C_6H_3I$ in 77% yield. The substitution pattern was evident from the ^{1}H NMR spectrum.

When Cl_2 gas was sparged through a $CF_3C_6H_5$ solution of 1,3,5-$(R_{f6})_2C_6H_3I$ at −30 °C to −35 °C, the sample turned bright yellow. Two aliquots were removed. The ^{1}H NMR spectrum of one (Figure 1b) showed two downfield shifted signals (cf. Figure 1a), which were attributed to the target molecule 1,3,5-$(R_{f6})_2C_6H_3ICl_2$. Integration indicated 77:23 and 75:25 $ArICl_2$/ArI ratios prior to and after solvent removal (room temperature, rotary evaporation). The isolated material was redissolved in $CF_3C_6H_5$ and kept at −35 °C. After 7 d, the solvent was again removed by rotary evaporation, giving a 65:35 $ArICl_2$/ArI mixture (Figure 1d). The solvent was removed from the second aliquot by oil pump vacuum at −40 °C. This gave a 35:65 $ArICl_2$/ArI mixture as a pale white solid (Figure 1c). A variety of attempts to achieve higher conversions or isolate pure 1,3,5-$(R_{f6})_2C_6H_3ICl_2$ were unsuccessful. It was concluded that 1,3,5-$(R_{f6})_2C_6H_3ICl_2$ was much more labile with respect to Cl_2 evolution than the fluorous aryliodine(III) dichlorides shown in Scheme 5, and that the 75–80% conversions reflected a thermodynamic limit.

Next, analogs of 1,3,5-$(R_{f6})_2C_6H_3ICl_2$ with less electron-deficient iodine atoms were sought. As shown in Scheme 1, related fluorous aryliodine(III) dichlorides with three-methylene spacers, $(R_{f8}CH_2CH_2CH_2)_2C_6H_3ICl_2$, had been isolated (the isomers **III**, **IV**) [17]. Recently, a potential precursor with two-methylene spacers, 1,3-$(R_{f8}CH_2CH_2)_2C_6H_4$, became readily available [49]. Accordingly, it could be iodinated with I_2/H_5IO_6 as shown in Scheme 6 (bottom) to give 1,2,4-$(R_{f8}CH_2CH_2)_2C_6H_3I$ [50] in 93% yield after work-up. The ^{1}H NMR spectrum clearly indicated the regioisomer in which the iodide is *ortho* and *para* to the two alkyl substituents. This contrasts with the iodination of 1,3-$(R_{f6})_2C_6H_4$, in which the substituents function as *meta* directing groups.

As shown in Scheme 6, reactions of C_6F_6 or perfluoroheptane solutions of 1,2,4-$(R_{f8}CH_2CH_2)_2C_6H_3I$ and NaOCl/HCl gave the corresponding iodine(III) dichloride 1,2,4-

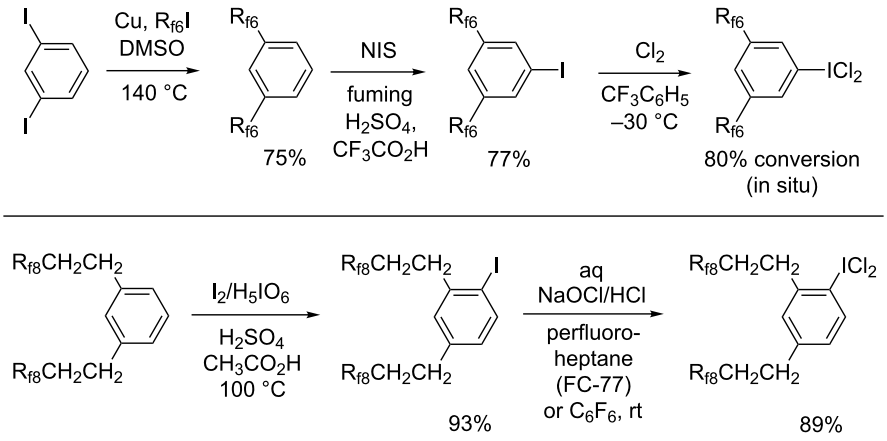

Scheme 6: Syntheses of aromatic fluorous compounds with two perfluoroalkyl groups.

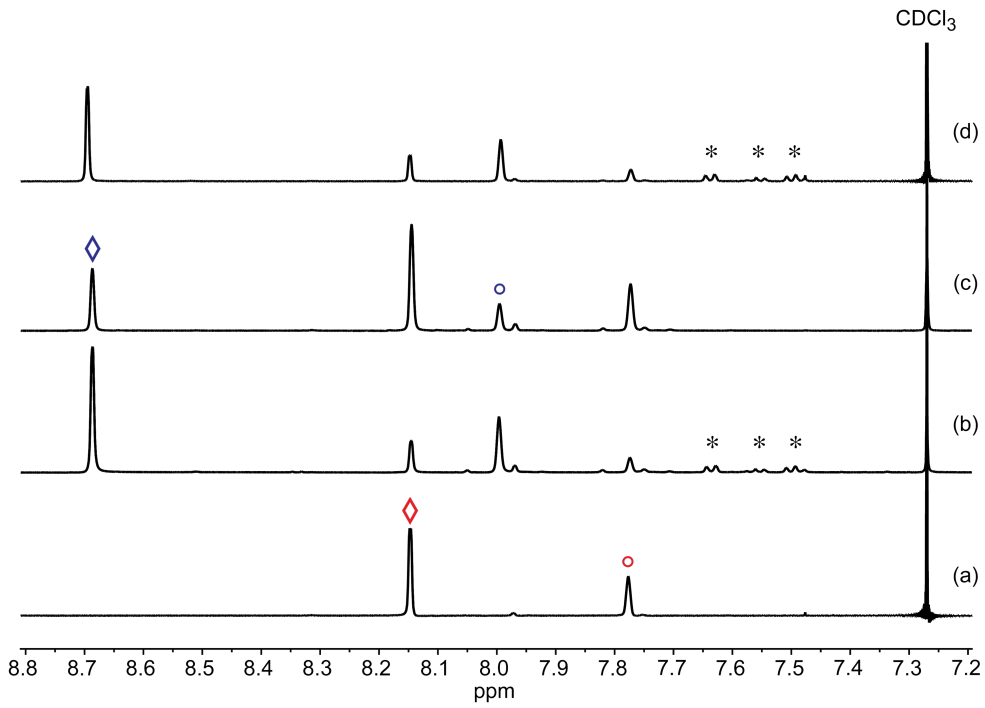

Figure 1: Partial ^{1}H NMR spectra (sp^2 CH, 500 MHz, $CDCl_3$) relating to the reaction of 1,3,5-$(R_{f6})_2C_6H_3I$ and Cl_2 in $CF_3C_6H_5$ at −30 to −35 °C: (a) starting 1,3,5-$(R_{f6})_2C_6H_3I$; (b) aliquot taken after 24 h and removing nearly all $CF_3C_6H_5$ (* = residual signals) by rotary evaporation (75:25 $ArICl_2$/ArI); (c) aliquot taken after 24 h and removing all solvents by oil pump vacuum at −40 °C (35:65 $ArICl_2$/ArI); (d) the sample from b, which was redissolved in $CF_3C_6H_5$, kept at −35 °C for 7 d, and worked up as in b (65:35 $ArICl_2$/ArI). The signals for the protons *para* and *ortho* to the iodine atoms are denoted ° and ◊ (red = ArI; blue = $ArICl_2$).

$(R_{f8}CH_2CH_2)_2C_6H_3ICl_2$ [50] as a white powder in 89% yield. This material was stable at room temperature and gave a microanalysis consistent with a monohydrate. Hence, the iodine atom in benzenoid compounds with two $R_{f8}CH_2CH_2$ substituents is sufficiently Lewis basic to support a dichloride, but analogs with two R_{f6} substituents are not.

Structural and computational data. Crystal structures of fluorous compounds were virtually unknown 20 years ago [51], so opportunities to acquire structural data are usually seized. Crystals of 1,3,5-$(R_{f6})_2C_6H_3I$ could be grown as described in the experimental section. X-ray data were collected, and the structure determined, as summarized in Table 1 and the experimental section. Two views of the molecular structure and key metrical parameters are provided in Figure 2. Two perspectives of the unit cell (Z = 8) are provided in Figure 3. There are some unusual features associated with the packing and space group, and these are treated in the discussion section.

In order to help interpret the accessibilities and/or stabilities of the various iodine(III) dichlorides described above, the gas phase free energies of chlorination

$$RI(g) \text{ or } ArI(g) + Cl_2(g) \longrightarrow RICl_2(g) \text{ or } ArICl_2(g) \quad (1)$$

were computed by DFT methods as described in the experimental section and summarized in Table S1 (Supporting Information File 1). The data are presented in "ladder format" in Figure 4, with the substrates that undergo more exergonic chlorinations placed higher. The energy difference between any pair of compounds is equal to that expressed by the corresponding isodesmic equation:

$$RI(g) \text{ or } ArI(g) + R'ICl_2(g) \text{ or } Ar'ICl_2(g) \longrightarrow RICl_2(g) \text{ or } ArICl_2(g) + R'I(g) \text{ or } Ar'I(g) \quad (2)$$

The validity of the data was supported by the good agreement of the computed structure of 1,3,5-$(R_{f6})_2C_6H_3I$ with the crystal structure (Figure 2). An overlay, provided in Figure S2 (Supporting Information File 1), shows only very slightly increasing conformational differences as the perfluorohexyl groups extend from the arene. For the aliphatic compounds ($R_{fn}I$, $R_{fn}CH_2I$, $R_{fOx}CH_2ICl_2$), the free energies of chlorination were calculated for a series of chain lengths. As summarized in Figure 4 and tabulated in Table S1 (Supporting Information File 1), the ΔG values within each series varied by less than 0.5 kcal/mol. In all cases, vertical ionization potentials (not presented) followed analogous trends.

Table 1: Summary of crystallographic data for 1,3,5-$(R_{f6})_2C_6H_3I$.

empirical formula	$C_{18}H_3F_{26}I$
formula weight	840.10
diffractometer	Bruker GADDS X-ray (three-circle)
temperature [K]	110(2)
wavelength [Å]	1.54178
crystal system	tetragonal
space group	*I*4
unit cell dimensions	
a [Å]	29.6474(9)
b [Å]	29.6474(9)
c [Å]	5.5976(2)
α [°]	90
β [°]	90
γ [°]	90
V [Å^3]	4920.1(3)
Z	8
ρ_{calcd} [Mg/m^3]	2.268
μ [mm^{-1}]	12.238
F(000)	3184
crystal size [mm^3]	0.40 × 0.02 × 0.02
θ limit [°]	2.11 to 59.94
index ranges [*h*, *k*, *l*]	−33, 32; −33, 33; −6, 5
reflections collected	53384
independent reflections	3568
R(int)	0.0540
completeness (%) to θ (°)	99.8 (59.94)
max. and min. transmission	0.7919 and 0.0843
data/restraints/parameters	3568/1/407
goodness-of-fit on F^2	0.991
R indices (final) [$I > 2\sigma(I)$]	
R_1	0.0156
wR_2	0.0355
R indices (all data)	
R_1	0.0172
wR_2	0.0357
largest diff. peak and hole [eÅ^{-3}]	0.227 and −0.532

The iodine(III) dichlorides formed in the more exergonic reactions (upper portion of Figure 4) would be expected to be more stable with respect to Cl_2 evolution. Thus, the data are consistent with the stability order $R_{fn}CH_2ICl_2$ >> $R_{fn}ICl_2$ evident from Scheme 2 and Scheme 4. However, they also imply that the ethereal systems $R_{fOx}CH_2ICl_2$ (Scheme 3; −0.65 kcal/mol, x = 1) should be more stable than $R_{fn}CH_2ICl_2$ (−0.53 to −0.59 kcal/mol, n = 4–8). All attempts to generate the former have been unsuccessful to date. Hence, there is either a kinetic barrier to the formation of $R_{fOx}CH_2ICl_2$ that is not overcome under the conditions of Scheme 3, or an unrecognized, presumably non-electronic, destabilizing feature.

In the same vein, there must be a mitigating factor, such as solubility, that allows the isolation of the dinitro-substituted aryliodine(III) dichloride **II**-Me in pure form (Scheme 1), but not the bis(perfluorohexyl) species 1,3,5-$(R_{f6})_2C_6H_3ICl_2$ (Scheme 6, Figure 1). The latter is derived from a more Lewis basic aryl iodide, with Cl_2 addition 0.83 kcal/mol more favorable. The *ortho* methyl group in **II**-Me plays a moderately stabilizing role, with Cl_2 addition to **I**-Me 0.73 kcal/mol more favorable than **I**. Otherwise, the computations (carried out with R_{f6} groups to aid comparability) nicely predict the relative stabilities of the fluorous aryliodine(III) dichlorides (1,2,4-$(R_{f8}CH_2CH_2)_2C_6H_3ICl_2$ [50] > 1,4-$R_{f6}C_6H_4ICl_2$ > 1,3-$R_{f6}C_6H_4ICl_2$ > 1,3,5-$(R_{f6})_2C_6H_3ICl_2$).

Discussion

The preceding experimental data define the stability limits associated with a broad range of fluorous aliphatic and aromatic

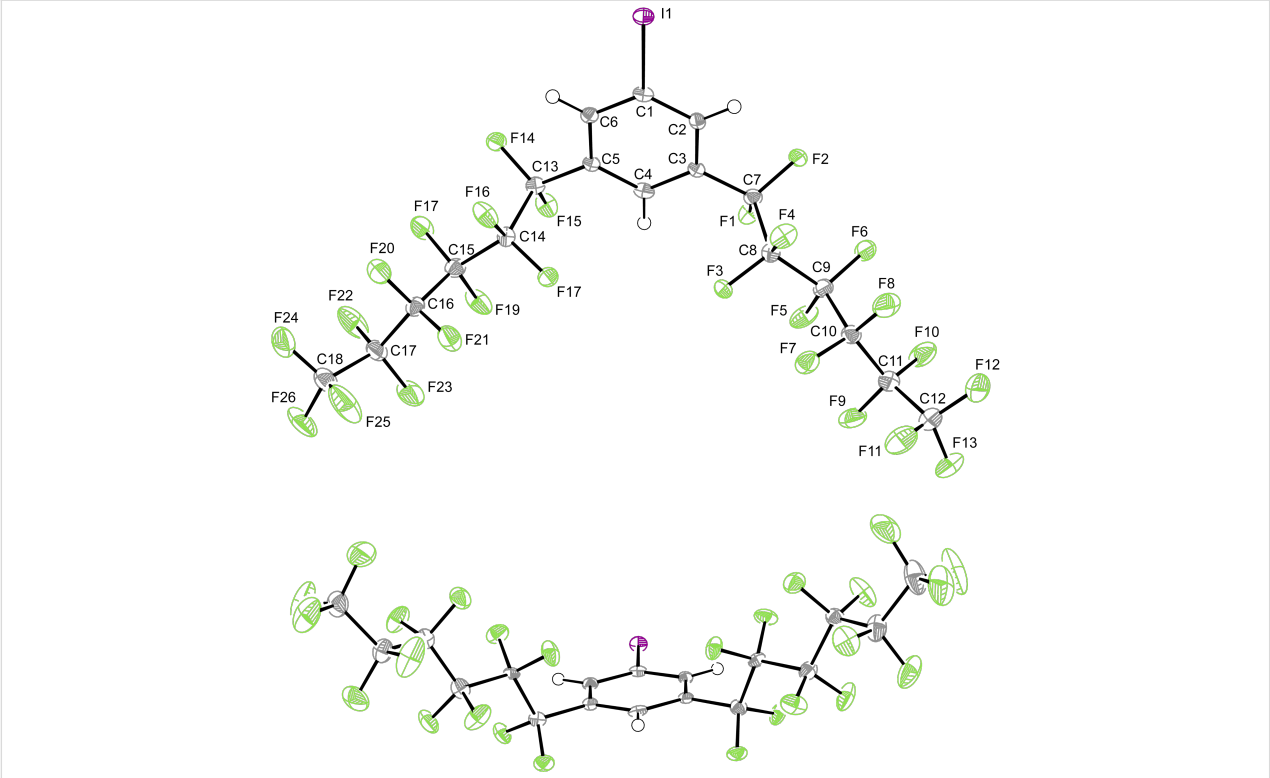

Figure 2: Two views of the molecular structure of 1,3,5-$(R_{f6})_2C_6H_3I$ with thermal ellipsoids at the 50% probability level. Key bond lengths (Å) and angles (°): C1–I1 2.099(3), C1–C2 1.391(4), C2–C3 1.386(4), C3–C4 1.393(4), C4–C5 1.387(4), C5–C6 1.393(4), C6–C1 1.394(4), C3–C7 1.501(4), C5–C13 1.508(4), average of 10 CF–CF 1.545(5), I1–C1–C2 119.0(2), C1–C2–C3 118.8(3), C2–C3–C4 121.0(3), C3–C4–C5 119.2(3), C4–C5–C6 121.1(3), C5–C6–C1 118.5(3), C6–C1–C2 121.4(3), C6–C1–I1 119.5(2), C2–C3–C7 119.7(2), C4–C3–C7 119.3(2), C4–C5–C13 119.6(2), C6–C5–C13 119.3(2), average of 8 CF–CF–CF 115.0(10).

iodine(III) dichlorides. Aliphatic compounds of the formula $R_{fn}ICl_2$ are clearly very unstable with respect to Cl_2 loss, although there is literature precedent for their synthesis and isolation from other iodine(III) precursors under exacting low temperature conditions [43]. When an insulating methylene group is introduced between the fluorous moiety and the ICl_2 group, the situation improves. Compounds of the formula $R_{fn}CH_2ICl_2$ can generally be isolated, although they are somewhat labile towards Cl_2 loss. In contrast, efforts to prepare the ethereal systems $R_{fOx}CH_2ICl_2$ by the chlorination of $R_{fOx}CH_2I$ have been unsuccessful. This poses a conundrum with respect to the DFT calculations; they seemingly possess sufficient Lewis basicity (Figure 4), but there appears to be a kinetic barrier.

In contrast, fluorous aromatic iodine(III) dichlorides bearing a single perfluoroalkyl group, $R_{fn}C_6H_4ICl_2$, are easily isolated in analytically pure form (Scheme 5), although they are still subject to slow Cl_2 loss in solution (Figure S1, Supporting Information File 1). However, it has not yet proved possible to quantitatively generate analogs with two perfluoroalkyl groups by chlorinations of iodine(I) precursors (Scheme 6, top); 75–80% conversions are the maximum realized to date. In contrast, chlorinations of the doubly substituted substrates $(R_{fn}(CH_2)_m)_2C_6H_3I$ (m = 2, 3) go to completion, as exemplified in Scheme 1 (bottom) and Scheme 6 (bottom). The intervening methylene groups partially insulate the iodine atoms from the electron-withdrawing perfluoroalkyl segments, enhancing Lewis basicities.

However, it has not yet proved possible to access related compounds with three $R_{fn}(CH_2)_m$ groups, at least when two of them are *ortho* to the iodine atom, as exemplified by **V** in Scheme 1 [17]. To probe this point, the DFT calculations were extended to the R_{f6} homologs of the precursors of the three aryliodine(III) dichlorides in Scheme 1. These correspond to **VII**, **VIII**, and **IX** in Scheme 7 (top). The ΔG values obtained were −3.40, −3.75, and −4.15 kcal/mol, respectively. Thus, the third $R_{fn}(CH_2)_3$ substituent enhances the exergonicity of Cl_2 addition. Hence, the failure to observe a reaction must represent a kinetic phenomenon. A second "ladder", augmented with the additional alkyl and aryl iodides analyzed in the discussion section, is provided in Figure S3 (Supporting Information File 1).

Interestingly, isodesmic reactions corresponding to Equation 2 in the preceding section can actually be carried out. For example, Cl_2 can be transferred from the fluorous aliphatic

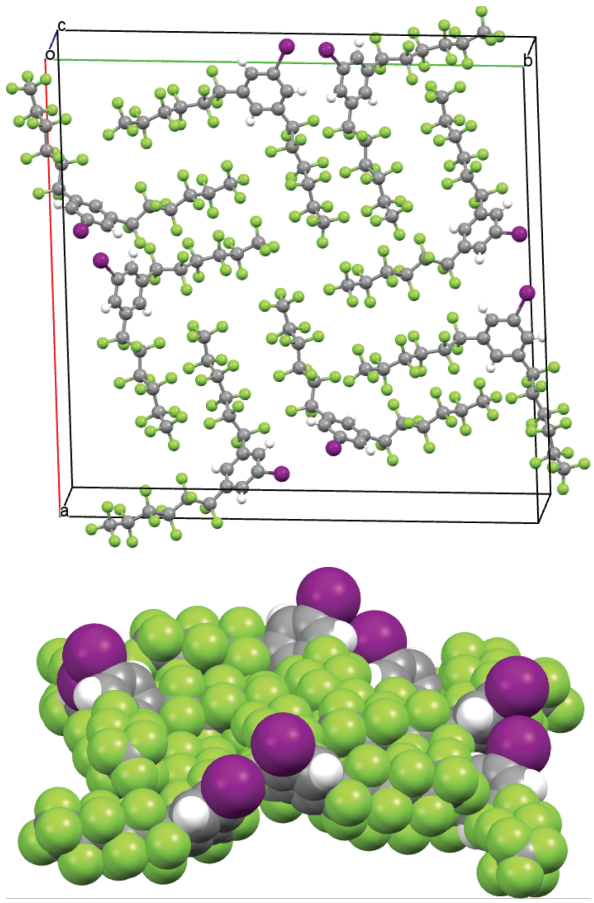

Figure 3: Ball-and-stick and space filling representations of the unit cell of 1,3,5-$(R_{f6})_2C_6H_3I$.

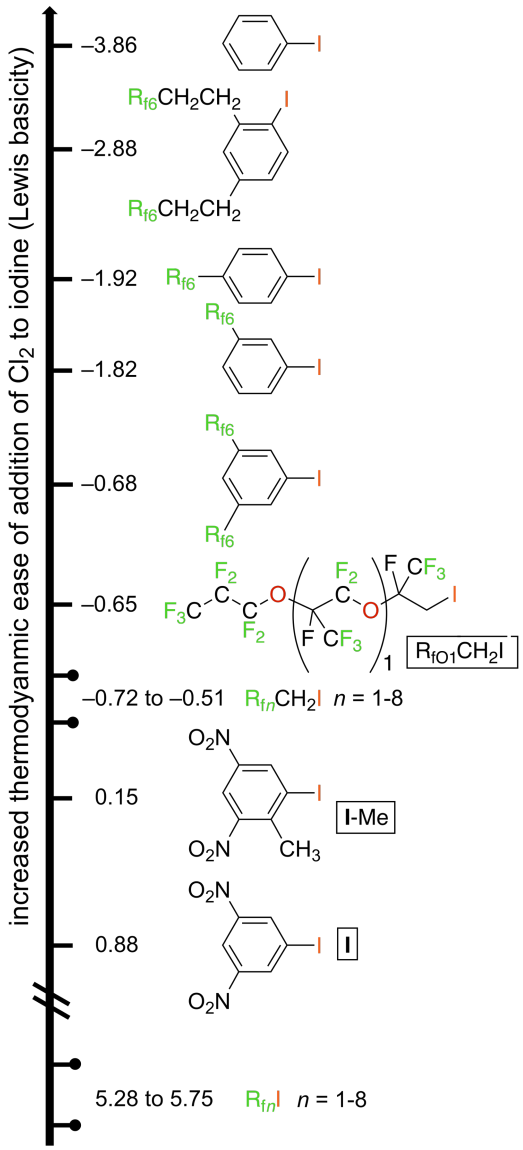

Figure 4: Free energies of chlorination of relevant aryl and alkyl iodides to the corresponding iodine(III) dichlorides in the gas phase (kcal/mol), presented in a ladder format (each iodide is more Lewis basic than that shown below it).

iodine(III) dichloride $R_{f1}CH_2ICl_2$ ($CF_3CH_2ICl_2$) to phenyl iodide as shown in Scheme 7 (middle) [52]. The ΔG value for the addition of Cl_2 to phenyl iodide is computed to be −3.86 kcal/mol, as compared to −0.72 kcal/mol for $R_{f1}CH_2I$. Curiously, the introduction of two $R_{fn}(CH_2)_3$ substituents that are *ortho*/*para* or *meta*/*para* to iodine is thermodynamically deactivating for Cl_2 addition (**VII**/**III** and **VIII**/**IV**; −3.40 to −3.75 kcal/mol), whereas the introduction of three that are *ortho*/*para*/*ortho* is activating (**IX**/**V**; −4.15 kcal/mol) but kinetically inhibiting for steric reasons.

As noted in the introduction, a long-standing goal has been to realize highly fluorophilic aliphatic and aromatic iodine(I) compounds and iodine(III) dichlorides. The preceding results raise the question, "*quo vadis*?" When the compounds $R_{fn}CH_2I$ and $R_{fn}CH_2ICl_2$ reach n = 15 (Scheme 2), they are close to approaching a practical solubility limit, although the former gives a highly biased $CF_3C_6F_{11}$/toluene liquid/liquid partition coefficient. Branched analogs may be more tractable. However, DFT calculations show that chlorinations of substrates such as $(R_{fn})_3CCH_2I$ **X** (Scheme 7) would be strongly endergonic (ΔG = 3.36 kcal/mol, n = 6). Related species, such as (1) $(R_{fn})_3CCF_2CF_2CH_2I$, which features a more remote branch site, or (2) $(R_{fn}CH_2)_3CCH_2I$, which features additional insulating methylene groups, would be more likely to give stabile iodine(III) dichlorides. Nonetheless, these types of species have never been described in the literature. Silicon has been used as a locus for branching, as exemplified by a variety of highly fluorophilic compounds of the formula $(R_{fn}CH_2CH_2)_3SiZ$ (see **XI** in Scheme 7, Z = 4-C_6H_5X [53,54]). However, these feature silicon–carbon and sp^3 carbon–hydrogen bonds that may be sensitive towards Cl_2.

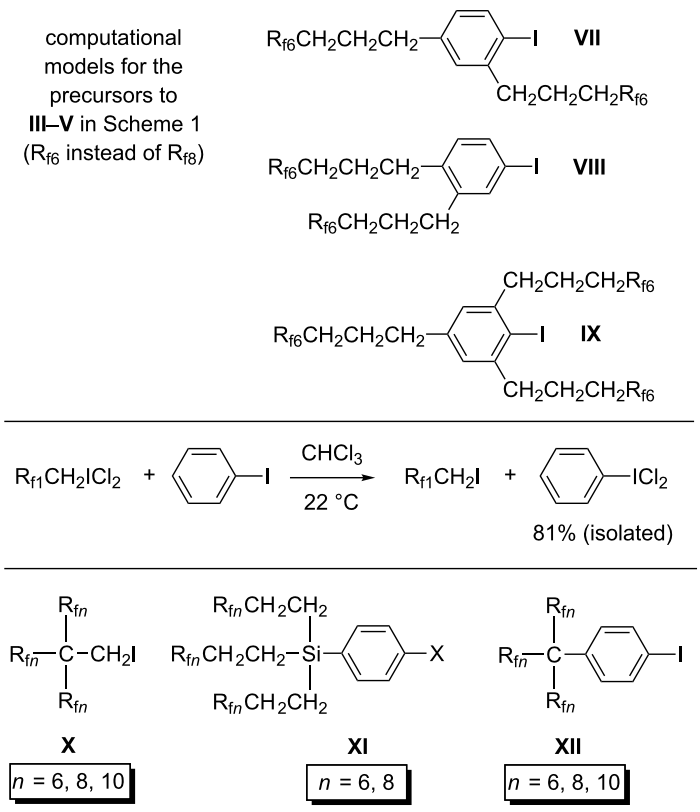

Scheme 7: Other relevant fluorous compounds and reactions.

The fluorous aryl iodides that are precursors to **III** and **IV** have rather modest fluorophilicities ($CF_3C_6F_{11}$/toluene partition coefficients (69.5–74.7):(30.5–25.3) [16]), and simply lengthening the R_{f8} segments to R_{f10} or even longer is unlikely to achieve biases of >99:<1. The same goes for 1,2,4-$(R_{f8}CH_2CH_2)_2C_6H_3I$ in Scheme 6. Accordingly, we suggest that branched fluorous aryl iodides of the formula $(R_{fn})_3CC_6H_4I$ (**XII**, Scheme 7) have particular promise. DFT calculations establish exergonic chlorinations, with ΔG values of −1.93 and −1.59 kcal/mol for n = 6 and 8. This implies that the corresponding iodine(III) dichlorides should have good stabilities, equal to or better than those of 1,3- and 1,4-$R_{f6}C_6H_4ICl_2$ in Scheme 5. However, this represents a currently unknown type of compound, and the synthesis is potentially challenging.

The following analysis of the crystal structure of 1,3,5-$(R_{f6})_2C_6H_3I$ is kept brief, as this compound crystallizes in the same space group and crystal system (*I*4, tetragonal) as the corresponding bromide 1,3,5-$(R_{f6})_2C_6H_3Br$ reported earlier [48]. The unit cell dimensions of the latter are virtually identical, with the cell volume ca. 1.5% lower (4851.7(4) vs 4920.1(3) Å^3), apropos to the smaller bromine atom. The space group is both chiral and polar, and the unit cell dimensions of both compounds feature c values (5.5976(2)–5.5624 Å) that are much smaller than the a and b values (29.6474(9)–29.5335(13) Å). As noted earlier and illustrated in Figure 2 (bottom), the sixteen perfluorohexyl groups associated with the eight molecules in the unit cell lie roughly in the a/b plane. They largely segregate, as seen for most fluorous molecules [44,51,55,56], into fluorous domains.

The eight arene rings in the unit cell tilt distinctly out of the a/b plane (average angle 49.1°). Furthermore, the eight iodine atoms are oriented on the same "side" or a/b face of the unit cell. In the neighboring unit cell that adjoins the a/b face, the iodine atoms are found on the opposite side (c direction). This represents the molecular basis for the polar nature of the crystal. Also, the C–C–C–C and F–C–C–F segments in the perfluorohexyl groups do not exhibit the idealized antiperiplanar and gauche conformations associated with saturated alkanes. Rather, the torsion angles for the roughly anti linkages average 164.4(1.6)° and 166.0(3.6)°, respectively. This leads to helical motifs as shown in Figure 5, which are furthermore reproduced by the computations. The basis for this deviation, as well as a more detailed presentation of the torsional relationships, is provided elsewhere [57-59]. In a given molecule, the C_6F_{13} groups exhibit opposite helical chiralities (see Figure S2, Supporting Information File 1), affording a *meso* stereoisomer.

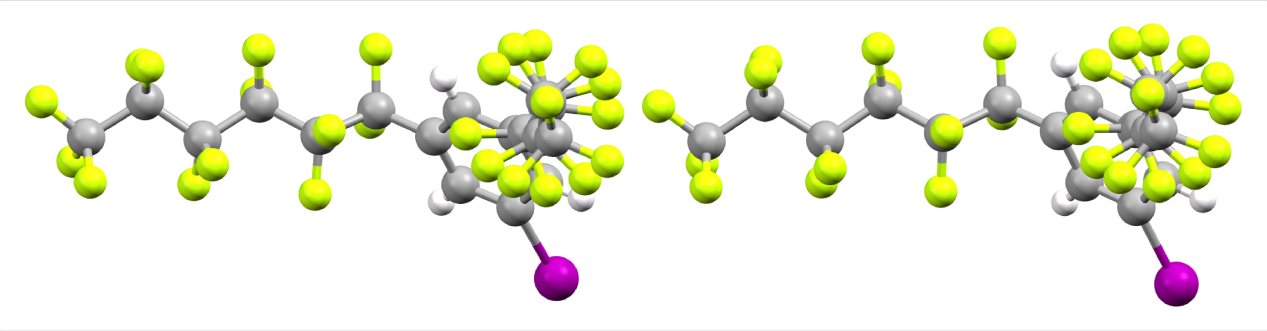

Figure 5: Views of the helical motif of the perfluorohexyl segments in crystalline 1,3,5-$(R_{f6})_2C_6H_3I$ (left) and the structure computed by DFT calculations (right).

Finally, attempts have been made to extend the preceding chemistry in several directions. In screening experiments, all of the fluorous iodine(III) dichlorides assayed, as well as $PhICl_2$, were competent for the free radical chlorination of methane [25]. Under certain conditions, uncommon selectivities were apparent, but the fluorophilicities of the dichlorides or precursor iodides studied were insufficient for certain target recycling strategies. As discussed above, it is not clear how to meet these challenges at this time, although the couple $R_{f13}CH_2ICl_2$/$R_{f13}CH_2I$ would be one of several with promise. Regardless, the fluorous iodides reported herein have numerous other uses, some of which will be communicated in the near future [23].

Conclusion

The preceding experimental and computational data have established a strong correlation between iodine atom Lewis basicity and the feasibility of oxidizing fluorous and non-fluorous aliphatic and aromatic iodides to the corresponding iodine(III) dichlorides. Although a few surprises are noted, these are attributed to special phenomena that can drive equilibria, such as precipitation (e.g., the conversion of **I**-Me to **II**-Me in Scheme 1), or kinetic barriers (inertness of $R_{fOx}CH_2I$ in Scheme 3 or the precursor to **V** in Scheme 1). With the fluorous iodides, the extent of chlorination generally provides a measure of the degree to which the electron-withdrawing perfluoroalkyl or perfluoroether segments are insulated from the Lewis basic site.

Experimental

Five syntheses that are representative of the types of transformations in this study are detailed in the main article. The remaining preparations are described in Supporting Information File 1, together with data on the solvents, starting materials, and instrumentation employed.

$R_{f11}CH_2OTf$. A Schlenk flask was flame dried, allowed to cool, charged with $R_{f11}CH_2OH$ (5.10 g, 8.52 mmol) and anhydrous $CF_3C_6H_5$ (50 mL) under a N_2 flow, capped, and placed in an ice bath. Then pyridine (1.0 mL, 1.0 g, 13 mmol) and (after 30 min) Tf_2O (3.0 mL, 5.3 g, 14 mmol) were added dropwise by syringe with stirring. The ice bath was allowed to warm to room temperature. After 16 h, H_2O (60 mL) was added. After 30 min, the organic phase was separated and dried ($MgSO_4$). The solvent was removed by rotary evaporation. The residue was dissolved in petroleum ether/ethyl acetate (4:1 v/v). The solution was filtered through a silica pad (3 × 5 cm) and the solvent was removed by rotary evaporation to give $R_{f11}CH_2OTf$ as a white solid (3.82 g, 5.21 mmol, 61%), mp 77.2–79.9 °C (capillary). Anal. calcd for $C_{13}H_2F_{26}O_3S$: C, 21.33; H, 0.28; F, 67.46; S, 4.38; found: C, 21.44; H, 0.31; F, 67.21; S, 4.15; ^{1}H NMR (500 MHz, acetone-d_6) δ 5.55 (t, $^3J_{HF}$ = 13 Hz, 2H, CH_2); ^{19}F{^{1}H} NMR (470 MHz, acetone-d_6) δ −75.5 (s, 3F, SO_2CF_3), −81.7 (t, $^4J_{FF}$ = 10 Hz [60-62], 3F, CF_3), −120.2 (m, 2F, CF_2), −122.2 (m, 12F, $6CF_2$), −123.2 (m, 4F, $2CF_2$), −126.7 (m, 2F, CF_2); ^{13}C{^{1}H} NMR (125 MHz, acetone-d_6, partial) δ 70.0 (t, $^2J_{CF}$ = 28 Hz, CH_2); IR (powder film, cm^{-1}): 2924 (w), 2855 (w), 1418 (m), 1202 (s), 1140 (s), 1103 (w), 1023 (m), 854 (m), 822 (m).

$R_{f11}CH_2I$. A round bottom flask was charged with $R_{f11}CH_2OTf$ (3.01 g, 4.11 mmol), NaI (10.2 g, 68.0 mmol), and acetone (30 mL), and fitted with a condenser. The flask was placed in a 75 °C oil bath and the mixture was stirred. After 1 d, the bath was removed and the mixture was allowed to cool. The solvent was removed by rotary evaporation. Then Et_2O (50 mL) and H_2O (40 mL) were added with stirring. After 5 min, the dark brown organic phase was separated, washed with saturated aqueous $Na_2S_2O_3$ until it became colorless, and dried (Na_2SO_4). The solvent was removed by rotary evaporation and the residue was dissolved in hexanes/ethyl acetate (20:1 v/v). The solution was kept at −35 °C until a precipitate formed. The solid was collected by filtration and washed with cold hexanes to give $R_{f11}CH_2I$ as a white solid (2.00 g, 2.82 mmol, 69%), mp (capillary): 97.8–98.2 °C. Anal. calcd for $C_{12}H_2F_{23}I$: C, 20.30; H, 0.28; F, 61.54; I, 17.87; found: C, 20.20; H, 0.16; F, 61.29; I, 17.68; ^{1}H NMR (500 MHz, acetone-d_6) δ 4.06 (t, $^3J_{HF}$ = 19 Hz,

2H, CH_2); $^{19}F\{^1H\}$ NMR (470 MHz, acetone-d_6) δ −81.6 (t, $^4J_{FF}$ = 10 Hz [60-62], 3F, CF_3), −107.0 (m, 2F, CF_2), −122.2 (m, 14F, $7CF_2$), −123.2 (m, 2F, CF_2), −126.7 (m, 2F, CF_2); $^{13}C\{^1H\}$ NMR (125 MHz, acetone-d_6, partial) δ −3.8 (t, $^2J_{CF}$ = 25 Hz, CH_2); IR (powder film, cm^{-1}): 2986 (w), 2874 (w), 1422 (w), 1373 (w), 1348 (w), 1234 (s), 1200 (s), 1140 (s), 1040 (m), 858 (m).

$R_{f11}CH_2ICl_2$. A round bottom flask was charged with $R_{f11}CH_2I$ (1.01 g, 1.42 mmol), C_6F_6 (1.4 mL), and CH_3CN (14 mL) with stirring. Aqueous NaOCl (2.5% w/w, 21 mL) and then conc. HCl (10 mL) were slowly added. After 2 h, a pale yellow precipitate began to form. After 5 h, the mixture was filtered. The filter cake was washed with hexane (10 mL) and air dried (4–5 h) to give $R_{f11}CH_2ICl_2$ as a pale yellow powder (0.90 g, 1.15 mmol, 81%), mp 122.1–125.4 °C (capillary). Anal. calcd for $C_{12}H_2F_{23}Cl_2I$: C, 18.46; H, 0.26; F, 55.96; Cl, 9.08; found: C, 16.76; H, 1.16; F, 50.15; Cl, 7.98 [63]; ^1H NMR (500 MHz, acetone-d_6) δ 5.44 (t, $^3J_{HF}$ = 17 Hz, 2H, CH_2); $^{19}F\{^1H\}$ NMR (470 MHz, acetone-d_6, partial) δ −106.7 (m, 2F, CF_2); IR (powder film, cm^{-1}): 3030 (w), 2970 (w), 1392 (w), 1373 (w), 1348 (w), 1315 (w), 1202 (s), 1148 (s), 1046 (m), 860 (m).

1,3-$R_{f6}C_6H_4I$. A Schlenk tube was charged with copper (1.26 g, 20.0 mmol) and DMSO (30 mL) and placed in a 105 °C oil bath. The mixture was sparged with N_2 with stirring (30 min), and 1,3-diiodobenzene (6.60 g, 20.0 mmol) was added. After a second sparge, $R_{f6}I$ (4.48 g, 10.0 mmol) was added in portions over 30 min under a N_2 flow with stirring. The tube was sealed and placed in a 110 °C oil bath. After 4 d, the mixture was cooled to room temperature and poured into H_2O (100 mL). Then Et_2O (100 mL) was added with stirring. After 1 h, the aqueous phase was separated and extracted with Et_2O (5 × 50 mL). The combined organic phases were dried (Na_2SO_4) and the solvent was removed by rotary evaporation. The residue was dissolved in CH_3CN (10 mL). The sample was extracted with perfluorohexane (5 × 5 mL). The fluorous layers were combined, concentrated to 2 mL, and extracted with acetone (5 × 3 mL). The solvent was removed from the extracts by oil pump vacuum to give 1,3-$R_{f6}C_6H_4I$ as a colorless oil (3.16 g, 6.05 mmol, 60% based upon $R_{f6}I$). Anal. calcd for $C_{12}H_4F_{13}I$: C; 27.61; H, 0.77; F, 47.31; found: C, 28.09; H, 0.67; F, 48.59 [63]. The solvent was removed from the concentrated perfluorohexane extract by oil pump vacuum to give 1,3-$(R_{f6})_2C_6H_4$ as a light yellow oil (1.07 g, 1.51 mmol, 15%) [48]. The ^1H NMR spectrum matched those in the literature [47,48]. ^1H NMR (500 MHz, CD_2Cl_2) δ 8.01 (s, 1H), 7.96 (d, $^3J_{HH}$ = 8 Hz, 1H), 7.61 (d, $^3J_{HH}$ = 8 Hz, 1H), 7.26 (t, $^3J_{HH}$ = 8 Hz, 1H); $^{19}F\{^1H\}$ (470 MHz, CD_2Cl_2) δ −82.0 (t, $^4J_{FF}$ = 9 Hz [60-62], 3F, CF_3), −111.7 (t, $^4J_{FF}$ = 15 Hz [60-62], 2F, CF_2), −122.1 (m, 2F, CF_2), −122.3 (m, 2F, CF_2), −123.5 (m, 2F, CF_2), −127.0 (m, 2F, CF_2); $^{13}C\{^1H,^{19}F\}$ (125 MHz, CD_2Cl_2) δ 141.9, 136.4, 130.8, 126.8, 118.0 (5 × s, C_6H_4), 116.1, 115.8, 112.0, 111.5, 111.1, 109.3 (5 × s, $5CF_2/CF_3$), 94.4 (s, CI).

1,3-$R_{f6}C_6H_4ICl_2$. A round bottom flask was charged 1,3-$R_{f6}C_6H_4I$ (0.523 g, 1.00 mmol), C_6F_6 (1 mL), and CH_3CN (10 mL) with stirring. Aqueous NaOCl (2.5% w/w, 10 mL) followed by conc. HCl (10 mL) were slowly added. After 30 min, a pale yellow precipitate began to form. After 3 h, the mixture was filtered. The filter cake was washed with H_2O (5 mL) and hexane (10 mL) and air dried (2 d) to give 1,3-$R_{f6}C_6H_4ICl_2$ as a pale yellow powder (0.477 g, 0.804 mmol, 80%). Anal. calcd for $C_{12}H_4F_{13}Cl_2I$: C, 24.31; H, 0.68; F, 41.65; found: C, 23.89; H, 0.38; F, 49.81 [63]; ^1H NMR (500 MHz, $CDCl_3/C_6F_6$) δ 8.54–8.52 (m, 2H), 7.94 (d, $^3J_{HH}$ = 8 Hz, 1H), 7.79 (t, $^3J_{HH}$ = 8 Hz, 1H); $^{19}F\{^1H\}$ NMR (470 MHz, $CDCl_3/C_6F_6$) δ −82.3 (t, $^4J_{FF}$ = 9 Hz [60-62], 3F, CF_3), −112.0 (t, $^4J_{FF}$ = 15 Hz [60-62], 2F, CF_2), −124.4 (m, 4F, $2CF_2$), −123.7 (m, 2F, CF_2), −127.3 (m, 2F, CF_2).

Partition coefficients. The following is representative. A 20 mL vial was charged with a $CF_3C_6F_{11}$ solution of $R_{fn}CH_2I$ (n = 11, 15; 5.0×10^{-2} M, 4.0 mL) and toluene (4.0 mL), capped, and vigorously stirred. After 10 min at room temperature (24 °C), aliquots were removed from the fluorous (2.0 mL) and organic (2.0 mL) phases. The solvent was evaporated from each, and the residues were dried under vacuum. A solution of Ph_2SiMe_2 (internal standard; 0.0055 mL) in acetone-d_6/$CF_3C_6H_5$ (1:1 v/v; 10.0 mL) was prepared. Each residue was dissolved in 1.00 mL of this solution and ^1H NMR spectra were recorded. The relative peak integrations gave the corresponding partition coefficients.

Crystallography. A solution of 1,3,5-$(R_{f6})_2C_6H_3I$ (ca. 0.05 g) in $CHCl_3/C_6F_6$ (1.0 mL, 4:1 v/v) in an NMR tube was allowed to concentrate. After 2 d, colorless needles with well defined faces were obtained. Data were collected as outlined in Table 1. Integrated intensity information for each reflection was obtained by reduction of the data frames with the program APEX2 [64]. Data were corrected for Lorentz and polarization factors, and using SADABS [65] for absorption and crystal decay effects. The structure was solved by direct methods using SHELXTL/XS [66,67]. Non-hydrogen atoms were refined with anisotropic thermal parameters. Hydrogen atoms were placed in idealized positions and refined using a riding model. The structure was refined (weighted least squares refinement on F^2) to convergence [66-68].

Calculations. Computations were performed with the Gaussian09 program package, employing the ultrafine grid

(99,590) to enhance accuracy [69]. Geometries were optimized using density functional theory (DFT). The B3LYP [70-72] functional was employed with an all-electron 6-311+G(d,p) [73] basis set on all atoms except iodine, which was treated using an effective core potential, SDD [74]. The optimized structures were subjected to frequency calculations (using the same functional and basis set as before) to confirm that all structures were local minima and to obtain the free energies of chlorination (Figure 4 and Table S1, Supporting Information File 1).

Supporting Information

Full details and product characterization for all the syntheses described in Schemes 2, 3, 5, and 6, information on the solvents, starting materials, and instrumentation employed, and additional spectroscopic, structural, and computational data, including a molecular structure file that can be read by the program Mercury [75] and contains the optimized geometries of all computed structures [76].

Supporting Information File 1

Experimental section continued.
[http://www.beilstein-journals.org/bjoc/content/supplementary/1860-5397-13-246-S1.pdf]

Supporting Information File 2

Molecular structure file.
[http://www.beilstein-journals.org/bjoc/content/supplementary/1860-5397-13-246-S2.mol2]

Acknowledgements

The authors thank the Qatar National Research Fund for support (project number 5-848-1-142), the Laboratory for Molecular Simulation and Texas A&M High Performance Research Computing for resources, Prof. Michael B. Hall and Dr. Lisa M. Pérez for helpful discussions, and Dr. Markus Jurisch for preliminary studies of $R_{f13}CH_2OTf$ and $R_{f13}CH_2I$.

ORCID® iDs

Tathagata Mukherjee - https://orcid.org/0000-0002-6369-8923
Andreas Ehnbom - https://orcid.org/0000-0002-7044-1712
Hassan S. Bazzi - https://orcid.org/0000-0002-5702-0091
John A. Gladysz - https://orcid.org/0000-0002-7012-4872

References

1. Gladysz, J. A.; Curran, D. P.; Horváth, I. T., Eds. *Handbook of Fluorous Chemistry;* Wiley-VCH: Weinheim, 2004.
2. Horváth, I. T., Ed. *Fluorous, Chemistry. Topics in Current Chemistry;* Springer, 2012.
3. Mukherjee, T.; Gladysz, J. A. *Aldrichimica Acta* **2015,** *48,* 25–28.
4. As of the submission date of this manuscript, a SciFinder search ($n \geq 6$) showed only 1,4-$R_{f6}C_6H_4I$ (Hong Kong Chemhere Co.).
5. Kysilka, O.; Rybáčková, M.; Skalický, M.; Kvíčalová, M.; Cvačka, J.; Kvíčala, J. *Collect. Czech. Chem. Commun.* **2008,** *73,* 1799–1813. doi:10.1135/cccc20081799
6. Lapčik, J.; Girnello, O.; Ladmiral, V.; Friesen, C. M.; Ameduri, B. *Polym. Chem.* **2015,** *6,* 79–96. doi:10.1039/C4PY00965G
7. Dolbier, W. R., Jr. *Chem. Rev.* **1996,** *96,* 1557–1584. doi:10.1021/cr941142c
8. Brace, N. O. *J. Fluorine Chem.* **2001,** *108,* 147–175. doi:10.1016/S0022-1139(01)00348-7
9. Cowell, A. B.; Tamborski, C. *J. Fluorine Chem.* **1981,** *17,* 345–356. doi:10.1016/S0022-1139(00)81780-7
10. Darses, S.; Pucheault, M.; Genêt, J.-P. *Eur. J. Org. Chem.* **2001,** 1121–1128. doi:10.1002/1099-0690(200103)2001:6<1121::AID-EJOC1121>3.0.CO;2-3
11. Miura, T.; Nakashima, K.; Tada, N.; Itoh, A. *Chem. Commun.* **2011,** *47,* 1875–1877. doi:10.1039/C0CC03149F
12. Jiang, D.-F.; Liu, C.; Guo, Y.; Xiao, J.-C.; Chen, Q.-Y. *Eur. J. Org. Chem.* **2014,** 6303–6309. doi:10.1002/ejoc.201402820
13. Alvey, L. J.; Rutherford, D.; Juliette, J. J. J.; Gladysz, J. A. *J. Org. Chem.* **1998,** *63,* 6302–6308. doi:10.1021/jo980692y
14. Alvey, L. J.; Meier, R.; Soós, T.; Bernatis, P.; Gladysz, J. A. *Eur. J. Inorg. Chem.* **2000,** 1975–1983. doi:10.1002/1099-0682(200009)2000:9<1975::AID-EJIC1975>3.0.CO;2-M
15. Wende, M.; Seidel, F.; Gladysz, J. A. *J. Fluorine Chem.* **2003,** *124,* 45–54. doi:10.1016/S0022-1139(03)00171-4
16. Rocaboy, C.; Gladysz, J. A. *Chem. – Eur. J.* **2003,** *9,* 88–95. doi:10.1002/chem.200390034
17. Podgoršek, A.; Jurisch, M.; Stavber, S.; Zupan, M.; Iskra, J.; Gladysz, J. A. *J. Org. Chem.* **2009,** *74,* 3133–3140. doi:10.1021/jo900233h
18. Tesevic, V.; Gladysz, J. A. *Green Chem.* **2005,** *7,* 833–836. doi:10.1039/b511951k
19. Tesevic, V.; Gladysz, J. A. *J. Org. Chem.* **2006,** *71,* 7433–7440. doi:10.1021/jo0612067
20. Bravo, P., III; Montanari, V.; Resnati, G.; DeMarteau, D. D. *J. Org. Chem.* **1994,** *59,* 6093–6094. doi:10.1021/jo00099a048
21. Lion, C. J.; Vasselin, D. A.; Schwalbe, C. H.; Matthews, C. S.; Stevens, M. F. G.; Westwell, A. D. *Org. Biomol. Chem.* **2005,** *3,* 3996–4001. doi:10.1039/B510240E
22. Zagulyaeva, A. A.; Yusubov, M. S.; Zhdankin, V. V. *J. Org. Chem.* **2010,** *75,* 2119–2122. doi:10.1021/jo902733f
23. Ghosh, S. K.; Gladysz, J. A.; Cummins, C. C. manuscript in preparation.
24. Cossairt, B. M.; Cummins, C. C. *New J. Chem.* **2010,** *34,* 1533–1536. doi:10.1039/c0nj00124d
25. Mukherjee, T.; El-Zoghbi, I.; Bazzi, S.; Gladysz, J. A. unpublished results.
26. Banks, D. F.; Huyser, E. S.; Kleinberg, J. *J. Org. Chem.* **1964,** *29,* 3692–3693. doi:10.1021/jo01035a504
27. Tanner, D. D.; van Bostelen, P. B. *J. Org. Chem.* **1967,** *32,* 1517–1521. doi:10.1021/jo01280a047
28. Gladysz, J. A. Catalysis Involving Fluorous Phases: Fundamentals and Directions for Greener Methodologies. In *Handbook of Green Chemistry;* Anastas, P.; Crabtree, R. H., Eds.; Chapter 2 (See section 2.5), Vol. 1: Homogeneous Catalysis; Wiley-VCH: Weinheim, 2009.

29. Kiss, L. E.; Kövesdi, I.; Rábai, J. *J. Fluorine Chem.* **2001,** *108,* 95–109. doi:10.1016/S0022-1139(01)00342-6
30. Rocaboy, C.; Rutherford, D.; Bennett, B. L.; Gladysz, J. A. *J. Phys. Org. Chem.* **2000,** *13,* 596–603. doi:10.1002/1099-1395(200010)13:10<596::AID-POC284>3.0.CO;2-M
31. Friedrich, K.; Amann, W.; Fritz, H. *Chem. Ber.* **1978,** *111,* 2099–2107. doi:10.1002/cber.19781110605
32. Exner, O. *Correlation Analysis in Chemistry*. Chapman, N. B.; Shorter, J., Eds.; Chapter 10; Plenum: New York, 1978.
33. Maul, J. J.; Ostrowski, P. J.; Ublacker, G. A.; Linclau, B.; Curran, D. P. *Top. Curr. Chem.* **1999,** *206,* 79–105. doi:10.1007/3-540-48664-X_4
34. Tesevic, V.; Gladysz, J. A. *Top. Organomet. Chem.* **2008,** *23,* 67–89.
35. Gladysz, J. A.; Emnet, C. Fluorous Solvents and Related Media. In *Handbook of Fluorous Chemistry;* Gladysz, J. A.; Curran, D. P.; Horváth, I. T., Eds.; Wiley-VCH: Weinheim, 2004; pp 11–23. doi:10.1002/3527603905
36. Zhao, X.-F.; Zhang, C. *Synthesis* **2007,** 551–557. doi:10.1055/s-2007-965889
37. Zhdankin, V. V. *Hypervalent Iodine Chemistry: Preparation, Structure, and Synthetic Applications of Polyvalent Iodine Compounds;* Chapter 2; John Wiley & Sons: New York, 2014.
38. The recipe employed in this work is also a function of location, as Cl_2 is very difficult to obtain in Qatar.
39. Hu, X. C.; Andrews, D. Q.; Lindstrom, A. B.; Bruton, T. A.; Schaider, L. A.; Grandjean, P.; Lohmann, R.; Carignan, C. C.; Blum, A.; Balan, S. A.; Higgins, C. P.; Sunderland, E. M. *Environ. Sci. Technol. Lett.* **2016,** *3,* 344–350. doi:10.1021/acs.estlett.6b00260 See for recent lead references.
40. Lo, A. S. W.; Horváth, I. T. *Green Chem.* **2015,** *17,* 4701–4714. doi:10.1039/C5GC01345C
41. Chu, Q.; Henry, C.; Curran, D. P. *Org. Lett.* **2008,** *10,* 2453–2456. doi:10.1021/ol800750q
42. Skalický, M.; Skalická, V.; Paterová, J.; Rybáčková, M.; Kvíčalová, M.; Cvačka, J.; Březinová, A.; Kvíčala, J. *Organometallics* **2012,** *31,* 1524–1532. doi:10.1021/om201062c
43. Minkwitz, R.; Berkei, M. *Inorg. Chem.* **1999,** *38,* 5041–5044. doi:10.1021/ic990441n
44. Rocaboy, C.; Hampel, F.; Gladysz, J. A. *J. Org. Chem.* **2002,** *67,* 6863–6870. doi:10.1021/jo011173p
45. McLoughlin, V. C. R.; Thrower, J. *Tetrahedron* **1969,** *25,* 5921–5940. doi:10.1016/S0040-4020(01)83100-8
46. Ishihara, K.; Kondo, S.; Yamamoto, H. *Synlett* **2001,** 1371–1374. doi:10.1055/s-2001-16788
47. van den Broeke, J.; Deelman, B.-J.; van Koten, G. *Tetrahedron Lett.* **2001,** *42,* 8085–8087. doi:10.1016/S0040-4039(01)01716-6
48. Ghosh, S. K.; Ojeda, A. S.; Guerrero-Leal, J.; Bhuvanesh, N.; Gladysz, J. A. *Inorg. Chem.* **2013,** *52,* 9369–9378. doi:10.1021/ic400945u
49. Su, H.-L.; Balogh, J.; Al-Hashimi, M.; Seapy, D. G.; Bazzi, H. S.; Gladysz, J. A. *Org. Biomol. Chem.* **2016,** *14,* 10058–10069. doi:10.1039/C6OB01980C
50. This formula is potentially ambiguous. For all benzenoid compounds in the paper, any iodine substituent is assigned the 1-position.
51. Guillevic, M.-A.; Arif, A. M.; Gladysz, J. A.; Horváth, I. T. *Angew. Chem., Int. Ed. Engl.* **1997,** *36,* 1612–1615. doi:10.1002/anie.199716121
52. Montanari, V.; DesMarteau, D. D.; Pennington, W. T. *J. Mol. Struct.* **2000,** *550-551,* 337–348. doi:10.1016/S0022-2860(00)00502-0
53. Richter, B.; de Wolf, E.; van Koten, G.; Deelman, B.-J. *J. Org. Chem.* **2000,** *65,* 3885–3893. doi:10.1021/jo991548v
54. de Wolf, E.; Riccomagno, E.; de Pater, J. J. M.; Deelman, B.-J.; van Koten, G. *J. Comb. Chem.* **2004,** *6,* 363–374. doi:10.1021/cc049959z
55. Corrêa da Costa, R.; Hampel, F.; Gladysz, J. A. *Polyhedron* **2007,** *26,* 581–588. doi:10.1016/j.poly.2006.08.015
56. Tuba, R.; Brothers, E. N.; Reibenspies, J. H.; Bazzi, H. S.; Gladysz, J. A. *Inorg. Chem.* **2012,** *51,* 9943–9949. doi:10.1021/ic301434g
57. See literature cited within references [55] and [56] and the more recent studies in references [58] and [59].
58. Quarti, C.; Milani, A.; Castiglioni, C. *J. Phys. Chem. B* **2013,** *117,* 706–718. doi:10.1021/jp3102145
59. Cormanich, R. A.; O'Hagan, D.; Bühl, M. *Angew. Chem., Int. Ed.* **2017,** *56,* 7867–7870. doi:10.1002/anie.201704112
60. The triplets commonly observed for $CF_2CF_2CF_3$ and $CF_2CF_2CF_2X$ signals have been shown to be four bond and *not* three bond (vicinal) couplings [61,62].
61. White, H. F. *Anal. Chem.* **1966,** *38,* 625–626. doi:10.1021/ac60236a025
62. Foris, A. *Magn. Reson. Chem.* **2004,** *42,* 534–555. doi:10.1002/mrc.1368
63. These microanalytical data feature one or more values outside of normally accepted ranges but are presented nonetheless as the best fit obtained to date, and/or to illustrate a point made in the text.
64. *APEX2. Program for Data Collection on Area Detectors;* BRUKER AXS Inc.: Madison, WI, USA.
65. *SADABS, Program for Absorption Correction of Area Detector Frames;* Sheldrick, G. M. BRUKER AXS Inc.: Madison, WI, USA.
66. Sheldrick, G. M. *Acta Crystallogr., Sect. A: Found. Crystallogr.* **2008,** *64,* 112–122. doi:10.1107/S0108767307043930
67. Sheldrick, G. M. *Acta Crystallogr., Sect. C: Struct. Chem.* **2015,** *71,* 3–8. doi:10.1107/S2053229614024218
68. Dolomanov, O. V.; Bourhis, L. J.; Gildea, R. J.; Howard, J. A. K.; Puschmann, H. *J. Appl. Crystallogr.* **2009,** *42,* 339–341. doi:10.1107/S0021889808042726
69. *Gaussian 09,* Revision D.01; Gaussian, Inc.: Wallingford CT, 2009.
70. Becke, A. D. *Phys. Rev. A* **1988,** *38,* 3098–3100. doi:10.1103/PhysRevA.38.3098
71. Becke, A. D. *J. Chem. Phys.* **1993,** *98,* 5648–5652. doi:10.1063/1.464913
72. Lee, C.; Yang, W.; Parr, R. G. *Phys. Rev. B* **1988,** *37,* 785–789. doi:10.1103/PhysRevB.37.785
73. Hariharan, P. C.; Pople, J. A. *Theor. Chim. Acta* **1973,** *28,* 213–222. doi:10.1007/BF00533485
74. Peterson, K. A.; Shepler, B. C.; Figgen, D.; Stoll, H. *J. Phys. Chem. A* **2006,** *110,* 13877–13883. doi:10.1021/jp065887l
75. Macrae, C. F.; Bruno, I. J.; Chisholm, J. A.; Edgington, P. R.; McCabe, P.; Pidcock, E.; Rodriguez-Monge, L.; Taylor, R.; van de Streek, J.; Wood, P. A. *J. Appl. Crystallogr.* **2008,** *41,* 466–470. doi:10.1107/S0021889807067908
76. Lichtenberger, D. L.; Gladysz, J. A. *Organometallics* **2014,** *33,* 835. doi:10.1021/om500109u

BEILSTEIN JOURNAL OF ORGANIC CHEMISTRY

One-pot three-component route for the synthesis of *S*-trifluoromethyl dithiocarbamates using Togni's reagent

Azim Ziyaei Halimehjani*[1], Martin Dračínský[2] and Petr Beier*[2]

Letter

Open Access

Address:
[1]Faculty of Chemistry, Kharazmi University, P. O. Box 15719-14911, 49 Mofateh St., Tehran, Iran and [2]The Institute of Organic Chemistry and Biochemistry of the Czech Academy of Sciences, Flemingovo namestí 2, 166 10 Prague 6, Czech Republic

Email:
Azim Ziyaei Halimehjani* - ziyaei@khu.ac.ir; Petr Beier* - beier@uochb.cas.cz

* Corresponding author

Keywords:
dithiocarbamates; electrophilic trifluoromethylation; Togni reagents

Beilstein J. Org. Chem. **2017,** *13,* 2502–2508.
doi:10.3762/bjoc.13.247

Received: 29 September 2017
Accepted: 16 November 2017
Published: 24 November 2017

This article is part of the Thematic Series "Organo-fluorine chemistry IV".

Guest Editor: D. O'Hagan

Abstract

A one-pot three-component route for the synthesis of *S*-trifluoromethyl dithiocarbamates by the reaction of secondary amines, carbon disulfide and Togni's reagent is described. The reactions proceed in moderate to good yields. A similar reaction using a primary aliphatic amine afforded the corresponding isothiocyanate in high yield. A variable temperature NMR study revealed a rotational barrier of 14.6, 18.8, and 15.9 kcal/mol for the C–N bond in the dithiocarbamate moiety of piperidine, pyrrolidine, and diethylamine adducts, respectively. In addition, the calculated barriers of rotation are in reasonable agreement with the experiments.

Introduction

Dithiocarbamates are well known for their manifold applications as pesticides, fungicides and crop protection agents in agriculture [1-3], as intermediates in synthetic organic chemistry [4-12], radical chain transfer agents in RAFT polymerization [13], sulfur vulcanization agents in rubber manufacturing [14] and valuable pharmacophores in medicine [15-17]. Beside traditional methods, a recent synthesis of dithiocarbamates via a one-pot reaction of an amine, CS_2 and an electrophile is of great interest due to its simplicity and environmental friendly procedure. Diverse electrophiles including alkyl halides [18], epoxides [19], alkenes [20-22], aldehydes [23], and alcohols [24] were applied for the synthesis of novel dithiocarbamates. Nevertheless, new synthetic methods towards dithiocarbamates are sought after and research in this area is still intense.

The introduction of a trifluoromethyl group into organic compounds is a very productive strategy of modification of molecules for various applications in the fields of pharmaceuticals, agrochemicals, and materials sciences. The key properties such as metabolic and chemical stability, polarity, bioavailability, viscosity and lipophilicity can be altered in molecules containing the CF_3 group in comparison with the nonfluorinated ana-

logues. Numerous methods have been reported to introduce the trifluoromethyl group in organic structures including nucleophilic, electrophilic, radical and transition metal-mediated trifluoromethylations. Among the electrophilic trifluoromethylation methods, reagents based on hypervalent iodine (Togni's reagents I and II, Scheme 1b) have been used extensively in trifluoromethylations of S-, P-, O-, and C-nucleophilic functionalities [25-32]. Although reports exist on the synthesis of fluorinated dithiocarbamates [33-35], the direct trifluoromethylation of dithiocarbamates has not been described. In 2001 Naumann and co-workers [36] have published a reaction of tetraethylthiuram disulfide with perfluoroorganosilver and perfluoroorganocadmium reagents proceeding most probably by a radical mechanism (Scheme 1a). This method suffers from several drawbacks such as extra reaction steps for the preparation of the thiuram disulfide and the use of expensive and environmentally problematic heavy metals. These observations prompted us to investigate the reaction of in situ prepared dithiocarbamic acid with Togni's reagents as a new route to *S*-trifluoromethyl dithiocarbamates (Scheme 1b).

Results and Discussion

We started our investigation with a one-pot, three-component reaction of piperidine, CS_2, and a cyclic hypervalent iodane (Togni's reagent I) as a model reaction to find the optimal reaction conditions for the preparation of *S*-trifluoromethyl dithiocarbamates (Table 1). In the first run, we observed that the reaction of piperidine (1 equiv) with CS_2 (2 equiv) in THF for 10 min followed by the addition of Togni's reagent I (1 equiv) and stirring for 2 hours at room temperature afforded the corresponding trifluoromethyl dithiocarbamate **4a** in 25% isolated yield and the corresponding thiuram disulfide **5a** (ratio of **4a**:**5a** 1.8:1) (Table 1, entry 1). Performing the same reaction at −78 °C and slow heating to ambient temperature over 2 hours increased the yield of **4a** to 35% with an increase in the **4a**:**5a** ratio to 2.4:1 (Table 1, entry 2). Using excess of both the amine (2 equiv) and CS_2 (3 equiv) a higher yield of **4a** was obtained, albeit the product ratio decreased (Table 1, entry 3). By further varying the equivalents of amines and CS_2, we found that when using 1.5 equivalents of piperidine and CS_2 and 1 equivalent of **3** in THF at −78 °C for 1 hour, the yield was improved to 45% with a product ratio of 2.5:1 (Table 1, entry 4). Using excess of **2** and **3** with piperidine as the limiting reagent led to significant yield reduction (Table 1, entry 5). The use of chloroform, dichloromethane, ethanol or water as solvents afforded the product, albeit in unsatisfactory yield (interestingly, in aqueous KOH the **4a**:**5a** ratio was the highest observed, Table 1, entries 6–10). In addition, using Togni's reagent II in THF gave low yields of **4a** (Table 1, entry 11). Using Et_3N as base in THF also afforded unsatisfactory results (Table 1, entry 12). Although with the potassium salt of piperidine dithiocarbamate in THF, water or DMF the product ratio increased to 5:1 (Table 1, entries 13–15), the yield of **4a** remained low compared to our one-pot three-component reaction in THF. In summary, stirring piperidine (1.5 equiv) and CS_2 (1.5 equiv) in THF at room temperature for 10 min, followed by cooling to −78 °C, addition of **3** (1 equiv) and additional stirring for one hour at −78 °C were considered as optimal reaction conditions for further derivatization.

In order to explore the scope of the reaction under the optimized reaction conditions, various commercially available secondary amines were investigated and moderate to good yields of products **4** were obtained (Scheme 2). The products were isolated from the reaction mixture by extraction with CH_2Cl_2 and purification was carried out by column chromatography on silica gel using CH_2Cl_2/*n*-pentane (1:9) as eluent. The structure of products was confirmed using IR, ^{1}H NMR, ^{13}C NMR, ^{19}F NMR and HRMS analysis. The dithiocarbamate moiety in *S*-trifluoromethyl dithiocarbamates appeared at 180–185 ppm in the ^{13}C NMR spectra, while this group usually can be found at 190–200 ppm for *S*-alkyl dithiocarbamates [4-12]. Also the car-

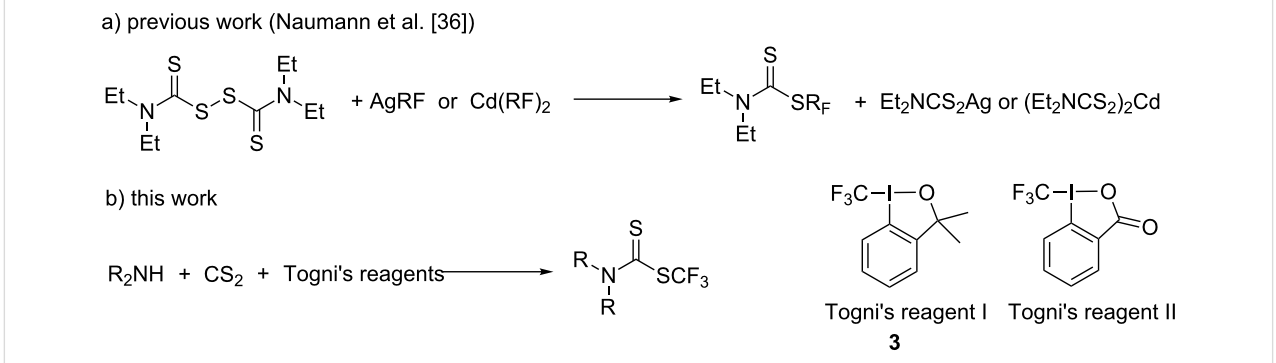

Scheme 1: Synthetic routes for the preparation of trifluoromethyl dithiocarbamates.

Table 1: Optimization of the reaction conditions.

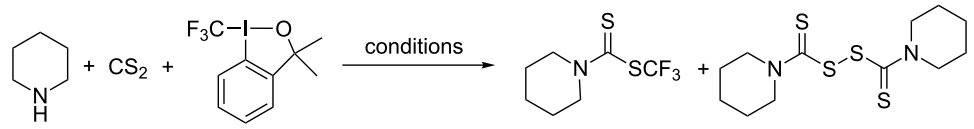

1a **2** **3** **4a** **5a**

Entry	**1a** (equiv)	**2** (equiv)	**3** (equiv)	Solvent	*T* (°C)	Time (h)	Yield **4a** (%)[a]	**4a**:**5a**[b]
1	1	2	1	THF	rt	2	25	1.8:1
2	1	2	1	THF	−78 to rt	2	35	2.4:1
3	2	3	1	THF	−78	1	40	1.75:1
4	1.5	1.5	1	THF	−78	1	**45**	**2.5:1**
5	1	2	1.2	THF	−78	1	22	1.6:1
6	1.5	2	1	$CHCl_3$	0-5	1	17	1:1.4
7	1	2	1	$CHCl_3$	rt	1	15	1.6:1
8	1.5	1.5	1	CH_2Cl_2	−78	2	13	1.1:1
9	1.2	1.2	1	EtOH	−78	2	15	1.7:1
10	1.5	1.5	1	H_2O	0 to rt	1	30	6:1[c]
11	1.5	1.5	1	THF	−78	1	10	1:1.8[d]
12	1.5	1.5	1	THF	−78 to rt	2	10	1:1[e]
13		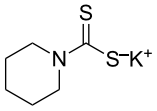 (1 equiv)	1	THF	−78 to rt	1.5	10	4:1
14		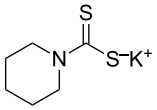 (1.5 equiv)	1	H_2O	0 to rt	2	25	5:1
15		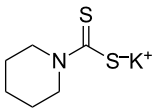 (1 equiv)	1	DMF	−55 to rt	1.5	12	1:1

[a]Isolated yield of **4a**. [b]The ratio of **4a**:**5a** was determined by ^{1}H NMR spectroscopy of the crude reaction mixture. [c]KOH (1.5 equiv) was used. [d]Togni's reagent II was used instead of Togni's reagent I (**3**). [e]Et_3N (1.5 equiv) was used.

bon of the CF_3 group was observed at around 128 ppm as quartet with a coupling constant of ≈308 Hz. In addition, a singlet at −40 ppm in the ^{19}F NMR spectra was assigned to the CF_3 group.

The one-pot reaction of benzylamine with CS_2 and Togni's reagent I under optimal reaction conditions was also investigated. Surprisingly, we observed that the corresponding benzyl isothiocyanate was obtained in high yield. This may be attributed to the low stability of the corresponding *S*-trifluoromethyl benzyldithiocarbamate. Alternatively, the iodane **3** can act as an oxidant towards the intermediate benzyl dithiocarbamic acid rather than an electrophilic trifluoromethylating reagent (Scheme 3). A similar behavior was recently reported by Schoenebeck [37] who showed that isothiocyanates are formed in reactions of primary amines with the $(Me_4N)SCF_3$ salt (through a different mechanism).

Interesting differences in the NMR spectra of compounds **4a**–**i** were observed. The nitrogen–carbon bond in the dithiocarbamate group [N–C(S)S] has a bond order higher than one leading to nonequivalence of the two alkyl substituents attached to the nitrogen atom. However, the rotational barrier of the N–C bond differs significantly for individual compounds and ^{1}H NMR spectra exhibit features of slow to intermediate chemical exchange with substantial signal broadening in some cases. Therefore, we performed a variable temperature NMR study to determine rotational barriers of compounds **4a**–**c**, and the exper-

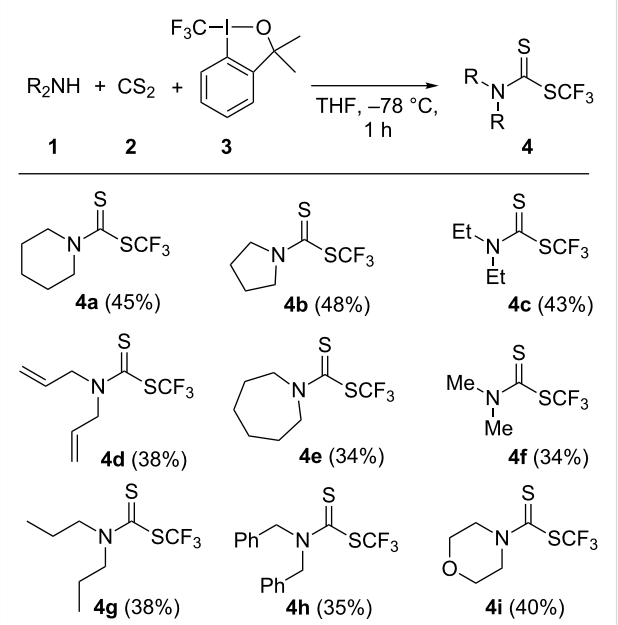

Scheme 2: Synthesis of *S*-trifluoromethyl dithiocarbamates. Isolated yields are given in parentheses.

imental data are compared to and rationalized by DFT calculations.

Figure 1 depicts variable temperature ^{1}H NMR spectra of compound **4c**. The coalescence of the methyl signals can be observed at 308 K, whereas the coalescence of the CH_2 signals would require an even higher temperature than 328 K. Complete lineshape analysis approach (dynamic NMR, dNMR) provided the rates of rotation around the N–C bond at all temperatures and the Eyring plot (Figure 2) allowed to determine the enthalpy and entropy of activation. The entropy of activation is small (−4.2 cal/K) and the free energy of activation (15.8 kcal/mol at 300 K) is dominated by the enthalpic term (14.6 kcal/mol). The rate of rotation k at coalescence temperature can also be determined by applying the equation $k = 2.22\Delta\nu$, where $\Delta\nu$ is the difference between resonance frequencies of the exchanging signals at slow exchange regime (at low temperature). The rotational barrier for compound **4c** determined using this approach (15.9 kcal/mol) is almost identical to that obtained by the dNMR approach and is higher compared to the corresponding nonfluorinated analogue [35,38,39].

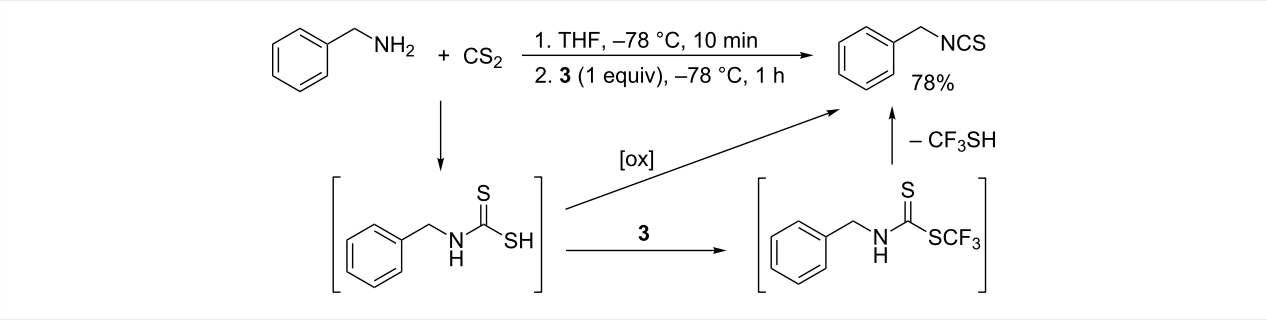

Scheme 3: Formation of benzyl isothiocyanate in a reaction with benzylamine.

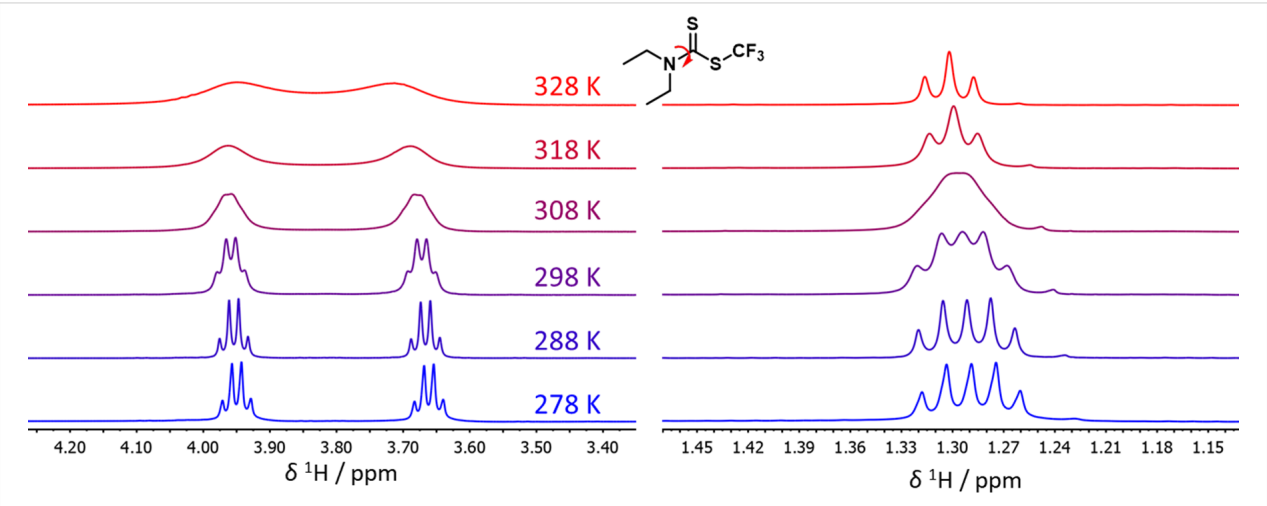

Figure 1: Variable temperature ^{1}H NMR spectra of compound **4c** (CH_2 region on the left and CH_3 region on the right); the sample was dissolved in $CDCl_3$.

The rotational barriers obtained for compounds **4a–c** are summarized in Table 2.

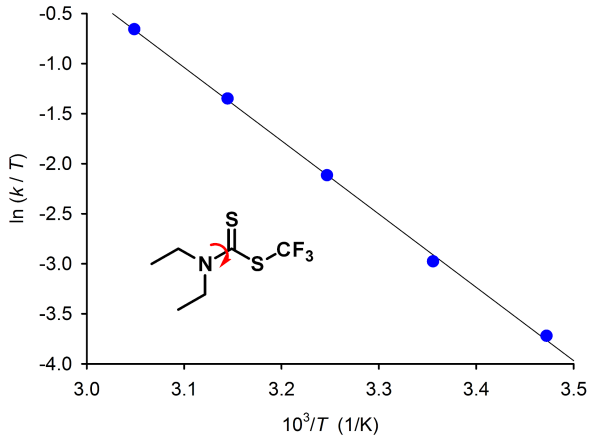

Figure 2: The Eyring plot obtained for the rotation around the N–C bond in compound **4c**.

Table 2: Experimental and calculated (B3LYP/6-31+g**) rotational barriers (kcal/mol) in compounds **4a–c**.

Compound	$\Delta G^{\#}_{exp}$	$\Delta E^{\#}_{calc}$
4a	14.6	14.6
4b	18.8	16.3
4c	15.9	15.0

The structures of compounds **4a–c** was optimized using DFT methods (B3LYP/6-31+g**). In all three cases, the carbon atoms attached to the nitrogen and the N–C(S)–S–C atoms of the dithiocarbamate group are almost in one plane and the torsion angle S=C–S–CF_3 is close to zero in the optimized structures. In the transition state corresponding to the rotation around the N–C bond, the plane with CH_2 carbon atoms attached to the nitrogen and the nitrogen atom is almost perpendicular to the N–C(S)–S–C plane. The calculated barriers of rotation are in reasonable agreement with experimental data (Table 2).

The rotational barrier in compound **4b** is both experimentally and computationally higher than in the other two compounds (**4a** and **4c**). This can be explained by the conformational strain in the five-membered ring in the transition state. In the ground state, the conformation of the pyrrolidine ring is $_4T^3$ with limited steric interactions between adjacent CH_2 hydrogen atoms (Figure 3). On the other hand, a ^1E conformation is found in the transition state structure. Hydrogen atoms are close to unfavorable syn-periplanar arrangement in this conformation, which leads to an increased energy demand for the pyrrolidine rotation.

Conclusion

In conclusion, we have reported a novel multicomponent reaction for the synthesis of *S*-trifluoromethyl dithiocarbamates from secondary amines, CS_2 and Togni's reagent in moderate to good yields. Under similar conditions, a primary amine afforded the corresponding isothiocyanate in excellent yield. The presence of dithiocarbamate and trifluoromethyl groups in a single structure generates a new family of compounds with potential application as agrochemicals or in drug design. A variable temperature NMR study allowed the determination of rotational barriers of 14.6, 18.8, and 15.9 kcal/mol for the C–N bond in the dithiocarbamate moiety of piperidine, pyrrolidine and diethylamine adducts, respectively. The results revealed that the rotational barrier in fluorinated dithiocarbamates is slightly higher than in the nonfluorinated analogue [35,38,39]. This may be attributed to a higher electron affinity of the trifluoromethyl group and an increased double bond character of the C–N bond.

Supporting Information

Supporting Information File 1

Experimantal procedures and characterization data of all products, copies of ^1H, ^{13}C, and ^{19}F NMR spectra of all compounds.
[http://www.beilstein-journals.org/bjoc/content/supplementary/1860-5397-13-247-S1.pdf]

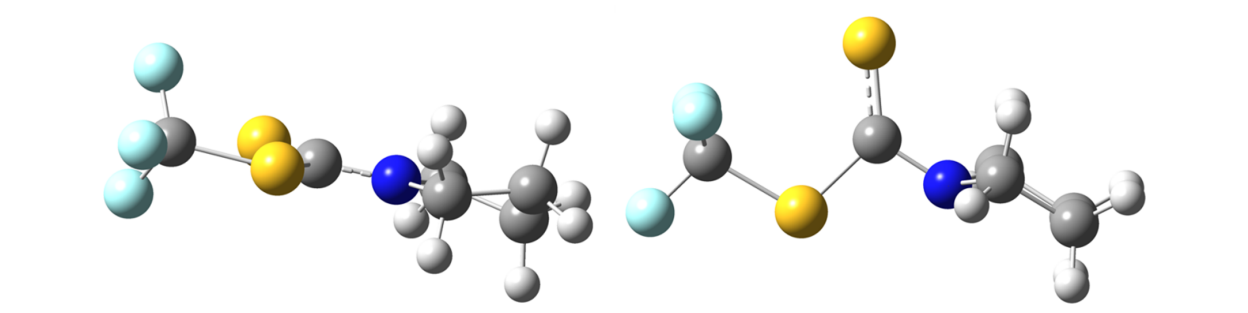

Figure 3: The optimized structure of compound **4b** (left) and the transition state structure for the rotation around the N–C bond (right).

Acknowledgements

We are grateful to the faculty of chemistry of Kharazmi University for supporting this work. This work was also supported by the Academy of Sciences of the Czech Republic (Research Plan RVO: 61388963) and Ministry of Education of the Czech Republic (Project LO1304, Program "NPU-I").

ORCID® iDs

Azim Ziyaei Halimehjani - https://orcid.org/0000-0002-0348-8959
Martin Dračínský - https://orcid.org/0000-0002-4495-0070
Petr Beier - https://orcid.org/0000-0002-0888-7465

References

1. Marinovich, M.; Viviani, B.; Capra, V.; Corsini, E.; Anselmi, L.; D'Agostino, G.; Di Nucci, A.; Binaglia, M.; Tonini, M.; Galli, C. L. *Chem. Res. Toxicol.* **2002,** *15,* 26–32. doi:10.1021/tx015538c
2. Malik, A. K.; Rao, A. L. J. *J. Agric. Food Chem.* **2000,** *48,* 4044–4047. doi:10.1021/jf991389g
3. Weissmahr, K. W.; Houghton, C. L.; Sedlak, D. L. *Anal. Chem.* **1998,** *70,* 4800–4804. doi:10.1021/ac980626w
4. Sugimoto, H.; Makino, I.; Hirai, K. *J. Org. Chem.* **1988,** *53,* 2263–2267. doi:10.1021/jo00245a025
5. Maddani, M.; Prabhu, K. R. *Tetrahedron Lett.* **2007,** *48,* 7151–7154. doi:10.1016/j.tetlet.2007.07.212
6. Das, P.; Kumar, C. K.; Kumar, K. N.; Innus, M.; Iqbal, J.; Srinivas, N. *Tetrahedron Lett.* **2008,** *49,* 992–995. doi:10.1016/j.tetlet.2007.12.022
7. Wong, R.; Dolman, S. J. *J. Org. Chem.* **2007,** *72,* 3969–3971. doi:10.1021/jo070246n
8. Guillaneuf, Y.; Couturier, J.-L.; Gigmes, D.; Marque, S. R. A.; Tordo, P.; Bertin, D. *J. Org. Chem.* **2008,** *73,* 4728–4731. doi:10.1021/jo800422a
9. Ziyaei Halimehjani, A.; Maleki, H.; Saidi, M. R. *Tetrahedron Lett.* **2009,** *50,* 2747–2749. doi:10.1016/j.tetlet.2009.03.127 and references therein.
10. Grainger, R. S.; Welsh, E. J. *Angew. Chem., Int. Ed.* **2007,** *46,* 5377–5380. doi:10.1002/anie.200701055
11. Ahmed, S.; Baker, L. A.; Grainger, R. S.; Innocenti, P.; Quevedo, C. E. *J. Org. Chem.* **2008,** *73,* 8116–8119. doi:10.1021/jo801652x
12. McMaster, C.; Bream, R. N.; Grainger, R. S. *Org. Biomol. Chem.* **2012,** *10,* 4752–4758. doi:10.1039/C2OB25434D
13. Lai, J. T.; Shea, R. *J. Polym. Sci., Part A: Polym. Chem.* **2006,** *44,* 4298–4316. doi:10.1002/pola.21532
14. Nieuwenhuizen, P. J.; Ehlers, A. W.; Haasnoot, J. G.; Janse, S. R.; Reedijk, J.; Baerends, E. J. *J. Am. Chem. Soc.* **1999,** *121,* 163–168. doi:10.1021/ja982217n
15. Imamura, H.; Ohtake, N.; Jona, H.; Shimizu, A.; Moriya, M.; Sato, H.; Sugimoto, Y.; Ikeura, C.; Kiyonaga, H.; Nakano, M.; Nagano, R.; Abe, S.; Yamada, K.; Hashizume, T.; Morishima, H. *Bioorg. Med. Chem.* **2001,** *9,* 1571–1578. doi:10.1016/S0968-0896(01)00044-X
16. Scozzafava, A.; Mastorlorenzo, A.; Supuran, C. T. *Bioorg. Med. Chem. Lett.* **2000,** *10,* 1887–1891. doi:10.1016/S0960-894X(00)00375-9
17. Hou, X.; Ge, Z.; Wang, T.; Guo, W.; Cui, J.; Cheng, T.; Lai, C.; Li, R. *Bioorg. Med. Chem. Lett.* **2006,** *16,* 4214–4219. doi:10.1016/j.bmcl.2006.05.085
18. Azizi, N.; Aryanasab, F.; Saidi, M. R. *Org. Lett.* **2006,** *8,* 5275–5277. doi:10.1021/ol0620141
19. Ziyaei-Halimjani, A.; Saidi, M. R. *Can. J. Chem.* **2006,** *84,* 1515–1519. doi:10.1139/v06-150
20. Ziyaei Halimehjani, A.; Zanussi, H. P.; Ranjbari, M. A. *Synthesis* **2013,** *45,* 1483–1488. doi:10.1055/s-0032-1318504
21. Ziyaei Halimehjani, A.; Marjani, K.; Ashouri, A. *Green Chem.* **2010,** *12,* 1306–1310. doi:10.1039/c004711b
22. Azizi, N.; Aryanasab, F.; Torkiyan, L.; Ziyaei, A.; Saidi, M. R. *J. Org. Chem.* **2006,** *71,* 3634–3635. doi:10.1021/jo060048g
23. Ziyaei Halimehjani, A.; Hajiloo Shayegan, M.; Hashemi, M. M.; Notash, B. *Org. Lett.* **2012,** *14,* 3838–3841. doi:10.1021/ol301598u
24. Chaturvedi, D.; Ray, S. *Tetrahedron Lett.* **2006,** *47,* 1307–1309. doi:10.1016/j.tetlet.2005.12.079
25. Charpentier, J.; Früh, N.; Togni, A. *Chem. Rev.* **2015,** *115,* 650–682. doi:10.1021/cr500223h
26. Václavík, J.; Zschoche, R.; Klimánková, I.; Matoušek, V.; Beier, P.; Hilvert, D.; Togni, A. *Chem. – Eur. J.* **2017,** *23,* 6490–6494. doi:10.1002/chem.201700607
27. Ismalaj, E.; Le Bars, D.; Billard, T. *Angew. Chem., Int. Ed.* **2016,** *55,* 4790–4793. doi:10.1002/anie.201601280
28. Zhang, C. *ARKIVOC* **2014,** No. i, 453–469. doi:10.3998/ark.5550190.p008.656
29. Shibata, N.; Matsnev, A.; Cahard, D. *Beilstein J. Org. Chem.* **2010,** *6,* No. 65. doi:10.3762/bjoc.6.65
30. Niedermann, K.; Früh, N.; Vinogradova, E.; Wiehn, M. S.; Moreno, A.; Togni, A. *Angew. Chem., Int. Ed.* **2011,** *50,* 1059–1063. doi:10.1002/anie.201006021
31. Bertrand, F.; Pevere, V.; Quiclet-Sire, B.; Zard, S. Z. *Org. Lett.* **2001,** *3,* 1069–1071. doi:10.1021/ol0156446
32. Matoušek, V.; Václavík, J.; Hájek, P.; Charpentier, J.; Blastik, Z. E.; Pietrasiak, E.; Budinská, A.; Togni, A.; Beier, P. *Chem. – Eur. J.* **2016,** *22,* 417–424. doi:10.1002/chem.201503531
33. Ashirbaev, S. S.; Levin, V. V.; Struchkova, M. I.; Dilman, A. D. *J. Fluorine Chem.* **2016,** *191,* 143–148. doi:10.1016/j.jfluchem.2016.07.018
34. Kitazume, T.; Sasaki, S.; Ishikawa, N. *J. Fluorine Chem.* **1978,** *12,* 193–202. doi:10.1016/S0022-1139(00)81585-7
35. Chniti, I.; Sanhoury, M. A. K.; Merlet, D.; Chehidi, I. *J. Fluorine Chem.* **2014,** *168,* 223–229. doi:10.1016/j.jfluchem.2014.10.015
36. Wessel, W.; Tyrra, W.; Naumann, D. *Z. Anorg. Allg. Chem.* **2001,** *627,* 1264–1268. doi:10.1002/1521-3749(200106)627:6<1264::AID-ZAAC1264>3.0.CO;2-J
37. Scattolin, T.; Klein, A.; Schoenebeck, F. *Org. Lett.* **2017,** *19,* 1831–1833. doi:10.1021/acs.orglett.7b00689
38. Pontes, R. M.; Basso, E. A.; dos Santos, F. P. *J. Org. Chem.* **2007,** *72,* 1901–1911. doi:10.1021/jo061934u
39. Holloway, C. E.; Gitlitz, M. H. *Can. J. Chem.* **1967,** *45,* 2659–2663. doi:10.1139/v67-435

BEILSTEIN JOURNAL OF ORGANIC CHEMISTRY

Palladium-catalyzed Heck-type reaction of secondary trifluoromethylated alkyl bromides

Tao Fan[1], Wei-Dong Meng[1] and Xingang Zhang[*2]

Full Research Paper

Open Access

Address:
[1]College of Chemistry, Chemical Engineering and Biotechnology, Donghua University, 2999 North Renmin Road, Shanghai 201620, China, and [2]Key Laboratory of Organofluorine Chemistry, Shanghai Institute of Organic Chemistry, Chinese Academy of Sciences, 345 Lingling Road, Shanghai 200032, China

Email:
Xingang Zhang[*] - xgzhang@mail.sioc.ac.cn.

* Corresponding author

Keywords:
alkenes; cross-coupling; Heck-type reaction; palladium; secondary trifluoromethylated alkyl bromides

Beilstein J. Org. Chem. **2017,** *13,* 2610–2616.
doi:10.3762/bjoc.13.258

Received: 30 September 2017
Accepted: 21 November 2017
Published: 06 December 2017

This article is part of the Thematic Series "Organo-fluorine chemistry IV".

Guest Editor: D. O'Hagan

Abstract

An efficient palladium-catalyzed Heck-type reaction of secondary trifluoromethylated alkyl bromides has been developed. The reaction proceeds under mild reaction conditions with high efficiency and excellent functional group tolerance, even towards formyl and hydroxy groups. Preliminary mechanistic studies reveal that a secondary trifluoromethylated alkyl radical is involved in the reaction.

Introduction

With the increasing number of applications of fluorinated compounds in life and materials science, developing efficient and straightforward methods for the synthesis of fluorinated compounds has become more and more important. Although great achievements have been made in the introduction of fluorine atom(s) into organic molecules over the past decade, investigations mainly focused on direct fluorination or fluoroalkylation of aromatics [1-5]. Fluoroalkylated alkenes are a kind of important fluorinated structural motifs and have wide applications in medicinal chemistry and advanced functional materials [6-9]. However, developing efficient methods for the synthesis of such valuable structures has received less attention [10-15].

Commonly, fluoroalkylated alkenes can be prepared through fluoroalkyl radical addition of alkynes via an atom transfer pathway [16,17] or cross-coupling of alkenyl halides with fluoroalkyl metal species [18-24]. Recently, we reported a palladium-catalyzed Heck-type reaction of fluoroalkyl bro-

mides, representing an efficient and straightforward alternative to access fluoroalkylated alkenes [25-27]. Preliminary mechanistic studies reveal that a fluoroalkyl radical via a single electron transition (SET) pathway is involved in the reaction. Inspired by this work, we question that whether secondary fluoroalkylated alkyl bromides are also suitable substrates for such a Heck-type reaction. To the best of our knowledge, the palladium-catalyzed Heck-type reaction of secondary fluoroalkylated alkyl bromides with alkenes remains a challenge and has not been reported so far [28-32] due to the sluggish oxidative addition [33] of alkyl halides to palladium and facile β-hydride elimination [34,35] of alkylpalladium species. Additionally, the resulting fluoroalkylated allylic compounds can serve as a versatile building block for the synthesis of complex fluorinated molecules [36,37]. Herein, we describe a palladium-catalyzed Heck-type reaction of secondary trifluoromethylated alkyl bromides. The reaction proceeds under mild reaction conditions with broad substrate scope and high efficiency. The reaction can also extend to secondary difluoroalkylated alkyl iodide. Preliminary mechanistic studies reveal that a secondary alkyl radical via a SET pathway is involved in the reaction.

Results and Discussion

We began this study by choosing styrene (**1a**) and 2-bromo-1,1,1-trifluorohexane (**2a**) as model substrates (Table 1). Initially, a 27% yield of product **3a** along with small amount of hydrodebrominated byproduct **3a′** (2% yield) were obtained when the reaction of **1a** (0.2 mmol, 1.0 equiv) with **2a** (2.0 equiv) was carried out in the presence of $PdCl_2(PPh_3)_2$ (5 mol %), Xantphos (10 mol %) and K_2CO_3 (2.0 equiv) in DCE for 16 h at 80 °C (Table 1, entry 1). After optimization of the reaction conditions (for details, see Supporting Information File 1), a dramatically improved yield of **3a** (83% yield upon isolation) was provided by using KOAc as a base (Table 1, entry 5). K_3PO_4 also led to a good yield of **3a** (Table 1, entry 6), but other bases, such as Na_2CO_3, Cs_2CO_3, NaOAc and KF were less effective (Table 1, entries 2–4 and 7). Among all the tested palladium salts (Table 1, entries 8–12), $PdCl_2(PPh_3)_2$ was proved to be the most effective catalyst and provided **3a** in 84% yield (Table 1, entry 5). The use of Xantphos was crucial for the reaction efficiency (Table 1, entry 5). Other ligands either led to low yield or showed no reactivity (Table 1, entry 13, for details, see Supporting Information File 1). The beneficial effect of Xantphos is probably due to its large bit angle to promote the reaction [38,39]. However, the exact role of Xantphos remains elusive. Finally, the optimal reaction conditions were identified by decreasing the loading amount of Xantphos from 10 mol % to 7.5 mol % with a higher concentration of **1a** and **2a**, providing **3a** in 88% yield upon isolation (Table 1, entry 14).

Table 1: Representative results for the optimization of Pd-catalyzed cross-coupling between **1a** and 2-bromo-1,1,1-trifluorohexane (**2a**)[a].

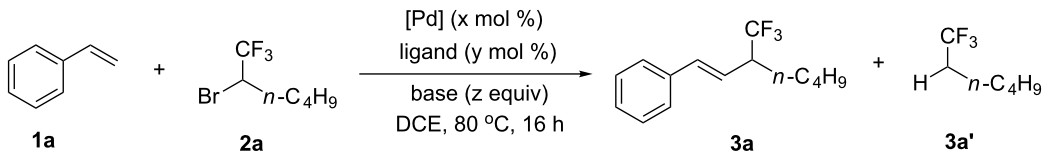

1a **2a** **3a** **3a'**

entry	[Pd] (mol %)	ligand (mol %)	base (equiv)	**3a**, yield (%)[b]
1	$PdCl_2(PPh_3)_2$ (5)	Xantphos (10)	K_2CO_3 (2)	27
2	$PdCl_2(PPh_3)_2$ (5)	Xantphos (10)	Na_2CO_3 (2)	5
3	$PdCl_2(PPh_3)_2$ (5)	Xantphos (10)	Cs_2CO_3 (2)	26
4	$PdCl_2(PPh_3)_2$ (5)	Xantphos (10)	NaOAc (2)	42
5	$PdCl_2(PPh_3)_2$ (5)	Xantphos (10)	KOAc (2)	84 (83)
6	$PdCl_2(PPh_3)_2$ (5)	Xantphos (10)	K_3PO_4 (2)	75
7	$PdCl_2(PPh_3)_2$ (5)	Xantphos (10)	KF (2)	37
8	$PdCl_2$ (5)	Xantphos (10)	KOAc (2)	18
9	$Pd(OAc)_2$ (5)	Xantphos (10)	KOAc (2)	51
10	$PdCl_2$·dppp (5)	Xantphos (10)	KOAc (2)	Trace
11	$PdCl_2$·dppf (5)	Xantphos (10)	KOAc (2)	69
12	$Pd(PPh_3)_4$ (5)	Xantphos (10)	KOAc (2)	64
13	$PdCl_2(PPh_3)_2$ (5)	dprephos	KOAc (2)	45
14[c]	$PdCl_2(PPh_3)_2$ (5)	Xantphos (7.5)	KOAc (2)	95 (88)

[a]Reaction conditions (unless otherwise specified): **1a** (0.2 mmol, 1.0 equiv), **2a** (2.0 equiv), base (2.0 equiv), DCE (3 mL), 16 h. [b]Determined by ^{19}F NMR using fluorobenzene as an internal standard (isolated yield in parentheses). [c]**1a** (0.4 mmol, 1.0 equiv), **2a** (2.0 equiv) and DCE (3 mL) were used.

With the optimized reaction conditions in hand, a variety of alkenes were examined. As shown in Scheme 1, reactions of **2a** with a series of styrene derivatives **1** proceeded smoothly and provided **3** in moderate to excellent yields (Scheme 1). Generally, substrates bearing electron-donating groups afforded higher yields than that of alkenes bearing electron-withdrawing groups. Various versatile functional groups, such as ester, cyano, and chloride showed good tolerance to the reaction (**3f–j**). Vinylnaphthalene also furnished the corresponding product efficiently (**3k**). The conjugated alkene did not interfere with the reaction efficiency, providing **3l** in 83% yield. The reaction was not restricted to aromatic alkenes, enamide was also applicable to the reaction and afforded **3m** in 61% yield.

To demonstrate the generality of this method further, reactions of alkenes with various secondary trifluoromethylated alkyl bromides were performed and provided the corresponding products **4** with high yield. As shown in Scheme 2, a variety of secondary trifluoromethylated alkyl bromides, including those substrates bearing base and nucleophile sensitive functional groups, such as hydroxy, aldehyde, and phthalimide (**4e**, **4f**, **4j** and **4k**), were all applicable to the reaction, thus offering good opportunities for downstream transformations and highlighting the utility of the current process further. (3-Bromo-4,4,4-trifluorobutyl)benzene and 4-bromo-5,5,5-trifluoropentyl benzoate were also successfully employed to couple with a conjugated alkene and afforded the corresponding products **4d** and **4h** in good yields. The current cross coupling was also applicable to the secondary difluoroalkylated alkyl halides as demonstrated by the representative reaction of secondary ethyl 2,2-difluoro-2-iodoacetate with *para*-methoxystyrene and *para*-fluorostyrene (**4l** and **4m**).

To probe whether a secondary trifluoromethylated alkyl radical is involved in the current reaction, radical inhibition experiments were performed (Table 2). When a reaction of **1a** with **2a** was carried out in the presence of $PdCl_2(PPh_3)_2$ (5 mol %), Xantphos (7.5 mol %) and KOAc in DCE at 80 °C, the addition

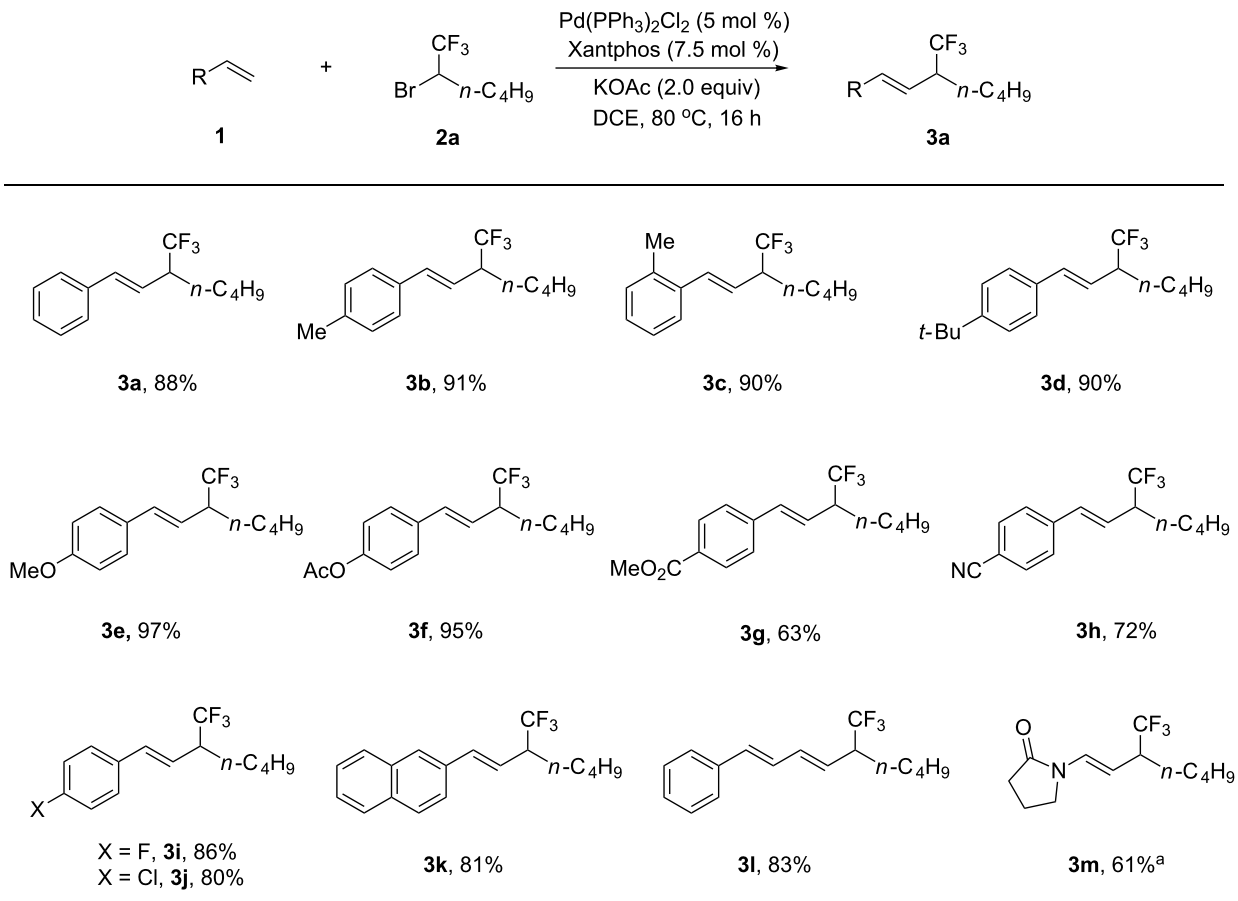

Scheme 1: Palladium-catalyzed Heck-type reaction of 2-bromo-1,1,1-trifluorohexane (**2a**) with alkenes **1**. Reaction conditions (unless otherwise specified): **1** (0.4 mmol, 1.0 equiv), **2a** (2.0 equiv), DCE (3 mL), 80 °C, 16 h. All reported yields are those of isolated products. [a]The reaction was conducted at 100 °C.

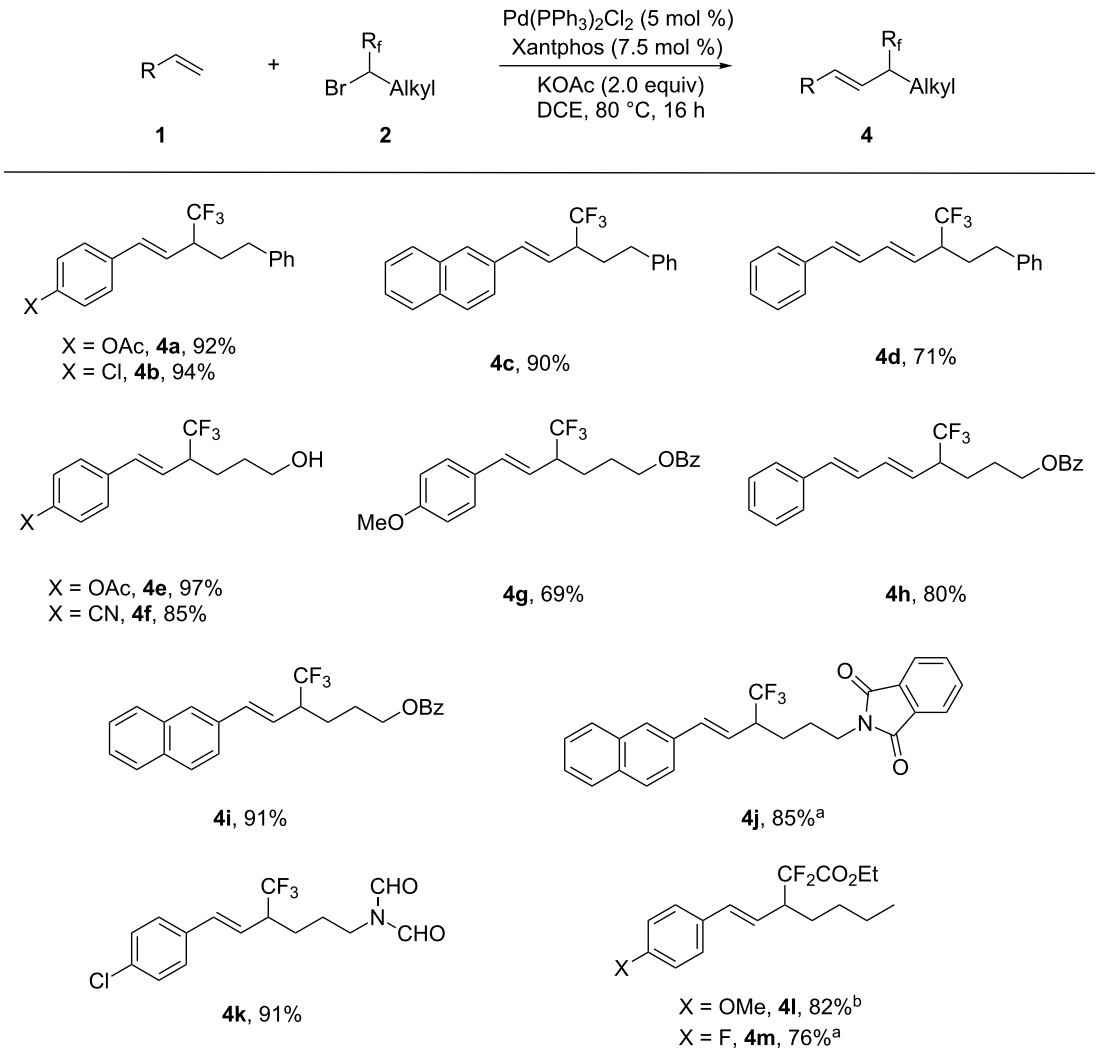

Scheme 2: Palladium-catalyzed Heck-type reaction of fluorinated secondary bromides (iodides) **2** with alkenes **1**. Reaction conditions (unless otherwise specified): **1** (0.4 mmol, 1.0 equiv), **2** (2.0 equiv), DCE (3 mL), 80 °C, 16 h. All reported yields are those of isolated products. [a]The reaction was carried out in 0.2 mmol scale. [b]Ethyl 2,2-difluoro-2-iodoacetate was used.

Table 2: Radical inhibition experiments of Pd-catalyzed cross-coupling between **1a** and 2-bromo-1,1,1-trifluorohexane (**2a**)[a].

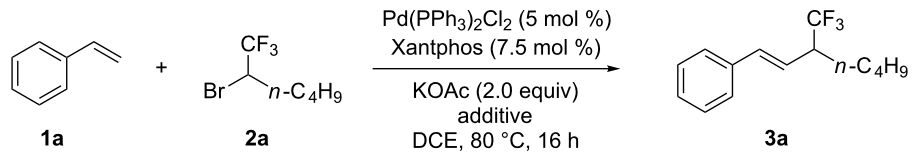

entry	additive (equiv)	**3a**, yield (%)[b]
1	none	95 (88)
2	1,4-dinitrobenzene (0.2)	22
3	1,4-dinitrobenzene (1.0)	5
4	hydroquinone (0.2)	0

[a]Reaction conditions: **1** (0.4 mmol, 1.0 equiv), **2a** (2.0 equiv), KOAc (2.0 equiv), DCE (3 mL), 16 h. [b]Determined by ^{19}F NMR using fluorobenzene as an internal standard.

of an electron transfer scavenger 1,4-dinitrobenzene [25-27] dramatically diminished the yield of **3a** (Table 2, entries 2 and 3), and catalytic amount of radical inhibitor hydroquinone totally shut down the reaction (Table 2, entry 4). Thus, these results suggest that a secondary trifluoromethylated alkyl radical via a SET pathway is likely involved in the reaction.

The existence of an alkyl radical species was further confirmed by the radical clock experiment. As illustrated in Scheme 3, when α-cyclopropylstyrene (**5**) [40] was subjected to the reaction, a ring-opened compound **6** was isolated in 55% yield, demonstrating that a secondary triflurometylated alkyl radical existed in the reaction is reasonable.

On the basis of these results and our previous reports [25-27], a plausible mechanism is proposed (Scheme 4). The reaction begins with the reaction of [$PdL_n(0)$] with secondary trifluoromethylated **2** via a SET pathway to generate alkyl radical **B**. **B** subsequently reacts with alkene to produce new radical species **D**, which then recombines with [L_nPd(I)Br] **C** to give the key palladium-complex **E**. Finally, a β-hydride elimination delivers trifluoromethylated allylic products **3** and **4**.

Conclusion

In conclusion, we have developed an efficient method for preparation of aliphatic alkenes branched with a trifluoromethyl group by palladium catalyzed Heck-type reaction of secondary trifluoromethylated alkyl bromides. The reaction proceeds under mild conditions and showed good functional group compatibility, even towards formyl and hydroxy groups, thus providing a facile route for applications in discovering biologically interesting molecules. Preliminary mechanistic studies reveal that a secondary trifluoromethylated alkyl radical is involved in the reaction.

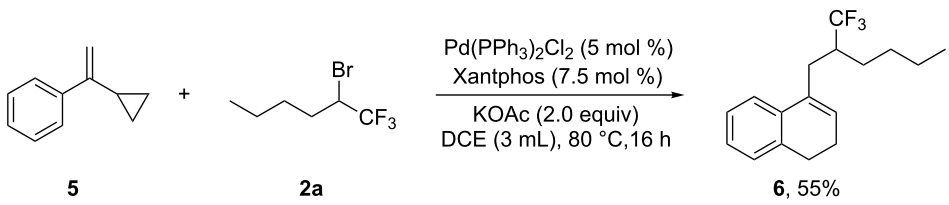

Scheme 3: Radical clock experiment for mechanistic studies.

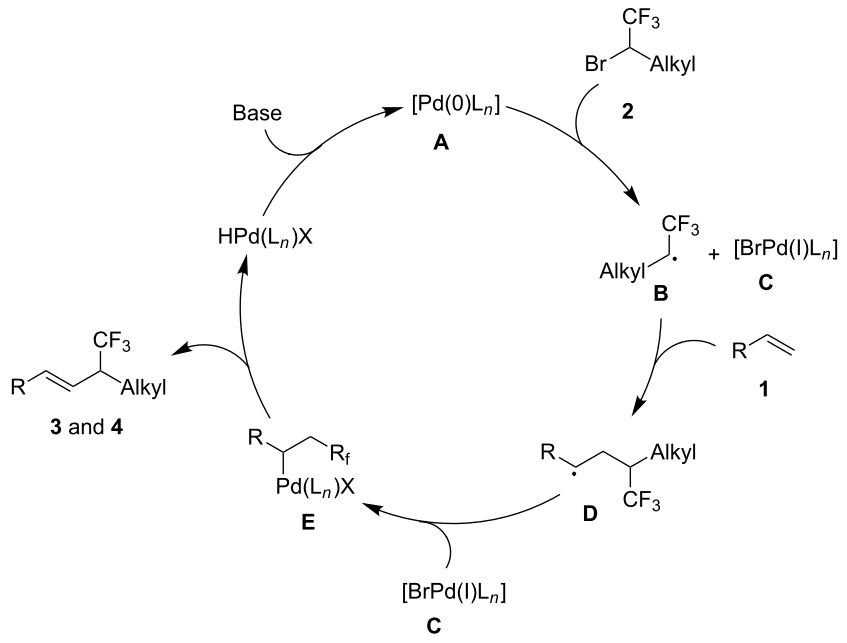

Scheme 4: Proposed mechanism.

Supporting Information

Supporting Information File 1

General experimental information, experimental details on the synthesis of compounds **2**–**4** and **6**; full characterization data as well as ^{1}H/ ^{19}F/ ^{13}C NMR spectra of all products.
[http://www.beilstein-journals.org/bjoc/content/supplementary/1860-5397-13-258-S1.pdf]

Acknowledgements

This work was financially supported by the National Natural Science Foundation of China (21425208, 21672238, 21332010, and 2141002), the Strategic Priority Research Program of the Chinese Academy of Sciences (No. XDB20000000), and Shanghai Institute of Organic Chemistry, Chinese Academy of Sciences.

ORCID® iDs

Xingang Zhang - https://orcid.org/0000-0002-4406-6533

References

1. Furuya, T.; Kamlet, A. S.; Ritter, T. *Nature* **2011,** *473,* 470. doi:10.1038/nature10108
2. Tomashenko, O. A.; Grushin, V. V. *Chem. Rev.* **2011,** *111,* 4475. doi:10.1021/cr1004293
3. Hollingworth, C.; Gouverneur, V. *Chem. Commun.* **2012,** *48,* 2929. doi:10.1039/c2cc16158c
4. Besset, T.; Schneider, C.; Cahard, D. *Angew. Chem., Int. Ed.* **2012,** *51,* 5048. doi:10.1002/anie.201201012
5. Qing, F.-L. *Chin. J. Org. Chem.* **2012,** *32,* 815. doi:10.6023/cjoc1202021
6. Wipf, P.; Henninger, T. C.; Geib, S. J. *J. Org. Chem.* **1998,** *63,* 6088. doi:10.1021/jo981057v
7. Xiao, J.; Weisblum, B.; Wipf, P. *J. Am. Chem. Soc.* **2005,** *127,* 5742. doi:10.1021/ja051002s
8. Couve-Bonnaire, S.; Cahard, D.; Pannecoucke, X. *Org. Biomol. Chem.* **2007,** *5,* 1151. doi:10.1039/b701559c
9. Narumi, T.; Hayashi, R.; Tomita, K.; Kobayashi, K.; Tanahara, N.; Ohno, H.; Naito, T.; Kodama, E.; Matsuoka, M.; Oishi, S.; Fujii, N. *Org. Biomol. Chem.* **2010,** *8,* 616. doi:10.1039/B917236J
10. Seyferth, D.; Simon, R. M.; Sepelak, D. J.; Klein, H. A. *J. Org. Chem.* **1980,** *45,* 2273. doi:10.1021/jo01299a055
11. Long, Z.-Y.; Chen, Q.-Y. *J. Org. Chem.* **1999,** *64,* 4775. doi:10.1021/jo9900937
12. Murakami, S.; Ishii, H.; Fuchigami, T. *J. Fluorine Chem.* **2004,** *125,* 609. doi:10.1016/j.jfluchem.2003.12.015
13. Ghattas, W.; Hess, C. R.; Iacazio, G.; Hardre, R.; Klinman, J. P.; Réglier, M. *J. Org. Chem.* **2006,** *71,* 8618. doi:10.1021/jo061022s
14. Yu, C.; Iqbal, N.; Park, S.; Cho, E. J. *Chem. Commun.* **2014,** *50,* 12884. doi:10.1039/C4CC05467A
15. Besset, T.; Poisson, T.; Pannecoucke, X. *Chem. – Eur. J.* **2014,** *20,* 16830. doi:10.1002/chem.201404537
16. Hu, C.-M.; Qiu, Y.-L.; Qin, F.-L. *J. Fluorine Chem.* **1991,** *51,* 295. doi:10.1016/S0022-1139(00)80300-0
17. Umemoto, T.; Kuriu, Y.; Miyano, O. *Tetrahedron Lett.* **1982,** *23,* 3579. doi:10.1016/S0040-4039(00)87675-3
18. Taguchi, T.; Kitagawa, O.; Morikawa, T.; Nishiwaki, T.; Uehara, H.; Endo, H.; Kobayashi, Y. *Tetrahedron Lett.* **1986,** *27,* 6103. doi:10.1016/S0040-4039(00)85409-X
19. Yokomatsu, T.; Suemune, K.; Murano, T.; Shibuya, S. *J. Org. Chem.* **1996,** *61,* 7207. doi:10.1021/jo960896j
20. Sato, K.; Kawata, R.; Ama, F.; Omate, M.; Ando, A.; Kumadaki, I. *Chem. Pharm. Bull.* **1999,** *47,* 1013. doi:10.1248/cpb.47.1013
21. Schwaebe, M. K.; McCarthy, J. R.; Whitten, J. P. *Tetrahedron Lett.* **2000,** *41,* 791. doi:10.1016/S0040-4039(99)02212-1
22. Chu, L.; Qing, F.-L. *Org. Lett.* **2010,** *12,* 5060. doi:10.1021/ol1023135
23. Fier, P. S.; Hartwig, J. F. *J. Am. Chem. Soc.* **2012,** *134,* 5524. doi:10.1021/ja301013h
24. Prakash, G. K. S.; Ganesh, S. K.; Jones, J.-P.; Kulkarni, A.; Masood, K.; Swabeck, J. K.; Olah, G. A. *Angew. Chem., Int. Ed.* **2012,** *51,* 12090. doi:10.1002/anie.201205850
25. Feng, Z.; Min, Q.-Q.; Zhao, H.-Y.; Gu, J.-W.; Zhang, X. *Angew. Chem., Int. Ed.* **2015,** *54,* 1270. doi:10.1002/anie.201409617
26. Feng, Z.; Min, Q.-Q.; Zhang, X. *Synthesis* **2015,** *47,* 2912. doi:10.1055/s-0035-1560457
27. Feng, Z.; Xiao, Y.-L.; Zhang, X. *Org. Chem. Front.* **2016,** *3,* 466. doi:10.1039/C6QO00005C
28. Firmansjah, L.; Fu, G. C. *J. Am. Chem. Soc.* **2007,** *129,* 11340. doi:10.1021/ja075245r
29. Bloome, K. S.; McMahen, R. L.; Alexanian, E. J. *J. Am. Chem. Soc.* **2011,** *133,* 20146. doi:10.1021/ja2091883
30. McMahon, C. M.; Alexanian, E. J. *Angew. Chem., Int. Ed.* **2014,** *53,* 5974. doi:10.1002/anie.201311323
31. Zou, Y.; Zhou, S. *Chem. Commun.* **2014,** *50,* 3725. doi:10.1039/C4CC00297K
32. Okano, T.; Sugiura, H.; Fumoto, M.; Matsubara, H.; Kusukawa, T.; Fujita, M. *J. Fluorine Chem.* **2002,** *114,* 91. doi:10.1016/S0022-1139(02)00002-7
33. Stille, J. K. In *The Chemistry of the Metal-Carbon Bond;* Patai, S., Ed.; chap. 9, Vol. 2; Wiley: New York, 1985; pp 625–787.
34. Ozawa, F.; Ito, T.; Yamamoto, A. *J. Am. Chem. Soc.* **1980,** *102,* 6457. doi:10.1021/ja00541a013
35. Hartwig, J. F. *Organotransition Metal Chemistry: From Bonding to Catalysis;* Chapter 10; University Science Books: Sausalito, CA, 2009; pp 397–416.
36. Taguchi, T.; Namba, R.; Nakazawa, M.; Nakajima, M.; Nakama, Y.; Kobayashi, Y.; Hara, N.; Ikekawa, N. *Tetrahedron Lett.* **1988,** *29,* 227. doi:10.1016/S0040-4039(00)80061-1
37. Jiang, B.; Lu, Y.; Zhou, W.-s. *J. Org. Chem.* **2000,** *65,* 6231. doi:10.1021/jo000059o
38. Grushin, V. V.; Marshall, W. J. *J. Am. Chem. Soc.* **2006,** *128,* 12644. doi:10.1021/ja064935c
39. Bakhmutov, V. I.; Bozoglian, F.; Gómez, K.; González, G.; Grushin, V. V.; Macgregor, S. A.; Martin, E.; Miloserdov, F. M.; Novikov, M. A.; Panetier, J. A.; Romashov, L. V. *Organometallics* **2012,** *31,* 1315. doi:10.1021/om200985g
40. Baldwin, J. E. *Chem. Rev.* **2003,** *103,* 1197. doi:10.1021/cr010020z

License and Terms

BEILSTEIN JOURNAL OF ORGANIC CHEMISTRY

Regioselective decarboxylative addition of malonic acid and its mono(thio)esters to 4-trifluoromethylpyrimidin-2(1*H*)-ones

Sergii V. Melnykov[1], Andrii S. Pataman[2], Yurii V. Dmytriv[2,3], Svitlana V. Shishkina[4,5], Mykhailo V. Vovk[1] and Volodymyr A. Sukach[*1]

Full Research Paper

Open Access

Address:
[1]Institute of Organic Chemistry, National Academy of Sciences of Ukraine, 5 Murmanska str., Kyiv 02660, Ukraine, [2]Enamine LTD, 78 Chervonotkats'ka str., Kyiv 02094, Ukraine, [3]National Technical University of Ukraine "Igor Sikorsky Kyiv Polytechnic Institute", 37 Peremohy ave., Kyiv 03056, Ukraine, [4]STC ''Institute for Single Crystals'', National Academy of Sciences of Ukraine, 60 Nauky ave., Kharkiv 61001, Ukraine and [5]Department of Inorganic Chemisrtry, V.M. Karasin Kharkiv National University, 4 Svobody sq, Kharkiv 61122, Ukraine

Email:
Volodymyr A. Sukach[*] - vsukach@gmail.com

* Corresponding author

Keywords:
ketimines; malonic acid; Michael- and Mannich-type decarboxylative addition; pyrimidin-2(1*H*)-ones; regioselectivity; trifluoromethyl group

Beilstein J. Org. Chem. **2017,** *13,* 2617–2625.
doi:10.3762/bjoc.13.259

Received: 03 August 2017
Accepted: 20 November 2017
Published: 07 December 2017

This article is part of the Thematic Series "Organo-fluorine chemistry IV".

Guest Editor: D. O'Hagan

Abstract

Background: Due to the high reactivity towards various C-nucleophiles, trifluoromethylketimines are known to be useful reagents for the synthesis of α-trifluoromethylated amine derivatives. However, decarboxylative reactions with malonic acid and its mono(thio)esters have been poorly investigated so far despite the potential to become a convenient route to β-trifluoromethyl-β-amino acid derivatives and to their partially saturated heterocyclic analogues.

Results: In this paper we show that 4-trifluoromethylpyrimidin-2(1*H*)-ones, unique heterocyclic ketimines, react with malonic acid under organic base catalysis to regioselectively provide either Michael- or Mannich-type decarboxylative addition products depending on solvent polarity. Malonic mono(thio)esters give exclusively Michael-type products. The two regioisomeric products can be converted into saturated (2-oxohexahydropyrimidin-4-yl)acetic acid derivatives by mild hydrogenation of the endocyclic C=C double bond in the presence of Pd/C as catalyst. The *cis*-stereoisomers selectively formed upon reduction of the Michael-type products were structurally determined by X-ray diffraction. As a result of this study, a number of novel acetic acid derivatives containing trifluoromethylated, partially or fully saturated 2-oxopyrimidine cores were prepared and characterized as promising building blocks.

Conclusions: Regio- and stereoselective protocols have been developed for the synthesis of novel isomeric 4(6)-trifluoromethylated 1,2,3,4-tetrahydro- and perhydro-(2-oxopyrimidin-4-yl)acetic acid derivatives.

Introduction

Organofluorine compounds now play an essential role in the development of new materials for solar cells [1-3], radiotracers for PET imaging [4], agrochemicals [5,6], sensitive chemical probes for ^{19}F nuclear magnetic resonance investigation of biological experiments [7,8], and are most widely used in the modern drug discovery and development area [9,10]. As a result of intensive research efforts over the last decades, efficient fluorination and fluoroalkylation methods have emerged to prepare previously challenging molecules decorated with fluorine atoms or fluorinated groups which make them practically useful [11-14]. A building-block approach remains an alternative strategy to the synthesis of fluorine-containing compounds. This complementary method takes advantage of specific reagents featuring original fluorinated motives and/or functional groups which affords more complex derivatives via conventional functionalization or (hetero)cyclization [15-17]. Among these reagents, trifluoromethylketimines have drawn much research interest in recent years as key starting materials for the synthesis of trifluoromethyl-substituted amines [18,19], α-amino acids [20-23] as well as nitrogen-containing heterocyclic compounds [24-29]. It should be noted that the presence of a strong electron-withdrawing trifluoromethyl group is responsible for the sufficient reactivity of the electrophilic ketimine function with various carbon nucleophiles in these reactions.

Recently, the decarboxylative addition of malonic acid mono(thio)esters to aldehydes and imines has become an increasingly popular synthetic strategy [28,30-36]. However, the utility of trifluoromethylketimines as electrophilic substrates in this reaction remains underinvestigated. The only published work from the group of Ma described the development of a chiral thiourea-catalyzed enantioselective decarboxylative Mannich reaction of malonic acid monoesters with 4-trifluoromethylquinazolin-2(1*H*)-ones as heterocyclic trifluoromethylketimine substrates for the preparation of enantioenriched 3,4-dihydroquinazolin-2(1*H*)-ones and the anti-HIV drug DPC 083 [28]. No examples of any ketimines reacting directly with malonic acid have been reported so far.

Here we present the results of the decarboxylative addition of malonic acid, malonic monoester **1a** and thioester **1b** to 4-trifluoromethylpyrimidin-2(1*H*)-ones **2** (Figure 1). These compounds are unique heterocyclic conjugated trifluoromethylketimines with two competing electrophilic centers which can enable either Michael- or Mannich-type nucleophilic additions. As found in our previous studies, organocatalytic addition of acetone [37], nitromethane [38] and trimethylsilyl cyanide [39] in most cases can be performed regioselectively after optimization of the reaction conditions (temperature, solvent, time and catalyst nature). In general, under kinetic reaction control, the Michael-type 1,4-adducts are the predominant products while under thermodynamic control, the regioisomeric Mannich-type 1,2-adducts are more likely to be formed. These observations allowed us to develop selective methods for the synthesis of functionalized partially saturated 4-trifluoromethyl-substituted pyrimidin-2(1*H*)-ones, in particular, 4,5-dihydroorotic acid analogues **3** [39]. Here we report the preparation of acid **3** homologues (with a methylene linker between the carboxylic group and the pyrimidine ring) and their isomers resulting from two alternative regioselective pathways for the decarboxylative nucleophilic addition of malonic acid and its mono(thio)esters.

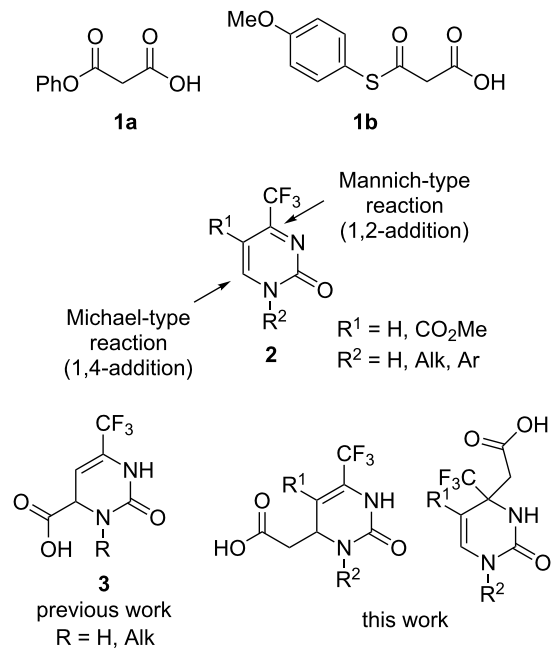

Figure 1: Summary of the present study.

Results and Discussion

We first screened organic base catalysts, solvents and temperature in the decarboxylative addition of malonic acid (nucleophilic component) to 1-methyl-4-trifluoromethylpyrimidin-2(1*H*)-one (**2a**, the simplest model substrate) aiming to find the optimal organocatalytic reaction conditions (Table 1). In the preliminary experiments, it was established that the reaction was quite slow; heating and a 5-fold excess of malonic acid were required to reach a reasonable conversion. Additionally, it was found that a stoichiometric amount of a model catalyst, triethylamine (TEA), was necessary for the reaction to proceed efficiently. Thus, heating the reaction mixture in toluene at 80 °C for 18 h in the presence of 1 equivalent of TEA resulted

Table 1: Screening of the reaction conditions for organic base-catalyzed malonic acid addition to 1-methyl-4-trifluoromethylpyrimidin-2(1*H*)-one (**2a**).

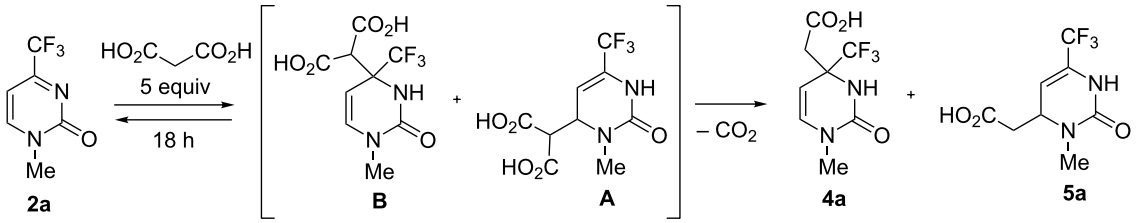

entry	base (1 equiv)	solvent	temp. (°C)	conv. (%)	**4a**:**5a** ratio (%)	product (isolated yield, %)
1	TEA	toluene	80	84	92:8	**4a** (68)
2	TEA	THF	65	97	13:87	**5a** (63)
3	TEA	DMSO	80	94	1:99	**5a** (85)
4	TEA	MeOH	63	46	21:79	–
5	DIEA	toluene	80	83	88:12	**4a** (66)
6	DBU	toluene	80	80	85:15	–
7	quinine	toluene	80	81	47:53[a]	–
8	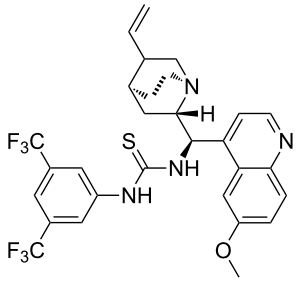 QT	toluene	80	62	34:66[a]	–

[a]The two regioisomers were racemic.

in a satisfactory 84% conversion and led to the Mannich-type product, (1-methyl-2-oxo-4-trifluoromethyl-1,2,3,4-tetrahydropyrimidin-4-yl)acetic acid (**4a**), along with a small amount of the Michael-type regioisomer **5a** (Table 1, entry 1). The reaction course and the ratio of the regioisomers formed were conveniently monitored by ^{19}F NMR spectroscopy. Acid **4a** precipitated in pure form on evaporating toluene and treating the residue with diluted hydrochloric acid. Performing the reaction in a more polar solvent such as THF drastically shifted the regioselectivity to the Michael-type adduct formation (Table 1, entry 2). Using DMSO as solvent and heating the reaction at 80 °C provided exclusively (3-methyl-2-oxo-6-trifluoromethyl-1,2,3,4-tetrahydropyrimidin-4-yl)acetic acid (**5a**) in high isolated yield (Table 1, entry 3). Methanol proved to be an unsuitable solvent for this reaction in terms of both conversion and selectivity (Table 1, entry 4). Likewise, diisopropylethylamine (DIEA) and 1,8-diazabicyclo[5.4.0]undec-7-ene (DBU) were found to be not superior to TEA as catalysts (Table 1, entries 5 and 6). Unfortunately, quinine and the chiral quinine-derived thiourea organocatalyst QT in toluene led to a mixture of racemic products along with 19% and 38% of unreacted starting material, respectively (Table 1, entries 7 and 8).

As seen from the screening results, the reaction regioselectivity is easily solvent controlled. Non-polar toluene is the preferential solvent for the Mannich-type decarboxylative addition to the C=N double bond while polar DMSO promotes the highly selective Michael-type addition to the C=C double bond. These observations are explained by the fact that the initially formed (kinetically controlled) Michael-type dicarboxylate adduct **A** is much more stable in a low-polar than in a high-polar solvent (Table 1). In the former case, the long-living intermediate **A** is gradually converted, via the reversible first reaction step, into the energetically advantageous (thermodynamically controlled) Mannich-type adduct **B**, followed by rapid irreversible decarboxylation of **B** into compound **4a**. Contrastingly, in a high-polar solvent, the intermediate **A** is so labile that it undergoes decarboxylation to product **5a** rather than rearrangement to **B**. The proposed reaction mechanism is supported by the known effect of solvent polarity on the decarboxylation rate of malonic acid derivatives which was claimed to be faster in polar media [40].

To study the substrate scope of the regioselective additions of malonic acid, we introduced substituted pyrimidones **2b**–**m** in

the reaction and performed it under optimal conditions using toluene or DMSO as solvent and TEA (1 equiv) as catalyst (Table 2). The alkyl substituent at the nitrogen atom of the substrate had no significant effect on the reaction course. In all cases, both regioisomers, **4b**–**i** and **5b**–**i**, were isolated in modest to high yields (Table 2, entries 1–16). The presence of the ester functionality at position 5 of the heterocycle led to product mixtures if toluene was used as solvent so that products **4j**–**m** could not be obtained selectively and separated. In DMSO solution, the corresponding Michael-type adducts **5j**–**m** were smoothly formed and obtained in 75–83% isolated yields (Table 2, entries 17–20). 4-Trifluoromethylpyrimidin-2(1*H*)-ones **2** lacking a substituent at position 1 (structures not shown) were found to be completely unreactive in the decarboxylative reaction under study.

With the aim of preparing the corresponding *N*1(3)-unsubstituted products **4j** and **5n**,**o**, we utilized *N*1(3)-(4-methoxybenzyl) derivatives **4i**, **5i**, **5k** in trifluoroacetic acid (TFA); the resulting cleavage of the 4-methoxybenzyl (PMB) group afforded the target compounds in good yields (see Table 2).

Next we studied the decarboxylative addition of reagent **1a** to model substrate **2a** (Table 3) to compare the reactivity of malonic acid and its monophenyl ester **1a**. It was proved again that the reaction proceeded sufficiently fast in toluene only in

Table 2: Regioselective decarboxylative addition of malonic acid to 4-trifluoromethylpyrimidin-2(1*H*)-ones **2b–m** and preparation of *N*1(3)-unsubstituted compounds **4j** and **5n,o**.

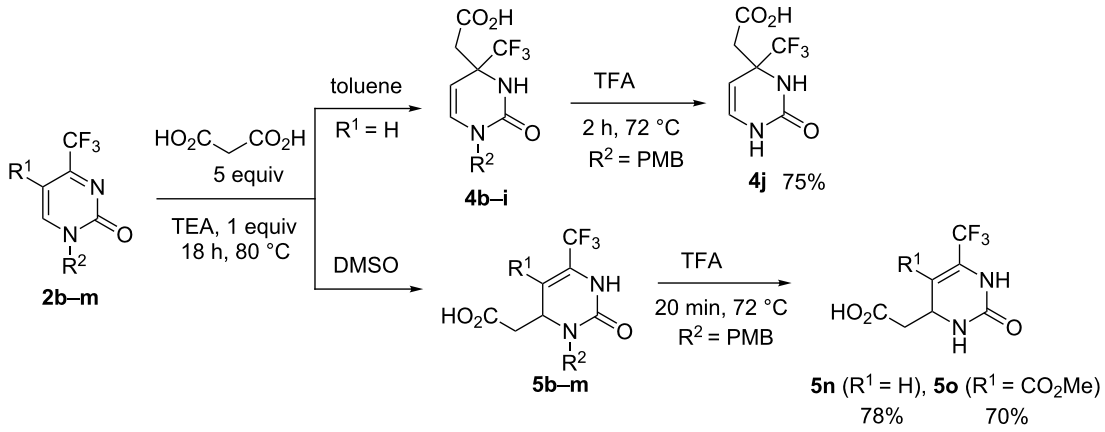

entry	comp. **2**	R^1	R^2	isol. product	yield (%)
1	**b**	H	Et	**4b**	62
2	**b**	H	Et	**5b**	58
3	**c**	H	*n*-Bu	**4c**	67
4	**c**	H	*n*-Bu	**5c**	55
5	**d**	H	Me_2CHCH_2	**4d**	57
6	**d**	H	Me_2CHCH_2	**5d**	51
7	**e**	H	$MeOCH_2CH_2$	**4e**	59
8	**e**	H	$MeOCH_2CH_2$	**5e**	64
9	**f**	H	CH_2=$CHCH_2$	**4f**	73
10	**f**	H	CH_2=$CHCH_2$	**5f**	82
11	**g**	H	Bn	**4g**	68
12	**g**	H	Bn	**5g**	89
13	**h**	H	4-$FC_6H_4CH_2$	**4h**	60
14	**h**	H	4-$FC_6H_4CH_2$	**5h**	80
15	**i**	H	4-$MeOC_6H_4CH_2$	**4i**	65
16	**i**	H	4-$MeOC_6H_4CH_2$	**5i**	82
17	**j**	CO_2Me	4-$FC_6H_4CH_2$	**5j**	75
18	**k**	CO_2Me	4-$MeOC_6H_4CH_2$	**5k**	83
19	**l**	CO_2Me	4-ClC_6H_4	**5l**	81
20	**m**	CO_2Me	4-$MeOC_6H_4$	**5m**	81

Table 3: Screening of the reaction conditions for organic base-catalyzed malonic acid monophenyl ester (**1a**) addition to 1-methyl-4-trifluoromethyl-pyrimidin-2(1*H*)-one (**2a**).

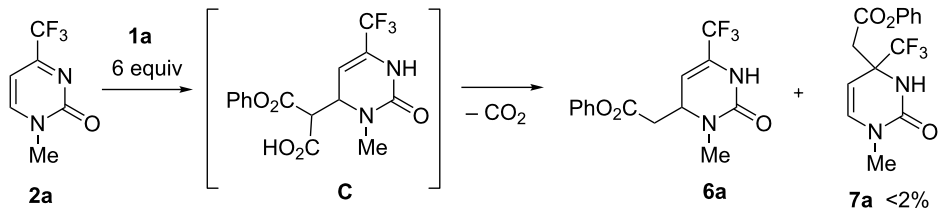

entry	solvent	base	temp. (°C)	time (h)	conv.	yield **6a** (%)[a]
1	toluene	TEA	80	4	98	81
2	toluene	DIEA	80	4	96	77
3	toluene	DBU	80	4	10	–
4	toluene	quinine	80	4	92	68[b]
5	toluene	QT	80	4	78	55[b]
6	CH_2Cl_2	TEA	40	8	94	75
7	THF	TEA	66	8	90	74
8	dioxane	TEA	80	4	91	80
9	DMSO	TEA	80	4	93	81

[a]The regioisomeric product **7a** was formed in a negligible amount in all cases; [b]Racemic product.

the presence of a stoichiometric amount of TEA or DIEA (Table 3, entries 1 and 2). Under these conditions the reaction provided the Michael-type adduct, phenyl 2-(3-methyl-2-oxo-6-trifluoromethyl-1,2,3,4-tetrahydropyrimidin-4-yl)acetate (**6a**). The presence of DBU caused substantial decarboxylation of starting reagent **1a** (Table 3, entry 3). This unwanted process necessitated using of up to 6 equivalents of **1a** to reach a reasonable conversion with TEA as catalyst. Quinine and QT were again found to be ineffective to promote the enantioselective reaction (Table 3, entries 4 and 5). In contrast to the reaction with malonic acid under similar conditions, just trace amounts of regioisomeric Mannich-type adduct **7a** were detected. Presumably, in this case, the kinetically controlled Michael-type intermediate **C** is even far more prone to decarboxylation than the dicarboxylate intermediate **A** (Table 1) and hence, the reaction is sufficiently regioselective irrespective of the solvent polarity (Table 3, entries 1, and 6–9). Performing the reaction in toluene in the presence of TEA (1 equiv) at 80 °C for 4 hours gave the best result in terms of regioselectivity and yield of **6a** (Table 3, entry 1), virtually the only product formed in all the solvents used here (as evidenced by ^{19}F NMR monitoring).

The addition of malonic acid monophenyl ester (**1a**) to substituted pyrimidones **2b**–**e** carried out in the presence of TEA in toluene for 8 h has shown that a substituent at position 1 of the pyrimidine ring can significantly influence the progress of the reaction (Table 4). Thus, *N*1-alkyl-substituted compounds **2b**–**e** exhibited a lower reactivity compared to **2a** and the corresponding products **6b**–**e** were not isolated due to low conversion and regioselectivity (Table 4, entries 1–4). These are likely caused by the enhanced steric hindrance around the neighboring electrophilic position 6 and also the lowered electrophilicity of the reaction center. Consequently, the nucleophilic attack on the C=N double bond becomes equally probable thus leading to the loss of regioselectivity. Fortunately, allyl and various benzyl or phenyl substituents in derivatives **2f**–**m** allowed the regioselective synthesis of products **6f**–**m** in high yields (Table 4, entries 5–12). We found that the ester group at position 5 significantly increases the electrophilicity of the endocyclic C=C double bond giving rise to faster addition of **1a** and higher regioselectivity of products **6j**–**m** (Table 4, entries 9–12). Like *N*3-unsubstituted compounds **5n**,**o**, their phenyl ester analogues **6n**,**o** were obtained by the cleavage of the *N*3-PMB substituent on short heating in TFA (see Table 4). It has been shown that acids **4a**,**f**–**m** can be synthesized alternatively by alkaline hydrolysis of esters **6a**,**f**–**m** (see Supporting Information File 1 for full experimental data). The ester group at position 5 remained intact during the hydrolysis.

Malonic acid monothioesters are known to be more reactive C-nucleophiles than the corresponding esters [41]. Therefore, we studied the decarboxylative addition of compound **1b** as representative example to substrates **2a**–**m** (Table 5). They were found to furnish Michael-type addition products **8a**–**m** on

Table 4: Regioselective decarboxylative addition of malonic acid monophenyl ester (**1a**) to 4-trifluoromethylpyrimidin-2(1*H*)-ones **2b–m** and preparation of *N*3-unsubstituted compounds **6n**,**o**.

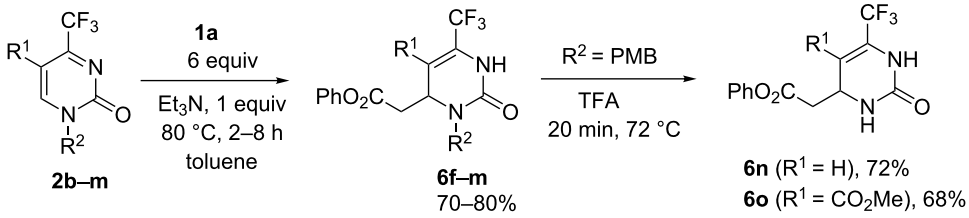

entry	comp. **2**, **6**	R^1	R^2	time (h)	conv.	yield **6** (%)
1	**b**	H	Et	8	50	–
2	**c**	H	*n*-Bu	8	55	–
3	**d**	H	Me_2CHCH_2	8	49	–
4	**e**	H	$MeOCH_2CH_2$	8	44	–
5	**f**	H	CH_2=$CHCH_2$	4	97	75
6	**g**	H	Bn	4	99	70
7	**h**	H	4-$FC_6H_4CH_2$	4	99	74
8	**i**	H	4-$MeOC_6H_4CH_2$	4	98	69
9	**j**	CO_2Me	4-$FC_6H_4CH_2$	2	99	80
10	**k**	CO_2Me	4-$MeOC_6H_4CH_2$	2	97	71
11	**l**	CO_2Me	4-ClC_6H_4	2	98	73
12	**m**	CO_2Me	4-$MeOC_6H_4$	2	99	75

Table 5: Regioselective decarboxylative addition of malonic acid mono-4-methoxyphenyl thioester (**1b**) to 4-trifluoromethylpyrimidin-2(1*H*)-ones **2a–m**.

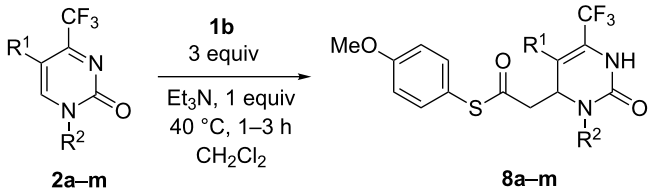

entry	comp. **2**, **8**	R^1	R^2	time (h)	yield **8** (%)
1	**a**	H	Me	3	83
2	**b**	H	Et	3	71
3	**c**	H	*n*-Bu	3	77
4	**d**	H	Me_2CHCH_2	3	77
5	**e**	H	$MeOCH_2CH_2$	3	75
6	**f**	H	CH_2=$CHCH_2$	3	73
7	**g**	H	Bn	3	74
8	**h**	H	4-$FC_6H_4CH_2$	3	71
9	**i**	H	4-$MeOC_6H_4CH_2$	3	70
10	**j**	CO_2Me	4-$FC_6H_4CH_2$	1	77
11	**k**	CO_2Me	4-$MeOC_6H_4CH_2$	1	75
12	**l**	CO_2Me	4-ClC_6H_4	1	81
13	**m**	CO_2Me	4-$MeOC_6H_4$	1	72

heating in CH_2Cl_2 at 40 °C in excellent yields. Moreover, 3 equivalents excess of **1b** was sufficient for the reaction to be completed within 1–3 hours.

Satisfactory conversion and regioselectivity were achieved even with substrates **2b**–**e** bearing ethyl, *n*-butyl, isobutyl and 2-methoxyethyl substituents which demonstrated low reactivity

in the addition reaction with ester analogue **1a**. It can thus be inferred that the substituents R^1 and R^2 have almost no impact on the outcome of the decarboxylative addition provided a highly reactive nucleophilic component such as malonic acid monothioester **1b** is used.

Importantly, representative compounds **6a**,**j** and **8f** readily reacted with benzylamine thus showing the possibility of esters **6** and thioesters **8** to be convenient amine acylating agents [32] and, hence, building blocks for direct preparation of the amide derivatives (see Supporting Information File 1 for examples of the corresponding amide syntheses).

In a next set of experiments, the endocyclic C=C double bond of the decarboxylative adducts **4**–**6** were hydrogenated to prepare compounds with a saturated 3,4,5,6-tetrahydropyrimidin-2(1*H*)-one ring functionalized with an acetic acid moiety and a trifluoromethyl group. Thus, the acids **4a**,**g**,**i** quantitatively yielded reduced products **9a–c** under mild catalytic conditions (when reacted with hydrogen at atmospheric pressure and room temperature for 3 hours in the presence of 10% Pd/C catalyst) as shown in Scheme 1. The simplest acetic acid derivative **9d** was synthesized from **9c** in a good yield by using the general procedure for *N*1-PMB cleavage. Likewise, regioisomeric acids **5a**,**g**,**i** and their phenyl esters **6a**,**g**,**i** were reduced to the respective saturated compounds **10a**–**c** and **11a**–**c**. In this case a high hydrogenation *cis*-stereoselectivity is provided when the Pd/C catalyst loading is smaller than 20 weight % (otherwise the reaction proceeds too fast leading to diastereomeric mixtures with a *cis*- to *trans*-ratio of up to 3:1).

The relative *cis*-configuration of the CF_3 and CH_2COOPh substituents in the prepared phenyl (2-oxo-6-trifluoromethylhexahydropyrimidin-4-yl)acetates **11a**–**c** was unambiguously corroborated by a single-crystal X-ray diffraction study of compound **11b** (Figure 2, see Supporting Information File 1 for full structure description and experimental data). The configuration-preserving conversion of ester **11b** into acid **10b** by simple alkaline hydrolysis has also confirmed the *cis*-geometry for acids **10a**–**c** obtained by direct hydrogenation of compounds **5a**,**g**,**i** (see Supporting Information File 1). *N*3-Unsubstituted compounds **10d** and **11d** with the preserved *cis*-configuration of the substituents were readily prepared from the corresponding *N*3-PMB derivatives **10c** and **11c** by using the general procedure for *N*1(3)-PMB cleavage (see Scheme 1).

Conclusion

In conclusion, it has been demonstrated that the efficient and highly regioselective organocatalytic decarboxylative addition of malonic acid or its derivatives to 4-trifluoromethylpyrimidin-2(1*H*)-ones **2** is perfectly feasible with a precise control of the reaction conditions. A remarkable solvent effect has been observed which governs the ratio of the resulting regioisomeric decarboxylated adducts **4** and **5** and allows their preparative selective isolation. This effect may well be attributed to a two-step mechanism of the decarboxylative nucleophilic addition which is characterized by a faster decarboxylation of kinetically-controlled Michael-type intermediates in high-polar solvents.

Though malonic monoester **1a** appears to be similar to malonic acid in reactivity towards compounds **2**, it produces exclusively

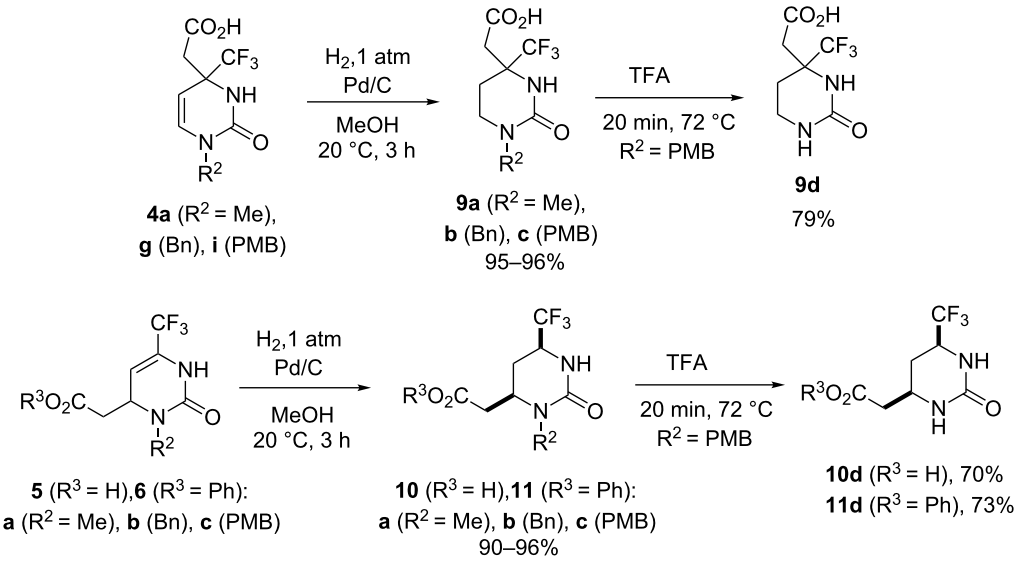

Scheme 1: Hydrogenation of compounds **4–6** and preparation of *N*1(3)-unsubstituted compounds **9–11d**.

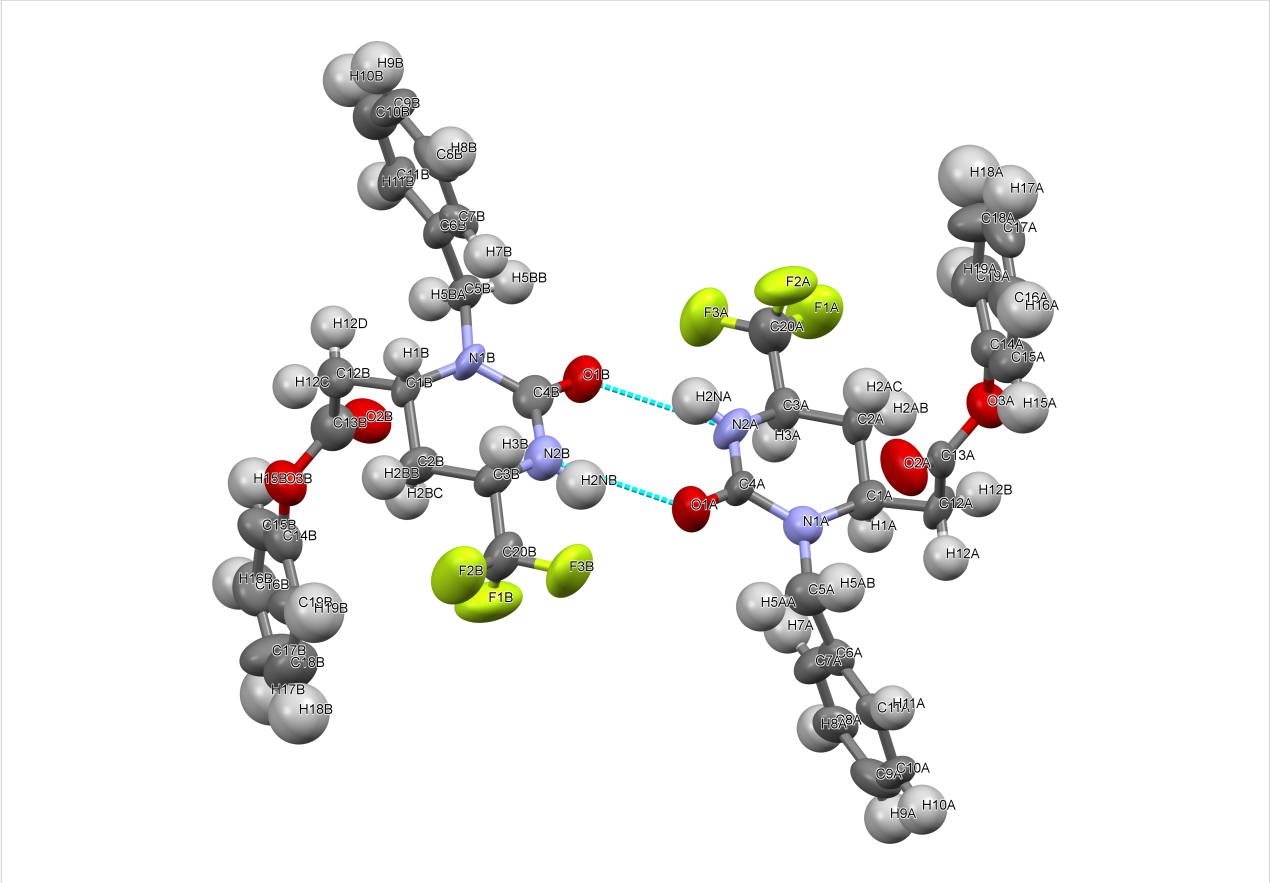

Figure 2: Molecular structure of compound **11b**. Two enantiomers form a heterochiral dimer in the crystal state. Intermolecular hydrogen bonds in the dimer are shown as dashed lines. Thermal ellipsoids are defined at 50% probability.

Michael-type adducts **6** regardless of the reaction conditions used. Likewise, the more reactive malonic mono thioester **1b**, when reacted with a broader scope of substrates **2** under milder conditions, gives rise only to analogous Michael-type products **8**. In general, the reactivity of substrates **2** can be increased by introduction of the ester functionality at position 5 as well as allyl, various benzyl or phenyl substituents at position 1 of the pyrimidine core. Notably, esters **6** and thioesters **8** are remarkable for their potential application as smooth amine acylating agents.

It has been shown that the 3,4-dihydropyrimidin-2(1*H*)-one ring in both Mannich- and Michael-type products **4** and **5**, **6** can be readily hydrogenated under mild catalytic conditions to furnish saturated compounds **9** and **10**, **11**, respectively. Products **10** and **11** featuring two stereogenic centers were obtained only as *cis*-isomers.

*N*1(3)-Unsubstituted products **4j**, **5n**,**o**, **6n**,**o**, and **9**–**11d**, unavailable by direct decarboxylative addition, are readily accessible by TFA-mediated cleavage of the corresponding *N*1(3)-PMB substituted precursors.

Supporting Information

Supporting Information File 1

Experimental procedures, characterization data and X-ray structure determination for compound **11b**.
[http://www.beilstein-journals.org/bjoc/content/supplementary/1860-5397-13-259-S1.pdf]

Supporting Information File 2

Copies of the ^{1}H, ^{13}C, and ^{19}F NMR spectra.
[http://www.beilstein-journals.org/bjoc/content/supplementary/1860-5397-13-259-S2.pdf]

ORCID® iDs

Svitlana V. Shishkina - https://orcid.org/0000-0002-3946-1061
Volodymyr A. Sukach - https://orcid.org/0000-0002-2891-343X

References

1. Liang, Y.; Feng, D.; Wu, Y.; Tsai, S.-T.; Li, G.; Ray, C.; Yu, L. *J. Am. Chem. Soc.* **2009,** *131,* 7792–7799. doi:10.1021/ja901545q

2. Son, H. J.; Wang, W.; Xu, T.; Liang, Y.; Wu, Y.; Li, G.; Yu, L. *J. Am. Chem. Soc.* **2011,** *133,* 1885–1894. doi:10.1021/ja108601g
3. Stuart, A. C.; Tumbleston, J. R.; Zhou, H.; Li, W.; Liu, S.; Ade, H.; You, W. *J. Am. Chem. Soc.* **2013,** *135,* 1806–1815. doi:10.1021/ja309289u
4. Brooks, A. F.; Topczewski, J. J.; Ichiishi, N.; Sanford, M. S.; Scott, P. J. H. *Chem. Sci.* **2014,** *5,* 4545–4553. doi:10.1039/C4SC02099E
5. Jeschke, P. *ChemBioChem* **2004,** *5,* 570–589. doi:10.1002/cbic.200300833
6. Jeschke, P. *Pest Manage. Sci.* **2010,** *66,* 10–27. doi:10.1002/ps.1829
7. Chen, H.; Viel, S.; Ziarelli, F.; Peng, L. *Chem. Soc. Rev.* **2013,** *42,* 7971–7982. doi:10.1039/c3cs60129c
8. Marsh, E. N. G.; Suzuki, Y. *ACS Chem. Biol.* **2014,** *9,* 1242–1250. doi:10.1021/cb500111u
9. Wang, J.; Sánchez-Roselló, M.; Aceña, J. L.; del Pozo, C.; Sorochinsky, A. E.; Fustero, S.; Soloshonok, V. A.; Liu, H. *Chem. Rev.* **2014,** *114,* 2432–2506. doi:10.1021/cr4002879
10. Zhou, Y.; Wang, J.; Gu, Z.; Wang, S.; Zhu, W.; Aceña, J. L.; Soloshonok, V. A.; Izawa, K.; Liu, H. *Chem. Rev.* **2016,** *116,* 422–518. doi:10.1021/acs.chemrev.5b00392
11. Liang, T.; Neumann, C. N.; Ritter, T. *Angew. Chem., Int. Ed.* **2013,** *52,* 8214–8264. doi:10.1002/anie.201206566
12. Yerien, D. E.; Bonesi, S.; Postigo, A. *Org. Biomol. Chem.* **2016,** *14,* 8398–8427. doi:10.1039/c6ob00764c
13. Yang, X.; Wu, T.; Phipps, R. J.; Toste, F. D. *Chem. Rev.* **2015,** *115,* 826–870. doi:10.1021/cr500277b
14. Bizet, V.; Besset, T.; Ma, J.-A.; Cahard, D. *Curr. Top. Med. Chem.* **2014,** *14,* 901–940. doi:10.2174/1568026614666140202205531
15. Percy, J. M. Building Block Approaches to Aliphatic Organofluorine Compounds. In *Organofluorine Chemistry, Techniques and Synthons;* Chambers, R. D., Ed.; Topics in Current Chemistry, Vol. 193; Springer: Berlin, 1998; pp 131–195. doi:10.1007/3-540-69197-9_4
16. Ren, X.; Wan, W.; Jiang, H.; Hao, J. *Mini-Rev. Org. Chem.* **2007,** *4,* 330–337. doi:10.2174/157019307782411662
17. Zhu, S. Z.; Wang, Y. L.; Peng, W. M.; Song, L. P.; Jin, G. F. *Curr. Org. Chem.* **2002,** *6,* 1057–1096. doi:10.2174/1385272023373635
18. Wu, Y.; Hu, L.; Li, Z.; Deng, L. *Nature* **2015,** *523,* 445–450. doi:10.1038/nature14617
19. Kutovaya, I. V.; Shmatova, O. I.; Tkachuk, V. M.; Melnichenko, N. V.; Vovk, M. V.; Nenajdenko, V. G. *Eur. J. Org. Chem.* **2015,** 6749–6761. doi:10.1002/ejoc.201500898
20. Morisaki, K.; Sawa, M.; Yonesaki, R.; Morimoto, H.; Mashima, K.; Ohshima, T. *J. Am. Chem. Soc.* **2016,** *138,* 6194–6203. doi:10.1021/jacs.6b01590
21. Sanz-Vidal, Á.; Miró, J.; Sánchez-Roselló, M.; del Pozo, C.; Fustero, S. *J. Org. Chem.* **2016,** *81,* 6515–6524. doi:10.1021/acs.joc.6b01139
22. Miró, J.; Sánchez-Roselló, M.; González, J.; del Pozo, C.; Fustero, S. *Chem. – Eur. J.* **2015,** *21,* 5459–5466. doi:10.1002/chem.201406224
23. Han, X.; Wu, H.; Wang, W.; Dong, C.; Tien, P.; Wu, S.; Zhou, H.-B. *Org. Biomol. Chem.* **2014,** *12,* 8308–8317. doi:10.1039/C4OB01333F
24. Lou, H.; Wang, Y.; Jin, E.; Lin, X. *J. Org. Chem.* **2016,** *81,* 2019–2026. doi:10.1021/acs.joc.5b02848
25. Zhou, B.; Jiang, C.; Rao Gandi, V.; Lu, Y.; Hayashi, T. *Chem. – Eur. J.* **2016,** *22,* 13068–13071. doi:10.1002/chem.201603105
26. Zhou, D.; Huang, Z.; Yu, X.; Wang, Y.; Li, J.; Wang, W.; Xie, H. *Org. Lett.* **2015,** *17,* 5554–5557. doi:10.1021/acs.orglett.5b02668
27. Yang, L.-J.; Li, S.; Wang, S.; Nie, J.; Ma, J.-A. *J. Org. Chem.* **2014,** *79,* 3547–3557. doi:10.1021/jo500356t
28. Yuan, H.-N.; Li, S.; Nie, J.; Zheng, Y.; Ma, J.-A. *Chem. – Eur. J.* **2013,** *19,* 15856–15860. doi:10.1002/chem.201303307
29. Shmatova, O. I.; Shevchenko, N. E.; Balenkova, E. S.; Röschenthaler, G.-V.; Nenajdenko, V. G. *Eur. J. Org. Chem.* **2013,** *15,* 3049–3058. doi:10.1002/ejoc.201201725
30. Ricci, A.; Pettersen, D.; Bernardi, L.; Fini, F.; Fochi, M.; Herrera, R. P.; Sgarzani, V. *Adv. Synth. Catal.* **2007,** *349,* 1037–1040. doi:10.1002/adsc.200600536
31. Li, X.-J.; Xiong, H.-Y.; Hua, M.-Q.; Nie, J.; Zheng, Y.; Ma, J.-A. *Tetrahedron Lett.* **2012,** *53,* 2117–2120. doi:10.1016/j.tetlet.2012.02.053
32. Bae, H. Y.; Sim, J. H.; Lee, J.-W.; List, B.; Song, C. E. *Angew. Chem., Int. Ed.* **2013,** *52,* 12143–12147. doi:10.1002/anie.201306297
33. Jia, C.-M.; Zhang, H.-X.; Nie, J.; Ma, J.-A. *J. Org. Chem.* **2016,** *81,* 8561–8569. doi:10.1021/acs.joc.6b01750
34. Saadi, J.; Wennemers, H. *Nat. Chem.* **2016,** *8,* 276–280. doi:10.1038/nchem.2437
35. Bernardi, L.; Fochi, M.; Franchini, M. C.; Ricci, A. *Org. Biomol. Chem.* **2012,** *10,* 2911–2922. doi:10.1039/C2OB07037E
36. Nakamura, S. *Org. Biomol. Chem.* **2014,** *12,* 394–405. doi:10.1039/C3OB42161A
37. Sukach, V. A.; Tkachuk, V. M.; Shoba, V. M.; Pirozhenko, V. V.; Rusanov, E. B.; Chekotilo, A. A.; Röschenthaler, G.-V.; Vovk, M. V. *Eur. J. Org. Chem.* **2014,** 1452–1460. doi:10.1002/ejoc.201301542
38. Tkachuk, V. M.; Sukach, V. A.; Kovalchuk, K. V.; Vovk, M. V.; Nenajdenko, V. G. *Org. Biomol. Chem.* **2015,** *13,* 1420–1428. doi:10.1039/C4OB02233E
39. Sukach, V. A.; Resetnic, A. A.; Tkachuk, V. M.; Lin, Z.; Kortz, U.; Vovk, M. V.; Röschenthaler, G.-V. *Eur. J. Org. Chem.* **2015,** 1290–1301. doi:10.1002/ejoc.201403495
40. Midyana, G. G.; Makitra, R. G.; Pal'chikova, E. Y. *Russ. J. Gen. Chem.* **2010,** *80,* 944–947. doi:10.1134/S1070363210050142
41. Bew, S. P.; Stephenson, G. R.; Rouden, J.; Godemert, J.; Seylani, H.; Martinez-Lozano, L. A. *Chem. – Eur. J.* **2017,** *23,* 4557–4569. doi:10.1002/chem.201605148

License and Terms

BEILSTEIN JOURNAL OF ORGANIC CHEMISTRY

Electrophilic trifluoromethylselenolation of terminal alkynes with *Se*-(trifluoromethyl) 4-methylbenzenesulfonoselenoate

Clément Ghiazza[1], Anis Tlili[*1] and Thierry Billard[*1,2]

Full Research Paper

Open Access

Address:
[1]Institute of Chemistry and Biochemistry, Univ Lyon, Université Lyon 1, CNRS, 43 Bd du 11 novembre 1918, F-69622 Villeurbanne, France and [2]CERMEP-In vivo Imaging, Groupement Hospitalier Est, 59 Bd Pinel, F-69003 Lyon, France

Email:
Anis Tlili[*] - anis.tlili@univ-lyon1.fr; Thierry Billard[*] - Thierry.billard@univ-lyon1.fr

* Corresponding author

Keywords:
alkynes; nucleophilic addition; perfluoroalkylselenolation; *Se*-(trifluoromethyl) 4-methylbenzenesulfonoselenoate; trifluoromethylselenolation

Beilstein J. Org. Chem. **2017,** *13,* 2626–2630.
doi:10.3762/bjoc.13.260

Received: 22 September 2017
Accepted: 21 November 2017
Published: 07 December 2017

This article is part of the Thematic Series "Organo-fluorine chemistry IV".

Guest Editor: D. O'Hagan

Abstract

Herein the nucleophilic addition of *Se*-(trifluoromethyl) 4-methylbenzenesulfonoselenoate, a stable and easy-to-handle reagent, to alkynes is described. This reaction provides trifluoromethylselenylated vinyl sulfones with good results and the method was extended also to higher fluorinated homologs. The obtained compounds are valuable building blocks for further syntheses of fluoroalkylselenolated molecules.

Introduction

Over the last decades, fluorinated compounds have been the subject of growing interest [1,2]. The specific properties introduced by fluorinated groups have contributed to the "success story" of fluorinated molecules. Nowadays, fluorinated compounds find applications in various fields, from life sciences to materials [3-15]. In the objective to design new molecules with specific properties, novel fluorinated substituents have been developed, such as diverse trifluoromethylchalcogeno groups, due to their particular electronic properties [16] and, more especially, to their high lipophilicity [17]. Whereas the CF_3O and CF_3S substituents have been largely studied [18-23], the CF_3Se group, albeit known, has gained only little attention until recently. However, selenylated derivatives present pertinent properties and have found some interest in materials [24], life sciences [25-33] and drug design [34-37]. Furthermore, very recently, the Hansch lipophilicity parameter of CF_3Se has been determined (π_R = 1.29) – a high value lying between that of CF_3O and CF_3S [38]. Consequently, trifluoromethylselenolated molecules could represent interesting alternatives in the modulation of properties for various applications.

Despite such potential interest for CF_3Se compounds, methods to their syntheses remain still limited [39]. Direct trifluoromethylselenolation reactions have recently gained renewed

interest and mainly follow two strategies. The nucleophilic approach is based on the use of the CF_3Se^- anion which must be prepared from stoichiometric amounts of metallic selenium [40-53]. Concerning the electrophilic approach, two reagents, that are easy to obtain, have been described: CF_3SeCl [38,54-67] and CF_3SeTs [68].

Results and Discussion

Recently, we have described the electrophilic addition of CF_3SeCl to alkenes to access α-chloro-β-trifluoromethylselenolated molecules [65]. These products are particularly interesting because the presence of the chlorine substituent opens the way to post-functionalization and thereby to syntheses of more elaborated compounds. However, the similar reaction with alkynes has failed and only a complex mixture was observed which is basically due to the high reactivity of CF_3SeCl.

To overcome this issue, we have developed another easier-to-use reagent with a more controlled reactivity to perform electrophilic trifluoromethylselenolations, namely *Se*-(trifluoromethyl) 4-methylbenzenesulfonoselenoate (**1a**). This reagent is easily obtained by reacting sodium toluenesulfinate with in situ formed CF_3SeCl [68]. With this reagent at hand we envisaged the trifluoromethylselenolation of alkynes.

To our delight, the addition of **1a** to phenylacetylene (**2a**) at room temperature, without any other practical precautions, lead to the expected addition product **3a** with good yield (Scheme 1).

Subsequently, the reaction was extended to various arylalkynes and afforded, in general, good yields. Satisfactory to excellent results were observed whatever the electronic character (donor or acceptor) of the substituents on the phenyl moiety were. Even highly electron-withdrawing groups led to satisfactory yields of the products **3h**–**j**. The reaction is also not too sensitive to steric hindrance because good results were obtained also with *ortho*-substituted substrates **3c**,**e**,**i**. Nevertheless, the reaction with aliphatic alkyne **2k**, resulted in a low yield (28%).

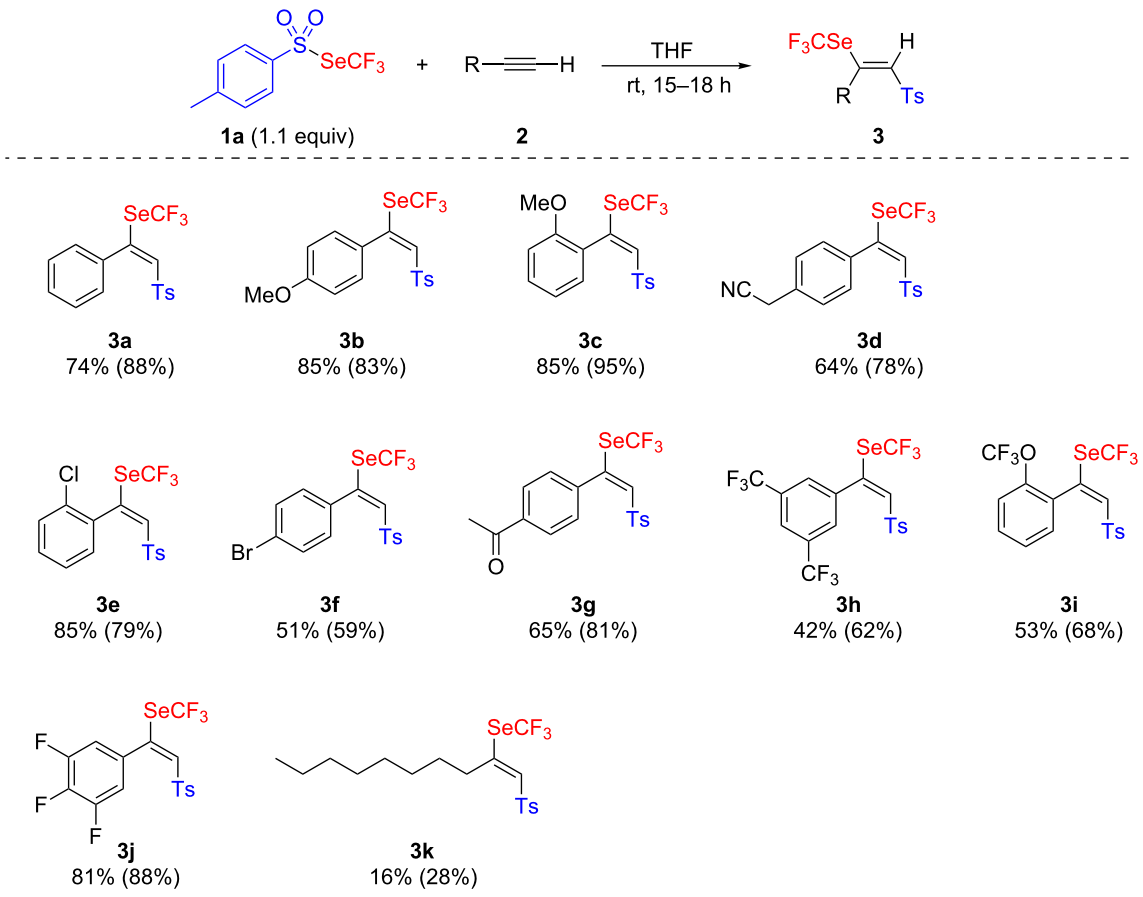

Scheme 1: Electrophilic addition of **1a** to alkynes. Yields shown are those of isolated products; yields determined by ^{19}F NMR spectroscopy with $PhOCF_3$ as an internal standard are shown in parentheses.

The reaction is stereoselective with the exclusive formation of the *trans*-isomers. Further, a high regioselectivity is observed but, surprisingly, the *anti*-Markovnikov regioisomers were obtained. The stereochemistry and regiochemistry were confirmed thanks to the X-ray structure of compound **3a** (Figure 1).

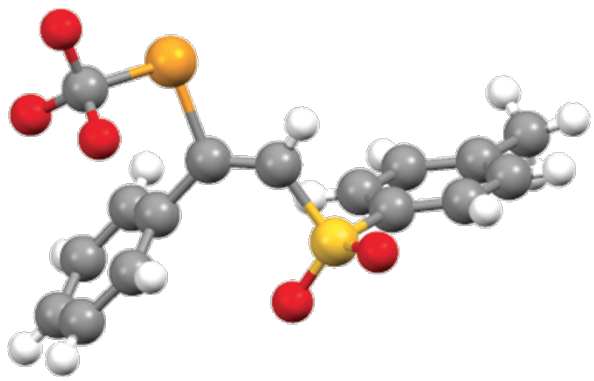

Figure 1: Single-crystal X-ray structure of **3a**.

From a mechanistic point of view, the reaction starts certainly with the intermediate formation of the trifluoromethylselenonium ion **I**. This is in accordance with the observed *trans*-selectivity due to the *anti* opening of **I** by the toluenesulfinate anion. The regioselectivity could be rationalized by the steric hindrance between the aromatic moiety and the large nucleophile (toluenesulfinate anion) which favors the attack on the less hindered side (Scheme 2, pathway a). Such sensitivity to steric hindrance of **I** was confirmed by the lack of reactions observed with internal alkynes.

Higher homologs of reagent **1a** are also available, the reaction was briefly performed with **1b** and **1c** (Scheme 3). The expected products were obtained with good yields. The tridecafluorohexylselenyl group in product **5a** makes this compound interesting because it opens the way to applications in the design of fluorinated polymers or surfactants.

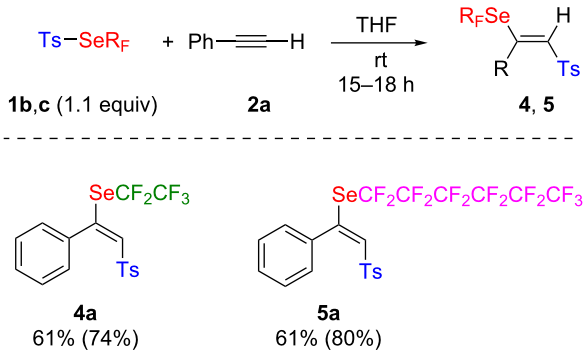

4a
61% (74%)

5a
61% (80%)

Scheme 3: Perfluoroalkylselenolation of alkynes. Yields shown are those of isolated products; yields determined by ^{19}F NMR spectroscopy with $PhOCF_3$ as an internal standard are shown in parentheses.

Conclusion

To conclude, *Se*-(trifluoromethyl) 4-methylbenzenesulfonoselenoate and *Se*-(perfluoroalkyl) 4-methylbenzenesulfonoselenoate have been confirmed as valuable bench-stable reagents to perform perfluoroalkylselenolations. Nucleophilic additions with alkynes to provide perfluoroalkylselenolated vinyl sulfones can easily be carried out. *Se*-(Trifluoromethyl) 4-methylbenzenesulfonoselenoate and *Se*-(perfluoroalkyl) 4-methylbenzenesulfonoselenoate constitute interesting building blocks for various applications.

Experimental

Typical procedure: To a flask equipped with a magnetic stir bar were added **1** (0.25 mmol, 1.1 equiv), alkyne **2** (0.23 mmol, 1.0 equiv), and anhydrous THF (1 mL). The reaction was stirred at 25 °C for 15–18 hours (conversion was checked by ^{19}F NMR with $PhOCF_3$ as internal standard). The crude residue was purified by chromatography to afford the desired products **3**–**5**.

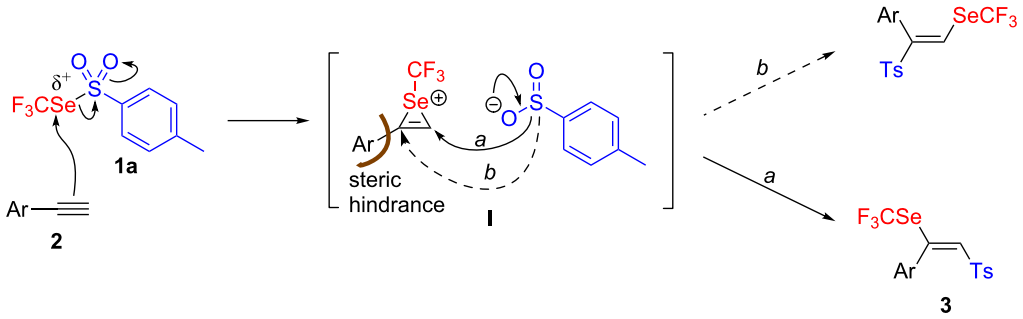

Scheme 2: Mechanism proposal.

Supporting Information

Supporting Information File 1

Additional experimental and analytical data and NMR spectra.
[http://www.beilstein-journals.org/bjoc/content/supplementary/1860-5397-13-260-S1.pdf]

Acknowledgements

Clément Ghiazza holds a doctoral fellowship from la Région Rhône Alpes. The authors are grateful to the CNRS and the French Ministry of Research for financial support. The French Fluorine Network is also acknowledged for its support. We thank Dr. Erwann Jeanneau (Centre de Diffractométrie Henri Longchambon) for collecting the crystallographic data and solving the structure of **3a**.

ORCID® iDs

Clément Ghiazza - https://orcid.org/0000-0002-1264-2559
Anis Tlili - https://orcid.org/0000-0002-3058-2043
Thierry Billard - https://orcid.org/0000-0002-2937-9523

References

1. Dolbier, W. R., Jr. *J. Fluorine Chem.* **2005,** *126,* 157–163. doi:10.1016/j.jfluchem.2004.09.033
2. Kirsch, P. Introduction. *Modern Fluoroorganic Chemistry,* 2nd ed.; Wiley-VCH: Weinheim, Germany, 2013; pp 1–24.
3. Becker, A. *Inventory of Industrial Fluoro-biochemicals;* Eyrolles: Paris, 1996.
4. Smart, B. E. *J. Fluorine Chem.* **2001,** *109,* 3–11. doi:10.1016/S0022-1139(01)00375-X
5. Hagmann, W. K. *J. Med. Chem.* **2008,** *51,* 4359–4369. doi:10.1021/jm800219f
6. Wang, J.; Sánchez-Roselló, M.; Aceña, J. L.; del Pozo, C.; Sorochinsky, A. E.; Fustero, S.; Soloshonok, V. A.; Liu, H. *Chem. Rev.* **2014,** *114,* 2432–2506. doi:10.1021/cr4002879
7. Gillis, E. P.; Eastman, K. J.; Hill, M. D.; Donnelly, D. J.; Meanwell, N. A. *J. Med. Chem.* **2015,** *58,* 8315–8359. doi:10.1021/acs.jmedchem.5b00258
8. Zhou, Y.; Wang, J.; Gu, Z.; Wang, S.; Zhu, W.; Aceña, J. L.; Soloshonok, V. A.; Izawa, K.; Liu, H. *Chem. Rev.* **2016,** *116,* 422–518. doi:10.1021/acs.chemrev.5b00392
9. Theodoridis, G. Chapter 4 Fluorine-Containing Agrochemicals: An Overview of Recent Developments. In *Advances in Fluorine Science;* Tressaud, A., Ed.; Elsevier: Amsterdam, 2006; Vol. 2, pp 121–175. doi:10.1016/S1872-0358(06)02004-5
10. Jeschke, P. *Pest Manage. Sci.* **2010,** *66,* 10–27. doi:10.1002/ps.1829
11. Fujiwara, T.; O'Hagan, D. *J. Fluorine Chem.* **2014,** *167,* 16–29. doi:10.1016/j.jfluchem.2014.06.014
12. Pagliaro, M.; Ciriminna, R. *J. Mater. Chem.* **2005,** *15,* 4981–4991. doi:10.1039/b507583c
13. Hird, M. *Chem. Soc. Rev.* **2007,** *36,* 2070–2095. doi:10.1039/b610738a
14. Chopra, D.; Row, T. N. G. *CrystEngComm* **2011,** *13,* 2175–2186. doi:10.1039/c0ce00538j
15. Berger, R.; Resnati, G.; Metrangolo, P.; Weber, E.; Hulliger, J. *Chem. Soc. Rev.* **2011,** *40,* 3496–3508. doi:10.1039/c0cs00221f
16. Hansch, C.; Leo, A.; Taft, R. W. *Chem. Rev.* **1991,** *91,* 165–195. doi:10.1021/cr00002a004
17. Leo, A.; Hansch, C.; Elkins, D. *Chem. Rev.* **1971,** *71,* 525–616. doi:10.1021/cr60274a001
18. Toulgoat, F.; Alazet, S.; Billard, T. *Eur. J. Org. Chem.* **2014,** 2415–2428. doi:10.1002/ejoc.201301857
19. Xu, X.-H.; Matsuzaki, K.; Shibata, N. *Chem. Rev.* **2015,** *115,* 731–764. doi:10.1021/cr500193b
20. Toulgoat, F.; Billard, T. Towards CF3S Group: From Trifluoromethylation of Sulfides to Direct Trifluoromethylthiolation. In *Modern Synthesis Processes and Reactivity of Fluorinated Compounds: Progress in Fluorine Science;* Groult, H.; Leroux, F.; Tressaud, A., Eds.; Elsevier Science: London, United Kingdom, 2017; pp 141–179. doi:10.1016/B978-0-12-803740-9.00006-8
21. Leroux, F. R.; Manteau, B.; Vors, J.-P.; Pazenok, S. *Beilstein J. Org. Chem.* **2008,** *4,* No. 13. doi:10.3762/bjoc.4.13
22. Besset, T.; Jubault, P.; Pannecoucke, X.; Poisson, T. *Org. Chem. Front.* **2016,** *3,* 1004–1010. doi:10.1039/C6QO00164E
23. Tlili, A.; Toulgoat, F.; Billard, T. *Angew. Chem.* **2016,** *128,* 11900–11909. doi:10.1002/ange.201603697
24. Romashov, L. V.; Ananikov, V. P. *Chem. – Eur. J.* **2013,** *19,* 17640–17660. doi:10.1002/chem.201302115
25. Wessjohann, L. A.; Schneider, A.; Abbas, M.; Brandt, W. *Biol. Chem.* **2007,** *388,* 997–1006. doi:10.1515/BC.2007.138
26. Bodnar, M.; Konieczka, P.; Namiesnik, J. *J. Environ. Sci. Health, Part C: Environ. Carcinog. Ecotoxicol. Rev.* **2012,** *30,* 225–252. doi:10.1080/10590501.2012.705164
27. Holben, D. H.; Smith, A. M. *J. Am. Diet. Assoc.* **1999,** *99,* 836–843. doi:10.1016/S0002-8223(99)00198-4
28. Brown, K. M.; Arhur, J. R. *Public Health Nutr.* **2001,** *4,* 593–599. doi:10.1079/PHN2001143
29. Kyriakopoulos, A.; Behne, D. *Rev. Physiol., Biochem. Pharmacol.* **2002,** *145,* 1–46. doi:10.1007/BFb0116430
30. Lu, J.; Holmgren, A. *J. Biol. Chem.* **2009,** *284,* 723–727. doi:10.1074/jbc.R800045200
31. Paculła, A. J.; Kaczor, K. B.; Wojtowicz, A.; Antosiewicz, J.; Janecka, A.; Długosz, A.; Janecki, T.; Ścianowski, J. *Bioorg. Med. Chem.* **2017,** *25,* 126–131. doi:10.1016/j.bmc.2016.10.018
32. Combs, G. F., Jr.; Gray, W. P. *Pharmacol. Ther.* **1998,** *79,* 179–192. doi:10.1016/S0163-7258(98)00014-X
33. Rayman, M. P. *Lancet* **2000,** *356,* 233–241. doi:10.1016/S0140-6736(00)02490-9
34. Abdulah, R.; Miyazaki, K.; Nakazawa, M.; Koyama, H. *J. Trace Elem. Med. Biol.* **2005,** *19,* 141–150. doi:10.1016/j.jtemb.2005.09.003
35. Angeli, A.; Tanini, D.; Viglianisi, C.; Panzella, L.; Capperucci, A.; Menichetti, S.; Supuran, C. T. *Bioorg. Med. Chem.* **2017,** *25,* 2518–2523. doi:10.1016/j.bmc.2017.03.013
36. Thangamani, S.; Younis, W.; Seleem, M. N. *Sci. Rep.* **2015,** *5,* No. 11596. doi:10.1038/srep11596
37. Singh, N.; Sharpley, A. L.; Emir, U. E.; Masaki, C.; Herzallah, M. M.; Gluck, M. A.; Sharp, T.; Harmer, C. J.; Vasudevan, S. R.; Cowen, P. J.; Churchill, G. C. *Neuropsychopharmacology* **2016,** *41,* 1768–1778. doi:10.1038/npp.2015.343
38. Glenadel, Q.; Ismalaj, E.; Billard, T. *Eur. J. Org. Chem.* **2017,** 530–533. doi:10.1002/ejoc.201601526

39. Zhang, C. *J. Chin. Chem. Soc.* **2017,** *64,* 457–463. doi:10.1002/jccs.201600861
40. Chen, C.; Ouyang, L.; Lin, Q.; Liu, Y.; Hou, C.; Yuan, Y.; Weng, Z. *Chem. – Eur. J.* **2014,** *20,* 657–661. doi:10.1002/chem.201303934
41. Rong, M.; Huang, R.; You, Y.; Weng, Z. *Tetrahedron* **2014,** *70,* 8872–8878. doi:10.1016/j.tet.2014.09.091
42. Zhu, P.; He, X.; Chen, X.; You, Y.; Yuan, Y.; Weng, Z. *Tetrahedron* **2014,** *70,* 672–677. doi:10.1016/j.tet.2013.11.093
43. Aufiero, M.; Sperger, T.; Tsang, A. S.-K.; Schoenebeck, F. *Angew. Chem.* **2015,** *127,* 10462–10466. doi:10.1002/ange.201503388
44. Hou, C.; Lin, X.; Huang, Y.; Chen, Z.; Weng, Z. *Synthesis* **2015,** *47,* 969–975. doi:10.1055/s-0034-1379972
45. Lefebvre, Q.; Pluta, R.; Rueping, M. *Chem. Commun.* **2015,** *51,* 4394–4397. doi:10.1039/C4CC10212F
46. Wang, Y.; You, Y.; Weng, Z. *Org. Chem. Front.* **2015,** *2,* 574–577. doi:10.1039/C5QO00045A
47. Wu, C.; Huang, Y.; Chen, Z.; Weng, Z. *Tetrahedron Lett.* **2015,** *56,* 3838–3841. doi:10.1016/j.tetlet.2015.04.088
48. Fang, W.-Y.; Dong, T.; Han, J.-B.; Zha, G.-F.; Zhang, C.-P. *Org. Biomol. Chem.* **2016,** *14,* 11502–11509. doi:10.1039/C6OB02107G
49. Matheis, C.; Krause, T.; Bragoni, V.; Goossen, L. J. *Chem. – Eur. J.* **2016,** *22,* 12270–12273. doi:10.1002/chem.201602730
50. Matheis, C.; Wagner, V.; Goossen, L. J. *Chem. – Eur. J.* **2016,** *22,* 79–82. doi:10.1002/chem.201503524
51. Tian, Q.; Weng, Z. *Chin. J. Chem.* **2016,** *34,* 505–510. doi:10.1002/cjoc.201600052
52. Wang, J.; Zhang, M.; Weng, Z. *J. Fluorine Chem.* **2017,** *193,* 24–32. doi:10.1016/j.jfluchem.2016.11.006
53. Dürr, A. B.; Fisher, H. C.; Kalvet, I.; Truong, K.-N.; Schoenebeck, F. *Angew. Chem., Int. Ed.* **2017,** *56,* 13431–13435. doi:10.1002/anie.201706423
54. Dale, J. W.; Emeléus, H. J.; Haszeldine, R. N. *J. Chem. Soc.* **1958,** 2939–2945. doi:10.1039/JR9580002939
55. Yarovenko, N. N.; Shemanina, V. N.; Gazieva, G. B. *Russ. J. Gen. Chem.* **1959,** *29,* 924–927.
56. Yagupol'skii, L. M.; Voloshchuk, V. G. *Russ. J. Gen. Chem.* **1966,** *36,* 173–174.
57. Voloshchuk, V. G.; Yagupol'skii, L. M.; Syrova, G. P.; Bystrov, V. P. *Russ. J. Gen. Chem.* **1967,** *37,* 105–108.
58. Yagupol'skii, L. M.; Voloshchuk, V. G. *Russ. J. Gen. Chem.* **1967,** *37,* 1463–1465.
59. Yagupol'skii, L. M.; Voloshchuk, V. G. *Russ. J. Gen. Chem.* **1968,** *38,* 2426–2429.
60. Marsden, C. J. *J. Fluorine Chem.* **1975,** *5,* 401–422. doi:10.1016/S0022-1139(00)82499-9
61. Haas, A.; Praas, H.-W. *Chem. Ber.* **1992,** *125,* 571–579. doi:10.1002/cber.19921250308
62. Magnier, E.; Vit, E.; Wakselman, C. *Synlett* **2001,** 1260–1262. doi:10.1055/s-2001-16050
63. Magnier, E.; Wakselman, C. *Collect. Czech. Chem. Commun.* **2002,** *67,* 1262–1266. doi:10.1135/cccc20021262
64. Glenadel, Q.; Ismalaj, E.; Billard, T. *J. Org. Chem.* **2016,** *81,* 8268–8275. doi:10.1021/acs.joc.6b01344
65. Ghiazza, C.; Glenadel, Q.; Tlili, A.; Billard, T. *Eur. J. Org. Chem.* **2017,** 3812–3814. doi:10.1002/ejoc.201700643
66. Ghiazza, C.; Tlili, A.; Billard, T. *Molecules* **2017,** *22,* 833–841. doi:10.3390/molecules22050833
67. Ghiazza, C.; Billard, T.; Tlili, A. *Chem. – Eur. J.* **2017,** *23,* 10013–10016. doi:10.1002/chem.201702028
68. Glenadel, Q.; Ghiazza, C.; Tlili, A.; Billard, T. *Adv. Synth. Catal.* **2017,** *359,* 3414–3420. doi:10.1002/adsc.201700904

License and Terms

BEILSTEIN JOURNAL OF ORGANIC CHEMISTRY

Recent progress in the racemic and enantioselective synthesis of monofluoroalkene-based dipeptide isosteres

Myriam Drouin and Jean-François Paquin*

Review

Open Access

Address:
Département de chimie, Université Laval, 1045 avenue de la Médecine, Pavillon Alexandre-Vachon, Québec (Québec) G1V 0A6, Canada

Email:
Jean-François Paquin* - jean-francois.paquin@chm.ulaval.ca

* Corresponding author

Keywords:
dipeptide isosteres; monofluoroalkene-based amide bonds; monofluoroalkenes; peptides; synthesis

Beilstein J. Org. Chem. **2017,** *13,* 2637–2658.
doi:10.3762/bjoc.13.262

Received: 27 September 2017
Accepted: 28 November 2017
Published: 12 December 2017

This article is part of the Thematic Series "Organo-fluorine chemistry IV".

Guest Editor: D. O'Hagan

Abstract

Monofluoroalkenes are fluorinated motifs that can be used to replace amide bonds. In order to be incorporated into peptides, it is normally necessary to first synthesize a dipeptide where the amide bond has been replaced with a monofluoroalkene. In that context, this review will present the racemic and enantioselective synthesis of monofluoroalkene-based dipeptide isosteres described since 2007. Some applications of those compounds will also be presented.

Introduction

Nowadays, the pharmaceutical industry is interested in the development of new categories of drugs. While small molecules were the principal targets in the last decades [1], larger biomolecules, such as peptides, are now widely studied [2,3]. The interest of these biopolymers originates, in part, from their high potency and selectivity towards the target, which results in a decrease of the toxicity and/or side effects. However, peptides have a poor metabolic stability [2].

A solution to enhance the stability of peptides is to modify their structure, in particular the amide bond linkage. Different moieties can be used as amide bond isosteres and some are illustrated in Figure 1 [4-6].

Of those amide bond isosteres, the monofluoroalkene is of particular interest as it possesses many relevant characteristics (Figure 2a). The resonance in the amide generates a double bond character between the carbon of the carbonyl and the nitrogen, which is responsible of the slow rotation around this bond. Furthermore, the negative charge is located on the oxygen atom and the dipole moment of the amide bond is 3.6 D [7]. The amide bond can also perform hydrogen bonds, with the oxygen atom as the hydrogen bond acceptor and N–H as hydrogen bond donor. This characteristic is important for the formation of secondary structures and folding into tertiary and quaternary structures. To have a good amide bond isostere, these different aspects should be reproduced, which is mostly the case

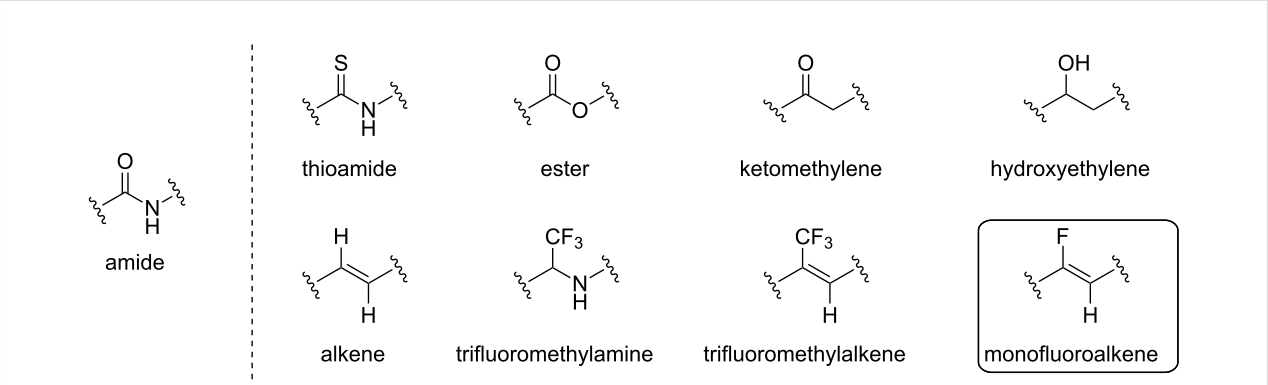

Figure 1: Selected amide bond isosteres.

with the monofluoroalkene moiety [8]. The monofluoroalkene is a rigid molecule as it possesses a double bond. Furthermore, the fluorine atom bears a partial negative charge, with a dipole moment of 1.4 D. Finally, the monofluoroalkene has the ability to accept a hydrogen bond through the fluorine atom [9]. Geometrically, the monofluoroalkene is quite similar to the amide bond. The C=O bond of the amide is 1.228 Å, compared to 1.376 Å for the C–F bond, and the C–N bond is 1.368 Å compared to 1.333 Å for the C=C bond [5,10-12]. Also, the amide structure is found in Nature as the s-*trans* or s-*cis* isomer, which can be in equilibrium (Figure 2b) [13]. However, most of the time it is found as the s-*trans* isomer to minimize steric interaction and to favour a linear and less hindered shape [14]. A notable exception is found in the case of the proline, where the s-*cis* isomer is favoured [15]. With the monofluoroalkene moiety, it is possible to mimic selectively one or the other isomer as no equilibrium exists between them. As such, the (*Z*)-monofluoroalkene is an analogue of the s-*trans* amide bond, while the (*E*)-monofluoroalkene mimics the s-*cis* form.

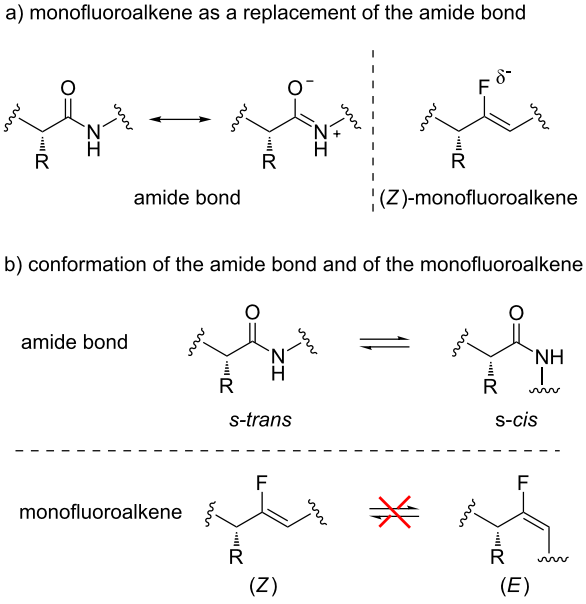

Figure 2: Monofluoroalkene as an amide bond isostere.

Considering those favourable properties, monofluoroalkenes constitute an interesting amide bond isostere, thus many researches have investigated their synthesis and application [16-22]. In order to be incorporated into peptides, it is normally necessary to first synthesize a dipeptide where the amide bond has been replaced with a monofluoroalkene. This review is the follow-up of the last one published by Taguchi and Yanai in 2009 which covered the literature until 2007 [5] and will discuss the new developments on the racemic and enantioselective synthesis of monofluoroalkene-based dipeptide isosteres from 2008 to September 2017. First, synthetic approaches to analogues in which there is no side chain or where the side chain stereochemistry is not controlled will be highlighted. This will be followed by the presentation of the synthesis of analogues where the side chain stereochemistry is controlled. In both cases, the review will be divided according to the monofluoroalkene-based dipeptide isosteres prepared. Finally, recent applications will be described.

Review

Analogues in which there is no side chain or where the side chain stereochemistry is not controlled

Gly-ψ[CF=CH]-Gly

The Gly-ψ[CF=CH]-Gly analogue is the simplest one, as it does not present side chains. Its synthesis was performed by two groups, using in both cases an olefination reaction. Sano's group was interested in the Horner–Wadsworth–Emmons (HWE) olefination to develop the synthesis of α-fluoro-α,β-

unsaturated ester **3**, which can be used as a precursor for the synthesis of monofluoroalkene-based dipeptide isosteres [23]. Cbz-Gly-ψ[(*Z*)-CF=CH]-Gly **5** was obtained in seven steps (Scheme 1). First, triethyl 2-fluoro-2-phosphonoacetate (**1**) was converted into the α-fluoro-α,β-unsaturated carbonyl **3** using the HWE olefination. The (*Z*)-isomer was obtained with complete selectivity. Then, reduction of the ester into the corresponding alcohol followed by a Mitsunobu reaction allowed the insertion of the NH-carboxybenzyl moiety to afford **4**. Finally, removal of the *tert*-butyldiphenylsilyl group using *tert*-*n*-butylammonium fluoride, followed by oxidation with the Jones reagent, provided the *C*-terminal carboxylic acid **5**.

In 2011, Lequeux and co-workers used rather the Julia–Kocienski olefination to access Phth-Gly-ψ[CF=CH]-Gly **9**, from benzothiazolyl fluoroaminosulfones (Scheme 2) [24,25]. The Julia–Kocienski olefination of 3-alkoxypropanal **7** with phthalimido sulfone **6** afforded the corresponding monofluoroalkene **8** as a (*Z*):(*E*) mixture (54:46). Removal of the benzyl group using titanium tetrachloride gave the free alcohol which was oxidized to provide the N-protected dipeptide isostere **9**. Some limitations were observed towards the compatibility of the N-protecting groups and in particular, *N*-*tert*-butoxycarbonyl-protected amines were not compatible with this methodology.

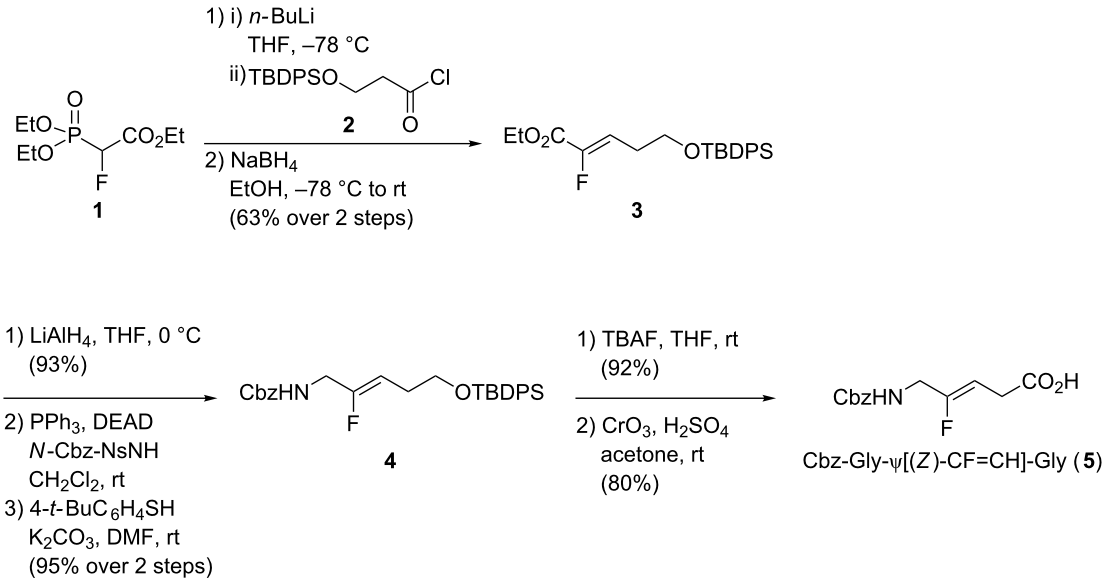

Scheme 1: Synthesis of Cbz-Gly-ψ[(Z)-CF=CH]-Gly using a HWE olefination by Sano and co-workers.

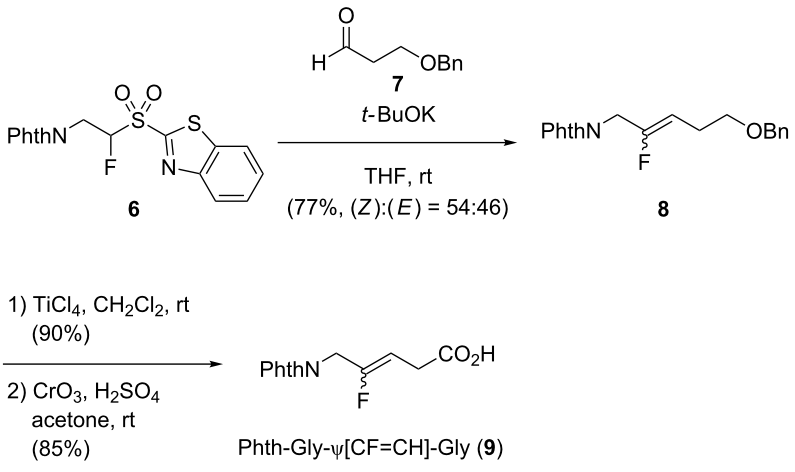

Scheme 2: Synthesis of Phth-Gly-ψ[CF=CH]-Gly using the Julia–Kocienski olefination by Lequeux and co-workers.

Xaa-ψ[CF=CH]-Gly

To access Xaa-ψ[CF=CH]-Gly isosteres, a S_N2' reaction upon 3,3-difluoropropene substrates can be used, as shown by Taguchi's group. The synthesis of monofluoroalkenes starting from 3,3-difluoropropenes and using trialkylaluminium reagents was developed. Using this methodology, they were able to prepare Boc-Nva-ψ[CF=CH]-Gly isostere [26] via a S_N2' reaction (Scheme 3). The defluorinative allylic alkylation of terminal 3,3-difluoropropene **10** with triethylaluminium selectively provided the corresponding (*Z*)-monofluoroalkene **11**. In this case, the use of Et_3Al allowed access to a norvaline (Nva) isostere. Then, alcohol **11** was converted into the trichloroimidate, and heating in xylenes permitted a [3,3]-sigmatropic rearrangement. At this stage, the trichloroimidate was transformed into an NHBoc moiety. Deprotection of the alcohol followed by Jones oxidation gave the final dipeptide isostere **13**.

Taguchi and co-workers proposed a variant of the defluorinative reaction using heteroatom nucleophiles using aluminum-based reagents such as Me_2AlCl and $(iPrO)_2AlN_3$, and (*Z*) selectivity was observed for the formation of the monofluoroalkene [27]. When dimethylaluminum chloride was used, the resulting allylic chloride reacted easily in a S_N2 reaction to give a more functionalized molecule. For example, treatment of the chlorinated monofluoroalkene with NaN_3 provided the corresponding N_3-containing monofluoroalkene. The azide group underwent a 1,3-dipolar cycloaddition to give a 1,2,3-triazole, which is also a peptide bond isostere [6]. Using this strategy, a mutant tripeptide containing two different peptide bond isosteres could be synthesized (Figure 3).

In 2016, Konno and co-workers developed a stereoselective chromium-mediated C–F bond cleavage followed by a C–C bond formation to access (*Z*)-monofluoroalkenes with excellent selectivity (Scheme 4) [28]. The chromium-mediated coupling of 1-bromo-4-(*tert*-butyldiphenylsiloxy)-1,1-difluorobutane (**15**) with aldehyde **16** led to the formation of monofluoroalkene **17**. This was then reacted with sodium azide and a further Staudinger reduction gave **18**. Boc protection of the resulting amine **18**, cleavage of the alcohol protecting group, Jones oxidation and formation of the methyl ester afforded the corresponding dipeptide isostere Boc-Ser(PMB)-ψ[(*Z*)-CF=CH]-Gly-OMe (**19**). In the same way, Boc-Val-ψ[(*Z*)-CF=CH]-Gly-OMe, Boc-Leu-ψ[(*Z*)-CF=CH]-Gly-OMe and Boc-Ala-ψ[(*Z*)-CF=CH]-Gly-OMe were prepared.

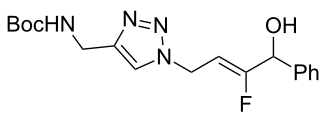

Figure 3: Mutant tripeptide containing two different peptide bond isosteres.

Xaa-ψ[CF=C]-Pro

The methodologies presented in the last decades used the olefination of cyclopentanone derivatives as the key step to access Xaa-ψ[CF=C]-Pro, via either a Peterson olefination or a HWE olefination [29-31]. In all cases, the selectivity was modest and the isomers had to be separated by flash chromatography. In 2014, Sano and co-workers reported a selective synthesis of Xaa-ψ[CF=C]-Pro with a new cyclopentanone derivative **20** bearing a bulky 2-(4-methyl-2,6,7-trioxabicyclo[2.2.2]octan-1-yl) group (OBO), which favoured the formation of the (*E*)-isomer in the HWE olefination (Scheme 5). The (*E*)-monofluoroalkene was thus obtained in an excellent selectivity using *n*-butyllithium in *tert*-butyl methyl ether. The resulting ester **21**

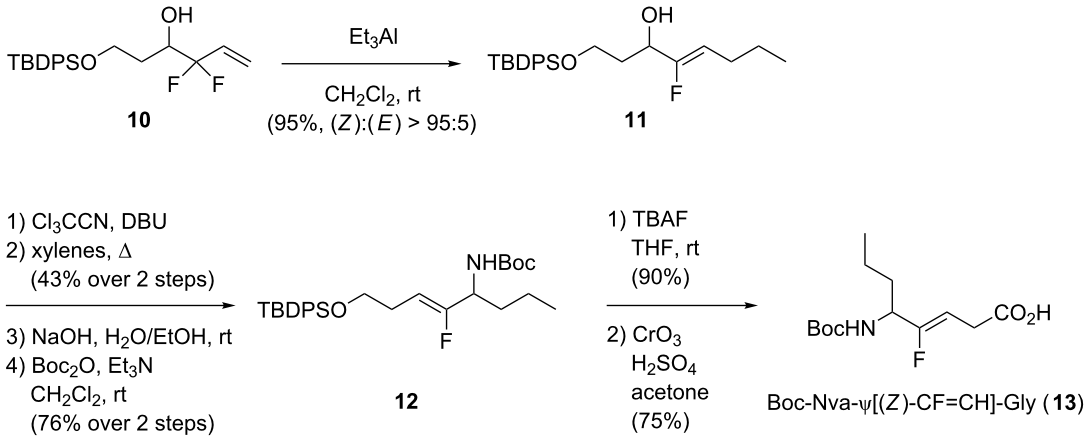

Scheme 3: Synthesis of Boc-Nva-ψ[(*Z*)-CF=CH]-Gly by Taguchi and co-workers.

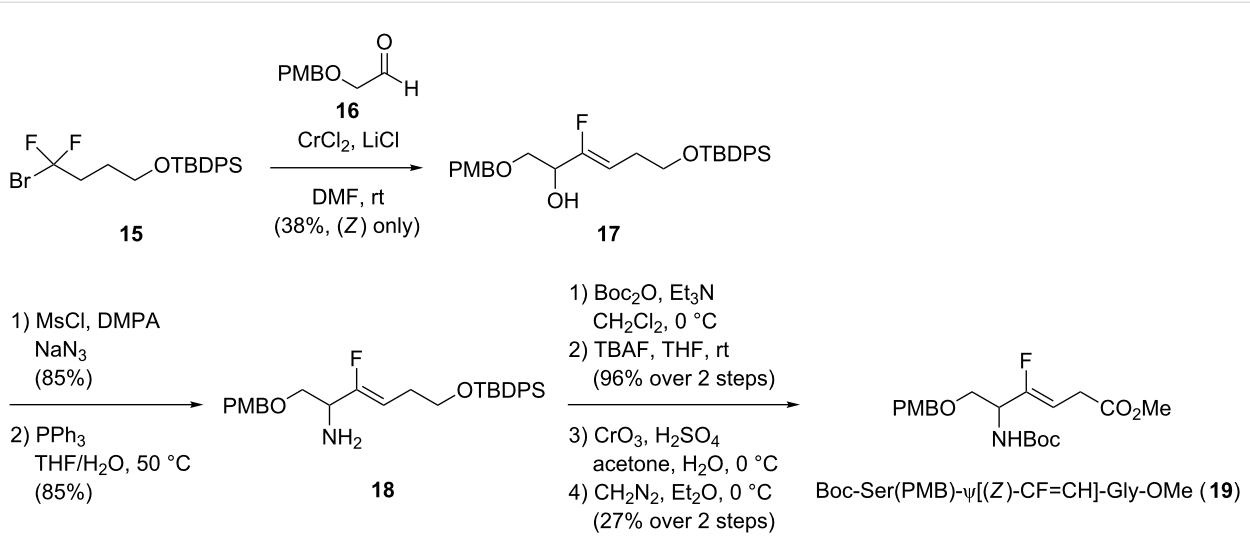

Scheme 4: Chromium-mediated synthesis of Boc-Ser(PMB)-ψ[(*Z*)-CF=CH]-Gly-OMe by Konno and co-workers.

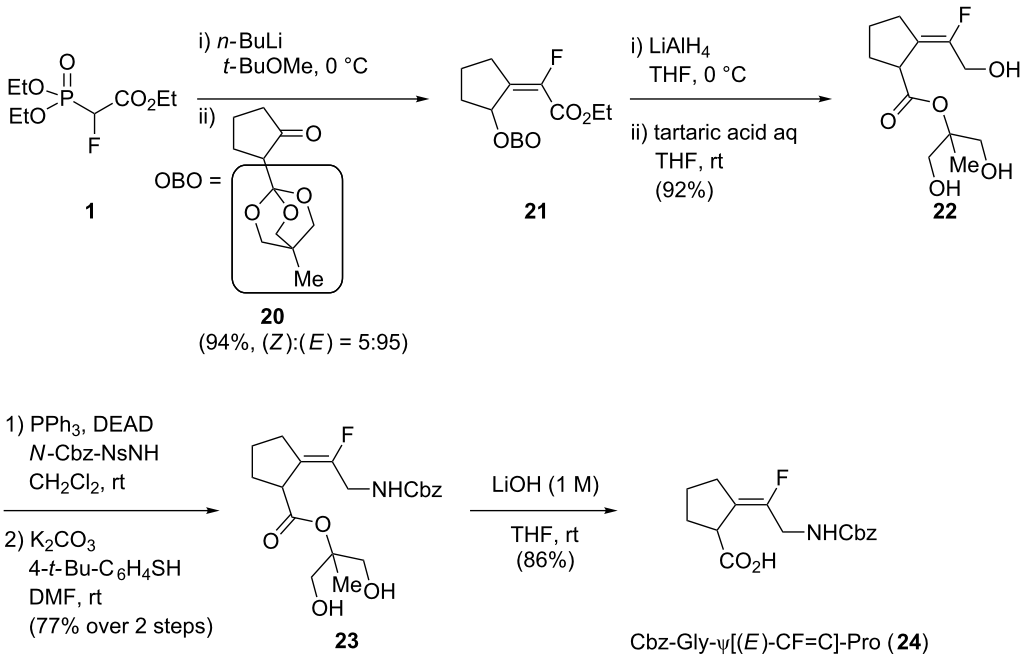

Scheme 5: Synthesis of Cbz-Gly-ψ[(*E*)-CF=C]-Pro by Sano and co-workers.

was reduced using lithium aluminum hydride, and treatment with tartaric acid deprotected the OBO, thus providing the free triol **22**. This was then converted into a protected amino group employing a Mitsunobu reaction. Finally, removal of the nosyl group, followed by hydrolysis using lithium hydroxide, afforded the targeted isostere **24**.

Sano and co-workers also worked on the Mg(II)-promoted stereoselective synthesis of (*Z*)-monofluoroalkenes (Scheme 6) [32,33]. HWE olefination promoted by Mg(II) of (diethoxyphosphoryl)fluoroacetic acid (**25**) with triisopropylsilyl-protected 2-hydroxymethylcyclopentanone **26** was realized with excellent yield and stereoselectivity. Esterification of the resulting carboxylic acid **27** into the corresponding methyl ester using trimethylsilyldiazomethane, followed by its reduction to the corresponding alcohol and a Mitsunobu reaction, permitted the incorporation of the N-terminal moiety. Then, removal of the Ns group of **28** and deprotection of the primary alcohol was

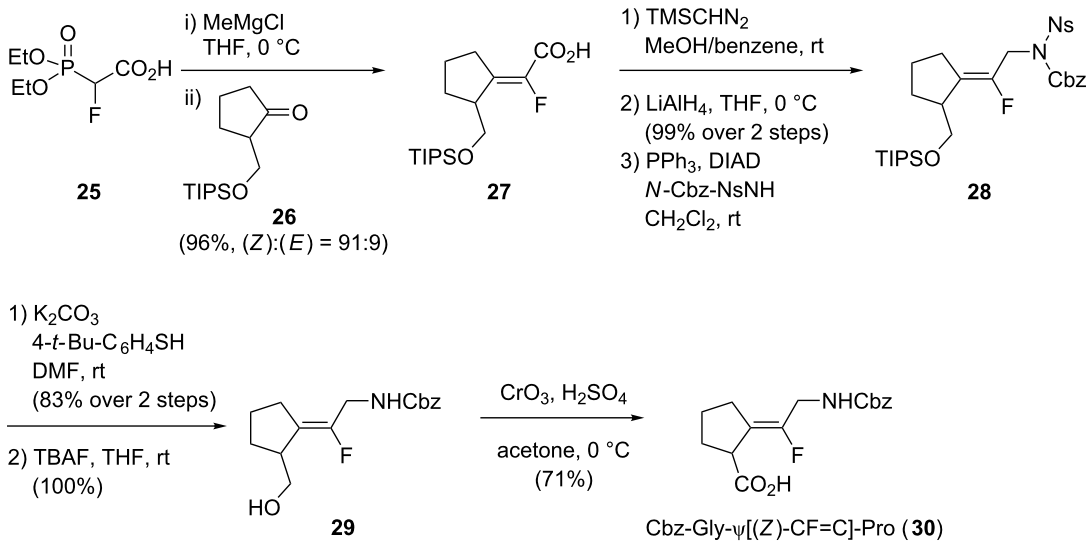

Scheme 6: Synthesis of Cbz-Gly-ψ[(*Z*)-CF=C]-Pro by Sano and co-workers.

performed to obtain **29** which underwent a Jones oxidation to give the final dipeptide isostere **30**.

Analogues in which the side chain stereochemistry is controlled

Gly-ψ[CF=CH]-Xaa

Different strategies have been used over the years to access Gly-ψ[CF=CH]-Xaa isosteres in which the side chain stereochemistry of the Xaa is controlled. This could be achieved using an olefination reaction, a metathesis reaction or a copper-mediated reduction of 3,3-difluoropropenes. Pannecoucke's group employed a chiral auxiliary, the Evans oxazolidinone, to prepare the non-racemic dipeptide isostere **35** (Scheme 7) [34]. Stereoselective alkoxymethylation on the oxazolidinone derivative **31** was first achieved with an excellent yield (88%) and diastereoselectivity (de > 95%). The chiral auxiliary was then removed and the free alcohol was oxidized to the corresponding aldehyde **32**. Alkene **33** was then obtained after olefination of **32** with low selectivity ((*Z*):(*E*) = 64:36). The resulting ester **33** was then reduced to the corresponding aldehyde, followed

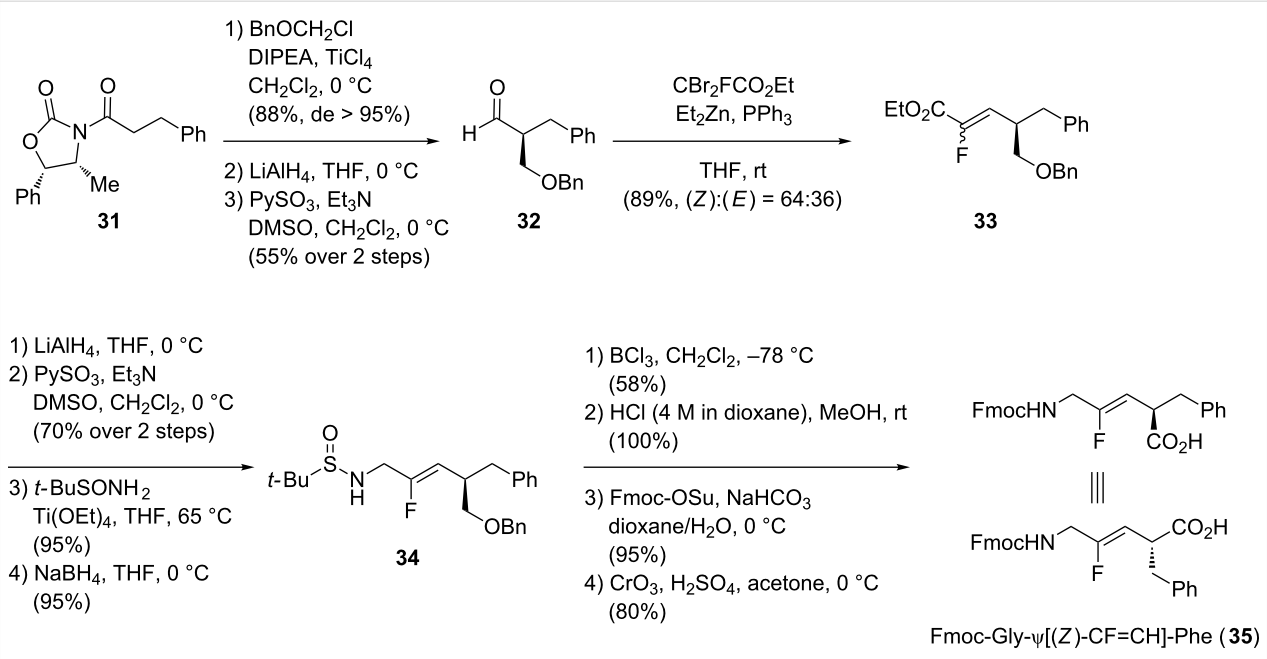

Scheme 7: Stereoselective synthesis of Fmoc-Gly-ψ[(*Z*)-CF=CH]-Phe by Pannecoucke and co-workers.

by the formation of the terminal imine and its subsequent reduction to access the N-terminal moiety of **34**. The alcohol and the amine deprotections were then achieved, followed by reprotection of the amine with a fluorenylmethyloxycarbonyl group. Oxidation of the remaining alcohol to the corresponding carboxylic acid provided the dipeptide isostere **35**.

Couve-Bonnaire and co-workers developed the preparation of (*E*)-monofluoroalkene dipeptide isosteres towards an intramolecular ring-closure metathesis (Scheme 8) [35]. The bis-alkene **36** underwent a ring-closure metathesis reaction in the presence of catalyst **37** under microwave irradiation to give lactam **38**. Deprotection of the amine followed by acidic opening of the ring gave the (*E*)-monofluoroalkene **39** in good yield. The reaction was also performed on the racemic starting material to confirm that the process did not induce any epimerization. This methodology was then extended to the synthesis Gly-ψ[(*E*)-CF=CH]-Gly (not shown).

Finally, Dory and co-workers reported the synthesis of Fmoc-Gly-ψ[(*Z*)-CF=CH]-Phe (Scheme 9) [36].Their work was inspired by the methodology reported by Fujii, Otaka and co-workers, which showed that the sultam moiety is a useful chiral auxiliary to control the stereochemistry during the incorporation of the lateral chain (see Scheme 15) [37]. The copper-mediated reduction of 3,3-difluoropropene **40** bearing a sultam (Xs) as a chiral auxiliary followed by α-alkylation afforded the monofluoroalkene **41**. Hydrolysis of the chiral auxiliary fol-

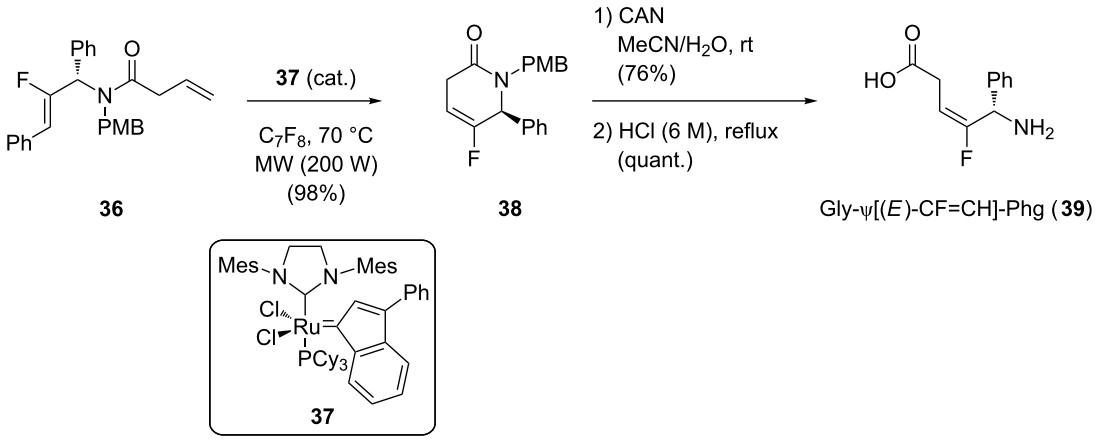

Scheme 8: Ring-closure metathesis to prepare Gly-ψ[(*E*)-CF=CH]-Phg by Couve-Bonnaire and co-workers.

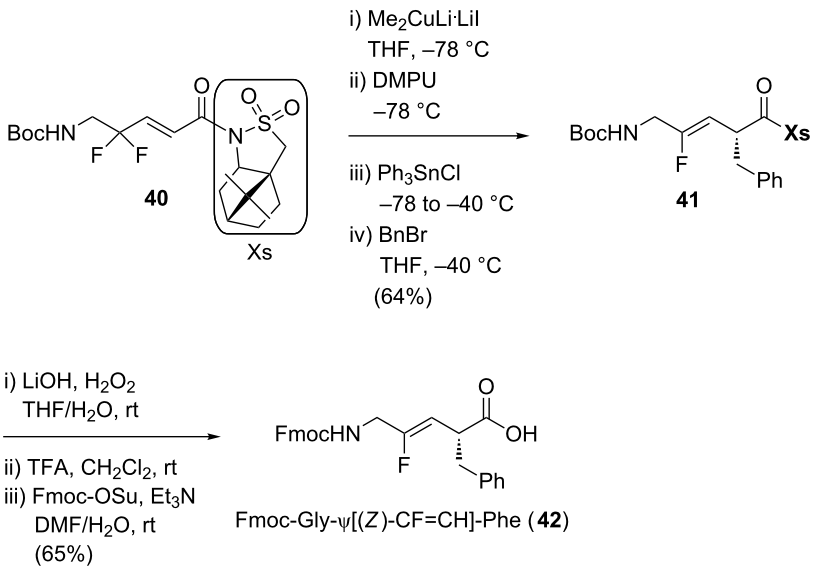

Scheme 9: Stereoselective synthesis of Fmoc-Gly-ψ[(*Z*)-CF=CH]-Phe by Dory and co-workers.

lowed by deprotection of the Boc-protected amine and its subsequent reprotection by a Fmoc group gave the final dipeptide isostere **42**.

Xaa-ψ[CF=CH]-Gly

The development of new methodologies to access Xaa-ψ[CF=CH]-Gly isosteres with control of the stereochemistry at the side chain will be discussed in this section. In particular, olefination reaction, defluorinative reduction of 3,3-difluoropropene derivatives and electrophilic fluorination of alkenylstannanes are presented. Pannecoucke's group described the synthesis of monofluoroalkenes from α-fluoro-α,β-unsaturated aldehydes **45**, which are more easily accessible than the corresponding enones (Scheme 10) [38]. Their synthesis started with the olefination of aldehyde **43** which gave the corresponding monofluoroalkene **44**. Reduction with subsequent oxidation of the ester gave the corresponding aldehyde **45** which was then transformed into the α-fluoroenimine **47**. This was selectively converted into the corresponding sulfinylamines using Grignard reagents to access (*S*)-amino acids **48**, while addition of organolithium reagents gave (*R*)-amino acids. A sequence of N- and O-deprotection, *N*-Fmoc-protection and oxidation to the carboxylic acid afforded the final Fmoc-Ala-ψ[(*Z*)-CF=CH]-Gly (**49**).

Then, it was discovered that the diastereoselectivity of the addition of the Grignard reagent on **47** was enhanced when dimethylzinc (Me_2Zn) was used as an additive (Table 1) [39]. Indeed, triorganozincates ($Me_2(R)ZnMgX$) were formed in situ and these reagents activated favourably the substrates towards the stereoselective addition of the alkyl chain.

To prepare Boc-Val-ψ[(*Z*)-CF=CH]-Gly-OEt, Otaka's group developed an intramolecular redox reaction of 3,3-difluoropropenes using N-heterocyclic carbenes (NHCs, Scheme 11) [40]. The reaction was first performed on the γ,γ-difluoro-α,β-enal **52** which was synthesized via a Wittig olefination of **50**. The resulting monofluoroalkene Boc-Val-ψ[(*Z*)-CF=CH]-Gly-OEt was obtained in good yield. Afterwards, the γ,γ-difluoro-α,β-enoylsilane **55**, obtained after HWE olefination using dimethyl phosphonoacylsilane **54**, was found to facilitate the NHC-catalyzed reduction and gave in this way the dipeptide isostere **56** in excellent yield.

The defluorinative reduction could also be performed using samarium iodide. Altman and co-workers proposed the synthesis of Boc-Tyr-ψ[(*Z*)-CF=CH]-Gly using a diastereoselective Reformatsky–Honda condensation, a (*E*)-selective HWE olefination and a SmI_2 reduction as key steps (Scheme 12) [41].

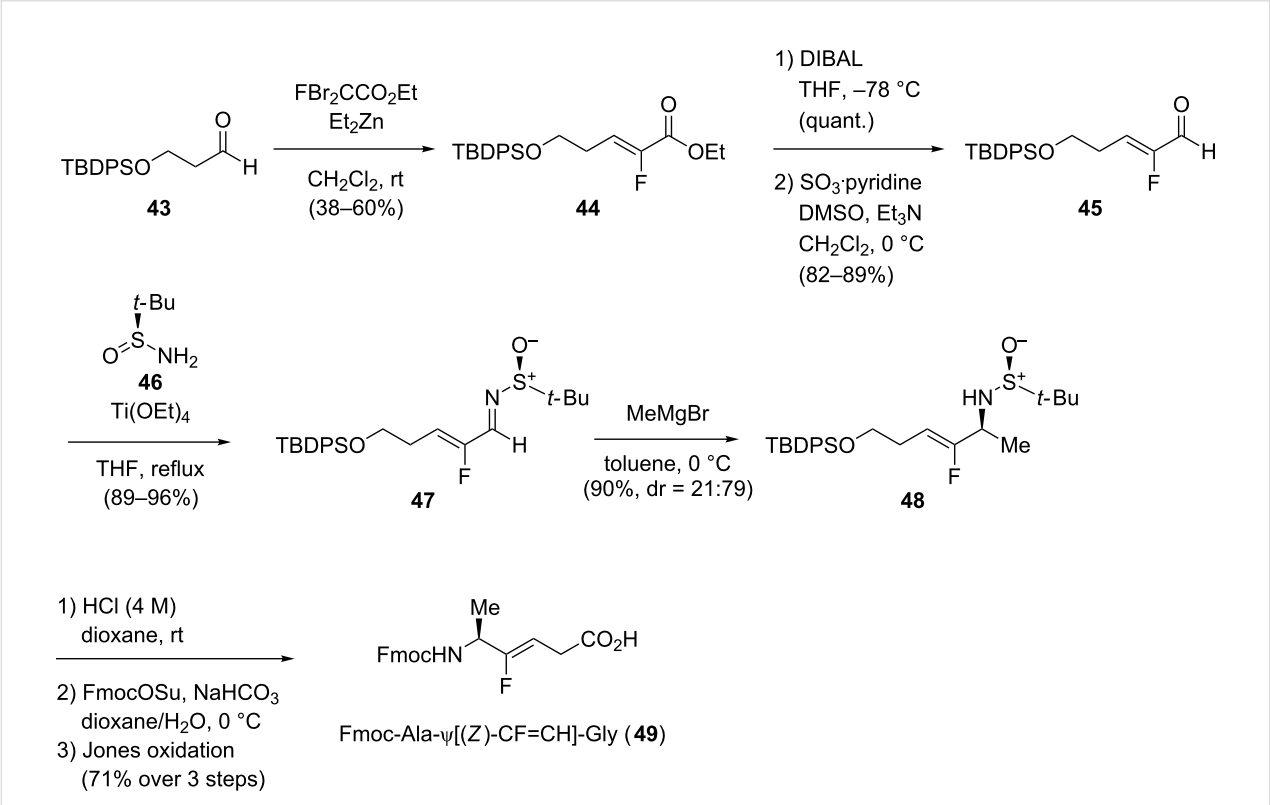

Scheme 10: Diastereoselective addition of Grignard reagents to sulfinylamines derived from α-fluoroenals by Pannecoucke and co-workers.

Table 1: Diastereoselective addition of Grignard reagents to sulfinylamines derived from α-fluoroenals with Me_2Zn as additive.

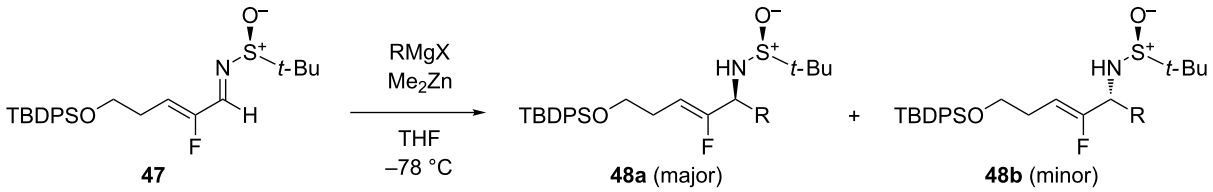

entry	RMgX	yield (%)	dr
1	iPrMgCl	63	93:7
2	iBuMgBr	75	98:2
3	BnMgCl	96	84:16
4	(allyl)MgBr	74	67:33
5	(vinyl)MgBr	98	91:9

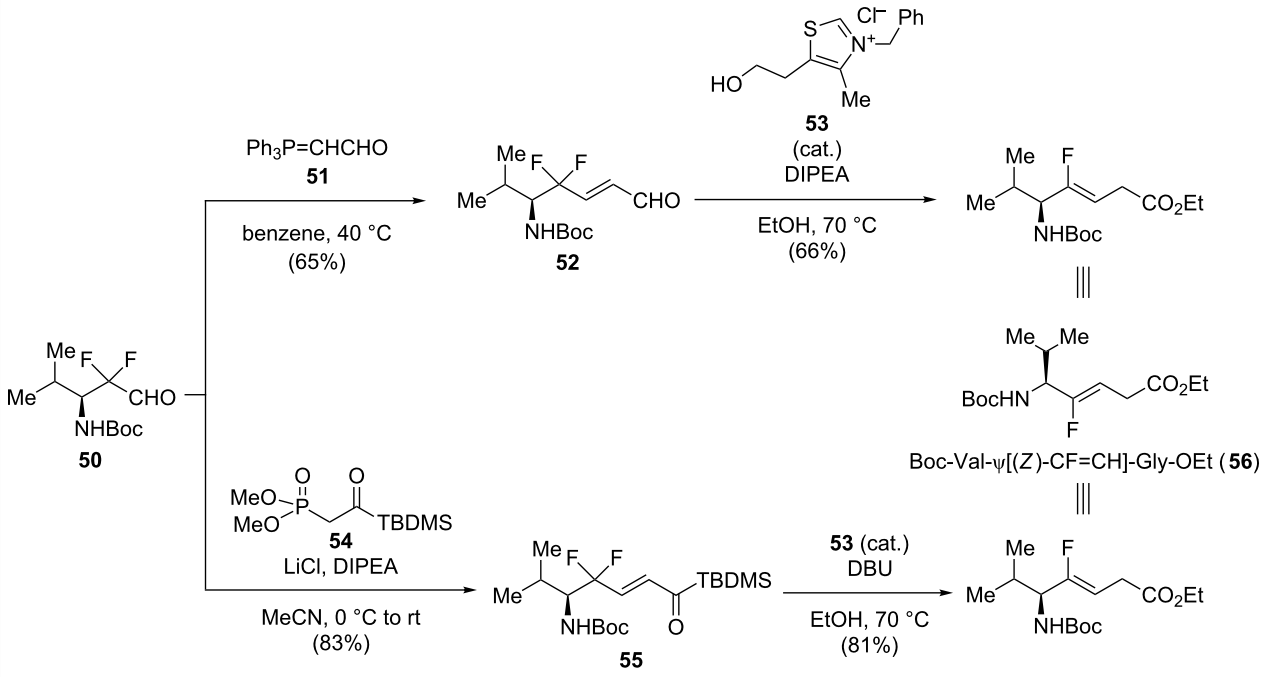

Scheme 11: NHC-mediated synthesis of monofluoroalkenes by Otaka and co-workers.

First, Reformatsky–Honda reaction of TIPS-protected phenylacetaldehyde **57** with the chiral auxiliary (*L*)-phenylglycine derivative **58** afforded **59**. Removal of the chiral auxiliary and subsequent Boc protection were then performed. Reduction of the ester followed by HWE olefination of the resulting aldehyde gave the 3,3-difluoropropene **60**. The latter was reduced in the presence of SmI_2 to furnish the (*Z*)-monofluoroalkene with good yield. A final saponification gave the monofluoroalkene-based dipeptide isostere **61**.

Finally, Fürstner's group developed the silver-mediated fluorination of functionalized alkenylstannanes to access monofluoroalkenes [42]. Hydrostannation of the N-protected ynamines **62** followed by electrophilic fluorination with Selectfluor gave the corresponding (*Z*)-monofluoroalkenes **64** in good yields (Table 2). The reported results showed that the methodology was suitable to replace an amide bond and could be used in late-stage fluorination to access monofluoroalkene-based dipeptide isosteres.

Xaa-ψ[CF=CH]-Xaa

The preparation of Xaa-ψ[CF-CH]-Xaa derivatives represents a synthetic challenge, as the stereochemistry of two side chains should be controlled during the synthesis. Here, the mono-

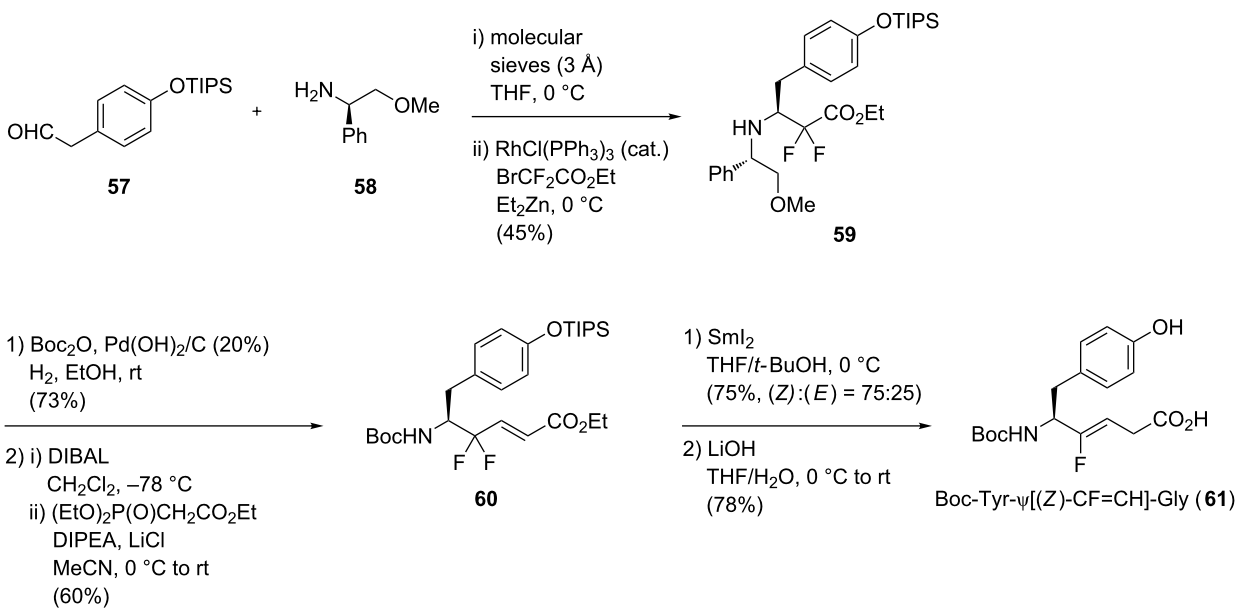

Scheme 12: Stereoselective synthesis of Boc-Tyr-ψ[(*Z*)-CF=CH]-Gly by Altman and co-workers.

Table 2: Silver-mediated fluorination of functionalized alkenylstannanes.

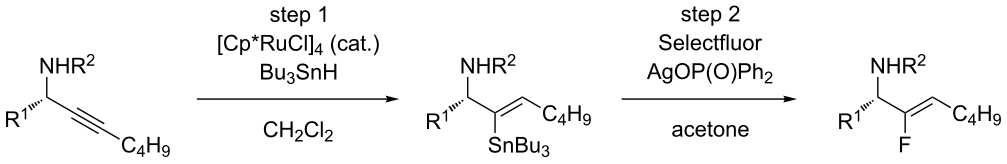

entry	R^1	R^2	yield (step 2, %)
1	iBu	Cbz	77
2	iBu	$P(O)(OPh)_2$	84
3	iBu	*t*-$BuSO_2$	81
4	iBu	Ns	54
5	iPr	Cbz	76
6	Ph	*t*-$BuSO_2$	76
7	Ph	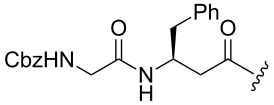	83

fluoroalkenes can be access either by an olefination reaction or a S_N2' reaction starting from 3,3-difluoropropenes. First, Miller reported the asymmetric synthesis of a monofluoroalkene using a chiral auxiliary (Scheme 13) [43]. The synthesis started with the alcohol protection of known compound **65** followed by chiral auxiliary removal and acylation of the resulting carboxylic acid. A HWE olefination was performed in two steps on **66** to give the (*Z*)-monofluoroalkene **67** as a single isomer (dr > 95:5). Conversion of the ester into the corresponding Weinreb amide, followed by addition of an organolithium reagent gave the corresponding ketone **69**. Four further steps gave the ring skeleton for the proline residue of **71**, i.e., formation of the chiral sulfinylimine, reduction into the corresponding sulfinylamine using DIBAL, deprotection of the terminal

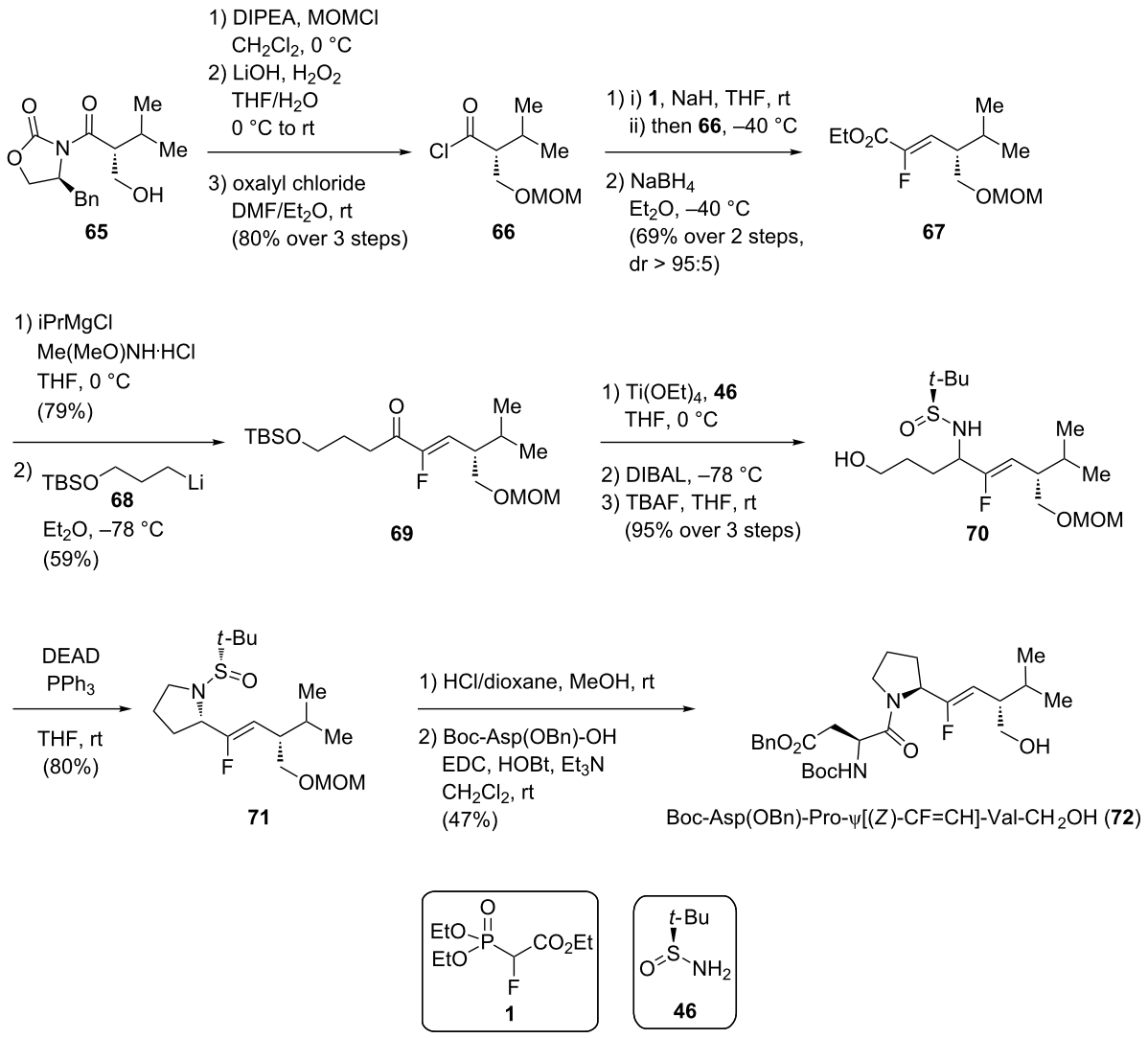

Scheme 13: Synthesis of the tripeptide Boc-Asp(OBn)-Pro-ψ[(*Z*)-CF=CH)-Val-CH_2OH by Miller and co-workers.

alcohol and Mitsunobu ring closure into the corresponding pyrrolidine derivative. Then, simultaneous deprotection of the amine and the alcohol in acidic conditions followed by coupling with Boc-Asp(OBn)-OH gave the final tripeptide isostere Boc-Asp(OBn)-Pro-ψ[(*Z*)-CF=CH)-Val-CH_2OH (**72**).

In the last years, Taguchi and co-workers described the synthesis of the monofluoroalkenes **74** by S_N2' reaction between 4,4-difluoro-5-hydroxyallylic alcohols **73** and Gilman reagent prepared in situ from trialkylaluminium reagents and CuLi (Scheme 14A) [44,45]. Even if the diastereoselectivity of the reaction was excellent, two problems remained. First, an excess of trialkylaluminium reagent and of copper had to be used. Second, trialkylaluminium reagents are not widely available. As an alternative, they proposed in 2011 a new synthetic route using Grignard reagents, which are widely available or can be easily synthetized in the laboratory (Scheme 14B) [46]. Unfortunately, these reagents did not react with the 4,4-difluoro-5-hydroxyallylic alcohols **73**. Terminal 3,3-difluoropropenes **76** were then prepared starting from the commercially available protected chiral hydroxyl ester **75**. Reduction to the aldehyde followed by coupling with bromodifluoropropene gave two diastereoisomers **76a** and **76b** separable by flash chromatography. Then, the copper-catalyzed defluorinative allylic alkylation using Grignard reagents was performed on **76a** and monofluoroalkenes **77** were obtained in good yields and high selectivity. Claisen rearrangement and further modifications (hydrolysis of the trichloroacetoamide, Boc protection of the free

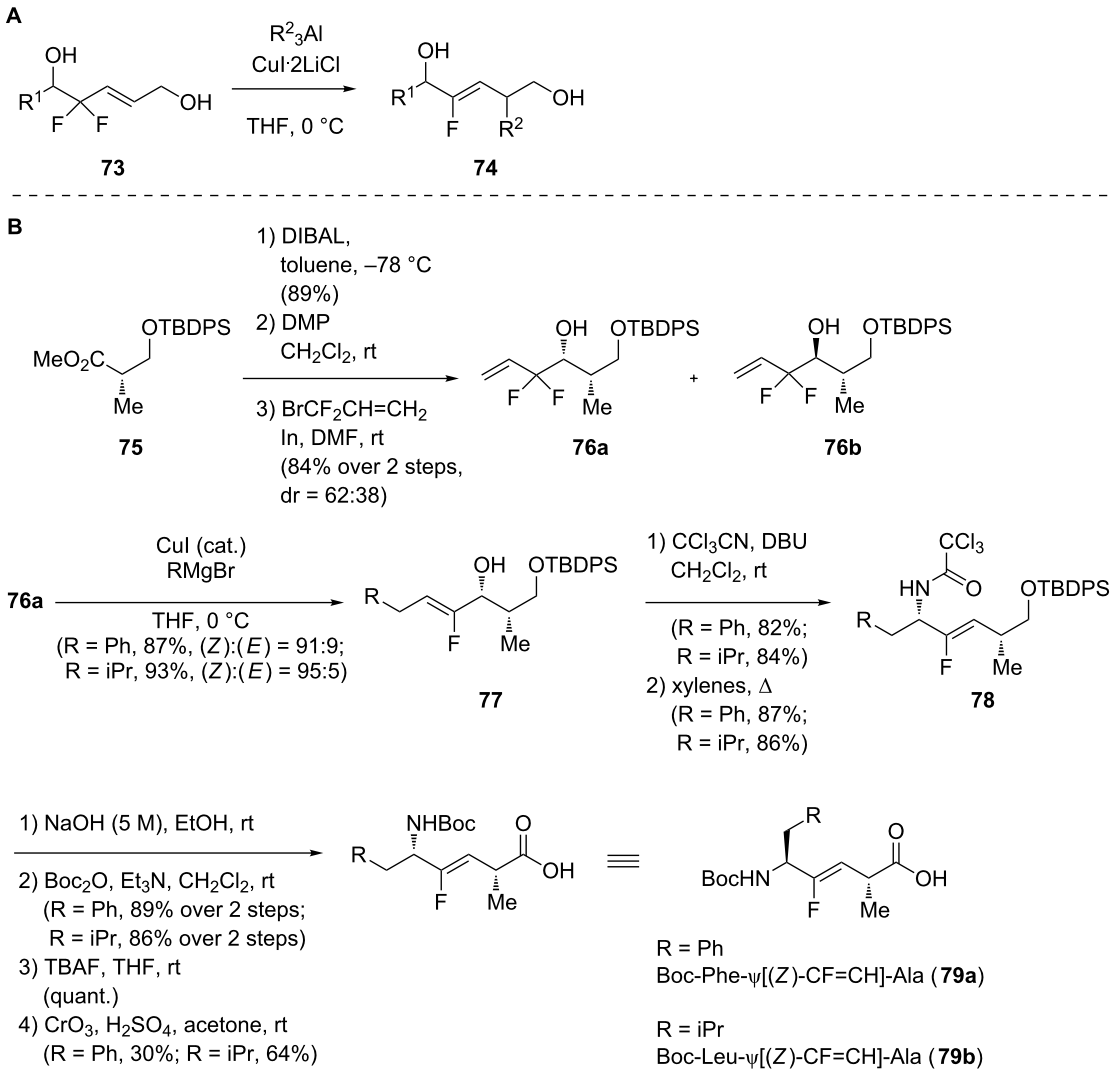

Scheme 14: Copper-catalyzed synthesis of monofluoralkenes by Taguchi and co-workers.

amine, deprotection of the alcohol and Jones oxidation to give the carboxylic acid) afforded the final dipeptide isosteres **79a** and **79b**.

The sultam Xs moiety has also been used as chiral auxiliary for the synthesis of Xaa-[CF=CH]-Xaa [37]. Otaka and co-workers developed a one-pot methodology to access amide isosteres at the *C*-terminal (Scheme 15) [47]. Cyanide-mediated reductive defluorination of γ,γ-difluoro-α,β-enoylsilane **80** in the presence of 18-crown-6 followed by addition of camphorsultam **81** gave the corresponding monofluoroalkene **82**. Then, α-alkylation of the amide with either allyl bromide or benzyl bromide provided the corresponding dipeptide isosteres **83a** and **83b**. Interestingly, different amino acids, such as H_2N-Gly-OEt, H_2N-Val-OMe and H_2N-Pro-OMe, could be used instead of the sultam **81** to access tripeptide isosteres in a racemic manner (not shown).

Fujii and co-workers also used the sultam Xs as a chiral auxiliary but started their synthesis with 3,3-difluoropropenes bearing a *N*-enoyl sultam moiety **84** instead. A 3-key step strategy involving a copper-mediated reduction, a transmetalation and an asymmetric alkylation was adopted for the preparation of monofluoroalkenes **85** (Scheme 16). After some synthetic modifications, Fmoc-Orn(Ns)-ψ[(*Z*)-CF=CH]-Orn(Ns) [48], Fmoc-Lys(Cbz)-ψ[(*Z*)-CF=CH]-Lys(Cbz) [49] and Fmoc-Orn(Ns)-ψ[(*Z*)-CF=CH]-Nal were obtained [50].

Fujii and co-workers also worked on the stereoselective synthesis of (*E*)-monofluoroalkenes (Scheme 17) [51]. To obtain a

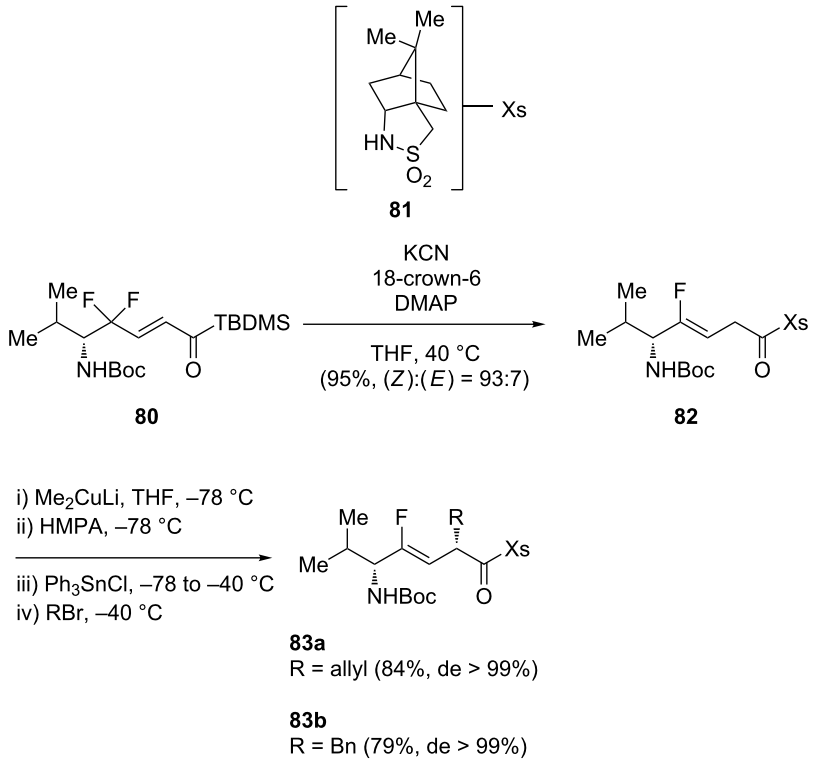

Scheme 15: One-pot intramolecular redox reaction to access amide-type isosteres by Otaka and co-workers.

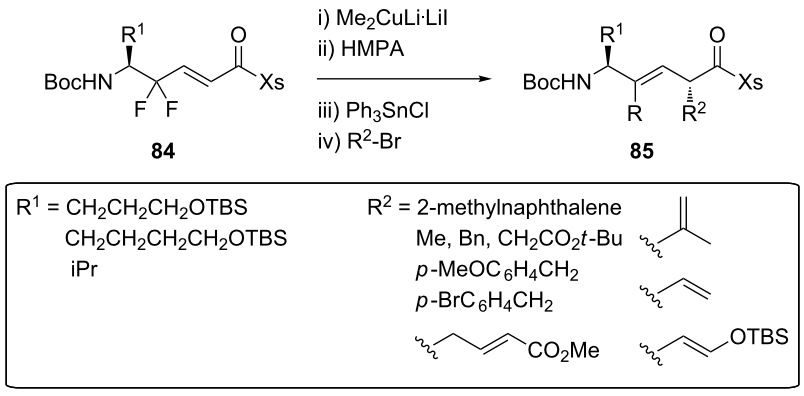

Scheme 16: Copper-mediated reduction, transmetalation and asymmetric alkylation by Fujii and co-workers.

good selectivity towards the (*E*)-alkene, they relied on the copper-mediated reduction and the α-alkylation on the γ,γ-difluoro-α,β-unsaturated δ-lactam **86**. Unfortunately, the α-alkylation provided a mixture of diastereoisomers **87a** and **87b** which was separable by flash chromatography. The dipeptide isostere **88** was finally obtained after the opening of the lactam **87b** in acidic conditions and *N*-Boc protection.

Xaa-ψ[CF=C]-Pro

The first asymmetric synthesis of Xaa-ψ[CF=C]-Pro was reported in 2012 by Chang's group with the synthesis of MeOCO-Val-ψ[(*Z*)-CF=C]-Pro **93** (Scheme 18) [52]. Their synthesis started with a stereoselective aldol reaction using (L)-threonine to furnish a chiral β-hydroxy cyclopentanone **90**. A HWE olefination converted **90** into (*Z*)-monofluoroalkene **91** without any

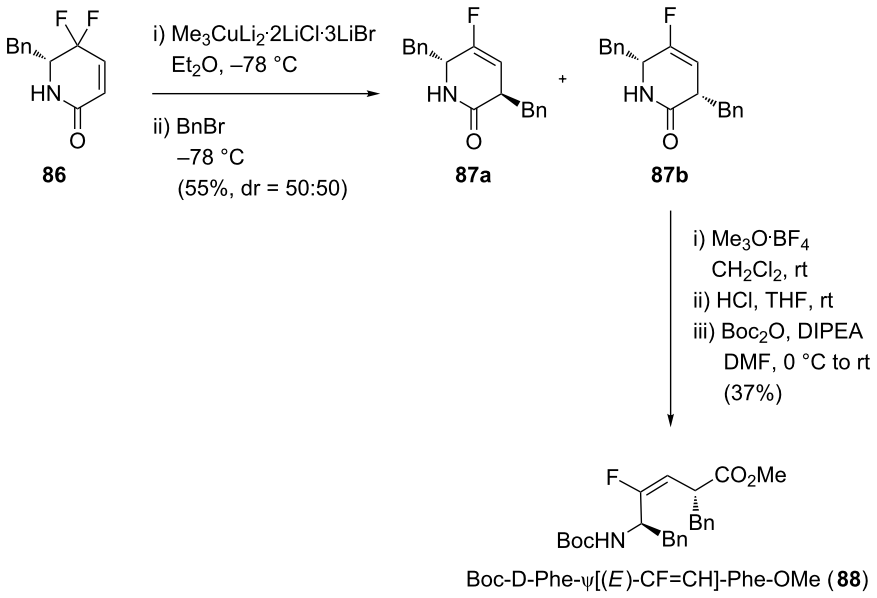

Scheme 17: Synthesis of (*E*)-monofluoroalkene-based dipeptide isostere by Fujii and co-workers.

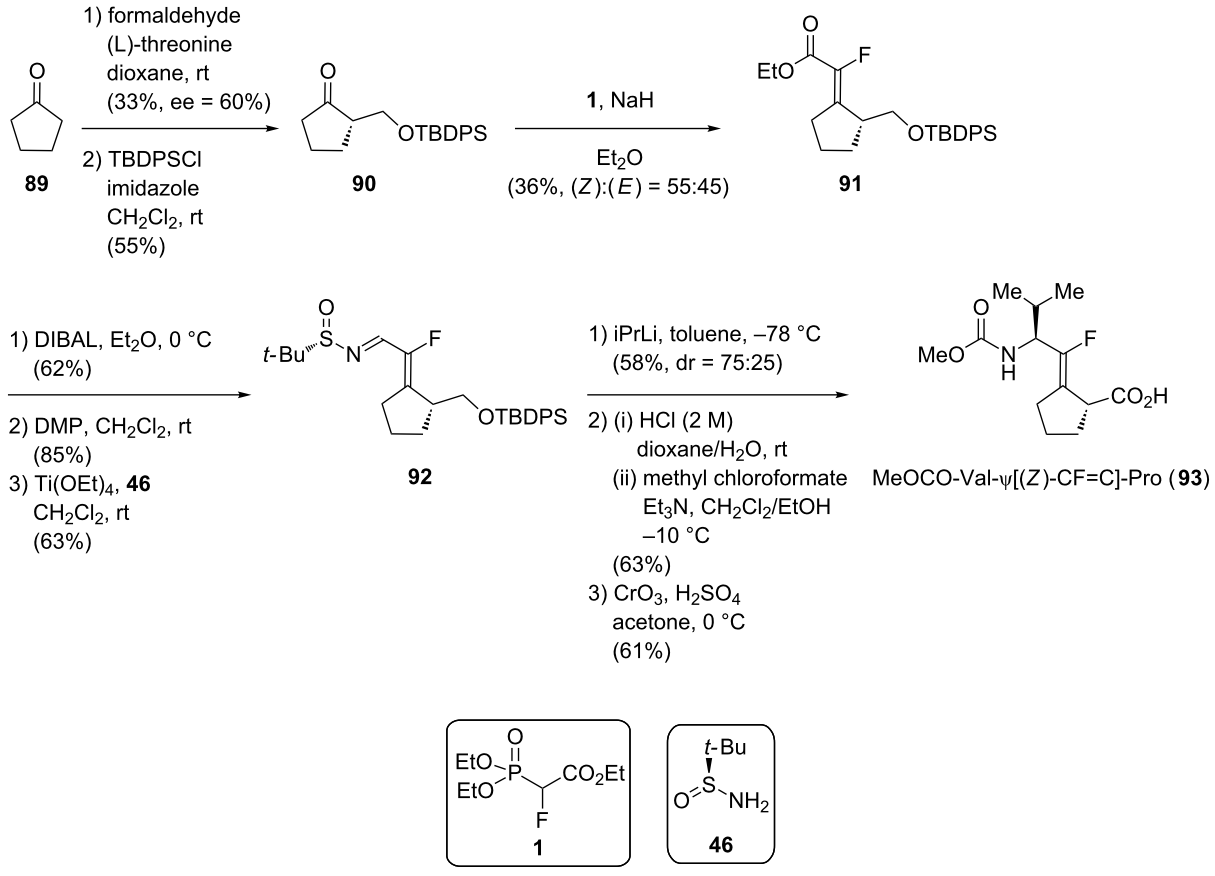

Scheme 18: Diastereoselective synthesis of MeOCO-Val-ψ[(*Z*)-CF=C]-Pro isostere by Chang and co-workers.

significant selectivity. The chiral Ellman's sulfinylimine **92** was obtained in 3 steps. The diastereoselective addition of isopropyllithium was then possible to afford the (L)-Leu residue with a moderate selectivity (dr = 75:25). Further modifications (removal of the sulfinyl group and the silyl protecting group in acidic conditions, transformation of the amine in methyl carbamate and oxidation of the primary alcohol into the corresponding carboxylic acid) gave the final isostere **93**.

In 2013, Pannecoucke and co-workers proposed a new strategy based on a chemoenzymatic reduction of ethyl 2-oxocyclopentanecarboxylate (**94**) using Baker's yeast to afford the corresponding chiral alcohol **95** (Scheme 19) [53]. Then, reduction of the ester into the primary alcohol, its selective protection by a silyl protecting group, oxidation of the secondary alcohol with pyridinium dichromate into the corresponding cyclopentanone derivative and subsequent olefination using CBr_3F gave the monofluoroalkene **96** with a modest selectivity towards the (*Z*)-alkene. A Negishi coupling then gave alkene **98**. Stereoselective reductive amination using a chiral sulfonamide as chiral auxiliary afforded **99** (de > 98:2). Finally, group manipulations, i.e., deprotection of the amine, Fmoc reprotection and oxidation gave the isostere **100**.

Then, Pannecoucke's group proposed a modified and more versatile approach where the monofluoroalkene **102** was synthesized by a HWE olefination of the chiral cyclopentanone **101** (Scheme 20) [54]. The resulting ester was converted into the

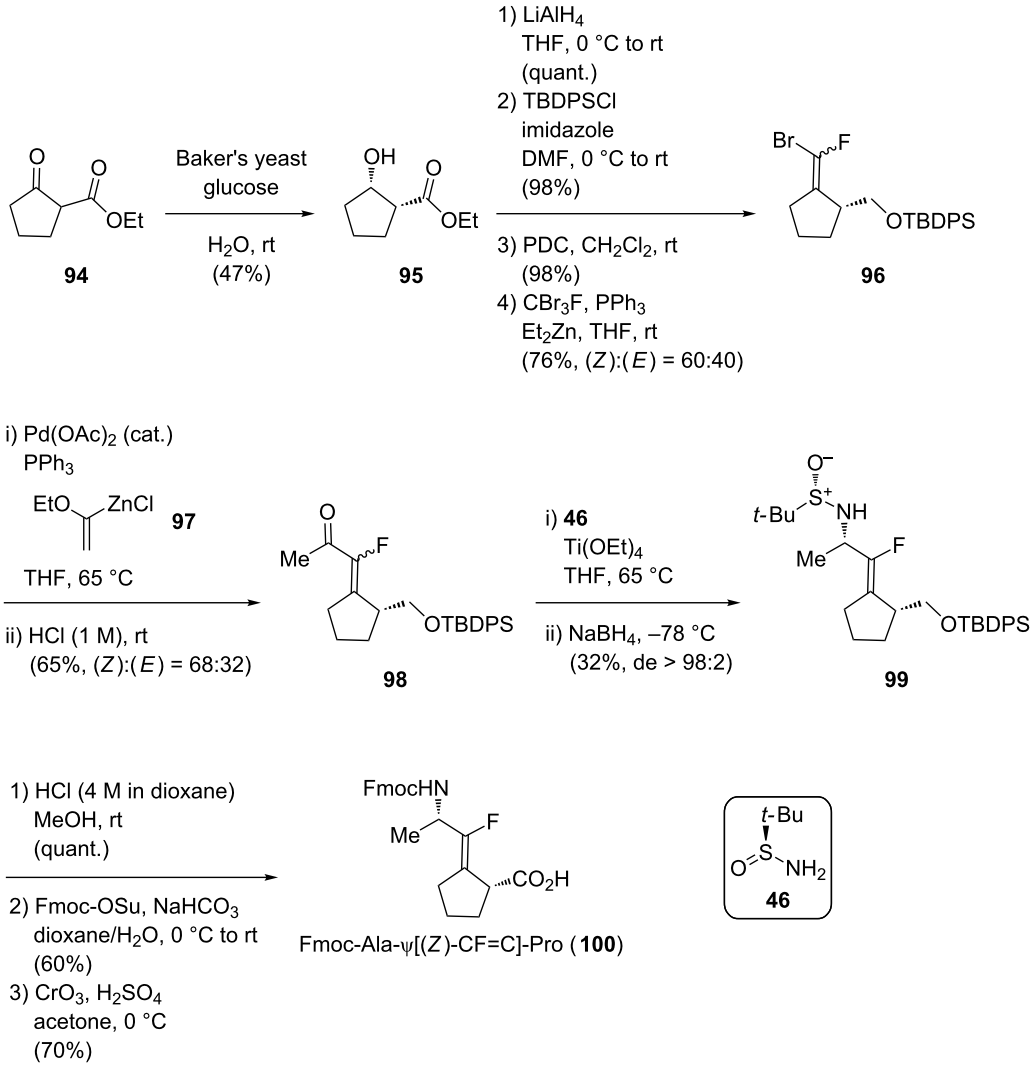

Scheme 19: Asymmetric synthesis of Fmoc-Ala-ψ[(*Z*)-CF=C]-Pro by Pannecoucke and co-workers.

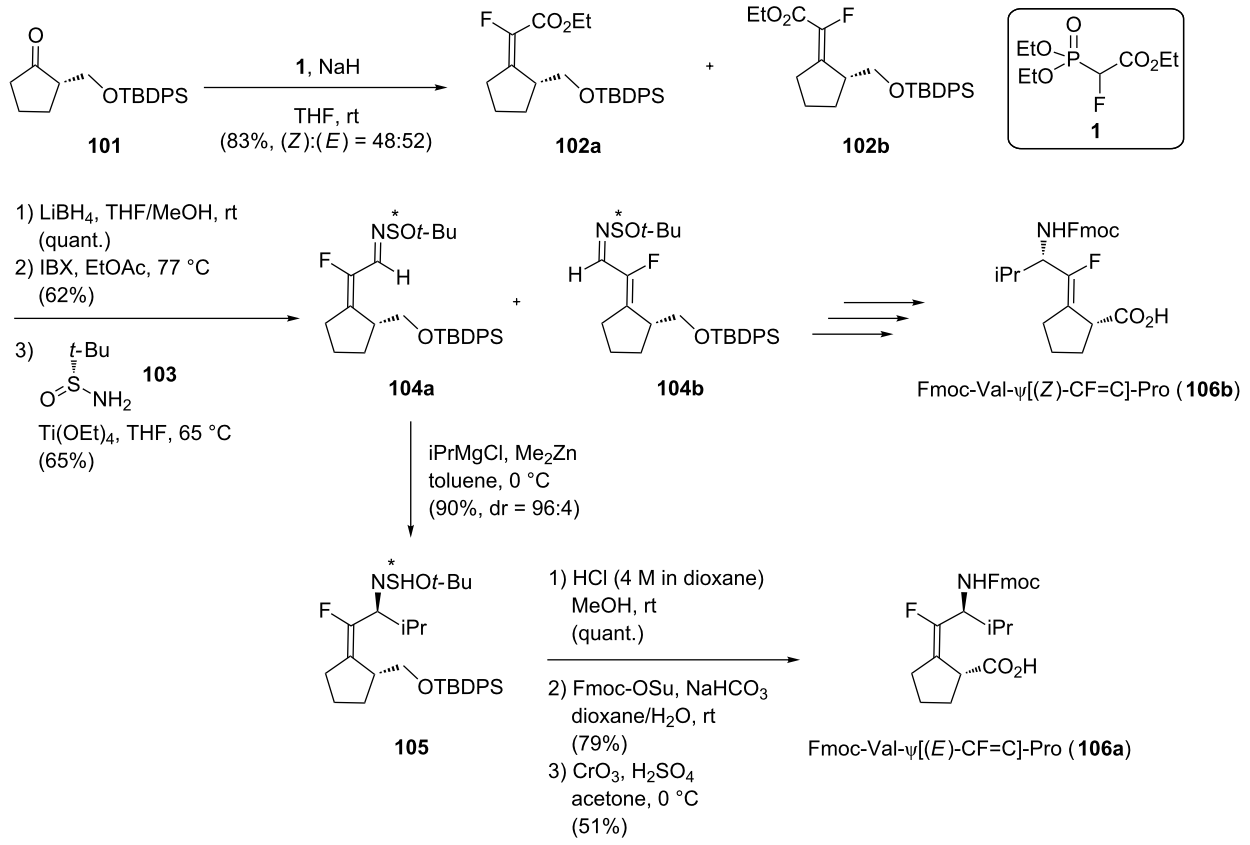

Scheme 20: Synthesis of Fmoc-Val-ψ[(*E*)-CF=C]-Pro by Pannecoucke and co-workers.

aldehyde and β-fluoroenimine **104** was obtained using Ellman's conditions. At this stage, the lateral chain of the N-terminal residue was added by an alkylation reaction using a Grignard reagent to give **105**. The last three steps (simultaneous deprotection of the amine and the alcohol in acidic conditions, Fmoc protection of the amine and oxidation of the alcohol into the corresponding carboxylic acid) led to the formation of three isosteres: Fmoc-Val-ψ[(*E*)-CF=C]-Pro (**106a**), Fmoc-Val-ψ[(*Z*)-CF=C]-Pro (**106b**) and Fmoc-Ala-ψ[(*Z*)-CF=C]-Pro.

Applications

In this section, recent applications of monofluoroalkene-based dipeptide isosteres will be briefly described.

Chang's group used the Val-ψ[(*Z*)-CF=C]-Pro isostere (see Scheme 18) to synthesize a fluorinated analogue of BMS-790052, which is a promising inhibitor of the non-structural protein NS5A, an interesting target of the chronic hepatitis C virus [52]. The monofluoroalkene replaced the amide group, and the use of a dipeptide isostere containing a proline residue favoured a γ-turn substructure which is necessary for the interaction with the NS5A protein. This fluorinated peptide isostere showed activity in the picomolar range against one genotype and did not exhibit any cytotoxicity (Figure 4).

Pannecoucke and co-workers synthesized three heptapeptides, Gly-Gly-ψ[(*Z*)-CF=CH]-Phe-Ser-Phe-Arg-Phe-NH_2, Gly-ψ[(*Z*)-CF=CH]-Gly-Phe-Ser-Phe-Arg-Phe-NH_2 and Gly-ψ[(*E*)-CF=CH]-Gly-Phe-Ser-Phe-Arg-Phe-NH_2 (see Scheme 7), representing the seven last amino acids of the neuropeptide 26Fra [34]. For the analogue containing the Gly-ψ[(*Z*)-CF=CH]-Phe isostere, epimerization was observed during last stages of the synthesis. The two diastereoisomers were separated after incorporation into the heptapeptide prior to biological studies, hence one had a D-Phe while the other had a L-Phe. The functional activity of the fluorinated mutants was evaluated by the calcium mobilizing response in GPR103-transfected cells. The peptides containing Gly-ψ[(*Z*)-CF=CH]-Gly or Gly-ψ[(*E*)-CF=CH]-Gly showed a higher activity than the non-fluorinated one, while an important decrease was observed for the peptides containing Gly-ψ[(*Z*)-CF=CH]-D-Phe and Gly-ψ[(*Z*)-CF=CH]-L-Phe (Table 3). These results underlined the

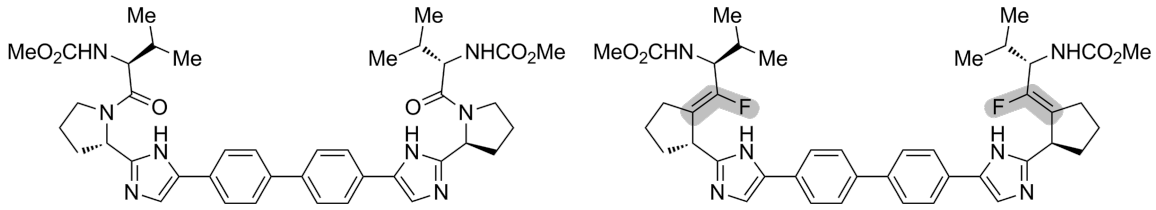

BMS-790052
EC_{50} genotype 1B = 0.009 nM
CC_{50} = 2 800 nM

fluorinated analogue
EC_{50} genotype 1B = 0.079 nM
CC_{50} = >10 000 nM

Figure 4: BMS-790052 and its fluorinated analogue.

Table 3: Activity towards the calcium mobilizing response in GPR103-transfected cells of different 26FRa analogues.

entry	pseudopeptides	EC_{50} (nM)
1	Gly-Gly-Phe-Ser-Phe-Arg-Phe-NH_2	(739 ± 149)
2	Gly-ψ[(*Z*)-CF=CH]-Gly-Phe-Ser-Phe-Arg-Phe-NH_2	(618 ± 104)
3	Gly-ψ[(*E*)-CF=CH]-Gly-Phe-Ser-Phe-Arg-Phe-NH_2	(538 ± 13)
4	Gly-Gly-ψ[(*Z*)-CF=CH]-D-Phe-Ser-Phe-Arg-Phe-NH_2	6752
5	Gly-Gly-ψ[(*Z*)-CF=CH]-L-Phe-Ser-Phe-Arg-Phe-NH_2	(1720 ± 1010)

importance of the Gly-Phe amide bond for the functional activity of the peptide. On the other hand, the fluorinated peptides showed a higher stability towards enzymatic degradation.

Fujii's group studied several applications of monofluoroalkene-based dipeptide isosteres. First, the affinity of the monofluoroalkene-based dipeptide isosteres Phe-ψ[(*Z*)-CF=CH]-Gly and Phe-ψ[(*E*)-CF=CH]-Gly for the peptide transporter PEPT1 was investigated (see Scheme 17) [51]. As the (*Z*)-monofluoroalkenes had a better bioactivity than the (*E*), the conclusion was that the transporter preferred the s-*trans* peptide bond. The K_i values obtained were also compared to the alkene analogues (Table 4).

Comparison between Phe-ψ[(*Z*)-CF=CH]-Gly and Phe-ψ[(*E*)-CF=CH]-Gly isosteres and their alkene analogues was also performed in an antagonist activity study towards GPR54. The fluorinated isosteres were incorporated into pentapeptides using Fmoc solid phase peptide synthesis (SPPS). Similar results as above were obtained in the sense that the activity of the s-*trans* peptide bond isostere was superior and that the fluorinated pseudopeptides were not more active than the natural peptide or the alkene-containing pseudopeptides (Figure 5) [55].

Fujii and co-workers also prepared, without isomerization or epimerization, cyclic pseudopeptides using Fmoc SPPS [48,50]. Biological studies were conducted on monofluoroalkene-containing analogues of FC131, which is a known antagonist of the chemokine receptor CXCR4. The latter has implications in cancer metastasis and HIV 1 infection. Anti-HIV 1 activity of the fluorinated antagonists showed an acceptable EC_{50} for the mutant containing Arg-ψ[(*Z*)-CF=CH]-Arg, while the one containing Arg-ψ[(*Z*)-CF=CH]-Nal (where NaI = L-3-(2-naphthyl)alanine) was not active (Table 5).

Finally, incorporation at different positions of the monofluoroalkene-based dipeptide isostere Lys-ψ[(*Z*)-CF=CH]-Lys into a fusion inhibitory peptide active against HIV 1, SC29EK, was investigated [49]. Weak to moderate anti-HIV activity was observed for the fluorinated analogues, but the potency was always lower than for SC29EK. This suggested than the H-bonding behaviour was important for the activity (Table 6). Conformational studies of the fluorinated peptide using circular dichroism also showed that the incorporation of the monofluoroalkene did not perturb the formation of the secondary structure of the peptide, which was a α-helix.

Dory and co-workers wanted to study the pentapeptide Leu-enkephaline, which can have analgesic properties when bounded to the DOPr receptor [36]. In order to study some derivative of the peptide, Fmoc-Gly-ψ[(*Z*-CF=CH]-Phe was synthesized (see Scheme 9). Using Fmoc SPPS, the fluorinated

Table 4: K_i values of Phe-Gly and analogues based on inhibition of [^{3}H]Gly-Sar uptake by PEPT1 in Caco-2 cells.

entry	pseudopeptides	K_i (mM)
1	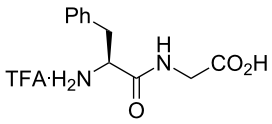	0.205
2	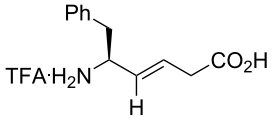	0.853
3	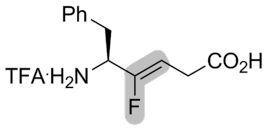	1.34
4	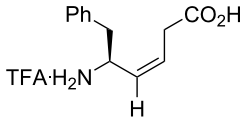	>10.0
5	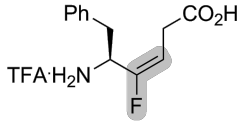	>10.0

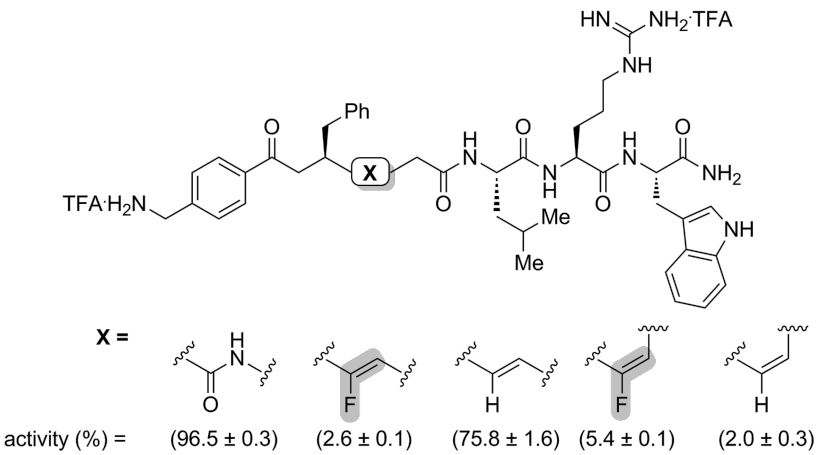

Figure 5: Bioactivities of pentapeptide analogues based on the relative maximum agonistic activity at 10 nM of the compound to 1 μM kisspeptin-10 (%). 100% = maximum agonistic activity at 1 μm kisspeptin-10.

mutant was incorporated in the sequence of the Leu-enkephaline to obtain Tyr-Gly-Gly-ψ[(*Z*)-CF=CH]-Phe-Leu. The fluorinated Leu-enkephaline presented a 6-fold decreased binding affinity towards the DOPr receptor that the non-fluorinated analogue, showing that a hydrogen bond acceptor is necessary at this position of the peptide (Figure 6). The fluorinated peptide also showed higher lipophilicity, which can improve its pharmacokinetic properties.

Altman and co-workers also studied a fluorinated mutant of the Leu-enkephaline [41]. The isostere Boc-Tyr-ψ[(*Z*)-CF=CH]-Gly (see Scheme 12) was coupled to a tripeptide to afford Boc-Tyr-ψ[(*Z*)-CF=CH]-Gly-Gly-Phe-Leu. Then, the opioid activity was calculated towards the DOPr receptor and an EC_{50} in the nanomolar range was observed (Figure 7). Even if this value represented a 60-fold decrease compared to the non-fluorinated peptide, it showed that the fluorinated peptide binds to the re-

Table 5: Anti-HIV activities of FC131 and its fluorinated derivatives against three HIV strains.

entry	pseudopeptides	EC50 (μM)		
		NL4-3	IIIB	Ba-L
1	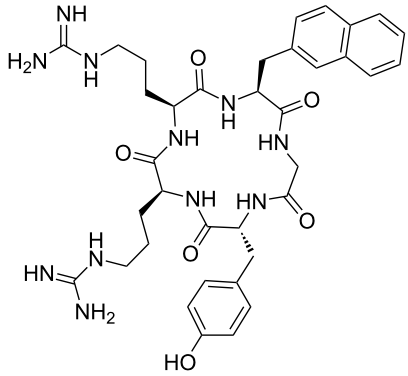	(0.014 ± 0.002)	(0.019 ± 0.003)	>10
2	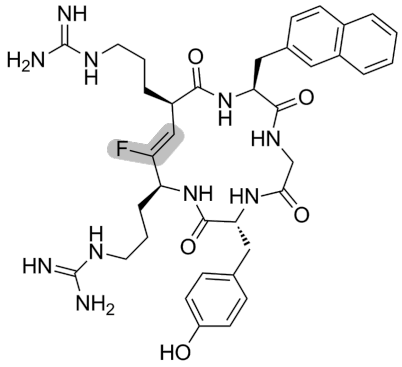	(0.332 ± 0.073)	(0.403 ± 0.051)	>10
3	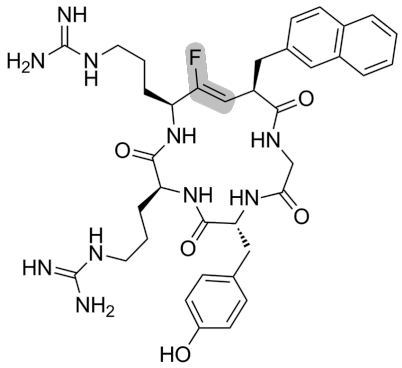	>10	>10	>10

Table 6: Anti-HIV activities of SC29EK and its fluorinated derivatives against three HIV strains. The number indicates the position of the dipeptide isostere.

entry	pseudopeptides	EC50 (nM)		
		NL4-3	IIIB	Ba-L
1	SC29EK	(2.2 ± 0.2)	(6.5 ± 0.9)	(1.9 ± 0.2)
2	SC29EK-6-Lys-ψ[(*Z*)-CF=CH]-Lys	(5220 ± 202)	>10 000	(5580 ± 1920)
3	SC29EK-13-Lys-ψ[(*Z*)-CF=CH]-Lys	(599 ± 96)	(3010 ± 554)	(600 ± 302)
4	SC29EK-20-Lys-ψ[(*Z*)-CF=CH]-Lys	(663 ± 242)	(2200 ± 712)	(527 ± 95)
5	SC29EK-27-Lys-ψ[(*Z*)-CF=CH]-Lys	(43 ± 7)	(237 ± 16)	(51 ± 7)

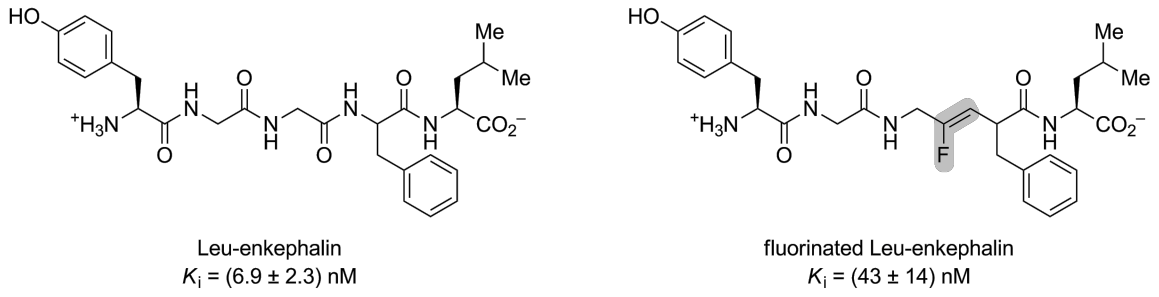

Figure 6: Structures and affinities of the Leu-enkephalin and its fluorinated analogue. The affinity towards DOPr was measured by competitive binding assays.

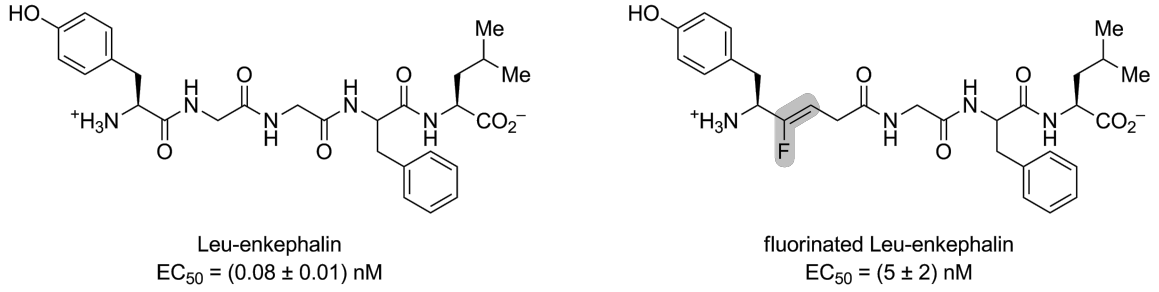

Figure 7: Activation of the opioid receptor DOPr by Leu-enkephaline and a fluorinated analogue.

ceptor and that the amide bond at this position was not necessary. Thus, Boc-Tyr-ψ[(*Z*)-CF=CH]-Gly-Gly-Phe-Leu is shown to be a better isostere than Tyr-Gly-Gly-ψ[(*Z*)-CF=CH]-Phe-Leu for interactions with the DOPr receptor. The activity was also tested for the MOPr receptor, where it was lower than the Leu-enkephaline, and no activity was shown for the KOPr receptor.

Conclusion

Different methodologies to synthesize monofluoroalkene-based dipeptide isosteres were developed since 2007. First, synthetic approaches to analogues in which there is no side chain or where the side chain stereochemistry is not controlled was discussed, either to obtain Gly-ψ[CF=CH]-Gly, Xaa-ψ[CF=CH]-Gly or Xaa-ψ[CF=C]-Pro. The synthesis of fluorinated isosteres with control of the stereochemistry at the side chain was then described, allowing the preparation of Gly-ψ[CF=CH]-Xaa, Xaa-ψ[CF=CH]-Gly, Xaa-ψ[CF=CH]-Xaa and Xaa-ψ[CF=C]-Pro. In both syntheses, control of the geometry of the fluoroalkene (i.e., *Z* vs *E*) was important. Finally, as the monofluoroalkene is of interest in medicinal chemistry as a non-hydrolyzable peptide bond isostere, some applications have been presented.

Acknowledgements

We acknowledge the financial support of NSERC, PROTEO and Université Laval. MD thanks NSERC for a Vanier Canada Graduate Scholarship.

ORCID® iDs

Myriam Drouin - https://orcid.org/0000-0001-6707-2357
Jean-François Paquin - https://orcid.org/0000-0003-2412-3083

References

1. Newman, D. J.; Cragg, G. M. *J. Nat. Prod.* **2012,** *75,* 311–335. doi:10.1021/np200906s
2. Craik, D. J.; Fairlie, D. P.; Liras, S.; Price, D. *Chem. Biol. Drug Des.* **2013,** *81,* 136–147. doi:10.1111/cbdd.12055
3. Vlieghe, P.; Lisowski, V.; Martinez, J.; Khrestchatisky, M. *Drug Discovery Today* **2010,** *15,* 40–56. doi:10.1016/j.drudis.2009.10.009
4. Choudhary, A.; Raines, R. T. *ChemBioChem* **2011,** *12,* 1801–1807. doi:10.1002/cbic.201100272
5. Taguchi, T.; Yanai, H. Fluorinated Moieties for Replacement of Amide and Peptide Bonds. In *Fluorine in Medicinal Chemistry and Chemical Biology;* Ojima, I., Ed.; Blackwell Publishing Inc., 2009; pp 257–290. doi:10.1002/9781444312096.ch10
6. Angell, Y. L.; Burgess, K. *Chem. Soc. Rev.* **2007,** *36,* 1674–1689. doi:10.1039/b701444a

7. Wipf, P.; Henninger, T. C.; Geib, S. J. *J. Org. Chem.* **1998,** *63,* 6088–6089. doi:10.1021/jo981057v
8. Abraham, R. J.; Ellison, S. L. R.; Schonholzer, P.; Thomas, W. A. *Tetrahedron* **1986,** *42,* 2101–2110. doi:10.1016/S0040-4020(01)87627-4
9. Champagne, P. A.; Desroches, J.; Paquin, J.-F. *Synthesis* **2015,** *47,* 306–322. doi:10.1055/s-0034-1379537
10. O'Hagan, D.; Rzepa, H. S. *Chem. Commun.* **1997,** 645–652. doi:10.1039/a604140j
11. Howard, J. A. K.; Hoy, V. J.; O'Hagan, D.; Smith, T. G. *Tetrahedron* **1996,** *52,* 12613–12622. doi:10.1016/0040-4020(96)00749-1
12. Urban, J. J.; Tillman, B. G.; Cronin, W. A. *J. Phys. Chem. A* **2006,** *110,* 11120–11129. doi:10.1021/jp062881n
13. Joseph, A. P.; Srinivasan, N.; de Brevern, A. G. *Amino Acids* **2012,** *43,* 1369–1381. doi:10.1007/s00726-011-1211-9
14. Ramachandra, G. N.; Sasisekharan, V. *Adv. Protein Chem.* **1968,** *23,* 283–437. doi:10.1016/S0065-3233(08)60402-7
15. Ramachandra, G. N.; Mitra, A. K. *J. Mol. Biol.* **1976,** *107,* 85–92. doi:10.1016/S0022-2836(76)80019-8
16. van Steenis, J. H.; van der Gen, A. *J. Chem. Soc., Perkin Trans. 1* **2002,** 2117–2133. doi:10.1039/b106187a
17. Zajc, B.; Kumar, R. *Synthesis* **2010,** 1822–1836. doi:10.1055/s-0029-1218789
18. Landelle, G.; Bergeron, M.; Turcotte-Savard, M.-O.; Paquin, J.-F. *Chem. Soc. Rev.* **2011,** *40,* 2867–2908. doi:10.1039/c0cs00201a
19. Yanai, H.; Taguchi, T. *Eur. J. Org. Chem.* **2011,** 5939–5954. doi:10.1002/ejoc.201100495
20. Hara, S. *Top. Curr. Chem.* **2012,** *327,* 59–86. doi:10.1007/128_2012_317
21. Pfund, E.; Lequeux, T.; Gueyrard, D. *Synthesis* **2015,** *47,* 1534–1546. doi:10.1055/s-0034-1380548
22. Champagne, P. A.; Desroches, J.; Hamel, J.-D.; Vandamme, M.; Paquin, J.-F. *Chem. Rev.* **2015,** *115,* 9073–9174. doi:10.1021/cr500706a
23. Sano, S.; Kuroda, Y.; Saito, K.; Ose, Y.; Nagao, Y. *Tetrahedron* **2006,** *62,* 11881–11890. doi:10.1016/j.tet.2006.09.096
24. Calata, C.; Pfund, E.; Lequeux, T. *J. Org. Chem.* **2009,** *74,* 9399–9405. doi:10.1021/jo901540c
25. Calata, C.; Pfund, E.; Lequeux, T. *Tetrahedron* **2011,** *67,* 1398–1405. doi:10.1016/j.tet.2010.12.061
26. Yanai, H.; Okada, H.; Sato, A.; Okada, M.; Taguchi, T. *Tetrahedron Lett.* **2011,** *52,* 2997–3000. doi:10.1016/j.tetlet.2011.03.148
27. Sato, A.; Yanai, H.; Suzuki, D.; Okada, M.; Taguchi, T. *Tetrahedron Lett.* **2015,** *56,* 925–929. doi:10.1016/j.tetlet.2014.12.128
28. Nihei, T.; Nishi, Y.; Ikeda, N.; Yokotani, S.; Ishihara, T.; Arimitsu, S.; Konno, T. *Synthesis* **2016,** *48,* 865–881. doi:10.1055/s-0035-1560390
29. Boros, L. G.; De Corte, B.; Gimi, R. H.; Welch, J. T.; Wu, Y.; Handschumacher, R. E. *Tetrahedron Lett.* **1994,** *35,* 6033–6036. doi:10.1016/0040-4039(94)88067-0
30. Welch, J. T.; Lin, J. *Tetrahedron* **1996,** *52,* 291–304. doi:10.1016/0040-4020(95)00912-R
31. Van der Veken, P.; Kertèsz, I.; Senten, K.; Haemers, A.; Augustyns, K. *Tetrahedron Lett.* **2003,** *44,* 6231–6234. doi:10.1016/S0040-4039(03)01542-9
32. Sano, S.; Matsumoto, T.; Nakao, M. *Tetrahedron Lett.* **2014,** *55,* 4480–4483. doi:10.1016/j.tetlet.2014.06.063
33. Sano, S.; Matsumoto, T.; Nanataki, H.; Tempaku, S.; Nakao, M. *Tetrahedron Lett.* **2014,** *55,* 6248–6251. doi:10.1016/j.tetlet.2014.09.077
34. Pierry, C.; Couve-Bonnaire, S.; Guilhaudis, L.; Neveu, C.; Marotte, A.; Lefranc, B.; Cahard, D.; Ségalas-Milazzo, I.; Leprince, J.; Pannecoucke, X. *ChemBioChem* **2013,** *14,* 1620–1633. doi:10.1002/cbic.201300325
35. Guérin, D.; Dez, I.; Gaumont, A.-C.; Pannecoucke, X.; Couve-Bonnaire, S. *Org. Lett.* **2016,** *18,* 3606–3609. doi:10.1021/acs.orglett.6b01631
36. Nadon, J.-F.; Rochon, K.; Grastilleur, S.; Langlois, G.; Hà Dao, T. T.; Blais, V.; Guérin, B.; Gendron, L.; Dory, Y. L. *ACS Chem. Neurosci.* **2017,** *8,* 40–49. doi:10.1021/acschemneuro.6b00163
37. Narumi, T.; Niida, A.; Tomita, K.; Oishi, S.; Otaka, A.; Ohno, H.; Fujii, N. *Chem. Commun.* **2006,** 4720–4722. doi:10.1039/b608596b
38. Pierry, C.; Zoute, L.; Jubault, P.; Pfund, E.; Lequeux, T.; Cahard, D.; Couve-Bonnaire, S.; Pannecoucke, X. *Tetrahedron Lett.* **2009,** *50,* 264–266. doi:10.1016/j.tetlet.2008.10.140
39. Pierry, C.; Cahard, D.; Couve-Bonnaire, S.; Pannecoucke, X. *Org. Biomol. Chem.* **2011,** *9,* 2378–2386. doi:10.1039/c0ob00773k
40. Yamaki, Y.; Shigenaga, A.; Tomita, K.; Narumi, T.; Fujii, N.; Otaka, A. *J. Org. Chem.* **2009,** *74,* 3272–3277. doi:10.1021/jo900134k
41. Karad, S. N.; Pal, M.; Crowley, R. S.; Prisinzano, T. E.; Altman, R. A. *ChemMedChem* **2017,** *12,* 571–576. doi:10.1002/cmdc.201700103
42. Sommer, H.; Fürstner, A. *Chem. – Eur. J.* **2017,** *23,* 558–562. doi:10.1002/chem.201605444
43. Jakobsche, C. E.; Peris, G.; Miller, S. J. *Angew. Chem., Int. Ed.* **2008,** *47,* 6707–6711. doi:10.1002/anie.200802223
44. Okada, M.; Nakamura, Y.; Saito, A.; Sato, A.; Horikawa, H.; Taguchi, T. *Tetrahedron Lett.* **2002,** *43,* 5845–5847. doi:10.1016/S0040-4039(02)01169-3
45. Nakumara, Y.; Okada, M.; Sato, A.; Horikawa, H.; Koura, M.; Saito, A.; Taguchi, T. *Tetrahedron* **2005,** *61,* 5741–5753. doi:10.1016/j.tet.2005.04.034
46. Watanabe, D.; Koura, M.; Saito, A.; Yanai, H.; Nakamura, Y.; Okada, M.; Sato, A.; Taguchi, T. *J. Fluorine Chem.* **2011,** *132,* 327–338. doi:10.1016/j.jfluchem.2011.03.007
47. Yamaki, Y.; Shigenaga, A.; Li, J.; Shimohigashi, Y.; Otaka, A. *J. Org. Chem.* **2009,** *74,* 3278–3285. doi:10.1021/jo900135t
48. Narumi, T.; Tomita, K.; Inokuchi, E.; Kobayashi, K.; Oishi, S.; Ohno, H.; Fujii, N. *Tetrahedron* **2008,** *64,* 4332–4346. doi:10.1016/j.tet.2008.02.076
49. Oishi, S.; Kamitani, H.; Kodera, Y.; Watanabe, K.; Kobayashi, K.; Narumi, T.; Tomita, K.; Ohno, H.; Naito, T.; Kodama, E.; Matsuoka, M.; Fujii, N. *Org. Biomol. Chem.* **2009,** *7,* 2872–2877. doi:10.1039/b907983a
50. Narumi, T.; Hayashi, R.; Tomita, K.; Kobayashi, K.; Tanahara, N.; Ohno, H.; Naito, T.; Kodama, E.; Matsuoka, M.; Oishi, S.; Fujii, N. *Org. Biomol. Chem.* **2010,** *8,* 616–621. doi:10.1039/B917236J
51. Niida, A.; Tomita, K.; Mizumoto, M.; Tanigaki, H.; Terada, T.; Oishi, S.; Otaka, A.; Inui, K.-i.; Fujii, N. *Org. Lett.* **2006,** *8,* 613–616. doi:10.1021/ol052781k
52. Chang, W.; Mosley, R. T.; Bansal, S.; Keilman, M.; Lam, A. M.; Furman, P. A.; Otto, M. J.; Sofia, M. J. *Bioorg. Med. Chem. Lett.* **2012,** *22,* 2938–2942. doi:10.1016/j.bmcl.2012.02.051
53. Dutheuil, G.; Pierry, C.; Villiers, E.; Couve-Bonnaire, S.; Pannecoucke, X. *New J. Chem.* **2013,** *37,* 1320–1325. doi:10.1039/C2NJ40891K
54. Villiers, E.; Couve-Bonnaire, S.; Cahard, D.; Pannecoucke, X. *Tetrahedron* **2015,** *71,* 7054–7062. doi:10.1016/j.tet.2015.06.093
55. Tomita, K.; Narumi, T.; Niida, A.; Oishi, S.; Ohno, H.; Fujii, N. *Biopolymers* **2007,** *88,* 272–278. doi:10.1002/bip.20676

BEILSTEIN JOURNAL OF ORGANIC CHEMISTRY

Ring-size-selective construction of fluorine-containing carbocycles via intramolecular iodoarylation of 1,1-difluoro-1-alkenes

Takeshi Fujita, Ryo Kinoshita, Tsuyoshi Takanohashi, Naoto Suzuki and Junji Ichikawa*

Full Research Paper

Open Access

Address:
Division of Chemistry, Faculty of Pure and Applied Sciences, University of Tsukuba, Tsukuba, Ibaraki 305-8571, Japan

Email:
Junji Ichikawa* - junji@chem.tsukuba.ac.jp

* Corresponding author

Keywords:
alkenes; carbocycles; cyclization; electrophilic activation; fluorine; iodine

Beilstein J. Org. Chem. **2017,** *13,* 2682–2689.
doi:10.3762/bjoc.13.266

Received: 03 October 2017
Accepted: 29 November 2017
Published: 14 December 2017

This article is part of the Thematic Series "Organo-fluorine chemistry IV".

Guest Editor: D. O'Hagan

Abstract

1,1-Difluoro-1-alkenes bearing a biaryl-2-yl group effectively underwent site-selective intramolecular iodoarylation by the appropriate cationic iodine species. Iodoarylation of 2-(2-aryl-3,3-difluoroallyl)biaryls proceeded via regioselective carbon–carbon bond formation at the carbon atoms in β-position to the fluorine substituents, thereby constructing dibenzo-fused six-membered carbocycles bearing a difluoroiodomethyl group. In contrast, 2-(3,3-difluoroallyl)biaryls underwent a similar cyclization at the α-carbon atoms to afford ring-difluorinated seven-membered carbocycles.

Introduction

As 1,1-difluoro-1-alkenes have an electron-deficient carbon–carbon double bond, they readily undergo intramolecular substitution of nucleophiles through an addition–elimination mechanism [1,2]. Thus, under basic conditions, they serve as useful precursors for ring-fluorinated heterocycles and carbocycles that are promising candidates for pharmaceuticals, agrochemicals, and functional materials. In contrast, the cationic cyclization of 1,1-difluoro-1-alkenes using electrophilic reagents (under acidic conditions) has been quite limited because of their low electron densities caused by fluorine substituents [3-5]. Despite the limitation, the cationic cyclization of difluoroalkenes possesses high potential for the synthesis of fluorine-containing cyclic compounds. Thus, the development of this type of cyclization is highly desirable to further expand the utility of difluoroalkenes in organic synthesis.

We have already achieved the metal-catalyzed and acid-mediated cationic cyclization of 1,1-difluoro-1-alkenes. In the former case, we reported the palladium [6-10], indium [10-13], and silver-catalyzed construction of ring-fluorinated carbocycles and heterocycles [14]. In the latter case, the domino-Friedel–Crafts-type cyclization proceeded via the cleavage of

two carbon–fluorine bonds to afford polycyclic aromatic hydrocarbons [15-21]. Both types of cationic cyclization proceeded exclusively at the carbon atoms α to the fluorine substituents, because the β-selective metalation or protonation of difluoroalkenes generates α-fluorocarbocations, which were stabilized by the resonance effect of fluorine substituents.

In the course of our studies on the cationic cyclization of 1,1-difluoro-1-alkenes, we undertook an investigation of their iodine-mediated cyclization. Three-membered iodonium intermediates generated in the reaction course were expected to exhibit switchable regioselectivities [22]. This is because their cationic charge might be less localized on the carbon atoms α to the fluorine substituents, as compared to the aforementioned cationic intermediates [23-27]. Thus, we examined and eventually achieved complete control over the regioselectivity at the carbon atoms in β-position as well as those in α-position to the fluorine in the intramolecular Friedel–Crafts-type iodoarylation of 1,1-difluoro-1-alkenes bearing a biaryl group. Among the 1,1-difluoro-1-alkenes examined, 2-(2-aryl-3,3-difluoroallyl)biaryls underwent cyclization at the carbon atoms in β-position to the fluorine substituents to construct six-membered carbocycles bearing a difluoroiodomethyl group (Scheme 1a). On the other hand the cyclization of 2-(3,3-difluoroallyl)biaryls proceeded at the α-carbon atoms to give ring-fluorinated seven-membered carbocycles (Scheme 1b) [28].

Results and Discussion

First, we sought an electrophilic iodine species suitable for the intramolecular iodoarylation of 2-(2-aryl-3,3-difluoroallyl)-biaryls **1** using 2-(2-phenyl-3,3-difluoroallyl)biphenyl (**1a**) as a model substrate. To generate a highly reactive, cationic iodine species, several iodine sources were used with acid or metal activators (Table 1, entries 1–3). Upon treatment with *N*-iodosuccinimide (NIS) and trimethylsilyl trifluoromethanesulfonate (TMSOTf) in a 1:1 mixed solvent of 1,1,1,3,3,3-hexafluoropropan-2-ol (HFIP) and dichloromethane, **1a** afforded the expected iodoarylation product **2a** and its overreacted product,

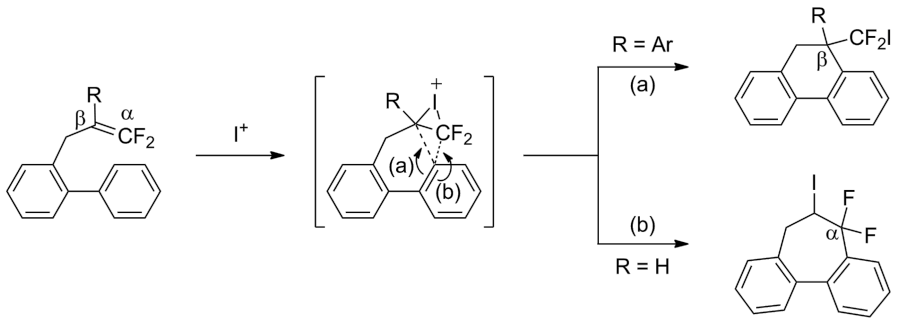

Scheme 1: Intramolecular site-selective iodoarylation of 1,1-difluoro-1-alkenes bearing a biaryl group.

Table 1: Screening of conditions for the iodoarylation of **1a**.

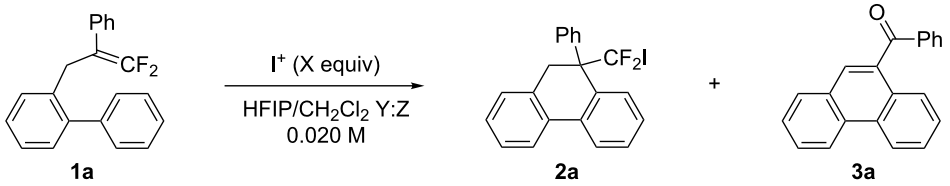

1a **2a** **3a**

entry	I^+ (X equiv)	Y:Z	conditions	**2a** (%)[a]	**3a** (%)[a]
1	NIS (1.2), TMSOTf (1.2)	1:1	0 °C, 40 min	34	15
2	IPy_2BF_4 (1.0), TfOH (2.0)	1:1	0 °C, 1.5 h	N.D.[b]	N.D.[b]
3	I_2 (1.2), AgOTf (1.2)	1:1	0 °C, 1.5 h	16	33
4	ICl (2.0)	1:1	0 °C, 20 min	N.D.[b]	43
5	PyICl (2.0)	1:1	0 °C, 1 h	31	N.D.[b]
6	PyICl (2.0)	9:1	0 °C, 1 h	85	12
7[c]	PyICl (2.0)	9:1	0 °C, 1 h	91	1

[a]Yield was determined by ^{19}F NMR spectroscopy using $PhCF_3$ as an internal standard. [b]N.D. = not detected. [c]0.075 M.

9-benzoylphenanthrene (**3a**), in 34% and 15% yields, respectively (Table 1, entry 1). Ketone **3a** was formed probably via the sequence consisting of iodide elimination from **2a**, 1,2-migration of the phenyl group, and deprotonation, followed by hydrolysis of the resulting doubly activated benzylic difluoromethylene unit (Scheme 2). Neither a combination of bis(pyridine)iodonium (IPy_2BF_4) and trifluoromethanesulfonic acid nor a combination of I_2 and silver(I) triflate improved the yield of **2a** (Table 1, entries 2 and 3). Although iodine monochloride, which is known as a cationic iodine species, afforded only ketone **3a** (Table 1, entry 4), its pyridine complex (PyICl) exclusively afforded the iodoarylation product **2a** in 31% yield (Table 1, entry 5). The use of a 9:1 mixed solvent of HFIP and CH_2Cl_2 improved the yield of **2a** to 85% (Table 1, entry 6). Lastly, increasing the concentration up to 0.075 M suppressed the formation of **3a** and selectively afforded **2a** in 91% yield (Table 1, entry 7). In this reaction, the nucleophilic benzene ring attacked the carbon atom β to the fluorine substituents of the cyclic iodonium intermediate, which was derived from **1a** and PyICl. This indicates that the cationic charge in the cyclic iodonium intermediate might be localized at the β-carbon atom because of stabilization by the proximal phenyl group [28].

Under the optimal conditions obtained above, iodoarylation of several 2-(2-aryl-3,3-difluoroallyl)biaryls **1** was examined (Table 2). Difluoroiodomethylated dihydrophenanthrenes, **2a** and **2b**, bearing a phenyl and a biphenyl-4-yl group were obtained in 79% and 74% isolated yields, respectively. 2-(2-Aryl-

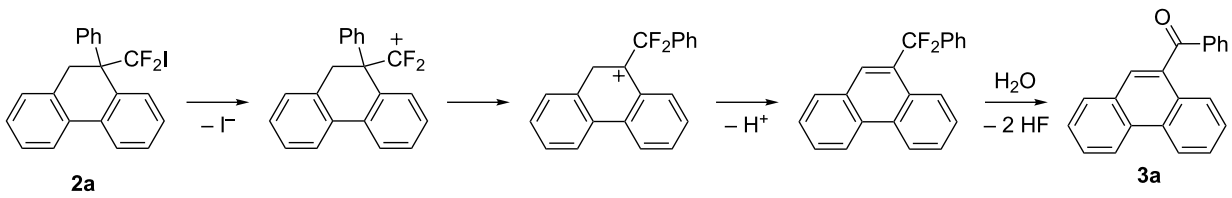

Scheme 2: Mechanism for formation of **3a**.

Table 2: Construction of six-membered carbocycles via iodoarylation of **1**.

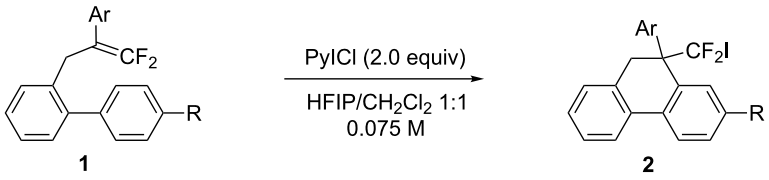

entry	1	2	time	yield (%)[a]
1[b]	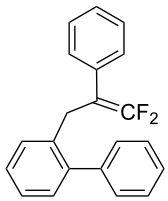 **1a**	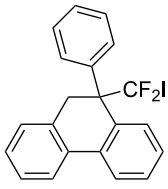 **2a**	1 h	79
2	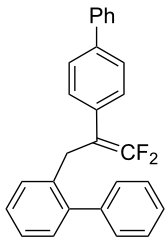 **1b**	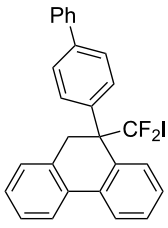 **2b**	2 h	74

Table 2: Construction of six-membered carbocycles via iodoarylation of **1**. (continued)

3	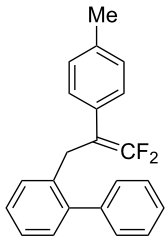 **1c**	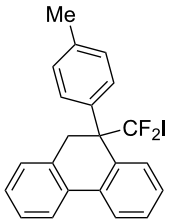 **2c**	35 min	82
4	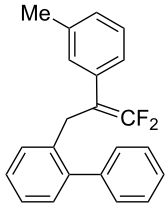 **1d**	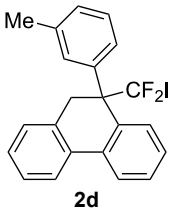 **2d**	1 h	53
5	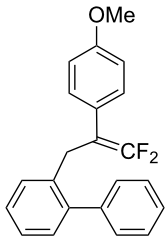 **1e**	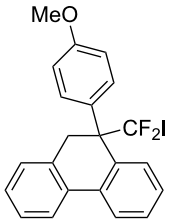 **2e**	25 min	83
6	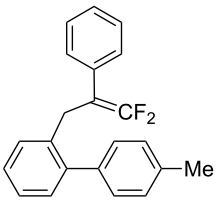 **1f**	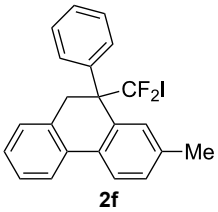 **2f**	1.5 h	54
7	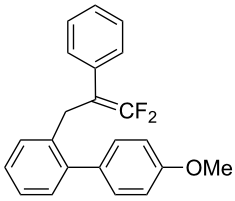 **1g**	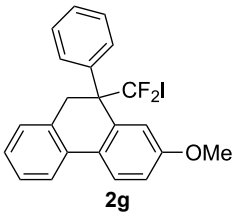 **2g**	1 h	80

[a]Isolated yield. [b]HFIP/CH_2Cl_2 9:1.

3,3-difluoroallyl)biaryls **1c**–**e** bearing electron-donating substituents (4-Me, 3-Me, and 4-MeO) on the benzene ring attached to the vinylic position successfully underwent iodoarylation to afford the corresponding dihydrophenanthrenes **2c**–**e**. In contrast, electron-withdrawing substituents on similar positions hardly promoted the iodoarylation, which was presumably because of inefficient cyclic iodonium formation. Substrates **1f** and **1g** bearing electron-donating groups on the nucleophilic aryl groups also participated in the iodoarylation to afford the corresponding difluoroiodomethylated dihydrophenanthrenes **2f** and **2g** in 54% and 80% yields, respectively. However, with substrates bearing a strong electron-withdrawing group (e.g., CF_3) on the nucleophilic benzene ring, the iodoarylation hardly proceeded. The unambiguous structural determination of the iodoarylation products **2** was accomplished by X-ray crystallographic analysis of **2a** (Figure 1), which revealed that the iodoarylation products **2** have six-membered carbocycles bearing a difluoroiodomethyl group.

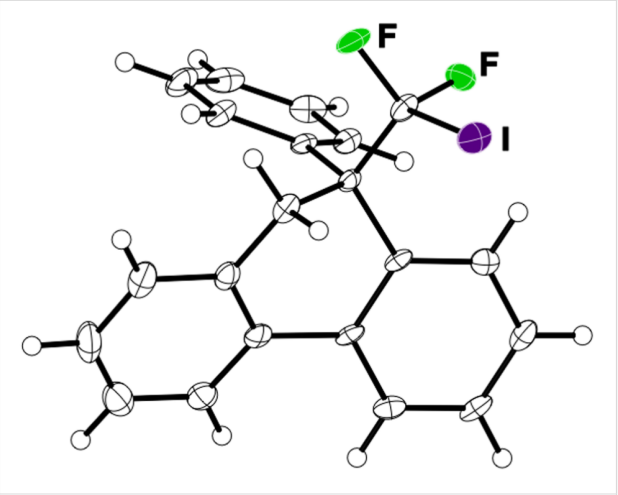

Figure 1: ORTEP diagram of **2a** with 50% ellipsoid probability.

Further transformation of the difluoroiodomethyl group of **2a** was achieved by heating (Scheme 3). Thus, refluxing a DMF solution of **2a** for 15 h induced iodine–hydrogen exchange to afford difluoromethylated dihydrophenanthrene derivative **4a** in almost quantitative yield [29,30]. A difluoromethyl group functions as a hydrogen-bond donor and a bioisostere of a hydroxy group, as a result of which difluoromethyl-bearing compounds attract much attention as bioactive materials [31,32]. This sequence provides ready access to these compounds.

Scheme 3: Transformation of a CF_2I group of **2a** into a CHF_2 group.

Next, 2-(3,3-difluoroallyl)biphenyl (**5a**), without an aryl group at its vinylic position, was subjected to the conditions examined in entries 1–3 of Table 1. In contrast to **1a**, iodoarylation of **5a** proceeded through C–C-bond formation exclusively at the carbon atoms α to the fluorine substituents to afford dibenzo-fused cycloheptane **6a** with geminal fluorine substituents on the ring in 92%, 38%, 49% yields, respectively. The thus-obtained selectivity might be attributed to the localization of the cationic charge at the carbon atoms α to the fluorine substituents in the three-membered iodonium intermediates. Since the combination of NIS and TMSOTf was found to be the best for an iodoarylation of **5**, the reactions of a couple of 2-(3,3-difluoroallyl)biaryls **5** were examined under the same conditions (Scheme 4). The iodoarylation of difluoroallylbiphenyl **5b**, bearing an electron-donating methyl group on the nucleophilic aryl group, was completed in 15 min to afford **6b** in 60% isolated yield. Brominated difluoroallylbiphenyl **5c** successfully underwent the same cyclization to afford the corresponding product **6c** in 62% isolated yield. The structural characterization of **6** was achieved by X-ray analysis using a single crystal of **6a** (Figure 2), and it was found that the iodoarylation products **6** have a seven-membered carbocycle bearing adjacent difluoromethylene and iodomethylene units.

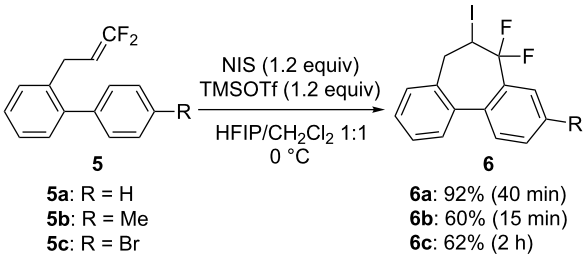

Scheme 4: Construction of seven-membered carbocycles via iodoarylation of **5**.

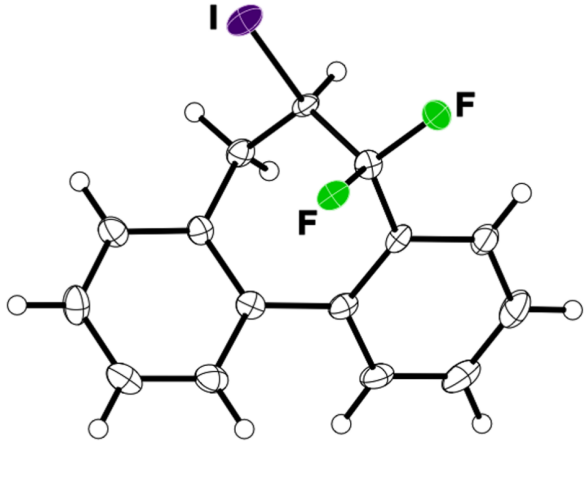

Figure 2: ORTEP diagram of **6a** with 50% ellipsoid probability.

In addition, a selective HI elimination from **6a** could be achieved by the choice of base, leading to the construction of a [7]annulene system (Scheme 5). The use of lithium bases, such as lithium diisopropylamide and lithium hexamethyldisilazide, induced HF eliminations as well as substantial HI elimination. However, 1,8-diazabicyclo[5.4.0]undec-7-ene (DBU) exclusively promoted HI elimination to afford ring-difluorinated dibenzo[*a*,*c*][7]annulene **7a** in an almost quantitative yield. Since dibenzo[*a*,*c*][7]annulenes serve as bioactive agents, this method would be of value in the research directed toward pharmaceutical and materials chemistry [33-35].

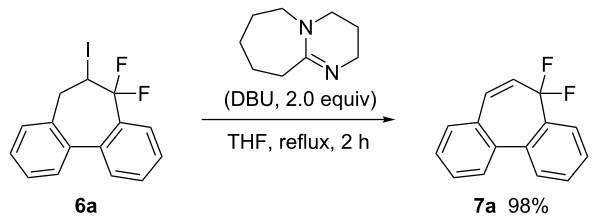

Scheme 5: Selective HI elimination from **6a**.

Conclusion

In summary, we demonstrated selective constructions of six and seven-membered carbocyclic rings through the intramolecular iodoarylation of 3,3-difluoroallylic biaryls. The size selectivity in the cyclization was drastically controlled by the presence or absence of an aryl group in the 2-position of the 3,3-difluoroallylic moiety, which might perturb cationic charge distribution in the corresponding cyclic iodonium intermediates. The aryl group in the 2-position (at the carbon atom in β-position to the fluorine substituents) promoted a six-membered-ring closure, most likely because of the localization of cationic charge stabilized by the aromatic ring. In contrast, seven-membered carbocycles were constructed probably as a result of the cationic charge localized at the 3-position of difluoroallylic moiety (at the α-carbon atom of the fluorine substituents) due to the α-cation-stabilizing effect of fluorine.

Experimental

General: ^{1}H NMR, ^{13}C NMR, and ^{19}F NMR spectra were recorded on a Bruker Avance 500 or a JEOL ECS-400 spectrometer. Chemical shift values are given in ppm relative to internal Me_4Si (for ^{1}H NMR: δ = 0.00 ppm), $CDCl_3$ (for ^{13}C NMR: δ = 77.0 ppm), C_6F_6 (for ^{19}F NMR: δ = 0.0 ppm), and $(4\text{-}MeC_6H_4)_2C(CF_3)_2$ (for ^{19}F NMR: δ = 97.9 ppm). IR spectra were recorded on a Horiba FT-300S spectrometer using the attenuated total reflectance (ATR) method. Mass spectra were measured on a JEOL JMS-T100GCV spectrometer. X-ray diffraction studies were performed on a Bruker APEXII ULTRA instrument equipped with a CCD diffractometer using Mo Kα (graphite monochromated, λ = 0.71069 Å) radiation. The CCDC deposition numbers of compounds **2a** and **6a** are 1556804 and 1556803, respectively. All the reactions were conducted under argon or nitrogen atmosphere.

Materials: Column chromatography and preparative thin-layer chromatography (PTLC) were conducted on silica gel (Silica Gel 60 N, Kanto Chemical Co., Inc. for column chromatography and Wakogel B-5F, Wako Pure Chemical Industries, Ltd. for PTLC). Tetrahydrofuran (THF), dichloromethane, and *N*,*N*-dimethylformamide (DMF) were purified by a solvent-purification system (GlassContour) equipped with columns of activated alumina and supported-copper catalyst (Q-5) before use. 1,1,1,3,3,3-Hexafluoropropan-2-ol (HFIP) was distilled from CaH_2 and stored over activated 4 Å molecular sieves. Unless otherwise noted, materials were obtained from commercial sources and used directly without further purifications.

Typical procedure for the iodoarylation of 2-(2-aryl-3,3-difluoroallyl)biaryls 1: To a HFIP (1.20 mL) and dichloromethane (0.13 mL) solution of 2-(2-phenyl-3,3-difluoroallyl)biphenyl (**1a**, 31 mg, 0.10 mmol) was added pyridine iodine monochloride (PyICl, 49 mg, 0.20 mmol) at 0 °C. After stirring at the same temperature for 1 h, the reaction was quenched with an aqueous $NaHCO_3$ solution. The organic materials were extracted with $CHCl_3$ three times. The combined extracts were washed with an aqueous $Na_2S_2O_3$ solution and brine, and dried over anhydrous Na_2SO_4. After removal of the solvent under reduced pressure, the residue was purified by PTLC (hexane/ethyl acetate 10:1) to give 9-(difluoroiodomethyl)-9-phenyl-9,10-dihydrophenanthrene (**2a**, 34 mg, 79%) as a white solid. ^{1}H NMR (500 MHz, $CDCl_3$) δ 3.68 (d, J = 15.8 Hz, 1H), 3.71 (d, J = 15.8 Hz, 1H), 7.07–7.08 (m, 3H), 7.15–7.24 (m, 5H), 7.42–7.49 (m, 2H), 7.52–7.54 (m, 1H), 7.79 (d, J = 7.5 Hz, 1H), 7.95 (d, J = 7.6 Hz, 1H); ^{13}C NMR (126 MHz, $CDCl_3$) δ 38.7, 59.5 (t, J_{CF} = 17 Hz), 110.6 (t, J_{CF} = 316 Hz), 123.6, 125.1, 127.2, 127.4, 127.50, 127.52, 128.0, 128.46, 128.50, 128.6 (t, J_{CF} = 4 Hz), 130.1, 132.7, 133.64, 133.64, 134.6, 136.8; ^{19}F NMR (470 MHz, $CDCl_3$) δ 124.7 (br s); IR (neat): 3068, 1489, 1454, 1126, 1147, 1097, 964, 850, 742, 696, 592 cm^{-1}; HRMS–EI (m/z): $[M]^+$ calcd for $C_{21}H_{15}F_2I$, 432.0186; found: 432.0166.

Typical procedure for the iodoarylation of 2-(3,3-difluoroallyl)biaryls 5: To a HFIP (2.5 mL) and dichloromethane (1.5 mL) solution of *N*-iodosuccinimide (NIS, 27 mg, 0.12 mmol) was added trimethylsilyl trifluoromethanesulfonate (22 μL, 0.12 mmol) at 0 °C. After stirring at the same temperature for 10 min, a dichloromethane (1.0 mL) solution of 2-(3,3-difluoroallyl)biphenyl (**5a**, 23 mg, 0.10 mmol) was added to the reaction mixture. After stirring at 0 °C for 40 min, the reaction was quenched with an aqueous $NaHCO_3$ solution. The organic materials were extracted with dichloromethane three times. The combined extracts were washed with an aqueous $Na_2S_2O_3$ solution and brine, and dried over anhydrous Na_2SO_4. After removal of the solvent under reduced pressure, the residue was purified by PTLC (hexane/ethyl acetate 10:1) to give 5,5-difluoro-6-iodo-6,7-dihydro-5*H*-dibenzo[*a*,*c*][7]annulene (**6a**, 33 mg, 92%) as a colorless liquid. ^{1}H NMR (500 MHz, $CDCl_3$) δ 3.06 (dd, J = 14.8, 4.9, 1H), 3.38 (dd, J = 14.8, 6.0 Hz, 1H), 4.91–4.98 (m, 1H), 7.28–7.35 (m, 2H), 7.41–7.44 (m, 3H), 7.47

(d, J = 7.8 Hz, 1H), 7.55–7.59 (m, 1H), 7.70 (d, J = 7.4 Hz, 1H); ^{13}C NMR (126 MHz, $CDCl_3$) δ 35.1 (dd, J_{CF} = 27 Hz), 41.7, 118.9 (dd, J_{CF} = 247 Hz), 125.2, 127.5, 128.0, 128.20, 128.23, 129.2, 129.7, 131.0, 131.4 (dd, J_{CF} = 24 Hz), 134.6, 138.6 (dd, J_{CF} = 5 Hz), 140.3; ^{19}F NMR (470 MHz, DMSO-d_6, 120 °C) δ 72.3 (d, J_{FF} = 236 Hz, 1F), 86.5 (d, J_{FF} = 236 Hz, 1F); IR (neat): 3068, 3030, 1450, 1149, 1055, 989, 752, 598 cm^{-1}; HRMS–EI (m/z): [M]$^+$ calcd for $C_{15}H_{11}F_2I$, 355.9873; found: 355.9866.

Supporting Information

Supporting Information File 1

Detailed experimental procedures and spectral data.
[http://www.beilstein-journals.org/bjoc/content/supplementary/1860-5397-13-266-S1.pdf]

Acknowledgements

This work was financially supported by JSPS KAKENHI Grant Number JP16H04105 in Grant-in-Aid for Scientific Research (B) (J.I.), JSPS KAKENHI Grant Number JP16H01002 in Precisely Designed Catalysts with Customized Scaffolding (J.I.), and JSPS KAKENHI Grant Number JP16K20939 in Grant-in-Aid for Young Scientists (B) (T.F.). We acknowledge the generous gifts of 1,1,1,3,3,3-hexafluoropropan-2-ol (HFIP, Central Glass Co., Ltd.), 2-bromo-3,3,3-trifluoroprop-1-ene, and dibromodifluoromethane (Tosoh Finechem Co.).

ORCID® iDs

Takeshi Fujita - https://orcid.org/0000-0001-9666-022X
Naoto Suzuki - https://orcid.org/0000-0003-0166-3909
Junji Ichikawa - https://orcid.org/0000-0001-6498-326X

References

1. Ichikawa, J. *Chim. Oggi* **2007,** *25,* 54–57.
2. Zhang, X.; Cao, S. *Tetrahedron Lett.* **2017,** *58,* 375–392. doi:10.1016/j.tetlet.2016.12.054
3. Suda, M. *Tetrahedron Lett.* **1980,** *21,* 2555–2556. doi:10.1016/0040-4039(80)80127-4
4. Morikawa, T.; Kumadaki, I.; Shiro, M. *Chem. Pharm. Bull.* **1985,** *33,* 5144–5146. doi:10.1248/cpb.33.5144
5. Kendrick, D. A.; Kolb, M. *J. Fluorine Chem.* **1989,** *45,* 273–276. doi:10.1016/S0022-1139(00)84152-4
6. Yokota, M.; Fujita, D.; Ichikawa, J. *Org. Lett.* **2007,** *9,* 4639–4642. doi:10.1021/ol702279w
7. Tanabe, H.; Ichikawa, J. *Chem. Lett.* **2010,** *39,* 248–249. doi:10.1246/cl.2010.248
8. Fuchibe, K.; Morikawa, T.; Shigeno, K.; Fujita, T.; Ichikawa, J. *Org. Lett.* **2015,** *17,* 1126–1129. doi:10.1021/ol503759d
9. Fuchibe, K.; Morikawa, T.; Ueda, R.; Okauchi, T.; Ichikawa, J. *J. Fluorine Chem.* **2015,** *179,* 106–115. doi:10.1016/j.jfluchem.2015.06.008
10. Fuchibe, K.; Shigeno, K.; Zhao, N.; Aihara, H.; Akisaka, R.; Morikawa, T.; Fujita, T.; Yamakawa, K.; Shimada, T.; Ichikawa, J. *J. Fluorine Chem.* **2017,** *203,* 173–184. doi:10.1016/j.jfluchem.2017.09.002
11. Fuchibe, K.; Mayumi, Y.; Zhao, N.; Watanabe, S.; Yokota, M.; Ichikawa, J. *Angew. Chem., Int. Ed.* **2013,** *52,* 7825–7828. doi:10.1002/anie.201302740
12. Fuchibe, K.; Mayumi, Y.; Yokota, M.; Aihara, H.; Ichikawa, J. *Bull. Chem. Soc. Jpn.* **2014,** *87,* 942–949. doi:10.1246/bcsj.20140128
13. Fuchibe, K.; Imaoka, H.; Ichikawa, J. *Chem. – Asian J.* **2017,** *12,* 2359–2363. doi:10.1002/asia.201700870
14. Fujita, T.; Watabe, Y.; Yamashita, S.; Tanabe, H.; Nojima, T.; Ichikawa, J. *Chem. Lett.* **2016,** *45,* 964–966. doi:10.1246/cl.160427
15. Ichikawa, J. *Pure Appl. Chem.* **2000,** *72,* 1685–1689. doi:10.1351/pac200072091685
16. Ichikawa, J.; Jyono, H.; Kudo, T.; Fujiwara, M.; Yokota, M. *Synthesis* **2005,** 39–46. doi:10.1055/s-2004-834910
17. Ichikawa, J.; Kaneko, M.; Yokota, M.; Itonaga, M.; Yokoyama, T. *Org. Lett.* **2006,** *8,* 3167–3170. doi:10.1021/ol060912r
18. Ichikawa, J.; Yokota, M.; Kudo, T.; Umezaki, S. *Angew. Chem., Int. Ed.* **2008,** *47,* 4870–4873. doi:10.1002/anie.200801396
19. Isobe, H.; Hitosugi, S.; Matsuno, T.; Iwamoto, T.; Ichikawa, J. *Org. Lett.* **2009,** *11,* 4026–4028. doi:10.1021/ol901693y
20. Fuchibe, K.; Jyono, H.; Fujiwara, M.; Kudo, T.; Yokota, M.; Ichikawa, J. *Chem. – Eur. J.* **2011,** *17,* 12175–12185. doi:10.1002/chem.201100618
21. Suzuki, N.; Fujita, T.; Ichikawa, J. *Org. Lett.* **2015,** *17,* 4984–4987. doi:10.1021/acs.orglett.5b02426
22. Saito, A.; Okada, M.; Nakamura, Y.; Kitagawa, O.; Horikawa, H.; Taguchi, T. *J. Fluorine Chem.* **2003,** *123,* 75–80. doi:10.1016/S0022-1139(03)00138-6
23. Freeman, F. *Chem. Rev.* **1975,** *75,* 439–490. doi:10.1021/cr60296a003
24. Rodriguez, J.; Dulcère, J.-P. *Synthesis* **1993,** 1177–1205. doi:10.1055/s-1993-26022
25. French, A. N.; Bissmire, S.; Wirth, T. *Chem. Soc. Rev.* **2004,** *33,* 354–362. doi:10.1039/b310389g
26. Denmark, S. E.; Kuester, W. E.; Burk, M. T. *Angew. Chem., Int. Ed.* **2012,** *51,* 10938–10953. doi:10.1002/anie.201204347
27. Nolsøe, J. M. J.; Hansen, T. V. *Eur. J. Org. Chem.* **2014,** 3051–3065. doi:10.1002/ejoc.201301400
28. See reference [16] for an α-cation-stabilizing effect of fluorine exceeding that of an aryl group.
29. Zhang, L.; Cradlebaugh, J.; Litwinienko, G.; Smart, B. E.; Ingold, K. U.; Dolbier, W. R., Jr. *Org. Biomol. Chem.* **2004,** *2,* 689–694. doi:10.1039/b313757k
30. Zhang, C.-P.; Chen, Q.-Y.; Xiao, J.-C.; Gu, Y.-C. *J. Fluorine Chem.* **2009,** *130,* 671–673. doi:10.1016/j.jfluchem.2009.05.005
31. Hu, J. *J. Fluorine Chem.* **2009,** *130,* 1130–1139. doi:10.1016/j.jfluchem.2009.05.016
32. Ichikawa, J. *J. Synth. Org. Chem., Jpn.* **2010,** *68,* 1175–1184. doi:10.5059/yukigoseikyokaishi.68.1175
33. Bergemann, S.; Brecht, R.; Büttner, F.; Guénard, D.; Gust, R.; Seitz, G.; Stubbs, M. T.; Thoret, S. *Bioorg. Med. Chem.* **2003,** *11,* 1269–1281. doi:10.1016/S0968-0896(02)00639-9
34. Büttner, F.; Bergemann, S.; Guénard, D.; Gust, R.; Seitz, G.; Thoret, S. *Bioorg. Med. Chem.* **2005,** *13,* 3497–3511. doi:10.1016/j.bmc.2005.02.059
35. Lin, H.-C.; Lee, S.-S. *J. Nat. Prod.* **2012,** *75,* 1735–1743. doi:10.1021/np300402k

BEILSTEIN JOURNAL OF ORGANIC CHEMISTRY

Development of a fluorogenic small substrate for dipeptidyl peptidase-4

Futa Ogawa[1], Masanori Takeda[1], Kanae Miyanaga[2], Keita Tani[2], Ryuji Yamazawa[1], Kiyoshi Ito[1], Atsushi Tarui[1], Kazuyuki Sato[1] and Masaaki Omote[*1]

Full Research Paper

Open Access

Address:
[1]Faculty of Pharmaceutical Sciences, Setsunan University, 45-1 Nagaotoge-cho, Hirakata, Osaka 573-0101, Japan and [2]Division of Natural Sciences, Osaka Kyoiku University, Asahigaoka, Kashiwara, Osaka 582-8582, Japan

Email:
Masaaki Omote[*] - omote@pharm.setsunan.ac.jp

* Corresponding author

Keywords:
dipeptidyl peptidase-4; fluorogenic substrate; fluorometry; small fluorescent molecule

Beilstein J. Org. Chem. **2017,** *13,* 2690–2697.
doi:10.3762/bjoc.13.267

Received: 26 September 2017
Accepted: 29 November 2017
Published: 14 December 2017

This article is part of the Thematic Series "Organo-fluorine chemistry IV".

Guest Editor: D. O'Hagan

Abstract

A series of aniline and *m*-phenylenediamine derivatives with electron-withdrawing 3,3,3-trifluoropropenyl substituents were synthesized as small and chemically stable fluorescent organic compounds. Their fluorescence performances were evaluated by converting 2,4-disubstituted aniline **1** to the non-fluorescent dipeptide analogue H-Gly-Pro-**1** for the use as a fluorogenic substrate for dipeptidyl peptidase-4 (DPP-4). The progress of the enzymatic hydrolysis of H-Gly-Pro-**1** with DPP-4 was monitored by fluorometric determination of **1** released into the reaction medium. The results suggest that **1** could be used as fluorophore in OFF–ON-type fluorogenic probes.

Introduction

Fluorescent organic probes have become indispensable for bioimaging or molecular imaging to visualize the presence of species such as particular enzymes and biologically important inorganic ions. In biomedicine, these probes are used for the detection of a wide range of significant biomarkers and are essential for the diagnosis of critical diseases [1-3]. Selective and accurate determinations of specific enzymes, including β-galactosidase [4-6], exoglycosidases [7], cyclooxygenases [8], and others [9-13], have been achieved using the OFF–ON-type fluorogenic probes with fluorescence that can be turned on by enzymatic transformations. These fluorescent probes can act as good sensors for enzymes but the fluorophore unit is usually large because fused aromatic rings and an elongated π-conjugated system are necessary to impart appropriate fluorescent properties to the probe [14]. The molecular size of the fluorescent probe is therefore large, which is sometimes inconvenient in terms of membrane permeability, water solubility, and inhibition of inherent interactions between the probe molecule and the target enzyme. We have developed a new OFF–ON probe with a small fluorescent core unit. The same approach was recently

used to produce a fluorophore for a push–pull system, which has a single benzene ring substituted by both electron-donating and electron-withdrawing groups [15-17]. We focused on the 3,3,3-trifluoropropenyl (TFPE) group, which is an electron-withdrawing substituent that is free of oxygen atoms, which would form hydrogen bonds in protic solvents. We assumed that the use of the oxygen-free TFPE group would eliminate hydrogen bonding with protic solvents, even water, to avoid attenuation of the fluorescent characteristics of the fluorophore. In this paper, we report the synthesis of a new fluorophore with TFPE groups and its application as an OFF–ON-type fluorogenic probe for determining dipeptidyl peptidase-4 (DPP-4) activity.

Results and Discussion

Synthesis of fluorescent compounds as fluorophores

It has been reported that the introduction of a TFPE group changes the properties of electron-rich aromatics and leads to a good fluorophore structure. This suggests that substitution with TFPE would be a reasonable approach to producing new fluorescent molecules. However, there are few methods for synthesizing TFPE-substituted compounds. In a previous study, we achieved the facile introduction of TFPE groups via Hiyama cross-coupling reactions of (*E*)-trimethyl-(3,3,3-trifluoroprop-1-enyl)silane and iodoanilines. This straightforward method is useful for TFPE introduction and a broad range of iodoanilines can be used without protection of the amino group. We used this approach to synthesize several aniline derivatives containing TFPE groups. The data in Table 1 show that Hiyama cross-coupling reactions gave the desired TFPE-anilines and TFPE-phenylenediamines (**1**–**4**) in moderate to good yields. This method has the advantage that complete substitution of diiodo- and triiodoarenes can proceed to give disubstituted (**1** and **3**) and trisubstituted (**2** and **4**) products in one synthetic operation.

Next, the fluorescence profiles of these products were investigated. The results are summarized in Figure 1 and Table 2. The number of amino groups and TFPE groups introduced into compounds **1**–**4** significantly affected the fluorescence profiles in

Table 1: Synthesis of TFPE-anilines **1**–**4** via Hiyama cross-coupling reactions of iodoanilines with (*E*)-trimethyl(3,3,3-trifluoroprop-1-enyl)silane.[a]

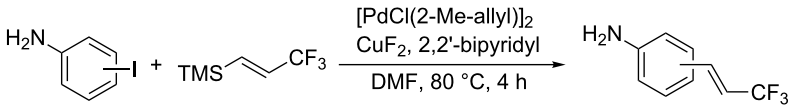

Entry	ArI	Product	Yield (%)[b]
1	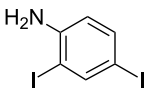	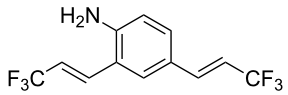 **1**	89
2	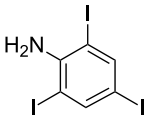	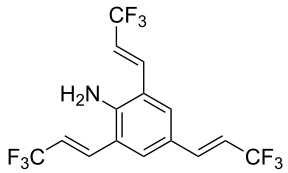 **2**	54
3	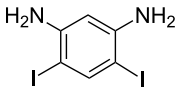	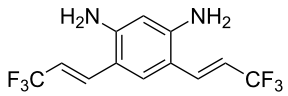 **3**	70
4	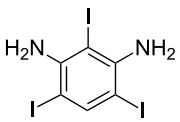	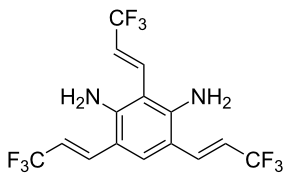 **4**	20

[a]Reaction conditions: ArI (1.0 mmol), (*E*)-trimethyl(3,3,3-trifluoroprop-1-enyl)silane (2 equiv), $[PdCl(2\text{-Me-allyl})]_2$ (10 mol %), CuF_2 (2 equiv), 2,2'-bipyridyl (2 equiv), DMF (6 mL). [b]Isolated yield.

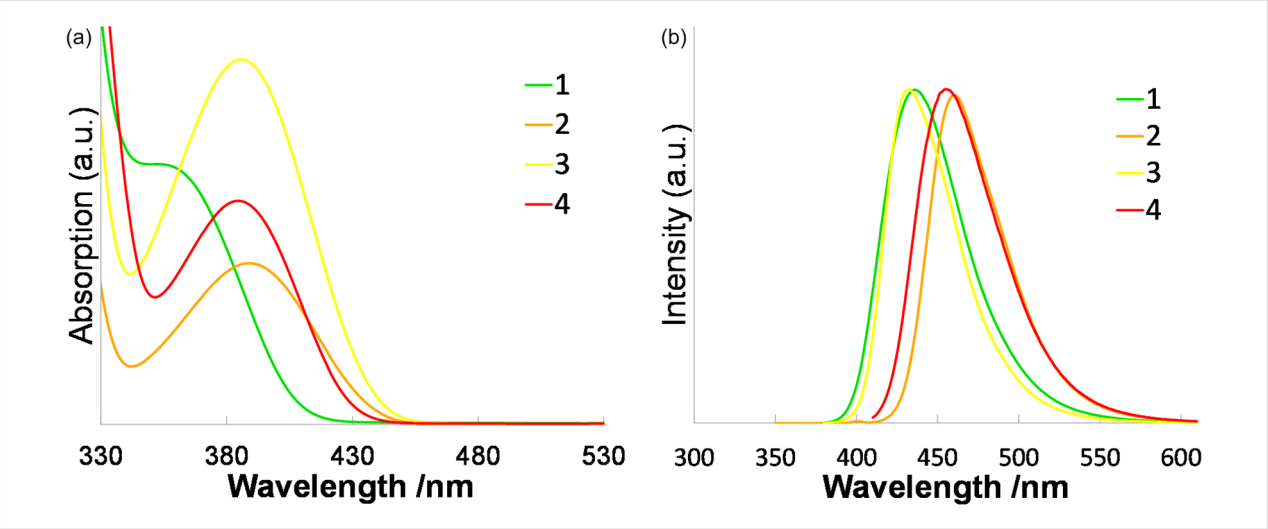

Figure 1: (a) UV–vis absorption and (b) fluorescence spectra of **1**–**4** in THF.

Table 2: UV–vis absorption and fluorescence data for **1**–**4** in THF.[a]

	$\lambda_{abs,peak}$ (nm)	ε ($M^{-1}cm^{-1}$)	$\lambda_{fl,peak}$ (nm)	φ[b]
1	359	4371	436	0.31
2	388	5763	460	0.30
3	373	7913	433	0.25
4	385	7004	455	0.03

[a]Measurement conditions:1.0 × 10^{-5} M in THF, excitation at λ = 370 nm for **1** and **3**, 400 nm for **2** and **4**. [b]Fluorescence quantum yield.

THF solution. TFPE-anilines **1** and **2** gave moderate fluorescence quantum yields of 0.31 and 0.30, respectively. In comparison with these, the fluorescence quantum yields of TFPE-phenylenediamine **3** was slightly lower, namely 0.25. The introduction of one more TFPE group into **3**, to give **4**, further decreased the quantum yield to 0.03. In spectroscopic terms, the fluorescence emission peaks of these compounds red-shifted with increasing TFPE substitution. Additionally, a large Stokes shift was observed for **1**, which is important in view of the biomedical use of fluorescent compounds. Next, we changed the solvent from THF to H_2O/DMSO (9:1) as shown in Figure 2 and Table 3. The fluorescence quantum yield of a fluorophore generally decreases significantly in an aqueous solvent because of release of energy in the excited state of the fluorophore by forming hydrogen bonds with water. However, in the cases of **1** and **3**, the decreases in the fluorescence quantum yield were small, namely 0.27 and 0.20, respectively. This is reasonable for **1** and **3** because the oxygen-free TFPE group is less likely to form hydrogen bonds, even in aqueous solution. Additionally, the emission peak of **1** is red-shifted from 436 to 461 nm. On the basis of the properties of **1**–**4**, we chose **1** for subsequent experiments involving enzymatic reactions.

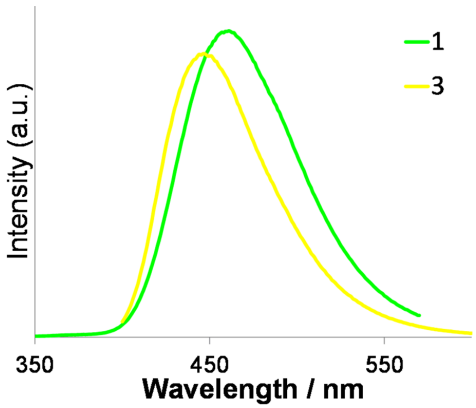

Figure 2: Fluorescence spectra of **1** and **3** in H_2O:DMSO (9:1).

Table 3: Fluorescence data for **1**–**3** in H_2O:DMSO (9:1).[a]

	$\lambda_{fl,peak}$ (nm)	φ[b]
1	461	0.27
2	-[c]	-[c]
3	447	0.20

[a]Measurement conditions: 1.0 × 10^{-5} M in H_2O:DMSO (9:1), excitation at λ = 330 nm for **1** and **3**. [b]Fluorescence quantum yield. [c]**2** is insoluble in H_2O:DMSO (9:1).

Design of fluorogenic probes

Fluorogenic OFF–ON-type probes for enzymes should be designed carefully to ensure that the fluorescence profiles before and after the enzymatic reaction are different, ideally, non-fluorescence and intensive fluorescence, respectively. On the basis of the structural features of **1**, we expected that its fluorescence

would disappear as a result of peptide derivatization of the amino group, because electron donation by the amino group would be attenuated and the fluorescence push–pull system would be destroyed. To confirm this, we modified **1** to provide a peptidic substrate for an enzyme. The serine protease DPP-4 was used as the test enzyme because its substrate specificity is clear: it hydrolyses the C-terminal of proline or alanine second to the N-terminal of the peptide [18]. Additionally, DPP-4 is a significant biomarker for the progress of diabetes, and several chromogenic or fluorogenic substrates for DPP-4 have been developed [19-21]. We therefore evaluated **1** as a fluorogenic probe for DPP-4 activity using the peptide analogue H-Gly-Pro-**1** as a substrate for DPP-4. The experimental strategy is summarized in Scheme 1; non-fluorescent H-Gly-Pro-**1** is hydrolysed specifically by DPP-4 to release **1**, enabling fluorometric measurements.

Synthesis of the fluorogenic substrate for DPP-4

The synthesis of H-Gly-Pro-**1** is shown in Scheme 2. In the synthesis, N-protected glycine was condensed with proline methyl ester under microwave irradiation. Subsequent hydrolysis of the ester gave N-protected Gly-Pro-OH (**6**). Condensation of dipeptide **6** with **1** was achieved using the corresponding acid chloride. Deprotection of the amino group was achieved by treatment with hydrazine, without disturbing the peptide bond structure, to give H-Gly-Pro-**1**.

DPP-4 activity measurement

The fluorescence spectra of **1** and H-Gly-Pro-**1** were recorded to confirm their fluorescence profiles; the spectra are shown in Figure 3. As expected, H-Gly-Pro-**1** was non-fluorescent because of the modification of the amino group to an amide

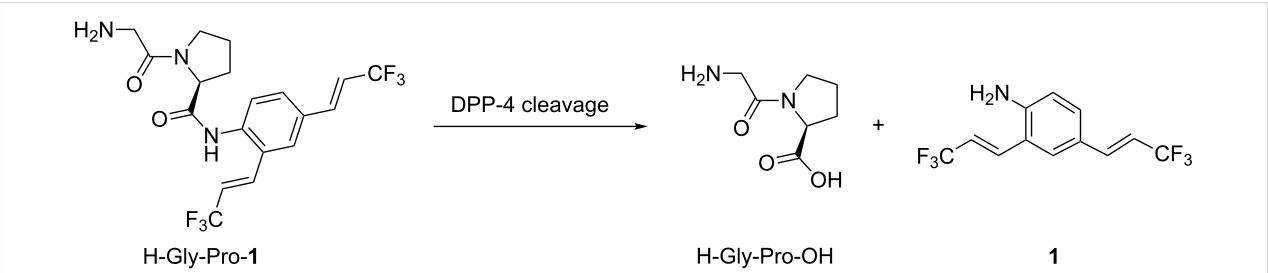

Scheme 1: Use of **1** as fluorogenic probe for DPP-4 activity.

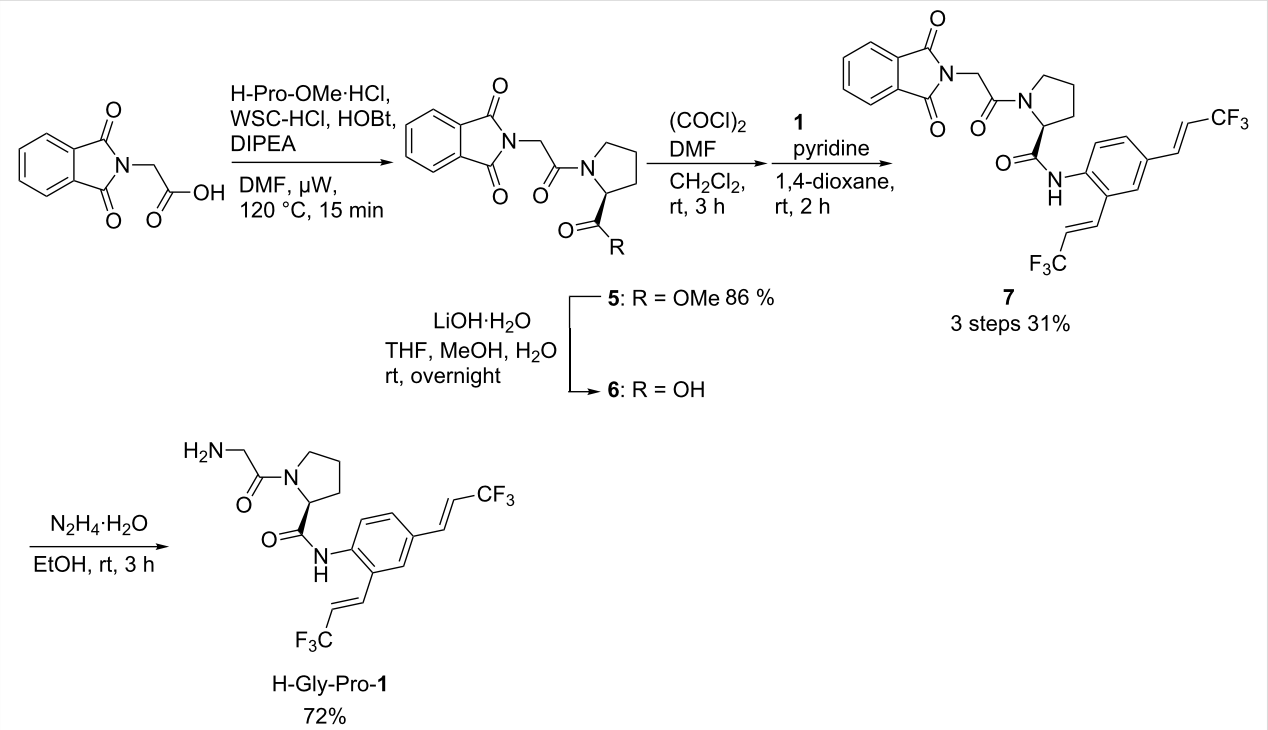

Scheme 2: Synthesis of fluorogenic probe H-Gly-Pro-**1**.

group. The loss of fluorescence is the result of attenuation of the electron-donating effect of the amino group to the benzene ring. In particular, a large difference between the fluorescence emissions of **1** and H-Gly-Pro-**1** at around 460 nm was observed. H-Gly-Pro-**1** can therefore be used as a fluorogenic substrate for DPP-4 to minimize spectral interference from the background state.

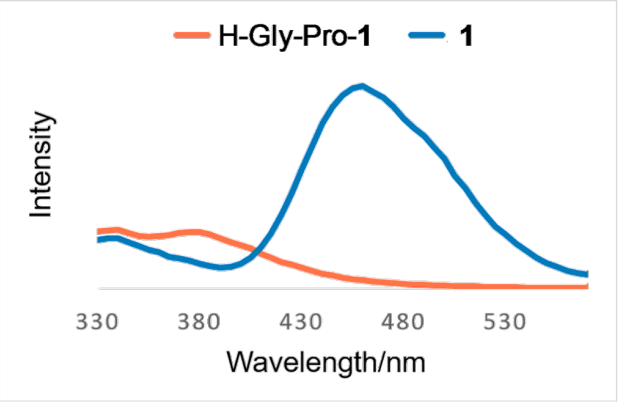

Figure 3: Fluorescence spectra of **1** and H-Gly-Pro-**1**. Measurement conditions: 1.0 × 10^{-5} M in H_2O:DMSO (9:1), excitation at λ = 300 nm.

Next, we determined whether or not DPP-4 could hydrolyse H-Gly-Pro-**1**. The hydrolysis experiments were conducted using H-Gly-Pro-**1** with DPP-4 concentrations of 0.07 and 7.00 μg/mL, and a control. The results are shown in Figure 4. Enzymatic hydrolysis occurred when the DPP-4 concentration was 7.00 μg/mL, as shown by the increased fluorescence intensity as the reaction proceeded. In contrast, hydrolysis was not observed in the absence of DPP-4 (control). The reaction did not proceed at a low concentration of DPP-4 (0.07 μg/mL). These results suggest that H-Gly-Pro-**1** could be used as an OFF–ON-type fluorogenic substrate for enzymatic reactions of DPP-4, with release of **1** as a fluorophore. In comparison with existing fluorogenic substrates containing rhodamine fluorophore, non-fluorescent characteristic of H-Gly-Pro-**1** have negligible background on the fluorometry to permit easy and clear identification of reaction progress. On the other hand, H-Gly-Pro-**1** needs some improvements in terms of the reaction rate for this enzymatic reaction.

Conclusion

We synthesized the small fluorescent compounds **1**–**4**. Among them, **1** showed a good fluorescence profile despite its small size. The use of **1** as a probe was investigated using the derivative H-Gly-Pro-**1** as a fluorogenic substrate for DPP-4. The enzymatic activity of DPP-4 was confirmed by measuring the fluorescence intensity of the reaction medium, in which fluorescent **1** accumulated as the reaction progressed. H-Gly-Pro-**1** behaves as an OFF–ON-type fluorogenic substrate for DPP-4. Further studies of the synthesis of different TFPE-aniline derivatives and fluorogenic substrates for other enzymes are underway.

Experimental

General information

All experiments were carried out under an argon atmosphere in flame-dried glassware using standard inert techniques for introducing reagents and solvents, unless otherwise noted. *N,N*-Dimethylformamide (DMF) was distilled over calcium hydride and stored in a bottle with activated molecular sieves (4 Å). All commercially available materials were used as received without further purification. ^{1}H NMR, ^{13}C NMR and ^{19}F NMR spectra were measured on a JEOL ECZS 400S spectrometer (^{1}H: 400MHz, ^{13}C: 100 MHz, ^{19}F: 376 MHz). Chemical shifts of ^{1}H NMR and ^{13}C NMR are reported in parts per million from tetramethylsilane (TMS), used as an internal standard at

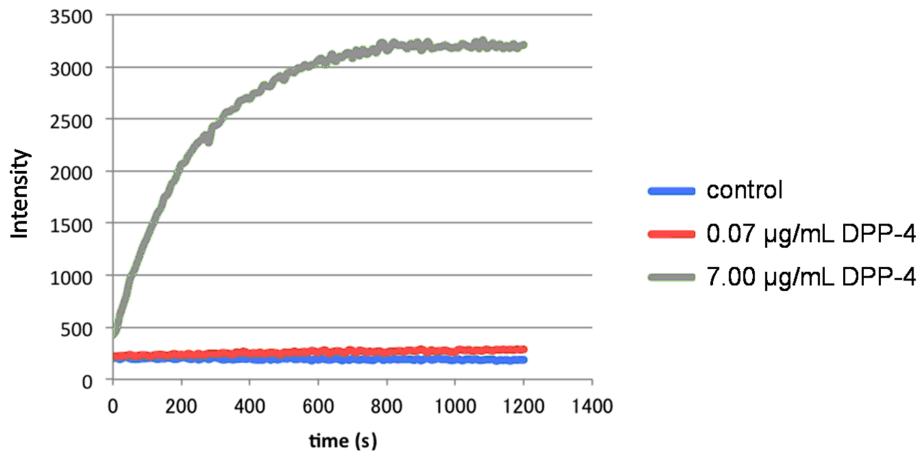

Figure 4: Fluorescence intensity changes of H-Gly-Pro-**1** on addition of DPP-4.

0 ppm. Chemical shifts of ^{19}F NMR are reported in parts per million from trichlorofluoromethane ($CFCl_3$), used as an internal standard at 0 ppm. All dates are reported as follows: chemical shifts, relative integration value, multiplicity (s = singlet, d = doublet, t = triplet, q = quartet, m = multiplet), and coupling constants (Hz). High-resolution mass spectroscopy (HRMS) experiments were performed with a double-focusing mass spectrometer with EI. Melting points were measured on Yanaco melting point apparatus MP-500V without correction. Microwave reactions were performed in microwave tubes with clip lids using a Biotage Initiator microwave reactor.

Typical procedure for the Hiyama cross-coupling reaction

Analogous as described in [24]. In a glovebox purged with argon gas, iodo aniline (1.0 mmol), (2-methylallyl)palladium(II) (0.1 mmol), CuF_2 (2.0 mmol), and 2,2'-bipyridyl (2.0 mmol) were placed in a flask. To the flask were added anhydrous DMF (6.0 mL) and (*E*)-trimethyl(3,3,3-trifluoroprop-1-enyl)silane (2.0 mmol), and mixture was stirred at 80 °C. After the reaction mixture was stirred for 4 h, it was poured into ice water. The mixture was extracted with CH_2Cl_2, and the organic layer was dried over anhydrous $MgSO_4$. After the solid was filtered, the solvent was removed in vacuo, and the residue was purified by silica gel column chromatography to give product.

2,4-Bis[(*E*)-3,3,3-trifluoroprop-1-enyl]aniline (1): The title product was purified by column chromatography and was obtained in 89% yield (251 mg). A light yellow solid: mp 106–107 °C (recrystallized from AcOEt and hexane); ^1H NMR ($CDCl_3$) δ 4.05 (s, 2H), 6.04 (qd, *J* = 6.6, 16.2 Hz, 1H), 6.19 (qd, *J* = 6.5, 15.8 Hz, 1H), 6.72 (d, *J* = 8.2 Hz, 1H), 7.03 (qd, *J* = 2.1, 16.2 Hz, 1H), 7.20 (qd, *J* = 2.1, 15.8 Hz, 1H), 7.30 (dd, *J* = 1.8, 8.2 Hz, 1H), 7.36 (d, *J* = 1.8 Hz, 1H); ^{13}C NMR ($CDCl_3$) δ 112.9 (q, *J* = 33.7 Hz), 116.8, 117.9 (q, *J* = 33.7 Hz), 119.2, 123.3 (q, *J* = 269.4 Hz), 123.9 (q, *J* = 269.4 Hz), 124.4, 127.9, 132.7 (q, *J* = 6.7 Hz), 136.8 (q, *J* = 6.7 Hz), 146.3; ^{19}F NMR ($CDCl_3$) δ 89.84 (dd, *J* = 2.2, 6.5 Hz, 3F), 90.47 (dd, *J* = 2.2, 6.5 Hz, 3F); MS *m*/*z*: M^+ 281, 242, 211; HRMS *m*/*z*: M^+ calcd for $C_{12}H_9F_6N$, 281.0639; found, 281.0634.

2,4,6-Tris((*E*)-3,3,3-trifluoroprop-1-en-1-yl)aniline (2): The title product was purified by column chromatography and was obtained in 54% yield (203 mg). A light yellow solid: mp 119–120 °C (recrystallized from AcOEt and hexane); ^1H NMR ($CDCl_3$) δ 4.20 (s, 2H), 6.11 (qd, *J* = 6.5, 16.0 Hz, 1H), 6.20 (qd, *J* = 6.4, 16.0 Hz, 2H), 7.05 (qd, *J* = 2.1, 16.0 Hz, 1H), 7.21 (qd, *J* = 2.1, 16.0 Hz, 2H), 7.40 (s, 2H); ^{13}C NMR ($CDCl_3$) δ 114.1 (q, *J* = 34.0 Hz), 119.8 (q, *J* = 33.6 Hz), 121.1, 123.0 (q, *J* = 269.4 Hz), 124.3, 124.7 (q, *J* = 269.2 Hz), 128.7, 132.3 (q, *J* = 6.8 Hz), 136.2 (q, *J* = 6.7 Hz), 143.9; ^{19}F NMR ($CDCl_3$) δ 89.59 (dd, *J* = 2.2, 6.5 Hz, 6F), 90.24 (dd, *J* = 2.2, 6.5 Hz, 3F); MS *m*/*z*: M^+ 375, 316, 266; HRMS *m*/*z*: M^+ calcd for $C_{15}H_{10}F_9N_3$, 375.0670; found, 375.0668.

4,6-Bis((*E*)-3,3,3-trifluoroprop-1-en-1-yl)-1,3-diaminobenzene (3): The title product was purified by column chromatography and was obtained in 70% yield (183.7 mg). A light brown solid: mp 165–167 °C (recrystallized from AcOEt and hexane); ^1H NMR ($CDCl_3$) δ 3.95 (s, 4H), 6.00 (s, 1H), 6.01 (qd, *J* = 6.6, 16.0 Hz, 2H), 7.09 (qd, *J* = 2.1, 16.0 Hz, 2H), 7.27 (s, 1H); ^{13}C NMR ($CDCl_3$) δ 102.3, 111.4, 113.9 (q, *J* = 33.4 Hz), 123.8 (q, *J* = 268.8 Hz), 128.6, 132.4 (q, *J* = 6.7 Hz), 147.5; ^{19}F NMR ($CDCl_3$) δ 89.83 (dd, *J* = 2.2, 6.5 Hz, 3F), 90.47 (dd, *J* = 2.2, 6.5 Hz, 3F). MS *m*/*z*: M^+ 296, 277, 257, 226, 187; HRMS *m*/*z*: M^+ calcd for $C_{12}H_{10}F_6N_2$, 296.2116; found, 296.0749.

2,4,6-Tris((*E*)-3,3,3-trifluoroprop-1-en-1-yl)-1,3-diaminobenzene (4): The title product was purified by column chromatography and was obtained in 20% yield (78 mg). A orange solid: mp 196 °C (recrystallized from AcOEt and hexane); ^1H NMR ($CDCl_3$) δ 4.12 (s, 4H), 6.04 (qd, *J* = 6.4, 15.9 Hz, 2H), 6.21 (qd, *J* = 6.1, 16.4 Hz, 1H), 7.02 (qd, *J* = 2.0, 16.4 Hz, 1H), 7.11 (qd, *J* = 2.0, 15.9 Hz, 2H), 7.28 (s, 1H); ^{13}C NMR ($CDCl_3$) δ 105.7, 111.1, 115.4 (q, *J* = 33.7 Hz), 122.6 (q, *J* = 270.3 Hz), 123.6 (q, *J* = 269.0 Hz), 124.9 (q, *J* = 33.7 Hz), 128.6, 131.0 (q, *J* = 6.7 Hz), 132.3 (q, *J* = 6.7 Hz), 144.5; ^{19}F NMR ($CDCl_3$) δ 89.18 (dd, *J* = 1.5, 5.8 Hz, 3F), 90.40 (dd, *J* = 1.5, 6.5 Hz, 6F); MS *m*/*z*: M^+ 390, 321; HRMS *m*/*z*: M^+ calcd for $C_{15}H_{11}F_9N_3$, 390.0779; found, 390.0783.

Fluorogenic substrate synthesis

1-[2-(1,3-Dihydro-1,3-dioxo-2*H*-isoindol-2-yl)acetyl]-L-proline methyl ester (5): *N*-Phtaloylglycine (4 mmol), 1-hydroxybenzotriazole (4.4 mmol) and *N*-ethyl-*N*'(3-dimethylaminopropyl)carbodiimide hydrochloride (10 mmol) were placed in a microwave vial. To the microwave vial was added anhydrous DMF (8 mL) and anhydrous *N*,*N*-diisopropylethylamine (20 mmol), and the mixture was stirred at room temperature. After the reaction mixture was stirred for 5 min, to the microwave vial was added L-proline methyl ester hydrochloride (4.8 mmol) and the mixture was heated by microwave irradiation for 20 min at 120 °C. The resulting mixture was quenched with water and extracted with AcOEt. The AcOEt layer was washed with brine and dried over $MgSO_4$. The solvent was removed in vacuo and the residue was purified by column chromatography to give 1-[2-(1,3-dihydro-1,3-dioxo-2*H*-isoindol-2-yl)acetyl]-L-proline methyl ester (**5**) in 86% yield (1.09 g, 3.4 mmol). A white solid: mp 166–167 °C ; ^1H NMR ($CDCl_3$) δ 1.90–2.36 (m, 4H), 3.60–3.83 (m, 5H), 4.40 (d, *J* = 16.5 Hz, 1H), 4.51–4.61 (m, 2H), 7.70–7.73 (m, 2H), 7.85–7.88 (m, 2H); ^{13}C NMR ($CDCl_3$) δ 24.8, 28.9, 39.7,

46.2, 52.3, 59.1, 123.5, 132.2, 134.0, 164.4, 167.8, 172.1; MS *m*/*z*: M^+ 316, 284, 257, 188, 160, 128; HRMS *m*/*z*: M^+ calcd for $C_{16}H_{16}N_2O_5$, 316.3086; found, 316.1051.

(*S*)-*N*-(2,4-Bis((*E*)-3,3,3-trifluoroprop-1-en-1-yl)phenyl)-1-(2-(1,3-dioxo-2*H*-isoindolin-2-yl)acetyl)pyrrolidine-2-carboxamide (7): **5** (2 mmol) and lithium hydroxide (12 mmol) were placed in a flask. To the flask was added THF (4.8 mL), methanol (1.5 mL), water (1.5 mL), and the mixture was stirred overnight at room temperature. The resulting solution was concentrated in vacuo, the residue was diluted with aq HCl and, extracted with $CHCl_3$:EtOH (2:1). The organic layer was washed with brine and dried over $MgSO_4$. The solvent was removed in vacuo to give **6**. To a solution of **6** (1 mmol) in anhydrous CH_2Cl_2 was added oxalyl chloride (2 mmol) and anhydrous DMF (1 drop) at 0 °C, and mixture was stirred at room temperature. After the reaction mixture was stirred for 3 h, it was concentrated in vacuo. To the residue was added **1** (0.3 mmol), anhydrous 1,4-dioxane (3 mL) and, anhydrous pyridine (0.45 mmol), and mixture was stirred at room temperature. After the reaction mixture was stirred for 2 h, it was quenched with sat. $NaHCO_3$ and, extracted with $CHCl_3$. The $CHCl_3$ layer was washed with water and dried over $MgSO_4$. The solvent was removed in vacuo and the residue was purified by column chromatography to give (*S*)-*N*-(2,4-bis((*E*)-3,3,3-trifluoroprop-1-en-1-yl)phenyl)-1-(2-(1,3-dioxo-2*H*-isoindolin-2-yl)acetyl)pyrrolidine-2-carboxamide (**7**) in 31% yield (71.9 mg, 0.12 mmol). A white solid: mp 181–182 °C; ^{1}H NMR ($CDCl_3$) δ 1.87–1.97 (m, 1H), 2.14–2.28 (m, 2H), 2.63–2.67 (m, 2H), 3.58–3.77 (m, 2H), 4.51 (d, *J* = 3.9 Hz, 2H), 4.82 (d, *J* = 7.8 Hz, 1H), 6.11 (qd, *J* = 6.4, 16.0 Hz, 2H), 7.08 (qd, *J* = 2.2, 16.0 Hz, 1H), 7.28 (qd, *J* = 2.1, 16.0 Hz, 1H), 7.44 (d, *J* = 6.6 Hz, 2H), 7.73–7.90 (m, 4H), 8.08 (d, *J* = 9.0 Hz, 1H), 9.46 (s, 1H); ^{13}C NMR ($CDCl_3$) δ 26.3, 29.7, 39.7, 46.9, 61.2, 115.8 (q, *J* = 33.9 Hz), 119.4 (q, *J* = 34.0 Hz), 122.7 (q, *J* = 270.0 Hz), 122.8, 123.5 (q, *J* = 269.0 Hz), 123.8, 125.8, 126.4, 129.9, 132.0, 132.7 (q, *J* = 6.7 Hz), 136.4, 137.6 (q, *J* = 6.8 Hz), 137.6, 167.2, 167.8, 168.5; ^{19}F NMR ($CDCl_3$) δ 89.32 (dd, *J* = 2.2, 6.6 Hz, 3F), 89.54 (dd, *J* = 2.2, 6.4 Hz, 3F); MS *m*/*z*: M^+ 565, 468, 285, 257, 188, 160; HRMS *m*/*z*: M^+ calcd for $C_{27}H_{21}F_6N_3O_4$, 565.1436; found, 595.1437.

***N*-(*S*)-1-(2-Aminoacetyl)-*N*-(2,4-bis((*E*)-3,3,3-trifluoroprop-1-en-1-yl)phenyl)pyrrolidine-2-carboxamide (H-Gly-Pro-1)**: To solution of **7** (0.05 mmol) in ethanol was added hydrazine hydrate (0.05 mmol), and mixture was stirred for 3 h at room temperature. The resulting precipitate was filtered, then the filtrate was concentrated in vacuo and the residue was purified by column chromatography to give *N*-(*S*)-1-(2-aminoacetyl)-*N*-(2,4-bis((*E*)-3,3,3-trifluoroprop-1-en-1-yl)phenyl)py-rolidine-2-carboxamide (H-Gly-Pro-**1**) in 72% yield (15.7 mg, 0.036 mmol). A light yellow solid: mp 129–130 °C; ^{1}H NMR (DMSO-d_6) δ 1.90–2.25 (m, 4H), 3.51–3.80 (m, 2H), 4.56 (d, *J* = 8.3 Hz), 6.75–6.95 (m, 2H), 7.21–7.53 (m, 4H), 7.75 (d, *J* = 8.2 Hz), 8.20 (s, 1H); ^{13}C NMR (DMSO-d_6) δ 24.8, 26.7, 46.2, 60.6, 70.3, 116.2 (q, *J* = 33.6 Hz), 117.2 (q, *J* = 33.3 Hz), 124.3 (q, *J* = 269.0 Hz), 124.6 (q, *J* = 269.0 Hz), 126.6, 127.2, 128.7, 130.4, 131.2, 134.1 (q, *J* = 7.0 Hz), 137.6 (q, *J* = 7.0 Hz), 138.4, 171.4; ^{19}F NMR (DMSO-d_6) δ 80.80 (dd, *J* = 2.2, 7.2 Hz, 3F), 80.91 (dd, *J* = 2.2, 7.2 Hz, 3F); MS *m*/*z*: M^+ 435, 281, 242, 174, 155, 127; HRMS *m*/*z*: M^+ calcd for $C_{19}H_{19}F_6N_3O_2$, 435.3635; found, 435,1382.

Assay of dipeptidyl peptidase activity using H-Gly-Pro-1 as a substrate

Stenotrophomonas dipeptidyl aminopeptidase IV was prepared from the E. coli DH5 containing pUC19-SDP4 as described previously [22]. The enzyme activity was assayed using H-Gly-Pro-**1** as a substrate following the procedure described previously [23]. The reaction mixture (total 100 μL) contained 0.1 M Tris–HCl (pH 8.0), 10–50 μM substrate and 10–400 ng of the enzyme. The reaction was initiated by the addition of the enzyme solution. Following incubation at 37 °C for 5 min in a 96-well plate inside a SH-9000 plate reader (Corona electric, Japan), the amount of **1** liberated was determined fluorometrically. The excitation and emission wavelengths used were 300 nm and 460 nm for **1**, respectively. The reaction velocities (μmol/min/mg protein) were compared.

Acknowledgements

We thank Helen McPherson, PhD, from Edanz Group (http://www.edanzediting.com/ac) for editing a draft of this manuscript.

ORCID® iDs

Keita Tani - https://orcid.org/0000-0002-9449-8406

References

1. Yang, Y.; Zhao, Q.; Feng, W.; Li, F. *Chem. Rev.* **2013,** *113,* 192–270. doi:10.1021/cr2004103
2. Lee, M. H.; Yang, Z.; Lim, C. W.; Lee, Y. H.; Dongbang, S.; Kang, C.; Kim, J. S. *Chem. Rev.* **2013,** *113,* 5071–5109. doi:10.1021/cr300358b
3. Yuan, L.; Lin, W.; Zheng, K.; Zhu, S. *Acc. Chem. Res.* **2013,** *46,* 1462–1473. doi:10.1021/ar300273v
4. Asanuma, D.; Sakabe, M.; Kamiya, M.; Yamamoto, K.; Hiratake, J.; Ogawa, M.; Kosaka, N.; Choyke, P. L.; Nagano, T.; Kobayashi, H.; Urano, Y. *Nat. Commun.* **2015,** *6,* No. 6463. doi:10.1038/ncomms7463
5. Kamiya, M.; Asanuma, D.; Kuranaga, E.; Takeishi, A.; Sakabe, M.; Miura, M.; Nagano, T.; Urano, Y. *J. Am. Chem. Soc.* **2011,** *133,* 12960–12963. doi:10.1021/ja204781t
6. Gu, K.; Xu, Y.; Li, H.; Guo, Z.; Zhu, S.; Zhu, S.; Shi, P.; James, T. D.; Tian, H.; Zhu, W.-H. *J. Am. Chem. Soc.* **2016,** *138,* 5334–5340. doi:10.1021/jacs.6b01705

7. Cecioni, S.; Vocadlo, D. J. *J. Am. Chem. Soc.* **2017,** *139,* 8392–8935. doi:10.1021/jacs.7b01948
8. Zhang, H.; Fan, J.; Wang, J.; Zhang, S.; Dou, B.; Peng, X. *J. Am. Chem. Soc.* **2013,** *135,* 11663–11669. doi:10.1021/ja4056905
9. Jia, Y.; Li, P.; Song, W.; Zhao, G.; Zheng, D.; Li, D.; Wang, Y.; Wang, J.; Li, C.; Han, K. *ACS Appl. Mater. Interfaces* **2016,** *8,* 25818–25824. doi:10.1021/acsami.6b09190
10. Shin, N.; Hanaoka, K.; Piao, W.; Miyakawa, T.; Fujisawa, T.; Takeuchi, S.; Takahashi, S.; Komatsu, T.; Ueno, T.; Terai, T.; Tahara, T.; Tanokura, M.; Nagao, T.; Urano, Y. *ACS Chem. Biol.* **2017,** *12,* 558–563. doi:10.1021/acschembio.6b00852
11. Wang, Y.; Li, J.; Feng, L.; Yu, J.; Zhang, Y.; Ye, D.; Chen, H.-Y. *Anal. Chem.* **2016,** *88,* 12403–12410. doi:10.1021/acs.analchem.6b03717
12. Luo, Z.; Feng, L.; An, R.; Duan, G.; Yan, R.; Shi, H.; He, J.; Zhou, Z.; Ji, C.; Chen, H.-Y.; Ye, D. *Chem. – Eur. J.* **2017,** *23,* 14778–14785. doi:10.1002/chem.201702210
13. Arian, D.; Harenberg, J.; Krämer, R. *J. Med. Chem.* **2016,** *59,* 7576–7583. doi:10.1021/acs.jmedchem.6b00652
14. Li, X.; Gao, X.; Shi, W.; Ma, H. *Chem. Rev.* **2014,** *114,* 590–659. doi:10.1021/cr300508p
15. Shimizu, M.; Takeda, Y.; Higashi, M.; Hiyama, T. *Chem. – Asian J.* **2011,** *6,* 2536–2544. doi:10.1002/asia.201100176
16. Shimizu, M.; Takeda, Y.; Higashi, M.; Hiyama, T. *Angew. Chem., Int. Ed.* **2009,** *48,* 3653–3656. doi:10.1002/anie.200900963
17. Beppu, T.; Tomiguchi, K.; Masuhara, A.; Pu, Y.-J.; Katagiri, H. *Angew. Chem., Int. Ed.* **2015,** *54,* 7332–7335. doi:10.1002/anie.201502365
18. Hopsu-Have, V. K.; Glenner, G. G. *Histochemie* **1966,** *7,* 197–201. doi:10.1007/BF00577838
19. Röhrborn, D.; Wronkowitz, N.; Eckel, J. *Front. Immunol.* **2015,** *6,* 386. doi:10.3389/fimmu.2015.00386
20. Boonacker, E.; Elferink, S.; Bardai, A.; Fleischer, B.; Van Noorden, C. J. F. *J. Histochem. Cytochem.* **2003,** *51,* 959–968. doi:10.1177/002215540305100711
21. Ho, N.-H.; Weissleder, R.; Tung, C.-H. *Bioorg. Med. Chem. Lett.* **2006,** *16,* 2599–2602. doi:10.1016/j.bmcl.2006.02.045
22. Nakajima, Y.; Ito, K.; Toshima, T.; Egawa, T.; Zheng, H.; Oyama, H.; Wu, Y.-F.; Takahashi, E.; Kyono, K.; Yoshimoto, T. *J. Bacteriol.* **2008,** *190,* 7819–7829. doi:10.1128/JB.02010-07
23. Mustafa, M. S. M.; Nakajima, Y.; Oyama, H.; Iwata, N.; Ito, K. *Biol. Pharm. Bull.* **2012,** *35,* 2010–2016. doi:10.1248/bpb.b12-00544
24. Omote, M.; Tanaka, M.; Tanaka, M.; Ikeda, A.; Tarui, A.; Sato, K.; Ando, A. *J. Org. Chem.* **2013,** *78,* 6196–6201. doi:10.1021/jo400859s

License and Terms

BEILSTEIN JOURNAL OF ORGANIC CHEMISTRY

CF_3SO_2X (X = Na, Cl) as reagents for trifluoromethylation, trifluoromethylsulfenyl-, -sulfinyl- and -sulfonylation. Part 1: Use of CF_3SO_2Na

Hélène Guyon, Hélène Chachignon and Dominique Cahard*

Full Research Paper

Open Access

Address:
UMR 6014 CNRS COBRA, Normandie Université, 1 rue Tesnière, 76821 Mont Saint Aignan, France

Email:
Dominique Cahard* - dominique.cahard@univ-rouen.fr

* Corresponding author

Keywords:
fluorine; sulfur; trifluoromethylation; trifluoromethylsulfenylation; trifluoromethylsulfonylation

Beilstein J. Org. Chem. **2017,** *13,* 2764–2799.
doi:10.3762/bjoc.13.272

Received: 20 September 2017
Accepted: 15 November 2017
Published: 19 December 2017

This article is part of the Thematic Series "Organo-fluorine chemistry IV".

Guest Editor: D. O'Hagan

Abstract

Sodium trifluoromethanesulfinate, CF_3SO_2Na, and trifluoromethanesulfonyl chloride, CF_3SO_2Cl, are two popular reagents that are widely used for the direct trifluoromethylation of a large range of substrates. Further, these two reagents are employed for the direct trifluoromethylsulfenylation and trifluoromethylsulfinylation, the introduction of the SCF_3 and the $S(O)CF_3$ group, respectively. In addition to the aforementioned reactions, the versatility of these two reagents is presented in other reactions such as sulfonylation and chlorination. This first part is dedicated to sodium trifluoromethanesulfinate.

Introduction

In organofluorine chemistry, the CF_3 group occupies a place of choice as privileged structural motif in the development of multifaceted catalysts and ligands for organic synthesis as well as in the design of pharmaceuticals, agrochemicals and specialty materials [1-4]. The trifluoromethyl group is most of the time linked to a carbon atom but can also be encountered with chalcogens (S, Se, O) and nitrogen. The CF_3S motif, which was till recently considered as an emerging substituent, is henceforth a tamed substituent as a result of abundant literature describing methods to prepare CF_3S-featuring molecules [5]. Its oxidised congeners $CF_3S(O)$ and CF_3SO_2 are also well-developed as structural units in biologically active compounds, catalysts for synthesis, and functional materials. The chemistry of CF_3Se derivatives is less developed but basically shares the same synthetic approaches with CF_3S analogues [6,7]. The CF_3O group is also of high interest but difficulties still exist to easily introduce this motif directly onto organic molecules [8]. The reasons behind such massive interest for the CF_3 group are due to the specific physical and chemical properties of the compounds that contain it. The CF_3 group has a large van der Waals volume somewhere between those of the iPr and the *t*-Bu groups [9]. Its electronegativity is comparable to that of oxygen

(4.0 versus 3.5 on the Pauling scale) and its hydrophobicity is large (0 for H, 0.51 for Me, and 1.07 for CF_3) [10]. In this respect, judicious installation of CF_3 group(s) in catalysts or ligands is an effective tool to tune their reactivity and selectivity in synthesis. As a pharmacophore, CF_3 substantially improves the catabolic stability, lipophilicity, and transport rate. In association with chalcogens (OCF_3, SCF_3, $SeCF_3$), the CF_3 group imparts enhanced lipophilicity of aromatic compounds in comparison with aryl–CF_3 analogues (Hansch's hydrophobic parameter $\pi(SCF_3) = 1.44$; $\pi(OCF_3) = 1.04$ versus $\pi(CF_3) = 0.88$). Trifluoromethyl sources are manifold displaying nucleophilic, electrophilic or radical reactivities [11]. The most popular nucleophilic trifluoromethylating reagent is certainly the trifluoromethyltrimethylsilane, CF_3SiMe_3, known as the Ruppert–Prakash reagent discovered in 1984 by Ruppert and applied for trifluoromethylation in 1989 by Prakash and Olah. More recently, renewed investigation on the use of fluoroform, CF_3H, as an ideal source of trifluoromethide offered new horizons for atom-economical, low-cost trifluoromethylation reactions. With regard to electrophilic CF_3 donors, *S*-(trifluoromethyl)sulfonium salts developed by Yagupolskii and Umemoto and hypervalent iodine(III)-CF_3 reagents developed by Togni are widely employed in a variety of trifluoromethylation reactions [12]. Traditional radical CF_3 sources include the gaseous trifluoroiodomethane CF_3I and trifluorobromomethane CF_3Br. More conveniently, the liquid trifluoromethanesulfonyl chloride CF_3SO_2Cl and the solid sodium trifluoromethanesulfinate CF_3SO_2Na that are commercially available at reasonable prices, are easy-to-handle sources of trifluoromethyl radicals. Remarkably, CF_3SO_2Na and CF_3SO_2Cl are multi-purpose reagents since they not only act as CF_3 donors by extrusion of SO_2, but also, under certain reaction conditions, the sulfur atom is retained for trifluoromethylsulfenylation (also named trifluoromethylthiolation), trifluoromethylsulfinylation, or trifluoromethylsulfonylation reactions. Typically, CF_3SO_2Na reacts under oxidative conditions whereas CF_3SO_2Cl requires reductive conditions. The advent of a new dynamism and the versatility of these two reagents have been recently demonstrated through several creative research articles; hence, this review aims to collect the recent progresses in the diverse uses of CF_3SO_2Na and CF_3SO_2Cl reagents. A special emphasis is placed on mechanistic studies. The review is divided in Part 1 and Part 2 that are published back-to-back. The literature is comprehensively covered through July 2017.

Review

Sodium trifluoromethanesulfinate (alternate names: sodium triflinate, trifluoromethanesulfinic acid sodium salt, Langlois reagent), CAS No. 2926-29-6, MW 156.06, is a stable white solid (mp 350 °C) soluble in water and slightly soluble in acetonitrile, methanol and acetone [13]. Although this reagent was prepared in 1955 by Haszeldine [14] and in 1976 by Roesky [15], it is only in 1991 that Langlois reported the trifluoromethylation of aromatic compounds under oxidative conditions [16]. Since then, the use of CF_3SO_2Na has grown considerably for the creation of C_{sp3}–CF_3, C_{sp2}–CF_3 and C_{sp}–CF_3 bonds [17-19]. This reagent is also conveniently used in trifluoromethylsulfinylation and trifluoromethylsulfonylation reactions. More recently, from 2015, CF_3SO_2Na has found a new application as source of SCF_3 for direct trifluoromethylsulfenylation.

1 Trifluoromethylation

C_{sp3}–CF_3 bond-forming reactions

Synthesis of α-trifluoromethyl ketones from alkenes: After their original reports on the trifluoromethylation of aromatics (see later in the text, Scheme 34) [16] and disulfides (Scheme 69) [20], Langlois and co-workers demonstrated that enol acetates **1a**–**c** were converted into the corresponding α-trifluoromethyl ketones upon treatment with CF_3SO_2Na with *tert*-butyl hydroperoxide (TBHP) and a catalytic amount of copper(II) triflate (Scheme 1) [21]. The scope was rather narrow and yields were moderate to poor. In particular, enol acetate **1b**, prepared from symmetrical undecan-6-one, gave a mixture of the desired α-CF_3 ketone and two isomeric enol acetates **1b'**. In 2014, Li, Duan and co-workers applied the conditions described by Langlois to a series of enol acetates **3** derived from aryl and heteroaryl ketones featuring a single enolizable position (Scheme 2) [22]. Notably, it was found that Cu(II) and Cu(I) salts gave similar yields. A radical trifluoromethylation was suggested for this transformation. The $CF_3^{\bullet}$, which was generated by reaction of *tert*-butyl hydroperoxide with CF_3SO_2Na in the presence of copper(I), reacted at the more electron-rich carbon atom of the C=C double bond to give the radical species **5** that was oxidised by copper(II) into the corresponding cationic intermediate **6** via a single electron transfer (SET). Finally, the acetyl cation was eliminated to provide the α-CF_3 carbonyl compound **4** (Scheme 3).

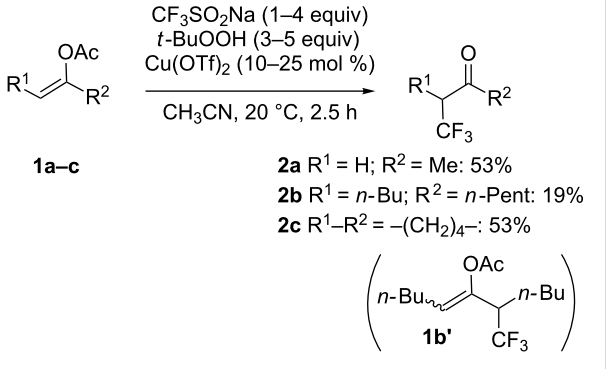

Scheme 1: Trifluoromethylation of enol acetates by Langlois.

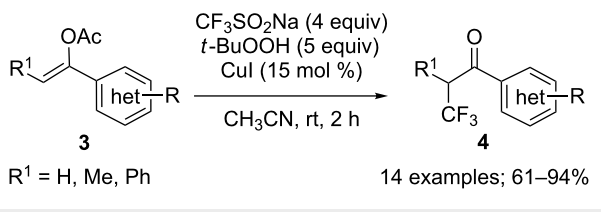

Scheme 2: Trifluoromethylation of (het)aryl enol acetates.

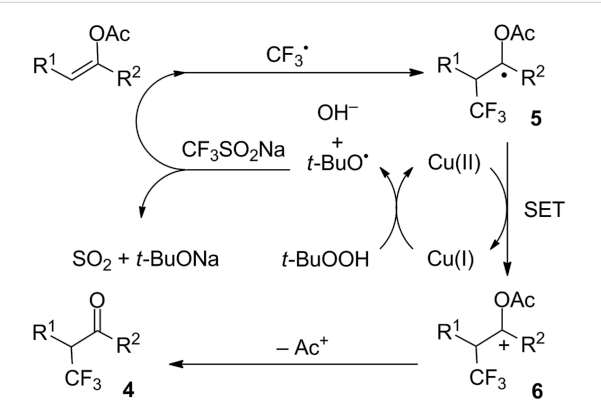

Scheme 3: Mechanism for the trifluoromethylation of enol acetates.

Unactivated olefins are widely available substrates prone to be transformed into α-trifluoromethyl carbonyl compounds under oxidative trifluoromethylation as first reported by Maiti and co-workers in 2013. The reaction is operationally simple, conducted under air at room temperature and presents a predictable reactivity pattern as well as a wide functional group tolerance. The substrate scope was evaluated on 33 styrenes, β-substituted styrenes, heteroaromatic olefins and vinyl cycloalkanes (Scheme 4). The trifluoromethyl radical was generated from CF_3SO_2Na by means of an oxidative system comprising catalytic amounts of silver(I) nitrate and potassium persulfate $K_2S_2O_8$. Both atmospheric oxygen and $K_2S_2O_8$ can be the source of the oxygen atom of the ketone moiety. A series of experiments that include the formation of TEMPO–CF_3 (TEMPO: 2,2,6,6-tetramethylpiperidine 1-oxyl), the detection of Ag(0) by X-ray photoelectron spectroscopy, the retardation of the reaction in absence of air and an ^{18}O-labeling reaction led the authors to propose the mechanism described in Scheme 4 [23].

Because some limitations appeared with heterocycles such as quinolone, indole, pyrimidine, thiophene, etc. the Maiti group reported an alternative approach toward α-trifluoromethyl ketones starting from (hetero)arylacetylenes **7** and also aliphatic terminal alkynes **8** (Scheme 5) [24]. The trifluoromethyl radical was generated from CF_3SO_2Na as indicated earlier, oxygen from air was the source of the oxygen atom, and *N*-methylpyrrolidine (NMP) acted as solvent and source of the hydrogen atom to convert the peroxo intermediate **9** to its hydroperoxo form **10**. As proof of the mechanism, *N*-methylsuccinimide (**11**) was identified in all these reactions.

Simultaneously to Maiti's work, Luo and co-workers reported a metal-free protocol for the trifluoromethylation of styrenes with CF_3SO_2Na, *tert*-butyl hydroperoxide and benzoquinone (BQ) as oxidant. The reactions were run at 80 °C for 16 h to give mixtures of α-trifluoromethyl ketones **12** and the corresponding alcohols **13** (Scheme 6) [25]. The scope was limited to simple substituted styrenes and yields were only moderate although super-stoichiometric amounts of reagents were used. The ratio **12**/**13** ranged from 31:69 to 66:34 but a subsequent reduction or

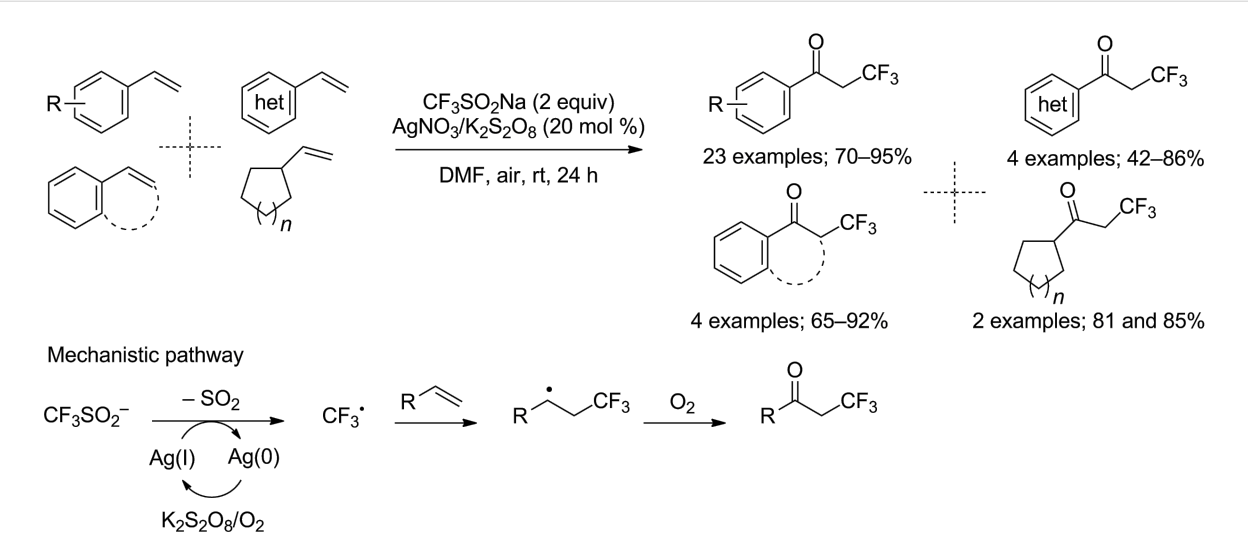

Scheme 4: Oxidative trifluoromethylation of unactivated olefins and mechanistic pathway.

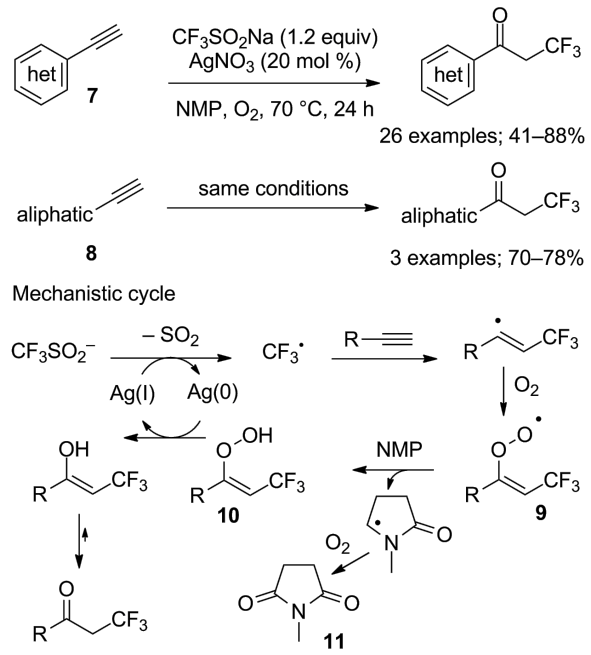

Scheme 5: Oxidative trifluoromethylation of acetylenic substrates.

oxidation allowed to access either the alcohol or the ketone exclusively.

The use of transition metal catalysts and/or a large excess of organic oxidants can be obstacles to production. In a quest for ideal conditions, Lei and co-workers exposed heteroatom-functionalised alkenes **14** to aerobic C_{vinyl}–heteroatom bond oxygenation under metal-free conditions, where oxygen from air worked in concert with a catalytic amount of potassium persulfate to activate CF_3SO_2Na (Scheme 7) [26]. The heteroatom must be a good leaving group or part of it (X = Br, Cl, NHCOMe, N_3, $OP(O)(OEt)_2$). A mechanistic investigation demonstrated the role of oxygen: 93% isotopic purity of the ketone product was obtained when using $^{18}O_2$; no reaction occurred under N_2 instead of O_2; $K_2S_2O_8$ rather than O_2 served as initiator; the radical $CF_3SO_2^•$ could either extrude SO_2 to $CF_3^•$ or react with O_2 to re-initiate the radical chain process (Scheme 7).

Vinyl azides were used by Liu and co-workers as precursors of α-trifluoromethylated ketones by reaction of CF_3SO_2Na under photoredox catalysis. The substrate scope was broad and the reaction proceeded with high functional group tolerance;

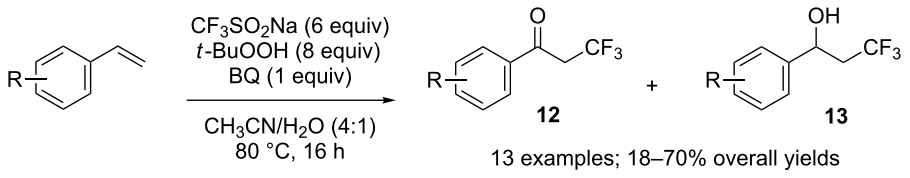

Scheme 6: Metal free trifluoromethylation of styrenes.

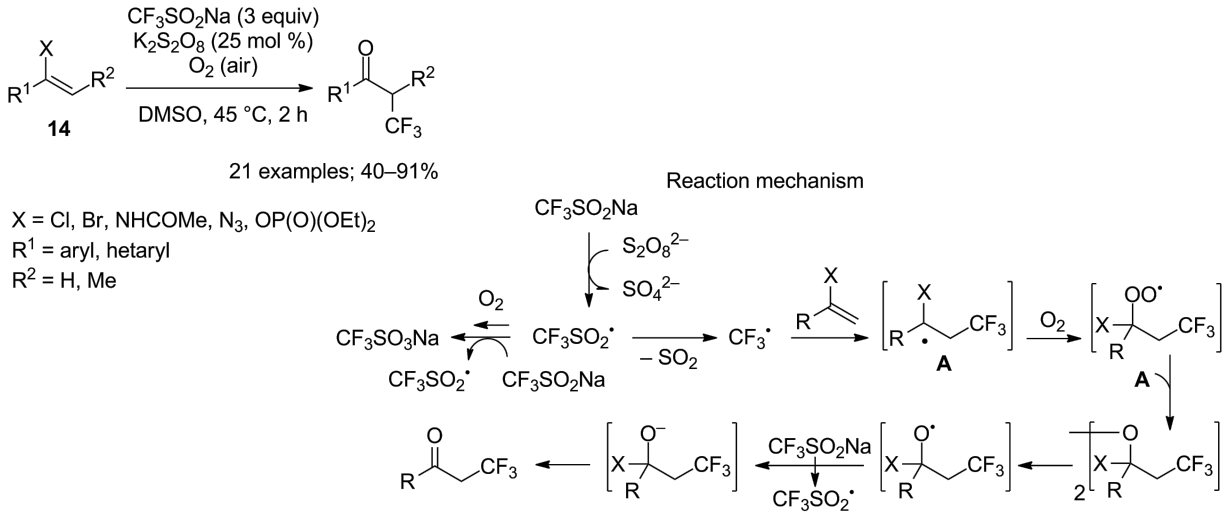

Scheme 7: Synthesis of α-trifluoromethylated ketones by oxytrifluoromethylation of heteroatom-functionalised alkenes.

indeed, aryl-, alkyl-, hetero-functionalised terminal as well as non-terminal vinyl azides **15** were compatible with the reaction conditions. In the presence of the organic photocatalyst *N*-methyl-9-mesitylacridinium (**17**), CF_3SO_2Na was converted into $CF_3^•$ upon visible-light irradiation. The $CF_3^•$ radical reacted with the vinyl azide to give the iminyl radical **18** that was reduced by Mes-Acr$^•$ (Mes-Acr: 9-mesityl-10-methylacridinium) into the iminyl anion **19**. After protonation and hydrolysis of the imine function, the α-trifluoromethylated ketones **16** were obtained in moderate to good yields (Scheme 8) [27].

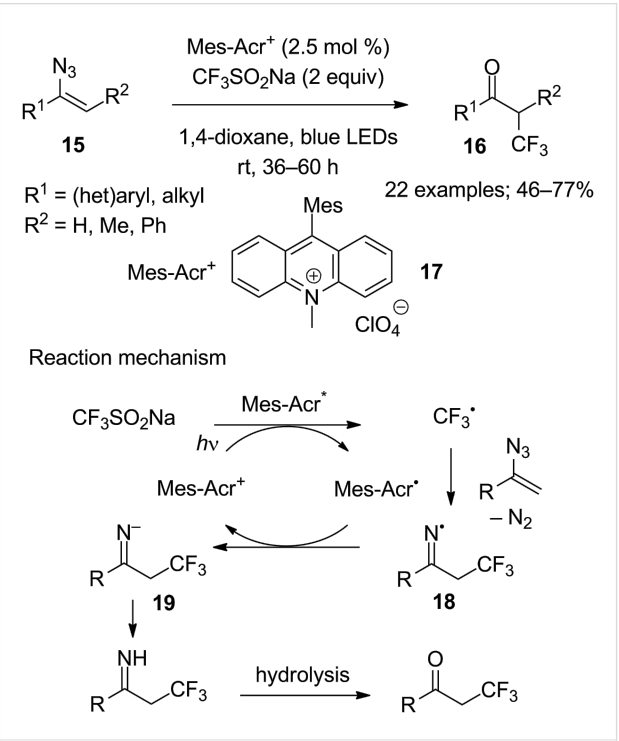

Scheme 8: Catalysed photoredox trifluoromethylation of vinyl azides.

Alkenyl MIDA (*N*-methylimidodiacetic) boronates **20**, as functionalised alkenes, were transformed into α-trifluoromethyl-α-boryl ketones **21** by oxidative trifluoromethylation with CF_3SO_2Na. In that case, 2-iodoxybenzoic acid (IBX) was used as the oxidant to generate the trifluoromethylated radical **22** and atmospheric oxygen was the oxygen source to form the ketone (Scheme 9) [28].

Synthesis of β-trifluoromethyl ketones from cyclopropanols: Moving away the CF_3 group by one carbon atom further from the carbonyl function would provide the corresponding β-trifluoromethyl ketones. For this aim, distally trifluoromethyl ketones were synthesised by the ring-opening of cyclopropanol derivatives by means of per- or polyfluorinated sulfonates, including CF_3SO_2Na. Kananovich and co-workers demonstrated that sodium triflinate, under Langlois' conditions, served as a

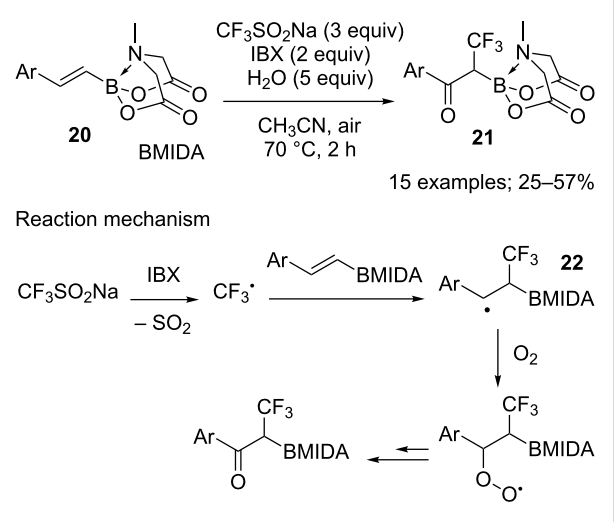

Scheme 9: Oxidative difunctionalisation of alkenyl MIDA boronates.

precursor of trifluoromethyl copper species that were involved in the ring-opening trifluoromethylation of tertiary cyclopropanols **23** (Scheme 10) [29]. The substrate scope was broad allowing access to various β-trifluoromethyl ketones **24** featuring aryl, alkyl, functionalised alkyl, alkenyl, acetal, silylated alcohol, pyran, and piperidine functionalities (R group in **24**). Mechanistic studies by ^{19}F NMR allowed to identify CF_3 complexes of copper(I) and copper(III) and the predominance of an electrophilic pathway (versus SET pathway) was suggested by regioselective trifluoromethylation of a case substrate. Although Cu(II) acetate was used, the authors mentioned that Cu(I) can be formed in situ by reduction with MeOH or the cyclopropanol. Concomitant mechanisms are depicted in Scheme 10.

β-Trifluoromethyl ketones could also be obtained from allylic alcohols **25** by a cascade trifluoromethylation/1,2-aryl migration. Yang, Xia and co-workers employed sodium triflinate under metal-free conditions with ammonium persulfate as the oxidant that was necessary to generate the CF_3 radical (Scheme 11) [30].

Amino- and azotrifluoromethylation of alkenes: Alkene trifluoromethylation was applied to the construction of indole, pyrazole and pyridazinone moieties via a multicomponent cascade reaction developed by Antonchick and Matcha in 2014 [31]. The method was based on the reaction between simple alkenes, sodium triflinate and diazonium salts. The CF_3 radical was produced from CF_3SO_2Na by oxidation with H_2O_2 in the presence of silver nitrate. Then, $CF_3^•$ was added to the terminal position of the alkene to give radical **26** that was trapped by the arenediazonium salt to form the radical cation **27**, which was reduced into **28** prior to be converted into nitrogen heterocycles

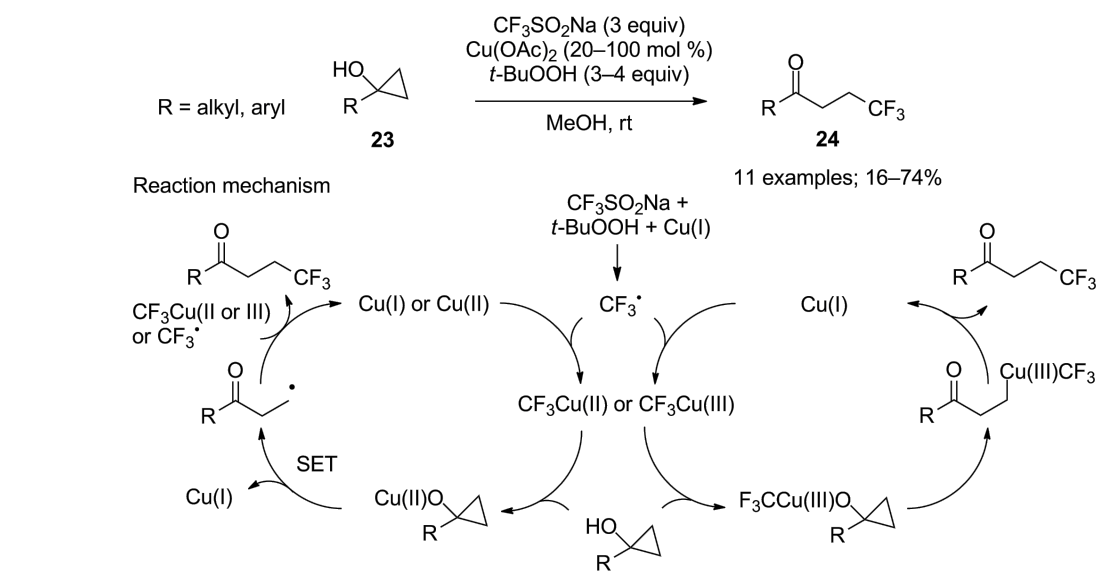

Scheme 10: Synthesis of β-trifluoromethyl ketones from cyclopropanols.

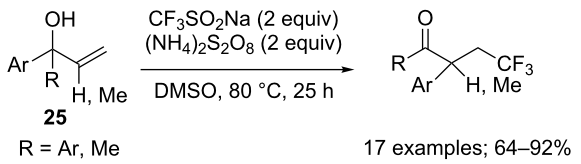

Scheme 11: Aryltrifluoromethylation of allylic alcohols.

via [1,3]-hydride shift and cyclisation steps (Scheme 12). The reaction was regioselective and had a broad scope. This application of alkene trifluoromethylation provided a convenient entry to trifluoromethylated nitrogen heterocycles.

Subsequently, a photoredox-catalysed azotrifluoromethylation of unactivated alkenes was developed by Chen, Xiao and co-workers [32]. The scope was broad for a variety of unactivated alkenes, functionalised or not, and aryldiazonium salts

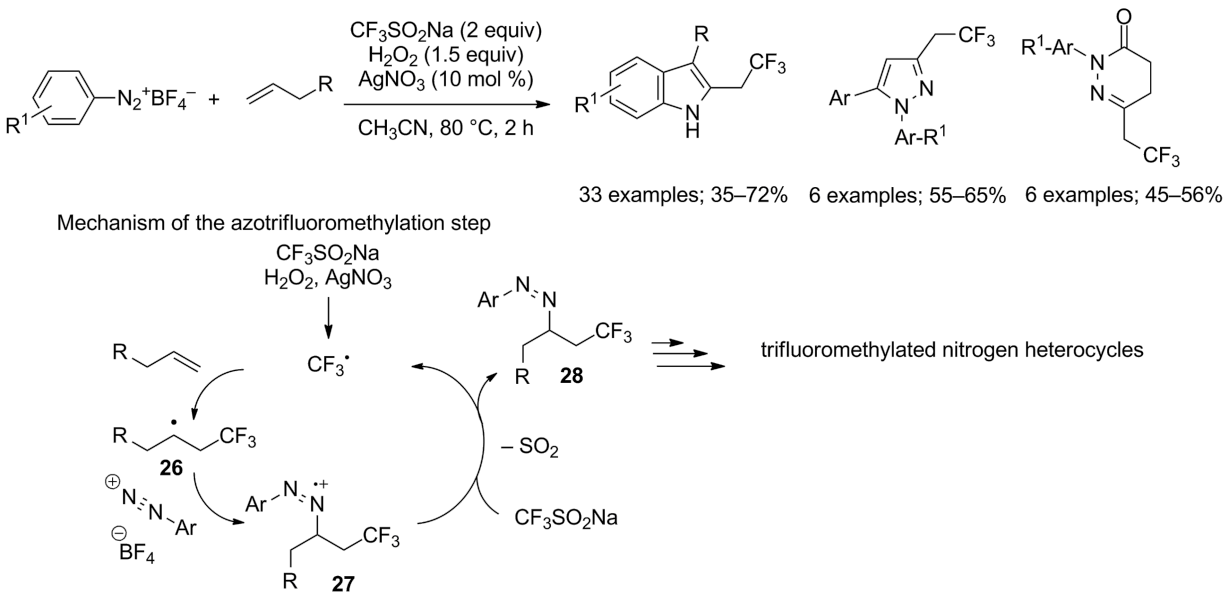

Scheme 12: Cascade multicomponent synthesis of nitrogen heterocycles via azotrifluoromethylation of alkenes.

(Scheme 13). Interestingly, the method did not require stoichiometric amounts of oxidant and further transformation of the azotrifluoromethyl products allowed a Fisher indole synthesis. From a mechanistic point of view, the excited photocatalyst was oxidised by the aryldiazonium salt to produce $[Ru(bpy)_3]^{3+}$ (bpy: 2,2'-bipyridine) as the oxidant to generate the CF_3 radical from CF_3SO_2Na with extrusion of SO_2. Then, $CF_3^{\bullet}$ underwent a radical addition to the alkene to form the radical **29**, which was trapped by the aryldiazonium salt to give the radical cation **30**. Finally, **30** was reduced by $[Ru(bpy)_3]^{2+*}$ to end up with the product **31** (Scheme 13).

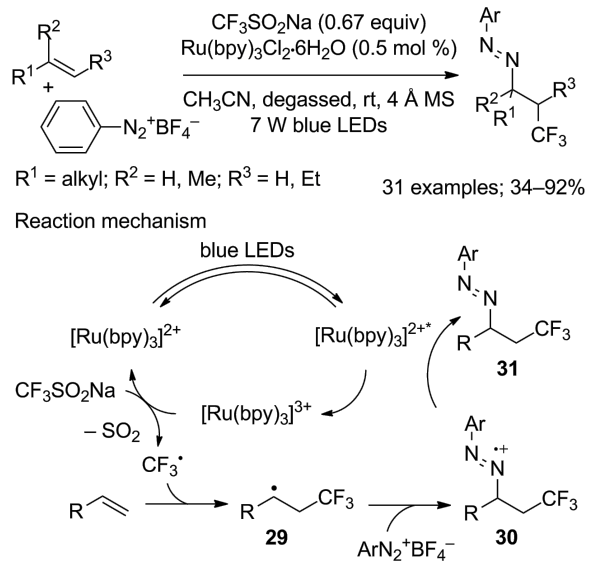

Scheme 13: Photocatalytic azotrifluoromethylation of alkenes with aryldiazonium salts and CF_3SO_2Na.

The aminotrifluoromethylation of alkenes in an intramolecular version was reported by Zhang and co-workers in 2017 (Scheme 14) [33]. Langlois' conditions with *tert*-butyl hydroperoxide and a catalytic amount of copper(II) triflate were used to prepare a series of CF_3-containing indoline, pyrrolidine, lactam and lactone.

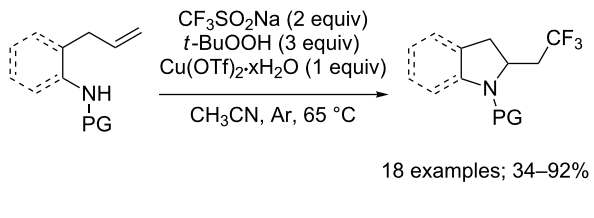

Scheme 14: Copper-promoted intramolecular aminotrifluoromethylation of alkenes with CF_3SO_2Na.

Oxytrifluoromethylation of alkenes: The difunctionalisation of alkenes including a trifluoromethylation step was extended to carbon–oxygen bond formation via oxytrifluoromethylation. We have already described some examples of such a reaction leading to α-trifluoromethyl ketones (vide supra) [26]. Now synthetic routes are presented leading to vicinal trifluoromethyl alcohols. In 2013 Qing and Jiang described the oxytrifluoromethylation of alkenes with hydroxamic acids **32** and CF_3SO_2Na under Langlois' conditions with the couple *t*-BuOOH/copper salt (Scheme 15) [34]. A competitive formation of two radicals, $CF_3^{\bullet}$ and the amidoxyl radical $[ArN(CO_2Me)O^{\bullet}]$ **33**, would lead to two regioisomeric oxytrifluoromethylated products. Fortunately, this issue was solved by the primary formation of the CF_3 radical and thus a regioselective addition. After optimization of the reaction conditions with styrene as model alkene, the method was applied to a wide range of alkenes featuring various functional groups. Further reduction of the N–O bond by $Mo(CO)_6$ gave the corresponding alcohols.

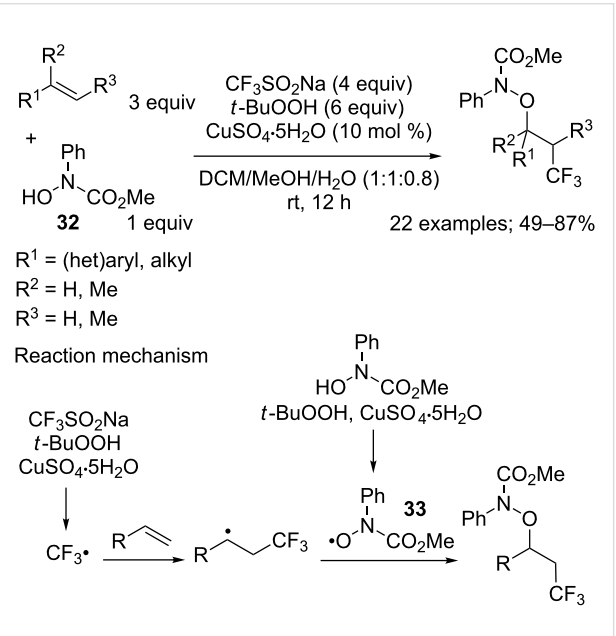

Scheme 15: Oxytrifluoromethylation of alkenes with CF_3SO_2Na and hydroxamic acid.

A protocol free of peroxide initiator was developed by Yang, Vicic and co-workers using a manganese salt and O_2 from air [35]. Styrene derivatives were transformed preferentially into hydroxytrifluoromethylated compounds **34** versus the corresponding ketones **35** in moderate to good selectivities (Scheme 16). In the case of 1,2-disubstituted alkenes, mixtures of *syn*- and *anti*-isomers were obtained. A radical pathway was supported by several observations: (i) addition of TEMPO suppressed the reaction; (ii) an induction period was observed

followed by acceleration with consumption of styrene; (iii) vinyl triflone was detected indicating the formation of $CF_3SO_2^{\bullet}$; (iv) formation of $CF_3SO_3^-$ via oxidation of $CF_3SO_2^{\bullet}$ (Scheme 16).

A metal-free approach with in situ generation of the peroxide from the combination of NMP and O_2 as the radical initiator was proposed by Lei and co-workers [36]. This method was based on a previous work by Maiti (see Scheme 5) [24] but did not require a metal to generate the CF_3 radical. Tertiary β-trifluoromethyl alcohols **36** were obtained in good yields from a variety of di- and trisubstituted alkenes (Scheme 17). Labelling and IR experiments were conducted to investigate the reaction mechanism as well as kinetic studies that revealed the reaction rate dependence on O_2 diffusion.

A case of intramolecular oxytrifluoromethylation of alkenes leading to oxazolines **37** was described by Fu and co-workers in

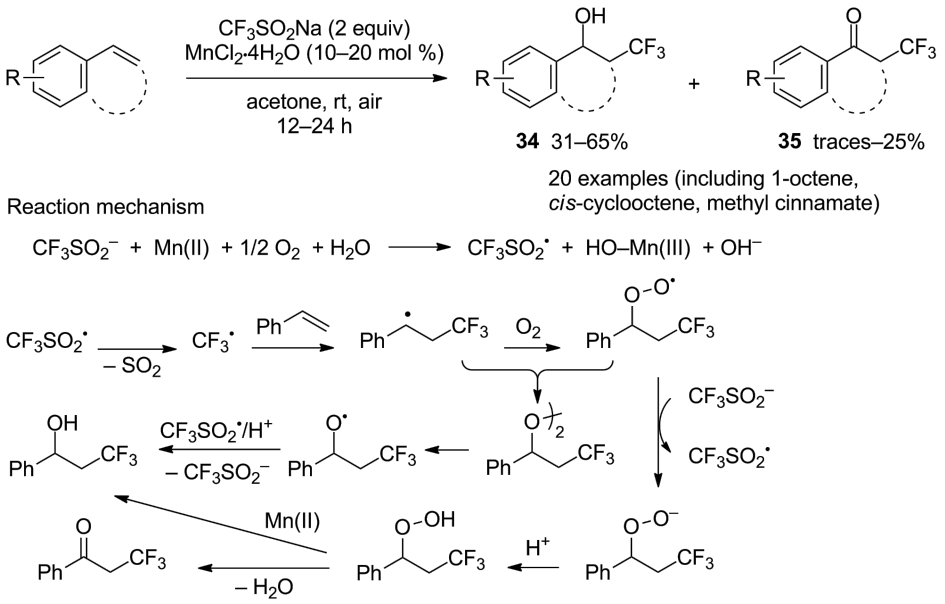

Scheme 16: Manganese-catalysed oxytrifluoromethylation of styrene derivatives.

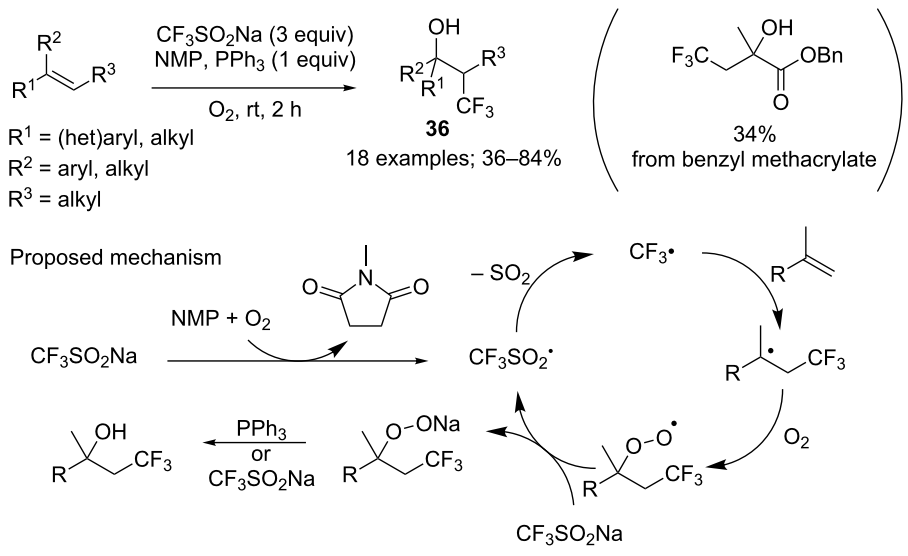

Scheme 17: Oxytrifluoromethylation of alkenes with NMP/O_2 and CF_3SO_2Na.

2014 [37]. In this work iodobenzene diacetate (PIDA) was used as the oxidant to generate the CF_3 radical from CF_3SO_2Na (Scheme 18).

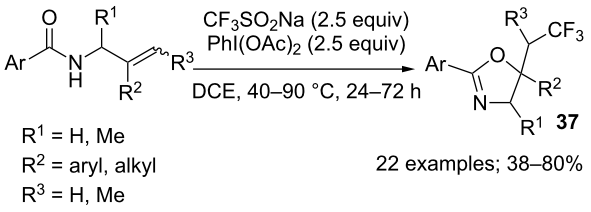

Scheme 18: Intramolecular oxytrifluoromethylation of alkenes.

Hydrotrifluoromethylation of alkenes: Direct alkene hydrotrifluoromethylation by means of CF_3SO_2K under electrochemical oxidation was first reported by Tommasino and co-workers in 2002 on three alkenes but yields were below 20% due to the formation of oxidised byproducts [38]. Nicewicz and co-workers in 2013 found suitable reaction conditions for the alkene hydrotrifluoromethylation using CF_3SO_2Na [39]. The single electron oxidation of CF_3SO_2Na was performed by visible-light activated *N*-methyl-9-mesitylacridinium as a photoredox catalyst. Two hydrogen atom donors, 20 mol % of methyl thiosalicylate **38** for aliphatic alkenes (or 1 equiv of thiophenol **39** for styrenyl alkenes) and 2,2,2-trifluoroethanol (TFE), worked in concert for the hydrogen atom transfer with complete suppression of the oxidised trifluoromethylated byproducts. The method was regioselective for mono-, di-, and trisubstituted aliphatic alkenes and styrenyl alkenes with a broad substrate scope (Scheme 19). As an exception, 1,2-disubstituted alkenes and chalcone gave low regioselectivities with mixed Markovnikov and anti-Markovnikov products.

The CF_3 radical is electrophilic in nature and, as such, not prone to readily react with electron-deficient alkenes. Nevertheless, Lefebvre, Hoffmann and Rueping reported that *N*-substituted maleimides, maleic anhydride and dimethyl maleate were hydrotrifluoromethylated with CF_3SO_2Na in the presence of 4,4'-dimethoxybenzophenone as photosensitiser under near-UV irradiation (350 nm) and hexafluoroisopropanol (HFIP) as a proton donor (Scheme 20) [40]. The reactions were performed in batch and under continuous flow conditions with rate enhancement for the latter setup. It was proposed that the CF_3 radical added onto the substrate while the ketyl radical **41** was protonated by HFIP. Then, hydrogen transfer gave the hydrotrifluoromethylated product **40** and the sensitiser was regenerated (Scheme 20). In the same paper, the authors also realised the same chemical transformation under visible light irradiation at 450 nm by means of the iridium photocatalyst $Ir[dF(CF_3)ppy]_2(dtbbpy)PF_6$ ([4,4'-bis(*tert*-butyl)-2,2'-bipyridine]bis[3,5-difluoro-2-[5-(trifluoromethyl)-2-pyridinyl]phenyl]iridium(III) hexafluorophosphate), which delivered comparable and even higher yields of the products in longer reaction times but with lower catalyst loading (1 mol %).

Both unactivated terminal alkenes and electron-deficient alkenes (Michael acceptors) were successfully hydrotrifluoromethylated under irradiation with 36 W blue LEDs in the presence of an iridium photoredox catalyst as reported by Zhu, Zhang and co-workers [41]. Of the photocatalysts tested, $Ir[dF(CF_3)ppy]_2(dtbbpy)PF_6$ had appropriate redox potentials and gave the best results. A wide range of terminal alkenes featuring several functional groups reacted with exclusive anti-Markovnikov selectivity. Notably, styrene failed to react under these conditions. A selection of α,β-unsaturated electron-withdrawing motifs that included a sulfone, esters, an amide, and a ketone were investigated for the first time and the β-addition products were obtained regioselectively in moderate to good

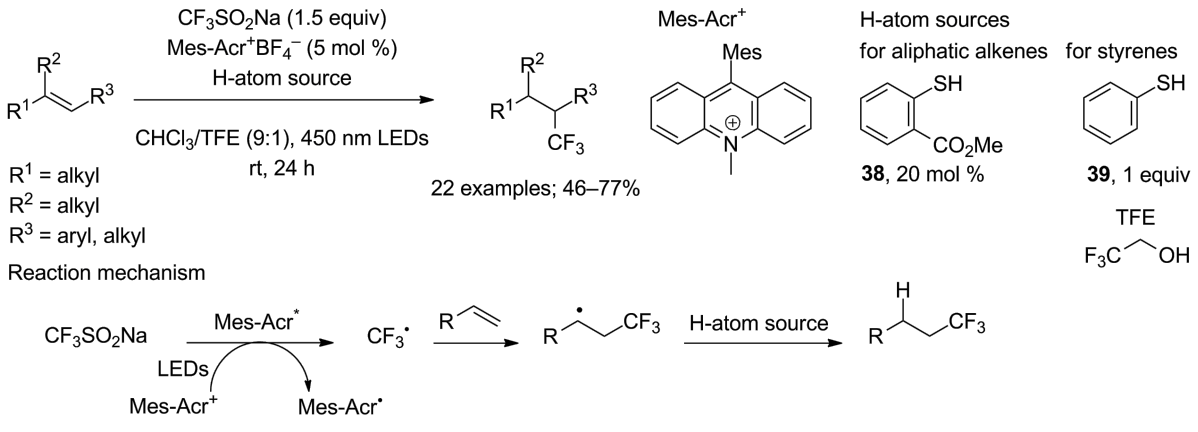

Scheme 19: Hydrotrifluoromethylation of styrenyl alkenes and unactivated aliphatic alkenes.

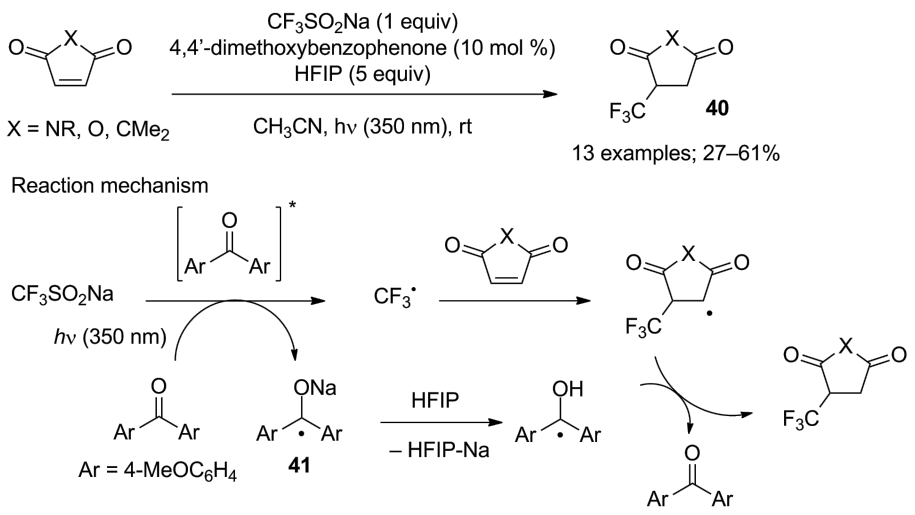

Scheme 20: Hydrotrifluoromethylation of electron-deficient alkenes.

yields (Scheme 21). It was suggested that the methylene radical formed by addition of the CF_3 radical onto the alkene was reduced by the sulfinate anion and the corresponding carbanion was protonated by methanol.

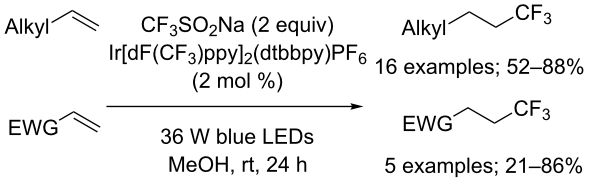

Scheme 21: Hydrotrifluoromethylation of alkenes by iridium photoredox catalysis.

Halo- and pseudohalotrifluoromethylation of alkenes: The direct iodotrifluoromethylation was previously achieved by means of gaseous CF_3I until Liu and co-workers reported the convenient use of CF_3SO_2Na and iodide pentoxide, I_2O_5, in combination for the iodotrifluoromethylation of alkenes and alkynes (see later in the text) [42]. After an optimisation with 4-chlorostyrene, the reaction was developed with a wide range of terminal and internal alkenes bearing diverse functional groups such as halogens, nitro, sulfonate, sulfamide, carboxylate, amide, ether, carbonyl, and hydroxy that were all well-tolerated (Scheme 22). A mixed solvent system of dichloromethane and water was used in a sealed tube at 110 °C. Mechanistic studies by electron spin resonance were carried out in which both the $CF_3^{\bullet}$ and the β-CF_3 alkyl radical intermediate were observed by using 2-methyl-2-nitrosopropane as a radical spin trap. A single-electron oxidative free-radical process was clearly ascertained. For the iodination step, the authors proposed that the β-CF_3 alkyl radical was intercepted by I_2, which was formed by a multistep redox process from I_2O_5. In continuation of this work, the same research group described the bromotrifluoromethylation of alkenes under similar reaction conditions but using sodium bromate, $NaBrO_3$, as a bromine source (Scheme 22) [43].

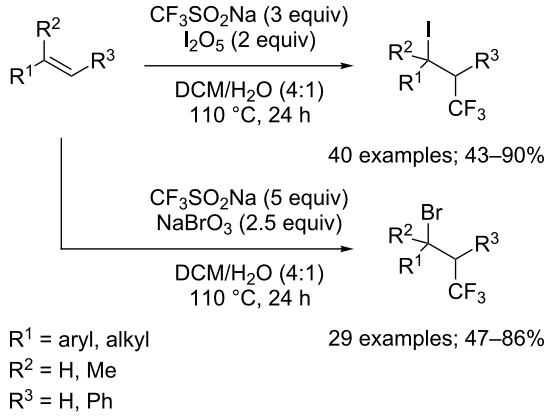

Scheme 22: Iodo- and bromotrifluoromethylation of alkenes by CF_3SO_2Na/I_2O_5 or CF_3SO_2Na / $NaBrO_3$.

The photoredox-catalysed chloro-, bromo- and also (trifluoromethylthio)trifluoromethylation of unactivated alkenes was studied by Liu and co-workers in 2017 (Scheme 23) [44]. The Langlois reagent was combined with *N*-halophthalimides **42a**,**b** or *N*-trifluoromethylthiosaccharin **43** in the presence of *N*-methyl-9-mesitylacridinium under visible light irradiation at room temperature. Terminal, internal, and *gem*-substituted alkenes bearing imide, ester, amide, ketone, aldehyde and electron-rich aryl functional groups were suitable substrates. Notably, diethyl 2,2-diallylmalonate as a diene gave the

cyclised product resulting of a radical cascade. It has to be noticed that the reactions were conducted in the presence of 2 equivalents of trifluoroacetic or *p*-toluenesulfonic acid; yet, there was no mention of hydrotrifluoromethylated side-products. The mechanism was similar to previous examples to generate the β-CF_3 alkyl radical intermediate **44**, which was trapped by halogen atom transfer from the halogenating agent. The nitrogen-centered radical **45** oxidised Mes-Acr* by a single-electron-transfer process to restart the catalytic cycle (Scheme 23).

Carbotrifluoromethylation of alkenes: The strategies for carbotrifluoromethylation of alkenes with CF_3SO_2Na are very much based on methods described earlier in the text: (i) reactions mediated by *tert*-butyl hydroperoxide and a catalytic amount of copper; (ii) metal-catalysed or metal-free reactions with $K_2S_2O_8$, I_2O_5 or a hypervalent iodine reagent, and (iii) photochemical activation. Most of the works concerned cascade intramolecular reactions in which a C–C bond is formed after the initial trifluoromethylation.

Therefore, Lipshutz and co-workers reported a copper-catalysed intramolecular carbotrifluoromethylation of *N*-arylacrylamides **46** with CF_3SO_2Na to produce oxindoles **47** [45]. Addition of the CF_3 radical to such an electron-deficient alkene should be unfavourable. However, the subsequent annulation step drove the cascade process toward oxindole synthesis. The reaction utilised Langlois' conditions with *tert*-butyl hydroperoxide and a catalytic amount of Cu(II), but with 10 mol % of tetramethylethylenediamine (TMEDA). Organic solvents were replaced by pure water and the aqueous medium can be recycled up to five times. The substrate scope was large when tertiary amides were used. A secondary arylamide failed to give the expected product. With a substituent at the *meta*-position of the aniline ring, a mixture of regioisomers was obtained. Various alkenes with substituents (R^3) were investigated and the oxindoles were obtained in moderate to high yields (Scheme 24).

Simultaneously, Lei and co-workers published the same reaction under slightly different conditions [46]. They used a combination CF_3SO_2Na/TBHP in the presence of catalytic amounts of copper chloride and triphenylphosphine. Trisubstituted alkenes (R^3 and $R^4 \neq H$) were employed as substrates and diastereoisomers were obtained. The *tert*-butoxyl radical was generated from TBHP and Cu(*n*) via a SET process, which then, it reacted

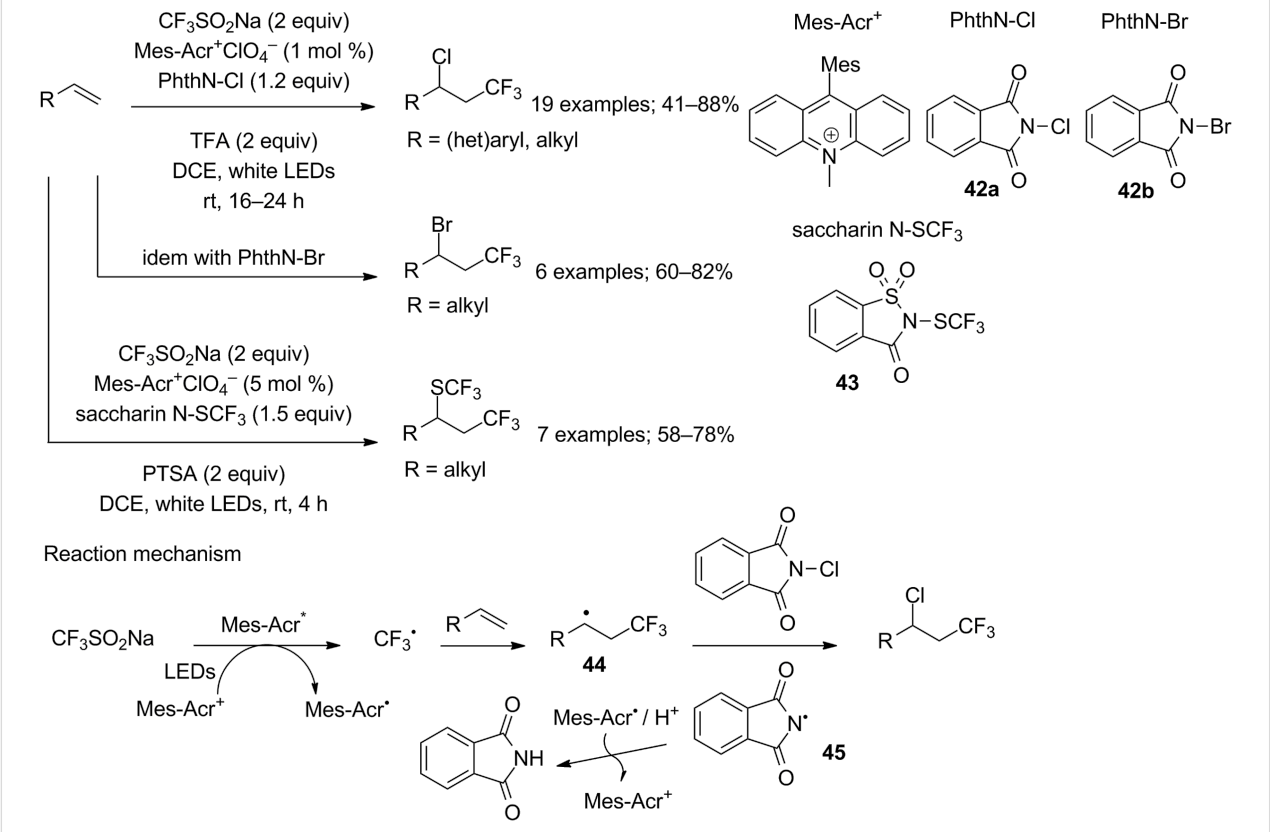

Scheme 23: *N*-methyl-9-mesityl acridinium and visible-light-induced chloro-, bromo- and SCF_3 trifluoromethylation of alkenes.

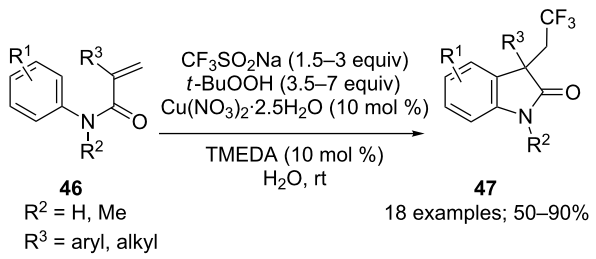

Scheme 24: Carbotrifluoromethylation of *N*-arylacrylamides with CF_3SO_2Na / TBHP by Lipshutz.

with CF_3SO_2Na to liberate $CF_3^•$. The subsequent addition of $CF_3^•$ to the β-position of the C=C bond of the acrylamide gave the intermediate **48**, which underwent an intramolecular radical annulation to produce the aryl radical **49**. Finally, oxidation of **49** by Cu(n + 1) and aromatisation afforded the oxindole and regenerated the copper catalyst (Scheme 25).

The same indoles bearing a 2,2,2-trifluoroethyl side-chain were also obtained in reactions performed with CF_3SO_2Na and $(NH_4)_2S_2O_8$ as the oxidant in the presence of a catalytic amount of $AgNO_3$ as reported by Tan and co-workers (Scheme 26) [47]. In the absence of $AgNO_3$ the reaction did not work. Notably, *N*-alkyl and *N*-aryl protected substrates worked well, whereas *N*-acyl and *N*–H derivatives failed to deliver the desired products. Mechanistically, Ag(I) was initially oxidised to Ag(II) by the persulfate anion; then, $CF_3SO_2^-$ was oxidised to $CF_3SO_2^•$ that generated $CF_3^•$ by release of SO_2. Addition of the CF_3 radical to the alkene led to the radical intermediate **50**, which underwent intramolecular cyclisation into **51**. The sulfate radical anion then oxidised intermediate **51** into the final oxindole (Scheme 26).

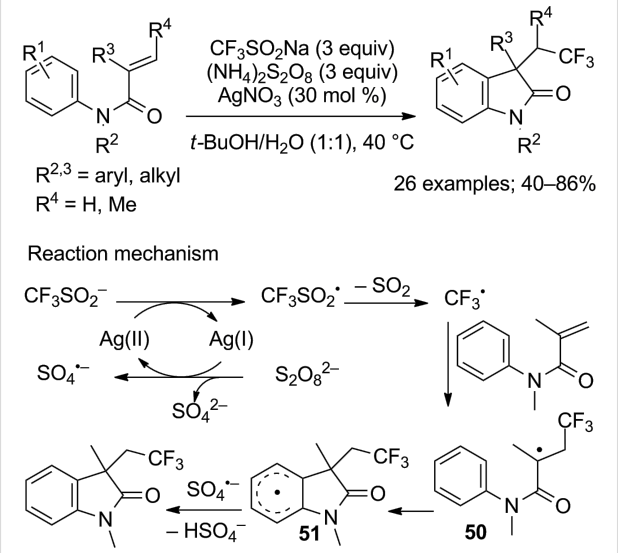

Scheme 26: Carbotrifluoromethylation of *N*-arylacrylamides with $CF_3SO_2Na/(NH_4)_2S_2O_8$.

In an independent work Wang and co-workers demonstrated that silver nitrate was not necessary for the reaction to proceed in acetonitrile and water at 80 °C (Scheme 27) [48]. Again, *N*-acyl and *N*–H derivatives failed to deliver the desired products and *meta*-substituted phenyl rings produced mixtures of regioisomers. Under these metal-free conditions, it was proposed that the CF_3 radical was formed uniquely by reaction of CF_3SO_2Na with $K_2S_2O_8$.

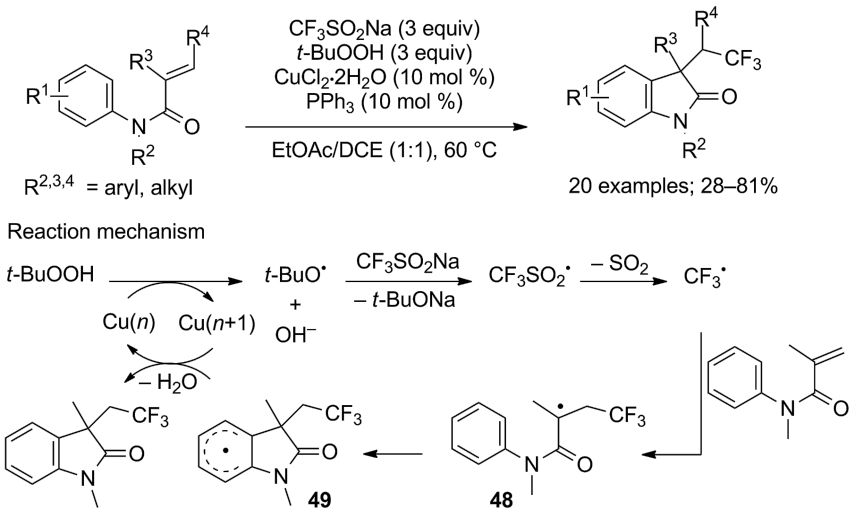

Scheme 25: Carbotrifluoromethylation of *N*-arylacrylamides with CF_3SO_2Na/TBHP reported by Lei.

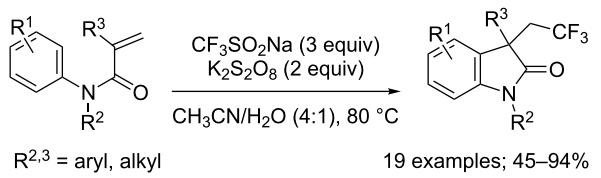

Scheme 27: Metal-free carbotrifluoromethylation of *N*-arylacrylamides with $CF_3SO_2Na/K_2S_2O_8$ reported by Wang.

N-Arylacrylamides could also react with CF_3SO_2Na under metal-free conditions by replacing *tert*-butyl hydroperoxide or the persulfate by hypervalent iodine oxidants such as iodobenzene diacetate (PIDA, Scheme 28) [49], or iodobenzene bis(trifluoroacetate) (PIFA) [50]. Fu and co-workers proposed the reaction mechanism depicted in Scheme 28. PIDA reacted with CF_3SO_2Na under heating conditions to produce two radicals: $CF_3^•$ along with PhI•OAc. Addition of the CF_3 radical to the alkene followed by intramolecular cyclisation mediated by PhI•OAc gave the desired oxindole with release of PhI and AcOH (Scheme 28) [49].

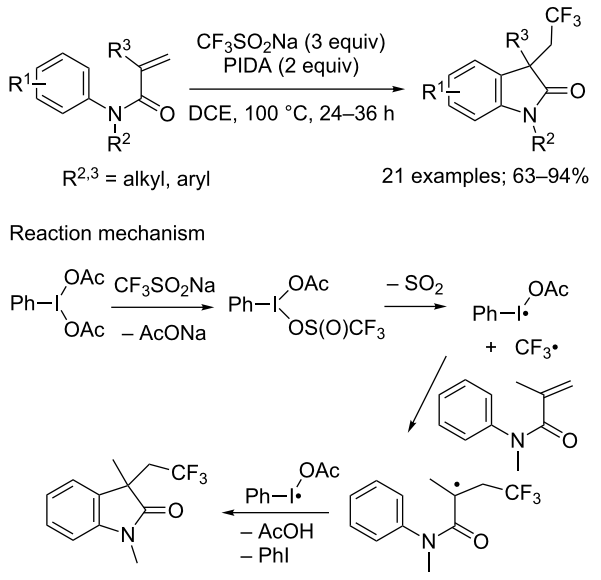

Scheme 28: Metal-free carbotrifluoromethylation of *N*-arylacrylamides with CF_3SO_2Na/PIDA reported by Fu.

For another metal-free trifluoromethylation/cyclisation of *N*-arylacrylamides by means of a different oxidant, Liu and co-workers reported the use of CF_3SO_2Na in combination with iodide pentoxide in a similar way to their iodotrifluoromethylation of alkenes (see earlier in the text) [42] (Scheme 29a) [51]. Interestingly, this cascade reaction was also applied to enynes for the synthesis of pyrrolidines **52** (Scheme 29b) [51]. A single-electron oxidative free-radical process was ascertained for the generation of $CF_3^•$. From enynes, the iodination step was realised by I_2, which was formed by a multistep redox process from I_2O_5.

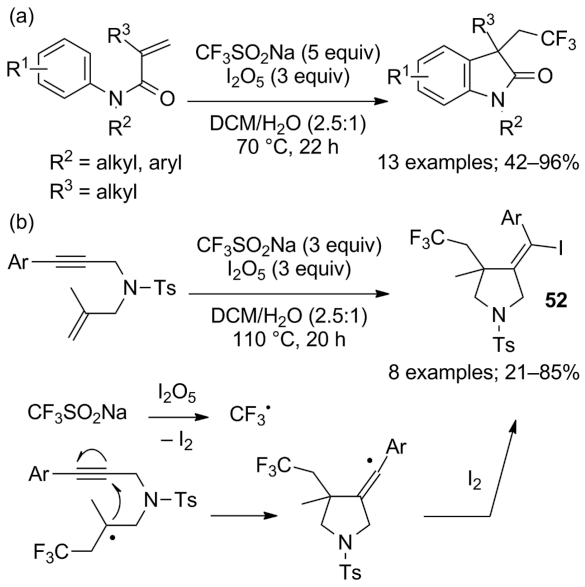

Scheme 29: Metal-free cascade trifluoromethylation/cyclisation of *N*-arylmethacrylamides (a) and enynes (b) with CF_3SO_2Na/I_2O_5.

The intramolecular carbotrifluoromethylations of alkenes from acrylamides and methacrylamides, so far described, provided oxindoles via a 5-*exo trig* cyclization. Starting from cinnamamides **53**, Mai, Xiao and co-workers reported a 6-*endo trig* cyclisation leading to 3,4-disubstituted dihydroquinolin-2(1*H*)-ones **54** (Scheme 30) [52]. Ag(I) was oxidised by the persulfate anion ($S_2O_8^{2-}$) to generate the Ag(II) cation and the sulfate radical anion; then, the Ag(II) oxidised CF_3SO_2Na into $CF_3^•$ with extrusion of SO_2. The CF_3 radical reacted with the C=C double bond of the cinnamamide leading to the intermediate **55** that underwent 6-*endo trig* cyclisation to **56** that finally aromatised to the desired product **54** *trans*-selectively (Scheme 30).

In 2016, Xia and co-workers described a metal-free, UV-light-mediated difunctionalisation of alkenes with CF_3SO_2Na for the synthesis of phenanthrene and anthrone derivatives [53]. The substrates were either α,β-unsaturated ketones **57** (Scheme 31a) or γ,δ-unsaturated ketones **58** (Scheme 31b). Benzophenone (BP) or anthracene-9,10-dione (AQ) were used as sensitizers under irradiation using a UV lamp at 280 nm. A radical pathway that involves $CF_3^•$ was established after a negative reaction in the presence of TEMPO (TEMPO–CF_3 was detected by GC–MS).

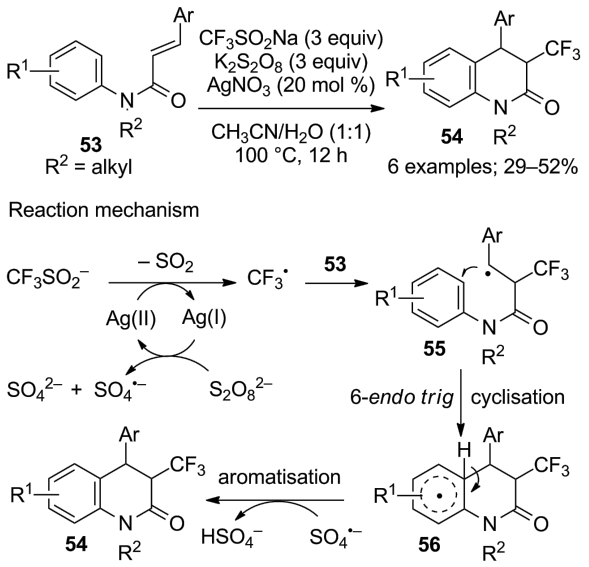

Scheme 30: Trifluoromethylation/cyclisation of *N*-arylcinnamamides: Synthesis of 3,4-disubstituted dihydroquinolin-2(1*H*)-ones.

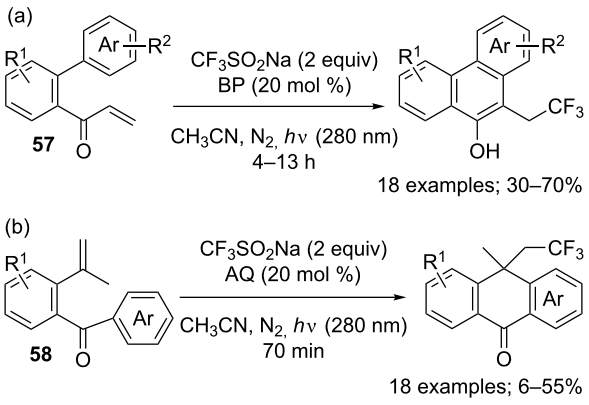

Scheme 31: Trifluoromethylation/cyclisation of aromatic-containing unsaturated ketones.

An example of difunctionalisation of unactivated alkenes with CF_3SO_2Na and an heteroaryl group in which the heteroarylation was realised by a distal heteroaryl *ipso*-migration was provided in 2017 by Zhu and co-workers (Scheme 32) [54]. A variety of nitrogen containing heteroaryl groups showcased the migratory aptitude selectively in the presence of an aryl or an alkyl group. The number of methylene units between the alkene and the tertiary alcohol function was studied: n = 0, 2, and 3 were suitable for generating thermodynamically favoured 3, 5, and 6-membered cyclic transition states; the reaction failed with n = 1, 4. Experimental and computational studies allowed the authors to propose the mechanism depicted in Scheme 32. First, the CF_3 radical was generated from CF_3SO_2Na and PIFA. Then, addition of $CF_3^•$ to the alkene gave the alkyl radical **59** that added to the *ipso* position of the heteroaryl group to form radical **60**. Next, homolysis of the C–C σ-bond in **60** provided the more stable hydroxyalkyl radical **61**. This radical was oxidised by PIFA to yield the cationic intermediate **62**, which finally lost a proton to furnish the reaction product.

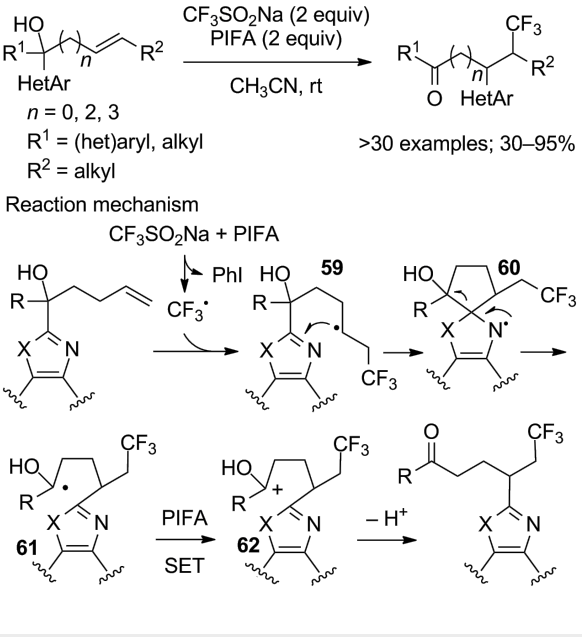

Scheme 32: Chemo- and regioselective cascade trifluoromethylation/heteroaryl *ipso*-migration of unactivated alkenes.

1,2-Bis-trifluoromethylation of alkenes: Alkenes were efficiently and chemoselectively bis-trifluoromethylated under Langlois' conditions with CF_3SO_2Na. Indeed, Qing and co-workers prepared 1,2-bis(trifluoromethylated) compounds **63** with in situ generated CF_3 radicals (Scheme 33). In order to avoid the formation of dimerised side products, it was demonstrated that an increase of the CF_3 radical concentration, obtained by increasing the amount of copper catalyst, was beneficial to the chemoselectivity. Both styrene derivatives and terminal unactivated alkenes were suitable substrates in this transformation but not internal alkenes [55].

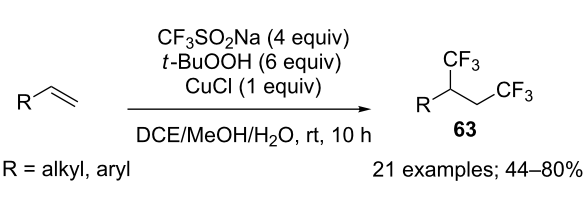

Scheme 33: Copper-mediated 1,2-bis(trifluoromethylation) of alkenes.

C_{sp2}–CF_3 bond-forming reactions

Direct trifluoromethylation of arenes and heteroarenes: In 1991, Langlois and co-workers reported the first trifluoromethylation of aromatic compounds with sodium trifluoromethanesulfinate under oxidative conditions (Scheme 34) [16]. The scope was quite narrow with electron-rich aromatics and mixtures of regioisomers were often obtained. For instance, from aniline, two isomers were obtained in 13% overall yield, and from 1,3-dimethoxybenzene, four products (regioisomers + bis-CF_3 compounds) were obtained in 90% overall yield. For this transformation, a radical process was proposed: the trifluoromethyl radical $CF_3^•$ was generated by reaction of *tert*-butyl hydroperoxide with CF_3SO_2Na in the presence of a copper(II) catalyst (Scheme 34).

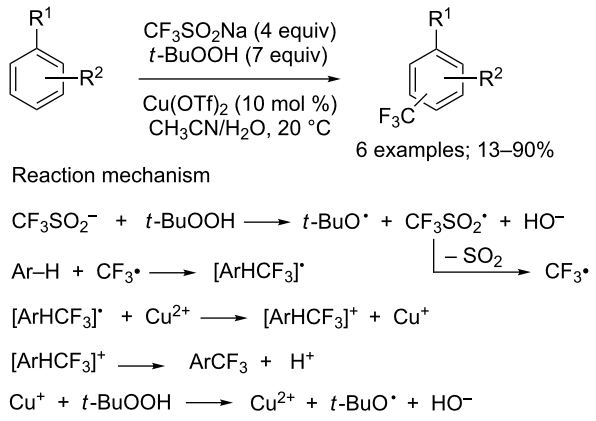

Scheme 34: Trifluoromethylation of aromatics with CF_3SO_2Na reported by Langlois.

Substrates with sensitive functional groups may not be tolerated under such reaction conditions and a large excess amount of peroxide was necessary to reach high yields. That is how, in 1998, Smertenko and co-workers described a milder electrochemical trifluoromethylation of a series of aromatic compounds using CF_3SO_2Na in acetonitrile [56]. Furthermore, the electrochemical oxidation of the trifluoromethylsulfinate anion (from CF_3SO_2K) generated the trifluoromethyl radical for the reaction of electron-rich aromatics and alkenes [38].

It is twenty years after Langlois' pioneering work that the direct trifluoromethylation of heteroaromatic compounds was re-investigated by Baran and co-workers in 2011 [57]. This group reported a C−H trifluoromethylation protocol that was operationally simple, scalable, achieved at room temperature, working with a variety of electron-deficient and -rich heteroaromatic systems tolerating various functional groups such as unprotected alcohols, amines, ketones, esters, halides and nitriles. Importantly, the trifluoromethylation proceeded at the innate reactive positions of the heterocycles; however, it was noticed that the regioselectivity can be tuned simply by solvent choice. Langlois and others employed catalytic metal salts for reaction initiation but Baran's group demonstrated that metal additives were not required for a productive reaction, only trace metals found in Langlois' reagent could be responsible for reaction initiation. The scope was evaluated on pyridines, pyrroles, indoles, pyrimidines, pyrazines, phthalazines, quinoxalines, deazapurine, thiadiazoles, uracils, xanthenes and pyrazolinopyrimidines (Scheme 35). The combination of previous studies with new observations allowed to propose a putative mechanism (Scheme 35) as well as unproductive pathways (formation of CF_3H from $CF_3^•$ by abstraction of a hydrogen atom or reaction of $CF_3^•$ with isobutene generated from *t*-BuOOH).

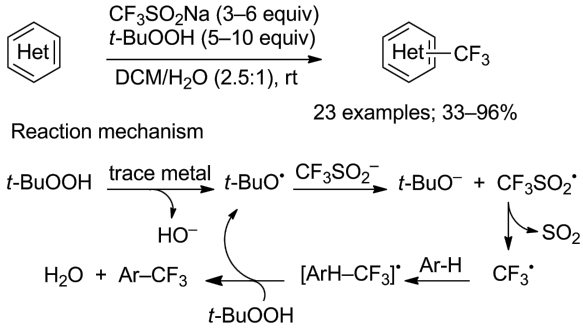

Scheme 35: Baran's oxidative C–H trifluoromethylation of heterocycles.

This oxidative trifluoromethylation method was exploited for the synthesis of modified nucleosides, in particular 8-CF_3-2'-deoxyguanosine and 8-CF_3-inosine in 39 and 73% yields, respectively [58].

The same copper-free method was applied for the trifluoromethylation of a variety of electron-deficient 4-substituted acetanilides or anilines (Scheme 36). In these reaction conditions, Cao's group reported that acetanilides or anilines featuring electron-donating substituents at the *para*-position of the acetamino group afforded mixtures of isomeric C−H trifluoromethylation products in moderate yields. However, with substrates bearing electron-withdrawing groups, *ortho*-CF_3 acetanilides or anilines were obtained as sole products [59].

To meet high expectations of environmentally low impact chemical reactions, Lipshutz and co-workers carried out the trifluoromethylation of heterocycles using aqueous micellar conditions based on the surfactant TPGS−750−M in water at room temperature. The trifluoromethyl radical was generated from CF_3SO_2Na and *t*-BuOOH. In comparaison to Baran's

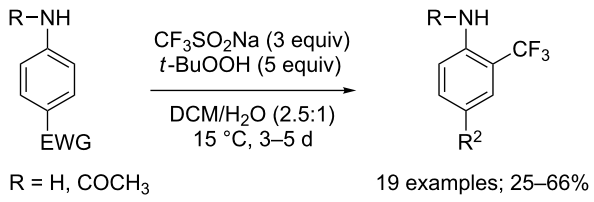

Scheme 36: Trifluoromethylation of acetanilides and anilines.

results, in all cases, the yields were improved. Advantageously, the aqueous medium can be recycled (Scheme 37) [60].

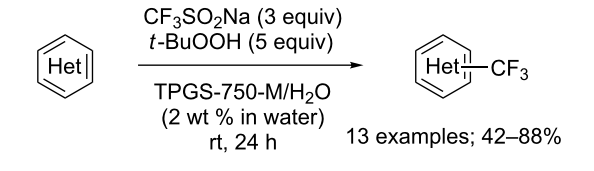

Scheme 37: Trifluoromethylation of heterocycles in water.

Even though it is a proven fact after 2011 and Baran's work that no-added metal trifluoromethylation with CF_3SO_2Na are highly efficient, the original Langlois' conditions were nevertheless applied to a series of heteroarenes. Li and co-workers reported the synthesis of 3-trifluoromethylcoumarins **64** by Cu(I)-catalysed trifluoromethylation with CF_3SO_2Na and *t*-BuOOH in a continuous-flow reactor [61]. After optimisation of the reaction conditions in batch, the optimal reaction conditions were established in a continuous-flow reactor at a flow rate of 100 μL min^{-1} at 60 °C for 40 min. The substrate scope was evaluated on 11 coumarins and showed that both electron-rich and electron-deficient functional groups were tolerated (Scheme 38).

Zou and co-workers applied the conditions described by Langlois or Baran (CF_3SO_2Na/*t*-BuOOH/cat. Cu(II) or CF_3SO_2Na/*t*-BuOOH, respectively) for the trifluoromethylation of coumarins but no reaction was observed. By testing other oxidants, they found that $Mn(OAc)_3$ was a good oxidant for this reaction and allowed to carry out the trifluoromethylation exclusively at the α-position of the carbonyl group in the pyranone ring. The substrate scope was large and included 17 coumarins, 2 quinolines and 3 pyrimidinones. With coumarins bearing electron-donating groups on the phenyl ring, the 3-trifluoromethylated compounds were obtained in 50–56% yields. However, coumarins bearing electron-withdrawing groups gave yields up to 70%. As for the mechanism, the trifluoromethyl radical was generated from CF_3SO_2Na and $Mn(OAc)_3$, then $CF_3^{\bullet}$ added regioselectively onto the coumarin to give intermediate radical **65**, which was oxidised by

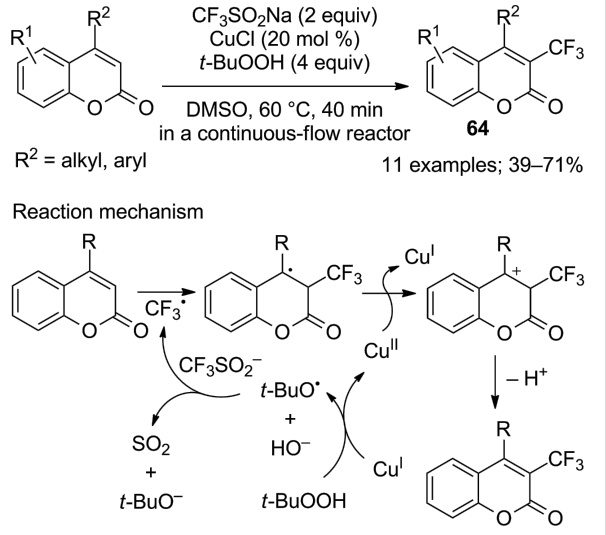

Scheme 38: Trifluoromethylation of coumarins in a continuous-flow reactor.

$Mn(OAc)_3$ to form the carbocation **66** and, after deprotonation, the trifluoromethyl compounds (Scheme 39) [62].

The same group also reported a straightforward method for the trifluoromethylation of pyrimidinones and pyridinones under the same reaction conditions. 5-Trifluoromethylpyrimidinones and 3-trifluoromethylpyridinones were selectively obtained in moderate to good yields (Scheme 40). It was observed that the substituent R^1 provided no stabilisation for the radical intermediate, so the less bulky substituents at 6-position of pyrimidinones or 4-position of pyridinones facilitated the trifluoromethyl radical attack [63].

Catalytic amounts of phosphovanadomolybdic acid, a heteropolyacid catalyst (HPA), was used by Mizuno, Yamaguchi and co-workers for the oxidative C−H trifluoromethylation of arenes and heteroarenes in the presence of CF_3SO_2Na and O_2 as the terminal oxidant. This method allowed the trifluoromethylation of arenes bearing electron-donating as well as electron-withdrawing groups in moderate to good yields (Scheme 41) [64]. It has to be noted that bis-CF_3 products as well as regioisomers were also characterised or detected in small amounts in most cases. A radical mechanism was proposed as described in Scheme 41.

Imidazopyridines have demonstrated many interesting features toward biological activities and the incorporation of a trifluoromethyl group into such architectures was expected to alter their properties. Therefore, Hajra and co-workers reported a direct and regioselective method for the trifluoromethylation of imidazopyridines **67** and other imidazoheterocycles **68** [65]. The

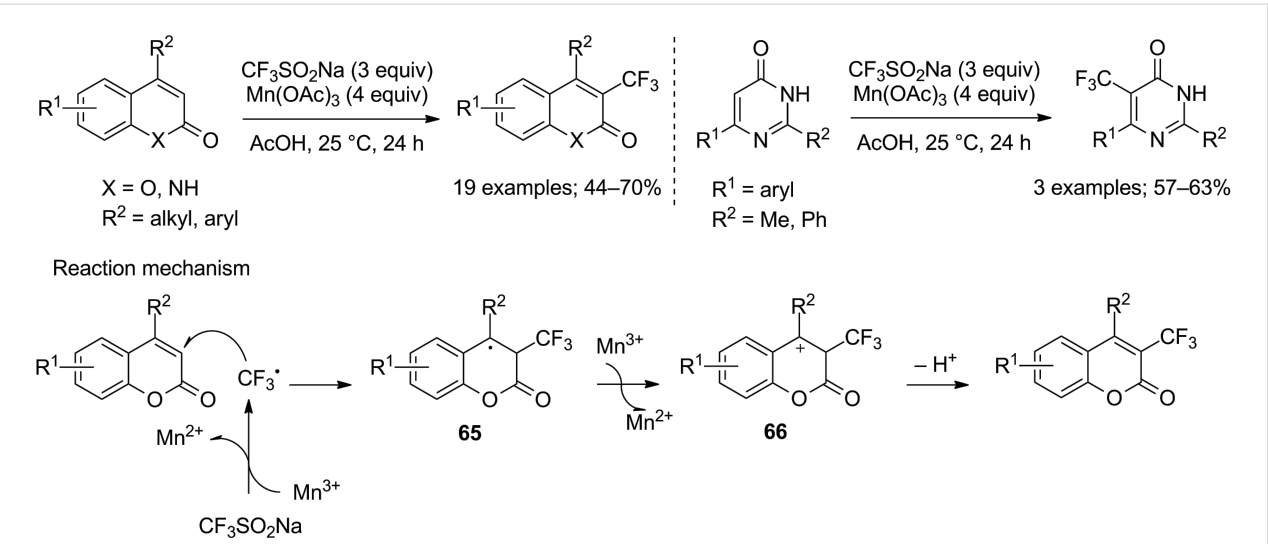

Scheme 39: Oxidative trifluoromethylation of coumarins, quinolines and pyrimidinones.

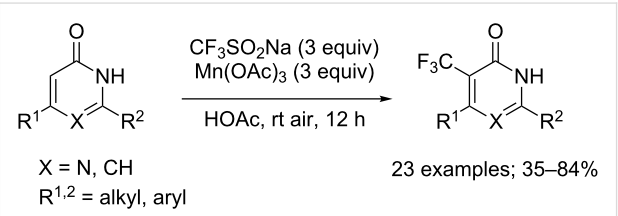

Scheme 40: Oxidative trifluoromethylation of pyrimidinones and pyridinones.

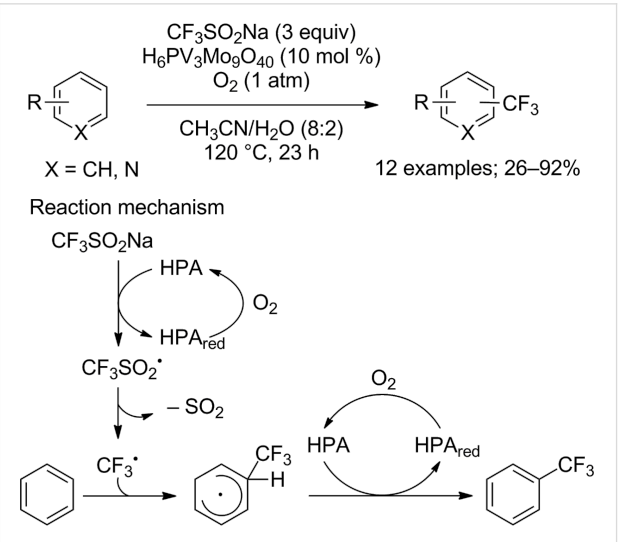

Scheme 41: Phosphovanadomolybdic acid-catalysed direct C−H trifluoromethylation.

combination CF_3SO_2Na/*t*-BuOOH/cat. $AgNO_3$ at room temperature under air was applied to 17 imidazopyridines and 3 imidazoheterocycles (Scheme 42). Good yields were obtained when the phenyl moiety was substituted by electron-donating groups. As a result of absence of reactivity in presence of the radical scavenger TEMPO, a radical pathway was proposed. Under argon atmosphere, only trace amounts of the CF_3 product were obtained clearly indicating the crucial role of aerial oxygen in the catalytic cycle (see mechanism in Scheme 42).

Simultaneously, Tang and co-workers reported a greener strategy for the trifluoromethylation of imidazoheterocycles with CF_3SO_2Na in a recyclable mixed medium of 1-butyl-3-methylimidazolium tetrafluoroborate ([Bmim]BF_4) and water [66]. The substrate scope was investigated on 11 imidazothiazoles, 13 imidazo[1,2-*a*]pyridines and 6 imidazoles (Scheme 43). The reaction was simple, achieved at room temperature and had a good tolerance for various functional groups. However, for the trifluoromethylation of imidazoles, it was essential to have a phenyl as a substituent in order to get good yields. A radical mechanism was proposed but the role of oxygen was not discussed.

Aminoquinoline derivatives are found in naturally occurring and synthetic bioactive compounds, most notable for their antimalarial activity. So, it was not surprising that trifluoromethyl analogues were prepared in particular by means of CF_3SO_2Na. Indeed, 5-trifluoromethyl-8-aminoquinoline derivatives **69** were regioselectively synthesised under various reaction conditions. Cai and co-workers reported the trifluoromethylation of 8-aminoquinolines selectively at position 5 by using CF_3SO_2Na, $CuBr_2$ in a catalytic amount and azobisisobutyronitrile (AIBN) as an oxidant (Scheme 44) [67]. This process had a broad tolerance toward a wide range of functional groups. Aliphatic amides, aromatic amides and carboxamides with hetero-

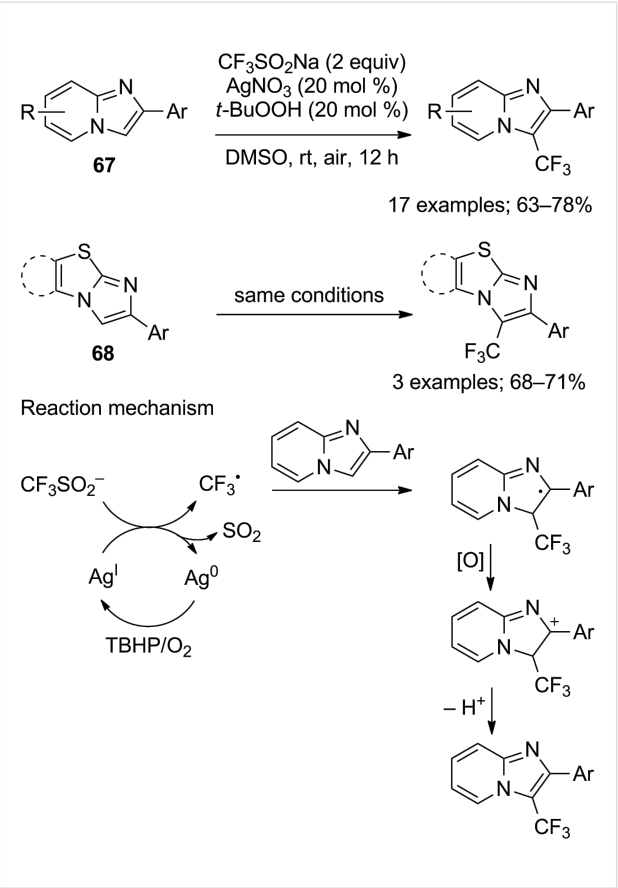

Scheme 42: Oxidative trifluoromethylation of imidazopyridines and imidazoheterocycles.

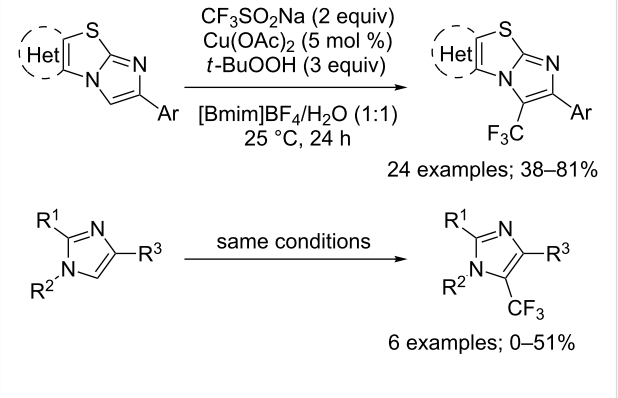

Scheme 43: Oxidative trifluoromethylation of imidazoheterocycles and imidazoles in ionic liquid/water.

cyclic substituents were compatible with the reaction conditions. A series of control experiments that included the inhibition of the reaction in the presence of TEMPO, deuteration and isotope effect experiments were carried out and led the authors to propose the single-electron transfer mechanism presented in Scheme 44.

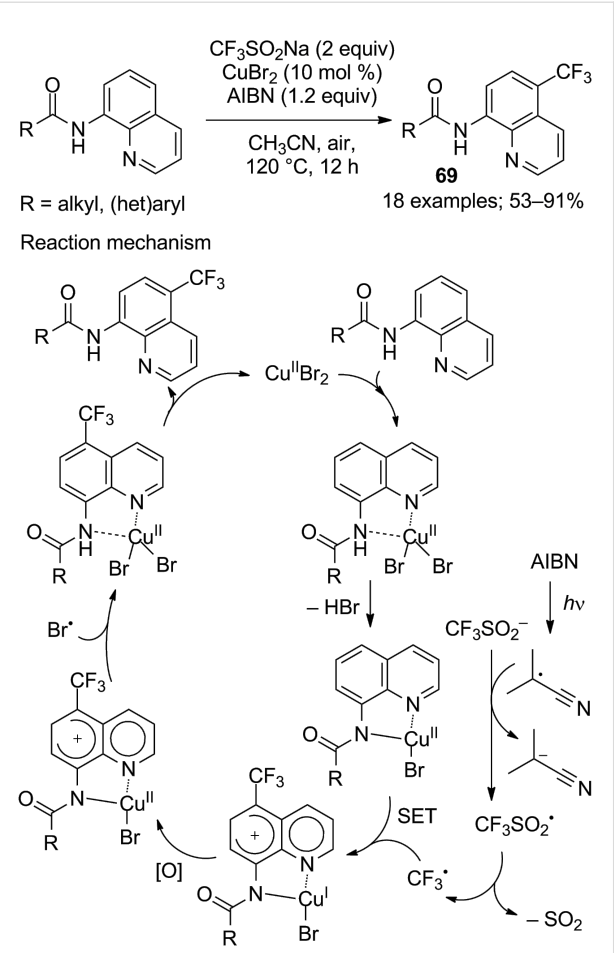

Scheme 44: Oxidative trifluoromethylation of 8-aminoquinolines.

Simultaneously, Shen, Zhang and co-workers reported a milder regioselective trifluoromethylation of 8-aminoquinolines using the supported catalyst CS@Cu(OAc)$_2$ (CS = chitosan), potassium persulfate as the oxidant and CF_3SO_2Na as the $CF_3^•$ source (Scheme 45) [68]. After optimisation of the reaction conditions, the authors studied the effect of structural variations in the substrate (R^1 = aryl, heteroaryl, alkyl; R^2 = H, 6-OMe, 2-Me). Aniline amides gave no conversion nor did quinoline having an ester group at the 8 position instead of the 8-amino group. The chitosan-based copper catalyst was efficiently reused in five cycles of this heterogeneous trifluoromethylation.

In 2017, Lu, Weng and co-workers reported a protocol for the *para*-selective trifluoromethylation of naphthylamide **70**, instead of the previously studied quinolines, with CF_3SO_2Na, *tert*-butyl hydroperoxide and Cu(OAc)$_2$·H$_2$O as oxidant (Scheme 46) [69].

tert-Butyl hydroperoxide could be replaced by sodium persulfate as demonstrated in 2016 by Gong and co-workers who re-

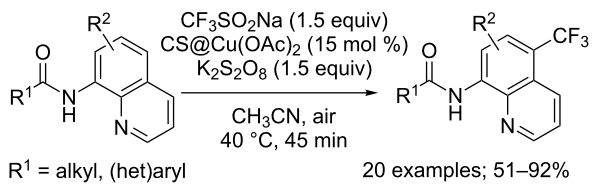

Scheme 45: Oxidative trifluoromethylation of various 8-aminoquinolines using the supported catalyst CS@Cu(OAc)$_2$.

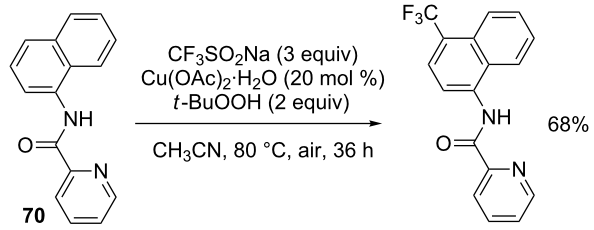

Scheme 46: Oxidative trifluoromethylation of the naphthylamide **70**.

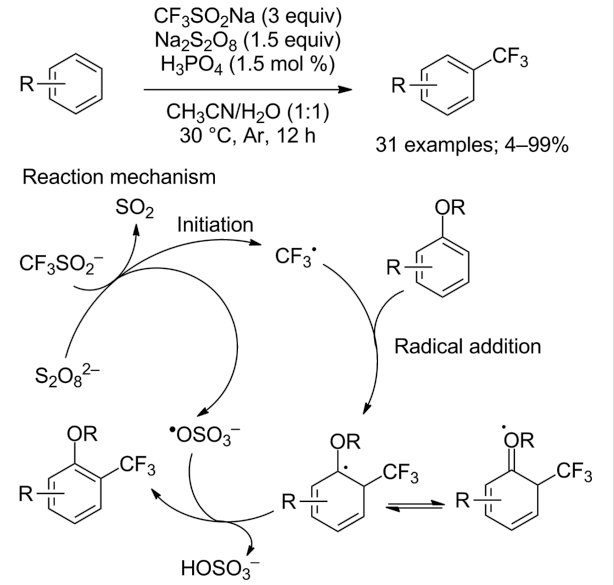

Scheme 47: Oxidative trifluoromethylation of various arenes in the presence of CF_3SO_2Na and sodium persulfate.

ported a direct C−H trifluoromethylation of arenes with CF_3SO_2Na in a mixture of water and acetonitrile (Scheme 47) [70]. Various trifluoromethylated arenes were obtained in moderate to excellent yields. However, to achieve high yields in this trifluoromethylation, one (or more) alkoxy group(s) must be present on the arenes in order to stabilise the free-radical intermediate (see mechanism in Scheme 47). Control experiments such as the trapping of the trifluoromethyl radical with the scavenger TEMPO or with benzoquinone were performed and a radical process was proposed. This mild and safe transformation had a good tolerance for various functional groups.

In 2013, Shibata and co-workers reported a transition-metal-free oxidative trifluoromethylation of arenes with CF_3SO_2Na and phenyliodine bis(trifluoroacetate) (PIFA) instead of *tert*-butyl hydroperoxide as the oxidant in hexafluoroisopropanol (HFIP) at room temperature [71]. In order to obtain good results for this transformation, it should be noted that the electron-donating nature of the aromatic substituents was a crucial point. In the case of unsymmetrical biaryl substrates, mixtures of regioisomers at C4 and C5 were obtained (Scheme 48). In the reaction mechanism, PIFA played a dual role in the activation of the arene via a π-complex and in the generation of the CF_3 radical from CF_3SO_2Na.

More recently, Maruoka and co-workers reported the synthesis of trifluoromethylated coumarin **71** and flavone **72** with CF_3SO_2Na (2 equiv), the hypervalent iodine F_5-PIFA (pentafluorophenyliodine bis(trifluoroacetate)) (2 equiv) and 2,3-dichloro-5,6-dicyano-1,4-benzoquinone (DDQ, 0.6 equiv). The

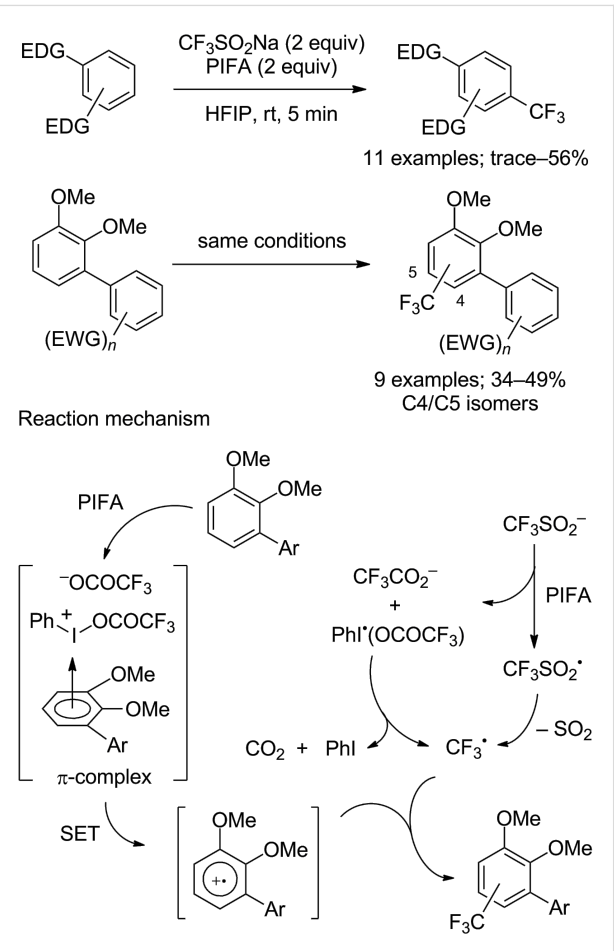

Scheme 48: Trifluoromethylation of electron-rich arenes and unsymmetrical biaryls with CF_3SO_2Na in the presence of PIFA.

trifluoromethylated compounds were obtained in moderate yields (Figure 1) [50].

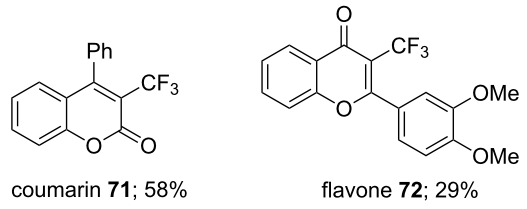

Figure 1: Trifluoromethylated coumarin and flavone.

To avoid the use of transition-metal catalysts and/or an excess amount of oxidants, the Itoh group reported a simple metal-free, direct trifluoromethylation of arenes and heteroarenes using a photoredox-based process under visible-light irradiation. This method used CF_3SO_2Na as source of the trifluoromethyl group and a catalytic amount of anthraquinone-2-carboxylic acid (AQN-2-CO_2H). The scope was achieved on arenes and heteroarenes (10 examples). Once more, electron-rich aromatic compounds were converted into the corresponding trifluoromethylated products in good yields (Scheme 49). The oxidation–reduction potentials were determined by cyclic voltammetry and a catalytic cycle was proposed in which the CF_3 radical was generated from CF_3SO_2Na via the organocatalyst AQN-2-CO_2H and visible light (Scheme 49) [72].

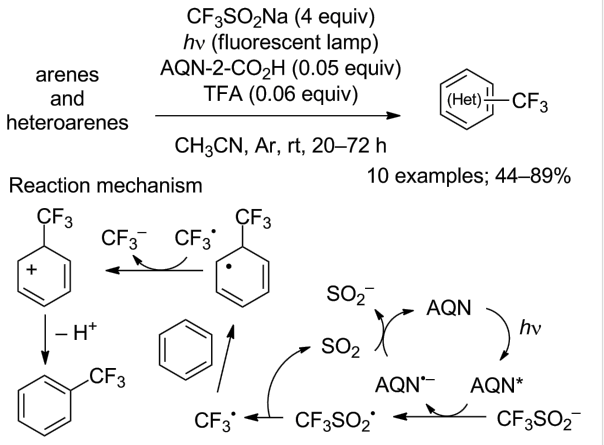

Scheme 49: Metal-free trifluoromethylation catalysed by a photoredox organocatalyst.

Rueping's group described three examples of prototypical (hetero)aromatic substrates that were trifluoromethylated with CF_3SO_2Na in the presence of 4,4'-dimethoxybenzophenone as photosensitiser under near-UV irradiation (350 nm) and HFIP as a proton donor [40]. More recently, Yuan and co-workers reported an efficient and operationally simple method for the direct trifluoromethylation of a wide variety of arenes and heteroarenes under visible-light irradiation [73]. The substrate scope was evaluated on 30 arenes and heteroarenes using 2,3-dichloro-5,6-dicyanobenzoquinone (DDQ) as photocatalyst and CF_3SO_2Na as the CF_3 radical source. The reaction conditions tolerated a broad range of functional groups and the yields ranged from 31 to 68% (Scheme 50). During the process, the quinone was converted into hydroquinone and a regeneration process was established by passing through a cartridge of MnO_2. A mechanism for this transformation was proposed as a result of electron paramagnetic resonance spectroscopy experiments (Scheme 50).

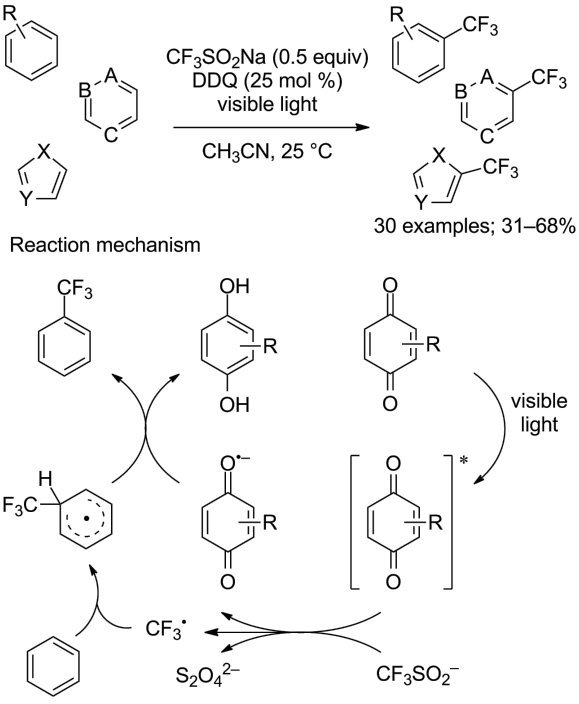

Scheme 50: Quinone-mediated trifluoromethylation of arenes and heteroarenes.

In 2016, Li, Mi and co-workers reported a simple and clean approach for the direct trifluoromethylation of unactivated arenes and heteroarenes through a photoreduction without any metal catalyst nor oxidant. The radical initiators were as simple as acetone or diacetyl for the generation of CF_3 radicals. Indeed, the authors demonstrated that photoexcited acetone was capable to trigger the trifluoromethylation reaction efficiently. So, acetone in this process was used as solvent and photosensitiser. The reactions were carried out under UV irradiation with either a 300 W xenon lamp (emission wavelengths between 200 and 1000 nm) or the photoreactor (λ = 254 nm). This photochemical process allowed the synthesis of trifluoromethylated arenes (Scheme 51), but also heteroarenes and nucleosides in good

yields [74]. Further to this work, it should be noted that Davies, MacMillan and co-workers have designed an integrated small-scale photoreactor that enabled acceleration of this photocatalytic reaction [75].

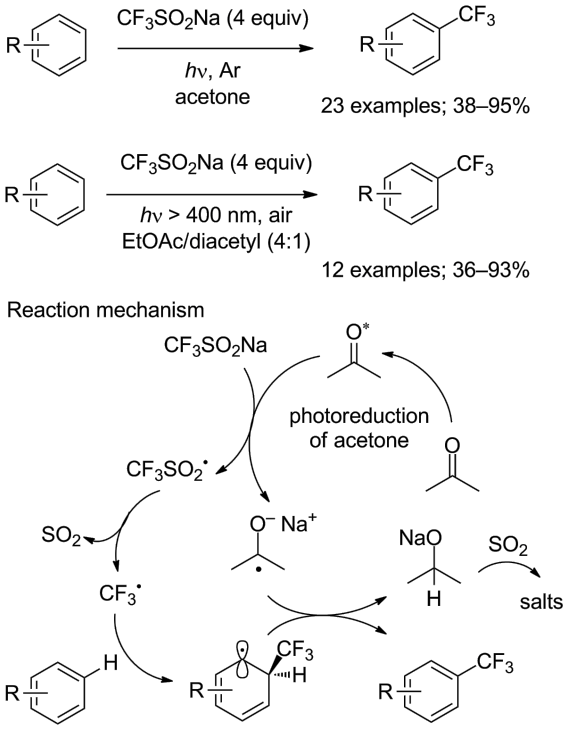

Scheme 51: Metal- and oxidant-free photochemical trifluoromethylation of arenes.

Trifluoromethylation of arenediazonium compounds: Langlois' conditions were applied in the copper-mediated Sandmeyer-type trifluoromethylation of aryldiazonium compounds. The scope of this reaction was investigated on 12 aryldiazonium compounds. The mild reaction conditions allowed the tolerance of various groups such as ester, aryl, nitrile, amine, ketone, nitro, sulfonate and bromo (Scheme 52). In this process, the CF_3 radical was stabilised by the presence of an excess amount of $CuBF_4(MeCN)_4$ and the tridentate ligand 2,2';6',2"-terpyridine (tpy) [76]. Notably, a change in the copper source caused the predominant trifluoromethanesulfonylation of the substrate (introduction of the SO_2CF_3 group, vide infra). A one-pot version starting from anilines was recently developed [77].

Trifluoromethylation of aryl-, vinyl-, alkynylboronic acids: In 2012, Sanford and co-workers reported, for the first time, the copper-mediated radical trifluoromethylation of aryl- and heteroarylboronic acids using CF_3SO_2Na and TBHP as an oxidant. The substrate scope was evaluated on 24 aryl and heteroaryl boronic acids. The process was compatible with

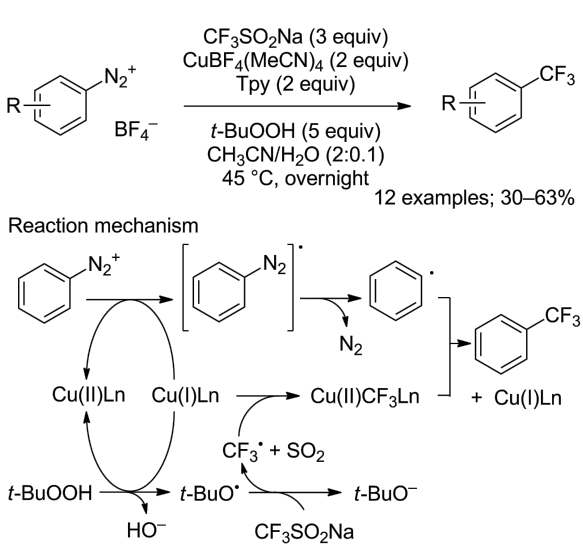

Scheme 52: Copper-mediated trifluoromethylation of arenediazonium tetrafluoroborates.

various functional groups. Arenes bearing electron-donating groups reacted in excellent yields under the CuCl-mediated conditions. However, arenes with electron-withdrawing substituents necessitated $(MeCN)_4CuPF_6$ and a base, $NaHCO_3$, to allow the trifluoromethylation to proceed in good yields (Scheme 53) [78].

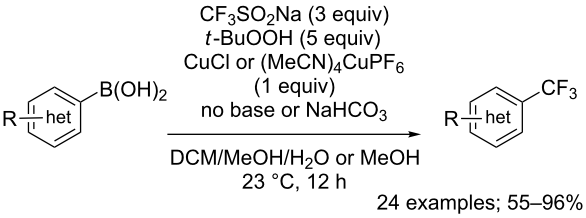

Scheme 53: Oxidative trifluoromethylation of aryl- and heteroarylboronic acids.

In the continuity of Sanford's work, Beller's group reported the synthesis of trifluoromethylated arenes from arylboronic acids as well as trifluoromethylated vinylarenes [79]. The substrate scope was realised on 17 arylboronic acids and 8 vinylboronic acids (Scheme 54). The protocol was robust and tolerated various functional groups. However, large excesses of both CF_3SO_2Na and TBHP were required. In this process, a ligand, 2,4,6-collidine, was used in order to increase the yield of the transformation. For the styrenylboronic acids, electron-withdrawing and electron-donating substituents on the aryl ring were compatible with the reaction conditions. Based on experimental observations, the authors proposed two possible mechanisms for this trifluoromethylation (Scheme 54). In path A,

transmetallation of the boronic acid with the active Cu(II) species **73** gave the arylcopper(II) complex **74**, which reacted with $CF_3^•$ to afford the arylcopper(III) complex **75**. Next, a reductive elimination gave the trifluoromethylated product with release of the Cu(I) complex **76** that was re-oxidised to the active copper(II) catalyst **73** to close the cycle. In path B, the copper(II) complex **73** reacted with $CF_3^•$ to form the copper(III) complex **77**, which after transmetallation with the boronicacid gave the same intermediate **75**.

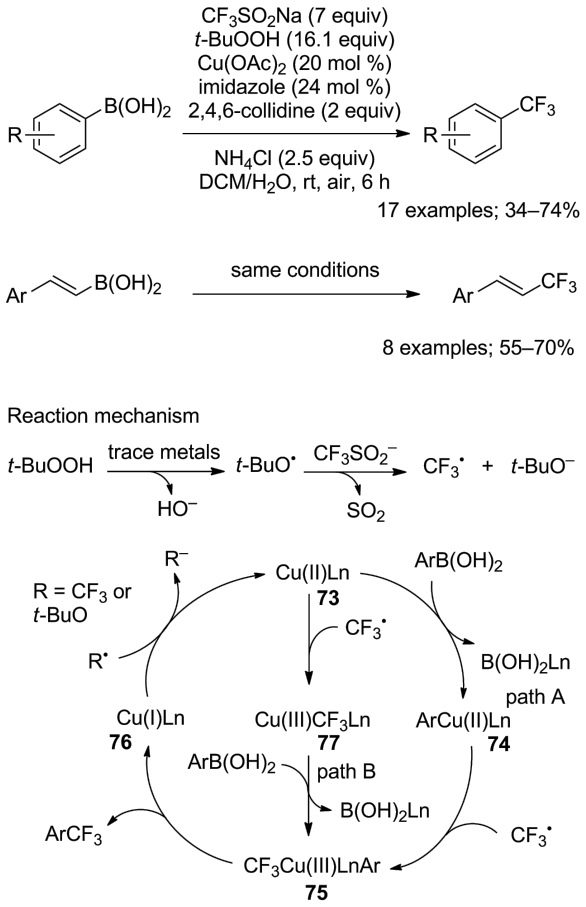

Scheme 54: Oxidative trifluoromethylation of aryl- and vinylboronic acids.

Trifluoromethylation of potassium organotrifluoroborates: In 2013, Molander, Rombouts and co-workers simply applied the reaction conditions described by Sanford for boronic acids to a series of unsaturated potassium organotrifluoroborates (Scheme 55) [80]. In the case of aryl- and heteroaryltrifluoroborates, electron-rich substrates were efficiently trifluoromethylated although the increase of the steric hindrance caused a decrease in yields. On the other hand, the yields obtained with electron-poor potassium organotrifluoroborates were lower. In the same paper, the preparation of trifluoromethyl-substituted alkynes and alkenes from alkynyl- and alkenyltrifluoroborates was demonstrated albeit in moderate yields. The yields of the trifluoromethylation of alkenyltrifluoroborates strongly depended on the substitution of the olefin (Scheme 55).

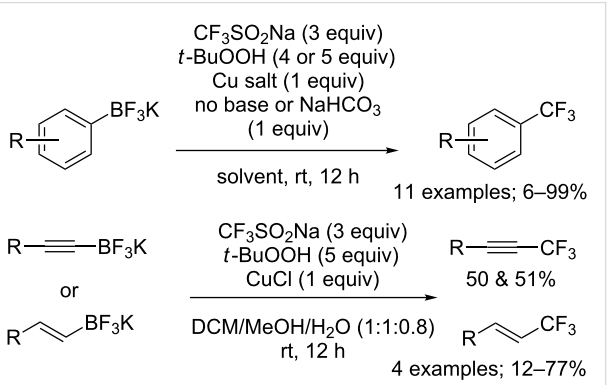

Scheme 55: Oxidative trifluoromethylation of unsaturated potassium organotrifluoroborates.

Simultaneously, Dubbaka and co-workers reported the trifluoromethylation of aryl-, heteroaryl-, and vinyltrifluoroborates with CF_3SO_2Na (Scheme 56) [81]. The authors used basically the same protocol as Sanford and Molander but observed that a more diluted reaction medium gave improved reaction yields.

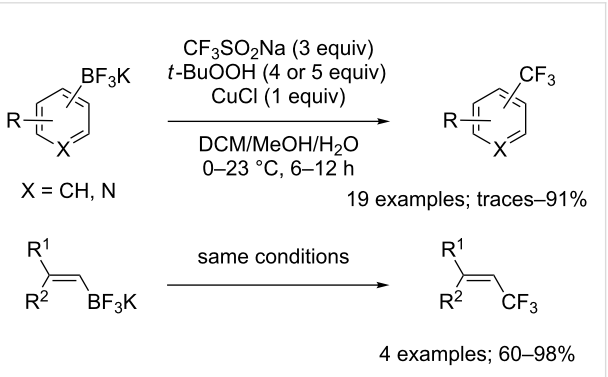

Scheme 56: Oxidative trifluoromethylation of (hetero)aryl- and vinyltrifluoroborates.

Trifluoromethylation of alkenes by decarboxylation: Liu and co-workers were the first to describe the copper-catalysed decarboxylative trifluoromethylation of α,β-unsaturated carboxylic acids in the presence of CF_3SO_2Na and TBHP [82]. Various (hetero)arenes were compatible with these reaction conditions (Scheme 57); nevertheless, cinnamic acids bearing electron-donating groups afforded the corresponding products in better yields. The stereoselectivity was moderate to high from 76:24 to 99:1. Interestingly, aryls bearing a nitro or a chloro substituent gave the corresponding α-trifluoromethyl ketones.

This process was interesting for the construction of C_{vinyl}–CF_3 bonds via a radical addition–elimination (Scheme 57).

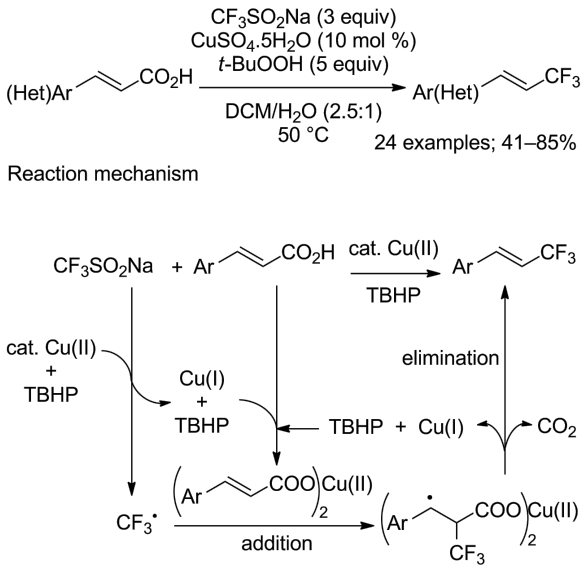

Scheme 57: Copper−catalysed decarboxylative trifluoromethylation of cinnamic acids.

Soon after, Maiti and co-workers reported an iron-mediated trifluoromethylation of α,β-unsaturated carboxylic acids with CF_3SO_2Na, iron(III) chloride and potassium persulfate as oxidant [83]. The substrate scope was evaluated on 10 cinnamic acids (Scheme 58). Under these conditions, both electron-rich or electron-poor arenes gave the vinylic CF_3 products in good yields and with excellent stereoselectivities. A mechanism was proposed starting from the generation of iron carboxylate and the reaction with the CF_3 radical followed by extrusion of CO_2 and radical coupling (Scheme 58).

Two major drawbacks appeared in the above-mentioned works: halo-substituted aryl derivatives failed to give the expected products and α,β-unsaturated carboxylic acids substituted at the β-position were not studied. Accordingly, Li, Duan and co-workers reported a copper/silver-catalysed decarboxylative trifluoromethylation of α,β-unsaturated carboxylic acids with CF_3SO_2Na that tolerated various substrates bearing halogens as well as α,β-unsaturated carboxylic acids substituted at the β-position (Scheme 59) [84]. It was even noticed that β-methyl or β-phenyl-substituted cinnamic acids gave better yields compared to unsubstituted cinnamic acid. All products were obtained with excellent stereoselectivity. To gain insight about the mechanism, the authors used TEMPO as a radical scavenger and concluded that CF_3 radical was involved in this reaction (Scheme 59).

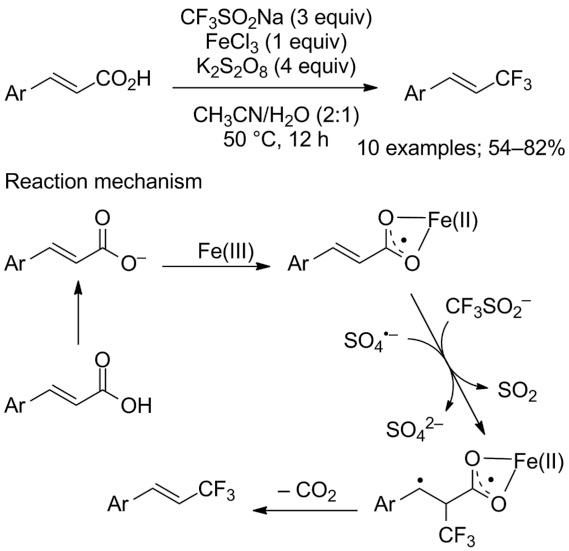

Scheme 58: Iron-mediated decarboxylative trifluoromethylation of α,β-unsaturated carboxylic acids.

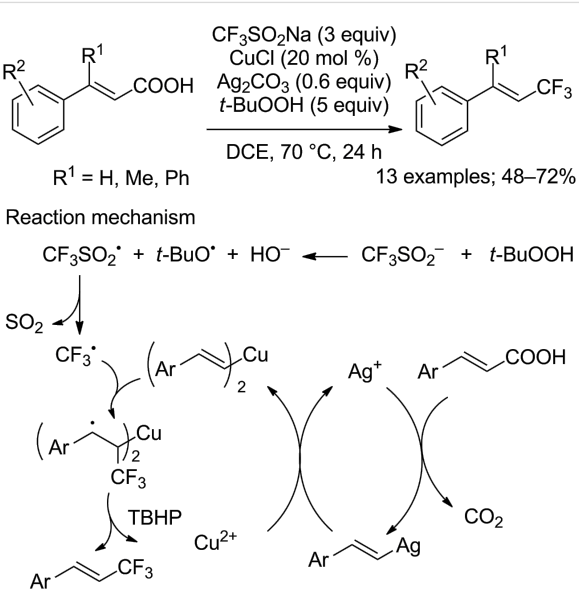

Scheme 59: Cu/Ag-catalysed decarboxylative trifluoromethylation of cinnamic acids.

A metal-free protocol for the decarboxylative trifluoromethylation of cinnamic acids with CF_3SO_2Na was reported by Shang, Liu and co-workers using iodine pentoxide (I_2O_5) as oxidant. The substrate scope was evaluated on 9 α,β-unsaturated carboxylic acids substituted by electron-rich aryls (Scheme 60) [85]. The mild conditions gave the trifluoromethylated products in excellent yields with high stereoselectivities. Nevertheless, the reaction conditions did not allow the formation of products with electron-withdrawing substituents on the aromat-

ic ring, such as the nitro group. The case of halogen-substituted cinnamic acids was not studied. Finally, mechanistic studies conducted by electron-spin resonance and by spin trapping technology suggested a free-radical addition– elimination process (Scheme 60).

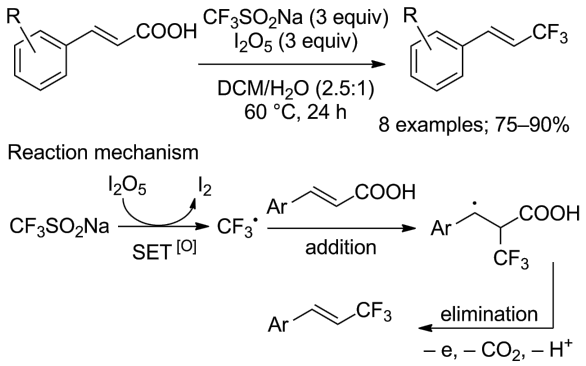

Scheme 60: I_2O_5-Promoted decarboxylative trifluoromethylation of cinnamic acids.

Trifluoromethylation of alkenes by denitration: Another route to the C_{vinyl}–CF_3 bond is the denitrative trifluoromethylation of β-nitrostyrenes. More generally, this transformation has attracted much attention as a useful method for the construction of C_{vinyl}–R moieties. In 2016, Li, Duan and co-workers reported this trifluoromethylation by means of CF_3SO_2Na catalysed by silver nitrate in the presence of a large excess of di-*tert*-butyl peroxide (DTBP) as the oxidant and tetrabutylammonium iodide (TBAI) as a phase-transfer catalyst (Scheme 61) [86]. The substrate scope was evaluated on 16 β-nitrostyrenes and substrates bearing electron-donating groups as well as halides afforded the corresponding trifluoromethylstyrenes in moderate to good yields. However, the substrates with electron-withdrawing groups (CN, NO_2) led to trifluoromethylated products in poor yields. This transformation was highly stereoselective, only (*E*)-isomers of the products were obtained. Experiments in the presence of 1,1-diphenylethylene as a radical scavenger led the authors to propose a radical process for the trifluoromethylation as described in Scheme 61.

Trifluoromethylation of styrene derivatives: An obviously simple route for the synthesis of trifluoromethylated styrene derivatives is the direct C–H trifluoromethylation of alkenes. Very recently, Shen, Loh and co-workers reported a copper-catalysed direct trifluoromethylation of the vinylic C_{sp2}–H bond of styrene derivatives with CF_3SO_2Na, di-*tert*-butyl peroxide, 10 mol % of copper(I) iodide, 1-methylimidazole (NMI) as ligand to copper and tetrabutylammonium iodide (TBAI) as additive (Scheme 62) [87]. The mild reaction conditions allowed a wide variety of functional groups to be tolerated and afforded a

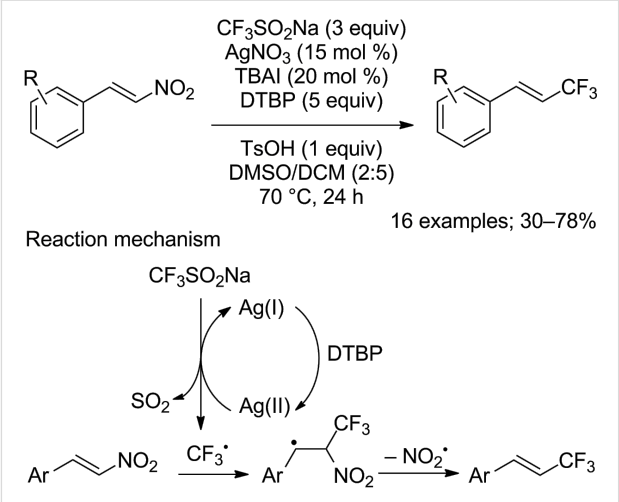

Scheme 61: Silver(I)-catalysed denitrative trifluoromethylation of β-nitrostyrenes.

series of trifluoromethylated styrenes in moderate to good yields and with excellent stereoselectivity. However, aliphatic alkenes or styrenes bearing electron-withdrawing groups were not suitable for this reaction. Based on control experiments, the authors proposed a radical pathway for this reaction (Scheme 62).

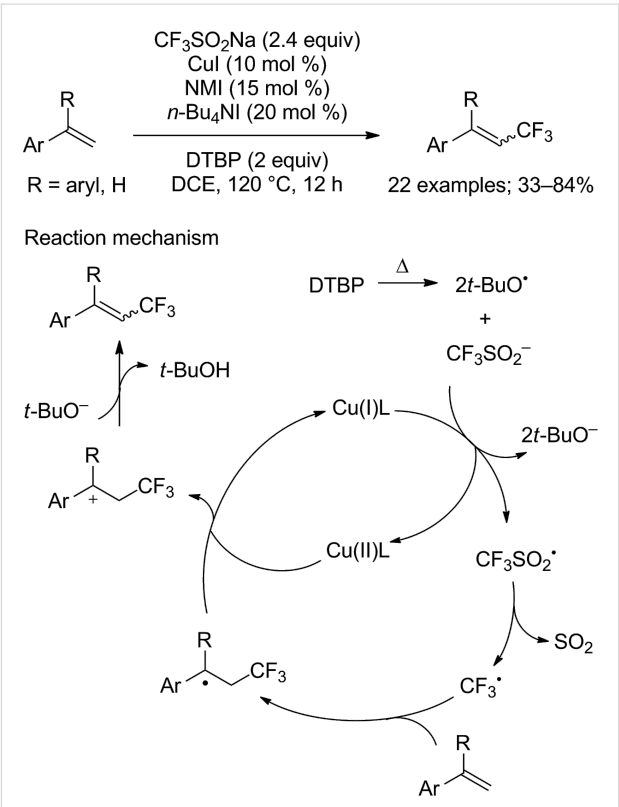

Scheme 62: Copper-catalysed direct trifluoromethylation of styrene derivatives.

Trifluoromethylation of enamines: Highly functionalised alkenes represented by (*Z*)-methyl-3-(phenylamino)acrylates **78** were subjected to Baran's conditions for the synthesis of β-trifluoromethylated enamines. Indeed, Jiang, Wu and co-workers reported mild, transition-metal-free conditions, insensitive to air and water, for the synthesis of a wide range of CF_3-enamines using CF_3SO_2Na and TBHP as initiator and oxidant (Scheme 63) [88]. Moderate to good yields were obtained and only (*E*)-isomers were observed. The authors carried out several experiments such as the use of TEMPO or 2,6-di-*tert*-butyl-4-methylphenol (BHT) as scavengers in order to investigate the mechanism of this reaction (Scheme 63).

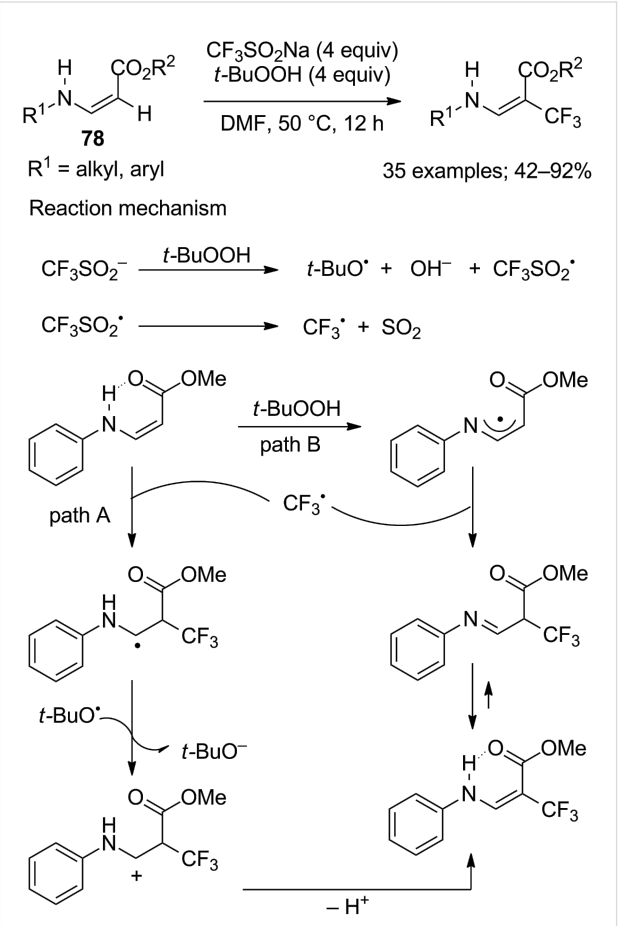

Scheme 63: Transition-metal-free synthesis of β-trifluoromethylated enamines.

Trifluoromethylation of alkynes: Together with the iodotrifluoromethylation of alkenes leading to C_{sp3}–CF_3 products (see Scheme 22), the Liu group extended the free-radical iodotrifluoromethylation to alkynes with the combination of CF_3SO_2Na/I_2O_5 and assistance of $NaHCO_3$ (Scheme 64) [42]. The substrate scope was carried out on various aryl-substituted alkynes and one propargylic ester; (*E*)-CF_3 alkenyl iodides were obtained stereoselectively in moderate to high yields via a free-radical process.

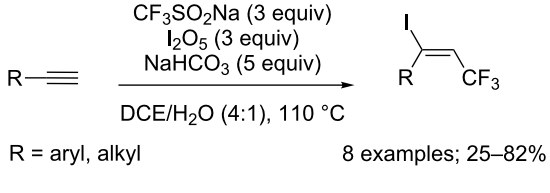

Scheme 64: I_2O_5-mediated iodotrifluoromethylation of alkynes.

Trifluoromethylation of isonitriles: The synthesis of trifluoromethylated phenanthridines **79** from aryl isonitriles has been the recent subject of several investigations as potential structural unit in pharmaceuticals. In this context, CF_3SO_2Na was used by Zhang and co-workers in a silver-catalysed tandem trifluoromethylation and cyclisation of aryl isonitriles (Scheme 65) [89]. A wide variety of aryl isocyanides were transformed into the corresponding phenanthridines in moderate to good yields; some regioisomers were obtained depending on the biphenyl substituents. Here again, a radical pathway was established for this transformation (Scheme 65).

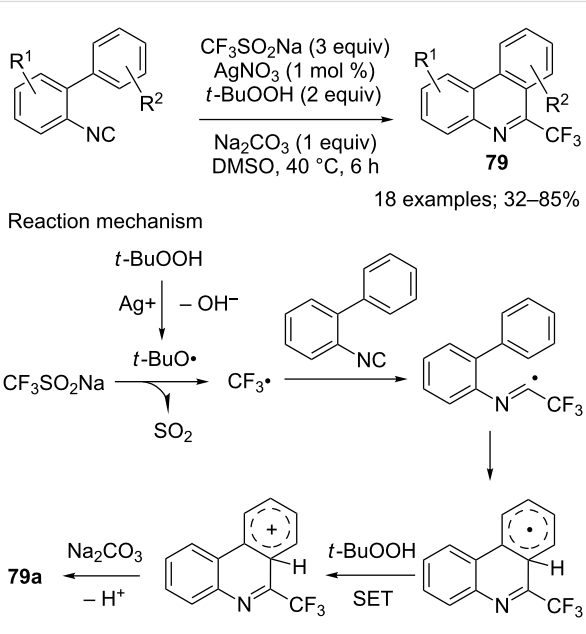

Scheme 65: Silver-catalysed tandem trifluoromethylation/cyclisation of aryl isonitriles.

Simultaneously, Lu and co-workers reported a transition-metal-free synthesis of the trifluoromethylphenanthridine **79a** in 58% yield using the system $CF_3SO_2Na/K_2S_2O_8/K_2CO_3$ in H_2O/CH_3CN at 80 °C [90]. In addition, Maruoka and co-workers used the system CF_3SO_2Na/PIFA/AcONa in AcOEt at room

temperature for 1.5 h to get **79a** in 74% yield [50]. Mid 2017, Ao, Liu and co-workers exploited the reaction conditions developed previously for the photoredox trifluoromethylation of vinyl azides (see Scheme 8) in the synthesis of fluorinated phenanthridines **79**. The yields were moderate to good and regioselectivity issues appeared depending on the biphenyl substituents (Scheme 66) [91].

Scheme 66: Photoredox trifluoromethylation of 2-isocyanobiphenyls.

C_{sp}–CF_3 bond-forming reactions

For the synthesis of trifluoromethylacetylenes **81**, a copper-mediated trifluoromethylation of potassium alkynyltrifluoroborates **80** with CF_3SO_2Na was developed by Dubbaka and co-workers (Scheme 67) [92]. The scope was large including aryl, heteroaryl, alkenyl, and aliphatic alkynyltrifluoroborates and the yields were moderate. Mechanistically, the CF_3 radical was generated under Langlois' conditions by means of *tert*-butyl hydroperoxide and CuCl.

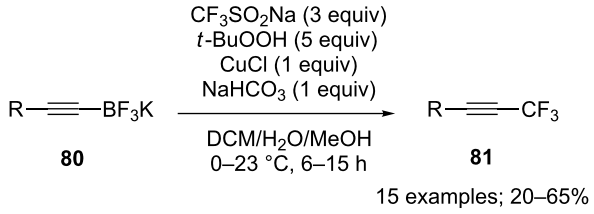

Scheme 67: Trifluoromethylation of potassium alkynyltrifluoroborates with CF_3SO_2Na.

N–CF_3 bond-forming reactions

C-, O-, and S-trifluoromethylated compounds are common in the field of biologically active molecules unlike the N–CF_3 motif despite the huge number of nitrogen-containing pharmaceuticals. In 2017, Selander and co-workers reported a chemoselective *N*-trifluoromethylation of nitrosoarenes **82** in the presence of CF_3SO_2Na, a catalytic amount of copper(II), *tert*-butyl hydroperoxide as oxidant and hydroquinone as additive [93]. No reaction was observed in the absence of the copper salt. The scope was evaluated on 14 nitrosoarenes featuring electron-poor and electron-rich groups. The reaction conditions were suitable with a wide variety of functionalised nitrosoarenes and the corresponding trifluoromethylated hydroxylamines **83** were obtained in moderate to good yields (Scheme 68). The authors proposed a radical mechanism with two pathways for the generation of the CF_3 radical, either by copper species or by *tert*-$BuO^{\bullet}$ (Scheme 68). Interestingly, N–CF_3 anilines were easily obtained after reduction of the N–O bond.

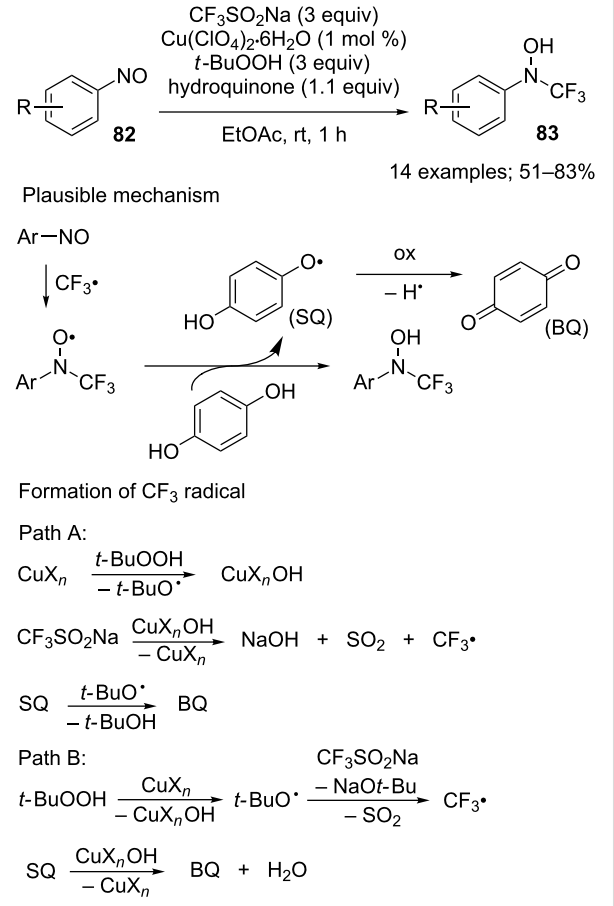

Scheme 68: *N*-trifluoromethylation of nitrosoarenes with CF_3SO_2Na (SQ: semiquinone).

S–CF_3 bond-forming reactions

Synthetic routes to trifluoromethylthiolated compounds are diverse, one is the S–CF_3 bond formation (see next section for C–SCF_3 bond formation). For this purpose, Langlois and co-workers used aliphatic and aromatic disulfides, RS–SR, which reacted with CF_3SO_2Na in the presence of an oxidant, *t*-BuOOH providing the best yields, to afford the trifluoromethyl thioethers (Scheme 69a) [20]. Other oxidants such as $K_2S_2O_8$ and $(NH_4)_2Ce(NO_3)_6$ displayed lower reactivity and selectivity. Only one sulfenyl moiety of the disulfide was trifluoromethylated in this approach, the second being oxidised without trifluoromethylation. Aryl disulfides exhibited a lower

reactivity and selectivity because side radical aryl C–H trifluoromethylation occurred competitively. This approach was applied to the synthesis of *S*-trifluoromethyl-containing amino acids **85** from dithio-amino acids **84** (Scheme 69b) [94].

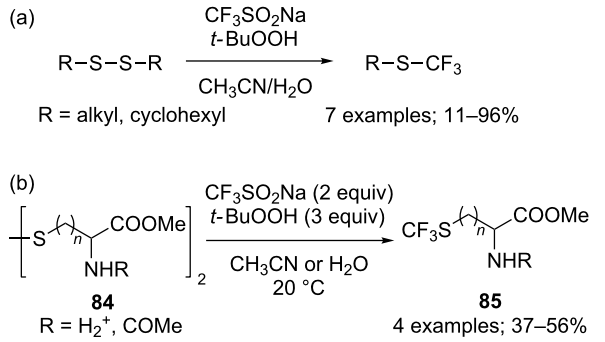

Scheme 69: Trifluoromethylation of disulfides with CF_3SO_2Na.

Apart from disulfides, thiols were also used as substrates by Yi and co-workers to produce several trifluoromethyl thioethers and aliphatic trifluoromethylthiols. Their contribution was inspired by the previous work of Liu, using iodine pentoxide as an inexpensive inorganic oxidant [42] to generate the CF_3 radical and release of iodine, which then reacted with the thiol to first form the corresponding disulfide **86** (detected as reaction intermediate) and further the sulfenyl iodide **87**. The final SCF_3 product was the result of the reaction of $CF_3^{\bullet}$ with either **86** or/and **87** (Scheme 70) [95]. The reaction performed well only at high reaction temperature (110 °C) for both thiophenols, benzylthiols and mercapto derivatives. The same research group recently reported different reaction conditions to obtain the same SCF_3 products by means of CF_3SO_2Na in the presence of potassium persulfate and a catalytic amount of silver nitrate at 80 °C in acetonitrile and water [96].

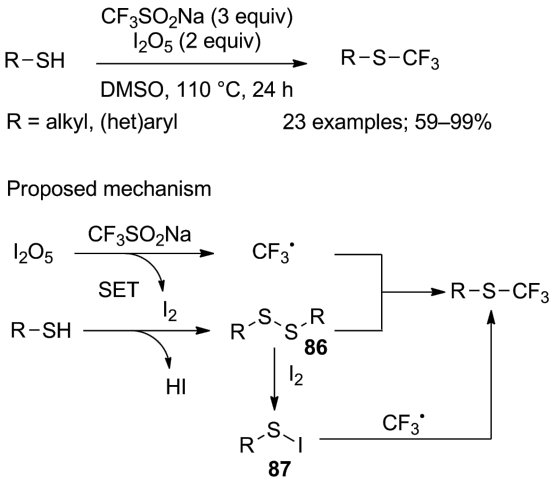

Scheme 70: Trifluoromethylation of thiols with CF_3SO_2Na/I_2O_5.

2 Trifluoromethylsulfenylation

In the early development of the direct electrophilic trifluoromethylthiolation, trifluoromethanethiol (CF_3SH), trifluoromethanesulfenyl chloride (CF_3SCl), and bis(trifluoromethyl) disulfide (CF_3SSCF_3) were the only reagents available, but their gaseous and toxic nature precluded a wider use. Fortunately, in the recent years, a collection of stable and easy-to-handle reagents was designed to perform efficient trifluoromethylthiolations [97]. Less sophisticated and suitable for large scale industrial use, CF_3SO_2Na was first used in trifluoromethylthiolation reactions in 2015 by Yi, Zhang and co-workers who reported the direct copper-catalysed trifluoromethylthiolation of indoles, pyrroles as well as enamines in the presence of $(EtO)_2P(O)H$ as reductant, CuCl and DMSO in toluene at 110 °C (Scheme 71) [98]. Unlike its use in trifluoromethylation reactions, here, no extrusion of SO_2 ocurred from CF_3SO_2Na thus allowing the transfer of the SCF_3 motif. Under these reaction conditions, indoles bearing an electron-donating group gave better yields compared to those with electron-rich groups. Using the same protocol, the trifluoromethylsulfenylated pyrroles and enamines were obtained in good to excellent yields. After mechanistic studies by ^{19}F NMR spectroscopy, the authors proposed that bis(trifluoromethyl) disulfide, CF_3SSCF_3, was generated in situ (Scheme 71, path B). The route through path A and CF_3SOH was also envisaged but should lead only to the formation of small amount of product.

The same authors further demonstrated that the trifluoromethylsulfenylation can be conducted under metal-free conditions by replacing CuCl with trimethylsilyl chloride (TMSCl) to generate the cation CF_3S^+ in the presence of $(EtO)_2P(O)H$ [99]. Again, the electrophilic trifluoromethylsulfenylation of indoles was studied but also the trifluoromethylthiolation of electron-rich arenes (Scheme 72). Using this protocol, trifluoromethylsulfenylated compounds were obtained in moderate to excellent yields. Compared to the CuCl-mediated approach, this method directly converted CF_3SOH into CF_3S^+ by reaction with TMSCl (Scheme 72).

Based on this above-mentioned work and simultaneously to the metal-free approach, Cai and co-workers reported the direct trifluoromethylsulfenylation of indoles, pyrroles and enamines, with CF_3SO_2Na, triphenylphosphine and *N*-chlorophthalimide without added metal and at room temperature (Scheme 73) [100]. In general, the substrates were successfully trifluoromethylsulfenylated in moderate to excellent yields by in situ generated CF_3SCl as suggested by ^{19}F NMR studies and previous literature reports.

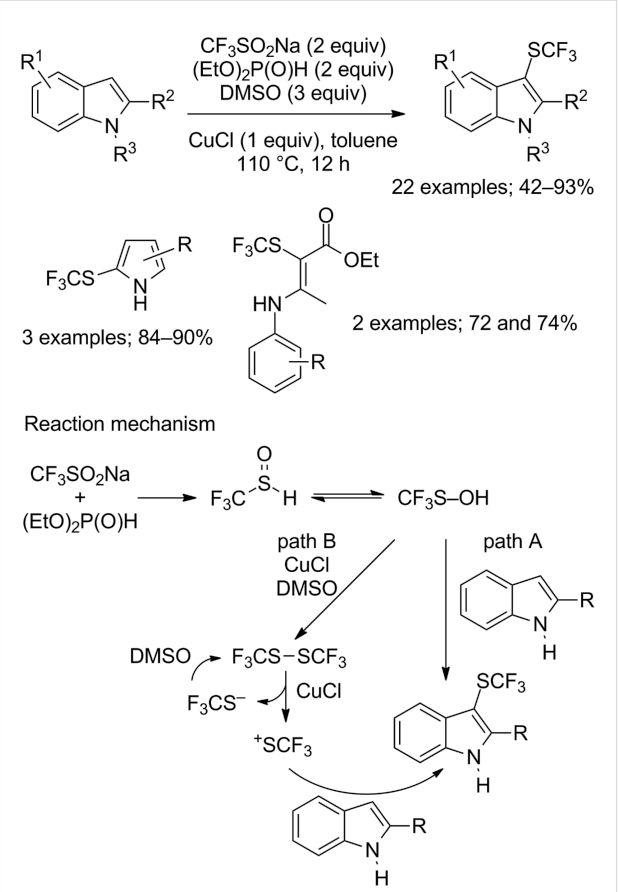

Scheme 71: Electrophilic trifluoromethylsulfenylation by means of $CF_3SO_2Na/(EtO)_2P(O)H/CuCl/DMSO$.

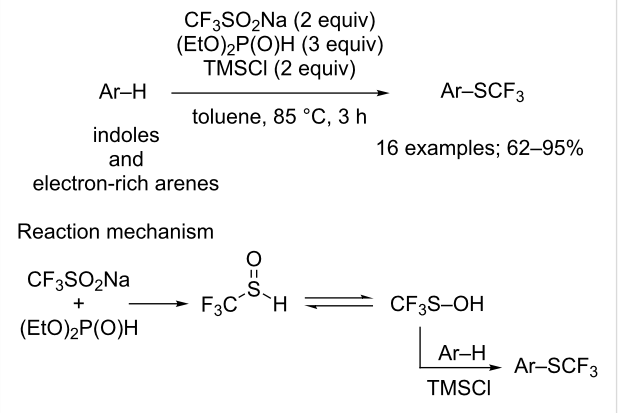

Scheme 72: Electrophilic trifluoromethylsulfenylation by means of $CF_3SO_2Na/(EtO)_2P(O)H/TMSCl$.

Different phosphorus reductive reagents were evaluated by Liu, Lin and co-workers. It was found that phosphorus trichloride (PCl_3) allowed to react with CF_3SO_2Na and a series of indoles afforded the corresponding 3-CF_3S derivatives selectively in good to excellent yields (Scheme 74) [101]. Unlike the work of

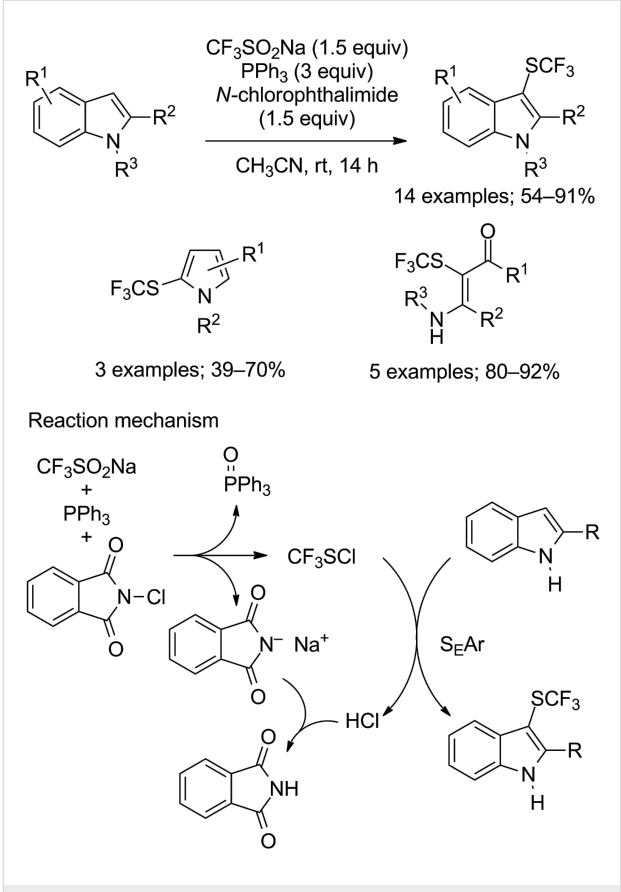

Scheme 73: Electrophilic trifluoromethylsulfenylation by means of $CF_3SO_2Na/PPh_3/N$-chlorophthalimide.

Cai using PPh_3 and *N*-chlorophthalimide, here, PCl_3 was used both as a reducing and chlorinating reagent. ^{19}F NMR investigation of reaction intermediates showed the signal of CF_3SCl, species which was interpreted as the key intermediate in the reaction system. Noteworthy, switching from PCl_3 to $P(O)Cl_3$ allowed the synthesis of the trifluoromethylsulfinyl derivatives instead of the trifluoromethylsulfenyl ones (see next section).

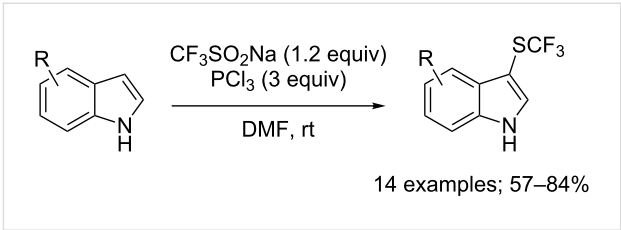

Scheme 74: Electrophilic trifluoromethylsulfenylation by means of CF_3SO_2Na/PCl_3.

At the same time, Zhao, Lu and co-workers described similar observations. The trifluoromethylsulfenylation of indoles and electron-rich aromatics was realised with CF_3SO_2Na in the presence of PCl_3 (1.2 instead of 3 equivalents) in acetonitrile at

60 °C (Scheme 75) [102]. The authors proposed a reaction mechanism that involved the 3-trifluoromethylsulfinyl intermediate **88** (Scheme 75). Consequently, a decrease of the amount of PCl_3 and the temperature was proposed to interrupt the reaction and to obtain **88** selectively (see next section).

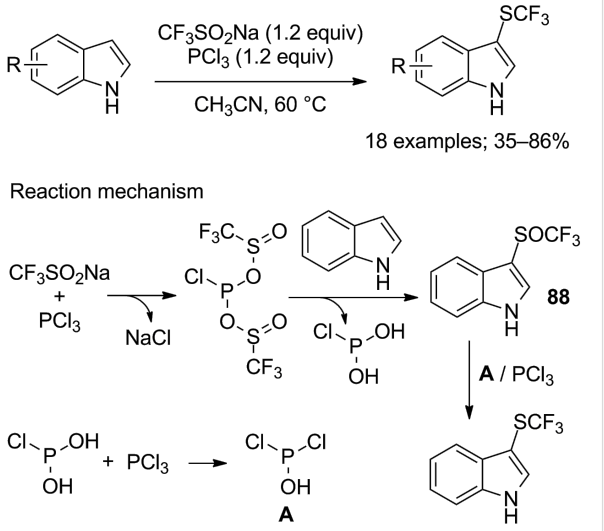

Scheme 75: Electrophilic trifluoromethylsulfenylation by means of CF_3SO_2Na/PCl_3.

Aryl iodides served as substrates in a programmable regioselective trifluoromethylsulfenylation by direct coupling with $CuSCF_3$ generated form CF_3SO_2Na in the presence of copper(I) chloride and triphenylphosphine. Indeed, Yang, Vicic and co-workers described the deoxygenative reduction of CF_3SO_2Na to form the ligand-free $CuSCF_3$ intermediate that reacted with a diverse array of aryl iodides in high yields (Scheme 76) [103]. In addition, $CuSCF_3$ was reacted with various ligands to furnish air-stable [$LCu(SCF_3)$] complexes as trifluoromethylsulfenylating agents.

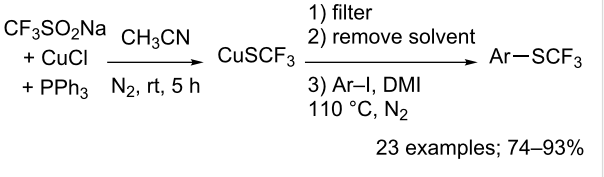

Scheme 76: Trifluoromethylsulfenylation of aryl iodides with in situ generated $CuSCF_3$ (DMI: 1,3-dimethyl-2-imidazolidinone).

3 Trifluoromethylsulfinylation

In 1999, Langlois and co-workers used the system $CF_3SO_2Na/POCl_3$ as an efficient and inexpensive equivalent of the $CF_3S(O)^+$ cation for the trifluoromethylsulfinylation of various amines, alcohols as well as carbon nucleophiles (Scheme 77) [104]. In the case of primary amines, the addition of one equivalent of diisopropylethylamine to the reaction medium was necessary to trap acidic phosphoric species coming from the reaction and to reach higher product yields. *N*-Methylpyrrole was used as an example of C-nucleophile affording the corresponding $S(O)CF_3$ product in 60% yield.

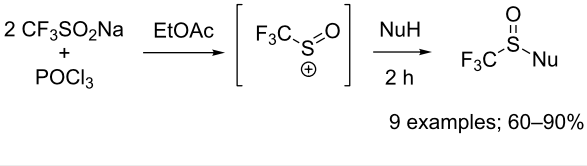

Scheme 77: Pioneering trifluoromethylsulfinylation of N, O, and C-nucleophiles.

A few years later, the same group reported the synthesis of the trifluoromethanesulfinamide **89** derived from (1*R*,2*S*)-ephedrine using the process described above (Scheme 78). Compound **89** was used as an efficient trifluoromethylating agent for a wide range of non-enolisable and enolisable carbonyl compounds [105].

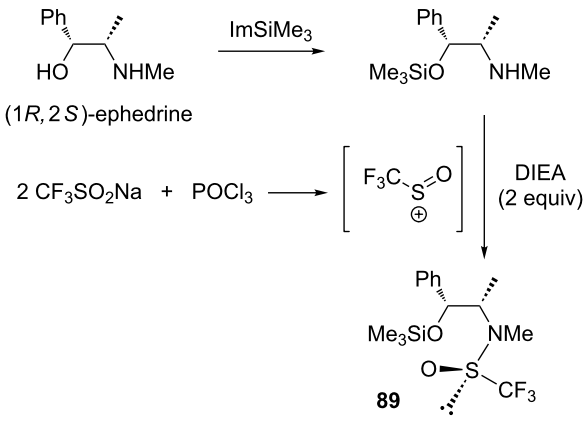

Scheme 78: Trifluoromethylsulfinylation of (1*R*,2*S*)-ephedrine (Im: imidazole; DIEA: *N*,*N*-diisopropylethylamine).

Other *N*-aryl- and *N*-alkyltrifluoromethanesulfinamides have been prepared from the corresponding anilines or aliphatic amines with CF_3SO_2Na and phosphoryl chloride for further reactions with arynes [106] or in the synthesis of trifluoromethylsulfonimidates [107].

Another direct trifluoromethylsulfinylation method was described by Wakselman's group in 2001 with CF_3SO_2Na in the presence of triflic acid (Scheme 79) [108]. This method was applied to simple aryls featuring a halogen atom, a OCF_3 group or an acetanilide function. In this reaction, *ortho*/*para* regio-

isomers were formed in ratios from 25:75 to 3:97. With regard to the mechanism, the sulfinate was protonated to generate the highly electrophilic $CF_3S(OH)_2^+$ species that underwent an S_EAr with arenes. A further development of the method consisted in the replacement of triflic acid with triflic anhydride in dichloromethane, and this strategy has been applied to the synthesis of trifluoromethylsulfonium salts, known as Umemoto's reagents [109-111].

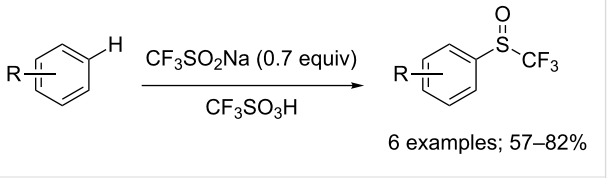

Scheme 79: Trifluoromethylsulfinylation of substituted benzenes with CF_3SO_2Na/CF_3SO_3H.

After these initial works, it is only in 2017 that new results using CF_3SO_2Na appeared in the field. As briefly mentioned in the preceding section, Liu, Lin and co-workers evaluated different phosphorus reductive reagents and found that PCl_3 (3 equiv) afforded the corresponding 3-CF_3S derivatives whereas $P(O)Cl_3$ (1 equiv) allowed to get selectively the trifluoromethylsulfinyl derivatives **90** (Scheme 80) [101].

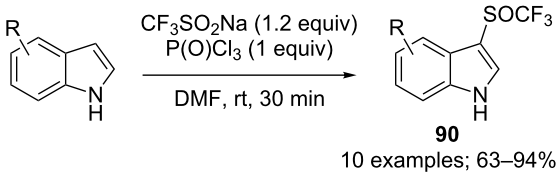

Scheme 80: Trifluoromethylsulfinylation of indoles with $CF_3SO_2Na/P(O)Cl_3$.

With the same objective of partial reduction of CF_3SO_2Na with phosphorus reagents for the selective trifluoromethylsulfinylation, Zhao, Lu and co-workers noticed that a decrease of the amount of PCl_3 and a slight lowering of the temperature were beneficial to the desired trifluoromethylsulfinylation (Scheme 81) [102].

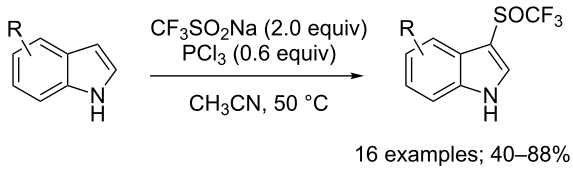

Scheme 81: Trifluoromethylsulfinylation of indoles with CF_3SO_2Na/PCl_3.

4 Trifluoromethylsulfonylation

The trifluoromethylsulfonyl motif (SO_2CF_3, Tf, triflyl) is highly electron-withdrawing (SO_2CF_3, $\sigma_m = 0.79$, $\sigma_p = 0.93$) and trifluoromethylsulfones (or triflones), in which the trifluoromethylsulfonyl group is attached to a carbon atom, are moderatly lipophilic (SO_2CF_3, $\pi = 0.55$ versus CF_3, $\pi = 0.88$). Therefore, the SO_2CF_3 group has been frequently employed in catalysts and ligands, as subunit of bioactive compounds, or as building block for advanced functional materials. Trifluoromethylsulfones have been prepared by several approaches [5], in particular by means of CF_3SO_2Na as compiled hereafter.

C_{sp3}–SO_2CF_3 bond-forming reactions

The trifluoromethanesulfinate, triflinate anion, possesses a low nucleophilicity thus affecting its potential in substitution reactions. Mainly primary bromides and some secondary ones (α-bromo ketones and esters) could be converted into trifluoromethylsulfones. From benzyl bromides, phase-transfer conditions [112] and/or high temperatures [113-115] were required to obtain the triflones in low to high yields (Scheme 82). Using benzyl chloride in propionitrile at reflux led to 90% yield of the corresponding triflone [115]. Methyl iodide was also used as substrate for the formation of methyl trifluoromethylsulfone [116]. The displacement of a tosyl group by CF_3SO_2Na in the presence of n-Bu_4NI in THF worked with 60 % yield [117].

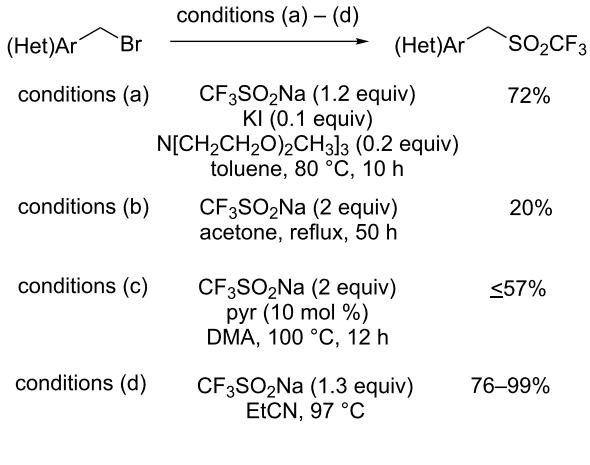

Scheme 82: Formation of triflones from benzyl bromides (DMA: dimethylacetamide).

α-Trifluoromethylsulfonyl ketones, esters, and amides were prepared by displacement of the corresponding bromide (Scheme 83a) [112,118] or chloride (Scheme 83b,c) [118,119] under various conditions. Long reaction times and high temperatures were often required.

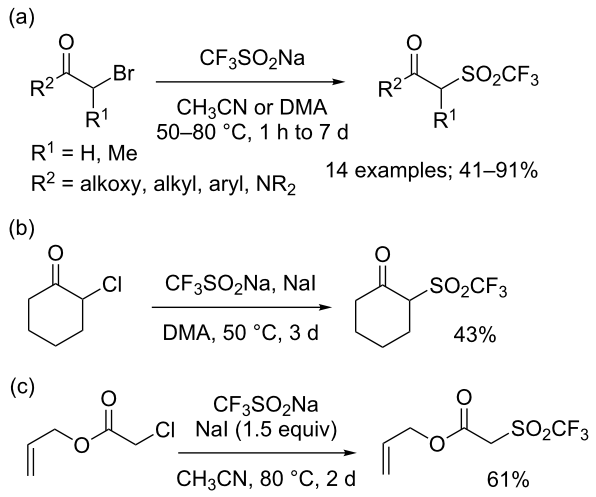

Scheme 83: Formation of α-trifluoromethylsulfonyl ketones, esters, and amides.

Allylic trifluoromethylsulfones could be prepared from aromatic allylic alcohols or esters and CF_3SO_2Na in the presence of *p*-toluenesulfonic acid at 100 °C in dioxane. The reaction was highly regioselective, worked well with primary, secondary and tertiary allylic alcohols, and tolerated a wide range of functions (Scheme 84) [120]. The reaction proceeded through an S_N1-type mechanism by the formation of a cationic Π-allyl intermediate by means of *p*-toluenesulfonic acid.

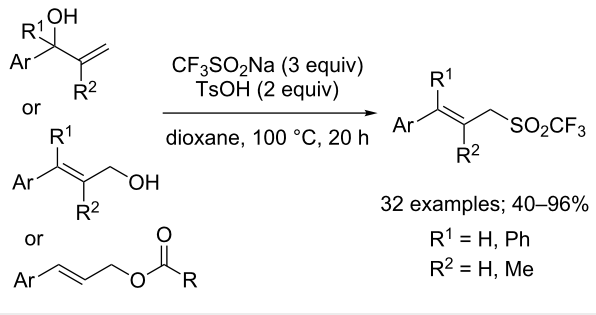

Scheme 84: Allylic trifluoromethanesulfonylation of aromatic allylic alcohols.

C_{sp2}–SO_2CF_3 bond-forming reactions

Aryl triflones: The synthesis of aryl trifluoromethylsulfones was investigated by Shekhar and co-workers in 2013. First, Pd- and Cu-catalysed coupling reactions with iodobenzene or arylboronic acids failed because of the poor nucleophilicity of CF_3SO_2Na [121]. It was next found that aryl iodonium salts reacted with CF_3SO_2Na in the presence of copper catalysts. In particular cuprous oxide in DMF gave the triflones in moderate to high yields from a variety of symmetrical and unsymmetrical (het)aryl iodonium salts **91** bearing various functional groups and counteranions (Scheme 85) [121]. The reaction was sulfonyl-retentive and was likely to proceed via a nonradical pathway, probably involving Cu(I)/Cu(III) intermediates.

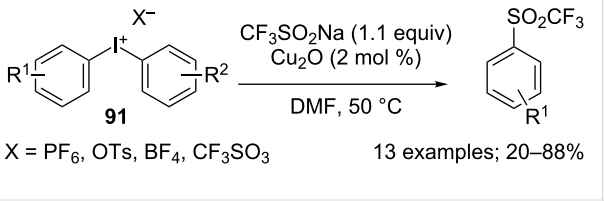

Scheme 85: Copper-catalysed couplings of aryl iodonium salts with CF_3SO_2Na.

Another example of trifluoromethanesulfonylation of a diaryl iodonium salt was reported by Li and co-workers as a single case, among several other nucleophiles, using 10 mol % of copper(II) triflate in dichloroethane at 80 °C [122]. The hypervalent iodine species could also be generated in situ [123].

In 2016, Shekhar's group finally succeeded in the trifluoromethanesulfonylation of the more readily available (het)aryl triflates and some aryl chlorides using a combination of $Pd_2(dba)_3$ and the bulky RockPhos phosphine ligand in toluene and tris(3,6-dioxaheptyl)amine (TDA) as phase-transfer catalyst to facilitate the reaction with the sparingly soluble CF_3SO_2Na (Scheme 86) [124].

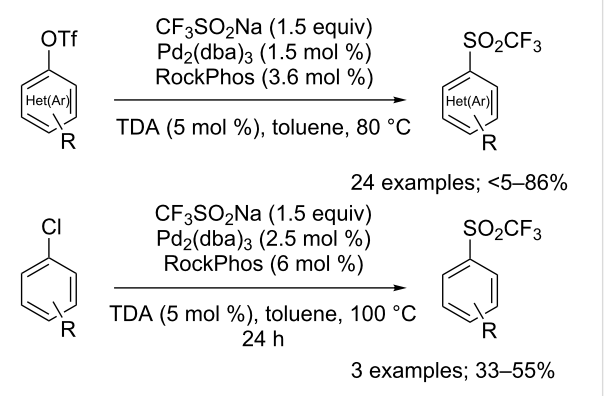

Scheme 86: Palladium-catalysed trifluoromethanesulfonylation of aryl triflates and chlorides with CF_3SO_2Na.

Arenediazonium tetrafluoroborates **92** were also suitable substrates for the formation of triflones. Xu, Qing and a co-worker demonstrated that CF_3SO_2Na produced triflones when engaged in a Cu-catalysed reaction in DMSO (Scheme 87) [76]. The reaction was sulfonyl-retentive whereas in the presence of the oxidant *tert*-butyl hydroperoxide the chemoselective trifluoromethylation was obtained (see Scheme 52).

Scheme 87: Copper-catalysed coupling of arenediazonium tetrafluoroborates with CF_3SO_2Na.

Finally, a metal-free protocol was reported by Singh and co-workers, in which in situ generated benzyne was reacted with CF_3SO_2Na (Scheme 88) [125].

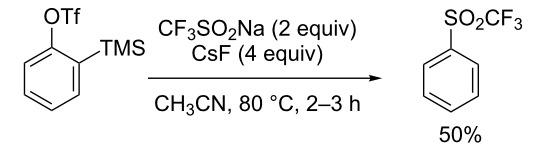

Scheme 88: Synthesis of phenyltriflone via coupling of benzyne with CF_3SO_2Na.

Vinyl triflones: The synthesis of two vinyl trifluoromethylsulfones was reported in 2004 by Ochiai and co-workers by treatment of λ^3-bromane **93** with CF_3SO_2Na in DCM at 0 °C (Scheme 89) [126]. The reaction also produced 1-alkynyltriflones as minor products. The 1-alkynyl-λ^3-bromanes acted as Michael acceptors for the sulfinate anion and underwent tandem Michael addition–carbene insertion reactions to yield the 1-trifluoromethanesulfonylcyclopentenes.

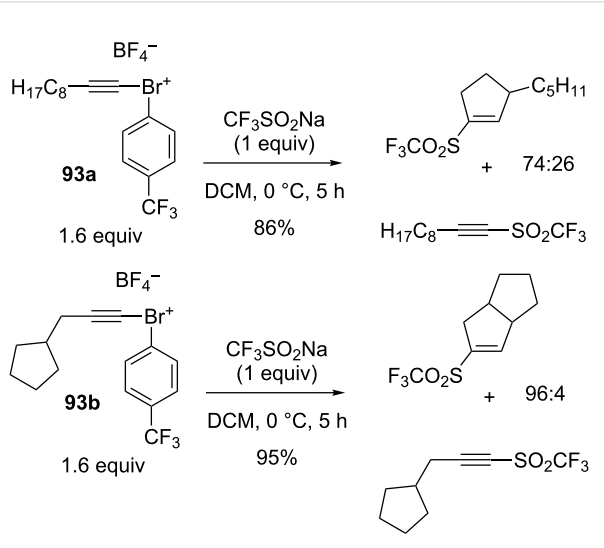

Scheme 89: Synthesis of 1-trifluoromethanesulfonylcyclopentenes from 1-alkynyl-λ^3-bromanes and CF_3SO_2Na.

Vinyl triflones with exclusive *E*-selectivity could also be prepared from allylic alcohols and CF_3SO_2Na under metal-free conditions as reported by Xu, Ji and co-workers (Scheme 90) [127]. Under acidic conditions, the π-allylic carbocation reacted with the sulfinyl anion leading to allylsulfone **95**, which underwent an electrophilic addition of PIDA and capture of the benzylic carbocation by water. Then, a concerted proton elimination and C–I bond cleavage occurred to give the triflylated allylic alcohol **94**.

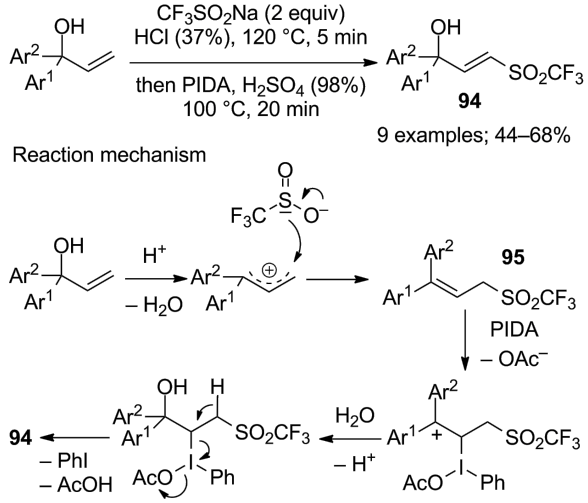

Scheme 90: One-pot synthesis of functionalised vinyl triflones.

Huang, Xu and co-workers demonstrated that styrenes, but also vinylbenzofuran and vinylthiophene, reacted with CF_3SO_2Na in the presence of iodine and CuCN to afford regioselectively the internal vinyl triflones **96** (Scheme 91) [128]. A cationic reaction mechanism was proposed by electrophilic addition of I_2 (or the in situ generated CF_3SO_2I) to the olefin. The highly strained iodonium bridge subsequently reacted with the sulfinyl anion to afford the iodotriflylated product, which eliminated HI to give the vinyl triflone. The role of CuCN was not precised at this stage.

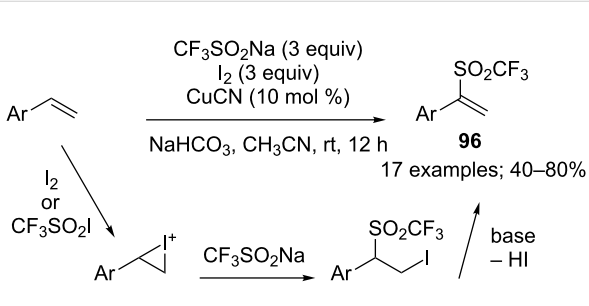

Scheme 91: Regioselective synthesis of vinyltriflones from styrenes.

C_{sp}–SO_2CF_3 bond-forming reactions

Apart from the side products described in Scheme 89, a variety of acetylenic triflones **98** was proposed by Zhang and co-workers. Alkynyl(phenyl) iodonium tosylates **97** reacted with CF_3SO_2Na in a transition metal-free protocol to furnish the acetylenic triflones under mild conditions (Scheme 92) [129]. The authors suggested that alkylidene carbene intermediates might be formed followed by a 1,2-rearrangement to yield the triflones. The reaction from ethynylbenzene and CF_3SO_2Na in the presence of Koser's reagent allowed to obtain the corresponding triflone albeit in a 33% yield.

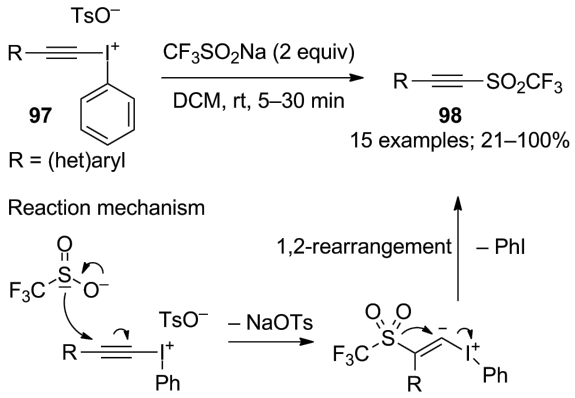

Scheme 92: Trifluoromethanesulfonylation of alkynyl(phenyl) iodonium tosylates by CF_3SO_2Na.

S–SO_2CF_3 and Se–SO_2CF_3 bond-forming reactions

Langlois' group prepared thiotrifluoromethanesulfonates **100** from sulfenyl chlorides **99** or disulfides **101** by two methods: first, sulfenyl chlorides were reacted with CF_3SO_2Na in DCM at room temperature [130]; second, a wider scope was obtained by reaction of disulfides with CF_3SO_2Na under oxidative conditions with either bromine [130] or PIFA [131] (Scheme 93a). These methodologies were extended to phenylselenyl chloride and diphenyl diselenide (Scheme 93b).

Conclusion

Sodium trifluoromethanesulfinate was used for the first time in direct radical trifluoromethylation under oxidative conditions by the Langlois group in 1991. Since that time its chemistry has evolved sporadically till 2011 and then immensely thanks to Baran's contribution. It enjoyed a rapid growth not only as donor of the trifluoromethyl group but also as a trifluoromethylsulfenylating agent, for the transfer of the whole SCF_3 motif, and as trifluoromethanesulfinylating agent for $S(O)CF_3$ transfer. CF_3SO_2Na is an easy-to-handle, inexpensive reagent that has became versatile for the construction of sophisticated fluorinated products in the pharmaceutical chemistry. It is the authors' hope that this review will contribute to stimulate further research toward new reactions and applications for this reagent that could include the formation of new bonds with other heteroatoms, novel tandem reactions, and the exploration of asymmetric reactions, so far absent with CF_3SO_2Na, to cite but a few examples.

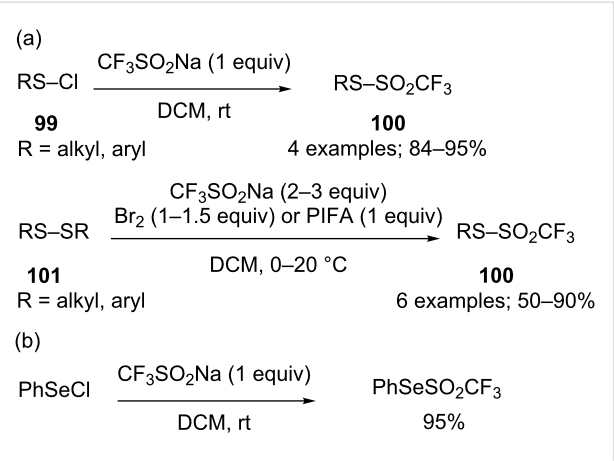

Scheme 93: Synthesis of thio- and selenotrifluoromethanesulfonates.

Acknowledgements

Our research was supported by the Centre National de la Recherche Scientifique CNRS, Normandy University, and Labex SynOrg (ANR-11-LABX-0029). H.C. thanks the French "Ministère de la Recherche et de l'Enseignement Supèrieur" for a doctoral fellowship. H.G. thanks Normandy University for a postdoctoral grant. The French Fluorine Network (GIS Fluor) is also acknowledged.

ORCID® iDs

Hélène Chachignon - https://orcid.org/0000-0001-6657-1728
Dominique Cahard - https://orcid.org/0000-0002-8510-1315

References

1. Kirsch, P. *Modern Fluoroorganic Chemistry;* Wiley-VCH: Weinheim, 2004.
2. Gillis, E. P.; Eastman, K. J.; Hill, M. D.; Donnelly, D. J.; Meanwell, N. A. *J. Med. Chem.* **2015,** *58,* 8315–8359. doi:10.1021/acs.jmedchem.5b00258
3. Harsanyi, A.; Sandford, G. *Green Chem.* **2015,** *17,* 2081–2086. doi:10.1039/c4gc02166e
4. Zhou, Y.; Wang, J.; Gu, Z.; Wang, S.; Zhu, W.; Aceña, J. L.; Soloshonok, V. A.; Izawa, K.; Liu, H. *Chem. Rev.* **2016,** *116,* 422–518. doi:10.1021/acs.chemrev.5b00392
5. Xu, X.-H.; Matsuzaki, K.; Shibata, N. *Chem. Rev.* **2015,** *115,* 731–764. doi:10.1021/cr500193b
6. Matheis, C.; Wagner, V.; Goossen, L. J. *Chem. – Eur. J.* **2016,** *22,* 79–82. doi:10.1002/chem.201503524
7. Glenadel, Q.; Ismalaj, E.; Billard, T. *Eur. J. Org. Chem.* **2017,** 530–533. doi:10.1002/ejoc.201601526

8. Besset, T.; Jubault, P.; Pannecoucke, X.; Poisson, T. *Org. Chem. Front.* **2016,** *3,* 1004–1010. doi:10.1039/c6qo00164e
9. Seebach, D. *Angew. Chem., Int. Ed. Engl.* **1990,** *29,* 1320–1367. doi:10.1002/anie.199013201
10. McClinton, M. A.; McClinton, D. A. *Tetrahedron* **1992,** *48,* 6555–6666. doi:10.1016/S0040-4020(01)80011-9
11. Ma, J.-A.; Cahard, D. *J. Fluorine Chem.* **2007,** *128,* 975–996. doi:10.1016/j.jfluchem.2007.04.026
12. Shibata, N.; Matsnev, A.; Cahard, D. *Beilstein J. Org. Chem.* **2010,** *6,* No. 65. doi:10.3762/bjoc.6.65
13. Ye, Y. e-EROS Encyclopedia of Reagents for Organic **2014,** 1–4. doi:10.1002/047084289X.rn01689
14. Haszeldine, R. N.; Kidd, J. M. *J. Chem. Soc.* **1955,** 2901–2910. doi:10.1039/JR9550002901
15. Roesky, H. W.; Holtschneider, G. *J. Fluorine Chem.* **1976,** *7,* 77–84. doi:10.1016/s0022-1139(00)83984-6
16. Langlois, B. R.; Laurent, E.; Roidot, N. *Tetrahedron Lett.* **1991,** *32,* 7525–7528. doi:10.1016/0040-4039(91)80524-a
17. Zhang, C. *Adv. Synth. Catal.* **2014,** *356,* 2895–2906. doi:10.1002/adsc.201400370
18. Langlois, B. R. Once Upon a Time Was the Langlois' Reagent: A “Sleeping Beauty”. In *Modern Synthesis Processes and Reactivity of Fluorinated Compounds;* Groult, H.; Leroux, F.; Tressaud, A., Eds.; Elsevier, 2017; pp 125–140.
19. Lefebvre, Q. *Synlett* **2017,** *28,* 19–23. doi:10.1055/s-0036-1588643
20. Clavel, J.-L.; Langlois, B.; Laurent, E.; Roidot, N. *Phosphorus, Sulfur Silicon Relat. Elem.* **1991,** *59,* 169–172. doi:10.1080/10426509108045716
21. Langlois, B. R.; Laurent, E.; Roidot, N. *Tetrahedron Lett.* **1992,** *33,* 1291–1294. doi:10.1016/s0040-4039(00)91604-6
22. Lu, Y.; Li, Y.; Zhang, R.; Jin, K.; Duan, C. *J. Fluorine Chem.* **2014,** *161,* 128–133. doi:10.1016/j.jfluchem.2014.01.020
23. Deb, A.; Manna, S.; Modak, A.; Patra, T.; Maity, S.; Maiti, D. *Angew. Chem., Int. Ed.* **2013,** *52,* 9747–9750. doi:10.1002/anie.201303576
24. Maji, A.; Hazra, A.; Maiti, D. *Org. Lett.* **2014,** *16,* 4524–4527. doi:10.1021/ol502071g
25. Luo, H.-Q.; Zhang, Z.-P.; Dong, W.; Luo, X.-Z. *Synlett* **2014,** *25,* 1307–1311. doi:10.1055/s-0033-1341057
26. Lu, Q.; Liu, C.; Huang, Z.; Ma, Y.; Zhang, J.; Lei, A. *Chem. Commun.* **2014,** *50,* 14101–14104. doi:10.1039/c4cc06328g
27. Qin, H.-T.; Wu, S.-W.; Liu, J.-L.; Liu, F. *Chem. Commun.* **2017,** *53,* 1696–1699. doi:10.1039/c6cc10035j
28. Lv, W.-X.; Zeng, Y.-F.; Li, Q.; Chen, Y.; Tan, D.-H.; Yang, L.; Wang, H. *Angew. Chem., Int. Ed.* **2016,** *55,* 10069–10073. doi:10.1002/anie.201604898
29. Konik, Y. A.; Kudrjashova, M.; Konrad, N.; Kaabel, S.; Jarving, I.; Lopp, M.; Kananovich, D. G. *Org. Biomol. Chem.* **2017,** *15,* 4635–4643. doi:10.1039/C7OB00680B
30. Huang, H.-L.; Yan, H.; Gao, G.-L.; Yang, C.; Xia, W. *Asian J. Org. Chem.* **2015,** *4,* 674–677. doi:10.1002/ajoc.201500096
31. Matcha, K.; Antonchick, A. P. *Angew. Chem., Int. Ed.* **2014,** *53,* 11960–11964. doi:10.1002/anie.201406464
32. Yu, X.-L.; Chen, J.-R.; Chen, D.-Z.; Xiao, W.-J. *Chem. Commun.* **2016,** *52,* 8275–8278. doi:10.1039/c6cc03335k
33. Zhang, H.-Y.; Huo, W.; Ge, C.; Zhao, J.; Zhang, Y. *Synlett* **2017,** *28,* 962–965. doi:10.1055/s-0036-1588400
34. Jiang, X.-Y.; Qing, F.-L. *Angew. Chem., Int. Ed.* **2013,** *52,* 14177–14180. doi:10.1002/anie.201307595
35. Yang, Y.; Liu, Y.; Jiang, Y.; Zhang, Y.; Vicic, D. A. *J. Org. Chem.* **2015,** *80,* 6639–6648. doi:10.1021/acs.joc.5b00781
36. Liu, C.; Lu, Q.; Huang, Z.; Zhang, J.; Liao, F.; Peng, P.; Lei, A. *Org. Lett.* **2015,** *17,* 6034–6037. doi:10.1021/acs.orglett.5b03035
37. Yu, J.; Yang, H.; Fu, H. *Adv. Synth. Catal.* **2014,** *356,* 3669–3675. doi:10.1002/adsc.201400144
38. Tommasino, J.-B.; Brondex, A.; Medebielle, M.; Thomalla, M.; Langlois, B. R.; Billard, T. *Synlett* **2002,** 1697–1699. doi:10.1055/s-2002-34210
39. Wilger, D. J.; Gesmundo, N. J.; Nicewicz, D. A. *Chem. Sci.* **2013,** *4,* 3160–3165. doi:10.1039/c3sc51209f
40. Lefebvre, Q.; Hoffmann, N.; Rueping, M. *Chem. Commun.* **2016,** *52,* 2493–2496. doi:10.1039/c5cc09881e
41. Zhu, L.; Wang, L.-S.; Li, B.; Fu, B.; Zhang, C.-P.; Li, W. *Chem. Commun.* **2016,** *52,* 6371–6374. doi:10.1039/c6cc01944g
42. Hang, Z.; Li, Z.; Liu, Z.-Q. *Org. Lett.* **2014,** *16,* 3648–3651. doi:10.1021/ol501380e
43. Liu, Z.-Q.; Liu, D. *J. Org. Chem.* **2017,** *82,* 1649–1656. doi:10.1021/acs.joc.6b02812
44. Fang, J.; Wang, Z.-K.; Wu, S.-W.; Shen, W.-G.; Ao, G.-Z.; Liu, F. *Chem. Commun.* **2017,** *53,* 7638–7641. doi:10.1039/c7cc01903c
45. Yang, F.; Klumphu, P.; Liang, Y.-M.; Lipshutz, B. H. *Chem. Commun.* **2014,** *50,* 936–938. doi:10.1039/c3cc48131j
46. Lu, Q.; Liu, C.; Peng, P.; Liu, Z.; Fu, L.; Huang, J.; Lei, A. *Asian J. Org. Chem.* **2014,** *3,* 273–276. doi:10.1002/ajoc.201300236
47. Liu, J.; Zhuang, S.; Gui, Q.; Chen, X.; Yang, Z.; Tan, Z. *Eur. J. Org. Chem.* **2014,** 3196–3202. doi:10.1002/ejoc.201400087
48. Wei, W.; Wen, J.; Yang, D.; Liu, X.; Guo, M.; Dong, R.; Wang, H. *J. Org. Chem.* **2014,** *79,* 4225–4230. doi:10.1021/jo500515x
49. Shi, L.; Yang, X.; Wang, Y.; Yang, H.; Fu, H. *Adv. Synth. Catal.* **2014,** *356,* 1021–1028. doi:10.1002/adsc.201300995
50. Sakamoto, R.; Kashiwagi, H.; Selvakumar, S.; Moteki, S. A.; Maruoka, K. *Org. Biomol. Chem.* **2016,** *14,* 6417–6421. doi:10.1039/c6ob01245k
51. Zhang, L.; Li, Z.; Liu, Z.-Q. *Org. Lett.* **2014,** *16,* 3688–3691. doi:10.1021/ol5014747
52. Mai, W.-P.; Wang, J.-T.; Yang, L.-R.; Yuan, J.-W.; Xiao, Y.-M.; Mao, P.; Qu, L.-B. *Org. Lett.* **2014,** *16,* 204–207. doi:10.1021/ol403196h
53. Li, B.; Fan, D.; Yang, C.; Xia, W. *Org. Biomol. Chem.* **2016,** *14,* 5293–5297. doi:10.1039/c6ob00912c
54. Wu, Z.; Wang, D.; Liu, Y.; Huan, L.; Zhu, C. *J. Am. Chem. Soc.* **2017,** *139,* 1388–1391. doi:10.1021/jacs.6b11234
55. Yang, B.; Xu, X.-H.; Qing, F.-L. *Org. Lett.* **2015,** *17,* 1906–1909. doi:10.1021/acs.orglett.5b00601
56. Smertenko, E. A.; Datsenko, S. D.; Ignat'ev, N. V. *Russ. J. Electrochem.* **1998,** *34,* 46–51.
57. Ji, Y.; Brueckl, T.; Baxter, R. D.; Fujiwara, Y.; Seiple, I. B.; Su, S.; Blackmond, D. G.; Baran, P. S. *Proc. Natl. Acad. Sci. U. S. A.* **2011,** *108,* 14411–14415. doi:10.1073/pnas.1109059108
58. Musumeci, D.; Irace, C.; Santamaria, R.; Montesarchio, D. *Med. Chem. Commun.* **2013,** *4,* 1405–1410. doi:10.1039/c3md00159h
59. Wu, M.; Ji, X.; Dai, W.; Cao, S. *J. Org. Chem.* **2014,** *79,* 8984–8989. doi:10.1021/jo501221h
60. Fennewald, J. C.; Lipshutz, B. H. *Green Chem.* **2014,** *16,* 1097–1100. doi:10.1039/c3gc42119h
61. Zhang, X.; Huang, P.; Li, Y.; Duan, C. *Org. Biomol. Chem.* **2015,** *13,* 10917–10922. doi:10.1039/c5ob01516b
62. Cao, X.-H.; Pan, X.; Zhou, P.-J.; Zou, J.-P.; Asekun, O. T. *Chem. Commun.* **2014,** *50,* 3359–3362. doi:10.1039/c3cc49689a

63. Zhang, P.-Z.; Li, C.-K.; Zhang, G.-Y.; Zhang, L.; Jiang, Y.-J.; Zou, J.-P. *Tetrahedron* **2016,** *72,* 3250–3255. doi:10.1016/j.tet.2016.04.048
64. Li, C.; Suzuki, K.; Yamaguchi, K.; Mizuno, N. *New J. Chem.* **2017,** *41,* 1417–1420. doi:10.1039/c6nj03654f
65. Monir, K.; Bagdi, A. K.; Ghosh, M.; Hajra, A. *J. Org. Chem.* **2015,** *80,* 1332–1337. doi:10.1021/jo502928e
66. Ji, X.-M.; Wei, L.; Chen, F.; Tang, R.-Y. *RSC Adv.* **2015,** *5,* 29766–29773. doi:10.1039/C5RA02888D
67. Jin, L.-K.; Lu, G.-P.; Cai, C. *Org. Chem. Front.* **2016,** *3,* 1309–1313. doi:10.1039/c6qo00369a
68. Shen, C.; Xu, J.; Ying, B.; Zhang, P. *ChemCatChem* **2016,** *8,* 3560–3564. doi:10.1002/cctc.201601068
69. Li, J.-M.; Wang, Y.-H.; Yu, Y.; Wu, R.-B.; Weng, J.; Lu, G. *ACS Catal.* **2017,** *7,* 2661–2667. doi:10.1021/acscatal.6b03671
70. Wang, D.; Deng, G.-J.; Chen, S.; Gong, H. *Green Chem.* **2016,** *18,* 5967–5970. doi:10.1039/c6gc02000c
71. Yang, Y.-D.; Iwamoto, K.; Tokunaga, E.; Shibata, N. *Chem. Commun.* **2013,** *49,* 5510–5512. doi:10.1039/c3cc41667d
72. Cui, L.; Matusaki, Y.; Tada, N.; Miura, T.; Uno, B.; Itoh, A. *Adv. Synth. Catal.* **2013,** *355,* 2203–2207. doi:10.1002/adsc.201300199
73. Chang, B.; Shao, H.; Yan, P.; Qiu, W.; Weng, Z.; Yuan, R. *ACS Sustainable Chem. Eng.* **2017,** *5,* 334–341. doi:10.1021/acssuschemeng.6b01682
74. Li, L.; Mu, X.; Liu, W.; Wang, Y.; Mi, Z.; Li, C.-J. *J. Am. Chem. Soc.* **2016,** *138,* 5809–5812. doi:10.1021/jacs.6b02782
75. Le, C. C.; Wismer, M. K.; Shi, Z.-C.; Zhang, R.; Conway, D. V.; Li, G.; Vachal, P.; Davies, I. W.; MacMillan, D. W. C. *ACS Cent. Sci.* **2017,** *3,* 647–653. doi:10.1021/acscentsci.7b00159
76. Zhang, K.; Xu, X.-H.; Qing, F.-L. *J. Org. Chem.* **2015,** *80,* 7658–7665. doi:10.1021/acs.joc.5b01295
77. Hong, J.; Wang, G.; Huo, L.; Zheng, C. *Chin. J. Chem.* **2017,** *35,* 1761–1767. doi:10.1002/cjoc.201700311
78. Ye, Y.; Künzi, S. A.; Sanford, M. S. *Org. Lett.* **2012,** *14,* 4979–4981. doi:10.1021/ol3022726
79. Li, Y.; Wu, L.; Neumann, H.; Beller, M. *Chem. Commun.* **2013,** *49,* 2628–2630. doi:10.1039/c2cc36554e
80. Presset, M.; Oehlrich, D.; Rombouts, F.; Molander, G. A. *J. Org. Chem.* **2013,** *78,* 12837–12843. doi:10.1021/jo4023233
81. Dubbaka, S. R.; Salla, M.; Bolisetti, R.; Nizalapur, S. *RSC Adv.* **2014,** *4,* 6496–6499. doi:10.1039/C3RA46837B
82. Li, Z.; Cui, Z.; Liu, Z.-Q. *Org. Lett.* **2013,** *15,* 406–409. doi:10.1021/ol3034059
83. Patra, T.; Deb, A.; Manna, S.; Sharma, U.; Maiti, D. *Eur. J. Org. Chem.* **2013,** 5247–5250. doi:10.1002/ejoc.201300473
84. Yin, J.; Li, Y.; Zhang, R.; Jin, K.; Duan, C. *Synthesis* **2014,** *46,* 607–612. doi:10.1055/s-0033-1338578
85. Shang, X.-J.; Li, Z.; Liu, Z.-Q. *Tetrahedron Lett.* **2015,** *56,* 233–235. doi:10.1016/j.tetlet.2014.11.076
86. Huang, P.; Li, Y.; Fu, X.; Zhang, R.; Jin, K.; Wang, W.; Duan, C. *Tetrahedron Lett.* **2016,** *57,* 4705–4708. doi:10.1016/j.tetlet.2016.09.016
87. Wu, L.-H.; Zhao, K.; Shen, Z.-L.; Loh, T.-P. *Org. Chem. Front.* **2017,** *4,* 1872–1875. doi:10.1039/c7qo00416h
88. Jiang, H.; Huang, W.; Yu, Y.; Yi, S.; Li, J.; Wu, W. *Chem. Commun.* **2017,** *53,* 7473–7476. doi:10.1039/c7cc03125d
89. Liu, Y.-R.; Tu, H.-Y.; Zhang, X.-G. *Synthesis* **2015,** *47,* 3460–3466. doi:10.1055/s-0034-1378810
90. Lu, S.; Gong, Y.; Zhou, D. *J. Org. Chem.* **2015,** *80,* 9336–9341. doi:10.1021/acs.joc.5b01518
91. Fang, J.; Shen, W.-G.; G.-Z., Ao; Liu, F. *Org. Chem. Front.* **2017,** *4,* 2049–2053. doi:10.1039/C7QO00473G
92. Dubbaka, S. R.; Nizalapur, S.; Atthunuri, A. R.; Salla, M.; Mathew, T. *Tetrahedron* **2014,** *70,* 2118–2121. doi:10.1016/j.tet.2014.02.005
93. van der Werf, A.; Hribersek, M.; Selander, N. *Org. Lett.* **2017,** *19,* 2374–2377. doi:10.1021/acs.orglett.7b00908
94. Langlois, B.; Montègre, D.; Roidot, N. *J. Fluorine Chem.* **1994,** *68,* 63–66. doi:10.1016/0022-1139(93)02982-k
95. Ma, J.-J.; Yi, W.-B.; Lu, G.-P.; Cai, C. *Catal. Sci. Technol.* **2016,** *6,* 417–421. doi:10.1039/c5cy01561h
96. Ma, J.-j.; Liu, Q.-r.; Lu, G.-p.; Yi, W.-b. *J. Fluorine Chem.* **2017,** *193,* 113–117. doi:10.1016/j.jfluchem.2016.11.010
97. Chachignon, H.; Cahard, D. *Chin. J. Chem.* **2016,** *34,* 445–454. doi:10.1002/cjoc.201500890
98. Jiang, L.; Qian, J.; Yi, W.; Lu, G.; Cai, C.; Zhang, W. *Angew. Chem., Int. Ed.* **2015,** *54,* 14965–14969. doi:10.1002/anie.201508495
99. Yan, Q.; Jiang, L.; Yi, W.; Liu, Q.; Zhang, W. *Adv. Synth. Catal.* **2017,** *359,* 2471–2480. doi:10.1002/adsc.201700270
100. Bu, M.-j.; Lu, G.-p.; Cai, C. *Org. Chem. Front.* **2017,** *4,* 266–270. doi:10.1039/c6qo00622a
101. Sun, D.-W.; Jiang, X.; Jiang, M.; Lin, Y.; Liu, J.-T. *Eur. J. Org. Chem.* **2017,** 3505–3511. doi:10.1002/ejoc.201700661
102. Zhao, X.; Wei, A.; Yang, B.; Li, T.; Li, Q.; Qiu, D.; Lu, K. *J. Org. Chem.* **2017,** *82,* 9175–9181. doi:10.1021/acs.joc.7b01226
103. Yang, Y.; Xu, L.; Yu, S.; Liu, X.; Zhang, Y.; Vicic, D. A. *Chem. – Eur. J.* **2016,** *22,* 858–863. doi:10.1002/chem.201504790
104. Billard, T.; Greiner, A.; Langlois, B. R. *Tetrahedron* **1999,** *55,* 7243–7250. doi:10.1016/s0040-4020(99)00364-6
105. Roussel, S.; Billard, T.; Langlois, B. R.; Saint-Jalmes, L. *Synlett* **2004,** 2119–2122. doi:10.1055/s-2004-831322
106. Liu, Z.; Larock, R. C. *J. Am. Chem. Soc.* **2005,** *127,* 13112–13113. doi:10.1021/ja054079p
107. Richards-Taylor, C. S.; Martinez-Lamenca, C.; Leenaerts, J. E.; Trabanco, A. A.; Oehlrich, D. *J. Org. Chem.* **2017,** *82,* 9898–9904. doi:10.1021/acs.joc.7b01628
108. Wakselman, C.; Tordeux, M.; Freslon, C.; Saint-Jalmes, L. *Synlett* **2001,** 550–552. doi:10.1055/s-2001-12316
109. Magnier, E.; Blazejewski, J.-C.; Tordeux, M.; Wakselman, C. *Angew. Chem., Int. Ed.* **2006,** *45,* 1279–1282. doi:10.1002/anie.200503776
110. Okazaki, T.; Laali, K. K.; Reddy, A. S. *J. Fluorine Chem.* **2014,** *165,* 91–95. doi:10.1016/j.jfluchem.2014.06.021
111. Umemoto, T.; Zhang, B.; Zhu, T.; Zhou, X.; Zhang, P.; Hu, S.; Li, Y. *J. Org. Chem.* **2017,** *82,* 7708–7719. doi:10.1021/acs.joc.7b00669
112. Eugene, F.; Langlois, B.; Laurent, E. *J. Fluorine Chem.* **1994,** *66,* 301–309. doi:10.1016/0022-1139(93)02909-x
113. Meshcheryakov, V. I.; Shainyan, B. A. *Russ. J. Org. Chem.* **2004,** *40,* 390–396. doi:10.1023/B:RUJO.0000034977.74026.b3
114. Hasegawa, A.; Naganawa, Y.; Fushimi, M.; Ishihara, K.; Yamamoto, H. *Org. Lett.* **2006,** *8,* 3175–3178. doi:10.1021/ol060939a
115. Hasegawa, A.; Ishikawa, T.; Ishihara, K.; Yamamoto, H. *Bull. Chem. Soc. Jpn.* **2005,** *78,* 1401–1410. doi:10.1246/bcsj.78.1401
116. Zhu, S.; Chu, Q.; Xu, G.; Qin, C.; Xu, Y. *J. Fluorine Chem.* **1998,** *91,* 195–198. doi:10.1016/s0022-1139(98)00240-1

117. Wu, W.-L.; Asberom, T.; Bara, T.; Bennett, C.; Burnett, D. A.; Clader, J.; Domalski, M.; Greenlee, W. J.; Josien, H.; McBriar, M.; Rajagopalan, M.; Vicarel, M.; Xu, R.; Hyde, L. A.; Del Vecchio, R. A.; Cohen-Williams, M. E.; Song, L.; Lee, J.; Terracina, G.; Zhang, Q.; Nomeir, A.; Parker, E. M.; Zhang, L. *Bioorg. Med. Chem. Lett.* **2013,** *23,* 844–849. doi:10.1016/j.bmcl.2012.11.047
118. Kong, H. I.; Crichton, J. E.; Manthorpe, J. M. *Tetrahedron Lett.* **2011,** *52,* 3714–3717. doi:10.1016/j.tetlet.2011.05.015
119. Kong, H. I.; Gill, M. A.; Hrdina, A. H.; Crichton, J. E.; Manthorpe, J. M. *J. Fluorine Chem.* **2013,** *153,* 151–161. doi:10.1016/j.jfluchem.2013.03.020
120. Liao, J.; Guo, W.; Zhang, Z.; Tang, X.; Wu, W.; Jiang, H. *J. Org. Chem.* **2016,** *81,* 1304–1309. doi:10.1021/acs.joc.5b02674
121. Cullen, S. C.; Shekhar, S.; Nere, N. K. *J. Org. Chem.* **2013,** *78,* 12194–12201. doi:10.1021/jo401868x
122. Xie, F.; Zhang, Z.; Yu, X.; Tang, G.; Li, X. *Angew. Chem., Int. Ed.* **2015,** *54,* 7405–7409. doi:10.1002/anie.201502278
123. Wang, F.; Yu, X.; Qi, Z.; Li, X. *Chem. – Eur. J.* **2016,** *22,* 511–516. doi:10.1002/chem.201504179
124. Smyth, L. A.; Phillips, E. M.; Chan, V. S.; Napolitano, J. G.; Henry, R.; Shekhar, S. *J. Org. Chem.* **2016,** *81,* 1285–1294. doi:10.1021/acs.joc.5b02523
125. Aithagani, S. K.; Yempalla, K. R.; Munagala, G.; Vishwakarma, R. A.; Singh, P. P. *RSC Adv.* **2014,** *4,* 50208–50211. doi:10.1039/c4ra07370c
126. Ochiai, M.; Tada, N.; Nishi, Y.; Murai, K. *Chem. Commun.* **2004,** 2894–2895. doi:10.1039/B410830B
127. Chu, X.-Q.; Meng, H.; Xu, X.-P.; Ji, S.-J. *Chem. – Eur. J.* **2015,** *21,* 11359–11368. doi:10.1002/chem.201500469
128. Hua, L.-N.; Li, H.; Qing, F.-L.; Huang, Y.; Xu, X.-H. *Org. Biomol. Chem.* **2016,** *14,* 8443–8447. doi:10.1039/C6OB01567K
129. Han, J.-B.; Yang, L.; Chen, X.; Zha, G.-F.; Zhang, C.-P. *Adv. Synth. Catal.* **2016,** *358,* 4119–4124. doi:10.1002/adsc.201600717
130. Billard, T.; Langlois, B. R.; Large, S.; Anker, D.; Roidot, N.; Roure, P. *J. Org. Chem.* **1996,** *61,* 7545–7550. doi:10.1021/jo960619c
131. Billard, T.; Langlois, B. R. *J. Fluorine Chem.* **1997,** *84,* 63–64. doi:10.1016/s0022-1139(97)00009-2

License and Terms

BEILSTEIN JOURNAL OF ORGANIC CHEMISTRY

CF_3SO_2X (X = Na, Cl) as reagents for trifluoromethylation, trifluoromethylsulfenyl-, -sulfinyl- and -sulfonylation and chlorination. Part 2: Use of CF_3SO_2Cl

Hélène Chachignon, Hélène Guyon and Dominique Cahard*

Full Research Paper

Open Access

Address:
UMR 6014 CNRS COBRA, Normandie Université, 1 rue Tesnière, 76821 Mont Saint Aignan, France

Email:
Dominique Cahard* - dominique.cahard@univ-rouen.fr

* Corresponding author

Keywords:
chlorination; fluorine; sulfur; trifluoromethylation; trifluoromethylsulfenylation; trifluoromethylsufinylation; trifluoromethylsulfonylation

Beilstein J. Org. Chem. **2017,** *13,* 2800–2818.
doi:10.3762/bjoc.13.273

Received: 20 September 2017
Accepted: 20 November 2017
Published: 19 December 2017

This article is part of the Thematic Series "Organo-fluorine chemistry IV".

Guest Editor: D. O'Hagan

Abstract

The recent progresses of the application of trifluoromethanesulfonyl chloride, CF_3SO_2Cl, in the formation of C–CF_3, C–SCF_3, C–$SOCF_3$, and C–Cl bonds are summarised in this second part of a two-part review published back-to-back on both sodium trifluoromethanesulfinate, CF_3SO_2Na, (Part 1) and trifluoromethanesulfonyl chloride, CF_3SO_2Cl (Part 2). There are many reactions in common between these two reagents but it should be noted that CF_3SO_2Cl reacts under reductive conditions while CF_3SO_2Na requires oxidative conditions. Electrophilic chlorination is obviously the exclusive preserve of CF_3SO_2Cl that has been exploited with emphasis in enantioselective chlorination.

Introduction

In the preceding paper, we described the various uses of sodium trifluoromethanesulfinate in direct trifluoromethylation, trifluoromethylsulfenylation, trifluoromethylsufinylation and trifluoromethylsulfonylation reactions. We now focused this second part of the review on the similarly diverse uses of trifluoromethanesulfonyl chloride plus chlorination. This review appears in two parts that are published back-to-back. We encourage the readers to refer to Part 1 for a general introduction in the field [1].

Review

Trifluoromethanesulfonyl chloride (alternate name: triflyl chloride), CAS No. 421-83-0, MW 168.53, is a colourless liquid (bp 29–32 °C) soluble in dichloromethane, tetrahydrofuran and

dioxane [2]. Up to recently, the predominant use of CF_3SO_2Cl was for triflate and triflamide formation. Indeed, CF_3SO_2Cl reacts with oxygen nucleophiles to generate triflate derivatives as highly electron-withdrawing substituent in order to act in nucleophilic substitutions and metal-catalysed coupling reactions as an excellent leaving group [2]. The reaction of CF_3SO_2Cl with nitrogen nucleophiles provides trifluoromethanesulfonamide (triflamide) derivatives, which are used in drugs and agrochemicals [3]. The *C*-trifluoromethylsulfonylation is less reported than the corresponding *O*- and *N*-trifluoromethylsulfonylations, although the resulting triflone group is an important synthetic tool for further functionalisation [4,5]. These sulfonylation reactions will not be further detailed hereafter. Instead, CF_3SO_2Cl, which is experiencing an advanced level of growth for the installation of the CF_3 moiety onto a wide range of substrates, alone or simultaneously with the chlorine atom or the sulfonyl group, is the focus of this review. The direct introduction of CF_3S and $CF_3S(O)$ motifs also occupies a prime position in this review.

1 Trifluoromethylation

C_{sp3}–CF_3 bond-forming reactions

Trifluoromethylation of silyl enol ethers and enol acetates: After their original reports on the trifluoromethylation of aromatics in 1990 (C_{sp2}–CF_3 bond-forming reactions; see later in the text, Scheme 24) [6,7], Kamigata and co-workers studied silyl enol ethers in 1997 in trifluoromethylation reactions. Kamigata's group reported that in the presence of $RuCl_2(PPh_3)_3$, in benzene at 120 °C, silyl enol ethers could furnish the corresponding α-trifluoromethylated carbonyls in low to moderate yields (Scheme 1) [8]. Nonetheless, important competition between the introduction of the CF_3 group or a Cl atom was invariably observed in various ratio depending on the nature of the substrates. As for the mechanism of the reaction, the authors proposed a radical pathway that involved Ru(II)/Ru(III) metallic species (Scheme 1).

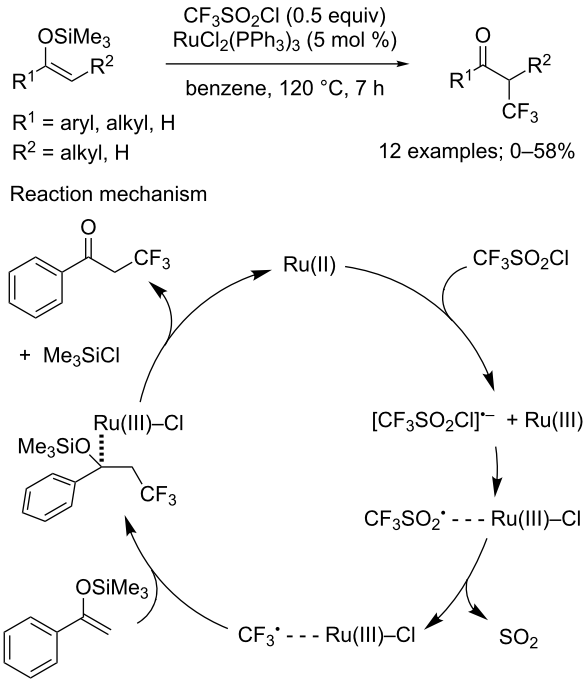

Scheme 1: Trifluoromethylation of silyl enol ethers.

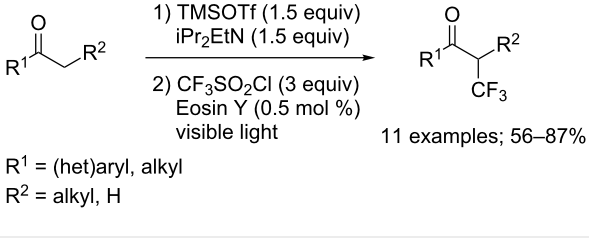

Scheme 2: Continuous flow trifluoromethylation of ketones under photoredox catalysis.

The trifluoromethylation of silyl enol ethers can also be adressed in a continuous-flow procedure. To do so, the appropriate ketones were transformed in situ into the corresponding silyl enol ethers, which were then reacted with CF_3SO_2Cl in the presence of Eosin Y under visible light irradiation (Scheme 2) [9]. Acetophenone derivatives with various substitution patterns as well as aliphatic or heteroaromatic ketones were equally well tolerated. This methodology offered the advantage of minimising the chlorination side reaction, consequently resulting in higher yields indifferently of the substrate.

Enol acetates as another type of masked enol(ates) also proved to be appropriate substrates to access α-trifluoromethylated ketones (Scheme 3) [10]. In the presence of 1 mol % of (4,4'-di-*tert*-butyl-2,2'-bipyridine)bis[(2-pyridinyl)phenyl]iridium(III) hexafluorophosphate, $Ir(ppy)_2(dtbbpy)PF_6$, various aryl enol acetates carrying electron-donating or electron-withdrawing groups were converted into the corresponding products in high yields. Moreover, the reaction was compatible with cyclic and acyclic branched enol acetates. Quite interestingly, when the reaction was performed using an aryl or alkylsulfonyl chloride, instead of trifluoromethanesulfonyl chloride, no extrusion of the SO_2 moiety was observed, and the sulfonated products were recovered. The reaction mechanism involved excitation of the iridium catalyst under visible light to generate an Ir(III)* species, which was then oxidatively quenched by CF_3SO_2Cl to furnish Ir(IV) and the CF_3 radical. Said radical was added on the substrate to form the radical species **1**, which yielded the cationic intermediate **2** through oxidation by Ir(IV). The oxidation of compound **1** by means of CF_3SO_2Cl, regenerating the

trifluoromethyl radical in the process, was also considered. Intermediate **2** was ultimately converted into the final product after liberating an acetyl cation, which was captured by a chloride anion to give acetyl chloride (Scheme 3).

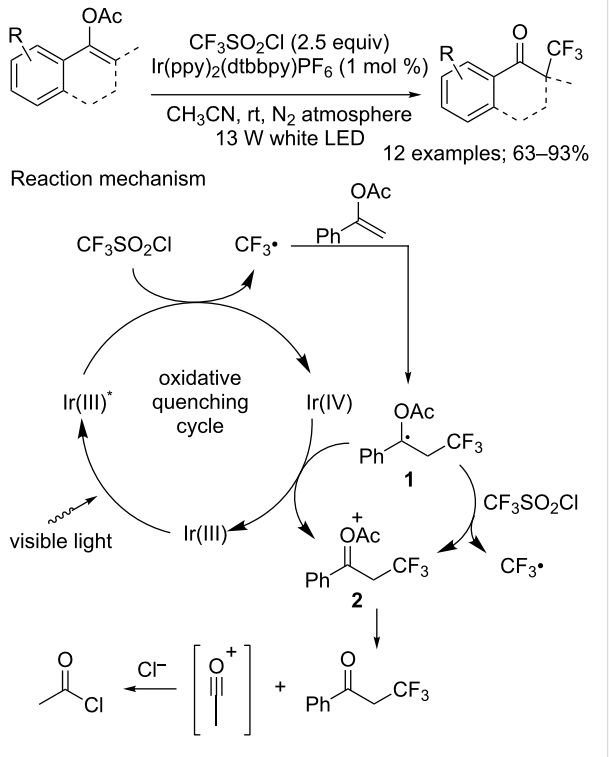

Scheme 3: Trifluoromethylation of enol acetates.

Trifluoromethylation of olefins with cascade reactions: The most widely described type of reactions in which CF_3SO_2Cl and molecules carrying a C=C double bond are involved are actually cascade reactions that include a cyclisation or a group migration step. In this context, the acrylamide motif was a notably popular object of research, and served in several tandem trifluoromethylation/cyclisation processes. Dolbier and co-workers first proposed the use of *N*-arylacrylamides **3** to access trifluoromethylated 3,3-disubstituted 2-oxindoles **4** under photocatalytic conditions (Scheme 4) [11]. In the presence of $Ru(phen)_3Cl_2$ (phen = phenanthroline), a variety of *N*-arylacrylamides *para*-substituted on their aryl moiety by electron-donating or electron-withdrawing groups were converted into the corresponding oxindoles with similarly good yields. However, the reaction was compatible only with acrylamides bearing methyl or phenyl as R^1 and R^2 groups; for example, *N*-acyl and *N*-sulfonyl amides failed to react.

Interestingly, Zhang and co-workers demonstrated that this reaction could be performed as well using bismuth oxybromide (BiOBr) nanosheets instead of a ruthenium complex as the photocatalyst (Scheme 5) [12]. The reaction unfortunately suffered from the same limitations. However, the scope of application was extended to substrates carrying more diverse R^2 groups such as ethers, esters or alcohols.

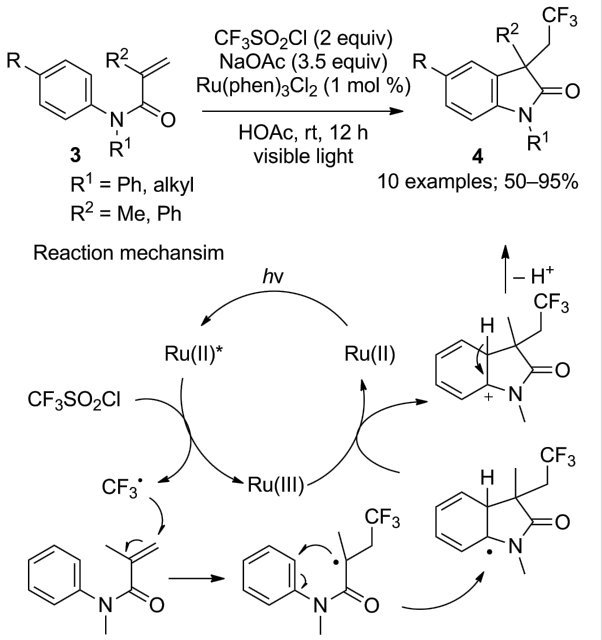

Scheme 4: Photoredox-catalysed tandem trifluoromethylation/cyclisation of *N*-arylacrylamides: a route to trifluoromethylated oxindole derivatives.

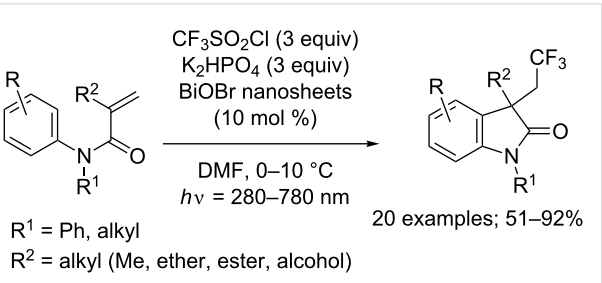

Scheme 5: Tandem trifluoromethylation/cyclisation of *N*-arylacrylamides using BiOBr nanosheets catalysis.

In 2015, Yang, Xia and co-workers reported that trifluoromethylated oxindole derivatives could also be accessed from *N*-tosylacrylamides **5**, via a similar pathway including an additional desulfonylation step (Scheme 6) [13]. Both electron-withdrawing and electron-donating groups on *para*-position of the aryl ring were tolerated, and provided comparable yields. On the other hand, the presence of a substituent in *meta*-position led to the formation of two regioisomers. As for *ortho*-substituted substrates, they furnished even more complex reaction mixtures, probably because of steric hindrance.

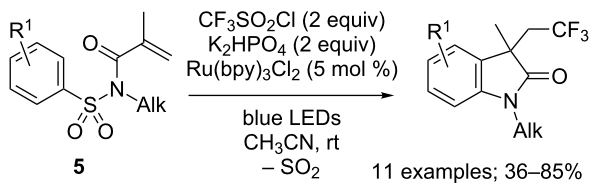

Scheme 6: Photoredox-catalysed trifluoromethylation/desulfonylation/cyclisation of *N*-tosyl acrylamides (bpy: 2,2'-bypyridine).

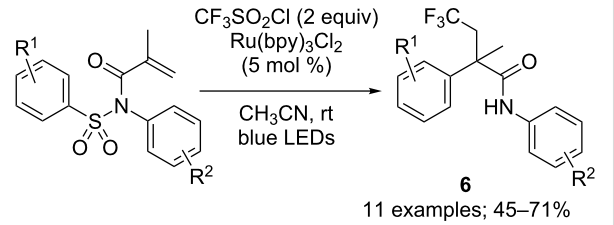

Scheme 7: Photoredox-catalysed trifluoromethylation/aryl migration/desulfonylation of *N*-aryl-*N*-tosylacrylamides.

The most influential parameter however proved to be the nature of the substituent linked to the nitrogen atom. Indeed, when replacing the alkyl group by an aryl moiety, a totally different product was obtained predominantly: the α-aryl-β-trifluoromethyl amide **6**. This compound was determined to be issued from a trifluoromethylation/1,4-aryl shift/desulfonylation cascade reaction (Scheme 7).

This reaction could be performed on various *N*-aryl,*N*-tosylacrylamides with moderate to good yields. The nature of the substituents of the sulfonamide group showed little influence on the efficiency of the process. On the contrary, better results were obtained when realising the reaction on substrates featuring electron-donating groups on the phenyl ring directly bound to the nitrogen atom. It was also shown that the reaction proceeded equally smoothly when using BiOBr nanosheets catalysis [14].

The proposed mechanism of these two reactions is represented in Scheme 8. Alongside the classical pathway, the trifluoromethyl radical was generated and added onto the *N*-tosylacrylamide. The obtained radical species **7** then underwent an aryl migration/desulfonylation cascade reaction to furnish intermediate **8**. In the case of an aryl substituted substrate, this nitrogen radical being stabilised, it directly performed an hydrogen

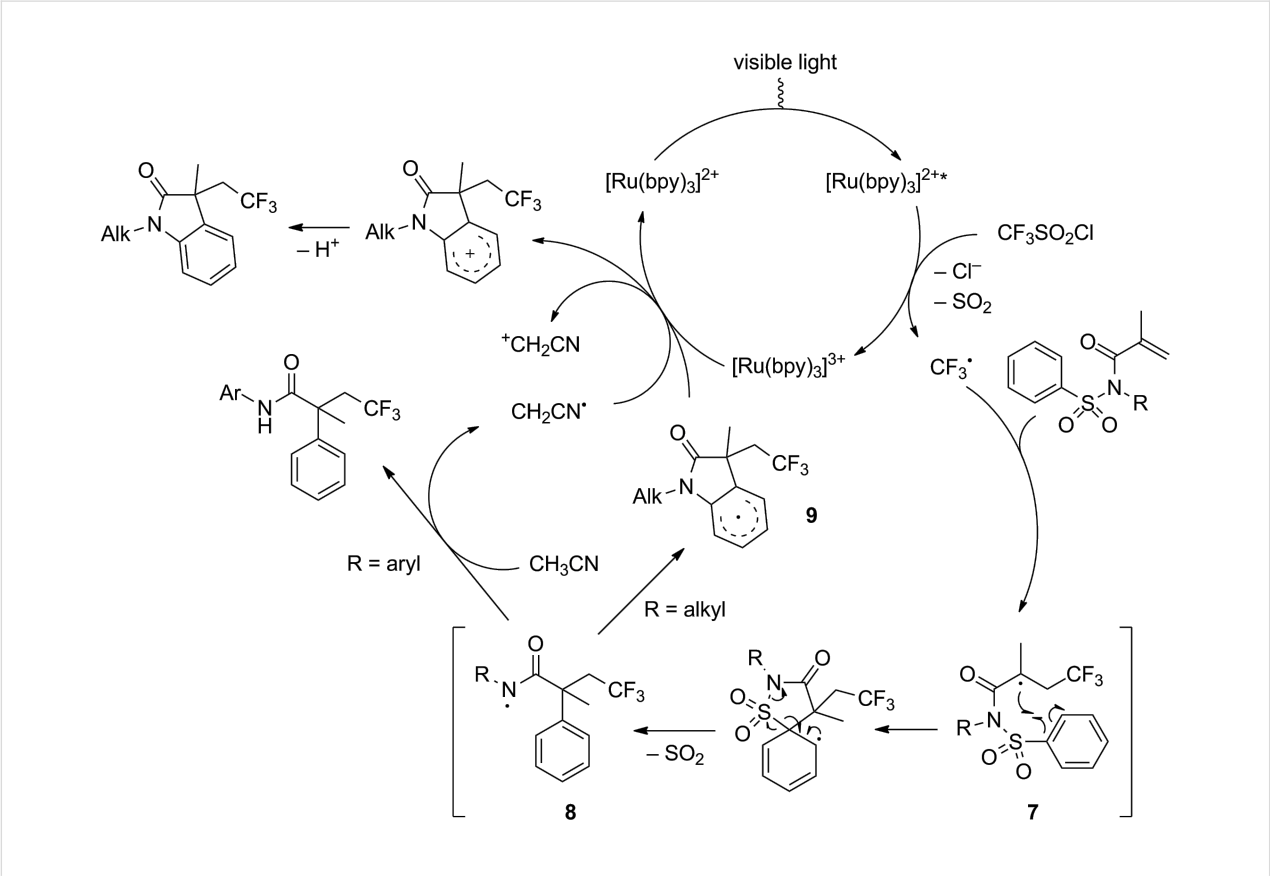

Scheme 8: Proposed mechanism for the trifluoromethylation/aryl migration/desulfonylation (/cyclisation) of *N*-tosylacrylamides.

abstraction on acetonitrile to lead to the corresponding α-aryl-β-trifluoromethyl amide. On the other hand, for *N*-alkylacrylamides, intermediate **8** preferentially cyclised to yield intermediate **9**, which ultimately gave access to the oxindole derivative product.

Yang, Xia and co-workers were also interested in structurally close substrates that are *N*-methacryloyl-*N*-methylbenzamide derivatives **9**. It was found out that such compounds could take part in similar catalytic cycles, without CO extrusion, to yield trifluoromethylated isoquinolindione derivatives **10** in moderate to good yields (Scheme 9).

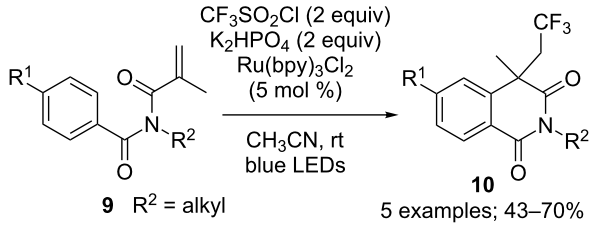

Scheme 9: Photoredox-catalysed trifluoromethylation/cyclisation of *N*-methacryloyl-*N*-methylbenzamide derivatives.

Additionally, Zhang and co-workers reported once again that BiOBr nanosheet catalysis was also suitable to carry out this reaction [12]. The same tendencies in term of reactivity of the substrates depending on their substitution pattern was observed, and similar yields were achieved (Scheme 10). Similarly, $Ir(ppy)_2(dtbbpy)PF_6$ was also described as an appropriate catalyst for this cascade reaction [15].

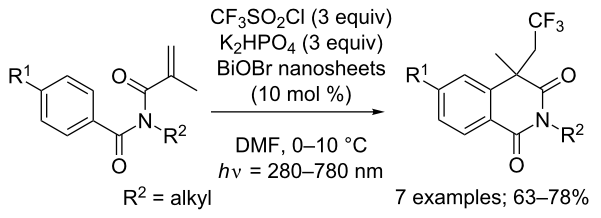

Scheme 10: Photoredox-catalysed trifluoromethylation/cyclisation of *N*-methylacryloyl-*N*-methylbenzamide derivatives using BiOBr nanosheets.

Another cyclisation pattern was observed for other benzylacrylamide derivatives: indeed, in the case of the *N*-benzylmethacrylamide derivative **11**, the formation of an azaspiro[4,5]decyl system through a dearomitising spirocyclisation was observed (Scheme 11) [16].

Other motifs than acrylamides were also investigated for the realisation of cascade reactions including a trifluoromethylation step. This was notably the case of unactivated alkenes: Dolbier and co-workers showed that such compounds could be involved in photoredox-catalysed trifluoromethylation reactions, followed by a 6-*exo* radical cyclisation, to yield the tetralin derivative **12** (Scheme 12) [17].

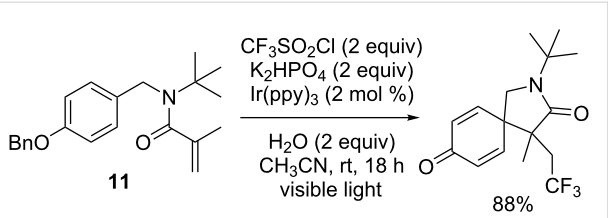

Scheme 11: Photoredox-catalysed trifluoromethylation/dearomatising spirocyclisation of a *N*-benzylacrylamide derivative (ppy = 2-phenylpyridyl).

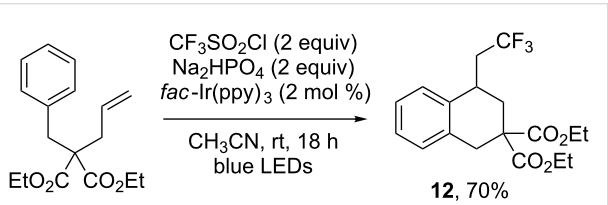

Scheme 12: Photoredox-catalysed trifluoromethylation/cyclisation of an unactivated alkene.

In 2017, Liu and co-workers focused on *N*-alkenylurea derivatives **13**, and from which they developed an asymmetric radical aminotrifluoromethylation methodology, based on a copper salt/chiral phosphoric acid dual-catalytic system [18,19]. This way, they could access a variety of α-tertiary pyrrolidines carrying a β-trifluoromethyl group, in high yields and enantioselectivities (Scheme 13). The reaction conditions were compatible with various substituents on both aryl rings, as well as with unbranched substrates. Interestingly, for some substrates, this method permitted to reach better results than with a previously developed approach using Togni's reagent. The authors proposed the mechanism represented on Scheme 13. First, the trifluoromethyl radical and the chiral mono or diphosphonate Cu(II) **14** or **15** were generated via a single-electron transfer (SET) between CF_3SO_2Cl and the association CuBr/chiral phosphoric acid. In the process, SO_2 and HCl were released, but the latter was scavenged by Ag_2CO_3, minimising its impact on the reaction process by notably avoiding hydroamination side reactions. The trifluoromethyl radical was then added onto the substrate, furnishing radical intermediate **16**, which was trapped by compounds **14** or **15** to form the radical copper species **17**. From this intermediate, two plausible pathways were considered. First, the alkyl radical can be trapped by copper phosphate to provide the copper(III) species **18**. During this step,

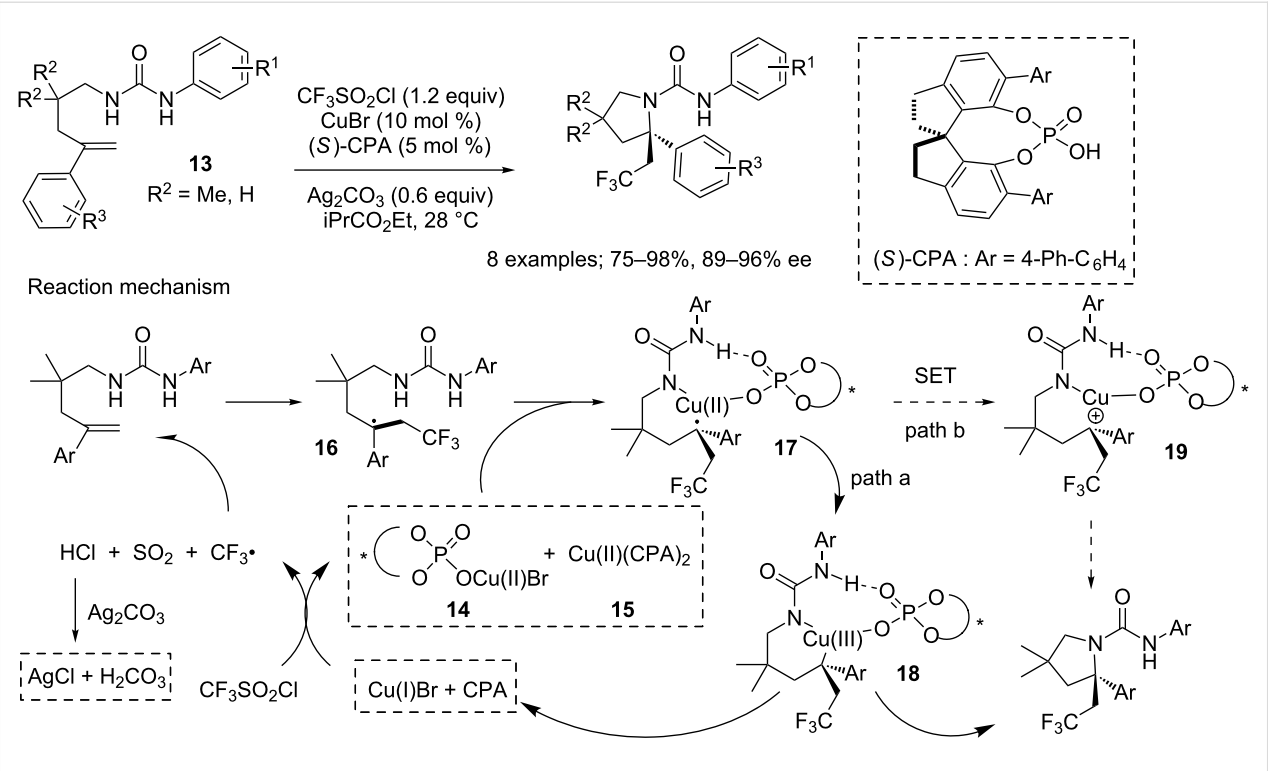

Scheme 13: Asymmetric radical aminotrifluoromethylation of *N*-alkenylurea derivatives using a dual CuBr/chiral phosphoric acid catalytic system.

facial selectivity originated partly from hydrogen-bonding interactions between the chiral phosphate and the N–H bond adjacent to the aryl group. Ion pairing interaction in a concerted transition state probably intervened in this phenomenon as well. The final product was then obtained after reductive elimination of species **18**. The other envisaged pathway was the oxidation of intermediate **17** through a SET to form the cationic species **19**, which would then afford the final product after a C–N bond formation.

Liu and co-workers also proposed a racemic version of this reaction, replacing the chiral phosphoric acid with diphenyl phosphate (Scheme 14) [20].

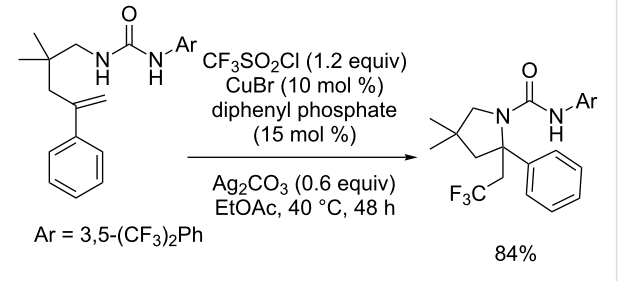

Scheme 14: Aminotrifluoromethylation of an *N*-alkenylurea derivative using a dual CuBr/phosphoric acid catalytic system.

Liu's research group was interested as well in 1,2-difunctionalisation of unactivated alkenes. In this context, they developed two distinct approaches allowing to perform radical-mediated 1,2-formyl- [21] or 1,2-cyanotrifluoromethylations [22] of alkenes under photoredox catalysis. These reactions proceeded through a formyl or a cyano group migration triggered by the addition of the trifluoromethyl radical onto the alkene moiety. Both methodologies were developed using Togni's hypervalent iodine reagent as the CF_3 source, but it was found that they also proceeded smoothly with CF_3SO_2Cl (Scheme 15).

Chlorotrifluoromethylation of alkenes: As clearly demonstrated in the works described above, CF_3SO_2Cl is a reliable CF_3 source under photoredox catalysis. However, its use under similar conditions can also allow the simultaneous introduction of the CF_3 moiety and a Cl atom onto alkenes or alkynes. Kamigata's group was the first to report such type of transformation in 1989 [23,24]. In the presence of $RuCl_2(PPh_3)_2$ at 120 °C, a variety of styrene derivatives as well as cyclic and acyclic alkenes were converted into their chlorotrifluoromethylated analogues (Scheme 16). Generally, the reaction proceeded particularly well with terminal and internal alkenes carrying an electron-withdrawing group. On the contrary, styrene derivatives bearing an electron-donating group provided less satisfying yields. Such results can be explained by the partial consumption of the expected product in a side dehydrochlorination reac-

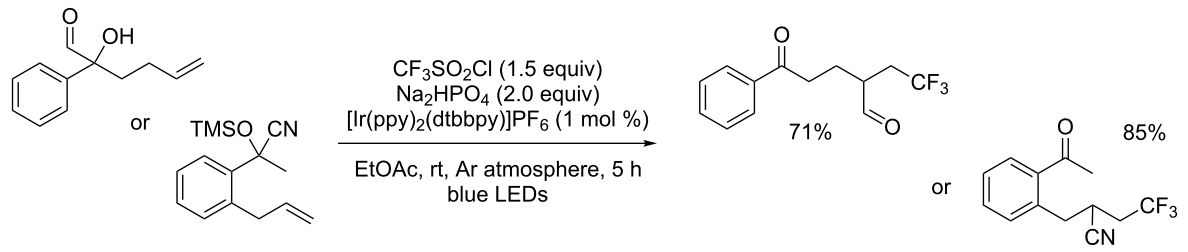

Scheme 15: 1,2-Formyl- and 1,2-cyanotrifluoromethylation of alkenes under photoredox catalysis.

tion. Likewise, the dehydrochlorinated product was recovered exclusively when performing the reaction on 1-phenyl-1,3-butadiene, which tended to indicate that such process was all the more favoured as the conjugation of the final product increased. Cyclic olefins and dienes proved to be more problematic substrates because they raised stereoselectivity issues and afforded poor yields. As for the mechanism, the reaction followed a similar pathway as the one proposed by the same group for the trifluoromethylation of silyl enol ethers (see Scheme 1); except that radical **20** underwent a chlorine atom abstraction to furnish the chlorotrifluoromethylated product (Scheme 16).

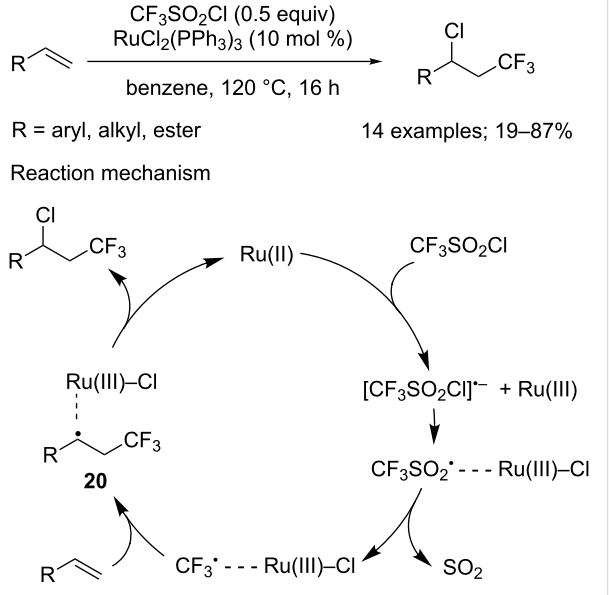

Scheme 16: First simultaneous introduction of the CF_3 moiety and a Cl atom onto alkenes.

Several years later this transformation of alkenes was re-investigated under photoredox catalysis by Jung, Han and co-workers [25]. By replacing $RuCl_2(PPh_3)_2$ with $Ru(phen)_3Cl_2$ (phen: phenanthroline) at room temperature and adding a base, a variety of alkenes furnished the corresponding chlorotrifluoromethylated products under much milder conditions and with higher yields (Scheme 17). Moreover, tuning of the reaction conditions allowed to broaden the scope of the reaction: Indeed, it was extended to terminal alkenes carrying various functional groups, such as protected amines, unprotected alcohols and aldehydes, as well as ether, ester, or amide moieties. Branched and internal alkenes also proved to be compatible with these conditions. Interestingly, no dehydrochlorination reaction was mentioned for any of the studied substrates. The reaction plausibly proceeded through a mechanism similar to the one previously proposed by Kamigata and co-workers. The SET generated CF_3 radical attacked preferentially the less hindered carbon of the alkene to provide the more stable tertiary radical **21**. Said radical was then oxidised by $Ru(phen)_3^{3+}$, yielding the cationic species **22**, which was subsequently trapped by a chloride anion to afford the expected product (Scheme 17). A chain propagation pathway involving the reduction of CF_3SO_2Cl by radical intermediate **21** was also considered. This, however, was

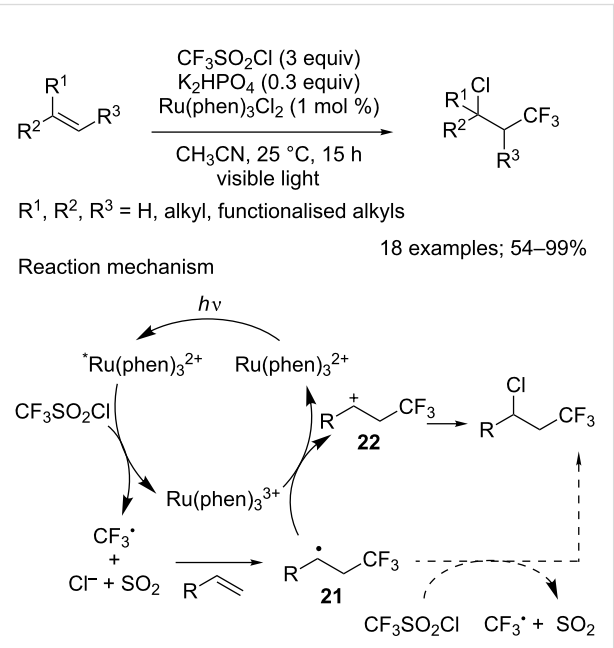

Scheme 17: Chlorotrifluoromethylaltion of terminal, 1,1- and 1,2-substituted alkenes.

declared unlikely as it was observed that the reaction needed continuous irradiation to proceed efficiently.

Unfortunately, Dolbier and co-workers demonstrated in 2015 that this catalytic system was inefficient when switching the substrates to electron-deficient alkenes [26]. Such compounds could nonetheless be converted into the corresponding chlorotrifluoromethylated products by replacing the Ru(II) catalyst by $Cu(dap)_2Cl$ (dap = 2,9-bis(*p*-anisyl)-1,10-phenanthroline) (Scheme 18). This change of reactivity can supposedly be attributed to the high reduction potential of $Cu(dap)_2Cl$ in the excited state, and its important ability to mediate the transfer of the Cl atom. Consequently, a variety of electron-deficient alkenes, such as *N*-arylacrylamides, acrylonitrile, acrylate and enone derivatives furnished their chlorotrifluoromethylated analogues in moderate to excellent yields. Interestingly, performing the reaction on 1,1-disubstituted alkenes did not impact the yield significantly, while 1,2-disubstituted alkenes provided slightly less satisfying results.

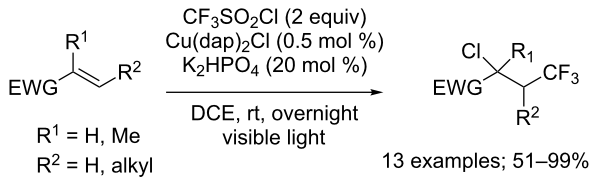

Scheme 18: Chorotrifluoromethylation of electron-deficient alkenes (DCE = dichloroethane).

Chlorotrifluoromethylation reactions can also be included in cascade radical addition/cyclisation processes, as demonstrated by Miyabe and co-workers [27]. Thus, in typical photoredox catalysis conditions, *N*-allyl-*N*-(benzyloxy)methacrylamide **23** could undergo the addition of the CF_3 radical, followed by a cyclisation step and a final chlorine abstraction to yield the corresponding cyclic compound, albeit in low yield and with poor regio- and diastereoselectivity (Scheme 19). Interestingly, the authors proposed a mechanism involving a chain propagation pathway, in contrast to the work of Jung and Han.

A similar cascade reaction was also performed on diethyl 2-allyl-2-(3-methylbut-2-en-1-yl)malonate (**24**) to yield a mixture of two cyclic CF_3 products, the main one being deprived of the chlorine atom (Scheme 20). Unfortunately, no more investigation was carried out on this type of cascade reactions.

Trifluoromethylchlorosulfonylation of alkenes: It was previously evocated that the system $CF_3SO_2Cl/[Cu(dap)_2]Cl$ could be used for the simultaneous introduction of the CF_3 moiety and a chlorine atom onto electron-deficient alkenes (see

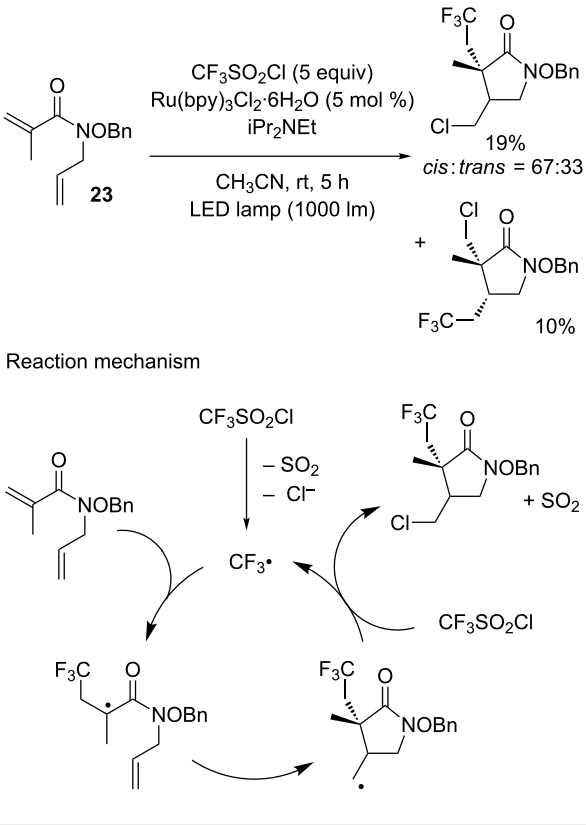

Scheme 19: Cascade trifluoromethylation/cyclisation/chlorination of *N*-allyl-*N*-(benzyloxy)methacrylamide.

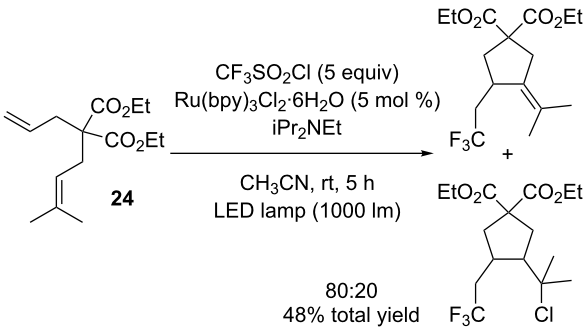

Scheme 20: Cascade trifluoromethylation/cyclisation (/chlorination) of diethyl 2-allyl-2-(3-methylbut-2-en-1-yl)malonate.

Scheme 18). However, Reiser and co-workers observed that such reagent combination could also be exploited for the trifluoromethylchlorosulfonylation of a limited range of alkenes [28]. Thus, allylbenzene derivatives carrying diverse substituents were successfully converted into the expected products with moderate to high yields, as well as cyclic or acyclic aliphatic alkenes (Scheme 21). Nevertheless, internal alkenes suffered from regio- and stereoselectivity issues, and often produced mixtures of isomers. On the other hand, when substrates

featuring a donor atom close to the C=C double bond were submitted to these reaction conditions, chlorotrifluoromethylation was predominantly observed, which was consistent with Dolbier's work. Moreover, similar results were obtained for styrene derivatives, although with a subsequent dehydrochlorination step. If the nature of the substrate undoubtedly played an important role in the reaction process, it was also the case of the catalyst. Indeed, the use of other usual photocatalysts such as $[Ru(bpy)_3]Cl_2$, $[Ir(ppy)_2(dtbbpy)]PF_6$ or Eosin Y favoured the introduction of the CF_3 group and a chlorine atom, with SO_2 extrusion. This phenomenon can be explained by the presumed ability of copper to coordinate SO_2Cl^- (intermediate **25**), preventing it from decomposing into SO_2 and Cl^- and consequently allowing it to be transferred as a whole onto radical **26**. However, this bonding interaction appeared to be weak enough to possibly be destabilised in the presence of a donor atom on the alkene substrate, thus favouring SO_2 extrusion and chlorotrifluoromethylation.

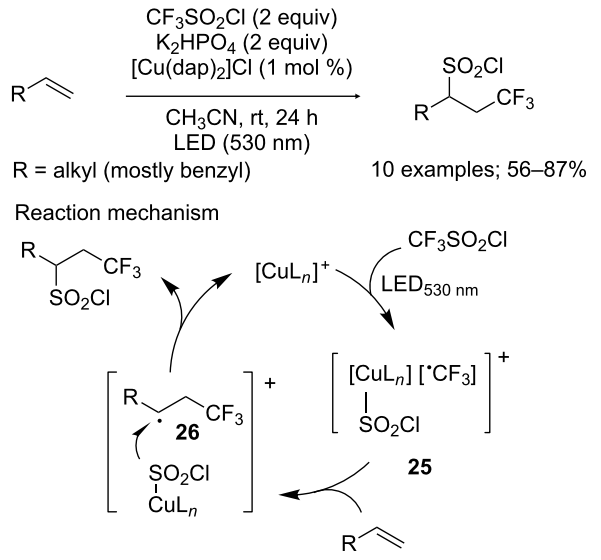

Scheme 21: Trifluoromethylchlorosulfonylation of allylbenzene derivatives and aliphatic alkenes.

The obtained CF_3-containing sulfonyl chloride derivatives could then be involved in another photocatalytic sequence in the presence of α-methylstyrene and water to access β-hydroxysulfones **27** in moderate to good yields (Scheme 22) [29]. Interestingly, this process can be realised in one-pot.

Reiser and co-workers also envisioned that using alkenols as substrates in their previously developed reaction conditions could open an access to trifluoromethylated sultones via a cascade trifluoromethylchlorosulfonylation/cyclisation process [30]. The reaction indeed proceeded smoothly, furnishing γ- and δ-sultones in good to excellent yields (Scheme 23). ε-Sultones, on the other hand, proved to be more difficult to obtain. The first step appeared to be the trickiest one, as it could be antici-

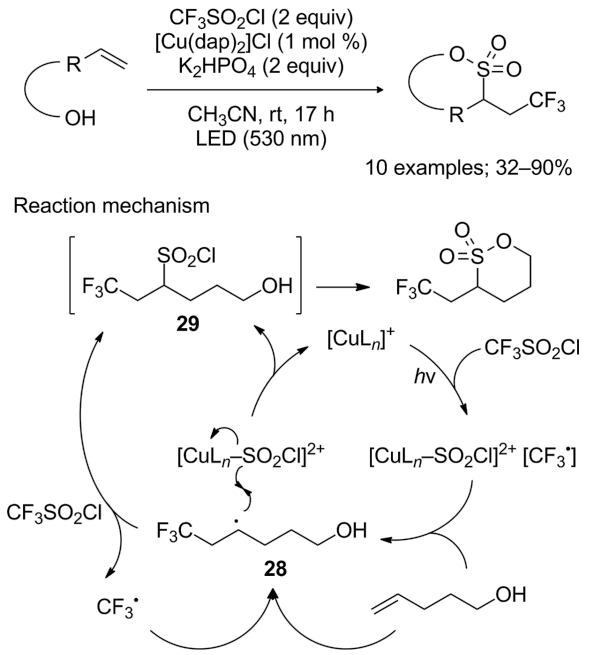

Scheme 23: Cascade trifluoromethylchlorosulfonylation/cyclisation reaction of alkenols: a route to trifluoromethylated sultones.

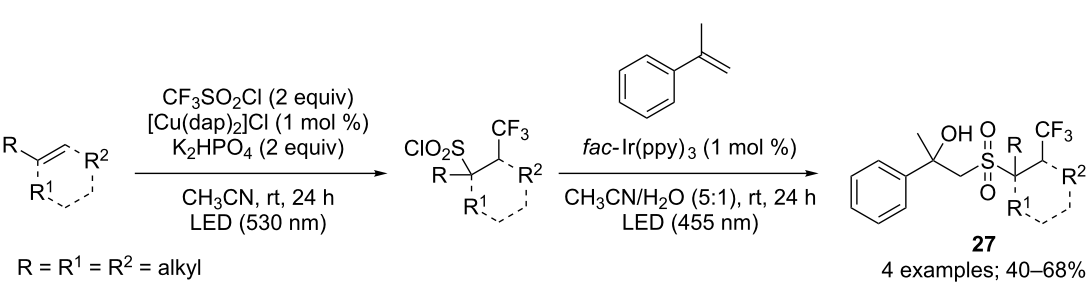

Scheme 22: Access to β-hydroxysulfones from CF_3-containing sulfonyl chlorides through a photocatalytic sequence.

pated considering Reiser's previous reports. Once again, the results were strongly substrate-dependant; indeed the reaction was particularly sensitive to steric effects. The use of alkenols bearing substituents on the double bond or close to it favoured the formation of the chlorotrifluoromethylated products. The mechanism of the reaction was supposedly identical to the one proposed for the trifluoromethylchlorosulfonylation of simple alkenes, although obviously including an additional step of intramolecular cyclisation. An alternative radical chain process was also considered this time, involving notably the reaction of radical **28** with CF_3SO_2Cl to produce $CF_3^{\bullet}$ and intermediate **29**.

C_{sp2}–CF_3 bond-forming reactions

Trifluoromethylation of arenes and heteroarenes: The pioneering example of such transformation was reported in 1990 by Kamigata and co-workers, and described the introduction of the CF_3 moiety onto arenes in the presence of a catalytic amount of $RuCl_2(PPh_3)_3$ (Scheme 24) [6,7]. This reaction, however, suffered from limitations, such as its poor regioselectivity in the case of monosubstituted arenes, and its incompatibility with aromatics bearing strong electron-withdrawing groups. The authors proposed the mechanism represented in Scheme 24. A redox-transfer reaction occurred between CF_3SO_2Cl and the Ru(II) catalyst producing radical anion **30**, which then furnished radical **31** through homolytic cleavage. After a step of SO_2 extrusion, the obtained trifluoromethyl radical **32** was added to the aromatic substrate to afford cyclohexadienyl radical **33**, which was converted into the expected product after a proton abstraction mediated by the R(III)–Cl species.

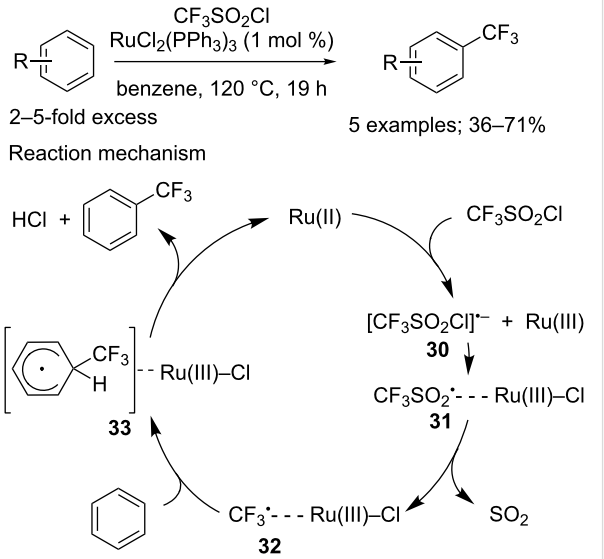

Scheme 24: First direct C–H trifluoromethylation of arenes and proposed mechanism.

The introduction of the CF_3 motif on unactivated arenes was studied in more detail by MacMillan's group in 2011 [31]. They proposed a new methodology based on the use of photoredox catalysts such as $Ru(phen)_3Cl_2$ or $Ir(Fppy)_3$, (Fppy = 2-(2,4-difluorophenyl)pyridine), under the irradiation of a simple household light bulb. This way, they were able to considerably extend the scope of application of the reaction. Indeed, electron-rich five-atom heteroarenes, electron-deficient six-atom heteroarenes as well as unactivated arenes were easily converted into their trifluoromethylated analogues in high yields (Scheme 25). Although the regioselectivity of the reaction was overall excellent for heteroarenes, it proved to be less satisfying for substituted arenes. Further investigations allowed the authors to propose a detailed mechanism, represented in Scheme 25. After excitation of the ruthenium catalyst through visible light irradiation, a first SET reduction of CF_3SO_2Cl occurred, ultimately leading to the formation of the stabilised trifluoromethyl radical after releasing SO_2 and chloride anion. This electron deficient radical was then added on the most electron-rich position of the arene substrate to yield cyclohexadienyl radical **34**, which was readily converted into the cationic species **35** through a second SET regenerating the Ru(II) catalyst. Finally, the cationic intermediate **35** underwent a simple re-aromatising deprotonation to yield the expected product.

Later Wolf and co-workers conducted electrochemical investigations on this type of reaction and proposed a slightly revised mechanism in which the second SET step involved directly the substrate instead of a trifluoromethylated radical such as species **34**. The CF_3 radical then coupled with the generated radical intermediate **36** (Scheme 26) [32].

Blechert and co-workers thereafter reported that the trifluoromethylation of (hetero)arenes could also be performed under heterogeneous catalysis [33]. To this aim, the Ru- or Ir-based catalysts were replaced with a mesoporous graphitic carbon nitride polymer (mpg-CN), which offers the advantage of being cheap, metal-free and recyclable. A variety of heteroarenes, like pyrroles, oxazoles, furanes, thiophenes, indoles and pyrazines were successfully converted into the corresponding trifluoromethylated products in moderate to good yields (Scheme 27). Remarkably, a side chlorination reaction was observed during the optimisation phase, which was possible to minimise by increasing the catalyst loading (see later in the text for other chlorinations with CF_3SO_2Cl).

Indirectly, CF_3SO_2Cl intervened in the trifluoromethylation of (hetero)arenes; indeed, when reacted with zinc in water, it afforded the zinc sulfinate salt $(CF_3SO_2)_2Zn$, which demonstrated great efficiency in introducing the CF_3 moiety on (hetero)aromatic rings [34].

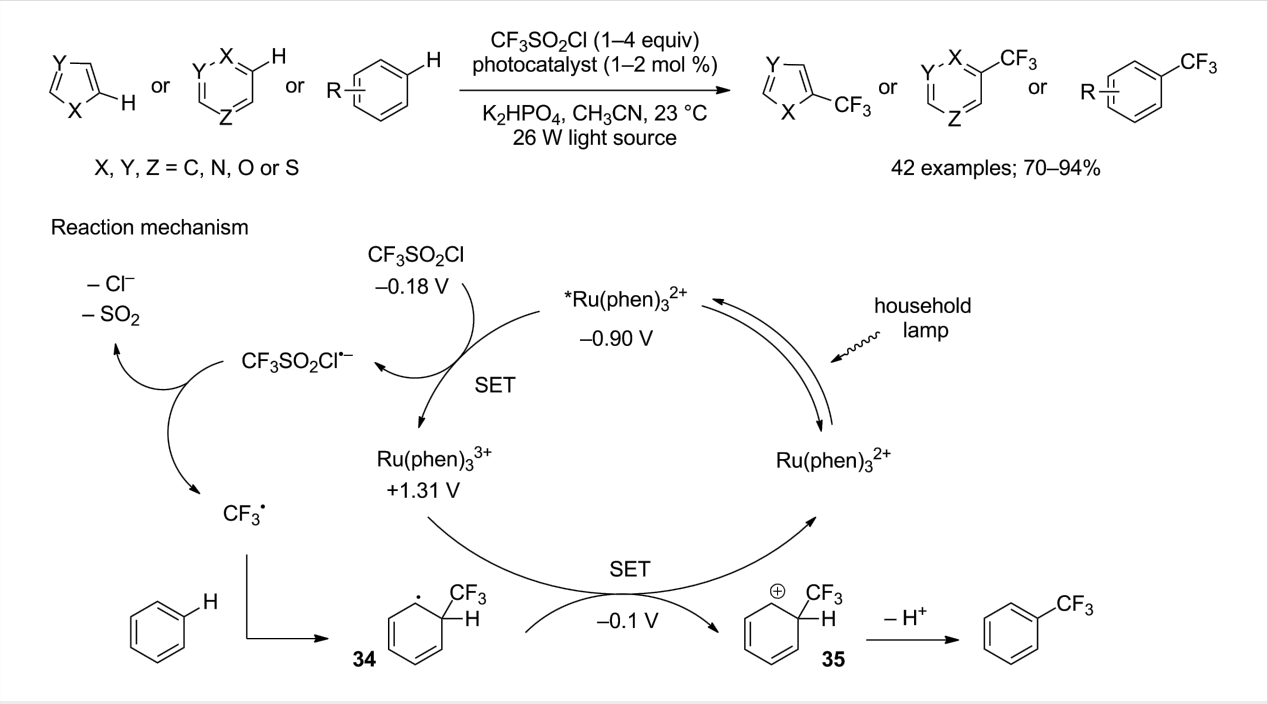

Scheme 25: Direct C–H trifluoromethylation of five- and six-membered (hetero)arenes under photoredox catalysis.

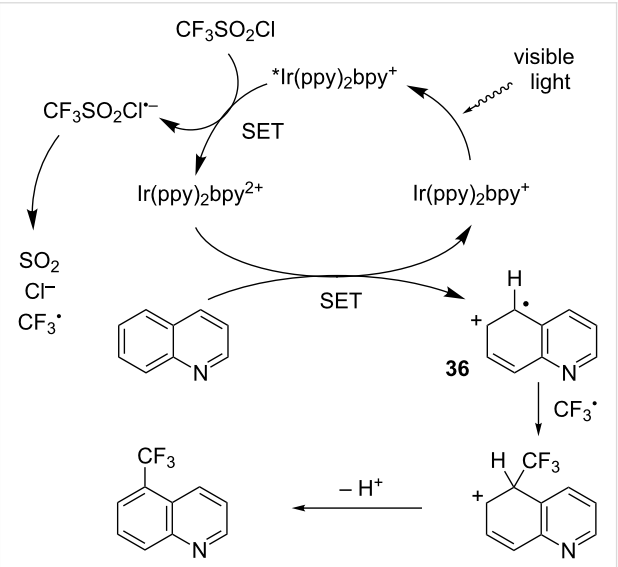

Scheme 26: Alternative pathway for the C–H trifluoromethylation of (hetero)arenes under photoredox catalysis.

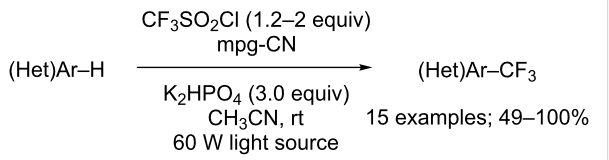

Scheme 27: Direct C–H trifluoromethylation of five- and six-membered ring (hetero)arenes using heterogeneous catalysis.

Trifluoromethylation of olefins: In 2005, Vogel and co-workers showed that terminal alkenes could be trifluoromethylated by means of CF_3SO_2Cl via a palladium-catalysed desulfitative Mizoroki–Heck reaction, in classical solvents or in an ionic liquid media, to yield the corresponding CF_3 alkenes (Scheme 28) [35,36].

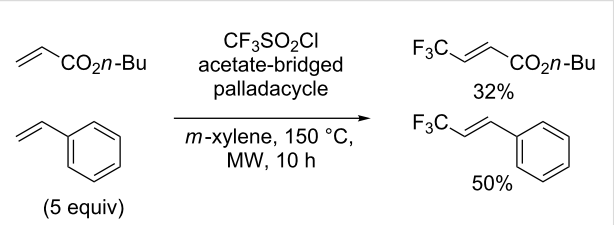

Scheme 28: Trifluoromethylation of terminal olefins.

As for Yu, Zhang and co-workers, they described the trifluoromethylation of two enamides under photocatalytic conditions, using similar conditions as those they proposed for the introduction of the CF_3 moiety on enol acetates (Scheme 29) [37].

Anecdotally, CF_3SO_2Cl was evaluated for the trifluoromethylation of allylsilanes, but, disappointingly, gave lower yields than Togni's hypervalent iodine reagent [38]. More recently, Balaraman and co-workers studied extensively the reaction of β-nitroalkenes with trifluoromethanesulfonyl chloride [39]. They found out that in the presence of the photocatalyst Eosin

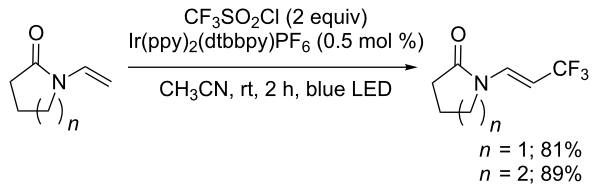

Scheme 29: Trifluoromethylation of enamides.

Y, under visible-light irradiation, such substrates could be selectively converted into (*E*)-1-trifluoromethylalkenes in moderate to good yields (Scheme 30). A plausible mechanism for this reaction was proposed: first, Eosin Y reached its photoexcited singlet state by visible light irradiation, then proceeded to reduce CF_3SO_2Cl through SET. As usual, the formed radical anion **37** immediately collapsed to give $CF_3^{\bullet}$, generating SO_2 and a chloride anion in the process. The trifluoromethyl radical then reacted with the β-nitroalkene to furnish radical intermediate **38**, which was reduced by the Eosin Y radical cation to yield the expected product after elimination of NO_2. This proposed mechanism can rationalise several limitations of the reaction, such as its incompatibility with aliphatic β-nitroalkenes because of the lower stability of the radical intermediate **38** generated. The variation of stability of this species also explained the higher yields obtained with β-nitrostyrene derivatives substituted by electron-withdrawing groups.

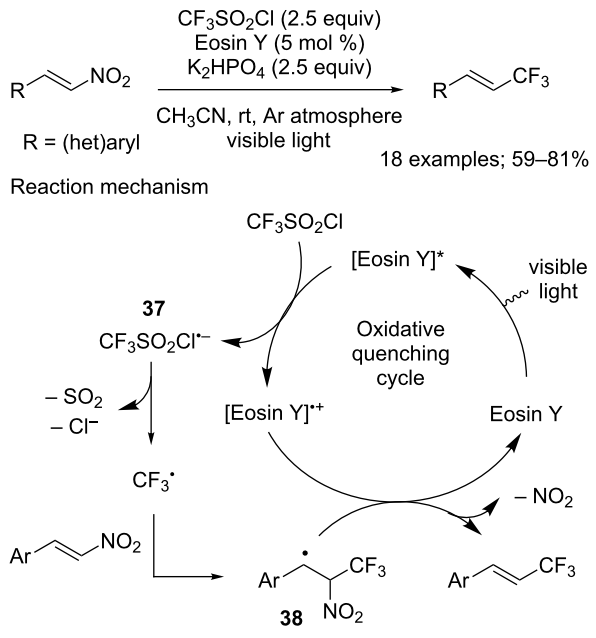

Scheme 30: (*E*)-Selective trifluoromethylation of β-nitroalkenes under photoredox catalysis.

Trifluoromethylation of alkynes: *o*-Azidoarylalkynes also proved to be interesting substrates for cascade reactions, allowing to obtain the 3-trifluoromethylated indole **39** albeit in low yield (Scheme 31) [40].

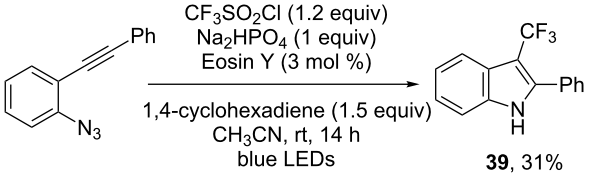

Scheme 31: Photoredox-catalysed trifluoromethylation/cyclisation of an *o*-azidoarylalkynes.

Chlorotrifluoromethylation of alkynes: In the continuity of their work on alkenes, Jung and Han got interested in the chlorotrifluoromethylation of internal alkynes [41]. In the presence of 2 mol % of $Ir(ppy)_3$ and Li_2CO_3, under blue LED irradiation, this type of substrate was easily converted into the corresponding alkenes through a mechanism similar to the one described for alkenes (Scheme 32). It is noteworthy that the introduction of the chlorine atom took selectively place from a direction anti to the CF_3 group, probably because of electrostatic repulsion. The reaction proceeded smoothly with prop-1-yn-1-ylbenzene derivatives, indifferently to the substitution pattern of the aryl moiety. As for the R group, alkyl, ester or amide moieties were well-tolerated. Terminal alkynes could also be

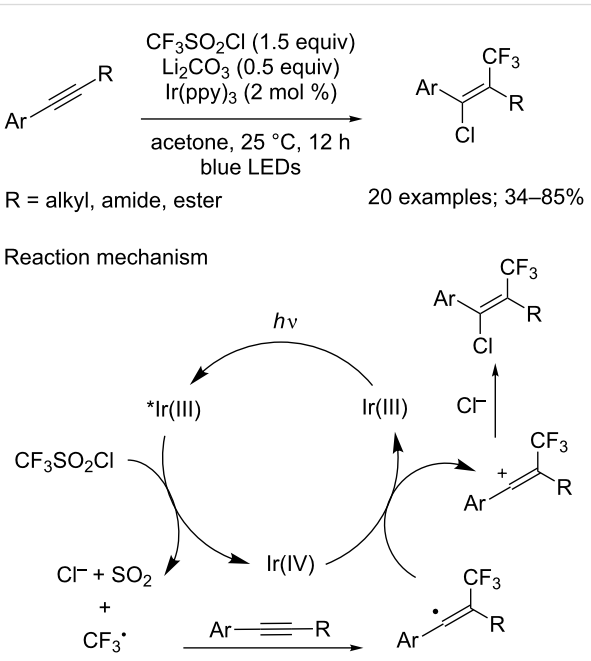

Scheme 32: Regio- and stereoselective chlorotrifluoromethylation of alkynes.

submitted to these conditions successfully, albeit in lower yields.

2 Trifluoromethylsulfenylation

In 2016, CF_3SO_2Cl was proposed for the first time as a new electrophilic trifluoromethylsulfenylation reagent by our research group [42]. To achieve that kind of transformation, said reagent was used under reductive conditions in order to generate in situ the highly reactive CF_3SCl, which could subsequently be trapped by nucleophiles.

Indole derivatives proved to be appropriate substrates for this reaction, and a variety of them were selectively converted into their 3-trifluoromethylated analogues in the presence of trimethylphosphine, with moderate to excellent yields (Scheme 33). The higher nucleophilicity of trimethylphosphine versus triphenylphosphine and the water solubility of trimethylphosphine oxide byproducts were essential elements in choosing the reducing agent. Both electron-withdrawing and donating groups were well-tolerated on various positions of the benzo-fused ring, without tremendous influence on the yields. Similarly, substrates featuring alkyl and aryl substituents in position 1 or 2 were compatible with the reaction conditions. On the other hand, 2-trifluoromethylsulfenylation did not occur with 3-substituted substrates. Other azaarenes, such as pyrrole derivatives, as well as enamines or silyl enol ethers were also compatible with these conditions, and furnished the corresponding products in moderate to good yields. The key step of the reaction comprises the formation of an halogen bond between the positive electrostatic potential on the outer side of the chlorine atom and the lone pair of the phosphorus atom of the phosphine. This phenomenon indeed triggered the cleavage of the S–Cl bond, producing chlorophosphonium sulfinate **40**, which was then readily converted into an *O*-sulfinatophosphonium chloride **41**. The latter finally gave access to the corresponding sulfinyl chloride through an Arbuzov collapse. The obtained

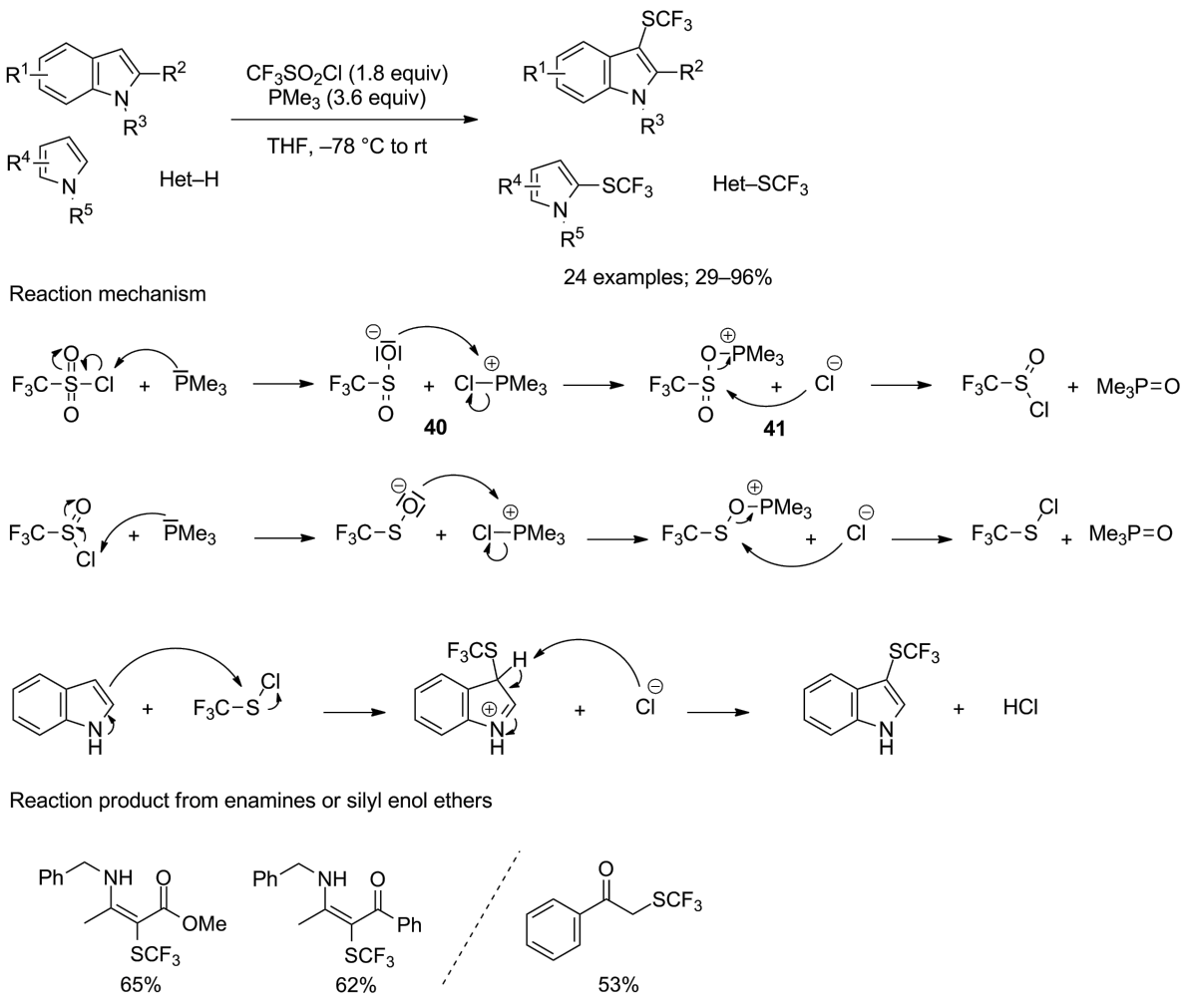

Scheme 33: PMe_3-mediated trifluoromethylsulfenylation by in situ generation of CF_3SCl.

sulfinyl chloride then underwent a similar sequence to yield CF_3SCl, which then reacted with the chosen nucleophile to provide the trifluoromethylsulfenylated analogue (Scheme 33).

Yi and co-workers reported that the reaction could also be performed in acetonitrile at 90 °C, with diethyl phosphite as the reducing agent (Scheme 34) [43]. These modifications allowed to get improved yields for the trifluoromethylsulfenylation of indole and pyrrole derivatives. Morevover, the scope could be extended to other substrates of interest, such as activated benzene derivatives and thiols.

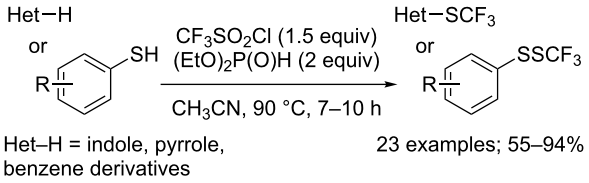

Scheme 34: $(EtO)_2P(O)H$-mediated trifluoromethylsulfenylation of (hetero)arenes and thiols.

Similarly, Lu, Zhao and co-workers found out that excellent yields could also be achieved for indole derivatives when replacing PMe_3 or $(EtO)_2P(O)H$ by cheap and stable triphenylphosphine in acetonitrile at 60 °C [44]. The addition of catalytic amounts of sodium iodide, while not being essential for the production of the trifluoromethylsulfenylated substrates, permitted to slightly increase the yields (Scheme 35). For that matter, excellent yields were achieved indifferently of the nature and position of the substrate substituents. Notably, this procedure allowed for the synthesis of 2-trifluoromethylsulfenylated 3-methylindole, which could not have been realised with the two previously evocated methodologies. The isolated yield was nonetheless quite low (38%). As opposed to previous reports, the proposed mechanism does not include the free phosphine as the reducing agent, but rather iodotriphenylphosphonium iodide **42**. This species was supposedly generated from PPh_3 and I_2, itself issued from the reaction of CF_3SO_2Cl, PPh_3 and NaI. Species **42** was able to reduce CF_3SO_2Cl through the nucleophilic attack of the sulfur atom by the iodine counter anion, leading to the formation of intermediate **43**, which ultimately furnished CF_3SOCl, regenerating I_2 in the process. A second reduction then took place, followed by the electrophilic trifluoromethylsulfenylation step. According to this proposed mechanism, bis(trifluoromethyl)disulfide (CF_3SSCF_3) was generated but its possible role in the trifluoromethylsulfenylation was not evoked.

A slight tuning of the reaction conditions, including notably a replacement of NaI by *n*-Bu_4NI, as well as the increase of reagents quantities permitted to perform the trifluoromethylsulfenylation of thiophenol derivatives at room temperature (Scheme 36) [45]. These conditions proved to be tolerant with variously substituted aryl thiols, but no conversion was observed for any aliphatic substrates.

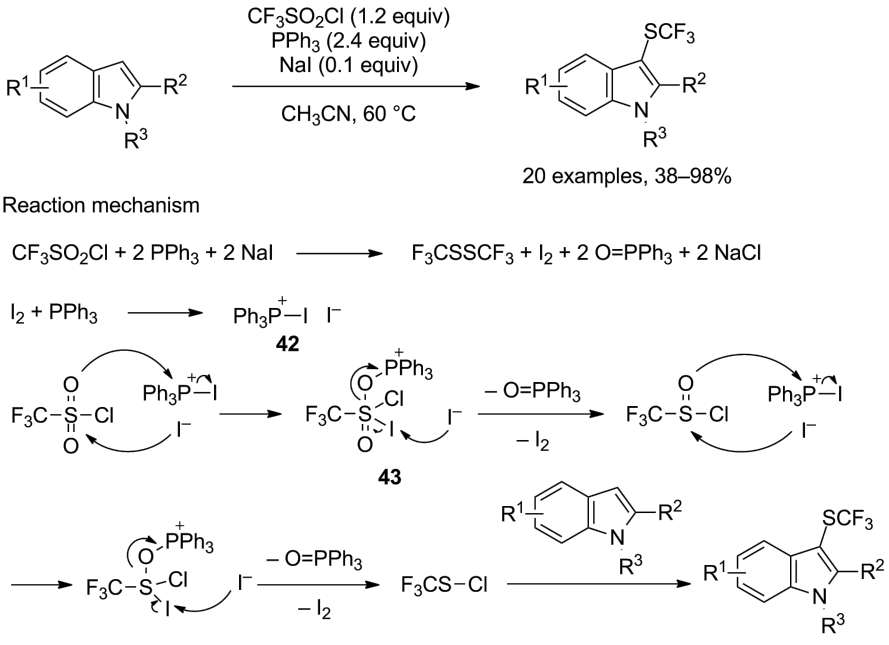

Scheme 35: PPh_3/NaI-mediated trifluoromethylsulfenylation of indole derivatives.

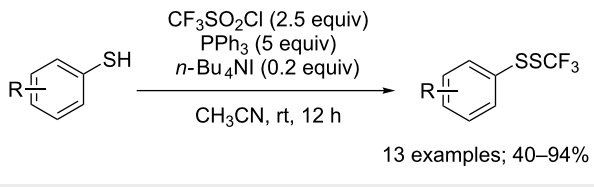

Scheme 36: PPh_3/*n*-Bu_4NI mediated trifluoromethylsulfenylation of thiophenol derivatives.

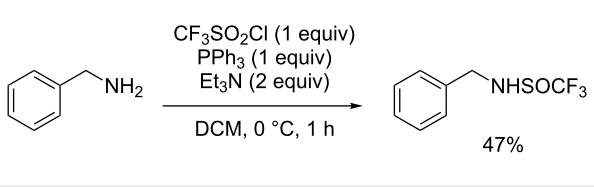

Scheme 37: PPh_3/Et_3N mediated trifluoromethylsulfinylation of benzylamine.

3 Trifluoromethylsulfinylation

Following a similar concept, CF_3SO_2Cl could also be used in an interrupted reduction to selectively furnish CF_3SOCl, thus allowing the trifluoromethylsulfinylation of nucleophiles. The first reports on the introduction of the $SOCF_3$ group using such strategy dated back to 2007 and 2009, but were, however, limited to benzylamine [46,47]. Using 1 equivalent of CF_3SO_2Cl and PPh_3 in the presence of 2 equivalents of Et_3N, benzylamine was converted into the corresponding product in 47% yield (Scheme 37).

A more extensive study of this type of reaction was carried out by our research group in 2017 [48]. Using 1.5 equivalents of CF_3SO_2Cl and tricyclohexylphosphine, the trifluoromethylsulfinylation of various indole and pyrrole derivatives featuring diverse functional groups, as well as other azaarenes could be achieved in low to excellent yields (Scheme 38a). Generally, indole derivatives provided better results than pyrrole derivatives, which were often involved in polymerisation and poly functionalisation side reactions. The scope of the reaction could as well be extended to aryl and alkylamines, albeit the products were obtained in reduced yields, which were partly due to the instability of the formed compounds in the reaction medium. As for phenol derivatives, their lower reactivities led to even further decreased yields (Scheme 38b). Interestingly, while the introduction of the $SOCF_3$ moiety occurred selectively on the nitrogen atom for amines, only the *C*-trifluoromethylsulfinylated products were isolated when performing the reaction on

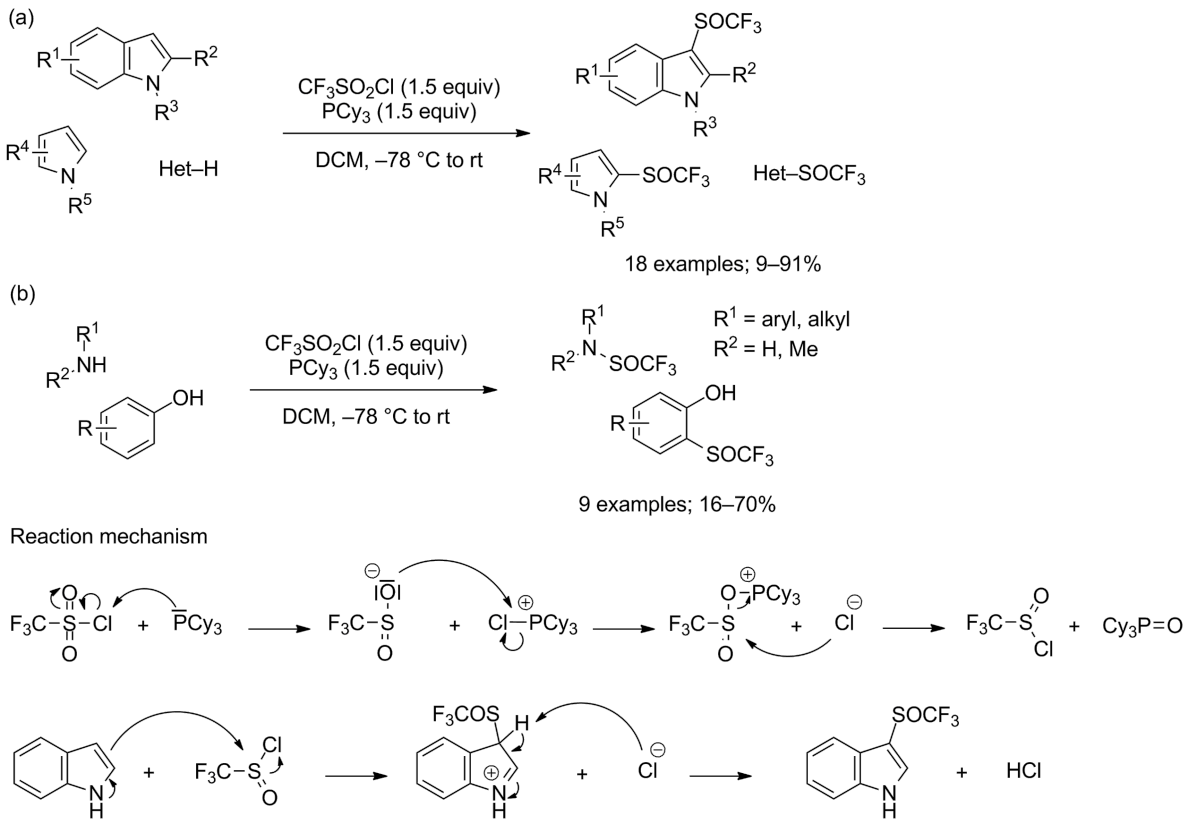

Scheme 38: PCy_3-mediated trifluoromethylsulfinylation of azaarenes, amines and phenols.

phenol derivatives. Such products were probably obtained through an *O*-trifluoromethylsulfinylation step, followed by a rearrangement. As for the mechanism of the reaction, we proposed a pathway similar to the one we previously described for the trifluoromethylsulfenylation of indoles, except that the nature of the phosphine as well as the stoichiometry between CF_3SO_2Cl and PCy_3 prevented the reduction of formed CF_3SOCl and therefore allowed its direct reaction with the substrate (Scheme 38).

4 Chlorination

Sparingly, CF_3SO_2Cl was employed as a chlorinating agent. The first example of such type of reaction was reported by Just and Hakimelahi in 1979 [49]. Their work was focused on the mono- or dichlorination of various carbon acids, in the pK_a range between dialkyl malonate and methyl dichloroacetate, as well as certain nucleophiles, were reacted with trifluoromethanesulfonyl chloride in the presence of a base, like Et_3N or DBU (1,8-diazabicyclo[5.4.0]undec-7-ene) in dichloromethane (Scheme 39). The chlorinated products were recovered in excellent yields. Interestingly, when the reactions were conducted in methanol, the selectivity proved to be quite high, as the rate of chlorination of carbanions was calculated to be more than 10^5 higher than that of the sulfonylation of methanol.

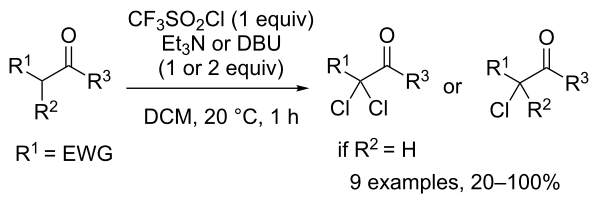

Scheme 39: Mono- and dichlorination of carbon acids.

However, forty years later, Shainyan and Danilevich reported that the process might not be that selective in regard to mono- versus dichlorination of compounds carrying two acidic protons [50]. Indeed, depending on the nature of the substrate, the introduction of one or two chlorine atoms occurred predominantly when performing the reaction with only 1.0 equivalent of CF_3SO_2Cl and Et_3N. Nonetheless, this transformation was utilised for the dichlorination of a cyclopentadiene-1-carbaldehyde derivative [51] and the monochlorination of (*N*-aryl-*N*-hydroxy)acylacetamides **44** (Scheme 40) [52]. In this case, some side *N*-chlorination was observed for certain substrates.

Anecdotally, CF_3SO_2Cl could also be involved in the chlorination of *ortho*-lithiated veratrole [53]. It also allowed the surprising formation of a 5'-chloro nucleoside, when used in an attempt to prepare the corresponding 5'-OTf nucleoside [54]. Moreover, considering the excellent selectivity of the combination CF_3SO_2Cl/Et_3N towards the chlorination of substrates displaying a hydroxy group, the reaction could be further exploited for cascade chlorination/cyclisation processes. For instance, diethyl malonates substituted by an alkyl chain bearing an alcohol or ether function could give access to tetrahydropyran or -furan derivatives [55]. Furthermore, this type of process also allowed the synthesis of diverse heterocycles fused with β-lactams (Scheme 41) [56]. The competition between mono- and dichlorination remained an issue in these transformations; but fortunately, increasing the bulkiness of the ester group permitted to limit the reaction to the introduction of only one chlorine atom. It was also possible to achieve the isolation of similar compounds starting from differently substituted β-lactams, notably carrying a malonate moiety linked to the nitrogen [57].

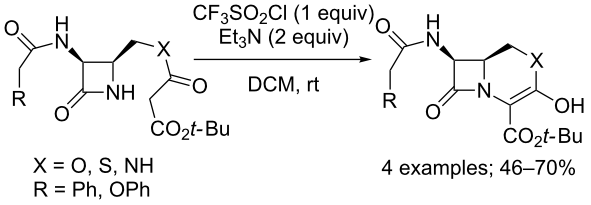

Scheme 41: Examples of the synthesis of heterocycles fused with β-lactams through a chlorination/cyclisation process.

More recently, CF_3SO_2Cl also found to be an appropriate reagent for the asymmetric introduction of a chlorine atom onto several substrates. For instance, Shibata, Toru and co-workers used CF_3SO_2Cl for the enantioselective chlorination of β-ketoesters and oxindoles in the presence of a dbfox-Ph/Ni(II)

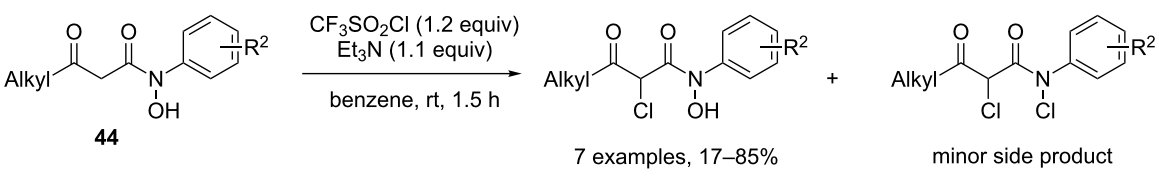

Scheme 40: Monochlorination of (*N*-aryl-*N*-hydroxy)acylacetamides.

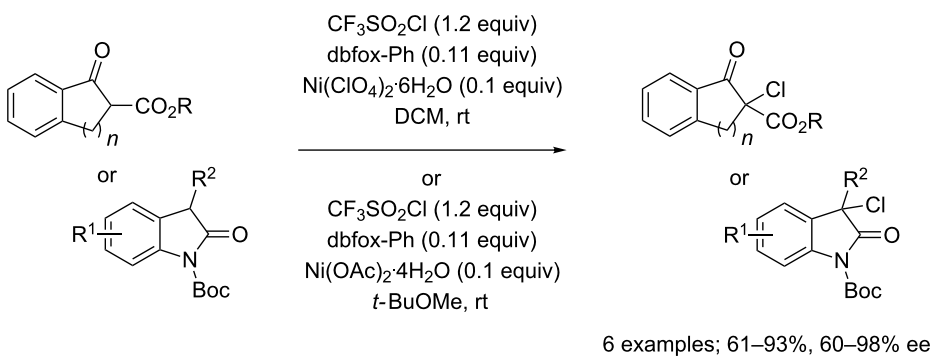

Scheme 42: Enantioselective chlorination of β-ketoesters and oxindoles.

system (dbfox-Ph = [(*R*,*R*)-4,6-dibenzofurandiyl-2,2'-bis(4-phenyloxazoline)]) (Scheme 42) [58]. The reaction proceeded in good to excellent yields and enantioselectivities.

In 2011, Sodeoka and co-workers reported that this reagent was also suitable for the asymmetric chlorination of 3-acyloxazolidin-2-one derivatives thanks to a trinary activation system (Scheme 43) [59]. The expected products were isolated in high yields and enantioselectivities, and no dichlorination reaction occurred. Interestingly, in both cases, it was observed that far lower ee values were reached when replacing CF_3SO_2Cl by *N*-chlorosuccinimide, which highlighted its great compatibility with asymmetric reactions.

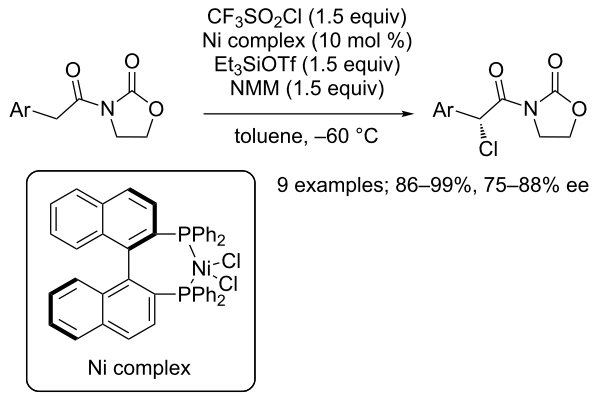

Scheme 43: Enantioselective chlorination of 3-acyloxazolidin-2-one derivatives (NMM = *N*-methylmorpholine).

Conclusion

Trifluoromethanesulfonyl chloride is an inexpensive versatile reagent indissociable from major achievements in the field of trifluoromethylation. Indeed, early discoveries by Kamigata in the nineties using ruthenium catalysis and, more recently in 2011, by MacMillan using photoredox catalysis for the direct trifluoromethylation of the inherently reactive positions of the substrates, paved the way to a dramatic acceleration of discoveries in the field. In addition, the recent breakthrough methods for direct trifluoromethylsufenylation and trifluoromethylsufinylation offer alternative accesses to SCF_3 and $S(O)CF_3$ compounds, respectively, bypassing the use of sophisticated SCF_3 donor reagents. Lastly, CF_3SO_2Cl has a demonstrated ability to transfer an electrophilic chlorine atom for efficient chlorination reactions including enantioselective chlorination. Current know-how and further exploration of the utility of this reagent will undoubtedly be beneficial for the pharmaceutical and agrochemical industries in which new opportunities for economical and sustainable development are eagerly sought after. Numerous applications and novel reactions are expected to appear, thus contributing to enrich the bright future of trifluoromethanesulfonyl chloride.

Acknowledgements

Our research was supported by the Centre National de la Recherche Scientifique CNRS, University of Rouen, INSA Rouen, and Labex SynOrg (ANR-11-LABX-0029). H.C. thanks the French "Ministère de la Recherche et de l'Enseignement Supérieur" for a doctoral fellowship. H.G. thanks Normandy University for a postdoctoral grant. The French Fluorine Network (GIS Fluor) is also acknowledged.

ORCID® iDs

Hélène Chachignon - https://orcid.org/0000-0001-6657-1728
Dominique Cahard - https://orcid.org/0000-0002-8510-1315

References

1. Guyon, H.; Chachignon, H.; Cahard, D. *Beilstein J. Org. Chem.* **2017,** *13,* 2764–2799. doi:10.3762/bjoc.13.272
2. Wender, P. A.; Smith, T. E.; Vogel, P.; Gerber-Lemaire, S. *e-EROS Encycl. Reagents Org. Synth.* **2001**. doi:10.1002/9780470842898.rt248.pub2
3. Shainyan, B. A.; Tolstikova, L. L. *Chem. Rev.* **2013,** *113,* 699–733. doi:10.1021/cr300220h

4. Zhu, S.; Qin, C.; Xu, G.; Chu, Q. *Tetrahedron Lett.* **1998,** *39,* 5265–5268. doi:10.1016/S0040-4039(98)01061-2
5. Müller, R.; Mulani, I.; Basson, A. E.; Pribut, N.; Hassam, M.; Morris, L.; van Otterlo, W. A. L.; Pelly, S. C. *Bioorg. Med. Chem. Lett.* **2014,** *24,* 4376–4380. doi:10.1016/j.bmcl.2014.08.020
6. Kamigata, N.; Fukushima, T.; Yoshida, M. *Chem. Lett.* **1990,** *19,* 649–650. doi:10.1246/cl.1990.649
7. Kamigata, N.; Ohtsuka, T.; Fukushima, T.; Yoshida, M.; Shimizu, T. *J. Chem. Soc., Perkin Trans. 1* **1994,** 1339–1346. doi:10.1039/P19940001339
8. Kamigata, N.; Udodaira, K.; Shimizu, T. *Phosphorus, Sulfur Silicon Relat. Elem.* **1997,** *129,* 155–168. doi:10.1080/10426509708031590
9. Cantillo, D.; de Frutos, O.; Rincón, J. A.; Mateos, C.; Kappe, C. O. *Org. Lett.* **2014,** *16,* 896–899. doi:10.1021/ol403650y
10. Jiang, H.; Cheng, Y.; Zhang, Y.; Yu, S. *Eur. J. Org. Chem.* **2013,** 5485–5492. doi:10.1002/ejoc.201300693
11. Tang, X.-J.; Thomoson, C. S.; Dolbier, W. R., Jr. *Org. Lett.* **2014,** *16,* 4594–4597. doi:10.1021/ol502163f
12. Liu, C.; Zhao, W.; Huang, Y.; Wang, H.; Zhang, B. *Tetrahedron* **2015,** *71,* 4344–4351. doi:10.1016/j.tet.2015.04.056
13. Zheng, L.; Yang, C.; Xu, Z.; Gao, F.; Xia, W. *J. Org. Chem.* **2015,** *80,* 5730–5736. doi:10.1021/acs.joc.5b00677
14. Liu, C.; Zhang, B. *RSC Adv.* **2015,** *5,* 61199–61203. doi:10.1039/c5ra08996d
15. Xia, X.-F.; Zhu, S.-L.; Wang, D.; Liang, Y.-M. *Adv. Synth. Catal.* **2017,** *359,* 859–865. doi:10.1002/adsc.201600982
16. Zhang, Z.; Tang, X.-J.; Dolbier, W. R., Jr. *Org. Lett.* **2016,** *18,* 1048–1051. doi:10.1021/acs.orglett.6b00168
17. Zhang, Z.; Martinez, H.; Dolbier, W. R. *J. Org. Chem.* **2017,** *82,* 2589–2598. doi:10.1021/acs.joc.6b03012
18. Li, X.-F.; Lin, J.-S.; Liu, X.-Y. *Synthesis* **2017,** *49,* 4213–4220. doi:10.1055/s-0036-1589044
19. Lin, J.-S.; Wang, F.-L.; Dong, X.-Y.; He, W.-W.; Yuan, Y.; Chen, S.; Liu, X.-Y. *Nat. Commun.* **2017,** *8,* No. 14841. doi:10.1038/ncomms14841
20. Li, X.-F.; Lin, J.-S.; Liu, X.-Y. *Synthesis* **2017,** *49,* 4213–4220. doi:10.1055/s-0036-1589044
21. Li, Z.-L.; Li, X.-H.; Wang, N.; Yang, N.-Y.; Liu, X.-Y. *Angew. Chem., Int. Ed.* **2016,** *55,* 15100–15104. doi:10.1002/anie.201608198
22. Wang, N.; Li, L.; Li, Z.-L.; Yang, N.-Y.; Guo, Z.; Zhang, H.-X.; Liu, X.-Y. *Org. Lett.* **2016,** *18,* 6026–6029. doi:10.1021/acs.orglett.6b02960
23. Kamigata, N.; Fukushima, T.; Yoshida, M. *J. Chem. Soc., Chem. Commun.* **1989,** 1559–1560. doi:10.1039/c39890001559
24. Kamigata, N.; Fukushima, T.; Terakawa, Y.; Yoshida, M.; Sawada, H. *J. Chem. Soc., Perkin Trans. 1* **1991,** 627–633. doi:10.1039/P19910000627
25. Oh, S. H.; Malpani, Y. R.; Ha, N.; Jung, Y.-S.; Han, S. B. *Org. Lett.* **2014,** *16,* 1310–1313. doi:10.1021/ol403716t
26. Tang, X.-J.; Dolbier, W. R., Jr. *Angew. Chem., Int. Ed.* **2015,** *54,* 4246–4249. doi:10.1002/anie.201412199
27. Yoshioka, E.; Kohtani, S.; Tanaka, E.; Hata, Y.; Miyabe, H. *Tetrahedron* **2015,** *71,* 773–781. doi:10.1016/j.tet.2014.12.068
28. Bagal, D. B.; Kachkovskyi, G.; Knorn, M.; Rawner, T.; Bhanage, B. M.; Reiser, O. *Angew. Chem., Int. Ed.* **2015,** *54,* 6999–7002. doi:10.1002/anie.201501880
29. Pagire, S. K.; Paria, S.; Reiser, O. *Org. Lett.* **2016,** *18,* 2106–2109. doi:10.1021/acs.orglett.6b00734
30. Rawner, T.; Knorn, M.; Lutsker, E.; Hossain, A.; Reiser, O. *J. Org. Chem.* **2016,** *81,* 7139–7147. doi:10.1021/acs.joc.6b01001
31. Nagib, D. A.; MacMillan, D. W. C. *Nature* **2011,** *480,* 224–228. doi:10.1038/nature10647
32. Ochola, J. R.; Wolf, M. O. *Org. Biomol. Chem.* **2016,** *14,* 9088–9092. doi:10.1039/c6ob01717g
33. Baar, M.; Blechert, S. *Chem. – Eur. J.* **2015,** *21,* 526–530. doi:10.1002/chem.201405505
34. Fujiwara, Y.; Dixon, J. A.; O'Hara, F.; Funder, E. D.; Dixon, D. D.; Rodriguez, R. A.; Baxter, R. D.; Herlé, B.; Sach, N.; Collins, M. R.; Ishihara, Y.; Baran, P. S. *Nature* **2012,** *492,* 95–99. doi:10.1038/nature11680
35. Dubbaka, S. R.; Vogel, P. *Chem. – Eur. J.* **2005,** *11,* 2633–2641. doi:10.1002/chem.200400838
36. Dubbaka, S. R.; Zhao, D.; Fei, Z.; Volla, C. M. R.; Dyson, P. J.; Vogel, P. *Synlett* **2006,** 3155–3157. doi:10.1055/s-2006-944198
37. Jiang, H.; Huang, C.; Guo, J.; Zeng, C.; Zhang, Y.; Yu, S. *Chem. – Eur. J.* **2012,** *18,* 15158–15166. doi:10.1002/chem.201201716
38. Mizuta, S.; Engle, K. M.; Verhoog, S.; Galicia-López, O.; O'Duill, M.; Médebielle, M.; Wheelhouse, K.; Rassias, G.; Thompson, A. L.; Gouverneur, V. *Org. Lett.* **2013,** *15,* 1250–1253. doi:10.1021/ol400184t
39. Midya, S. P.; Rana, J.; Abraham, T.; Aswin, B.; Balaraman, E. *Chem. Commun.* **2017,** *53,* 6760–6763. doi:10.1039/C7CC02589K
40. Gu, L.; Jin, C.; Wang, W.; He, Y.; Yang, G.; Li, G. *Chem. Commun.* **2017,** *53,* 4203–4206. doi:10.1039/c6cc10305g
41. Han, H. S.; Lee, Y. J.; Jung, Y.-S.; Han, S. B. *Org. Lett.* **2017,** *19,* 1962–1965. doi:10.1021/acs.orglett.7b00470
42. Chachignon, H.; Maeno, M.; Kondo, H.; Shibata, N.; Cahard, D. *Org. Lett.* **2016,** *18,* 2467–2470. doi:10.1021/acs.orglett.6b01026
43. Jiang, L.; Yi, W.; Liu, Q. *Adv. Synth. Catal.* **2016,** *358,* 3700–3705. doi:10.1002/adsc.201600651
44. Lu, K.; Deng, Z.; Li, M.; Li, T.; Zhao, X. *Org. Biomol. Chem.* **2017,** *15,* 1254–1260. doi:10.1039/c6ob02465c
45. Zhao, X.; Li, T.; Yang, B.; Qiu, D.; Lu, K. *Tetrahedron* **2017,** *73,* 3112–3117. doi:10.1016/j.tet.2017.04.032
46. Harmata, M.; Zheng, P.; Huang, C.; Gomes, M. G.; Ying, W.; Ranyanil, K.-O.; Balan, G.; Calkins, N. L. *J. Org. Chem.* **2007,** *72,* 683–685. doi:10.1021/jo062296i
47. Revés, M.; Riera, A.; Verdaguer, X. *Eur. J. Inorg. Chem.* **2009,** 4446–4453. doi:10.1002/ejic.200900521
48. Chachignon, H.; Cahard, D. *J. Fluorine Chem.* **2017,** *198,* 82–88. doi:10.1016/j.jfluchem.2016.11.020
49. Hakimelahi, G. H.; Just, G. *Tetrahedron Lett.* **1979,** *20,* 3643–3644. doi:10.1016/S0040-4039(01)95485-1
50. Shainyan, B. A.; Danilevich, Yu. S. *Russ. J. Org. Chem.* **2009,** *45,* 1412–1413. doi:10.1134/s1070428009090176
51. Hafner, K.; Stowasser, B.; Sturm, V. *Tetrahedron Lett.* **1985,** *26,* 189–192. doi:10.1016/s0040-4039(00)61876-2
52. Sato, K.; Kinoto, T.; Sugai, S. *Chem. Pharm. Bull.* **1986,** *34,* 1553–1560. doi:10.1248/cpb.34.1553
53. Wang, T.; Rabe, P.; Citron, C. A.; Dickschat, J. S. *Beilstein J. Org. Chem.* **2013,** *9,* 2767–2777. doi:10.3762/bjoc.9.311
54. Amiable, C.; Pochet, S. *Tetrahedron* **2015,** *71,* 2525–2529. doi:10.1016/j.tet.2015.03.020
55. Hamimelai, G. H.; Just, G. *Tetrahedron Lett.* **1979,** *20,* 3645–3648. doi:10.1016/S0040-4039(01)95486-3
56. Hakimelahi, G. H.; Hwu, J. R.; Tsay, S.-C.; Ramezani, Z.; Hwu, J. R. *Helv. Chim. Acta* **1996,** *79,* 813–819. doi:10.1002/hlca.19960790323
57. Hwu, J. R.; Hakimelahi, S.; Lu, K.-L.; Tsay, S.-C. *Tetrahedron* **1999,** *55,* 8039–8044. doi:10.1016/s0040-4020(99)00423-8

58. Shibata, N.; Kohno, J.; Takai, K.; Ishimaru, T.; Nakamura, S.; Toru, T.; Kanemasa, S. *Angew. Chem., Int. Ed.* **2005,** *44,* 4204–4207. doi:10.1002/anie.200501041
59. Hamashima, Y.; Nagi, T.; Shimizu, R.; Tsuchimoto, T.; Sodeoka, M. *Eur. J. Org. Chem.* **2011,** 3675–3678. doi:10.1002/ejoc.201100453

License and Terms

BEILSTEIN JOURNAL OF ORGANIC CHEMISTRY

The use of 4,4,4-trifluorothreonine to stabilize extended peptide structures and mimic β-strands

Yaochun Xu[1], Isabelle Correia[2], Tap Ha-Duong[1], Nadjib Kihal[1], Jean-Louis Soulier[1], Julia Kaffy[1], Benoît Crousse[1], Olivier Lequin[*2] and Sandrine Ongeri[*1]

Full Research Paper

Open Access

Address:
[1]Molécules Fluorées et Chimie Médicinale, BioCIS, Univ. Paris-Sud, CNRS, Université Paris Saclay, 5 rue Jean-Baptiste Clément, 92296 Châtenay-Malabry Cedex, France and [2]Sorbonne Universités, UPMC Univ Paris 06, Ecole Normale Supérieure, PSL Research University, CNRS, Laboratoire des Biomolécules, 4 place Jussieu, 75252 Paris Cedex 05, France

Email:
Olivier Lequin[*] - olivier.lequin@upmc.fr; Sandrine Ongeri[*] - Sandrine.ongeri@u-psud.fr

* Corresponding author

Keywords:
aggregation; beta-sheet; fluorine; peptide; unnatural amino acid

Beilstein J. Org. Chem. **2017,** *13,* 2842–2853.
doi:10.3762/bjoc.13.276

Received: 28 September 2017
Accepted: 13 December 2017
Published: 21 December 2017

This article is part of the Thematic Series "Organo-fluorine chemistry IV".

Guest Editor: D. O'Hagan

Abstract

Pentapeptides having the sequence R-HN-Ala-Val-**X**-Val-Leu-OMe, where the central residue **X** is L-serine, L-threonine, (2*S*,3*R*)-L-CF_3-threonine and (2*S*,3*S*)-L-CF_3-threonine were prepared. The capacity of (2*S*,3*S*)- and (2*S*,3*R*)-CF_3-threonine analogues to stabilize an extended structure when introduced in the central position of pentapeptides is demonstrated by NMR conformational studies and molecular dynamics simulations. CF_3-threonine containing pentapeptides are more prone to mimic β-strands than their natural Ser and Thr pentapeptide analogues. The proof of concept that these fluorinated β-strand mimics are able to disrupt protein–protein interactions involving β-sheet structures is provided. The CF_3-threonine containing pentapeptides interact with the amyloid peptide $A\beta_{1\text{-}42}$ in order to reduce the protein–protein interactions mediating its aggregation process.

Introduction

It is estimated that 20% of administered drugs contain fluorine atoms or fluoroalkyl groups, representing 150 fluorinated molecules, and this trend is expected to increase to about 30% in the early future as a new generation of fluorinated compounds is currently in Phase II−III clinical trials [1]. In parallel, pharmaceutical peptides are attracting increasing interest as around 100 peptides are on the pharmaceutical market [2]. Peptide fluorination has appeared as a general and effective strategy to enhance the stability against enzymatic, chemical and thermal denaturation while generally retaining the original structure and biological activity [3,4]. Fluorinated amino acids can also be used as powerful ^{19}F NMR probes for the study of protein–ligand interactions and enzymatic activities [5-8]. However, the development of fluorinated peptides as drug candidates seems to be largely under-exploited. Investigation on the influence of a fluorinated substituent incorporated in the side-

chain of amino acids on peptide conformations has recently raised attention [9]. While the effect of fluorinated analogs of hydrophobic aliphatic and aromatic amino acids has been prominently studied, the influence of fluorinated polar amino acids has been rarely explored. To our knowledge, only one example of conformational studies of a peptide containing a (2*S*,3*S*)-CF_3-threonine has been conducted by Kitamoto et al. [7,10]. These authors reported a significant conformational difference between an enkephalin-related hexapeptide derivative and its fluorinated analogue containing a (2*S*,3*S*)-CF_3-threonine at its C-terminus. NMR studies demonstrated that the natural hexapeptide adopted a folded conformation while for the trifluoromethylated analogue an extended backbone conformation predominated.

In the present study, our objective was to evaluate the capacity of both (2*S*,3*S*)- and (2*S*,3*R*)-CF_3-threonine analogues (the (2*S*,3*S*)- analogue being the exact analogue of the natural threonine residue, see Figure 1A) to stabilize an extended structure when introduced in the central position of pentapeptides, with the intent of designing inducer or stabilizer of β-strand mimics. Indeed, β-strand mimics have a particular interest as ligand of

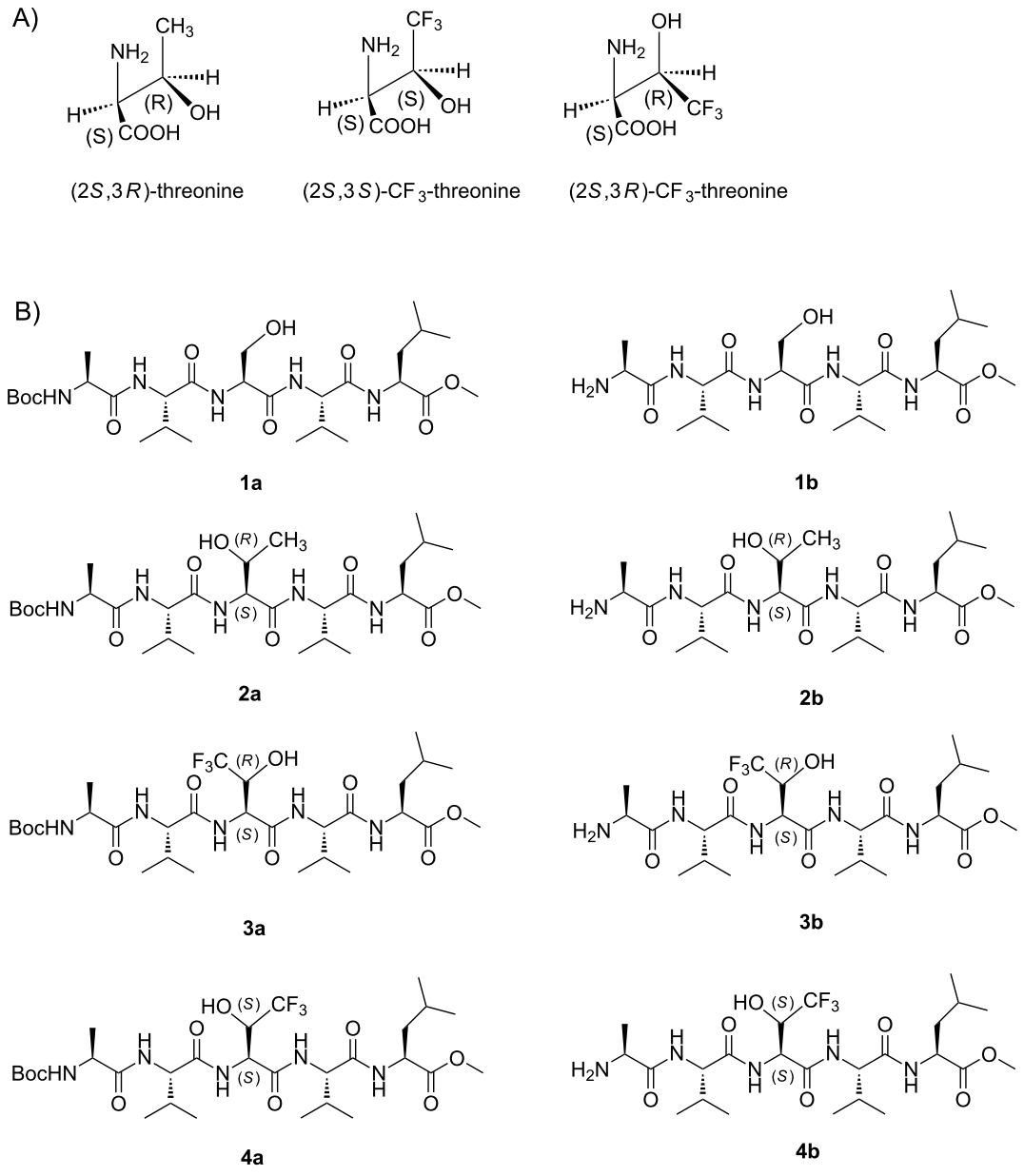

Figure 1: A) Natural threonine and its trifluoromethyl analogues sawhorse projections. B) Structure of Boc-protected pentapeptides **1a**–**4a** and free amine pentapeptides **1b**–**4b**.

β-sheet structures and as potential inhibitors of protein–protein interactions involving β-sheet structures [11-13]. For example, β-strand mimics have been successfully introduced in inhibitors of amyloid proteins aggregation characterized by ordered β-sheet structure assemblies [14,15]. In this context, we synthesized and analyzed, by NMR and molecular modeling, the conformational preferences of eight pentapeptides, containing a L-serine, a L-threonine, a (2*S*,3*R*)-L-*allo*-CF_3-threonine or a (2*S*,3*S*)-L-CF_3-threonine in the third position. Both *N*-Boc protected (compounds **1a**–**4a**) and *N*-deprotected pentapeptides (**1b**–**4b**) were studied.

Results and Discussion

Synthesis. First, we synthesized the two (2*S*,3*R*)- and (2*S*,3*S*)-CF_3-Thr analogues. An enantioselective synthesis of (2*S*,3*R*)-Boc-CF_3-Thr was proposed in 2003 [16] from propargylic alcohol in ten steps, based on the trifluoromethylation key step of 1-(((*E*)-3-bromoallyloxy)methyl)benzene to obtain (*E*)-1-benzyloxy-4,4,4-trifluoro-2-butene. The sequence then involved Sharpless asymmetric dihydroxylation, nucleophilic opening of cyclic sulfate with NaN_3, palladium-catalyzed selective hydrogenation, and oxidation. Zeng et al. described the synthesis of the enantiomer (2*R*,3*S*)-Boc-CF_3-Thr(Bzl) in four steps from the (*S*)-Garner's aldehyde [17,18]. The enantiomer (2*S*,3*R*)-Boc-CF_3-Thr(Bzl) was not described by Zeng et al. However, we decided to follow this more straightforward methodology and we have adapted Zeng's synthesis starting from the (*R*)-Garner's aldehyde. (2*S*,3*R*)-Boc-CF_3-Thr(Bzl) was obtained with satisfactory yields (Scheme 1). In this synthetic pathway, the key intermediate **6** was obtained, as a mixture of two diastereoisomers (9:1, evaluated by ^{19}F NMR) via a nucleophilic trifluoromethylation reaction of Ruppert's reagent on the (*R*)-Garner's aldehyde **5** in THF and in the presence of a catalytic amount of TBAF. Benzylation of the alcohol of **6** was then performed to obtain the desired intermediate as two diastereoisomers **7a** and **7b** that were easily separated at this stage by column chromatography. The major diastereomer **7a** was used in the following steps. Hydrolysis of the oxazolidine, followed by Jones oxidation of the alcohol **8**, allowed us to recover the desired acid **9** in good yield (90%). The optical rotation of a solution of the product **9** (2*S*,3*R*), dissolved in MeOH was measured at 25 °C. The value obtained was equal to −13° and opposite to the value (+13°) described by Zeng et al. [17] for the enantiomer (2*R*,3*S*).

The synthesis of (2*S*,3*S*)-CF_3-threonine has been described in several publications [7,10,19-22]. Among these approaches, we followed a general procedure to access to (2*S*,3*S*)-CF_3-threonine through an aldol reaction of CF_3CHO with the Ni(II) complex of the chiral Schiff base of glycine which was introduced by Belokon et al. [23,24]. The chiral auxiliary (*S*)-*N*-(2-benzoylphenyl)-1-benzylpyrrolidine-2-carboxamide (**11**) was obtained in good yield starting from the *N*-benzylation of L-proline in the presence of KOH, then activation of the carboxylic acid functionality of **10** using $SOCl_2$ at low temperature, followed by condensation with 2-aminobenzophenone (Scheme 2). Complexation of **11** with nickel nitrate and glycine under basic conditions gave the nickel Schiff base complex **12**

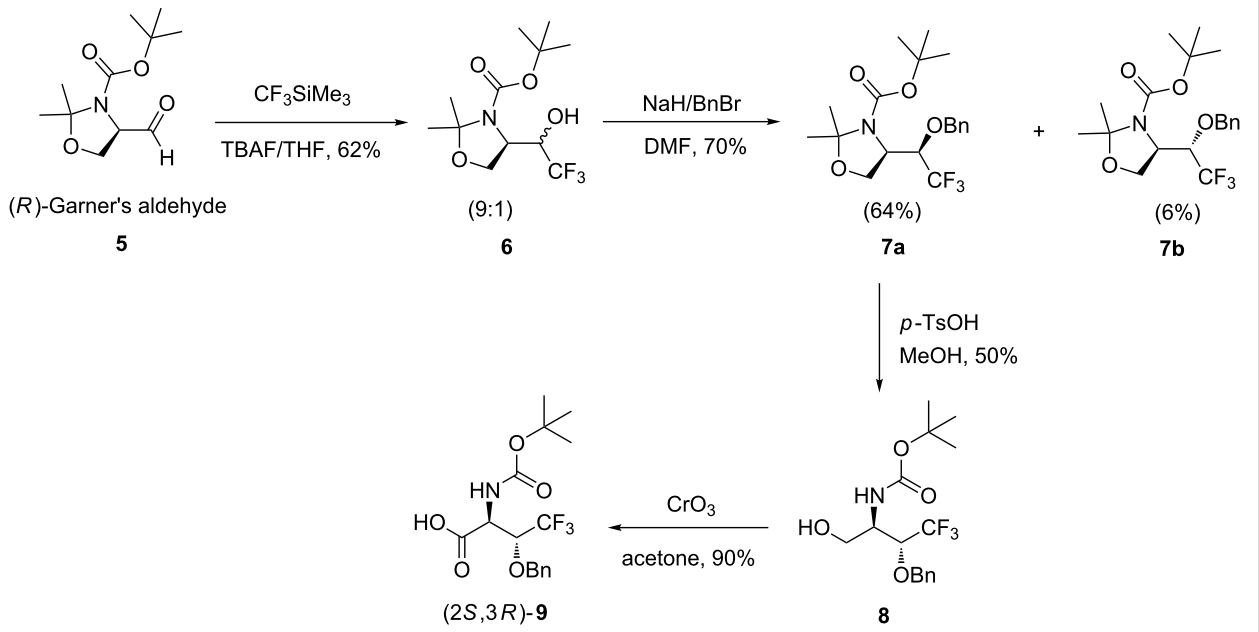

Scheme 1: Synthesis of (2*S*,3*R*)-Boc-CF_3-Thr(Bzl) **9**.

in 71% yield as red crystals. The nucleophilic glycine equivalent **12** went through the aldol reaction with trifluoroacetaldehyde to give complex **13** in moderate yield (66%). Further hydrolysis of complex **13** led to the recovery of the chiral auxiliary **11** and release of free (2*S*,3*S*)-CF_3-threonine whose diastereoselectivity was determined to be about 96% by ^{19}F NMR. Although in most of the reported cases, the free amino acid was released into the aqueous phase, and then purified by ion-exchange chromatography, we purified the free (2*S*,3*S*)-CF_3-threonine by another way. We first managed to remove the Ni(II) by addition of 2.0 equivalents of NaSCN and 4.0 equivalents of pyridine to form the complex $Ni(Py)_4(SCN)_2$, which precipitated from the aqueous phase. After filtration, we protected the free amino acid using Boc_2O under basic conditions. The Boc-(2*S*,3*S*)-CF_3-threonine **14** was then purified by silica column chromatography and was obtained in 43% yield after three steps from **13** (Scheme 2).

Classical peptide synthesis in solution was used to prepare pentapeptides **1a**–**4a** (Scheme 3). Boc-L-Val-OH was activated by isobutylchloroformate (IBCF) and then coupled with L-Leu-OMe to afford dipeptide **15**. Acidic hydrolysis of **15** using TFA, and coupling with the third amino acid (Boc-L-Ser(Bzl)-OH, Boc-L-Thr(Bzl)-OH, (2*S*,3*R*)-Boc-CF_3-Thr, (2*S*,3*S*)-Boc-CF_3-Thr), using HBTU/HOBt in the presence of DIPEA in DMF, afforded tripeptides **16a**–**d** in good yields (48–83%). The tripeptides **16a**–**d** were deprotected using TFA, and the salt of the free amine was coupled to Boc-L-Val-OH using HBTU/HOBt/DIPEA or DMTMM(Cl^-)/NMM to afford tetrapeptides **17a**–**c** and **17d** respectively, in satisfactory yields (61–87%). The pentapeptides **18a**–**c** and **4a** were obtained by deprotecting tetrapeptides **17a**–**d** with TFA and then performing the coupling reaction with Boc-L-Ala-OH in the presence of HBTU/HOBt/DIPEA or DMTMM(Cl^-)/NMM. Catalytic hydrogenation, using 10% Pd/C or $Pd(OH)_2$, under H_2 atmosphere, gave pentapeptides **1a**–**3a** in moderate to quantitative yield. After acidic removal of the Boc group, the pentapeptide salts **1b**–**4b** were obtained in quantitative yield.

Conformational studies. The conformational properties of the eight pentapeptides (**1a**–**4a** and **1b**–**4b**) were examined by NMR analyses in a protic solvent, which is more challenging than in aprotic organic solvents for maintaining intramolecular hydrogen bond network. Methanol was used because of the limited solubility of these compounds in aqueous solutions. The ^1H and ^{13}C chemical shifts of these pentapeptides were assigned using 1D ^1H, 2D ^1H,^1H-TOCSY, 2D ^1H,^1H-ROESY, 2D ^1H,^{13}C-HSQC, and 2D ^1H,^{13}C-HMBC spectra. The ^1H and ^{13}C chemical shift assignments of the 8 pentapeptides at 298 K are given in Tables S1–S8 (Supporting Information File 1). A single set of chemical shifts was observed for all deprotected pentapeptides **1b**–**4b**, whereas for the Boc-protected pentapeptides **1a**–**4a**, two chemical shift sets could be detected. This chemical shift heterogeneity involved in particular the *t*-Bu protons of the Boc group and the amide proton of the residue Ala[1]. The chemical shift set of weaker intensity was assigned more easily by cooling down to 271 K because of significant broadening near room temperature. Exchange peaks were ob-

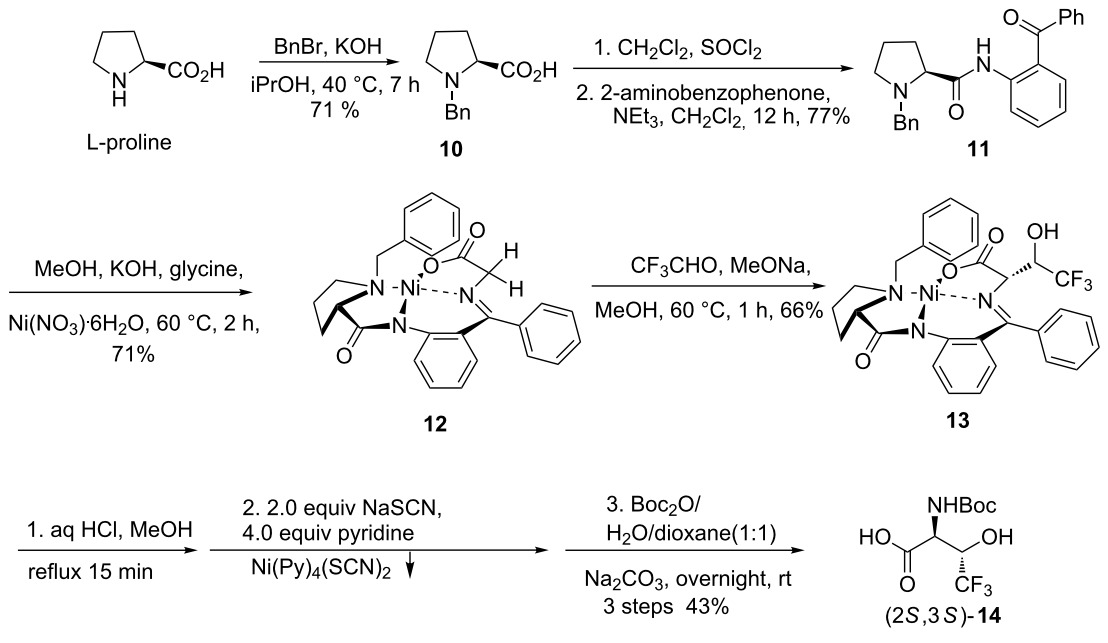

Scheme 2: Synthesis of (2*S*,3*S*)-Boc-CF_3-Thr **14**.

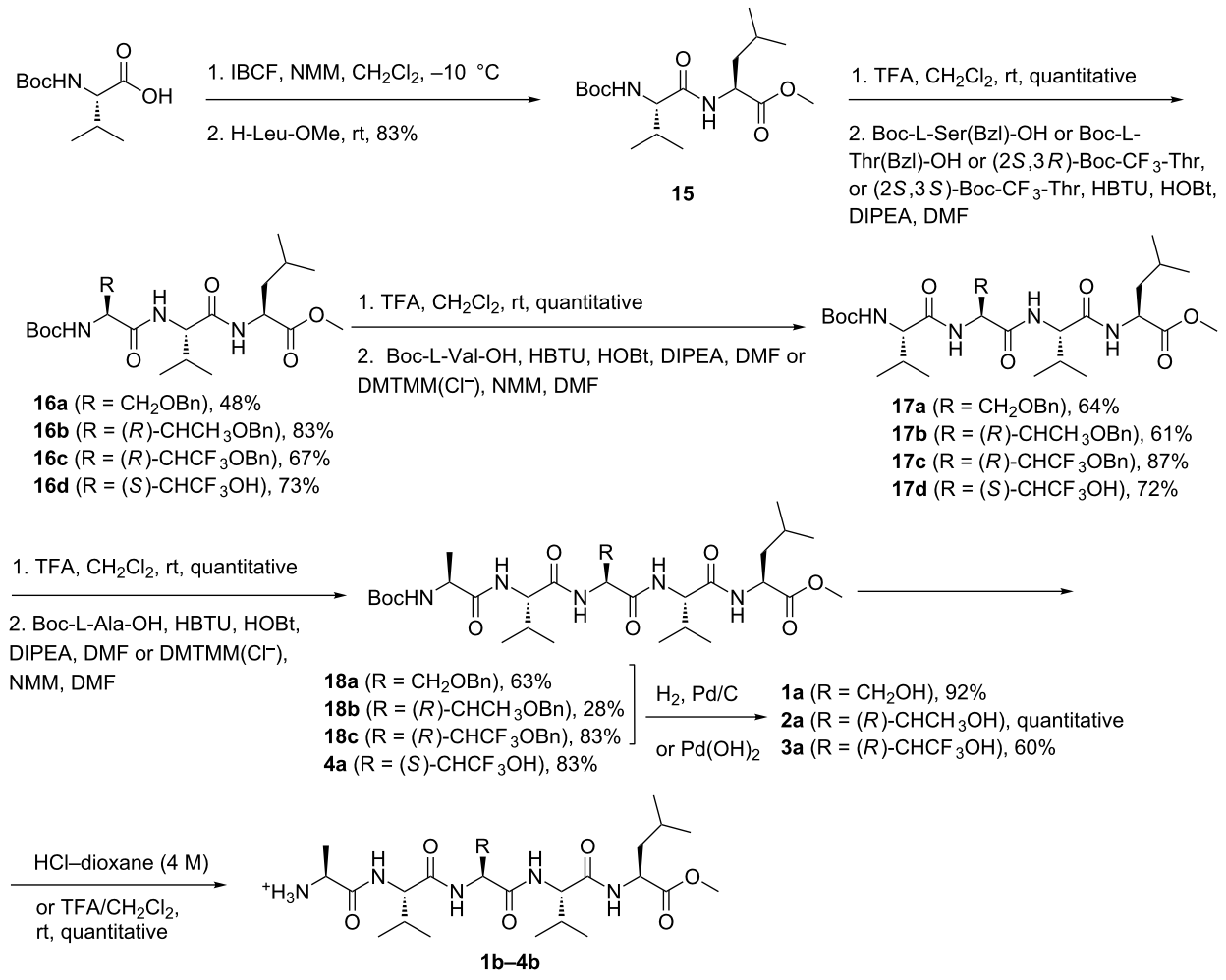

Scheme 3: Synthesis of pentapeptides **1a**–**4a** and **1b**–**4b**.

served on ROESY spectra at 271 K (300 ms mixing time), proving that the two forms interconvert in a slow exchange regime on the ^{1}H NMR time scale. This equilibrium was ascribed to the existence of the *syn*- and *anti*-rotamers of the carbamate group. The more stable forms (about 85% population at 271 K) were assigned to *anti*-rotamers based on literature results [25].

Different NMR parameters were examined to analyze backbone conformational propensities, namely $^1H_\alpha$ and $^{13}C_\alpha$ chemical shift deviations (CSD), vicinal $^3J_{HN\text{-}H\alpha}$ coupling constants, H^α-HN ROE correlations and temperature coefficient ($\Delta\delta_{HN}/\Delta T$) of the amide protons. The $^1H^\alpha$ and $^{13}C^\alpha$ chemical shift deviations (CSD) from random coil values provide information on backbone conformational space for each amino acid [26-31]. The terminal Ala^1 and Leu^5 residues were excluded from this CSD analysis because of the absence of a neighboring residue, as well as fluorinated Thr residues because of the absence of known random coil values. The analysis of $^1H_\alpha$ and $^{13}C_\alpha$ CSDs for residues Val^2 and Val^4 in all of the eight pentapeptides (Table 1 and Table 2) supports the predominance of extended conformations, as shown by downfield shifted Hα protons (positive CSD values between 0.09 and 0.22 ppm, Table 1) and upfield shifted Cα carbons (negative CSD values in the range of −2.5 to −1.6 ppm, Table 2).

The high propensity for exploring extended backbone conformations was further confirmed for these pentapeptides by the analysis of Hα–HN ROE correlations, showing that sequential $H\alpha_i$–HN_{i+1} ROEs have much higher intensities than intra-residual $H\alpha_i$–HN_i ROEs. Few sequential HN–HN ROEs with weak intensities could be observed, indicating that turn or helical conformers are sparsely populated.

Because of its Karplus dependence upon main chain φ dihedral angle, the vicinal $^3J_{HN\text{-}H\alpha}$ coupling constant is also a valuable descriptor of peptide backbone conformations [32]. The coupling constants in all pentapeptides (Table 3) exhibit large

Table 1: ^{1}Hα chemical shift deviations (CSD) of residues in pentapeptides **1a**–**4a** and **1b**–**4b** in CD_3OH (298 K).

Peptide	Boc-protected (**1a**–**4a**)					Non-protected (**1b**–**4b**)				
	Ala^1	Val^2	**X^3**	Val^4	Leu^5	Ala^1	Val^2	**X^3**	Val^4	Leu^5
R-Ala-Val-Ser-Val-Leu-OMe (**1**)	−0.23	0.09	**0.01**	0.15	0.09	−0.35	0.14	**0.04**	0.15	0.08
R-Ala-Val-Thr-Val-Leu-OMe (**2**)	−0.20	0.13	**0.04**	0.13	0.11	−0.41	0.14	**0.05**	0.12	0.07
R-Ala-Val-(2*S*,3*R*)-CF_3-Thr-Val-Leu-OMe (**3**)	−0.22	0.09	**–**	0.17	0.07	−0.33	0.14	**–**	0.18	0.07
R-Ala-Val-(2*S*,3*S*)-CF_3-Thr-Val-Leu-OMe (**4**)	−0.19	0.13	**–**	0.15	0.09	−0.35	0.22	**–**	0.17	0.08

Table 2: ^{13}Cα chemical shift deviations (CSD) of residues in pentapeptides **1a**–**4a** and **1b**–**4b** in CD_3OH (298 K).

Peptide	Boc-Protected (**1a**–**4a**)					Non-Protected (**1b**–**4b**)				
	Ala^1	Val^2	**X^3**	Val^4	Leu^5	Ala^1	Val^2	**X^3**	Val^4	Leu^5
R-Ala-Val-Ser-Val-Leu-OMe (**1**)	−0.6	-2.0	**−1.6**	−2.1	−2.8	−2.1	−1.7	**−1.8**	−2.2	−2.8
R-Ala-Val-Thr-Val-Leu-OMe (**2**)	−0.9	−2.0	**−1.8**	−2.2	−2.9	−2.1	−1.6	**−1.9**	−2.3	−2.9
R-Ala-Val-(2*S*,3*R*)-CF_3-Thr-Val-Leu-OMe (**3**)	−0.8	−2.5	**–**	−2.4	−2.7	−2.2	−2.0	**–**	−2.4	−2.7
R-Ala-Val-(2*S*,3*S*)-CF_3-Thr-Val-Leu-OMe (**4**)	−0.8	−1.6	**–**	−1.9	−2.9	−2.1	−2.0	**–**	−2.4	−2.8

Table 3: Coupling constants $^{3}J_{HN-H\alpha}$ (Hz) of residues in pentapeptides **1a**–**4a** and **1b**–**4b** in CD_3OH (271 K for most residues, * indicates values measured at 298 K).

Peptide	Boc-protected (**1a**–**4a**)					Non-protected (**1b**–**4b**)				
	Ala^1	Val^2	**X^3**	Val^4	Leu^5	Ala^1	Val^2	**X^3**	Val^4	Leu^5
R-Ala-Val-Ser-Val-Leu-OMe (**1**)	6.8	8.2	**7.5**	8.9	7.8	–	8.3	**7.6***	8.6*	7.6*
R-Ala-Val-Thr-Val-Leu-OMe (**2**)	6.9*	8.3*	**8.4***	8.8*	7.8*	–	broad peak	**8.4**	8.7	7.7
R-Ala-Val-(2*S*,3*R*)-CF_3-Thr-Val-Leu-OMe (**3**)	7.1	8.9	**9.1**	9.2	7.6	–	8.7	**9.0**	8.2	7.4
R-Ala-Val-(2*S*,3*S*)-CF_3-Thr-Val-Leu-OMe (**4**)	6.8	7.7	**8.6**	9.0	7.7	–	8.9	**9.0**	8.9	7.6

values (6.8–9.2 Hz range), that are systematically higher than average values found in the coil library (6.1, 7.0, and 7.5 Hz for Ala, Leu and Val, respectively) [33]. This clearly reflects a preference of all backbone dihedral angles φ for values within the range of −160° to −110°, as expected for extended conformations. The three central residues presented higher $^{3}J_{HN-H\alpha}$ coupling constants than terminal Ala^1 and Leu^5 residues, thus demonstrating stronger extended conformational propensities. Interestingly, the conformation of the central residue gets more extended upon substitution of Ser ($^{3}J_{HN-H\alpha}$ of 7.5 Hz) by the β-branched Thr residue ($^{3}J_{HN-H\alpha}$ 8.4 Hz) and trifluoromethylation of Thr further stabilizes extended conformations ($^{3}J_{HN-H\alpha}$ between 8.6 and 9.1 Hz).

We next examined the values of vicinal $^{3}J_{H\alpha-H\beta}$ coupling constants which yield information on side-chain χ1 dihedral angle space (Table 4) [34]. Most residues exhibit average values that indicate conformational equilibria between different side-chain rotamers. Notably, the (2*S*,3*S*)-CF_3-Thr residue in peptides **4a** and **4b** has a small coupling constant, indicating a *gauche* relationship between Hα and Hβ protons. The analysis of intraresidual and sequential Hβ-HN ROEs led to the identification of the χ1 *gauche*+ (+60°) conformation as the major side-chain rotamer. As the local conformational space appears to be more restricted for both backbone and side chain of (2*S*,3*S*)-CF_3-Thr residue, we further characterized its conformation by recording ^{1}H,^{19}F heteronuclear NOEs in 1D ^{1}H{^{19}F} and 2D

Table 4: $^3J_{H\alpha-H\beta}$ coupling constants (Hz) for peptides **1a**–**4a** and **1b**–**4b** in CD_3OH. Coupling constants were extracted from 1D ^1H spectra on multiplets of Hβ protons for Ala or Hα protons for other residues.

Peptide	Boc-protected (**1a**–**4a**)					Non-protected (**1b**–**4b**)				
	Ala[1]	Val[2]	**X**[3]	Val[4]	Leu[5]	Ala[1]	Val[2]	**X**[3]	Val[4]	Leu[5]
R-Ala-Val-Ser-Val-Leu-OMe (**1**)	7.1	6.7	**6/6**	6.6	5.1/10.6	7.2	6.6	**7.5/7.5**	6.6	5.3/10.3
R-Ala-Val-Thr-Val-Leu-OMe (**2**)	7.2	7.3	**4.9**	6.9	5.0/10.6	7.2	7.1	**4.6**	7.1	5.6/10.0
R-Ala-Val-(2*S*,3*R*)-CF_3-Thr-Val-Leu-OMe (**3**)	7.3	7.1	**6.4**	6.5	6/10	7.3	7.3	**6.7**	7.0	5.3/10.3
R-Ala-Val-(2*S*,3*S*)-CF_3-Thr-Val-Leu-OMe (**4**)	7.0	7.0	**2.5**	7.1	5.0/10.5	7.2	8.2	**2.0**	7.5	5.4/10.5

^1H,^{19}F-HOESY experiments (Figures S19 and S20, Supporting Information File 1). Heteronuclear NOEs involving the CF_3 group confirmed the previous assignment of χ1 rotamer and revealed an i/i+2 interaction with the Ala[1] methyl group, as expected in peptides exploring major β-strand like conformations (Figure S21, Supporting Information File 1).

The chemical shift of amide protons generally displays a temperature dependence [35,36] which can be used to get information on the presence and the stability of hydrogen bonds [37]. In aqueous and alcoholic solvents, small negative temperature coefficients ($\Delta\delta_{HN}/\Delta T > -4.5$ ppb K^{-1}) usually characterize amide protons that are engaged in intramolecular hydrogen bonds, while more negative values ($\Delta\delta_{HN}/\Delta T < -6$ ppb K^{-1}) rather indicate that they are exposed to solvent. The analysis of the temperature coefficient of the amide bond NH protons ($\Delta\delta_{HN}/\Delta T$) reveals negative values in the range of −9.0 ppb/K to −5.0 ppb/K for most protons, which indicates that they are not engaged in stable intra- (or inter-)molecular hydrogen bonds with carbonyl groups (Table 5). Interestingly, residue Val[4] displays the smallest temperature coefficient (around –4.5 ppb K^{-1}) in pentapeptides **4a** and **4b** while residue Val[2] shows intermediate values of −5.5 and −5.9 ppb K^{-1}. This i/i+2 periodicity may reflect transient intermolecular β-strand contacts involving hydrogen bonding through Val[2] and Val[4] residues (Figure S16, Supporting Information File 1). However, no long-range HN/HN or Hα/Hα ROEs could be detected in the 8 pentapeptides, indicating that transient intermolecular association, if any, is too fast to be detected by ROE magnetization transfer.

In summary, the NMR analysis shows that the pentapeptides with the sequence RNH-Ala-Val-**X**-Val-Leu-OMe (X = Ser, Thr, (2*S*,3*R*)-CF_3-Thr and (2*S*,3*S*)-CF_3-Thr) explore predominantly extended backbone conformations in CD_3OH. No major difference could be observed between the Boc protected pentapeptides **1a**–**4a** and their respective deprotected amine analogues **1b**–**4b**. This β-propensity can be ascribed to the presence of two Val residues, as β-branched residues are known to explore more extended conformations [38]. Such an effect is also observed for the central residue upon replacement of Ser by the β-branched Thr residue and the incorporation of a trifluoromethyl group in Thr or *allo*-Thr further increases the β-propensity of these residues. The presence of self-association involving intermolecular β-sheet formation was not detectable. Nevertheless, the unique i/i+2 periodicity of amide proton temperature coefficients in peptides **4a**–**4b** incorporating the (2*S*,3*S*)-CF_3-threonine residue might be explained by transient intermolecular β-strand contacts.

In order to gain a more detailed insight into the structural behavior of the pentapeptides according to their central fluori-

Table 5: Temperature coefficients $\Delta\delta/\Delta T$ (ppb K^{-1}) for HN protons in pentapeptides **1a**–**4a** and **1b**–**4b** in CD_3OH (298 K).

Peptide	Boc-protected (**1a**–**4a**)					Non-protected (**1b**–**4b**)				
	Ala[1]	Val[2]	**X**[3]	Val[4]	Leu[5]	Ala[1]	Val[2]	**X**[3]	Val[4]	Leu[5]
R-Ala-Val-Ser-Val-Leu-OMe (**1**)	−7.8	−6.4	**−7.7**	−8.0	−7.4	–	−6.1	**−7.8**	−7.8	−7.0
R-Ala-Val-Thr-Val-Leu-OMe (**2**)	−7.4	−5.8	**−7.5**	−7.6	−7.9	–	−5.5	**−8.1**	−8.0	−7.7
R-Ala-Val-(2*S*,3*R*)-CF_3-Thr-Val-Leu-OMe (**3**)	−6.5	−5.3	**−7.4**	−7.4	−5.0	–	−6.6	**−8.5**	−9.0	−6.0
R-Ala-Val-(2*S*,3*S*)-CF_3-Thr-Val-Leu-OMe (**4**)	−7.4	−5.9	**−8.9**	−4.5	−9.0	–	−5.5	**−8.3**	−4.6	−7.9

nated or non-fluorinated residue, all-atom molecular dynamics (MD) simulations were performed using the GROMACS 4.5 package, with the OPLS-AA force field in combination with the SPC/E water model (for a complete description of the method, see Supporting Information File 1).

The conformational ensembles generated for each of the eight pentapeptides in water, were first characterized by the average coupling constants $^3J_{HN\text{-}H\alpha}$ of their five residues and then compared to available NMR measurements at 298 K (Figure S23, Supporting Information File 1). Water solvent was chosen in order to better anticipate the peptide conformations in a solvent closer to physiological conditions. Nevertheless, we verified for compounds **2b** and **4b** that the simulations conducted in MeOH and in water were very similar (Figure S23, Supporting Information File 1). Overall, the theoretical $^3J_{HN\text{-}H\alpha}$ coupling values are in fair agreement with the experimental ones, indicating that the peptide conformational ensembles were sampled quite faithfully by the MD trajectories. Excepting the first residue Ala[1], all the theoretical coupling constants have high values above 7 Hz, confirming that the pentapeptides have locally extended backbone conformations. It could be noted that the $^3J_{HN\text{-}H\alpha}$ experimental value of the central residue in compounds **3a**, **3b**, and **4b** are significantly higher than in the simulations. This discrepancy between the NMR and MD $^3J_{HN\text{-}H\alpha}$ coupling values for the fluorinated central residues indicates that their conformations are less frequently extended in the simulations than in experiments. However, the $^3J_{HN\text{-}H\alpha}$ coupling constants alone cannot unambiguously discriminate between α- or β-structures for each residues and, above all, cannot determine the peptide global structure. In that context, MD simulations can provide useful complementary structural information.

In particular, MD trajectories revealed significant differences between the conformations of the fluorinated and non-fluorinated peptides. Indeed, when their end-to-end distances are analyzed (Figure 2), it can be noted that both the Boc-protected and non-protected peptides **4a** and **4b** have significantly larger populations of extended conformations than the other three sequences whose distributions are broader and shifted toward lower values.

This global structural characteristic is reflected at a local level when the distributions of the backbone ψ dihedral angle values are examined (Figure 3). In contrast with other peptides, all the three central ψ dihedral angles of peptides **4a** and **4b** clearly have a higher propensity to populate the β basin (90° to 180°) than the α region (−70° to +40°), endowing it with the aforementioned extended conformations. More specifically, the probability of each residue to be in α- or β-conformation can be quantified by calculating the area under the peaks of the ψ distribution functions centered around −30° or +140°, respectively. The probability of the three central residues to be in β-conformation is reported in Table 6 for all studied peptides. It can be seen that, except the (2S,3*R*)-CF_3-Thr residue in the Boc-protected peptide **3a**, all central residues predominantly adopt local β-conformations, with probabilities ranging from 50 to 92%, in agreement with the NMR CSDs and $^3J_{HN\text{-}H\alpha}$ coupling constant values. The probability of each peptide to have all its three central residues in β-conformation (which is equal to the product of the three central residue probabilities) is a good indication of its propensity to adopt a global extended structure. According to this criterion, almost 50% of the **4a** and **4b** conformations are globally extended, whereas less than 30% of the other sequence conformations are in that case (Table 6).

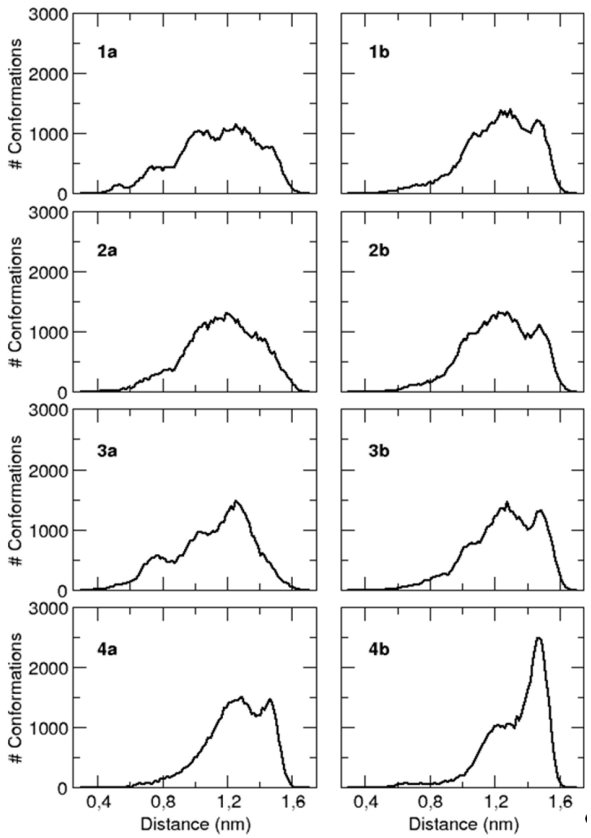

Figure 2: Probability distribution of the peptide conformations as a function of end-to-end distance (defined as the distance between the nitrogen of residue Ala[1] and the carbon of the *C*-terminal carbonyl).

The most prevalent conformations of each peptide were determined by clustering their conformational ensembles, using the "gromos" method implemented in GROMACS with a RMSD threshold of 0.2 nm. Visual inspections of the representative structure of the most populated clusters (Figures S24 and S25,

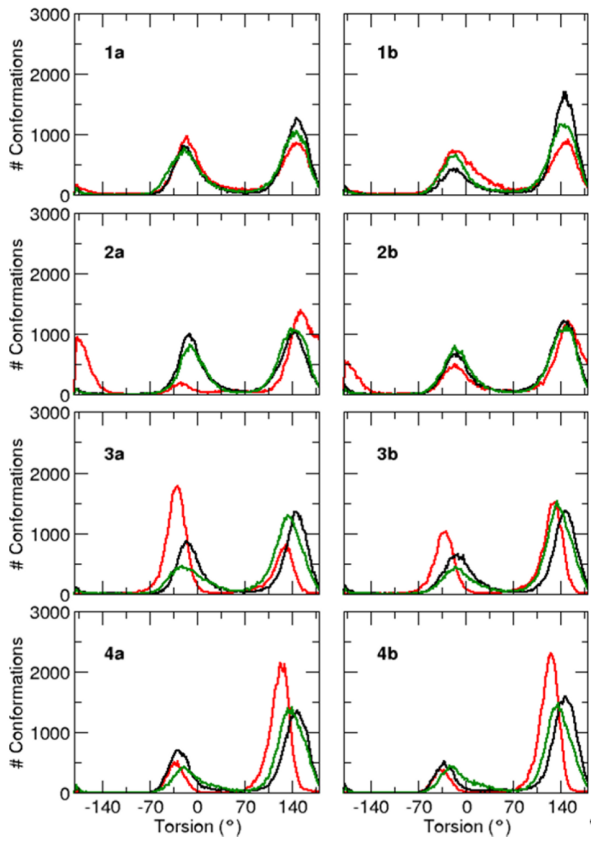

Figure 3: Probability distribution of the peptide dihedral angles ψ for the three central residues Val^2 (black), X^3 (red) and Val^4 (green).

Supporting Information File 1SI) confirm that the peptides **4a** and **4b** visit extended β-strand-like structures more frequently than the other three which have higher propensities to form compact α-helix-like conformations.

All together, the theoretical study shows that the replacement of the methyl group of the threonine side chain in the RNH-Ala-Val-Thr-Val-Leu-OMe pentapeptide by a trifluoromethyl induces an increase of the population of global extended conformations.

Inhibition of $A\beta_{1-42}$ fibrillization. In the frame of our interest in modulators of protein–protein interactions involving β–sheet structures, in particular in the field of $A\beta_{1-42}$ peptide aggregation involved in Alzheimer's disease [15,39-42], we evaluated the activity of the pentapeptides on this process. The objective of this preliminary study was to analyze the influence of the trifluoromethyl group and of the propensity of the pentapeptides to adopt an extended structure, on their ability to modulate $A\beta_{1-42}$ peptide aggregation. For that purpose, the classical fibrillization assay was performed using thioflavin-T (ThT) fluorescence spectroscopy [14,15,39-42]. The fluorescence curve of the control peptide ($A\beta_{1-42}$ 10 μM, purple curve, Figure S26, Supporting Information File 1) displayed a typical sigmoid pattern with a lag phase corresponding to the nucleation process, an elongation phase and a final plateau linked to the morphology and the amount of fibrils formed at the end of the aggregation process. Compounds **1a**–**4a** and **1b**–**4b** were tested at compound/$A\beta_{1-42}$ ratios of 10:1 and 1:1. None of the Boc-*N*-protected pentapeptides **1a**–**4a** displayed inhibitory activity even at a 10:1 compound/$A\beta_{1-42}$ ratio (data not shown) while some *N*-deprotected compounds displayed inhibitory activity at this ratio, by decreasing the fluorescence plateau at 40 hours (see Supporting Information File 1, Table S9). This result is in accordance with our previous demonstration that a free amine is crucial to establish ionic interactions with acidic residues of $A\beta_{1-42}$ [15,39-41]. No activity was observed at a 1:1 ratio for the fluorinated compounds **3b** and **4b**, while an increase of the fluorescence plateau was observed in the presence of the Ser and Thr containing compounds **1b** and **2b**. At a 10:1 compound/$A\beta_{1-42}$ ratio the less extended Ser containing pentapeptide **1b** was found to be inactive (Figure 4 and Table S9, Supporting Information File 1). The Thr containing pentapeptide **2b** reduced the fluorescence plateau intensity by 22%, suggesting a slight reduction of the amount of fibrils formed after 40 hours (Figure 4 and Table S9, Supporting Information File 1). The reduction of the fluorescence intensity after 40 hours was much more pronounced for the two CF_3-Thr derivatives **3b** and **4b**, reaching 60% (Figure 4 and Table S9, Supporting Information File 1), indicating that the presence of fluorine atoms probably increased the interaction of pentapep-

Table 6: Probability (%) of the three central residues of the eight studied peptides to be in β-conformation. The column P indicates the probability for each peptide to have all its three central residues in β-conformation.

peptide	Boc-protected (**1a**–**4a**)				Non-protected (**1b**–**4b**)			
	Val^2	X^3	Val^4	P	Val^2	X^3	Val^4	P
RNH-Ala-Val-Ser-Val-Leu-OMe (**1**)	59.9	51.4	55.8	**17.2**	76.5	50.3	64.9	**25.0**
RNH-Ala-Val-Thr-Val-Leu-OMe (**2**)	53.5	91.1	61.0	**29.7**	64.8	73.5	59.1	**28.2**
RNH-Ala-Val-(3*R*)-CF_3-Thr-Val-Leu-OMe (**3**)	59.7	31.7	69.9	**13.2**	63.3	59.4	74.7	**28.1**
RNH-Ala-Val-(3*S*)-CF_3-Thr-Val-Leu-OMe (**4**)	67.1	82.7	75.6	**42.0**	77.9	85.6	74.8	**49.9**

tides with $A\beta_{1-42}$ and their inhibitory effect on $A\beta_{1-42}$ aggregation.

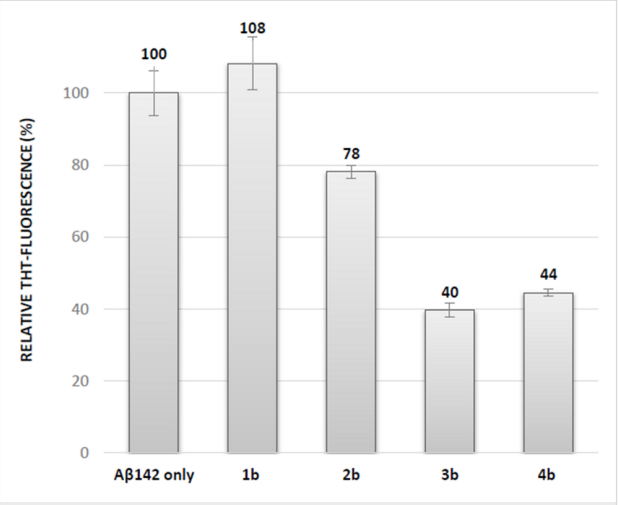

Figure 4: Effects of compounds **1–4** on $A\beta_{1-42}$ fibrillization assessed by ThT-fluorescence spectroscopy at 10:1 compound/Aβ ratios (the concentration of $A\beta_{1-42}$ is 10 μM) and compared to the values obtained for $A\beta_{1-42}$ alone. (See Supporting Information File 1 for the calculation of the change of fluorescence intensity at the plateau).

Conclusion

We synthesized eight pentapeptides **1a**–**4a** and **1b**–**4b** having the sequence RHN-Ala-Val-**X**-Val-Leu-OMe, where the central residue **X** is L-serine, L-threonine, (2*S*,3*R*)-L-CF_3-threonine and (2*S*,3*S*)-L-CF_3-threonine, respectively. The fluorinated amino acid (2*S*,3*R*)-Boc-CF_3-Thr(Bzl) was prepared through a nucleophilic trifluoromethylation of Ruppert's reagent on the (*R*) Garner's aldehyde, while (2*S*, 3*S*)-Boc-CF_3-Thr (mimic of the natural threonine) was obtained through the aldol reaction of trifluoroacetaldehyde with the Ni(II) complex of the chiral Schiff base of glycine.

The conformational analysis of these pentapeptides was conducted by the combined use of NMR spectroscopy and molecular dynamics simulations. NMR conformational studies showed that the eight pentapeptides (**1a**–**4a** and **1b**–**4b**) adopt mainly extended backbone conformations in a polar solvent (CD_3OH). The MD simulated conformations were in fair agreement with the NMR results. Overall we conclude that the CF_3-Thr-containing pentapeptides were experimentally found more extended than the L-Ser-, L-Thr derivatives, with the (2*S*,3*S*)-CF_3-Thr-residue more prone to induce extended conformations than the (2*S*,3*R*)-CF_3-Thr, as suggested by MD simulations. The temperature coefficients observed in both Boc-protected and deprotected (2*S*,3*S*)-CF_3-Thr pentapeptides (**4a** and **4b**) suggest that these pentapeptides could transiently form intermolecular β-strand contacts. This higher propensity of **4a** and **4b** to adopt extended structures can be explained by a strong hydrophobic interaction of the trifluoromethyl group with the Ala^1 methyl group side chain, as observed in $^1H,^{19}F$ heteronuclear NOEs in 1D $^1H\{^{19}F\}$ and 2D $^1H,^{19}F$ HOESY experiments. Thus, both conformational studies demonstrated the trifluoromethyl effect on peptide conformations that promotes an extended conformation in order to mimic a β-strand structure. Interestingly in the MD results, we found that the deprotected pentapeptides **1b**, **3b** and **4b** showed increased propensities to adopt extended conformations compared to the Boc-protected counterparts **1a, 3a** and **4a** (a similar propensity to be in β-conformation was observed for **2a** and **2b**).

The structural information obtained in this study provides valuable insights to explore novel β-strand mimics containing trifluoromethylated analogues of threonine as inhibitors of protein–protein interactions involving β-sheet structures. As a proof of concept, we demonstrated that the incorporation of the CF_3-Thr residues in hydrophobic pentapeptides allowed their interaction with the amyloid protein $A\beta_{1-42}$, in order to reduce its aggregation process. The inhibitory effect seems more pronounced by combining both the use of extended pentapeptides and the introduction of fluorine atoms. This positive effect of the trifluoromethylation can be due to the increased polarity of the hydroxy group in the CF_3-Thr residue, acting as a β-sheet breaker element and thus preventing the interactions between Aβ species [15].

The introduction of such fluorinated peptides in larger structures, such as glycopeptide or β-hairpin compounds can be envisaged. Indeed we have previously demonstrated that small peptides/peptidomimetics that displayed inhibitory activity at high ratios show greater aggregation inhibitory activity at 1:1 ratio or even less, when they are incorporated in such designed structures [15,39-41].

Supporting Information

Supporting Information File 1

Description of synthetic procedures and characterization of compounds. Additional NMR data, computational methods and additional figures and tables. Experimental procedure for fluorescence-detected ThT binding assay and representative curves of ThT fluorescence assays.
[http://www.beilstein-journals.org/bjoc/content/supplementary/1860-5397-13-276-S1.pdf]

Acknowledgements

Central Glass Co. Ltd. is gratefully acknowledged for kindly providing fluoral. The China Scholarship Council is thanked for financial support for Yaochun Xu. The Laboratory BioCIS is a

member of the Laboratory of Excellence LERMIT supported by a Grant from ANR (ANR-10-LABX-33).

ORCID® iDs

Benoît Crousse - https://orcid.org/0000-0002-2042-9942
Olivier Lequin - https://orcid.org/0000-0001-5307-3068
Sandrine Ongeri - https://orcid.org/0000-0002-2118-7324

References

1. Zhou, Y.; Wang, J.; Gu, Z.; Wang, S.; Zhu, W.; Aceña, J. L.; Soloshonok, V. A.; Izawa, K.; Liu, H. *Chem. Rev.* **2016,** *116,* 422–518. doi:10.1021/acs.chemrev.5b00392
2. Uhlig, T.; Kyprianou, T.; Martinelli, F. G.; Oppici, C. A.; Heiligers, D.; Hills, D.; Calvo, X. R.; Verhaert, P. *EuPa Open Proteomics* **2014,** *4,* 58–69. doi:10.1016/j.euprot.2014.05.003
3. Buer, B. C.; Marsh, E. N. G. *Protein Sci.* **2012,** *21,* 453–462. doi:10.1002/pro.2030
4. Marsh, E. N. G. *Acc. Chem. Res.* **2014,** *47,* 2878–2886. doi:10.1021/ar500125m
5. Meng, H.; Kumar, K. *J. Am. Chem. Soc.* **2007,** *129,* 15615–15622. doi:10.1021/ja075373f
6. Zanda, M. *New J. Chem.* **2004,** *28,* 1401–1411. doi:10.1039/b405955g
7. Kitamoto, T.; Marubayashi, S.; Yamazaki, T. *Tetrahedron* **2008,** *64,* 1888–1894. doi:10.1016/j.tet.2007.11.085
8. Vulpetti, A.; Dalvit, C. *Drug Discovery Today* **2012,** *17,* 890–897. doi:10.1016/j.drudis.2012.03.014
9. Salwiczek, M.; Nyakatura, E. K.; Gerling, U. I.; Ye, S.; Koksch, B. *Chem. Soc. Rev.* **2012,** *41,* 2135–2171. doi:10.1039/C1CS15241F
10. Kitamoto, T.; Marubayashi, S.; Yamazaki, T. *Chem. Lett.* **2006,** *35,* 1264–1265. doi:10.1246/cl.2006.1264
11. Pelay-Gimeno, M.; Glas, A.; Koch, O.; Grossmann, T. N. *Angew. Chem., Int. Ed.* **2015,** *54,* 8896–8927. doi:10.1002/anie.201412070
12. Watkins, A. M.; Arora, P. S. *ACS Chem. Biol.* **2014,** *9,* 1747–1754. doi:10.1021/cb500241y
13. Milroy, L.-G.; Grossmann, T. N.; Hennig, S.; Brunsveld, L.; Ottmann, C. *Chem. Rev.* **2014,** *114,* 4695–4748. doi:10.1021/cr400698c
14. Cheng, P.-N.; Liu, C.; Zhao, M.; Eisenberg, D.; Nowick, J. S. *Nat. Chem.* **2012,** *4,* 927–933. doi:10.1038/nchem.1433
15. Kaffy, J.; Brinet, D.; Soulier, J.-L.; Correia, I.; Tonali, N.; Fera, K. F.; Iacone, Y.; Hoffmann, A. R. F.; Khemtémourian, L.; Crousse, B.; Taylor, M.; Allsop, D.; Taverna, M.; Lequin, O.; Ongeri, S. *J. Med. Chem.* **2016,** *59,* 2025–2040. doi:10.1021/acs.jmedchem.5b01629
16. Jiang, Z.-X.; Qin, Y.-Y.; Qing, F.-L. *J. Org. Chem.* **2003,** *68,* 7544–7547. doi:10.1021/jo0344384
17. Zeng, C.-m.; Kerrigan, S. A.; Katzenellenbogen, J. A.; Slocum, C.; Gallacher, K.; Shomali, M.; Lyttle, C. R.; Hattersley, G.; Miller, C. P. *Tetrahedron Lett.* **2010,** *51,* 5361–5363. doi:10.1016/j.tetlet.2010.07.147
18. Qing, F.-L.; Pen, S.; Hu, C.-M. *J. Fluorine Chem.* **1998,** *88,* 79–81. doi:10.1016/S0022-1139(97)00155-3
19. Soloshonok, V. A.; Kukhar, V. P.; Galushko, S. V.; Svistunova, N. Yu.; Avilov, D. V.; Kuz'mina, N. A.; Raevski, N. I.; Struchkov, Y. T.; Pysarevsky, A. P.; Belokon, Y. N. *J. Chem. Soc., Perkin Trans. 1* **1993,** 3143–3155. doi:10.1039/P19930003143
20. Kitazume, T.; Lin, J. T.; Yamazaki, T. *Tetrahedron: Asymmetry* **1991,** *2,* 235–238. doi:10.1016/S0957-4166(00)80041-5
21. Scolastico, C.; Conca, E.; Prati, L.; Guanti, G.; Banfi, L.; Berti, A.; Farina, P.; Valcavi, U. *Synthesis* **1985,** 850–855. doi:10.1055/s-1985-31363
22. Sting, A. R.; Seebach, D. *Tetrahedron* **1996,** *52,* 279–290. doi:10.1016/0040-4020(95)00895-F
23. Belokon, Y. N.; Tararov, V. I.; Maleev, V. I.; Savel'eva, T. F.; Ryzhov, M. G. *Tetrahedron: Asymmetry* **1998,** *9,* 4249–4252. doi:10.1016/S0957-4166(98)00449-2
24. Soloshonok, V. A.; Avilov, D. V.; Kukhar, V. P.; Tararov, V. I.; Savel'eva, T. F.; Churkina, T. D.; Ikonnikov, N. S.; Kochetkov, K. A.; Orlova, S. A.; Pysarevsky, A. P.; Struchkov, Y. T.; Raevsky, N. I.; Belokon, Y. N. *Tetrahedron: Asymmetry* **1995,** *6,* 1741–1756. doi:10.1016/0957-4166(95)00220-J
25. Marcovici-Mizrahi, D.; Gottlieb, H. E.; Marks, V.; Nudelman, A. *J. Org. Chem.* **1996,** *61,* 8402–8406. doi:10.1021/jo961446u
26. Szilagyi, L.; Jardetzky, O. *J. Magn. Reson.* **1989,** *83,* 441–449.
27. Spera, S.; Bax, A. *J. Am. Chem. Soc.* **1991,** *113,* 5490–5492. doi:10.1021/ja00014a071
28. Wishart, D. S.; Sykes, B. D. *Methods Enzymol.* **1994,** *239,* 363–392. doi:10.1016/S0076-6879(94)39014-2
29. Wishart, D. S.; Sykes, B. D. *J. Biomol. NMR* **1994,** *4,* 171–180. doi:10.1007/BF00175245
30. Wishart, D. S.; Bigam, G. C.; Holm, A.; Hodges, R. S.; Sykes, B. D. *J. Biomol. NMR* **1995,** *5,* 67–81. doi:10.1007/BF00227471
31. Smith, L. J.; Fiebig, K. M.; Schwalbe, H.; Dobson, C. M. *Folding Des.* **1996,** *1,* R95–R106. doi:10.1016/S1359-0278(96)00046-6
32. Vuister, G. W.; Bax, A. *J. Am. Chem. Soc.* **1993,** *115,* 7772–7777. doi:10.1021/ja00070a024
33. Avbelj, F.; Grdadolnik, S. G.; Grdadolnik, J.; Baldwin, R. L. *Proc. Natl. Acad. Sci. U. S. A.* **2006,** *103,* 1272–1277. doi:10.1073/pnas.0510420103
34. Schmidt, J. M. *J. Biomol. NMR* **2007,** *37,* 287–301. doi:10.1007/s10858-006-9140-8
35. Ohnishi, M.; Urry, D. W. *Biochem. Biophys. Res. Commun.* **1969,** *36,* 194–202. doi:10.1016/0006-291X(69)90314-3
36. Kopple, K. D.; Onishi, M.; Go, A. *J. Am. Chem. Soc.* **1969,** *91,* 4264–4272. doi:10.1021/ja01043a040
37. Cierpicki, T.; Otlewski, J. *J. Biomol. NMR* **2001,** *21,* 249–261. doi:10.1023/A:1012911329730
38. Minor, D. L., Jr.; Kim, P. S. *Nature* **1994,** *367,* 660–663. doi:10.1038/367660a0
39. Pellegrino, S.; Tonali, N.; Erba, E.; Kaffy, J.; Taverna, M.; Contini, A.; Taylor, M.; Allsop, D.; Gelmi, M. L.; Ongeri, S. *Chem. Sci.* **2017,** *8,* 1295–1302. doi:10.1039/C6SC03176E
40. Kaffy, J.; Brinet, D.; Soulier, J.-L.; Khemtémourian, L.; Lequin, O.; Taverna, M.; Crousse, B.; Ongeri, S. *Eur. J. Med. Chem.* **2014,** *86,* 752–758. doi:10.1016/j.ejmech.2014.09.031
41. Vahdati, L.; Kaffy, J.; Brinet, D.; Bernadat, G.; Correia, I.; Panzeri, S.; Fanelli, R.; Lequin, O.; Taverna, M.; Ongeri, S.; Piarulli, U. *Eur. J. Org. Chem.* **2017,** 2971–2980. doi:10.1002/ejoc.201700010
42. LeVine, H., III. *Methods Enzymol.* **1999,** *309,* 274–284. doi:10.1016/S0076-6879(99)09020-5

BEILSTEIN JOURNAL OF ORGANIC CHEMISTRY

Position-dependent impact of hexafluoroleucine and trifluoroisoleucine on protease digestion

Susanne Huhmann, Anne-Katrin Stegemann, Kristin Folmert, Damian Klemczak, Johann Moschner, Michelle Kube and Beate Koksch*

Full Research Paper

Open Access

Address:
Department of Chemistry and Biochemistry, Freie Universität Berlin, Takustraße 3, 14195 Berlin, Germany

Email:
Beate Koksch* - beate.koksch@fu-berlin.de

* Corresponding author

Keywords:
fluorinated amino acids; hexafluoroleucine; peptide drugs; protease stability; trifluoroisoleucine

Beilstein J. Org. Chem. **2017,** *13,* 2869–2882.
doi:10.3762/bjoc.13.279

Received: 29 September 2017
Accepted: 13 December 2017
Published: 22 December 2017

This article is part of the Thematic Series "Organo-fluorine chemistry IV".

Guest Editor: D. O'Hagan

Abstract

Rapid digestion by proteases limits the application of peptides as therapeutics. One strategy to increase the proteolytic stability of peptides is the modification with fluorinated amino acids. This study presents a systematic investigation of the effects of fluorinated leucine and isoleucine derivatives on the proteolytic stability of a peptide that was designed to comprise substrate specificities of different proteases. Therefore, leucine, isoleucine, and their side-chain fluorinated variants were site-specifically incorporated at different positions of this peptide resulting in a library of 13 distinct peptides. The stability of these peptides towards proteolysis by α-chymotrypsin, pepsin, proteinase K, and elastase was studied, and this process was followed by an FL-RP-HPLC assay in combination with mass spectrometry. In a few cases, we observed an exceptional increase in proteolytic stability upon introduction of the fluorine substituents. The opposite phenomenon was observed in other cases, and this may be explained by specific interactions of fluorinated residues with the respective enzyme binding sites. Noteworthy is that 5,5,5-trifluoroisoleucine is able to significantly protect peptides from proteolysis by all enzymes included in this study when positioned N-terminal to the cleavage site. These results provide valuable information for the application of fluorinated amino acids in the design of proteolytically stable peptide-based pharmaceuticals.

Introduction

Peptide-based drugs are promising pharmaceuticals since they offer several advantages including high selectivity, specificity, and efficacy for recognizing and binding to their targets [1-6]. However, their application as drugs is often limited due to low oral bioavailability and a short half-life attributable in part to proteases of the digestive system and blood plasma [1-8]. Effi-

cient approaches to overcome these limitations have been developed including the incorporation of non-natural amino acids, such as D-amino acids, backbone-extended or chemically modified amino acids [1]. In this regard, the incorporation of fluorine into amino acids has become a promising strategy. Fluorine's unique properties, namely low polarizability, a strong inductive effect, and high electronegativity, as well as its small size, result in strong, short C–F bonds and perturb the acidity and basicity of adjacent functional groups. Moreover, these changes may strongly influence hydrogen bonding and electrostatic interactions that are crucial for binding to receptors or, in context of protease stability, enzymes. Thus, when introduced in the form of fluorinated amino acids, this unique element can alter the biophysical, chemical and pharmaceutical properties of proteins and peptides including their interaction with proteases [9,10].

Several laboratories have focused on introducing highly fluorinated analogues of hydrophobic amino acids and have studied the effects on stability of the resulting proteins towards thermal and chemical denaturation [9,11-22]. These studies prompted further investigation into the extent to which fluorinated amino acids stabilize peptides and proteins against proteolytic degradation in particular. Meng and Kumar reported that the incorporation of 5,5,5,5',5',5'-hexafluoroleucine (HfLeu) into the antimicrobial peptides magainin 2 amide and buforin enhanced their resistance towards proteolytic degradation by trypsin [23]. They also introduced HfLeu into the glucagon-like-peptide-1 (GLP-1), which is an attractive lead compound for the treatment of diabetes mellitus type 2. Unfortunately, the clinical use of the wild-type peptide is severely hampered due to rapid digestion (≈2 min) by the serine protease dipeptidyl peptidase [24-26]. Satisfyingly, the fluorinated GLP-1 analogues displayed higher proteolytic stability against this enzyme [27].

Usually, the enhanced proteolytic stability of fluorinated peptides is explained by their greater hydrophobicity and altered secondary structure compared to the parent, non-fluorinated peptide. A further reason is the increased steric bulk of the fluorinated amino acid, meaning protection from protease degradation is a result of the steric occlusion of the peptide from the active site [23,28]. In contrast, the Marsh lab found that the introduction of HfLeu into the antimicrobial peptide MSI-78 only renders it more stable towards proteolysis by trypsin and chymotrypsin in the presence of liposomes [29]. In the absence of liposomes, the fluorinated variants were as rapidly degraded as the non-fluorinated control, suggesting that the incorporation of HfLeu is not the only factor that prevents the peptide from being digested by proteases [29]. Fluorinated aromatic amino acids were also investigated regarding their impact on peptide proteolysis. For instance, incorporation of monofluorinated phenylalanine variants into the histone acetyltransferase protein tGN5 resulted in destabilization in a chymotrypsin digestion assay [30]. Substitution of tryptophan, tyrosine, and phenylalanine residues in a glycosylation-deficient mutant of *Candida antarctica* lipase B, CalB N74D, by their monofluorinated analogues, left the resistance to proteolytic degradation by proteinase K unchanged [31]. Incorporation of α-fluoroalkyl-substituted amino acids can also lead to proteolytically stable peptides, and proteases can even be used to synthesize α-fluoroalkyl-substituted peptides [32-38].

These results indicate that the influence of fluorinated amino acids on the proteolytic stability of peptides and proteins remains difficult to predict. In an attempt to systematically study the influence of fluorinated amino acids on the proteolytic stability of peptides, a 10-amino acid peptide (FA) was previously designed in our group, comprising the substrate specificities of the proteases α-chymotrypsin and pepsin [39,40]. 2-Aminobutanoic acid (Abu) and its fluorinated analogues 2-amino-4,4-difluorobutanoic acid (DfeGly) and 2-amino-4,4,4-trifluorobutanoic acid (TfeGly) were individually incorporated at either the P2, the P1' or the P2' position [41] to give nine different analogues of FA. In prior studies, we observed that the introduction of fluorine atoms into the Abu side chain can significantly improve or dramatically reduce resistance to hydrolysis by different enzymes and human blood plasma, depending upon the fluorine content of the side chain, the position of the substitution relative to the cleavage site and the particular protease [39,40].

Here, we extend these studies to include highly fluorinated, sterically demanding HfLeu, and 5,5,5-trifluoroisoleucine (TfIle) and to investigate their effects on proteolytic stability towards the serine proteases α-chymotrypsin, elastase, and proteinase K, and the aspartate protease pepsin.

Results and Discussion

Peptide design and structure

To elucidate the impact of fluorination on proteolytic stability we previously designed the peptide FA (Figure 1b) that comprises the substrate specificities of α-chymotrypsin and pepsin [39,40]. Consequently, the P1 position is occupied by a phenylalanine residue. Lysine residues were introduced at both ends of the peptide sequence to enhance solubility, and *o*-aminobenzoic acid (Abz) at the N-terminus serves as a fluorescence label. Alanine residues in positions P3, P3', and P4' act as spacers as the peptide binds in an extended conformation to the enzyme's active site [42]. The positions P2, P1' and P2' at or adjacent to the cleavage site [41] carry the key residues for the recognition of the substrate by the protease and serve as substitution sites.

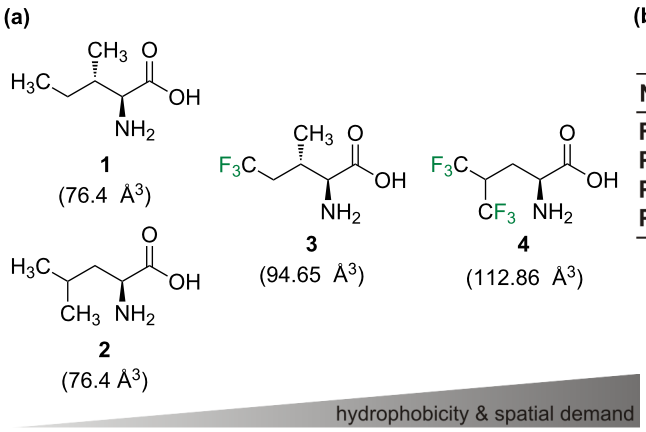

(b)

Name		P3	P2	P1	P1'	P2'	P3'	P4'	
FA	Abz	K	A	A	F	A	A	A	A	K
P2-XaaFA	Abz	K	A	**Xaa**	F	A	A	A	A	K
P1'-XaaFA	Abz	K	A	A	F	**Xaa**	A	A	A	K
P2'-XaaFA	Abz	K	A	A	F	A	**Xaa**	A	A	K

Figure 1: (a) Structures of isoleucine (**1**), leucine (**2**), and their fluorinated analogues 5,5,5-trifluoroisoleucine (**3**, TfIle) and 5,5,5,5',5',5'-hexafluoroleucine (**4**, HfLeu). The van der Waals volumes given in parentheses correspond to the side chains (starting at α-carbon), and were calculated according to Zhao et al. [43]; (b) Names and amino acid sequences of the studied peptides; the substitution positions are marked as Xaa; Xaa = Leu, HfLeu, Ile or TfIle. Positions are named according to Schechter and Berger nomenclature [41].

The alanines at P2, P1' or P2' positions were substituted individually with either TfIle or HfLeu (Figure 1a). Ile and Leu variants were also included in this study as non-fluorinated controls. This led to a library of 12 FA variants (Figure 1b).

Leu and Ile are larger and more hydrophobic than Ala. The fluorinated amino acids are even larger and more hydrophobic than their hydrocarbon analogues [44,45]. Furthermore, fluorine substitution has been shown to polarize neighboring C–H bonds (here the γ-hydrogens) that could affect noncovalent interactions [9,11]. Since the amino acids used here (Figure 1a) differ in their degree of fluorination, spatial demand and hydrophobicity, it is expected that they will have different impacts on the enzyme's binding pocket, reflected by different behavior in the proteolysis assay.

Determination of proteolytic stability

All peptides were incubated with the four different proteases and their proteolytic degradation was followed over a period of 24 h. Both, α-chymotrypsin [46-49] and pepsin [50-54] are well characterized digestive proteases. They are, together with trypsin, the main enzymes of the human digestive system. Elastase possesses a wide substrate specificity for non-aromatic, neutral side chains [55,56] and is found in the human pancreas and in blood serum. Proteinase K, an enzyme widely used for inactivation and degradation studies of proteins, was included here since it shows a broad substrate specificity and high activity and, thus, is able to digest numerous native proteins, even in the presence of detergents [57]. These four enzymes have different preferences at their subsites, thus providing a broad scope for our investigations.

The course of proteolytic digestion was characterized by an analytical HPLC-assay with fluorescence detection [39,40]. For quantification of substrate degradation, integration of the corresponding HPLC peak was conducted. Cleavage products were identified by ESI–ToF mass spectrometry (see Supporting Information File 1, Tables S4–S7). Figure S2 (Supporting Information File 1) shows the time course of all of the digestion experiments. A detailed description of the results for the individual enzymes is given in the following sections.

Proteolytic stability towards α-chymotrypsin (EC 3.4.21.1)

α-Chymotrypsin is a serine endopeptidase with broad specificity. It preferably cleaves peptide bonds C-terminal to large hydrophobic residues such as phenylalanine, tyrosine, tryptophan, and leucine in the P1 position. Secondary hydrolysis also occurs at the carbonyl end of isoleucine, methionine, serine, threonine, valine, histidine, glycine, and alanine [47,58-60].

The S2 subsite of α-chymotrypsin generally prefers to accommodate hydrophobic residues [59,61]. We observed that the fluorinated P2 variants show a smaller amount of digestion after 120 min compared to their hydrocarbon analogues, while all variants are more stable than the control FA (Figure 2). After 24 h, all P2 peptides except for P2-LeuFA are still more stable than FA. Incorporation of Leu into P2 leads to complete proteolysis compared to FA, in which Ala occupies this position. However, incorporation of six fluorine substituents into Leu (resulting in HfLeu) results in an almost 100% gain in proteolytic stability. Ile is not as highly preferred in P2 as Leu, but also here the introduction of three fluorine substituents leads to a

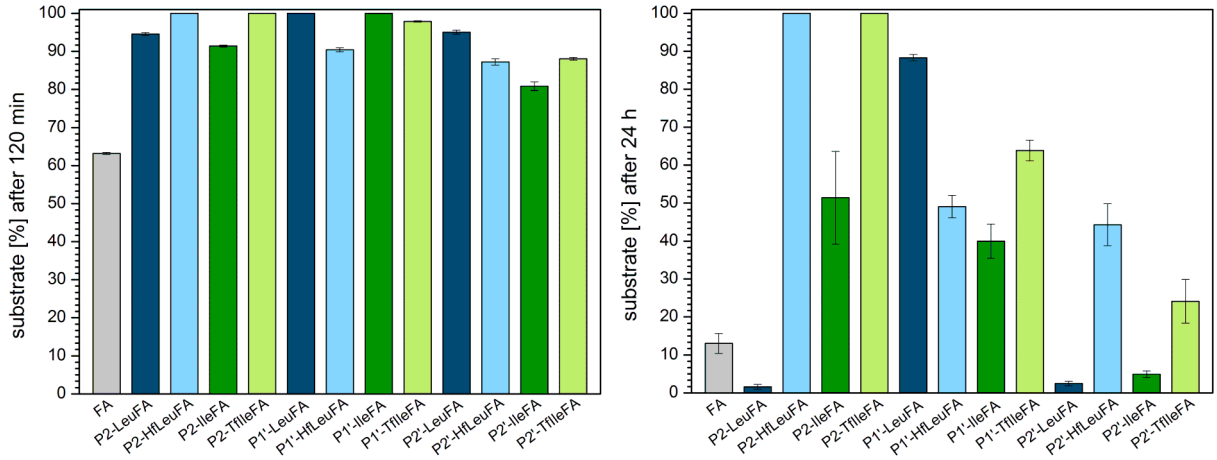

Figure 2: Percentage of substrate remaining after incubation for 120 min (left) and 24 h (right) with α-chymotrypsin in 10 mM phosphate buffer, pH 7.4, at 30 °C. The data shown represent the average of three independent measurements. Errors are derived from the standard deviation.

50% gain in stability. P2-HfLeuFA and P2-TfIleFA are not digested at all, suggesting that HfLeu and TfIle are not favored within the S2 pocket of α-chymotrypsin.

P1'-substituted peptides are all more stable towards digestion than the control peptide FA, while Leu seems to provide the best protection from proteolysis. Here, introduction of fluorine makes the peptide prone to degradation. The opposite is true for Ile as TfIle leads to less efficient degradation. The S1' subsite of α-chymotrypsin usually accommodates basic residues with long side chains [59,62,63]. Ile, as a branched amino acid, is obviously not well accommodated in this position for steric reasons. A further increase in side chain volume with TfIle exacerbates this effect. In the case of HfLeu, however, fluorine substituents seem to engage in favorable interactions with amino acid residues of the binding site, thus making P1'-HfLeuFA a better substrate than the non-fluorinated Leu peptide. Several such interactions are possible, as described in our previous work [39,40,64].

The S2' subsite of α-chymotrypsin exhibits a hydrophobic character and thus prefers to accommodate hydrophobic residues [59,65]. However, the more hydrophobic peptides P2'-LeuFA, P2'-HfLeuFA, P2'-IleFA, P2'-TfIleFA are more stable against digestion by α-chymotrypsin compared to FA after 120 min of incubation. After 24 h, only the fluorinated analogues are less degraded than the control FA. Full length P2'-HfLeuFA and P2'-TfIleFA are present at percentages up to 44% and 24%, respectively, while substitution by Leu and Ile in P2' position leads to accelerated proteolysis compared to FA. Thus, both HfLeu and TfIle have a protective effect towards proteolysis in this position.

ESI–ToF mass analysis confirms that the position P1 bearing Phe is the main cleavage site for α-chymotrypsin (Figure 3). Cleavage C-terminal to Leu and HfLeu in P1'-LeuFA and P1'-HfLeuFA is also observed (Figure 3, see Supporting Information File 1, Table S4), which means that the cleavage site was shifted towards the C-terminus by one residue. This is likely a consequence of α-chymotrypsin's preference for not only aromatic residues but also bulky hydrophobic residues in the S1 pocket, thus, HfLeu is accepted by the P1 binding pocket of α-chymotrypsin.

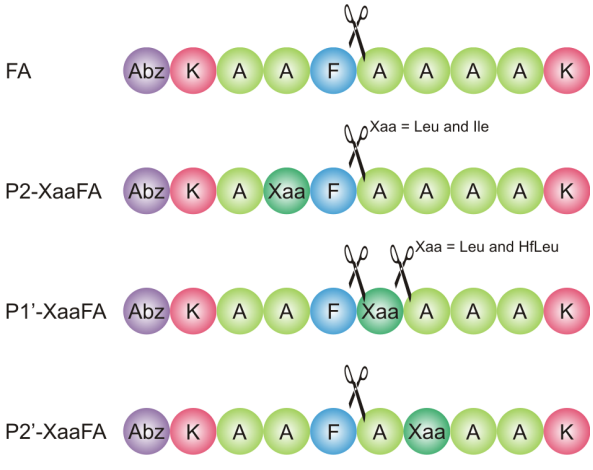

Figure 3: Cleavage positions observed in the digestion of library peptides with α-chymotrypsin.

In summary, the introduction of fluorinated Leu and Ile analogues into a α-chymotrypsin specific peptide sequence can

improve proteolytic stability mainly at the P2 and P2’ positions, with the strongest effects observed for the P2 position.

Proteolytic stability towards pepsin (EC 3.4.23.1)

Pepsin is an aspartic endopeptidase and one of the main digestive enzymes in humans. It exhibits specificity for hydrophobic, especially aromatic residues like Phe, Trp, and Tyr at the P1 and P1’ positions [50-54]. It has an extended active site that can bind at least seven residues [66,67], and peptide bond cleavage occurs N-terminal to the residue at position P1. The cleavage efficiency heavily depends upon the identity of this amino acid, with Phe and Leu being the most favored residues. At the P1’ position aromatic amino acid residues are preferred, however, the influence of the P1’ position on proteolytic cleavage is not as significant [68]. Pepsin typically does not cleave at Val, Ala, or Gly linkages [60].

The S2 subsite of pepsin preferentially accommodates hydrophobic residues such as Leu, Ala or norleucine as well as the β-branched species Ile and Val, but can also bind charged residues [69,70]. Except for P2-TfIleFA, we observed that the P2-modified peptides are degraded more rapidly than the control peptide FA and that these peptides are almost or completely degraded after 120 min (Figure 4). For example, whereas after 24 h FA is also almost completely degraded, P2-TfIleFA is still detected at a level of 100%. Incorporation of Leu or Ile leads to complete proteolysis. Remarkably, the introduction of six fluorine atoms into Leu doesn’t change this behavior. In sharp contrast yet equally remarkable, the incorporation of three fluorine substituents into Ile results in a 100% gain in proteolytic stability. These results indicate that Leu, HfLeu, as well as Ile are well accommodated in the S2 subsite of pepsin. In contrast, TfIle, although smaller than HfLeu [44], doesn’t appear to fit well into the S2 pocket of pepsin.

To compare the P1’ substituted peptides, only P1’-HfLeuFA shows the same persistence after 120 min as the control peptide FA, while all other sequences are digested faster. Here, the introduction of fluorine into Leu seems to stabilize the peptide by about 20%. Interestingly, after 24 h this trend is reversed, and the P1’-HfLeuFA peptide is destabilized to an amount of 17% compared to the hydrocarbon analogue, but both peptides are somewhat more stable than the control FA. The incorporation of TfIle into this position doesn’t show a significant impact. Although the fluorine substituents slow down the digestion process (see Supporting Information File 1, Figure S2b), the TfIle containing peptide as well as its hydrocarbon analogue are fully digested after 24 h. The S1’ subsite has hydrophobic character and thus prefers to accommodate hydrophobic or aromatic residues [71]. Ile and TfIle are obviously well accommodated in this position, while Leu and HfLeu are not.

The S2’ subsite of pepsin favors hydrophobic amino acids, but also accepts charged polar amino acids like Glu and Thr [52,72]. After 120 min peptides P2’-LeuFA, P2’-IleFA and P2’-TfIleFA are degraded faster than the control FA. Instead, P2’-HfLeuFA is only digested up to 5%. This effect is even more pronounced after 24 h. While all other P1’ substituted peptides, along with the control peptide FA, are almost or completely digested, P2’-HfLeuFA is still present to about 76%. In this case fluorination leads to protection against proteolysis by pepsin. Hfleu is obviously not well accommodated in this position. As already observed for position P1’, the introduction of

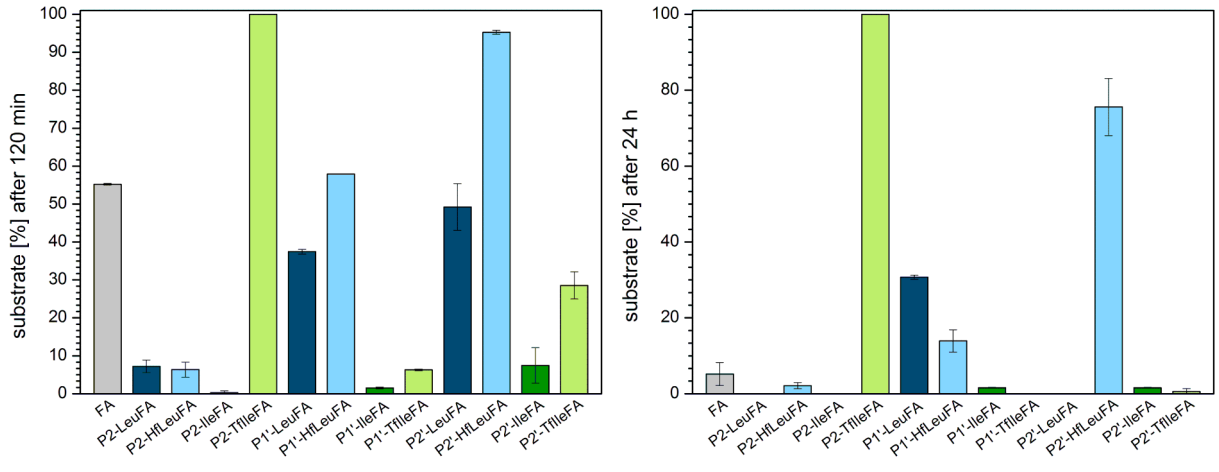

Figure 4: Percentage of substrate remaining after incubation for 120 min (left) and 24 h (right) with pepsin in 10 mM acetate buffer, pH 4.0, at 30 °C. The data shown represent the average of three independent measurements. Errors are derived from the standard deviation.

three fluorine atoms into Ile slows down proteolysis, although both peptides are completely digested after 24 h.

For almost all peptides of our library, we observed the expected cleavage pattern with Phe in the P1 position (Figure 5, see Supporting Information File 1, Table S5). Only P2'-HfLeuFA is not hydrolyzed at the designed cleavage site, instead cleavage occurs exclusively N-terminal to the HfLeu residue, thus demonstrating that HfLeu occupies the P1' position. In the case of P2'-TfIle we found two further peptide bonds that are cleaved by pepsin, namely N-terminal cleavage to TfIle and to Phe. These findings indicate that the S1' subsite accommodates bulky hydrophobic residues more readily than does the S2' site of pepsin. For P1'-LeuFA and P1'-HfLeuFA we found an additional cleavage site at which the peptide bonds Leu$^{P1'}$-Ala$^{P2'}$, and HfLeu$^{P1'}$-Ala$^{P2'}$ are hydrolyzed, respectively, which means that the cleavage site was shifted towards the C-terminus by one residue. This cleavage pattern was also detected for α-chymotrypsin before, and indicates that HfLeu is well accepted by pepsin in its S1 binding site. Furthermore, we identified a second cleavage site for P2-HfLeuFA at which the peptide bond N-terminal to Phe is proteolytically cleaved as well. This means that the cleavage site is shifted such that HfLeu occupies the P1 and Phe the P1' position. However, this perfectly matches the specificity of pepsin that prefers bulky hydrophobic and aromatic amino acids both up- and downstream of the scissile bond.

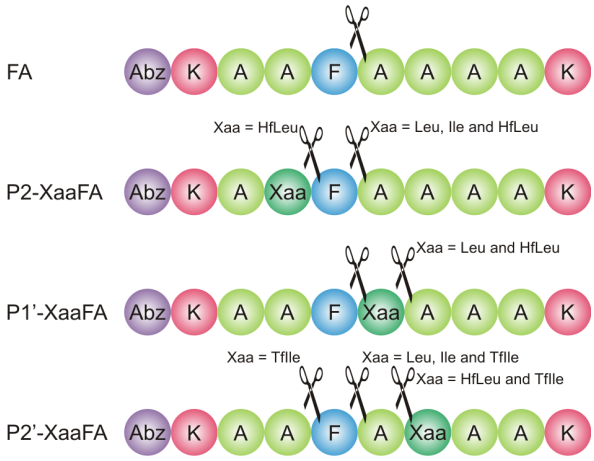

Figure 5: Cleavage positions for digestion of the different peptides with pepsin.

In summary, the introduction of fluorinated Leu into a pepsin specific peptide sequence can improve the proteolytic stability at the P2' position, whereas the incorporation of a fluorinated Ile into the P2 position shows the strongest effect in protection from proteolysis.

Proteolytic stability towards elastase (EC 3.4.21.36)

Elastase is a serine endopeptidase, and has a wide specificity for non-aromatic uncharged side chains. It preferentially cleaves peptide bonds C-terminal to small uncharged non-aromatic amino acid residues such as glycine, alanine and serine, but also valine, leucine, isoleucine [56,73]. Its binding site extends over eight subsites (S5 to S1, and S1' to S3') [74].

The fact that in this study larger and more hydrophobic amino acids [44,45] were introduced may explain why degradation of most of the variants during the first 120 min of incubation with elastase is hardly observed (Figure 6). Only P2'-LeuFA, P2'-

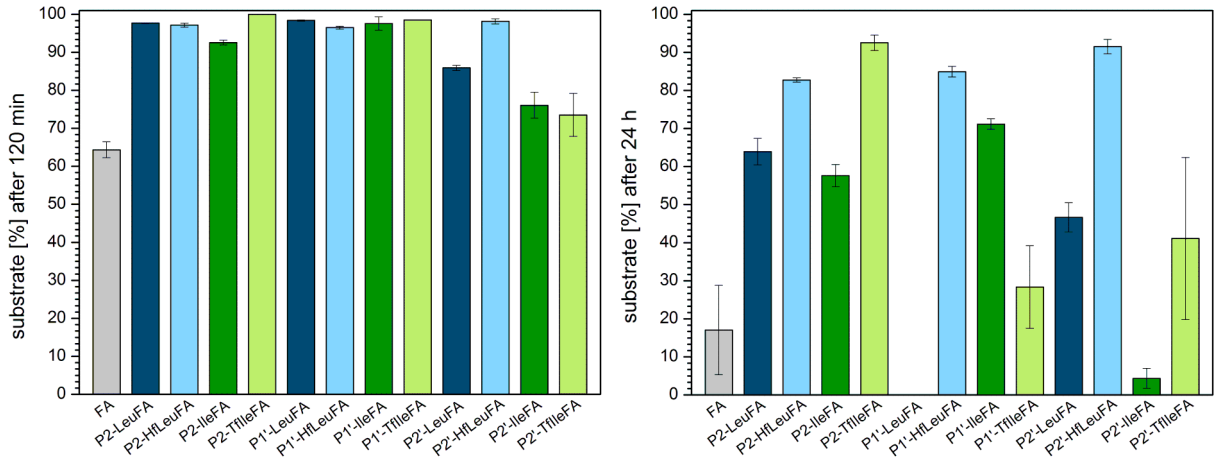

Figure 6: Percentage of substrate remaining after incubation for 120 min (left) and 24 h (right) with elastase in 100 mM Tris/HCl buffer, pH 8.4, at 37 °C. The data shown represent the mean of three independent measurements. Errors are derived from the standard deviation.

IleFA, and P2'-TfIleFA were somewhat digested during this time, however, all of the modified peptides are more stable than the control FA.

After 24 h all P2 peptide variants are more stable than the control FA (Figure 6), while TfIle provides the best protection from elastase digestion. Leu and Ile are not quite as preferred in P2 position as is Ala. Fluorination of Leu leads to an increase in stability of around 19%. With 35% this effect is even higher when three fluorine atoms are introduced into Ile.

Modification of the P1' postion renders P1'-HfLeuFA and P1'-IleFA more stable than the control peptide FA, while P1'-TfIleFA is comparably stable. Incorporation of Leu into P1' leads to complete digestion. However, introducing six fluorine atoms into Leu results in an 85% gain in stability. The opposite is observed for Ile, where TfIle accelerates enzymatic degradation.

Except for P2'-IleFA, all P2' modified variants are more stable compared to the control peptide FA after 24 h. Leu is not as preferred in this position as Ala. Introduction of fluorine strengthens this effect and effectively doubles the stability. In contrast, introduction of Ile leads to almost complete proteolysis. However, substitution by TfIle slows down the degradation rate and results in a stabilization of around 37%. In P2', fluorination shows in both cases a protective effect towards hydrolysis by elastase.

Elastase preferably hydrolyses peptide bonds C-terminal to uncharged non-aromatic amino acids and mainly between Ala–Ala and Ala–Gly bonds [56,73]. Since Ala is the main residue present in the peptides studied here, we observed various cleavage products in the ESI–ToF analysis (Figure 7, see Supporting Information File 1, Table S6). For none of the peptides were fragments with Phe in the P1 position observed. Since elastase has a constricted S1 pocket, the binding of aromatic amino acids at P1 is deleterious [75]. Here, we also observed that Leu appears to never occupy the P1 position, although it is known to occupy this position in other substrates [73]. Interestingly, the larger fluorinated variant was found in the P1 position in one case, while Ile and its fluorinated analogue occupy this position in two of the three peptide analogues.

The S2' subsite of elastase has a marked specificity for Ala, and can accommodate bulkier residues only with some difficulty [74]. Thus, we did not find the fluorinated amino acids HfLeu and TfIle binding to the S2' subsite of the enzyme as expected, whereas for the Leu and Ile variants this was observed only in one case each.

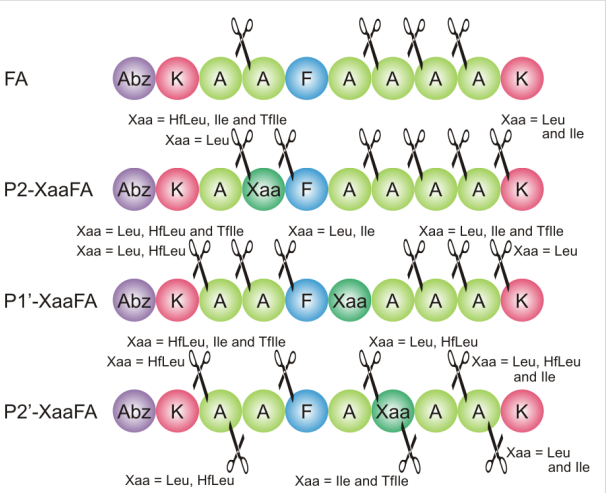

Figure 7: Cleavage positions for digestion of the different peptides with elastase.

The S1' subsite usually prefers Lys residues, and to a lesser extent Ala or Glu [74,76]. Indeed, we found a fragment cleaved off corresponding to a Lys in P1', but primarily detected fragments with Ala in P1' and also Phe that was even more favored than Lys. We observed that Ile as well as its fluorinated analogue TfIle are not accommodated in this subsite, probably due to their β-branched topology.

The S3' pocket in elastase is known to have a high aromatic specificity [74]. Interestingly, in our cases Phe in P3' was less favored. Instead, mainly Lys occupied this position.

Ala is favored in P2. Its carboxyl group can form a hydrogen bond with the amide nitrogen of Gly193 in the S2 pocket, and Ala's methyl group faces the solvent [76].

Occupation of the S4 subsite is important for efficient catalysis [76,77]. Thus elastase might not easily split the first three bonds at the amino terminus of a peptide chain, since interactions of a residue with S4 is necessary [77]. Indeed, we only observed a low amount of cleavage proximal to the N-terminus, while most of the hydrolysis occurred at the C-terminal end of the peptides. The S3 subsite seems to accommodate bulkier hydrophobic amino acids well, as we observed cleavage products containing Ile and Leu in P3 position for all the peptides modified with these residues, as well as their fluorinated analogues for two of the three substituted peptides each.

In summary, introduction of HfLeu in different positions of a peptide can enhance the proteolytic stability up to 85% compared to the corresponding Leu analogues. Replacing Ile with TfIle can increase the stability against elastase as well, although not as efficiently as HfLeu.

Proteolytic stability towards proteinase K (EC 3.4.21.64)

Proteinase K is a non-specific serine endopeptidase and the main proteolytic enzyme produced by the fungus *Tritirachium album Limber* [78]. It has a broad substrate specificity, cleaving peptide bonds C-terminal to a number of amino acids, however, prefers aromatic or aliphatic hydrophobic amino acids in position P1 [57,78]. Furthermore, Ala is favored in position P2 and enhances cleavage efficiency [79,80]. Proteinase K possesses a very high proteolytic activity [79]. Its active center contains an extended binding region consisting of several subsites, at least four or five subsites on the N-terminal side of the scissile bond (S1 to S4/S5) and three subsites C-terminal to the scissile bond (S1' to S3') [81-83]. The "bottom" of substrate recognition site is predominantly hydrophobic and there is evidence that not the sequence of the substrate is of importance in the recognition but only the volume of the side chains [84].

Substitution of Ala in position P2 with Ile and Leu leads to a greater or comparable amount of degradation after 120 min. Introducing fluorine atoms in both cases slows down the digestion process, most pronounced for P2-TfIleFA with a gain of 60% in stability compared to its non-fluorinated analogue. Ile is not preferred to the extent that Leu is, and the introduction of fluorine enhances this effect. While all other peptides are almost completely or entirely degraded after 24 h, P2-TfIleFA is the only peptide that is still left after 24 h of incubation (Figure 8).

Introduction of Leu at the P1' position leads to an amount of digestion comparable to FA after 120 min. Fluorination of the Leu side chain leads to a small acceleration in digestion. Ile at this position is not as preferred as is Leu and this enhances the stability to a small extent compared to FA. Introducing three fluorine atoms at the Ile side chains strengthens the stability against proteinase K even further.

As already observed for the other two Leu containing peptides, also substitution of Ala at position P2' with Leu does not change the resistance against proteinase K significantly. Interestingly, when six fluorine atoms are introduced, the digestion process is faster and P2'-HfLeuFA is almost completely degraded after 120 min. The opposite is observed for the fluorination of Ile. While P2'-IleFA is as stable as FA, P2'-TfIleFA shows a small gain in stability of around 12%.

Thus, in the case of P1' as well as P2' peptide variants, only fluorination of Ile leads to a slower digestion by proteinase K, while introducing even more fluorine atoms into the Leu side chain leads to more rapid hydrolysis compared to the non-fluorinated analogues. Ile seems in all investigated cases not as preferred as Leu, since less efficient digestion is observed. Introduction of three fluorine atoms even enhances this protective effect.

Based on the wide substrate specificity of proteinase K and its preference for alanine, and since our studied peptides have a high number of alanine residues present, there are multiple cleavage sites possible in addition to the designed site between Phe^{P1} and $Xaa^{P1'}$. Indeed, multiple cleavage patterns are observed, especially cleavage C-terminal to Ala (Figure 9, see Supporting Information File 1, Table S7). Thus, Ala mainly occupies the S1 subsite, but is also found to bind to the S2 site

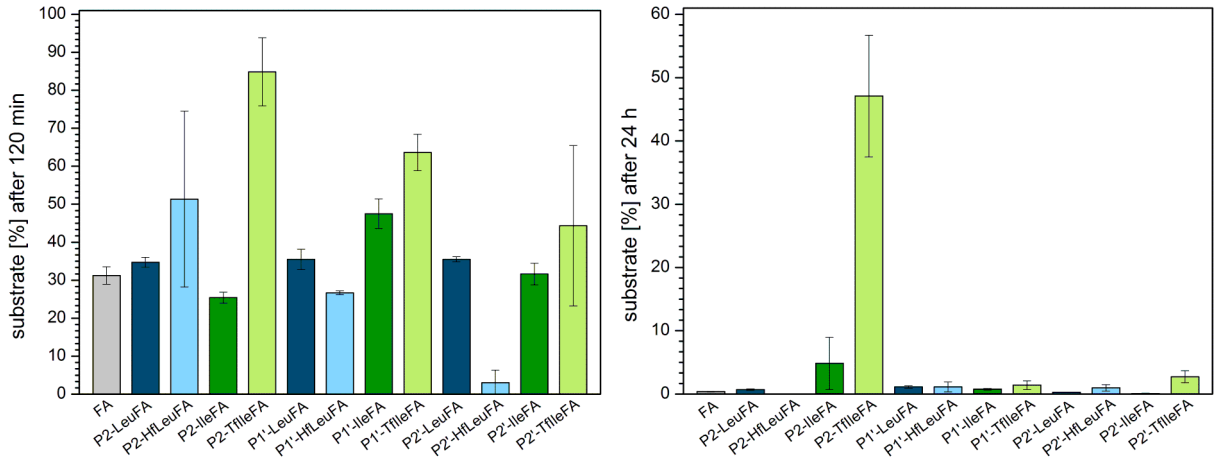

Figure 8: Percentage of substrate remaining after incubation for 120 min (left) and 24 h (right) with proteinase K in 50 mM Tris/HCl buffer, containing 10 mM $CaCl_2$ pH 7.5, at 37 °C. The data shown represent the mean of three independent measurements. Errors are derived from the standard deviation.

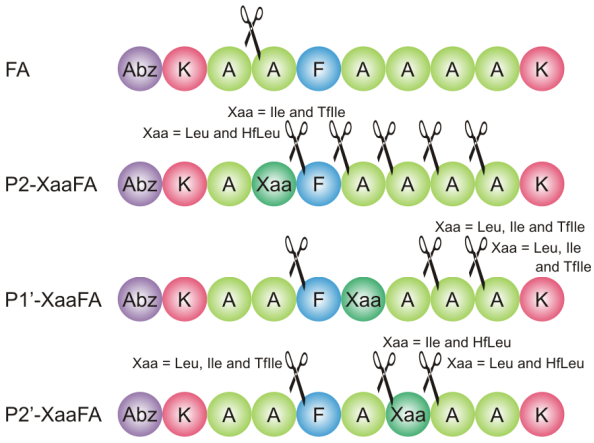

Figure 9: Cleavage positions found with proteinase K.

to a greater extent. Ala is most effective in P2 [80] as the S2 subsite is a small and narrow cleft, which limits the possibilities for effective side chain substitutions [79]. However, Ile and TfIle are well accepted here. A negative or positive charge at S2 is not preferred and hampers the formation of the enzyme substrate complex [82]. Thus, it can be concluded that Lys is poorly accepted at this position. HfLeu, the most sterically bulky amino acid investigated here, is not observed to occupy the S2 subsite. Instead, HfLeu is mainly found to bind to the S1 pocket. Leu is also found to occupy the S1 site of proteinase K, which is large and has mainly hydrophobic character [82,83,85]. It does not impose too strong steric limitations on the amino acid side chain but prefers hydrophobic and aromatic residues, with a specificity for Ala [78,81,83,86]. Charged side chains of Glu and Lys are very poorly accepted, as are β-branched functional groups, because the entrance to the S1 subsite is too narrow to allow their passage [79]. Thus, Lys is not observed to occupy the S1 subsite. Neither Ile nor TfIle can be accommodated by the S1 pocket due to their β-branching. Phe is found in S1 in only two cases in our study, and mainly occupies the S3 and S1' pockets. The S3 pocket has a wide specificity due to its location at the protein surface, but exhibits preference for aromatic side chains in P3 (Trp, Phe) [79]. S1' shows a slight preference for smaller residues like Ala and Gly, but also bulkier residues such as Phe and Leu are hydrolyzed to a significant extent [81]. In this study Leu apparently does not bind to the S1' site at all, and this is also true of TfIle. Additionally, Lys is not well accommodated here. Phe is also found to occupy S4 to a great extent, and this subsite is known to have an affinity for aromatic groups, especially a marked preference for Phe [79]. S4–P4 interactions are primarily hydrophobic in nature [79], which might explain why we observed that Lys is only poorly accepted in this position. The S3 subsite cannot be defined as a "cleft" or "pocket" [79]. The P3 residue of the peptide substrate lies on the protein surface and the side chain of P3 should be directed toward the solvent [79]. This arrangement might explain the broad specificity of S3 [79]. We observed that all the residues used in this study can occupy the P3 position, mainly Phe and Lys. Leu, Ile and TfIle are also found to a great extent in P3.

In summary, fluorination of an Ile residue N-terminal to the cleavage site can help to protect a peptide against proteolysis by proteinase K. Due to its broad specificity and high activity, proteinase K typically digests peptides quickly [57]. This was also observed in this work in experiments in which all peptides, except for P2-TfIleFA, a remarkably stable species, were completely degraded after an incubation time of 24 h.

Conclusion

The bulky side-chain fluorinated amino acids HfLeu and TfIle have the power to significantly stabilize peptides against proteolytic degradation. The impact of their incorporation on the proteolytic stability of peptides does not follow a general trend but rather depends on a combination of factors including the nature of the fluorinated amino acid, the substitution position relative to the cleavage site and the studied protease. Also, in contrast to proteolytic studies published before [23,27,28], the expectation of a general increase in proteolytic stability as a result of steric occlusion of the peptide from the active site upon incorporation of sterically demanding fluorinated amino acids could not be verified based on the results of our current study. We found a significant stabilization towards proteolysis in 13 of a total of 24 peptides of the library studied here upon introduction of either HfLeu or TfIle (Figure 10). However, we observed that even these sterically demanding fluorinated amino acids show in some cases favorable interactions with the enzymes binding sites resulting in a more rapid digestion as the non-fluorinated control.

The introduction of fluorinated Leu and Ile analogues into P2 and P2' position improved the proteolytic stability towards α-chymotrypsin. When introduced in the P1' position a stabilization was still observed for TfIle, while incorporation of HfLeu made the peptide more prone to proteolytic digestion compared to the non-fluorinated control. Incorporation of HfLeu had a significantly stabilizing effect towards hydrolysis by pepsin only in P2' position, while TfIle develops a protective effect only when incorporated in P2 position.

As both, elastase and proteinase K possess a broad specificity, preferring C-terminal cleavage to Ala, we observed here a rather unspecific cleavage pattern for both enzymes with multiple cleavage products, in which the intended designed

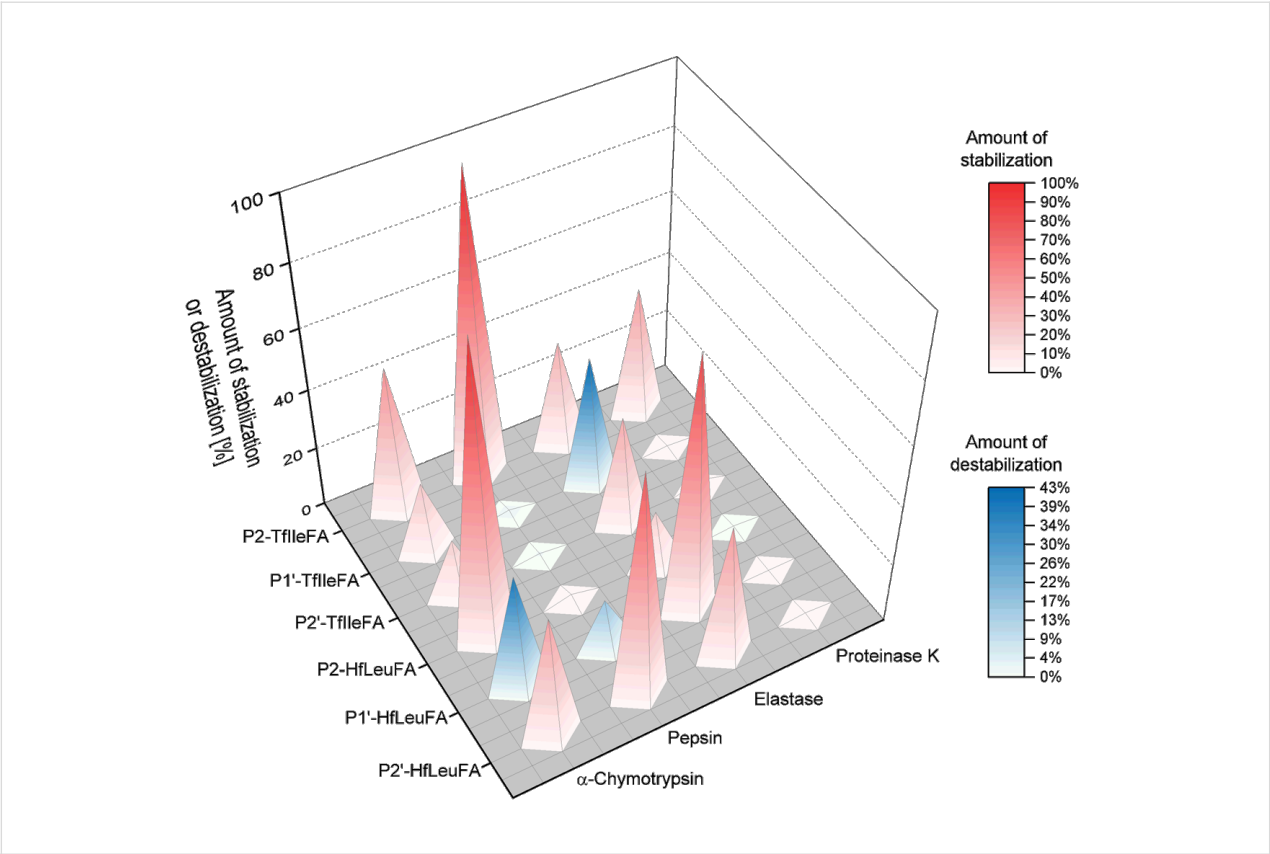

Figure 10: Dimension of stabilization or destabilization upon TfIle or HfLeu incorporation compared to the non-fluorinated analogues containing Ile or Leu, respectively, for all four different enzymes studied here and measured after 24 h of incubation.

cleavage site with Phe in P1 position wasn't affected. However, we observed that the introduction of HfLeu has a general protective effect against degradation by elastase, whereas the effect of TfIle depends on the substitution position. Although the introduction of fluorine substituents generally affected the rate of hydrolysis by proteinase K, only fluorination of an Ile residue N-terminal to the cleavage site effectively protected the peptide from digestion. Particularly noteworthy is the effect of fluorination of the Ile side chain in P2 position. The P2-TfIleFA peptide was the most resistant substrate towards proteolysis by all four proteases applied in this study. In contrast, destabilization due to fluorination was only observed when TfIle and HfLeu were incorporated into the P1' position.

In future studies, we will focus on a more precise characterization of the interaction of fluorinated substrates with proteolytic enzymes to which multiple factors contribute. The steric demand or conformation of the side chain, hydrophobicity, fluorine induced polarity and significant pK_a-value changes of neighboring groups [9,10] can lead to fluorine-specific interactions between substrate and enzyme binding sites as well as to an exclusion of the cleavage-relevant peptide bonds from the active site.

Furthermore, our investigations show that fluorine's impact on proteolytic stability needs to be investigated always case-by-case as there is no general trend to be concluded. Nevertheless, the results of this current study provide valuable knowledge on how bulky fluorinated amino acids can help to increase the proteolytic stability of peptides, and show that upon smart design, these fluorinated amino acids can be used to engineer peptide drug candidates.

Experimental

Materials

Fmoc-L-amino acids were purchased from ORPEGEN Peptide Chemicals GmbH (Heidelberg, Germany). Fmoc-Lys(Boc)Wang resin was from Novabiochem (Merck Chemicals GmbH, Darmstadt, Germany). All solvents were used from VWR (Darmstadt, Germany) without further purification. All other chemicals were bought from Acros (Geel, Belgium), abcr GmbH (Karlsruhe, Germany), fluorochem (Hadfield, United Kingdom), VWR (Darmstadt, Germany) or Merck (Darmstadt, Germany) at highest commercially available purity and used as such. A detailed synthetic strategy for Fmoc-TfIle-OH is described in literature [44]. For the synthesis of Fmoc-HfLeu-OH see Supporting Information File 1.

Peptide synthesis, purification and characterization

Peptides were synthesized manually in a 0.05 mmol scale on a solid support by means of an Fmoc/*tert*-butyl protecting group strategy on a preloaded Fmoc-Lys(Boc)Wang resin (0.57 mmol/g loading) using 10 mL polypropylene reactors. HfLeu containing peptides were synthesized with an Activo-P11 automated peptide synthesizer (Activotec, Cambridge, United Kingdom). Couplings of non-fluorinated amino acids were performed in dimethylformamide (DMF) with the Fmoc-L-amino acid, 1-hydroxybenzotriazole (HOBt) and *N,N'*-diisocarbodiimide (DIC) in an eight-fold excess with respect to the resin amount. In order to ensure completion of the reaction the couplings were performed twice for 1 h each. The fluorinated amino acids and coupling reagents 1-hydroxy-7-azabenzotriazole (HOAt)/DIC were used in 1.2-fold excess, and the coupling was carried out manually one time overnight. In the case of an insufficient coupling, the coupling was repeated for 3 h with 0.5 equivalents. Prior to the Fmoc deprotection of the fluorinated amino acids, free N-termini were capped by adding a mixture of acetic anhydride (Ac_2O, 10% (v/v)) and *N,N*-diisopropylethylamine (DIPEA, 10% (v/v)) in DMF (3 × 10 min). Fmoc deprotection was achieved by treatment with 20% (v/v) piperidine in DMF (3 × 10 min). All peptides were N-terminally labeled with *o*-aminobenzoic acid (Abz) to enable photometric detection. The resin was washed between each step with DMF and dicholoromethane (DCM, 3 × 2 mL each). After the synthesis, the peptides were cleaved from the resin by treatment with a solution (2 mL) containing triisopropylsilane (TIS, 10% (v/v)), water (1% (v/v)), and trifluoroacetic acid (TFA) (89% (v/v)) for 3 h. The resin was washed twice with TFA (1 mL) and DCM (1 mL) and excess solvent was removed by evaporation. The crude peptide was precipitated with ice-cold diethyl ether (80 mL), and after centrifugation dried by lyophilization. Purification of the synthesized peptides was performed on a LaPrepΣ low-pressure HPLC system (VWR, Darmstadt, Germany) using a Kinetex RP-C18 endcapped HPLC column (5 µM, 100 Å, 250 × 21.2 mm, Phenomenex®, USA). A Security GuardTM PREP Cartridge Holder Kit (21.20 mm, ID, Phenomenex®, USA) served as pre-column. As eluents deionized water (Milli-Q Advantage® A10 Ultrapure Water Purification System, Millipore®, Billerica, MA, USA) and acetonitrile (ACN), both containing 0.1% (v/v) TFA were used. HPLC runs were performed starting with an isocratic gradient of 5% ACN over 5 min, flow rate: 10 mL/min, continuing with a linear gradient of 5–70% ACN over 25 min, flow rate: 20.0 mL/min. UV-detection occurred at 220 nm. Data analysis was performed with an EZChrom Elite-Software (Version 3.3.2 SP2, Agilent Technologies, Santa Clara, CA, USA). The fractions containing pure peptide were combined, reduced in vacuo and lyophilized to give the peptides as a white powder. The purity of the peptides was controlled by analytical HPLC (LUNA^{TM} C8 (2) column, 5 µm, 250 × 4.6 mm, Phenomenex®, Torrance, CA, USA), and the products were identified by high-resolution ESI–ToF–MS (see Supporting Information File 1).

Protease digestion assay

All peptides employed in the degradation studies were used as the TFA salts obtained after lyophilization. Stock solutions of α-chymotrypsin (from bovine pancreas, EC 3.4.21.1, ≥40.0 units/mg of protein, Sigma Aldrich, St. Louis, MO, USA), and pepsin (from porcine stomach mucosa, EC 3.4.23.1, ≥250 units/mg of protein, Sigma Aldrich, St. Louis, MO, USA) were prepared at concentrations of 1 mg/mL in phosphate buffer (10 mM, pH 7.4), or in acetate buffer (10 mM, pH 4.0), respectively. For proteinase K (from tritirachium album, EC 3.4.21.64, ≥30 units/mg of protein, Sigma Aldrich, St. Louis, MO, USA) and elastase (from porcine pancreas, EC 3.4.21.36, 6.2 units/mg of protein, Sigma Aldrich, St. Louis, MO, USA) stock solutions were prepared also at concentrations of 1 mg/mL in tris/HCl (50 mM) + $CaCl_2$ (10 mM) buffer (pH 7.5), or in tris/HCl buffer (100 mM, pH 8.4), respectively. Peptides (0.002 mmol) were prepared as stocks in DMSO (100 µL) and incubated with the respective enzyme at 30 °C (for α-chymotrypsin and pepsin) or 37 °C (for proteinase K and elastase) with shaking at 300 rpm in a thermomixer over a period of 24 h. The reaction mixture consisted of DMSO (15 µL), corresponding buffer (25 µL), peptide solution (5 µL) and the corresponding enzyme solution (5 µL). The concentration of enzyme was optimized so that the hydrolysis of the control peptide FA was about 40% after 120 min. Aliquots of 5 µL were taken at fixed time points (0, 15, 30, 60, 90, 120 min as well as 3 h and 24 h) and either quenched with ACN containing 0.1% (v/v) TFA (95 µL), in the case of α-chymotrypsin, proteinase K and elastase, or 2% aqueous ammonia (95 µL), in the case of pepsin. All samples were subjected to analytical HPLC on a LaChrom-ELITE-HPLC-System equipped with a fluorescence detector (VWR International Hitachi, Darmstadt, Germany). A monolithic reversed-phase C8 Chromolith® Performance HPLC column (100 × 4.6 mm, Merck KGaA, Darmstadt, Germany) was used to resolve and quantify the products of digestion. The used system and gradients are described in detail in Supporting Information File 1. Detection based on the Abz label was carried out using a fluorescence detector with λ_{ex} = 320 nm and λ_{em} = 420 nm. In all cases, the peaks corresponding to the starting materials (full-length peptides) or the N-terminal fragments (products) were integrated and used to determine the velocity of the reaction (see Supporting Information File 1). The FA peptide was used as a reference. Each fragment cleaved from the full-length peptide was identified by ESI–ToF mass analysis on an Agilent 6220 ESI–ToF–MS spec-

trometer (Agilent Technologies, Santa Clara, CA, USA, see Supporting Information File 1). All experiments were performed in triplicate.

Supporting Information

Supporting Information File 1

Characterization and identification of synthesized peptides, characterization of the enzymatic digestion reactions, and identification of proteolytic cleavage products, HPLC methods, and synthesis protocol for Fmoc-HfLeu-OH.
[http://www.beilstein-journals.org/bjoc/content/supplementary/1860-5397-13-279-S1.pdf]

Acknowledgements

This work has been generously supported by the DFG in the context of the Research Training Group 1582 “Fluorine as Key Element”. Special thanks go to Dr. Holger Erdbrink and Prof. Dr. Constantin Czekelius for providing the fluorinated amino acid Boc-TfIle-OH. The authors thank Dr. Allison Ann Berger for carefully proofreading the manuscript.

References

1. Vlieghe, P.; Lisowski, V.; Martinez, J.; Khrestchatisky, M. *Drug Discovery Today* **2010,** *15,* 40–56. doi:10.1016/j.drudis.2009.10.009
2. Sato, A. K.; Viswanathan, M.; Kent, R. B.; Wood, C. R. *Curr. Opin. Biotechnol.* **2006,** *17,* 638–642. doi:10.1016/j.copbio.2006.10.002
3. Albericio, F.; Kruger, H. G. *Future Med. Chem.* **2012,** *4,* 1527–1531. doi:10.4155/fmc.12.94
4. Uhlig, T.; Kyprianou, T.; Martinelli, F. G.; Oppici, C. A.; Heiligers, D.; Hills, D.; Calvo, X. R.; Verhaert, P. *EuPa Open Proteomics* **2014,** *4,* 58–69. doi:10.1016/j.euprot.2014.05.003
5. Fosgerau, K.; Hoffmann, T. *Drug Discovery Today* **2015,** *20,* 122–128. doi:10.1016/j.drudis.2014.10.003
6. Santos, G. B.; Ganesan, A.; Emery, F. S. *ChemMedChem* **2016,** *11,* 2245–2251. doi:10.1002/cmdc.201600288
7. Jäckel, C.; Koksch, B. *Eur. J. Org. Chem.* **2005,** 4483–4503. doi:10.1002/ejoc.200500205
8. Latham, P. W. *Nat. Biotechnol.* **1999,** *17,* 755–757. doi:10.1038/11686
9. Salwiczek, M.; Nyakatura, E. K.; Gerling, U. I. M.; Ye, S.; Koksch, B. *Chem. Soc. Rev.* **2012,** *41,* 2135–2171. doi:10.1039/C1CS15241F
10. Berger, A. A.; Völler, J.-S.; Budisa, N.; Koksch, B. *Acc. Chem. Res.* **2017,** *50,* 2093–2103. doi:10.1021/acs.accounts.7b00226
11. Salwiczek, M.; Samsonov, S.; Vagt, T.; Nyakatura, E.; Fleige, E.; Numata, J.; Cölfen, H.; Pisabarro, M. T.; Koksch, B. *Chem. – Eur. J.* **2009,** *15,* 7628–7636. doi:10.1002/chem.200802136
12. Huhmann, S.; Nyakatura, E. K.; Erdbrink, H.; Gerling, U. I. M.; Czekelius, C.; Koksch, B. *J. Fluorine Chem.* **2015,** *175,* 32–35. doi:10.1016/j.jfluchem.2015.03.003
13. Marsh, E. N. G. Designing Fluorinated Proteins. In *Methods in Enzymology;* Vincent, L. P., Ed.; Academic Press, 2016; Vol. 580, pp 251–278. doi:10.1016/bs.mie.2016.05.006
14. Vukelić, S.; Moschner, J.; Huhmann, S.; Fernandes, R.; Berger, A. A.; Koksch, B. Synthesis of Side Chain Fluorinated Amino Acids and Their Effects on the Properties of Peptides and Proteins. In *Modern Synthesis Processes and Reactivity of Fluorinated Compounds;* Leroux, F. R.; Tressaud, A., Eds.; Elsevier, 2017; pp 427–464. doi:10.1016/B978-0-12-803740-9.00015-9
15. Buer, B. C.; Meagher, J. L.; Stuckey, J. A.; Marsh, E. N. G. *Protein Sci.* **2012,** *21,* 1705–1715. doi:10.1002/pro.2150
16. Buer, B. C.; Meagher, J. L.; Stuckey, J. A.; Marsh, E. N. G. *Proc. Natl. Acad. Sci. U. S. A.* **2012,** *109,* 4810–4815. doi:10.1073/pnas.1120112109
17. Jäckel, C.; Salwiczek, M.; Koksch, B. *Angew. Chem., Int. Ed.* **2006,** *45,* 4198–4203. doi:10.1002/anie.200504387
18. Tang, Y.; Tirrell, D. A. *J. Am. Chem. Soc.* **2001,** *123,* 11089–11090. doi:10.1021/ja016652k
19. Tang, Y.; Ghirlanda, G.; Petka, W. A.; Nakajima, T.; DeGrado, W. F.; Tirrell, D. A. *Angew. Chem., Int. Ed.* **2001,** *40,* 1494–1496. doi:10.1002/1521-3773(20010417)40:8<1494::AID-ANIE1494>3.0.CO;2-X
20. Tang, Y.; Ghirlanda, G.; Vaidehi, N.; Kua, J.; Mainz, D. T.; Goddard, W. A., III; DeGrado, W. F.; Tirrell, D. A. *Biochemistry* **2001,** *40,* 2790–2796. doi:10.1021/bi0022588
21. Yoder, N. C.; Kumar, K. *Chem. Soc. Rev.* **2002,** *31,* 335–341. doi:10.1039/b201097f
22. Bilgiçer, B.; Xing, X.; Kumar, K. *J. Am. Chem. Soc.* **2001,** *123,* 11815–11816. doi:10.1021/ja016767o
23. Meng, H.; Kumar, K. *J. Am. Chem. Soc.* **2007,** *129,* 15615–15622. doi:10.1021/ja075373f
24. Deacon, C. F.; Nauck, M. A.; Toft-Nielsen, M.; Pridal, L.; Willms, B.; Holst, J. J. *Diabetes* **1995,** *44,* 1126–1131. doi:10.2337/diab.44.9.1126
25. Holst, J. J.; Deacon, C. F. *Curr. Opin. Pharmacol.* **2004,** *4,* 589–596. doi:10.1016/j.coph.2004.08.005
26. Drucker, D. J. *Curr. Pharm. Des.* **2001,** *7,* 1399–1412. doi:10.2174/1381612013397401
27. Meng, H.; Krishnaji, S. T.; Beinborn, M.; Kumar, K. *J. Med. Chem.* **2008,** *51,* 7303–7307. doi:10.1021/jm8008579
28. Akçay, G.; Kumar, K. *J. Fluorine Chem.* **2009,** *130,* 1178–1182. doi:10.1016/j.jfluchem.2009.09.002
29. Gottler, L. M.; Lee, H.-Y.; Shelburne, C. E.; Ramamoorthy, A.; Marsh, E. N. G. *ChemBioChem* **2008,** *9,* 370–373. doi:10.1002/cbic.200700643
30. Voloshchuk, N.; Zhu, A. Y.; Snydacker, D.; Montclare, J. K. *Bioorg. Med. Chem. Lett.* **2009,** *19,* 5449–5451. doi:10.1016/j.bmcl.2009.07.093
31. Budisa, N.; Wenger, W.; Wiltschi, B. *Mol. BioSyst.* **2010,** *6,* 1630–1639. doi:10.1039/c002256j
32. Bordusa, F.; Dahl, C.; Jakubke, H.-D.; Burger, K.; Koksch, B. *Tetrahedron: Asymmetry* **1999,** *10,* 307–313. doi:10.1016/S0957-4166(98)00508-4
33. Koksch, B.; Sewald, N.; Burger, K.; Jakubke, H.-D. *Amino Acids* **1996,** *11,* 425–434. doi:10.1007/BF00807946
34. Koksch, B.; Sewald, N.; Hofmann, H.-J.; Burger, K.; Jakubke, H.-D. *J. Pept. Sci.* **1997,** *3,* 157–167. doi:10.1002/(SICI)1099-1387(199705)3:3<157::AID-PSC94>3.0.CO;2-W
35. Smits, R.; Koksch, B. *Curr. Top. Med. Chem.* **2006,** *6,* 1483–1498. doi:10.2174/156802606777951055
36. Thust, S.; Koksch, B. *J. Org. Chem.* **2003,** *68,* 2290–2296. doi:10.1021/jo020613p

37. Thust, S.; Koksch, B. *Tetrahedron Lett.* **2004,** *45,* 1163–1165. doi:10.1016/j.tetlet.2003.12.007
38. Sewald, N.; Hollweck, W.; Mütze, K.; Schierlinger, C.; Seymour, L. C.; Gaa, K.; Burger, K.; Koksch, B.; Jakubke, H. D. *Amino Acids* **1995,** *8,* 187–194. doi:10.1007/BF00806491
39. Asante, V.; Mortier, J.; Schlüter, H.; Koksch, B. *Bioorg. Med. Chem.* **2013,** *21,* 3542–3546. doi:10.1016/j.bmc.2013.03.051
40. Asante, V.; Mortier, J.; Wolber, G.; Koksch, B. *Amino Acids* **2014,** *46,* 2733–2744. doi:10.1007/s00726-014-1819-7
41. Schechter, I.; Berger, A. *Biochem. Biophys. Res. Commun.* **1967,** *27,* 157–162. doi:10.1016/S0006-291X(67)80055-X
42. Davies, D. R. *Annu. Rev. Biophys. Biophys. Chem.* **1990,** *19,* 189–215. doi:10.1146/annurev.bb.19.060190.001201
43. Zhao, Y. H.; Abraham, M. H.; Zissimos, A. M. *J. Org. Chem.* **2003,** *68,* 7368–7373. doi:10.1021/jo034808o
44. Erdbrink, H.; Nyakatura, E. K.; Huhmann, S.; Gerling, U. I. M.; Lentz, D.; Koksch, B.; Czekelius, C. *Beilstein J. Org. Chem.* **2013,** *9,* 2009–2014. doi:10.3762/bjoc.9.236
45. Samsonov, S. A.; Salwiczek, M.; Anders, G.; Koksch, B.; Pisabarro, M. T. *J. Phys. Chem. B* **2009,** *113,* 16400–16408. doi:10.1021/jp906402b
46. Blow, D. M.; Birktoft, J. J.; Hartley, B. S. *Nature* **1969,** *221,* 337–340. doi:10.1038/221337a0
47. Blow, D. M. The Structure of Chymotrypsin. In *The Enzymes;* Paul, D. B., Ed.; Academic Press, 1971; Vol. 3, pp 185–212. doi:10.1016/S1874-6047(08)60397-2
48. Derewenda, Z. S.; Derewenda, U.; Kobos, P. M. *J. Mol. Biol.* **1994,** *241,* 83–93. doi:10.1006/jmbi.1994.1475
49. Polgár, L. *Cell. Mol. Life Sci.* **2005,** *62,* 2161–2172. doi:10.1007/s00018-005-5160-x
50. Fruton, J. S. The Specificity and Mechanism of Pepsin Action. In *Advances in Enzymology and Related Areas of Molecular Biology;* Nord, F. F., Ed.; John Wiley & Sons, Inc., 1970; Vol. 33, pp 401–443. doi:10.1002/9780470122785.ch9
51. Fruton, J. S. Pepsin. In *The Enzymes;* Paul, D. B., Ed.; Academic Press, 1971; Vol. 3, pp 119–164. doi:10.1016/S1874-6047(08)60395-9
52. Dunn, B. M. *Chem. Rev.* **2002,** *102,* 4431–4458. doi:10.1021/cr010167q
53. Antonov, V. K. New Data on Pepsin Mechanism and Specificity. In *Acid Proteases:Structure, Function, and Biology;* Tang, J., Ed.; Springer US: Boston, MA, 1977; pp 179–198. doi:10.1007/978-1-4757-0719-9_11
54. Powers, J. C.; Harley, A. D.; Myers, D. V. Subsite Specificity of Porcine Pepsin. In *Acid Proteases:Structure, Function, and Biology;* Tang, J., Ed.; Springer US: Boston, MA, 1977; Vol. 92, pp 141–157. doi:10.1007/978-1-4757-0719-9_9
55. Largman, C.; Brodrick, J. W.; Geokas, M. C. *Biochemistry* **1976,** *15,* 2491–2500. doi:10.1021/bi00656a036
56. Shotton, D. M. Elastase. *Methods in Enzymology;* Academic Press, 1970; Vol. 19, pp 113–140. doi:10.1016/0076-6879(70)19009-4
57. Sweeney, P. J.; Walker, J. M. Proteinase K (EC 3.4.21.14). In *Enzymes of Molecular Biology;* Burrell, M. M., Ed.; Humana Press: Totowa, NJ, 1993; pp 305–311. doi:10.1385/0-89603-234-5:305
58. Czapinska, H.; Otlewski, J. *Eur. J. Biochem.* **1999,** *260,* 571–595. doi:10.1046/j.1432-1327.1999.00160.x
59. Hedstrom, L. *Chem. Rev.* **2002,** *102,* 4501–4524. doi:10.1021/cr000033x
60. Sweeney, P. J.; Walker, J. M. Proteolytic Enzymes for Peptide Production. In *Enzymes of Molecular Biology;* Burrell, M. M., Ed.; Humana Press: Totowa, NJ, 1993; pp 277–303. doi:10.1385/0-89603-234-5:277
61. Brady, K.; Abeles, R. H. *Biochemistry* **1990,** *29,* 7608–7617. doi:10.1021/bi00485a010
62. Schellenberger, V.; Jakubke, H.-D. *Biochim. Biophys. Acta, Protein Struct. Mol. Enzymol.* **1986,** *869,* 54–60. doi:10.1016/0167-4838(86)90309-2
63. Schellenberger, V.; Turck, C. W.; Rutter, W. J. *Biochemistry* **1994,** *33,* 4251–4257. doi:10.1021/bi00180a020
64. Ye, S.; Loll, B.; Berger, A. A.; Mülow, U.; Alings, C.; Wahl, M. C.; Koksch, B. *Chem. Sci.* **2015,** *6,* 5246–5254. doi:10.1039/C4SC03227F
65. Antal, J.; Pál, G.; Asbóth, B.; Buzás, Z.; Patthy, A.; Gráf, L. *Anal. Biochem.* **2001,** *288,* 156–167. doi:10.1006/abio.2000.4886
66. Sampath-Kumar, P. S.; Fruton, J. S. *Proc. Natl. Acad. Sci. U. S. A.* **1974,** *71,* 1070–1072. doi:10.1073/pnas.71.4.1070
67. Fruton, J. S. *Acc. Chem. Res.* **1974,** *7,* 241–246. doi:10.1021/ar50080a001
68. Hamuro, Y.; Coales, S. J.; Molnar, K. S.; Tuske, S. J.; Morrow, J. A. *Rapid Commun. Mass Spectrom.* **2008,** *22,* 1041–1046. doi:10.1002/rcm.3467
69. Rao, C.; Dunn, B. M. Evidence for Electrostatic Interactions in the S2 Subsite of Porcine Pepsin. In *Aspartic Proteinases: Structure, Function, Biology, and Biomedical Implications;* Takahashi, K., Ed.; Springer US: Boston, MA, 1995; pp 91–94. doi:10.1007/978-1-4615-1871-6_10
70. Fujinaga, M.; Chernaia, M. M.; Mosimann, S. C.; James, M. N. G.; Tarasova, N. I. *Protein Sci.* **1995,** *4,* 960–972. doi:10.1002/pro.5560040516
71. Kageyama, T. *Cell. Mol. Life Sci.* **2002,** *59,* 288–306. doi:10.1007/s00018-002-8423-9
72. Dunn, B. M.; Hung, S.-H. *Biochim. Biophys. Acta, Protein Struct. Mol. Enzymol.* **2000,** *1477,* 231–240. doi:10.1016/S0167-4838(99)00275-7
73. Naughton, M. A.; Sanger, F. *Biochem. J.* **1961,** *78,* 156–163. doi:10.1042/bj0780156
74. Renaud, A.; Lestienne, P.; Hughes, D. L.; Bieth, J. G.; Dimicoli, J. L. *J. Biol. Chem.* **1983,** *258,* 8312–8316.
75. Qasim, M. A. *Protein Pept. Lett.* **2014,** *21,* 164–170. doi:10.2174/09298665113206660093
76. Atlas, D. *J. Mol. Biol.* **1975,** *93,* 39–48. doi:10.1016/0022-2836(75)90358-7
77. Atlas, D.; Levit, S.; Schechter, I.; Berger, A. *FEBS Lett.* **1970,** *11,* 281–283. doi:10.1016/0014-5793(70)80548-8
78. Ebeling, W.; Hennrich, N.; Klockow, M.; Metz, H.; Orth, H. D.; Lang, H. *Eur. J. Biochem.* **1974,** *47,* 91–97. doi:10.1111/j.1432-1033.1974.tb03671.x
79. Georgieva, D.; Genov, N.; Voelter, W.; Betzel, C. *Z. Naturforsch., C: J. Biosci.* **2006,** *61,* 445–452. doi:10.1515/znc-2006-5-623
80. Morihara, K.; Tsuzuki, H. *Agric. Biol. Chem.* **1975,** *39,* 1489–1492. doi:10.1080/00021369.1975.10861790
81. Brömme, D.; Peters, K.; Fink, S.; Fittkau, S. *Arch. Biochem. Biophys.* **1986,** *244,* 439–446. doi:10.1016/0003-9861(86)90611-9
82. Kraus, E.; Femfert, U. *Hoppe-Seyler's Z. Physiol. Chem.* **1976,** *357,* 937–947. doi:10.1515/bchm2.1976.357.2.937
83. Betzel, C.; Singh, T. P.; Visanji, M.; Peters, K.; Fittkau, S.; Saenger, W.; Wilson, K. S. *J. Biol. Chem.* **1993,** *268,* 15854–15858.
84. Wolf, W. M.; Bajorath, J.; Müller, A.; Raghunathan, S.; Singh, T. P.; Hinrichs, W.; Saenger, W. *J. Biol. Chem.* **1991,** *266,* 17695–17699.
85. Betzel, C.; Bellemann, M.; Pal, G. P.; Bajorath, J.; Saenger, W.; Wilson, K. S. *Proteins: Struct., Funct., Genet.* **1988,** *4,* 157–164. doi:10.1002/prot.340040302

86. Kraus, E.; Kiltz, H.-H.; Femfert, U. F. *Hoppe-Seyler's Z. Physiol. Chem.* **1976,** *357,* 233–237. doi:10.1515/bchm2.1976.357.1.233

License and Terms

BEILSTEIN JOURNAL OF ORGANIC CHEMISTRY

The synthesis of the 2,3-difluorobutan-1,4-diol diastereomers

Robert Szpera, Nadia Kovalenko, Kalaiselvi Natarajan, Nina Paillard and Bruno Linclau*

Full Research Paper

Open Access

Address:
Chemistry, University of Southampton, Highfield, Southampton SO17 1BJ, United Kingdom

Email:
Bruno Linclau* - bruno.linclau@soton.ac.uk

* Corresponding author

Keywords:
acetal isomerization; deoxyfluorination; epoxide opening; fluorinated building block; vicinal difluoride

Beilstein J. Org. Chem. **2017,** *13,* 2883–2887.
doi:10.3762/bjoc.13.280

Received: 05 October 2017
Accepted: 13 December 2017
Published: 27 December 2017

This article is part of the Thematic Series "Organo-fluorine chemistry IV".

Guest Editor: D. O'Hagan

Abstract

The diastereoselective synthesis of fluorinated building blocks that contain chiral fluorine substituents is of interest. Here we describe optimisation efforts in the synthesis of *anti*-2,3-difluorobutane-1,4-diol, as well as the synthesis of the corresponding *syn*-diastereomer. Both targets were synthesised using an epoxide opening strategy.

Introduction

The introduction of fluorine in organic compounds usually results in the modification of a range of chemical, physical and biological properties [1]. Fluorine incorporation is therefore a common strategy to optimise the properties of drugs/agrochemicals, as well as materials [2-6].

Many methods exist for the stereoselective introduction of the C–F group [7-11]. An alternative and often time-efficient approach is the use of fluorinated building blocks, where fluorine is introduced as part of a carbon containing fragment, sometimes also bearing other functionality [12,13]. The development of novel fluorinated building blocks is therefore of interest, particularly those that can be synthesised conveniently on a multigram scale. Interestingly, the majority of currently commercially available fluorinated building blocks do not contain stereogenic C–F bonds.

The *vicinal*-difluoride motif is known to exert conformational control through the fluorine *gauche* effect [14,15], and so building blocks containing this motif are of interest [16,17]. We have previously reported on the gram-scale synthesis of *meso*-2,3-difluorobutane-1,4-diol (*anti*-**5**) starting from commercially available *cis*-but-2-ene-1,4-diol (Scheme 1) [17]. The *vicinal*-difluoride group was introduced by a two-step sequence, with initial nucleophilic epoxide [18] opening by a fluoride source [19], followed by nucleophilic deoxyfluorination [9-11].

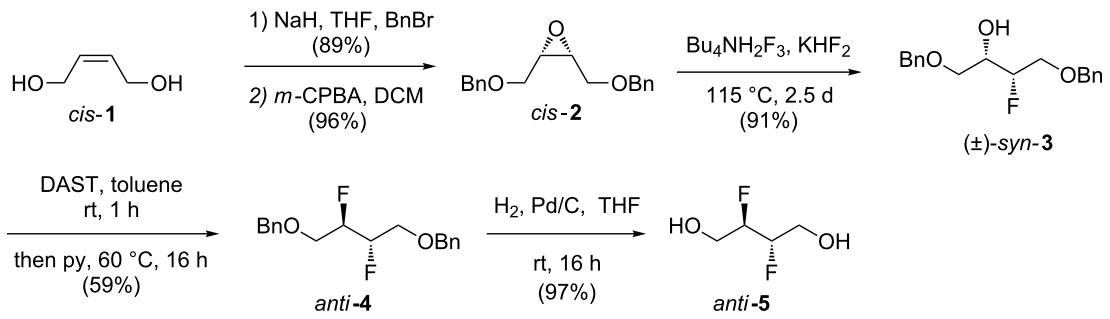

Scheme 1: The synthesis of *anti*-2,3-difluorobutan-1,4-diol (*anti*-**5**) [17].

In this contribution, we report on work directed at the further optimisation of the synthesis of *anti*-**5**, as well as on a gram-scale synthesis of its diastereomer (±)-*syn*-**5**, a novel compound.

Results and Discussion

Optimisation of the synthesis of *anti*-5

While the synthesis of *anti*-**5** as described in Scheme 1 was high-yielding [17], two disadvantages were apparent. First, the epoxide opening takes 2.5 days at 115 °C and uses an expensive fluoride source (Landini's reagent [18]: $Bu_4NH_2F_3$). It was found that $Bu_4NH_2F_3$ made in-house gave significantly reduced yields. Second, the use of the benzyl ether protecting group resulted in a significant increase in mass, and therefore, chromatographic purification of the protected intermediates upon scale-up was inconvenient.

As previously reported [17], epoxide opening of *cis*-**2** with Olah's reagent (HF·py) led to an 80% yield of the fluorohydrin after just three hours, however, the product was obtained as a mixture of both the *syn*- and *anti*-diastereomers. Whilst no mechanistic studies were conducted, it is possible that competing S_N1 and/or anchimeric assistance by the benzyloxy group occurred. Work by Schlosser has shown that 1,2-disubstituted epoxide opening with $Et_3N{\cdot}3HF$ proceeds with excellent diastereoselectivity [19]. $Et_3N{\cdot}3HF$ is less acidic than Olah's reagent, disfavouring S_N1 and rearrangement pathways [20,21]. Indeed, the use of this reagent for the epoxide opening of *cis*-**2** led to (±)-*syn*-**3** in excellent yield (Scheme 2), with no significant isomerisation (see Supporting Information File 1). Epoxide opening with the recently described TBAF/KHF_2 [22] was also possible, but in lower yield (75%, not shown). Incidentally, it was also found that the subsequent deoxofluorination reaction was somewhat higher yielding when DAST was added at rt over just 5 min, immediately followed by the addition of pyridine and heating at 70 °C.

It should be noted that DAST is known to undergo decomposition at temperatures above 90 °C [23]. Here we use DAST in solution. The initial mixing is at room temperature, and heating doesn't exceed 70 °C, and therefore, the procedure is deemed to have low risk. Nonetheless, care must be taken and the reaction was run with the protection of a blast shield.

In order to reduce the relative contribution of the protecting group to the overall weight of the intermediates, the use of an acetonide was explored. Given the starting alkene was *cis*-configured, its introduction was possible from the start (Scheme 3).

Hence, following literature procedures [24-26], the reaction of *cis*-**1** with 2,2-dimethoxypropane and subsequent epoxidation led to **7**. However, epoxide opening with $Et_3N{\cdot}3HF$ was accompanied by acetonide rearrangement to afford fluorohydrin (±)-**9**, containing the thermodynamically favoured five-membered ring [24]. This is clearly indicated by the appearance of a doublet of doublets for the primary alcohol OH proton. DAST-mediated deoxofluorination then led to (±)-**10**, in which an alkyl fluoride signal at −232 ppm confirmed the presence of a primary fluoride.

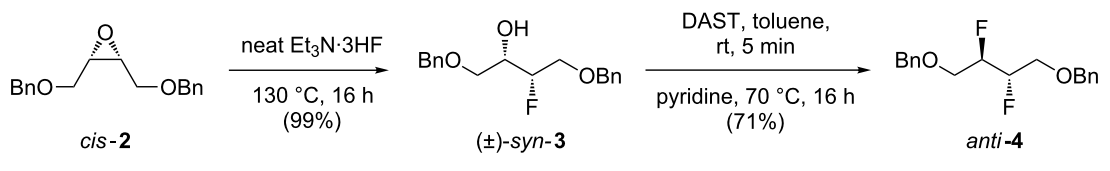

Scheme 2: Improved epoxide opening and deoxofluorination conditions.

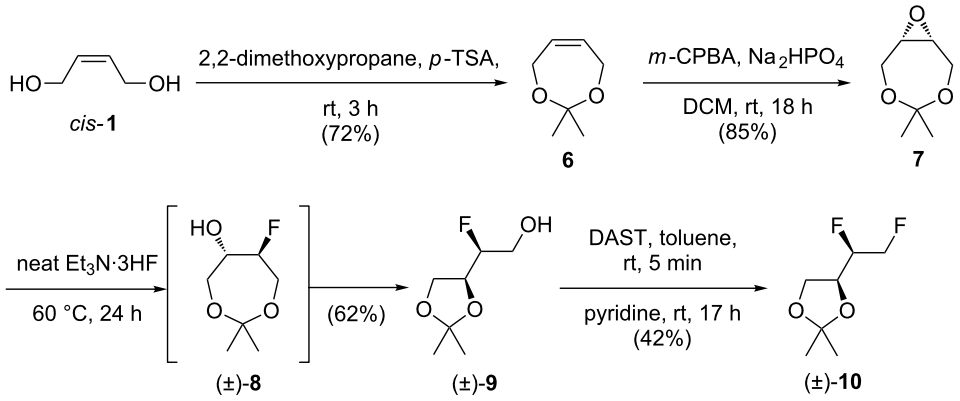

Scheme 3: Attempted synthesis of *anti*-**5** via acetonide protection.

Hence, non-acidic epoxide opening conditions were investigated to circumvent the rearrangement (Scheme 4). Both the use of $Bu_4NH_2F_3$ [18] and of the TBAF/KHF_2 reagent combination [22] were successful (56% and 64%, respectively). While subsequent fluorination using PyFluor only led to the formation of the 2-pyridinesulfonate intermediate (±)-**12**, the use of DAST at 60 °C proved successful. The difluoride *meso*-**11** was not isolated due to its low boiling point, but was immediately subjected to acid hydrolysis to give *anti*-**5**. Unfortunately, the yield for this two-step process was only moderate (30%).

Synthesis of (±)-*syn*-5

The synthesis of (±)-*syn*-**5** (Scheme 5) was achieved starting from the *trans*-configured but-2-ene-1,4-diol (**1**), which is not commercially available in geometrically pure form.

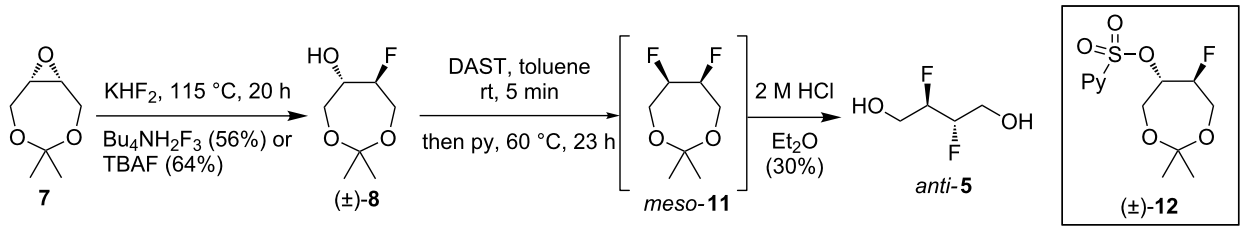

Scheme 4: Completion of the synthesis of *anti*-**5**.

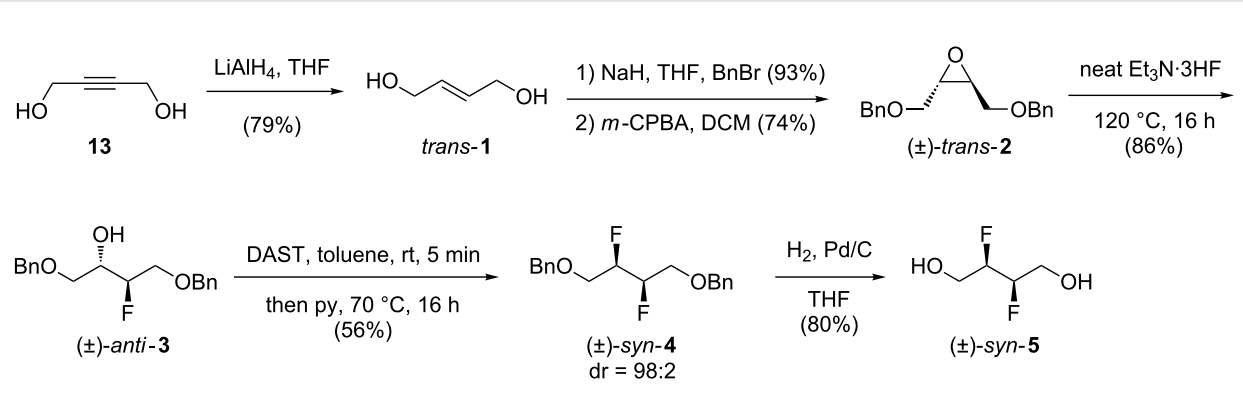

Scheme 5: Synthesis of (±)-*syn*-**5**.

Hence, according to literature procedures, reduction of 1,4-butynediol (**13**) by $LiAlH_4$ to give *trans*-**1** [27] was followed by benzylation [28] and epoxidation with *m*-CPBA to give (±)-*trans*-**2** [28]. When the reaction was performed on a small scale, excess *m*-CPBA and the byproduct 3-chlorobenzoic acid were removed by extraction with a saturated $Na_2S_2O_3$ solution. However, on scale-up this proved inconvenient due to the large volumes of solvent required, and so these impurities were precipitated out the reaction mixture by cooling to 0 °C and collected by filtration through Celite. After work-up, the obtained epoxide was of high purity and no additional chromatographic purification was required, which was convenient on scale. The reaction of (±)-*trans*-**2** with neat $Et_3N{\cdot}3HF$ at 120 °C for 16 h led, after aqueous work-up, to (±)-*anti*-**3** in high diastereomeric purity (see Supporting Information File 1). The ^{19}F shift of −195.3 ppm is different compared to that of (±)-*syn*-**3** (−204.4 ppm) [17]. Upon scale-up of the reaction to 10 g of (±)-*trans*-**2**, a similarly high yield of 90% (crude) was obtained, which again could be used directly in the next step without purification. Conversion of fluorohydrin (±)-*anti*-**3** to difluoride (±)-*syn*-**4** under the same conditions as shown in Scheme 2 resulted in 56% yield after column chromatography. ^{19}F NMR analysis of the crude product showed a dr of 98:2 in favour of (±)-*syn*-**4**. However, given a diastereomerically pure starting material was used, this indicates that S_N1 or neighbouring group participation pathways may have occurred, although only to a very small extent. Separation of the diastereomers proved not possible. Finally, deprotection of (±)-*syn*-**4** by palladium catalysed hydrogenolysis led to (±)-*syn*-**5**. Recrystallization to remove the minor diastereomer was not successful.

Conclusion

A gram-scale synthesis of both *syn*- and *anti*-2,3-difluorobutan-1,4-diol diastereomers is described. The key steps involve epoxide opening and subsequent deoxyfluorination. For the first step, $Et_3N{\cdot}3HF$ was found to be the best reagent, giving an excellent yield with no formation of diastereomeric byproducts. Unfortunately it was found that the subsequent DAST-mediated deoxyfluorination gives rise to a small amount of the undesired diastereomer. The primary alcohol groups require protection, for which the benzyl group has been employed. While this group is effective for this purpose, there is a significant mass increase upon its introduction (roughly three fold increase). An investigation to use the much smaller acetonide protecting group, which can be used for the *cis*-1,4-butenediol starting material, was carried out. It was found that the use of $Et_3N{\cdot}3HF$ for the epoxide opening step also lead to acetal rearrangement, leading to a more stable 1,3-dioxolane ring. While the use of $Bu_4NH_2F_3/KHF_2$ and TBAF/KHF_2 achieves epoxide opening without acetonide rearrangement, the subsequent deoxyfluorination/deprotection sequence is low yielding (30%). Overall, the protocols provided will be of use for the large-scale synthesis of both *syn*- and *anti*-2,3-difluorobutan-1,4-diol building blocks.

Supporting Information

Supporting Information File 1

Experimental part and NMR spectra.
[http://www.beilstein-journals.org/bjoc/content/supplementary/1860-5397-13-280-S1.pdf]

Acknowledgements

We thank the University of Southampton and the EPSRC (core capability EP/K039466/1) for funding.

ORCID® iDs

Robert Szpera - https://orcid.org/0000-0003-1351-1750
Nina Paillard - https://orcid.org/0000-0003-0109-5403
Bruno Linclau - https://orcid.org/0000-0001-8762-0170

References

1. Gillis, E. P.; Eastman, K. J.; Hill, M. D.; Donnelly, D. J.; Meanwell, N. A. *J. Med. Chem.* **2015,** *58,* 8315. doi:10.1021/acs.jmedchem.5b00258
2. Zhou, Y.; Wang, J.; Gu, Z.; Wang, S.; Zhu, W.; Aceña, J. L.; Soloshonok, V. A.; Izawa, K.; Liu, H. *Chem. Rev.* **2016,** *116,* 422. doi:10.1021/acs.chemrev.5b00392
3. Wang, J.; Sánchez-Roselló, M.; Aceña, J. L.; del Pozo, C.; Sorochinsky, A. E.; Fustero, S.; Soloshonok, V. A.; Liu, H. *Chem. Rev.* **2014,** *114,* 2432. doi:10.1021/cr4002879
4. Fujiwara, T.; O'Hagan, D. *J. Fluorine Chem.* **2014,** *167,* 16. doi:10.1016/j.jfluchem.2014.06.014
5. O'Hagan, D. *J. Fluorine Chem.* **2010,** *131,* 1071. doi:10.1016/j.jfluchem.2010.03.003
6. Kirsch, P.; Bremer, M. *ChemPhysChem* **2010,** *11,* 357. doi:10.1002/cphc.200900745
7. Champagne, P. A.; Desroches, J.; Hamel, J.-D.; Vandamme, M.; Paquin, J.-F. *Chem. Rev.* **2015,** *115,* 9073. doi:10.1021/cr500706a
8. Liang, T.; Neumann, C. N.; Ritter, T. *Angew. Chem., Int. Ed.* **2013,** *52,* 8214. doi:10.1002/anie.201206566
9. Yerien, D. E.; Bonesi, S.; Postigo, A. *Org. Biomol. Chem.* **2016,** *14,* 8398. doi:10.1039/C6OB00764C
10. Al-Maharik, N.; O'Hagan, D. *Aldrichimica Acta* **2011,** *44,* 65.
11. Hu, W.-L.; Hu, X.-G.; Hunter, L. *Synthesis* **2017,** *49,* 4917. doi:10.1055/s-0036-1590881
12. Percy, J. M. Building Block Approaches to Aliphatic Organofluorine Compounds. In *Organofluorine Chemistry: Techniques and Synthons;* Chambers, R. D., Ed.; Topics in Current Chemistry, Vol. 193; Springer: Berlin, Heidelberg, 1997; pp 131–196.
13. Harsanyi, A.; Sandford, G. *Org. Process Res. Dev.* **2014,** *18,* 981. doi:10.1021/op500141c
14. Thiehoff, C.; Rey, Y. P.; Gilmour, R. *Isr. J. Chem.* **2017,** *57,* 92. doi:10.1002/ijch.201600038
15. Hunter, L. *Beilstein J. Org. Chem.* **2010,** *6,* No. 38. doi:10.3762/bjoc.6.38
16. O'Hagan, D.; Rzepa, H. S.; Schüler, M.; Slawin, A. M. Z. *Beilstein J. Org. Chem.* **2006,** *2,* No. 19. doi:10.1186/1860-5397-2-19

17. Linclau, B.; Leung, L.; Nonnenmacher, J.; Tizzard, G. *Beilstein J. Org. Chem.* **2010,** *6,* No. 62. doi:10.3762/bjoc.6.62
18. Landini, D.; Penso, M. *Tetrahedron Lett.* **1990,** *31,* 7209. doi:10.1016/S0040-4039(00)97281-2
19. Hamatani, T.; Matsubara, S.; Matsuda, H.; Schlosser, M. *Tetrahedron* **1988,** *44,* 2875. doi:10.1016/S0040-4020(88)90023-3
20. Haufe, G. *J. Fluorine Chem.* **2004,** *125,* 875. doi:10.1016/j.jfluchem.2004.01.023
21. Wölker, D.; Haufe, G. *J. Org. Chem.* **2002,** *67,* 3015. doi:10.1021/jo016331r
22. Yan, N.; Lei, Z.-W.; Su, J.-K.; Liao, W.-L.; Hu, X.-G. *Chin. Chem. Lett.* **2016,** *28,* 467. doi:10.1016/j.cclet.2016.10.006
23. Lal, G. S.; Pez, G. P.; Pesaresi, R. J.; Prozonic, F. M.; Cheng, H. *J. Org. Chem.* **1999,** *64,* 7048. doi:10.1021/jo990566+
24. Elliott, W. J.; Fried, J. *J. Org. Chem.* **1976,** *41,* 2469. doi:10.1021/jo00876a027
25. Al-Dulayymi, A.; Li, X.; Neuenschwander, M. *Helv. Chim. Acta* **2000,** *83,* 1633. doi:10.1002/1522-2675(20000705)83:7<1633::AID-HLCA1633>3.0.CO;2-5
26. Mischitz, M.; Kroutil, W.; Wandel, U.; Faber, K. *Tetrahedron: Asymmetry* **1995,** *6,* 1261. doi:10.1016/0957-4166(95)00158-L
27. Organ, M. G.; Cooper, J. T.; Rogers, L. R.; Soleymanzadeh, F.; Paul, T. *J. Org. Chem.* **2000,** *65,* 7959. doi:10.1021/jo001045l
28. Hachiya, I.; Matsumoto, T.; Inagaki, T.; Takahashi, A.; Shimizu, M. *Heterocycles* **2010,** *82,* 449. doi:10.3987/COM-10-S(E)16

License and Terms

BEILSTEIN JOURNAL OF ORGANIC CHEMISTRY

Conformational preferences of α-fluoroketones may influence their reactivity

Graham Pattison

Full Research Paper

Open Access

Address:
Department of Chemistry, University of Warwick, Gibbet Hill Road, Coventry CV4 7AL, UK

Email:
Graham Pattison - graham.pattison@warwick.ac.uk

Keywords:
α-halogenated ketones; conformational analysis; reactivity; stereoelectronic effects

Beilstein J. Org. Chem. **2017,** *13,* 2915–2921.
doi:10.3762/bjoc.13.284

Received: 23 October 2017
Accepted: 12 December 2017
Published: 29 December 2017

This article is part of the Thematic Series "Organo-fluorine chemistry IV".

Guest Editor: D. O'Hagan

Abstract

Fluorine has been shown in many cases to impart specific and predictable effects on molecular conformation. Here it is shown that these conformational effects may have an influence on reactivity through studying the relative reactivity of various α-halogenated ketones towards borohydride reduction. These results demonstrate that the α-fluoro ketones are in fact a little less reactive than the corresponding α-chloro and α-bromo derivatives. It is suggested, supported by computation, that this effect is due to reactive conformations in which the C–X bond is orthogonal to the carbonyl group for good orbital overlap being disfavoured in the case of fluoro ketones.

Introduction

α-Halogenated ketones are widely used electrophiles in organic synthesis, being highly reactive in both nucleophilic addition to the carbonyl group and in S_N2 nucleophilic displacements [1]. Our research group has recently been exploring the synthesis and reactivity of α-fluorinated ketones [2-4] and here their reactivity relative to other halogenated ketones is compared.

It is well established that the halogen leaving groups in these substrates are highly activated by orbital overlap with the adjacent carbonyl group, making α-halogenated ketones one of the most reactive classes of electrophiles available to synthetic chemists for S_N2 substitution [5]. The orbital overlap in α-halogenated ketones also provides activation to the carbonyl group, making it more reactive towards nucleophilic addition than non-halogenated carbonyl compounds [6]. However, relatively little work has been performed previously to quantify the effects that different α-halogen atoms have on carbonyl reactivity.

This paper aims to examine some of the effects that α-halogenation can impart on carbonyl reactivity with a particular emphasis on the effects of α-fluorination. As the most electronegative element, fluorine is often involved in introducing

unusual properties to organic molecules, whether by its strong inductive effect, interactions of its tightly-held lone pairs or through the strong dipole moment it can induce in molecules [7].

To begin to quantify the effects of α-halogenation on carbonyl reactivity we wished to measure the relative reactivity of various α-halogenated ketones towards nucleophilic addition. As these are highly reactive systems obtaining rate profiles can be difficult due to the short time-scales for measurements, so instead relative reactivity was measured through a series of competition experiments. A competition experiment between two substrates stopped at low conversion (<20%) provides a good approximation for the relative initial rates of reaction of the two substrates through measurement of the relative amounts of the two products formed.

These competition reactions should proceed cleanly, with minimal byproduct formation, and in the case of examining the reactivity of the carbonyl group of α-halogenated ketones, should show very high regioselectivity for nucleophilic addition to the carbonyl group rather than nucleophilic displacement of the halogen atom. Another important consideration in this scenario is that the nucleophilic addition to the carbonyl group should not be reversible. The choice of nucleophile for study should take all of these important considerations into account. The nucleophilic addition of sodium borohydride to various α-halogenated ketones was therefore chosen for examination as borohydride addition is irreversible and shows a very high preference for direct addition to the carbonyl group.

Results and Discussion

The initial focus of this work was on comparing the reactivity of various α-monohalogenated ketones to examine the effects of different halogen atoms on the reactivity. The reactivity of α-fluoroacetophenone was compared to α-chloro- and α-bromoacetophenone in sodium borohydride reductions, using 0.2 equiv of $NaBH_4$ to 1.0 equiv of α-fluoroacetophenone and 1.0 equiv of the second α-haloacetophenone to ensure the reaction stopped at low conversion. The relative ratios of reduced products were then compared using ^1H NMR spectroscopy (Scheme 1). All results are the average of at least two repetitions, with the NMR integrals, set to the fluorinated peak equal to 1.00, consistent to at least ±0.1.

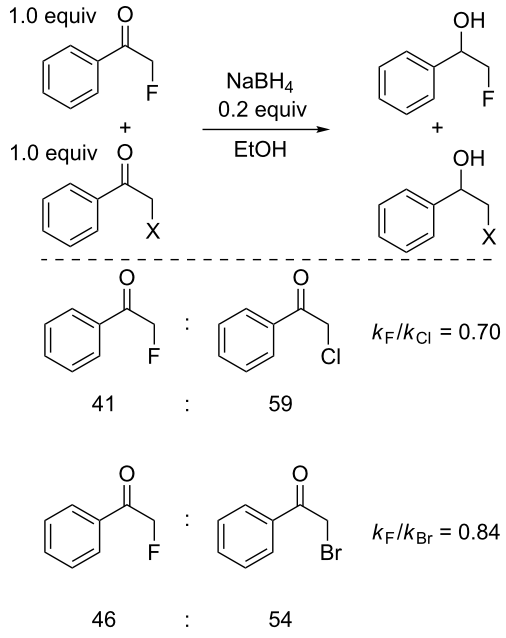

Scheme 1: Relative reactivity of α-fluoroacetophenone to α-chloroacetophenone and α-bromoacetophenone.

Interestingly, both experiments showed α-fluoroacetophenone to be less reactive than both α-chloroacetophenone and α-bromoacetophenone, with a slightly larger difference in reactivity for α-chloroacetophenone. The reactivity of α-iodoacetophenone was not examined as it proved to be unstable under the reaction conditions. This higher reactivity of the non-fluorinated ketones was not the expected outcome through simple arguments of electronegativity differences. Comparison of the reactivity of each α-haloacetophenone to non-halogenated acetophenone showed the halogenated derivatives to be significantly more reactive (no reduction of acetophenone could be observed) (Scheme 2).

Potential reasons behind the lower than expected reactivity of α-fluoroacetophenone were then considered. It is known that fluorine can dramatically influence the conformational prefer-

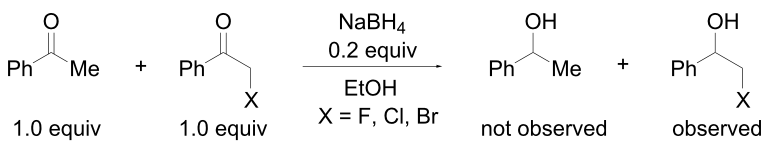

Scheme 2: Competitive reduction of haloacetophenones and acetophenone.

ences of molecules [8,9], so began by simulating the conformational energy profile of each α-haloacetophenone, calculating the energy of each compound as the carbon–halogen bond is rotated through 10° increments in both the gas phase and in ethanol as reaction solvent (Figure 1) [10].

The fluorinated acetophenone showed significant differences in conformational energy to the chlorinated and brominated variants. The energy minimum for α-fluoroacetophenone was displayed at an O=C–C–X dihedral angle of around 140° in the gas phase, whilst the chloro- and bromoacetophenones both showed minima around 110°. Highly polar conformations which place the C–X bond in the same plane as the carbonyl group were favoured in the polar solvent ethanol; indeed in ethanol the lowest energy conformation of α-fluoroacetophenone is calculated be a *cis*-conformation with a O=C–C–X dihedral angle of 0°. Figure 2 shows equivalent 3-dimensional views along the C–C bond between the carbonyl group and C–X bond emphasising the smaller dihedral angle preferred by the chlorinated derivative in the gas phase. Figure 3 compares the lowest energy conformations of α-fluoroacetophenone and α-chloro-acetophenone in the polar solvent ethanol. Experimental work by Olivato amongst others supports these conformational preferences [11-15]. IR spectroscopy was used to show an increased preference for a *cis* (0° dihedral angle) compared to a *gauche* (150°) conformation in α-fluoroacetophenone compared to α-chloroacetophenone [16].

This has significant implications for the orbital overlap in these systems as it would be expected that the best orbital overlap between the C=O π* orbital and C–X σ* orbital which is necessary for high reactivity would be achieved when the O=C–C–X dihedral angle is 90° (Figure 4). Previous calculations by Paddon-Row on nucleophilic additions to fluoroethanal and 2-fluoropropanal have suggested that additions to this conformation lead to the most stabilized transition state [17], whilst experimentally, nucleophilic addition of $NaBH_4$ to 2-fluoropropiophenone leads to the *anti*-diastereoisomer that would be expected by polar Felkin–Anh addition to this conformation [18]. However, around a 90° dihedral angle in the conformational energy profiles, the fluorinated derivative is around 10 kJ·mol^{-1} higher in relative energy than the brominated and chlorinated

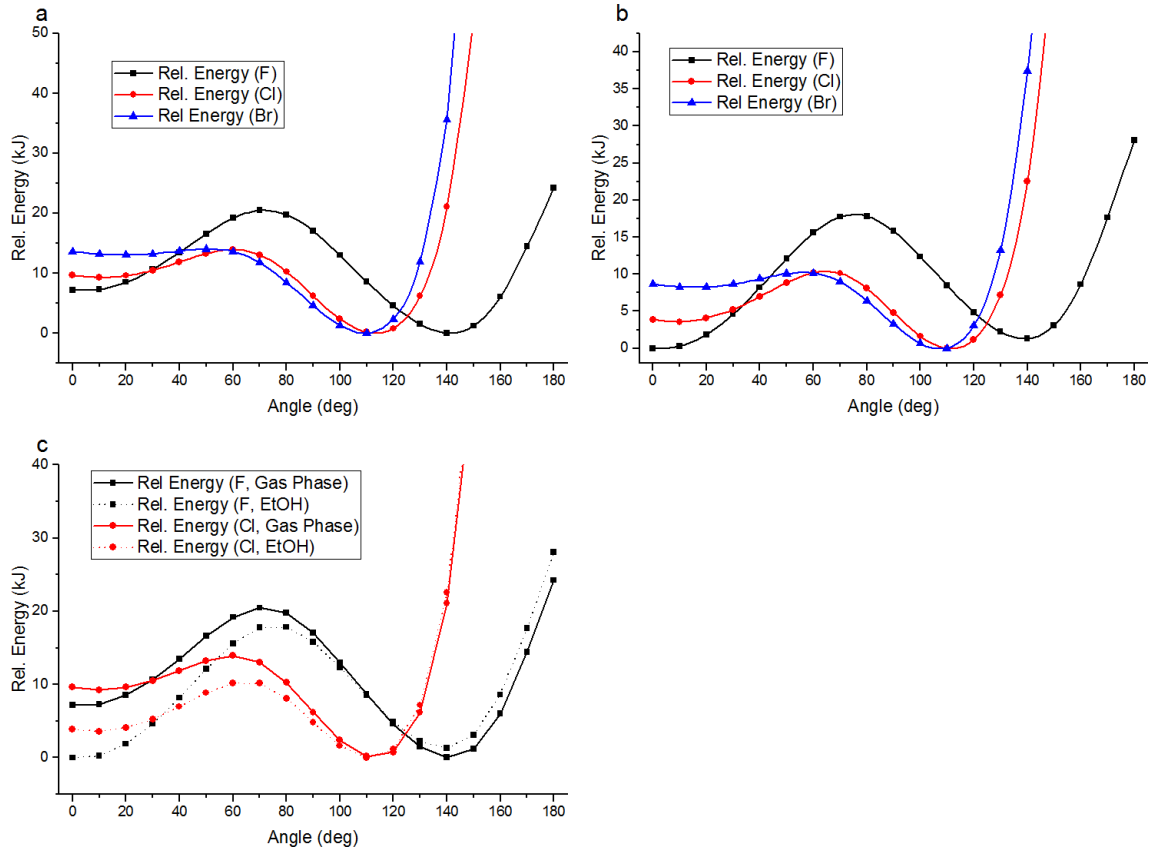

Figure 1: Conformational energy profiles of halogenated acetophenones (a) in gas phase; (b) in EtOH; (c) overlay of gas phase and EtOH for F and Cl.

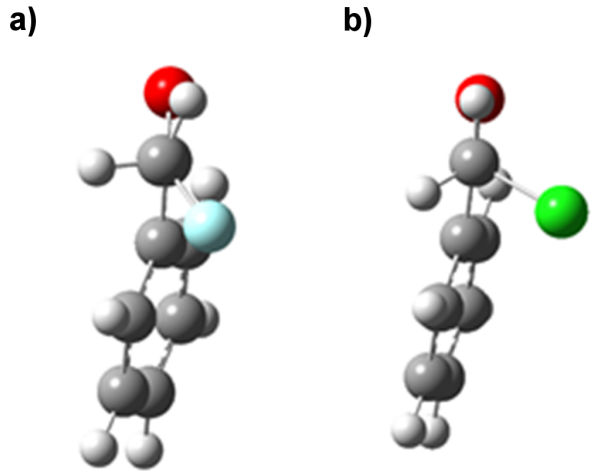

Figure 2: Optimised gas phase geometries of (a) α-fluoroacetophenone and (b) α-chloroacetophenone emphasising the smaller dihedral angle preferred by the chlorinated derivative.

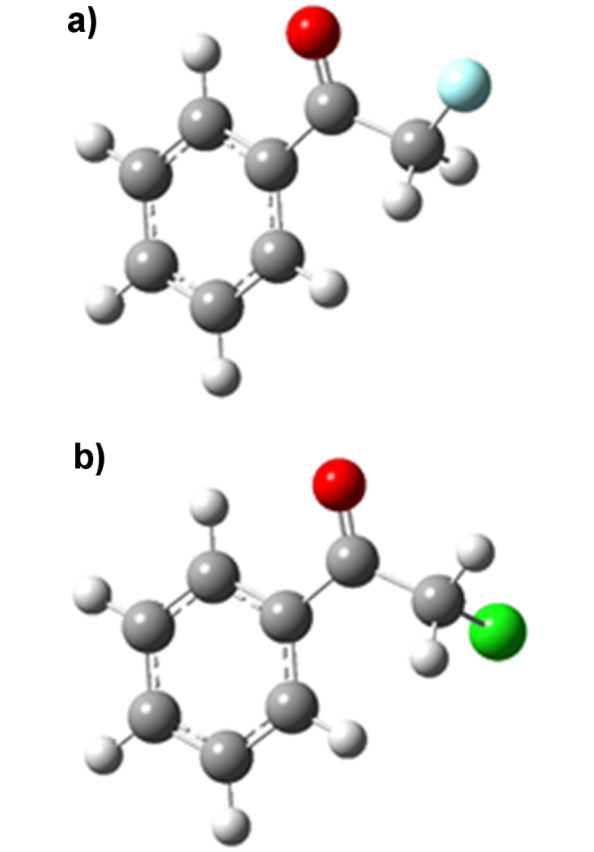

Figure 3: Most stable conformations of (a) α-fluoroacetophenone and (b) α-chloroacetophenone in ethanol.

analogues, suggesting that it will be energetically unfavourable for α-fluoroacetophenone to access these particularly reactive conformations.

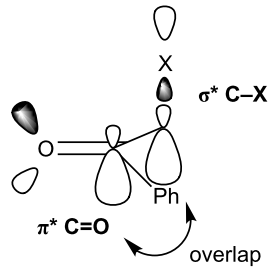

Figure 4: Expected reactive conformation of halo-acetophenones.

Orbital interactions with the C=O π* orbital are possible at dihedral angles other than 90°. For example in a *gauche* conformation (120–150° O=C–C–X dihedral angle), overlap between the halogen atom lone pairs and the C=O π* orbital is possible, weakening the π-bond and increasing the reactivity towards nucleophilic attack (Figure 5). It would be expected that of all the halogens, fluorine's lone pairs would overlap most strongly with the carbonyl π*-orbital and decrease its bond order. However, particularly in polar solvents like ethanol, it is the *cis* conformation (0° O=C–C–X dihedral angle) which is preferred for α-fluoroacetophenone, which places the C–F bond in the same plane as the C=O bond, making orbital interactions impossible. Although orbital interactions between chlorine's lone pairs and the C=O π* orbital are expected to be weak, at least α-chloro-acetophenone has a lowest energy *gauche* conformation where these orbital interactions are possible, which may provide some degree of electronic activation.

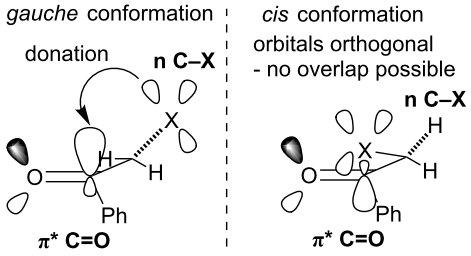

Figure 5: Orbital interactions in *gauche*- and *cis*-conformations of haloacetophenones.

The variability of the relative reactivity of α-fluoroacetophenone and α-chloroacetophenone with temperature were then investigated (Table 1). The same methodology using competition experiments stopped at low conversion was used at 20 °C temperature increments from 0 to 60 °C. This showed an increase in the relative reactivity of the fluorinated derivative as the temperature was increased. One potential reason for this is that increased conformational freedom at higher temperatures makes more reactive conformations more accessible to the fluorinated acetophenone.

Table 1: Relative reactivity of α-fluoroacetophenone and α-chloroacetophenone at different temperatures.

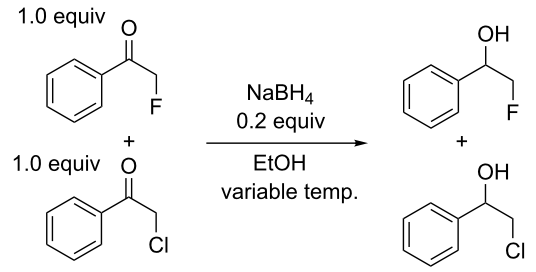

Temperature [°C]	k_F/k_{Cl}
0	0.58
20	0.70
40	0.77
60	0.86

Potential reasons for the different conformational preferences of the α-halogenated acetophenones were then examined. One possibility is that the increased electronegativity of fluorine induces a high dipole moment at small O=C–C–X dihedral angles and that therefore larger dihedral angles are favoured as this minimizes the molecule's overall dipole moment. However, computational analysis of the angular variation of the dipole moment of each α-haloacetophenone did not show a significant variation between the different halogens (Figure 6).

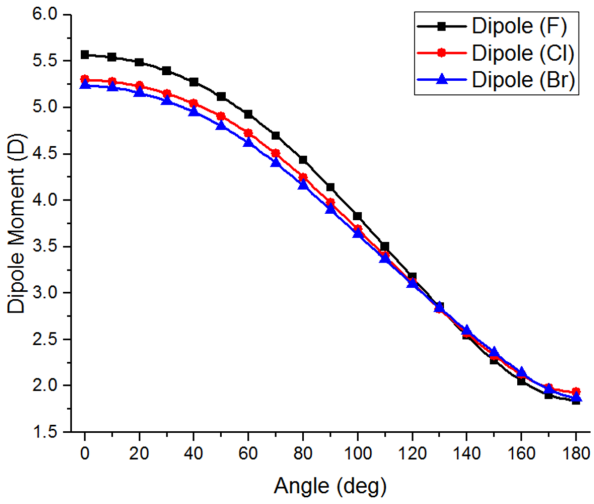

Figure 6: Variation of dipole moment with angle for haloacetophenones.

The highest energy conformations of α-haloacetophenones have a O=C–C–X dihedral angle of 60–70° and place the C–X bond roughly aligned with the π-system of the carbonyl group and aromatic ring (Figure 7). It may well be that in this conformation there is significant repulsion between the halogen lone pairs and the filled C=O π-orbital. The higher polarizability of higher halogens such as chlorine and bromine may be able to reduce this repulsion, however, the tightly held, non-polarizable lone pairs of fluorine are likely to experience this repulsive effect most strongly. The shorter C–F bond length may also play a role in this interaction, placing the fluorine atom closer to the carbonyl group. This will disfavour these conformations in the fluorinated derivatives, which also happen to be the most reactive conformations.

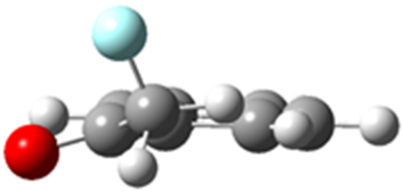

Figure 7: Highest energy conformation of fluoroacetophenone, emphasizing the closeness of approach of fluorine atom to carbonyl π-orbital.

We then wanted to establish whether this lower reactivity of α-fluoro ketones compared to α-chloro ketones was transferable to other systems than acetophenones, and chose to compare the reactivity of fluoroacetone and chloroacetone (Scheme 3). The higher volatility of the reduced products in this case meant the reactions were performed directly in deuterated methanol before taking NMR of the reaction mixture without isolation.

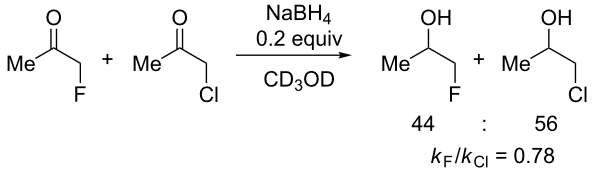

Scheme 3: Competitive reduction of fluoroacetone and chloroacetone.

This again showed the α-fluoroacetone to be slightly less reactive than the α-chloroacetone. A similar conformational analysis of the bond rotation of the O=C–C–X dihedral angle for the chloro and fluoro derivatives was performed (Figure 8). This showed that, whist both molecules were most stable in an *anti*-conformation [19-21], the barrier to rotation of fluoroacetone was significantly higher than of chloroacetone, and the reactive conformations in which the halogen was orthogonal to the carbonyl group for C–X σ*/C=O π* overlap were significantly

higher in energy for the fluorinated derivative. This offers further support to the theory that this may be a significant factor in slightly reducing reactivity of the fluorinated system relative to the chlorinated.

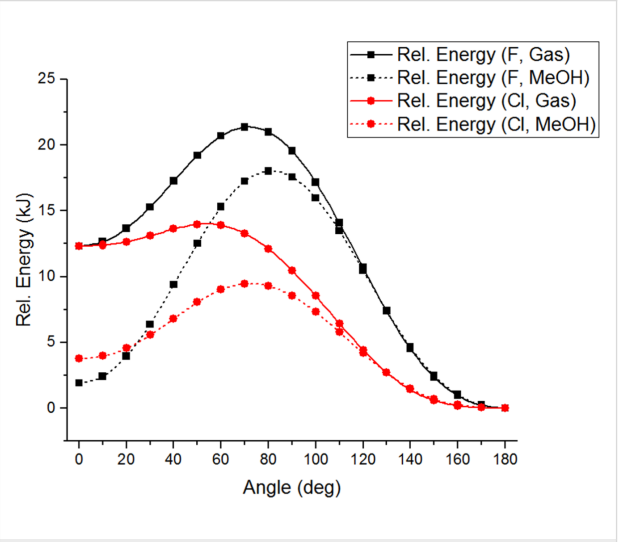

Figure 8: Conformational energy profiles of halogenated acetones in gas phase and in MeOH.

Again, as for the haloacetophenones, the *cis*-arrangement was significantly stabilized in methanol, particularly for fluoroacetone, although in this case a *trans*-arrangement was still more stable. Neither *cis*- nor *trans*-arrangements of the C=O and C–X bonds can offer any stabilization by donation of halogen lone pairs into the C=O π* orbital, so this orbital interaction is not relevant in the case of haloacetones. This conformational analysis is supported by previous work by Abraham and Rittner who used NMR coupling constants and theory to demonstrate that a *trans*-conformation of fluoroacetone is always most favourable, but that the energy difference to the *cis*-conformation decreases on solvation [22]. Work on related halo-acetaldehyde systems suggested that steric repulsions were the key contributing factor in determining these preferred conformations [23].

Finally, the conformational profiles of fluoroacetone and fluoroacetophenone were compared by overlaying on the same graph (Figure 9). This showed a similar maximum energy for both, around the same angle, supporting the hypothesis that this is due to repulsion of fluorine lone pairs with the carbonyl π-system. Between 80° and 140° dihedral angles fluoroacetophenone is stabilized relative to fluoroacetone, likely due to overlap between the carbonyl C=O π-orbital and the aromatic ring π-system beginning to develop. However, at high dihedral angles (150–180°) fluoroacetophenone is significantly destabilized, likely due to steric interactions between the fluorine atom and *ortho*-hydrogens of the aromatic ring.

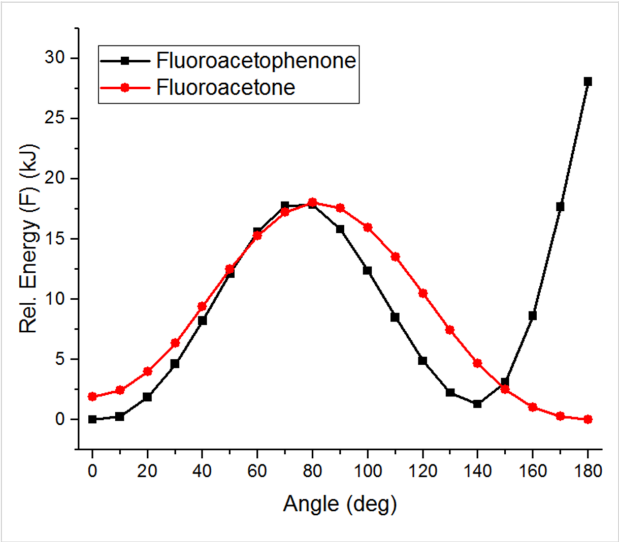

Figure 9: Overlay of conformational energy profiles of fluoroacetone and fluoroacetophenone.

Conclusion

The relative reactivity of various halogenated ketones in borohydride reduction have been studied, which established that the fluorinated derivatives display slightly lower reactivity than the chlorinated and brominated derivatives. This is the opposite that would be expected from simple electronegativity arguments and can be potentially explained by the higher energy barrier in the fluoro ketones to access reactive conformations which place C–X and C=O bonds at 90° to each other for optimal orbital overlap. The reason for this higher energy barrier in the fluorinated derivatives compared to other halogenated ketones is not fully understood, although could be related to repulsion between fluorine's lone pairs and the carbonyl π-system, which will be reduced for other halogens due to their higher polarizability. A final factor which may explain the unexpectedly lower reactivity of fluorinated ketones is that they show a high preference in polar solvents to attain a *cis*-conformation, which place C=O and C–F bonds in the same plane and unable to undergo favourable orbital interactions.

Experimental

NMR analysis was performed on a Bruker Avance III HD-400 system. Computational calculations were performed using the Gaussian-03 package using a MP2/6-311G++(d,p) basis set.

Procedure for competition experiments

Acetophenones. A mixture of 2-fluoroacetophenone (69.1 mg, 0.5 mmol) and either 2-chloroacetophenone (77.3 mg, 0.5 mmol) or 2-bromoacetophenone (99.5 mg, 0.5 mmol) was dissolved in ethanol (1 mL) and heated/cooled to the appropriate temperature. Sodium borohydride (3.8 mg, 0.1 mmol) was added and the mixture stirred for 15 minutes. After this

period HCl (1 M, 1 mL) was added, followed by diethyl ether (2 mL). The organic layer was separated, dried over $MgSO_4$ and evaporated. ^1H NMR in $CDCl_3$ was measured of this crude mixture.

Acetones. A mixture of chloroacetone (46.3 mg, 0.5 mmol) and fluoroacetone (38.0 mg, 0.5 mmol) was dissolved in CD_3OD at room temperature. Sodium borohydride (3.8 mg, 0.1 mmol) was added and the mixture stirred for 15 minutes. ^1H NMR was measured of this crude mixture.

Supporting Information

Supporting Information File 1

Copies of NMR spectra showing ratios of fluorinated and halogenated products.
[http://www.beilstein-journals.org/bjoc/content/supplementary/1860-5397-13-284-S1.pdf]

Supporting Information File 2

Details of computational conformational analysis.
[http://www.beilstein-journals.org/bjoc/content/supplementary/1860-5397-13-284-S2.zip]

Acknowledgements

G.P. was a Warwick IAS Global Research Fellow. The author would like to thank the University of Warwick and Royal Society for Research Grants.

ORCID® iDs

Graham Pattison - https://orcid.org/0000-0003-0116-8457

References

1. Erian, A. W.; Sherif, S. M.; Gaber, H. M. *Molecules* **2003,** *8,* 793–865. doi:10.3390/81100793
2. Dobson, L. S.; Pattison, G. *Chem. Commun.* **2016,** *52,* 11116–11119. doi:10.1039/C6CC05775F
3. Leng, D. J.; Black, C. M.; Pattison, G. *Org. Biomol. Chem.* **2016,** *14,* 1531–1535. doi:10.1039/C5OB02468D
4. Nash, T. J.; Pattison, G. *Eur. J. Org. Chem.* **2015,** 3779–3786. doi:10.1002/ejoc.201500370
5. Thorpe, J. W.; Warkentin, J. *Can. J. Chem.* **1973,** *51,* 927–935. doi:10.1139/v73-137
6. Bach, R. D.; Coddens, B. A.; Wolber, G. J. *J. Org. Chem.* **1986,** *51,* 1030–1033. doi:10.1021/jo00357a016
7. O'Hagan, D. *Chem. Soc. Rev.* **2008,** *37,* 308–319. doi:10.1039/B711844A
8. Hunter, L. *Beilstein J. Org. Chem.* **2010,** *6,* No. 38. doi:10.3762/bjoc.6.38
9. Zimmer, L. E.; Sparr, C.; Gilmour, R. *Angew. Chem., Int. Ed.* **2011,** *50,* 11860–11871. doi:10.1002/anie.201102027
10. Fiorin, B. C.; Basso, E. A.; Tormena, C. F.; Rittner, R.; Abraham, R. J. *J. Phys. Chem. A* **2009,** *113,* 2906–2913. doi:10.1021/jp808048s
11. Jones, R. N.; Spinner, E. *Can. J. Chem.* **1958,** *36,* 1020–1027. doi:10.1139/v58-145
12. Krueger, P. J. *Can. J. Chem.* **1973,** *51,* 1363–1367. doi:10.1139/v73-203
13. RamaRao, M.; Bothner-By, A. A. *Org. Magn. Reson.* **1976,** *8,* 329–331. doi:10.1002/mrc.1270080702
14. Distefano, G.; Granozzi, G.; Bertoncello, R.; Olivato, P. R.; Guerrero, S. A. *J. Chem. Soc., Perkin Trans. 2* **1987,** 1459–1463. doi:10.1039/P29870001459
15. Olivato, P. R.; Guerrero, S. A.; Santos, P. S. *Spectrosc. Lett.* **1989,** *22,* 675–692. doi:10.1080/00387018908053927
16. Olivato, P. R.; Guerrero, S. A.; Hase, Y.; Rittner, R. *J. Chem. Soc., Perkin Trans. 2* **1990,** 465–471. doi:10.1039/P29900000465
17. Wong, S. S.; Paddon-Row, M. N. *J. Chem. Soc., Chem. Commun.* **1990,** 456–458. doi:10.1039/C39900000456
18. Mohanta, P. K.; Davis, T. A.; Gooch, J. R.; Flowers, R. A., II. *J. Am. Chem. Soc.* **2005,** *127,* 11896–11897. doi:10.1021/ja052546x
19. Saegebarth, E.; Krisher, L. C. *J. Chem. Phys.* **1970,** *52,* 3555. doi:10.1063/1.1673522
20. Guerrero, S. A.; Barros, J. R. T.; Wladislaw, B.; Rittner, R.; Olivato, P. R. *J. Chem. Soc., Perkin Trans. 2* **1983,** 1053–1058. doi:10.1039/P29830001053
21. Olivato, P. R.; Guerrero, S. A.; Modelli, A.; Granozzi, G.; Jones, D.; Distefano, G. *J. Chem. Soc., Perkin Trans. 2* **1984,** 1505–1509. doi:10.1039/p29840001505
22. Abraham, R. J.; Jones, A. D.; Warne, M. A.; Rittner, R.; Tormena, C. F. *J. Chem. Soc., Perkin Trans. 2* **1996,** 533–539. doi:10.1039/p29960000533
23. Pontes, R. M.; Fiorin, B. C.; Basso, E. A. *Chem. Phys. Lett.* **2004,** *395,* 205–209. doi:10.1016/j.cplett.2004.07.066

License and Terms

BEILSTEIN JOURNAL OF ORGANIC CHEMISTRY

Microfluidic radiosynthesis of [^{18}F]FEMPT, a high affinity PET radiotracer for imaging serotonin receptors

Thomas Lee Collier*[1,2], Steven H. Liang[1], J. John Mann[3], Neil Vasdev[2] and J. S. Dileep Kumar[3]

Full Research Paper

Open Access

Address:
[1]Division of Nuclear Medicine and Molecular Imaging, Massachusetts General Hospital & Harvard Medical School, Boston, MA, USA, [2]Advion, Inc., Ithaca, NY, USA and [3]Molecular Imaging and Neuropathology Division, New York State Psychiatric Institute, New York, NY, USA

Email:
Thomas Lee Collier* - tcollier@mgh.harvard.edu

* Corresponding author

Keywords:
agonist; fluorine-18; 5-HT$_{1A}$; microfluidics; PET

Beilstein J. Org. Chem. **2017,** *13,* 2922–2927.
doi:10.3762/bjoc.13.285

Received: 27 October 2017
Accepted: 18 December 2017
Published: 29 December 2017

This article is part of the Thematic Series "Organo-fluorine chemistry IV".

Guest Editor: D. O'Hagan

Abstract

Continuous-flow microfluidics has shown increased applications in radiochemistry over the last decade, particularly for both pre-clinical and clinical production of fluorine-18 labeled radiotracers. The main advantages of microfluidics are the reduction in reaction times and consumption of reagents that often result in increased radiochemical yields and rapid optimization of reaction parameters for ^{18}F-labeling. In this paper, we report on the two-step microfluidic radiosynthesis of the high affinity partial agonist of the serotonin 1A receptor, [^{18}F]FEMPT (pK_i = 9. 79; K_i = 0.16 nM) by microfluidic radiochemistry. [^{18}F]FEMPT was obtained in ≈7% isolated radiochemical yield and in >98% radiochemical and chemical purity. The molar activity of the final product was determined to be >148 GBq/μmol (>4 Ci/μmol).

Introduction

The development of serotonin 1A receptor (5-HT$_{1A}$R) agonist radiotracers for applications in molecular imaging with positron emission tomography (PET) has been avidly sought over the past two decades, albeit with limited success. The current status of serotonin-targeting radiopharmaceuticals was recently reviewed by Paterson et al. [1] and their conclusion was that "the development of PET and single-photon emission computed tomography (SPECT) radioligands to image serotonergic targets is of high interest, and successful evaluation in humans is leading to invaluable insight into normal and abnormal brain function". A further review by us focusing on 5-HT$_{1A}$R overviewed a number of PET and SPECT tracers that have been tested in vivo with varying efficacy [2]. A few representative compounds which show the structures that have been tested as radiotracers are shown in Figure 1.

The 5-HT$_{1A}$R is implicated in the pathophysiology of a variety of neuropsychiatric and neurodegenerative disease states as well

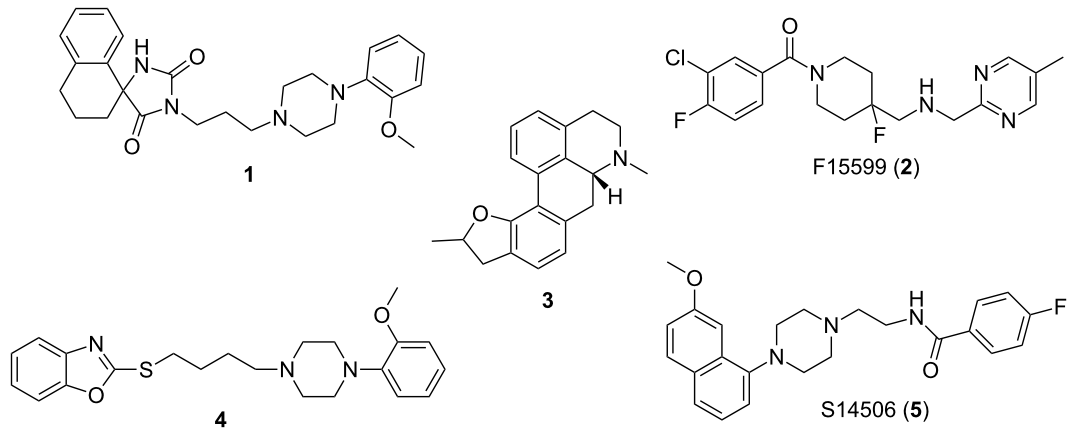

Figure 1: Representative examples of recent 5-HT_{1A}R agonists [3-9].

as in the mechanism of action of antidepressants. The 5-HT_{1A}R exists in low and high agonist affinity states. The antagonist ligands have similar affinity to the low affinity (LA) and high affinity (HA) conformations of 5-HT_{1A}R. However, agonist ligands prefer binding to the HA state of the receptor. This is coupled to G-protein and thus agonist binding gives a more meaningful functional measure of the 5-HT_{1A}R that can reflect desensitization and supersensitivity. Significant research has been directed at the differences between agonist and antagonist binding to 5-HT_{1A} receptors in Alzheimer's disease [10] and this interest has led to the development of a high-resolution in vivo atlas for four of the human brain's serotonin receptors and transporters [11].

Antagonist 5-HT_{1A}R PET tracers can detect the total receptor binding, but not modifications in the high affinity 5-HT_{1A}R binding in disease states or in the context of treatment functionally larger and earlier effects of antidepressants. The development of 5-HT_{1A}R agonist PET tracers for the past 2 decades has met with limited success. An arylpiperazine derivative of 3,5-dioxo-(2*H*,4*H*)-1,2,4-triazine radiolabeled with carbon-11 ($t_{½}$ = 20.4 min), [^{11}C]MPT, is the first successful agonist PET tracer reported for 5-HT_{1A}R in non-human primates. The binding of [^{11}C]MPT in baboon brain was in excellent agreement with the known distribution of the 5-HT_{1A}R. Despite the excellent binding profile of [^{11}C]MPT, the slow washout in baboons limits this radiotracer from advancing to human studies. Our recent efforts have focused on the development of fluorine-18 ($t_{½}$ = 109.7 min) labelled MPT derivatives, as the longer half-life enables imaging protocols that can provide a better match of the pharmacokinetics of binding to the half-life of the radionuclide, as well as simplified radiochemistry protocols and the long-term goal of distribution for multicenter clinical trials.

Several reports on the use of continuous flow microfluidics for radiofluorination have shown higher yields, with less amount of reagents and shorter reaction times compared to traditional vessel-based techniques [12]. Microfluidic techniques also allow for cost-effective and rapid optimization of reaction parameters for new radiotracers as simultaneous reactions can be carried out. We have recently shown that continuous flow microfluidics is suitable for ^{18}F-radiopharmaceutical production studies [13] and have applied this technique in human PET imaging studies [14]. Herein we present the microfluidic synthesis and evaluation of [^{18}F]FEMPT as an agonist PET ligand for 5-HT_{1A}R.

Results and Discussion

Synthesis and binding affinity of FEMPT

Desmethyl-MPT, the radiolabeling precursor, was synthesized as described previously [15]. The reference standard FEMPT (**7**) was synthesized in 70% by reacting desmethyl-MPT (**6**) with 1-bromo-2-fluoroethane in the presence of K_2CO_3 (Scheme 1 and Supporting Information File 1).

The in vitro binding assays to establish the potency and selectivity of FEMPT towards 5-HT_{1A}R and various other biogenic amines, brain receptors, and transporters were evaluated by the National Institute of Mental Health Psychoactive Drug Screening Program (NIMH-PDSP). FEMPT shows 0.2 nM binding affinity (K_i) to 5-HT_{1A}R. The next closest bindings for MPT are $Sigma_2$ PC12, H1, 5-HT_7, and 5-HT_{1B} (Table 1) and are >50 times higher than 5-HT_{1A}R. The K_i values for several other brain receptors and transporters were low (0.1 to 10 μM). Agonist properties of FEMPT on 5-HT_{1A}R were estimated by [^{35}S]GTPγS binding in membranes of CHO cells which stably express human 5-HT_{1A}R. A dose-dependent increase in [^{35}S]GTPγS binding was induced by FEMPT. Maximal FEMPT

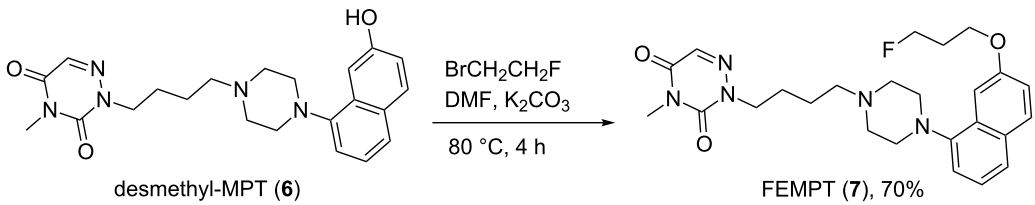

Scheme 1: Synthesis of FEMPT (**7**).

Table 1: K_is of FEMPT for receptors and transporters.

Targets	K_i values (nM)	Targets	K_i values (nM)	Targets	K_i values (nM)
5-HT_{1A}	0.2	adrenergic$_{\alpha 1}$	180	D_1	>10,000
5-HT_{1B}	122.5	adrenergic$_{\alpha B}$	196	D_2	80
5-HT_{2A}	406	adrenergic$_{\alpha D}$	142	D_3	35
5-HT_{2B}	12	adrenergic$_{\alpha 2A}$	346	D_4	24
5-HT_{2C}	343	adrenergic$_{\alpha 2B}$	403	D_5	>10,000
5-HT_3	>10,000	adrenergic$_{\alpha 2C}$	400	DAT	407.4
5-HT_{5A}	2340	adrenergic$_{\beta 1}$	1300	sigma$_2$ PC12	10
5-HT_6	71	adrenergic$_{\beta 2}$	202	DAT	407.4
5-HT_7	11	adrenergic$_{\beta 3}$	564	DOR	>10,000
A_2, A_3, A_4	>10,000	H_1	11	EP	>10,000
BZP	>10,000	H_2	1364	GABA	>10,000
Ca^{2+}	>10,000	H_3, H_4	>10,000	smoothened	>10,000
AMPA	>10,000	hERG	>10,000	Y_2	>10,000
NET	6980	KOR	1423	SERT	6144
NK	>10,000	M	>10,000	sigma$_2$	>10,000
sigma$_1$	1014	MDR1	>10,000	$VMAT_{1,2}$	>10,000
V_1, V_2	>10,000	MOR	>10,000	NT_1	>10,000
Na^+ channel	>10,000	mGluR	>10,000	imidazoline	>10,000
CB_1, CB_2	>10,000	NMDA	>10,000		
5-HT_{1A}R E_{max}	100%	EC_{50}	85 nM		

stimulated [^{35}S]GTPγS binding E_{max} was 100% of that seen with 5-HT and an EC_{50} of 85 nM.

Microfluidic chemistry

Reaction optimization of radiofluorination methods vary depending on the microfluidic systems being used but we can typically optimize ^{18}F-labeling reaction conditions in one or two days from a single batch of [^{18}F]fluoride. This is significantly more efficient than classical vial-based radiofluorination methods which, generally involves several experimental days and analysis as each reaction, including azeotropic drying of [^{18}F]fluoride, must be carried out individually. The microfluidic radiosynthesis of [^{18}F]FEMPT was optimized by treating the reactions as 2 individual steps, using the Discovery mode of the Advion NanoTek® microfluidic synthesizer [16]. The first step is the preparation of the labeling reagent [^{18}F]fluoroethyltosylate (**10**) via tetraethylammonium fluoride ([^{18}F]TEAF). The second step is the reaction of the [^{18}F]fluoroethyltosylate (**10**), with the FEMPT precursor **8** (Scheme 2).

Step 1: Synthesis of [^{18}F]fluoroethyltosylate (**10**)

Using the NanoTek Discovery mode, in the 1-step configuration, the synthesis of [^{18}F]fluoroethyltosylate (**10**) was optimized, initially using the reported methods which used up to 32 mg/mL of the ditosylate **9** [17], At this concentration of ditosylate **9**, up to 55% radiochemical conversion (RCC) were noted (Figure 2A). However, if this high concentration is used for the 2-step preparation, it would lead to low product yields due to the competition of the large amounts of unreacted ditosylate with the precursor **8**. By altering the ratios between the [^{18}F]fluoride and the ditosylate precursor **9**, the minimum concentration of the ditosylate precursor could be rapidly determined (Figure 2B). The reaction of [^{18}F]TEAF with ethylene glycol ditosylate (4 mg/mL, 10 μmol/mL) in DMSO in the first

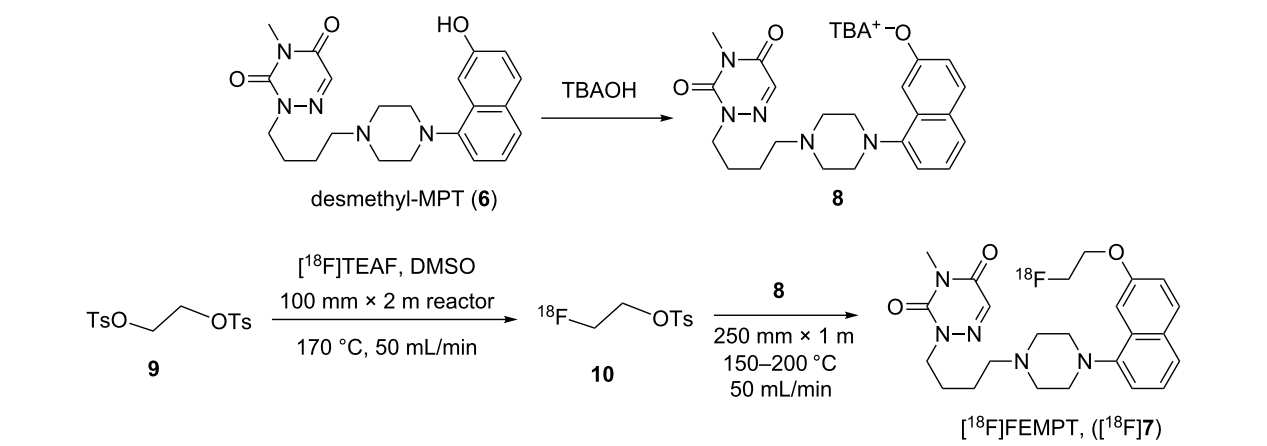

Scheme 2: Radiosynthetic scheme for the microfluidic flow synthesis of [^{18}F]fluoroethyltosylate (**10**) and [^{18}F]FEMPT (**7**).

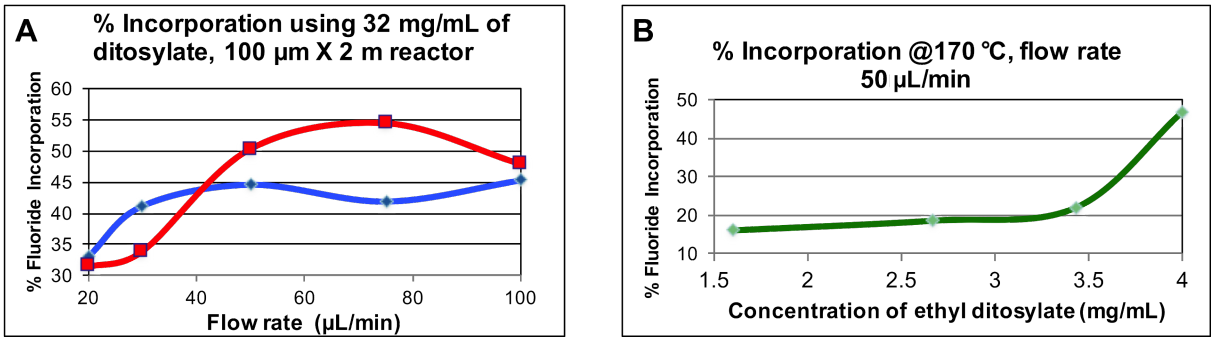

Figure 2: (A) Incorporation yield of [^{18}F]fluoride versus flow rate, red line 180 °C, blue line 150 °C, moderately high yields can be obtained; (B) Incorporation yield of [^{18}F]fluoride versus ditosylate concentration. An incorporation yield of almost 50% was obtained with only 4 mg/mL.

reactor resulted in a final solution concentration of 5 µmol/mL of the ethylene ditosylate, and still yielded ≈45% RCC.

Step 2: Reaction of [^{18}F]fluoroethyltosylate (**10**) with FEMPT precursor **8**

The [^{18}F]fluoroethyltosylate solution, prepared in the first step of the reaction was then mixed with the precursor phenolate **8** (2 mg/mL, 5 µmol/mL) at various flow rates, temperatures and ratios using the Discovery mode of the Advion NanoTek software. The concentration of the precursor was selected such that at a 1:1 ratio, the [^{18}F]fluoroethyltosylate and ditosylate solution would not completely consume the precursor during the second step, as there is no purification of the [^{18}F]fluoroethyltosylate from the ditosylate prior to the second step. Selected results are shown in Table 2.

The final product was then purified on a Phenomenex Luna column, 10 × 250 mm, 5 µm, with a mobile phase of 55% MeCN: 45% 10 mM phosphate at a flow rate of 5 mL/min. The HPLC fraction containing the product was collected and diluted with 20 mL of sterile water for injection, then this diluted solution was trapped on a HLB SPE light cartridge, washed with 10 mL of water, eluted from the HLB cartridge with 1 mL ethanol and diluted with 10 mL of 0.9% NaCl solution (saline). [^{18}F]FEMPT was obtained in ≈7% isolated radiochemical yield and in >98% radiochemical and chemical purity. The identity of the radiotracer was confirmed by co-injection with the standard (see Supporting Information File 1). The use of microfluidics allowed the optimization of the radiosynthesis in one day. The molar activity of the final product was determined to be >148 GBq/µmol (>4 Ci/µmol) by both UV spectroscopy and mass spectrometry methods and both methods were found to be in agreement. The chemical purity was determined using both UV spectroscopy and mass spectrometry and little chlorinated (<0.1%) and no elimination product was seen by mass spectrometry.

To determine the products being formed during the radiosynthesis the final formulation was analyzed by LC–MS using 1 mL of the final product solution trapped on a concentration

Table 2: Selected reaction conditions for two-step continuous-flow radiosynthesis.

Flow rate (μL/min)		Reactor temperature (°C)		P2 : Reaction 1 ratio	% Radiochemical yield
P1 and P3 combined	P2	Reactor 1	Reactor 2		
50	70	170	150	2	10
50	100	170	125	1	4
50	100	170	170	1	7
50	50	170	170	1	12
50	50	170	150	1	22

system, which consists of the replacement of the injection loop with a trapping cartridge (Valco Instruments Co. Inc, Houston, TX, Fingertight cartridge assembly #SFECH412, packed with Waters HLB SPE packing material) and the rest of the system remains as standard for the chromatography system. In the UV chromatogram observed on the HPLC system from the direct injection almost no signal is observed. However, when 1 mL of the solution of the purified radiotracer was injected via the trapping system, the UV traces indicate the presence of a number of species with retention times close to the desired product (Figure 3).

A number of the observed impurities were able to be identified using LC–MS and the major impurities observed were the expected elimination product and the hydroxy product. However, all of these materials were below the mass seen for the desired FEMPT and the combined signals were used in the molar activity calculation. Also seen was the presence of tetrabutylammonium salt, which appeared through the semi-preparative purification and the reformulation step. However, the signal for the tetrabutylammonium salt corresponds to <10 μg/mL.

Conclusion

In summary, [^{18}F]FEMPT was efficiently synthesized by continuous flow microfluidics. This protocol is generally applicable for the implementation of a suitable microfluidic process to optimize classical ^{18}F-radiofluorination reactions. Preclinical PET imaging studies with this radiotracer are underway.

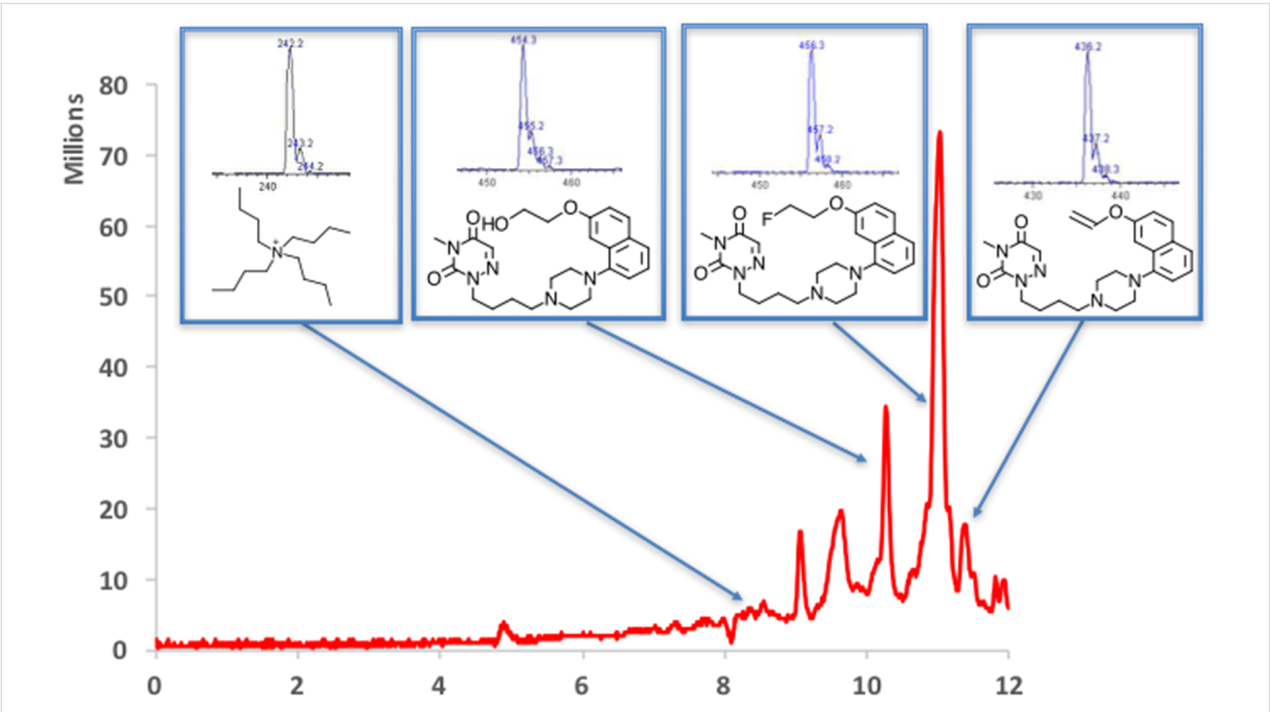

Figure 3: Analysis of the final formulated product by LC–MS, using the trapping system to improve the sensitivity. Red line is the UV spectra observed at 254 nm. Column = 3 μm, 4.6 × 150 mm C18, Phenomenex, Luna. Solvent MeCN:0.1% formic acid, Flow rate = 1 mL/min, Gradient from 20% ACN to 95% ACN at 10 minutes, hold for 2 minutes at 95% MeCN. Insets are the structures identified using the MS data. Mass spectra obtained using an Expression-L Compact Mass Spectrometer (Advion Inc., USA), APCI ion source operating in positive ion mode and corona discharge of 5 μA, *m*/*z* scan range: 200–500.

Supporting Information

Supporting Information File 1

Experimental part.
[http://www.beilstein-journals.org/bjoc/content/supplementary/1860-5397-13-285-S1.pdf]

ORCID® iDs

Thomas Lee Collier - https://orcid.org/0000-0002-3757-4855
Steven H. Liang - https://orcid.org/0000-0003-1413-6315
Neil Vasdev - https://orcid.org/0000-0002-2087-5125
J. S. Dileep Kumar - https://orcid.org/0000-0001-6688-3991

References

1. Paterson, L. M.; Kornum, B. R.; Nutt, D. J.; Pike, V. W.; Knudsen, G. M. *Med. Res. Rev.* **2013,** *33,* 54. doi:10.1002/med.20245
2. Kumar, J. S. D.; Mann, J. J. *Cent. Nerv. Syst. Agents Med. Chem.* **2014,** *14,* 96. doi:10.2174/1871524914666141030124316
3. Valhondo, M.; Marco, I.; Martin-Fontecha, M.; Vázquez-Villa, H.; Ramos, J. A.; Berkels, R.; Lauterbach, T.; Benhamú, B.; López-Rodriguez, M. L. *J. Med. Chem.* **2013,** *56,* 7851. doi:10.1021/jm400766k
4. Fornaretto, M. G.; Caccia, C.; Marchi, G.; Brambilla, E.; Mantegani, S.; Post, C. *Ann. N. Y. Acad. Sci.* **1997,** *812,* 226. doi:10.1111/j.1749-6632.1997.tb48184.x
5. Dawson, L. A.; Watson, J. M. *CNS Neurosci. Ther.* **2009,** *15,* 107. doi:10.1111/j.1755-5949.2008.00067.x
6. Dounay, A. B.; Barta, N. S.; Bikker, J. A.; Borosky, S. A.; Campbell, B. M.; Crawford, T.; Denny, L.; Evans, L. M.; Gray, D. L.; Lee, P.; Lenoir, E. A.; Xu, W. *Bioorg. Med. Chem. Lett.* **2009,** *19,* 1159. doi:10.1016/j.bmcl.2008.12.087
7. Siracusa, M. A.; Salerno, L.; Modica, M. N.; Pittalà, V.; Romeo, G.; Amato, M. E.; Nowak, M.; Bojarski, A. J.; Mereghetti, I.; Cagnotto, A.; Mennini, T. *J. Med. Chem.* **2008,** *51,* 4529. doi:10.1021/jm800176x
8. Franchini, S.; Prandi, A.; Sorbi, C.; Tait, A.; Baraldi, A.; Angeli, P.; Buccioni, M.; Cilia, A.; Poggesi, E.; Fossa, P.; Brasili, L. *Bioorg. Med. Chem. Lett.* **2010,** *20,* 2017. doi:10.1016/j.bmcl.2010.01.030
9. Liu, Z.; Zhang, H.; Ye, N.; Zhang, J.; Wu, Q.; Sun, P.; Li, L.; Zhen, X.; Zhang, A. *J. Med. Chem.* **2010,** *53,* 1319. doi:10.1021/jm9015763
10. Vidal, B.; Sebti, J.; Verdurand, M.; Fieux, S.; Billard, T.; Streichenberger, N.; Troakes, C.; Newman-Tancredi, A.; Zimmer, L. *Neuropharmacology* **2016,** *109,* 88. doi:10.1016/j.neuropharm.2016.05.009
11. Beliveau, V.; Ganz, M.; Feng, L.; Ozenne, B.; Højgaard, L.; Fisher, P. M.; Svarer, C.; Greve, D. N.; Knudsen, G. M. *J. Neurosci.* **2017,** *37,* 120. doi:10.1523/JNEUROSCI.2830-16.2016
12. Pascali, G.; Watts, P.; Salvadori, P. A. *Nucl. Med. Biol.* **2013,** *40,* 776. doi:10.1016/j.nucmedbio.2013.04.004
13. Liang, S. H.; Yokell, D. L.; Jackson, R. N.; Rice, P. A.; Callahan, R.; Johnson, K. A.; Alagille, D.; Tamagnan, G.; Collier, T. L.; Vasdev, N. *MedChemComm* **2014,** *5,* 432. doi:10.1039/C3MD00335C
14. Liang, S. H.; Yokell, D. L.; Normandin, M. D.; Rice, P. A.; Jackson, R. N.; Shoup, T. M.; Brady, T. J.; Fakhri, G. E.; Collier, T. L.; Vasdev, N. *Mol. Imaging* **2014,** *13,* 7290201400025.
15. Kumar, J. S. D.; Majo, V. J.; Hsiung, S.-C.; Millak, M. S.; Liu, K.-P.; Tamir, H.; Prabhakaran, J.; Simpson, N. R.; Van Heertum, R. L.; Mann, J. J.; Parsey, R. V. *J. Med. Chem.* **2006,** *49,* 125. doi:10.1021/jm050725j
16. Pascali, G.; Matesic, L.; Collier, T. L.; Wyatt, N.; Fraser, B. H.; Pham, T. Q.; Salvadori, P. A.; Greguric, I. *Nat. Protoc.* **2014,** *9,* 2017. doi:10.1038/nprot.2014.137
17. Pascali, G.; Mazzone, G.; Saccomanni, G.; Manera, C.; Salvadori, P. A. *Nucl. Med. Biol.* **2010,** *37,* 547. doi:10.1016/j.nucmedbio.2010.03.006

License and Terms

BEILSTEIN JOURNAL OF ORGANIC CHEMISTRY

Stereochemical outcomes of C–F activation reactions of benzyl fluoride

Neil S. Keddie‡[1], Pier Alexandre Champagne‡[2], Justine Desroches[2], Jean-François Paquin*[2] and David O'Hagan*[1]

Full Research Paper

Open Access

Address:
[1]School of Chemistry, Biomedical Sciences Research Complex, University of St Andrews, North Haugh, St Andrews, Fife KY16 9ST, United Kingdom and [2]PROTEO, CCVC, Département de chimie, 1045 Avenue de la Médecine, Université Laval, Québec, QC G1V 0A6, Canada

Email:
Jean-François Paquin* - jean-francois.paquin@chm.ulaval.ca;
David O'Hagan* - do1@st-andrews.ac.uk

* Corresponding author ‡ Equal contributors

Keywords:
benzylic fluorides; C–F activation; chiral liquid crystal; ^{2}H NMR; PBLG; stereochemistry

Beilstein J. Org. Chem. **2018,** *14,* 106–113.
doi:10.3762/bjoc.14.6

Received: 20 October 2017
Accepted: 12 December 2017
Published: 09 January 2018

This article is part of the Thematic Series "Organo-fluorine chemistry IV".

Associate Editor: J. A. Murphy

Abstract

In recent years, the highly polar C–F bond has been utilised in activation chemistry despite its low reactivity to traditional nucleophiles, when compared to other C–X halogen bonds. Paquin's group has reported extensive studies on the C–F activation of benzylic fluorides for nucleophilic substitutions and Friedel–Crafts reactions, using a range of hydrogen bond donors such as water, triols or hexafluoroisopropanol (HFIP) as the activators. This study examines the stereointegrity of the C–F activation reaction through the use of an enantiopure isotopomer of benzyl fluoride to identify whether the reaction conditions favour a dissociative (S_N1) or associative (S_N2) pathway. [^{2}H]-Isotopomer ratios in the reactions were assayed using the Courtieu ^{2}H NMR method in a chiral liquid crystal (poly-γ-benzyl-L-glutamate) matrix and demonstrated that both associative and dissociative pathways operate to varying degrees, according to the nature of the nucleophile and the hydrogen bond donor.

Introduction

The C–F bond is the strongest carbon–halogen bond known [1]. Its low reactivity, in comparison to other C–X bonds, means that it is inert to all but the most harsh reaction conditions, and fluorine can generally be carried through multistep syntheses without concern over side reactions (the exception being S_NAr reactions). In recent years, there has been an increasing interest in C–F bond activation [2], with a view to using organic bound fluoride as a leaving group in substitution reactions that typically require more activated leaving groups. Such an approach could circumvent the requirement for protecting groups in multistep synthesis by capitalizing on the low reactivity of the C–F bond. Paquin et al. have published extensively on non-

metal based methods for benzylic C–F bond activation [3-7]. The reactivity relies on protic activation driven by the capacity of organic fluoride to form hydrogen bonds [8,9]. Protocols using water/isopropanol [3], optimally coordinated triols [4,5], and hexafluoroisopropanol (HFIP) [6,7] as the corresponding hydrogen bond donors have shown considerable success. This mode of activation has been demonstrated for amination [3-5] and Friedel–Crafts reactions [6,7] on benzylic fluoride substrates (Figure 1), producing the corresponding substituted products in moderate to good yields. The water/isopropanol system was also shown to be amenable to phenolate and thiolate nucleophiles [3].

Previously, Paquin et al. undertook density functional theory (DFT) studies on the mechanism of C–F amination reactions employing water/isopropanol [3] and triols [4,5] as hydrogen-bond donor activators. Through these studies, the authors suggested that multiple donors (even when using a triol) surround the fluorine atom of the benzyl fluoride, thus stabilising the transition state through substantial F···HOR hydrogen bond interactions, rather than through electrostatic stabilisation only [3]. This stabilisation was suggested to lead to a purely associative bimolecular (S_N2) mechanism. The authors also studied the C–F activated Friedel–Crafts reactions [6,7] using very strong hydrogen bond donors, namely HFIP, in the presence or absence of trifluoroacetic acid (TFA). For both of these activators, Paquin et al. proposed a dissociative unimolecular (S_N1) mechanism, whereby the strong hydrogen bond donor associates with the benzyl fluoride, leading to ionisation of the molecule, generating a benzylic carbocation and a formal equivalent of HF (which behaves in an autocatalytic manner as a stronger hydrogen bond donor than HFIP or TFA).

Overall, there are three possible mechanistic pathways that these C–F activation reactions could follow: S_N1, S_N2, and a mixed S_N1/S_N2 pathway. Typically, benzylic substitutions would be expected to display a significant level of S_N1 character. However, given the particularly poor properties of fluoride as a leaving group, developing a better understanding of the dissociative nature of these transformations remains of considerable interest. A direct bimolecular S_N2 substitution would result in a complete inversion of configuration of the stereocenter and perfect enantiospecificity, while an S_N1 mechanism would yield a fully racemized product. Any mixed pathway would generate products with partially racemized stereocenters. In this context, we decided to explore the stereointegrity of the aforementioned reactions using enantiopure 7-[$^2H_1$]-(*R*)-benzyl fluoride ((*R*)-**1,** Figure 2) as a primary, yet chiral electrophile [10].

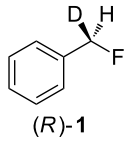

(*R*)-**1**

Figure 2: 7-[$^2H_1$]-(*R*)-Benzyl fluoride ((*R*)-**1**).

Substitution reactions of benzyl fluoride (**1**) will generate substituted products that retain the deuterium atom, and the degree of stereointegrity can be determined by examining the enantiopurity of the isotopically labelled product. Quadrupolar ^{2}H-nuclei can serve as a particularly useful NMR probe for assaying enantiopurity. If the ^{2}H NMR is recorded in a lyotropic liquid crystalline solvent, where tumbling of the solute is restricted, then the ^{2}H NMR signal splits into a doublet due to differential interactions of the quadrupolar nuclei with the electric field gradient associated with the oriented media [10]. When placed in an enantiomerically enriched liquid crystalline environment, the enantiomeric isotopomers interact unequally with the electric field gradients associated with the orientated media, creating anisotropy and resolving into two sets of doublets. If there is sufficient resolution between these quadrupolar couplings, then the enantiomeric ratio can be recorded. We have used poly-γ-benzyl-L-glutamate (PBLG) previously as the liquid-crystalline matrix for the determination of ee of samples of deuterated benzyl alcohols, benzyl fluorides, and esters of fluoroacetic acid [11] by ^{2}H NMR and found it to be effective for the resolution of enantiomers. In this study, we explore various nucleophilic substitutions and a Friedel–Crafts reaction on enantiomerically labelled [$^2H_1$]benzyl fluoride.

Results and Discussion

Highly enantiomerically enriched 7-[$^2H_1$]-(*R*)-benzyl fluoride ((*R*)-**1**) was synthesised in two steps from benzaldehyde (**2**), as

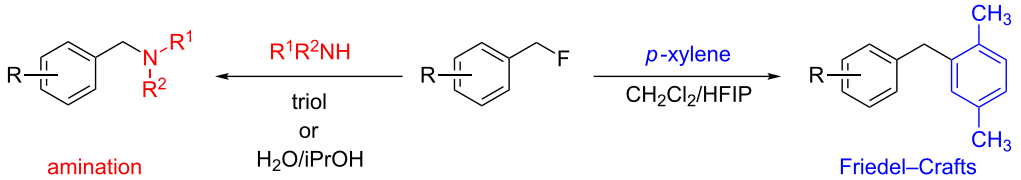

Figure 1: C–F activation of benzylic fluorides to generate benzylamine or diarylmethane products.

described previously [11]; the procedure is summarised in Scheme 1.

Aldehyde **2** was reduced under Noyori's conditions [12] using (*S*,*S*)-Ru(DPEN)$_2$ as catalyst and [$^2H_2$]-formic acid as the deuterium source. This afforded the corresponding 7-[$^2H_1$]-(*S*)-benzyl alcohol ((*S*)-**3**) in moderate yield (81%) and high ee (95%), as evidenced by ^{2}H-PBLG-NMR. Benzyl alcohol **3** was converted to the corresponding benzyl fluoride (**1**) using a modification of Bio's method [13,14] to promote the S_N2 reaction exclusively, using TMS-morpholine and DAST, in moderate yield (51%) and high ee (94%).

The isotopically enriched [$^2H_1$]-benzyl fluoride ((*R*)-**1**, 95% ee) was then subjected to a range of C–F activation reactions using a mixture of nucleophiles (for direct substitutions) and aryls (for Friedel–Crafts reactions) to give products **5**–**9**. The nucleophilic substitution reactions of **1** are shown in Table 1 and Table 2, and were all conducted using either a mixture of water/isopropanol, or tris(hydroxymethyl)propane as the activating hydrogen bond donor. In addition, three reactions of racemic substrates (Table 1, entries 1–3), were performed in order to ensure that sufficient resolution could be obtained in the ^{2}H{^{1}H}-PBLG-NMR, therefore allowing the ee of the products to be determined. A representative example of the ^{2}H NMR spectra (107.5 MHz) is displayed in Figure 3, using *N*-methylaniline as a nucleophile, showing the spectra of both a racemic sample (Figure 3A) and an enantioenriched sample (Figure 3B) of **6**. However, as evidenced by entry 3 (Table 1), and entries 3 and 7 (Table 2), the analysis revealed that some nucleophiles (such as *N*-methylbenzylamine and morpholine [not shown]) were unsuitable for this study, as the resulting products **7** could not be resolved in the ^{2}H NMR with PBLG assay.

Two different activator systems were investigated for the nucleophilic substitution of **1**: a mixture of water and isopropanol (Table 2, entries 1–5) and tris(hydroxymethyl)propane (Table 2, entries 6–8). Using water/isopropanol as the activator afforded the benzylated products **5**–**9** in moderate yields after 18 h. The ee values of all of the resulting products was

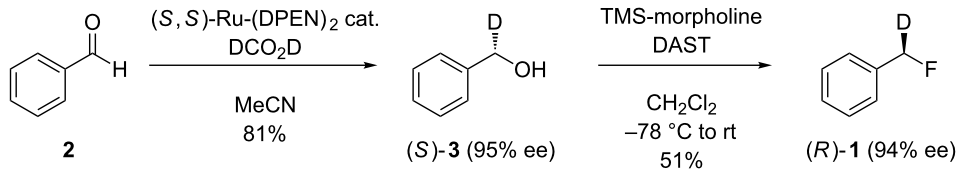

Scheme 1: Synthesis of enantioenriched 7-[$^2H_1$]-(*R*)-benzyl fluoride ((*R*)-**1**) from benzaldehyde (**2**).

Table 1: Nucleophilic substitution reactions of racemic 7-[$^2H_1$]-benzyl bromide (**4**).

Entry	Reaction	ee (%)
1	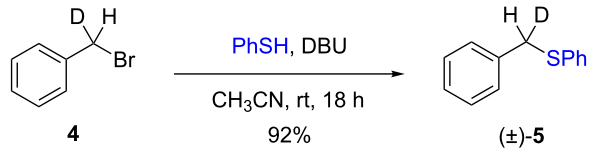	racemic
2	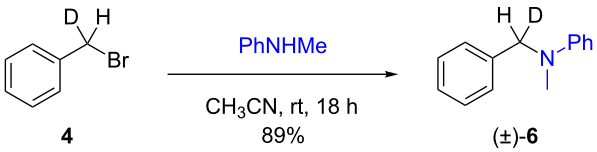	racemic
3	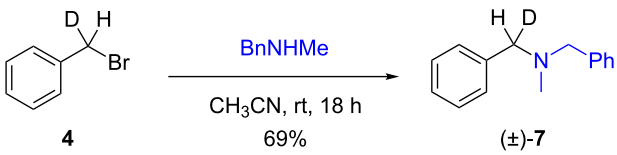	nd[a]

[a]ee could not be determined as a result of poor ^{2}H{^{1}H} NMR resolution.

Table 2: Nucleophilic substitution reactions of 7-[$^2H_1$]-(*R*)-benzyl fluoride ((*R*)-**1**).

Entry	Reaction	ee (%)
1	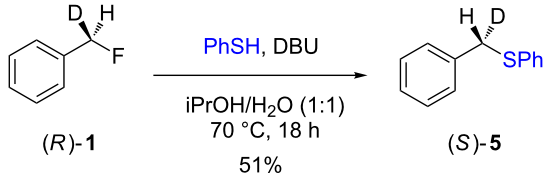 (*R*)-**1** → (*S*)-**5**	94
2	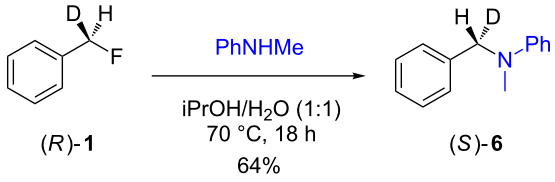 (*R*)-**1** → (*S*)-**6**	90
3	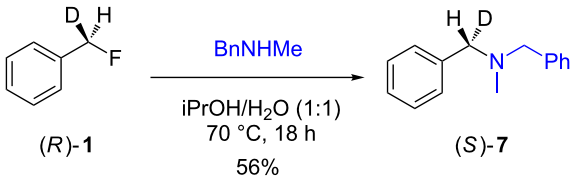 (*R*)-**1** → (*S*)-**7**	nd[a]
4	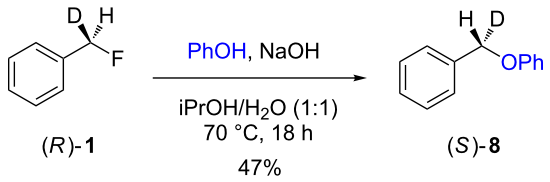 (*R*)-**1** → (*S*)-**8**	93
5	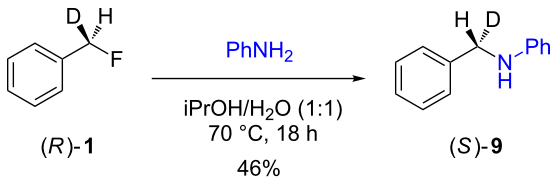 (*R*)-**1** → (*S*)-**9**	91
6	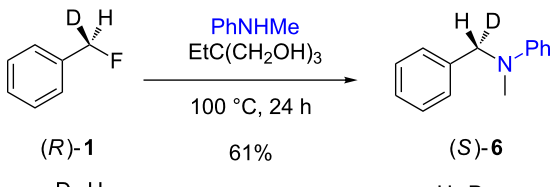 (*R*)-**1** → (*S*)-**6**	87
7	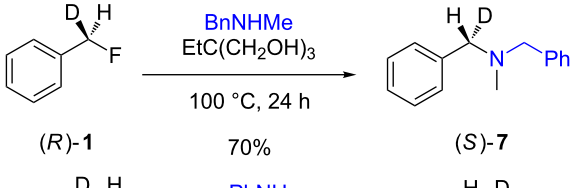 (*R*)-**1** → (*S*)-**7**	nd[a]
8	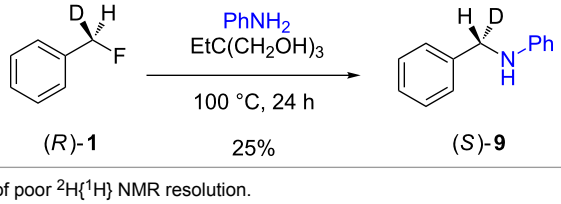 (*R*)-**1** → (*S*)-**9**	89

[a]ee could not be determined as a result of poor $^2H\{^1H\}$ NMR resolution.

very close to that of the original benzyl fluoride ((*R*)-**1**, 95%), indicating that a highly associative S_N2-like pathway was operating, where the incoming nucleophile must have approached on a coordinate anti to the C–F bond resulting in an inversion of the configuration. These results are in good agreement with the transition state proposed by Paquin [3-5]. Unfortunately,

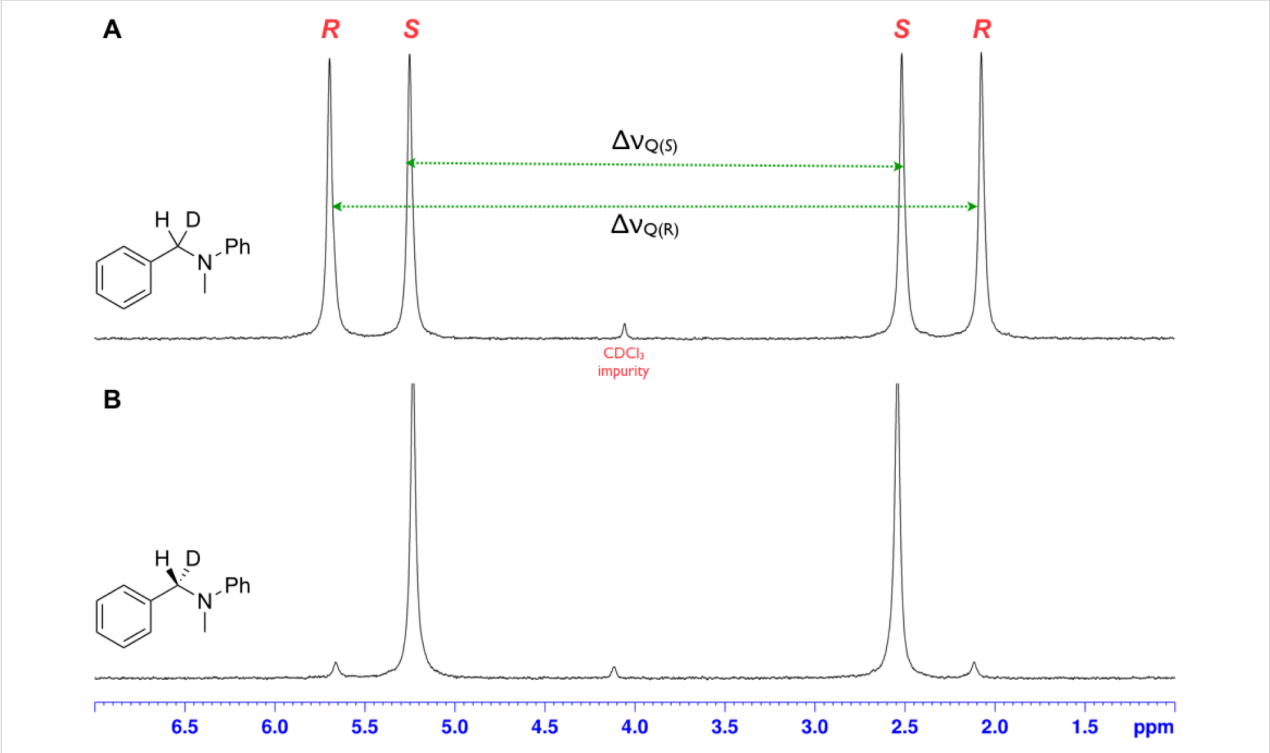

Figure 3: Partial $^2H\{^1H\}$ NMR (107.5 MHz) with PBLG in $CHCl_3$ (13% w/w). (A) racemic sample of **6** (from Table 1, entry 2) and (B) enantioenriched sample of **6** (from Table 2, entry 2). The magnitude of the quadrupolar splittings for the (*R*)- and (*S*)-enantiomers are labelled $\Delta\nu_{Q(ent)}$. The ee of each sample was determined by deconvolution of the line shapes and subsequent integration.

N-methylbenzylamine (Table 2, entry 3) afforded a product **7** that did not resolve by ^2H NMR, and thus the ee could not be determined.

Changing the activator from water/isopropanol to tris(hydroxymethyl)propane was anticipated to increase the stability of the triol–benzyl fluoride complex, and hence a tendancy towards an associative mechanism was expected. However, on performing the reactions with nitrogen nucleophiles (Table 2, entries 6 and 8) and the triol as the hydrogen bond donor, slightly lower ee's were obtained relative to those obtained using the same nucleophiles with the water/isopropanol system (Table 2, entries 2 and 5). These minor differences in ee may be due to the higher temperature leading to a minor, but noticeable dissociative pathway. Once again, using *N*-methylbenzylamine as the nucleophile (Table 2, entry 7) afforded **7**, which could not be resolved by ^2H NMR. Overall, the nucleophilic substitution of **1**, using either of the described hydrogen bond activating systems, afforded enantioenriched benzylated products with little erosion in stereointegrity.

In contrast to the above nucleophilic substitutions, which all proceeded with good stereointegrity, the Friedel–Crafts reactions of **1** with *p*-xylene gave very different results, as shown in Table 3.

At room temperature (Table 3, entry 1), benzyl fluoride (*R*)-**1** was activated by HFIP, affording biarylmethane **10** in a good yield (88%) after 18 h. The ee of the product was low (24%), but not racemic. The proposed stereochemistry of the product was verified by independent synthesis of the (*S*)-isomer from the unsymmetric diphenyl ketone **11** (Scheme 2).

Corey–Bakshi–Shibata reduction of diaryl ketone **11**, afforded the (*R*)-alcohol **12** in moderate to good yield and moderate ee [15,16]. The absolute stereochemistry of **12** was confirmed by X-ray crystallography of the 4-bromophenyl ester derivative **13**. Alcohol **12** was activated as the tosyl ester at −20 °C, and then immediately displaced by $LiAlD_4$ [17], inverting the stereocenter to afford the (*S*)-diarylmethane **10** isotopomer in 18% ee. $^2H\{^1H\}$ NMR in a PBLG matrix indicated that the dominant isomer was the same as was produced in entry 1, Table 3. Therefore, this analysis showed that the dominant enantiomer of **10** arose from an inversion, rather than retention, of configuration of the original stereocenter of **1**.

There may be four different reaction mechanisms operating in these Friedel–Crafts reactions as shown in Figure 4. (A) Coordination of the fluorine atom with the hydrogen bond donor, followed by backside attack of the nucleophile leads to S_N2 reaction and inversion of configuration. (B) Hydrogen bond donor

Table 3: Friedel–Crafts reactions of 7-[$^2H_1$]-(*R*)-benzyl fluoride ((*R*)-**1**).

Entry	Reaction	ee (%)
1	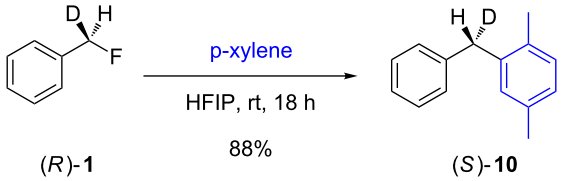 (*R*)-**1** → (*S*)-**10**	24
2	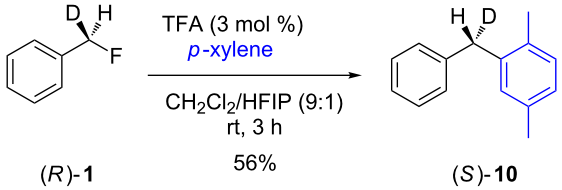 (*R*)-**1** → (*S*)-**10**	19
3	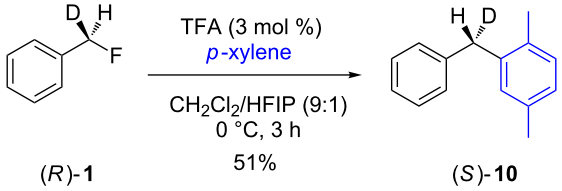 (*R*)-**1** → (*S*)-**10**	28

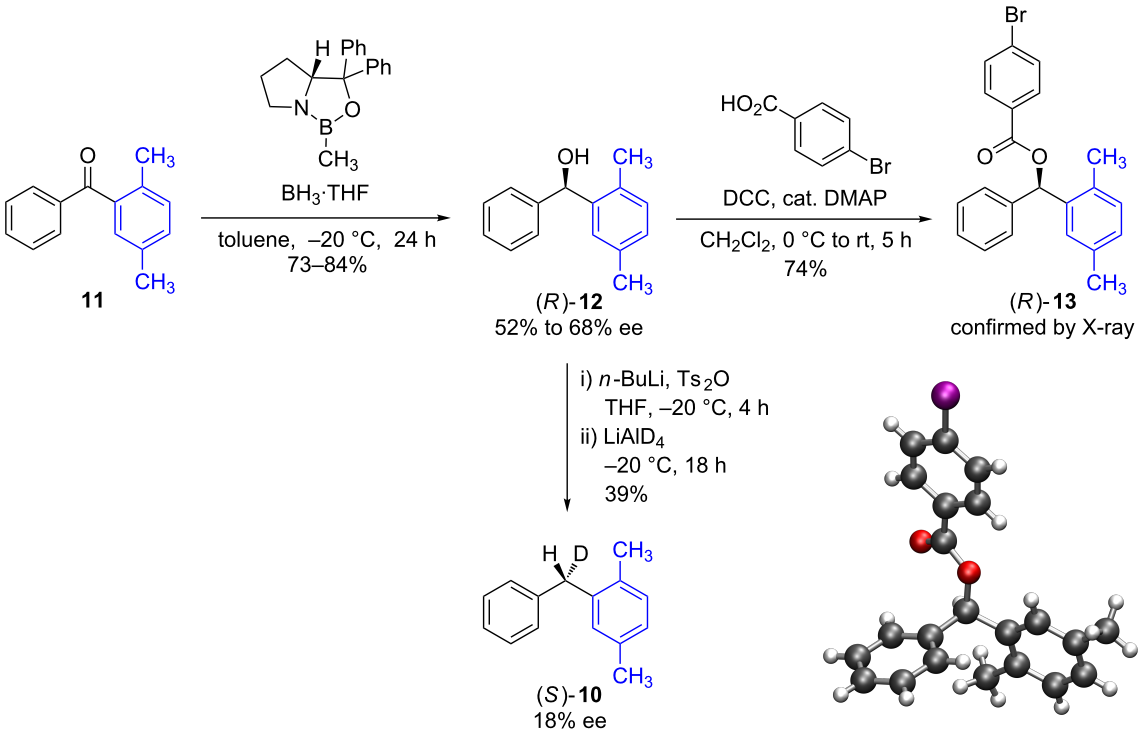

Scheme 2: Synthesis of enantioenriched (*S*)-diarylmethane **10** from diaryl ketone **11** and confirmation of configuration of (*R*)-**13** by single crystal X-ray structure.

coordination to fluorine leads to ionisation of **1**, producing an intimate ion pair, which only permits backside attack of the nucleophile on the benzylic cation. (C) If the nucleophile is poor and $k_4 > k_3$, a solvent-separated ion pair will be formed, where the HBD-coordinated fluorine atom is loosely associated with the solvated cation, allowing a nucelophilic attack to occur

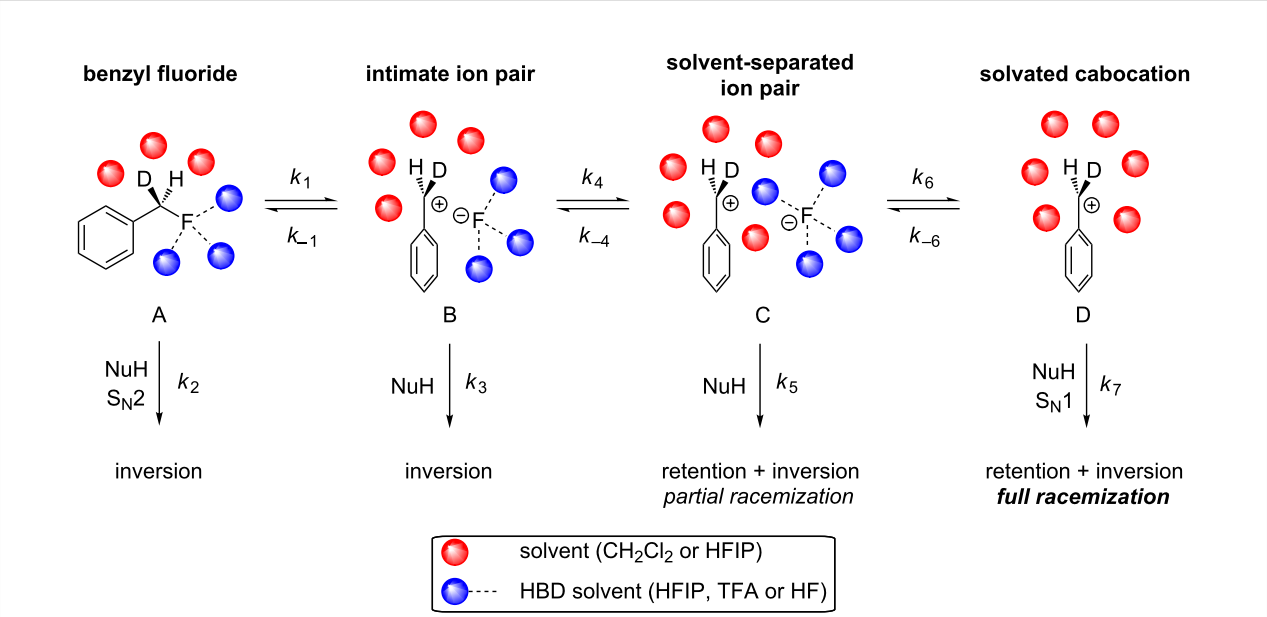

Figure 4: Possible reactive intermediates for C–F activation of benzyl fluoride **1** with strong hydrogen bond donors.

from more trajectories, leading to a mixture of inversion (predominant) and retention products. (D) Fully solvated cation, where attack of the nucleophile can freely occur from either face, leading to racemization of the product in an S_N1 reaction.

We propose that the actual attack of the nucleophile does not occur on the coordinated benzyl fluoride (A), or the fully solvated carbocation (D), as these scenarios would incur 100% or 0% enantiospecificity, respectively. Rather, the data suggest that attack occurs on a mixture of intimate (B) and solvent-separated (C) ion pairs. The partial racemization observed in Table 3 suggests that the solvent-separated ion-pair intermediate (C) is most likely the reactive species, as it would naturally lead to a partial racemization of the substrate stereocenter.

When the activator was changed from HFIP to a mixed system of HFIP and TFA (3 mol %, Table 3, entries 2 and 3), the reactions were complete in a significantly shorter time, i.e., the initial induction period observed when only HFIP was used [7] disappeared in each case. The ee of entry 2 was lower (19%), showing that the increased hydrogen bonding strength of the TFA, and thus the more rapid generation of HF (vide infra), promotes a dissociative pathway via the solvent-separated ion pair. The greater ionic strength of the solution may also play a part in stabilising the partially dissociated carbocation. Pleasingly, decreasing the temperature (Table 3, entry 3) did not slow the reaction down, and it completed after 3 h. However, the decreased temperature lead to a slightly higher ee (28%) for **10**, suggesting that at lower temperatures the separation of the ions is less favoured in solution, presumably for entropic reasons.

The nature of the poorer nucleophile, coupled with the stronger hydrogen bond donor in the Friedel–Crafts reaction allows the solvent-separated ion-pair mechanism to predominate, significantly eroding the stereointegrity of the biarylmethane products **10**. However, the products were not racemic, showing that the nucleophilic attack also occurs via an associated ion pair, rather than the fully solvated carbocation.

Conclusion

In summary, we have analyzed the stereochemical outcomes of substitution and Friedel–Crafts reactions of 7-[$^2H_1$]-(*R*)-benzyl fluoride ((*R*)-**1**), mediated by C–F activation using hydrogen-bond donors. When strong nucleophiles are used in conjunction with hydroxyl-based donors, an associative S_N2-like reaction mechanism predominates, with almost complete inversion of the configuration at the stereogenic center. Poorer aryl nucleophiles can be used for Friedel–Crafts reactions if strong hydrogen bond donors (such as HFIP or TFA) are used to activate the C–F bond. In these cases, a dissociative mechanism operates, probably via a solvent-separated ion pair, rather than a fully solvated benzylic carbocation. The products arising from this mechanism are only partially enantioenriched, suggesting that there is still a steric influence for backside attack of the nucleophile in the solvent-separated ion pair, arising from the large, congested hydrogen bond networks around the fluorine atom.

Supporting Information

The Supporting Information features experimental protocols and ^{1}H, ^{19}F (where appropriate) and $^{2}H\{^{1}H\}$ NMR spectra of benzyl fluoride **1** and adducts **5–10**. The methods for measurement of the ee by $^{2}H\{^{1}H\}$ NMR are also described.

Supporting Information File 1

Experimental protocols.
[http://www.beilstein-journals.org/bjoc/content/supplementary/1860-5397-14-6-S1.pdf]

Supporting Information File 2

^{2}H NMR analysis of enantiopurity.
[http://www.beilstein-journals.org/bjoc/content/supplementary/1860-5397-14-6-S2.pdf]

Acknowledgements

NK and DOH acknowledge support from the University of St Andrews, Engineering and Physical Sciences Research Council (EPSRC, Grant No.: EP/L017911/1), and the EPSRC UK National Mass Spectrometry Facility at Swansea University. This work was also supported by the Natural Sciences and Engineering Research Council of Canada (NSERC), the FRQNT Centre in Green Chemistry and Catalysis (CGCC), and the Université Laval.

ORCID® iDs

Neil S. Keddie - https://orcid.org/0000-0002-9502-5862
Jean-François Paquin - https://orcid.org/0000-0003-2412-3083

References

1. Blanksby, S. J.; Ellison, G. B. *Acc. Chem. Res.* **2003,** *36,* 255–263. doi:10.1021/ar020230d
2. Amii, H.; Uneyama, K. *Chem. Rev.* **2009,** *109,* 2119–2183. doi:10.1021/cr800388c
3. Champagne, P. A.; Pomarole, J.; Thérien, M.-E.; Benhassine, Y.; Beaulieu, S.; Legault, C. Y.; Paquin, J.-F. *Org. Lett.* **2013,** *15,* 2210–2213. doi:10.1021/ol400765a
4. Champagne, P. A.; Saint-Martin, A.; Drouin, M.; Paquin, J.-F. *Beilstein J. Org. Chem.* **2013,** *9,* 2451–2456. doi:10.3762/bjoc.9.283
5. Champagne, P. A.; Drouin, M.; Legault, C. Y.; Audubert, C.; Paquin, J.-F. *J. Fluorine Chem.* **2015,** *171,* 113–119. doi:10.1016/j.jfluchem.2014.08.018
6. Champagne, P. A.; Benhassine, Y.; Desroches, J.; Paquin, J.-F. *Angew. Chem., Int. Ed.* **2014,** *53,* 13835–13839. doi:10.1002/anie.201406088
7. Hemelaere, R.; Champagne, P. A.; Desroches, J.; Paquin, J.-F. *J. Fluorine Chem.* **2016,** *190,* 1–6. doi:10.1016/j.jfluchem.2016.08.003
8. Schneider, H.-J. *Chem. Sci.* **2012,** *3,* 1381–1394. doi:10.1039/c2sc00764a
9. Champagne, P. A.; Desroches, J.; Paquin, J.-F. *Synthesis* **2015,** *47,* 306–322. doi:10.1055/s-0034-1379537
10. Canet, I.; Courtieu, J.; Loewenstein, A.; Meddour, A.; Pechine, J. M. *J. Am. Chem. Soc.* **1995,** *117,* 6520–6526. doi:10.1021/ja00129a015
11. Wadoux, R. D. P.; Lin, X.; Keddie, N. S.; O'Hagan, D. *Tetrahedron: Asymmetry* **2013,** *24,* 719–723. doi:10.1016/j.tetasy.2013.05.001
12. Yamada, I.; Noyori, R. *Org. Lett.* **2000,** *2,* 3425–3427. doi:10.1021/ol0002119
13. Bio, M. M.; Waters, M.; Javadi, G.; Song, Z. J.; Zhang, F.; Thomas, D. *Synthesis* **2008,** 891–896. doi:10.1055/s-2008-1032181
14. Bresciani, S.; O'Hagan, D. *Tetrahedron Lett.* **2010,** *51,* 5795–5797. doi:10.1016/j.tetlet.2010.08.104
15. Corey, E. J.; Helal, C. J. *Tetrahedron Lett.* **1996,** *37,* 5675–5678. doi:10.1016/0040-4039(96)01198-7
16. The enantiomeric excess varied slightly when the reaction was run on different scales, due to variations in temperature.
17. Bolshan, Y.; Chen, C.-y.; Chilenski, J. R.; Gosselin, F.; Mathre, D. J.; O'Shea, P. D.; Roy, A.; Tillyer, R. D. *Org. Lett.* **2003,** *6,* 111–114. doi:10.1021/ol0361655

BEILSTEIN JOURNAL OF ORGANIC CHEMISTRY

Gram-scale preparation of negative-type liquid crystals with a CF_2CF_2-carbocycle unit via an improved short-step synthetic protocol

Tatsuya Kumon, Shohei Hashishita, Takumi Kida, Shigeyuki Yamada, Takashi Ishihara and Tsutomu Konno*

Full Research Paper

Open Access

Address:
Faculty of Molecular Chemistry and Engineering, Kyoto Institute of Technology, Matsugasaki, Sakyo-ku, Kyoto 606-8585, Japan

Email:
Tsutomu Konno* - konno@kit.ac.jp

* Corresponding author

Keywords:
gram-scale preparation; liquid crystals; short-step preparation; tetrafluorinated cyclohexadiene; tetrafluorinated cyclohexane

Beilstein J. Org. Chem. **2018,** *14,* 148–154.
doi:10.3762/bjoc.14.10

Received: 26 October 2017
Accepted: 05 December 2017
Published: 15 January 2018

This article is part of the Thematic Series "Organo-fluorine chemistry IV".

Guest Editor: D. O'Hagan

Abstract

Herein, we demonstrate an improved short-step protocol for the synthesis of multicyclic molecules having a CF_2CF_2-containing cyclohexadiene or cyclohexane framework in a mesogenic structure. These molecules are promising candidates for vertical alignment (VA)-mode liquid crystal (LC) display devices owing to their large negative dielectric constant. The tetrafluorinated multicyclic molecules were successfully obtained in only five or six reaction steps without the need for special handling techniques, as is generally required for thermally unstable organometallic species, representing a reduction of three reaction steps. The improved short-step synthetic protocol was also amenable to the multigram preparation of these promising molecules, which may contribute significantly to the development of novel negative-type LC molecules containing CF_2CF_2 carbocycles.

Introduction

Fluorine-containing organic compounds have attracted much attention in various areas, such as the medicinal, agrochemical, and materials science fields [1-3], due to the unique characteristics of the fluorine atom [4-6]. It is well known that fluorine atoms incorporated into organic substances very often lead to intriguing physical as well as chemical properties. Therefore, considerable attention has been devoted to the development of efficient synthetic protocols for fluorine-containing organic compounds.

Owing to the fascinating molecular properties of organofluorine compounds exerted by the fluorine atom, our research group has devoted sustained effort to the development of novel biologically active fluorinated substances and high-functional

fluorinated materials thus far [7-9]. Our recent interest inspired by the discovery of fluorinated liquid-crystalline (LC) molecules [10,11] led to the rational molecular design and synthesis of a family of novel fluorinated LC molecules that possess large negative dielectric anisotropy (Δε). In fact, as shown in Figure 1, tricyclic molecules containing a CF_2CF_2 carbocycle, e.g., the 5,5,6,6-tetrafluorocyclohexa-1,3-diene [12] or the 1,1,2,2-tetrafluorocyclohexane motif [13], were successfully synthesized and found to exhibit a large negative Δε value (−7.3 for **1c** and −9.4 for *trans*-**2c**) [14]. This indicated that these compounds are promising candidates for vertical alignment (VA)-type display materials.

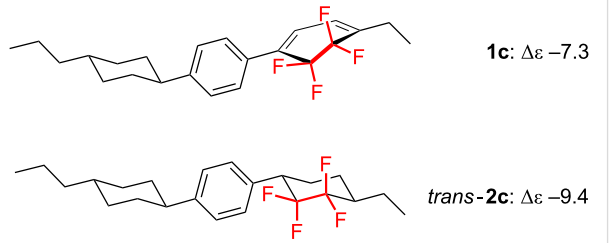

Figure 1: Typical examples of previously reported negative-type liquid crystals containing a CF_2CF_2-carbocycle.

In spite of their valuable utility, synthetic procedures for generating the aforementioned CF_2CF_2-containing LC molecules inevitably require a multistep protocol, viz. eight steps for **1** and nine steps for **2**, which is a substantial drawback for the practical application of these compounds. Therefore, for practical use of fluorine-containing LC molecules, the development of more efficient synthetic protocols is highly necessary. Herein, an improved short-step synthetic protocol for obtaining promising LC molecules containing the CF_2CF_2 fragment is demonstrated, where the improved methodology enables us to prepare the CF_2CF_2-containing cyclohexadiene **1a** and the corresponding cyclohexane **2c**, as selected examples, on the multigram scale.

Results and Discussion

Improved synthetic design

In order to establish an improved synthetic protocol, we initially designed a method for the multicyclic mesogens **1** and **2** containing a CF_2CF_2 carbocycle which is shown in Scheme 1.

The desired multicyclic molecules **1** with a tetrafluorocyclohexadiene or **2** with a tetrafluorocyclohexane moiety could be prepared starting from the same precursor, e.g., tetrafluorocyclohexane-1,4-diol **3**: through dehydration in the case of **1** or radical reduction through the corresponding bisxanthate derivative in the case of **2**. The required diol **3** could be obtained through a simultaneous hydrogenation of both, the cyclohexene and vinyl moieties of 1-aryl-4-vinyl-5,5,6,6-tetrafluorocyclohex-2-ene-1,4-diol **4**. The latter could be constructed through ring-closing metathesis of the corresponding precursor, e.g., 4,4,5,5-tetrafluoroocta-1,7-diene **5**, using a Grubbs' catalyst. The octa-1,7-diene **5** could be obtained through a nucleophilic addition of a vinylic Grignard reagent to the γ-keto ester **6**. Lastly, the γ-keto ester **6** could be prepared by an addition–elimination reaction of commercially available tetrafluorosuccinic acid diester **7**.

The designed reaction protocol enabled the construction of the target multicyclic molecules in only five or six steps, which is a more efficient protocol with three reaction steps less than the previous method. In addition, the present synthetic protocol involves several standard organic transformations, such as hydrogenation and dehydration, which are advantageous for a large-scale synthesis of the target compounds. Thus, we attempted a detailed examination of the short-step manipulations for obtaining the CF_2CF_2-containing multicyclic molecules **1** and **2**.

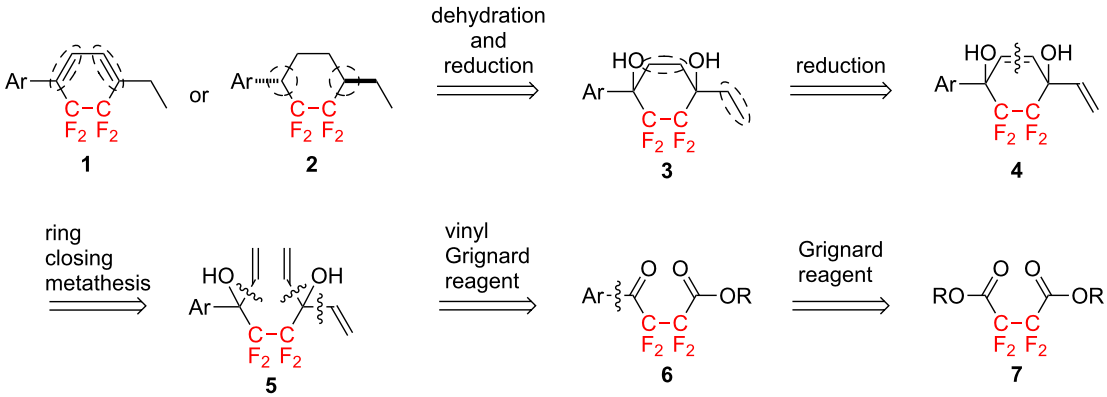

Scheme 1: Improved short-step synthetic protocol for multicyclic mesogens **1** and **2**.

Scope and limitation

The synthetic route was initiated by the sequential addition–elimination reaction of 4-*n*-propylphenylmagnesium bromide (4-*n*-PrC$_6$H$_4$MgBr) with commercially available dimethyl tetrafluorosuccinate (**7**, Scheme 2) and the results are summarized in Table 1.

Thus, the treatment of 1.0 equiv of **7** with 2.0 equiv of 4-*n*-PrC$_6$H$_4$MgBr in THF at −78 °C overnight gave the corresponding γ-keto ester **6a** in 85% isolated yield. Interestingly, although using an excess amount of Grignard reagent in this reaction, no adducts by over-reactions, e.g., **A**, **B**, **C**, etc. (Figure 2a), were observed.

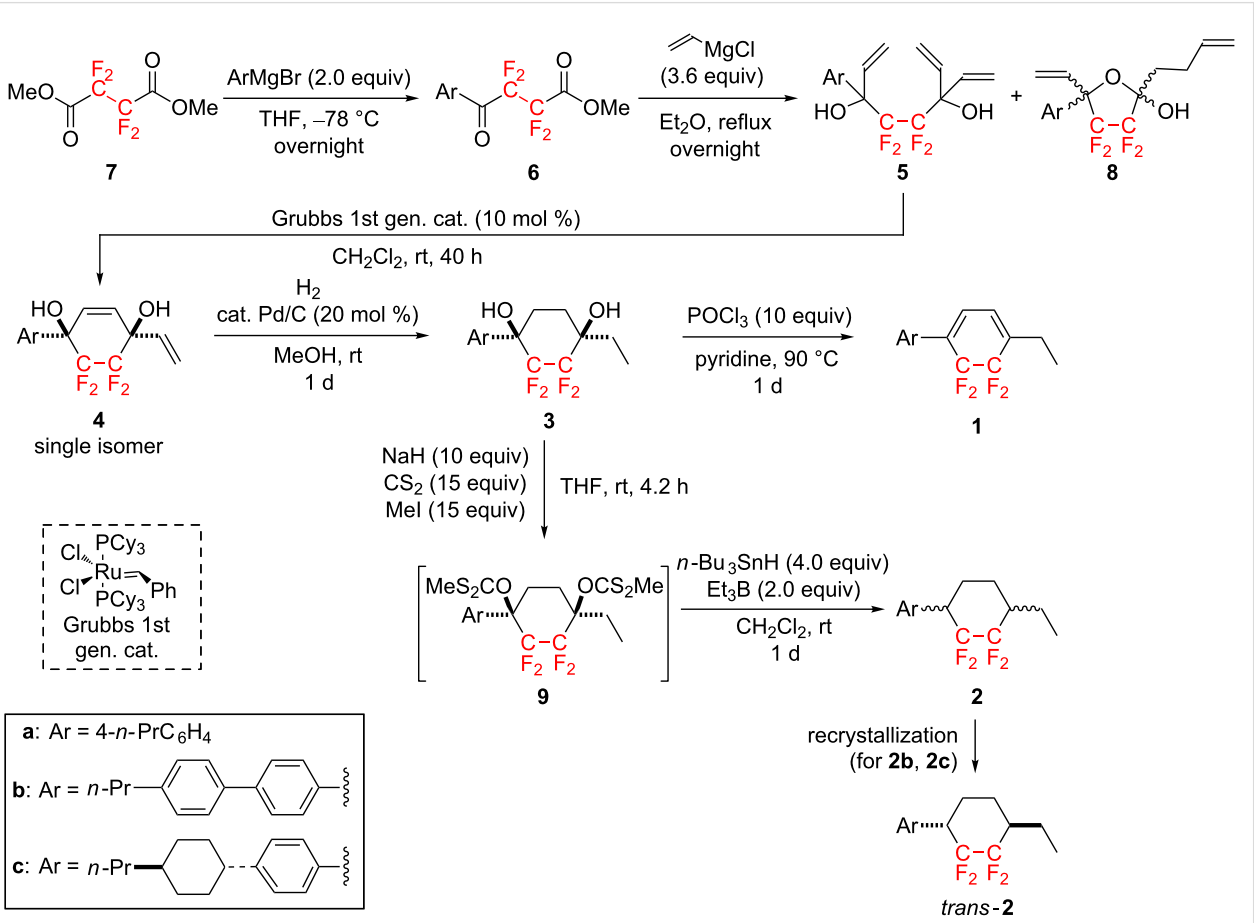

Scheme 2: Short-step approach to CF_2CF_2-containing carbocycles.

Table 1: Yields of all reaction steps in Scheme 2.

	Isolated yield [%]					
	6	**5/8**	**4**	**3**	**1**	**2** (*trans*/*cis*)[a]
n-Pr– (a)	85	46/42	75	99	82	47 (79/21)
n-Pr– (**b**)	67	43/47	59	96	96	59[b] (72/28[b]→100/0[c])[d]
n-Pr– (**c**)	86	38/46	71	100	74	59[b] (87/13[b]→100/0[c])[d]

[a]Determined by ^{19}F NMR. [b]Before recrystallization. [c]After recrystallization. [d]Previously reported in [13].

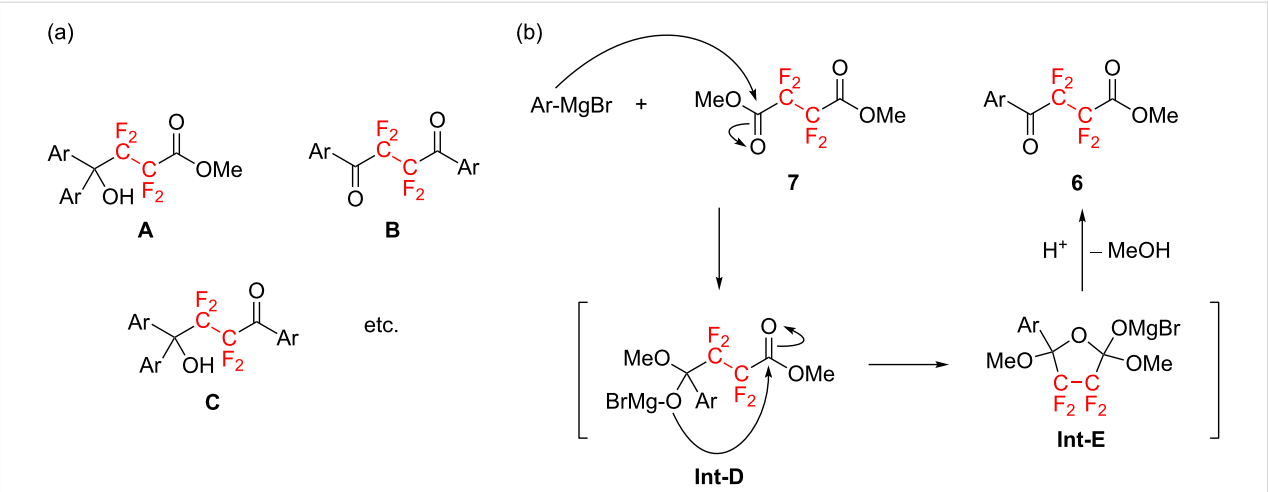

Figure 2: (a) Expected products of over-reaction in the Grignard reaction of dimethyl tetrafluorosuccinate (**7**) with 4-*n*-propylmagnesium bromide (reaction step **7**→**6**). (b) Mechanism for the **7**→**6** reaction step.

The suppression of the formation of the over-reacted products **A**–**C** may be brought about by the following possible reaction pathway (Figure 2b): (i) the nucleophilic attack of the Grignard reagent on the ester carbonyl functionality leads to the formation of the corresponding magnesium acetal **Int-D**, (ii) the alkoxide attacks another ester carbonyl moiety in the molecule to form the corresponding 5-membered ring acetal intermediate (**Int-E**) [15-17], after which immediate hydrolysis leads to the exclusive formation of the corresponding monosubstituted product **6**. The intermediate **Int-E** may be quite stable at −78 °C and in equilibrium with **Int-D** at the stated temperature because of the high electrophilicity of the carbonyl moiety derived from the strong electron-withdrawing effect of the perfluoroalkylene fragment [18,19]. Accordingly, the over-reactions did not occur, and the γ-keto ester **6a** was exclusively obtained after acid treatment of the reaction mixture.

As shown in Scheme 2, the isolated γ-keto ester **6a** was treated with a large excess (3.6 equiv) of the vinyl Grignard reagent in diethyl ether at reflux overnight to afford the corresponding octa-1,7-diene **5a** in only 46% yield. In this case, the 5-membered lactol derivative **8a** was also obtained in 42% yield as a side-product. A proposed reaction mechanism for the formation of **5a** and **8a** is shown in Scheme 3.

Thus, the nucleophilic addition reactions of vinylmagnesium chloride with the γ-keto ester **6** furnishes the corresponding magnesium alkoxide **Int-F**, which can be easily converted to the 5-membered ring intermediate, **Int-G**, as already discussed in the reaction of **7**→**6** (Figure 2b). However, the reaction at a higher temperature may lead to the elimination of MeOMgCl, generating the lactone **Int-H**. Accordingly, **Int-H** could undergo a second Grignard reaction with vinylmagnesium chloride present in the reaction mixture, resulting in the formation of **Int-I**. The latter intermediate, **Int-I** which is also in equilibrium with **Int-J** at reflux temperature, can react with the vinylic Grignard reagent through two possible pathways. As indicated by the blue arrow in Scheme 3, when vinylmagnesium chloride attacks the carbonyl carbon of **Int-I**, the corresponding adduct **Int-K** is formed in situ; this adduct can be smoothly converted into the desired octa-1,7-diene **5a** after acid hydrolysis. On the other hand, the β-carbon at the α,β-unsaturated carbonyl moiety of **Int-I** may be susceptible to attack by the vinylic Grignard reagent, as shown by the purple arrow in Scheme 3, because of the high electrophilicity and lack of steric hindrance. As a consequence, **Int-I** also undergoes conjugate addition reaction, a Michael addition reaction, giving rise to the corresponding magnesium enolate **Int-L**. The subsequent hydrolysis of **Int-L** then leads to the γ-hydroxyketone **8a'**, which easily tautomerizes into the more stable 5-membered hemiacetal **8a**.

From the above insight into the reaction mechanism, if the 1,2-addition reaction of **Int-I** proceeds in preference to the conjugate addition reaction, the desired octa-1,7-diene **5a** should be produced in higher yield. However, no significant improvement was observed after various attempts such as employing a more nucleophilic lithium reagent instead of the Grignard reagent [20] or the addition of a Lewis acid to the reaction mixture [21,22]. Fortunately, **5a** and **8a** are easily separable by silica gel column chromatography, and the obtained octa-1,7-diene **5a** was employed in the ensuing reaction without further attempts to improve its yield.

The subsequent ring-closing metathesis [23-25] of **5a** under the influence of less than 10 mol % of a Grubbs 1st generation catalyst did not proceed to completion, resulting in recovery of the

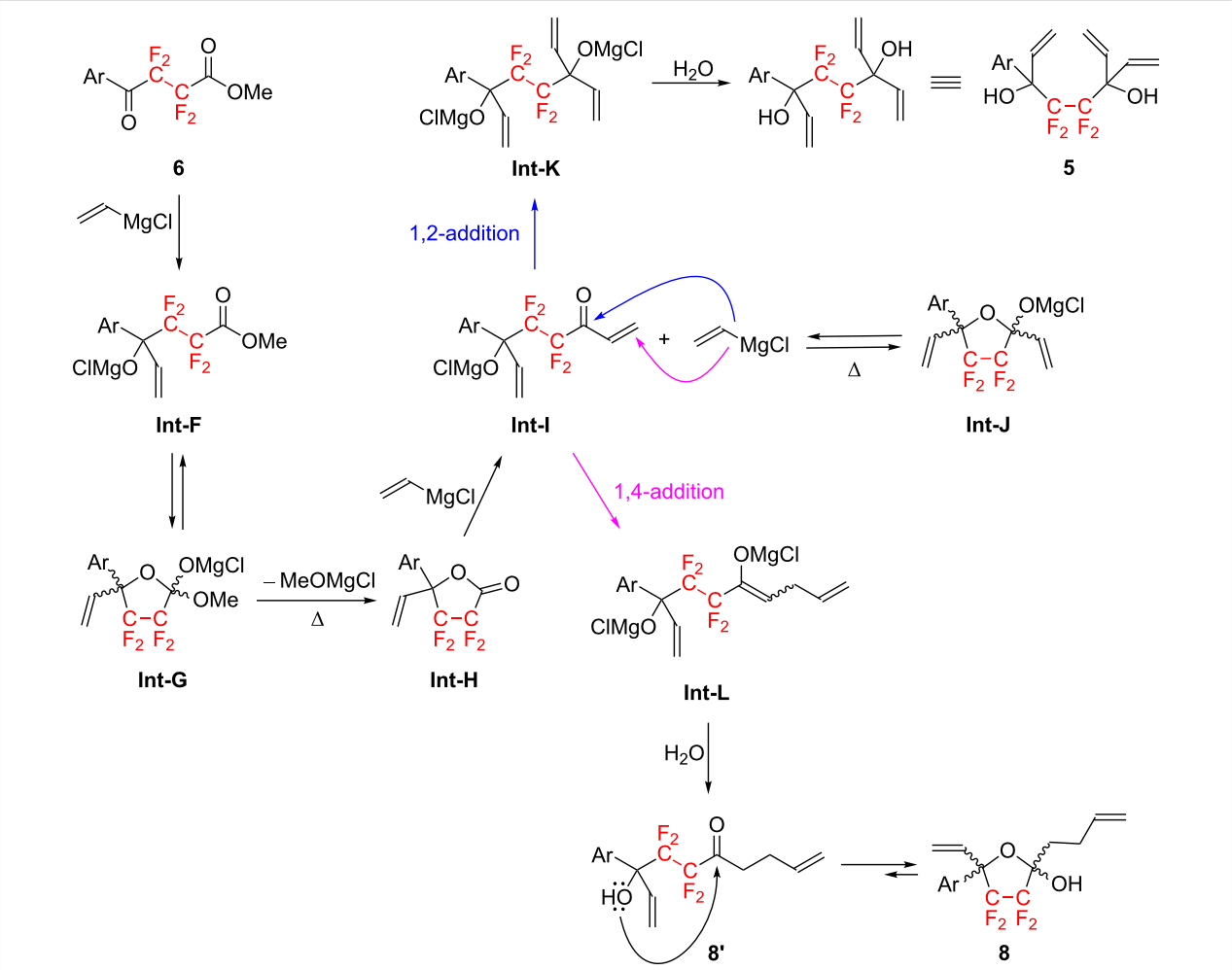

Scheme 3: Mechanism for the reaction of γ-keto ester **6** with vinyl Grignard reagents.

starting material along with the desired adduct **4a**. Increasing the reaction temperature did not lead to satisfactory results. However, performing the reaction in the presence of 10 mol % of the catalyst for 40 h drove the reaction to completion. Intriguingly, the ring-closing metathesis proceeded in a highly diastereoselective manner and produced the corresponding cyclized adduct **4a** as a single isomer [26].

Finally, with compound **4a** in hand, the successive hydrogenation in the presence of 20 mol % of Pd/C in methanol was performed for 1 d and generated the corresponding tetrafluorinated cyclohexane-1,4-diol **3a** in quantitative yield. Compound **3a** could be converted to the cyclohexadiene **1a** in 82% isolated yield under the influence of a large amount of phosphorus oxychloride in pyridine at 90 °C for 1 d according to the previous literature [12]. On the other hand, **4a** could also be transformed into the corresponding bisxanthate derivative **9a** according to the literature procedure [13]. Without further purification, **9a** was treated with 4.0 equiv of *n*-Bu_3SnH and 2.0 equiv of Et_3B in dichloromethane at room temperature for 1 d to afford the desired reduction products **2a** as an inseparable diastereomeric mixture in a *trans*/*cis* ratio of ca. 80:20 in 47% isolated yield [27].

With the established short-step protocol, we subsequently synthesized **1b**, **1c**, **2b**, and **2c** using the corresponding Grignard reagents, e.g., (4-*n*-PrC_6H_4)C_6H_4MgBr or 4-(*trans*-4-*n*-Pr-*c*-C_6H_{10})C_6H_4MgBr, instead of 4-*n*-PrC_6H_4MgBr. As shown in Table 1, all reactions proceeded well to afford the corresponding adducts in acceptable to excellent yields. Tricyclic cyclohexanes containing the CF_2CF_2 fragment, e.g., **2b** and **2c**, were also obtained as a mixture of *trans*/*cis* diastereomers, but careful recrystallization enabled the isolation of the *trans* isomers in a pure form. A noteworthy advantage of the current synthetic protocol is that starting from the commercially available fluorine-containing substance **7**, multigram-scale preparation of the promising negative-type LC molecules could be firstly achieved and ca. 2.0 g each of tetrafluorocyclohexadiene

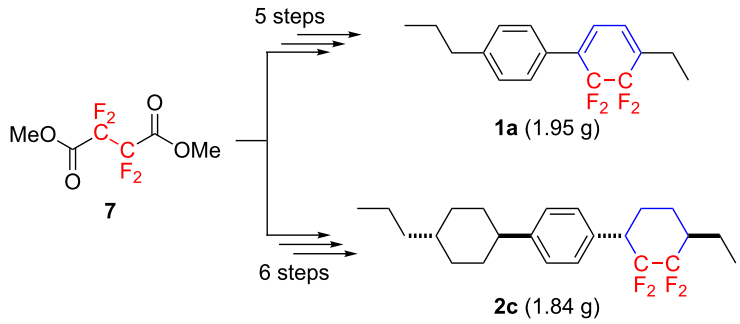

Scheme 4: First multigram-scale preparation of CF_2CF_2-containing multicyclic mesogens.

1a and the cyclohexane derivative **2c** (Scheme 4) were obtained. This achievement may lead to a significant contribution to the LC display industry.

The stereochemistry in the ring-closing metathesis step **5**→**4** was determined as follows. As depicted in Table 2, it has been generally recognized that the melting points of *trans*-1,4-disubstituted cyclohexane-1,4-diols are much higher than those of the corresponding *cis*-counterparts [28].

Table 2: Melting points of various 1,4-disubstituted cyclohexane-1,4-diol derivatives.

R	Melting point (mp) [°C]	
	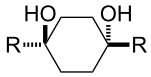 *trans*	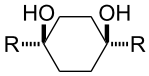 *cis*
H	143	100–102
CH_3	199–200	166–167
Ph	234.5–235	150.5–151
$HC{\equiv}CCH_2$	193	131
$CH_2{=}CHCH_2$–	133	72

As shown in Scheme 5, diastereomeric mixtures of *trans*- and *cis*-1-ethyl-2,2,3,3-tetrafluoro-4-[4-(4-*n*-propylphenyl)phenyl]cyclohexane-1,4-diol (**3b**) or 1-ethyl-2,2,3,3-tetrafluoro-4-[4-(*trans*-4-*n*-propylcyclohexyl)phenyl]cyclohexane-1,4-diol (**3c**) were obtained through an alternative procedure, starting from commercially available 4-bromo-3,3,4,4-tetrafluorobut-1-ene [12,13]. Fortunately, the *trans*/*cis* diastereomers **3b** and **3c** could be separated from each other through silica gel column chromatography. The careful thermal analyses of the diastereomers **3b** and **3c** [12] revealed that the melting points of the less polar products were approximately 20–50 °C higher than those of the more polar products, indicating that the former and the latter could be successfully assigned as the *trans*- and *cis*-isomer, respectively. On the other hand, the products **3b** and **3c** obtained in the present study were found to be identical to the more polar adducts based on comparison of various physical data, such as the ^1H, ^{13}C, ^{19}F nuclear magnetic resonance (NMR) signals, retardation factors (R_f values), melting points, etc. From these analyses, **3b** and **3c** obtained by the present protocol were eventually determined to be the *cis*-isomer in both cases.

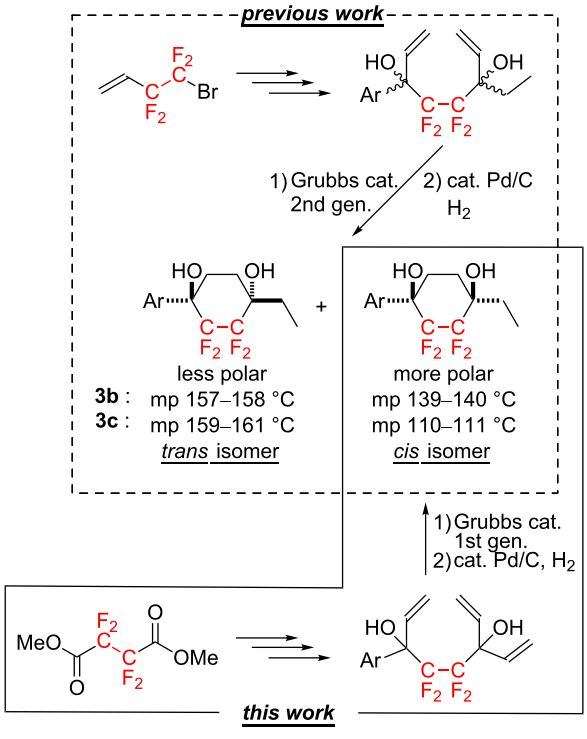

Scheme 5: Stereochemical assignment of the ring-closing metathesis products.

Conclusion

In summary, we demonstrated the efficient short-step, gram-scale preparation of tetrafluorinated cyclohexadiene or cyclo-

hexane derivatives, which are very promising negative-type LC molecules, starting from commercially available dimethyl 2,2,3,3-tetrafluorosuccinate (**7**). A total of only five or six steps were required for the synthesis of the cyclohexadiene or cyclohexane derivatives, respectively. It should also be noted that the present reaction pathways did not require specific techniques or sensitive reagents, and gram-scale preparation was successfully achieved. The present synthetic protocol is promising for the development of a wide range of negative-type LC molecules containing CF_2CF_2 carbocycles by the selection of the starting Grignard reagent and should contribute to further evolution of VA-type LC display molecules.

Supporting Information

Supporting Information File 1

Experimental procedures, characterization data, and copies of ^{1}H, ^{13}C and ^{19}F NMR spectra.
[http://www.beilstein-journals.org/bjoc/content/supplementary/1860-5397-14-10-S1.pdf]

ORCID® iDs

Shigeyuki Yamada - https://orcid.org/0000-0002-6379-0447
Tsutomu Konno - https://orcid.org/0000-0002-5146-9840

References

1. Charpentier, J.; Früh, N.; Togni, A. *Chem. Rev.* **2015,** *115,* 650–682. doi:10.1021/cr500223h
2. Campbell, M. G.; Ritter, T. *Chem. Rev.* **2015,** *115,* 612–633. doi:10.1021/cr500366b
3. Ni, C.; Hu, M.; Hu, J. *Chem. Rev.* **2015,** *115,* 765–825. doi:10.1021/cr5002386
4. Zhou, Y.; Wang, J.; Gu, Z.; Wang, S.; Zhu, W.; Aceña, J. L.; Soloshonok, V. A.; Izawa, K.; Liu, H. *Chem. Rev.* **2016,** *116,* 422–518. doi:10.1021/acs.chemrev.5b00392
5. Ni, C.; Hu, J. *Chem. Soc. Rev.* **2016,** *45,* 5441–5454. doi:10.1039/C6CS00351F
6. O'Hagan, D. *Chem. Soc. Rev.* **2008,** *37,* 308–319. doi:10.1039/B711844A
7. Konno, T. *Synlett* **2014,** *25,* 1350–1370. doi:10.1055/s-0033-1340867
8. Konno, T.; Ishihara, T. In *Advances in Organic Synthesis, Modern Organofluorine Chemistry–Synthetic Aspects;* Rahman, A.-U.; Laali, K. K., Eds.; Bentham Science Publishers, Ltd.: The Netherlands, 2006; Vol. 2, pp 491–522.
9. Konno, T.; Ishiahra, T. A New Aspect of Fluoroalkylated Acetylenes: Synthesis and Applications—Hydrometallation and Carbometallation. In *Fluorine-Containing Synthons;* Soloshonok, V. A., Ed.; ACS Publication Division and Oxford University Press: Washington DC, 2005; Vol. 911, pp 190–203. doi:10.1021/bk-2005-0911.ch009
10. Kirsch, P. *J. Fluorine Chem.* **2015,** *177,* 29–36. doi:10.1016/j.jfluchem.2015.01.007
11. Hird, M. *Chem. Soc. Rev.* **2007,** *36,* 2070–2095. doi:10.1039/b610738a
12. Yamada, S.; Hashishita, S.; Asai, T.; Ishihara, T.; Konno, T. *Org. Biomol. Chem.* **2017,** *15,* 1495–1509. doi:10.1039/C6OB02431A
13. Yamada, S.; Hashishita, S.; Konishi, H.; Nishi, Y.; Kubota, T.; Asai, T.; Ishihara, T.; Konno, T. *J. Fluorine Chem.* **2017,** *200,* 47–58. doi:10.1016/j.jfluchem.2017.05.013
14. The Δε values were obtained in a binary mixture of the guest fluorinated molecule (10%) and host LC molecule (90%, MLC-6608 (Merck)) by means of extrapolation technique. The experimentally details were described in previous reports; see references [12,13].
15. Bonnac, L.; Lee, S. E.; Giuffredi, G. T.; Elphick, L. M.; Anderson, A. A.; Child, E. S.; Mann, D. J.; Gouverneur, V. *Org. Biomol. Chem.* **2010,** *8,* 1445–1454. doi:10.1039/b922442d
16. Timofte, R. S.; Linclau, B. *Org. Lett.* **2008,** *10,* 3673–3676. doi:10.1021/ol801272e
17. Boydell, A. J.; Vinader, V.; Linclau, B. *Angew. Chem., Int. Ed.* **2004,** *43,* 5677–5679. doi:10.1002/anie.200460746
18. Kaneko, S.; Yamazaki, T.; Kitazume, T. *J. Org. Chem.* **1993,** *58,* 2302–2312. doi:10.1021/jo00060a055
19. Pierce, O. R.; Kane, T. G. *J. Am. Chem. Soc.* **1954,** *76,* 300–301. doi:10.1021/ja01630a097
20. Amoah, E.; Dieter, R. K. *J. Org. Chem.* **2017,** *82,* 2870–2888. doi:10.1021/acs.joc.6b02769
21. Pace, V.; Castoldi, L.; Hoyos, P.; Sinisterra, J. V.; Pregnolato, M.; Sánchez-Montero, J. M. *Tetrahedron* **2011,** *67,* 2670–2675. doi:10.1016/j.tet.2011.01.067
22. Liu, H.-J.; Shia, K.-S.; Shang, X.; Zhu, B.-Y. *Tetrahedron* **1999,** *55,* 3803–3830. doi:10.1016/S0040-4020(99)00114-3
23. Vougioukalakis, G. C.; Grubbs, R. H. *Chem. Rev.* **2010,** *110,* 1746–1787. doi:10.1021/cr9002424
24. Nolan, S. P.; Clavier, H. *Chem. Soc. Rev.* **2010,** *39,* 3305–3316. doi:10.1039/b912410c
25. Coquerel, Y.; Rodriguez, J. *Eur. J. Org. Chem.* **2008,** 1125–1132. doi:10.1002/ejoc.200700696
26. Wallace, D. J. *Tetrahedron Lett.* **2003,** *44,* 2145–2148. doi:10.1016/S0040-4039(03)00161-8
27. Our previous report cited in [13] reported that a catalytic hydrogenation of tetrafluorocyclohexa-1,3-diene provided the corresponding cyclohexane moiety in a *cis*-selective manner. After careful investigations, the present methodology was successful to obtain the desired tetrafluorocyclohexane unit with a *trans*-selective manner.
28. Courtot, P.; Kinastowski, S.; Lumbroso, H. *Bull. Soc. Chim. Fr.* **1964,** 489–494.

License and Terms

BEILSTEIN JOURNAL OF ORGANIC CHEMISTRY

Progress in copper-catalyzed trifluoromethylation

Guan-bao Li[1], Chao Zhang[1], Chun Song[*1] and Yu-dao Ma[*2]

Review

Open Access

Address:
[1]School of Pharmaceutical sciences, Shandong University, 44 West Culture Road, Jinan 250012, PR China and [2]Department of chemistry, Shandong University, 27 Shanda South Road, Jinan 250100, PR China

Email:
Chun Song[*] - chunsong@sdu.edu.cn; Yu-dao Ma[*] - ydma@sdu.edu.cn

* Corresponding author

Keywords:
copper; fluorine; trifluoromethylation

Beilstein J. Org. Chem. **2018,** *14,* 155–181.
doi:10.3762/bjoc.14.11

Received: 19 October 2017
Accepted: 04 January 2018
Published: 17 January 2018

This article is part of the Thematic Series "Organo-fluorine chemistry IV".

Guest Editor: D. O'Hagan

Abstract

The introduction of trifluoromethyl groups into organic molecules has attracted great attention in the past five years. In this review, we describe the recent efforts in the development of trifluoromethylation via copper catalysis using nucleophilic, electrophilic or radical trifluoromethylation reagents.

Introduction

The fluorine atom has a strong electronegativity and a small atomic radius, and the incorporation of fluoroalkyl groups into molecules imparts a variety of features. The trifluoromethyl group, as the most significant common used fluoroalkyl group, could improve molecular properties such as metabolic stability, lipophilicity and permeability [1-4]. Therefore, organic molecules bearing trifluoromethyl groups are widely used in pharmaceuticals and agrochemicals, such as the antidepressant fluoxetine, the anti-ulcer drug lansoprazole and so on (Figure 1).

The specific roles of the trifluoromethyl group (CF_3) in biologically active molecules promote the development of novel methods to construct C–CF_3 bonds in the past few years. Among the many methods developed, copper-catalyzed trifluoromethylation has gained enormous interest due to its high efficiency and cheapness.

Recently, several reviews on trifluoromethylation were disclosed. Xu, Dai [5] and Shen [6] mainly discussed progress in copper-mediated trifluoromethylation before 2013. Other works focus on the trifluoromethylation of alkynes [7] or on the C(sp^3)−CF_3, C(sp^2)−CF_3, and C(sp)−CF_3 bond construction [8]. This minireview mainly focuses on the copper-mediated or -catalyzed trifluoromethylations from 2012 to 2016. And some previous pioneering works were included to gain a comprehensive understanding of the development of the diverse synthetic methods over the time. Throughout this minireview, compounds **1** are the trifluoromethylation reagents.

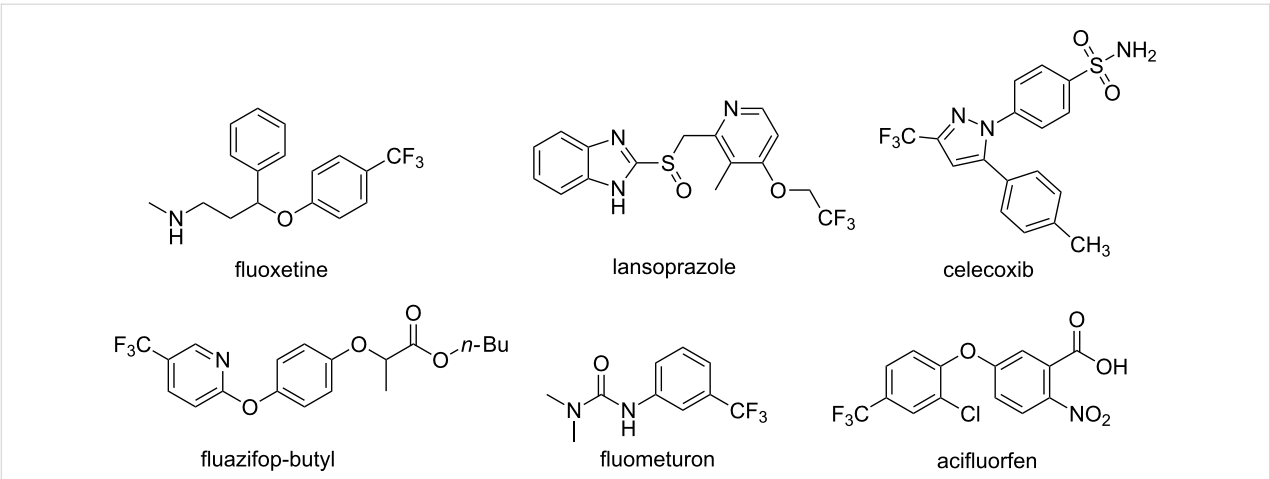

Figure 1: Selected examples of pharmaceutical and agrochemical compounds containing the trifluoromethyl group.

Review

Copper-catalyzed trifluoromethylation of aryl and alkyl halides

The first example of copper-promoted perfluoroalkylation of aromatic halides was presented in a US patent 1968 [9]. Since then, the copper-catalyzed trifluoromethylation of aromatic compounds has entered a stage of rapid development. Many reviews [6,10] have been published on this subject, so this part mainly discussed trifluoromethylations using several new trifluoromethylation reagents and some important examples using traditional trifluoromethylation reagents were also involved.

Trifluoromethylation of aryl halides with traditional trifluoromethylation reagents and a trifluoromethyl-substituted sulfonium ylide as a new reagent

The CuI-mediated cross-coupling protocol using $TESCF_3$ was firstly reported by Urata and Fuchikami [11]. The proposed mechanism of this reaction was demonstrated in Scheme 1. But it was found that the generation rate of trifluoromethyl anions is

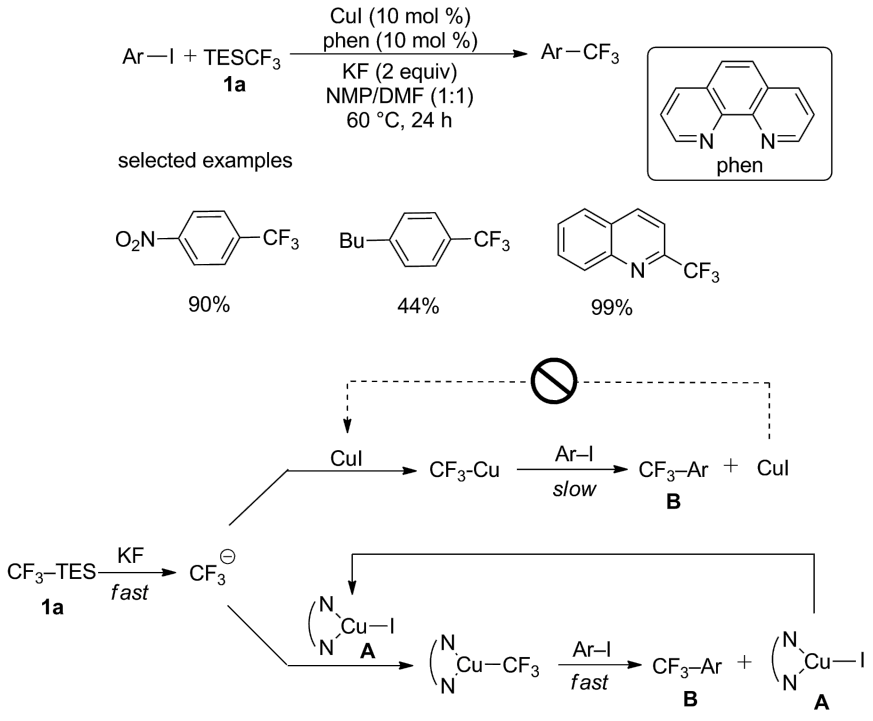

Scheme 1: Introduction of a diamine into copper-catalyzed trifluoromethylation of aryl iodides.

much higher than the second step affording **B** and CuI. Thus, there is no sufficient recirculated CuI to react with trifluoromethyl before its decomposition. Optimizations were then performed to overcome this shortcoming in 2009 [12], a series of diamine ligands such as 1,10-phenanthroline (phen) were discovered. These diamines were able to accelerate the second step to regenerate sufficient amounts of reusable complexes **A** utilizing copper(I)-diamine complexes (Scheme 1), thus accelerating the trifluoromethylation of aryl/heteroaryl iodides.

Although this catalytic reaction worked efficiently, the trifluoromethyl source $TESCF_3$ was expensive and relatively inaccessible, which made this process less economic, especially for large-scale synthesis.

In 2014, Novák, Kotschy and co-workers [13] developed a new procedure with the relatively cheap and readily available $TMSCF_3$ (Scheme 2). Similarly, the recycling of CuI was inefficient and led to the degradation of excessive trifluoromethyl anions. Differently, a novel strategy was developed to solve this problem, a Lewis acid such as trialkyl borate was added for the temporary trapping of the in situ generated trifluoromethyl anion and suppress its rapid decomposition (Scheme 2).

S-(Trifluoromethyl)diphenylsulfonium salts, as commonly used electrophilic trifluoromethylation reagents, were orginally developed by the group of Yagupolskii [14]. When iodo-substituted aromatics and heteroaromatics were employed as the substrates, Xiao and co-workers [15] firstly used *S*-(trifluoromethyl)diphenylsulfonium salts in the presence of copper powder to convert the substrates into the corresponding trifluoromethylated compounds in high yield. The $CuCF_3$ intermediate was formed in this process, as confirmed by ^{19}F NMR spectroscopy and ESIMS. It was proposed that $[CuCF_3]$ was generated through reduction of *S*-(trifluoromethyl)diphenylsulfonium triflate by Cu^0 through a single-electron transfer (SET) process (Scheme 3).

In 2015, the group of Lu and Shen [16] developed a new electrophilic trifluoromethylation reagent, trifluoromethyl-substituted sulfonium ylide, which was prepared by a Rh-catalyzed carbenoid addition to trifluoromethyl thioether (Scheme 4). This process was conducted in dichloromethane at 40 °C for 4 h with a catalyst loading of 100 ppm. Moreover, this new reagent was easily scaled-up and stable to moisture and air. This reagent was applied in trifluoromethylation of aryl iodides. A variety of aryl and heteroaryl iodides were converted to the corresponding ana-

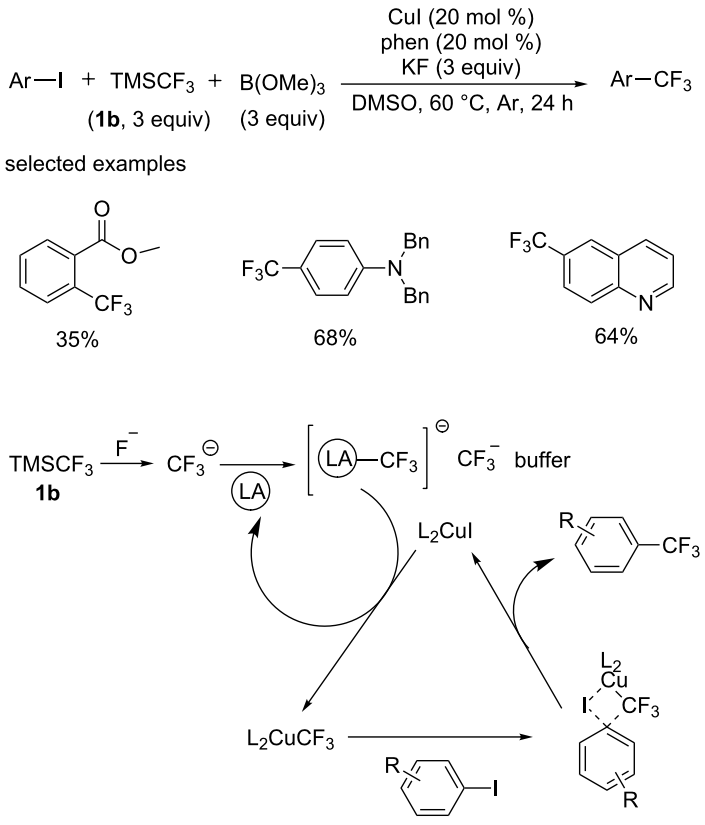

Scheme 2: Addition of a Lewis acid into copper-catalyzed trifluoromethylation of aryl iodides and the proposed mechanism.

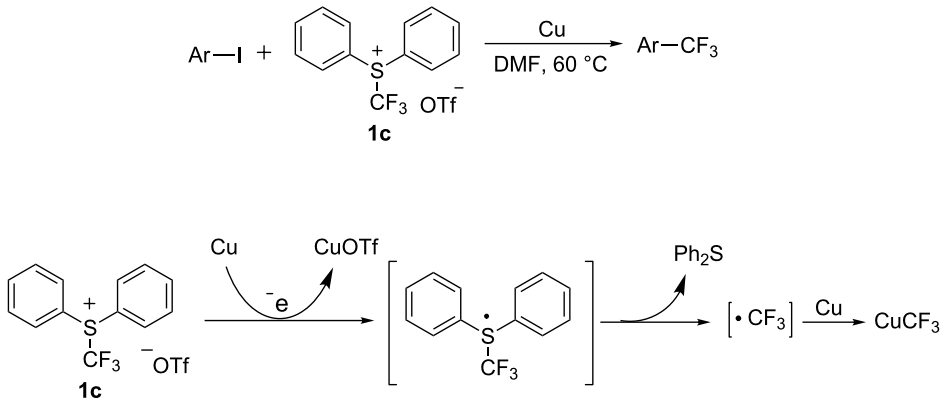

Scheme 3: Trifluoromethylation of heteroaromatic compounds using *S*-(trifluoromethyl)diphenylsulfonium salts as a trifluoromethyl source.

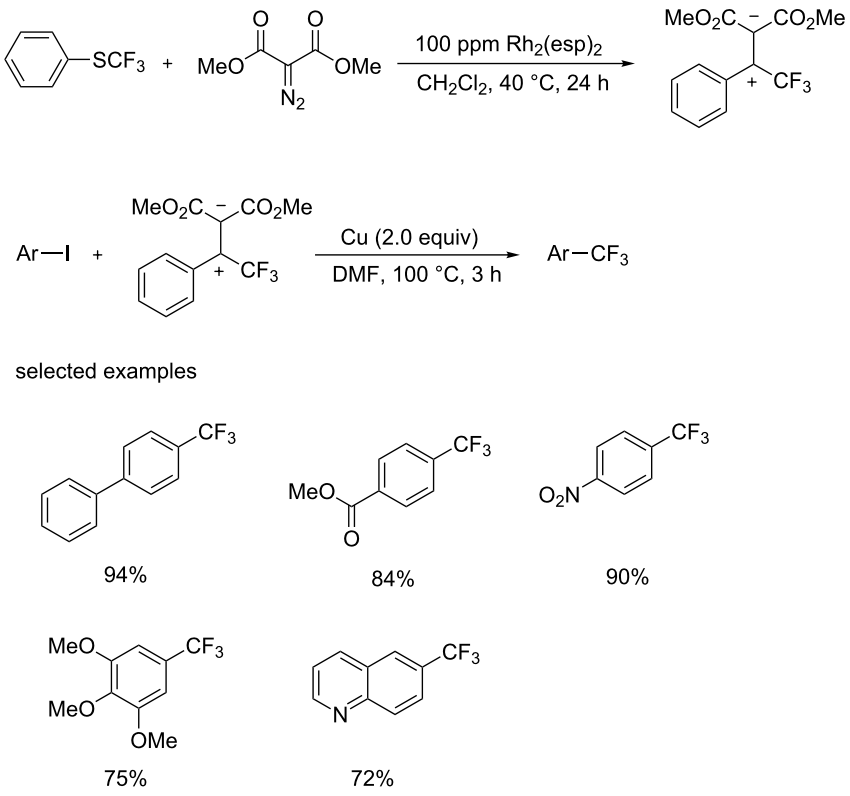

Scheme 4: The preparation of a new trifluoromethylation reagent and its application in trifluoromethylation of aryl iodides.

logues in high yields. Both electron-donating and -withdrawing groups including methoxy, nitro and ester groups, were tolerated.

Trifluoromethylation of aryl halides using trifluoroacetates as the trifluoromethyl source

Reactions employing expensive electrophilic CF_3 species such as Umemoto's reagent or Togni's reagent, were unpractical and limited on a large-scale synthesis. After comparison of the prices of different CF_3 reagents, attention was paid on trifluoroacetates. Trifluoroacetate is readily available and one of the cheapest and most convenient sources of the trifluoromethylation for both industrial and medicinal purposes.

In 2011, a practical and ligand-free Cu-catalyzed decarboxylative trifluoromethylation of aryl iodides was reported by the

group of Li and Duan, with sodium trifluoroacetate as the trifluoromethyl source and using Ag_2O as a promoter (Scheme 5) [17].

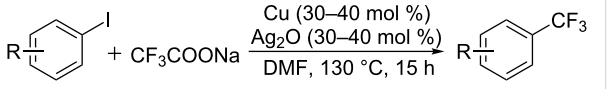

Scheme 5: Trifluoromethylation of aryl iodides using CF_3CO_2Na as a trifluoromethyl source.

Subsequently, Beller and co-workers [18] finished a copper-catalyzed trifluoromethylation of aryl iodides with inexpensive methyl trifluoroacetate (MTFA) (Scheme 6). However, it was found that the generation of the trifluoromethyl anion proceeds faster than the subsequent transfer of CF_3 to the aromatic halide. Subsequently, the problem was solved by using a slow addition mode that adjusted the rate of decarboxylation step to the rate of the consumption of CF_3 in the aromatic trifluoromethylation step.

The attractive prospect of trifluoroacetate as the trifluoromethyl source for the preparation of trifluoromethylarenes prompted the investigation of the mechanism of this reaction. A mechanistic study indicated that $CuCF_3$ was formed by decarboxylation of the trifluoroacetate (Scheme 6), followed by oxidative addition with aryl iodides and the trifluoromethylated products were delivered through reductive elimination.

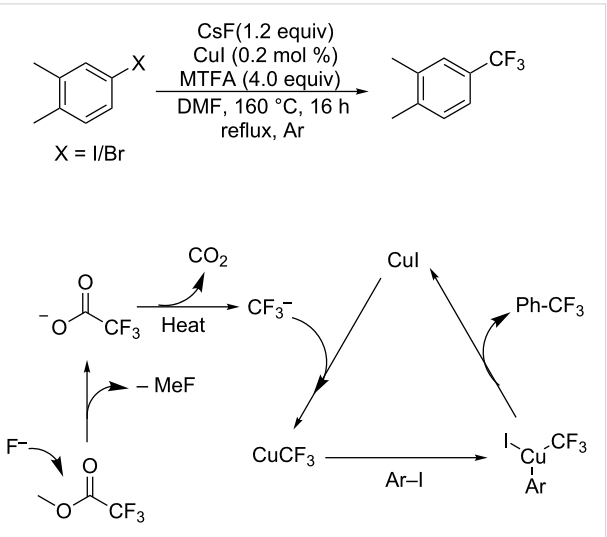

Scheme 6: Trifluoromethylation of aryl iodides using MTFA as a trifluoromethyl source.

Later, Buchwald and co-worker [19] firstly developed an efficient, scalable technique to introduce a trifluoromethyl group into aryl iodides with CF_3CO_2K as the CF_3 source (Scheme 7). High temperature was required to accelerate the rate of the decarboxylation of CF_3CO_2K and the increased pressure occurred during the process, which brought problems under batch conditions. Buchwald and co-worker deal with it through combining flow chemistry. Under flow conditions, reaction parameters such as temperature, pressure and residence times could be readily managed. Besides, very short reaction times (16 minutes) were required to achieve full conversion of (hetero)aryl starting materials in this protocol.

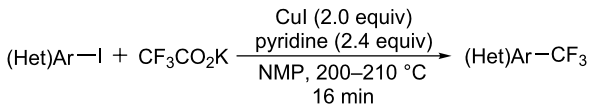

Scheme 7: Trifluoromethylation of aryl iodides using CF_3CO_2K as a trifluoromethyl source.

More recently, Weng and co-workers [20] reported a new economic decarboxylative trifluoromethylation reagent [$Cu(phen)O_2CCF_3$], which was prepared from readily available and inexpensive starting materials (Scheme 8). Treatment of copper *tert*-butoxide with phen, followed by addition of trifluoroacetic acid afforded the air-stable [$Cu(phen)O_2CCF_3$] complex, which was characterized by X-ray crystallography. Aryl iodides, which contained nitrile, ketone, aldehyde, ester, methyl, phenyl groups, etc., were successfully reacted with this trifluoromethylation reagent to give the corresponding products in moderate to high yields. Also, a broad spectrum of heteroaryl bromides proceeded smoothly to form the corresponding products. A late-stage trifluoromethylation of an estradiol derivative and a gram-scale reaction were performed with this protocol demonstrating the applicability of this protocol to other pharmaceutically relevant molecules and its scalability.

Trifluoromethylation of aryl halides using difluorocarbene precursors as the trifluoromethyl source

The trifluoromethyl sources employed in the above-mentioned trifluoromethylations were mainly CF_3-containing reagents. Besides, some examples employing difluorocarbene precursors as the trifluoromethylation reagents were reported recently.

In 2015, the group of Lin, Zheng and Xiao [21] disclosed a trifluoromethylation reagent, the difluorocarbene precursor difluoromethyltriphenylphosphonium bromide (DFPB), which could be applied in the trifluoromethylation of aromatic iodides without addition of external fluoride (Scheme 9). It was found that DBU can promote the decomposition of difluorocarbene to give fluoride which then reacts with difluorocarbene to a trifluoromethyl anion. Both electron-rich and electron-deficient sub-

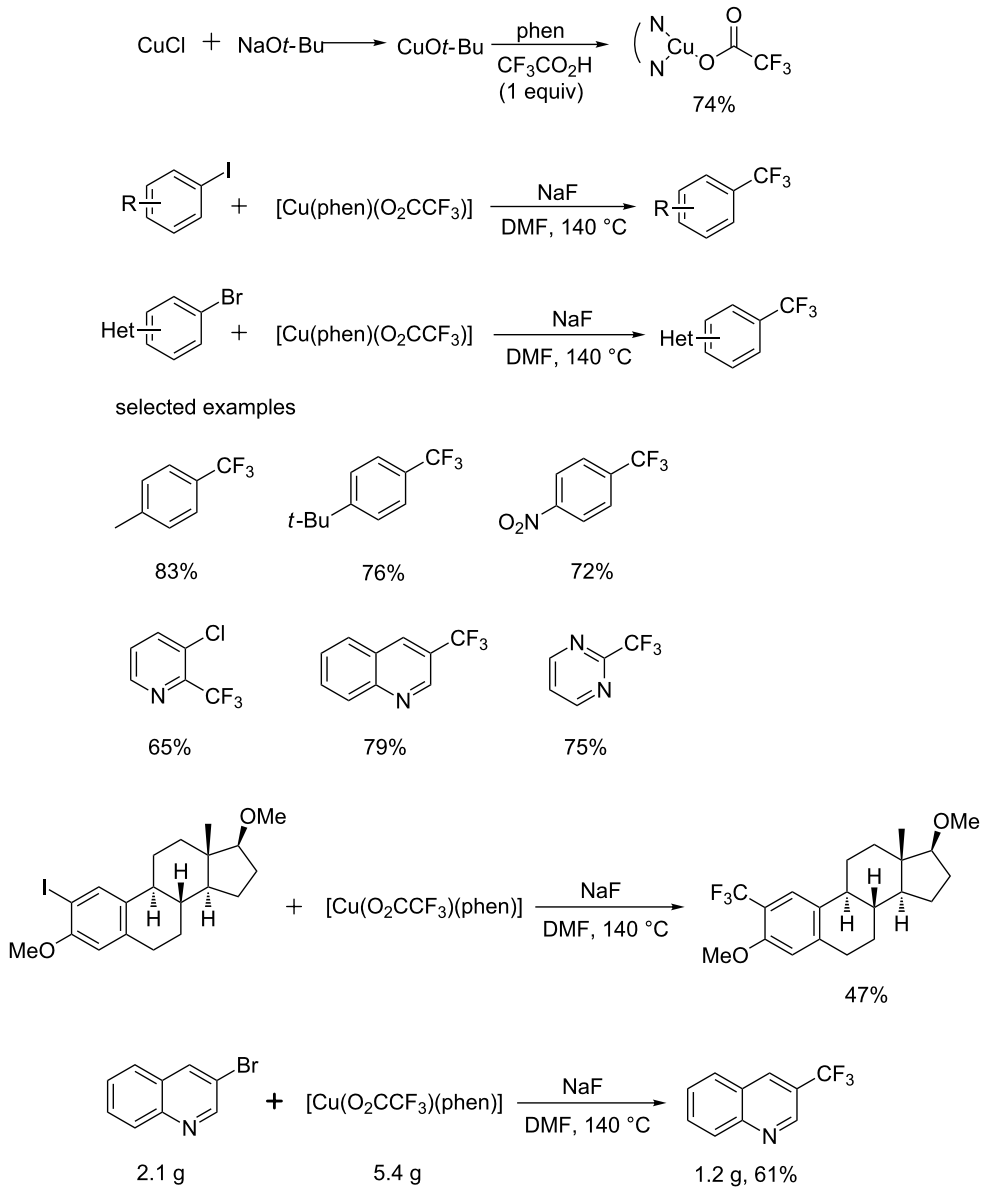

Scheme 8: Trifluoromethylation of aryl iodides and heteroaryl bromides using [Cu(phen)(O_2CCF_3)] as a trifluoromethyl source.

strates were converted to the corresponding analogues in moderate to good yields, without producing byproducts from a pentafluoroethylation.

The proposed reaction mechanism is depicted in Scheme 9. First, a phosphonium ylide is formed after treating DFPB with DBU, and then dissociated to generate a difluorocarbene. The difluorocarbene reacts with DBU affording nitrogen ylide **I**, followed by a rearrangement to give unstable difluoromethyl amine **II**. Decomposition of **II** produces intermediate **III** by releasing a fluoride ion which was trapped by difluorocarbene affording the trifluoromethyl anion. The latter reacts with copper to $CuCF_3$. The desired Ar–CF_3 was formed by the reaction of $CuCF_3$ with the aromatic iodide. Additionally, the intermediate **III** is also unstable and decomposes to intermediate **IV** in the presence of water. And DBU is regenerated after the elimination of HF and decarbonylation.

Then, the group of Zhang [22] from GlaxoSmithKline designed trimethylsilyl chlorodifluoroacetate (TCDA) as a novel reagent, which was demonstrated to efficiently introduce a CF_3 group via cooperative interaction of AgF and CuI (Scheme 10). In order to develop a practical process, the expensive AgF was replaced by KF. Under improved conditions, a broad range of aryl iodides were applicable to this protocol. The utility of this new reagent for the late-stage trifluoromethylation

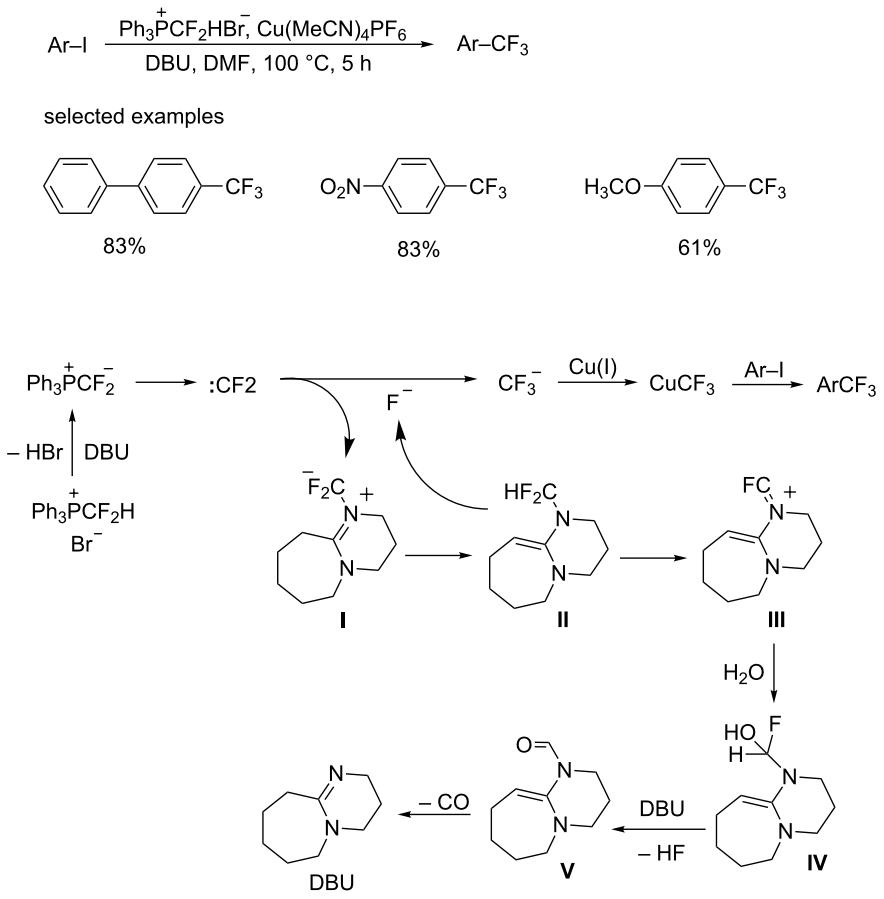

Scheme 9: Trifluoromethylation of aryl iodides with DFPB and the proposed mechanism.

was demonstrated by the preparation of drug-related molecules, Boc-fluoxetine, fluvoxamine, and flutamide in decagram scale.

In 1989, the group of Chen [23] developed the first catalytic trifluoromethylation reaction of haloarenes with $FSO_2CF_2CO_2Me$ in the presence of CuI. It is proposed that the reaction pathway involved the formation of corresponding $Cu(I)(O_2CCF_2SO_2F)$. Later in 2016 [24], they sought to isolate and characterize the intermediate. During the study, they accidently prepared $Cu(II)(O_2CCF_2SO_2F)_2$ instead of the desired $Cu(I)(O_2CCF_2SO_2F)$, the former was demonstrated to be an efficient and mild trifluoromethylating reagent. It is a blue solid and can be conveniently prepared from inexpensive starting materials on a large scale.

In this literature, the author proposed a plausible mechanism (Scheme 11). First, **1d** in DMF decomposed into Cu^{2+}, difluorocarbene and fluoride with the release of SO_2 and CO_2. Then, difluorocarbene and fluoride combined into a CF_3 species in the presence of Cu^{2+} and Cu. In contrast with the majority of previously reported copper-mediated trifluoromethylation reactions of haloarenes, $CuCF_3$ generated in situ without any ligand reacts with the haloarenes to provide the corresponding products in good to excellent yields with good functional group compatibility.

Copper-catalyzed trifluoromethylation of alkyl halides

Considerable efforts have been devoted to the trifluoromethylation of aryl halides in the past years. In contrast, successful examples of copper-catalyzed trifluoromethylation of alkyl halides are quite limited.

In 2011, the group of Shibata [25] firstly reported the copper-mediated chemoselective trifluoromethylation at the benzylic position with shelf-stable electrophilic reagent **1c** (Scheme 12). In this protocol, benzyl bromides reacted with reactive $[CuCF_3]$ generated in situ from the reduction of **1c**. A broad range of benzyl bromides were found to be compatible with the reaction conditions, giving the corresponding products in good to high yields.

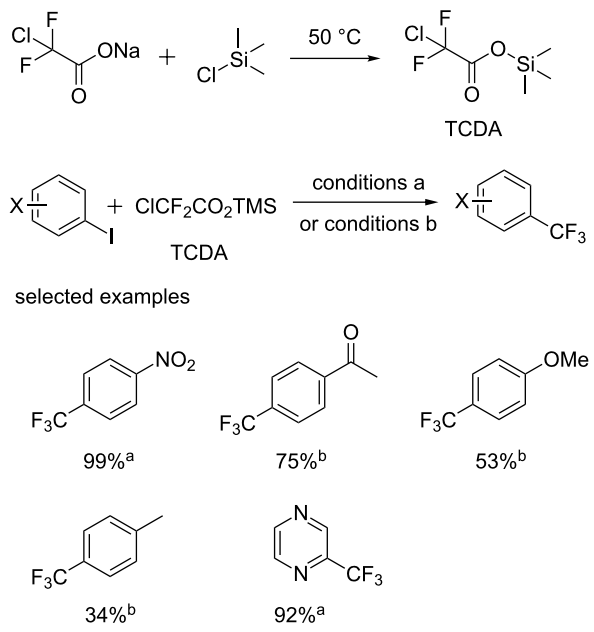

Scheme 10: Trifluoromethylation of aryl iodides using TCDA as a trifluoromethyl source. Reaction conditions: [a] CuI (1.5 equiv), KF (5.0 equiv), TCDA (2.0 equiv) DMF/trimethylamine, 90 °C, 4 h, N_2; [b] CuI (1.5 equiv), AgF (4.0 equiv), TMEDA (1.5 equiv), TCDA (2.0 equiv), DMF, 100 °C, 6 h.

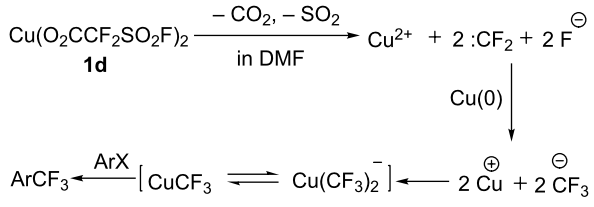

Scheme 11: The mechanism of trifluoromethylation using $Cu(II)(O_2CCF_2SO_2F)_2$ as a trifluoromethyl source.

Subsequently, a copper-catalyzed nucleophilic trifluoromethylation of allylic halides was developed by the group of Nishibayashi [26] (Scheme 13). Various cinnamyl halides bearing methyl, chloro, methoxy or ester groups proceeded smoothly to give the corresponding analogues in good yields. Other primary and secondary allylic halides were also subjected to these conditions. It is notable that the trifluoromethyl group was introduced at the α position of the carbon–halogen bond with complete regioselectivity.

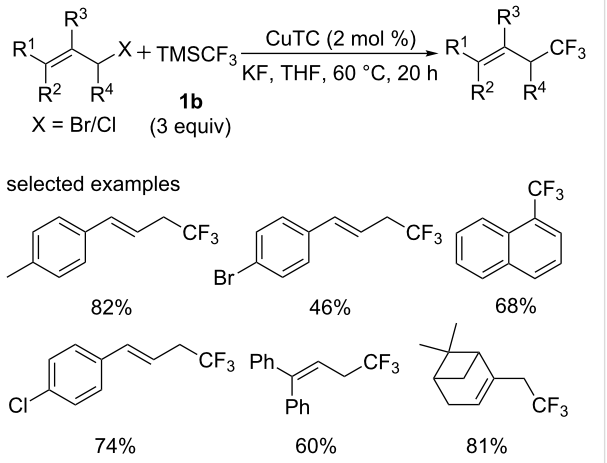

Scheme 13: Trifluoromethylation of allylic halides and propargylic halides reported by the group of Nishibayashi.

Later, they extended these conditions to propargylic halides [27] and succeeded in synthesizing the corresponding analogues from primary propargylic chlorides (Scheme 14), while the trifluoromethylated allenes can be obtained from reactions of secondary propargylic chlorides.

Moreover, in 2014, the primary and secondary benzylic chlorides [28] were investigated under similar conditions, which

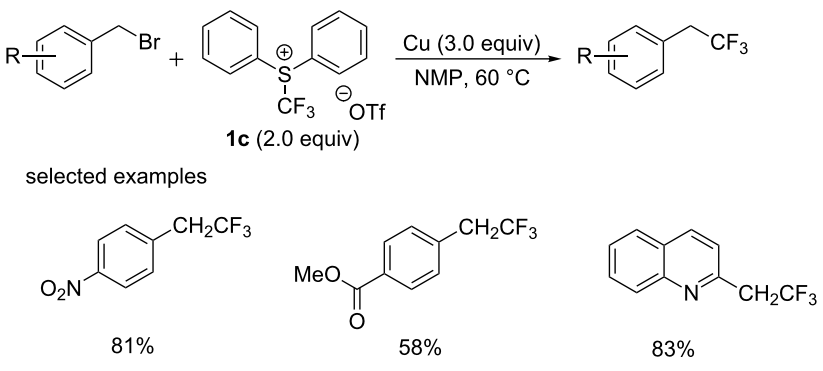

Scheme 12: Trifluoromethylation of benzyl bromide reported by Shibata's group.

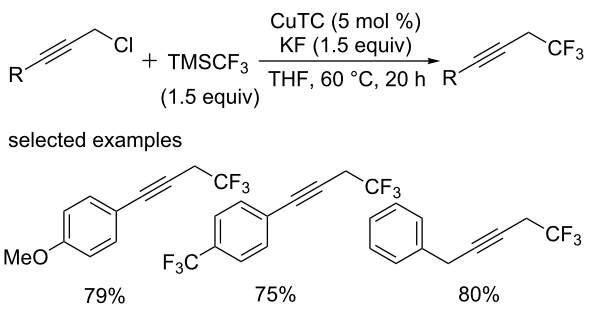

Scheme 14: Trifluoromethylation of propargylic halides reported by the group of Nishibayashi.

proceeded smoothly to give the corresponding trifluoromethylated products in high yields (Scheme 15). But applicable substrates were limited to benzylic chlorides bearing electron-donating groups. The methodology described by the group of Nishibayashi could provide an efficient strategy for the synthesis of CF_3-containing compounds at the allylic, propargylic, benzylic position, which were useful building blocks in pharmaceuticals.

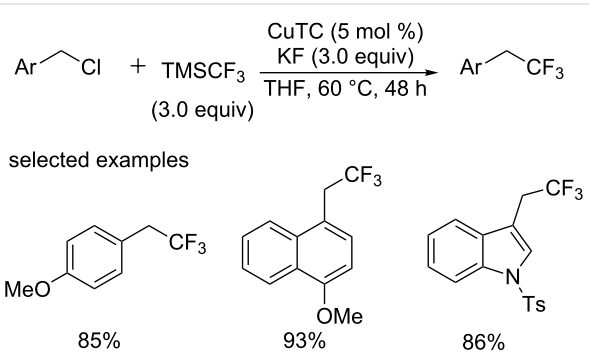

Scheme 15: Trifluoromethylation of alkyl halides reported by Nishibayashi's group.

Building on a pioneering work, substantial progress has recently been made in the trifluoromethylation of aryl and alkyl halides, including the development of new trifluoromethylation reagents or improved processes. But, there still exist several limitations in the trifluoromethylation of alkyl halides, such as limited substrate species and some unclarified mechanisms. The application of copper-catalyzed trifluoromethylation of alkyl halides remains in its infancy and has a lot of promise for the future.

Copper-catalyzed trifluoromethylation of boronic acid derivatives

Boronic acid derivatives are common building blocks in organic chemistry due to its commercial availability, and stability to heat, air, and water. Several examples of trifluoromethylation of boronic acid derivatives with nucleophilic, electrophilic or radical trifluoromethylation reagents were reported.

Trifluoromethylation of boronic acid derivatives with nucleophilic trifluoromethylation reagents

Protodeborylation was found to be the main side reaction in the copper-catalyzed trifluoromethylation of arylboronic acids [29,30]. In 2012, the group of Gooßen [31] designed a new protocol replacing the boronic acids with the corresponding pinacol esters to minimize side reaction (Scheme 16). This reaction proceeded smoothly to form the corresponding analogues in moderate to high yields using the shelf-stable, and easy-to-handle potassium (trifluoromethyl)trimethylborate $K^+[CF_3B(OMe)_3]^-$ as a CF_3 source, molecular oxygen as the oxidant. However, another side reaction, substitution of the boronate by methoxy groups originating from the CF_3 source, arose in this transformation.

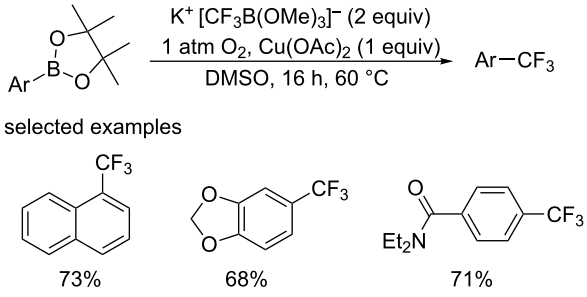

Scheme 16: Trifluoromethylation of pinacol esters reported by the group of Gooßen.

At the same year, the group of Fu explored the trifluoromethylation of primary and secondary alkylboronic acids with the Ruppert–Prakash reagent ($TMSCF_3$) (Scheme 17) [32]. These alkylboronic acids were prepared from the corresponding alkyl halides or tosylates by using their previously developed Cu-catalyzed borylation method [33]. Both primary and secondary alkylboronic acids underwent the trifluoromethylation well under different optimized conditions.

Trifluoromethylation of boronic acid derivatives with electrophilic trifluoromethylation reagents

CF_3^+ reagents were also explored in the trifluoromethylation of boronic acid derivatives. In 2011, the group of Liu [34] achieved the copper-catalyzed trifluoromethylation of aryl, heteroaryl, and vinylboronic acids at room temperature or 0 °C with Umemoto's reagent **1e** (Scheme 18). Of importance, this process was not sensitive to moisture, unlike the former trifluoromethylation reaction involved CF_3^- reagents. Moreover, this process showed good functional group compati-

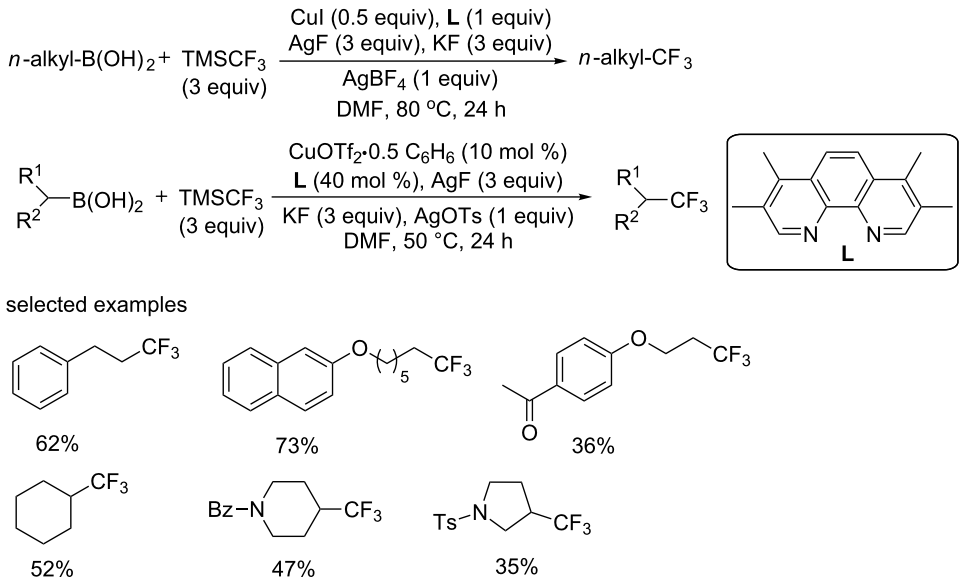

Scheme 17: Trifluoromethylation of primary and secondary alkylboronic acids reported by the group of Fu.

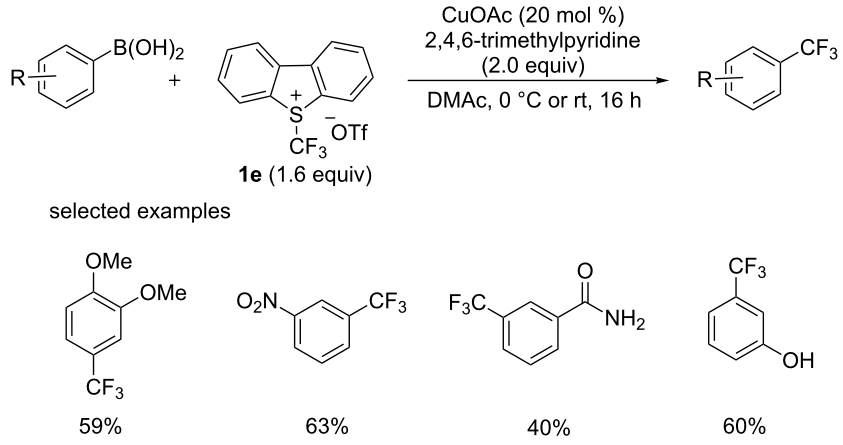

Scheme 18: Trifluoromethylation of boronic acid derivatives reported by the group of Liu.

bility and even some unprotected OH and NH groups were tolerated.

Subsequently, the group of Huang [35] reported an efficient copper-catalyzed trifluoromethylation of organotrifluoroborates (Scheme 19). This reaction was accomplished under base-free conditions by using Togni's reagent **1f** as the trifluoromethylation reagent at room temperature. Organotrifluoroborates were attractive alternatives to boronic acids for its superior characteristic, such as ease of handling, storability, and robustness under harsh reaction conditions. It was found that ligands and molecular sieves were essential for the efficient conversion. Various aryltrifluoroborates bearing electron-donating and electron-withdrawing substituents at different positions were converted to the desired products. And substrates bearing electron-withdrawing groups suffered from lower yields.

Recently, the group of Shibata [36] reported a catalytic trifluoromethylation of aryl- and vinylboronic acids using **1g** as a trifluoromethyl source (Scheme 20), which had not been actively investigated due to its instability in some solvents [37]. Solvent screening results indicated that ethyl acetate was the best solvent for the target transformations. Substrates regardless of bearing electron-donating (OMe) or electron-withdrawing

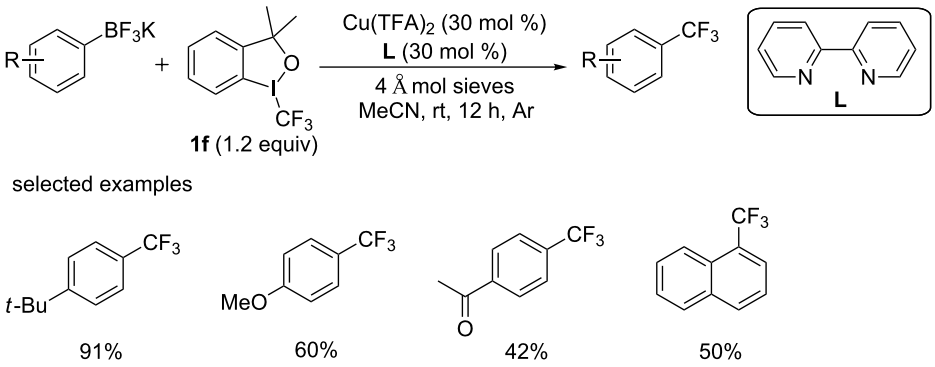

Scheme 19: Trifluoromethylation of organotrifluoroborates reported by the group of Huang.

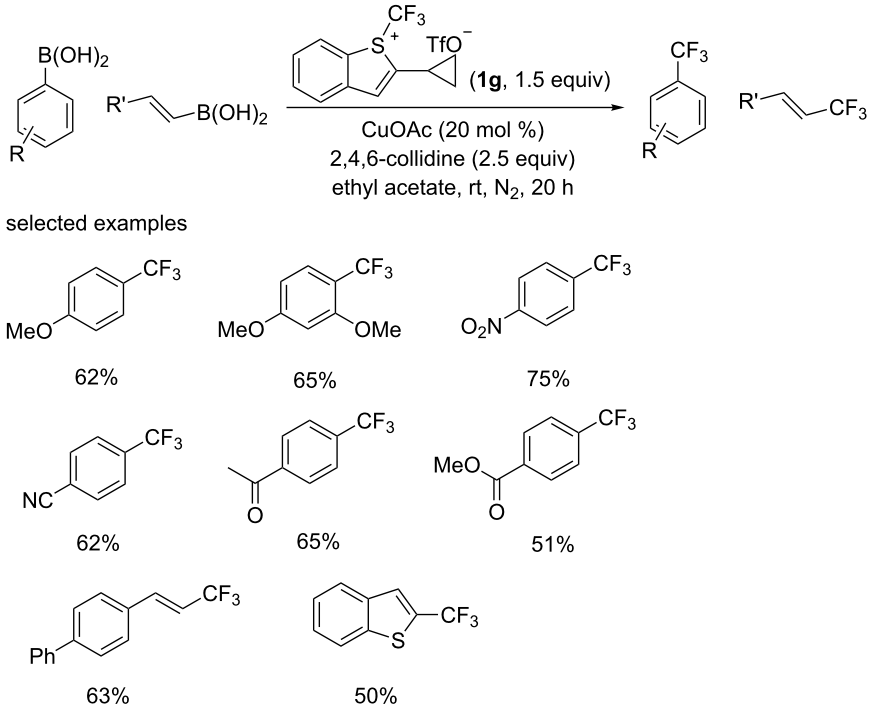

Scheme 20: Trifluoromethylation of aryl- and vinylboronic acids reported by the group of Shibata.

groups (NO_2, CN, carbonyl, and ester) were tolerated in this conversion. Moreover, vinylboronic acids and heteroaryl substrates were also acceptable.

Trifluoromethylation of boronic acid derivatives with radical trifluoromethylation reagents

The trifluoromethylation of boronic acid derivatives through a radical pathway was explored since the CF_3 radical can be generated under mild, neutral conditions from commercially available and relatively inexpensive CF_3I. Besides, the easy conversion of CF_3I to CF_3 radical at room temperature with visible light developed by MacMillan facilitated these method [38,39].

On the basis of the former work, the group of Sanford [40] designed the cross-coupling of arylboronic acids with CF_3I via the merger of photoredox and Cu catalysis (Scheme 21). In this protocol, the CF_3 radical was generated by visible light photoredox, then Cu aryl species were generated through Cu catalysis. Aromatic boronic acids bearing either electron-donating or electron-withdrawing substituents underwent trifluoromethylation smoothly to give the corresponding products in

high yield. It represented a new example of combining transition metal and photoredox catalysis to achieve the trifluoromethylation of (hetero)aromatic boronic acids.

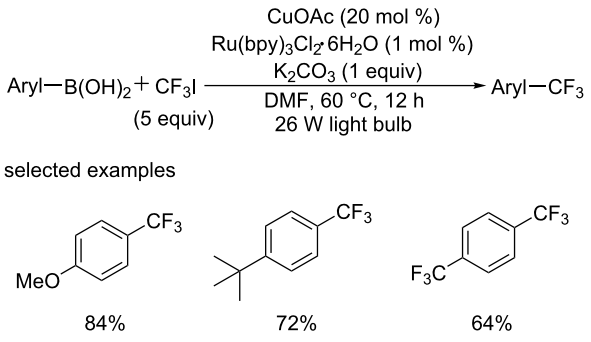

Scheme 21: Trifluoromethylation of arylboronic acids via the merger of photoredox and Cu catalysis.

Then, the same group [41] chose a more practical CF_3 source, CF_3SO_2Na (Langlois' reagent, **1h**, Scheme 22), which can generate trifluoromethyl radicals at room temperature in the presence of ambient air and moisture when combined with TBHP. Electron-neutral and -rich boronic acids proceeded smoothly to give the corresponding products in excellent yields. An addition of $NaHCO_3$ was required for the conversion of electron-deficient derivatives. Besides, sterically hindered boronic acids were also tolerated in this reaction. This protocol was simplified and easy-to-handle and no protodeboronation byproduct was observed under these conditions, while the major side product (the corresponding hydroxylated arene) was readily removable by extraction or column chromatography.

Later, the group of Beller [42] described another example of copper-catalyzed trifluoromethylation reactions of aryl- and vinylboronic acids with CF_3SO_2Na as the trifluoromethyl source (Scheme 23). The trifluoromethyl radical was generated from CF_3SO_2Na in the presence of TBHP at room temperature using a mixture of water and DCM as solvent. Arylboronic acids with electron-donating substituents proceeded smoothly to give the corresponding products in good yields. Common hydroxy protecting groups (Bn and TBS) were well-tolerated in this process. Also, the vinylboronic acids were compatible with the reaction, which were less sensitive towards the influence of the substituents.

Great advances have been made in the trifluoromethylation of boronic acid derivatives. However, some side reaction existed and the substrate scope was still need to be expanded. Therefore, more efficient and practical methods were desirable.

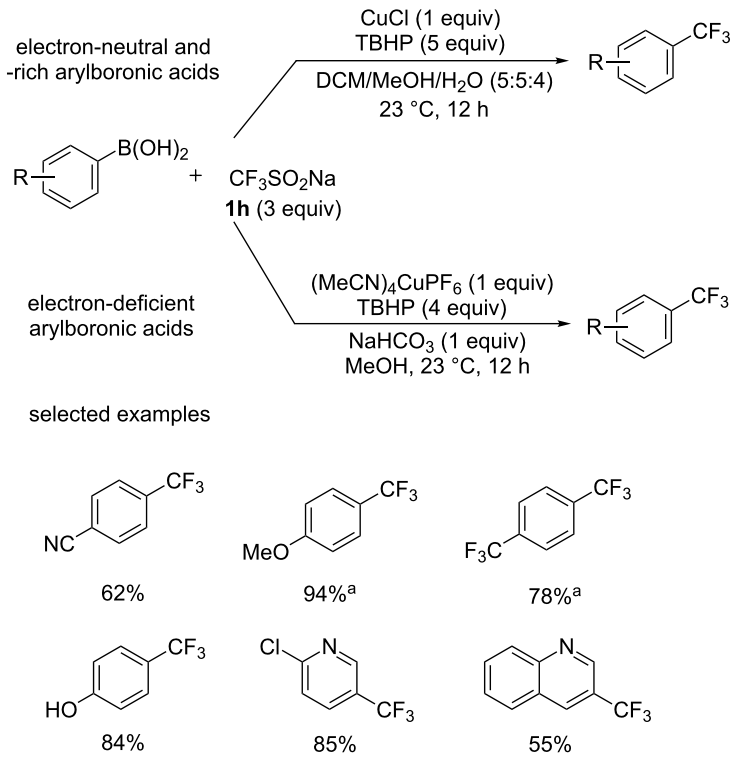

Scheme 22: Trifluoromethylation of arylboronic acids reported by Sanford's group. Isolated yield. [a]Yields determined by ^{19}F NMR analysis.

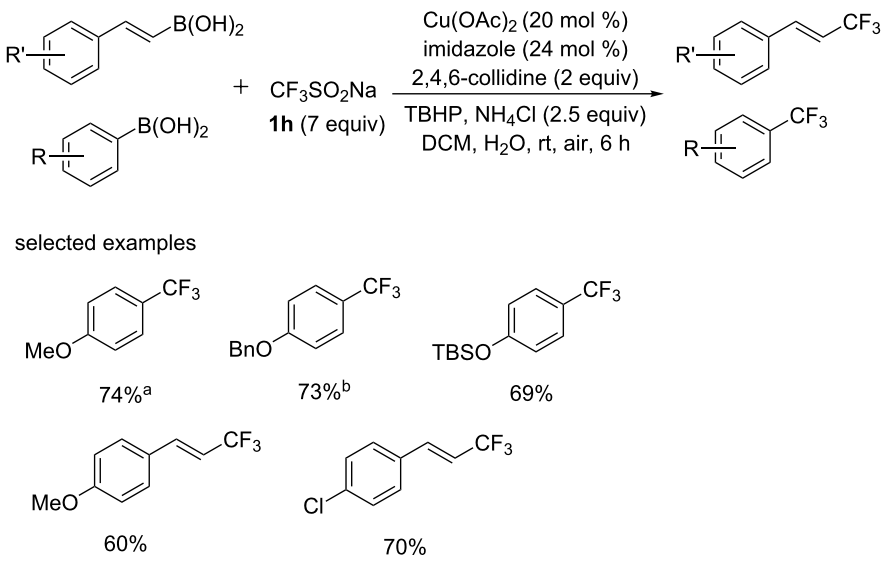

Scheme 23: Trifluoromethylation of arylboronic acids and vinylboronic acids reported by the group of Beller. Yields determined by ^{19}F NMR analysis. [a]GC yield. [b]Isolated yield.

Trifluoromethylation of aryldiazonium salts (Sandmeyer type trifluoromethylation)

Aromatic amines, which are available in great structural diversity, are prevalent chemicals in organic chemistry. The amino group can be easily transformed into numerous functional groups including halides or cyano groups, which is known as the Sandmeyer reaction. This transformation contained two steps: Diazotization of aromatic amines led to aryldiazonium salt, followed by conversion of diazonium group into target functional groups. Recently, several examples of conversion of anilines into trifluoromethylated arenes, named Sandmeyer type trifluoromethylation, were disclosed. This protocol offered a complementary method for the synthesis of trifluoromethylated arenes from the corresponding aromatic amines.

In 2013, Fu [43], Gooßen [44] and Wang [45] almost simultaneously reported Sandmeyer type trifluoromethylations. The group of Fu [43] accomplished a copper-mediated Sandmeyer trifluoromethylation reaction for the conversion of aromatic amines into trifluoromethylated arenes (Scheme 24). This reaction was conducted under mild conditions using Umemoto's reagent as the trifluoromethylation agent in the presence of isoamyl nitrite (iAmONO). The reaction proceeded smoothly with various arylamines under these conditions to give the corresponding products in modest to good yields. The reaction exhibits good tolerance to many functional groups, such as unsaturated double bonds, triple bonds and even unprotected OH group. Different heteroaromatic amines were also amenable to this conversion, including pyridines and pyrazoles.

A mechanistic study indicated that an aryl radical and $CuCF_3$ were involved in this conversion. A plausible mechanism is proposed in Scheme 24. First, the CF_3 radical, generated from Umemoto's reagent through copper-mediated single electron transfer (SET), reacts with copper affording $CuCF_3$. Second, Ar–CF_3 was formed by the reaction of $CuCF_3$ with the aryl radical derived from the aryldiazonium ion, which is generated in situ from the corresponding arylamine.

At the same time, a copper-catalyzed Sandmeyer trifluoromethylation of arenediazonium tetrafluoroborates was also reported by the group of Gooßen (Scheme 25) [44]. This reaction was conducted under mild conditions using $TMSCF_3$ as the trifluoromethyl source. It is notable that no desired product was observed in the absence of copper or basic additives. Both electron-rich and electron-deficient substrates were smoothly converted into the corresponding analogues in high yields except for some simple, low-boiling substrates. Additionally, various heterocycles were also compatible with this approach. The reaction can tolerate many common groups, including methoxy, iodo and carboxyl groups. The majority of products were produced in sufficiently pure form to permit straightforward isolation.

Gooßen assumed that this conversion proceeded via radical intermediates (Scheme 25), which is analogous to Sandmeyer halogenations of diazonium salts. First, the trifluoromethyl copper(I) species is generated from $TMSCF_3$ and copper salt. Then, Cu(I)CF_3 transfers one electron to the diazonium salt

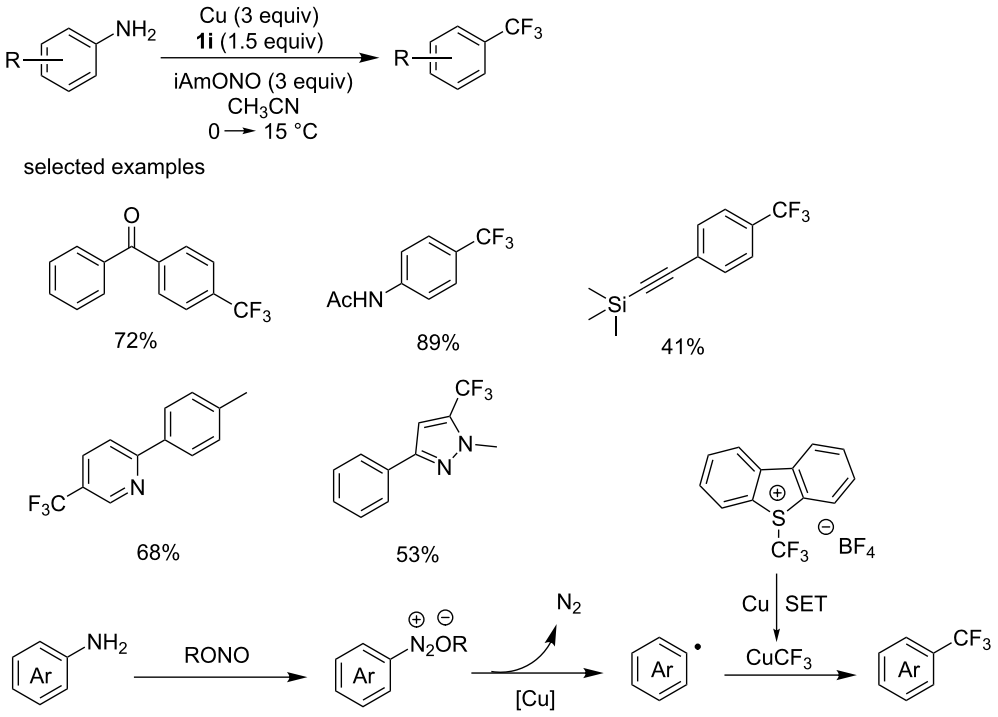

Scheme 24: Copper-mediated Sandmeyer type trifluoromethylation using Umemoto's reagent as a trifluoromethylation reagent and the proposed mechanism.

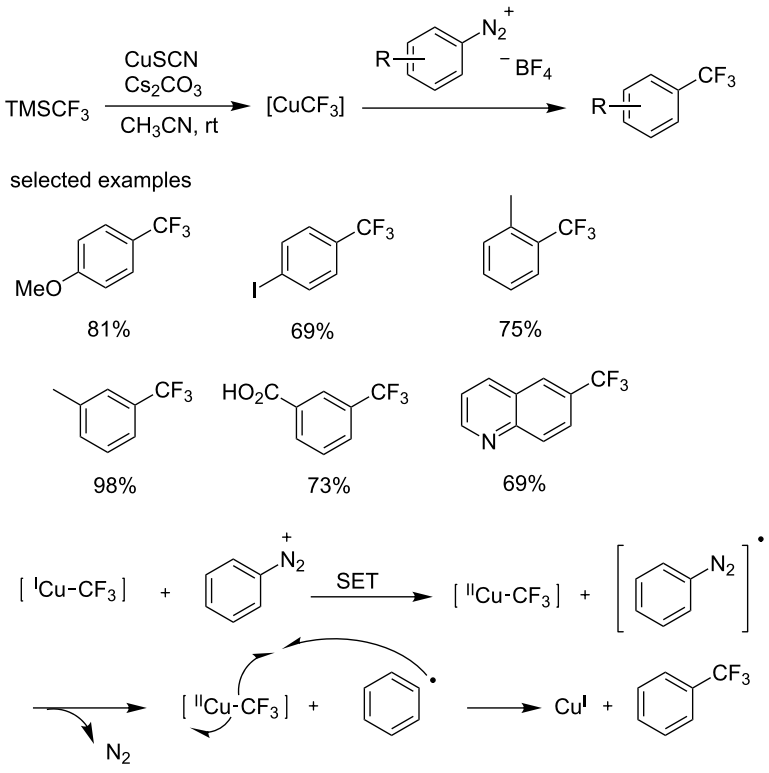

Scheme 25: Copper-mediated Sandmeyer type trifluoromethylation using $TMSCF_3$ as a trifluoromethylation reagent and the proposed mechanism.

affording Cu(II)CF_3 and a diazo radical following by the formation of an aryl radial from the diazo radical through the release of nitrogen. Finally, the aryl radical reacts with Cu(II)CF_3 furnishing the trifluoromethylated product along with copper(I) salt.

Compared with Fu's method, this process needs an extra step to generate the diazionium salt. Later, the same group developed a one-pot Sandmeyer trifluoromethylation combining the diazotization and the Sandmeyer reaction (Scheme 26) [46]. This reaction proceeded smoothly using *tert*-butyl nitrite as the diazotization reagent, $TMSCF_3$ as the trifluoromethylation reagent in the presence of anhydrous *para*-toluenesulfonic acid and catalytic amounts of copper reagent (0.5 equiv). Diversely substituted aromatic amines and heterocyclic amines were all converted in high yields. The majority of products were produced in sufficiently pure form to allow for simple isolation.

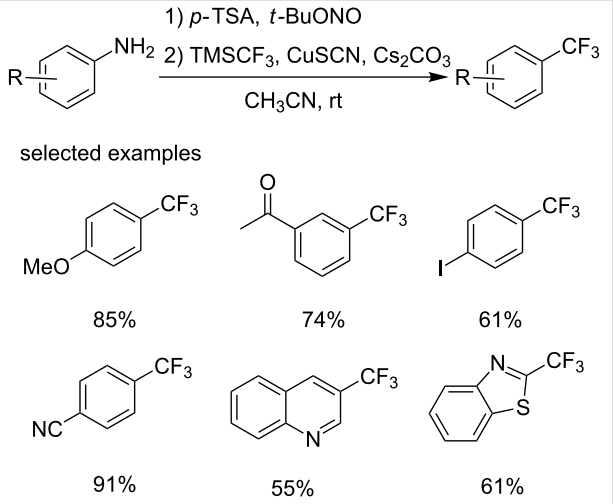

Scheme 26: One-pot Sandmeyer trifluoromethylation reported by the group of Gooßen.

Note that the CF_3 reagents employed in the aformentioned examples were all moisture sensitive. Therefore, it required anhydrous conditions, which limits the large-scale application. In order to overcome this problem, the group of Grushin [47] developed a copper-catalyzed trifluoromethylation of arenediazonium salts in aqueous media (Scheme 27).

Initially, they investigated the trifluoromethylation of preisolated arenediazonium salts 4-$XC_6H_4N_2^+$ BF_4^- (X = MeO, Br, NO_2). But the main product was the reduction product XC_6H_5, which could be largely suppressed using MeCN as a co-solvent. Then, they examined the reaction of $CuCF_3$ with ArN_2^+ X^- generated in situ from the corresponding aniline. It was found that *t*-BuONO and aromatic amines decomposed $CuCF_3$. Acid was added to make the diazonium substrate fully preformed prior to the reaction with $CuCF_3$. Finally, they explored the possibility of reaction of hydrolysable $CuCF_3$ reagent with aqueous solutions of arenediazonium salts. Although it seemed unwise, the desired $ArCF_3$ product was produced. Subsequent condition optimization provided a high-yielding process. The reaction can tolerate a variety of synthetically important functional groups, such as Me, MeO, NO_2, I. A mechanistic study revealed that a radical mechanism was involved in this transformation.

Recently, the group of Qing [48] accomplished a Sandmeyer trifluoromethylation of aryldiazonium derivatives with $NaSO_2CF_3$ in the presence of TBHP (Scheme 28). The yield was improved by adding the tridentate ligand 2,2′,6′,2″-terpyridine (tpy) and a

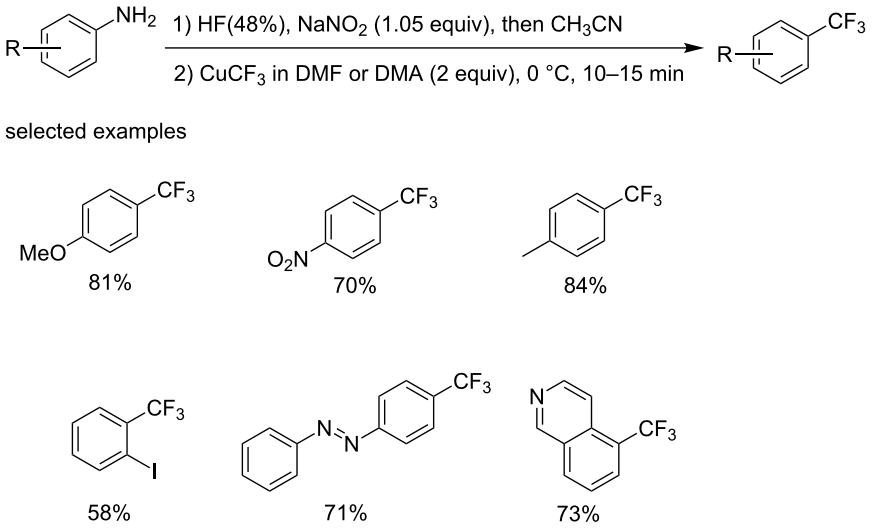

Scheme 27: Copper-catalyzed trifluoromethylation of arenediazonium salts in aqueous media.

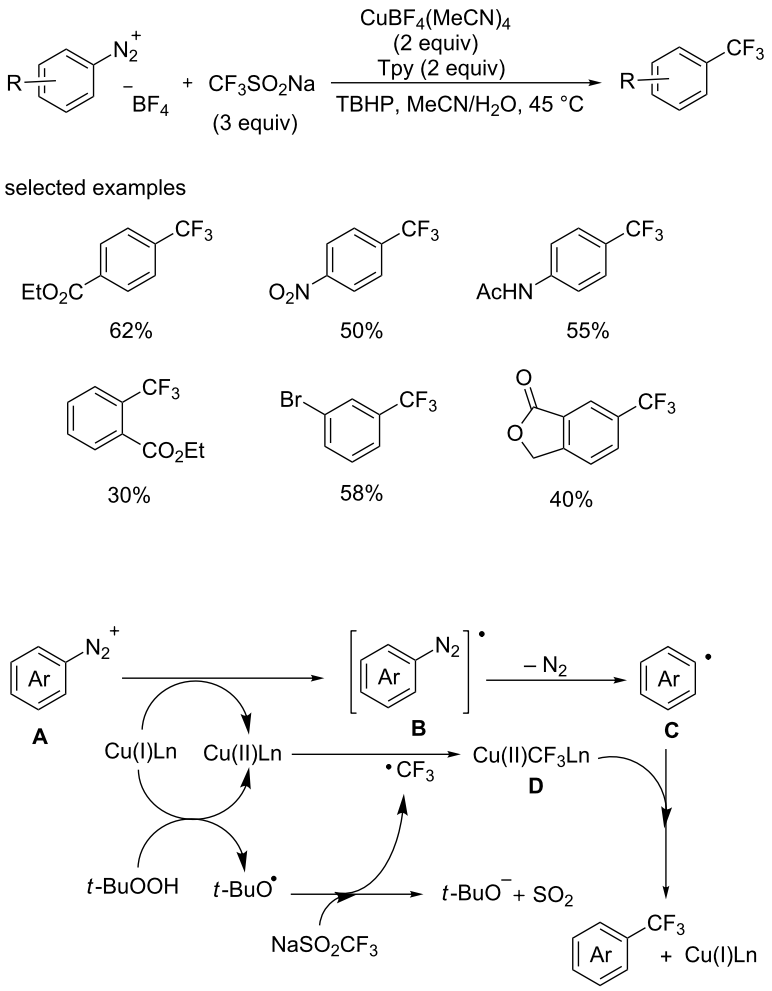

Scheme 28: Copper-mediated Sandmeyer trifluoromethylation using Langlois' reagent as a trifluoromethyl source and the proposed mechanism.

small amount of water as the co-solvent. A range of arenediazonium tetrafluoroborates were smoothly converted to the corresponding analogues in acceptable yields.

A mechanistic study indicated that a radical process was involved in this conversion (Scheme 28). First, the diazo radical, generated through copper-mediated single electron transfer from diazonium salt **A**, released nitrogen gas affording the aryl radical **C**. On the other hand, the CF_3 radical was generated through the reaction of TBHP with $NaSO_2CF_3$ in the presence of Cu(I) species. Then, the CF_3 radical reacted with the Cu(I) species to provide the complex Cu(II)CF_3Ln. Finally, the reaction of aryl radical **C** with complex **D** gave the desired Ar–CF_3 product along with the Cu(I) species.

Copper-catalyzed direct trifluoromethylation of C–H bonds

The above-mentioned strategies to introduce a trifluoromethyl group into organic compound were based on the use of prefunctionalized substrates. Instead, the direct trifluoromethylation of C–H bonds of arenes and heteroarenes was a more efficient and ideal protocol due to its atom and step economy. However, the direct trifluoromethylation of C–H bonds was not simple. And only in recent years, extensive research was reported including direct trifluoromethylation of C(sp^3)–H, C(sp^2)–H, C(sp)–H bonds in various substrates.

Copper-catalyzed direct trifluoromethylation of C(sp^3)–H

Molecules containing allylic CF_3 functional groups are versatile precursors for the synthesis of different types of CF_3-containing molecules. Traditional methods that were described for the preparation of CF_3-containing molecules required harsh reaction conditions and pre-functionalized starting materials such as allyl bromides or fluorosulfones. The past years had witnessed many advances in constructing allylic CF_3 bonds from olefins. Following examples described the straightforward trifluoromethylation of terminal alkenes via allylic C(sp^3)–H

bond activation generating allylic trifluoromethylated compounds.

In 2011, the group of Fu and Liu [49] described an unprecedented type of a Cu-catalyzed trifluoromethylation reaction of terminal alkenes through C(sp^3)–H activation (Scheme 29). Many substrates underwent the trifluoromethylation smoothly using Umemoto's reagent **1e** as a trifluoromethyl source and CuTC as catalyst under mild conditions. This reaction was tolerant to moisture and was compatible to different functional groups. But the reaction was sensitive to the steric hindrance of the olefin substrates, and 2-substituted terminal alkenes or internal (including cyclic) alkenes were not applicable to this protocol. A mechanistic study showed that the reaction may proceed through a Heck-like four-membered-ring transition state. Note that the presence of an olefin moiety in the product promised further conversion to other types of CF_3-containing molecules.

Later, the group of Wang [50] employed cheap copper chloride as the catalyst and a hypervalent iodine(III) reagent **1j** as both the oxidant and the CF_3 source in allylic trifluoromethylation (Scheme 30). It was found that allyl substrates bearing an aromatic moiety showed relatively low efficiency.

At the same year, the group of Li [51] achieved a copper-catalyzed trifluoromethylation via oxidation of C(sp^3)–H bonds adjacent to nitrogen atom in tetrahydroisoquinoline derivatives using DDQ and Ruppert–Prakash reagent (Scheme 31). A variety of amines proceeded smoothly to give the corresponding products in 15–90% yields under mild conditions.

Based on previous literature, the author proposed a possible mechanism in Scheme 31. Firstly, oxidation of *N*-substituted tetrahydroisoquinoline with DDQ generates dihydroquinoline salt **A**. Next, $CuCF_3$, generated by the reaction of CuI and CF_3TMS/KF, undergoes a nucleophilic addition with **A** affording the desired products and the copper salt. The generated copper salt would be reused to form $CuCF_3$ in the nucleophilic step again. So, only a catalytic amount of copper salt was required in this reaction.

The hydrogens on the *ortho* and *para* positions of phenols have higher reactivity. Thus, undesired side reactions were often involved in the trifluoromethylation of less substituted phenols, including oxidative dimerization and oligomerization. Although phenols were widely used building blocks in bioactive compounds, only a few examples introducing a CF_3 have been reported.

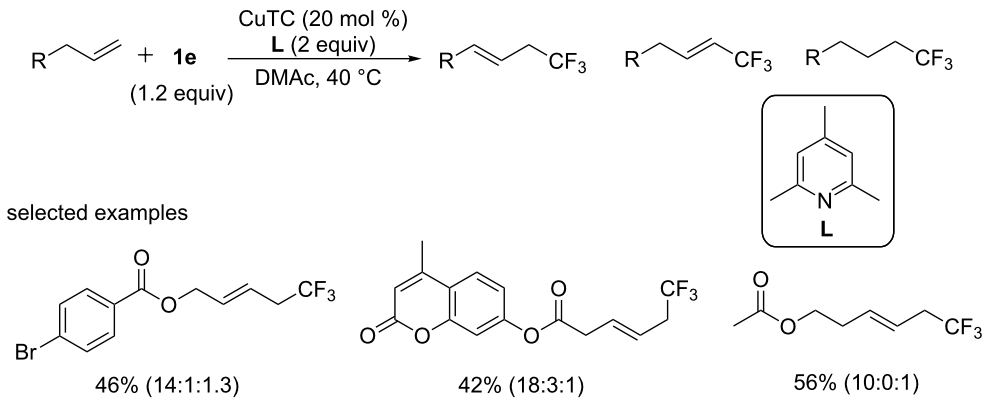

Scheme 29: Trifluoromethylation of terminal alkenes reported by the group of Liu.

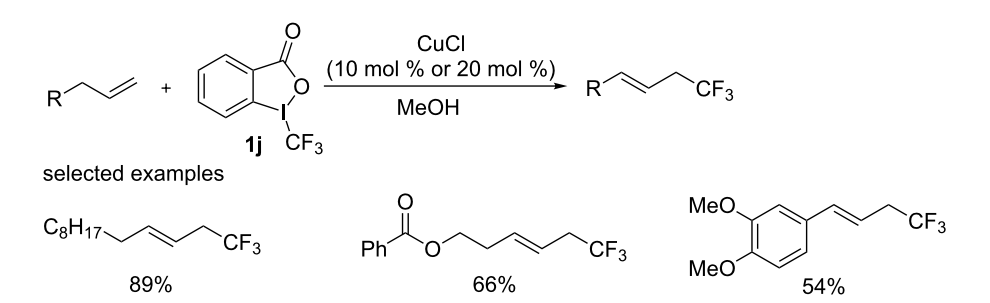

Scheme 30: Trifluoromethylation of terminal alkenes reported by the group of Wang.

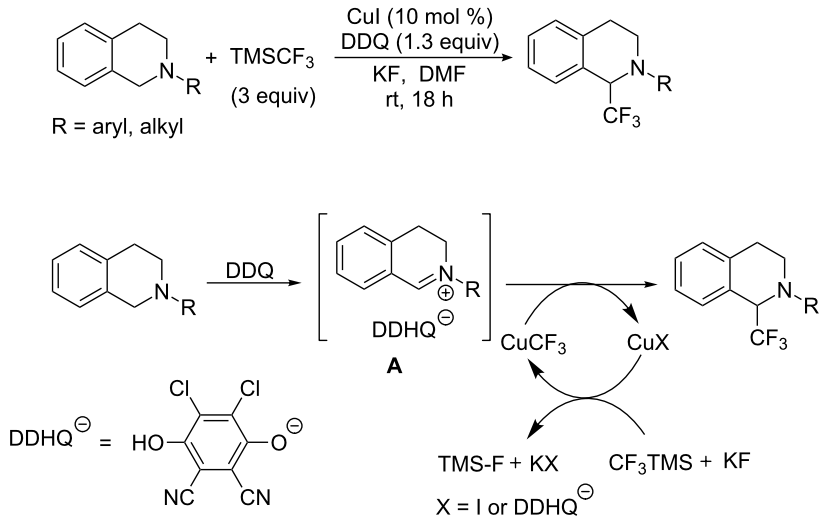

Scheme 31: Trifluoromethylation of tetrahydroisoquinoline derivatives reported by Li and the proposed mechanism.

In 2015, the group of Hamashima [52] achieved a direct C–H trifluoromethylation of phenol derivatives with high regioselectivity. The CF_3 was selectively incorporated into the *para*-benzylic position of the hydroxy group (Scheme 32). It is notable that the bulky *tert*-butyl group was introduced to suppress side reactions, which could be removed under acidic conditions. The solvent was critical in terms of product switching; the trifluoromethylation of aromatic C–H occurred in alcoholic solvents. The author accomplished the synthesis of a potent enoyl-acyl carrier protein reductase (Fab I) inhibitor in high yield under this conditions, demonstrating the practical utility of this process.

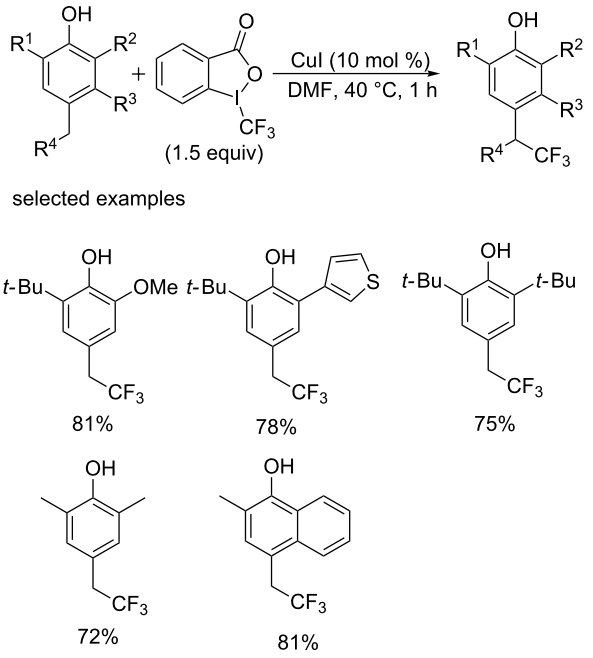

Scheme 32: Trifluoromethylation of phenol derivatives reported by the group of Hamashima.

Copper-catalyzed direct trifluoromethylation of C(sp^2)–H

Direct trifluoromethylation of C(sp^2)–H with a electrophilic trifluoromethylation reagent (Togni's reagent): *N,N*-Dialkylhydrazones were widely used in organic chemistry, including using as synthetic equivalents of carbonyl compounds, as precursors to substituted hydrazines or primary amines. In 2013, Baudoin and co-workers [53] firstly achieved the incorporation of CF_3 into *N,N*-dialkylhydrazones using Togni's reagent as a trifluoromethyl source in the presence of simple copper chloride (Scheme 33). Various hydrazones with an electron-donating dialkylamino group including 1-piperidinyl and 4-morpholinyl participated efficiently in this reaction. Irrespective of the phenyl group was substituted by an electron-withdrawing or -donating group, the reaction proceeded smoothly to afford the desired products in high yields. Besides, several heterocyclic hydrazones including pyridinyl, pyrazolyl and furyl were also applicable under this conditions. It is of importance, that the trifluoromethylated hydrazones were formed exclusively as the *Z* isomers.

The proposed mechanism [53] is shown in Scheme 33. Activation of Togni's reagent by CuI through single-electron transfer (SET) initiates the reaction pathway to generate the CF_3 radical donor, copper(II) species **A**. The latter reacts with the hydrazone to the trifluoromethylated aminyl radical intermediate **C** which is stabilized by the lone pair of the adjacent nitrogen atom, and (2-iodobenzoyloxy)copper(II) chloride (**B**). Finally, intermediate **C** is oxidized by copper(II) to restore the hydrazone functional group and copper(I).

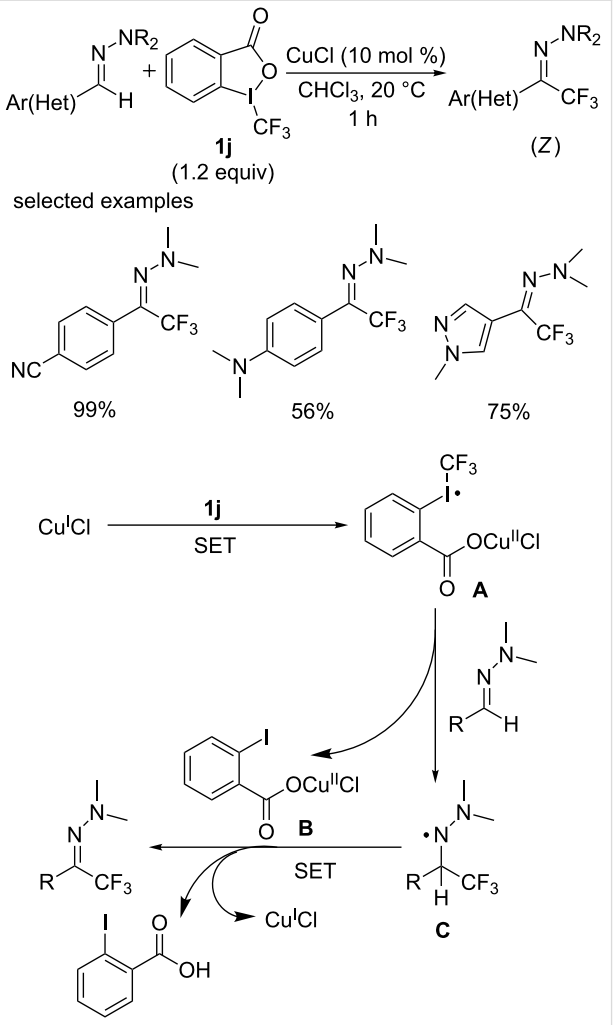

Scheme 33: Trifluoromethylation of hydrazones reported by the group of Baudoin and the proposed mechanism.

Benzamides were widely used building blocks in medicinal chemistry. In 2014, Dai and Yu [54] achieved an elegant copper-mediated *ortho*-selective trifluoromethylation of benzamides assisted by an *N*-phenyloxazoline group. But one major problem was the low selectivity, and that the ditrifluoromethylation product was formed as well. Recently, Tan and co-workers [55] designed a highly mono-selective *ortho*-trifluoromethylation of benzamides assisted with an 8-aminoquinoline directing group. This reaction employed simple copper salt CuBr as the promoter and Togni's reagent II as a CF_3 source (Scheme 34). Addition of water benefited the yield. A variety of functional groups such as methyl, ethyl, ester, fluoro, chloro, bromo, phenyl, methoxy, ethoxy as well as trifluoromethyl groups were well tolerated on the phenyl ring of benzamides and various *ortho*-trifluoromethylated benzamides were efficiently synthesized in 36–82% yields.

Direct trifluoromethylation of C(sp^2)–H with a nucleophilic trifluoromethylation reagent ($TMSCF_3$): Previously, the radical and electrophilic trifluoromethylation of arenes and heteroarenes were often limited to substrates bearing electron-donating substituents and generate mixture of regioisomers in some cases. In 2012, the group of Qing [56] designed a copper-catalyzed oxidative trifluoromethylation of heteroarenes and electron-deficient arenes with $TMSCF_3$ through direct C−H activation (Scheme 35).

At first, the oxidative trifluoromethylation of 1,3,4-oxadiazoles proceeded smoothly using $TMSCF_3$ as a trifluoromethyl source and air as an oxidant to give the corresponding products in high yields. Various 1,3,4-oxadiazoles bearing electron-donating and electron-withdrawing groups at the *para* position on the aryl rings were well tolerated, although the latter showed lower efficiency.

Then, they extended the substrate scope to 1,3-azoles and perfluoroarenes. Di-*tert*-butyl peroxide was chosen as a suitable oxidant instead of air. Functional groups, such as chloro and bromo, were compatible in this reaction, providing a complementary platform for further conversion. Notably, electron-deficient pentafluorobenzene was highly reactive under these

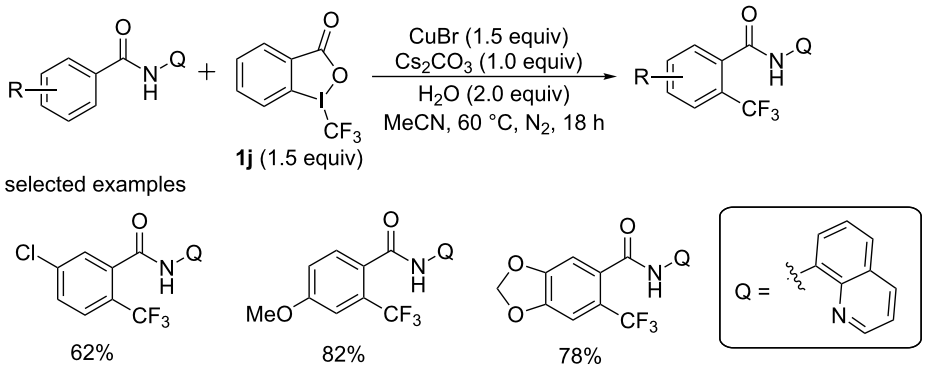

Scheme 34: Trifluoromethylation of benzamides reported by the group of Tan.

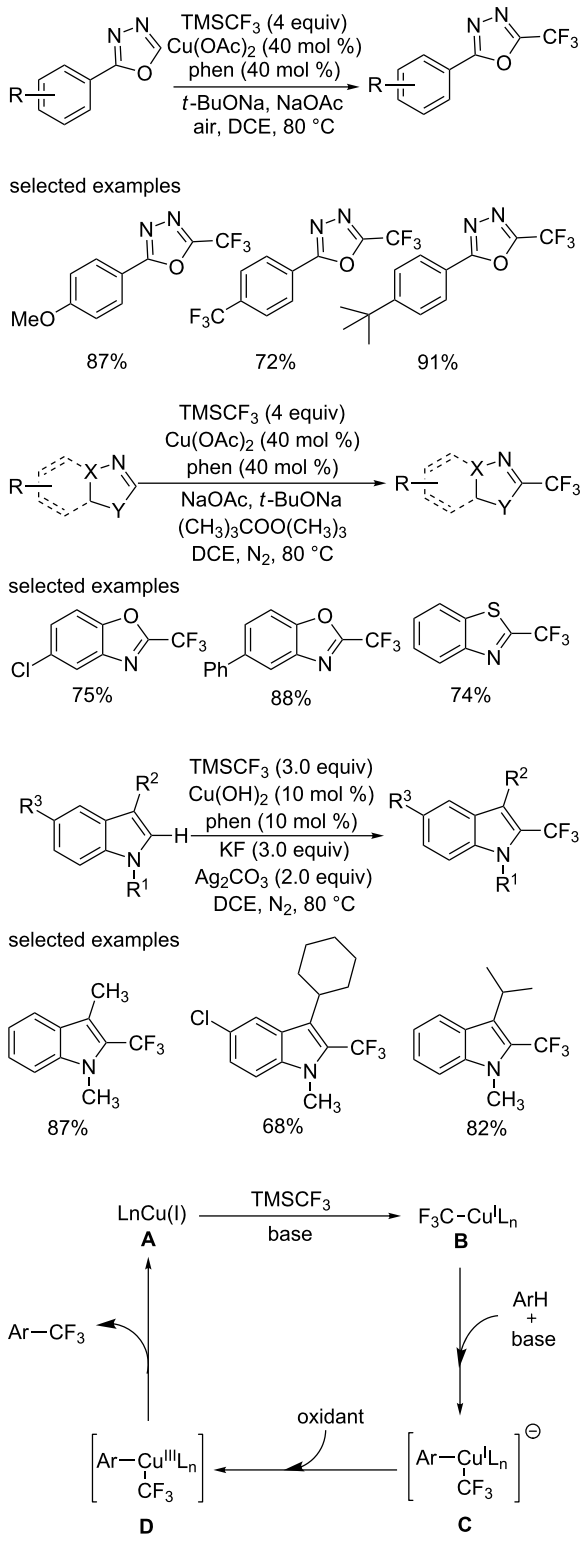

Scheme 35: Trifluoromethylation of heteroarenes and electron-deficient arenes reported by the group of Qing and the proposed mechanism.

reaction conditions to afford octafluorotoluene in excellent yield, which provided a promising model for functionalizations of electron-deficient arenes.

Furthermore, electron-rich indoles were applicable in these conditions and $Cu(OH)_2$ and Ag_2CO_3 were the best catalyst and oxidant, respectively. The electron density of the pyrrole ring had impact on the efficiency. *N*-Tosylindole and indole bearing the CO_2Me group on C3 position were nearly unreactive.

A plausible mechanism was proposed based on preliminary mechanistic studies (Scheme 35). First, the key intermediate $CF_3Cu^{I}Ln$ is generated in situ by the reaction of $TMSCF_3$ with Cu(II) reagent, followed by transmetalation with activated Ar−H generating the (aryl)$Cu^{I}(CF_3)$ species **C**, which might be oxidized to the corresponding (aryl)$Cu^{III}(CF_3)$ intermediate **D**. Finally, reductive elimination of the intermediate **D** would afford the desired product and regenerate Cu(I) catalyst to restart the catalytic cycle.

Direct trifluoromethylation of C(sp^2)–H with a radical trifluoromethylation reagent (CF_3SO_2Na): The radical trifluoromethylation via direct C(sp^2)–H activation also have made significant progress in recent years. Among them, the most studied methods were trifluoromethylations using Langlois' reagent (CF_3SO_2Na) as the trifluoromethyl source, which was inexpensive and readily available.

In 2014, the group of Liang and Lipshutz [57] explored a copper-catalyzed trifluoromethylation of *N*-aryl acrylamides using Langlois' reagent (CF_3SO_2Na) as a trifluoromethyl source and water as the reaction medium (Scheme 36). A variety of CF_3-containing oxindoles bearing a quaternary carbon center were formed under this conditions. Furthermore, more CF_3SO_2Na (3.0 equiv) and TBHP (7.0 equiv) were employed by highly water-insoluble solid substrates and substrates bearing electron-withdrawing groups.

This protocol exhibited several noteworthy features, such as the inexpensive and readily available catalyst and the trifluoromethylation reagent, and the ease of handing all components in air, the environmentally friendly nature, and the recycling of the aqueous medium.

Subsequently, the group of Li and Duan [58] reported an efficient method for the synthesis of α-trifluoromethyl ketones via addition of CF_3 to aryl(heteroaryl)enol acetates using readily available CF_3SO_2Na (Scheme 37). This reaction was experimentally simple and set out at room temperature under ambient conditions, affording the corresponding products in good to excellent yields with wide functional group tolerance.

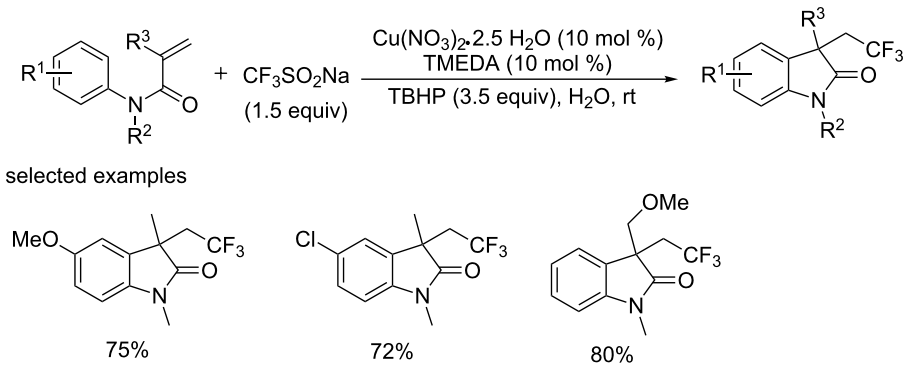

Scheme 36: Trifluoromethylation of *N*-aryl acrylamides using CF_3SO_2Na as a trifluoromethyl source.

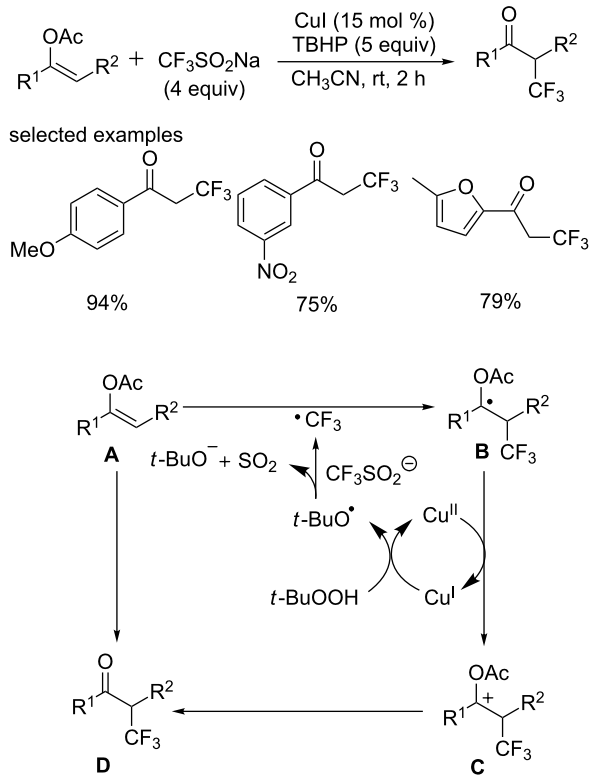

Scheme 37: Trifluoromethylation of aryl(heteroaryl)enol acetates using CF_3SO_2Na as the source of CF_3 and the proposed mechanism.

The mechanism research suggested that the CF_3 radical was involved in this transformation (Scheme 37). Firstly, the trifluoromethyl radical was generated in situ by the reaction of *tert*-butyl hydroperoxide with CF_3SO_2Na in the presence of catalytic amounts of CuI. Next, the addition of the CF_3 radical to the electron-rich α-position of the substrates formed the radical species **B**. Subsequent oxidation by Cu(II) produced cationic intermediate **C** and regenerated Cu(I) to restart the catalytic cycle. Finally, cationic intermediate **C** lost an acetyl cation affording the desired product.

Imidazoheterocycles were privileged skeletons in commercially available drugs, such as alpidem, olprinone, necopidem, which were developed by the modification of imidazoheterocyclic skeletons.

In 2015, the group of Tang [59] developed a regioselective C–H trifluoromethylation of imidazoheterocycles with Langlois' reagent at room temperature (Scheme 38). In order to figure out the insolubility problem of imidazoheterocycles and meet the guiding principles of green chemistry, this reaction was conducted in a recyclable mixed medium of 1-butyl-3-methylimidazolium tetrafluoroborate ([Bmim]BF_4) and water.

In the presence of catalytic amounts of cupric acetate and TBHP, various substrates, such as 6-arylimidazo[2,1-*b*]thiazoles and imidazopyridines, were compatible with this reaction conditions affording the corresponding analogues in moderate to good yields.

The proposed reaction mechanism is shown in Scheme 38. Initially, the trifluoromethyl radical is generated in situ by the reaction of TBHP with CF_3SO_2Na in the presence of copper reagent. Then, the trifluoromethyl radical reacts with substrates affording intermediate **A**, which may be oxidized to a carbocation **B**, followed by an oxidative dehydrogenation process delivering the target product.

Copper-mediated/catalyzed direct trifluoromethylation of C(sp)–H

Trifluoromethylated acetylenes were widely used in medicinal, agrochemical, and material science. In 2010, Qing and coworkers [60] firstly reported a copper-mediated trifluoromethylation of terminal alkynes using $TMSCF_3$ as a trifluoro-

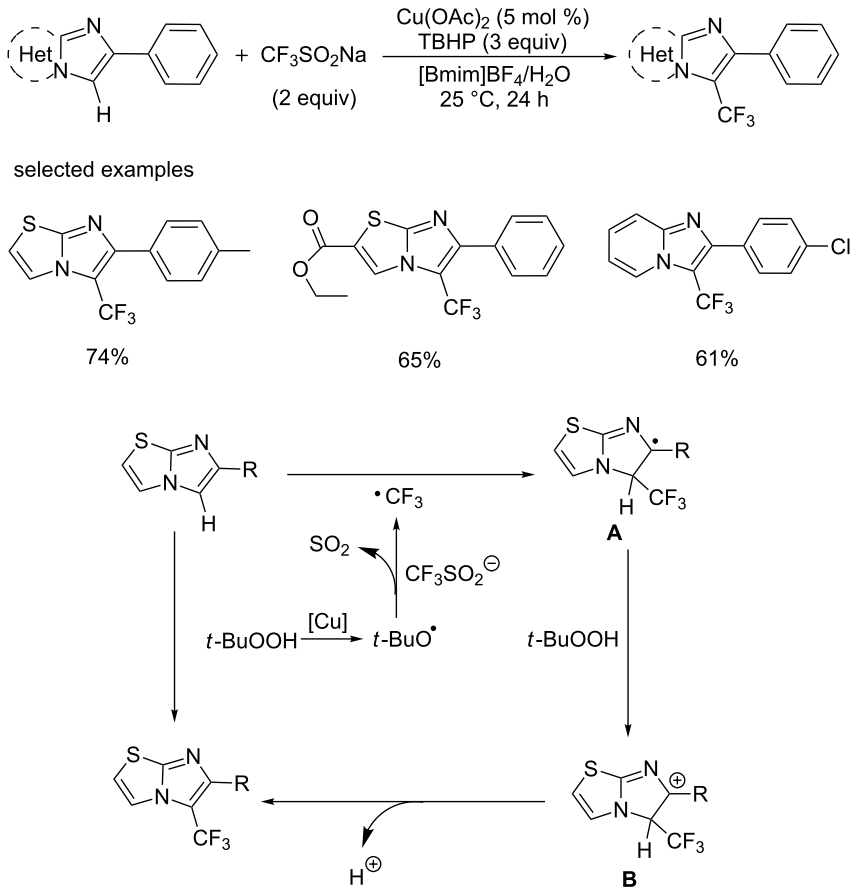

Scheme 38: Trifluoromethylation of imidazoheterocycles using CF_3SO_2Na as a trifluoromethyl source and the proposed mechanism.

methyl source. (Scheme 39). At the beginning of the experiment, undesired diyne byproduct was formed as major product instead of **E**. The author attributed this phenomenon to the competitive formation of bis-alkynyl–Cu complex **D**, which would produce the undesired diyne byproduct (Scheme 39). In order to solve this problem, the substrates were added by using a syringe pump over a period of 4 h to pregenerated $CuCF_3$. Furthermore, phen was introduced to this system to improve the yield. An excess of $TMSCF_3$ was required to get a high yield due to the decomposition of $TMSCF_3$ under this reaction condition. Aromatic alkynes as well as aliphatic alkynes worked well to give the corresponding products in moderate to good yields. This reaction can tolerate a variety of functionalities, such as alkoxy, amino, ester, and nitro groups.

However, a reaction temperature up to 100 °C and the requirement of excessive $TMSCF_3$ (bp 55 °C) rendered the former reaction less than ideal. In 2012, the same group [61] developed an improved procedure for the efficient copper-mediated trifluoromethylation of terminal alkynes (Scheme 40). This reaction was conducted at room temperature with a smaller amount of $TMSCF_3$.

However, the above-mentioned reaction still required stoichiometric amounts of copper. It is desirable to find novel methods to reduce the Cu loadings to catalytic quantities.

The preliminary mechanistic studies on the above-mentioned work indicated that $CuCF_3$ was generated in that transformation. It was found that the generation rate of trifluoromethyl anion was much higher than the next step affording B and CuI. Thus, there is no sufficient recirculated CuI to react with trifluoromethyl before its decomposition. And stoichiometric amounts of copper were required in this conversion. To obviate the problem, Qing and co-workers [62] adopted a new addition method. Adding a portion of $TMSCF_3$ (2 equiv) to the mixture afforded $CuCF_3$. And both terminal alkynes and the rest of $TMSCF_3$ were added to the reaction mixture slowly using a syringe pump. Various arylalkynes bearing electron-donating or -withdrawing groups were converted to the desirable products in good to high yields (Scheme 41).

In 2012, the group of Weng and Huang [63] achieved a trifluoromethylation of terminal alkynes using Togni's reagent (Scheme 42). This reaction was conducted at room temperature

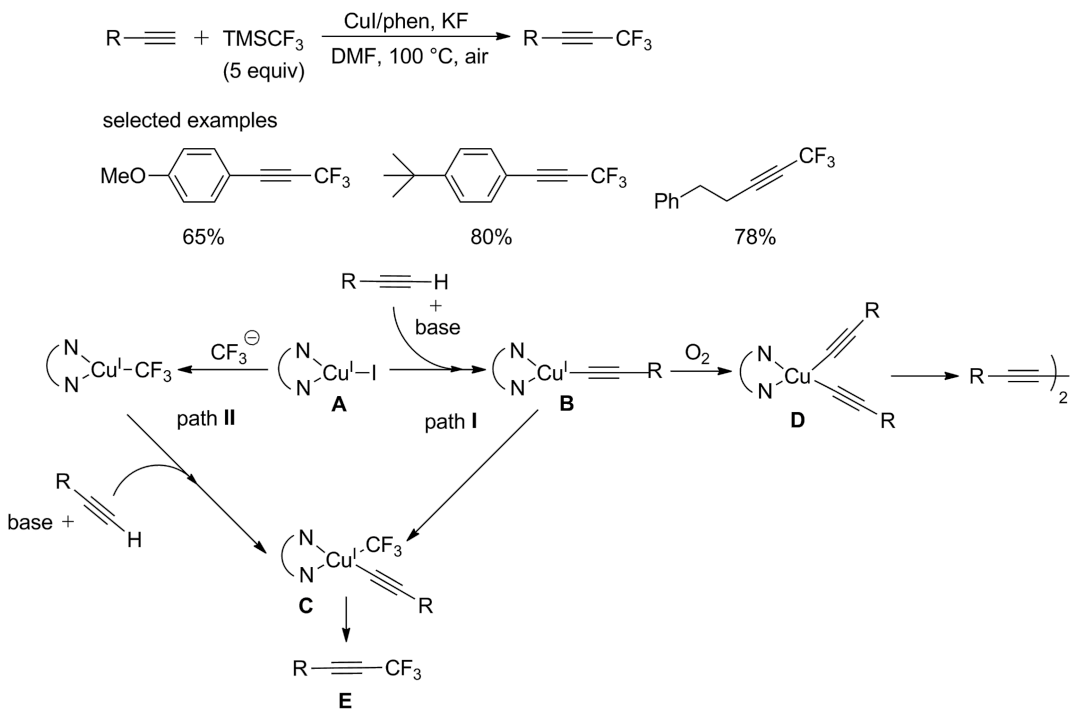

Scheme 39: Copper-mediated trifluoromethylation of terminal alkynes using $TMSCF_3$ as a trifluoromethyl source and the proposed mechanism.

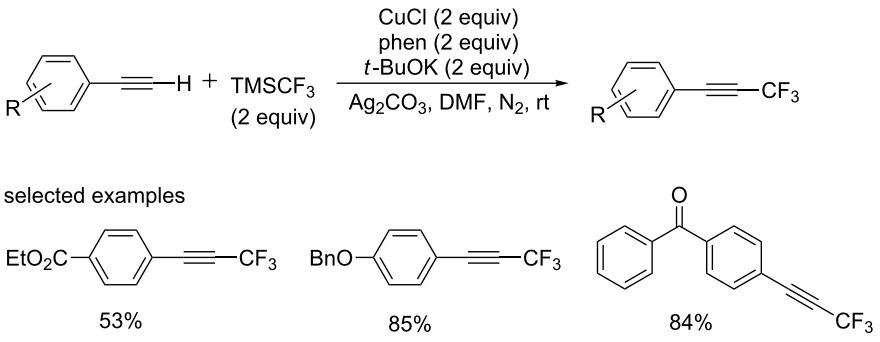

Scheme 40: Improved copper-mediated trifluoromethylation of terminal alkynes reported by the group of Qing.

with catalytic amounts of copper salt. The high reactivity was observed with phenylacetylenes bearing electron-donating groups. This reaction can tolerate a variety of functionalities, such as alkoxy, amino and halide groups.

The author proposed a plausible mechanism depicted in Scheme 42. At first, a dinitrogen ligated complex (*N,N*)CuX **A** is generated in situ by the reaction of CuI with phen. Then, a copper(I)-acetylide species **B** is formed through the coordination/deprotonation of the alkyne in the presence of base, followed by oxidative addition of CF_3^+ and reductive elimination providing the desired product. The copper complex **A** was regenerated to complete the catalytic cycle.

In the same year, the group of Fu and Guo [64] described a trifluoromethylation reaction of terminal alkynes using Umemoto's reagent as a trifluoromethyl source (Scheme 43). Various terminal alkynes underwent smoothly to provide the corresponding products in moderate to good yields at room temperature. Many synthetically important functional groups were tolerated in these conditions, such as sulfonate, nitro, ester, amide, ether, and even unprotected hydroxy groups. In addition,

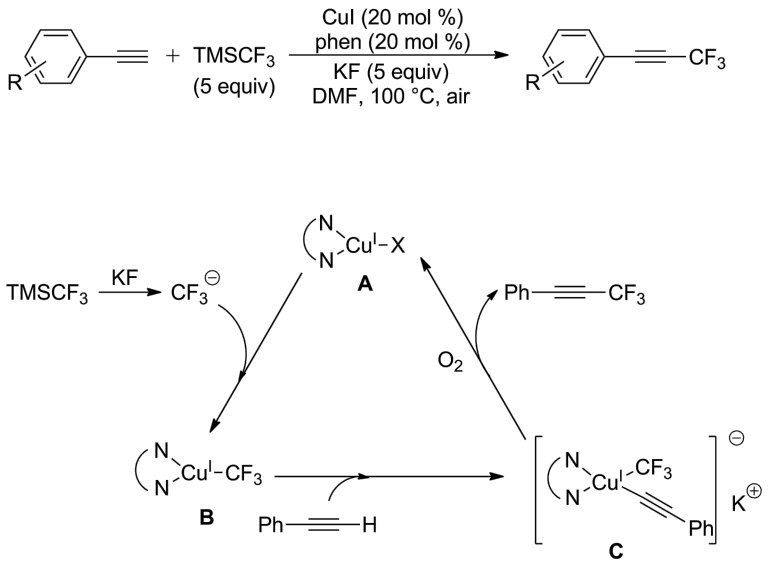

Scheme 41: Copper-catalyzed trifluoromethylation of terminal alkynes reported by the group of Qing.

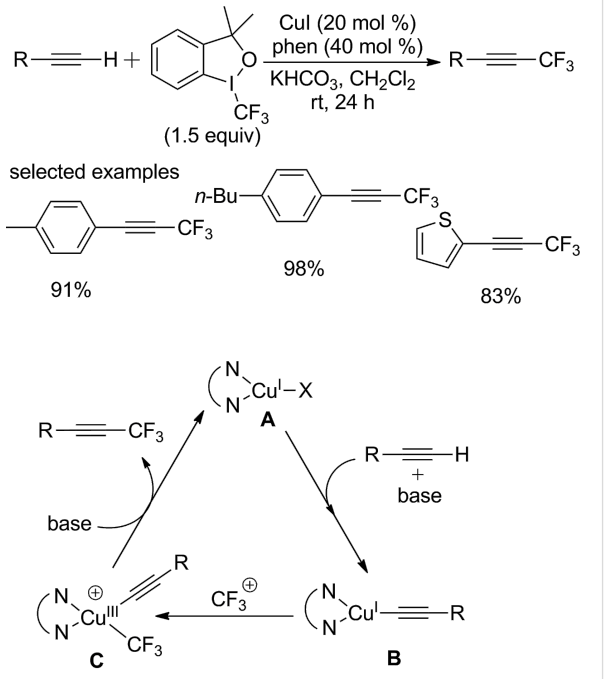

Scheme 42: Copper-catalyzed trifluoromethylation of terminal alkynes using Togni's reagent and the proposed mechanism.

arene rings bearing chloro and iodo groups did not interfere with the transformation, which promised further conversion at the halogenated positions. It was notable that substrates bearing sulfonate group had a high reactivity.

Recently, the group of Xiao and Lin [65] developed a copper-catalyzed C–H trifluoromethylation of 3-arylprop-1-ynes to provide (trifluoromethyl)allenes and propargyl trifluoromethanes (Scheme 44). This reaction was the first reported example for selective construction of allenic $C(sp^2)–CF_3$ and propargyl $C(sp^3)–CF_3$ bonds by modifying the reaction conditions. The ratio of propargyl trifluoromethanes increased dramatically when a solution of allenic products under conditions A was further heated. Compared with previous reactions of construction of allenic $C(sp^2)–CF_3$ and propargyl $C(sp^3)–CF_3$ bonds, this method combined selectivity and efficiency and showed atom economy by avoiding the requirement of the prefunctionalization of the substrates.

Regarding the reaction mechanism, the authors postulated the following plausible reaction pathways (Scheme 44). Initially, the CF_3 radical is generated by the reaction of Togni's reagent with Cu(I) salt, which is trapped by 3-arylprop-1-yne to produce the radical intermediate **B**. Then, oxidation occurs to intermediate **B** by Cu(II) providing the cationic intermediate **C** and CuI, followed by the deprotonation of a benzyl proton in intermediate **C** giving the allenic product **D**. At high temperature, deprotonation of allene **D** prefers to form anion **E** in the presence of KF, which is converted to anion **F** through a resonance effect. Protonation of intermediate **F** would then furnish the propargyl trifluoromethanes.

Conclusion

In the past few years, the field of copper-mediated trifluoromethylation of aromatic and aliphatic compounds including heterocycles have experienced significant advances. In parallel with this field, the trifluoromethylation catalyzed by other transition metals like Pd, Ag, Fe and photocatalysts, metal-free

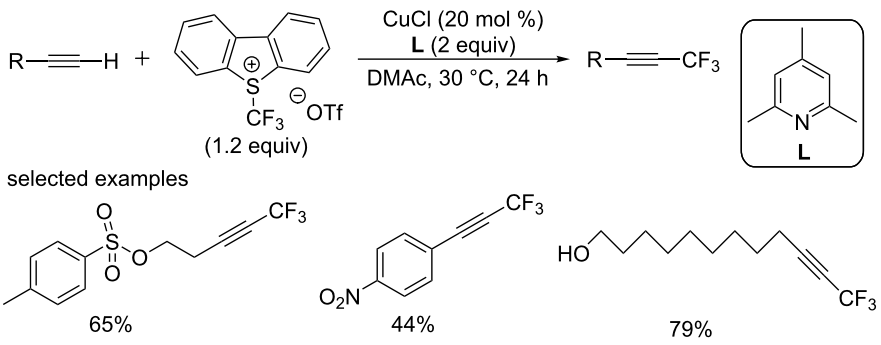

Scheme 43: Copper-catalyzed trifluoromethylation of terminal alkynes using Umemoto's reagent reported by the group of Fu and Guo.

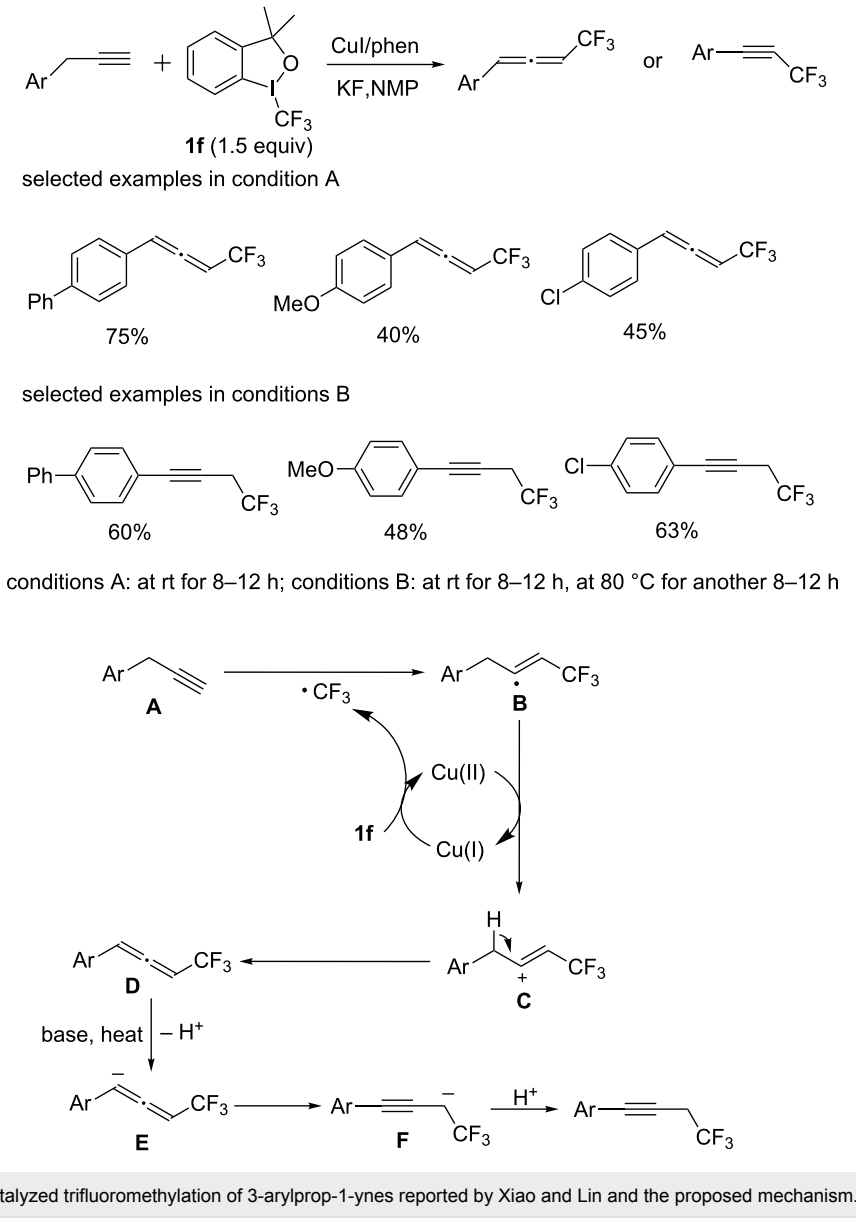

Scheme 44: Copper-catalyzed trifluoromethylation of 3-arylprop-1-ynes reported by Xiao and Lin and the proposed mechanism.

methods also have made tremendous advance. For trifluoromethylation of prefunctionalized substrates, these developments have expanded the substrate scope and provided milder conditions, but this field still suffered from limited and expensive trifluoromethylation reagents. Moreover, despite great progress have been made, current methods still lack enough efficiency for their general use in practical large-scale manufacturing.

Likewise, recently the direct trifluoromethylation of aliphatic and aromatic hydrocarbons as well as heterocycles are just starting out and remain a challenge. These methods have often the drawback of generating mixtures of regioisomers. Future efforts will be focus on developing efficient and less expensive reagents, along with a better understanding of mechanisms, improving the regioselectivity and enantioselectivity in these trifluoromethylation processes.

Acknowledgements

This research was supported financially by the National Natural Science Foundation of China 81473085; Major Project of Shandong 2015ZDXX0301A03; the Natural Science Foundation of Shandong 2013ZRE27169.

References

1. Kirsch, P. *Modern fluoroorganic chemistry: synthesis, reactivity, applications;* Wiley-VCH: Weinheim, Germany, 2004.
2. Müller, K.; Faeh, C.; Diederich, F. *Science* **2007,** *317,* 1881–1886. doi:10.1126/science.1131943
3. Purser, S.; Moore, P. R.; Swallow, S.; Gouverneur, V. *Chem. Soc. Rev.* **2008,** *37,* 320–330. doi:10.1039/B610213C
4. Furuya, T.; Kamlet, A. S.; Ritter, T. *Nature* **2011,** *473,* 470–477. doi:10.1038/nature10108
5. Wang, G.; He, X.; Dai, J.; Xu, H. *Chin. J. Org. Chem.* **2014,** *34,* 837–851. doi:10.6023/cjoc201311012
6. Liu, T.; Shen, Q. *Eur. J. Org. Chem.* **2012,** 6679–6687. doi:10.1002/ejoc.201200648
7. Gao, P.; Song, X.-R.; Liu, X.-Y.; Liang, Y.-M. *Chem. – Eur. J.* **2015,** *21,* 7648–7661. doi:10.1002/chem.201406432
8. Alonso, C.; Martinez de Marigorta, E.; Rubiales, G.; Palacios, F. *Chem. Rev.* **2015,** *115,* 1847–1935. doi:10.1021/cr500368h
9. Richard, M. V. C.; John, T. Manufacture of organic compounds containing fluorine. U.S. Patent 3,408,411, Oct 29, 1968.
10. Roy, S.; Gregg, B. T.; Gribble, G. W.; Le, V.-D.; Roy, S. *Tetrahedron* **2011,** *67,* 2161–2195. doi:10.1016/j.tet.2011.01.002
11. Urata, H.; Fuchikami, T. *Tetrahedron Lett.* **1991,** *32,* 91–94. doi:10.1016/S0040-4039(00)71226-3
12. Oishi, M.; Kondo, H.; Amii, H. *Chem. Commun.* **2009,** 1909–1911. doi:10.1039/b823249k
13. Gonda, Z.; Kovács, S.; Wéber, C.; Gáti, T.; Mészáros, A.; Kotschy, A.; Novák, Z. *Org. Lett.* **2014,** *16,* 4268–4271. doi:10.1021/ol501967c
14. Yagupolskii, L.; Kondratenko, N.; Timofeeva, G. *J. Org. Chem. USSR* **1984,** *20,* 103–106.
15. Zhang, C.-P.; Wang, Z.-L.; Chen, Q.-Y.; Zhang, C.-T.; Gu, Y.-C.; Xiao, J.-C. *Angew. Chem., Int. Ed.* **2011,** *50,* 1896–1900. doi:10.1002/anie.201006823
16. Liu, Y.; Shao, X.; Zhang, P.; Lu, L.; Shen, Q. *Org. Lett.* **2015,** *17,* 2752–2755. doi:10.1021/acs.orglett.5b01170
17. Li, Y.; Chen, T.; Wang, H.; Zhang, R.; Jin, K.; Wang, X.; Duan, C. *Synlett* **2011,** 1713–1716. doi:10.1055/s-0030-1260930
18. Schareina, T.; Wu, X.-F.; Zapf, A.; Cotté, A.; Gotta, M.; Beller, M. *Top. Catal.* **2012,** *55,* 426–431. doi:10.1007/s11244-012-9824-0
19. Chen, M.; Buchwald, S. L. *Angew. Chem., Int. Ed.* **2013,** *52,* 11628–11631. doi:10.1002/anie.201306094
20. Lin, X.; Hou, C.; Li, H.; Weng, Z. *Chem. – Eur. J.* **2016,** *22,* 2075–2084. doi:10.1002/chem.201504306
21. Wei, Y.; Yu, L.; Lin, J.; Zheng, X.; Xiao, J. *Chin. J. Chem.* **2016,** *34,* 481–484. doi:10.1002/cjoc.201500543
22. Wang, J.; Zhang, X.; Wan, Z.; Ren, F. *Org. Process Res. Dev.* **2016,** *20,* 836–839. doi:10.1021/acs.oprd.6b00079
23. Chen, Q.-Y.; Wu, S.-W. *J. Chem. Soc., Chem. Commun.* **1989,** 705–706. doi:10.1039/c39890000705
24. Zhao, G.; Wu, H.; Xiao, Z.; Chen, Q.-Y.; Liu, C. *RSC Adv.* **2016,** *6,* 50250–50254. doi:10.1039/C6RA09011G
25. Kawai, H.; Furukawa, T.; Nomura, Y.; Tokunaga, E.; Shibata, N. *Org. Lett.* **2011,** *13,* 3596–3599. doi:10.1021/ol201205t
26. Miyake, Y.; Ota, S.-i.; Nishibayashi, Y. *Chem. – Eur. J.* **2012,** *18,* 13255–13258. doi:10.1002/chem.201202853
27. Miyake, Y.; Ota, S.-i.; Shibata, M.; Nakajima, K.; Nishibayashi, Y. *Chem. Commun.* **2013,** *49,* 7809–7811. doi:10.1039/c3cc44434a
28. Miyake, Y.; Ota, S.-i.; Shibata, M.; Nakajima, K.; Nishibayashi, Y. *Org. Biomol. Chem.* **2014,** *12,* 5594–5596. doi:10.1039/C4OB00957F
29. Chu, L.; Qing, F.-L. *Org. Lett.* **2010,** *12,* 5060–5063. doi:10.1021/ol1023135
30. Senecal, T. D.; Parsons, A. T.; Buchwald, S. L. *J. Org. Chem.* **2011,** *76,* 1174–1176. doi:10.1021/jo1023377
31. Khan, B. A.; Buba, A. E.; Gooßen, L. J. *Chem. – Eur. J.* **2012,** *18,* 1577–1581. doi:10.1002/chem.201102652
32. Xu, J.; Xiao, B.; Xie, C.-Q.; Luo, D.-F.; Liu, L.; Fu, Y. *Angew. Chem.* **2012,** *124,* 12719–12722. doi:10.1002/ange.201206681
33. Yang, C. T.; Zhang, Z. Q.; Tajuddin, H.; Wu, C. C.; Liang, J.; Liu, J. H.; Fu, Y.; Czyzewska, M.; Steel, P. G.; Marder, T. B.; Liu, L. *Angew. Chem.* **2012,** *124,* 543–547. doi:10.1002/ange.201106299
34. Xu, J.; Luo, D.-F.; Xiao, B.; Liu, Z.-J.; Gong, T.-J.; Fu, Y.; Liu, L. *Chem. Commun.* **2011,** *47,* 4300–4302. doi:10.1039/c1cc10359h
35. Huang, Y.; Fang, X.; Lin, X.; Li, H.; He, W.; Huang, K.-W.; Yuan, Y.; Weng, Z. *Tetrahedron* **2012,** *68,* 9949–9953. doi:10.1016/j.tet.2012.09.083
36. Arimori, S.; Shibata, N. *Org. Lett.* **2015,** *17,* 1632–1635. doi:10.1021/acs.orglett.5b00164
37. Mizuta, S.; Verhoog, S.; Wang, X.; Shibata, N.; Gouverneur, V.; Médebielle, M. *J. Fluorine Chem.* **2013,** *155,* 124–131. doi:10.1016/j.jfluchem.2013.07.006
38. Nagib, D. A.; Scott, M. E.; MacMillan, D. W. C. *J. Am. Chem. Soc.* **2009,** *131,* 10875–10877. doi:10.1021/ja9053338
39. Pham, P. V.; Nagib, D. A.; MacMillan, D. W. C. *Angew. Chem., Int. Ed.* **2011,** *50,* 6119–6122. doi:10.1002/anie.201101861
40. Ye, Y.; Sanford, M. S. *J. Am. Chem. Soc.* **2012,** *134,* 9034–9037. doi:10.1021/ja301553c
41. Ye, Y.; Künzi, S. A.; Sanford, M. S. *Org. Lett.* **2012,** *14,* 4979–4981. doi:10.1021/ol3022726
42. Li, Y.; Wu, L.; Neumann, H.; Beller, M. *Chem. Commun.* **2013,** *49,* 2628–2630. doi:10.1039/c2cc36554e

43. Dai, J.-J.; Fang, C.; Xiao, B.; Yi, J.; Xu, J.; Liu, Z.-J.; Lu, X.; Liu, L.; Fu, Y. *J. Am. Chem. Soc.* **2013,** *135,* 8436–8439. doi:10.1021/ja404217t
44. Danoun, G.; Bayarmagnai, B.; Grünberg, M. F.; Gooßen, L. J. *Angew. Chem., Int. Ed.* **2013,** *52,* 7972–7975. doi:10.1002/anie.201304276
45. Wang, X.; Xu, Y.; Mo, F.; Ji, G.; Qiu, D.; Feng, J.; Ye, Y.; Zhang, S.; Zhang, Y.; Wang, J. *J. Am. Chem. Soc.* **2013,** *135,* 10330–10333. doi:10.1021/ja4056239
46. Bayarmagnai, B.; Matheis, C.; Risto, E.; Goossen, L. J. *Adv. Synth. Catal.* **2014,** *356,* 2343–2348. doi:10.1002/adsc.201400340
47. Lishchynskyi, A.; Berthon, G.; Grushin, V. V. *Chem. Commun.* **2014,** *50,* 10237–10240. doi:10.1039/C4CC04930F
48. Zhang, K.; Xu, X.-H.; Qing, F.-L. *J. Org. Chem.* **2015,** *80,* 7658–7665. doi:10.1021/acs.joc.5b01295
49. Xu, J.; Fu, Y.; Luo, D.-F.; Jiang, Y.-Y.; Xiao, B.; Liu, Z.-J.; Gong, T.-J.; Liu, L. *J. Am. Chem. Soc.* **2011,** *133,* 15300–15303. doi:10.1021/ja206330m
50. Wang, X.; Ye, Y.; Zhang, S.; Feng, J.; Xu, Y.; Zhang, Y.; Wang, J. *J. Am. Chem. Soc.* **2011,** *133,* 16410–16413. doi:10.1021/ja207775a
51. Mitsudera, H.; Li, C.-J. *Tetrahedron Lett.* **2011,** *52,* 1898–1900. doi:10.1016/j.tetlet.2011.02.038
52. Egami, H.; Ide, T.; Kawato, Y.; Hamashima, Y. *Chem. Commun.* **2015,** *51,* 16675–16678. doi:10.1039/C5CC07011B
53. Pair, E.; Monteiro, N.; Bouyssi, D.; Baudoin, O. *Angew. Chem., Int. Ed.* **2013,** *52,* 5346–5349. doi:10.1002/anie.201300782
54. Shang, M.; Sun, S.-Z.; Wang, H.-L.; Laforteza, B. N.; Dai, H.-X.; Yu, J.-Q. *Angew. Chem., Int. Ed.* **2014,** *53,* 10439–10442. doi:10.1002/anie.201404822
55. Hu, L.; Chen, X.; Gui, Q.; Tan, Z.; Zhu, G. *Chem. Commun.* **2016,** *52,* 6845–6848. doi:10.1039/C6CC02412B
56. Chu, L.; Qing, F.-L. *J. Am. Chem. Soc.* **2012,** *134,* 1298–1304. doi:10.1021/ja209992w
57. Yang, F.; Klumphu, P.; Liang, Y.-M.; Lipshutz, B. H. *Chem. Commun.* **2014,** *50,* 936–938. doi:10.1039/C3CC48131J
58. Lu, Y.; Li, Y.; Zhang, R.; Jin, K.; Duan, C. *J. Fluorine Chem.* **2014,** *161,* 128–133. doi:10.1016/j.jfluchem.2014.01.020
59. Ji, X.-M.; Wei, L.; Chen, F.; Tang, R.-Y. *RSC Adv.* **2015,** *5,* 29766–29773. doi:10.1039/C5RA02888D
60. Chu, L.; Qing, F.-L. *J. Am. Chem. Soc.* **2010,** *132,* 7262–7263. doi:10.1021/ja102175w
61. Zhang, K.; Qiu, X.-L.; Huang, Y.; Qing, F.-L. *Eur. J. Org. Chem.* **2012,** 58–61. doi:10.1002/ejoc.201101550
62. Jiang, X.; Chu, L.; Qing, F.-L. *J. Org. Chem.* **2012,** *77,* 1251–1257. doi:10.1021/jo202566h
63. Weng, Z.; Li, H.; He, W.; Yao, L.-F.; Tan, J.; Chen, J.; Yuan, Y.; Huang, K.-W. *Tetrahedron* **2012,** *68,* 2527–2531. doi:10.1016/j.tet.2011.12.085
64. Luo, D.-F.; Xu, J.; Fu, Y.; Guo, Q.-X. *Tetrahedron Lett.* **2012,** *53,* 2769–2772. doi:10.1016/j.tetlet.2012.03.107
65. Ji, Y.-L.; Luo, J.-J.; Lin, J.-H.; Xiao, J.-C.; Gu, Y.-C. *Org. Lett.* **2016,** *18,* 1000–1003. doi:10.1021/acs.orglett.6b00120

License and Terms

BEILSTEIN JOURNAL OF ORGANIC CHEMISTRY

Nucleophilic fluoroalkylation/cyclization route to fluorinated phthalides

Masanori Inaba[1], Tatsuya Sakai[1], Shun Shinada[1], Tsuyuka Sugiishi[1], Yuta Nishina[2], Norio Shibata[3] and Hideki Amii[*1]

Full Research Paper

Open Access

Address:
[1]Division of Molecular Science, Graduate School of Science and Technology, Gunma University, 1-5-1 Tenjin-cho, Kiryu, Gunma, 376-8515, Japan, [2]Research Core for Interdisciplinary Sciences, Okayama University, 3-1-1 Tsushimanaka, Kita-ku, Okayama 700-8530, Japan and [3]Department of Nanopharmaceutical Sciences, Department of Life Science and Applied Chemistry, Nagoya Institute of Technology Gokiso, Showa-ku, Nagoya 466-8555, Japan

Email:
Hideki Amii[*] - amii@gunma-u.ac.jp

* Corresponding author

Keywords:
cyclization; fluorine; lactone; phthalide; trifluoromethylation

Beilstein J. Org. Chem. **2018,** *14,* 182–186.
doi:10.3762/bjoc.14.12

Received: 26 September 2017
Accepted: 04 January 2018
Published: 19 January 2018

This article is part of the Thematic Series "Organo-fluorine chemistry IV".

Guest Editor: D. O'Hagan

Abstract

Discribed in this article is a versatile and practical method for the synthesis of C3-perfluoroalkyl-substituted phthalides in a one-pot manner. Upon treatment of KF or triethylamine, 2-cyanobenzaldehyde reacted with (perfluoroalkyl)trimethylsilanes via nucleophilic addition and subsequent intramolecular cyclization to give perfluoroalkylphthalides in good yields.

Introduction

Phthalides (1(3*H*)-isobenzofuranones) are frequently found in natural products and exhibit a range of bioactivity (Scheme 1) [1,2]. Substituted phthalides have been used as building blocks for the synthesis of useful bioactive compounds. There is a growing interest in the usefulness of phthalides and their derivatives. Organofluorine compounds often show attractive physical, chemical, and biological properties and are widely used in many fields, such as pharmaceuticals, agrochemicals, and materials [3-10]. Selective incorporation of fluorine or a fluoroalkyl group into a molecule is a topic of significant interest in organic chemistry. Fluorinated phthalides are considered to be one of the most fascinating organofluorine compounds. However, to our best knowledge, there have been few reports on the preparation of fluoroalkyl phthalides [11-19]. The first synthesis of 3-(trifluoromethyl)phthalides was accomplished by Reinecke and Chen in 1993. They studied *ortho*-lithiation of phenyloxazolines and the subsequent reactions with pentafluoroacetone and hexafluoroacetone to give 3-(trifluoromethyl)phthalide derivatives [11]. In 2006, Pedrosa et al. reported the nucleophilic trifluoromethylation of protected *ortho*-phthalaldehyde, followed by deprotection and oxidation to afford 3-(trifluoromethyl)phthalide [12]. Pohmakotr et al. demonstrated the nucleophilic trifluoromethylation of acid anhydrides to produce γ-hydroxy-γ-trifluoromethyl-γ-butyrolactones, which acted as

good precursors in the synthesis of γ-trifluoromethyl-γ-butyrolactones with organometallic reagents [16]. All these protocols involve multiple steps to obtain trifluoromethylphthalides. An operational simple procedure for a short-step synthesis of 3-(trifluoromethyl)phthalide is required due to their great potential in a variety of applications. Herein, we wish to report a general and convenient synthesis of 3-(perfluoroalkyl)phthalides **1** by nucleophilic perfluoroalkylation of 2-cyanobenzaldehyde (**2**) and subsequent intramolecular cyclization.

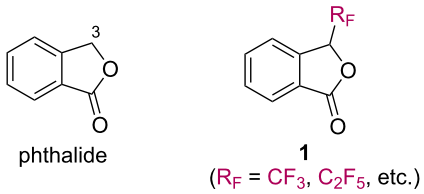

Scheme 1: Phthalide and fluorinated phthalides (**1**).

Results and Discussion

The reaction procedure is very simple. A mixture of 2-cyanobenzaldehyde (**2**), CF_3–$SiMe_3$ (so-called Ruppert–Prakash reagent) [20,21], and a catalytic amount of KF in anhydrous DMF was stirred at room temperature for 1 h. After work-up under acidic conditions, 3-(trifluoromethyl)-1(3*H*)-isobenzofuranone (**1a**) was obtained in 99% NMR yield (95% isolated yield) (Table 1, entry 1). As a good alternative activator of CF_3–$SiMe_3$, the use of a Lewis base such as triethylamine [22,23] worked well for the synthesis of 3-(trifluoromethyl)phthalide (**1a**, Table 1, entries 2–4). When aldehyde **2** was treated with CF_3–$SiMe_3$ in the presence of Et_3N at 50 °C, the cascade trifluoromethylation/cyclization proceeded smoothly to afford phthalide **1a** in 70% isolated yield (Table 1, entry 4).

Table 1: Trifluoromethylation/cyclization of 2-cyanobenzaldehyde.

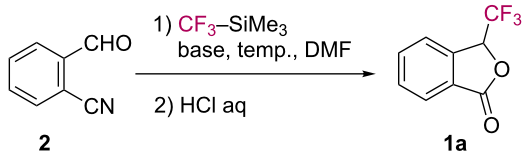

Entry	Base (equiv)	Conditions	Yield of **1a** (%)[a,b]
1	KF (0.1)	rt, 1 h	99 (95)
2	Et_3N (0.5)	rt, 1 h	80
3	Et_3N (0.5)	50 °C, 1 h	86
4	Et_3N (1.0)	50 °C, 1 h	91 (70)

[a]Yields were determined by ^{19}F NMR analysis using 1,3-bis(trifluoromethyl)benzene as an internal standard. [b]The values in parentheses indicate the isolated yield of **1a**.

The formation of phthalide **1a** can be explained by assuming the pathway shown in Scheme 2. The formyl group in aldehyde **2** undergoes nucleophilic trifluoromethylation triggered by a catalytic amount of KF to give the *ortho*-cyanobenzyl silyl ether **3**. Upon treatment with aq HCl, the subsequent lactonization of **4** takes place to afford trifluoromethylphthalide **1a**.

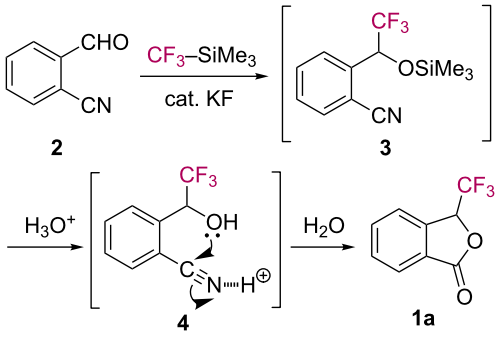

Scheme 2: Plausible reaction mechanism for the formation of phthalide **1a**.

Other examples of the one-pot synthesis of fluorinated phthalides **1** are given in Scheme 3. The reactions of 2-cyanobenzaldehyde (**2**) with organosilicon compounds (R_F–$SiMe_3$) proceeded cleanly by the use of KF (conditions A) or Et_3N (conditions B). As a consequence, pentafluoroethyl, heptafluo-

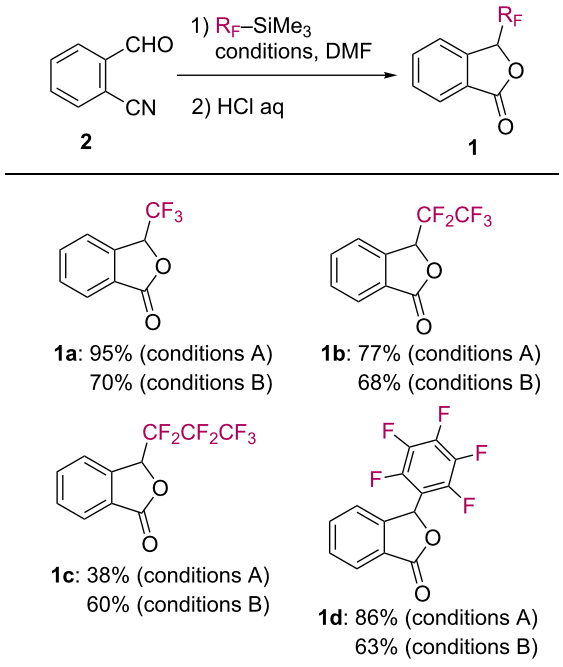

Scheme 3: Synthesis of fluorinated phthalides **1**.

ropropyl, and pentafluorophenyl [24,25] groups were successfully installed at the C3-position of phthalides **1b–d**.

Thus, the selective formation of fluorinated phthalides **1** represents a synthetic usefulness for further applications. In particular, the asymmetric synthesis of C3-substituted phthalides is of considerable importance in chemistry [26-32]. Enantioselective fluoroalkylation/lactonization reactions are worth investigating since a new stereogenic carbon center next to the fluoroalkyl groups is generated in products **1**. To the best of our knowledge, only one successful example of an asymmetric synthesis of 3-(trifluoromethyl)phthalide (**1a**) using a chiral auxiliary was published to date. In 2006, Pedrosa and co-workers discribed the diastereoselective nucleophilic trifluoromethylation of aldehyde **5**, which was prepared by condensation of *ortho*-phthalaldehyde with (−)-8-benzylaminomenthol (Scheme 4) [12]. Only diastereoisomer **6** was detected in the NMR analysis. Acid-promoted deprotection of hemiaminal **6** and subsequent oxidation of acetal **7** gave the enantiopure phthalide **1a** in good yield.

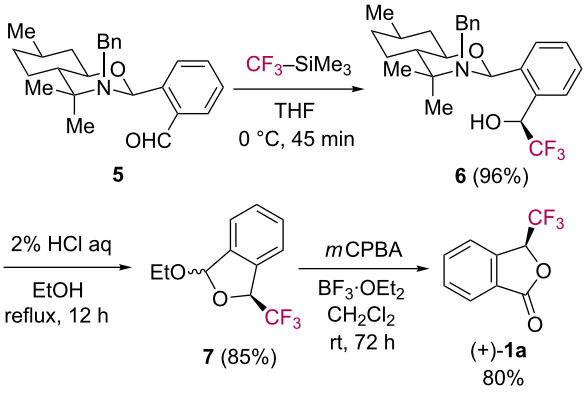

Scheme 4: Asymmetric synthesis of **1a** using a chiral auxiliary.

Although a high control of diastereoselectivity (using stoichiometric auxiliary strategy) was achieved for the asymmetric synthesis of trifluoromethylphthalide **1a**, it is desirable to reduce the amount of the chiral sources. Next, we undertook the development of a catalytic asymmetric synthesis of **1** in a one-pot manner. The results of our trial are summarized in Table 2.

For the catalytic asymmetric synthesis of **1**, we carried out the nucleophilic trifluoromethylation of **2** employing a small

Table 2: Trifluoromethylation/cyclization of 2-cyanobenzaldehyde (**2**) in the presence of chiral catalysts.

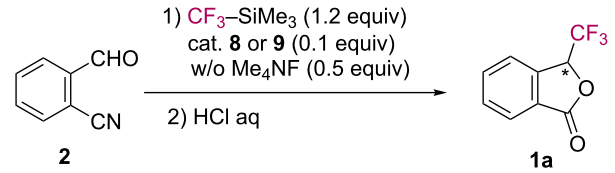

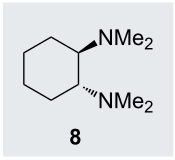

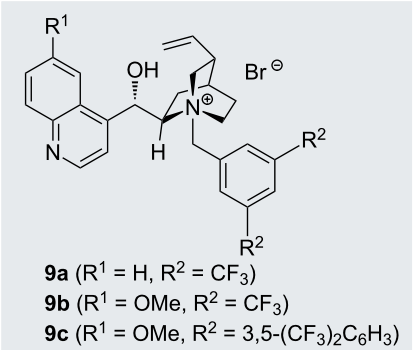

9a (R^1 = H, R^2 = CF_3)
9b (R^1 = OMe, R^2 = CF_3)
9c (R^1 = OMe, R^2 = 3,5-$(CF_3)_2C_6H_3$)

Entry	Catalyst	Solvent	Conditions	Yield of **1a** (%)[a]	% ee[b]
1	**8**	DMF	rt, 1 h	79	0
2	**8**	DMF	0 °C, 1 h	62	0
3	**9a**	toluene/CH_2Cl_2 (2:1)	−60 °C, 24 h	61	0
4	**9b**	toluene/CH_2Cl_2 (2:1)	−60 °C, 24 h	51	12
5	**9c**	toluene/CH_2Cl_2 (2:1)	−60 °C, 24 h	76	6

[a]Isolated yield of **1a**. [b]Each enantiomeric excess (ee) was determined by HPLC analyses.

amount of chiral tertiary amines. However, the use of (1*R*,2*R*)-(*N*,*N*,*N'*,*N'*-tetramethyl)-1,2-diaminocyclohexane (**8**) as a chiral catalyst resulted in the formation of a racemic mixture of **1a** (Table 2, entries 1 and 2).

Previously, Shibata et al. reported a cinchona alkaloid/Me_4NF-catalyzed nucleophilic enantioselective trifluoromethylation of carbonyl compounds [33-35]. Initially, we tried to conduct the reaction of 2-cyanobenzaldehyde (**2**) with CF_3–$SiMe_3$ in the presence of cinchona alkaloids **9**/TMAF combination (Table 2, entries 3–5). By employing catalyst **9b**, the reaction proceeded at −60 °C to give phthalide **1a** in 51% yield with 12% ee (Table 2, entry 4).

To improve the enantioselectivity of the present nucleophilic trifluorometylation/lactonization, we surveyed suitable conditions for the catalytic asymmetric transformation. After many experiments, we found that the use of ethyl 2-formylbenzoate (**10**) [36] instead of nitrile **2** resulted in the formation of **1a** with 27% ee upon exposure to organocatalyst **9b** (0.1 equiv) and tetramethylammonium fluoride (0.5 equiv, Scheme 5).

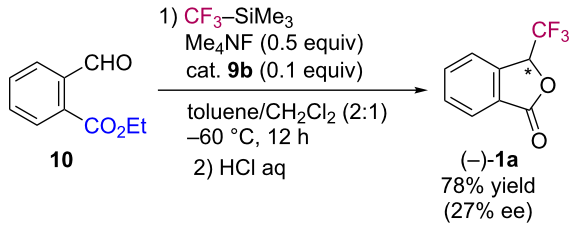

Scheme 5: Catalytic asymmetric synthesis of **1a**.

Conclusion

In summary, we have demonstrated a convenient route to fluorinated phthalides from 2-cyanobenzaldehyde or 2-formylbenzoates in a one-pot manner. In the transformations, installation of fluorinated substituents at the C3-position of phthalides has been achieved. The issue of the low stereoselectivity of the catalytic asymmetric fluoroalkylation should be solved in the future. Further examples for the promising utilization of fluorinated phthalides as building blocks can be found in [37].

Supporting Information

Supporting Information File 1

General methods, synthetic procedures, ^1H and ^{19}F NMR spectra for known compound **1a** and full characterization of all new compounds.
[https://www.beilstein-journals.org/bjoc/content/supplementary/1860-5397-14-12-S1.pdf]

Acknowledgements

This article is dedicated to the memory of Professor Yoshihiko Ito (1937-2006) on the occasion of the 10th anniversary of his sudden death. The financial support of JSPS KAKENHI Grant No. JP 16H04143 (Grant-in-Aid for Scientific Research (B)), JP16H01003 in Precisely Designed Catalysts with Customized Scaffolding, JP16H01129 in Middle Molecular Strategy, and Japan Science and Technology Agency (JST) (ACT-C: Creation of Advanced Catalytic Transformation for the Sustainable Manufacturing at Low Energy, Low Environmental Load) is acknowledged. We would like to thank Prof. Hiroshi Sano (Gunma University) for his useful suggestions.

ORCID® iDs

Norio Shibata - https://orcid.org/0000-0002-3742-4064

References

1. Lin, G.; Chan, S.-K. S.; Chung, H.-S.; Li, S.-L. Chemistry and biological activities of naturally occurring phthalides. In *Studies in Natural Products Chemistry;* Atta-ur-Rahman, Ed.; Elsevier: Amsterdam, 2005; Vol. 32, pp 611–670.
2. Knepper, K.; Ziegert, R. E.; Bräse, S. *Tetrahedron* **2004,** *60,* 8591–8603. doi:10.1016/j.tet.2004.05.111
3. Hiyama, T.; Kanie, K.; Kusumoto, T.; Morizawa, Y.; Shimizu, M. In *Organofluorine Compounds: Chemistry and Applications;* Yamamoto, H., Ed.; Springer-Verlag: Berlin, 2000. doi:10.1007/978-3-662-04164-2
4. Kirsch, P. *Modern Fluoroorganic Chemistry: Synthesis, Reactivity, Applications;* Wiley-VCH: Weinheim, Germany, 2004. doi:10.1002/352760393X
5. Chambers, R. D. *Fluorine in Organic Chemistry;* Blackwell: Oxford, 2004.
6. Uneyama, K. *Organofluorine Chemistry;* Blackwell: Oxford, 2006.
7. Bégué, J.-P.; Bonnet-Delpon, D. *Bioorganic and Medicinal Chemistry of Fluorine;* John Wiley & Sons, Inc.: Hoboken, NJ, 2008. doi:10.1002/9780470281895
8. Ojima, I., Ed. *Fluorine in Medicinal Chemistry and Chemical Biology;* Wiley-Blackwell: Chichester, West Sussex, 2009. doi:10.1002/9781444312096
9. *Fluorine in Pharmaceutical and Medicinal Chemistry: From Biophysical Aspects to Clinical Applications;* Gouverneur, V.; Müller, K., Eds.; Molecular Medicine and Medicinal Chemistry, Vol. 6; Imperial College Press: London, 2012. doi:10.1142/p746
10. Wang, J.; Sánchez-Roselló, M.; Aceña, J. L.; del Pozo, C.; Sorochinsky, A. E.; Fustero, S.; Soloshonok, V. A.; Liu, H. *Chem. Rev.* **2014,** *114,* 2432–2506. doi:10.1021/cr4002879
11. Reinecke, M. G.; Chen, L.-J. *Acta Chem. Scand.* **1993,** *47,* 318–322. doi:10.3891/acta.chem.scand.47-0318
12. Pedrosa, R.; Sayalero, S.; Vicente, M. *Tetrahedron* **2006,** *62,* 10400–10407. doi:10.1016/j.tet.2006.08.058
13. Zonov, Y. V.; Karpov, V. M.; Platonov, V. E.; Rybalova, T. V.; Gatilov, Y. V. *J. Fluorine Chem.* **2006,** *127,* 1574–1583. doi:10.1016/j.jfluchem.2006.08.006
14. Kinoshita, K.; Yamada, S.; Iwama, S.; Kawasaki-Takasuka, T.; Yamazaki, T. 20th International Symposium on Fluorine Chemistry, Kyoto, Japan, July 22–27, 2012; Abstr., No. P-41.

15. Shi, X.; Li, C.-J. *Adv. Synth. Catal.* **2012,** *354,* 2933–2938. doi:10.1002/adsc.201200690
16. Masusai, C.; Soorukram, D.; Kuhakarn, C.; Tuchinda, P.; Reutrakul, V.; Pohmakotr, M. *J. Fluorine Chem.* **2013,** *154,* 37–42. doi:10.1016/j.jfluchem.2013.06.006
17. Xu, L.; Jiang, H.; Hao, J.; Zhao, G. *Tetrahedron* **2014,** *70,* 4373–4378. doi:10.1016/j.tet.2014.04.072
18. Egami, H.; Asada, J.; Sato, K.; Hashizume, D.; Kawato, Y.; Hamashima, Y. *J. Am. Chem. Soc.* **2015,** *137,* 10132–10135. doi:10.1021/jacs.5b06546
19. Fustero, S.; Moscardó, J.; Sánchez-Rosselló, M.; Rodriguez, E.; Barrio, P. *Org. Lett.* **2010,** *12,* 5494–5497. doi:10.1021/ol102341n
20. Prakash, G. K. S.; Krishnamurti, R.; Olah, G. A. *J. Am. Chem. Soc.* **1989,** *111,* 393–395. doi:10.1021/ja00183a073
21. Prakash, G. K. S.; Yudin, A. K. *Chem. Rev.* **1997,** *97,* 757–786. doi:10.1021/cr9408991
22. Hagiwara, T.; Kobayashi, T.; Fuchikami, T. *Nippon Kagaku Kaishi* **1997,** 869–875. doi:10.1246/nikkashi.1997.869
23. Hagiwara, T.; Kobayashi, T.; Fuchikami, T. *Main Group Chem.* **1997,** *2,* 13–15. doi:10.1080/13583149712331338829
24. Brogan, S.; Carter, N. B.; Lam, H. W. *Synlett* **2010,** 615–617. doi:10.1055/s-0029-1219159
25. Du, G.-F.; Xing, F.; Gu, C.-Z.; Dai, B.; He, L. *RSC Adv.* **2015,** *5,* 35513–35517. doi:10.1039/C5RA05487G
26. Kitamura, M.; Okhuma, T.; Inoue, S.; Sayo, N.; Kumobayshi, H.; Akutagawa, S.; Ohta, T.; Takaya, H.; Noyori, R. *J. Am. Chem. Soc.* **1988,** *110,* 629–631. doi:10.1021/ja00210a070
27. Ramachandran, P. V.; Chen, G.-M.; Brown, H. C. *Tetrahedron Lett.* **1996,** *37,* 2205–2208. doi:10.1016/0040-4039(96)00260-2
28. Witulski, B.; Zimmermann, A. *Synlett* **2002,** 1855–1859. doi:10.1055/s-2002-34883
29. Kosaka, M.; Sekiguchi, S.; Naito, J.; Uemura, M.; Kuwahara, S.; Watanabe, M.; Harada, N.; Hiroi, K. *Chirality* **2005,** *17,* 218–232. doi:10.1002/chir.20156
30. Chang, H.-T.; Jeganmohan, M.; Cheng, C.-H. *Chem. – Eur. J.* **2007,** *13,* 4356–4363. doi:10.1002/chem.200601880
31. Phan, D. H. T.; Kim, B.; Dong, V. M. *J. Am. Chem. Soc.* **2009,** *131,* 15608–15609. doi:10.1021/ja907711a
32. Yasukawa, T.; Kobayashi, S. *Chem. Lett.* **2017,** *46,* 98–100. doi:10.1246/cl.160862
33. Mizuta, S.; Shibata, N.; Akiti, S.; Fujimoto, H.; Nakamura, S.; Toru, T. *Org. Lett.* **2007,** *9,* 3707–3710. doi:10.1021/ol701791r
34. Kawai, H.; Kusuda, A.; Nakamura, S.; Shiro, M.; Shibata, N. *Angew. Chem., Int. Ed.* **2009,** *48,* 6324–6327. doi:10.1002/anie.200902457
35. Kawai, H.; Mizuta, S.; Tokunaga, E.; Shibata, N. *J. Fluorine Chem.* **2013,** *152,* 46–50. doi:10.1016/j.jfluchem.2013.01.032
36. Cai, C.; Chen, T. Preparation method of 3-trifluoromethyl phthalide. Chin. Pat. Appl CN 2016-11198471, Dec 22, 2016.
While this article was in preparation, on May 17, 2017, a related observation using 2-formylbenzoates was reported in the above stated patent.
37. Hamura, T.; Nakayama, R. *Chem. Lett.* **2013,** *42,* 1013–1015. doi:10.1246/cl.130398

License and Terms

BEILSTEIN JOURNAL OF ORGANIC CHEMISTRY

Syn-selective silicon Mukaiyama-type aldol reactions of (pentafluoro-λ^6-sulfanyl)acetic acid esters with aldehydes

Anna-Lena Dreier[1], Andrej V. Matsnev[2], Joseph S. Thrasher[2] and Günter Haufe[*1,3]

Full Research Paper

Open Access

Address:
[1]Organisch-Chemisches Institut, Universität Münster, Corrensstraße 40, 48149 Münster, Germany, [2]Department of Chemistry, Advanced Materials Research Laboratory, Clemson University, 91 Technology Drive, Anderson, South Carolina 29625, United States of America and [3]Cells-in-Motion Cluster of Excellence, Universität Münster, Waldeyerstraße 15, 48149 Münster, Germany

Email:
Günter Haufe[*] - haufe@uni-muenster.de

* Corresponding author

Keywords:
aldol reaction; ester enolate; fluorine; SF_5 compounds; stereochemistry

Beilstein J. Org. Chem. **2018,** *14,* 373–380.
doi:10.3762/bjoc.14.25

Received: 24 December 2017
Accepted: 26 January 2018
Published: 08 February 2018

This article is part of the Thematic Series "Organo-fluorine chemistry IV".

Guest Editor: D. O'Hagan

Abstract

Aldol reactions belong to the most frequently used C–C bond forming transformations utilized particularly for the construction of complex structures. The selectivity of these reactions depends on the geometry of the intermediate enolates. Here, we have reacted octyl pentafluoro-λ^6-sulfanylacetate with substituted benzaldehydes and acetaldehyde under the conditions of the silicon-mediated Mukaiyama aldol reaction. The transformations proceeded with high diastereoselectivity. In case of benzaldehydes with electron-withdrawing substituents in the *para*-position, *syn*-α-SF_5-β-hydroxyalkanoic acid esters were produced. The reaction was also successful with *meta*-substituted benzaldehydes and *o*-fluorobenzaldehyde. In contrast, *p*-methyl-, *p*-methoxy-, and *p*-ethoxybenzaldehydes led selectively to aldol condensation products with (*E*)-configured double bonds in 30–40% yields. In preliminary experiments with an SF_5-substituted acetic acid morpholide and *p*-nitrobenzaldehyde, a low amount of an aldol product was formed under similar conditions.

Introduction

The classical acid- or base-catalyzed directed cross aldol reaction of an aldehyde and an enolizable second carbonyl compound is one of the most powerful and reliable carbon–carbon bond-forming transformations in organic synthesis applied most successfully for the construction of natural products and their analogs [1,2]. Later this type of reaction was extended to enolized carboxylic acid derivatives, particularly to silylated ketene acetals, as reaction partners for carbonyl active compounds [3-5]. Mild and highly selective reaction conditions could be developed in parallel with the progress in under-

standing the mechanism of these transformations [6-9]. Also, aldol reactions with fluorinated substrates, particularly with trifluoromethyl-containing ones, were investigated [10-13].

In recent years, the pentafluoro-λ^6-sulfanyl (SF_5) substituent has come into the focus of chemists because of the remarkable effects of this substituent on the physical and chemical properties of compounds, which are important for agricultural and medicinal chemistry as well as for materials sciences. While aromatic [14,15] and heteroaromatic [16,17] SF_5 compounds have become readily available and many applications have been described [18,19], the chemistry of aliphatic analogs is still underdeveloped [20]. Generally, the incorporation of SF_5 groups into aliphatic positions is based on radical addition of SF_5X (X = Cl, Br, SF_5) across π-bonds. The unconventional conditions usually required were overcome by Dolbier's elegant triethylborane initiation [21]. Recently, the radical arylation of a SF_5-substituted alkene was realized in order to gain access to SF_5-containing dihydrobenzofurans and indolines [22]. There are not many transformations of aliphatic SF_5 compounds described in the literature. Among them are the preparation and derivatization of SF_5-aldehydes [23], Diels–Alder reactions [24-26], the "click reaction" of SF_5-acetylenes with azides to form triazoles [27], and 1,3-dipolar cycloadditions of azomethine ylides with pentafluoro-λ^6-sulfanyl-substituted acrylic esters and amides [28].

A couple of years ago, we became interested in SF_5-substituted ester enolates as reaction intermediates. Thus, in 2016 we reported a highly *anti*-selective aldol addition of SF_5-substituted acetic ester-based boron enolates to aromatic and aliphatic aldehydes to form *anti*-2-pentafluoro-λ^6-sulfanyl-3-hydroxyalkylcarboxylic acid esters [29]. Quite similar results were published independently by Carreira et al. a couple of weeks before us [30].

Recently, we discovered that silylated enolates can be formed as mixtures of (*E*)- and (*Z*)-isomers from SF_5-substituted acetic acid esters of aliphatic terminal allylic alcohols at low temperature. At slightly elevated temperature, the latter diastereomers are transformed to γ,δ-unsaturated α-pentafluoro-λ^6-sulfanyl alkanoic acids in an Ireland–Claisen rearrangement [31]. Under slightly modified conditions, this type of rearrangement was also successful for SF_5-substituted acetic esters of cinnamyl alcohols [32].

Herein we describe our results [33] of highly *syn*-diastereoselective silicon Mukaiyama-type aldol reactions of SF_5-acetic acid esters with different aldehydes. While our research was well underway, Ponomarenko and Röschenthaler et al. reported similar Ti(IV)-mediated aldol reactions proceeding via titanium enolates and some succeeding or competing reactions of intermediates or products [34].

Results and Discussion

As a model for our investigations we chose the reaction of the less volatile octyl 2-(pentafluoro-λ^6-sulfanyl)acetate (**1**) with *p*-nitrobenzaldehyde. Analogously to a protocol used by Ishihara et al. [35] for an Evans aldol reaction of trifluoropropanoic amides, we refluxed 1 equiv of ester **1** with 1.5 equiv trimethylsilyl trifluoromethanesulfonate (TMSOTf) and 1.5 equiv triethylamine (Et_3N) in dichloromethane for 4 hours. Then the mixture was cooled down to 0 °C and 1 equiv of *p*-nitrobenzaldehyde and 0.3 equiv of $TiCl_4$ were added under stirring. Stirring at room temperature was continued for 15 hours. Then the reaction was quenched by the addition of ice-water. After workup 22% of the aldol addition products were formed in a *syn*/*anti*-ratio of 97:3 as determined by ^{19}F NMR spectroscopy (Scheme 1). Subsequently, the reaction conditions were optimized (Table 1).

Elevation of the reaction temperature (15 h reflux) led to an increase of the yield, while the *syn*/*anti*-ratio was not changed (Table 1, entry 2). Elongation of the reaction time resulted in the formation of more side products, drop of aldol products' yield and selectivity (Table 1, entry 3). A lower amount of

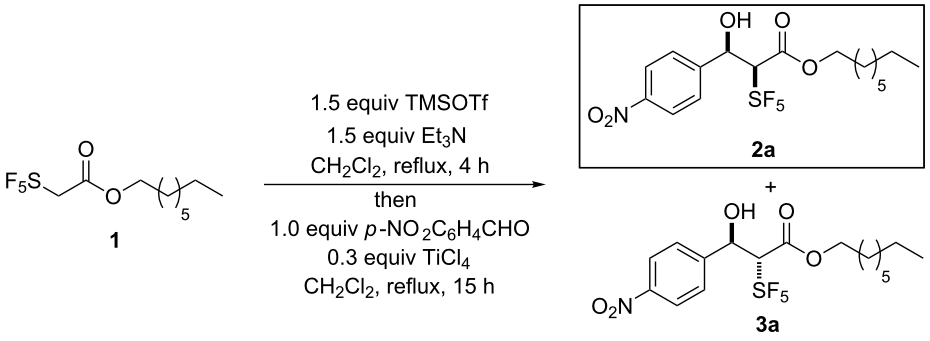

Scheme 1: Silicon-mediated Mukaiyama-type aldol reaction of octyl 2-(pentafluoro-λ^6-sulfanyl)acetate (**1**) with *p*-nitrobenzaldehyde.

Table 1: Optimization of the reaction conditions for the silicon Mukaiyama-type aldol reaction of ester **1** with *p*-nitrobenzaldehyde.

Entry	TMSOTf [equiv]	Et_3N [equiv]	Lewis acid [equiv]	Temp.	Time [h]	Yield **2** + **3** [%][a] (**2**:**3**-ratio)
1	1.5	1.5	0.3 $TiCl_4$	rt	15	22 (93:7)
2	1.5	1.5	0.3 $TiCl_4$	reflux	15	53 (93:7)
3	1.5	1.5	0.3 $TiCl_4$	reflux	3 days	40 (78:22)
4	1.2	1.5	0.3 $TiCl_4$	reflux	15	61 (73:27)
5	1.5	3.0	0.3 $TiCl_4$	reflux	15	0
6	1.5	1.5	1.0 $TiCl_4$	reflux	15	67 (81:19)
7	1.5	1.5	0.3 $BF_3{\cdot}OEt_2$	reflux	15	0
8	1.5	1.5	1.0 $BF_3{\cdot}OEt_2$	reflux	15	0
9	1.5	1.5	1.3 $BF_3{\cdot}OEt_2$	reflux	15	0

[a]Determined by ^{19}F NMR spectroscopy of the crude product mixture.

TMSOTf (1.2 equiv) led to increased yield but lower selectivity (Table 1, entry 4). Application of excess Et_3N delivered a complex mixture of products including fluorine-free ones. Only traces of the aldol products were detected (Table 1, entry 5). Increasing the amount of $TiCl_4$ to 1.0 equiv resulted in an increased yield (67%), but lower selectivity (81:19, Table 1, entry 6). All attempts to catalyze the reaction with $BF_3{\cdot}OEt_2$ as a Lewis acid failed. Aldol products were not found (Table 1, entries 7–9). Thus, the conditions of entry 2 presented the best compromise regarding the yield and selectivity. Therefore, these conditions were used for the reactions of other aromatic and aliphatic aldehydes (Table 2).

Table 2: Results of reactions of ester **1** with different aldehydes.

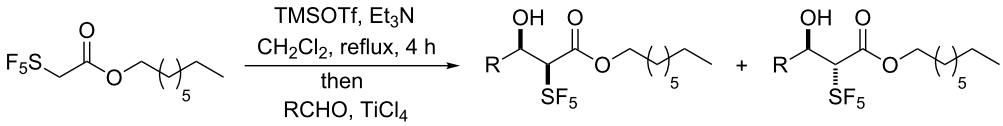

1 **2** **3**

Entry	Compounds	R	Yield **2** + **3** [%][a]	**2** : **3** ratio[b]
1	**a**	*p*-NO_2-C_6H_4	53 (40)	93:7 (99:1)
2	**b**	C_6H_5	44 (30)	86:14 (93:7)
3	**c**	*p*-F-C_6H_4	44 (37)	86:14 (91:9)
4	**d**	*p*-Cl-C_6H_4	38 (19)	81:19 (87:13)
5	**e**	*p*-Br-C_6H_4	39 (19)	83:17 (86:14)
6	**f**	*p*-SF_5-C_6H_4	42 (22)	95:5 (95:5)
7	**g**	*p*-CH_3-C_6H_4	0	–
8	**h**	*p*-CH_3O-C_6H_4	0	–
9	**i**	*p*-C_2H_5O-C_6H_4	0	–
10	**j**	*m*-NO_2-C_6H_4	61 (44)	90:10 (90:10)
11	**k**	*m*-CH_3-C_6H_4	57 (41)	73:27 (84:16)
12	**l**	*m*-CH_3O-C_6H_4	35 (26)	88:12 (99:1)
13	**m**	*o*-F-C_6H_4	69 (56)	83:17 (90:10)
14	**n**	*o*-Br-C_6H_4	0	–
15	**o**	2,6-Cl_2-C_6H_3	0	–
16	**p**	2,4-$(NO_2)_2$-C_6H_3	0	–
17	**q**	CH_3	58 (37)	87:13 (89:11)
18	**r**	*cyclo*-C_6H_{11}	0	–
19	**s**	CH_2=CH	0	–
20	**t**	CH_3-CH=CH	0	–

[a]Combined yield determined by ^{19}F NMR spectroscopy of the crude mixture, isolated yield after repeated chromatography in parentheses; [b]*syn/anti*-ratio of the crude product, ratio after chromatographic purification in parentheses determined by ^{19}F NMR spectroscopy.

Table 2 shows that benzaldehyde and five of its derivatives substituted with electron withdrawing groups in *para*-position gave the desired aldol addition products in fair yields and with diastereoselectivities between 81:19 and 95:5 in favor of the *syn*-products (Table 2, entries 1–6). In contrast, from the reactions of **1** with benzaldehydes bearing electron-donating substituents (methyl-, methoxy-, ethoxy-) no aldol addition products could be isolated (Table 2, entries 7–9), but the aldol condensation products **4g–i** were isolated in fair yields (see below). On the other hand, *meta*-substituted benzaldehydes gave mainly the *syn*-aldolates **2j–l** and small amounts of the *anti*-isomers **3j–l** regardless of the electronic nature of the aryl substituent (Table 2, entries 10–12). 2-Fluorobenzaldehyde gave the highest yield (69%) and 83:17 diastereoselectivity (Table 2, entry 13), while 2-bromo-, 2,6-dichloro- and 2,4-dinitrobenzaldehydes failed to give any aldol products (Table 2, entries 14–16). Besides the starting materials, only minor amounts of SF_5-containing side products of unknown structure were detected in the ^{19}F NMR spectra of the crude product mixtures. Among the saturated and unsaturated aliphatic aldehydes, only acetaldehyde gave the expected aldolates (58% yield, ratio 87:13, Table 2, entry 17), while cyclohexane carbaldehyde, acrolein, and crotonaldehyde did not give any aldol products (Table 2, entries 18–20).

During the aldol addition, two stereocenters were formed giving either the *syn*-**2** or the *anti*-isomers **3**. In all reactions one of the diastereomers was formed in large excess. In most cases, this isomer was isolated in an almost pure form after repeated chromatography, which explains the low isolated yields.

Unfortunately, all products are oils and could not be crystallized. Thus, in order to determine the relative stereochemistry, we analyzed the vicinal coupling constants of the protons attached to the stereocenters. In the *syn*-isomers **2** these protons are *anti* to each other, while in the *anti*-isomers **3** these protons are in a *syn*-arrangement (Figure 1). Such an arrangement was found in the crystalline state of an *anti*-aldol product we obtained as a result of a boron-mediated aldol reaction of the benzyl ester analog of compound **1** with benzaldehyde [29]. This product and a couple of its aryl-substituted analogs exhibited coupling constants of 2.4–4.0 Hz. The products **3** produced as minor compounds in the present study had coupling constants between 3.3 and 4.0 Hz, which is typical for a gauche arrangement of the coupling nuclei according to the Karplus equation. Also the other NMR data agree with those found for authentic *anti*-aldol addition products. Thus, the minor products of the silicon Mukaiyama aldol reactions are the *anti*-isomers **3**.

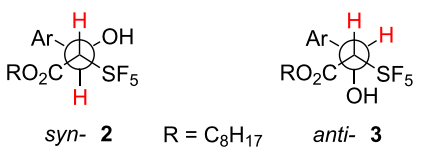

Figure 1: Newman projections of the *syn*- and the *anti*-diastereomeric aldol addition products.

On the other hand, the vicinal coupling constants of the major products were found between 8.5 Hz for the *p*-nitro derivative **2a** to about 9.4 Hz for derivatives **2b–e** with less electron-withdrawing substituents in *para*- and *meta*-positions, showing that these protons are in *anti*-position to each other as shown for compounds **2** in Figure 1. Thus, the major products are *syn*-isomers. Almost identical coupling constants and chemical shifts were also found for the aldol addition products of methyl SF_5-acetate with benzaldehyde, *p*-nitro-, and *p*-methoxybenzaldehyde as described recently by Ponomarenko and Röschenthaler et al. [34].

Considering our earlier results [31] on TMSOTf-mediated Claisen-type rearrangements of SF_5-acetates of allyl alcohols, we favor the initial formation of (*Z*)-enolates (ketene silylacetals) **5** in the aldol reactions (Scheme 2).

From this enolate, two transition states **A** and **B** can be formed for the aldol reactions. **B** should be less favored due to the steric (and may be also electronic) repulsion of the aryl and the SF_5 groups. Consequently, the *syn*-products resulting from transition state **A** are the major products of the aldol addition reactions.

As mentioned above, aldol addition products were not isolated from the reaction of **1** with electron rich *p*-methyl-, *p*-methoxy-, and *p*-ethoxybenzaldehydes. Here, aldol condensation products **4g–i** were obtained as single isomers after chromatography (Scheme 3).

In order to ascertain the configuration of our products, we performed a heteronuclear Overhauser effect (^1H,^{19}F-correlation spectrum (gHOESY), see Supporting Information File 1 for a copy of the spectrum). From this spectrum it becomes clear that the four equatorial fluorine atoms do interact with the vinylic proton. Thus, these atoms must be located in spatial proximity. This is possible only in the (*E*)-configuration of the double bond. A second proof for this configuration is the signal of the vinylic proton at δ = 7.41 ppm, which is a singlet. This was also found in the spectra of the analogous methyl esters, while for the corresponding (*Z*)-products a multiplet was identified, which is formed by $^4J_{H,F}$ coupling with the four equatorial fluorine atoms of the SF_5 group [34].

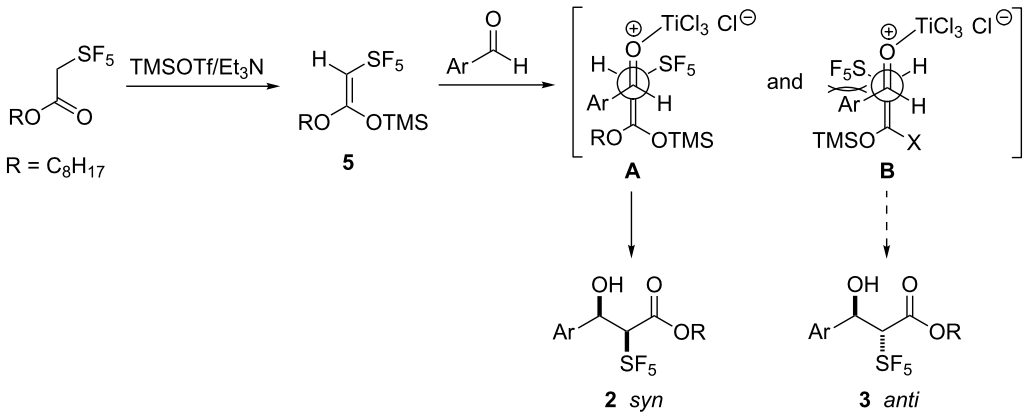

Scheme 2: Mechanism of the formation of aldol addition products.

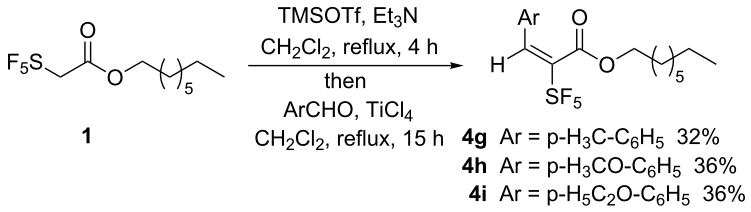

Scheme 3: Formation of (*E*)-configured aldol condensation products.

The formation of the condensation products might occur via two alternative mechanisms. Both variants depend on the initial formation of aldol addition products. These products could undergo acid catalyzed dehydration during aqueous work-up. Due to the presence of Lewis acids, which will be hydrolyzed, water would most probably eliminate via an intermediate benzyl cation, which would be stabilized by the electron-donating substituents in *p*-position. Consequently, the formation of a mixture of *E*/*Z*-isomers would be expected. Therefore, we were in favor of an alternative mechanism involving elimination subsequent to the addition step. According to Denmark's mechanism [5] for the silicon Mukaiyama aldol reaction (see above), the nucleophilic attack of the silicon enolate (in our case the ketene silylacetal) at the $TiCl_4$-activated aldehyde results in the formation of intermediate **6**. Under the influence of the electron-donating substituent, the elimination of titanium oxide dichloride ($Ti(O)Cl_2$) is favored under liberation of a chloride. For the formed oxonium ion, two conformers **A** and **B** are possible due to free rotation around the single bond neighboring the SF_5 group and the former benzylic carbon atom (Scheme 4).

Due to the possible repulsive interaction of the SF_5 group with the quinoid ring in conformer **A**, conformer **B** should be favored. Assisted by the chloride, this species is deprotonated forming the condensation product **4h** with an (*E*)-configured double bond. Obviously, this formal dehydration is possible only in the presence of electron-donating *para*-substituents in the benzaldehyde. In order to evaluate this assumption, we performed the following NMR experiment: the ester **1** was dissolved in CD_2Cl_2 and TMSOTf and Et_3N were successively added at room temperature. Then the mixture was refluxed for 4 hours, cooled down to ambient temperature, and *p*-anisaldehyde and $TiCl_4$ were added. This mixture was heated to 40 °C in a sealed tube overnight and directly investigated by ^1H and ^{19}F NMR spectroscopy showing the formation of product **4h**. Thus, a concerted mechanism seems to be responsible for the exclusive formation of the (*E*)-configured products.

Finally, we attempted to incorporate SF_5-substituted acetamides into aldol additions with the intension of applying amides in Evans-type substrate directed asymmetric C–C-bond forming reactions. Therefore, 2-(pentafluoro-λ^6-sulfanyl)acetic morpholide (**8**) was prepared by reaction of SF_5-$CH_2C(O)Cl$ (**7**) [36,37] with morpholine (Scheme 5).

According to the general protocol, the morpholide **8** was treated with TMSOTf and Et_3N and refluxed in CH_2Cl_2 for 4 hours. Then this mixture was treated with *p*-nitrobenzaldehyde and

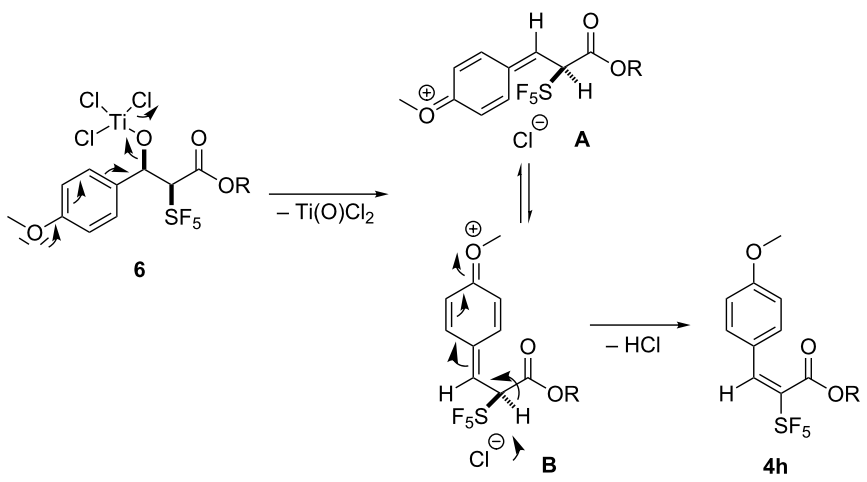

Scheme 4: Anticipated mechanism of formation of aldol condensation products.

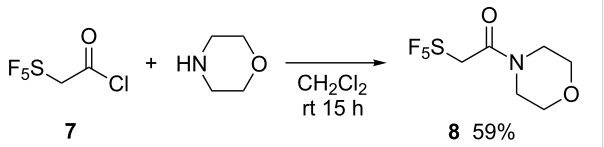

Scheme 5: Synthesis of SF_5-substituted acetmorpholide **8**.

$TiCl_4$ and refluxed in CH_2Cl_2 in a sealed tube for 15 hours. However, after aqueous work-up, the starting amide **8** and *p*-nitrobenzaldehyde were mainly recovered. A new SF_5-containing compound was detected (^{19}F NMR) in the crude product mixture, but we were unable to isolate this product. The following ^{19}F NMR data were found δ = 57.7 ppm (dm, $^2J_{F,F}$ = 147.6 Hz, 4F) and δ = 74.7 ppm (qn, $^2J_{F,F}$ = 147.6 Hz, 1F), which are different from the starting material and from the corresponding carboxylic acid [36]. Therefore, we repeated the reaction in an NMR tube and treated the morpholide **8** with TMSOTf and Et_3N in CD_2Cl_2 at room temperature. After a short period of time, the ^1H and ^{19}F NMR spectra showed the exclusive formation of the (*Z*)-ketene aminal. Signals of **8** were not found any more (Scheme 6).

The structure of this intermediate became evident from its NMR data (see Supporting Information File 1). In particular a quintet ($^3J_{H,F}$ = 7.0 Hz) at δ = 5.15 ppm in the ^1H NMR spectrum is indicative of a vinylic proton. A quintet ($^2J_{C,F}$ = 19.4 Hz) at δ = 106.1 ppm in the ^{13}C NMR spectrum can be assigned to the SF_5-substituted carbon atom, and for the second carbon atom of the double bond a quintet ($^3J_{C,F}$ = 4.6 Hz) appears at δ = 156.9 ppm. From the poorly resolved multiplets at 91.6 ppm and 74.1 ppm in the ^{19}F NMR spectrum one can reason that the SF_5 group is attached to a double bond. Its (*Z*)-configuration was deduced from a $^1H,^{19}F$-correlation spectrum (gHOESY) showing an interaction of the equatorial fluorine atoms of the SF_5 group and protons of the TMS group (see Supporting Information File 1 for a copy of the spectrum). Consequently, these two substituents must be located at the same side of the double bond.

Subsequently, the reaction mixture was treated with *p*-nitrobenzaldehyde and $TiCl_4$ and allowed to remain at room temperature for 3 days while new peaks appeared in NMR spectra. Besides signals of *p*-nitrobenzaldehyde, triethylamine hydrochloride, and several silicon compounds, the aforementioned

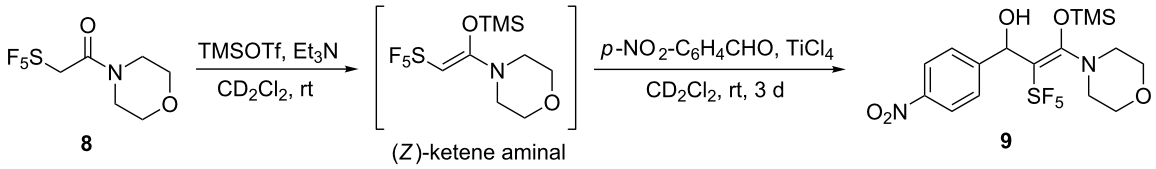

Scheme 6: Intermediate formation of the (*Z*)-ketene aminal from morpholide **8** with TMSOTf/ Et_3N and subsequent transformation to an aldol addition product **9** with *p*-nitrobenzaldehyde.

additional signals were found. From two new doublets for two protons each of a 1,4-disubstituted benzene ring (δ = 8.32 and δ = 7.96), a multiplet for one proton at δ = 4.62 ppm, a broad singlet of one proton at δ = 6.29 ppm, and the two multiplets of the morpholine ring for four protons each at δ = 3.37 ppm and δ = 3.28 ppm, one can reason the formation of an aldol addition product **9**. This assignment is supported by a multiplet for one axial fluorine atom at δ = 75.39 ppm (J = 147 Hz) and a doublet (of multiplets) for four fluorine atoms at δ = 57.6 ppm (J = 147 Hz) in the ^{19}F NMR spectra (overlapping with a doublet of another compound). Unfortunately, after work-up, we have not yet been able to isolate this product. Starting amide **8** was a major component of the crude reaction product.

In summary, the formation of the intermediate ketene aminal occurred very fast and was highly (*Z*)-selective. Unfortunately, the aldol product, which was formed after treatment with *p*-nitrobenzaldehyde, could not yet be isolated. Anyway, the preliminary results using morpholide **8** are promising. We expect that optimization of the reaction conditions and application of enantiopure Lewis acids or SF_5-substituted acetamides bearing a chiral auxiliary will result in asymmetric aldol addition reactions in the future.

Conclusion

From octyl SF_5-acetate and TMSOTf/Et_3N, a (*Z*)-enolate (ketene silylacetal) was preferentially formed as has already been shown in our earlier investigations. The C–C bond forming step proceeded preferably via a transition state with a *syn*-arrangement of the SF_5 and OTMS groups resulting in the formation of *syn*-aldol products in case of aldehydes with electron-withdrawing substituents in the *para*-position or any substituents in the *meta*-position. In contrast, aldols derived from aldehydes with electron-donating substituents in the *para*-position were not stable under the reaction conditions. A formal Lewis acid ($TiCl_4$)-assisted elimination of water produced the (*E*)-configured aldol condensation products. Preliminary results of formation of an aldol addition product from the reaction of an SF_5-substituted acetmorpholide and *p*-nitrobenzaldehyde are promising, and successful asymmetric reactions may be expected.

Supporting Information

Supporting Information File 1

General procedure, synthesis of the aldol products, spectroscopic data, and copies of ^{1}H, ^{13}C, and ^{19}F NMR spectra.
[https://www.beilstein-journals.org/bjoc/content/supplementary/1860-5397-14-25-S1.pdf]

Acknowledgements

We are grateful to the Deutsche Forschungsgemeinschaft (Ha 2145/12-1, AOBJ 588585) and the U.S. National Science Foundation (CHE-1124859) for financial support.

ORCID® iDs

Andrej V. Matsnev - https://orcid.org/0000-0003-4522-3059
Joseph S. Thrasher - https://orcid.org/0000-0003-1479-1897
Günter Haufe - https://orcid.org/0000-0001-8437-9035

References

1. Mukaiyama, T. *Org. React.* **1982,** *28,* 203–331. doi:10.1002/0471264180.or028.03
2. Mahrwald, R., Ed. *Modern Aldol Reactions;* Wiley-VCH: Weinheim, 2004; Vol. 1 and 2.
3. Saigo, K.; Osaki, M.; Mukaiyama, T. *Chem. Lett.* **1975,** *4,* 989–990. doi:10.1246/cl.1975.989
4. Reetz, M. T.; Kunisch, F.; Heitmann, P. *Tetrahedron Lett.* **1986,** *27,* 4721–4724. doi:10.1016/S0040-4039(00)85047-9
5. Denmark, S. E.; Beutner, G. L.; Wynn, T.; Eastgate, M. D. *J. Am. Chem. Soc.* **2005,** *127,* 3774–3789. doi:10.1021/ja047339w
6. Gawronski, J.; Wascinska, N.; Gajewy, J. *Chem. Rev.* **2008,** *108,* 5227–5252. doi:10.1021/cr800421c
7. Beutner, G. L.; Denmark, S. E. *Angew. Chem., Int. Ed.* **2013,** *52,* 9086–9096. doi:10.1002/anie.201302084
8. Kann, S. B. J.; Ng, K. K.-H.; Peterson, I. *Angew. Chem., Int. Ed.* **2013,** *52,* 9097–9108. doi:10.1002/anie.201303914
9. Matsuo, J.-i.; Murakami, M. *Angew. Chem., Int. Ed.* **2013,** *52,* 9109–9118. doi:10.1002/anie.201303192
10. Lefebvre, O.; Brigaud, T.; Portella, C. *J. Org. Chem.* **2001,** *66,* 1941–1946. doi:10.1021/jo001549j
11. Sato, K.; Sekiguchi, T.; Ishihara, T.; Konno, T.; Yamanaka, H. *Chem. Lett.* **2004,** *33,* 154–155. doi:10.1246/cl.2004.154
12. Itoh, Y.; Yamanaka, M.; Mikami, K. *J. Am. Chem. Soc.* **2004,** *126,* 13174–13175. doi:10.1021/ja046518a
13. Ramachandran, P. V.; Parthasarathy, G.; Gagare, P. D. *Org. Lett.* **2010,** *12,* 4474–4477. doi:10.1021/ol1016178
14. Umemoto, T.; Garrick, L. M.; Saito, N. *Beilstein J. Org. Chem.* **2012,** *8,* 461–471. doi:10.3762/bjoc.8.53
15. Kirsch, P. The pentafluorosulfanyl group and related structures. *Modern Fluoroorganic Chemistry,* 2nd ed.; Wiley-VCH: Weinheim, 2013; pp 179–191. doi:10.1002/9783527651351
16. Kosobokov, M.; Cui, B.; Balia, A.; Matsuzaki, K.; Tokunaga, E.; Saito, N.; Shibata, N. *Angew. Chem., Int. Ed.* **2016,** *55,* 10781–10785. doi:10.1002/anie.201605008
17. Das, P.; Tokunaga, E.; Shibata, N. *Tetrahedron Lett.* **2017,** *58,* 4803–4815. doi:10.1016/j.tetlet.2017.11.015
18. Altomonte, S.; Zanda, M. *J. Fluorine Chem.* **2012,** *143,* 57–93. doi:10.1016/j.jfluchem.2012.06.030
19. Savoie, P. R.; Welch, J. T. *Chem. Rev.* **2015,** *115,* 1130–1190. doi:10.1021/cr500336u
20. Kirsch, P.; Röschenthaler, G.-V. Functional Compounds Based on Hypervalent Sulfur Fluorides. In *Current Fluoroorganic Chemistry. New Synthetic Directions, Technologies, Materials, and Biological Applications;* Soloshonok, V. A.; Mikami, K.; Yamazaki, T.; Welch, J. T.; Honek, J. F., Eds.; ACS Symposium Series, Vol. 949; American Chemical Society: Washington, DC, 2007; pp 221–243. doi:10.1021/bk-2007-0949.ch013

21. Aït-Mohand, S.; Dolbier, W. R., Jr. *Org. Lett.* **2002,** *4,* 3013–3015. doi:10.1021/ol026483o
22. Desroches, J.; Gilbert, A.; Houle, C.; Paquin, J.-F. *Synthesis* **2017,** *49,* 4827–4844. doi:10.1055/s-0036-1589514
23. Ngo, S. C.; Lin, J.-H.; Savoie, P. R.; Hines, E. M.; Pugliese, K. M.; Welch, J. T. *Eur. J. Org. Chem.* **2012,** 4902–4905. doi:10.1002/ejoc.201200763
24. Dolbier, W. R., Jr.; Mitani, A.; Xu, W.; Ghiviriga, I. *Org. Lett.* **2006,** *8,* 5573–5575. doi:10.1021/ol0622662
25. Brel, V. K. *Synthesis* **2006,** 339–343. doi:10.1055/s-2005-918508
26. Duda, B.; Lentz, D. *Org. Biomol. Chem.* **2015,** *13,* 5625–5628. doi:10.1039/C5OB00610D
27. Huang, Y.; Gard, G. L.; Shreeve, J. M. *Tetrahedron Lett.* **2010,** *51,* 6951–6954. doi:10.1016/j.tetlet.2010.10.149
28. Falkowska, E.; Tognetti, V.; Joubert, L.; Jubault, P.; Bouillon, J.-P.; Pannecoucke, X. *RSC Adv.* **2015,** *5,* 6864–6868. doi:10.1039/C4RA14075C
29. Friese, F. W.; Dreier, A.-L.; Matsnev, A. V.; Daniliuc, C. G.; Thrasher, J. S.; Haufe, G. *Org. Lett.* **2016,** *18,* 1012–1015. doi:10.1021/acs.orglett.6b00136
30. Joilton, A.; Plancher, J.-M.; Carreira, E. M. *Angew. Chem., Int. Ed.* **2016,** *55,* 2113–2117. doi:10.1002/anie.201510380
31. Dreier, A.-L.; Matsnev, A. V.; Thrasher, J. S.; Haufe, G. *J. Fluorine Chem.* **2014,** *167,* 84–90. doi:10.1016/j.jfluchem.2014.05.006
32. Dreier, A.-L.; Beutel, B.; Mück-Lichtenfeld, C.; Matsnev, A. V.; Thrasher, J. S.; Haufe, G. *J. Org. Chem.* **2017,** *82,* 1638–1648. doi:10.1021/acs.joc.6b02805
33. Dreier, A.-L. Darstellung von α-(Pentafluorsulfanyl)-substituierten Carbonylverbindungen mittels Ireland-Claisen-Umlagerungen sowie Mukaiyama-Aldolreaktionen. Ph.D. Thesis, University of Münster, Münster, Germany, 2015.
34. Ponomarenko, M. V.; Grabowsky, S.; Pal, R.; Röschenthaler, G.-V.; Fokin, A. A. *J. Org. Chem.* **2016,** *81,* 6783–6791. doi:10.1021/acs.joc.6b00946
35. Shimada, T.; Yoshioka, M.; Konno, T.; Ishihara, T. *Org. Lett.* **2006,** *8,* 1129–1131. doi:10.1021/ol0531435
36. Kleemann, G.; Seppelt, K. *Chem. Ber.* **1979,** *112,* 1140–1146. doi:10.1002/cber.19791120409
37. Martinez, H.; Zheng, Z.; Dolbier, W. R., Jr. *J. Fluorine Chem.* **2012,** *143,* 112–122. doi:10.1016/j.jfluchem.2012.03.010

License and Terms

BEILSTEIN JOURNAL OF ORGANIC CHEMISTRY

Synthesis and stability of strongly acidic benzamide derivatives

Frederik Diness*[1,2], Niels J. Bjerrum[3] and Mikael Begtrup[1]

Full Research Paper

Open Access

Address:
[1]Department of Drug Design and Pharmacology, University of Copenhagen, Universitetsparken 2, DK-2100 Copenhagen, Denmark, [2]Present address: Department of Chemistry, University of Copenhagen, Universitetsparken 5, DK-2100 Copenhagen, Denmark and [3]Department of Energy Conversion and Storage, Technical University of Denmark, Kemitorvet, Building 207, room 042, DK-2800 Kgs. Lyngby, Denmark

Email:
Frederik Diness* - fdi@chem.ku.dk

* Corresponding author

Keywords:
benzoic acid; cross-coupling; hydrolysis; S_NAr; trifluoromethanesulfonamide

Beilstein J. Org. Chem. **2018,** *14,* 523–530.
doi:10.3762/bjoc.14.38

Received: 17 December 2017
Accepted: 13 February 2018
Published: 27 February 2018

This article is part of the Thematic Series "Organo-fluorine chemistry IV".

Guest Editor: D. O'Hagan

Abstract

Reactivity studies of strong organic acids based on the replacement of one or both of the oxygens in benzoic acids with the trifluoromethanesulfonamide group are reported. Novel derivatives of these types of acids were synthesized in good yields. The generated *N*-triflylbenzamides were further functionalized through cross-coupling and nucleophilic aromatic substitution reactions. All compounds were stable in dilute aqueous solutions. Studies of stability under acidic and basic conditions are also reported.

Introduction

Very strong organic acids are interesting as catalysts for chemical reactions [1,2] and for facilitation of proton conduction [3]. In order to enable their incorporation into functional materials (e.g., polymers), these acids need additional functionality in the form of a reactive group, and the chemistry applied for functionalization must be compatible with their strong acidic nature. Many types of strong organic acids such as triflic acid (**7**) or trifluoroacetic acid (**3**) are not readily modified, and changing substituents on these acids will heavily impact their pK_a value (Figure 1). In contrast, halogenated benzoic acid derivatives are easily functionalized through cross-coupling [4,5] or nucleophilic aromatic substitution reactions (S_NAr) [6,7]. Benzoic acids (e.g., **2**) are relatively weak acids, even with highly electron-withdrawing substituents on the aromatic core [8]. Very strong benzoic acid derivatives (e.g., **4** and **6**) have been synthesized by replacing one or both of the oxygens of the carboxylate group with the trifluoromethanesulfonamide (**1**) group [9-11].

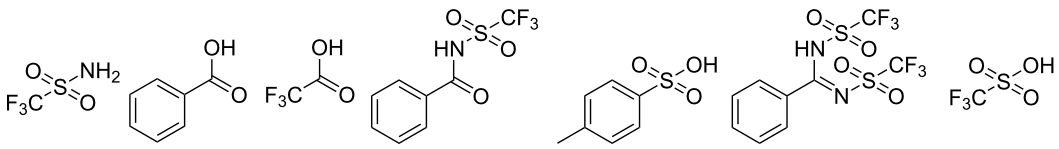

	1	2	3	4	5	6	7
pK_a in acetonitrile :	nr	21.5	12.7	11.1	8.6	6.2	0.7
pK_a in water :	5.8	4.3	0.2	nr	-2.8	nr	–14.7

Figure 1: Acid strength (p*K*a) of various organic acids in acetonitrile or water (nr = not reported) [12-14].

Interestingly, these types of compounds have attracted little attention and have not thoroughly been explored with regards to their applications. Few publications report the application of *N*-triflylbenzamides as benzoic acid bioisosteres in receptor antagonists and enzyme inhibitors (Figure 2) [15-18]. The reported derivatives all displayed activity, but only with similar or reduced potency compared to the corresponding benzoic acid derivatives. Application of deprotonated *N*-triflylbenzamide derivatives as counter anions in supramolecular crown ether compounds for metal ion extraction has also been reported by one group (Figure 2) [19-25]. All the *N*-triflylbenzamide constructs generated for this purpose have proved superior to the corresponding benzoate derivatives with regards to metal ion extraction capability.

The *N*-triflylbenzamides are simple to generate by the reaction between trifluoromethanesulfonamide (**1**) and an activated benzoyl derivative such as benzoyl chlorides (e.g., **8a**, Scheme 1) [9,15]. The reactions are generally high yielding and the products are simple to isolate in their protonated form by recrystallization. The generation of *N*-triflylbenzamides by direct reaction of various triflyl derivatives with benzamides or benzoic acids has been less systematically explored. Most compounds synthesized by these approaches are N-alkylated or N-arylated and have been formed unintentionally as byproducts [26-33]. Finally, two examples of syntheses via palladium-catalyzed carbonylation of trifluoromethanesulfonamide (**1**) have been reported [34,35]. The *N*-triflylbenzamides have only been explored as substrates in a few reactions. A recent report describes using *N*-triflylbenzamide as a directing group in a ruthenium-catalyzed C–H activation reaction [36]. Most other reported transformations pass via the imidoyl chloride intermediates (equivalent to **10**) to the amidine derivatives, which have been used in rearrangement reaction studies [9,37-39]. By these means also *N*,*N*'-bis(triflyl)benzimidamides (also termed benzamidines) have been generated, but only one report describes their syntheses [10]. The *N*-triflylbenzamides are stronger acids than any of the carboxylic acids, including trifluoroacetic acid (**3**). The *N*,*N*'-bis(triflyl)benzimidamides are very strong organic acids, much stronger than *p*-toluenesulfonic acid (**5**) which is commonly used as a soluble organic acid catalyst in chemical reactions. Remarkably, neither the *N*-triflylbenzamides nor the *N*,*N*'-bis(triflyl)benzimidamides have been studied as Brønsted acid catalysts. Their chemical stability including compatibility with conditions applied to common chemical transformations has not been described. With the prospect of using these strong benzoic acid derivatives for enhancing proton conductivity in proton-exchange membrane (PEM) fuel cells [3,40] we have examined their compatibility with chemical transformations as well as their stability towards hydrolytic conditions.

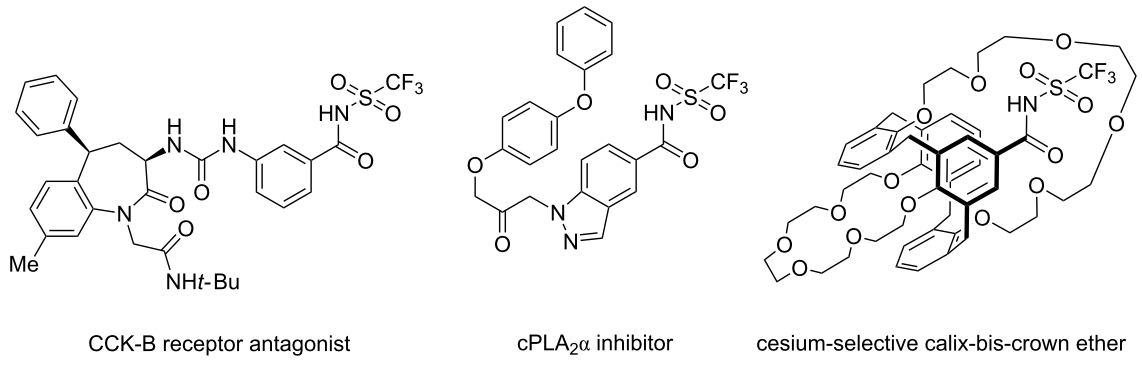

CCK-B receptor antagonist | cPLA$_2\alpha$ inhibitor | cesium-selective calix-bis-crown ether

Figure 2: Examples of functional molecules containing an *N*-triflylbenzamide.

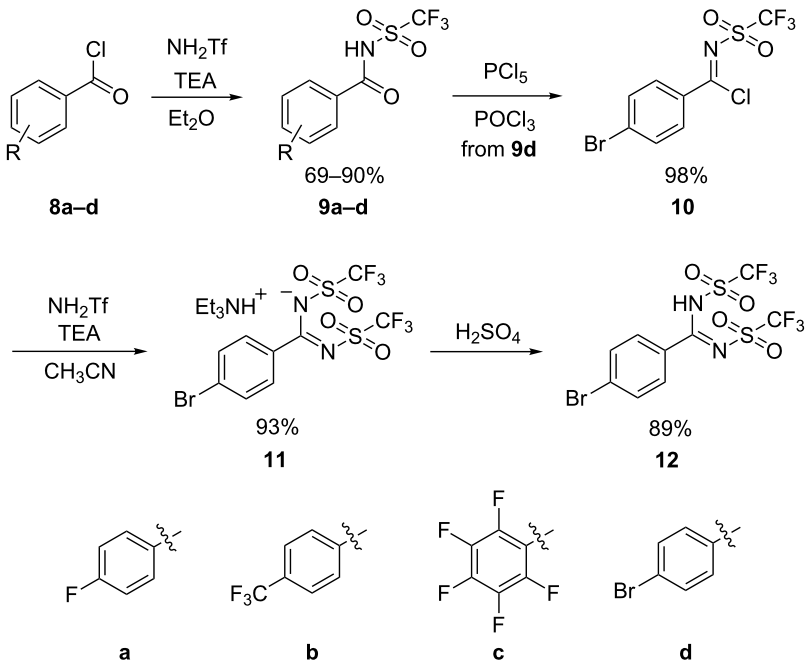

Scheme 1: Synthesis of the strongly acidic benzamide derivatives.

Results and Discussion

In these studies, four substituted *N*-triflylbenzamides **9a**–**d** were synthesized by the reaction of the corresponding benzoyl chloride with trifluoromethanesulfonamide (**1,** Scheme 1). The known 4-fluoro-*N*-triflylbenzamide (**9a**) was synthesized according to the previously reported method [9] and with few adjustments this methodology was also applied for the generation of three new derivatives **9b**–**d**, which were obtained in good yields. The 4-bromo derivative **9d** was further converted into the *N*,*N*'-bis(triflyl)benzimidamide **12** by formation of the corresponding imidoyl chlorides **10** with PCl_5 in $POCl_3$, followed by the additional reaction with trifluoromethanesulfonamide (**1**) and protonation by sulfuric acid (Scheme 1) [10].

In recent years, we have reported high yielding catalyst-free N-arylation by S_NAr reaction of mono- or perfluorobenzene derivatives [41-43]. Hence, it was proposed that the 4-fluoro and the pentafluorobenzamide derivatives **9a** and **9c** could be functionalized through S_NAr reactions. Thus, compounds **9a** and **9c** were reacted with benzimidazole under previously developed conditions (Scheme 2) [41,42]. The benzimidazole was chosen as model nucleophile for polybenzimidazole, a polymer commonly applied as a membrane in PEM fuel cells [40]. These reactions provided the 4-benzimidazolyl derivatives **13** and **14** in good yields and the *N*-triflylbenzamide group proved to be stable under these reaction conditions. Gratifyingly it was possible to perform selective mono-substitution of the pentafluoro derivative regioselectively in the 4-position, affording only compound **14**. This is in line with previous observations of S_NAr reactions on pentafluorobenzene derivatives [42]. Due to the zwitterionic nature of the products, reversed-phase chromatography was chosen to simplify the purifications.

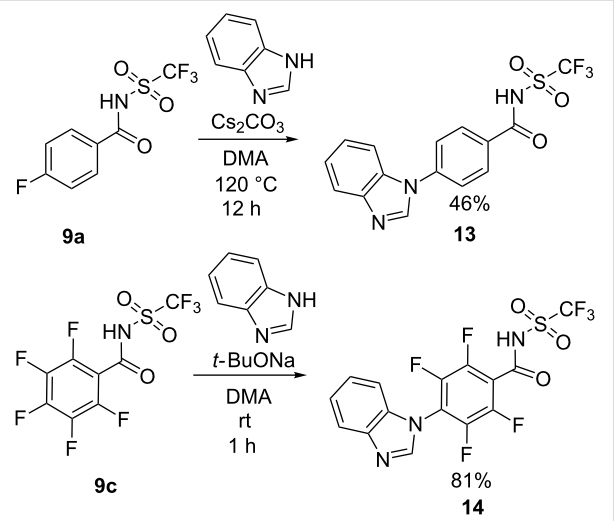

Scheme 2: S_NAr reactions of fluoro-substituted benzamide derivatives.

The *N*-triflylbenzamide group also proved stable to cross-coupling reaction conditions, as exemplified by a palladium-catalyzed Suzuki–Miyaura reaction of the 4-bromo-substituted derivative **9d** (Scheme 3). The corresponding *N*,*N*'-bis(triflyl)benzimidamide derivative **12** was also tested under

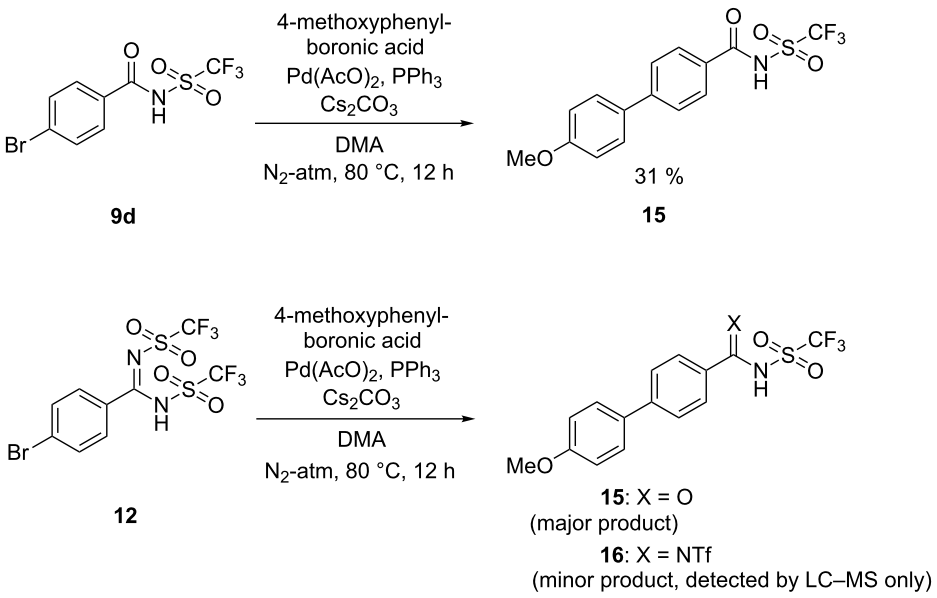

Scheme 3: Cross-coupling reactions of *N*-triflylbenzoic acid derivatives.

identical conditions. The reaction proceeded with high conversion, but surprisingly the major product of this reaction was also the *N*-triflylbenzamide **15**. Additional experiments revealed that the *N*,*N*'-bis(triflyl)benzimidamide group was unstable in aqueous basic conditions.

This led to concerns about the stability of the products in general. In addition, during characterization by NMR it was also noted that some samples of the *N*-triflylbenzamide products contained small amounts of the parent benzoic acid, despite prior purification by recrystallization. Further studies revealed that the content of benzoic acid increased over time in the solutions and the conversion rate was concentration dependent, the reason being simple hydrolysis auto-catalyzed by the acids themselves. This phenomenon was also observed for *N*,*N*'-bis(triflyl)benzimidamide **12** but at slower rate. Hence, an elaborated study of the products' stability towards acid or base promoted hydrolysis was undertaken (Scheme 4). Dilute aqueous solutions (0.5 mg/mL) of the *N*-triflylbenzamides displayed no sign of degeneration even after 24 h. The compounds also remained fully intact in 0.5 M aqueous NaOH. In solutions of 0.5 M aqueous HCl the compounds very slowly degraded over weeks. The *N*,*N*'-bis(triflyl)benzimidamide **12** was also stable in dilute aqueous solutions and was even more stable in 0.5 M aqueous HCl than the corresponding *N*-triflylbenzamide **9d**. Hence, in the acid-catalyzed hydrolysis reaction of **12** the 4-bromo-*N*-triflylbenzamide (**9d**) was only detected as a trace as **9d** converted faster to 4-bromobenzoic acid than compound **12** converted to **9d**. In contrast, 0.5 M aqueous NaOH rapidly hydrolyzed the *N*,*N*'-bis(triflyl)benzimidamide **12** to yield the base-stable *N*-triflylbenzamide **9d**.

Neither the mono-substituted *N*-triflylbenzamides **9a** and **9b** nor the 4-bromo-*N*,*N*'-bis(triflyl)benzimidamide (**12**) were stable in heated methanolic phosphoric acid, which is commonly used for operating PEM fuel cells (Figure 3) [44]. However, most surprisingly, the pentafluoro *N*-triflylbenzamide (**9c**) was found to be much more stable under these conditions, which is promising for future applications in proton conducting materials.

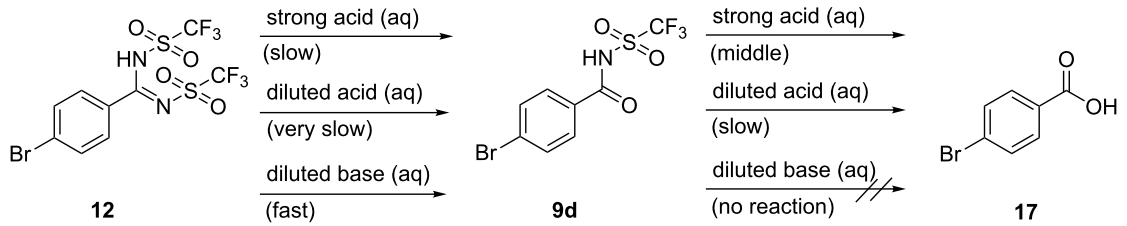

Scheme 4: Hydrolysis rates of the 4-bromobenzoic acid derivatives.

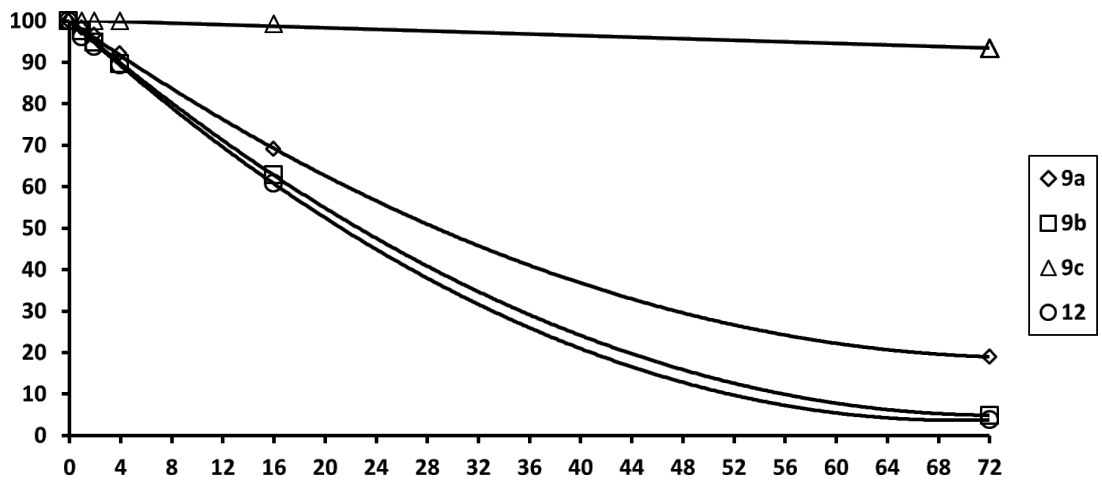

Figure 3: Content (percent) of super acids (0.5 mg/mL) over time (hours) in H_3PO_4/H_2O/MeOH 17:3:20 at 50 °C.

Conclusion

In summary, it has been demonstrated that novel mono- or bis-trifluoromethanesulfonamide derivatives of benzoic acids bearing a reactive group (bromine or fluorine) may be generated in good yields and further functionalized through nucleophilic aromatic substitution or cross-coupling reactions. It was found that the products were stable in dilute aqueous solutions, but they slowly hydrolyzed in concentrated solutions or in the presence of other strong acids. The *N*-triflylbenzamides **9a**–**d** were stable in basic aqueous solutions whereas the tested bromo-*N*,*N*'-bis(triflyl)benzimidamide **12** rapidly hydrolyzed to the corresponding bromo-*N*-triflylbenzamide **9d**. Under conditions simulating ambient PEM fuel cells operation the 4-substituted benzamide derivatives **9a**,**b**,**d** and **12** were about 50% degraded within 24 h, whereas the pentafluoro *N*-triflylbenzamide (**9c**) under the same conditions was less than 5% degraded.

Experimental

General aspects

All purchased chemicals were used without further purification. All solvents were HPLC grade. NMR data were recorded on a Bruker 500 MHz spectrometer at 298 K with methanol-d_4, DMSO-d_6 or hexafluorobenzene as internal standard. High-resolution mass spectrometry (HRMS) was performed on a Bruker MALDI–TOF spectrometer.

General procedure

Benzoyl chloride (10.0 mmol) in Et_2O (10 mL) was added dropwise to a solution of trifluoromethanesulfonamide (1.5 g, 10.0 mmol) and triethylamine (3.5 mL, 25 mmol) in Et_2O (30 mL) at 0 °C over 10 min. The mixture was stirred for 30 min and then heated to reflux for 2 h. The reaction was filtered and the solvent was removed from the filtrate. The crude product was mixed with 50% H_2SO_4 (aq, 50 mL) and the mixture stirred for 30 min. The precipitate was isolated and dried overnight. The product was purified by recrystallization from toluene.

4-Fluoro-*N*-((trifluoromethyl)sulfonyl)benzamide (9a) [9]: Synthesized by general procedure. The product was obtained as small clear crystalline flakes (1.88 g, 69%). mp 152–154 °C; ^{1}H NMR (500 MHz, methanol-d_4) δ 7.99 (dd, J = 9.0, 5.2 Hz, 2H), 7.29 (t, J = 8.8 Hz, 2H); ^{13}C NMR (126 MHz, methanol-d_4) δ 167.6 (d, J = 254.3 Hz), 166.0, 132.8 (d, J = 9.6 Hz), 129.1 (d, J = 3.1 Hz), 121.0 (q, J = 321.5 Hz), 117.1 (d, J = 22.7 Hz); ^{19}F NMR (470 MHz, methanol-d_4) δ −76.93 (s, 3F), −105.75 (s, 1F); HRMS (TOF) m/z: $[M - H]^-$ calcd for $C_8H_4F_4NO_3S^-$, 269.9854; found, 269.9888.

4-Trifluoromethyl-*N*-((trifluoromethyl)sulfonyl)benzamide (9b): Synthesized by general procedure. The product was obtained as white powder (2.83 g, 88%). mp 174–179 °C; ^{1}H NMR (500 MHz, methanol-d_4) δ 8.09 (d, J = 8.0 Hz, 1H), 7.86 (d, J = 8.1 Hz, 1H); ^{13}C NMR (126 MHz, methanol-d_4) δ 166.3, 136.5, 136.0 (q, J = 32.6 Hz), 130.6, 127.0 (q, J = 4.0 Hz), 125.0 (q, J = 271.9 Hz), 121.0 (q, J = 321.5 Hz); ^{19}F NMR (470 MHz, methanol-d_4) δ −64.31 (s, 3F), −77.06 (s, 3F); HRMS (TOF) m/z: $[M - H]^-$ calcd for $C_9H_4F_6NO_3S^-$, 319.9822; found, 319.9869.

Pentafluoro-*N*-((trifluoromethyl)sulfonyl)benzamide (9c): Synthesized by general procedure. The product was obtained as clear needle-shaped crystal (2.40 g, 70%). mp 129–131°C; ^{13}C NMR (126 MHz, methanol-d_4) δ 158.6, 145.4 (dm, J = 257.0 Hz), 144.5 (dm, J = 256.8 Hz), 139.1 (dm, J = 250.0

Hz), 121.0 (q, J = 321.4 Hz), 111.9 (t, J = 17.6 Hz); ^{19}F NMR (470 MHz, methanol-d_4) δ −78.15 (s, 3F), −142.78 (d, J = 17.9 Hz, 2F), −152.25 (t, J = 19.2 Hz, 1F), −162.65 (t, J = 18.3 Hz, 2F); HRMS (TOF) m/z: [M − H]$^-$ calcd for $C_8F_8NO_3S^-$, 341.9477; found, 341.9520.

4-Bromo-*N*-((trifluoromethyl)sulfonyl)benzamide (9d): Synthesized by general procedure. The product was obtained as white powder (2.98 g, 90%). mp 156–158 °C; ^{1}H NMR (500 MHz, methanol-d_4) δ 7.83 (d, J = 8.8 Hz, 2H), 7.73 (d, J = 8.7 Hz, 2H); ^{13}C NMR (126 MHz, methanol-d_4) δ 166.5, 133.3, 131.9, 131. 6, 129.9, 121.0 (q, J = 321.5 Hz); ^{19}F NMR (470 MHz, MeOD) δ −77.00 (s); HRMS (TOF) m/z: [M − H]$^-$ calcd for $C_8H_4{}^{79}BrF_3NO_3S^-$, 329.9053; found, 329.9095.

Triethylamine salt of 4-bromo-*N*,*N*'-bis((trifluoromethyl)-sulfonyl)benzimidamide (11): 4-Bromo-*N*-((trifluoromethyl)-sulfonyl)benzamide (**9d**, 1.68 g, 5.0 mmol) was mixed with $POCl_3$ (3 mL) and PCl_5 (1.11 g). The reaction mixture was stirred at rt for 2 h and then at 50 °C for 30 min. The solvent was removed and the imidoyl chloride was recrystallized from heptane (1.71 g, 98%). The imidoyl chloride (1.06 g) was dissolved in dry acetonitrile (4 mL) and the solution was added dropwise to a mixture of trifluoromethanesulfonamide (450 mg) and triethylamine (0.85 mL) in dry acetonitrile (8 mL) at 0 °C. The mixture was stirred at 0 °C for 30 min and then at rt for 5 h. The solvent was removed in vacuo and the residue was mixed with CH_2Cl_2 (30 mL) and 10% HCl (aq, 50 mL). The organic phase was separated and the water phase was extracted with CH_2Cl_2 (30 mL). The combined organic phase was washed with saturated $NaHCO_3$ (aq) and dried with $MgSO_4$. The solvent was removed in vacuo and the product was isolated as white powder (1.58 g, 93%). ^{1}H NMR (500 MHz, methanol-d_4) δ 7.73 (d, J = 8.7 Hz, 2H), 7.60 (d, J = 8.6 Hz, 2H), 3.20 (q, J = 7.3 Hz, 6H), 1.30 (t, J = 7.3 Hz, 9H); ^{13}C NMR (126 MHz, methanol-d_4) δ 170.0, 137.8, 132.3, 132.0, 127.6, 121.1 (q, J = 319.2 Hz), 48.0, 9.3; ^{19}F NMR (470 MHz, MeOD) δ −80.67 (s); HRMS (TOF) m/z: [M − H]$^-$ calcd for $C_9H_4{}^{79}BrF_6N_2O_4S_2^-$, 460.8706; found, 460.8769.

4-Bromo-*N*,*N*'-bis((trifluoromethyl)sulfonyl)benzimidamide (12): The trimethylamine salt of 4-bromo-*N*,*N*'-bis((trifluoromethyl)sulfonyl)benzimidamide (**11,** 0.50 g, 0.89 mmol) was mixed with H_2SO_4 (96%, 1.0 mL). The mixture was shaken for 30 min and extracted with CH_2Cl_2 (5 × 6 mL). The extract was dried with $MgSO_4$ and the solvent removed in vacuo. The crude product was recrystallized from toluene and heptane to yield **12** as a white crystalline powder (367 mg, 0.79 mmol, 89%). ^{1}H NMR (500 MHz, methanol-d_4) δ 7.72 (d, J = 8.7 Hz, 2H), 7.59 (d, J = 8.6 Hz, 2H); ^{13}C NMR (126 MHz, methanol-d_4) δ 170.1, 137.6, 132.23, 131.9, 127.6, 121.02 (q, J = 319.3 Hz); ^{19}F NMR (470 MHz, MeOD) δ −80.60 (s); HRMS (TOF) m/z: [M − H]$^-$ calcd for $C_9H_4{}^{79}BrF_6N_2O_4S_2^-$, 460.8706; found. 460.8766.

4-(1*H*-Benzo[*d*]imidazol-1-yl)-*N*-((trifluoromethyl)sulfonyl)benzamide (13): Cesium carbonate (163 mg, 5 equiv) was added to a glass vial containing benzimidazole (17.7 mg, 1.5 equiv) and 4-fluoro-*N*-((trifluoromethyl)sulfonyl)benzamide (**9a**, 27.1 mg, 0.1 mmol) in dry dimethylacetamide (1.0 mL). The reaction was heated to 120 °C for 12 h. The reaction was quenched with 1.0 M HCl (aq, 100 µL) and the solvent removed in vacuo. The crude product was dissolved in acetonitrile/water 1:1 and filtered through a Teflon syringe filter. The solution was transferred to a C18 gel column and purified by vacuum liquid chromatography (VLC, 0 to 90% CH_3CN in 0.01 M HCl). After lyophilization the product was obtained as a white powder (17 mg, 46%). ^{1}H NMR (500 MHz, DMSO-d_6) δ 9.64 (s, 1H), 8.20 (d, J = 8.5 Hz, 2H), 7.99–7.90 (m, 1H), 7.81 (d, J = 8.5 Hz, 3H), 7.64–7.53 (m, 2H), 4.53 (s, 2H); ^{13}C NMR (126 MHz, DMSO-d_6) δ 168.5, 142.3, 138.4, 136.0, 134.8, 131.4, 130.3, 126.0, 125.6, 124.0, 120.3 (q, J = 324.8 Hz), 116.6, 112.6; ^{19}F NMR (470 MHz, DMSO-d_6) δ −79.75 (s); HRMS (TOF) m/z: [M − H]$^-$ calcd for $C_{15}H_9F_3N_3O_3S^-$, 368.0322; found, 368.0367.

4-(1*H*-Benzo[*d*]imidazol-1-yl)-2,3,5,6-tetrafluoro-*N*-((trifluoromethyl)sulfonyl)benzamide (14): Sodium *tert*-butoxide (21 mg, 2.2 equiv) was added to a glass vial containing benzimidazole (11.8 mg, 0.1 mmol) in dry dimethylacetamide (1.0 mL). The mixture was stirred at rt for 1 min. The mixture was cooled to 0 °C and added to a solution of **9c** (37.7 mg, 0.11 mmol) in dry dimethylacetamide (1.0 mL) under stirring at 0 °C. The reaction was allowed to reach rt and stirred for 1 h. The reaction was quenched with 1.0 M HCl (aq, 20 µL) and the solvent removed in vacuo. The crude product was dissolved in acetonitrile/water 1:1 and filtered through a Teflon syringe filter. The solution was transferred to a C18 gel column and purified by vacuum liquid chromatography (VLC, 0 to 90% CH_3CN in 0.01 M HCl). After lyophilization the product was obtained as a white powder (30 mg, 81%). ^{1}H NMR (500 MHz, DMSO-d_6) δ 8.70 (s, 1H), 7.83 (dt, J = 7.3, 3.6 Hz, 1H), 7.66–7.57 (m, 1H), 7.47–7.34 (m, 2H); ^{13}C NMR (126 MHz, DMSO) δ 161.34, 143.9, 143.6 (dddd, J = 246.1, 13.0, 8.4, 4.1 Hz), 142.2 (ddm, J = 252.7, 16.4 Hz), 141.3, 137.6 (dm, J = 254.1 Hz), 133.1, 124.5, 123.6, 121.4 (t, J = 21.9 Hz), 120.0 (q, J = 323.7 Hz), 119. 5, 114.1 (t, J = 14.6 Hz), 111.3; ^{19}F NMR (470 MHz, DMSO-d_6) δ −80.53 (s), −145.56 (dd, J = 25.2, 12.3 Hz), −148.81 (dd, J = 24.1, 11.3 Hz); HRMS (TOF) m/z: [M − H]$^-$ calcd for $C_{15}H_5F_7N_3O_3S^-$, 439.9945; found, 434.0006.

4'-Methoxy-*N*-((trifluoromethyl)sulfonyl)-[1,1'-biphenyl]-4-carboxamide (15): Palladium(II) acetate (6 mg, 27 μmol), triphenylphosphine (20 mg, 76 μmol) and H_2O (0.5 μL, 28 μmol) were mixed in degassed dimethylacetamide (1.0 mL). The catalyst was preformed by heating the mixture in a closed screw cap vial to 100 °C for 1 min (color changed from yellow to deep red). A part of the catalyst mixture (0.2 mL) was added to a microwave glass vial containing a degassed mixture of **9d** (33.1 mg, 0.1 mmol), 4-methoxyphenylboronic acid (22.8 mg, 0.15 mmol, 1.5 equiv) and cesium carbonate (100 mg, 3 equiv) in dimethylacetamide (0.8 mL). The vial was closed with a teflon cap and heated to 80 °C for 12 h under stirring. The reaction was quenched with 1.0 M HCl (aq, 100 μL) and the solvent removed in vacuo. The crude product was dissolved in acetonitrile/water 1:1 and filtered through a Teflon syringe filter. The solution was transferred to a C18 gel column and purified by vacuum liquid chromatography (VLC, 0 to 90% CH_3CN in 0.01 M HCl). After lyophilization the product was obtained as a white powder (11 mg, 31%). ^{1}H NMR (500 MHz, DMSO-d_6) δ 7.96 (d, J = 8.3 Hz, 2H), 7.69–7.59 (m, 4H), 7.03 (d, J = 8.8 Hz, 2H), 3.80 (s, 3H); ^{13}C NMR (126 MHz, DMSO-d_6) δ 169.5, 159.2, 142.0, 135.7, 131.8, 129.2, 127.9, 125.4, 120.4 (q, J = 325.3 Hz). 114.4, 55.2; ^{19}F NMR (470 MHz, DMSO-d_6) δ −79.57 (s); HRMS (TOF) m/z: $[M - H]^-$ calcd for $C_{15}H_5F_7N_3O_3S^-$, 358.0366; found, 358.0408.

Supporting Information

Supporting Information File 1

NMR spectra of synthesized compounds.
[https://www.beilstein-journals.org/bjoc/content/supplementary/1860-5397-14-38-S1.pdf]

Acknowledgements

The Danish Strategic Research Foundation of Energy and Environment is acknowledged for supporting this research (Grant 2104-05-0026). Lundbeck A/S is acknowledged for supporting research within nucleophilic aromatic substitution reactions.

References

1. Akiyama, T. *Chem. Rev.* **2007,** *107,* 5744–5758. doi:10.1021/cr068374j
2. Akiyama, T.; Mori, K. *Chem. Rev.* **2015,** *115,* 9277–9306. doi:10.1021/acs.chemrev.5b00041
3. Peighambardoust, S. J.; Rowshanzamir, S.; Amjadi, M. *Int. J. Hydrogen Energy* **2010,** *35,* 9349–9384. doi:10.1016/j.ijhydene.2010.05.017
4. Miyaura, N.; Suzuki, A. *Chem. Rev.* **1995,** *95,* 2457–2483. doi:10.1021/cr00039a007
5. Suzuki, A. *J. Organomet. Chem.* **1999,** *576,* 147–168. doi:10.1016/S0022-328X(98)01055-9
6. Dehe, D.; Munstein, I.; Reis, A.; Thiel, W. R. *J. Org. Chem.* **2011,** *76,* 1151–1154. doi:10.1021/jo102063s
7. Keipour, H.; Hosseini, A.; Afsari, A.; Oladee, R.; Khalilzadeh, M. A.; Ollevier, T. *Can. J. Chem.* **2016,** *94,* 95–104. doi:10.1139/cjc-2015-0300
8. Hansch, C.; Leo, A.; Taft, R. W. *Chem. Rev.* **1991,** *91,* 165–195. doi:10.1021/cr00002a004
9. Yagupolskii, L. M.; Shelyazhenko, S. V.; Maletina, I. I.; Petrik, V. N.; Rusanov, E. B.; Chernega, A. N. *Eur. J. Org. Chem.* **2001,** 1225–1233. doi:10.1002/1099-0690(200104)2001:7<1225::AID-EJOC1225>3.0.CO;2-6
10. Yagupolskii, L. M.; Petrik, V. N.; Kondratenko, N. V.; Sooväli, L.; Kaljurand, I.; Leito, I.; Koppel, I. A. *J. Chem. Soc., Perkin Trans. 2* **2002,** 1950–1955. doi:10.1039/B204172C
11. Koppel, I. A.; Burk, P.; Koppel, I.; Leito, I. *J. Am. Chem. Soc.* **2002,** *124,* 5594–5600. doi:10.1021/ja0255958
12. Leito, I.; Kaljurand, I.; Koppel, I. A.; Yagupolskii, L. M.; Vlasov, V. M. *J. Org. Chem.* **1998,** *63,* 7868–7874. doi:10.1021/jo981124l
13. Raamat, E.; Kaupmees, K.; Ovsjannikov, G.; Trummal, A.; Kütt, A.; Saame, J.; Koppel, I.; Kaljurand, I.; Lipping, L.; Rodima, T.; Pihl, V.; Koppel, I. A.; Leito, I. *J. Phys. Org. Chem.* **2013,** *26,* 162–170. doi:10.1002/poc.2946
14. Trummal, A.; Lipping, L.; Kaljurand, I.; Koppel, I. A.; Leito, I. *J. Phys. Chem. A* **2016,** *120,* 3663–3669. doi:10.1021/acs.jpca.6b02253
15. Lowe, J. A., III; Drozda, S. E.; McLean, S.; Bryce, D. K.; Crawford, R. T.; Zorn, S.; Morrone, J.; Appleton, T. A.; Lombardo, F. *Bioorg. Med. Chem. Lett.* **1995,** *5,* 1933–1936. doi:10.1016/0960-894X(95)00327-P
16. Hamada, Y.; Abdel-Rahman, H.; Yamani, A.; Nguyen, J.-T.; Stochaj, M.; Hidaka, K.; Kimura, T.; Hayashi, Y.; Saito, K.; Ishiurac, S.; Kiso, Y. *Bioorg. Med. Chem. Lett.* **2008,** *18,* 1649–1653. doi:10.1016/j.bmcl.2008.01.058
17. Cervi, G.; Magnaghi, P.; Asa, D.; Avanzi, N.; Badari, A.; Borghi, D.; Caruso, M.; Cirla, A.; Cozzi, L.; Felder, E.; Galvani, A.; Gasparri, F.; Lomolino, A.; Magnuson, S.; Malgesini, B.; Motto, I.; Pasi, M.; Rizzi, S.; Salom, B.; Sorrentino, G.; Troiani, S.; Valsasina, B.; O'Brien, T.; Isacchi, A.; Donati, D.; D'Alessio, R. *J. Med. Chem.* **2014,** *57,* 10443–10454. doi:10.1021/jm501313x
18. Althaus, J.; Hake, T.; Hanekamp, W.; Lehr, M. *J. Enzyme Inhib. Med. Chem.* **2016,** *31,* 131–140. doi:10.1080/14756366.2016.1178246
19. Talanov, V. S.; Talanova, G. G.; Bartsch, R. A. *Tetrahedron Lett.* **2000,** *41,* 8221–8224. doi:10.1016/S0040-4039(00)01457-X
20. Talanov, V. S.; Talanova, G. G.; Gorbunova, M. G.; Bartsch, R. A. *J. Chem. Soc., Perkin Trans. 2* **2002,** 209–215. doi:10.1039/b109638a
21. Talanov, V. S.; Talanova, G. G.; Gorbunova, M. G.; Bartsch, R. A. *Tetrahedron Lett.* **2002,** *43,* 1629–1631. doi:10.1016/S0040-4039(02)00096-5
22. Surowiec, M.; Custelcean, R.; Surowiec, K.; Bartsch, R. A. *Tetrahedron* **2009,** *65,* 7777–7783. doi:10.1016/j.tet.2009.07.006
23. Yang, Y.; Arora, G.; Fernandez, F. A.; Crawford, J. D.; Surowiec, K.; Lee, E. K.; Bartsch, R. A. *Tetrahedron* **2011,** *67,* 1389–1397. doi:10.1016/j.tet.2010.12.006
24. Boston, A. L.; Lee, E. K.; Surowiec, K.; Gega, J.; Bartsch, R. A. *Tetrahedron* **2012,** *68,* 8789–8794. doi:10.1016/j.tet.2012.07.103
25. Zhou, H.; Connery, K. E.; Bartsch, R. A.; Moyer, B. A.; Haverlock, T. J.; Delmau, L. H. *Solvent Extr. Ion Exch.* **2013,** *31,* 683–696. doi:10.1080/07366299.2013.806754

26. Hendrickson, J. B.; Bergeron, R.; Giga, A.; Sternbach, D. *J. Am. Chem. Soc.* **1973,** *95,* 3412–3413. doi:10.1021/ja00791a072
27. Hendrickson, J. B.; Bergeron, R. *Tetrahedron Lett.* **1973,** *14,* 4607–4610. doi:10.1016/S0040-4039(01)87289-0
28. Benati, L.; Nanni, D.; Spagnolo, P. *J. Org. Chem.* **1999,** *64,* 5132–5138. doi:10.1021/jo9901541
29. Pampín, M. C.; Estévez, J. C.; Estévez, R. J.; Maestro, M.; Castedo, L. *Tetrahedron* **2003,** *59,* 7231–7243. doi:10.1016/S0040-4020(03)01073-1
30. Shainyan, B. A.; Tolstikova, L. L.; Bel'skikh, A. V. *Russ. J. Org. Chem.* **2008,** *44,* 1121–1125. doi:10.1134/S1070428008080022
31. Moskalik, M. Y.; Meshcheryakov, V. I.; Shainyan, B. A. *Russ. J. Org. Chem.* **2009,** *45,* 1644–1650. doi:10.1134/S1070428009110116
32. Cody, J. A.; Ahmed, I.; Tusch, D. J. *Tetrahedron Lett.* **2010,** *51,* 5585–5587. doi:10.1016/j.tetlet.2010.08.058
33. Wu, C.; Li, P.; Shi, X.; Pan, X.; Wu, J. *Acta Crystallogr., Sect. E: Struct. Rep. Online* **2011,** *67,* o382. doi:10.1107/S1600536811001085
34. Wu, X.; Rönn, R.; Gossas, T.; Larhed, M. *J. Org. Chem.* **2005,** *70,* 3094–3098. doi:10.1021/jo050080v
35. Urriolabeitia, E. P.; Laga, E.; Cativiela, C. *Beilstein J. Org. Chem.* **2012,** *8,* 1569–1575. doi:10.3762/bjoc.8.179
36. Petrova, E.; Rasina, D.; Jirgensons, A. *Eur. J. Org. Chem.* **2017,** 1773–1779. doi:10.1002/ejoc.201601582
37. Yagupolskii, L. M.; Shelyazhenko, S. V.; Maletina, I. I.; Sokolenko, L. V.; Chernega, A. N.; Rusanov, E. B.; Tsymbal, I. F. *J. Fluorine Chem.* **2007,** *128,* 515–523. doi:10.1016/j.jfluchem.2007.01.002
38. Yagupolskii, L. M.; Maletina, I. I.; Sokolenko, L. V.; Vlasenko, Y. G.; Buth, S. A. *J. Fluorine Chem.* **2008,** *129,* 486–492. doi:10.1016/j.jfluchem.2008.03.001
39. Yagupolskii, L. M.; Maletina, I. I.; Sokolenko, L. V.; Vlasenko, Y. G.; Drozdova, M. V.; Polovinko, V. V. *J. Fluorine Chem.* **2010,** *131,* 238–247. doi:10.1016/j.jfluchem.2009.10.019
40. Asensio, J. A.; Sánchez, E. M.; Gómez-Romero, P. *Chem. Soc. Rev.* **2010,** *39,* 3210–3239. doi:10.1039/b922650h
41. Diness, F.; Fairlie, D. P. *Angew. Chem., Int. Ed.* **2012,** *51,* 8012–8016. doi:10.1002/anie.201202149
42. Diness, F.; Begtrup, M. *Org. Lett.* **2014,** *16,* 3130–3133. doi:10.1021/ol5012554
43. Jacobsen, C. B.; Meldal, M.; Diness, F. *Chem. – Eur. J.* **2017,** *23,* 846–851. doi:10.1002/chem.201604098
44. Wang, J.-T.; Wainright, J. S.; Savinell, R. F.; Litt, M. *J. Appl. Electrochem.* **1996,** *26,* 751–756. doi:10.1007/bf00241516

License and Terms

BEILSTEIN JOURNAL OF ORGANIC CHEMISTRY

Copper-catalyzed asymmetric methylation of fluoroalkylated pyruvates with dimethylzinc

Kohsuke Aikawa, Kohei Yabuuchi, Kota Torii and Koichi Mikami*

Full Research Paper

Open Access

Address:
Department of Chemical Science and Engineering, School of Materials and Chemical Technology, Tokyo Institute of Technology, O-okayama, Meguro-ku, Tokyo 152-8552, Japan

Email:
Koichi Mikami* - mikami.k.ab@m.titech.ac.jp

* Corresponding author

Keywords:
asymmetric methylation; chiral phosphine ligand; copper catalyst; dimethylzinc; trifluoropyruvate

Beilstein J. Org. Chem. **2018,** *14,* 576–582.
doi:10.3762/bjoc.14.44

Received: 30 October 2017
Accepted: 19 February 2018
Published: 07 March 2018

This article is part of the Thematic Series "Organo-fluorine chemistry IV".

Guest Editor: D. O'Hagan

Abstract

The catalytic asymmetric methylation of fluoroalkylated pyruvates is shown with dimethylzinc as a methylating reagent in the presence of a copper catalyst bearing a chiral phosphine ligand. This is the first catalytic asymmetric methylation to synthesize various α-fluoroalkylated tertiary alcohols with CF_3, CF_2H, CF_2Br, and n-C_nF_{2n+1} (n = 2, 3, 8) groups in good-to-high yields and enantioselectivities. Axial backbones and substituents on phosphorus atoms of chiral phosphine ligands critically influence the enantioselectivity. Moreover, the methylation of simple perfluoroalkylated ketones is found to be facilitated by only chiral phosphines without copper.

Introduction

The introduction of fluorine atoms into organic compounds plays an important role in the discovery of lead candidates with unique biological and physicochemical properties [1,2]. Therefore, the development of novel synthetic methods for the introduction of fluorinated fragments, such as trifluoromethyl (CF_3), difluoromethyl (CF_2H), and difluoromethylene (-CF_2-), has attracted a great deal of attention from synthetic organic chemists [3-6]. Among these methods, many researchers including us have studied the catalytic asymmetric synthesis of optically active α-trifluoromethylated tertiary alcohols [7,8]. In these cases, one of commercially available and versatile trifluoromethyl sources, trifluoropyruvate, has been utilized for a variety of catalytic asymmetric carbon–carbon bond forming reactions, providing efficiently α-trifluoromethylated tertiary alcohols in high enantioselectivities [9-19]. Over the past decade we have also investigated several catalytic asymmetric reactions using trifluoropyruvate as an electrophile in the presence of a chiral Lewis acid complex [20-27]. However, the synthetic method for chiral α-trifluoromethylated tertiary alcohols via methylation of trifluoropyruvate is quite limited, although several drug candidates bearing this chiral trifluoromethylated moiety have so far been reported [7,28-30]. In 2007, Gosselin and Britton et al. re-

ported that treatment of ethyl trifluoropyruvate (**1a**) with (*R*)-BINOL-mediated organozincate as a chiral methylating regent provided the corresponding methylated tertiary alcohol **2a** in moderate enantioselectivity (Scheme 1, reaction 1) [31]. Kinetic resolution of racemic α-trifluoromethylated tertiary alcohols **2a** by an enzyme is also reported to give the corresponding alcohols **2a** in high enantioselectivity (Scheme 1, reaction 2) [32]. However, there has been no report for catalytic asymmetric methylation of trifluoropyruvate. Herein, we disclose the catalytic asymmetric methylation of trifluoropyruvate derivatives as electrophiles and dimethylzinc as a methylating nucleophile by a chiral copper catalyst. This method is also applicable to the asymmetric synthesis of various α-fluoroalkylated tertiary alcohols bearing CF_2H, CF_2Br, and n-C_nF_{2n+1} (n = 2, 3, 8) groups.

Results and Discussion

Our initial investigation was focused on the methylation of ethyl trifluoropyruvate (**1a**) with Me_2Zn in the presence of a copper salt bearing a chiral bidentate phosphine ligand (Table 1). We were delighted to find that the reaction proceeded smoothly in the presence of CuTC (TC: 2-thiophenecarboxylate, 2.5 mol %) and (*R*)-BINAP (2.7 mol %) in Et_2O at −78 °C, furnishing the methylated product **2a** in 99% yield with 38% ee (Table 1, entry 1). The effect of the Cu salt was also surveyed. The use of CuOAc resulted in slightly decreased enantioselectivities, and (CuOTf)·C_6H_6 and CuI led to a racemic product (Table 1, entries 2–4). Chiral phosphine ligands instead of BINAP were further assayed with the aim of enhancing the enantioselectivity. Indeed, the investigation of the effect of axial backbones and substituents on the phosphorus atoms led to an increase in the enantioselectivity. In the case of a biphenyl backbone, MeO-BIPHEP showed the same level of enantioselectivity as BINAP, while lower enantioselectivity was obtained by SEGPHOS (Table 1, entries 5 and 6). Exploring the effect of substituents on phosphorus, DM-BINAP slightly exceeded the level attained by BINAP, although Cy-BINAP and DTBM-BINAP decreased the enantioselectivities (Table 1, entries 7–9). In sharp contrast to BINAP derivatives, DTBM-SEGPHOS and DTBM-MeO-BIPHEP with extremely bulky aryl groups increased the enantioselectivities (Table 1, entries 10 and 11). Additionally, DTB-MeO-BIPHEP provided the desired alcohol in 84% yield with 60% ee (Table 1, entry 12). In toluene and CH_2Cl_2 as noncoordinating solvents (Table 1, entries 14 and 15), the reaction gave lower enantioselectivities, but TBME gave the best result in 90% yield and 67% ee (Table 1, entry 16). The use of methyl trifluoropyruvate (**1b**) instead of **1a** resulted in a lower enantioselectivity (Table 1, entry 17). The absolute configuration of **2b** was determined to be *S* by comparison with the optical rotation of reported data [32]. The absolute configurations of other alcohol products **2a** and **2c–k** were tentatively assigned by analogy to **2b**.

Additionally, the reaction conditions were fine-tuned as exemplified in Table 2. It was found that reactions without CuTC and phosphine ligand (Table 2, entry 1) or only without phosphine ligand (Table 2, entry 2) provided the alcohol as a racemic mixture even at −78 °C. In contrast, the chiral product was obtained in 64% yield in the absence of a copper salt but in low enantioselectivity (Table 2, entry 3). Therefore, decreasing the amount of phosphine ligand (2.4 mol %) to less than that of

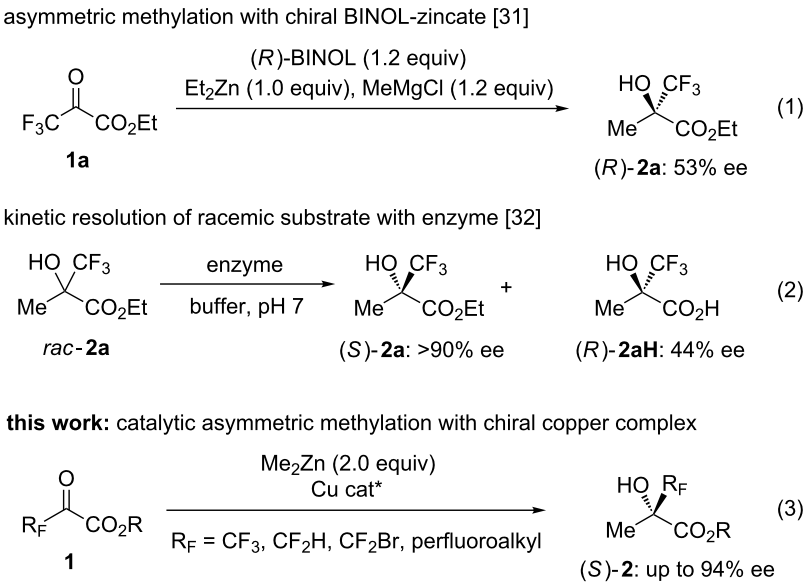

Scheme 1: Synthesis of chiral α-fluoroalkylated tertiary alcohols.

Table 1: Copper-catalyzed asymmetric methylation.

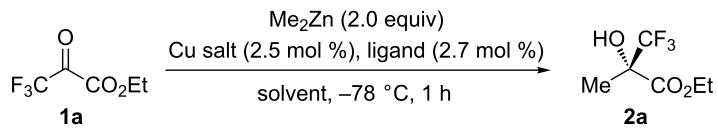

entry	ligand	Cu salt	solvent	yield (%)[a]	ee (%)
1	(*R*)-BINAP	CuTC	Et_2O	99	38
2	(*R*)-BINAP	CuOAc	Et_2O	43	36
3	(*R*)-BINAP	$(CuOTf)\cdot C_6H_6$	Et_2O	13	0
4	(*R*)-BINAP	CuI	Et_2O	38	0
5	(*R*)-SEGPHOS	CuTC	Et_2O	81	26
6	(*R*)-MeO-BIPHEP	CuTC	Et_2O	85	38
7	(*R*)-Cy-BINAP	CuTC	Et_2O	92	3
8	(*R*)-DM-BINAP	CuTC	Et_2O	70	41
9	(*R*)-DTBM-BINAP	CuTC	Et_2O	73	17
10	(*R*)-DTBM-SEGPHOS	CuTC	Et_2O	67	55
11	(*R*)-DTBM-MeO-BIPHEP	CuTC	Et_2O	99	50
12	(*R*)-DTB-MeO-BIPHEP	CuTC	Et_2O	84	60
13	(*R*)-DTB-MeO-BIPHEP	CuTC	THF	85	57
14	(*R*)-DTB-MeO-BIPHEP	CuTC	toluene	98	38
15	(*R*)-DTB-MeO-BIPHEP	CuTC	CH_2Cl_2	90	9
16	(*R*)-DTB-MeO-BIPHEP	CuTC	TBME	90	67
17[b]	(*R*)-DTB-MeO-BIPHEP	CuTC	TBME	71	59 (*S*)

[a]Yields were determined by ^{19}F NMR analysis using benzotrifluoride (BTF) as an internal standard. [b]Methyl trifluoropyruvate (**1b**) was used instead of ethyl trifluoropyruvate (**1a**).

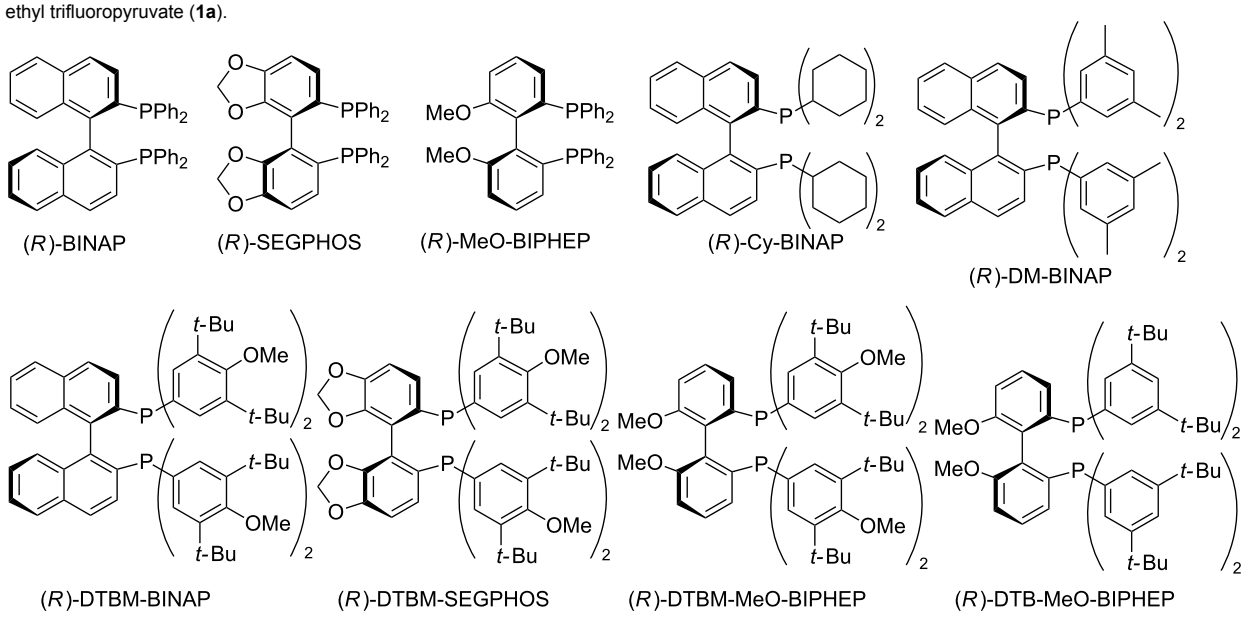

copper salt led to an enhancement of the enantioselectivity to 70% ee (Table 2, entries 4 vs 5). In addition, the selection of BTFM-Garphos instead of DTB-MeO-BIPHEP afforded a higher enantioselectivity (Table 2, entry 6), and consequently, a lower reaction temperature (−90 °C) gave the best result with 86% yield and 89% ee (Table 2, entry 7).

Various fluoroalkylated pyruvates were applicable to this catalytic transformation under the optimized reaction conditions (Scheme 2). Alkyl substituents on the ester moiety of the trifluoropyruvate were found to influence the stereoselectivity drastically. The reaction of trifluoropyruvates (**1c**–**e**) bearing sterically demanding substituents such as isopropyl, cyclopentyl,

Table 2: Optimization of reaction conditions.

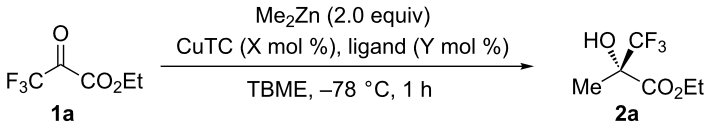

entry	X (mol %/Cu)	Y (mol %/ligand)	ligand	yield (%)[a]	ee (%)
1	0	0	–	17	–
2	2.5	0	–	15	–
3	0	2.5	(*R*)-DTB-MeO-BIPHEP	64	7
4	2.5	2.7	(*R*)-DTB-MeO-BIPHEP	90	67
5	2.5	2.4	(*R*)-DTB-MeO-BIPHEP	94	70
6	2.5	2.4	(*R*)-BTFM-Garphos	88	73
7[b]	2.5	2.4	(*R*)-BTFM-Garphos	86	89

[a]Yields were determined by ^{19}F NMR analysis using benzotrifluoride (BTF) as an internal standard. [b]Reaction temperature was −90 °C.

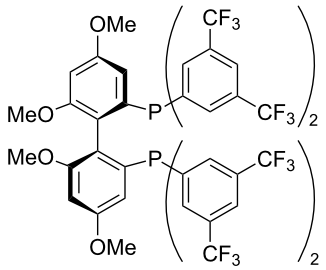

(*R*)-BTFM-Garphos

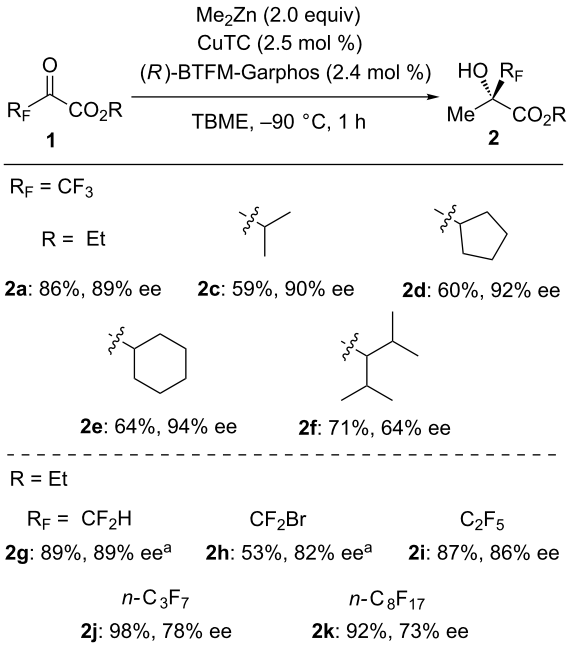

Scheme 2: Scope of fluoroalkylated pyruvates. Yields were determined by ^{19}F NMR analysis using benzotrifluoride (BTF) as an internal standard. [a]Reaction temperature was −78 °C.

and cyclohexyl led to a higher level of enantioselectivities (90–94% ee), compared to the corresponding ethyl ester **1a**. In contrast, trifluoropyruvate **1f** with an extremely bulky substituent caused a decrease of enantioselectivity. Ethyl difluoropyruvate (**1g**) and ethyl bromodifluoropyruvate (**1h**) also underwent the reactions in good enantioselectivities, although a slight decrease in yield was observed due to the steric hindrance of the CF_2Br group. Significantly, ethyl perfluoropyruvates **1i–k** with longer alkyl chains were also converted to the desired tertiary alcohols in good enantioselectivities.

The catalytic asymmetric methylation using the simple perfluoroalkylated ketone **3a** instead of pyruvate derivatives was further examined (Scheme 3). In contrast to the pyruvate system, the combination of CuTC and BINAP did not facilitate the reaction even at −78 °C, but also afforded the racemic product (25% yield, 0% ee). Interestingly, the use of only BINAP without CuTC led to higher reactivity and enantioselectivity (54% yield, 8% ee), while BTFM-Garphos decreased the reactivity (7% yield, 8% ee). After screening of phosphines, DTB-MeO-BIPHEP was found to smoothly catalyze the asymmetric methylation to give the desired alcohol **4a** in 87% yield and 24% ee.

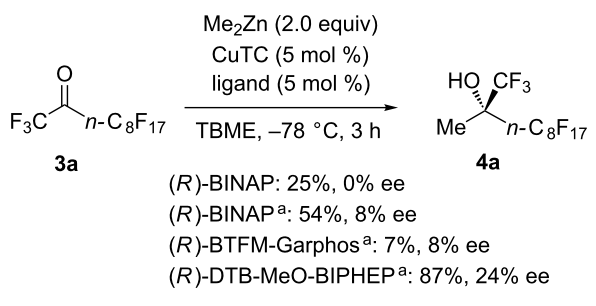

Scheme 3: Catalytic asymmetric methylation of the simple perfluoroalkylated ketone **3a**. Yields were determined by ^{19}F NMR analysis using benzotrifluoride (BTF) as an internal standard. [a]Reaction was carried out without CuTC.

Conclusion

In summary, we have succeeded in the catalytic enantioselective methylation of fluoroalkylated pyruvates in the presence of chiral diphosphine–copper complexes, providing the corresponding tertiary alcohols with an R_F group such as CF_3, CF_2H, CF_2Br, and n-C_nF_{2n+1} (n = 2, 3, 8) in good-to-high yields and enantioselectivities. This is the first report on catalytic asymmetric methylation with fluoroalkylated pyruvates. Moreover, a simple perfluoroalkyl ketone was also found to be methylated enantioselectively with dimethylzinc and a catalytic amount of a chiral diphosphine, but without copper.

Experimental

Typical procedure for copper-catalyzed asymmetric methylation of fluoroalkylated pyruvates: To a mixture of CuTC (1.0 mg, 0.005 mmol) and (*R*)-BTFM-Garphos (5.7 mg, 0.0048 mmol) was added CH_2Cl_2 (1.0 mL) at room temperature under an argon atmosphere, and the solution was stirred for 12 h. The solvent was removed under reduced pressure, and the prepared catalyst was dissolved in TBME (0.5 mL) under an argon atmosphere. After the solution was cooled to −90 °C, Me_2Zn (1.0 M in heptane, 0.4 mL, 0.4 mmol) followed by fluoroalkylated pyruvate **1** (0.2 mmol) in TBME (0.5 mL) were added over 30 min. The reaction mixture was stirred at the same temperature for 1 h. The reaction mixture was quenched with saturated aq NH_4Cl solution. The organic layer was separated and the aqueous layer was extracted twice with Et_2O. The combined organic layer was dried over anhydrous Na_2SO_4 and evaporated under reduced pressure (350 mmHg). The concentrated solution was used without purification for the next protection reaction. The yield of alcohol product **2** was determined by ^{19}F NMR analysis using benzotrifluoride (BTF) as an internal standard.

To a solution of DMAP (2.4 mg, 0.02 mmol) and the crude alcohol **2** in CH_2Cl_2 (2.0 mL) was added NEt_3 (56 µL, 0.4 mmol) at room temperature under an argon atmosphere. After the reaction mixture was cooled to 0 °C, *p*-nitrobenzoyl chloride (56 mg, 0.3 mmol) was added. Then the mixture was warmed to room temperature and stirred for 1 h. After 1 N HCl (5.0 mL) was added to the reaction mixture, the organic layer was separated and the aqueous layer was extracted twice with Et_2O. The combined organic layer was washed with saturated aq. $NaHCO_3$, water, and brine, and then dried over anhydrous $MgSO_4$ and evaporated under reduced pressure. The residue was purified by silica gel column chromatography to give *p*-nitrobenzoylated alcohol **2'**. The enantiomeric excess was determined by chiral HPLC analysis.

(*S*)-3-Ethoxy-1,1,1-trifluoro-2-methyl-3-oxopropan-2-yl 4-nitrobenzoate (**2a'**)

The yield of alcohol **2a** (86%) was determined by ^{19}F NMR analysis. *p*-Nitrobenzoylated alcohol **2a'** was purified by silica-gel column chromatography (EtOAc/hexane 1:40) as a colorless liquid (53% yield for 2 steps, 89% ee). ^{1}H NMR (300 MHz, $CDCl_3$) δ 8.34–8.31 (m, 2H), 8.24–8.20 (m, 2H), 4.33 (q, 4H, J = 6.9 Hz), 1.97 (d, 3H, J = 0.9 Hz), 1.28 (t, 3H, J = 7.0 Hz); ^{13}C NMR (75 MHz, $CDCl_3$) δ 164.3, 162.3, 151.1, 134.0, 131.2, 123.7, 122.7 (q, $J_{C\text{-}F}$ = 282.9 Hz), 80.7 (q, $J_{C\text{-}F}$ = 30.4 Hz), 63.2, 16.6, 13.8; ^{19}F NMR (282 MHz, $CDCl_3$) δ −78.4 (s, 3F); HRMS (APCI-TOF): $[M]^{-\cdot}$ calcd for $C_{13}H_{12}F_3NO_6$, 335.0617; found, 335.0623; FTIR (neat, cm^{-1}) 784, 813, 849, 876, 927, 1011, 1109, 1149, 1273, 1342, 1387, 1452, 1525, 1602, 1740, 1763, 2857, 2920, 2952, 2996, 3087, 3116; $[\alpha]_D^{22}$ −28.94 (*c* 0.20, $CHCl_3$); HPLC (column, CHIRALCEL OJ-3, hexane/2-propanol 91:9, flow rate 0.6 mL/min, 20 °C detection UV 254 nm) t_R of major isomer 13.1 min, t_R of minor isomer 23.8 min.

(*S*)-1-Ethoxy-3,3-difluoro-2-methyl-1-oxopropan-2-yl benzoate (**2g'**)

Reaction temperature was −78 °C. The yield of alcohol **2g** (89%) was determined by ^{19}F NMR analysis. In the protection of alcohol, benzoyl chloride was used instead of *p*-nitrobenzoyl chloride. Benzoylated alcohol **2g'** was purified by silica gel column chromatography (EtOAc/hexane 1:40) as a colorless liquid (41% yield for 2 steps, 89% ee). ^{1}H NMR (300 MHz, $CDCl_3$) δ 8.05 (dd, J = 8.3, 1.3 Hz, 2H). 7.61 (tt, J = 6.7, 1.3 Hz, 1H), 7.49–7.44 (m, 2H), 6.30 (dd, $J_{H\text{-}F}$ = 56.8, 54.8 Hz, 1H), 4.29 (q, J = 7.1 Hz, 2H), 1.77 (t, $J_{H\text{-}F}$ = 1.6 Hz, 3H), 1.27 (t, J = 7.1 Hz, 3H); ^{13}C NMR (75 MHz, $CDCl_3$) δ 167.6, 164.8, 133.7, 130.0, 128.8, 128.5, 122.9 (dd, $J_{C\text{-}F}$ = 250.0, 245.0 Hz), 79.7 (dd, $J_{C\text{-}F}$ = 27.5, 21.9 Hz), 62.3, 14.6 (t, $J_{C\text{-}F}$ = 3.2 Hz) 13.9; ^{19}F NMR (282 MHz, $CDCl_3$) δ −128.40 (dd, J = 290.2 Hz, $J_{F\text{-}H}$ =54.7 Hz, 1F), −132.76 (dd, J = 289.90 Hz, $J_{F\text{-}H}$ = 56.4 Hz, 1F); HRMS (APCI-TOF): $[M + Na]^+$ calcd for $C_{13}H_{14}F_2NaO_4$, 295.0758; found, 295.0761; FTIR (neat, cm^{-1}) 1026, 1093, 1114, 1216, 1279, 1388, 1452, 1602, 1730, 1747,

2938, 2985, 3021; $[\alpha]_D^{25}$ −7.47 (*c* 1.01, $CHCl_3$); HPLC (column, CHIRALCEL OJ-3, hexane/2-propanol 99:1, flow rate 0.6 mL/min, 20 °C detection UV 220 nm) t_R of major isomer 21.2 min, t_R of minor isomer 22.6 min.

(*S*)-1-Bromo-3-ethoxy-1,1-difluoro-2-methyl-3-oxopropan-2-yl 4-nitrobenzoate (**2h'**)

Reaction temperature was −78 °C. The yield of alcohol **2h** (53%) was determined by ^{19}F NMR analysis. *p*-Nitrobenzoylated alcohol **2h'** was purified by silica gel column chromatography (EtOAc/hexane 1:50) as a white solid (32% yield for 2 steps, 82% ee). ^1H NMR (300 MHz, $CDCl_3$) δ 8.34–8.31 (m, 2H), 8.25–8.21 (m, 2H), 4.32 (q, 2H, *J* = 7.2 Hz), 2.02 (s, 3H), 1.29 (t, 3H, *J* = 7.0 Hz); ^{13}C NMR (75 MHz, $CDCl_3$) δ 164.3, 162.4, 151.2, 134.3, 131.3, 123.9, 121.0 (t, $J_{C\text{-}F}$ = 311.6 Hz), 84.8 (dd, $J_{C\text{-}F}$ = 25.6, 23.4 Hz), 63.4, 18.4, 14.0; ^{19}F NMR (282 MHz, $CDCl_3$) δ −56.9 (d, 1F, *J* = 168.6 Hz), −58.9 (d, 1F, *J* = 165.3 Hz); HRMS (APCI-TOF): $[M]^{-\cdot}$ calcd for $C_{13}H_{12}BrF_2NO_6$, 394.9816; found, 394.9835; FTIR (KBr pellet, cm^{-1}) 716, 843, 876, 961, 1020, 1106, 1146, 1280, 1347, 1446, 1528, 1610, 1751, 2866, 2936, 2988; $[\alpha]_D^{22}$ −11.99 (*c* 1.55, $CHCl_3$); HPLC (column, CHIRALCEL OD-3, hexane/2-propanol 91:9, flow rate 0.6 mL/min, 20 °C detection UV 254 nm) t_R of major isomer 18.2 min, t_R of minor isomer 12.5 min.

(*S*)-1-Ethoxy-3,3,4,4,4-pentafluoro-2-methyl-1-oxobutan-2-yl *p*-nitrobenzoate (**2i'**)

The yield of alcohol **2i** (87%) was determined by ^{19}F NMR analysis. *p*-Nitrobenzoylated alcohol **2i'** was purified by silica gel column chromatography (EtOAc/hexane 1:40) as a white solid (48% yield for 2 steps, 86% ee). ^1H NMR (300 MHz, $CDCl_3$) δ 8.35–8.30 (m, 2H) 8.21–8.16 (m, 2H), 4.37–4.27 (m, 2H), 2.04 (q, $J_{H\text{-}F}$ = 0.6 Hz, 3H), 1.28 (t, *J* = 7.1 Hz, 3H); ^{13}C NMR (75 MHz, $CDCl_3$) δ 164.2, 162.2 (d, $J_{C\text{-}F}$ = 2.0 Hz), 151.0, 134.1, 131.0, 123.8, 118.6 (qt, $J_{C\text{-}F}$ = 286.1, 35.6 Hz), 112.0 (tq, $J_{C\text{-}F}$ = 263.0, 36.8 Hz), 81.3 (t, $J_{C\text{-}F}$ = 25.4 Hz), 63.3, 16.6, 13.7; ^{19}F NMR (282 MHz, $CDCl_3$) δ −79.19 (s, 3F), −121.42 (d, *J* = 280.9 Hz, 1F), −122.98 (d, *J* = 279.7 Hz, 1F); HRMS (APCI-TOF): $[M]^{-\cdot}$ calcd for $C_{14}H_{12}F_5NO_6$, 385.0585; found, 385.0582; FTIR (KBr pellet, cm^{-1}) 1014, 1142, 1208, 1222, 1281, 1350, 1385, 1533, 1747, 2942, 2987, 3059; $[\alpha]_D^{25}$ −27.75 (*c* 1.02, $CHCl_3$); HPLC (column, CHIRALCEL OJ-3, hexane/2-propanol 99:1, flow rate 0.6 mL/min, 20 °C detection UV 220 nm) t_R of major isomer 16.2 min, t_R of minor isomer 31.4 min.

(*S*)-1-Ethoxy-3,3,4,4,5,5,5-heptafluoro-2-methyl-1-oxopentan-2-yl *p*-nitrobenzoate (**2j'**)

The yield of alcohol **2j** (98%) was determined by ^{19}F NMR analysis. *p*-Nitrobenzoylated alcohol **2j'** was purified by silica-gel column chromatography (EtOAc/hexane 1:50) as a colorless oil (48% yield for 2 steps, 78% ee). ^1H NMR (300 MHz, $CDCl_3$) δ 8.35–8.31 (m, 2H) 8.21–8.16 (m, 2H), 4.36–4.29 (m, 2H), 2.07 (q, $J_{H\text{-}F}$ = 1.3 Hz, 3H), 1.28 (t, *J* = 7.1 Hz, 3H); ^{13}C NMR (75 MHz, $CDCl_3$) δ 164.2 162.2, 151.0, 134.1, 131.0, 123.8, 117.6 (qt, $J_{C\text{-}F}$ = 286.9, 33.9 Hz), 113.6 (tt, $J_{C\text{-}F}$ = 263.9, 30.9 Hz), 122.9 (tq, $J_{C\text{-}F}$ = 266.9, 37.4 Hz), 82.2 (t, $J_{C\text{-}F}$ = 25.7 Hz), 63.4, 16.8, 13.7; ^{19}F NMR (282 MHz, $CDCl_3$) δ −80.65 (m, 3F), −117.75 (d, *J* = 288.5 Hz, 1F), −119.60 (d, *J* = 288.2 Hz, 1F), −123.882 (s, 2F); HRMS (APCI-TOF): $[M]^{-\cdot}$ calcd for $C_{15}H_{12}F_7NO_6$, 435.0553; found, 435.0547; FTIR (neat, cm^{-1}) 1090, 1140, 1200, 1233, 1349, 1387, 1534, 1609, 1744, 1761, 2942, 2988, 3059; $[\alpha]_D^{25}$ −22.60 (*c* 0.94, $CHCl_3$); HPLC (column, CHIRALCEL OJ-3, hexane/2-propanol 99:1, flow rate 0.6 mL/min, 20 °C detection UV 220 nm) t_R of major isomer 12.2 min, t_R of minor isomer 15.5 min.

(*S*)-1-Ethoxy-3,3,4,4,5,5,6,6,7,7,8,8,9,9,10,10,10-heptadecafluoro-2-methyl-1-oxodecan-2-yl *p*-nitrobenzoate (**3k'**)

The yield of alcohol **2k** (92%) was determined by ^{19}F NMR analysis. *p*-Nitrobenzoylated alcohol **2k'** was purified by silica-gel column chromatography (EtOAc/hexane 1:50) as a white solid (85% yield for 2 steps, 73% ee). ^1H NMR (300 MHz, $CDCl_3$) δ 8.36–8.31 (m, 2H), 8.20–8.16 (m, 2H), 4.36–4.29 (m, 2H), 2.08 (s, 3H), 1.28 (t, 3H, *J* = 7.3 Hz); ^{13}C NMR (75 MHz, $CDCl_3$) δ 164.3, 162.4, 151.2, 134.3, 131.2, 123.9, 118.4–104.7 (m), 117.3 (qt, $J_{C\text{-}F}$ = 288.4, 33.2 Hz), 82.8 (t, $J_{C\text{-}F}$ = 25.4 Hz), 63.5, 17.1, 13.8; ^{19}F NMR (282 MHz, $CDCl_3$) δ –80.7 (m, 3F), –116.4 to −126.0 (m, 14F); HRMS (APCI-TOF): $[M]^{-\cdot}$ calcd for $C_{20}H_{12}F_{17}NO_6$, 685.0393; found, 685.0362; FTIR (KBr pellet cm^{-1}) 847, 969, 1009, 1142, 1214, 1246, 1297, 1472, 1530, 1613, 1732, 1757, 2339, 2360, 2860, 2922, 2997, 3112, 3454, 3493; $[\alpha]_D^{22}$ −11.93 (*c* 0.48, $CHCl_3$); HPLC (column, CHIRALPAK AD-3 and AD-H, hexane/2-propanol 99.5:0.5, flow rate 0.6 mL/min, 20 °C detection UV 254 nm) t_R of major isomer 16.8 min, t_R of minor isomer 24.4 min.

Supporting Information

Supporting Information File 1

Experimental details and characterization data of new compounds with copies of ^1H, ^{13}C and ^{19}F NMR spectra.
[https://www.beilstein-journals.org/bjoc/content/supplementary/1860-5397-14-44-S1.pdf]

Acknowledgements

This work was financially supported by JST (ACT-C: Advanced Catalytic Transformation program for Carbon utilization), JSPS KAKENHI Grant Number 25410036, and the

Noguchi Institute. We thank Central Glass Co., Ltd. for the gift of ethyl trifluoropyruvate (**1a**).

References

1. Müller, K.; Faeh, C.; Diederich, F. *Science* **2007,** *317,* 1881–1886. doi:10.1126/science.1131943
2. Hagmann, W. K. *J. Med. Chem.* **2008,** *51,* 4359–4369. doi:10.1021/jm800219f
3. Kirsch, P. *Modern Fluoroorganic Chemistry: Synthesis, Reactivity, Applications,* 2nd ed.; Wiley-VCH: Weinheim, Germany, 2013. doi:10.1002/9783527651351
4. Tomashenko, O. A.; Grushin, V. V. *Chem. Rev.* **2011,** *111,* 4475–4521. doi:10.1021/cr1004293
5. Liang, T.; Neumann, C. N.; Ritter, T. *Angew. Chem., Int. Ed.* **2013,** *52,* 8214–8264. doi:10.1002/anie.201206566
6. Sugiishi, T.; Amii, H.; Aikawa, K.; Mikami, K. *Beilstein J. Org. Chem.* **2015,** *11,* 2661–2670. doi:10.3762/bjoc.11.286
7. Nie, J.; Guo, H.-C.; Cahard, D.; Ma, J.-A. *Chem. Rev.* **2011,** *111,* 455–529. doi:10.1021/cr100166a
8. Mikami, K.; Itoh, Y.; Yamanaka, M. *Chem. Rev.* **2004,** *104,* 1–16. doi:10.1021/cr030685w
9. Gathergood, N.; Zhuang, W.; Jørgensen, K. A. *J. Am. Chem. Soc.* **2000,** *122,* 12517–12522. doi:10.1021/ja002593j
10. Zhuang, W.; Gathergood, N.; Hazell, R. G.; Jørgensen, K. A. *J. Org. Chem.* **2001,** *66,* 1009–1013. doi:10.1021/jo001176m
11. Török, B.; Abid, M.; London, G.; Esquibel, J.; Török, M.; Mhadgut, S. C.; Yan, P.; Prakash, G. K. S. *Angew. Chem., Int. Ed.* **2005,** *44,* 3086–3089. doi:10.1002/anie.200462877
12. Suri, J. T.; Mitsumori, S.; Albertshofer, K.; Tanaka, F.; Barbas, C. F., III. *J. Org. Chem.* **2006,** *71,* 3822–3828. doi:10.1021/jo0602017
13. Doherty, S.; Knight, J. G.; Smyth, C. H.; Harrington, R. W.; Clegg, W. *J. Org. Chem.* **2006,** *71,* 9751–9764. doi:10.1021/jo062023n
14. Rueping, M.; Theissmann, T.; Kuenkel, A.; Koenigs, R. M. *Angew. Chem., Int. Ed.* **2008,** *47,* 6798–6801. doi:10.1002/anie.200802139
15. Zhao, J.-F.; Tjan, T.-B. W.; Tan, B.-H.; Loh, T.-P. *Org. Lett.* **2009,** *11,* 5714–5716. doi:10.1021/ol902507x
16. Ogawa, S.; Iida, N.; Tokunaga, E.; Shiro, M.; Shibata, N. *Chem. – Eur. J.* **2010,** *16,* 7090–7095. doi:10.1002/chem.201000911
17. Ohshima, T.; Kawabata, T.; Takeuchi, Y.; Kakinuma, T.; Iwasaki, T.; Yonezawa, T.; Murakami, H.; Nishiyama, H.; Mashima, K. *Angew. Chem., Int. Ed.* **2011,** *50,* 6296–6300. doi:10.1002/anie.201100252
18. Dong, X.; Sun, J. *Org. Lett.* **2014,** *16,* 2450–2453. doi:10.1021/ol500830a
19. Morisaki, K.; Morimoto, H.; Mashima, K.; Ohshima, T. *Heterocycles* **2017,** *95,* 637–661. doi:10.3987/REV-16-SR(S)4
20. Aikawa, K.; Kainuma, S.; Hatano, M.; Mikami, K. *Tetrahedron Lett.* **2004,** *45,* 183–185. doi:10.1016/j.tetlet.2003.10.137
21. Mikami, K.; Kawakami, Y.; Akiyama, K.; Aikawa, K. *J. Am. Chem. Soc.* **2007,** *129,* 12950–12951. doi:10.1021/ja076539f
22. Aikawa, K.; Hioki, Y.; Mikami, K. *Org. Lett.* **2010,** *12,* 5716–5719. doi:10.1021/ol102541s
23. Mikami, K.; Aikawa, K.; Aida, J. *Synlett* **2011,** 2719–2724. doi:10.1055/s-0031-1289540
24. Aikawa, K.; Hioki, Y.; Shimizu, N.; Mikami, K. *J. Am. Chem. Soc.* **2011,** *133,* 20092–20095. doi:10.1021/ja2085299
25. Aikawa, K.; Asai, Y.; Hioki, Y.; Mikami, K. *Tetrahedron: Asymmetry* **2014,** *25,* 1104–1115. doi:10.1016/j.tetasy.2014.06.013
26. Aikawa, K.; Kondo, D.; Honda, K.; Mikami, K. *Chem. – Eur. J.* **2015,** *21,* 17565–17569. doi:10.1002/chem.201503631
27. Aikawa, K.; Yoshida, S.; Kondo, D.; Asai, Y.; Mikami, K. *Org. Lett.* **2015,** *17,* 5108–5111. doi:10.1021/acs.orglett.5b02617
28. Aicher, T. D.; Anderson, R. C.; Bebernitz, G. R.; Coppola, G. M.; Jewell, C. F.; Knorr, D. C.; Liu, C.; Sperbeck, D. M.; Brand, L. J.; Strohschein, R. J.; Gao, J.; Vinluan, C. C.; Shetty, S. S.; Dragland, C.; Kaplan, E. L.; DelGrande, D.; Islam, A.; Liu, X.; Lozito, R. J.; Maniara, W. M.; Walter, R. E.; Mann, W. R. *J. Med. Chem.* **1999,** *42,* 2741–2746. doi:10.1021/jm9902584
29. Aicher, T. D.; Anderson, R. C.; Gao, J.; Shetty, S. S.; Coppola, G. M.; Stanton, J. L.; Knorr, D. C.; Sperbeck, D. M.; Brand, L. J.; Vinluan, C. C.; Kaplan, E. L.; Dragland, C. J.; Tomaselli, H. C.; Islam, A.; Lozito, R. J.; Liu, X.; Maniara, W. M.; Fillers, W. S.; DelGrande, D.; Walter, R. E.; Mann, W. R. *J. Med. Chem.* **2000,** *43,* 236–249. doi:10.1021/jm990358+
30. Bebernitz, G. R.; Aicher, T. D.; Stanton, J. L.; Gao, J.; Shetty, S. S.; Knorr, D. C.; Strohschein, R. J.; Tan, J.; Brand, L. J.; Liu, C.; Wang, W. H.; Vinluan, C. C.; Kaplan, E. L.; Dragland, C. J.; DelGrande, D.; Islam, A.; Lozito, R. J.; Liu, X.; Maniara, W. M.; Mann, W. R. *J. Med. Chem.* **2000,** *43,* 2248–2257. doi:10.1021/jm0000923
31. Gosselin, F.; Britton, R. A.; Mowat, J.; O'Shea, P. D.; Davies, I. W. *Synlett* **2007,** 2193–2196. doi:10.1055/s-2007-984911
32. Konigsberger, K.; Prasad, K.; Repič, O. *Tetrahedron: Asymmetry* **1999,** *10,* 679–687. doi:10.1016/S0957-4166(99)00017-8

License and Terms